FILE COPY

ARO 25645.2-GS-CF

②

AD-A213 199

Second International Conference on Case Histories in Geotechnical Engineering

June 1-5, 1988

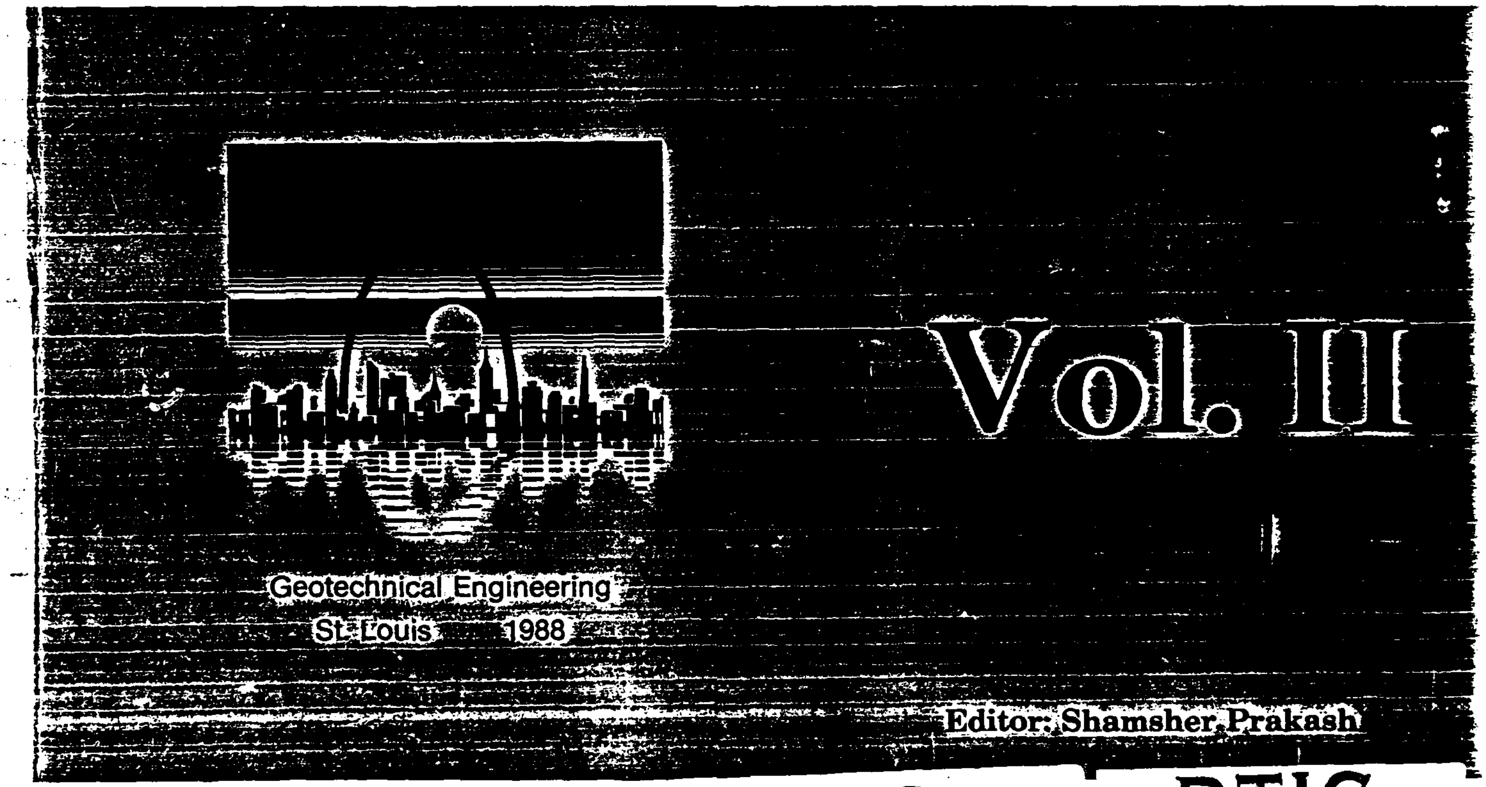
Geotechnical Engineering
St. Louis 1988

Vol. II

Editor: Shamsher Prakash

This document has been approved for public release and sale; its distribution is unlimited.

University of Missouri-Rolla
Rolla, Missouri

DTIC
ELECTE
OCT 10 1989
S E D

89 10 10 210

UNCLASSIFIED MASTER COPY - FOR REPRODUCTION PURPOSES

SECURITY CLASSIFICATION OF THIS PAGE

REPORT DOCUMENTATION PAGE

1a. REPORT SECURITY CLASSIFICATION
Unclassified

1b. RESTRICTIVE MARKINGS

2a. SECURITY CLASSIFICATION AUTHORITY

2b. DECLASSIFICATION / DOWNGRADING SCHEDULE

3. DISTRIBUTION / AVAILABILITY OF REPORT
Approved for public release;
distribution unlimited.

4. PERFORMING ORGANIZATION REPORT NUMBER(S)

5. MONITORING ORGANIZATION REPORT NUMBER(S)
ARO 25645.2-GS-CF

6a. NAME OF PERFORMING ORGANIZATION
Univ. of Missouri at Rolla

6b. OFFICE SYMBOL *(If applicable)*

7a. NAME OF MONITORING ORGANIZATION
U. S. Army Research Office

6c. ADDRESS *(City, State, and ZIP Code)*
Rolla, MO 65401-0149

7b. ADDRESS *(City, State, and ZIP Code)*
P. O. Box 12211
Research Triangle Park, NC 27709-2211

8a. NAME OF FUNDING / SPONSORING ORGANIZATION
U. S. Army Research Office

8b. OFFICE SYMBOL *(If applicable)*

9. PROCUREMENT INSTRUMENT IDENTIFICATION NUMBER
DAAL03-87-G-0129

8c. ADDRESS *(City, State, and ZIP Code)*
P. O. Box 12211
Research Triangle Park, NC 27709-2211

10. SOURCE OF FUNDING NUMBERS

PROGRAM ELEMENT NO.	PROJECT NO.	TASK NO.	WORK UNIT ACCESSION NO.

11. TITLE *(Include Security Classification)*
Second International Conference on Case Histories in Geotechnical Engineering, Volume II

12. PERSONAL AUTHOR(S)
Shamshear Prakash

13a. TYPE OF REPORT
Final

13b. TIME COVERED
FROM 1/1/88 TO 6/30/89

14. DATE OF REPORT *(Year, Month, Day)*

15. PAGE COUNT
1612

16. SUPPLEMENTARY NOTATION
The view, opinions and/or findings contained in this report are those of the author(s) and should not be construed as an official Department of the Army position, policy, or decision, unless so designated by other documentation.

17. COSATI CODES

FIELD	GROUP	SUB-GROUP

18. SUBJECT TERMS *(Continue on reverse if necessary and identify by block number)*
Geotechnical Engineering, Case Histories, Soil Dynamics, Rock Mechanics, Earthquake Engineering, Dams, Embankments, Slopes, Radioactive Waste, Hazardous Waste, Soil Structure

19. ABSTRACT *(Continue on reverse if necessary and identify by block number)*

The conference papers and state-of-the-art reports have been printed in two volumes which will be issued before the conference. The third volume containing reports, discussions, authors' replies, speeches and special programs, will be issued after the conference. The first volume contains 136 papers, and the second volume contains 100 papers and six state-of-the-art papers.

20. DISTRIBUTION / AVAILABILITY OF ABSTRACT
☐ UNCLASSIFIED/UNLIMITED ☐ SAME AS RPT. ☐ DTIC USERS

21. ABSTRACT SECURITY CLASSIFICATION
Unclassified

22a. NAME OF RESPONSIBLE INDIVIDUAL

22b. TELEPHONE *(Include Area Code)*

22c. OFFICE SYMBOL

83 APR edition may be used until exhausted.
All other editions are obsolete.

SECURITY CLASSIFICATION OF THIS PAGE
UNCLASSIFIED

Second
International Conference
on
Case Histories in
Geotechnical Engineering

June 1-5, 1988

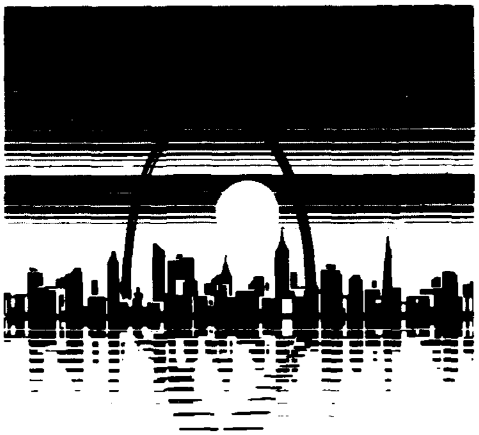

Geotechnical Engineering
St. Louis 1988

Vol. II

Editor: Shamsher Prakash

University of Missouri-Rolla
Rolla, Missouri

Disclaimer

"The views, opinions, and or findings contained in these proceeding volumes are those of the author(s) and should not be construed as an official Department of the Army or University of Missouri-Rolla position, policy, or decision, unless so designated by other documentation."

Preface

The University of Missouri-Rolla had hosted a very successful International Conference on Case Histories in Geotechnical Engineering in May 1984. The Second Conference in the series was planned in 1985, and a Call for Papers was issued in December 1986. The conference has been co-sponsored and partially funded by the U.S. Army Department of Research. It has been organized in cooperation with the International Society for Soil Mechanics and Foundation Engineering, International Association of Earthquake Engineering, Earthquake Engineering Research Institute, Association of Engineering Geologists, United States Committee on Large Dams, United States National Committee for Rock Mechanics, Transportation Research Board, American Society of Civil Engineers—Mid-Missouri Section, Association of Soil and Foundation Engineers, and Engineering Geology Division of the Geological Society of America.

The Call for Papers was issued in December 1986 and papers were contributed from 47 countries: Australia, Austria, Brazil, Bulgaria, Canada, China, Denmark, Egypt, France, Germany, Ghana, Greece, Hong Kong, India, Indonesia, Iraq, Ireland, Israel, Italy, Japan, Jordan, Kenya, Korea, Libya, Mexico, Netherlands, New Zealand, Nigeria, Norway, Pakistan, Panama, Peru, Portugal, Puerto Rico, Romania, Saudi Arabia, Singapore, South Africa, Sri Lanka, Sweden, Taiwan, Turkey, United Kingdom, United States, U.S.S.R., Vietnam, and Yugoslavia, making this conference a truly international one. The large number of papers received were reviewed by a panel of 12 international experts.

The conference papers and state-of-the-art reports have been printed in two volumes which will be issued before the conference. The third volume containing reports, discussions, authors' replies, speeches and special programs, will be issued after the conference. The first volume contains 136 papers, and the second volume contains 100 papers and six state-of-the-art papers.

The organizing committee was always ready to assist in matters of organization. In the initial stages of planning, guidance was obtained from W.D. Liam Finn, E. D'Appolonia, Norbert O. Schmidt, and Allen W. Hatheway. The University of Missouri-Rolla staff has been very cooperative throughout, especially personnel of the Engineering Continuing Education unit. In addition, our secretaries, particularly Janet Pearson, worked hard to keep pace with the paperwork associated with such a venture. Their work is especially appreciated since everyone knows how difficult it would be to handle such a monumental work without the active cooperation of these people.

The timely printing of the proceedings has been made possible through the efforts of personnel at UMR Centralized Printing Office. Without the expertise and technical assistance of these individuals, the proceedings would not exist in their present form.

We now look forward to a successful conference in St. Louis during the week of June 1-5, 1988.

JANUARY 3, 1988

Shamsher Prakash, Editor
and Conference Chairman

Accession For
NTIS GRA&I ☒
DTIC TAB ☐
Unannounced ☐
Justification
By
Distribution/
Availability Codes
Dist | Avail and/or Special
A-1

Table of Contents

Volume I

Session I

"Case Histories of Geotechnical and Hydrological Management of Solid, Hazardous, and Radioactive Wastes"

		Page No.
W.C.B. Gates (USA)	Use of Deeply Weathered Rock as Landfill Cover Material, Patacon Landfill, Republic of Panama. 1.05	1
D. Raghu H.N. Hsieh (USA)	Disposal of Phenolic Waters from a Producer Gas Plant. 1.06	7
D. McGrane (USA)	Complementing Radiologic Data with Geology—A Case History. 1.07	13
W.M. Kilkenny (England)	A Low-Rise Hospital Development on Restored Opencast Fill. 1.08	19
J.A. Caldwell R.E. Rager L. Coons (USA)	Geotechnical and Groundwater Site Characterization on the Umtra Project. 1.09	25
D.E. Mills D.A. Cordell (USA)	Evaluation of Remedial In-Waste Lechate Head Reduction. 1.10	35
H. Dezfulian (USA)	Site Assessment and Remediation of an Oil-Producing Property. 1.11	43
D. Raghu R.J. Van Orden (USA)	Failure and Reconstruction of a Waste Containment Pond Slope. 1.13	51
M.D. Huag J. Atwater R.B. Knight P. Kozicki A. Lissey (Canada)	Implementation of Remedial Measure to Contain a PCB Spill. 1.14	55
P.J. Bosscher T.B. Edil (USA)	Performance of Lightweight Waste Impoundment Dikes. 1.17	63
G.H. Cramer (USA)	A Study of Contamination Migration at a Hazardous Waste Facility in Louisiana. 1.21	71
R.V. Sarsby (England)	Control of Uplift from Ground Water. 1.22	75
A.S. Burgess M.S. Leonard G.S. Laird (USA)	Design and Construction of a Soil Bentonite Slurry Wall Around an Operating Facility Superfund Site. 1.23	81

Session I continued Page No.

G.S. Laird, A.M. Gurevich, W.B. Lozier (USA) — A Modified Field Infiltrometer Test for Clay Liners. 1.25 89

S.M. Testa (USA) — Hazardous Waste Disposal Site Hydrogeologic Characterization. 1.26 97

Session II
"Case Histories in Geological Engineering and Rock Mechanics"

S.C. Bandis (Greece) — Engineering Design of Rock Slope Reinforcement Based on Non-Linear Joint Strength Model. 2.03 107

J. Pitts (Singapore) — Stability of a Rock Slope at Bukit Batok New Town Singapore. 2.07 115

J.K.P. Kwong (USA), L.J. Endicott (Hong Kong), A.C. Lumsden (England) — Slope Stability Evaluation for an Existing Steep Cut in Weathered Volcanics Hong Kong. 2.08 123

N.M. Patel (India) — Distress in a Hill and Remedial Measures. 2.11 127

Z.Q. Wang, R.X. Zhang (China) — Case Study—Ground Failures and Ruptures in Xian City. 2.12 131

G.A. Hu (China) — On a New Problem of High Speed Landslides. 2.13 137

K.D. Weaver, D.J. Gross, L.T. Bauer (USA) — Slope Stabilization Measures for Kirkwood Penstock, Early Intake California. 2.14 143

B. Prabhakar, J.L. Jethwa, B. Singh (India) — A Case History of Tehri Tunnels. 2.15 147

C. Rodriquez-Perez, L. Vazquez Castillo, C. Rodriquez-Molina, A. Vazquez Castillo (Puerto Rico) — A Study of a Road Landslide in Puerto Rico. 2.16 151

Z.R. Fattohi (Iraq) — Simultaneous Velocity Measurements with Uniaxial Loading on Weak Sandstone from Iraq. 2.18 159

		Page No.
A.C. Van Besien N.B. Aughenbaugh (USA)	Johnston City School, Mine Subsidence or Shallow Foundation Problem. 2.19	163
L. Jiayou M. Jianyun (China)	The Successful Construction of a High Gravity Dam on Complex Rock Formations. 2.20	167
M.G. Karfakis B.A. Suprenant (USA)	Ground Failure Investigation Over Abandoned Coal Mines: A Case Study. 2.21	173
R.K. Goel J.L. Jethwa B. Singh (India)	Case History of Maneri—Uttarkashi Power Tunnel. 2.22	177
J.G. Cabrera (USA)	Foundation Investigation and Treatment for the Main Dam, Itaipu Project. 2.23	185
D. Raghu D.A. Antes J.L. Lifrieri (USA)	Grouting a Water Tower Foundation in a Carbonate Formation. 2.24	195
R.D. Prager G.S. Grainger R.L. Butts (USA)	Rock Response in a 12-M Tunnel Through a Zone of Low Strength. 2.25	201
P.S. Khare S.G. Kulkarni S.L. Mokhashi (India)	Stability Check of Escarpment Using Finite Element Method. 2.28	207
A.K. Dube B. Singh (India)	Rock Mass Behaviour Assessment for Large Cavern in Rock. 2.29	211
J.A. Larson (USA) D.P. Richards (Turkey)	Support Over Cavities of Unknown Depth for Underground Facility. 2.34	215
R.C. Ilsley S.B. Fradkin E.F. Shorey (USA)	Evaluation of the Site Investigation and Construction Related Aspects of the Milwaukee Crosstown Deep Tunnel. 2.36	221
J.M. Descour R.J. Miller (USA)	Microseismic Activity in an Open Pit Lignite Mine. 2.37	229
A.O. Erol A.W. Dhowian (Saudi Arabia)	Foundation Failures Associated with Salt Rock and Surrounding Coastal Plain. 2.39	237

Session II continued

		Page No.
G.S. Mehrotra R.K. Bhandari (India)	A Geological Appraisal of Slope Instability and Proposed Remedial Measures at Kaliasaur Slide on National Highway Garhwal Himalaya. 2.40	245
Y.P. Chugh K. Chandrashekhar R. Missavage (USA)	Subsidence Movements and Structural Damage Related to an Abandoned Coal Mine. 2.41	253
T. Ramamurthy V.M. Sharma (India)	Performance of Some Tunnels in Squeezing Rocks of Himalayas. 2.42	263
B. Hasan (Pakistan)	Effects of Geology and Geotechnical Properties of Rocks for the Selection of Type of Dams. 2.44	271
A.M. Jokhyo (Pakistan)	Slopes in Weak Rocks. 2.46	279
K.K. Kapoor S.C. Patodiya (India)	Construction of a Hydel Power House in Weak Rocks. 2.47	285
M.C. Betournay C. Mirza K.C. Lau (Canada)	Coring of Soft Soil-Like Rock Materials. 2.49	291
K. Anguelov (Bulgaria)	The Great Landslides in the East-Maritza Open-cast Mines (Bulgaria)—A Theoretical Paradox in the Engineering Geology. 2.50	299
H.C. Nainwal Y.P. Sundriya C. Prasad (India)	Study of Some Debris Avalanches in Garhwal Himalaya, India. 2.52	305
R.S. Mithal (India)	Lithotectonic Landslides and Hazards in Parts of Garhwal-Kumaon Himalaya. 2.55	311
M.A. El-Sohby S.O. Mazen (Egypt)	Geotechnical Characterization of Subsoil Deposits at Cairo. 2.56	321
D.M. Pancholi K.E. Modhwadia P.H. Vaidya (India)	Geo-Engineering Problems in the Spillway Foundations and Their Treatment at Guhai Reservoir Project in Gujarat, India. 2.58	327
R.K. Bhandari (India)	A Novel Low Cost Drum Diaphragm Wall for Landslide Control in The Himalaya. 2.60	333
M. Christos (Greece)	Prevision of the Bearing Capacity of Superficial Foundation on Jointed Rock. 2.61	337
K. H. Earley D. Rudenko (USA)	Use of Geophysical Methods in a Geotechnical Investigation. 2.64	341

Session III
"Case Histories of Dams, Embankments, and Slopes"

		Page No.
D. Abolhassani F. Bahrami-Samani (Iran) R.P. Brenner (Switzerland)	Unusual Behaviour of An Earth-Rockfill Dam. 3.01	347
J.W. Erwin G.R. Baer (USA)	Seepage Incident, St. Stephen Powerhouse, St. Stephen, S.C. 3.04	355
T.K. Natarajan A V.S.R. Murty D. Chandra (India)	Control of Surficial Slides by Different Erosion Control Techniques. 3.05	361
T.K. Natarajan P.J. Rao (India)	Restoration of the Stability of Retaining Wall. 3.06	365
Z.V. Solymar G.C. MacTavish W.G. Matthews (Canada)	Some Design Aspects and Performance of an Embankment Dam. 3.08	369
K. Kogure K. Matsuo (Japan)	Settlement Measurements of Peat Deposits as Embankment Foundation. 3.09	377
L. Knuppel F. McLean A. Roodsari (USA)	Underseepage Control Measures at Painted Rock Dam. 3.10	383
R.B. Smith W.O. Yandell (Australia)	Prediction and Field Performance of an Instrumented Road. 3.11	395
R.C. Findlay (USA)	Hydrostatic Pressure at a Soil-Structure Interface. 3.12	401
V.K. Singh B.D. Baliga B. Singh (India)	Openpit Mine Slope Stability—A Case Study. 3.13	407
H.J. Von M. Harmse F.A. Gerber (South Africa)	A Proposed Procedure for the Identification of Dispersive Soils. 3.14	411
Z.J. Ke C.H. Yong Y.H. Chang (China)	Failure and Repair of the Slope of Railway Embankments and Expansive Soils. 3.15	417

Session III continued

Page No.

M.C. Goel (India) D. Mudjihardjo (Indonesia)	Performance Evaluation of Rarem Dam. 3.16	423
M.C. Goel (India) A. Zainiko J.L. Surabaya (Indonesia)	Colbond Drains for Rapid Consolidation at Manggar Besar Dam. 3.17	433
K.V. Rupchang (India)	Problems and Behaviour of a Dam Founded on a Weak Zone. 3.18	437
D.G. Anderson J.G. Dehner T.B. King (USA)	Performance of a Harbor Embankment. 3.20	443
T. Smith C.E. Deal (USA)	Cracking Studies at Sand H Basin by the Finite Element Method. 3.21	451
J. Christodoulias H. Giannaros (Greece)	Failure of Railway Embankment. 3.22	457
H. Hejazi (USA)	Construction Problems with an Earth and Rockfill Dam. 3.24	461
J. Alberro G. Macedo L. Montanez F. Gonzalez-Valencia (Mexico)	Penitas Dam—In Situ Stress-Strain Characteristics of Materials. 3.26	467
M.D. Scott R.C. Lo E.J. Klohn K.K. Lum (Canada)	Overview of Highland Valley Tailings Storage Facility. 3.27	479
B. Bailey E. Bloom T.R. West J.A. Mundell (USA)	Excessive Seepage Losses at Westwood Lake Dam. 3.29	489
D.R. East J.W. Ransone W.A. Cincilla (USA)	Testing of the Homestake Mine Tailings Deposit. 3.30	495
J.R. Lambrechts E.B. Kinner (USA)	The Great Salt Lake Causeway—A Calculated Risk Revisited. 3.31	503

Session III continued

Page No.

J. Binquet
U. Zappi
(France)
Wadi Qattarah Dams Case History. 3.32 511

J.L. Llopis
C.M. Deaver
D.K. Butler
S.C. Hartung
(USA)
Comprehensive Seepage Assessment: Beaver Dam, Arkansas. 3.33 519

R.K. Katti
D.R. Katti
A.R. Katti
(India)
Remedial Measures to Seepage and Instability Aspect of a Dam Near Bombay. 3.34 527

R.J. Termaat
E.O.F. Calle
R.O. Petschl
(The Netherlands)
The Probability of Failure of an In Stages Constructed Embankment on Soft Soil. 3.37 533

J.A. van Herpen
J. de Pee
(The Netherlands)
Dike Reconstruction Polder Oudendijk. 3.38 541

J. Dekker
(The Netherlands)
Evaluation of the Failure of an Important Dike in the Netherlands. 3.39 547

R.C. Chaney
D.C. Tuttle
(USA)
Coastal Bluff Retreat at Big Lagoon, *California*. 3.40 555

P.L.R. Pang
Y.C. Chan
(Hong Kong)
Investigation of Settlements of a Trunk Road Embankment in Hong Kong. 3.41 559

W.R. Stroman
R.R.W. Beene
P.D. Thornhill
(USA)
Kerrville Ponding Dam, Guadalupe River, Texas. 3.42 567

Z. Shixuan
(China)
A Case Study of Success to Structures Founded on Expansive Soils. 3.44 575

T. Sivapatham
(Sri Lanka)
Behaviour of Inginimitiya Embankment Dam. 3.45 581

T. Mathur
R. Willis
(USA)
Performance of an Instrumented Earth Dam With Fat Clay Core. 3.46 587

B.D. Leonard
J.M. Olsen
(USA)
A Finite Element Analysis of the Utah "Thistle" Failure. 3.48 593

Session III continued

		Page No.
F. Colleselli P. Simonini M. Soranzo (Italy)	Improvement of Mechanical Properties of Soft Soils by Use of a Pre-Loading Embankment. 3.51	599
T. Ramamurthy S.L. Jain (India)	Deformation Response of Some Earth and Rockfill Dams. 3.52	607
B.V.K. Lavania (India)	History of Tehri Rockfill Dam Design. 3.53	615
B.V.K. Lavania (India)	Treatment of Left Bank Slopes of Ichari Dam. 3.54	621
A.J.T. Gilchrist (United Kingdom)	Design and Construction of Geocell Mattress as Embankment Foundation. 3.56	627
N.H. Wade L.F. Wei L.R. Courage R.A. Keys (Canada)	Performance of an Earthdam and Cut-off Through Deep Alluvium. 3.57	635
K.B. Agarwal (India)	An Undrained Failure in the Foundation of an Earthdam. 3.58	645
J.R. Schneider R.W. Lindquist (USA) G.K. Sammy (West Indies)	Design and Performance of Arena Dam. 3.59	651
K.K. Kapoor S.C. Patodiya (India)	Case History of a Partially Underground Power House. 3.60	657
I.I. Corda (Romania)	Iron Gates II: Design and Performance of Dams—Geotechnical Considerations 3.63	663
St. Christoulas E. Gassios N. Kalteziotis G. Tsiambaos (Greece)	Slope Stability Problems Related to a Semi-Bridge Construction. 3.65	671
J.A. Posse R.P. Hermosilla J.M.M. Santamaria (Spain)	Monitoring of the Canales Dam and Its Control During Construction Period. 3.66	677
D.C. Cowherd V.G. Perlea A. Coulson (USA)	Performance of a Coal Refuse Embankment. 3.68	683

Session III continued

		Page No.
R. Azevedo L.A. Santos (Brazil)	Field Observation and Finite Element Analysis of a Subway Excavation. 3.70	689
A. Marsland (England)	Failure of Flood Banks Due to Under Seepage. 3.72	695
J.D. Nelson (USA) B.P. Wrench (South Africa)	Construction of Road Embankments Over Very Soft Soils Using Band Drains and Preloading. 3.73	699
Izhar-ul-Haq (Pakistan)	Seepage Problems and Remedies—Hub Dam. 3.77	705
A.I. Harsulescu (Romania)	The Behaviour in Time of Ripa Albastra Dam Impervious Bentonitic Core. 3.78	711
F. J. Gichaga F.S. Atibu B.K. Sahu (Kenya)	Horizontal and Vertical Movements of Red Clay Highway Embankments. 3.79	717

Session IV
"Case Histories of Geotechnical Earthquake Engineering and Soil Dynamics"

Y. Koga O. Matsuo (Japan)	Stability Analysis of Seismically Damaged Embankments. 4.01	721
S. Chonggang (China)	Some Experiences from Damages of Embankments During Strong Earthquakes in China. 4.03	729
I. Rosenthal M. Itskowitch (Israel)	Vibration Response of Railway Bridge Piers to Nearby Pile Driving. 4.04	737
P. Fulan (China)	Theory and Experiment of Hammer Foundation Vibration. 4.05	743
T. Zhen-Yu T. Fang-Fu (China)	Stress Field Under a Reservoir and Its Induced Earthquake. 4.06	749
W. Xikang (China)	On Properties of Damping of Bases. 4.07	755
W. Xikang D. Shiwei Y. Xianjinan (China)	On Propagation of Elastic Surface Wave in Soil. 4.08	759

		Page No.
Q. Taiping L. HuiShan (China)	Influence of Piling on Characteristics of Liquefiable Soils. 4.10	765
W. Yuqing (China)	The Simplified Formulas for Predicting Seismic Liquefaction of Saturated Clayey Silt Site 4.11	769
D. Shiwei (China)	The Effect of Foundation Shape on Dynamic Parameter of Bases. 4.12	773
L.S. Srivastava (India)	Landslides in Rock Slopes During January 19, 1975 Kinnaur Earthquake in Himachal Pradesh, India. 4.14	779
T.F. Wolff G.L. Hempen M.M. Dirnberger B.H. Moore (USA)	Probabilistic Analysis of Earthquake-Induced Pool Release. 4.15	787
M. Lew J.C. Bowman, Jr. (USA)	Case History of Seismic Base Isolation of a Building—The Foothill Communities Law and Justice Center. 4.16	795
K.V. Rodda C.W. Perry R.E. Tepel (USA)	Upgrading the Seismic Resistance of Stevens Creek Dam. 4.18	801
M.B. Ray D.K. Ghosh (India)	Seismic Response Analysis of Forebay Structure for C.W. Pump House of a Nuclear Power Project. 4.20	807
G. Maurath D. Amick (USA)	Characterization of Liquefaction Sites/Features in the Charleston, S.C. Area. 4.21	811
P. Kvasnicka T. Ivsic A. Kiricenko (Yugoslavia)	Analysis and Measurement of Foundation Vibrations at Two Compressor Stations in Yugoslavia. 4.23	819
A. Bapat (India)	Seismosedimentation and Lives of Reservoirs. 4.24	825
R.C. Lo W.G. Milne E.J. Klohn G.T. Handford (Canada)	Seismic Assessment of Syncrude Tailings Dyke. 4.26	829
S. Bandyopadhyay M.K. Gupta A.S. Arya (India)	Reliability of the Wave Equation Analysis in the Estimation of Static Bearing Capacity of Vertical Pile—a Case Study. 4.27	837

M.D. Gillon (New Zealand) — The Observed Seismic Behavior of the Matahina Dam. 4.29 841

P.S. Seco e Pinto (Portugal) — Soil Liquefaction Potential of a Highway Bridge Foundation. 4.31 849

P. Srinivasulu, N. Lakshnaman, K. Muthumani, B.S. Sarma (India) — A Study of Dynamic Pile-Soil Interaction. 4.33 855

P.M. Byrne, H. Vaziri, U. Atukorala, D. Fraser (Canada) — Model Tests on Seismic Stability of an Approach Fill Embankment, Annacis Island Bridge Project Vancouver, Canada. 4.34 863

V.D. Miglani (India) — In-Situ Determination of Dynamic Properties of Soil for Foundation of a Turbo-Generator. 4.36 871

F. Ciuffi (Italy) — Geotechnical Services for a Bridge in a Seismic Area. 4.40 877

Author Index 883

Volume II

Session V

"New Solutions to Traditional Geotechnical Problems [Case Histories]"

		Page No.
H. Grice E.T. Mosley R.M. Perry (USA)	Vertical Excavation Below Footing Solved by Compaction Grouting. 5.01	885
T.V. Nhiem (France)	Recent Examples of Cut and Fill Reinforcement on A41-Highway in France. 5.02	889
B. Wietek (Austria)	Drainage Walling as Excavation Support. 5.03	905
T.J. Lyman M.J. Robison D.S. Lance (USA)	Compaction and Chemical Grouting Phoenix Drain Tunnels. 5.04	911
R.P. Kummerle (USA) J.C. Dumas (Canada)	Soil Improvement Using Dynamic Compaction for the Bristol Resource Recovery Facility. 5.05	921
G.E. Blight (South Africa)	Effects of Collapse Settlement of Fill on Reinforced Earth Walls. 5.06	929
H.O. Chukweze (Nigeria)	Pavement Failure Caused by Soil Erosion. 5.10	935
T.B. Celestino O.A. Ferrari C.T. Mitsuse L.C. Dominque (Brazil)	Progress in the Use of NATM for the Sao Paulo Subway. 5.12	941
C. Mastrantuono A. Tomiolo E. Arcangeli (Italy)	Effectiveness of Sand Drains in Peaty Soil in a Case of Differential Settlement Recovering. 5.13	947
H. Meissner G. Borm (Germany)	Construction of a Double Tunnel with Ground Windows. 5.14	953
W. Yuqing Z. Weiquan Q. Taiping (China)	Evaluation of the Effect of Saturated Silty and Fine Sand Foundation Improved by Vibroflotation in Seismic Area. 5.15	963
B. Song (Korea) M. Gambin (France)	Dynamic Compaction—An Unusual Application. 5.16	969

		Page No.
L.W. Franks J.M. Duncan S.A. Collins J. Fowler J.F. Peters V.R. Schaefer (USA)	Use of Reinforcement at Mohicanville Dike No. 2. 5.17	977
C.T. Yih R.P. Khera (USA)	Slurry Wall Instrumentation and Monitoring in Taipai. 5.18	985
L.D. Johnson (USA)	Deformation Behavior of Wilford Hall Hospital Mat. 5.19	989
J.E. Laier R.M. Mattox (USA)	Oversteepened Slopes Reinforced with Tensar Geogrid. 5.21	993
S.J. Kravits H.C. Harrel (USA)	Demonstrating Borehole Drilling Accuracy at the Navajo Dam. 5.23	997
S. DeFour A.S. Judge P. Lafleche (Canada)	Design and Monitoring of Earth Embankments over Permafrost. 5.25	1001
W. Schubert (Austria) T.L. Richardson (USA)	Soft Ground Tunneling on the Seoul Subway Using NATM. 5.27	1011
J.R. Davie M.R. Lewis L.W. Young (USA)	Accelerated Consolidation of Soft Clays Using Wick Drains. 5.29	1019
J.C. Neyer K.M. Swaffar H.R. Price (USA)	Tunnel Repair Using Cement-Stabilized Flyash. 5.30	1025
M.D. Boscardin (USA)	Impact of Tunneling on Two Brick-Bearing-Wall Structures. 5.31	1029
G. Guatteri (Brazil) J.L. Kauschinger (USA) A.C. Doria (Brazil) E.B. Perry (USA)	Advances in the Construction and Design of Jet Grouting Methods in South America. 5.32	1037

		Page No.
W. Fan M. Shi Y. Qiu (China)	Ten Years of Dynamic Consolidation in China. 5.33	1047
N. Ghosh M.M. Tabba (England)	Experience in Ground Improvement by Dynamic Compaction and Preloading at Half Moon Bay—Saudia Arabia. 5.35	1055
R.L. Curtis V.E. Chouery-Curtis D.A. Miller (USA)	Geogrid Reinforced Soil Retaining Wall on Compressible Soil. 5.35	1063
R.D. Charles (USA)	Performance of Prefabricated Drains in Soft Soils. 5.36	1069
K.R. Datye M.R. Madhav (India)	Case Histories of Foundations with Stone Columns. 5.37	1075
D.J. Hardin M.L. Byington S.V. Mills (USA)	The Rehabilitation of Terminal 2—A Case History. 5.40	1087
B.R. Christopher A.B. Wagner (USA)	A Geotextile Reinforced Embankment for a Four Lane Divided Highway U.S. Hwy 45 West Bend, Wisconsin. 5.42	1093
T. Matsui K.C. San T. Amano Y. Otani (Japan)	Field Measurement on a Slope Cutting With Tensile Inclusions. 5.43	1099
D.L. Jones G.J. Macdonald M.H. Golder (United Kingdom)	The Performance Behaviour of a Grain Silo Foundtion in Jeddah Supported on Stone Columns. 5.44	1107
K.Y.C. Chung (USA)	Designing Geotextile Support for Submarine Power Cables. 5.45	1113
K.S.A. Rahim A.W. Dhowian (Saudi Arabia)	Foundations on Stone Columns Resting on Coral Limestone. 5.46	1117
D.A. Bruce F. Gallavresi (Italy)	Special Tunnelling Methods for Settlement Control: Infilaggi and Premilling. 5.48	1121
J. Paul (United Kingdom)	Reinforced Soil in the Repair of Embankment and Cutting Slip Failures. 5.51	1127

Session V continued		Page No.
M.L. Ohri A. Singh G.R. Chowdhary (India)	Distribution of Contact Pressure and Stresses Under Skirted Footings. 5.53	1133
D. Cazzuffi A. Pagotto. P. Rimoldi (Italy)	Behaviour of a Geogrid Reinforced Embankment Over Waste Material. 5.55	1137
E.R. Farrel T.L.L. Orr T. O'Donovan (Ireland)	Performance of LPG Storage Tanks on Ground Improved by Stone Columns. 5.56	1145
H.D. Sharma P. Kozicki (Canada)	The Use of Synthetic Liner and/or Soil-Bentonite Liner for Groundwater Protection. 5.61	1149
R.F. Reed P. Wright (USA)	Long Term Building Performance Over An Injected Subgrade. 5.64	1159
A.V. Shroff D.P. Amin D.L. Shah (India)	Epoxy Resin Grout System for Solutions to Traditional Geotechnical Problems. 5.66	1165

Session VI
"Case Histories of Soil Structure Interaction"

Con[illegible]
(See [illegible])

P.D. Long N. Van Quang (Vietnam) B. Berggren (Sweden)	Partial Underpinning of a Five-Storey Building. 6.02	1169
A. Ghinelli G. Vannucchi (Italy)	Damage to Masonry Structures in the Historic Center of Arezzo (Italy) Following the Excavation of Sewer Tunnel. 6.05	1173
A.H. Wu (USA)	Structural Damage Arrested by Stabilization of Landfill. 6.06	1179
R.B. Seed C.Y. Ou (USA)	Compaction-Induced Distress of a Long-Span Culvert Overpass Structure. 6.10	1183
L.W. Abramson W.H. Hansmire (USA)	Three Examples of Innovative Retaining Wall Construction. 6.11	1191
J.J. Grosch K.S. Al-Yahyai (Saudi Arabia)	Anchored Bulkhead Failure on the Arabian Gulf. 6.13	1201

Session VI continued		Page No.
R. Cameron C.A. Carr (Canada)	The Influence of Thin Clay Layers on the Design and Performance of a Flexible Cantilever Retaining Wall. 6.16	1209
S.I. Tsien (China)	Some Case Histories in Urban and Rural Geotechnical Engineering. 6.20	1219
W. Yiji (China)	Treatment of KARST Subgrade by Deep Drilled Pile Foundations. 6.24	1225
G.E. Barnes (United Kingdom)	Diagnosis of Structural Damage and Movement Due to More Than One Cause. 6.25	1229
M.R. Lewis M.M. Blendy (USA)	Pressure-Injected Footings—a Case History. 6.26	1233
V.K. Garga (Canada)	Anchor Failures at a Deep Excavation. 6.27	1239
S. Dovnarovitch Y. Ivanov (USSR)	The Failure of Oil Storage Tanks and Their Control. 6.28	1245
J.M. Keaveny P.M. Aas F. Nadim (Norway)	GBS Platform Evaluation Using Field Instrumentation. 6.29	1249
T.K. Kiu C. Soydemir M.P. Mitsch (USA)	Underpinning of an 11-Storey Building in Boston—A Case Study. 6.31	1257
R. Riker D. Dailer (USA)	Design, Construction, and Performance of a Deep Excavation in Soft Clay. 6.32	1263
A.V. Chummar (India)	Failure of an Oil Storage Tank. 6.33	1271
C.J.F.P. Jones (United Kingdom)	The Effects of Mining Subsidence on a Motorway Bridge. 6.35	1275
H.O. Chukweze (Nigeria)	Correlation Between the Actual and Predicted Settlements of Structures on Tropical Soil Foundation. 6.36	1279
X. Sheng-sun (China)	Bearing Capacity of Pile Foundation. 6.37	1285
J.K. Jain R.K. Khare (India)	Stress Analysis of Gravity Dam Founded on Rock Mass Having Horizontal Seam (A Case Study of Bargi Dam in Madhya Pradesh, India). 6.39	1289
W.B. Ferguson E.F. Glynn (USA)	A Foundation Failure in Philadelphia. 6.42	1293

		Page No.
R.J. Finno (USA) D.K. Atmatzidas (Greece) S.M. Nerby (USA)	Ground Response to Sheet Pile Installation in Clay. 6.43	1297
S.A. Bucher R.J. Krizek (USA) D.K. Atmatzidis (Greece)	Full-Scale Load Test of Caisson on Chicago Hardpan. 6.44	1303
J.R. Davie M.R. Lewis (USA)	Settlement of Two Tall Chimney Foundations. 6.45	1309
M.A. Gouda I.W. Lippincott D. Raghu (USA)	Distress to Structures on Loose Ash and Cinders Fills. 6.49	1315
N.P. Angeles U.W. Stoll (USA)	Design and Field Monitoring of 70-Foot High Tied Anchor Retaining Wall. 6.50	1319
D.P. Gado G.P. Kelley J.J. McElroy (USA)	Performance of Foundations and Retaining Structures. 6.51	1327
S. Hansbo (Sweden)	Common-Sense Foundation Design. 6.54	1337
S.S.M. Cheng S.A. Ahmad (Canada)	Dynamic Testing Versus Static Load Test: Five Case Histories. 6.55	1343
R.C. Hepworth J. Langfelder (USA)	Settlement and Repairs to Cement Plant in Central Utah. 6.56	1349
K.D. Tucker (USA)	Performance Evaluation of Pile Foundation Using CPT Data. 6.58	1355
D. Sharma (India)	Foundation Failure of the St. Thomas Church, New Delhi. 6.59	1365
Z.S. Zhang D.Z. Luan X.X. Zhang (China)	The Case Record of Ba-Yu-Quan Anchor Slab Retaining Wall. 6.60	1371
T.L. Cooling J.B. Hummert, Jr. (USA)	Drilled Pier Load Test, Fort Collins, Colorado. 6.61	1375

Session VI continued

		Page No.
B.R. Christopher C.N. Baker, Jr. (USA)	Caisson Load Test and Instrumentation Program—Sohio Corporate Headquarters. 6.62	1383
C.N. Baker, Jr. S.B. Steinberg W. Lam (USA)	Building Design and Construction Over Organic Soil. 6.63	1389
M.R. Lewis J.R. Davie C.L. Weaver (USA)	Differential Settlement of Nuclear Power Plant Foundations. 6.64	1395
G. Hannink (The Netherlands)	Reconstruction of the Settlement History of Buildings. 6.67	1403
G. Hannink A.F. van Tol (The Netherlands)	Large Horizontal Displacements of Houses in Rotterdam. 6.68	1409
K.M. Chua L.J. Petroff (USA)	Predicting Performance of Large-Diameter Buried Flexible Pipe: Learning from Case Histories. 6.72	1417
J.C. Li H.L. Yao L.P. Shi B.I. Shy (Taiwan)	Behavior of Ground Anchors for Taipei Sedimentary Soils. 6.73	1421
A.J. Nicholson, Jr. J.R. Wolosick (USA)	Post-Tensioned Caissons Permit Interstate Construction: A Case History. 6.74	1425
A.S. Stipho (Saudi Arabia)	Model Test of Reinforced Earth Retaining Wall. 6.76	1433
S. Abdel-Salam M. Mashhour (Egypt)	Repair and Rehabilitation of a Residential Building at Nile River in Cairo. 6.77	1437
Y.S. Kim P.Y. Thompson (USA)	Behavior of Buried Concrete Box Culvert. 6.79	1443
R.H. Borden W.J. Sullivan W. Lien (USA)	Settlement Predictions in Residual Soils by Dilatometer, Pressuremeter and One-Dimensional Compression Tests: Comparison with Measured Field Response. 6.83	1449
M.P. Luong (France)	Collapsing Peak up of a Large Highway Steel Pipe-Arch. 6.88	1455
A. Kropp (USA)	Existing Pile Load Capacity Evaluation. 6.89	1471

R. Azevedo
N. Consoli
(Brazil)
Comparisons Between Field and Analytical Behavior of an Experimental Excavation. 6.90 1465

D.C. Cowherd
S.M. Thrasher
V.G. Perlea
J.O. Hurd
(USA)
Actual and Predicted Behavior of Large Metal Culverts. 6.92 1471

E.A. Nowatzki
(USA)
B.P. Wrench
(South Africa)
Geotechnical Investigation into Causes of Failure of a Gabion Retaining Wall. 6.96 1477

S.V. Nathan
(USA)
Two Case Histories: Performance of Shallow Foundations on Sand. 6.97 1483

P.K. Jain
B. Singh
G.C. Nayak
(India)
Geotechnical Studies of Foundation of a Tilted Tank at Parikshatgarh, India. 6.98 1489

R.J. Rapp
J.S. Schwenk
(USA)
Lock and Dam No. 26 R, Lock Cofferdam, Construction Sequencing. 6.99 1495

X.H. Zhao
Y.A. Yin
Y.P. Qian
J.G. Dong
W.Y. Shen
(China)
A Study of 15 Cases of Soil-Structure Interaction in China. 6.100 1501

I. Houssamy
M.M. Daman
(USA)
Simultation of Drilled Pier Behavior Under Three-Dimensional Loading. 6.101 1505

G. Ranjan
S.K. Kaushik
V.K. Gupta
(India)
Health of Ammonia Horton Spheres and Foundations—a Case Study. 6.102 1509

State-of-the-Art Papers

		Page No.
B.B. Broms (Singapore)	Design and Construction of Anchored and Strutted Sheet Pile Walls in Soft Clay.	1515
C.S. Desai (USA)	Case Studies Through Material Modelling and Computation.	1551
G.F. Sowers (USA)	Movement in the Powerhouse Excavation Saguling Project, Indonesia.	1567
J. Ramage (USA)	Lipari Landfill: Lechate Containment System—Geotechnical Considerations.	1577
W.D.L. Finn (Canada)	Case Histories in Seismic Response Analysis.	1585
G.W. Clough (USA)	Review of River Bank Stability Processes in Stabilizing Measures.	1597
M.L. Silver* (USA)	Lessons Learned from Case History Performance of Earth Dams, Embankments and Natural Slopes.	
Author Index		1609

*To be printed in Volume III

Session V

“New Solutions to Traditional Geotechnical Problems [Case Histories]”

Proceedings: Second International Conference on Case Histories in Geotechnical Engineering, June 1-5, 1988, St. Louis, Mo., Paper No. 5.01

Vertical Excavation below Footing Solved by Compaction Grouting

Harry Grice
Vice President, Rembco Engineering Corporation, Knoxville, Tennessee

Richard M. Berry
President, Rembco Engineering, Knoxville, Tennessee

Ernest T. Mosley
Senior Engineer, Raamot Associates, Inc., New York, New York

Synopsis: One of the problems regularly facing engineers in designing additions to buildings or other structures is dealing with excavating for footings directly adjoining existing footings but at a deeper level.

This was accomplished in sandy soils economically and quickly for a noted Conference Center in 1983 by using compaction grouting. Compaction piles were utilized to pick up existing loads as well as the horizontal loads which would normally allow the building to tip, settle and crack. We believe this was the first use of compaction piles as "anchor" piles to pick up horizontal loads. By using this process, the sandy soils along the excavation stood without other support when excavating with a backhoe.

The paper presents the criteria used in developing this method, summarizes the critical loads, and explains the operation. There has been no settlement at the site.

One of the problems regularly facing architects and engineers designing additions to buildings or other structures is dealing with excavation directly adjoining present structures where new footings need to be placed below the existing foundation level. That typical problem presented itself at the Harrison Conference Center in Glen Cove, NY, on the north shore of Long Island.

An addition incorporating an indoor sports center was planned to attach directly to a two story wing used as sleeping quarters at the Center. The exterior walls for the existing two story brick structure were supported by continuous spread footings on natural soils, a mixture of loose to medium dense glacially deposited beach sand, stones, and silt. The ground floor was a slab on grade. The addition was to be connected at its enclosed stairwell to allow direct passage to the second story of the new addition. The new section was a three story structure set so the roof lines would match. The new basement was to be placed below the level of the existing first floor with the new continuous strip footings to be placed from 6.5 to 13.5 feet below the existing footings.

The existing building was about eight years old at the time. It had been well constructed. Examination showed no evidence of settlement and no cracks, internal or external. Existing continuous footing loads ranged from about 2.1 to 3.6 kips/lin. ft. The site is some 200 feet in elevation above ocean level. Soil borings showed the soils to be well-drained.

The most common method of providing support for an existing structure where a new structure is to be built next to it, but at a lower level, is to underpin it with concrete piers. Pier holes at relatively wide spacing are excavated below the existing footings to a depth below the excavation level required for the new structure, then lagged with timber prior to placing reinforcement and filling them with concrete. After the first set of piers have sufficient strength, additional piers are constructed in between in a similar manner until a continuous wall exists. This work requires hand labor and is slow and tedious. Even though great care is taken, loss of ground during the excavation for the piers often occurs which results in settlement of the existing structure.

Compaction grouting has the attributes to solve the potential problems associated with this situation. Compaction piles are placed through small 2 inch diameter holes which create no potential for settlement during pile placement. No excavation for the new building takes place until the compaction piles are in place. During the grouting, the soil is compacted and densified so that when excavation does take place, neither settlement nor lateral failure can occur.

The concept for the Conference Center project was to provide vertical support for the existing building footings by using compaction piles placed through those footings. These piles extended a suitable distance below the eventual excavation depth. The piles were angled slightly inward so that excavation equipment would not cut into them. Horizontal support to the soils and support to prevent lateral movement of the building was provided by 45 degree anchor piles. The bases of these piles were placed beyond the shear line of the soil, and the top end anchored into the foundation. Each pile was attached to the footing by a threaded reinforcing bar extending through a hole cored in the footing, and the whole assembly epoxied in place.

After the grouting was complete, the existing building was fully supported on its own piles. Soils for the new excavation were then cut away adjacent to the existing structure, and there was no need for backfill nor to allow for the usual, eventual settlement.

The general plan of the existing footing is shown in Figure 1. That plan shows the pattern of piles placed under the building. Pile and soil calculations were based on three criteria:

- Settlement potential of the existing soil
- Lateral pressure and forces
- Bending forces on the piles

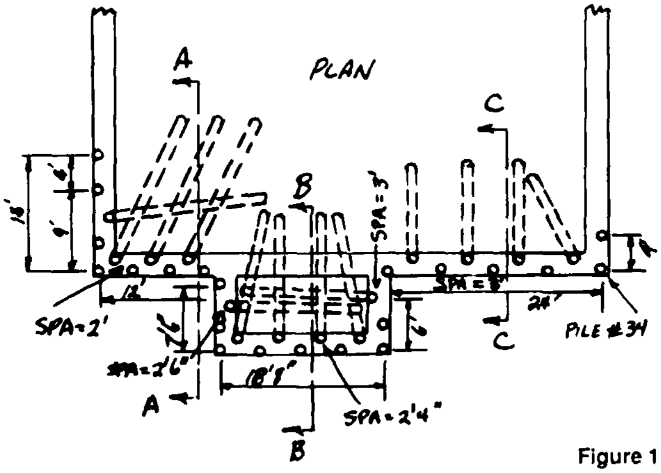

Figure 1

It was judged that a pile with a nominal and minimal diameter of one foot was reasonable to attain in these soils. When the first trial calculations were completed, it was evident that the lateral forces would govern and would become the limiting design criteria.

The advantages of the compaction grouting method are that loss of ground and subsidence during the underpinning operation are virtually eliminated. Furthermore, the underpinning can be completely installed prior to excavating to a level below the existing structure's foundation.

Grouting an anchor pile

For the Glen Cove project, compaction grout piles were designed to provide both vertical support for the existing continuous spread footing foundation and lateral support to the wedge of soil beneath the existing structure which would tend to slide into the excavation if not restrained. Vertical support was provided by compaction grout piles on 4 to 6 foot centers having a batter of 1 horizontal to 10 vertical. The purpose of the batter was to minimize their intrusion into the area of the new structure. It was not considered necessary to make the piles form a continuous wall since the water table was below the depth to be excavated. These piles were designed for both axial compression and flexure. The tops of the 1:10 batter piles were restrained laterally by compaction piles having a batter of 1 horizontal to 1 vertical. The 1:1 batter piles were located midway between the 1:10 batter piles and were designed for tension.

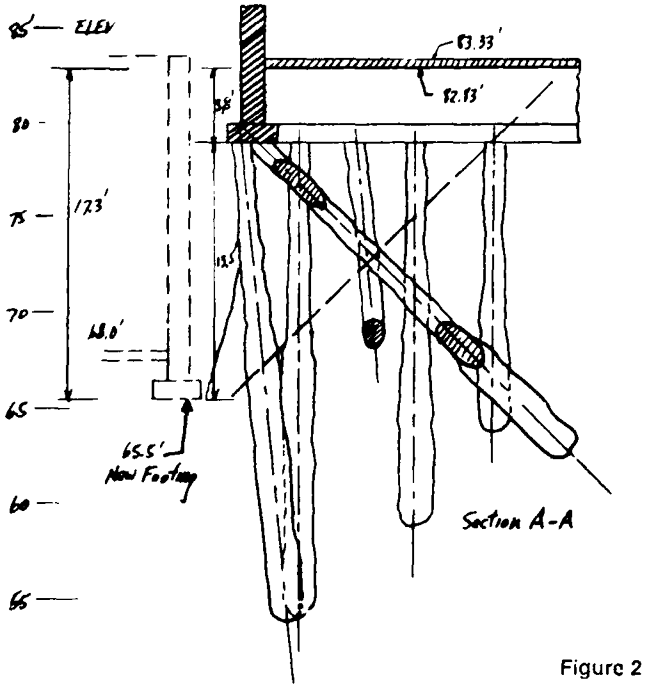

Figure 2

Both types of piles were reinforced with a single steel threaded bar over their full length. All bars extended through the existing footings. The bars had bearing plates at the top, and were grouted into the top of the footings. Either no. 8 or no. 10 bars were used depending on the design requirements. The 1:10 batter piles were designed for a diameter of approximately 12 inches at the top, increasing to 15 inches at 5 feet, to 20 inches at 10 feet, and continued at that diameter to the tip. The 1:1 batter piles were designed for a diameter of approximately 12 inches for the first 10 feet, increasing to 15 inches at 15 feet, to 20 inches at 20 feet, and continuing at 20 inches. Pile lengths ranged from 15 to 25 feet. The required grout strength was 3000 psi and grade 60 steel reinforcement was used.

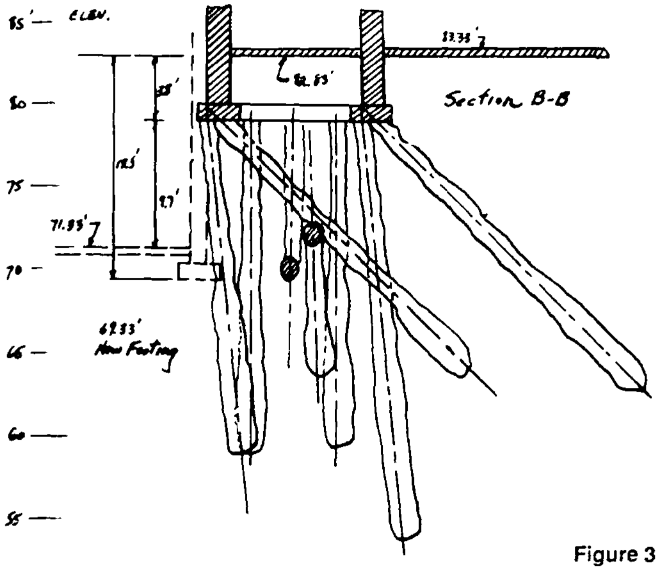

Figure 3

Design loading for the piles was based on a lateral earth pressure loading of one-half the vertical pressure from the underside of the existing floor slab to the underside of the existing footings. Below this level, the lateral pressure was assumed to remain constant to the depth where it is equal to the active pressure; that active earth pressure was assumed to be one-quarter of the vertical pressure.

Grout casings and drilling

The calculations for the design axial loads at the top of the piles were calculated based on the assumption: the lateral earth pressure, from the level of the existing floor subgrade to a level midway between the bottom of the existing footing and the excavation level of the new footing, will be supported by the 1:1 batter piles. The lateral earth pressure below this was assumed to be supported by the embedded portion of the 1:10 batter piles below the level of the new excavation.

The 1:1 batter tension piles had calculated design loads ranging from

17.5 to 20 kips. Their design length was such that they extended approximately 14 feet past a 1:1 slope up from the nearest excavation level. The calculated pile friction in this zone was in excess of three times the calculated design load.

Excavation done by backhoe

The 1:10 batter compression piles had calculated axial design loads ranging from 22.5 to 35 kips. Since the end bearing capacity of a 20 inch diameter pile in compact sand is much greater than the axial design loads, the lateral loading governed the required pile penetration below the new excavation level. The calculated lateral load to be supported by the embedded portion of the pile ranged from 5 to 12 kips depending on the depth of the excavation. Using laterally loaded pile analysis methods, it was found that penetrations of 9 to 12 feet were suitable. Maximum bending moments resulting from this analysis determined a suitable pile diameter, size for reinforcing steel, and required concrete strength.

The selection of pile size and length took into account the compressibility of the soil. In the vicinity of the existing foundation and floor slab, the size of the pile was to be no larger than 12 inches since the ground may not have been able to compress that much and heave of the structure may have occurred. The diameter of the lower portion of the piles was increased up to 20 inches to meet design requirements.

Corner showing sewer connection

The resulting layout is shown in Figure 1 and sections through the footings and shown in figures 2-4. Load calculations are summarized in the Table below:

Criteria	Units	Req'd	Design SF=3	Excess over SF
End bearing				
Min. dia. = 1 ft	tons	17.5	87.0	69.5
Bending (max case)				
Rebar size	sq. in.	1.04	1.27	0.23
Concrete strength	psi	2,200	3,000	800
Lateral earth pressure				
Rebar size (tension)	sq. in.	0.63	0.79	0.16
Min. embedment depth	ft.	7.6	18.8	11.2

Final excavation before new footings

In order to obtain adequate support directly under the existing strip footing and to get the minimum 1 foot diameter at shallow depths, stage grouting from the top down was chosen as the best technique. This is often done in compaction grouting where exceptional support near the bottom surface of the existing footings is needed and where confinement of the surrounding soil may be inadequate. The procedure minimizes the tendency for grout return, ground heave, and floor lift before the desired amount of material can be introduced near the surface.

Holes were drilled in the footing and 2 inch diameter grout casing installed. Earth drills then carried a pilot hole to about 5 feet below the footing and the first stage of grouting began. Grout slump was 0 to 1 inch. The grout was allowed to set, usually overnight for operational convenience. The casing was then drilled out and drilling continued through the first stage and into the earth below for another 5 feet. The next stage of grout was placed below the first and the process continued by approximately 5 foot stages until the design level was reached. After the second stage, there is minimal danger of uplift because point forces of injection are being transferred to such a large mass above. This is particularly important on the 1:1 batter piles where the upper restraint is provided only by a light floor slab.

During the last and deepest stage of grouting, the reinforcing bar was placed in the hole and grouted in place. The top of the threaded rebar extending through the footing had washers and nuts placed on them. The

1:1 batter rebar had bearing plates placed over the ends at 45 degrees and the nuts drawn up tight to accept the tension loads.

During grouting on one end of the building, an unexpected perched water zone was encountered at a depth of about 20 feet. The sand and gravel turned to a flowable mush and drilled pilot holes would not stay open for the next stage grout. Conventional methods of holding a hole open with drilling fluids do not work with compaction grouting where the grout is near zero slump and injection pressures run to several hundred psi. In order to get past this obstacle, the grout holes from the 20 foot level down were cased to the bottom, the reinforcing bar installed, and the bottom of the pile grouted from bottom up by pulling the casing in 1 foot increments. This turn about method was used on 12 piles where the perched water was encountered.

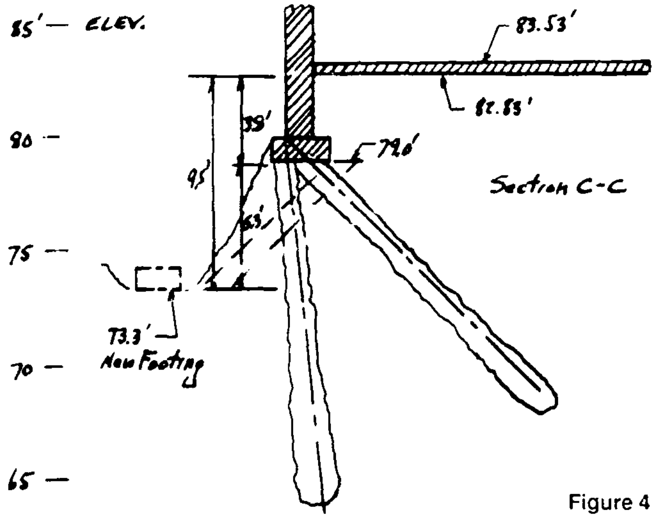

Figure 4

During excavation, a few piles were partially exposed. Close digging in the area of section B scraped against the grout at the top. On the right corner, pile number 34 was hit during excavation by earth moving equipment breaking away sizable sections. In the end, no harm was done and the digging contractor returned to using a backhoe rather than a bulldozer for excavation near the structure. It is interesting that the shape of the exposed pile, number 34, is roughly square rather than roughly round as might be surmised.

No special precautions were observed during excavation. Because of construction scheduling, the vertical face was exposed and unsupported for about a month. The soil between the piles along the face had been compressed so densely during grouting that there was no noticeable difference in appearance after the month passed.

When the new footings and walls were in, the space behind the new walls was filled with concrete to prevent any major migration of soil from beneath the building. However, no attempt was made to pump the space full so the end of the old structure will remain supported only on its compaction pile base.

Pile #34 bracing is for personal protection, not structural support

No settlement has occurred. Minor cosmetic cracking to the inner floor and some inner walls resulted from small uplift during the upper stages during the grouting process. Use of compaction grouting on this project gave a solid and probably the best technical solution to this common construction problem, and with no settlement. The project was completed in about one-third the time estimated for conventional underpinning and at 52% of the contractor's budgeted cost for the best alternate.

Proceedings: Second International Conference on Case Histories in Geotechnical Engineering, June 1-5, 1988, St. Louis, Mo., Paper No. 5.02

Recent Examples of Cut and Fill Reinforcement on A41-Highway in France

Trân Vô Nhiêm
Expert in Soil Mechanics, Spie-Batignolles, France

SYNOPSIS : At EVIRES PASS, between ANNECY and MONT BLANC in FRANCE, subsoil is made up of unstable clayey natural versants and marly bedrock affected by previous or current slidings. The problems encountered during the new A41-Highway construction were aggravated by the proximity of Road and Railway located on top of the same versant. The final Design consisted of succession of cuts and embankments with special soil reinforcement techniques to improve stability. So two existing unstable Railway embankments were promptly consolidated by "soil nailing" with driven steel dowel-piles which were either anchored or not. Two other high cuts in marls and sandstones affected by previous landslides were reinforced by incorporation of several ranges of anchored concrete slabs. A high embankment on inclined Soft Soil was founded on stone-columns made of crushed limestone strongly compacted in order to provide safety against sliding. Control instruments were installed prior and after performance of works, with a wiew to observe the actual behaviour of the performed reinforcements and to adapt the Project if necessary.

1 - INTRODUCTION

The versants at COL D'EVIRES between ANNECY and MONT BLANC in FRANCE (Fig. 1.1), are generally gentle slopes made of plastic clays and silts covering the inclined substratum of marly sandstone named "Molasse". During the wet seasons, and more particularly during thawings, the overburden becomes unstable, especially where the dip of the underlaying rock is unfavourably oriented towards the Valley. The marl interbeds were even the cause of ancient collapses of versants that are today either almost obliterated, or still the seat of active layer-on-layer slidings.

The problems encountered during the new A41-Highway construction were aggravated by the proximity of a main Road or of a Railway located on upstream side of the same unstable versant.

A realistic Highway Project was designed consisting of a succession of cuts and fills along the critical versant with special precautions being taken to reduce the problems :

- "split-level-carriage-ways" to minimize the height of excavations and embankments, following the natural slope as close as possible ;
- prior reinforcement of the existing Road and Railway at the specific locations of critical stability ;
- prior soil improvement below the embankments ;
- prior and permanent drainage of the site ;
- monitoring and control of the site and the works during and after the construction ;
- arrangement of permanent accesses to the reinforced areas with a view to be able to quickly execute additional reinforcements later on if necessary.

Chosen reinforcement techniques had to satisfy 2 main Design Criteria :

- use of light equipment and machine ;
- design of solutions which are easily adaptable to the specific soil conditions during the performance of works.

The related Examples of executed soil reinforcements are :

- Reinforcement of the existing unstable Railway embankment at 2 locations by "soil nailing" with several rows of driven steel dowel-piles, whose tops were either tied together by horizontal beams, or anchored to the bedrock by inclined prestressed tie-rods.
- reinforcement of 2 new high cut slopes below the existing Railway or Road by several levels of reinforced concrete slabs which were anchored to the stable rock stratum by 100-tons

Fig. 1.1 - View of worksite at EVIRES Pass

prestressed tie-backs. In these cases, the sites were affected by ancient versant collapse or by current sliding of rock mass.
- Soil improvement by means of stone-columns for the foundation of a new high embankment on unsteady versant.

2 - EXAMPLE OF SLOPE NAILING BY DRIVEN STEEL DOWEL-PILES

2.1 Les Houches' site

Along the critical zone named "Les Houches" (fig. 2.1), the existing Railway embankment is in average of 4m height and of precarious stability, although the clayey versant has a gentle slope of only about 15 %.

Soil investigations and tests revealed suitable characteristics of the clayey overburden, with a thickness of 5 to 6m :

C_u = 40 kPa with $\varnothing_u$ = 0°
$\varnothing'$ = 32° with C' = 25 kPa from triaxial tests
P_l = 300 to 500 kPa from pressuremeter tests
GWL at about 3 to 4m below GL.

The underlaying sandy clay was found to be stiff and marly sandstone encountered at 14m depth.

2.2 Highway Design (Fig. 2.2)

The Highway was designed to be in a slight split-level cut located at a 85m distance downstream from the Railway in order to minimize the problems. However, the relocation of a local road necessitated a cut down to 7m in depth at distance of 40 m from the Railway.

The stability analysis concerning circular sliding surface of large radius and based on the above measured soil characteristics showed a sufficient safety coefficient at short-term (F_u = 1,45 with high GWL) and a superabundant long-term security (F' = 2,6).

Nevertheless, it was decided to improve the general stability of the versant and cut slopes by means of heavy draining masks made of limestone quarry-run placed against the cut slopes, and of sub-horizontal bored drains to lower the water-table. In addition, topographical bench marks and inclinometer tubes were set up over the worksite, especially along the Railway in order to continually observe the ground behaviour during the earthworks.

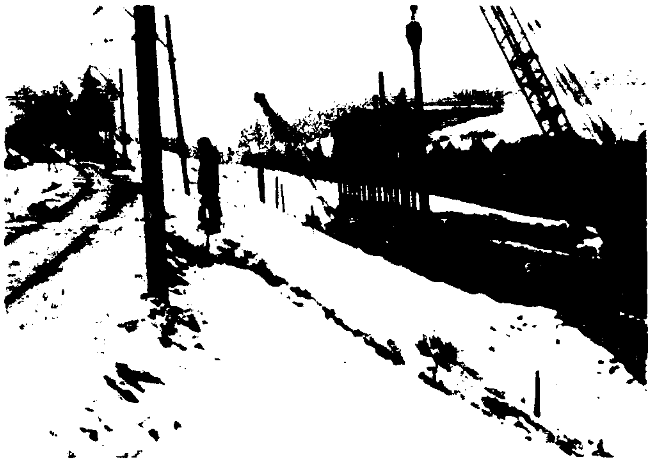

Fig. 2.1 - Railway embankment during Nailing

2.3 Unexpected slope sliding

Right from the beginning of the earthworks, consisting of few meters of cutting at 40m distance from the railway (fig. 2.2), the versant showed signs of instability : displacement of bench marks, deformation of inclinometers.

In addition, heavy rains in Autumn after a long dry season, contributed to accelerate the ground movements causing the shearing off of some inclinometers at 5m depth and important settlements of the Railway embankment at the location of a "bulge" on the versant which in fact was a "reversed relief" formed by an ancient sliding along a "fossile thalweg".

2.4 Emergency measures for stabilization

As the settlements of the Railway persited and necessitated important recharging of ballast, it was necessary to stop the earthworks and to stabilize the railway embankment without delay.

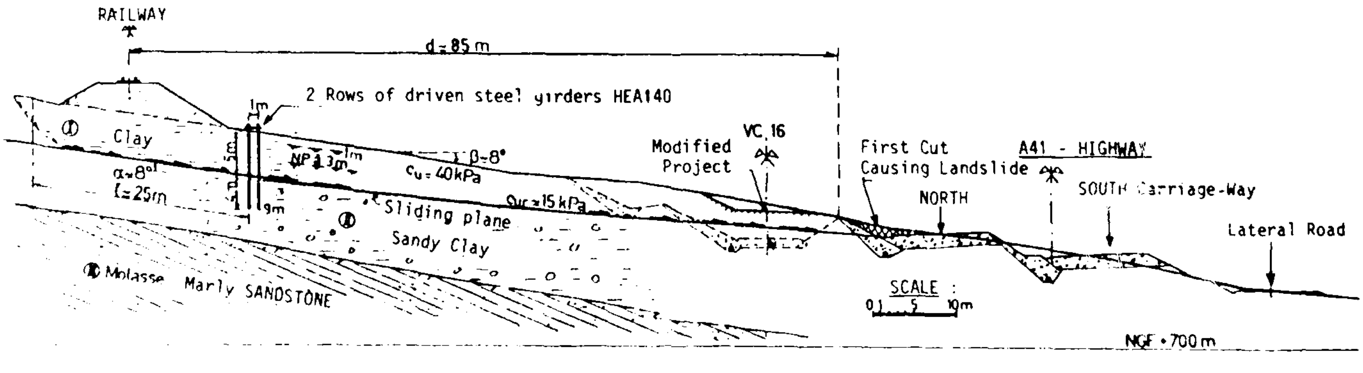

Fig. 2.2 - Soil Profile at "Les Houches" Zone with Highway and Soil nailing Project

In the first place, the toe of the sliding zone was overloaded with a heavy heap of quarry-run while additional control instruments were installed on the site. Once this effected, the instable versant was "nailed" by driving a number of HEA-steel girders, acting as vertical dowels, along the toe of the Railway embankment. Subsequent additional soil improvements, such as partial substitution and drainage, were performed under cover of the above nailing system.

2.5 Preliminary Design of the dowel-piles

Topographical survey and inclinometric measurements revealed that the sliding of the clayey overburden practically occured on a inclined plane surface located at a depth of about 5m (fig. 2.3). Hence the residual shearing resistance of soil along this sliding plane could be estimated to be only of Cur=15kPa (corresponding to the short-term safety Fu = 1), instead of Cu=40kPa measured in the overbuden itself.

As no suitable analysis method was available at the time of the works, the nailing piles network was approximately designed with respect to the following assumption : the necessary number of steel girders had to be such that their shearing resistance would compensate the lack of shearing resistance along the sliding plane in order to obtain a safety factor of $F + \Delta F > 1$.

It was thus estimated that by nailing HEA-140 steel girders, 4 nos per linear meter of the unstable embankment, it would be possible to increase the safety factor F up to 20%, i.e. :

$$F + \Delta F \# \frac{\Delta T}{\gamma_h \cdot h_A L_A \sin\alpha \,.\, \cos\beta} = 1{,}2$$

with $\Delta T = 4 \times 76$ kN for HEA-140 girders
$h_A = 5$ m $\quad L_A = 100$m $\quad \alpha = \beta = 8°$

In fact, the above summary analysis meant that the dowel-piles were capable of contributing the maximum of their shearing resistance, and that the unstable soil located downsteam had to offer a sufficient lateral subgrace reaction in such a way that the piles would not fail by bending moment excess.

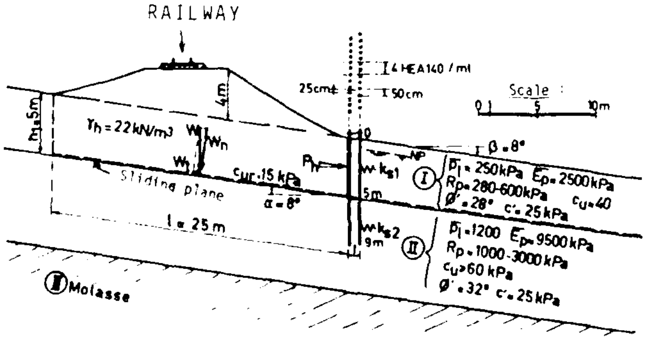

Fig. 2.3 - Simplified scheme for dowel-piles calculations

2.6 Executed slope nailing

A total of 300 nos of HEA-140 steel girders of 9m average length, were driven down every 50cm distance along 2 parallel rows, 1m apart, and 75m long at the toe of the Railway embankment (fig. 2.1)

The steel girders were set in place in the clayey overburden by low-frequency vibro-driving method, then driven down into the lower compact layer with the help of a 15 kN PAJOT Hammer. After driving, the girders heads were linked together by longitudinal and transversal HEA-160 beams (fig. 2.4) in order to distribute more uniformly the uneven earth pressures over the complete nailing-piles system.

2.7 Additional reinforcements

As soon as the first 40 nos of girders were nailed in over the 75m length, the sliding displacements slowed down considerably.

After setting in the whole of 300 girders, the Railway embankment and the downstream versant were practically stabilized. However, in order to improve the general stability of the whole site even more, additional works and reinforcements were undertaken under cover of the nailing piles network :

- raising the longitudinal profile of the lateral local road in order to reduce the cut depth (Fig. 2.1) ;
- improving the drainage of the Railway embankment by means of a longitudinal 5m depth draining trench, placed along upstream side ;
- reinforcement of the downstream clayey overburden by means of cast-in-situ frictional buttresses (or "hard core drains") made of 0/400m quarry-run backfilled in 4m wide, 5m deep and 60m long trenches running perpendiculary to the dowel-piles curtain ;

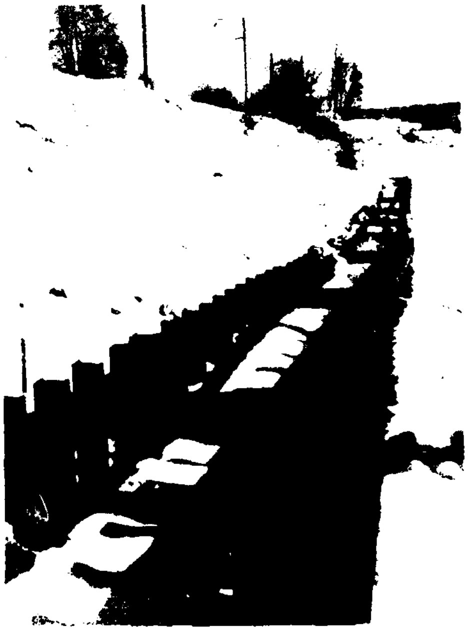

Fig. 2.4 - View of 2 dowel-piles rows with link beams

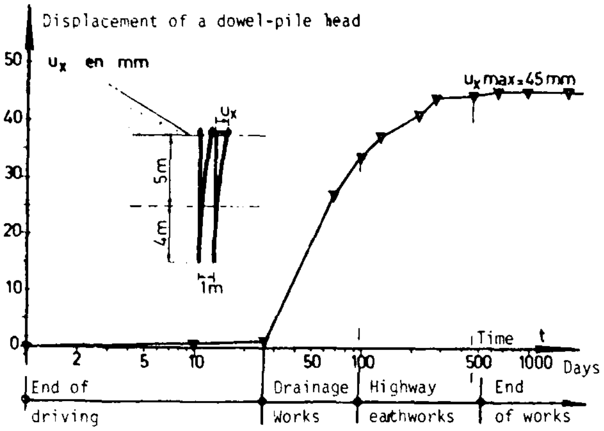

Fig. 2.5 - Pile head displacement versus time

- sub-horizontal bored drains, 40m long, in 4 fan-shaped networks belows the Railway embankment base.

Draining trenches and frictional buttresses were executed inside a telescopic KRINGS sheeting and by successive sections.

2.8 Follow-up and evolution

Since the completion of the two rows of dowel-piles, the site has been perfectly stabilized. Some displacements of the pile heads were only observed during the execution of additional draining and frictional buttresses (fig. 2.5).

However, regular inclinometric measurements revealed that the clayey overburden was still moving very slightly : 1 to 3mm of displacement in 2 years at a depth of 5 to 6m below the GL.

2.9 Posterior Analysis of dowel-piles stability

The computer Program "POP" evolved by SPIE-BATIGNOLLES now allows to calculate the intern efforts and displacements of piles which are subject to any sollicitations of whatever type (vertical/horizontal forces, overturning moment,

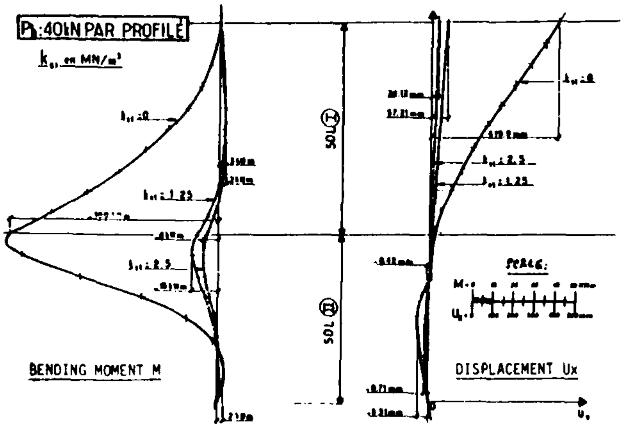

Fig. 2.6 - Computed Bending Moment M and Displacement Ux of a Dowel-pile subjected to Ph = 40 kN

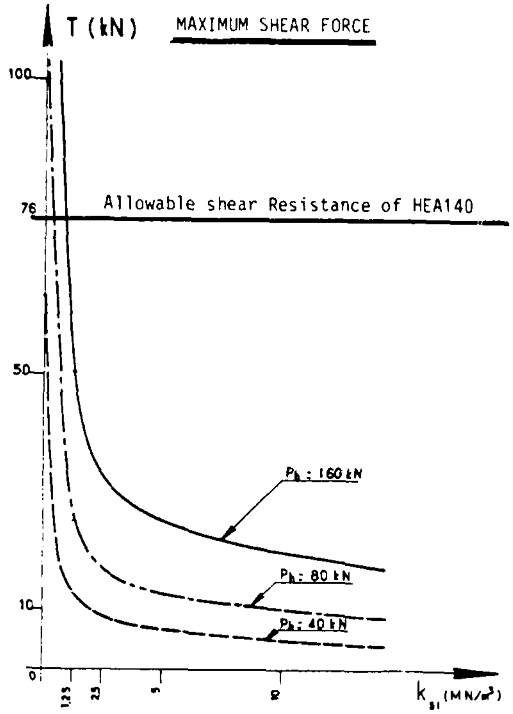

Fig. 2.7 - Calculated shear Force Tmax in a dowel-pile in terms of modulus ks1 for various earth pressure Ph

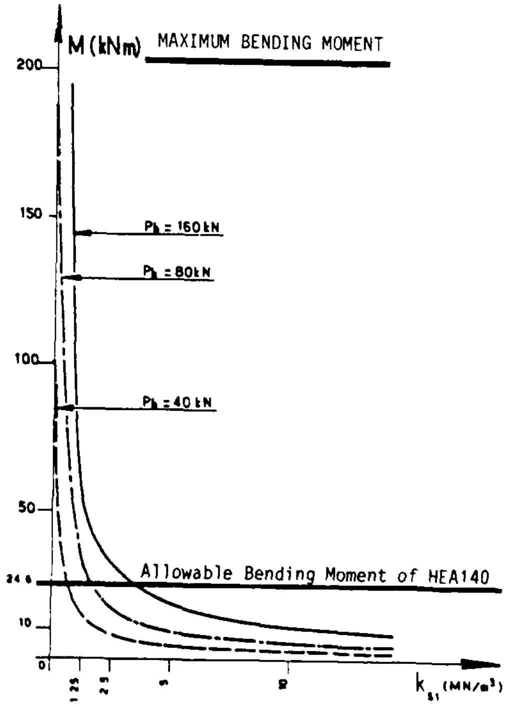

Fig. 2.8 - Calculated Bending Moment Mmax in a dowel-pile in terms of modulus ks1 for various earth pressure Ph

lateral earth pressures etc...), and embedded in a multilayer-soil having lateral subgrade reaction modulus ks.

The simplified scheme for calculation of the earth pressure Ph due to the unstable overburden and Railway embankment on the dowel-piles is shown on Fig. 2.3.

Fig. 2.6 shows the computed curves of bending moments M and of displacement Ux of a dowel pile sujected to the earth pressure Ph = 40 kN and supported by different subgrade reactions Ks1 = 0, 1,25 ; 2,5 kN/m³ and Ks2 = 50 KN/m³.

Fig. 2.7 and 2.8 show the variation of the calculated maximum bending moment Mmax and the maximum shear force Tmax in terms of the subgrade reaction modulus Ks1 of the overburden.

From the above POP Analysis, the performed dowel-piles system would fail rather by bending moment excess, than by shearing force when the downstream part of the unstable overburden tends to steal away (i.e. $Ks1 \rightarrow 0$). But a negligible subgrade reaction of the unstable soil was found sufficient to insure the stability of the dowel-piles. Such a fact was effectively observed on the site. This is in view of preserving this essential subgrade reaction, that additional soil reinforcements were undertaken downstream of the dowel-piles.

2.10 Posterior analysis of nailed slope stability.

It is presently possible to analyse the effect of the nailing piles on the general stability of the versant, using the recent "TALREN" Program evolved by TERRASOL (Paris).

Basically, the method consists in applying the general stability Analysis with failure surfaces such as circular one or wedges. Efforts mobilized in the resistant Inclusions are taken into account in the general equilibrium of forces (weight of soil, shear strength along failure surface, external forces) in order of calculate the overall safety factor F against sliding. The TALREN Program considers the general case of both retaining structures and slopes stability, and takes into account 4 failure criteria related to the strength of the materials (soil and inclusions) and to the interaction phenomena between them. These 4 criteria are (fig. 2.9) :

- Tensile and Shear strengths, and bending in the Inclusions,
- Shear Resistance in the soil
- Longitudinal interaction, i.e. lateral Friction between Soil and Inclusions,
- Transversal interaction i.e. lateral Earth pressure on the Inclusions.

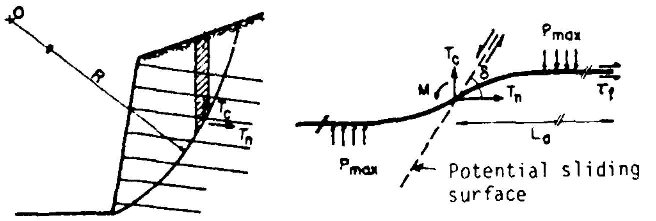

Fig. 2.9 - Principles of TALREN Program for stability Analyse of a nailed slope

In the present case, the short-term and long-term safety coefficients have been calculated with the soil characteristics corresponding to observed plane failure surface before reinforcement and to safety coefficient F = 1 :

$\emptyset u = 0$ with $Cu = 13$ kPa at short-term
$\emptyset' = 13°$ with $C' = 0$ at long-term.

The computation Results of several examined cases are summarized in Table I.

Table I : Results from TALREN program

examined cases	Safety Factor F	
	Short term	Long term
- Stable natural versant	1,08	-
- after cut causing slide	0,98	1,01
- versant with 1 row of dowel-piles	1,01	1,03
- versant with 2 rows of dewel piles	1,04	1,07
- with lavering of the GWL	-	-
- with GWL lowering and buttresses	-	1,68

The most outstanding Result is that the observed stabilization of the versant following on the nailing of dowel-piles, corresponds to a very slight increase of the safety Factor : 3% to 6%. This result is in agreement with the observations and conclusions presented by other Authors, that stabilization by nailing of an unstable slope could be obtained with an improvement of the safety Factor of only about 5%.

It is also to be noted that the most efficient and durable technique for the long-term stability in this present case consists in drainage by draining trenches, and in partial soil susbtitution by frictional buttresses.

3 - EXAMPLE OF NAILING BY ANCHORED DOWEL-PILES

3.1 "Chez Louiset" site

The site named "chez Louiset" was comparable to the previous one named "Les Houches" : unsteady Railway embankment, settled slope at exact location of a "bulge" on the versant having gentle slope of only 10 %.

Actually, additional soil investigations carried out subsequently to the "Les Houches" experience, revealed the existence of an overdeepening fossile thalweg of the marly Sandstone substratum at the location of the observed "bulge" in topography, which in fact is a "reversed relief". This ancient thalweg was covered with soft plastic clay (undrained cohesion of Cu = 20 to 30 kPa) and remolded marls (probably slided), 7m to 8m thick (Fig. 2.1).

3.2 The Highway Design

The Highway was designed in slight split-level cut placed at 50m distance from the Railway. In order to avoid excessive settlement of the

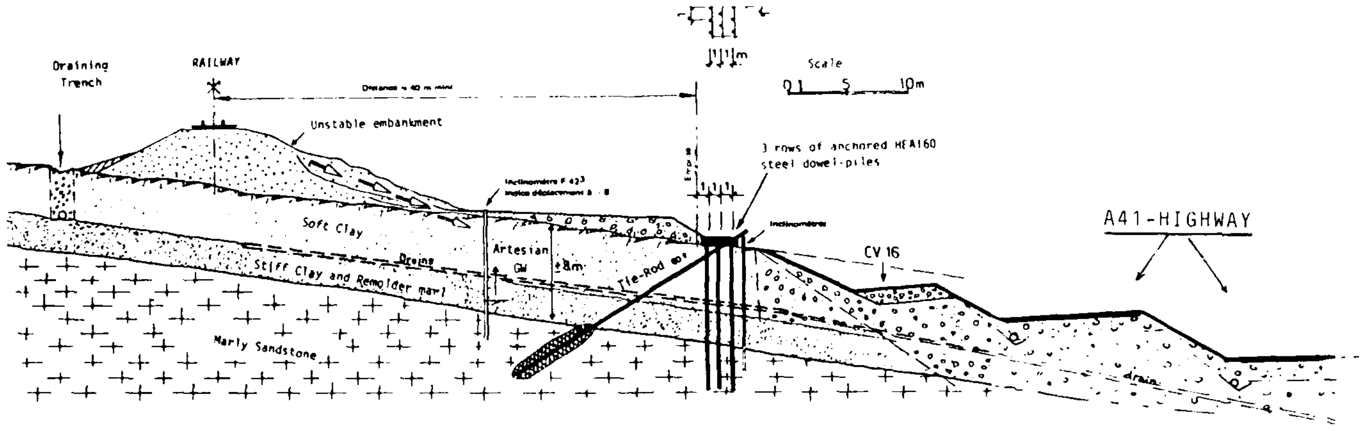
Draining Trench
RAILWAY
Distance ≈ 40 m mini
Scale
0 1 5 10m
1 1 1m
Unstable embankment
3 rows of anchored HEA160 steel dowel-piles
Inclinomètre F 42³ Indice déplacement
Inclinomètre
A41-HIGHWAY
CV 16
Soft Clay
Drains
Stiff Clay and Remolder marl
Artesian GW
8m
Tie-Rod
Marly Sandstone
drain

Fig. 3.1 - Soil profile at "Chez Louiset" Zone with soil reinforcement by anchored dowel-piles

Highway pavement and at the same time to improve the stability of the Railway embankment, it was planned to remove away the unstable clay and marl along the fossile thalweg, up to the toe of the Railway embankment, then to blackfill with coarse draining material.

Even by working by successive sections, such a substitution down to 7m depth could well cause disorders to the Railway.

3.3 Studied Solutions for soil reinforcement

Thanks to the preceding experience at Les Houches zone, it was decided to first of all improve the Railway stability by a soil reinforcement technique which was to stand up to the following criteria :

- possible execution with rather light equipment on unsteady versant ;
- assured safety for the Railway during the reinforcement works and soil substitution along the fossile thalweg ;
- no excessive induced settlement to the Railway embankment.

The considered Solution was to nail the soil with a curtain made of several rows of steel dowel-piles which were fitted into the marly bedrock and head-anchored by semi-prestressed tie-backs.

Two locations for the curtain were examined :

- at the toe itself of the Railway embankment :
- or at a minimum distance fo 40m from the Railway (Fig. 2.1).

Stability Analysis on the basis of residual soil characteristics led to the following designs :

- the first case, by nailing at the toe of Railway embankment, it was necessary to 3 nos of HEB-180 steel girders per lin meter, and to anchor with 300 kN tie-rods at 4m intervals. steel girders HEB-160 type per linear meter, with 300 kN tie rods every 4m distance, were necessary.

Fig. 3.2 - Sealing of dowel-piles in vertical borings

With a view to definitively stabilize the Railway, obviously the first nailing Solution at the toe appeared to be the most efficient one. However, the concerned Owner prefered the adoption of a temporary stabilisation by the far-off nailing layout.

3.4 Excuted nailing structure

The executed network of anchored dowel-piles consisted of 3 rows of 50m long and 1m apart, of HEA-160 steel girders nailed in soil every 1m distance. The steel girders were sealed into the marly bedrock by cement grout in vertical borings of 200mm diameter and 12m depth (Fig. 3.2) A reinforced concrete coping beam allowed the anchoring of the girder heads with 13 inclined 600 KN SIF tie-rods which were partly tensioned up to 300 kN in order to limit further deformations of the nailing system.

The control device included :

- topographical bench marks ;

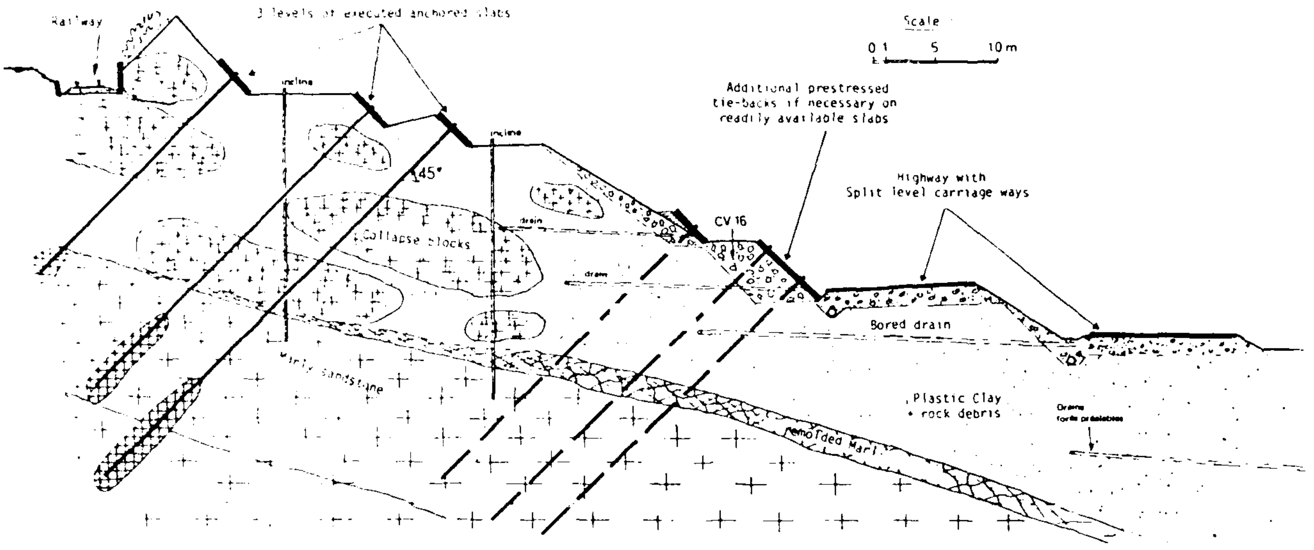
Railway
3 levels of executed anchored slabs
Scale
0 1 5 10 m
incline
incline
45°
Additional prestressed tie-backs if necessary on readily available slabs
Highway with Split level carriage ways
drain
Collapse blocks
CV 16
drain
Bored drain
Marly sandstone
Plastic Clay + rock debris
Drains forés préalables
Remolded Marl

Fig. 4.1 - Soil profile at "Chez Jacquet" Zone with designed anchored-slabs

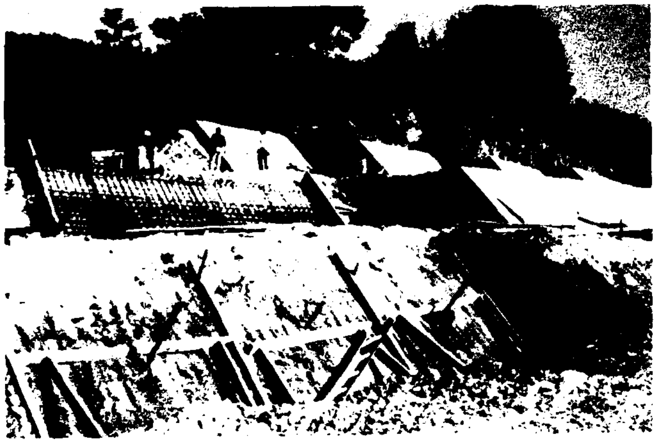

Fig. 4.2 - Execution of 3 upper levels of concrete slabs

Fig. 4.3 - Execution of 1000 kN anchor-rods

The adopted reinforcement technique that was used in this case consisted of several levels of reinforced concrete slabs anchored to the marly sandstone substratum by inclined prestressed tie-backs (Fig. 4.1).

Theoretically, the adopted multi-anchored slabs system allowed a degree of movement freedom to a potential circular sliding surface. But in the conceivable hypothesis of a quasi-rectilinear sliding of the overburden mass on the inclined plane of bedrock roof, such a system could be justified. Therefore, the Design of the necessary prestressed anchors has been computed considering that their introduced tensions in the soil would compensate the deficit of shear resistance along the potential sliding plane in order to obtain the adequate increase of safety factor.

4.4 Executed reinforcement works (Fig. 4.1).

The cut slope reinforcement finally consisted of

- 3 levels of strip concrete slabs 3,5m wide, 50m long, cast in place on slopes of 45° inclination (Fig. 4.2)
- 50 active 1000 kN-SIF anchor rods, 45° inclination and 3m apart, 35m to 40m length with minimum 6m of sealing length in the marly sandstone bedrock (Fig. 4.3).

The anchor rods were fixed on the supporting slabs with an extra length at head allowing a further re-tensioning if necessary. In addition, reservation holes (recess) were provided for supplementary anchor rods on the same slabs. All the works were excuted by successive descending phases from the top of the Hillock.

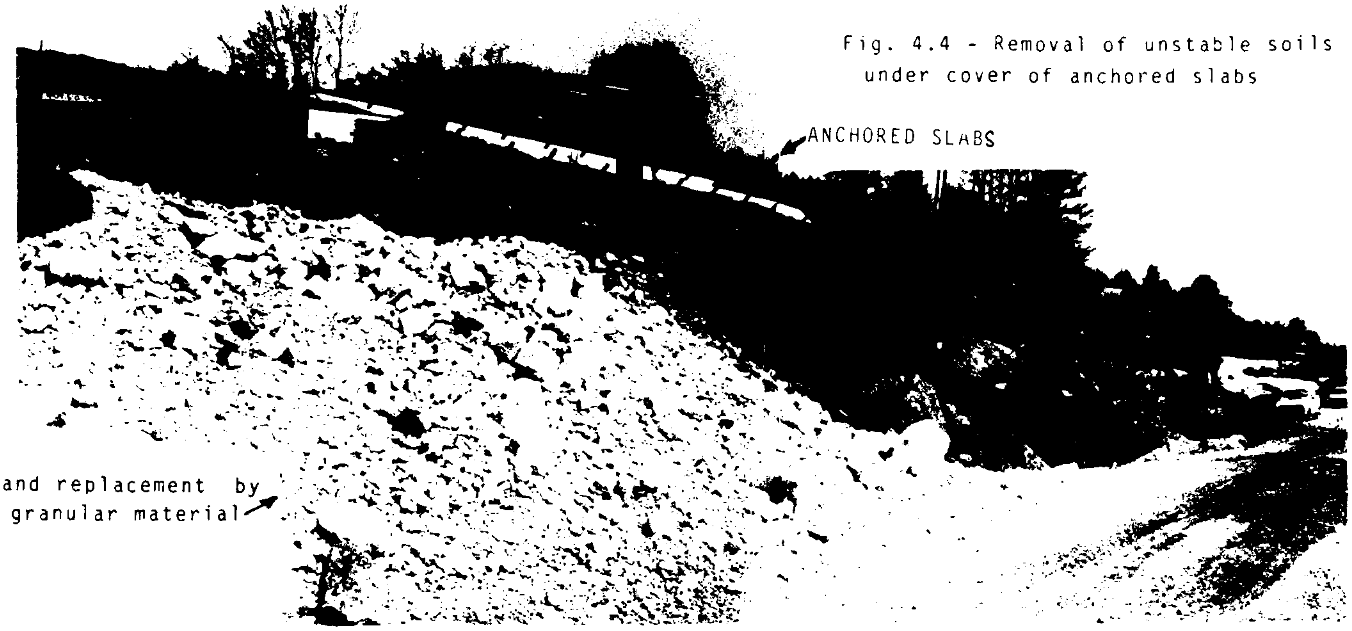

Fig. 4.4 - Removal of unstable soils under cover of anchored slabs

and replacement by granular material

It is to be noted that the performed reinforcement with 3 upper levels of anchored slabs was only sufficient to insure the stability of the Railway, but the Design allowed for a possible entension of the reinforcement system at the lower part of the Highway cut by including at least 3 additional levels of anchored slabs, for the event of observed stability insufficiency.

4.5 Additional reinforcement works

Under cover of the above anchored slabs, various traditional reinforcement works have been undertaken in the lower part of the cut :

- removal of unstable soils and replacement by granular material (Fig. 4.4) ;
- heavy draining masks made of quarry-run placed against the cut slope ;
- deep underground drainage by long subhorizontal bored drains (up to 50m long) at different levels from the Highway plateform.

In addition, 20 readily available concrete slabs were placedon the lower slope with a view to be able to promptly reinforce the stability of the cut by 50 extra anchor rods, if rendered necessary, without stoppage of Highway traffic (Fig. 4.5).

4.6 Follow-up and evolution of reinforced cut

The behaviour of the whole reinforced cut was monitored by a topographical bench marks network, inclinometer and piezometer tubes placed in deep boreholes down to the bedrock, Glötzl dynamometer cells at the anchor rod heads, and extensometers device on the concrete slabs.

During the whole delicate phase of earthworks in the lower part of the cut and until today, no significant movement were observed. During that period, the tension of the anchor rods did only show a slight variation around the nominal value of 1000KN and the Railway was quite safe.

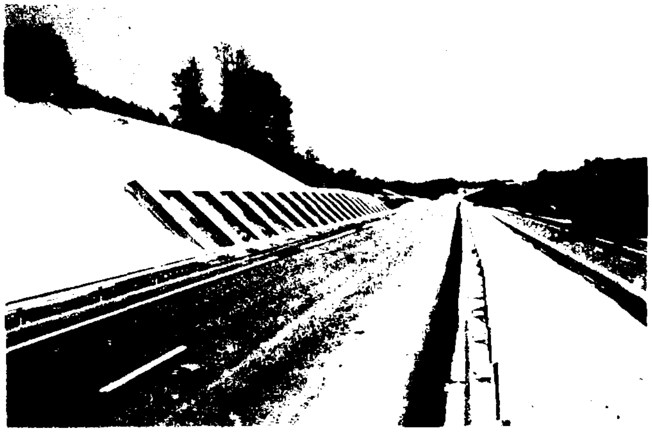

Fig. 4.5 - View of reinforced cut and Highway after completion of works

5 - EXAMPLE OF STABILISATION OF A SLIDEN CUT BY MULTI-ANCHORED SLABS

5.1 Slope sliding at "Les Damets" site.

A 25m high cut was designed below the existing RN203 main Road in the sandstone hillside at the so-called "Les Damets" zone. While the earthworks were in progress on the upper part of the cut, just below the main Road, a slope slide started at the location of a faulted area (Fig. 5.1). *The earthworks were immediately* stopped and the sliding temporary stemmed with the help of a heavy stockpile of rock material at the toe of the slope. Simultaneously, detailed geological survey and additional boring were undertaken on the site.

The soil investigation results quickly led to the conclusion that this was a quasi-plane sliding of the upper part of weathered and fractured marly sandstone on the inclined roof of the stable sandstone substratum. The marl and sandstone layers were dipping about 12° to 15° towards the valley, but the unfavourable effect of the dip was attenuated by the fact that the strike direction of bedding was oblique with respect to the Highway route.

5.2 Stabilization Project.

Basing on the fact that the sliding was a plane one made of a rock mass on an inclined stable substratum located at about 15m depth, the rock nailing technique by a network of high capacity anchor-rods with supporting slabs was considered to be the most adequate stabilization solution (Fig. 5.2).

In order to reduce the cost, the expensive system of multi-anchored slabs was only to be applied to the upper part of the cut slope where the main Road safety had to be urgently assured. Under cover of such prior upper rock reinforcement, the lower part of the cut could be stabilized by flattening the slope, removing the unstable material, draining the ground water and placing a heavy-mask made of quarry-run on the slope toe.

Obviously, the preceding reinforcement experience at "chez Jacquet" site has influenced the adoption of a solution. But in this present case, the rock reinforcement technique by multi-anchored slabs was applied subsequently to the cut failure (i.e. F=1 already), while the cut reinforcement at "chez Jacquet" was rather a preventive measure.

5.3 Executed reinforcement works

The first reinforcement works carried-out on the upper part of the cut slope and below the existing main Road comprised for a 100m length :

- a preliminary retaining structure by soil nai-

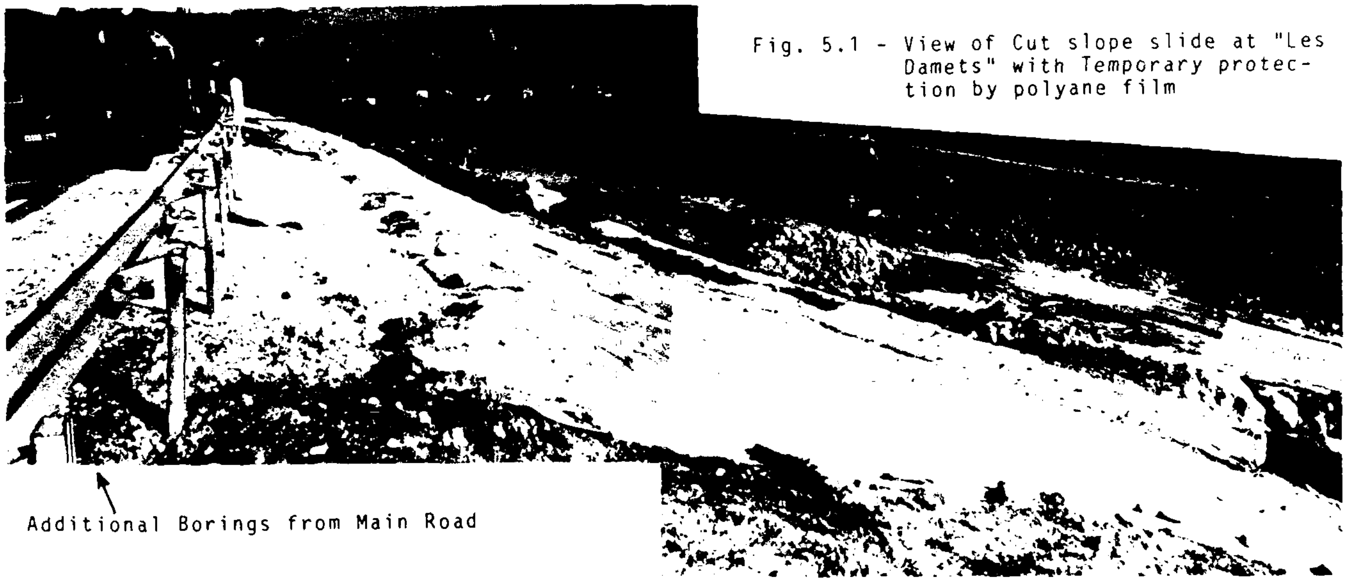
Additional Borings from Main Road

Fig. 5.1 - View of Cut slope slide at "Les Damets" with Temporary protection by polyane film

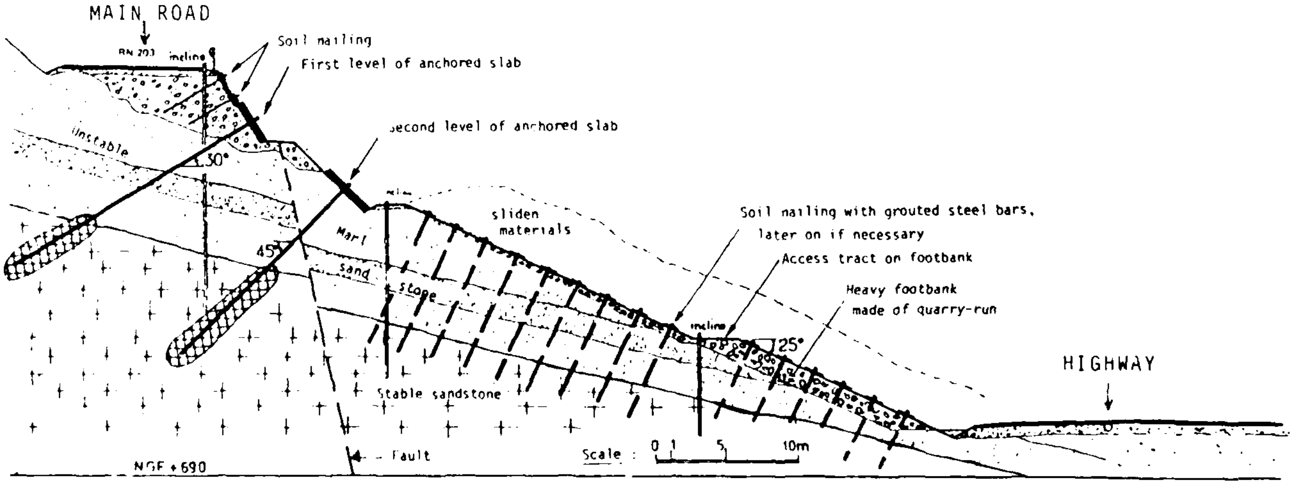
MAIN ROAD
RN 203
incline
Soil nailing
First level of anchored slab
Unstable
30°
second level of anchored slab
sliden materials
Marl
sand
stone
45°
Stable sandstone
Fault
NGF +690
Soil nailing with grouted steel bars, later on if necessary
Access tract on footbank
Heavy footbank made of quarry-run
incline
25°
HIGHWAY
Scale : 0 1 5 10m

Fig. 5.2 - "Les Damets" soil profile with design slope nailing and anchored slabs

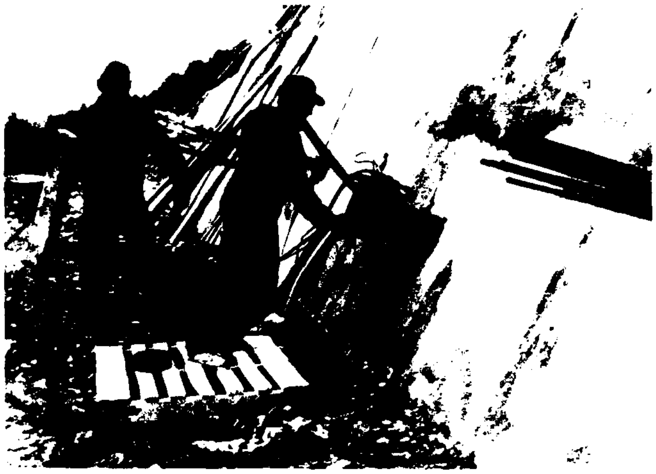

Fig. 5.4 - Tensioning of tie-rods on first anchored slab

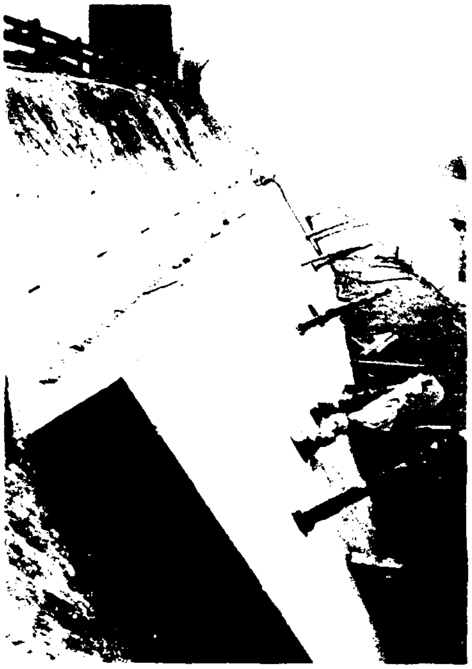

Fig. 5.3 - View of sol nailing and first anchored slab below main Road

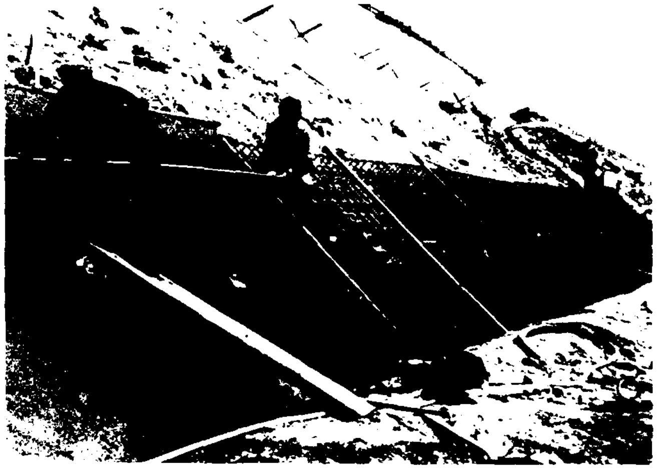

Fig. 5.5 - Concreting of second anchored-slab inclined by 45°

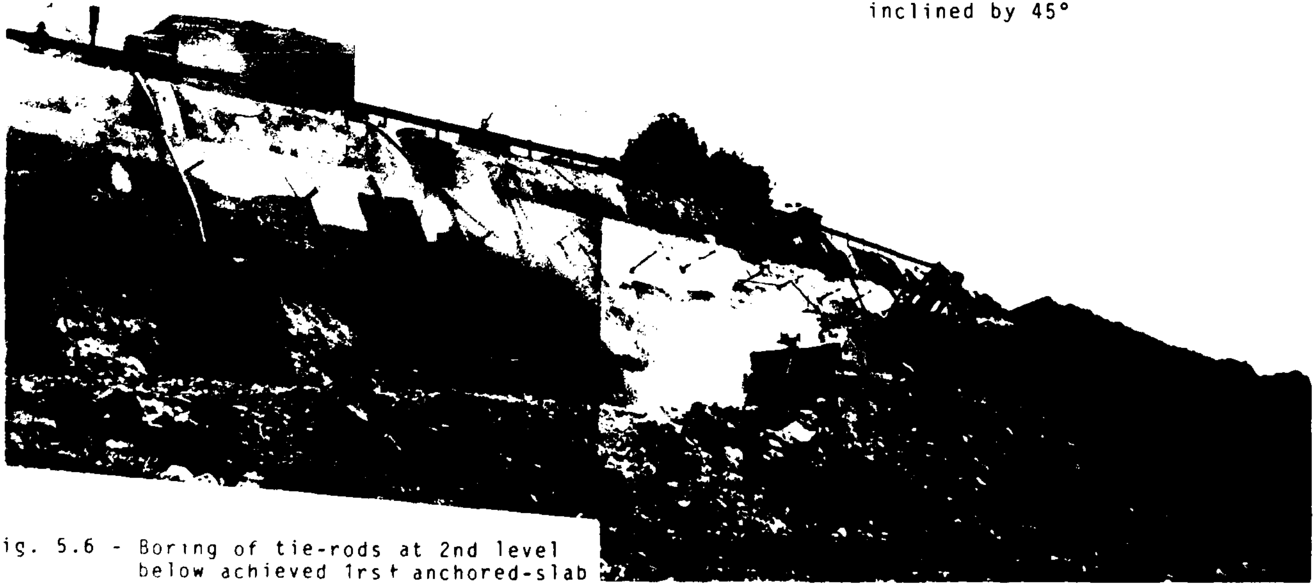

Fig. 5.6 - Boring of tie-rods at 2nd level below achieved 1rst anchored-slab

ling of the cut slope top, at the border of the existing Road, by 2 levels of steel bars T32mm, 4 and 6m long, 2m apart, sealed in predrilled boreholes with cement grout. The facing, or "skin", necessary to ensure local soil stability between the nailing bars, consisted of 10cm thick shotcrete on welded mesh and fitted with cross-drains (Fig. 5.3) ;

- and a stong rock reinforcement system by 2 split levels of strip concrete slabs which were cast in place on inclined slopes (Fig. 5.6) and anchored to the stable bedrock by prestressed 1000 kN anchor rods (Fig. 5.4). For theoretical and practical reasons, the upper slab was inclined by 60° with respect to the horizon (Fig. 5.3) and anchored with tie-backs inclined at 30° and 3m apart, and the lower slab inclined by 45° (Fig. 5.5) with anchor rods at 45° and 3m apart.

The subsequent stabilisation works on the lower part of the cut slope consisted of traditional techniques (Fig. 5.7).

- flattening of the slope to 25° with removal away and substitution of sliden materials by coarse and draining quarry-run.

- surcharging of the lower part of the flattened slope by a heavy mask and a massive 7m high 4m wide footbank made of 0/400 mm quarry-run.

- deep underground draining by 40m long subhorizontal drains bored at various levels.

The Design procedure was the following : as the sliding had already occured, it was possible to calculate the residual effective characteristic

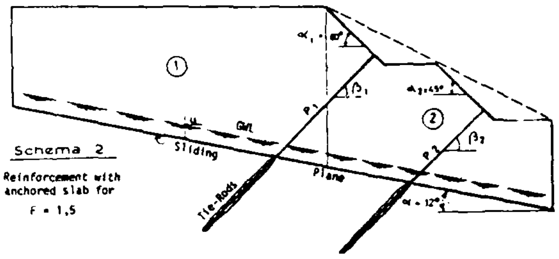

Fig. 5.8 - Calculations scheme

Ø' & C' of the marl on the inclined sliding plane, by posterior Analysis for safety factor value F=1. Then the number and the arrangement of the 1000 kN-anchor rods were determined in such a way as to compensate the lack of shearing resistance of the marl on the sliding plane and to increase the safety coefficient F from 1 to at least 1,5 (Fig. 5.8).

5.4 Monitoring and evolution

The behaviour of the multi-anchored slabs system and of the whole cut was checked at regular intervals by means of the following control instruments :

- 8 deep inclinometer tubes cast in boreholes at various levels ;
- 8 dynamometer cells at anchor-rod heads ;
- 2 extensometer devices on lower anchor slab ;
- topographical bench marks over the site.

Up to day, the inclinometric control measurement showed that some very slight "readjustment" movements would exist in the sandstone substratum below the reinforced zone, whereas the dynamometric records gave evidence that the tension in the anchor rods has always been quite stable (variations of only 10 to 20 kN around the nominal value of 1000 kN).

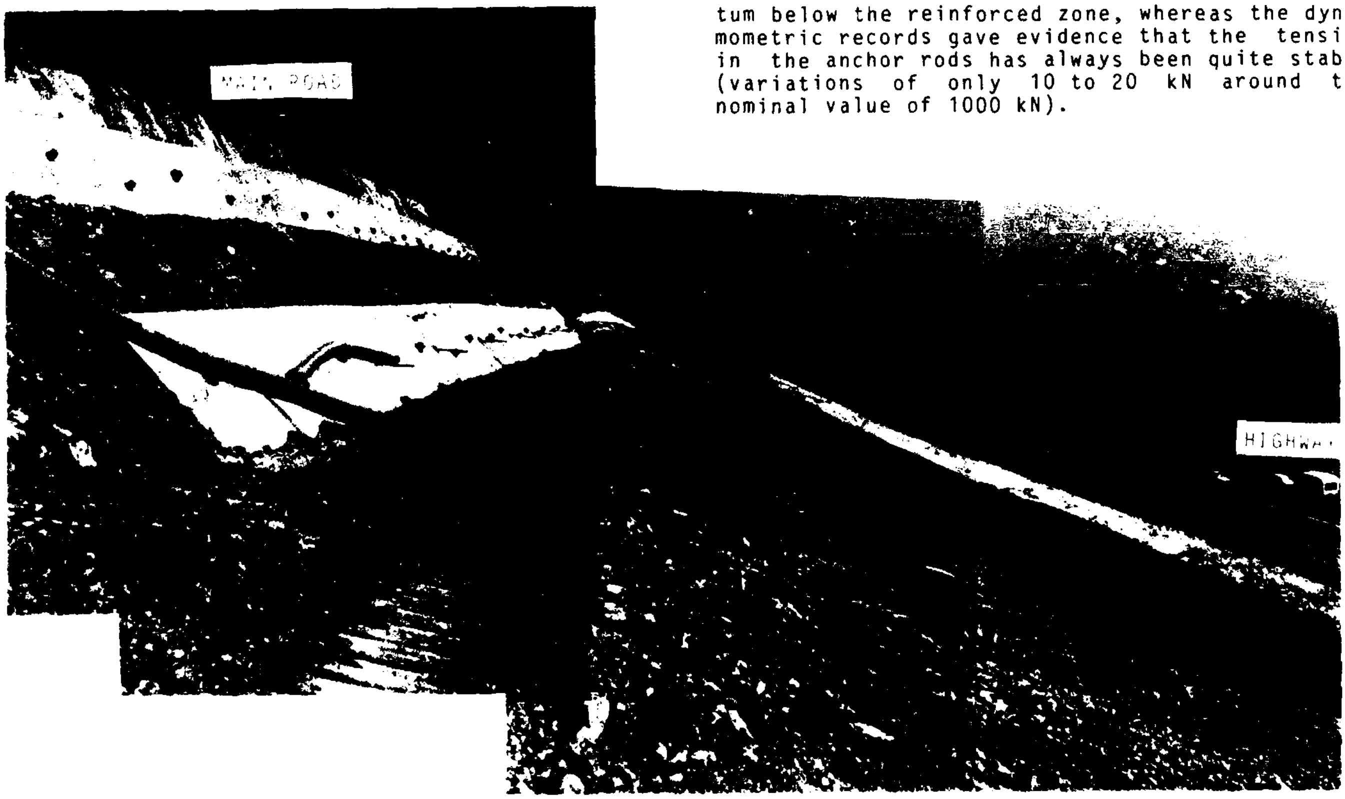

Fig. 5.7 - View of reinforced and masked cut slope after completion of works

6 - EXAMPLE OF EMBANKMENT FOUNDATION ON STONE COLUMNS

6.1 "Chez Vavert" Site (Fig. 6.1).

In that zone named "chez Vavert", the Highway was designed to cross over a depression in natural versant, by an embankment of 12m in height. This hollow area probably corresponds to the subsidence of the upper part of an ancient lanslide presently stabilized.

In fact, the soil investigation results demonstrated that the overburden of 3 to 12m in thickness, bearing a water table at 2m depth, was constituted mostly of soft clay (undrained cohesion of Cu = 30 to 50 kPa) and of remolded marl laying on the inclined marly bedrock (dip of about 25° towards valley.

6.2 Soil improvement solution (Fig. 6.2)

Theoretically, the short term stability of the designed embankment impplied that the clayey overburden had an undrained cohesion of at least Cu=70kPa. As the actual cohesion was lower or equal to Cu=50kPa, a soil replacement or improvement appeared to be necessary before erecting the embankment.

A possible solution would have consisted of a quasi-total substitution of the soft clay and remolded marl by a granular material forming a frictional and draining foundation seating for the high embankment. Such solution presented some difficulties and risks during the works due to the depth of the temporary excavation (down to 12m) and to the proximity of a Farm.

Therefore the technique of soil reinforcement by "stone-columns", was preferred because it offered the following advantages :

- suppression of the difficult and dangerous excavation for substitution works on the versant
- obtaining bearing improvement of bearing capacity and consolidation speeding-up of foundation soil ;

Fig. 6.1 - General view of "Chez Vavert" Site at Beginning of works

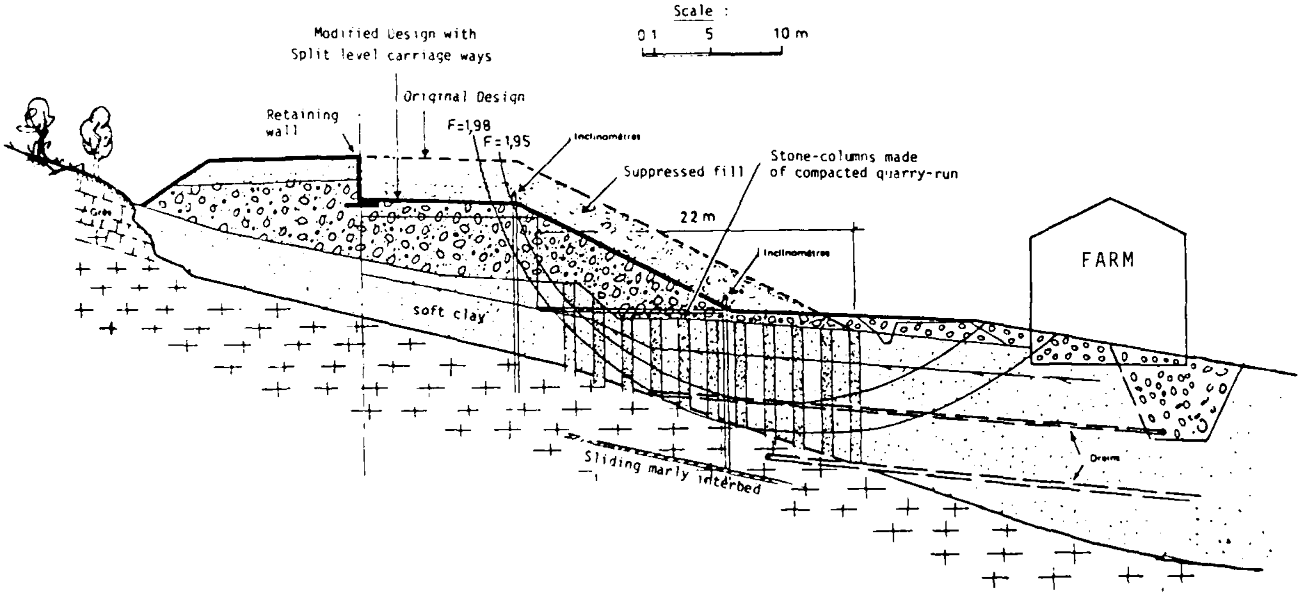
Scale :
0 1 5 10 m
Modified Design with
Split level carriage ways
Original Design
Retaining wall
F=1,98
F=1,95
Inclinomètres
Suppressed fill
Stone-columns made
of compacted quarry-run
22 m
Inclinomètres
FARM
soft clay
Sliding marly interbed
Drains

Fig. 6.2 - Soil profil at "Chez Vavert" Zone with designed embankment on stone-columns

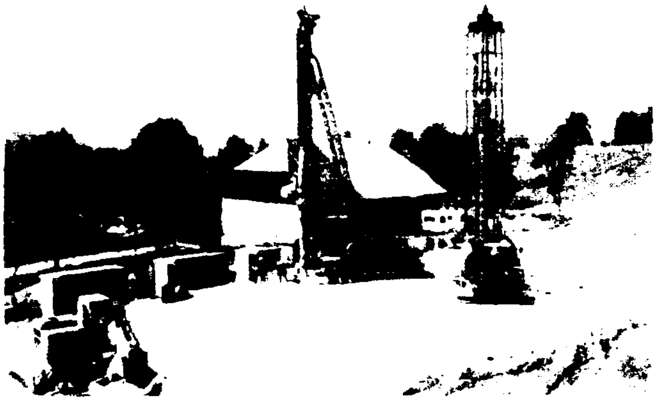

Fig. 6.3 - Execution of stone-columns using FRANKI equipment

- easy adaptation of the improvement depth by varying on demand the length of stone-columns in accordance with the unevenness of the bedrock surface.

6.3 Design of the stone-columns network

The Design of the embankment founded on stone-columns was realized in 2 phases :

- first phase : preliminary dimensioning of the required stone-columns network ;
- Second phase : general stability analysis of the embankment with the predimensioned stone-columns network.

The preliminary dimensioning study was based on the simplified analysis of the bearing capacity of stone-columns which are constituted of granular material having an angle of internal friction Øcol and embedded in a cohesive foundation soil having an apparent cohesion Csol. The density of columns (rumber of necessary columns of diameter B per unit surface of foundation soil) was then determined in such a way that they could alone bear the designed embankment with a safety coefficient of only F = 1.

The second design stage of general stability analysis with failure surfaces, either circular or not, necessitated the use of a computer Program and the simulation of the stone-colums (which are discontinuous i.e. "ponctual" in the foundation layer) as an equivalent network of "stone diaphragm-walls" made of the same frictional material with a reduced width. These simulated stone-walls were introduced into the computer Program as a series of vertical layers of soil having the internal friction Øcol and alternating with other vertical layers of natural soil having the cohesion Csol.

In fact, such computation was conservative, for it would have been more correct to also introduce the "concentration factor" of loads on the stone-columns which would increase the shearing resistance of these stone-columns in the same ratio (up to about 4 in the present case).

6.4 Final Design of stone-columns network

Theorical computations and practical considerations led to the following final Design of the stone-columns (Fig. 6.2).

- columns of diameter B=80cm made of limestone quarry-run having the angle of internal friction Øcol-40° ;
- grid layout implantation spaced 2mx2,5m, hence density of 1 column per $5m^2$ of soil surface, i.e. "replacement ratio" of a = 0,10.
- stone-columns placed along 11 rows, 2m apart, below the dowstream slope of the embankment (where the potential sliding surfaces reached the compact substratum).
- draining blanket over the stone-columns network with a view to assure the drainage at the base of the embankment.

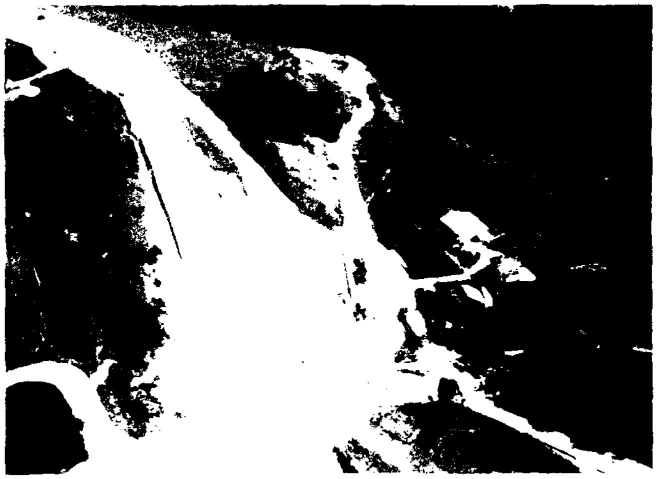

Fig. 6.4 - Aerial view of worksite during first consolidation phase

6.5 Execution of the stone-columns

Two techniques were considered for the execution of the designed stone-columns network :

1) The usual technique of cast in-situ piles, for instance FRANKI piling system (Fig. 6.3), where a steel casing is rammed down and filled with stone while the casing is removing up and the stone strongly tamped.
2) The modern technique, using KELLER electric vibrator or BAUER hydraulic one, with water jetting to create the hole and keep it open when the vibrator is lowered down.

The first technique using FRANKI piling equipment was finally adopted for the following practical reasons : elimination of jetting water which could pollute the site and soften the clayey foundation soil ; avoidance of soft soil removal to place the columns. So there is compaction of in-place soft soil when driving the casing ; strong compaction of stony material to form large and dense columns.

Using 2 piling rigs of 80HP, the network including 395 stone-columns of 8m in average length was executed in 7 weeks, incorporating a volume of $1800m^3$ of 0/60mm quarry-run into the ground (Fig. 6.3).

6.6 Control and instrumentation

In-situ tests, such as static penetrometer tests and Ménard pressuremeter tests in boreholes, were carried-out on the site before and after execution of the stone-columns. Contrarily to all expectation, the strong tamping of stone-columns without removal of the in-place soft soils, did not involve a significative improvement of the consistency of these soils. In fact, as the soft soils were clayey and saturated, the forced incorporation of the 1800m³ of quarry-run has rather caused some 40 cm heave of the working plate-form.

With a view to monitore the behaviour of the embankment on improved subsoil, control instruments were installed on the site prior to the embankment construction such as : hydraulic settlement cells on the plate-form, pore-pressure cells, piezometer and inclinometer tubes in the ground, topographical bench marks, etc...

6.7 Findings

As an additional precaution, it was decided to construct the embankment in three successive phases with periods of resk after each phase allowing consolidation of the reinforced subsoil :

- first phase : of 6m height of fill.
- second phase : up to 8m (Fig. 6.5)
- third phase : up to the final height of 12m (this phase was suppressed).

As a matter of fact, after completion of the second phase earthmoving, the inclinometric surveys did disclose an unexpected slight and slow sliding movement in a marly interbed below the stone-columns base at about 18 m in depth. In the meantime, the piezometric measurements pointed out that the excess pore pressure in the clayey soil between stone-columns was remaining at high values : the columns, made of draining

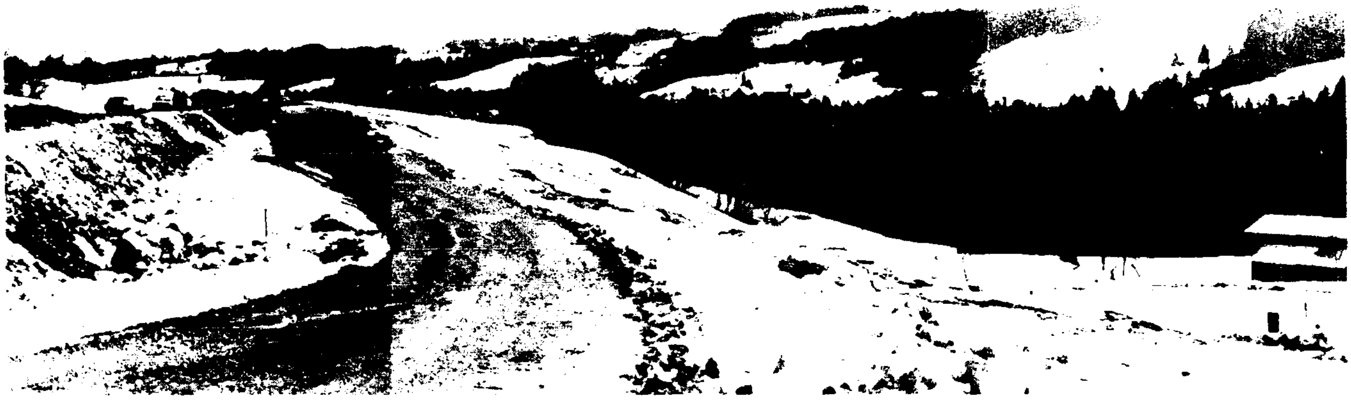

Fig. 6.5 - Second consolidation phase (8 m of embankment) during winter

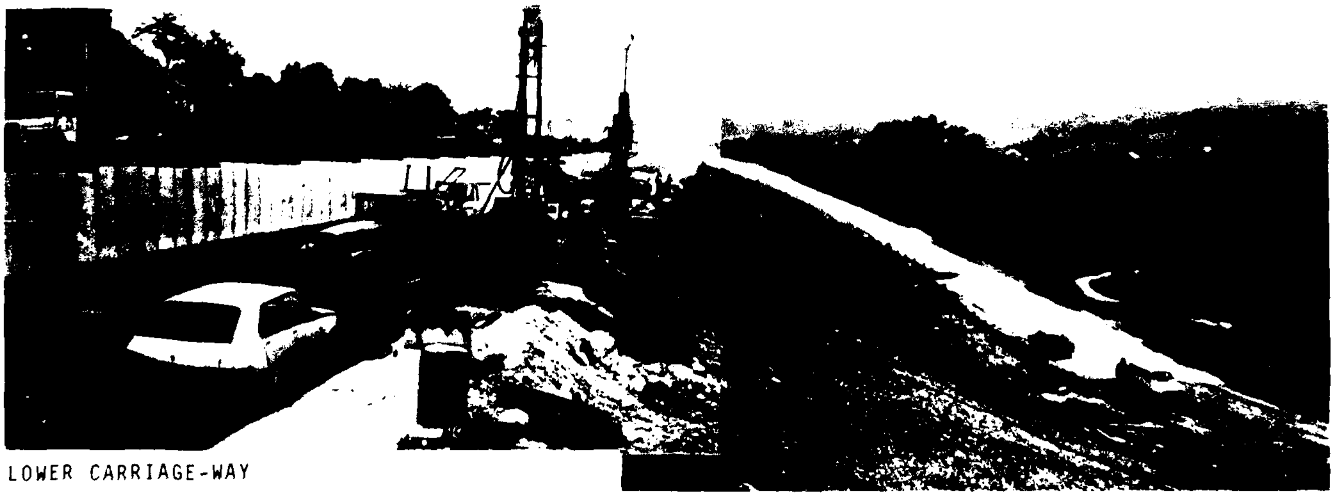

LOWER CARRIAGE-WAY

Fig. 6.6 - Plit-levelling of carriage-ways by precast retaining wall and placing of inclinometer tubes to observe the constructed embankment behaviour

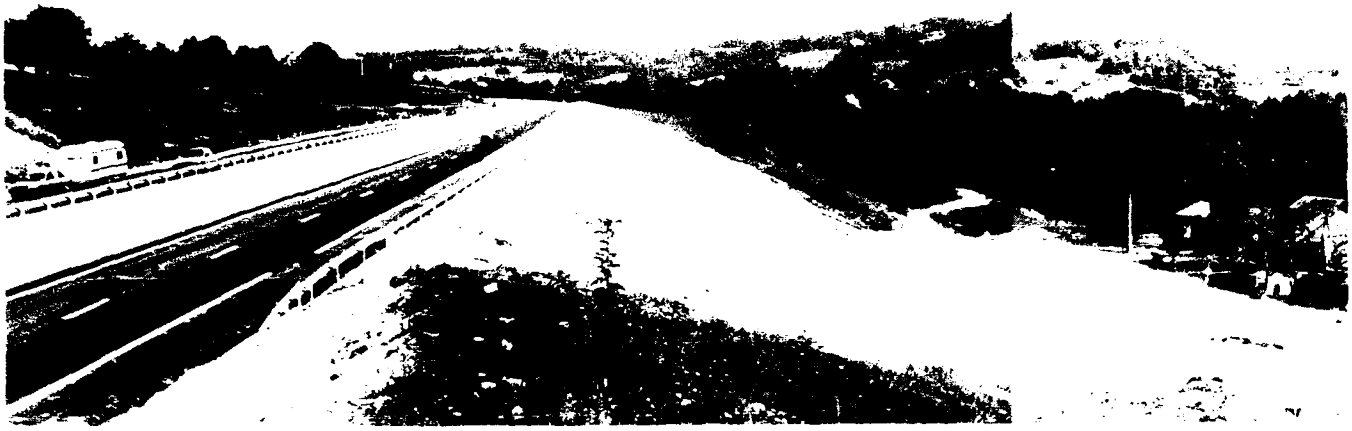

Fig. 6.7 - General view of "Chez Vavert" embankment after achievement of works and with Highway in operation

material, seemed unable to speed-up the underground drainage. Furhtermore, these columns having been strongly compacted had a high bearing capacity, which consequently did transfer most of the embankment weight directly to the substratum and were so causing some equilibrium disturbance within the marly interbed at about 15 m of depth.

6.3 Project adaptation and additional works.

The above unexpected findings led to the decision to make several modifications to the Design and to undertake additional works on the site :

- Reduction of the Highway embankment volume, hence weight, by placing the downstream carriage way (on Valley side) at a level lower by 3m, with respect to the upstream one. This split-levelling, obtained by construction of a cantilever retaining wall (Fig. 6.6), of precast concrete CHAPSOL type wall, required only a rather smal volume of additional fill compare to the already in place embankments (Fig. 6.5).

- Improvement of the underground drainage, hence soil consolidation, by adding 2 fan-shapes networks of subhorizontal drains. These drains were bored from 2 temporary excavations located at the stone-columns base level. The catchment waters were then collected and evacuated along a deep "French draining trench" down to the valley (Fig. 6.7). It is to be noted that thanks to the bored drains, the observed lowering height of the groundwater table was 7m in average.

- After achievement of the works, additional inclinometer tubes were installed through the fill and down to the bedrock (Fig. 6.6), with a view to observe the long term behaviour of the so constructed embankment on stone-columns.

Fig. 6.7 gives the général views of the Highway after completion of the works.

7 - CONCLUSION

The various reinforcement systems which have been excuted used mostly steel inclusions in the ground. This was intended principally to strengthen or to stabilize an existing main Road or Railway prior to the general Highway earthworks. Such steel inclusions, passive or tensioned. were rather flexible and slender in comparison with the soil mass to be reinforced. But appropriately conceived and correctly designed, they could really form efficient reinforcement systems offering the advantage to be executable with rather light equipment on quite unsteady inclined versant and at proximity of an existing traffic way. Furthermore, these reinforcement systems could be easily adaptable to the ground irregularity and could also be extended in case of further requirements.

But concerning the general stability problem of natural clayey versants or of ancient sliding, the most efficient and economical stabilisation techniques are the classical ones, such as : underground drainage, substitution of unstable soils, heavy draining masks on cut slop, frictional "hard core drains" running up and down the versant, etc... In the hereabove examples, such classical techniques were always applied under cover of a previously installed special reinforcement system.

The Design of the cited reinforcement examples was based on simplified schemes of soil failure, but it also took into account as much as possible all the failure criteria related to the strenght of soil and inclusions and also the interaction phenomena between those. As the subsoil frequently offers numerous enigmas mainly on the areas of ancient sliding, the actual behaviour of the executed soil reinforcement systems was checked by control instruments. This allowed to judiciously introduce corrections to the Design and works when and where it was found necessary.

Proceedings: Second International Conference on Case Histories in Geotechnical Engineering, June 1-5, 1988, St. Louis, Mo., Paper No. 5.03

Drainage Walling as Excavation Support

Bernhard Wietek
Professor (HTL), Dipl. Ing., Wietek Geotechnical Consulting Engineers, Innsbruck, Austria

SYNOPSIS: In practice there are different processes which are used to support excavations and to maintain the groundwater level in excavations which go down to this level. In urban areas the diaphragm wall is frequently used to protect the excavation and as underground water packing against groundwater flowing in form the side. In addition, the lowering of groundwater is necessary using a well point within the excavation.

A new fondation trench sheeting has been developed by the author of this paper. This new method is an improvement on the diaphragm wall by which not only is the earth shored up, but the lowering of the groundwater within the excavation can also be carried out. In accordance with the function of this method, we refer to the new type of foundation trench sheeting as drainage walling. This drainage walling is manufactured in a similar way to the diaphragm wall.

We have observed drainage walling on building sites which differ greatly from each other. The results of our observations are intended to demonstrate the advantages and also the problems involved in this new process to the planning and project engineers.

INTRODUCTION

A planning engineer is continually faced with the task of choosing a method of excavation support for a given structure. He then has to decide on all ensuing details. It is not until building has been completed that it becomes clear whether the correct choice was made and whether the building methods were economically viable.

The choice of excavation support is not easy as the choice is dependent not only on technical factors but also on non-technical factors and conditions. By technical factors we mean such factors as the size and depths of the excavation, a possible adjoining excavation and the type of subsoil. The non-technical factors, such as the necessity of there being no change in the underground water level outside the excavation can be numerous and of import.

The many demands made on an excavation mean that there is a tendancy to set up various types of support next to each other. The required conditions are thus met locally, but this method is highly unsatisfactory as far as the whole excavation is concerned. For this reason a diaphragm wall and a grouting wall are often combined with a sheet pile or another kind of support. This leads to various subgrade surfaces beneath the structure and usually to difficulties such as differences in settlement which then have to be equalized.

If one compiles a list of the demands made on excavation support, it soon becomes clear that there are numerous solutions available at present but that these are unsatisfactory in certain cases. This report aims at introducing a new type of excavation support which should close this gap to building specialists. I intend to base my explanations of this new type of excavation support on current practices and thus show the necessary basis for planning. This method of excavation will then be demonstrated by an existing example.

EXCAVATIONS BELOW GROUNDWATER LEVEL

Nowadays there are many different types of excavation support available. If the excavation is more than two storeys in depth, the number of possibilities is reduced. This is especially the case in an urban area, as vertical excavation walls are required here in general.

These deep excavations frequently reach the groundwater level. The excavation must be free from water for construction work, which means that the groundwater must not be allowed to penetrate into the excavation, but must be diverted before this can happen. It is possible to seal off the groundwater. In the following diagram normal procedures are shown which are independent of the type of support.

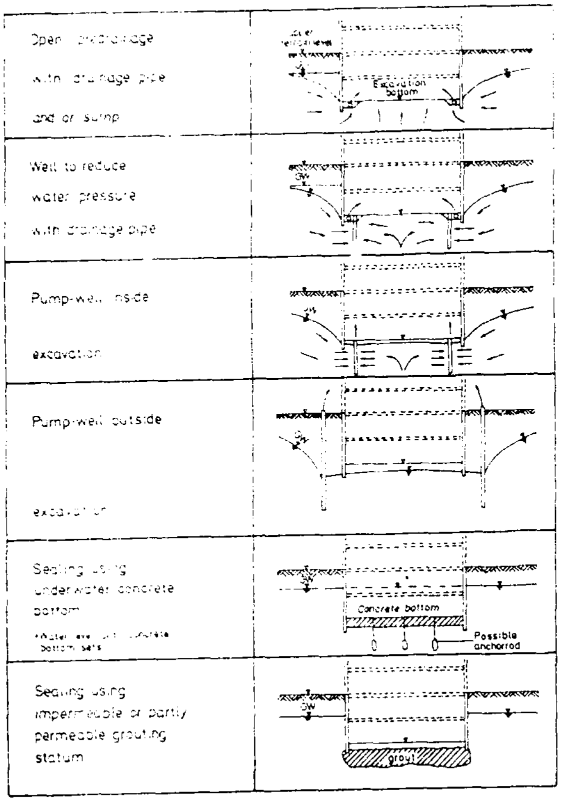

Fig 1: excavations below groundwater level

- open dewatering with drainage conduit and/or sump. Simplest type but groundwater lowering only possible up to 1-2 metres at a maximum; danger of hydraulic seepage into the excavation bottom.
- well to reduce tension with drainage conduit: especially advantageous in excavations where coheseive and pebbly soils alternate; lowering of groundwater possible up to a maximum of three metres.

-pump well inside the excavation; groundwater can be lowered to any depth; watertight excavation support has additional advantages; hydraulic seepage is largely avoided; the preparation of watertight foundation slab can cause hindrances.

- pump well outside the excavation; groundwater can be lowered to any depth; extreme depths mean large amounts of water which have to be pumped off; any type of excavation support can be applied; no hindrance caused by the preparation of watertight foundation slab.

- sealing off using underwater concrete bottom: watertight excavation support necessary; underwater concrete is introduced after completion of underwater excavation; buoyancy anchor rods may be necessary as an extra buoyancy guarantee; the lowering of the groundwater level should not take place until buoyancy reliability has been obtained.

- impermeable grouting bottom: watertight excavation support necessary; excavation down the groundwater level; production of grounting element, strength and depth depend on buoyancy security.

- partly permeable grouting bottom, production as above although it merely serves as a braking stratum (comparable to a cohesive interim stratum); remaining water has to be pumped off using open predrainage.

The main difficulty with excavations below the groundwater level is avoiding hydraulic seepage. This can be done using pump wells (inside or outside the excavation) or tail water concrete bottom and a grouting stratum. It must be borne in mind here that the latter two methods often tend to be expensive. The use of the pump well within the excavation ensures good control of the groundwater lowering but it is relatively difficult to seal the foundation slab against pressure from the groundwater. The reason for this is that the wells are in full use during building. This problem does not occur with wells outside the excavation. It is, however, often difficult to arrange wells outside the excavation, as excavation support is often situated at the edge of the building site and the wells would have to be set up on adjoining building sites.

PRINCIPLE OF DRAINAGE WALLING

Taking the possibilities of supporting deep excavations with predrainage as a starting point, it becomes apparent that the above-mentioned solutions often do not correspond with the wishes of the builders and contractors or with the building conditions. For this reason the demands made by deep excavations below the groundwaterlevel have been listed:

- The excavation should be deeper than foundations of directly adjoining buildings

- The excavation bottom should be flat to ensure full use of the lowest storey (as a storeroom or carpark).

- The excavation or excavation support should be set up directly along the edge of the plot.

- A terracing of the excavation bottom is not permitted as this would mean the loss of otherwise usuable volume of building work.

- The excavation must be completely open during building, i.e. no shoring should reach into the excavation.

- It is not permitted to make demands on neighbouringbuilding sites, although this may be possible for a short period during a difficult stage of building.

- A predrainage of the groundwater must not be allowed to infringe on building work and the excavation bottom in particular should be kept clear.

- No hydraulic seepage in the excavation must be allowed to occur through predrainage.

- The excavation support should be at least technically watertight so that a later sealing of the lower groundfloors against groundwater would not have to be carried out in entirety.

- The excavation support should be includes into the planned structure as far as possible in order to keep costs down.

- The foundation slab must be adjoined to the excavation support in such a way as to be watertight.

- As soon as buoyancy of the structure is guaranteed, predrainage should be stopped.

- The possibility of a later groundwater lowering should be left open to avoid subsequent work on the foundation slab and cellar walls leading to flooding.

- A continuous drawing off of groundwater is to be reckoned with to ensure that available water for washing plants and heat pumps etc. is available.

- Groundwater must not seep into cellars when water is being made available for use.

If one accepts these points, excavation support must fulfil five different requirements:

1. Support of the excavation against soil.
2. Predrainage of groundwater.
3. Sealing against groundwater.
4. Removal of building loads.
5. Possibility of later drawing off of water for use.

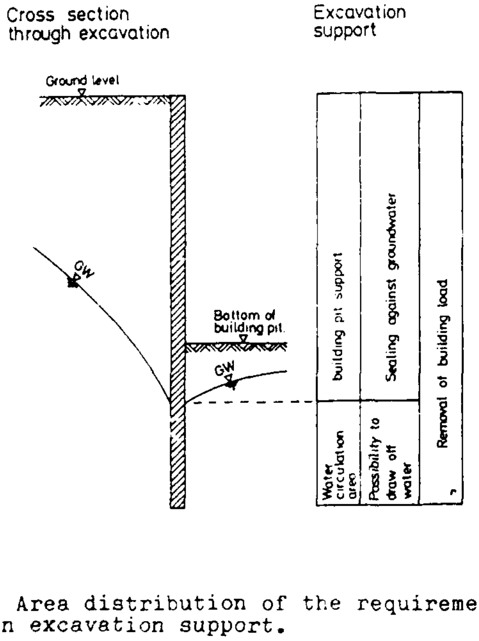
Cross section through excavation
Excavation support
Ground level
GW
Bottom of building pit
GW
building pit support
Sealing against groundwater
Removal of building load
Water circulation area
Possibility to draw off water

Fig 2: Area distribution of the requirements made on excavation support.

Excavation in present general use cannot fulfil these requirements. In order to find a new solution, the area distribution of the requirements must be looked at from the excavation support. Figure 2 is included for this reason.

Area A: Support of the excavation, sealing against groundwater and removal of building loads; in such cases ordinary excavation support such as a diaphragm wall or an overlapping bored pile wall can be used.

Area B: Groundwater lowering, subsequent drawing off of water for use and removal of building loads; the well function and bearing capacity can be combined with a permeable load-bearing building material for development of this area. Pervious concrete is a possible permeable building material with load-bearing qualities.

A type of axcavation support shich fulfils both of these conditions is known as drainage walling. In principle, the diaphragm wall, pile wall or single pile could be used as axcavation support. Figure 3 shows a cross-section of drainage piles.

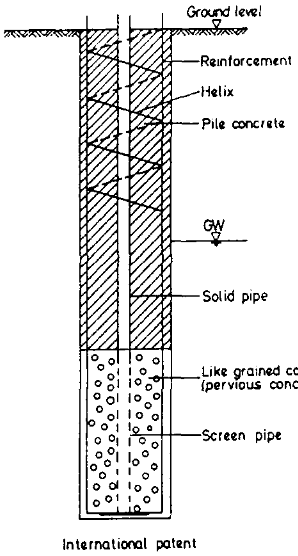
Ground level
Reinforcement
Helix
Pile concrete
GW
Solid pipe
Like grained concrete (pervious concrete)
Screen pipe
International patent

Fig 3: Structure of drainage piles

As opposed to the ordinary pile, a drainage pipe is additionally built into the middle. The lower part of this pipe (via which the groundwater lowering should take place) consists of a screen pipe and the upper part of a solid pipe. In addition, pervious concrete is built into the lower part instead of the normal pile concrete. This enables underground draining to take place via the pipe in addition to the fact that the pile has a load-bearing capacity and is able to absorb bending moments.

The same structure can of course be carried out on one element of a diaphragm wall. In this case we speak of a single drainage wall.

APPLICATION

The new drainage walling represents an extension of excavation support in general use at present. Using the drainage pile described above as a starting points, four different types of drainage support can be listened here.

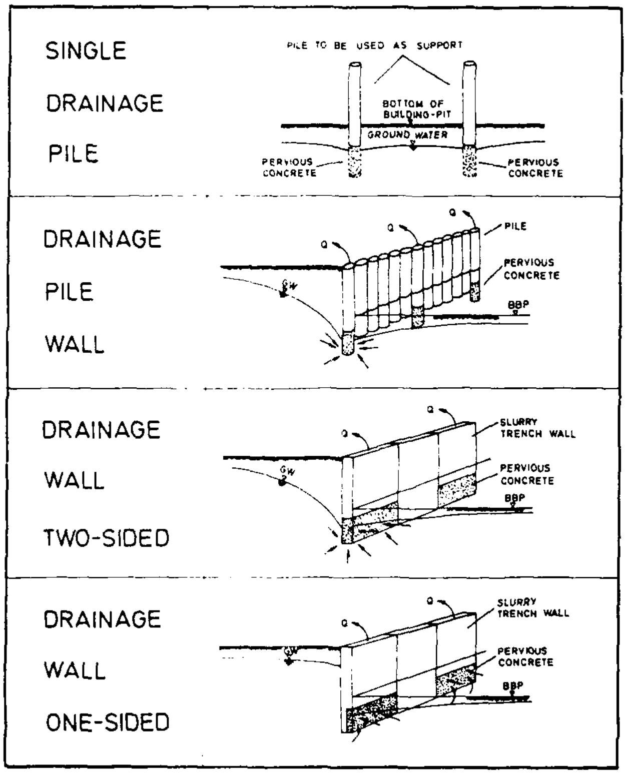
SINGLE DRAINAGE PILE
PILE TO BE USED AS SUPPORT
BOTTOM OF BUILDING-PIT
GROUND WATER
PERVIOUS CONCRETE
PERVIOUS CONCRETE
DRAINAGE PILE WALL
Q
Q
Q
PILE
PERVIOUS CONCRETE
GW
BBP
DRAINAGE WALL TWO-SIDED
Q
Q
SLURRY TRENCH WALL
PERVIOUS CONCRETE
GW
BBP
DRAINAGE WALL ONE-SIDED
Q
Q
SLURRY TRENCH WALL
PERVIOUS CONCRETE
GW
BBP

Fig 4: Drainage walling Systems

Single Drainage Pile: Any single pile can be built into a drainage pile and it does not necessarily have to be used as excavation support. The single drainage pile is of especial interest for covered-in building methods, as it ensures that very large excavations can be opened and the surface course, which is appropriate to the terrain, supports itself in the deeper building plot by this drainage pile. At the same time the whole predraining process can be carried out by means of the drainage piles.

Drainage Pile Wall: Single drainage piles can be arranged in the pile wall as excavation support to ensure the predrainage of the excavation. In Fig. 5 we can see a drainage wall under construction. Whether the drainage pile has to be deeper than the other piles or not now depends entirely on the subsoil conditions. A decisive reason for making the drainage pile deeper is the pressure of the groundwater and the permeability of the subsoil.

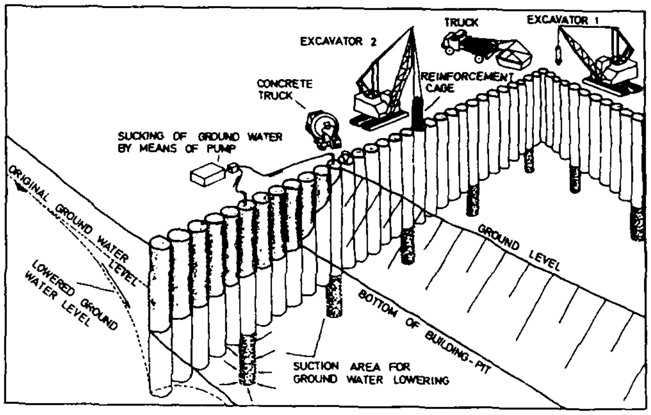
TRUCK
EXCAVATOR 1
EXCAVATOR 2
CONCRETE TRUCK
REINFORCEMENT CAGE
SUCKING OF GROUND WATER BY MEANS OF PUMP
ORIGINAL GROUND WATER LEVEL
LOWERED GROUND WATER LEVEL
GROUND LEVEL
BOTTOM OF BUILDING-PIT
SUCTION AREA FOR GROUND WATER LOWERING

Fig 5: Construction of Drainage Pile Wall

Drainage Wall Two sided: As in the drainage pile wall a drainage element is built into the lower part of the diaphragm wall. In this way the same effect is attained as in the drainage pile wall. A diagram did not appear necessary in this case.

Drainage Wall One-sided: Using the diaphragm wall as a departing point, a drainage element is built into single elements of the lower part on one side only. This, of course, demands very great precision in all stages of work. The advantages are, however, of great import. The one-sided sinking arrangments make it possible to extract water from within the excavation and more or less retain the level of the groundwater outside the excavation at the same time. This method is of special importance in urban excavations where a normal lowering of the groundwater would lead to settlement of adjoining buildings. A one-sided drainage wall under construction can be seen in Fig. 6.

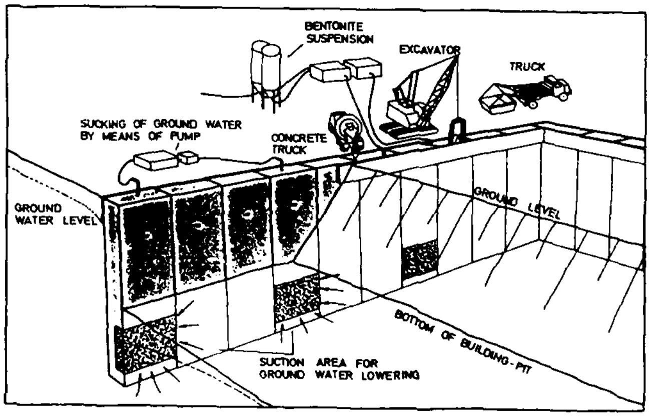
BENTONITE SUSPENSION
EXCAVATOR
TRUCK
SUCKING OF GROUND WATER BY MEANS OF PUMP
CONCRETE TRUCK
GROUND WATER LEVEL
GROUND LEVEL
BOTTOM OF BUILDING-PIT
SUCTION AREA FOR GROUND WATER LOWERING

Fig 6: Construction of one-sided Drainage Wall

The one-sided drainage wall is not only advantageous for the excavation itself but also for environmental reasons. For example, the natural groundwater stream underneath a rubbish tip or a contaminated waste depot can be cut off by using a one-sided drainage wall and an artificial stream underneath the tip can be forced. In this way the groundwater which has been soiled by seepage water can be drawn off and a filter plant can be put into use.

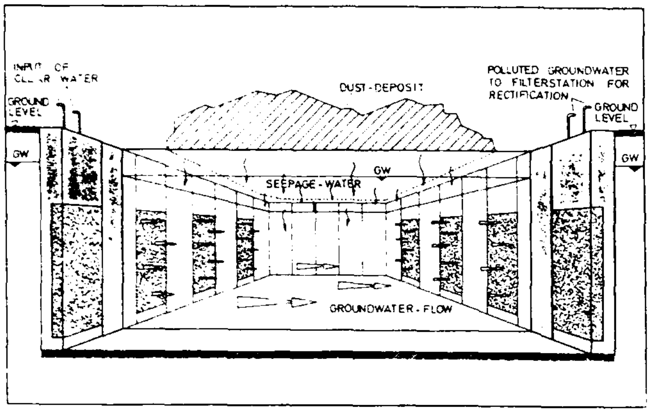
INPUT OF CLEAR WATER
GROUND LEVEL
GW
DUST-DEPOSIT
POLLUTED GROUNDWATER TO FILTERSTATION FOR RECTIFICATION
GROUND LEVEL
GW
SEEPAGE-WATER
GW
GROUNDWATER-FLOW

Fig 7: Drainage Wall under Rubbish Tip

The one-sided drainage wall can also be used to an advantage in the case of a tank store as shown in Fig. 8. Should a leak occur in the tank, then soiled groundwater can be pumped off and purification carried out.

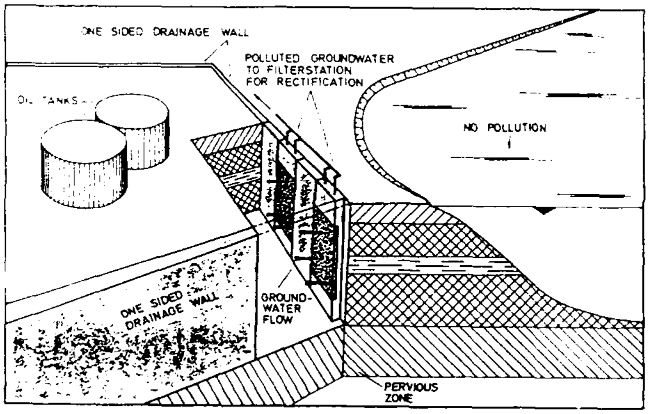
ONE SIDED DRAINAGE WALL
POLLUTED GROUNDWATER TO FILTERSTATION FOR RECTIFICATION
OIL TANKS
NO POLLUTION
ONE SIDED DRAINAGE WALL
GROUND-WATER FLOW
PERVIOUS ZONE

Fig 8: Drainage Walling as a Security Mesure with Oil Tanks

The different uses of a drainage wall have certainly not yet been fully recognized. Future use will bring a number of improvements in technical realazation and production. It is, therefore, especially important for the future that engineers and contracting firms work closely together during production and calculation of drainage walls.

SITUATION OF BUILDING SITE

Drainage walling was first put into use at an excavation for the construction of a power plant in Wald in Salzburg. The excavation support was intended for the first building phase at a depth of approx. 12 metres. The soil to be supported in this area consists mainly of boulder detritius on a slope consisting of all particle sizes ranging from silt and stones to large stones. The subsoil is densely compacted. which means relatively good characteristic values for the dimensioning of the excavation support. Fig. 9 shows a cross-section through the excavation giving the most important data.

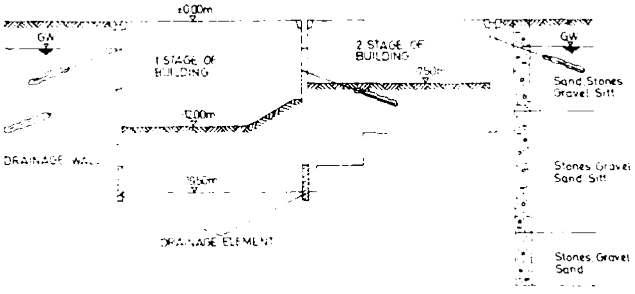
±0.00m
GW
1 STAGE OF BUILDING
2 STAGE OF BUILDING
-7.50m
-12.00m
DRAINAGE WALL
-19.50m
DRAINAGE ELEMENT
GW
Sand Stones Gravel Silt
Stones Gravel Sand Silt
Stones Gravel Sand

Fig 9: Cross-section through an excavation

An additional lowering of the groundwater was necessary for excavating since the groundwater level was measured at approx. 1.5 metres below the upper edge of the excavation. As far as permeability was concerned, the subsoil in and unter the bottom of the excavation was relatively dense. From the beginning it was not necessary to reckon with high groundwater flow as the permeability was k = 0.0005cm/sec. For this reason it was decided to arrange four drainage elements in the chosen diaphragm wall in order to relieve tension on the subsoil from groundwater pressure in the excavating phase

Because of the detailed soil stratum water pressure of between 2 and 5 l/sec. maximum was calculated for the entire excavation. The water should then be drawn off from the subsoil via the four drainage elements. A pumping off of the water found in the excavation area was also provided for during excavation via additional open predrainage. The entire excavation should then be kept dry by using the four built-in drainage elements.

CONSTRUCTION OF THE DRAINAGE WALL

As mentioned above a diaphragm wall was intended from the beginning as excavation support. The difference between this and drainage walling lies merely in the integrating of the drainage element into an element of the diaphragm wall. Few extra construction steps were necessary in addition to the construction of a normal diaphragm wall to construct this drainage element which was arranged in all four cases at a depth of between 17.5 and 20.5 metres. Drainage piping was inserted into every one of the four elements as shown in Fig. 10. The drainage piping consisted of a 4 metre long filter pipe with a solid pipe above. The filter element was thus only placed within the area of the drainage element.

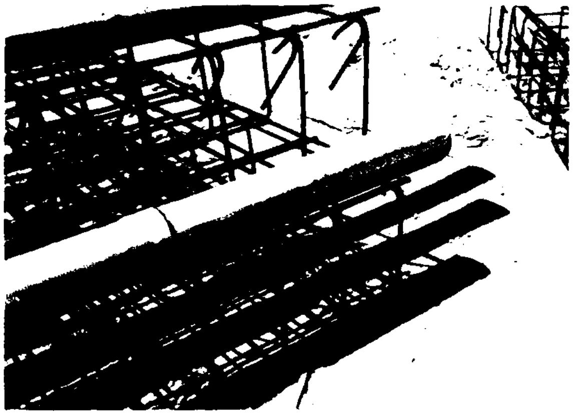

Fig 10: Drainage Pipe and Reinforcement for the Diaphragm Wall

Fig. 11 shows the drainage wall element before concreting. As can be seen from the diagram two concreting pipes were used to obtain a constant pouring level for the filter concrete. Filter concrete was then inserted via the concrete pipe. The filter concrete consisted of filter gravel 4-32 mm and 250 kilos of cement per cubic metre of precast-concrete. An additive was included before concreting which fixed the cement glue to the gravel grains.

Fig 11: Preparation for Concreting for a Drainage Element

After bringing the filter concrete into the desired position the remaining part was concreted with normal precast-concrete as with ordinary diaphragm walls. After hardening over a period of approx. ten days, the bentonite suspension was removed from the drainage pipe and the layer of precast-concrete. This was achieved by extremely powerful shocking (powerful, rapid pressure changes) as when sand is removed from a well. Immersion pumps were then built into the drainage piping and pumping off of the groundwater could commence. In Fig. 12 we can see water pumped off using a drainage element. The pumped off water amounts corresponded approx. to those previously calculated theoretically for reducing the groundwater level.

Fig 12: Pumped off Groundwater using a Drainage Element

CONCLUSION

This paper aims to introduce a new type of excavation support to specialists. Taking present solutions as a starting point, this excavation support represents an extension whereby groundwater lowering can be carried out within the excavation support for the first time.

It was possible to use this new type of drainage support for an excavation used for a power plant. The pumped off amounts of water corresponded exactly with these which had been previously theoretically calculated.

It is hoped that this new possibility of groundwater lowering will be used in future in structures and in connection with excavation support. It is also hoped that the economic viability will thus be proved.

REFERENCES

Wietek, P. (1982), "Drainagepfahl und Drainagewand", Tiefbau-Ingenieurbau-Straßenbau, Heft 10

Wietek, P. (1983), "Drainageverbau", Tiefbau- Ingenieurbau-Straßenbau, Heft 5, Jahrgang 1983

Proceedings: Second International Conference on Case Histories in Geotechnical Engineering, June 1-5, 1988, St. Louis, Mo., Paper No. 5.04

Compaction and Chemical Grouting for Drain Tunnels in Phoenix

T.J. Lyman
Vice President, Brierley & Lyman, Inc., Arizona

M.J. Robison
Sr. Geotechnical Engineer, Brierley & Lyman, Inc., Arizona

D.S. Lance
Deputy District Engineer, Arizona Department of Transportation, Arizona

SYNOPSIS: Ground runs during mining of the Papago Freeway Drain Tunnels posed significant potential risk to utilities, street pavement, and buildings located above and adjacent to one of the three tunnel alignments. Ground response to the larger ground runs resulted in open chimneys and settlement of the ground surface of up to several feet. Modifications to the tunneling machine included addition of poling plates and breasting boards. Further modification to the tunneling method included use of compaction grouting in conjunction with mining for the entire length of one tunnel alignment, and use of chemical grouting to prestabilize the ground surrounding the tunnel opening in areas of high risk utilities and in areas where subsurface conditions suggested that running ground would be encountered during mining.

This paper presents a summary of the ground behavior with and without the compaction and chemical grouting and describes the grouting methods.

INTRODUCTION

This paper presents a case history of soft ground tunneling for the Papago Freeway Drainage Tunnels in Phoenix, Arizona constructed from the spring of 1984 through mid-1987. Specific objectives are to describe the subsurface conditions, tunneling methods, the ground behavior in response to tunneling. The case history includes a description of compaction and chemical grouting methods that were used in conjunction with tunnel excavation over part of the project. The grouting allowed for rapid tunnel excavation while minimizing surface settlements above the tunnel thereby reducing the risk to overlying utilities, pavements, streets and adjacent buildings.

The Papago Freeway Drainage Tunnels are part of a drainage system for the highway expansion and improvements undertaken by the Arizona Department of Transportation in the greater Phoenix metropolitan area. Large sections of the highway system are depressed below existing ground elevations to minimize visual and noise impacts. The tunnels are part of an inverted siphon designed to carry surface runoff from intense rainfall. The system carries water to the Salt River and provides drainage for an approximately 40 square mile area. Tunnels were selected because of the disruption that cut and cover construction of alternatives would have caused to the utilities, traffic, streets, and adjacent business located along or near the system alignment.

The entire highway project is managed by the Arizona Department of Transportation (ADOT). The drainage tunnels were designed by Howard Needles Tammen and Bergendoff (HNTB), construction was done by the consortium of Shank-Artukovich-Ohbayashi (S-A-O) and construction management was provided by CRS Sirrine (CRSS).

The tunnel project consisted of three tunnels, the North, East and West Tunnels, shown in Figure 1. The total length of the three tunnels is approximately 6.5 miles making this one of the largest soft-ground tunneling projects in North America. The North Tunnel runs east and west, is 6,700 ft long, has a finished diameter of 14 ft and an excavated diameter of 17 ft. The East and West Tunnels run north and south, are 13,550 and 13,970 ft long respectively, have a finished diameter of 21 ft, and an excavated diameter of 25 ft. The North Tunnel slopes gently toward the center where it intersects with the West Tunnel. The East and West Tunnels slope gently from north to south. The depth of cover of the North Tunnel was between 25 and 40 ft. The depth of cover at the East and West Tunnels was between 33 and 45 ft. Each tunnel is connected to a concrete inlet or outlet structure at each end

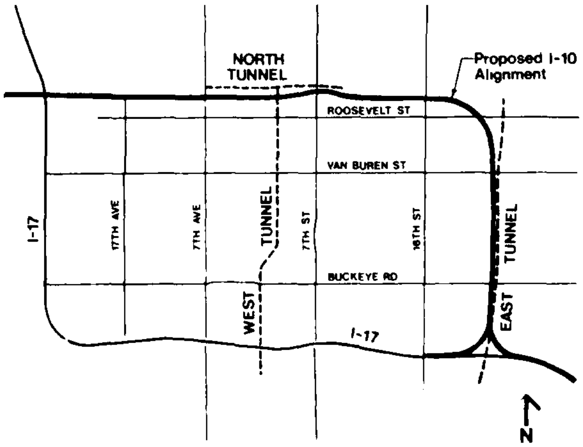

FIGURE 1 - PROJECT LOCATION

and to a number of concrete drop structures located along each tunnel alignment. The North Tunnel alignment includes several 800 to 1,000 ft radius curves and the West Tunnel is straight except for a reverse curve section with two 1,200 ft radius curves.

The remainder of this discussion deals exclusively with construction of the East and West Tunnels. No further considerations of the North Tunnel are included.

The tunnels were excavated using a shield with digger manufactured by Hitachi Zosen of Japan. The East Tunnel was driven first and was excavated from south to north. Upon completion of East Tunnel excavation, the shield was disassembled, moved and reassembled at the south shaft of the West Tunnel, and used to excavate the West Tunnel.

Almost immediately after the shield mined out of the south shaft at the East Tunnel, a series of large ground runs occurred. The runs resulted in large surface settlements of the order of 6 to 10 ft and in large open chimneys to the ground surface.

As a result of these ground runs, modifications were made to the shield. These modifications included addition of poling plates to the upper half of the shield and breasting boards inside the upper half of the shield. The poling plates were installed from springline to springline and were capable of extending 8 ft beyond the leading edge of the shield. The breasting boards extended from upper quarter arch to quarter arch and could also be extended beyond the face of the shield.

After these shield modifications, excavation of the East Tunnel was completed within a period of eight months. During excavation however, approximately five percent of the tunnel experienced significant ground runs. Individual losses associated with these runs ranged from approximately 5 to 250 cubic yards. These ground losses occurred at the top of the face and above the forward edge of the shield. Surface settlement above the tunnel of up to 10 ft and open chimneys from 3 to 10 ft in maximum dimension resulted from these ground losses.

The surface expression of the ground losses had little impact at the East Tunnel which was constructed primarily below cleared highway right-of-way. However, surface settlement and open chimneys at the West Tunnel represented unacceptable risk to overlying utilities, streets, pavements and adjacent buildings. Consequently, further modifications were added to the tunneling method including 1) compaction grouting to redensify soils loosened by ground losses during mining and to fill voids from ground runs at the face, and 2) chemical grouting to prestabilize the ground surrounding the tunnel.

Compaction grouting was used in conjunction with excavation of the entire length of the West Tunnel. The grouting was integrated with the tunnel excavation and implemented continuously and concurrently with tunnel excavation. Chemical grouting was used in section totalling 1,441 ft of the 13,970 ft of the West Tunnel. A total of 41 ft of this chemical grouting was done to prestabilize the ground, to reduce risk to utilities or adjacent buildings, and 1,400 ft was done in areas where subsurface information indicated a high probability that running ground conditions would be encountered during tunnel excavation.

GEOLOGIC INVESTIGATIONS AND SUBSURFACE CONDITIONS

The subsurface conditions along the tunnel alignments were determined by existing rotary borings, percussion borings, and four large diameter borings (LDB's) and by additional LDB's and tunnel face-mapping performed during tunnel construction. These methods allowed for a characterization of ground conditions during design and bidding for project construction, and for further detailed characterization of subsurface conditions during construction.

Rotary borings are difficult to advance to depth because of the coarse alluvial deposits characteristic of the area. Therefore, no subsurface data at tunnel depth were available from these borings. Percussion borings using reverse-circulation drills were used to investigate subsurface conditions. These borings advanced well through the coarse alluvial deposits but the results were difficult to interpret as little or no sampling is typically conducted with this boring method. Careful observation of the diesel hammer blows required to advance these borings in one foot increments allowed for some useful interpretation of subsurface conditions. Several existing borings drilled using this method extended to tunnel invert and were used to interpret subsurface conditions within the tunnel horizon. A total of four LDB's were drilled at selected locations along the tunnel alignments during site inspections for prospective contractors. Down-hole inspections were available for representatives of each prospective contractor from within casing lowered to full depth of each boring.

A total of 27 LDB's were drilled on 500-ft centers along the West Tunnel alignment and five LDB's were drilled at selected locations along the East Tunnel alignment. These borings consisted of drilling three foot diameter holes to the elevation of tunnel springline, setting a steel casing to the bottom of each boring, and inspecting and sampling from tunnel springline to a point 10-ft above tunnel crown.

The five LDB's drilled at the East Tunnel were located to determine, 1) the conditions at areas where significant ground losses had occurred in the completed portion of the tunnel and 2) to determine ground conditions at an instrumented section of the tunnel. The 27 LDB's at the West Tunnel were drilled to determine detailed subsurface conditions along that alignment and to compare and contrast those conditions to those encountered at the East Tunnel.

The project lies within the Basin and Range physiographic province. The Phoenix Basin consists of between 500 and 1,200 ft of variably consolidated alluvial sediments. These sediments are generally coarse and are the result of rapid infilling of the broad graben-like basin characteristic of the Basin and Range.

The general subsurface conditions at the East and West Tunnels are as follows:

UNIT A - Thin surface layer of fine-grained soils consisting of silty-clay, sandy clay, silt and silty sand with small amounts of gravel. Variable lime cementation (caliche) varying from strong to none was observed. The thickness of this unit varied from 0 to 20 ft with an average thickness of 15 ft.

UNIT B - Transitional sand and gravel underlying Unit A and consisting primarily of relatively clean sands, sand and gravel mixtures, and occasional silty sands. This unit occurred erratically and was not present in many areas.

UNIT C - Lower sand, gravel, cobble (SGC) underlying Unit B. All tunnels were constructed in this unit. This unit was distinguished from Unit B soils by the presence of cobbles. The unit includes highly variable alluvial deposits of gravelly coarse to fine sand, silty gravel, gravelly cobbles, sandy gravel, cobbly gravel, sand, some clay lenses, and sand and cobbles. All deposits vary in fines content from clean to trace silt or clay. Manganese oxide staining was often observed on loose gravel lenses. Variable cementation was observed in some SGC caused by calcium carbonate and clay-fraction. Clay content generally increased below a depth of 35 ft.

Groundwater generally occurred below the tunnel invert except in the southern third of the East and West Tunnel alignments. Groundwater levels followed regional trends and occurred approximately 10-ft above tunnel crown at the south shaft of the East and West Tunnels. Groundwater levels were drawn-down to below tunnel invert using several large diameter, high-capacity wells.

GROUND RESPONSE TO TUNNELING WITHOUT GROUTING

Ground response to tunneling without grouting was measured at 14 sites located along the East Tunnel alignment. Thirteen of the 14 sites were located in "normal" ground, where significant ground losses did not occur. One site was located in a zone of "running" ground. No grouting was used during construction of this tunnel.

In general, instrumentation at the East Tunnel consisted of subsurface settlement markers, multiple point borehole extensometers, and surface settlement points. In addition, inclinometers were installed at three of the fourteen instrumentation sites to measure horizontal movements.

Figure 2 presents the general ground behavior based on data from the 13 "normal" ground sites. This figure illustrates typical instrument locations relative to the excavated tunnel, the zone of influence of the tunnel, and the Generalized Surface Settlement Profile.

Vertical soil displacements shown by this figure for "normal" ground conditions indicate that displacements occur within a limited zone directly above the tunnel, that displacement is generally symmetrical about the tunnel centerline, and that maximum displacement varies from 12 inches at a point 5 ft above tunnel crown to 1.2 inches at ground surface. Most significant vertical displacements (greater than one-quarter inch) are confined within a zone equal to the width of the tunnel and all movement occurs within a zone extending from tunnel springline upward to ground surface at an angle of 20 degrees from vertical.

Instrumentation data from the only running ground site and observation of settlement troughs and open chimneys indicated the settlement was limited to the width of the tunnel, the larger depression or chimneys were generally symmetrical about tunnel centerline, and the width of the open chimneys was less in the uppermost fine grained soils than in the SGC below.

When large settlement troughs or open chimneys developed to the ground surface, the following conditions were noted:

1. Loose soils above the shield ran into the heading creating a void above and slightly behind the leading edge of the shield.
2. The loss of soil from above the shield occurred when uniform or gap graded, loose native soils were encountered at the tunnel crown.
3. In general, soils ahead of the tunnel face did not run into the face.
4. Significant settlement troughs or open chimneys developed at the ground surface and generally occurred within minutes or up to several hours after the run in the tunnel heading.
5. The surface width of settlement troughs and/or open chimneys is less than the width of the tunnel.
6. The size of the surface settlement trough and/or open chimney is directly related to the total volume of running ground removed from within the tunnel.
7. The surface expression of open chimneys or surface settlement troughs is symmetrical about tunnel centerline.

Settlement was studied as a function of distance from the instrument to the tunnel face· this indicated that the total settlement can be divided into four categories based on

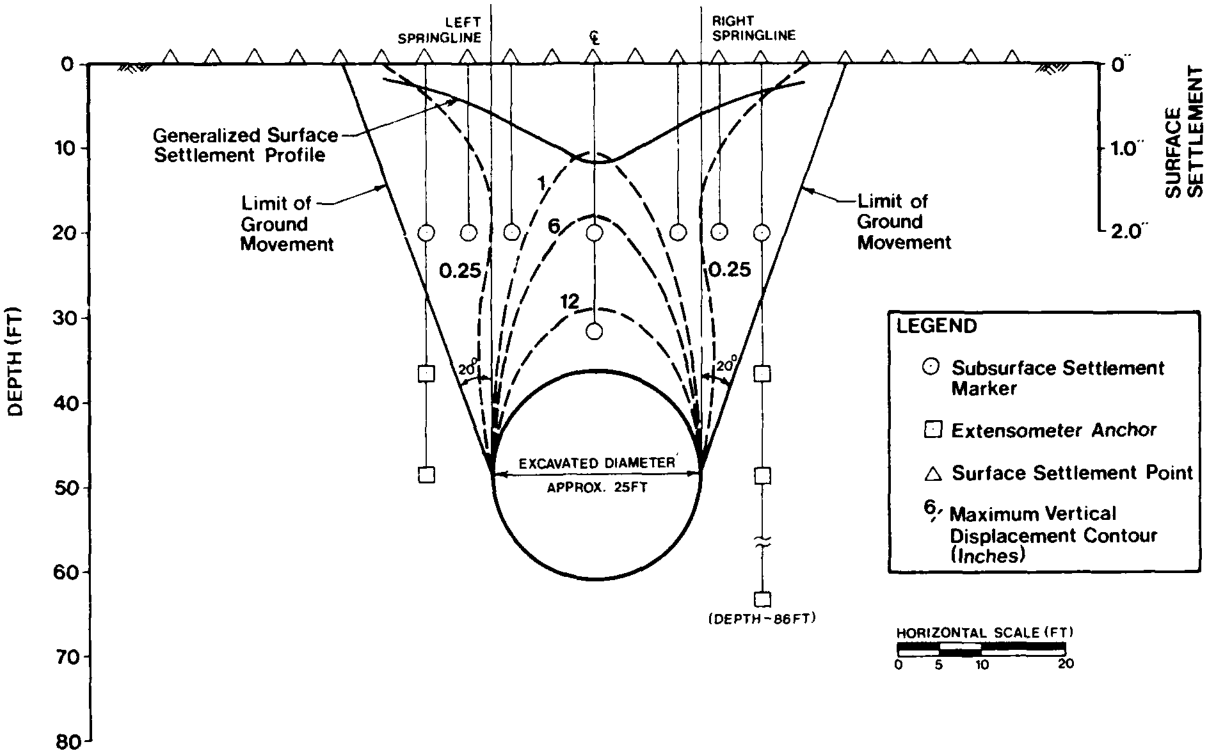
LEFT SPRINGLINE
℄
RIGHT SPRINGLINE
0
10
20
30
40
50
60
70
80
DEPTH (FT)
Generalized Surface Settlement Profile
Limit of Ground Movement
Limit of Ground Movement
1
6
12
0.25
0.25
20°
20°
EXCAVATED DIAMETER APPROX. 25FT
(DEPTH~86FT)
0"
1.0"
2.0"
SURFACE SETTLEMENT
LEGEND
○ Subsurface Settlement Marker
☐ Extensometer Anchor
△ Surface Settlement Point
6⁄ Maximum Vertical Displacement Contour (Inches)
HORIZONTAL SCALE (FT)
0
5
10
20

FIGURE 2 - EAST TUNNEL - GENERALIZED GROUND BEHAVIOR PROFILE

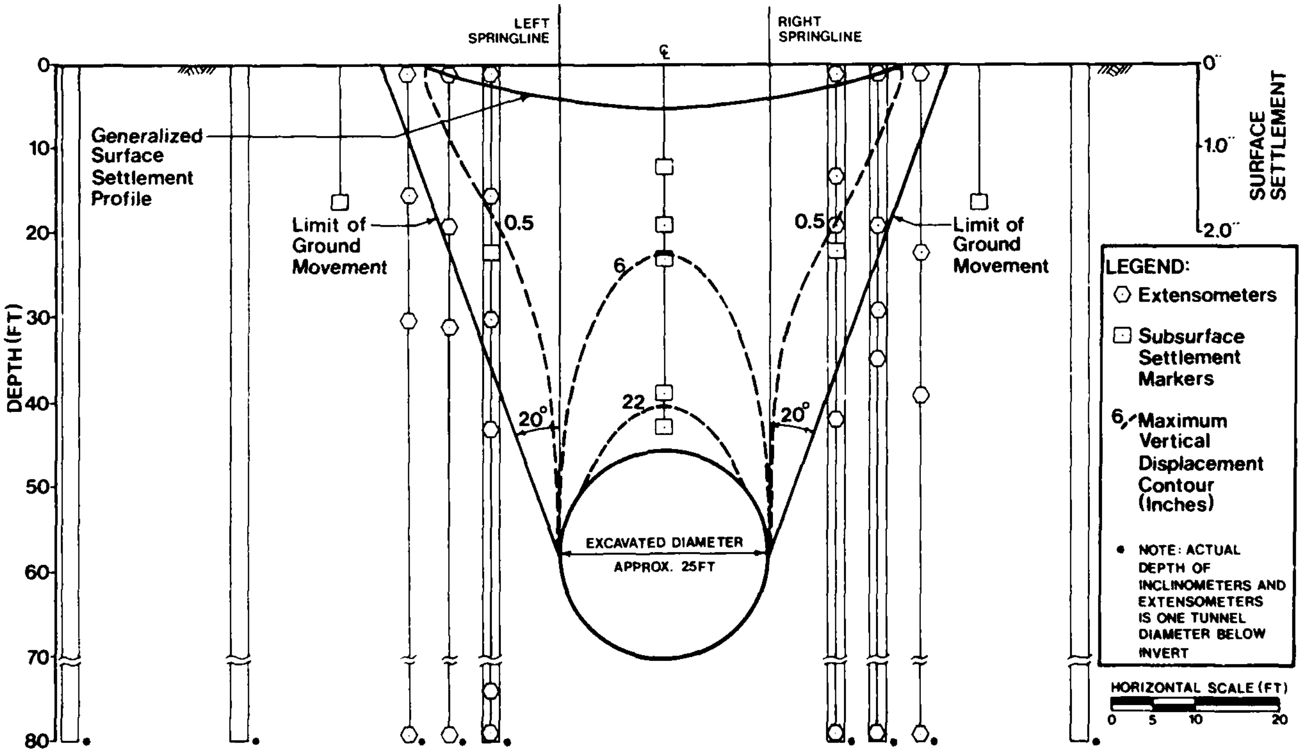
LEFT SPRINGLINE
℄
RIGHT SPRINGLINE
0
10
20
30
40
50
60
70
80
DEPTH (FT)
Generalized Surface Settlement Profile
Limit of Ground Movement
Limit of Ground Movement
0.5
0.5
6
22
20°
20°
EXCAVATED DIAMETER APPROX. 25FT
0"
1.0"
2.0"
SURFACE SETTLEMENT
LEGEND:
⬡ Extensometers
☐ Subsurface Settlement Markers
6⁄ Maximum Vertical Displacement Contour (Inches)
• NOTE: ACTUAL DEPTH OF INCLINOMETERS AND EXTENSOMETERS IS ONE TUNNEL DIAMETER BELOW INVERT
HORIZONTAL SCALE (FT)
0
5
10
20

FIGURE 3 - WEST TUNNEL - GENERALIZED GROUND BEHAVIOR PROFILE

loss mechanisms within the tunnel, as follows:

- Face losses - losses ahead of the tunnel face.
- Shield losses - losses above the shield.
- Tail losses - losses as soils load the initial lining.
- Long term losses - losses due to compaction of the ground after mining is complete.

The majority of settlement is tail loss and some settlement also occurs as shield loss. Settlements from both face loss, and long term loss are negligible.

Based upon field observations, ground losses in general occurred vertically above and behind the shield, and did not extend laterally beyond springline nor ahead into the face.

GROUND MODIFICATION PROGRAM

Introduction

Potential ground losses during mining presented considerable risk to utilities, streets, pavements, and possibly buildings located above and adjacent to the West Tunnel alignment. Based upon an analysis of this risk, a ground modification program consisting of compaction grouting and chemical grouting was recommended for mining the West Tunnel. This section describes the risk analysis and presents details of the ground modification program.

Risk Analysis

The risk analysis was made with considerable input from the owner. The utilities, buildings and streets/pavements in the vicinity of the tunnel were grouped into four levels of risk, designated Low, Moderate, High or Very High, depending upon the anticipated consequences of settlement, ground loss or failure of the utility.

The Low Risk category included:

1. Service gas lines, less than 2 psi.
2. Small water lines, less than 12 inch diameter.
3. Small sanitary sewer lines, less than 18 inch diameter.
4. Small storm sewers, less than 30 inch diameter.
5. Service electric lines.
6. Low volume telephone lines.
7. Irrigation lines for residences.
8. Residential buildings and one story commercial buildings.
9. Streets/pavements with low traffic volumes.
10. Sidewalks.

The Moderate Risk category included:

1. Irrigation lines for farms.
2. Two to three story commercial buildings.

The High Risk category included:

1. Gas distribution lines, 2 to 60 psi.
2. Large water lines, 12 to 30 inch diameter.
3. Sanitary sewers, 18 to 30 inch diameter.
4. Large storm sewers, equal to or greater than 30 inch diameter.
5. Electric distribution lines, 7 to 12.5 KV.
6. Multi-story commercial buildings and municipal buildings.
7. Buildings containing machinery sensitive to settlement.
8. Streets/pavements with high traffic volumes.
9. Interstate highways.
10. Railroad lines.

The Very High Risk category was assigned to utilities which, if severed, could result in loss of life or significant repair costs. The Very High Risk category included:

1. High pressure gas lines, greater than 60 psi.
2. Large water lines, greater than 30 inch diameter.
3. Large sanitary sewers, greater than 30 inch diameter.
4. High voltage electric lines, 230 KV.
5. High volume telephone lines.

In order to determine the risk areas along the West Tunnel alignment, the utilities, buildings and streets/ pavements located within the tunneling zone of influence were reviewed. Utility locations were determined through a review of the Utility Plans and Profiles in the Contract Drawings and through discussions with utility companies. Eight Very High Risk utilities were identified, as follows:

1. One 66 inch sanitary sewer
2. Two 30 inch sanitary sewers
3. One 10 inch, 300 psi gas line
4. One 230 KV electric line
5. One 42 inch water line
6. One Transcontinental Light Guide (fiber-optic) telecommunication cable
7. One jet fuel line.

Engineering recommendations were presented to minimize the potential for significant ground surface settlement, ground loss and open chimneys to the ground surface based upon the soil conditions, the anticipated ground behavior, and the level of risk assigned to utilities, buildings and streets/pavements within the tunneling zone of influence. These recommendations are summarized in the following paragraphs.

Good tunneling techniques were recommended during mining. Good tunneling techniques included control of the shield alignment to minimize the pitch, yaw and roll of the machine. Good tunneling also included careful excavation techniques to minimize ground losses during tunneling.

To supplement good tunneling techniques, a ground modification program was recommended consisting of compaction grouting and chemical grouting. Compaction grouting was recommended along the entire length of the West Tunnel to minimize ground settlement by re-densifying loosened soil behind the tail shield and replacing lost ground during tunneling.

Chemical grouting was recommended at specific areas of active, very high risk utilities crossing the West Tunnel. Chemical grouting was considered necessary to minimize risk to these active utilities by pre-stabilizing the soil around the tunnel below these utilities. Pre-stabilizing the soil further reduced settlement potential by reducing the likelihood of significant ground losses at utility locations. Where a very high risk utility could be deactivated during tunnel mining below, chemical grouting was not recommended.

Compaction Grouting

Purpose

Compaction grouting consisted of injecting low slump soil or soil/cement grout to form a bulb above the crown of the tunnel. Compaction grouting was used along the entire length of the West Tunnel, due to the risk associated with settlement of moderate to high-traffic volume streets, and overlying buildings. The purpose of the compaction grouting program was to minimize potential ground settlement by densifying loosened soil behind the tail shield, and replacing ground lost at the tunnel face.

Procedures

Compaction grouting was accomplished by drilling holes from ground surface at 10 ft centers along tunnel centerline to within approximately 10 ft above the tunnel crown, and inserting a 3 inch pipe into each hole. After the tail shield passed, a low slump, soil grout was injected to form a bulb, which densified any loosened soil above the initial precast lining. During grout injection, lining deflection was monitored and used as a criterion for termination of grouting. When large ground runs occurred, the grouting operation was moved directly over the shield, cement was added to the soil grout, and a large volume of grout was injected to rapidly replace lost ground.

During compaction grouting, voice communication was maintained between the grout technician on the surface and the tunnel technician underground. Constant communication was necessary to monitor grouting progress, to stop grout injection when temporary lining deflections reached tolerable limits, and to adjust grouting operations to events in the tunnel.

Initially the grout consisted of well graded silty sand having at least 20 percent but not more than 50 percent passing the U.S. NO. 200 sieve, flyash, and water with a slump of approximately 2 inches. Due to the availability of a native sandy silt, vandalism of the flyash silo, and problems with sand blockage during grouting, the grout mix was changed to silt with greater than 50 percent passing the U.S. No. 200 sieve, and use of flyash was discontinued.

When grouting in areas of ground losses in excess of 100 cubic yards, one bag of portland cement was added to every 2 yards of grout mix to strengthen the grout and reduce the chances of grout flowing into the heading around the face of the shield.

Compaction grouting was performed using two shifts in conjunction with mining of the West Tunnel. The grout was pumped until one of the following grouting termination criteria was met:

1. For initial precast concrete lining segments located approximately 40 ft behind the tail of the shield that were loose (i.e., tolerate 0.08 feet of deflection and still meet final lining specifications), grout was injected until 0.08 feet of deflection occurred in one of the segments. The grout pipe was raised several feet and pumped again until additional deflection occurred.
2. For initial precast concrete lining segments located approximately 40 ft behind the tail of the shield that were tight (i.e., tolerate less than 0.08 feet of deflection and still meet final lining specifications), grout was injected until all tolerable deflection occurred. The grout pipe was raised several feet and pumped again until additional deflection occurred.
3. Segments and/or keyblocks below the active grout pipe began to crack.
4. Heave of the ground or street surface near the active grout pipe was observed.
5. Pressures in excess of 500 psi developed at the top of the active grout pipe.

When large ground runs occurred, the tunnel technician radioed the grout technician to report the volume of the ground run and its location. The grout crew responded by halting normal grouting behind the shield, identifying the grout pipe closest to the run, and moving the grouting equipment forward. Pumping of compaction grout continued until one of the following grouting termination criteria was met:

1. Grout was observed at the face or tail of the shield.
2. Segments and/or keyblocks at the tail of the shield cracked.
3. Pumping pressure exceeded 300 psi or back pressures exceed 150 psi.
4. Surface heave was observed.
5. 100 percent of the reported ground run volume was injected.

Once a run had been filled, a normal grouting sequence resumed.

On several occasions, a ground run surfaced, which resulted in collapse of the street pavement. When this occurred the void was backfilled with either pea gravel, aggregate base course (ABC), tunnel muck or a combination of these materials.

Results

Compaction grouting of the sand-gravel-cobble alluvium encountered was effective. Compaction grouting densified the loosened soils over the crown of the tunnel, minimized surface settlements, and rapidly backfilled voids, thereby minimizing tunnel excavation downtime.

Compaction grouting during normal tunneling generally resulted in placement of between 0.1 and 0.5 cubic yards of compaction grout per linear foot of tunnel. During normal tunneling and normal ground behavior, the compaction grout densified the soil above the tunnel resulting in deflection of the precast concrete segment. In most cases, segment deflection resulted in grout termination under normal tunneling conditions.

When compaction grout was used to fill large voids from ground losses due to running ground, grout volume placed was between 50 and 90 percent of the ground loss. In most cases ground heave occurred prior to deflection of the precast concrete segments and determined when grout injection was stopped.

The total cost for the compaction grouting, including hole drilling, grouting, backfilling and placing a cold patch at street level was $2,191,680 or about $160 per linear foot of tunnel. Additional project costs not included in this figure were costs for tunnel crew standby time during grouting, repair of the asphalt surface, and repair of utilities damaged during grout hole drilling.

Chemical Grouting

Purpose

The chemical grouting program consisted of the injection of sodium silicate grout using "flood grouting" methods prior to tunnel excavation. Chemical grouting was used in areas of active, very high risk utilities and in areas of anticipated running ground. The purpose of the chemical grout was to strengthen the alluvial soils by increasing their cohesion, in order to minimize the potential for large ground losses and associated surface settlement.

Chemical grouting to stabilize the loose, cohesionless soil conditions was accomplished through the injection of a sodium silicate solution from the ground surface prior to tunnel excavation through the particular zone of concern. The ground was saturated with the low viscosity solution, which set-up to form a stiff gelatinous solid. This gel provided cohesive strength to the loose sand, gravel, and cobble soils.

Procedure

In general, chemical grouting was performed using the grout pipes installed for compaction grouting. In some instances, additional holes were drilled. For combination compaction and chemical grouting, the grout pipes consisted of 3 inch I.D., schedule 40, open end steel pipe. The annulus at the upper 10 ft of the pipe was backfilled with portland cement grout to provide a seal. Additional chemical grout holes were cased with 1-1/2 inch I.D., schedule 40, closed end PVC pipe with four 1/4 inch perforations on 1 ft centers along the lower 10 to 15 ft of pipe. The pipes were drilled to within 5 to 7 ft of tunnel crown, and the annulus backfilled with pea gravel to cover perforations and then filled to the street surface with portland cement grout.

Liquid sodium silicate was clear Grade 40, with a silica to soda ratio of 3.22 and a specific gravity of 41.5 degrees Baume. Initially, the grout mixture consisted of a 30 percent sodium silicate solution. This was modified to 40 percent to reduce grout set time. A number of different activators were used including glyceryl diacetate and sodium bicarbonate. When glyceryl diacetate was used as the activator, calcium chloride was added as an accelerator. With each chemical grout mixture, a series of tests were performed, to identify the mixture which would give the desired 30 to 45 minute gel time.

Chemical grouting was performed using flood grouting procedures and batch mixing methods. Grouting was accomplished by flooding three holes simultaneously with predetermined quantities of chemical grout. Flow rates and pressure to each hole was adjusted by valves until injection was approximately equal. Generally the following grouting procedure was used:

- o A concentrated activator solution (50 lbs of sodium bicarbonate in 100 gallons of water) was injected into each hole to cause quick gel of subsequent grout in areas of open gravels.
- o 1,000 gallons of sodium bicarbonate/sodium silicate grout was injected into each hole as quickly as possible to saturate the soil mass in the target zone.
- o 100 gallons of concentrated activator was injected into each hole.
- o Another 1,000 gallons of grout was injected into each hole.
- o A final 200 gallons of concentrated activator was injected into each hole.

Grout samples were taken periodically during the above process to check gel time of the grout. The process was crude in terms of mixing and delivering grout solutions to the ground and relied on alternately flooding a target zone in the ground with sodium silicate/sodium bicarbonate grout and accelerator. The process allowed for rapid placement of chemical grout in the general area desired.

Results

Chemical grouting of the sand-gravel-cobble alluvium by injecting sodium silicate grouts was effective. The grouting process was continually adapted as information was obtained after the tunnel was mined through each grouted section. The design objective, strengthening the alluvial soils to prevent large ground runs into the tunnel heading and unacceptable surface subsidence, was accomplished.

No ground losses were observed at any of the sewer crossings that received treatment with chemical grout. A total of 1,400 linear feet of West Tunnel alignment was grouted in 11 zones that had been identified as having potentially unstable, cohesionless ground and high probability of ground runs. Significant ground runs, greater than 5 cubic yards lost during one "push" of the shield, occurred in only two of these 11 zones. The first area was at Second Street and Polk Street, in front of the Arizona Republic and Gazette Building. At this location, a total of 55 cubic yards of ground was lost over a 50 ft interval within a chemically grouted zone. Extensive, very porous, gravel lenses existed in this area. The second area was between Filmore and Pierce on Second Street. At this location, a total of approximately 500 cubic yards of ground were lost over a 30 ft interval within a chemically grouted zone. Ground conditions within this zone included a 3 to 4 ft thick lens of dry, loose sand at the tunnel crown. Tunnel progress was halted, additional holes were drilled in front of the excavated face and more chemical grout was injected. Upon resumption of tunneling, the sand lens was stable and was excavated in large cemented chunks. No large losses of ground occurred after tunneling was resumed following injection of the additional chemical grout.

Small ground runs, less than 5 cubic yards lost during one "push" of the shield, occurred over approximately one third of the chemical grout zones. Grout pipes terminated 10 ft above the tunnel crown and these losses appeared to consist of material located between the tunnel crown and the grouted soil.

In many instances along the West Tunnel alignment ground runs occurred immediately before and/or after a chemical grout zone. This suggested that the ground was loose and prone to running, that the grout prevented runs, and that the ground would probably have run if the chemical grouting had not been performed.

The effectiveness of grouting to permeate the soil within the tunnel face was tested as the tunnel was mined using phenolphthalein to indicate the presence of high pH grout in the soil. This testing revealed that the soils at the tunnel face were generally well saturated with grout solution where grout pipes extended below tunnel crown. No grout saturation was found within the tunnel face in areas where grouting was done through compaction grout holes which terminated 10 ft above tunnel crown. These observations suggest that the chemical grout did effectively saturate a soil zone near the base of the grout pipes.

The total cost for chemical grouting was $410,000 or about $250 per foot of tunnel that was grouted. In most cases, chemical grouting was done through existing holes drilled and cased for compaction grouting, therefore, this cost does not include the cost of drilling grout holes from the ground surface.

GROUND RESPONSE TO TUNNELING WITH GROUTING

Ground response to tunneling with grouting was measured at 14 sites along the West Tunnel alignment. All of the sites were located in "normal" ground and no ground runs occurred within 20 ft of any instruments along the West Tunnel alignment.

In general, instrumentation used at the West Tunnel was simpler than that used at the East Tunnel. West Tunnel instrumentation had two purposes, to determine ground movements in soils surrounding the tunnel during mining, and to provide documentation of ground behavior in the vicinity of critical structures. Because of the magnitude of movements observed at the East Tunnel, subsurface settlement markers were primarily used to measure subsurface ground movements. Extensometers and inclinometers were generally used to provide information only at critical structures.

Based on the data obtained from the 14 sites a Generalized Ground Behavior Profile was developed as shown in Figure 3. This figure illustrates typical instrument locations relative to the tunnel excavation. The figure also contains approximate vertical displacement contours to illustrate the soil movements observed. Vertical soil displacements shown by this figure for "normal" ground conditions indicate that displacement occurs within a limited zone directly above the tunnel, that displacement is generally symmetrical about the tunnel centerline, and that the magnitude of maximum displacement ranges from 22 inches, 5 ft above tunnel centerline to less than one-half inch at ground surface. No measurable horizontal movements were indicated by inclinometers installed between 20 and 60 ft from tunnel centerline.

Comparing the vertical ground movements at the West Tunnel with those observed in normal ground at the East Tunnel indicates the following:

- The magnitude of displacement at 5 ft above tunnel crown is almost one foot larger at the West Tunnel, yet displacement at 20 to 25 ft above tunnel crown and at ground surface is generally less at the West Tunnel. Larger movement close to tunnel crown resulted from larger teeth installed on the shield and from other tunneling procedures. Compaction grouting limited the upward limit of these larger displacements and reduced the amount of vertical displacement observed at ground surface.

- The limit of vertical ground displacements is defined by a line extending from tunnel springline upwards to intersect the ground surface at an angle of 20 degrees from vertical.

- No horizontal soil movements were observed in any instrument within 8.5 ft of tunnel springline. This was consistent at both the East and West Tunnels.

Several areas of the West Tunnel experienced significant ground runs during excavation. These runs involved between 20 and 500 yards of material. Generally, ground runs were backfilled with compaction grout before surface subsidence or open chimneys developed. In a few areas at the northern end of the tunnel and at the beginning of the reverse curve, ground losses in the tunnel resulted in surface settlement and/or development of open chimneys. As at the East Tunnel, these were limited to the width of the tunnel.

SUMMARY AND CONCLUSIONS

A total of approximately 27,000 ft of 25 ft diameter tunnels were excavated at depths of about 45 ft in coarse alluvial sand-gravel-cobble deposits in downtown Phoenix.

Ground movements resulting from running ground conditions encountered during mining posed unacceptable risk of damage to utilities and streets overlying the West Tunnel alignment. In order to reduce these risks, chemical and compaction grouting techniques were amended to the contract provisions during construction and were utilized during mining of the West Tunnel. Chemical grouting was performed prior to mining, by placing sodium silicate/sodium bicarbonate grout using flood grouting methods to place grout at or above the tunnel crown. Chemical grout was used to prestabilize the ground at the location of two active utilities which could not be effectively shut-off or re-routed if they were disrupted by ground movements around the tunnel. Chemical grouting was also used at areas of the alignment where subsurface information suggested that running ground would occur during tunnel excavation. The chemical grouting was successfully applied and no significant ground losses occurred within areas treated by chemical grouting prior to tunnel excavation.

Compaction grouting was performed concurrently with tunnel excavation along the entire length of the West Tunnel. Grout was injected along tunnel centerline using soil or soil/cement grout to redensify soil loosened around the tunnel during mining or to fill voids above the tunnel shield immediately after ground runs occurred at the tunnel face. Compaction grouting successfully reduced soil movements around the tunnel and minimized potential damage to utilities, street pavement and nearby buildings.

Comparison of generalized ground movements above the East Tunnel where no grouting was performed and the West Tunnel where both chemical grouting and compaction grouting was performed shows that:

- Several large ground runs occurred along the West Tunnel with little or no corresponding near-surface ground movement. Ground runs of similar magnitude at the East Tunnel resulted in large surface settlement or open chimneys.

- The average surface settlement at tunnel centerline along the West Tunnel under "normal" ground conditions was 0.75 inches and 1.20 inches at the East Tunnel. Both settlement profiles were symmetrical about the tunnel centerline. No surface settlement was generally observed beyond 20 to 25 ft from tunnel centerline.

Generally, the grouting performed in conjunction with excavation of the West Tunnel was effective in limiting near surface ground movements. This effectively minimized the risk of damage to utilities, street pavement, and nearby building throughout most of the West Tunnel alignment.

ACKNOWLEDGEMENTS

The authors wish to thank the Arizona Department of Transportation for permission to publish this paper and for use of information and many reports developed during project construction.

Proceedings: Second International Conference on Case Histories in Geotechnical Engineering, June 1-5, 1988, St. Louis, Mo., Paper No. 5.05

Soil Improvement Using Dynamic Compaction for Bristol Resource Recovery Facility

Richard P. Kummerle
Principal, Tectonic Engineering Consultants, USA

Jean C. Dumas
President, Geopac Inc., Canada

SYNOPSIS: The paper discusses in detail the specifics of the dynamic compaction procedures implemented at the Bristol Resource Recovery Facility, and correlations developed between the two verification test methods, the advantages and disadvantages of these methods and how the verification testing aided in modifying the original approach, while still maintaining a difficult schedule. The paper further discusses the estimated bearing capacities and settlements calculated from each test method. Finally, the paper provides recommendations for specifying, performing and verifying dynamic compaction based on the experience and data obtained from this project.

INTRODUCTION

The Bristol Resource Recovery Facility is a 650 ton per day refuse to energy plant, located in Bristol, Connecticut. The site is an irregular shaped area located between an industrial park and the City of Bristol landfill. The turn key project team consisted of Ogden Martin Systems, the Owner/Operator, Burns and Roe Enterprises, the Architect/Engineer, and J. A. Jones, the Contractor.

Preliminary geotechnical data provided by the City of Bristol with the bid package recommended that H-Piles driven to rock should be used for establishing the design and construct costs during the bidding phase.

The initial site investigation revealed essentially a two-soil layer system overlying rock. In general, the upper soils were loose to medium sands, which were underlain by a dense to very dense silty fine sand with gravel. The depth to rock varied from 45 to 55 feet below existing grade.

Because of the apparent very dense nature and the presence of gravel and boulders in the lower dense silty sand stratum, there was concern regarding the ability to consistently advance the H-Piles to the top of rock. However, it was necessary to bid the project based on the recommendations contained to the request for proposal.

After being awarded the project, the design team performed a detailed review of the existing subsurface data. This review resulted in the recommendation that dynamic compaction would be the most prudent and cost-effective method of foundation support for the main plant structures; and that a detailed subsurface investigation be performed to confirm this recommendation. This investigation confirmed that dynamic compaction could be implemented at the site permitting the use of shallow foundations and a $400,000 savings.

SITE AND SUBSURFACE CONDITIONS

Prior to construction, the ground surface sloped from elevation 214 at the northern limit to about elevation 205 at the southern limit of the site where a marshy area was present.

The detailed subsurface investigation consisted of thirty-five borings performed using Standard Penetration Testing at 5-foot intervals and at many locations continuously. These borings were performed to delineate a detailed subsurface profile, confirm the viability of dynamic compaction, and thereby establish the dynamic compaction guidelines.

The subsurface profiles from grade to a depth of 18 to 30 ft is a coarse to fine sand, with varying amounts of coarse to fine gravel, and trace amounts of silt. Typically, SPT values ranged from 6 to 15 blows/foot. Underlying this stratum to the top of rock is a very distinct layer of fine sand with some silt and fine to coarse gravel. Silt content ranged from 20 to 30% at depths of 20 to 30 feet. Typically, SPT values ranged from 50 to more than 100 blows/foot. The contact between the loose soils and the very compact soils was found to be very sharp. It occurred at a depth of 18 feet at the northern limit, and 30 feet at the southern limit.

A medium dense to dense horizon between 2 to 8 feet thick also occurred through most of the site within a depth interval from 2 to 10 feet below existing grade.

These overburden soils extend to depth of 44 to 56 feet at which an arkosic sandstone was encountered.

The groundwater table varied from elevation 207 to 205 MSL.

DYNAMIC COMPACTION CRITERIA

The specification developed for this project required a Contractor experienced in dynamic compaction. The Contractor was required to provide a lump sum price for compaction of approximately 150,000 square feet and performing verification testing to document that the process had achieved the performance requirements. The requirements the dynamic compaction was required to achieve were:

1) For isolated footings founded at elevation 212, and allowable bearing capacity of not less than 5 kips per square foot.
2) The allowable total settlement of structures not exceeding three-quarters of an inch.
3) The allowable differential settlement of structures not to exceed one-half inch between structural columns spaced 25 feet apart.

For calculation of bearing capacity and settlement at a maximum column load of 800 kips, a maximum footing width of 12 feet was to be used. This approach, in our opinion, is more viable than the approach of specifying a degree of soil improvement, such as specifying a minimum N value after compaction. In most cases, the real purpose is to treat the soils in order to obtain adequate bearing capacity and settlement characteristics.

The verification testing program specified was quite extensive, and required the Contractor to use two different test methods. Allowing for two methods of testing is advantageous in difficult applications. Insitu testing methods all have limitations, and when used exclusively, can send the wrong signals. One of the required methods was Standard Penetration Testing, with the alternate methods of Pressuremeter Testing or Cone Penetrometer Testing. Pressuremeter Testing was used and, therefore, Geopac was required to perform precompaction PMT at the locations of the initial SPT testing, to establish precompaction correlations between the test methods. After completion of the dynamic compaction work, correlations again were developed between the two methods during initial testing; and thereafter, verification testing was performed by the Contractor selection option, in this case PMT.

Dynamic compaction results in vibrations resulting from the impact; therefore the Contractor was required to monitor vibration levels to ensure vibrations would not endanger existing structures. The Contractor was required to maintain vibration levels less than 2-in/sec at the closest property boundary.

DYNAMIC COMPACTION PROGRAM

Prior to performing the dynamic compaction, all organic material and vegetation was excavated from the site. In order to ensure that the dynamic compaction was performed with the groundwater table at least 5 feet below the working surface, granular fill was placed on the site. This fill was not compacted during placement because of the use of dynamic compaction to compact the underlying naturally occurring soils.

Compaction commenced with a 13.5-ton octogonal weight falling from 60 to 70 feet in the northern part of the site where the thickness of loose soils was the least. At the onset, it became evident that considerable amount of compactive energy was required to punch through the dense layer near surface. To insure maximum energy penetration, first the number of blows was increased and, second, the weight was increased to 15 tons for compaction south of the pit area.

Finally, when it became amply evident, with the results of the final verification testing that the ironing pass was not required over most of the site, it was decided that compaction at depth would be further enhanced by transferring the compactive energy planned for that pass to the initial high energy passes. The ironing pass was nevertheless maintained in the marshy areas at the south end.

The total amount of compactive energy applied was 14.6 x 10^9 ft-lb compared to 13.9 x 10^9 ft-lb as originally planned.

The lifting plant was a Manitowoc 3900 crawler crane equipped with a 100-foot boom.

The typical grid patterns for the high energy phases as well as the distribution of compactive energy are shown on Drawing Figure 1.

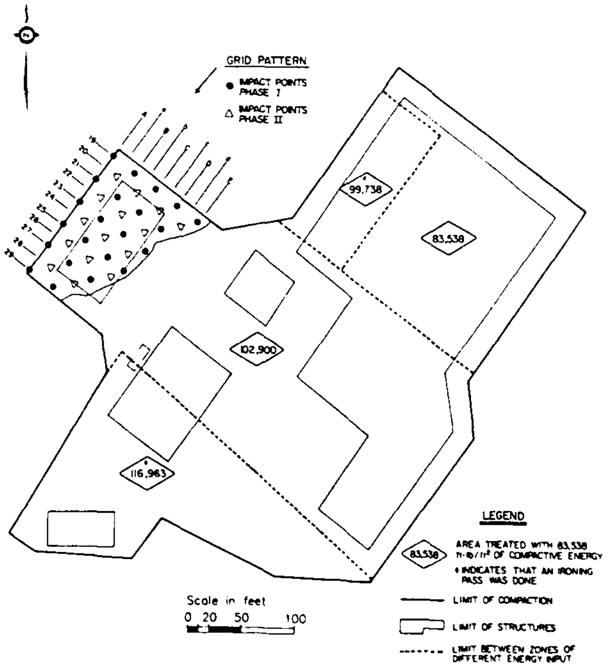

Fig. 1 Compaction Program

The area compacted by Geopac amounted to 141,900 square feet. This included a 20-foot zone beyond the imprint of all the structures.

Geopac undertook the preliminary pre-compaction testing with the pressuremeter on October 7 and commenced its dynamic compaction work on October 11, 1985.

Except for a pass of ironing at the south end on November 11, dynamic compaction was all done by November 6.

Final verification testing began October 23 and was completed November 18.

VERIFICATION TESTING

Pressuremeter Testing

A total of 26 pressuremeter tests at 5 locations before treatment, and 128 tests at 20 locations following treatment.

The tests before compaction were done next to SPT boreholes BP-4, BR-10, BR-14, BR-18 and BR-26 so as to allow a comparison between pressuremeter and SPT values.

A truck-mounted drill rig and Menard pressuremeter apparatus was employed with tests carried inside a calibrated slotted AW casing. Location of boreholes is shown on Drawing Figure 2.

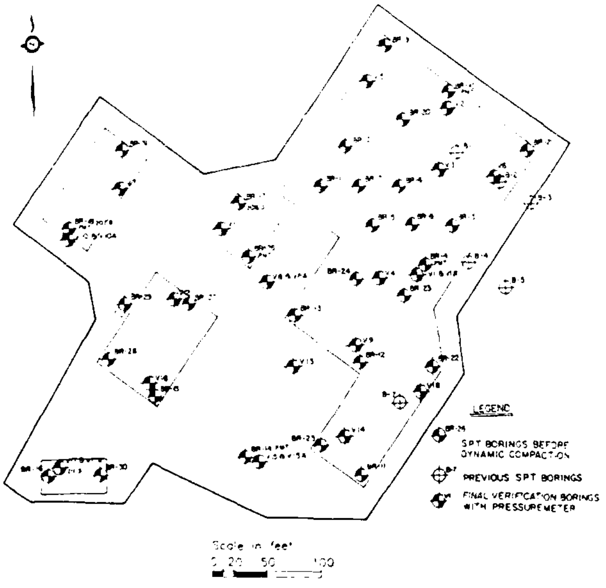
LEGEND
SPT BORINGS BEFORE DYNAMIC COMPACTION
PREVIOUS SPT BORINGS
FINAL VERIFICATION BORINGS WITH PRESSUREMETER
Scale in feet
0 20 50 100

Fig. 2 Verification Testing Locations

As a method of foundation engineering, the pressuremeter has a number of advantages, one of which is that it measures deformation properties of the soil in addition to a rupture or limit resistance. The test models the way in which actual foundations behave, which is particularly true with respect to spread footings where the maximum or limit resistance of the ground as measured by the pressuremeter is very close to the ultimate capacity of the footing.

A particularly interesting aspect of pressuremeter testing is that the quality of the test can be judged from the experimental curve and that, even in the case of lower quality tests, the results can usually be partially, if not completely, exploited.

At Bristol, examination of the experimental curves shows that the overall quality of testing was excellent. Of the 128 pressuremeter tests performed following dynamic compaction, only 16 or 12.5 per cent had to be rejected. Another 13 tests or 10 per cent of the total had deficiencies which did not prevent their use for settlement characteristics.

With very few exceptions, these deficiencies were encountered at a depth of 24 feet or greater where stresses increase due to foundation loads are less than 15 per cent. Their impact on measurement of the settlement characteristics of the foundation soils are therefore minimal (settlement calculation for a 12 foot square footing using the formula developed by Schmertmann (1970) does not take into account the characteristics of soils below 24 feet).

Nevertheless, these occurrences were investigated by additional SPT and pressuremeter testing. In essence, the problems encountered in testing were in most cases related to remolding of the borehole walls which occurred as a result of sand flowing inside the slotted tube during its expansion. This, as shown by sampling, occurred in fine silty sand layers or clean sand layers overlaid by silty horizons, where a condition of slight excess pore pressure, probably worsened by the driving of the slotted tube, still persisted. Where the reason for the lower values could not be ascertained, the existence of a weak layer was assumed for the calculation of the theoretical settlement, as shown later.

SPT Testing

Five of the 20 locations tested by pressuremeter following treatment were also tested by the Standard Penetration Test method using the same drill rig and same crew.

SPT tests were also performed at other locations to verify pressuremeter tests.

Correlation between pressuremeter and SPT values

Correlation between post-compaction N values, the SPT resistance to penetration corrected for overburden pressure, and p_1, the pressuremeter pressuremeter limit, is given in Figure 3. Correlation between E and P_1 is given in Figure 4.

Figure 3 shows $N:P_1$ ratios generally varying between 1 and 3. The best-fit curve indicates a ratio of 2.5 near surface, which should correspond to coarser sands, and of 1.5 at a depth of 24 feet which would correspond to siltier sands. This variation in our view fits very well the soil stratigraphy at the Bristol site. For sands only Baguelin, Jezequel and

Shields Ref. 2 recommend a N:P_l ratio of 2. On a project where more than 400 SPT borings and 400 static cone soundings were performed Dames & Moore Ref. 3 showed N:P_l ratios for sand to vary between 2 and 3.

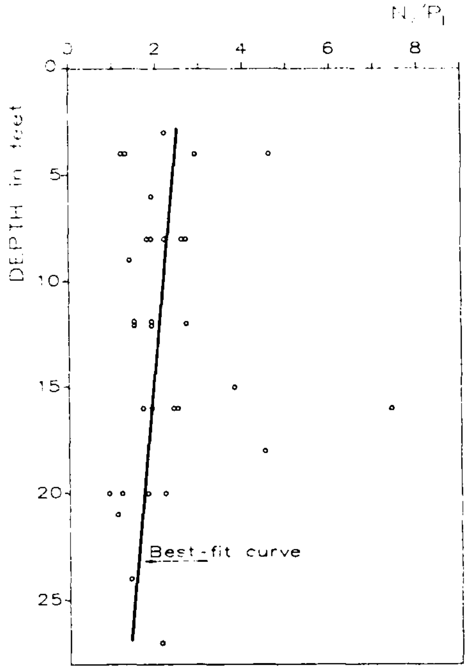

Fig. 3 Correlation Between Post-Compaction N Values Corrected For Overburden Pressure and Pressuremeter Limit

The E:P_l ratio for normally consolidated sand has generally been found to be 10. For silty sand, this may decrease to 6. High E:P_l ratio for sand indicate some degree of overconsolidation. It will be seen from Figure 4 that the highest E:P_l ratios are found at a depth of 8 feet. Which corresponds to the level of maximum improvement. Again, the lower E:P_l values below 15 feet probably reflect siltier conditions.

Evaluation of Enforced Settlement

Elevation surveys were carried out before each pass of energy input and an initial elevation was recorded for each point. Following each pass of the treatment a survey of the crater depth and crater diameter were taken and the data recorded on a site plan.

Table 1 gives the average energy input for each pass of compaction and the corresponding induced settlement calculated from the volume of the craters.

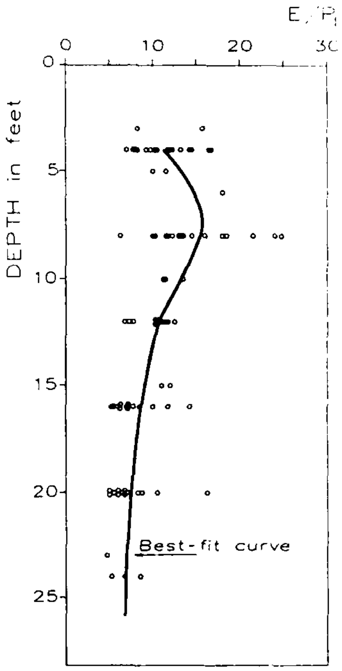

Fig. 4 E:P_l Ratios Versus Depth

TABLE 1. Induced Settlement VS Energy Input

Pass No.	Average Energy Input ft-lb/ft^2	Average Induced Settlement ft
1	61 058	0.53
2	36 635	0.31
Ironing	3 084	0.08
		0.92

Vibration Monitoring

A total of 528 measurements were taken on the northern border of the site and 17 additional measurements on the building situated at the corner of Crystal Pond Place and Horizon Drive which, at a distance of 400 feet, was the building closest to the operations.

The highest peak particle velocity measured at the northern border of the site was 0.146 inch per second. The highest peak particle velocity measured on the building at the corner of Crystal Pond Place and Horizon Drive was 0.0241 inch per second. This is many times lower than the accepted safe limit of 2.0 inch per second and cannot possibly constitute any risk of damage.

SOIL CHARACTERISTICS AFTER TREATMENT

Allowable Bearing Capacity

The calculation of bearing capacity is made according to the rules stated by Menard (1960) and using the results of pressuremeter tests performed after dynamic compaction.

Allowable bearing capacity is given by the relation:

$$q_a = \frac{k p_{le}}{3} \qquad (1)$$

where q_a = is the allowable bearing capacity
p_{le} = is the geometric mean of limit pressure values measured over a depth range equal to 1.5 times the width of the footing
k = is a shape factor based on the size and embedment of the footing.

Based on this equation, an allowable bearing in excess of 5 tsf is available.

Settlement

Post-construction settlements were calculated using the pressuremeter values measured in boreholes V-1 to V-20 and SPT values measured in boreholes V-1A, V-8A, V-10A, V-15A and V-17A.

Using pressuremeter data in accordance with Menard (1960), the settlement under finite footings is given by the relation:

$$S = \frac{1.33\ p\ Ro}{3E_B}\left(\frac{\lambda'\ R}{Ro}\right)^{\alpha} + \frac{\alpha\ p\lambda''R}{4.5\ E_A}$$

S = is settlement
p = is bearing stress
E_A, E_B = is consolidation and distortion modulus
R = is half the footing width in cm
Ro = is a reference width equal to 30 cm
λ', λ'' = are shape factors for footings
α = is a rheological factor

Where low pressuremeter results were encountered and could not be clearly attributed to a defect in the method of testing, the presence of a weak layer was assumed and settlement was computed according to the relation:

$$S = S_1 + S_2 \qquad (3)$$

Where S_1 is the settlement which is calculated from the general relation (2) and which would occur if the soft layer was the same as the surrounding soil, and where S_2 is the additional settlement due to the consolidation of the soft layer, which is computed from the relation:

$$S_2 = \alpha_{(z)}\ Z \left(\frac{1}{\bar{E}_z} - \frac{1}{\bar{E}_m}\right) q^*(z) \qquad (4)$$

Where

α_z = the rheological factor at depth z
Z = is the thickness of the soft layer
E = is the modulus of the soft layer
E^{z}_{m} = is the modulus of the surrounding soil
$q^*(z)$ = is the pressure increase calculated on the assumption that the soil is an elastic homogeneous half-space

In case of the 16 rejected tests previously mentioned, settlement calculations were performed using pressuremeter values derived from SPT tests performed at corresponding elevations, using the correlations shown in Figures 3 and 4.

Using SPT data, the settlement under finite footings has been calculated with the developed by Schmertmann (1970) formula.

$$S = 0.5\ S_1 \qquad (5)$$

$$S_1 = C1\ C2 \Delta p \sum_{1}^{n} \frac{I_z}{x\ q_c} \Delta z \qquad (6)$$

S1 = settlement calculated by Schmertmann's formula for first loading cases
C1 = correction factor for depth of embedment
C2 = correction factor for secondary creep settlement
Δp = net foundation pressure increase at bottom of footing
I_z = strain influence factor at centerheight of each sublayer
n = number of qc sublayers
Δz = thickness of sublayers
x = factor by which to multiply CPT qc to obtain equivalent Young's modulus
qc = resistance to static cone penetration

Table 2 summarizes the results of settlement calculations at the location of each post-compaction pressuremeter and SPT boreholes for a 12 foot square footing bearing a total load of 800 kips.

The most important feature of Table 2 is that calculations using the results of two different methods of control provide clear confirmation that the requirements of the specifications with regard to total and differential settlement were met.

Total settlement calculated by the Schmertmann formula is higher than that calculated with the pressuremeter method, on the other hand, differential settlement is lower. Explanation for these differences could be attributed to:

1. The qc/N correlation factor for this site has not been established. A factor of 4 is used for this report but Robertson & Campenella (1983) have shown that for medium and coarse sand the factor could actually vary between 4.5 and 7.

2. A higher factor would in effect reduce the settlement calculated with the Schmertmann formula. With a factor of 6 for instance, the average calculated settlement would be the same as that calculated by the pressuremeter method.

3. Settlement calculation for a square footing using the Schmertmann formula ignores the soils at depths lower than two times the width of the footing. The pressuremeter method on the other hand accounts for soils down to a depth equal to 8 times the width of the footing. The fact that the Schmertmann formula ignores the weaker layer found below 24 feet may explain the lesser differential settlement.

Table 2. Calculated Settlement

Calculation Using Pressuremeter Values		Calculation using SPT Values	
Borehole No.	Settlement In	Borehole No.	Settlement In
V-1	0.20	V-1A	0.50
V-2	0.27		
V-3	0.21		
V-4	0.17		
V-5	0.17		
V-6	0.41		
V-7	0.30		
V-8	0.19	V-8A	0.49
V-9	0.22		
V-10	0.29	V-10A	0.39
V-11	0.54		
V-12	0.31		
V-13	0.30		
V-14	0.46		
V-15	0.31	V-15A	0.38
V-16	0.44		
V-17	0.27	V-17A	0.55
V-18	0.16		
V-19	0.36		
V-20	0.49		

Two more comments must be made about the calculated settlements given in Table 2.

The first comment is that the driving of the slotted tube into the soil causes a certain degree of disturbance which in effect tends to lower the modulus values. Using these values for calculation leads to a conservative evaluation of post-construction settlement.

The second comment concerns the fact that because of the demands of the construction schedule, verification testing had to be performed immediately following compaction. As a result, important time dependent strength gains may have been overlooked in the process. Mitchell and Solymar Ref. 7 have demonstrated that sands freshly densified by vibro-compaction, dynamic compaction and compaction by explosives may exhibit substantial stiffening and strength increase with times up to several months.

Ground Improvement Achieved

The induced settlement is the tangible proof that the treatment has achieved densification. Its importance depends on the efficiency of the compaction plan but also upon the nature of the soil and its initial degree of compactness. Experience has shown that for a natural soil it usually varies between 4 and 6 per cent of the thickness of the compressible soils.

Table 1 shows that the average enforced settlement resulting from the treatment at Bristol amounts to 0.92 feet. Since the average thickness of the loose soils (N 20) as determined from pre-compaction SPT boreholes, was 15.5 feet, the enforced settlement represents 5.9 per cent of the thickness of loose soils, which must be considered satisfactory for this site.

The comparison between pre and post-compaction test results shown in Figures 5 and 6 is evidence that the treatment achieved very substantial improvement down to elevation 182, or down to about the top of the compact layer.

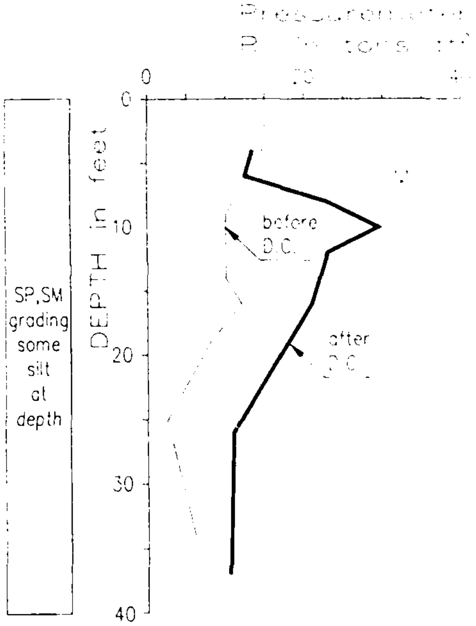

Fig. 5 Comparison of Average P_l Values Before and after treatment

CONCLUSIONS AND RECOMMENDATIONS

The ground improvement work was extensively monitored with Pressuremeter and Standard Penetration Test Testing performed before and after compaction. Both verification control methods demonstrates conclusively that the requirements of the specifications, in terms of allowable bearing capacity, maximum total settlement and maximum differential settlement were satisfied.

The induced settlement and the comparison of pre and post-compaction test results further demonstrate the improvement achieved.

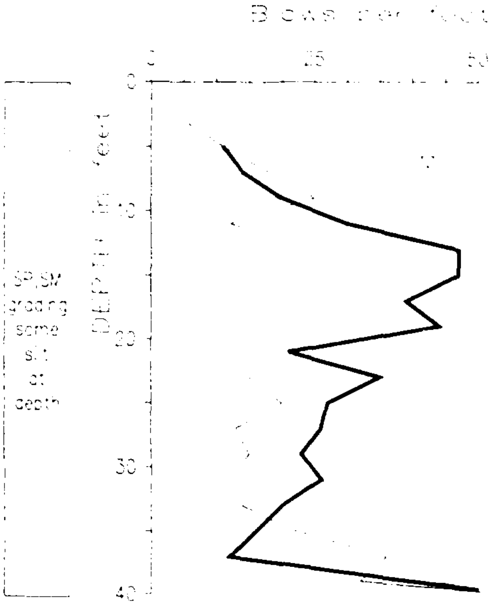

Fig. 6 Comparison of Average N Values Before and After Treatment

Extensive ground vibrations monitored showed that the operation was safe and did not constitute any risk for adjacent structures.

The plant is now in operation and all recorded settlement levels are well below the specification requirements.

The success of this project and the increasing number of failures at other sites where dynamic compaction has been employed reinforces the need for the engineer to specify meaningful compaction criteria, and to require extensive verification testing.

Dynamic compaction requirements should stipulate that the Contractor achieve certain performance goals, such as allowable bearing capacity and/or settlement. Furthermore, because of the limitations of various verification testing methods and the subsurface conditions, at least two methods should be used to ensure the Owner/Engineer that the contractor has obtained the specification requirements.

REFERENCES

Baquelin, F., Jezequel, J.F. and Shields, D.H. (1978), "The Pressuremeter and Foundation Engineering", D. Van Nostrand Company Inc., Publisher.

Dames & Moore (1978), "Geotechnical Consultancy Related to Dynamic Compaction Ashuganj Fertilizer Plant, Ashuganj Cornilla, Bengladesh", Vol. 1.

Menard, Louis (1975), "Interpretation and Application of Pressuremeter Test Results", General Notice D. 60. An, Soils Soils no. 26 1975.

Mitchell, James K. and Solymar, Zoltan V. (1984), "Time Dependent Strenght Gains in Freshly Deposited or Densified Sand", ASCE Journal of Geotechnical Engineering, Nov. 1984.

Robertson, P.K. and Campanella, R.G. (1983), "Interpretation of Cone Penetration Tests, Part I sand", Canadian Geotechnical Journal, Vol 20, 1983

Schmertmann, John H. (1970), "Settlement Calculation in Granular Soils", may 1970, Journal of Geotechnical Engineering.

Schmertmann, John H. (1978), "Guidelines for CPT Performance and Design", US Department of Transportation, FHWA-TS-78-209

Proceedings: Second International Conference on Case Histories in Geotechnical Engineering, June 1-5, 1988, St. Louis, Mo., Paper No. 5.06

Effects of Collapse Settlement of Fill on Reinforced Earth Walls

G.E. Blight
Professor of Construction Materials, University of the Witwatersrand,
Johannesburg, South Africa

SYNOPSIS

Two case histories illustrate the effects that collapse settlement of the fill forming a Reinforced Earth wall can have on the structure.

Pre-requisites for collapse settlement are inadequate compaction, compaction at too low a water content, or a combination of these. Collapse settlement occurs subsequently when the water content of the fill is increased by infiltration.

The effects of collapse settlement identified in this paper are:

(i) a temporary release of friction on the reinforcing strips with the result that the wall facing moves outwards; and

(ii) relative settlement between the fill and the wall facing with the result that the reinforcing strips become inclined to the horizontal and their tension increases.

EFFECTS OF COLLAPSE SETTLEMENT OF FILL ON STRIP FRICTION

A loose fill has an unstable structure that is maintained by capillary stresses. In clayey fills the structure will consist of an assemblage of clods that behaves like a granular mass. Each clod maintains its integrity by means of strength imparted by capillary stresses acting within it. The void space between clods is large relative to the void space within each clod, i.e. individual clods are compact relative to the overall soil. In sand fills the unstable structure will be maintained by capillary stresses between individual grains or groups of grains.

When water later infiltrates the fill, the capillary stresses are released. Clods lose strength and compact into the surrounding voids and sand grain assemblages break down. The net effect is a settlement of the fill that has been defined as collapse settlement. The amount of collapse settlement that occurs depends on the quantity of water infiltrating and the time-settlement relationship depends on the distribution of the infiltration with time. The transient effect of the settlement on friction between the reinforcing strips and the soil will be illustrated by a case history:

A reinforced earth wall was built at Koingnaas on the west coast of South Africa. The climate is desert with an average annual precipitation of 90 mm and an annual pan evaporation of 1950mm. The wall supports a fill of uniform fine dune sand which was placed without control on moisture content and with little compaction. Shortly after a high pressure sea water hose had burst on the platform at the top of the wall, the wall abruptly moved forward a distance of 150mm to 200mm and then again came to rest.

The sand was uniform in grading, having a d_{10} size of 0.1mm and a ratio $d_{60}/d_{10} = 3.2$. An investigation in the laboratory showed that the angle of shearing resistance of the sand was high ($\phi' = 43°$) although the angle of friction of the loose dry sand on the surfaces of the smooth galvanized steel reinforcing strips was surprisingly low ($\delta = 13°$). When the sand was inundated in the shear box, the angle of friction increased to 19°.

A re-analysis of the stability of the wall showed that for $\delta = 13°$ the factor of safety against pull-out of the strips from the fill would be as low as 1.1 at a distance of 2.5m below the top of the wall, increasing to 1.5 at 4.5m and to close to 2.0 at 6m, the base of the wall. Because the effect of wetting was ultimately to increase the factor of safety against a pull-out of the strips, it appeared that some transient phenomenon had occurred, presumably as the wetting front, arising from the burst hose, passed through the fill.

The phenomenon was modeled in the laboratory by loading a dry sand-to-galvanized steel surface in the shear box, to a factor of safety of 2 against shear failure. The sand was then inundated and the movement of the sand and the shear load were recorded on a UV recorder. A typical result of such a test is shown in Figure 1.

AB in the figure represents the stage during which the dry sand was loaded to a factor of safety of about 2 (actual $\delta = 6.1°$). At B the loading was stopped and the sand inundated. At C it appears that the water reached the sand-galvanized steel interface and the shear stress reduced (C to D) to an angle of friction of less than 1°. Simultaneously the sand settled, although most

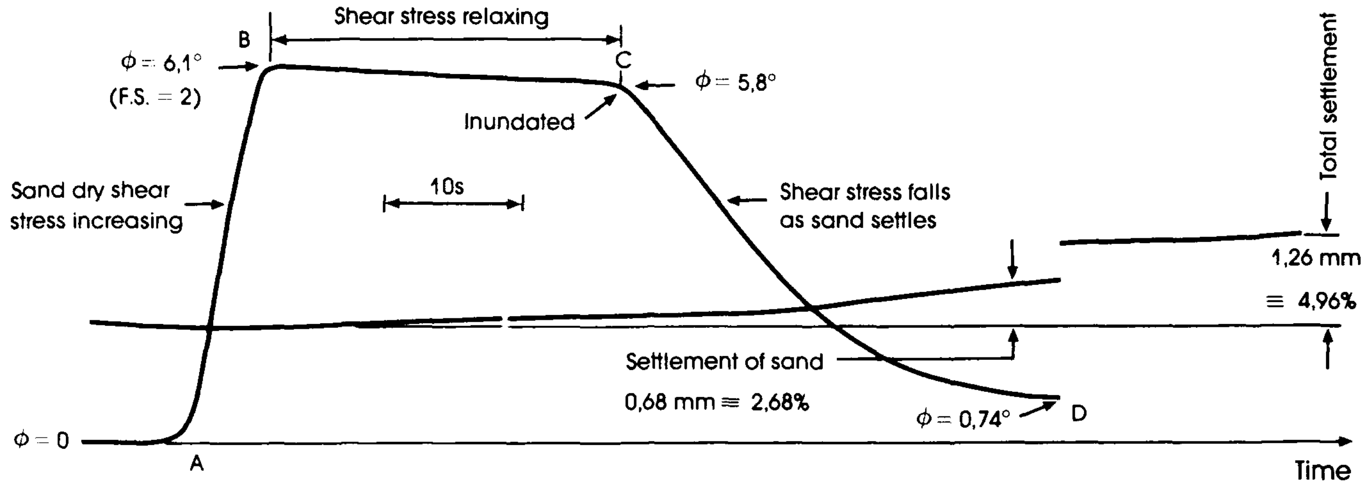

Figure 1: Variation of shear load at sand-steel interface when dry sand is inundated.

of the settlement occurred after the frictional resistance at the sand-steel interface had been lost.

It can be inferred from Figure 1 that as the wetting front moved downwards through the fill, successive layers of reinforcing strips temporarily lost their shear resistance and allowed the pressure in the fill to move the wall facing forward. As the wetting front passed, shear resistance was re-established, possibly at a greater angle of friction, and the wall facing re-stabilized.

The effect of saturating the fill on strip friction has previously been investigated by the Reinforced Earth Company. Although they found that saturation reduces the frictional coefficient between a dune sand and a steel reinforcing strip, the transient phenomenon illustrated in Figure 1 appears not to have been identified at that time.

A possible secondary effect of water entry is that water pressure may develop in the fill, thus reducing its shear strength and precipitating a rotational shear failure. In the Koingnaas case, this did not occur because the quantity of water was limited and the fill was relatively free-draining.

EFFECT OF COLLAPSE SETTLEMENT OF FILL ON STRIP TENSION

The collapse settlement of a poorly compacted fill has its effect on strip tension by dragging the reinforcing strips down relative to the wall facing. If the latter consists of concrete panels, the facing is stiff in a vertical plane, relative to the fill, once the 20mm joints between the concrete elements have closed up. This closure corresponds to 1.3% of post construction settlement of the fill.

There is also the possible secondary effect of water pressure to consider, if sufficient water enters the fill and if the fill is not free-draining.

The effect of collapse settlement on strip tension is a complex geometrical one, which depends on:

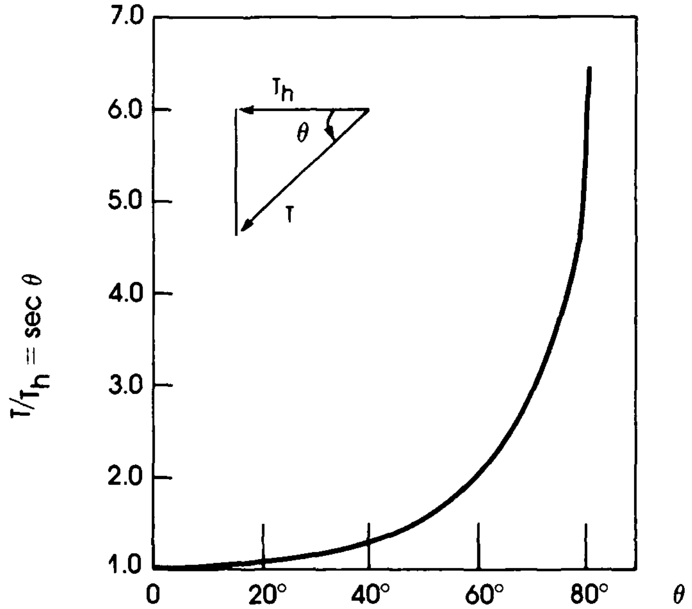

Figure 2: Strip tension T required to exert horizontal component T_h for various inclinations θ.

- the relative settlement of the reinforcing strip to the tie strip taking into account the ability of the cladding to compress in the vertical plane
- the movement of the reinforcing strip required to mobilise the friction in the loose fill along the length of the strip.

As a result of the relative settlement, the strips become inclined adjacent to the wall. For an inclined strip to exert a horizontal tension component T_h, the tension in the strip has to be (see Figure 2)

$$T = T_h \sec \theta$$

As shown by Figure 2, T increases rapidly with increasing θ. If the design factor of safety against yield of a reinforcing strip is 1.6, a strip inclination of 51° will cause yield. If the factor of safety against tensile fracture is 2, an inclination of 60° will result in fracture.

The occurrence of this effect of fill settlement will also be illustrated by a case history:

At the Grootgeluk Coal Mine in the north-west Transvaal province of South Africa, the two arms of a U-shaped crusher complex were constructed of Reinforced Earth walls.

The walls support the earth ramps that provide access for 250T haul trucks to tip their loads from the base of the U into a primary crusher. Eight years after construction one of the side walls (the south wall) of the U failed, a wedge of fill sliding out together with a section of the concrete panel facing. The height of the section that failed was 16m. A view of the failure is shown in Figure 3.

Early in the life of the wall complex there had been concern because the facing of the north arm of the U had been found to be moving outwards. The movement of the wall was monitored for fifteen months, but when the rate of movement was seen to be moderate (between 10 and 20mm per year), measurements were stopped. At the same time, the wall that ultimately failed was monitored over a period of five months. The observed movement was only 1mm and hence measurements were stopped. The observed movements of the north wall over the period 1979 to 1984 are illustrated in Figure 4. The 1984 measurements seem to show that the rate of movement of the wall had been almost constant with time.

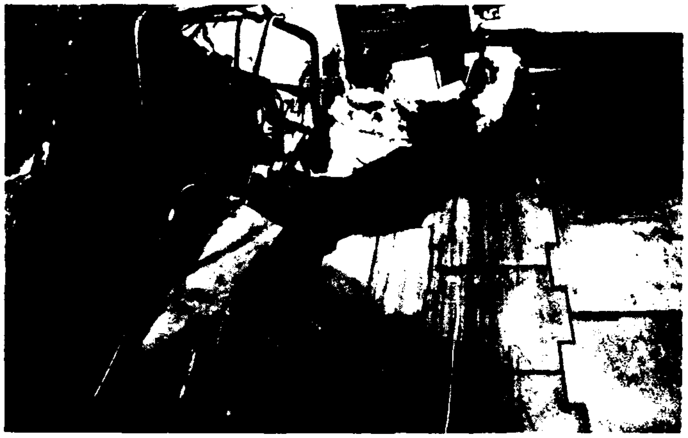

Figure 3: Frontal view of the failure at Grootgeluk Mine

An examination of the failure showed the following:

(i) A water pipe in the failed area had been leaking for an unknown period, discharging water into the fill.

(ii) The fill consisted of a sandy gravel which contains a considerable proportion of clay. It was certainly not free-draining but had an estimated permeability of only 1m/year. Penetration of water into the fill by infiltration of rainwater would have been slow. Equally, water fed into the fill by the leaking pipe would not readily have dispersed.

(iii) Several reinforcing strips had never been placed in the wall. For example, one facing panel was attached to four instead of the required six strips. In other cases 60mm x 3mm strips had been used instead of 80mm x 3mm strips.

(iv) Strips in the wall adjacent to the failed section were found to be inclined at steep angles to the horizontal. Inclinations as steep as 90° were found. It is surmised that a similar situation applied to the section of wall that failed. Figure 5 shows a row of inclined strips uncovered in the post-failure examination.

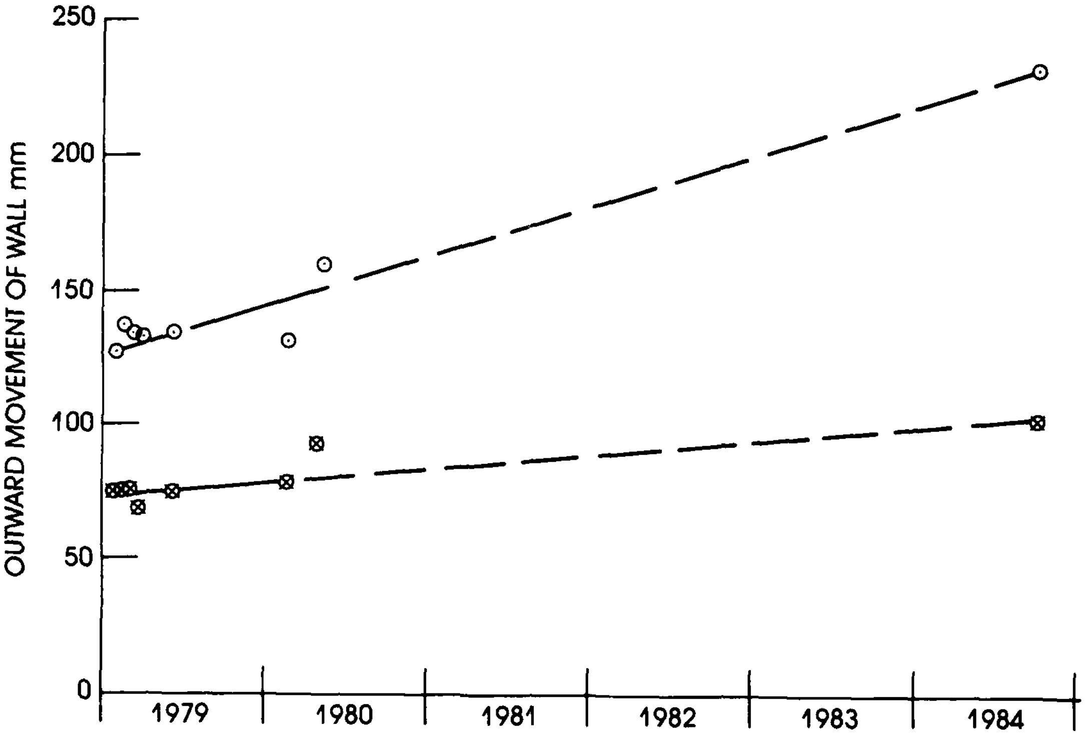

Figure 4: Observed movements of north wall at Grootgeluk Primary Crushing Plant.

The inclination of the strips may have resulted from setting the facing slabs too far ahead of the fill with the result that the unsupported reinforcing strips drooped down to rest on the fill surface. On the other hand, the observed progressive movements of the north wall were probably caused by a similar mechanism, involving collapse settlement, to the movement of the Koningnaas wall. Because of the relatively low permeability of the fill, the process of progressive release of friction would have taken place slowly over the years as each seasonal wetting front progressed through the fill. The same process was probably taking place on the south wall, but was unobserved.

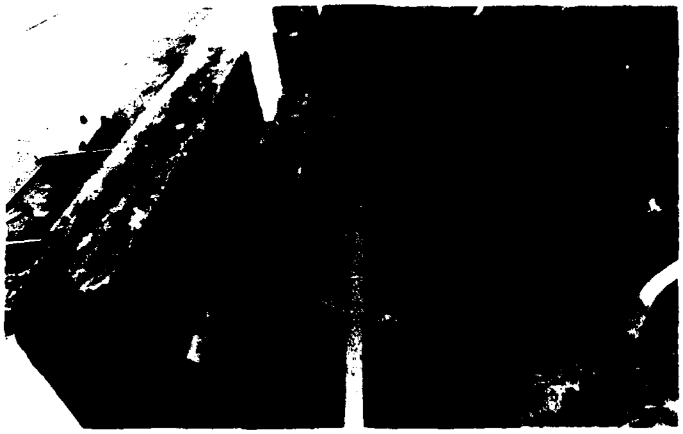

Figure 5: Inclined reinforcing strips uncovered during post-failure examination

(v) A deep rut in the surface of the fill showed that a heavy wheel load had been applied to the surface of the failed area shortly before the failure occurred.

(vi) Several of the strips supporting the failed section had clearly broken some time previously, as the fracture surfaces had rusted.

An engineering failure seldom stems from a single cause. It is usually the concatenation of a number of circumstances that results in a failure. The Grootgeluk failure was obviously no exception. All the above factors would have pushed the condition of the wall nearer to failure.

Accepting the various construction errors mentioned above, a likely scenario for the failure is the following:

Because of progressive collapse settlement and construction errors, the factor of safety of the section of wall that failed may have been close to unity before the water pipe started to leak. The penetration of the fill by water from the leak would have resulted in further collapse settlement and an increasing inclination of the reinforcing strips in this zone. Simultaneously, the accumulation of water would have reduced the shear strength of the fill. The last straw may have been the straying of a heavy vehicle onto the surface of the fill above this zone, now in a critical state. As often happens in engineering failures, there was no coherent eye-witness account of the failure.

Observations at Grootgeluk indicated that reinforcing strips were dragged down over a distance of 500mm to 750mm back from the wall facing. If one sets the acceptable angle of inclination at 37° (a 25 per cent increase in strip tension), then the maximum permissible settlement of the backfill relative to the wall facings is 375mm. Hence the limitation on settlement or misplacement of strips in elevation is not severe. Relative displacements of less than 375mm over a fill height of 16m should be easily possible with good supervision and careful compaction.

CONCLUDING REMARKS

The case histories described above, illustrate the importance of applying the usual control norms during the construction of Reinforced Earth structures, as well as the necessity for adequate compaction of the fill. As shown by measurements on Reinforced Earth structures, the tensions in reinforcing strips at a particular level can vary widely (Blight, Dane and Smith (1)). Circumstances that result in increasing strip tensions may cause certain strips to break, thus reducing the overall factor of safety of the structure. Recognition of these facts will lead to the building of safe, durable structures.

ACKNOWLEDGEMENTS

The information on the Koningnaas wall is published by kind permission of the Anglo American Corporation of South Africa Limited.

The Grootgeluk case history is published by permission of Iscor Limited.

REFERENCES

1. Blight, G.E., Dane, M.S.W. and Smith, A.C.S., "The progressive deterioration of a Reinforced Earth wall complex", submitted to Geotechnique, 1987.

Proceedings: Second International Conference on Case Histories in Geotechnical Engineering, June 1-5, 1988, St. Louis, Mo., Paper No. 5.10

Pavement Failures Caused by Soil Erosion

H.O. Chukweze
University of Nigeria, Nsukka, Nigeria

SUMMARY: The paper examines the failures of road pavements in Nigeria, caused by soil erosion by water. Field evidences reveal that the failures could be grouped into three types collectively known as incision, routing and rutting respectively. Incision and routing both involve the progressive destruction of the road-shoulder to the pavement layers leading to the ultimate failure of the surfacing. The rutting of the pavement involves the weakening of the pavement structure by the accummulated erosion debris. All three types are governed by the soil properties.

It is deduced that the pavements could be protected from erosion by water by applying the fundamental principles of soil mechanics only recognising the peculiar nature of the pavement structure, coupled with the carefully designed post construction management strategies.

INTRODUCTION

Perhaps the developing countries suffer most from the devastating activities of soil erosion by the virtue of the fact that those countries rely greatly on agriculture for **their** economic growth. The activities of soil erosion do not stop at washing away the plant nutrient but may proceed to deface the ground with ugly ditches and crevices.

Often these erosion units are cut through roads and highways thereby limiting human movements and diverting the traffic.

Often, the roads are paved in order to extend their life span. Although some of these paved roads have been designed with special features, erosion has often succeeded in destabilizing them.

This paper presents a few casesof failures of the paved roads in the Southern parts of Nigeria, which have been caused by soil erosion. The examples cited are used to illustrate the mechanisms of the destabilization of paved roads by soil erosion and the principles of the control of the failures.

THEORY

The earliest mathematical model of soil erosion is the so-called universal soil loss equation which was developed in America (soil conservation, 1952), i.e.

A = soil loss (mass per unit area)

$$= R.C.L.K.P.M. \qquad (1)$$

where

R = rainfall factor

C = cropping factor

L = slope length

K = soil factor

p = control factor

M = management factor

Eq. (1) is highly empirical and so leaves room for manipulation as values are assigned arbitrarily to each of the factors contained therein.

More recently other mathematical models have been introduced which can account for the erosion of both clay and other soil types. For example Mitchell and Arulanandan (1968), Partheniades and Paawell (1970) and Kandia (1975) show that the sodium absorption ratio, SAR, which is related to the cation exchange capacity of the soil is directly proportional to the dispersiveness of the soil immersed in water hence to the susceptibility to erosion of the soil. Thus a soil that exhibits high SAR is more susceptible to erosion than the soil with a lower value of SAR under the same environmental conditions.

It is deduced, therefore, that the use of SAR to evaluate soil erodibility is likely to fall through when the surface-active particles in the soil (clay fraction) tend to zero. See also Chukweze (1986).

An alternative equation to the use of SAR is due to Creod (1981). Here the rate of the clay particle detachment, c_e is given by the equation;

$$\dot{\varepsilon} = A\overset{o}{E} \qquad (2)$$

where

$$A = \frac{0.07\,\rho_s}{1+n}\;\frac{V_o\,n}{v\,\delta} \qquad (2a)$$

$$\overset{o}{e} = P.\ \exp.\ K$$

$$K = \frac{\rho \tau \lambda L}{NRT} - \frac{\Delta E}{RT} \qquad (2b)$$

ρ_s = soil particle density

v_o = water flow velocity

v = shear flow velocity

δ = thickness of the boundary layer

P = particle energy

τ = shear stress

λ = interparticle displacement

E = activation energy

T = absolute temperature

R = universal soil constant

N = no. of bonds per m^2 of soil

Several authors have discussed eq. 2 eg. Blandamir et al (1982), Ra dkivi & Tan (1984) and Arulanadan et al (1973). In general many of the parameters of eq. 2 are too difficult to determine thus making eq. 2 unusable.

In another attempt, Chukweze (1987) visualises soil erosion as a composite of the three separate events, vis:

(i) particle detachment

(ii) buoyancy

(iii) viscous drag; and shows that the rate of soil erosion may be estimated from a knowledge of the critical detachment energy, $\overset{o}{E}$ of the rainfall, the crital viscous resistance, τ_v and the relative density, ρ_r of the detached soil particle. (Chukweze, 1987). ie.

$$\overset{o}{E} = \frac{\gamma_{w}.g}{2A^2} \left(\frac{V}{t}\right)^3 \qquad (3)$$

$$\tau_v = \nu \frac{\delta y}{\delta x} \qquad (4)$$

where

γ_w = unit weight of the soil

g = gravitational constant

A = area of exposure to rain fall impact energy

V = volume of water collected

t = time interval

ν = fluid viscosity

$\frac{\delta y}{\delta x}$ = acceleration of flow

In addition to particle detachment by the flowing water, land slides also occur where preexisting slopes exceed the critical height (Chukweze, 1986; Morgenstein & Price, 1965; Bishop & Morgenstein, 1960).

In drainage channels, the water emerges in a localised torrent at the lower end of the culvert and tends to degrade the stream bed there, thereby undermining and undercutting the culvert structure. Such failures may be studied by using the equation due to Caesar et al (1983) i.e.

$$K = D^1 a\, (F)^b \qquad (5)$$

where

K - maximum dimension of the scour hole

D^1 = diameter of the culvert

$F = \frac{q}{g} \left(\frac{1}{2} D^1\right)^{5/2}$

g = gravitational constant

q = discharge of water through culvert

a, b = factors dependent on the maximum scour hole diameter (Caesar, 1981). Thus it may be concluded from the available literature, that the erosion of road pavement by water cannot be isolated from the general principles of soil erosion but the control strategy should always recognise the nature of the road pavement structures.

FIELD EVIDENCES

The area covered by the present study is shown in fig. 1.

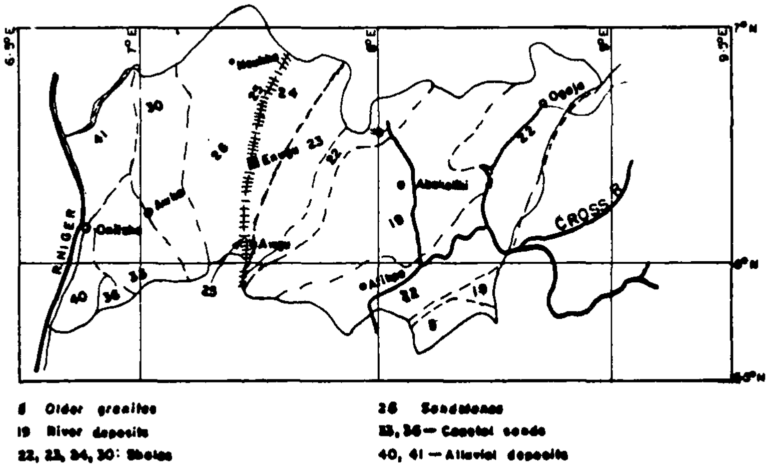

Fig. 1. The geology of the Anambra State, Nigeria.

The major rock associations found here are the shales, false-bedded sandstones containing some coal seams and the river sands and alluvial deposits. The area is drained by several rivers flowing essentially south ward. Some photographs have been taken to show the different types of pavement destructions associated with the erosion activities in the area.

PAVEMENT INCISION

Fig. 2.0 shows a flexible, bituminous pavement the edge of which has been cut by a shallow channel running parallel to it. The small channel started as a rill around September, 1986

and has since grown to a destabilizing unit of the present dimensions: 0.12m at the widest point at the top and more than 1.40m deep at the deepest point.

Hereby called incision the erosion activity carefully cuts through the grassed shoulder and then undermines and undercuts the hard slab of the pavement surfacing.

PAVEMENT ROUTING

Fig. 3 shows the routing of a new road by soil

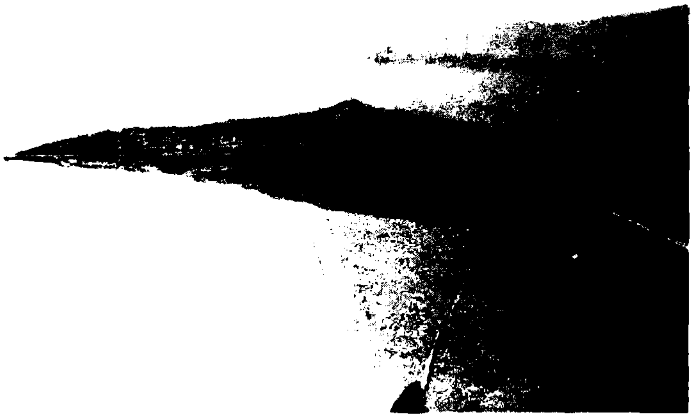

erosion. Here the road is cut across by a large gorge making it impossible for further use. The phenomenon started as a culvert erosion. As the culvert is undermined and undercut it collapses with the superjacent soil mass. As the collapsed soil mass is removed by flowing water and the culvert is further exposed and undermined that section again collapses with the superjacent soil mass and the gorge so created grows across the highway and the road is put out of use. Pavement routing is common in Nigeria and has occurred near Enugu, Awka, Aghara (near Okigwe) and near Onitsha.

PAVEMENT RUTTING

Figs. 4 and 5 show the different modes of failure of a road by the mass accummulation of erosion debris.

Fig. 4 shows a paved road in Nsukka which

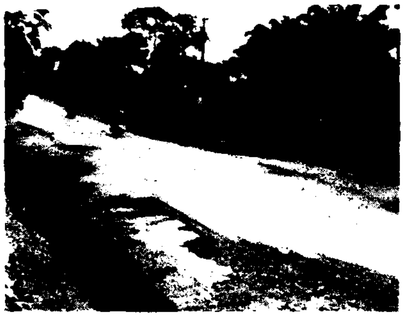

has been completely closed with erosion debris including blocks of broken concrete walls. Incessant flooding of this section of the road has caused the pavement here to weaken and rut. The cyclic deposition of flood materials has helped the pavement rutting by further closing up the drainage channels. Note the thick deposit of erratics.

Fig. 5 shows another case of rutting of

the road pavement along the Awka-Onitsha road. The setting is also typical for the 4th mile from 9th Mile (near Enugu) to Makurdi road. Here the road cut has collapsed and the soil materials are deposited on the road pavement which ruts and weakens with time.

DISCUSSIONS

Pavement failures resulting from soil erosion have been grouped here into three illustrated categories: Incision, routing and rutting.

The commonest of the three forms of pavement destruction is by incision. It occurs both on the pavement shoulders and the edge of the side slopes. It is easily detected by the deep, narrow, nearly straight channels.

It is believed that pavement incision is basically caused by inadequate and inefficient post construction management and maintenance strategies. As a result of neglect the flowing water gradually develops a flow line which grows with age.

Pavement incision may be readily controlled principally by carefully planned maintenance work programme. The rate of maintenance work may be reduced by inserting run-off break-walls (Chukwueze, 1987) at right angles to the sloping direction of the ground. These walls will prevent the removal of loose or detached soil particles by the runoff. The runoff break walls may be supported with grassing and occasional maintenance works.

Pavement routing though devastating is not common. It is associated with areas of the pavement where there are culverts or V - channel junctions (like the situation in the 9th Mile Corner near Enugu). The development of the gorge which grows across the highway is conceived as shown in fig. 6. It is seen that the development of the gorge requires two factors:

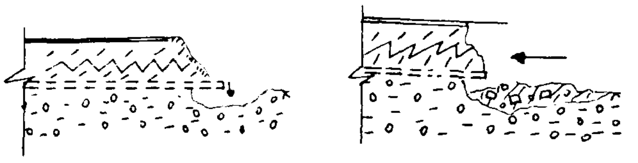
(a) Initial underscouring stages

(b) Advanced stage: progressive failure in the direction of arrow.

Fig 6. Pavement routing initiated by culvert erosion. This can be prevented partially by using monolithically cast culvert chamber (dotted line).

(i) Scouring current

(ii) Transporting current

In many instances the directions of flow of the water currents are orthogonal to each other as illustrated in fig. 7. Thus to control the pavement routing the gorge (if any) which has developed must be refilled; the scouring checked and the transporting current controlled.

Eq. 5 may be used to reduce the scour. The soil characteristics may be altered with the aid of eqs. 3 & 4 so that the effect of the transporting current is controlled. Alternatively monolithically cast culvert chambers instead of the segmented types may be used with the run-off break walls erected at the appropriate points to completely eliminate the incidence of pavement routing.

Fig. 7

The incidence of pavement rutting emanates principally from poor design and construction. Fig. 4 illustrates the case of a drainage channel in a soil whose erodibility varies with the depth of excavation. The channel deepens with age and the sides (slope) collapse into and undermine the functions of the drainage channel.

Fig. 5 illustrates the case of incompetent design of the slopes. It is seen that part of the slope is matted with thin cement layer which acts merely as a protective skin but not slope retainer.

Pavement rutting may thus be prevented by providing designs suitable for retaining the slopes at cuts along the pavement and providing adequate, uninterrupted drainage at culverts and side slopes. The detailed requirements can only be determined with a thorough understanding of the principles of soil behaviour.

These steps when taken in addition to providing well organised post-construction maintenance management schemes, should prevent the destruction of road pavements by soil erosion.

It is seen from the foregoing that the destruction of road pavements by soil erosion is caused by factors ranging from the inadequate involvements of the experts in soil engineering to inefficient and inadequate post construction maintenance management strategies.

CONCLUSIONS

The destruction of road pavements by soil erosion may be grouped into three major types: incision, routing and rutting.

Pavement incision is the most common of all but all the types of pavement destruction may be controlled by applying the principles of soil erosion for all soils coupled with adequate post-construction management programme.

ACKNOWLEDGEMENT

The author is grateful to his friends Dr. Pat Ndukwe and Don Ibe who made the field trip and taking the necessary photographs possible.

REFERENCES

Arulanadan, K. (1975), "Fundamental aspects of erosion of cohesive soils", Journal of Hydraulic Div., A.S.C.E., Vol. 101, H5 pp. 635 - 639.

Arulanadan, K. Sargunam, A., Leganathan, P. and Knon, R.B. (1973) "Application of chemical and electrical parameters to prediction of erodibility; Causes, Mechanisms, Prevention and Control", H.R.B. Spec. Report, 135, pp. 42-51.

Bishop, A.W. (1955), "The use of the slip circle in the stability analysis of slopes". Geotechnique 5, No. 7.

Bishop, A.W. and Morgenstein, N. (1960)," Stability Coefficients for earth slope", Geotechnique, 10, 129-150.

El Ndamir, M.J., Robertson, R.E. and Scott, J.M.V. (1983), "Dependence of equilibrium and rate constant on temperature and pressure", chemical Rev., June, Vol. 3.

British Standards Institution (1975), "Methods of testing soils for civil engineering purposes", B.S. 1377, HMSC., Publ. London.

Chesar, N., Steven, R. and Jones, F. (1983) "Head-wall influence on scour at culvert outlets", Journal of Hydraulics Div., ASCE., Vol. 109, No. 7, pp. 1056-1060.

Chukweze, H.O. (1975), "Some principal engineering geological properties of typical Nigerian laterites", M.Sc. University of Ife, Nigeria.

Chukweze, H.O. (1986), "A case study of the Agulu-Nanka erosion control scheme", Proc. National Workshop on Ecological Disaster: Erosion, 8-12 Sept., Fed. Ministry of Sci. & Techn., Lagos. sub-theme 3, paper 6.

Chukweze, H.O. (1987), "Soil erosion control measures for Aguata, Nigeria Proc. 9th regional Conf. S.M.F.E., Vol. 2, 15-17 Sept., Lagos, Nigeria.

Creod, R.H. (1981), "Physics of erosion in cohesive soils", Ph.D. thesis, Department of Civil Engineering, University of Aukland, N.Z.

Morgenstein, N.R. and Price, V.E. (1965), "The analysis of the stability of general slip surface", Geotechnique, 15, pp. 79-93.

Raudkivi, K. and Tan, S. (1984), "Erosion of Cohesive Soils", Journal of Hydraulics Research, I.A.H.R., Vol. 22, No. 4, pp 217-233.

Sargunam, A. (1973), "Influence of Mineralogy, Porefluid composition and structure on erosion of cohesive soils", Ph.D. thesis, Univ. of California, Davis.

Slot, R.E. (1984)", Terminal velocity formula for objectis in a viscous fluid", Journal of Hydraulics Research, I.A.H.R., Vol 22, No. 4, pp.235-243.

Proceedings: Second International Conference on Case Histories in Geotechnical Engineering, June 1-5, 1988, St. Louis, Mo., Paper No. 5.12

Progress in the Use of NATM for the São Paulo Subway

T.B. Celestino
Head of Department, Themag Engenharia, São Paulo, Brazil

C.T. Mitsuse
Civil Engineer, Themag Engenharia, São Paulo, Brazil

O.A. Ferrari
Project Engineer, Cia do Metropolitano de São Paulo, Brazil

L.C. Domingues
Civil Engineer, Themag Engenharia, São Paulo, Brazil

SYNOPSIS: The first time that the New Austrian Tunnelling Method (NATM) was used for underground works in the São Paulo Subway was in 1981. Since that time, significant progress has been achieved in successfully optimizing the support and lowering the construction costs. This paper will describe the latest experience of two single-track parallel tunnels excavated in 1986 through tertiary stiff clay. All the experience accumulated in previous jobs led to design improvements, such as (1) no steel ribs for support along 72% of the tunnels length (2) no temporary invert, and (3) no spiles, forepoles, soil grouting or any other type of ground improvement. Significant cost and time reduction were the practical result. A method for quick and efficient storage and graphical interpretation of instrumentation readings was developed and implemented in a network of microcomputers installed at the construction site, owner's and engineers' offices.

INTRODUCTION

Since 1981 the New Austrian Tunnelling Method (NATM) has been used for tunnel construction in connection with the extension of the North Line of the São Paulo Subway. In the first case, two parallel 60-m long single-track tunnels (6-m diameter) were excavated through tertiary stiff clay and soft organic clay. Face instability problems already related previously (Celestino et al., 1982) occurred in the soft clay. The solution basically consisted on the use of long grouted spiles.

In the second case, a 200-m long double-track (12-m diameter) tunnel was excavated through stiff tertiary clay, with overburden varying between 5 and 13 m. This construction was completely successful (Celestino et al., 1985) and new cost standards for underground works were established for the São Paulo Subway. (Before the use of NATM, only cut-and-cover and shield had been used for local underground construction). The double-track tunnel was excavated underneath poorly constructed old buildings. In the most critical case the foundations of a 5-storey masonry building (with no concrete or steel structure) were only 5 m above the tunnel crown (Mitsuse et al., 1985) and no damage other than minor cracks occurred. Tenants kept occupying the building normally during tunnel construction.

Due to design optimizations of support and final lining of the double-track tunnel, the contract was finished with fund surplus. The Subway Company decided to use those funds for the construction of two 63-m long single-track tunnels, also along the extension of the North Line, the construction of which is currently underway. This paper describes the performance during the construction of these tunnels, design optimizations that could be adopted based on instrumentation results, and the final cost.

It is important to emphasize that design optimizations during construction could only result in cost reduction due to the flexibility of the contract, as described elsewhere (Cruz et al., 1985).

Being NATM an observational method, (Rabcewicz, 1964) optimizations are heavily dependent on efficient instrumentation interpretation. Mathematical models have been used for the jobs mentioned above, and they have been upgraded as construction progressed in order to obtain good agreement between their results and instrumentation readings. Calibrated models helped to evaluate beforehand the consequences of design optimization measures and the resulting safety.

DESIGN DATA

The tunnels were excavated through tertiary stiff fissured clay. Above the West tunnel, quaternary deposits of soft clay with sand lenses occurred. Figure 1 shows a cross section through the portals. The overburden varies from 18 m at portals to 14 m at the end of the tunnels, 63 m away. The thickness of stiff clay above the crowns of the tunnels also decreases slightly to a minimum of 2 m. The pillar between the tunnels is about 5 m wide. The excavation progressed from a shaft towards the dead end of existing tunnels already in operation.

The stiff clay is randomly fissured. In some locations, no fissures could be noticed on the tunnel face; in others, spacing varied from a few to tens of centimeters. Their attitudes were also randomly distributed. They were usually slickensided, having very low strength. Unstable blocks were sometimes formed at the excavation face, and this was one of the critical problems that had to be looked at during construction. The SPT penetration

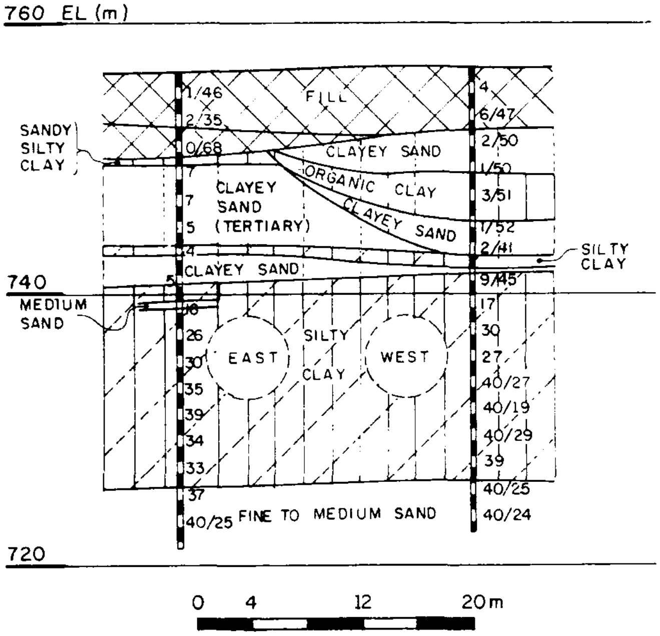
760 EL (m)
SANDY SILTY CLAY
FILL
CLAYEY SAND
ORGANIC CLAY
CLAYEY SAND (TERTIARY)
CLAYEY SAND
SILTY CLAY
740
MEDIUM SAND
EAST
WEST
SILTY CLAY
FINE TO MEDIUM SAND
720
1/46
2/35
0/68
7
7
5
26
30
35
39
34
33
37
40/25
4
6/47
2/50
1/50
3/51
1/52
2/41
9/45
17
30
27
40/27
40/19
40/29
39
40/25
40/24
0 4 12 20m

FIGURE 1 - Geological Cross Section Through the Portals

resistance of the clay (blows/foot), also indicated in Figure 1, is in the range of 20 to 40. The modulus of elasticity, and the coefficient of earth pressure at rest, both inferred from instrumentation results during the excavation and mathematical models, were 100 MPa and 1.0 respectively. The latter is also in agreement with theories of earth pressure for overconsolidated clays (e.g. Brooker and Ireland 1965) with an overconsolidation ratio of 5.

Eventhough not important for face stability the deposit of soft clay above the West tunnel played an important role for surface settlements. With a natural void ratio in the range of 2 to 3, the material undergoes appreciable consolidation under minor stress changes.

There are two water tables: one gravitational, approximately at elevation 750 m, and the other one artesian, in the sand deposit below elevation 723 m. Due to the low permeability of the stiff clay, no dewatering was necessary.

In spite of being in urban environment, there were no important buildings directly above the tunnels. However, several buildings were within the area of influence of the work.

Both support and final lining consisted of shotcrete, as indicated in Figure 2, with thicknesses of 15 cm and 10 cm respectively, and 2.2 kg/m2 CA-60B steel wire mesh. According to the design, 4-inch I steel sets would be used for support every 80 cm in the initial and final 10 m long stretches of the tunnels. Both at the portal and next to the dead end of previously excavated tunnels, non-symmetrical loads could be anticipated due to previous disturbance and loosening of the soil mass. Lengths of stretches where steel sets were actually installed were different, as described later on.

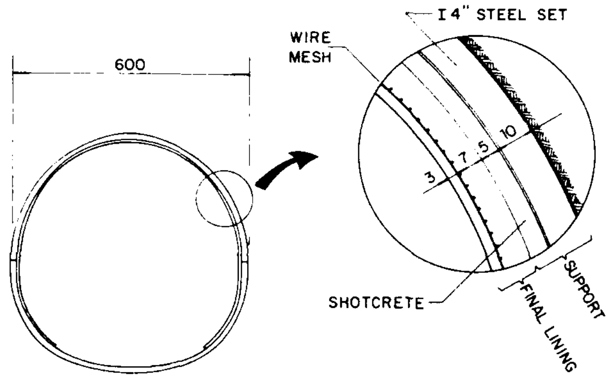
600
I 4" STEEL SET
WIRE MESH
10
7.5
3
SHOTCRETE
SUPPORT
FINAL LINING

(a) PORTAL ZONES

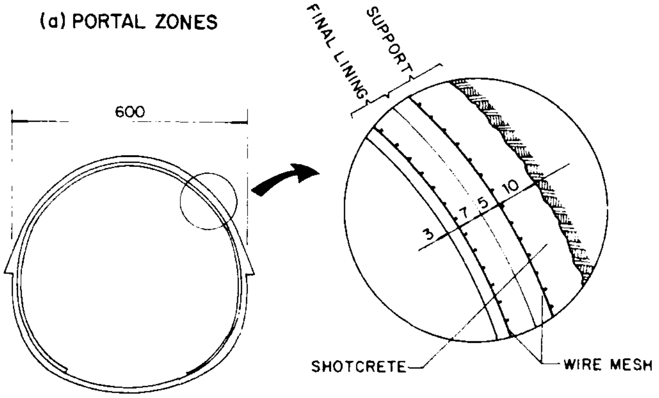
FINAL LINING
SUPPORT
600
10
7.5
3
SHOTCRETE
WIRE MESH

(b) AWAY FROM PORTALS

FIGURE 2 - Support and Final Lining (Thicknesses in Millimeters)

The tunnels were top-heading and bench excavated, with 0.8 m advance and distance from bench to face varying from 3.6 to 5.2 m. A core was left at the face in order to minimize problems of unstable blocks formed by slickensided. No global face stability problems were anticipated. Support and final lining were designed with basis on interaction diagrams (bending moment versus normal force) obtained from the mathematical model. The model reproduced the different excavation phases, placement of support and its hardening with time. Long term condition was simmulated by (a) introducing a factor of safety (equal to 2) on the effective strength parameters of the soil, thus causing soil relaxation and increase in load transferred to the shotcrete lining; (b) considering a 2-m increase in the elevation of the water table due to long-term fluctuations; and (c) considering surface and deep loads to be transferred to the soil mass by foundations of future buildings. An example of interaction diagrams is presented in Figure 3. Shown there are bending moment (Md) versus thrust (Nd) envelops for all cross sections of the lining and the moment-thrust interaction diagrams for the support and final lining.

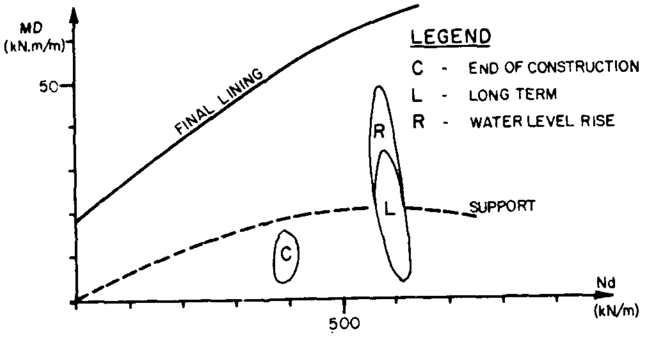

FIGURE 3 - Moment-Thrust Diagram for Support and Final Lining

MONITORING

Instrumentation was very simple and consisted of 7 control sections of surface and deep settlement devices.

A Full control section is shown in Figure 4, with two levels of deep as well as surface settlement devices. Some sections were more simple and had only one surface and one deep settlement devices.

Also shown in Figure 4 are other parameters that will be used later on:

s: maximum settlement;

i: distance to point of inflection of settlement trough, as defined by Peck (1969); referred to as settlement trough width for simplicity;

Vs: volume of settlement trough;

Ve: excavation volume;

π = Vs/Ve (%): percentage of settlement volume.

Settlements of nearby buildings were also controlled. Besides settlements, internal convergence of the tunnels was also measured.

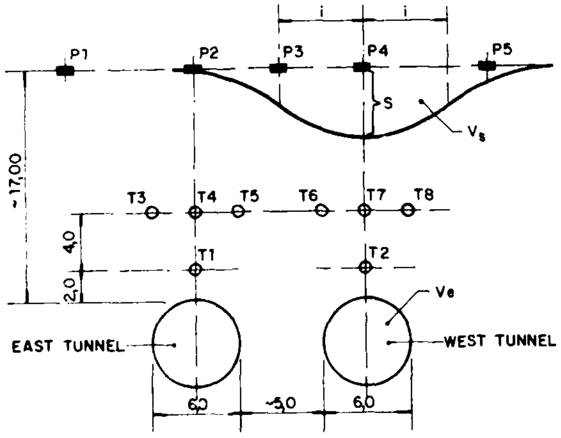

FIGURE 4 - Typical Control Section and Settlement Parameters

In order to speed up the interpretation of instrumention results, a system was developed for storage, retrieval and graphical presentation of instrument readings and general construction occurrences. A network of microcomputers was installed at the construction site, owner's office and engibeers' office so that the data could be remotely transmitted. This system allowed interpretation graphs to be available at the offices a few minutes after reading the instruments at the construction site.

Graphs of readings versus time or readings versus excavation progress can be obtained at scales easily chosen by the user. Annotations of construction occurrences are also shown. Other types of graphs are being implemented now. Domingues et al. (1987) present a general description of the system.

PERFORMANCE DURING CONSTRUCTION AND COST

Eventhough other tunnels have been excavated in soil without steel sets as part of the support both in Brazil (e.g. Negro and Eisenstein 1978; Teixeira, 1985) and abroad (e.g. Ocampo-Franco, 1982), no tunnels had yet been excavated without steel sets for the São Paulo Subway. At the time they were first used, steel sets represented significant progress for the practice of tunnel support. More recently, after other types of support have come up, for instance shotcrete, the use of steel sets has been questioned by some authors (e.g. Kramers, 1978; Rabcewicz, 1979). Important conclusions of the instrumentation program of the Du Pont Circle Station construction, Washington Metro (Brierly and Cording, 1976) show only limited action of steel sets. It was therefore decided to eliminate steel sets at the central portions of the tunnels, except where previous disturbance of the soil mass might cause the need for (a) support shortly after excavation, or (b) support element to withstand concentrated or non-symmetric load.

The West tunnel was excavated first, and only when it reached the end did the East tunnel excavation start. When the face of the West tunnel reached progressive 35 m, settlements started to increase. According to the design, steel sets were not being used for support. It was noticed that the quality of shotcrete (the only support element) was very poor. Time of initial setting and time of end of setting were far beyond design requirements. A large block (4 m wide, 0.9 m high) fell off the roof, and steel sets were again locally adopted. In this mean time, laboratory tests determined that the cement and admixture used were incompatible due to recent increase in the contents of blast furnace slag. Untill new compatible cement and admixture were found, a minimum of 10 hours was established between initiation of subsequent advances, so that the shotcrete could gain enough strength.

Figure 5 shows the contours of equal surface settlements caused by the excavation of the West Tunnel. Values for i, s and π along the tunnel axis are also shown. A deep trough (68.7 mm) can be seen at the location of the unstable block. It is interesting to notice that the

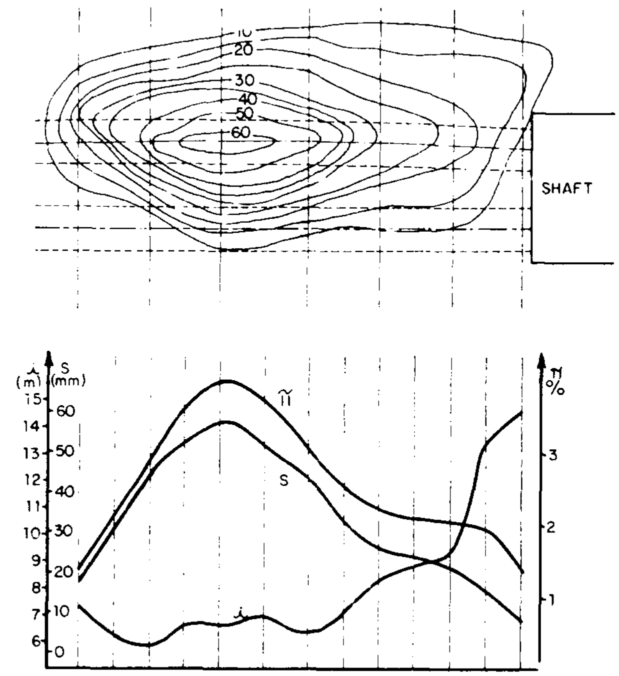

FIGURE 5 - Surface Settlements Caused by West Tunnel: Contours and Parameters i, s and π.

settlement trough becomes narrower at the location of the unstable block, indicating the tendency for plug-like mechanism. Trough width and settlement volume percentage have exactly opposite behaviors (one increases as the other decreases).

When the East tunnel excavation started, there was no more restriction about the time between advances, since new compatible cement and admixture had been found. Steel sets were only used in the initial 10 m according to the design. No problem of unstable block was found. The use of steel sets was conditioned to the maximum observed shear strain in the soil mass, inferred from the reading of the deepest settlement device. The limit was never reached and the excavation progressed successfully without steel sets.

Figure 6 shows settlements caused by the East tunnel. No pronounced peak of π or s exists. It can also be noticed that the settlements are significantly smaller than for the West tunnel. This is true not only at the location of the unstable block, but even in the first 30 m, where no serious problem of shotcrete occurred for the West tunnel.

This tendency is also observed for the deep settlement devices, that do not include consolidation of the soft clay above the West tunnel. East tunnel settlements were only 50% to 65% of West tunnel settlements.

The decrease in settlement caused by the second tunnel is opposite to what had been found by Cording and Hansmire (1975). They compiled data from several tunnels excavated with shield that showed a clear increase in settlement for the

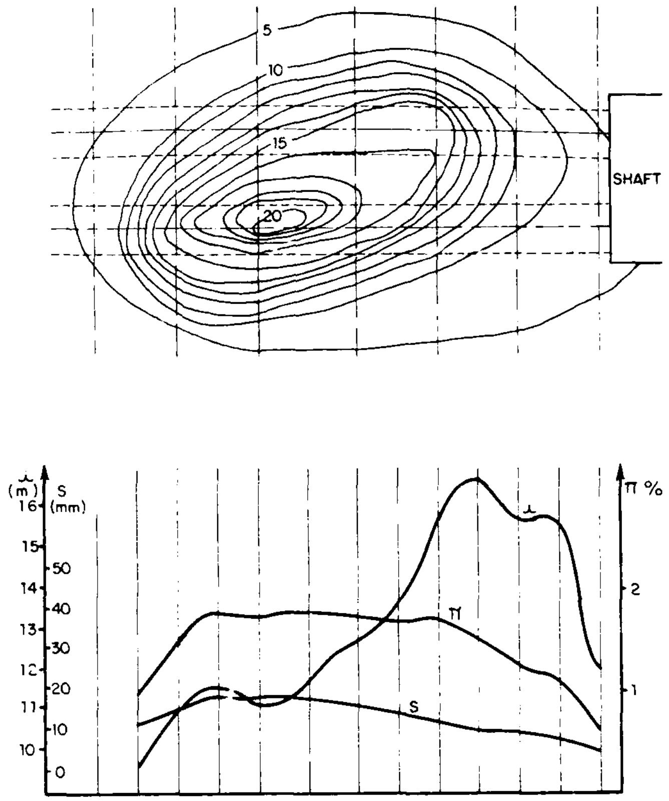

FIGURE 6 - Surface Settlements Caused by East Tunnel: Contours and Parameters i, s and π.

second tunnel. It is probable that the already completed shotcrete support of the first tunnel, interacting with the soil mass, is stiffer than the mass by itself. Similar results were found by Celestino et al. (1985), analyzing data of settlements caused by large dimension tunnels excavated in sequences of side and central galleries.

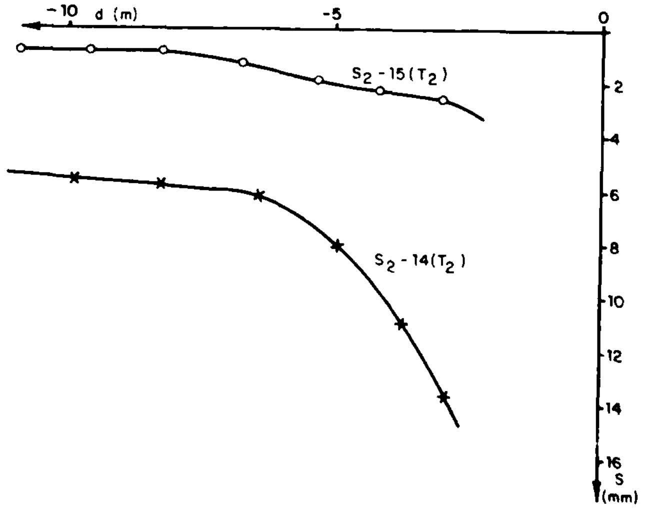

FIGURE 7 - Deep Settlements as a Function of the Distance to Excavation Face: S2-15 Above Pre-Existing Tunnel; S2-14 Above Soil Mass.

Another evidence of this fact was found in connection with the longitudinal arching as the East tunnel approached the dead end of the previously completed tunnel. Figure 7 shows the settlements measured at the deep settlement devices of section S2-15 (above pre-existing tunnel) and S2-14 (ca 15 m before) as function of their distance to the tunnel face. It can be clearly seen again that the interaction between soil mass and tunnel lining shows stiffer behavior (lower settlement) than the soil by itself.

As a result of this observation, the number of steel sets at that location was decreased from what had been specified in the design.

As a result of the measures adopted: (a) no steel sets along 72% of the length of the tunnels, (b) no temporary invert, (c) no ground improvement, and (d) shotcrete for final lining, the cost of the tunnels (excavation, support and final lining including floor slab) came out the lowest ever reached for the São Paulo Subway: only $5,300 per linear meter. For comparison, the cost of the double-track tunnel previously mentioned was of the order of magnitude of $16,000 per linear meter. The first application (single-track tunnels) had a wide variation of cost, due to problems already mentioned above. The lowest cost at problem-free regions was $12,000 per linear meter.

CONCLUSIONS

Despite serious problems with the quality of shotcrete that had to be coped with during the excavation of the second half of the West tunnel, the remainder of the tunnels could be successfully excavated without steel ribs and temporary invert. The cost presented is the lowest for tunnels of the São Paulo Subway.

Settlement data caused by twin tunnels showed tendency contrary to what had been previously reported, i.e. the interaction between the support of the first tunnel and the soil mass seems to contribute to decrease subsequent settements. Settlement caused by the second tunnel was smaller than the ones caused by the first tunnel.

ACKNOWLEDGMENTS

The authors wish to acknowledge the São Paulo Subway Campany, for the incentive and permission to publish the data presented here.

REFERENCES

Brierly, G.S. and E.J. Cording, (1976), "The Behavior During Construction of the Du Pont Circle Subway Station Lining", II Int. Conf. Shotcrete for Underground Support, Easton, ASCE/ACI, pp. 675-712.

Broker, E.W. and H.O. Ireland, (1965) "Earth Pressures at Rest Related to Stress History", Canadian Geot. Journal, Vol. 11, pp. 1-15.

Celestino, T.B., C.T. Mitsuse, C. Casarin and F. Fujimura, (1982), "NATM in Soft Soil for the São Paulo Subway", IVth International Conference on Shotcrete for Underground Support, Paipa, (Eng. Fdn. Conf.).

Celestino, T.B., L.C.S. Domingues, C.T. Mitsuse, K. Hori and O.A. Ferrari, (1985), "Recalques Decorrentes da Construção por NATM de um Túnel Urbano de Grandes Dimensões e Pequena Cobertura", 2. Simpósio Sobre Escavações Subterrâneas, ABGE Rio de Janeiro.

Cording, E.J. and W.H. Hansmire, (1975), "Displacements Around Soft Ground Tunnels", State of the Art Report, 5th Panamerican Conf. Soil Mech. Fdn. Eng., Vol. III, pp. 571-633.

Cruz, H.J.V., K. Hori, O.A. Ferrari and A.A. Ferreira, (1985), "A Construção em NATM e em área urbana, de um túnel de grande seção - o túnel de via dupla do prolongamento norte", 2o Simpósio Sobre Escavações Subterrâneas, ABGE, Rio de Janeiro.

Domingues, L.C.S., S.M. Burin, T.B. Celestino, C.T. Mitsuse, E.R. Esquivel, O.A. Ferrari and A.P. Horta, (1987), "SACI - A System for Instrumentation Control and Follow-up", 6th Int. Conference on Numerical Methods in Geomechanics, Innsbruck (in press).

Kramers, M., (1978), "The Swedish Approach to Tunnel Support", Water Power & Dam Construction, Sept., pp. 31-35.

Mitsuse, C.T., L.C.S. Domingues, T.B. Celestino, K. Hori and O.A. Ferrari, (1985), "Travessia Crítica de um Túnel NATM de Grandes Dimensões em Região de Baixa Cobertura no Metrô de São Paulo", 2o Simpósio Sobre Escavações Subterrâneas, ABGE Rio de Janeiro.

Negro, A. and Z. Eisenstein, (1981), "Ground Control Techniques Compared in Three Brazilian Water Tunnels. Part 2". Tunnels & Tunnelling, Nov. 1981, pp. 52-54.

Ocampo-Franco, M.R. (1982), "The Use of Shotcrete as Temporary Support and Final Lining in Tunnels of Line 7 Mexico City Subway", Int. Conf. Shotcrete for Underground Support, Paipa.

Peck, R.B., (1969), "Deep Excavation and Tunnelling in Soft Ground", 7th Int. Cong. Soil Mech. Fdn. Eng., Mexico State of the Art Report, Vol. II, pp. 225-290.

Rabcewicz, L. (1964), "The New Austrian Tunnelling Method", Water Power, pp. 453-457, 511-515.

Rabcewicz, L.V.; (1979), "Principles and Modes of Application of NATM With Special Regard to the Geotechnical and Topographical Brazilian Conditions" (in Portuguese), Translation n. 8, Brazilian Association Eng. Geology, São Paulo.

Teixeira, A.H. (1985), "Comunicação", 2o Simp. Sobre Escavações Subterrâneas, ABGE, Rio de Janeiro.

Proceedings: Second International Conference on Case Histories in Geotechnical Engineering, June 1-5, 1988, St. Louis, Mo., Paper No. 5.13

Effectiveness of Sand Drains in Peaty Soil in a Case of Differential Settlement Recovering

C. Mastrantuono
Geotechnical Consultant, Milano, Italy

E. Arcangeli
Engineer, RODIO S.p.A., Casalmaiocco, Milano, Italy

A. Tomiolo
Director, Solvo s.r.l. Engineering Services, Milano, Italy

SYNOPSIS: The result obtained in a case history of differential settlement recovery are reported. The effectiveness of sand drains in peaty soil is questioned. The importance and the mutual influence of the primary and secondary settlement are discussed. Remarks are made on the value of secondary settlement coefficient.

INTRODUCTION

The authors presented to the First International Conference on Case Histories in Geotechnical Engineering a paper concerning the recovering of differential settlements in a large six storey building by means of vertical drains and partial overloading of the foundation mat.

The details of the design together with general soil characteristics, settlement measurements up to November 1983 and observational analysis of settlements are reported in the mentioned paper. But the limited available space did not allow an accurate analysis of the settlements behaviour with respect to the soil characteristics: this will be done in this paper. Furthermore an other measurement of the settlements has been made in July 87, so that more precise forecast for the future behaviour is now possible.

SOIL CHARACTERISTICS

The general soil characteristics have been reported in the previous paper. It has to be stressed that the area was a marshland until a few years before the building construction and that propably the building was located on the border of the said area. In fig. 1 the lay-out of the foundation mat is reported with the boreholes and CPTs performed at the time of the intervention (1974). Borehole 1 and CPTs A and B showed a soil with characteristics substantially different from those of borehole 2 and CPTs C and D (see previous paper). In fact the side of the building interested by these latter tests was close to the water stream flowing at about the center of the marshy area.

In 1978 a new investigation was performed, consisting of one borehole, one electric CPT and one DMT (Marchetti Dilatometer Test). These tests were made in the vicinity of the existing borehole 2 (fig. 1) but at a sufficient distance from the building not to be affected by its load.

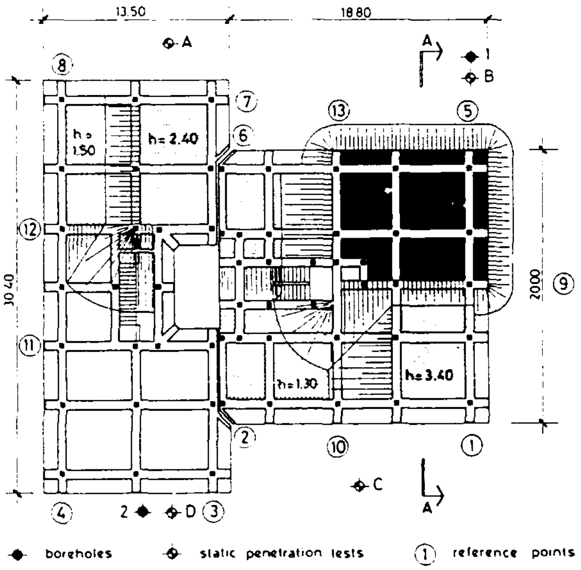

Fig. 1 Lay-out of the Foundation Mat with the Height (h) of Sand Loading and Reference Points

In fig. 2 are reported the profiles of CPT and DMT. In the borehole samples some characteristics resulted as follows:

sample depth (m)	peat content (%)	γ_0 (t/m^3)	W_0 (%)	W_L (%)	W_P (%)	C_U (t/m^2)	C_R
2.15 - 2.55	-	1.83	39	55	18	2.6	0.153
4.00 - 4.35	-	1.58	103	-	-	-	-
4.35 - 4.55	-	1.79	43	57	17	2.3	0.196
6.00 - 6.60	17.4	1.60	65	103	29	2.9	0.306
10.50 - 11.05	13.5	1.77	43	67	18	3.4	0.246
14.70 - 15.25		1.70	50	74	21	4.2	0.272
20.00 - 20.55	11.6	1.66	54	83	22	6.0	0.323
23.10 - 23.60	-	1.80	38	70	19	5.3	0.230
29.20 - 29.60		1.88	31	59	17	3.4	0.166
32.30 - 32.80	-	1.68	29	38	18	5.5	0.172

The values of cu were determined by laboratory vane tests: the trend is linear from 2 t/m2 at 2m depth to 4 t/m2 at 15 m. The samples resulted slightly overconsolidated down to about 10 m. C_R is the compression ratio ($\frac{\Delta H}{H}$ /log t) on the virgin curve in the compression range ($p > p_c$). As far as the peat content is concerned, and hence the compressibility, the layer between 5 and 10 m approximately resulted critical; this is in accordance with what had been obtained for borehole 2.

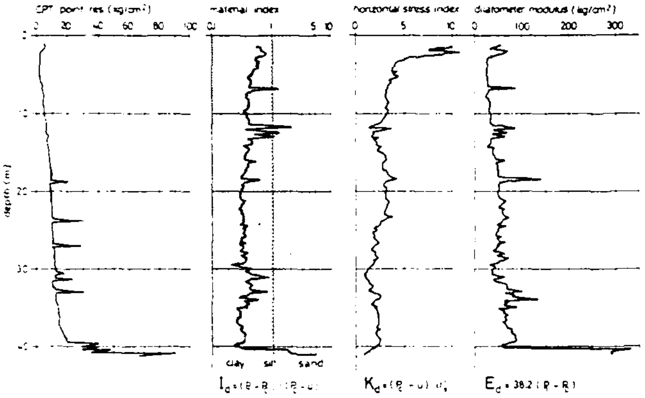

Fig. 2 CPT and DMT Tests in the Vicinity of Borehole 2

SETTLEMENT BEHAVIOUR

The drains were installed from 1st August to mid October 1974; in fig. 3 are sketched the diagrams of settlement for two opposite corners of the building, together with the drains execution period and the four loading steps. These steps with reference to the maximum height of sand loading on the foundation mat (fig. 1) were:

1st step Hmax = 1.10 m
2nd step = 2.20 m
3rd step = 3.50 m
4th step = 4.50 m

The partial unloading refers to a reduction of the maximum height of sand to 2.20 m all over the area; the partial reloading refers to a restatement of the height of 4.50 m in proximity to point 5 (fig. 1), but without the external embankment. On the diagrams in fig. 3 some interesting remarks can be done:

1. during the drains execution, which began from the corner of point 5, the point 4 showed a heave: this was due to the great rigidity of the building structure
2. after the 4th loading step, which interested only the area near to point 5, point 4 showed a complete stop of settlement for about two months (March and April 75), but afterwards it started again to settle. Point 5 in correspondence of the partial unloading

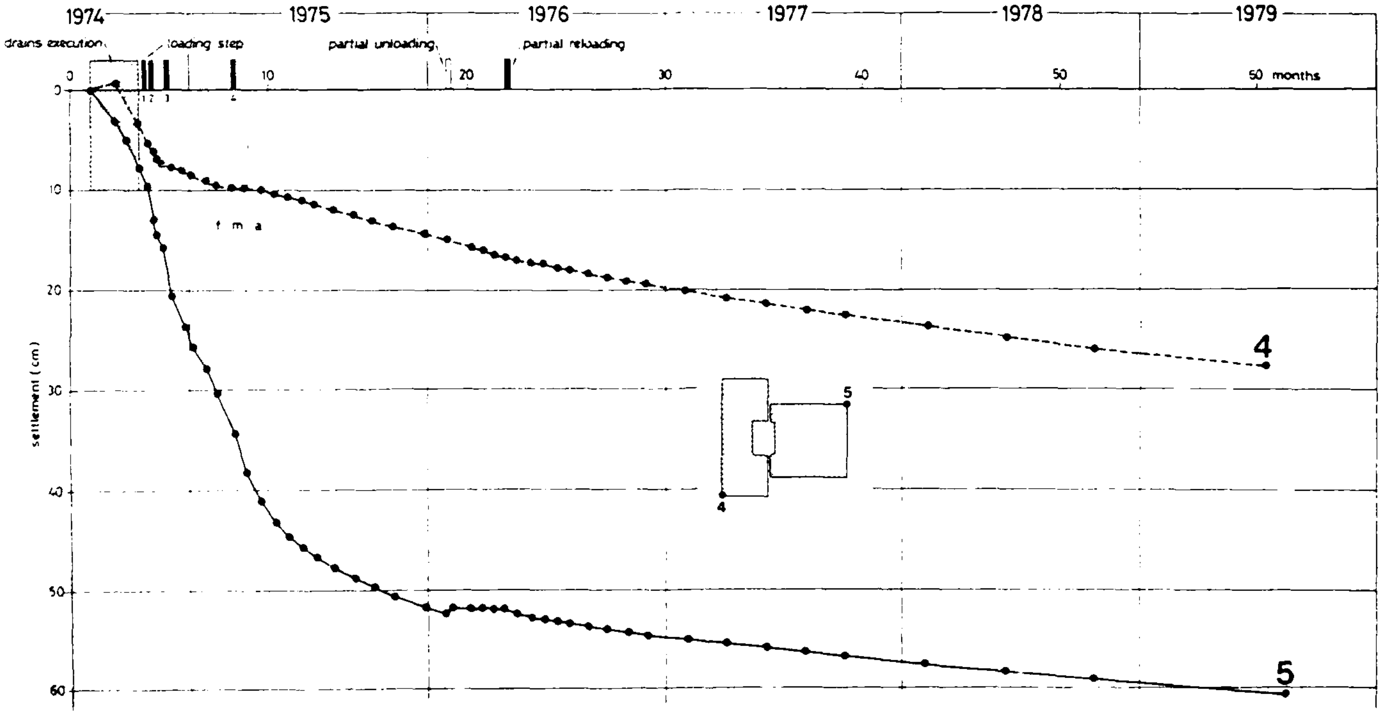

Fig. 3 Settlements of Two Opposite Corners of the Building

(from 4.50 m height of sand loading to 2.20 m) experienced a slight heave and then a complete stop of settlement. This phenomenon has been observed by many authors (e.g. Veder and Prinzl, 1983) and is employed in the technique of soft clays overloading, mainly to reduce secondary settlement

3. the settlement rate of point 4 was affected by the presence of the drains only during and immediately after their execution. From middle 1975 to 1979 the settlement behaviour seemed to be insensitive to the presence of the drains. In the previous paper it was attributed to the clogging of the drains by organic matter. The authors believe that this deduction and hence the questionability of the use of small diameter (10 cm) sand drains in peaty soil must be maintained

4. it is important to outline that the settlement behaviour was controlled not only by the soil characteristics, but also by the building rigidity. In Fig. 4 are reported the isochrones of settlement at July 79, which are almost perfectly parallel. The settlement recovering at that time between points 4 and 5 was about 32 cm.

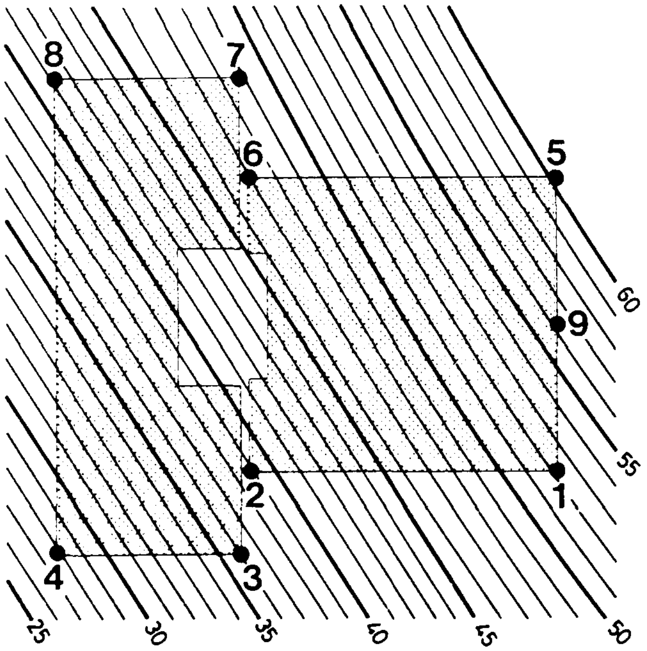

Fig. 4 Isochrones of Settlement at July 79

PRIMARY AND SECONDARY SETTLEMENT

The question about the settlement behaviour of point 4 was whether or not this was essentially secondary settlement. The primary settlement was calculated on the basis of the compression ratio values obtained from oedometer tests (in fig. 5 is reported the oedometer curve for the sample at depth 8.70-9.30 m). The stresses induced by the foundation were calculated by the method of Fox. The settlement calculation was limited to 28 m depth.

In the following table are reported the data of the calculation:

layer	thickness (m)	C_R	P_0 (kg/cm^2)	ΔP (kg/cm^2)	settlement (m)
1	2,00 - 4.65	0.2117	0.256	0.85	35.55
2	4.65 - 6.10	0.2588	0.412	0.76	17.04
3	6.10 - 11.10	0.3189	0.612	0.66	50.66
4'	11.10 - 16.00	0.1785	0.934	0.53	17.07
4"	16.00 - 20.10	0.1785	1.257	0.43	9.35
5	20.10 - 28.00	0.3388	1.682	0.32	20.24
					149.91

A calculation of the primary consolidation rate was done without drains and taking into account the presence of a layer of fine silty sand at 18-20 m depth. So the following scheme of consolidation was assumed:

- layer 1 from 2 to 10 m flow upward

  $C_{Vav} = 2,25 \ . \ 10^{-4} \ cm^2/sec.$

- layer 2 from 10 to 18 m flow downward

  $C_{Vav} = 1,01 \ . \ 10^{-3} \ cm^2/sec.$

- layer 3 from 20 to 28 m flow upward

  $C_{Vav} = 4,2 \ . \ 10^{-4} \ cm^2/sec.$

It resulted that at July 74 (14,5 years after the beginning of the construction) about 40 cm of the primary settlement had yet to develop, of which 35 cm due to layer 1 and 5 cm to layer 3, while layer 2 had almost completed primary consolidation.

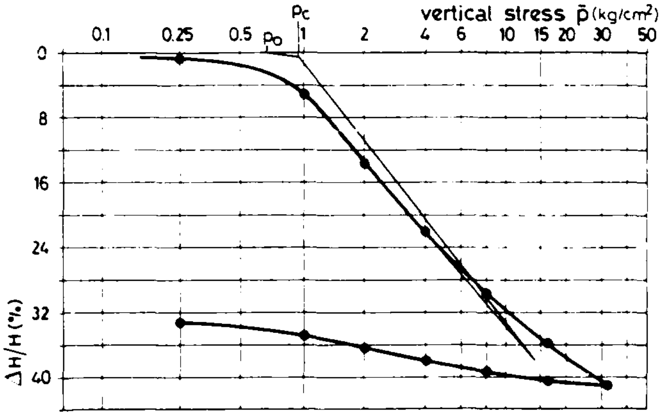

Fig. 5 Oedometer Curve for the Sample at Depth 8.70-9.30 m

In fig. 6 are reported the settlements from August 74 to July 87 of four significant points.
In fig. 7 the settlements of point 4 are reported versus log time. The estimated settlement of 130 cm at July 74 is based on:

1. out of level of 90 cm measured at July 74 between points 4 and 5
2. estimated settlement of 30 cm for point 5 (rough measurements made by the owner of the building gave 16 cm from January 63 to July 74)
3. evaluated immediate settlement of about 15 cm.

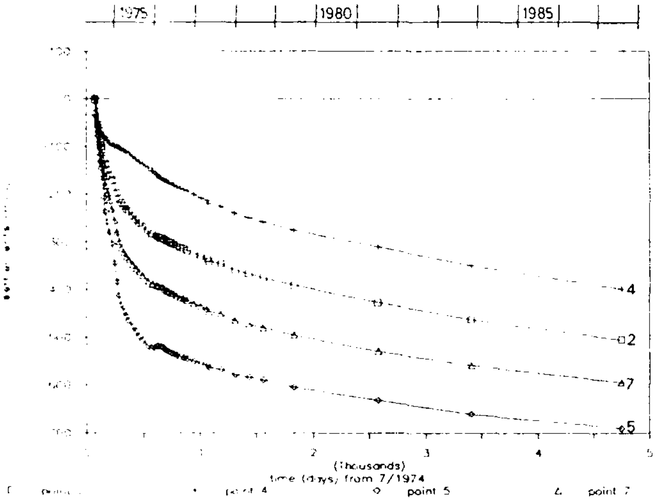

Fig. 6 Measured Settlements of Four Points

The curve in fig. 7 indicates:

1. the drains had little influence on the settlement rate of point 4, as also Asaoka analysis showed (see previous paper)
2. the primary and secondary parts of the curve seem to be well distinct. It is likely that the primary consolidation has been completed at about the end of 1979, 20 years after the beginning of the construction . The value of the primary settlement from August 74 to the end of 79 (40 cm approx.) fits very well with the calculation of the consolidation settlement amount and rate above reported.

In the previous paper a forecast of the secondary settlement rate was done, based on the values of the coefficient of secondary compression c_α given by the oedometer tests. The measurement of July 87 has invalidated that forecast and a new one is reported in fig. 7.
This new forecast corresponds to a value of $c_\alpha = 0.0125$, but this value in laboratory has been obtained as a maximum only for the sample at 8.60 - 9.30 m depth. For the other samples, values vary from 1/3 to 2/3 of the above maximum value.

Thus we must conclude that the in situ creep is in our case remarkably higher than the laboratory one.
This has already been noted in many case histories and the most likely reason is the collapse of the soil structure as the effective stress approaches the final value (Chang, 1981). It has to be noted that in our case the coefficient of mobilization of the ultimate strength was high ($c_u \simeq 2$ t/m2; net pressure $q = 0.85$ kg/cm2; coefficient of mobilization $f = 0.75$).

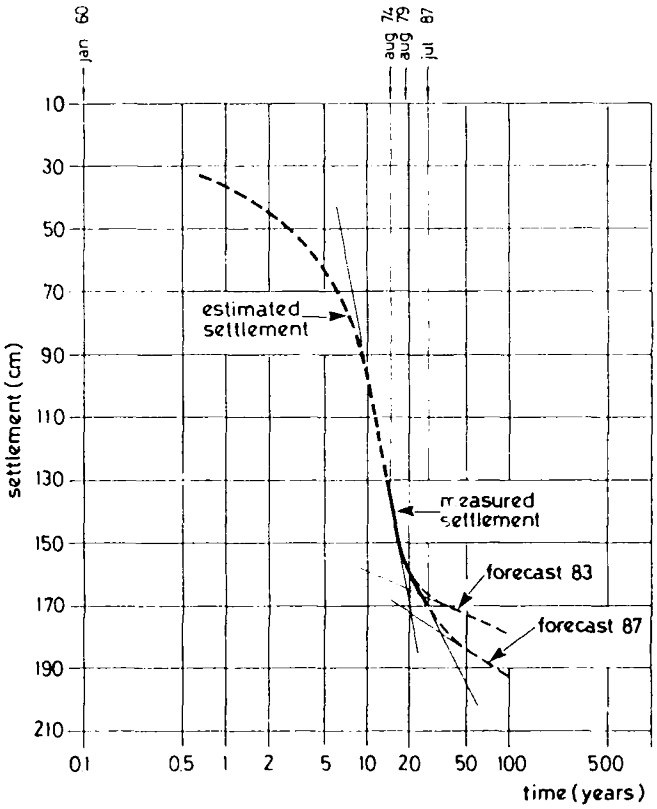

Fig. 7 Tentative Curve of the Settlement of Point 4 versus Log Time

CONCLUSIONS

The use of small diameter sand drains resulted not effective in the area affected by medium-high peat contents. On the contrary in the remaining part of the foundation the results were fully satisfactory.

The consolidation settlement and its rate, calculated on the basis of the parameters obtained from incremental oedometer tests, were well fitting with the measured values. It has to be said that it was very attractive to use the Bjerrum's concept of instant and delayed settlement to explain the unexpected settlement of point 4; but the agreement of calculated and measured values seems to be in accordance with the conclusions of Mesri and Choi (1985) about the uniqueness of end of primary consolidation.

Secondary settlement in situ resulted sensibly higher than in laboratory tests. This is an already known phenomenon and has to be attributed mainly to the high coefficient of mobilization of ultimate strength.

REFERENCES

Asaoka, A. (1978), "Observational Procedure of Settlement Prediction". Soils and Foundations, Vol. 18, no. 4

Bjerrum, L. (1967), "Engineering Geology of Norvegian Normally Consolidated Marine Clays as Related to Settlements of Buildings". 7th Rankine Lecture, Géotechnique, 17, 81-118.

Chang, Y. C. E. (1981), "Long Term Consolidation Beneath the Test Fills at Väsby, Sweden. Swedish Geotechnical Institute, Report no. 13.

Jamiolkowski, M., Ladd, C. C., Germaine, J. T. and Lancellotta, R. (1985), "New Developments in Field and Laboratory Testing of Soils". Theme Lecture, Vol. 1, XI ICSMFE, San Francisco.

Mastrantuono, C., Tomiolo, A. and Arcangeli E. (1984), "Recovering Differential Settlements by Vertical Drains". Proc. Int. Conf. on Case Histories in Geotechnical Engineering, St. Louis, MO, Vol. 1, 87-92.

Mesri, G. and Choi, Y. K. (1985), "The Uniqueness of the End-of-Primary (EOP) Void Ratio - Effective Stress Relationships". Proc. XI ICSMFE, San Francisco Vol. 2, 587-590.

Veder, C. and Prinzl, F. (1983), "The Avoidance of Secondary Settlements through Overconsolidation". Proc. VIII ECSMFZ, Helsinki, Vol. 2, 697-706.

Proceedings: Second International Conference on Case Histories in Geotechnical Engineering, June 1-5, 1988, St. Louis, Mo., Paper No. 5.14

Construction of a Double Tunnel with Ground Windows

Helmut Meissner
Prof. Dr.-Ing., Soil Mechanics und Foundation Engineering,
University of Kaiserslautern, Kaiserslautern, West Germany

Günter Borm
Priv.Doz.Dr.rer.nat., Rock Mechanics, University of Karlsruhe,
Karlsruhe, West Germany

SYNOPSIS: A double tunnel of 6.3 m height has been driven in loess underground of low friction and relatively large capillary cohesion. To attain a tunnel climate corresponding to natural underground conditions, earth windows were provided along the side walls of the tunnel.

The portal was supported by steel profiles, anchors and a shotcrete layer. The stability of the retaining construction was ensured by two independent methods. A preexcavation of the tunnel was found to be necessary. The works were performed simultaneously with excavation of the hillside facing the portal. The tunnel lining consists of reinforced shotcrete. The bearing behaviour of the lining was investigated through different finite element analyses assuming both a single tunnel and the double tunnel. For the latter case, a simultaneous excavation as well as successive individual excavations were studied.

The support system of the final tunnel faces is presented. A comparison of both measured and calculated convergences is given. During excavation of the hillside facing the portal a crack occurred in the supported ground. Good agreement was obtained between the observed crack course and the one presumed in the stability analyses.

INTRODUCTION

For the natural storage of wine a double tunnel was constructed in 1984/85 at one of the most famous vineyards of S-Germany at the Kaiserstuhl Mountain. The individual tunnels have a height of 6.3 m and an almost circular crosssection. The length of each tube is about 50 m.

The ground consists of loess with small angles of friction and large capillary cohesion. This cohesion, however, vanishes nearly totally with saturation of the soil.

The primary requirement of the owner was that the climate of the tunnel should agree fairly well with the natural conditions of the ground. In order to achieve this, special earth windows were foreseen at about half of the total area of the side wall.

The design and construction of the tunnels will be reported below. The displacements measured as well as the course of cracks observed during an unplanned state of construction were compared to the design data.

The retaining wall of the tunnel portal consists of anchored and drilled steel sheet piles and of shotcrete. Different failure mechanisms were used for stability analysis. A major effort was made to reduce the number of anchors in the tunnel cross section. As will be shown below, the support can considerably be reduced, if the excavation is carried out by asynchronously advancing tunnel facings. In this case, the retaining wall is subjected to a three-dimensional earth-pressure.

To provide supports for the excavations as well as for the final design of the tunnels, a thin lining of shotcrete was foreseen. The displacements and internal forces of the liner were obtained by finite element analyses. It was found that a system anchoring would have no significant influence on the stability of the tunnel. On the other hand, separate driving of the two tubes would affect substantially the tangential forces and bending moments of the lining. These forces and moments were to be compared with the corresponding values of a simultaneous excavation of both tubes.

The final faces of the double tunnel were supported by anchored concrete beams and shotcrete slabs. Accordingly, the construction was subjected to a three-dimensional earth pressure. To reduce this pressure, it was decided to excavate, in advance, a top heading of 3m length.

The construction of the double tunnel has been supervised. A detailed record of performance of the different stages of excavation is given below.

GEOLOGICAL SYSTEM AND TUNNEL DIMENSIONS

The Kaiserstuhl Mountain is a volcanic massif located in the Upper Rhine River Valley near Freiburg in SW-Germany. The elevation above the bottom of the valley is about 400 m. The hillside is covered with loess, an eolian sediment. Most of the extraordinary warm and sunny hillside is used by vineyards.

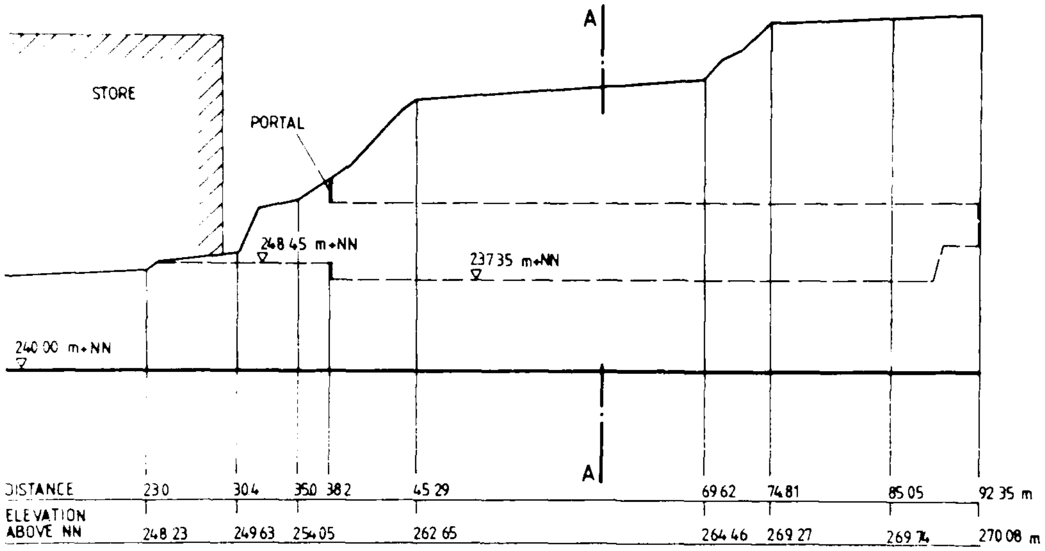
STORE
PORTAL
A
A
248 45 m+NN
237 35 m+NN
240 00 m+NN
DISTANCE
230
30 4
35 0
38 2
45 29
69 62
74 81
85 05
92 35 m
ELEVATION ABOVE NN
248 23
249 63
254 05
262 65
264 46
269 27
270 08 m

Fig. 1 Longitudinal Profile of Double Tunnel

A famous wine producer of that region decided to drive a double tunnel into the Kaiserstuhl as an unique winecellar, where the temperature and humidity agree with the natural conditions of the ground.

The profile of the hillside as well as the contour lines of the double tunnel are illustrated in Fig.1

The cross sectional view A-A of the double tunnel is shown in Fig.2. The floors of both tubes are filled with sand. The thickness of the shotcrete lining is 15 cm. In order to minimize the bending moments, a nearly circular shape is adopted for the tunnels. Radii of distinct circular sections composing the whole cross-section are indicated at the right part of Fig.2.

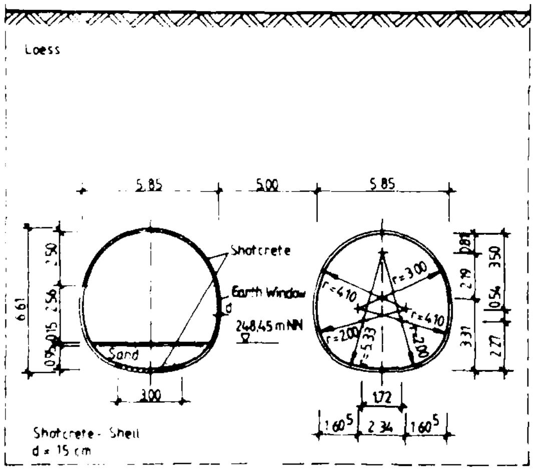
Loess
5.85
5.00
5.85
Shotcrete
Earth Window
248.45 m NN
Sand
3.00
6.61
r=3.00
r=4.10
r=4.10
r=2.00
r=2.00
r=5.33
1.72
1.60⁵
2.34
1.60⁵
3.50
3.31
2.27
Shotcrete - Shell
d = 15 cm

Fig. 2 Cross-Section A-A of Fig.1

Fig.3 shows the layout of the double tunnel. A retaining wall is provided at the portal. The total length of the tunnel is about 50 m.

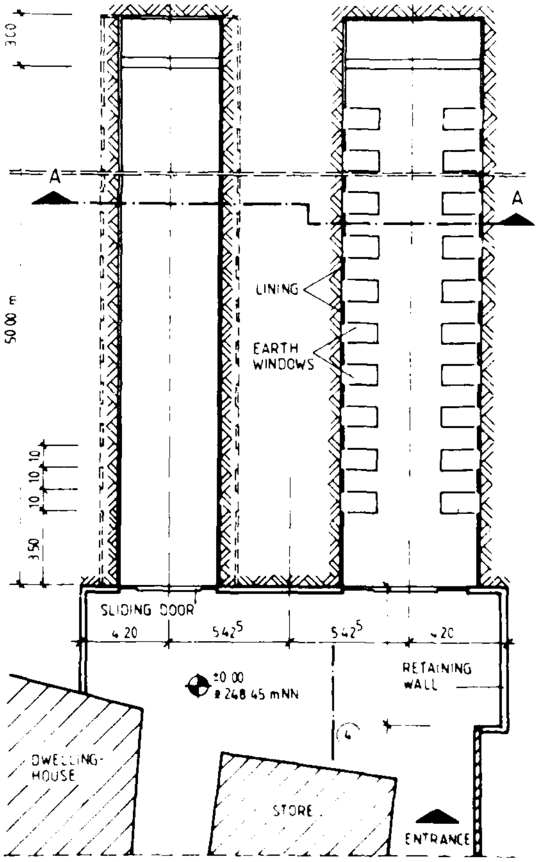
3.00
A
A
50.00 m
LINING
EARTH WINDOWS
10 10 10
3.50
SLIDING DOOR
4 20
5 42⁵
5 42⁵
4 20
±0.00
≙ 248 45 m NN
RETAINING WALL
DWELLING-HOUSE
STORE
ENTRANCE

Fig. 3 Layout of the Double Tunnel

In the right part of Fig.3, the earth windows are shown; they transfer the natural climate of the ground into the tunnel. Each of the earth windows has a width of 1 m; between them lining shells of 1 m width are provided.

SOIL PROPERTIES AND MATERIAL LAW

To obtain both the strength characteristics and the stress-strain behaviour of the soil, triaxial laboratory tests were performed on undisturbed samples. Some of the test results are shown in Table 1.

Table 1. Properties of Loess

Grain Size	d_{10} =	0,003 mm
Grain Size	d_{60} =	0,03 mm
Lime Content	V_{CA} =	34-40 %
Unit Weight	γ =	17,6 KN/m^3
Water Content	w =	17 %
Capillary Cohesion	c =	25 KPa (depth < 6m) 50 KPa (depth > 6m)
Angle of Friction	φ =	21°
Pseudo Elastic Modulus		
for Primary Loading:	E =	10 MPa
for Un- and Reloading:	E =	48 MPa

Analyses concerning the stability of the tunnel lining were performed using the finite element method. In these, the constitutive law for the soil is the one of plasticity. A non-associated flow rule is applied. Strain hardening as well as strain softening are taken into account. The six-fold yield surface used in the three-dimensional stress space is shown in Fig. 4.

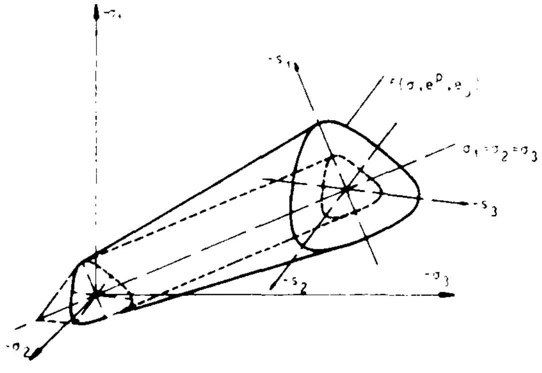

Fig. 4 Yield Surface in 3/D Stress Space

For both, a stress sum $I_\sigma > 0$, and a deviatoric stress path $II_{s,c}^{1/2}$, an elastic material model was used. However, if $I_\sigma < 0$ and $\sqrt{II_s} > \sqrt{II_{s,c}}$, plastic strains occur. The yield function used is given by

$$f = II_s^{1/2} - II_{s,c}^{1/2} - A\,I_\sigma \left(1 - B\frac{III_s}{II_s^{3/2}}\right)^{-m} \qquad (1)$$

where II_S and III_S are the second and third invariants of the deviatoric stress tensor, respectively, and A, B, and m are material parameters depending on plastic strains, stress invariants, and void ratio of the soil. A detailed description of tests necessary to determine the material parameters as well as a presentation of the total plastic model is given elsewhere (Meißner, 1988).

In the present context, only the stress path $\sqrt{II_{SC}}$ is illustrated, which is defined by means of the capillary cohesion c as

$$II_{s,c}^{1/2} = c\left(\frac{(1 + B/\sqrt{6})}{(1 - B\frac{III_s}{II_s^{3/2}})}\right)^m \quad ; \quad B < 0 \qquad (2)$$

According to Eq.(2), the limit of the extensional stress paths is less than that for the compressional stress paths.

For computational purposes, the material parameters of the reinforced shotcrete were adopted as

Elastic modulus	E_B =	15000 MPa
Poisson s ratio	ν_B =	0.25
Unit weight	γ_B =	25 KN/m

Since in the numerical analysis the boundary value problem was restricted to plane deformation, the effect of earth windows in the lining stiffness was taken into account by decreasing the elastic modulus to E_B = 7500 MPa.

DESIGN OF PORTAL SUPPORT AND TUNNEL DRIVING

A plan and a typical cross section of the portal construction are shown in Figs. 5a and 5b, respectively. The retaining structure of the portal consists of steel profiles][300 and reinforced concrete.

Boreholes of 90 cm diameter were provided, and steel profiles were put into them from the surface level. Below the final road surface, the boreholes were filled with concrete, while they were filled with dry sand above this level. The excavation of the hillside was performed thereafter in several steps in the following manner:

1. Excavation until level I (Fig. 5),
2. Construction of the cross girder,
3. Preparation of the anchors,
4. Concreting,
5. Tensioning of the anchors.

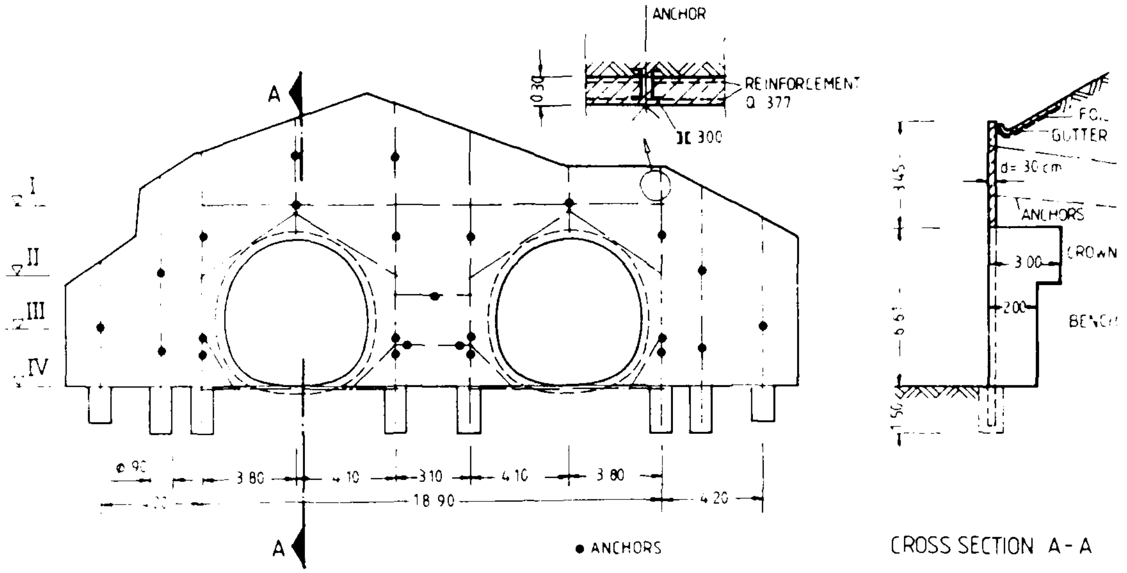
ANCHOR
0.30
REINFORCEMENT
Q 377
][300
A
A
I
II
III
IV
Φ 90
3 80
4 10
3 10
4 10
3 80
18 90
4 20
● ANCHORS
FOIL
GUTTER
d= 30 cm
ANCHORS
CROWN
3 00
200
BENCH
3 45
6 65
1 50
CROSS SECTION A-A

Fig.5 Elevation and Cross-Section of the Portal Support

This sequence was repeated for each level indicated in Fig.5. However, from level II onwards, both the crown and the bench of the tunnel were driven as shown in Fig.5b. Therefore, supporting of the tunnel face was not necessary, and anchoring in the tunnel section could also be avoided. It is self-evident that the anchors in the surrounding of the tunnel wall are spreaded.

The grouting length of the anchors allowed for tension forces of 390 KN per individual anchor and likewise per anchor in a group. Each anchor (System Bilfinger & Berger) consisted of 3 to 5 tendons.

The tunnel excavation was performed using full face heading. An unsupported span of ca. 2m was made possible without risk of loosening of the soil.

Prior to the shotcreting, the tunnel walls were supported by lattice girders spaced 1 m. A lining of 15 cm reinforced shotcrete deemed to be sufficient. However, it was required that the total lining was casted into the cross section within a period of 12 hours.

The final tunnel face was designed as shown in Fig.6. The supporting system consists of both chained beams and anchors. In order to provide a place for winetests as well as to stiffen the base of the crown lining, the choir was covered by a reinforced concrete slab.

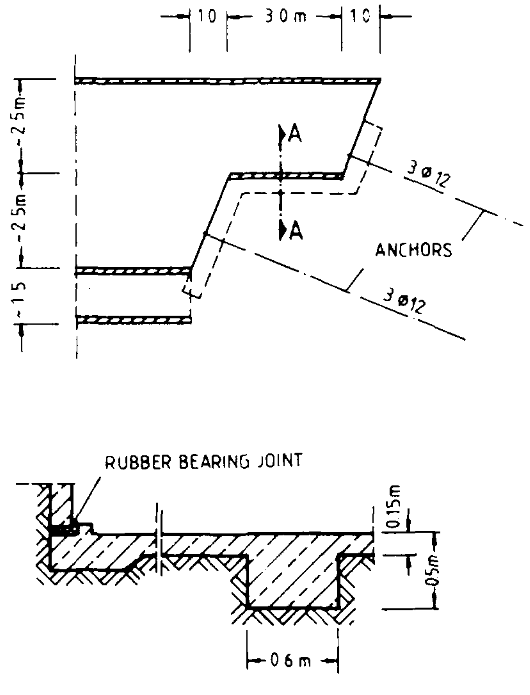
1 0
3 0 m
1 0
2 5m
2 5m
1 5
A
A
3 ø 12
ANCHORS
3 ø 12
RUBBER BEARING JOINT
0 15m
0 5m
0 6 m

CROSS-SECTION A-A

Fig. 6 Supporting System of Final Tunnel Face

EARTH STATICAL ANALYSIS

The supporting system of the portal as well as that of the final tunnel face were designed according to conventional methods.

A major effort was made to reduce the amount of anchors. The layout of the supporting system of the portal is shown in Fig.5.

The distribution of the earth pressure shown in Fig.7 was obtained for a typical cross-section. It was assumed that the capillary cohesion increased from zero at the surface to a total of 25 KPa at the tunnel roof. Below the roof, the cohesion attained 50 KPa. Furthermore, it was assumed that the earth pressure acting on the face of the tunnel pre-cut would completely be transferred through the liner to the steel profiles adjacent to the cross sections.

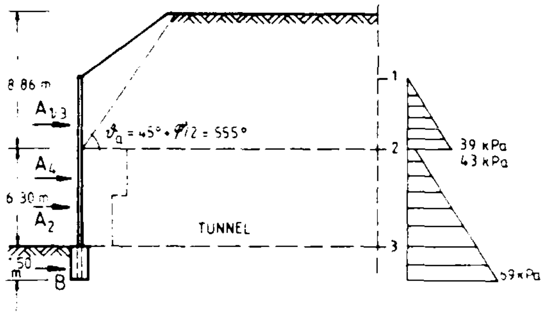

Fig. 7 Loads Acting on the Portal System

For analysis of base and slope failure, different methods were applied. Fig.8 shows the critical slipcircle based on the method of Bishop (1954). The global stability coefficient reads:

$$\eta = \frac{r\sum_i T_i + \sum M_s}{r\sum G_i \sin\alpha_i + \sum M} \tag{3}$$

where T_i is defined by:

$$T_i = \frac{G_i \tan\varphi_i + c_i b_i}{\cos\vartheta_i + \frac{1}{\eta}\tan\varphi_i \sin\vartheta_i} \tag{4}$$

The parameters ϑ_i, G_i, c_i, and b_i of Eq.(8) are illustrated in Fig.8. ΣM_S denotes summation of moments due to the forces acting on the sliding surface.

According to Bishop's theory the actual moments M_S must be divided by η. Hence, the expression for both the anchor forces and resisting earth pressure reads:

$$\sum M_s = r\frac{\tan\varphi}{\eta}\sum_{i=1}^{n} A_i \cos\beta_i \cos\varepsilon_i + E_{pm}\cdot r_E \tag{5}$$

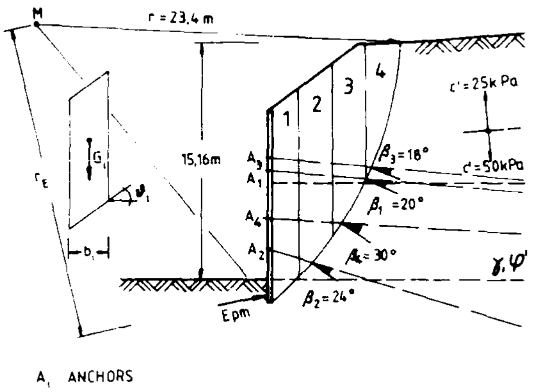

Fig. 8 Critical Slipcircle

In Eq.(5), ε_i denotes the spreading angle of the anchors in horizontal plane. The earth pressure E_{pm} is calculated with the reduced shear parameters defined as

$$\tan(\mathrm{cal}\,\varphi) = \tan(\varphi/\eta_r)$$

$$\mathrm{cal}\,c = c/\eta_c$$

E_{pm} is calculated with regard to three-dimensional state of deformation in front of the embeded length h. Referring to the pile width b, the passive earth pressure for plane conditions is given by

$$E^{*}_{pm} = E_{pg} + E_{pc}$$

The spatial conditions are regarded by the emempirical shape factors

$$\mu_{pg} = 1 + 0.3\cdot h/b \quad \text{and} \qquad \text{where} \quad h/b < 3.3$$
$$\mu_{pc} = 1 + 0.9\cdot h/b$$

Finally, the passive earth pressure is written as

$$E_{pm} = E_{pg}\cdot\mu_{pg} + E_{pc}\cdot\mu_{pe}$$

Obviously, it must be proven in all cases that for a fixed pile distance the three-dimensional earth pressure does not exceed that one of the plane conditions.

The expression ΣM in Eq.(3) denotes the summation of the anchor moments at the center of the slipcircle. Hence,

$$\sum M = -r\sum_{i=1}^{n} A_i \sin\beta_i \tag{6}$$

For the critical slipcircle presented in Fig.8, the stability coefficient yields

$$\eta = 1.32 > 1.30$$

In an additional computation, a failure mechanism consisting of distinct sliding planes was used (Gudehus, 1972). The system is illustrated in Fig.9a; Fig.9b shows both a displacement and a force polygon. To obtain force equilibrium, the failure motive ΔT_{20} is introduced which actually represents the decrease of cohesion c in sliding plane π_{20}. The external work W is obtained by multiplying the weight vectors by the displacement vectors. With respect to the notations of Fig.9, the work W is given by

$$W = G_1 u_{1z} + G_2 u_{2z} + \sum_i A_{iz} u_{iz} - \sum_i A_{iz} u_{iz} \qquad (7)$$

where A_i denote the anchor forces. Furthermore, in the sliding planes $\pi_{1,0}$, $\pi_{2,0}$, as well as in $\pi_{1,2}$, a dissipation work D arises as

$$D = T_{10} u_{10} + T_{20} u_{20} + T_{21} u_{21} + E_{pmh} u_{2x} \qquad (8)$$

In Eq.(8), the forces T_{ij} act within the sliding planes. The values of T_{ij} are computed according to

$$T_{ij} = C_{ij} + Q_{ij} \sin\varphi \qquad (9)$$

Obviously, the dissipation work of ΔT_{20} is not regarded in Eq.(8).

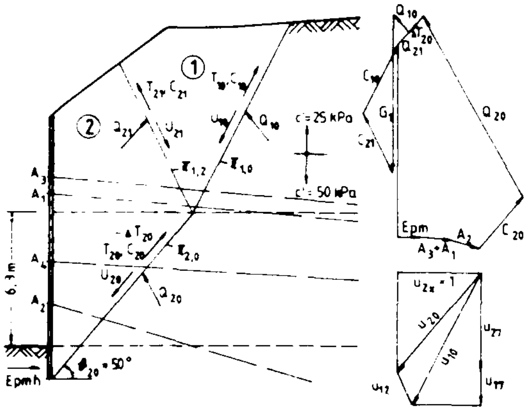

Fig. 9 Composed Failure Mechanism

It is interesting to note, that for the passive earth pressure a separate failure mechanism can be developed. However, for the given situation, an earth pressure as calculated by means of Eq.(8) deems to be sufficient.

The calculations were performed with the actual shear parameters φ and c. Therefore, a stability coefficient η > 1.0 was required.

This stability coefficient is defined by

$$\eta = \frac{D}{W} \qquad (10)$$

where D and W are the parameters calculated in Eqs.(7) and (8).

In terms of the plastic collapse theorems, the calculated external loads are an upper bound of the true collapse ones. Therefore, the failure mechanism must be varied until a minimum value of based on Eq.(10) is obtained. According to the mechanism in Fig.(9) the variational parameter is ϑ_{20} . However, for ϑ_{20} = 55 one obtains:

a. without pre-cut of the tunnels: η = 1,0
b. with pre-cut of about 2,5 m : η = 1,08

Obviously, in connection with the chosen anchor forces, a pre-cut of the tunnels was necessary for a sufficient global stability of the portal support system.

The supporting system of the final tunnel faces is shown in Fig.6. The faces are subjected to the spatial earth pressure. In the calculation, the latter is reduced by the resistance of the core in the bench.
Regarding the dimensioning of the tunnel lining three distinct cases are observed, namely:

1. Excavation of a single tunnel at a time;
2. After excavation of the single tunnel, the second tube is driven;
3. Simultaneous excavation of both tunnels.

Precalculations showed that a system anchoring with nails of 2.5 m length would have no significant influence on the stability of the tunnel. Therefore, it was decided that a system anchoring could be omitted.

A first estimate of the stability of an unsupported tunnel can be obtained by an expression of Kolymbas (1982). Accordingly, the required minimum support resistance p of a tunnel with circular cross-section would be

$$p_i = h \frac{\gamma r (1 - \sin\varphi) - c \cos\varphi}{r(1 - \sin\varphi) + h \sin\varphi} \qquad (11)$$

where h is the height of the overburden, and r is the tunnel radius. Assuming p to be zero, the minimum cohesion required for tunnel stability is given by

$$c_g = \frac{\gamma r (1 - \sin\varphi)}{\cos\varphi} = \frac{17.6 \cdot 3.25 (1 - \sin 21°)}{\cos 21°} = 39.3 \text{ kPa} \qquad (12)$$

Based on this value and on experience with that kind of ground, it could be expected that the stability of the tunnel wall was given at least for a few meters close to the face and at least for some hours. Therefore, it has been decided that the length of the crown heading should be about 2m, and the total lining should be casted into each section within 12 hours.

FINITE ELEMENT ANALYSIS

The numerical analyses were performed by a geotechnical finite element program (e.g. Borm et al., 1976). For the soil, plastic material behaviour was assumed, while for concrete linear elastic behaviour was adopted.

Plastic flow in the shell occurs when the ultimate stress of the concrete is achieved. Only a plane deformation problem was investigated. For this purpose, considering both the influence of the tunnel face and the stiffening time of the shotcrete, a residual lining resistance of 50% was taken into account. Consequently, the shotcrete shell was subjected to forces resulting from the factors mentioned above. However, the presumed lining resistance depends on the displacements arising from the face advance of the tunnel when the concrete shell has already been completed.

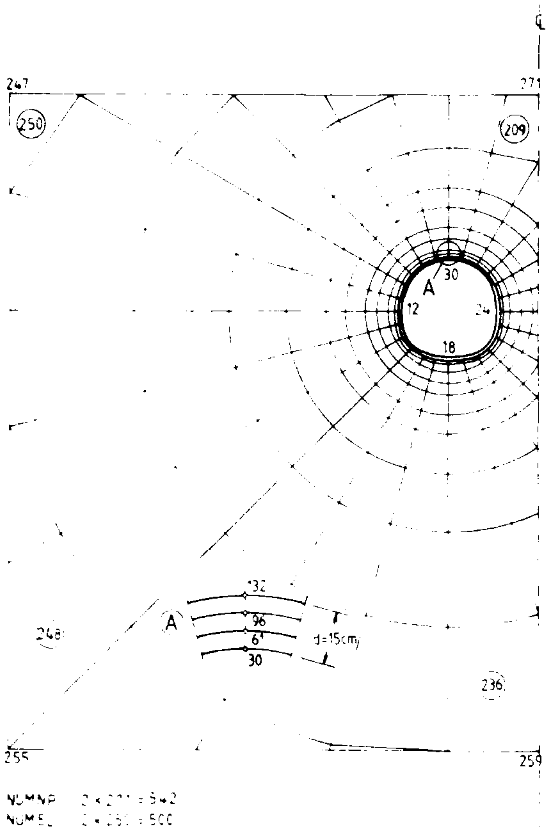

Fig.10 Finite Element Mesh of Left Tunnel

The finite element mesh used is shown in Fig.10. The reference state of stress and strain is the state of rest earth pressure.

Excavation is simulated by stepwise decrease of the balance forces determined for grid points at the surface of the tunnel. After a reduction of these supporting loads to 50%, the elements of the concrete shell were activated.

Simultaneous excavation of the two tunnels was chosen as driving process. The distribution of tangential forces and moments within the tunnel shell are shown in Figs.11 and 12, respectively.

Comparison of the results obtained from variation of both the excavation process and the decreasing factor of initial balance loads showed significant changes in the intersection forces. While the stresses and moments depend approximately on the inverse of the reduction factor, the difference in results obtained for various excavation processes is limited to about 20%.

It can be concluded that the dominant factor in this project is the reduction factor. If extensive three dimensional stress-/strain- analyses are to be avoided, further research work is necessary to determine correct shape factors for plane computations.

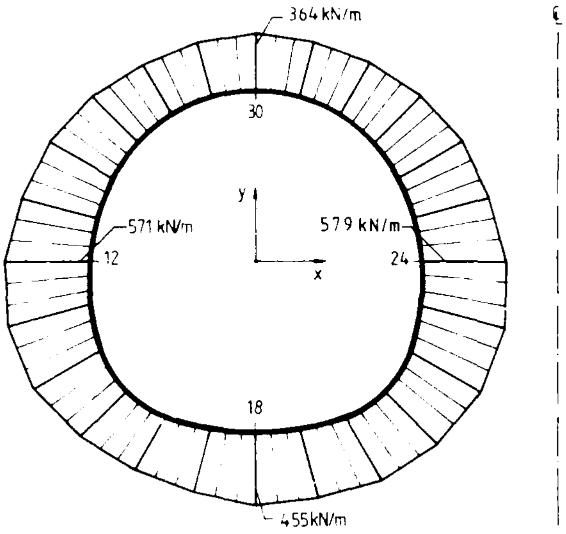

Fig.11 Distribution of Tangential Forces in the Tunnel Lining

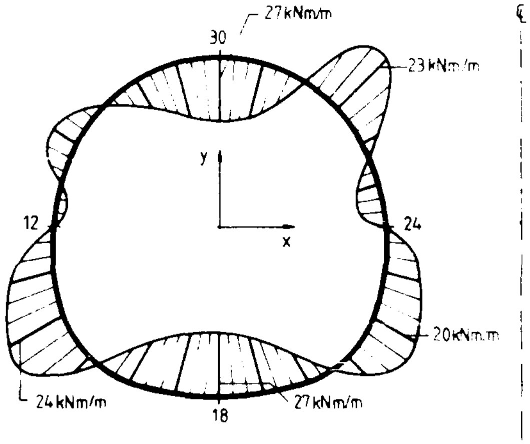

Fig.12 Distribution of Bending Moments in the Tunnel Lining

Actually, both the dimensioning and the reinforcement of the shotcrete were predicted using an assumed reduction factor of 50%. To control the effect of the design data on the stability of the lining in situ, an extensive measurement program as well as some geological profile registrations were executed. As usual in tunneling, convergences of distinct cross sections were determined, where the roof displacements were recorded by use of laser beams.

It was decided that the dimensions of the liner were subject to change if substantial deviation between field data and predictions arose. However, an alteration was finally not needed. The measured maximum convergences of 3 mm were less than the predicted ones of about 8 mm.

CONSTRUCTION PROCESS

Supervision of the construction works was provided as needed. The first visit was made, when both a crack in the tunnel lining occurred and settlements of about 5 cm of the steel profiles were recorded. At that time the hillside facing the portal was excavated.

The design required the installation of anchors in ditches excavated in different levels as illustrated in Fig.5. However, the excavation was actually performed in one step from level II to level IV without installation of the anchors in the corresponding layers. According to Eq.(10), in this case the stability coefficient will decrease to $\eta = 1.0$, i.e., that the limit of the stability of the supporting system has already been reached (see Fig.13).

Though the crack width was only of some millimeters, its development could have been detected easily during the course of excavation. By comparison of the observations with the failure mechanism illustrated in Fig.9, a good quantitative agreement between theory and large scale test is achieved. Moreover, the stability coefficient of $\eta = 1.0$ indicates that the magnitude of the capillary cohesion c has been determined correctly.

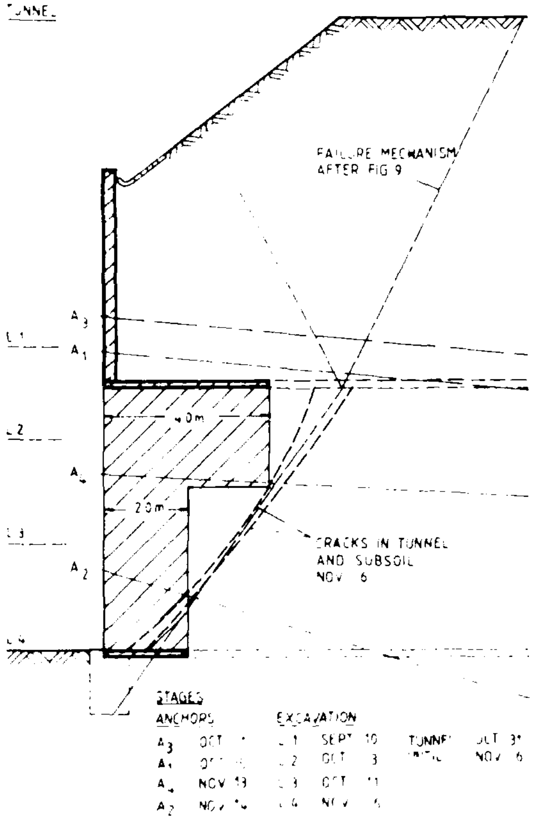

Fig.13 Stages of Construction and Crack Rise

It is well known that a change in magnitude of the cohesion affects the failure mechanism only slightly. Consequently, two independent conclusions could be drawn from the large scale test:

1. The failure mechanism of composed sliding planes described the collapse kinematics realistically;

2. The magnitudes of the capillary cohesion determined by laboratory tests were correct.

The crack was sealed later on in order to prevent seepage of water into the ground. The rate of excavation of the tunnels was about 1.8m per day. A crown heading of 2m span was provided along the total length of the tunnel as well as in sections with heavily fissured material.

Shutter elements were provided in order to protect the earth windows during shotcreting. Except the crack problem, the work has been performed as planned.

CONCLUSION

A double tunnel has been driven into a hillside of loess. The design and the construction process of both the portal and the tunnel are discussed in the present paper. The following conclusions can be drawn from this case history:

1. The capillary cohesion can be taken into account in tunnel construction, if the natural climate of the underground is preserved.

2. For stability analysis of the portal support system, the failure mechanism with composed sliding planes is suitable.

3. Pre-cut of the tunnel section substantially affects the stability of the portal support system. Moreover, in this case anchoring or nailing in the tunnel section may be avoided.

4. A final tunnel face may additionally be supported by an earth core in the bench, if it is possible.

5. For double tunnels, the sequence of excavation of the two tubes affects the intersection forces substantially. In plane finite element calculations, the dominant influence factor on these forces is the assumed residual resistance factor.

   Through this scale factor, both the actually three-dimensional stress state at the tunnel face as well as the time dependent stiffening process of the shotcrete were approached in the plane deformation analyses.

6. With respect to the uncertainty in magnitude of the residual resistance factor, additional research is needed. Otherwise, rigorous three-dimensional computations must be performed for a realistic treatment of the subject.

AD-A213 199 INTERNATIONAL CONFERENCE ON CASE HISTORIES IN 2/8
GEOTECHNICAL ENGINEERING (2..(U) MISSOURI UNIV-ROLLA
S PRAKASH 30 JUN 89 ARO-25645.2-GS-CF DAAL03-87-G-0129
UNCLASSIFIED F/G 13/2 NL

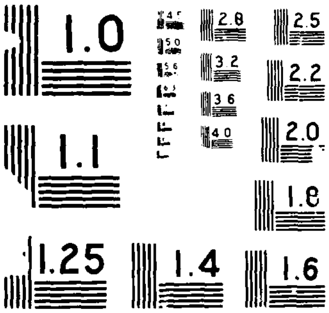
1.0
2.8
2.5
3.2
2.2
3.6
4.0
2.0
1.1
1.8
1.25
1.4
1.6

ACKNOWLEDGEMENT

The double tunnel was built by F. Keller, Oberbergen, W.-Germany. The construction works discussed were performed by the Bilfinger & Berger A.G., Mannheim, W.-Germany. The design of this project and the dimensioning of the reinforced concrete was the responsibility of Ingenieurbüro Fritz, Urach, Germany. The authors gratefully acknowledge participation in that interesting project.

REFERENCES

Bishop, A.W. (1954) "The Use of the Slipcircle in the Analysis of Slopes", Proc., European Conference on Stability of Earth Slopes, V.I Stockholm.

Borm, G., B.Fröhlich, and C.Nabold (1976) "Cost Evaluation of Some Modern Tunnel Design", Proc., Internat. Symposium Numerical Methods in Soil and Rock Mechanics, 367-384, University of Karlsruhe.

Gudehus, G. (1972), "Lower and Upper Bounds for Stability of Earth-Retaining Structures", Proc. 5th European Conference on Soil Mechanics and Foundation Engineering, Madrid.

Kolymbas, D. (1982) "Vereinfachte statische Berechnung der Firste eines Tunnels in massigem Fels", Rock Mechanics 14, 201-207.

Meißner, H. (1988) "Ground Movements by Tunnel Driving in the Protection of Frozen Shells", Proc., 6th International Conference Numerical Methods in Geomechanics. G.Swoboda (ed), A.A.Balkema, Rotterdam.

Proceedings: Second International Conference on Case Histories in Geotechnical Engineering, June 1-5, 1988, St. Louis, Mo., Paper No. 5.15

Evaluation of the Effect of Saturated Silty and Fine Sand Foundation Improved by Vibro-Flotation in Seismic Area

Wang Yuqing
Senior Research Engineer, the Central Research Institute of Building and Construction, MMI, Beijing, China

Qiao Taiping
Deputy Chief Engineer, Basic Construction Office CCP of Shanxi Province, Taiyuan, China

Zhang Weiquan
Engineer, the Central Research Institute of Building and Construction, MMI, Beijing, China

SYNOPSIS: The improvement of liquefaction foundations in seismic region has been concerning many engineers. The authors had carried out experimental studies on the improvement of saturated silty and fine sand foundtions at the suburbs of Beijing by vibroflotation method. The test results are described and the improvement effects are evaluated in this paper.

INTRODUCTION

Numbers of seismic disasters Liaonan, Tangshan, Tanjing as well as those abroad indicate that structure on loose saturated sand foundation had failed occasionally due to foundation liquefaction. Methods, both analytical and experimental, for evaluating liquefaction potential of liquefiable foundation have been well developed in the past twenty years. However, the measures for treating liquefiable soil deposit have not achieved so much progress. Among the common measures preventing sand liquefaction, vibroflotation is one of the adequate methods and has experienced a number of earthquakes. However, the mechanism of vibroflotation, the evaluation of its improvement effects and the criterion of aseismic design and analysis of vibroflotation improvement have not been understood very well. In engineering practice the design parameters are often determined by in-situ tests which have been proved very expensive. Therefore, it is quite necessary to raise the understanding for the vibroflotation mechanism, improve the design and construction methods and properly evaluate the vibroflotation effect through a great number of experiment research both in situ and laboratory. The authors had carried out vibroflotation tests in three experimental sites at the suburbs of Beijing including the in-situ measurement of soil dynamic response during vibroflotation, standard penetration test before and after vibroflotation improvement and static loading test. The conclusions of these three test are described.

EXPERIMENTAL SITES AND TEST METHODS

Sites.

The experimental sites locate at the southeastern suburbs of Beijing with subsoil layers of loose sand. Within 10m under the ground surface is mainly silty fine sand intercalated with cohesive soil intercalations of various thickness and consists of sand of about 30m thick, free water surface 1-3m. The silt fraction in the surface silt and sand is less than 10%, coefficient of uniformity less than 5, mean diameter D50 about 0.1mm, natural relative density 50-55%, standard penetration test blow count less than 10 within 8m under ground surface. The seismic intensity of the sites is VIII. The foundation is considered liquefiable according to the criterion of Chinese code. The subsoil profiles are shown in Fig. 1.

Test Methods.

The soil dynamic response (acceleration and excess pore water pressure) are mainly measured in site A and the routine soil tests (bearing test , standard penetration test and static cone penetration test) were made in site B and site C.

The ZCQ--II vibroflot was employed with exciting force of 7t and 10t. The soil dynamic response during vibroflotation was measured by two methods : (1) Single hole vibrating with measurement done at different distances form the hole. (2) The measuring devices were fixed at certain spots with vibroflotation from distance approaching the measuring spots. The data measured included ground surface acceleration of three directions X,Y,Z, soil acceleration and dynamic pore water pressure.

TEST RESULTS

The Variation of Ground Surface Acceleration.

Fig.2-5 show the ground surface acceleration at different distance from the different depth. It can be seen that the surface acceleration attenuated with the increase of the measuring distance and the attenuation may law be approximately expressed by exponential function. The measuring records showed that the vibration energy of the vibroflots distributed within soil in a wave form with larger amplitude in all X,Y and Z directions.

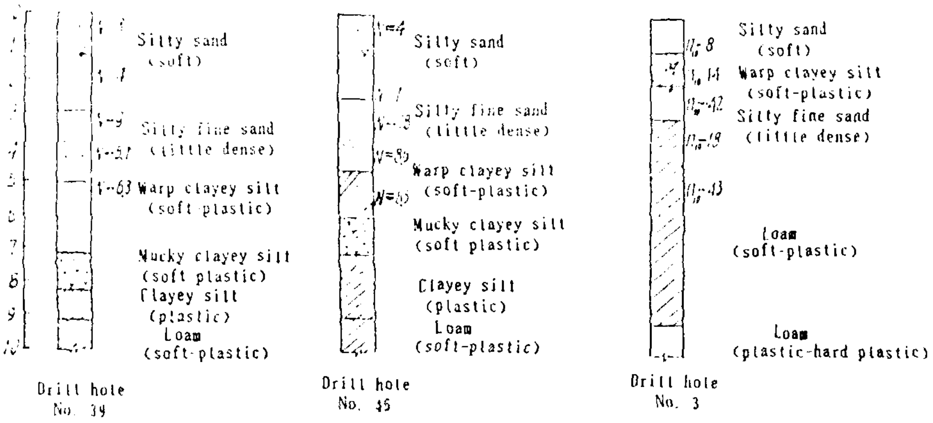
Silty sand
(soft)
Silty fine sand
(little dense)
Warp clayey silt
(soft plastic)
Mucky clayey silt
(soft plastic)
Clayey silt
(plastic)
Loam
(soft-plastic)
Drill hole
No. 39
N=4
Silty sand
(soft)
Silty fine sand
(little dense)
Warp clayey silt
(soft-plastic)
Mucky clayey silt
(soft plastic)
Clayey silt
(plastic)
Loam
(soft-plastic)
Drill hole
No. 45
Silty sand
(soft)
Warp clayey silt
(soft-plastic)
Silty fine sand
(little dense)
Loam
(soft-plastic)
Loam
(plastic-hard plastic)
Drill hole
No. 3

Fig. 1 Profiles of experimental sites
N standard penetration blow count n_u: sounding blow count

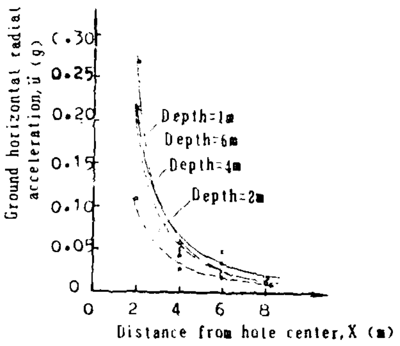

Fig. 2 Distribution of ground horizonal radial acceleration nearby the vibroflotation hole (site B)

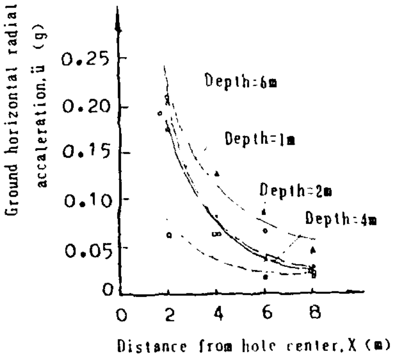

Fig. 3 Distribution of ground horizontal radial acceleration nearby the vibroflotation hole (Site c)

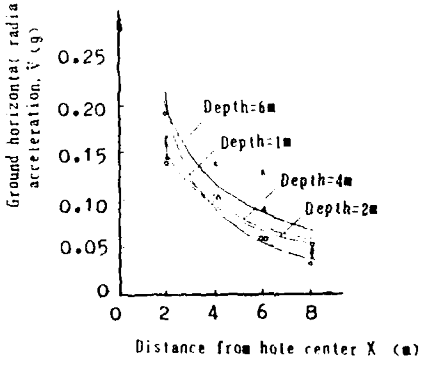

Fig. 4 Distribution of ground tangential acceleration near by the vibroflotation hole (Site C)

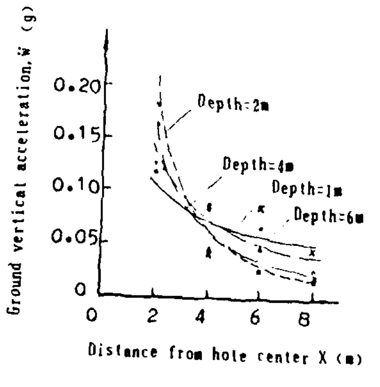

Fig. 5 Distribution of ground vertical acceleration near by vibroflotation hole (Site C)

The Variation of Dynamic Pore Water Pressure and Acceleration in Soil.

Fig. 6 shows the relationship between the excess pore water pressure at 2m below ground surface and the distance from the vibroflot hole during vibroflotation. Due to the difference of the soil properties in the two sites, the pore water pressure measured at site A and site C were somewhat different while the attenuation laws of excess pore pressure and acceleration were basically consistent. Fig. 7 has shown the histories of the horizontal radial acceleration and excess pore pressure at 2m deep below ground surface when the vibroflot penetrated uniformly into 6m deep and than drew back to the ground surface. It can been seen that the acceleration and excess pore pressure in soil 0.875m away from the center of vibroflotation hole reached maximum (amax=0.35g, umax=0.32kg/cm², pore pressure ratio u/σ_v =0.99) and the soil completely liquefied when the vibroflot penetrated 3m deep into the ground. However the pore pressure ratio 1.05m away from the hole center was only 0.48. It can be thus concluded that the liquefaction range located within 0.875-1.05m from the center of vibroflot hole in the C site condition during vibroflotation operation. Pore water pressure ratio at 2m deep maintained high during the process of continuing penetration and drawing back to the ground surface without filling.

Ground Acceleration and Excess Pore Pressure before and after Vibroflotation Improvement.

The changes of horizontal radial acceleration of ground surface in site B before and after vibroflotation improvement are demonstrated in Table 1.

Table 1. Ground Surface Acceleration Changes before and after Vibroflotation Improvement (g)

Distance m	Measuring spot	Vibroflotation time (sec.) Begin	10	30	60	120
4.6	before vibroflotation	.019	.027	.031	.031	.039
4.6	between piles	.129	.105	.105	.116	.129
4.6	pile top	.172	.172	.172	.164	.140

The excess pore pressure changes in site A before and after vibroflotation improvement are shown in Table 2.

Table 1 and Table 2 show that after vibroflotation the ground acceleration increased while the excess pore pressure reduced remarkably, while indicate that the vibration of vibroflots had made the surrounding soil denser and the pile-soil composite foundation stiffer.

Table 2. Pore Pressure Ratio before and after Vibroflotation

case	Distance (m)	2m below A pore ratio	2m below A press. (KPa)	2m below B pore ratio	2m below B press. (KPa)	3.6m Below B pore ratio	3.6m Below B press. (KPa)
I	8.6	0.90	4.5	1.25	3.6	3.65	4.0
	8.6	0.20	4.5	0.35	3.6	0.90	4.0
II	5.9	2.10	10.	2.50	12.	5.90	5.9
	5.9	0.20	10.	0.20	12.	1.00	5.9
III	3.6	4.20	4.2	5.00	3.5	12.60	3.6
	3.6	1.00	4.2	1.40	3.5	3.50	3.6

* In each case, the first and the second line are the data before and after vibroflotation respectively.

Effects of Foundation after Vibroflotation Improvement [1].

The P-S curves of bearing test before and after vibroflotation improvement are shown in Fig. 8 Foundation allowable bearing capacity are listed in Table 3. It can be seen that the bearing capacity after vibroflotation improvement had increased by more than 60%, the deformation had reduced by 1/3--2/3 and the allowable bearing capacity of the pile--soil composite foundation had multiplied more than 2.3 times.

The results of static cone penetration test are shown in Fig. 9 which indicates that the effects of vibroflotation were unremarkable in the surface layer, sandy loam intercalation and mucky soil but remarkable if the bearing stratum was fine sand, Ps average value tripled. The standard penetration results were roughly consistant with those of static cone penetration test. The blow count in fine sand might raise from 7.6 before vibroflotation to the maximum of 24 after improvement, relative density Dr to 85% [1].

Table 3. Bearing Test Results before and after Vibroflotation

Type			Allowable bearing capacity [R] and compression modulus Es [R] (KPa)	Es (KPa)
soil	No.1	B*	196.13	8727.90
		A*	319.70	14808.04
	No.2	B*	171.62	9316.32
		A*	317.74	15690.64
pile	NO.1		588.40	26576.02
	No.2		661.95	29616.08

B*: before vibroflotation
A*: after vibroflotation

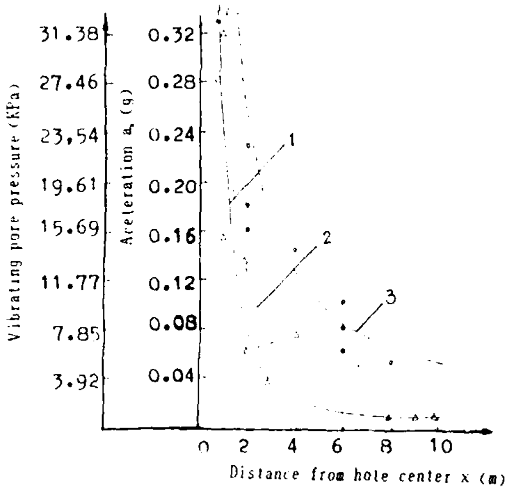

Fig.6 Distribution of vibrating pore pressure at 2m depth

1. Pore pressure in site C
2. The measured pore pressure in site A
3. The average of acceleration a,

o The average of aueajured a, in site C

△ The measured pore pressure P in site C

• The horizontal radial acceleration at the depth of 2m in site C

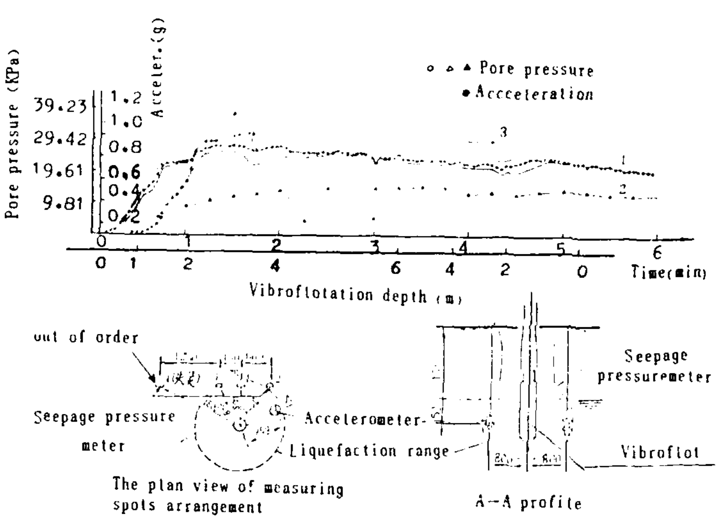

Fig.7 Variation of acceleration and pore pressure within soil

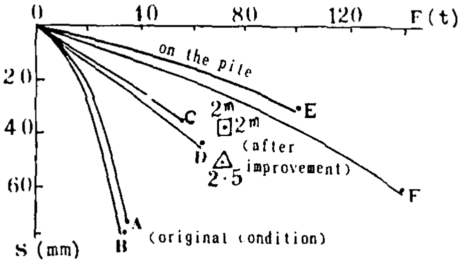

Fig.8 Bearing test results before and after vibroflotation improvment

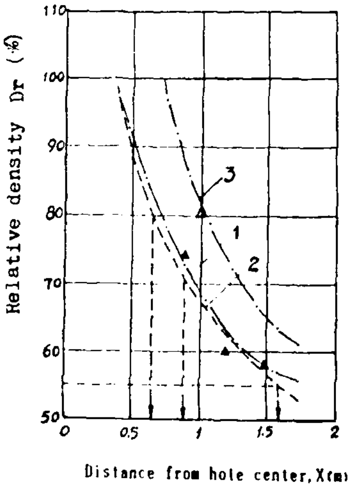

1. D'appolonia's single pile curve. (D_r is the average of these at 1.2, 1.8, 2.5m depth)
2. D'appolonia's densified curve, distanse between holes 2.44m .
3. D'appolonia's densified curve, distance between hole 1.83m .

▲ Predicted according to the single pile in Dongfang Chemical plant, Beijing (D_r is the average within 1~4 depth)

△ Data from Dongfang Chemical Plant, Beijing, distance between holes 1.80m .

Fig.9 S.C.P. test results before and after vibroflotation

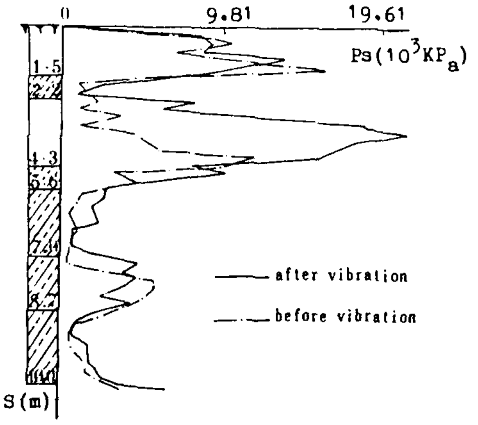

Fig.10 Relationship between distance and relative desnsity of sand surrounding the piles

EVALUATION OF SOIL LIQUEFACTION RESISTANCE AFTER VIBROFLOTATION IMPROVEMENT

Densification Effect.

According to the test results the sand within 0.5 m radius from the center of vibroflotation hole had completely liquefied subjected to vibroflotation by 10t ZCQ--II and consequently densified significantly under the composite function of vibroting force, confining pressure and the vibrating compacting of fillings. The soil 0.9m away from the hole center, despite influenced remarkably by vibration did not reach liquefaction condition. It can be assumed therefore the density of the surrounding soil decreased rapidly with the increase of the distance from the holes.

In order to evaluate quantitatively the changes of density in sand after gravel pile improvement, D'appolonia [2] assumed the density curves of soil surrounding single pile as shown in Fig. 10. The vibroflotation test results in a chemical plant in Beijing are also shown in the figure, which are more or less conformable with D'appolonia's. Accordingly, from the point of view of liquefaction resistance, the effective range of vibroflotation improvement should be predicted in the light of the anti-liquefaction critical relative density of sand in various countries and regions. According to the creteria suggested by Engineering Mechanics Institute, SINICA, the anti-liquefaction relative density of sand Dr is 50%, 70% and 80% for the earthquake intensity zone VII, VIII and IX respectively. The effective improvement range surrounding single pile to resist liquefaction may be obtained from Fig. 10 as 1.6m for seismic intensity zone VII, 0.9m for VIII and 0.66m for IX. The effective range should be enlarged moderately when pile group effect is considered [3].

Dranage Effect of Gravel Piles.

After vibroflotation improvement the sand surrounding vibroflotation holes had densified, the foundation stiffness enhanced and the excess pore water pressure lowered obviously. It was known through in-situ data that all of the recorded excess pore pressure had reduced more than 3.5 time after locating the gravel piles. During actural earthquake the percolation path would be shortened due to the location of gravel piles, which makes the excess pore pressure induced by earthquakes dissipate easier and consequently decreases the soil liquefaction potential.

Effect of Pre-vibration.

The laboratory tests indicated that the liquefaction resistance of sand foundation may be increased after being subjected to vibrations [4]. The vibroflots operated by vibration force of 10t were generally arranged within distance less than 2.5m. the ground acceleration 2m away from vibroflots was 0.27g and 0.019g for those 8m away, which means that the surrounding soil would undergo times of previbratings for some dozens of minutes during the whole operation. These previbrations would be beneficial to decreasing liquefaction potential.

The Influence of Vibroflotation Operation on the Nearby Building.

The influence of vibroflotation operation on the nearby buildings depends upon the magnitude of vibration force, site condition and the allowable vibration standard of the building. The test records in this site shows that the minimum safety distance for common building should be more than 5m when 10t ZCQ--II vibroflots are employed [5].

CONCLUSIONS

The following conclusions could be drawn from this study:

1. Before and after the vibroflotation, the dynamic response of soil foundation appears remarkable difference during the action of the same vibration force. Comparing the gravel pile-soil composite foundation improved with the nature foundation, as its enhanced stiffness and shortened percolation path, increased vibrating acceleration, reduced dynamic strain and the excess pore water pressure in the soil layer lowered more than 3.5 times for the composite foundation.

2. Under the condition of applied vibroflot the effective improving radius (from the center of the pile) of anti-liquefaction around the single-pile are 1.6m, 0.9m and 0.6m with the earthquake intensity of VII,VIII and IX, respectively.

3. Modification should be taken when the application of the influence coefficient curves proposed by D'appolonia,E to evaluating the relative density of the center of piles group.

4. After vibroflotation. the measured N-value of loose saturated silty and fine sand layer is higher than the liquefaction critical value Ncr of earthquake intensity VIII. the bearing capacity of soil between the piles is 60% more and the composite foundation is 2.3 times more than natural foundation, the compressing a modulus Es increases 50-70%.

5. Since the soil properties have taken place considerable changes after improvement of vibroflotation, the effect of the soil parameter change must be considered in seismic response analysis when the large area foundation improved by the vibroflotation.

REFERENCES

[1] Han, Z.Q. (1977), "Soft and Liquefiable Foundation Improvement by Vibroflotation Method",Proceedings of the Third Conference on Soil Mechanics and Foundation Engineering, China Civil Engineering Society, Held in December, 1979,Hangzhou, China,pp270-277.
[2] D'appolonia,E, "Loose Sands-Their Compaction by Vibroflotation", Symposium on Dynamic Testing of Soils.
[3] Wang Yuqing,Qiao Taiping and Zhang Weiquan, (1981), "Dynamic Response of Ground during Reinforcing it with Vibroflotation", Selections of Conference on Foundation Treatment in 1980, Chinese Architectural Society, Committee of Soils and Foundations,1981.

[4] Seed H.B.Mori E. and Chan C.K. (1975), "Influence of Seismic History on the Liquefaction Characteristics of Sands", Report EEEC-- 75-25, EERC, Univ. OF California, Berkeley.

[5] Wang Yuqing and Zhang Weiquan, (1981) "Effect of Vibroflotation Operation on the Environment Buildings, Metallurgical Architecture", 1981, No.5.

Proceedings: Second International Conference on Case Histories in Geotechnical Engineering, June 1-5, 1988, St. Louis, Mo., Paper No. 5.16

Dynamic Compaction—An Unusual Application

Byongmu Song
Civil Engineer, U.S. Army Corps of Engineers, San Francisco, California

Michel Gambin
Ingénieur Civil, Solentanche, Nanterre, France

SYNOPSIS: The site for the U.S. Air Force 750-bed medical contingency complex which is located approximately 10 miles west of Pusan, Korea is geotechnically adverse. Approximately 30 feet of saturated loose fine sand overlies about 180 feet of Pleistocene fluvial and marine sediments. The upper 90 feet of Pleistocene sediments are in a state of under-consolidation, and moisture contents are generally higher than the liquid limits with SPT N values of about three. 30 feet of loose sand was densified by dynamic compaction and the test results indicated that foundation performance satisfied the contract specifications. A considerable economy, in both cost and time, was achieved.

INTRODUCTION

The 750-bed U.S. Air Force medical contingency complex is currently being constructed on a geotechnically adverse site approximately 10 miles west of Pusan, Korea. The site is located within a polder with approximate plan dimensions of nine miles (N-S) by three miles (E-W). The complex consists of eight single story buildings with steel frame and pre-engineered walls and roofs (about 240 feet by 50/60 feet in plan dimensions) and a main building (approximately 240 feet by 360 feet) located in the central area. The entire complex is located in a site with plan dimensions of about 600 feet by 940 feet. The maximum column loads are about 47 kips for the main building and 18 kips for the other buildings.

The cost and technical difficulties precluded the use of concrete piles. Within the loose sand layer and very soft cohesive layers, concrete piles would often fall without control upon the impact by a pile driving hammer rendering splicing operation to be impractical. The dynamic compaction method was adapted and resulted in a considerable economy in both cost and time.

GEOTECHNICAL DATA

In order to explore the site subsurface conditions, 38 borings were initially placed throughout the site. Existing ground surface was at an elevation of about eight feet above the Mean Sea Level and groundwater table was encountered at a depth of about two feet. The entire surface of the polder is used for rice growing. Consequently, the top one to five feet of soil was a very soft silty material (ML) which was to be removed and replaced. Bedrock is believed to be at a depth of about 210 feet below the existing ground surface, and all materials above bedrock are considered to be Pleistocene and younger sediments. The subsurface materials may be described as about 30 feet of loose fine sand with occasional silt/clay lenses (SPT N value ranges from two to 12) overlying approximately 90 feet of a very soft sandy clay layer with the SPT N average of about three. The sediment is in a state of under-consolidation and has moisture

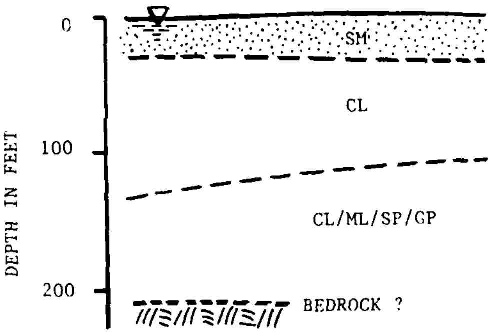

FIGURE 1. GENERALIZED SUBSURFACE SECTION

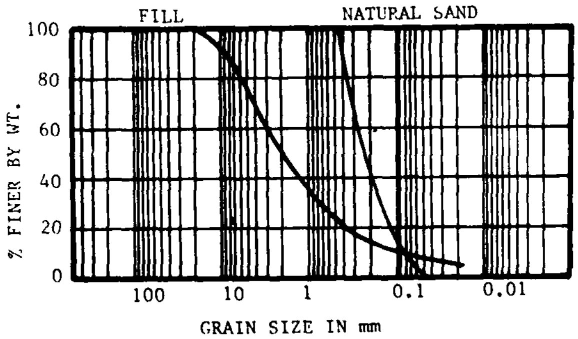

FIGURE 2. GRADATION CURVES

contents generally higher than the liquid limits. Approximately 90 feet of relatively good silt/clay/sand/gravel layers were encountered below the very soft sandy clay layer. The site subsurface condition is presented on Figure 1. Grain size distribution for the top sand layer and fill material is presented on Figure 2. The site subsurface conditions are relatively uniform except for minor variations in the thickness of cohesive lenses. In one area (B3-176), however, the thickness of soft material was greater and a special treatment was provided in this area in order to maintain the uniformity.

SOIL IMPROVEMENT

The proposed structures are relatively light and could tolerate some settlement and differential settlement. However, several factors which were adverse indicated that the existing foundation conditions, without modifications, would not provide the necessary support for the proposed structures. The adverse factors considered were: 1) Presence of a loose and wet top sand layer; 2) About 90 feet of very soft sandy clay layer immediately beneath the top sand layer; 3) Long and narrow configuration of the proposed structures; and 4) Heterogeneity of the top sand layer with respect to SPT N values and consequent potential differential settlement.

Two basic methods were considered: 1) Pile foundations with structural slabs; and 2) Densification of the top sand layer including fill material and slab-on-grade. Piles would have to be very long, and during the installation, piles would often "run" without control, and splicing of piles would present a formidable obstacle. There are more than 400 columns with axial loads ranging from 18 kips to 47 kips. The allowable axial load of a 350-millimeter concrete pile is 132 kips. More than half would be 18-kip columns. This is considered uneconomical and impractical. The dynamic compaction method developed by Louis Menard is now well known (Mitchell, 1981). Taking into consideration the various case-histories which can be found in the open literature, the U.S. Army Corps of Engineers, Far East District envisaged that the top sand layer and fill materials could be densified to the desired degree by dynamic compaction. The energy per unit area was estimated to be 300 t-m/m^2, and the specialist contractor was requested to perform a pilot test to verify the initial design assumptions. A considerable economy in both cost and time was achieved by the selection of the dynamic compaction method over the pile foundations with structural slab.

The densification criteria used for the top sand layer were:

1) The allowable bearing capacity within the treated area at depths up to 6.5 feet below the bottom of footings at any location shall be at least 1,500 pounds per square foot with a factor of safety of three. Computations will be based on a footing size of 6.5 feet by 6.5 feet in plan dimensions;

2) Total settlement at any location within the treated area shall be less than one inch under a loading intensity of up to 1,500 pounds per square foot on a footing size of 6.5 feet by 6.5 feet in plan dimensions; and

3) Differential settlement between the footings within the treated area shall be less than 0.002L where L is the distance between the footings.

Bearing capacity and settlement/differential settlement characteristics were to be evaluated by SPT, plate bearing tests, settlement gages, and other means. For the acceptance of DC work at the site, the following criteria were to be met initially:

1) For the depth 1B below the bottom of the footing (B is the width of footing), N shall not be less than 15;

2) From the depth of 1B to 1.5B, N shall not be less than eight; and

3) For the depth greater than 1.5B, N shall be greater than five. Settlement was to be measured and recorded continuously by six settlement gages.

PILOT TEST

Before dynamic compaction production could start, there had to be a test section to check the validity of the values taken for each tamping parmeters at the design stage, such as:

- weight of pounder,
- height of fall,
- pounder surface area,
- spacing of print centers,
- total energy per unit area,
- excess pore water pressure dissipation time lag.

As a matter of fact, there can be various types of test sections. On a routine type of job, a test section will only include visual observations of soil response to impacts in a 9-print-square-area, so as to check adequacy of print center spacing and pounder surface area. This test is performed at the start of each pass or coverage. This is necessary to evaluate the energy loss which appears as peripheral heave around the prints and to help take steps to decrease this loss as shown on Figure 3.

In the case of unusual soil, the test section can be a full size pilot test area carried out until obtaining the acceptance test values, just as in a preloading pilot test exercise.

For the medical contingency complex soil treatment project, the contract specified that the total energy had to be 300 t-m/m2 unless the specialist contractor could demonstrate that less energy could meet the acceptance criteria. Then it was necessary to complete the treatment on a representative pilot test area. This area must be of the right size so as to yield satisfactory results. Taking into consideration the energy distribution at depth below impact centers, for a 30-foot thick

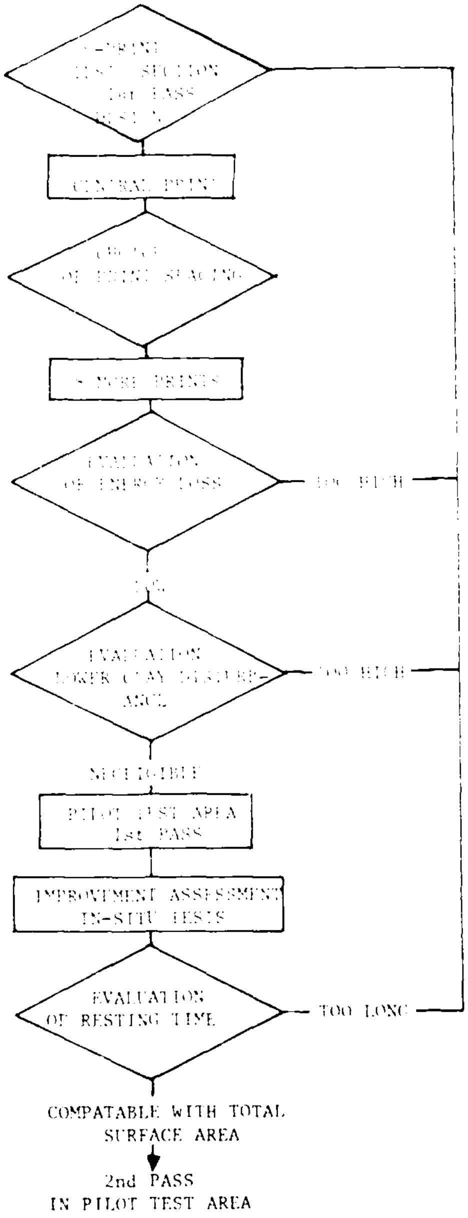
CENTRAL PRINT
CHOICE OF PRINT SPACING
8 MORE PRINTS
EVALUATION OF ENERGY LOSS
TOO HIGH
EVALUATION LOWER CLAY DISTURBANCE
TOO HIGH
NEGLIGIBLE
PILOT TEST AREA 1st PASS
IMPROVEMENT ASSESSMENT IN-SITU TESTS
EVALUATION OF RESTING TIME
TOO LONG
COMPATABLE WITH TOTAL SURFACE AREA
2nd PASS IN PILOT TEST AREA

FIGURE 3. TYPICAL PILOT TEST FLOW CHART

layer to be treated, the test pad must be at least 105 x 105-foot in size and conclusive tests must be taken within the center 35 x 35-foot square area.

The pilot test area will be successively subjected to the same number of passes as the main project. The trial was based on a reduced energy level, as proposed by Solentanche-Pumyang design office and included a first coverage with 10 drops followed by a second one with 2 drops. Plan lay-out of the test section area is shown on Figure 4. Spacing of the first pass impact prints was chosen between 20 and 25 ft, to match the proposed building columns pattern and the spacing of the second pass was estimated to be half way. First coverage was undertaken on Thursday 11 Nov 86. Soil response was observed at each print location by recording crater depth (Figure 5) and volume as well as possible surrounding ground surface heave by leveling 4 series of pegs (Figure 6). To measure excess pore water pressure as well as its dissipation period and to check that the

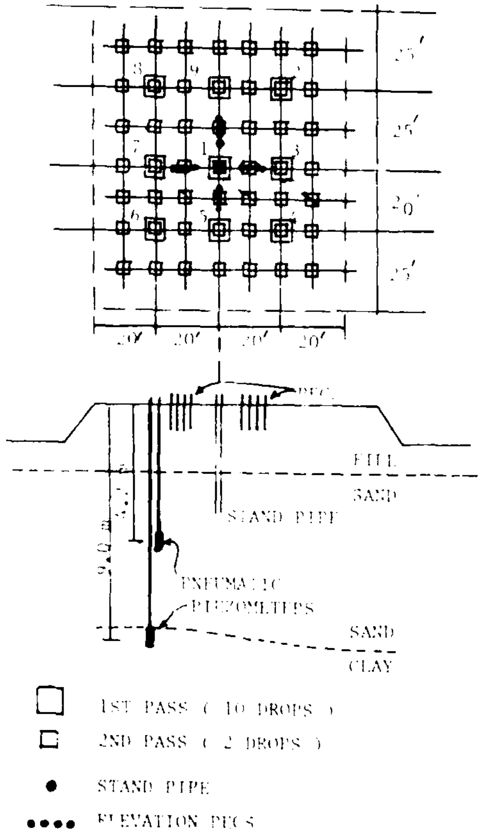
25'
25'
20'
25'
20'
20'
20'
20'
PEG
FILL
SAND
STAND PIPE
9.0 m
PNEUMATIC PIEZOMETERS
SAND
CLAY
1ST PASS (10 DROPS)
2ND PASS (2 DROPS)
STAND PIPE
ELEVATION PEGS

FIGURE 4. PLAN AND CROSS SECTION PILOT TEST AREA

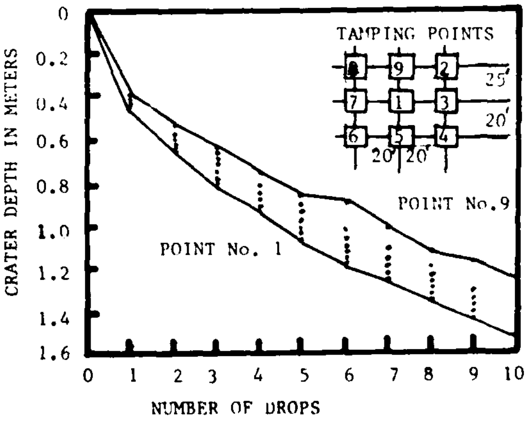

FIGURE 5. CRATER DEPTH vs NO. OF DROPS

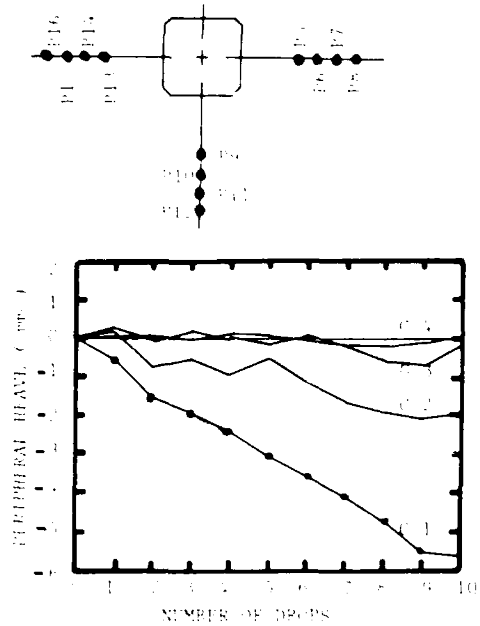

FIGURE 6. PERIPHERAL HEAVE vs NUMBER OF DROPS

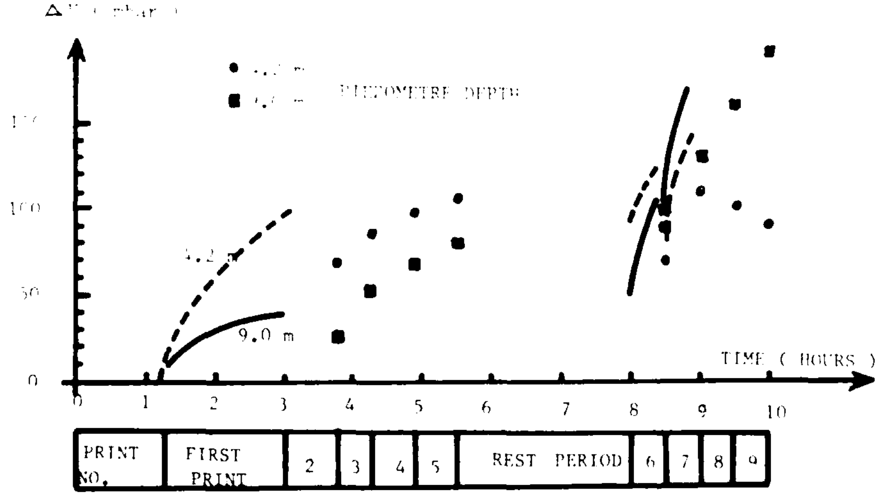

FIGURE 7. TREND OF Δu WITH TIME (FIRST PASS IN NINE POINT SECTION)

underlying clay layer was not disturbed during treatment, several piezometers were installed in one of the pre-treatment S.P.T. borehole (Figure 4). As it can be seen, depth of crater was evolving in a similar way for each tamping center and no heave at all of the surrounding ground was observed either close to the tamping crater or at a distance. However no real "refusal" was observed after 10 blows which was considered as corresponding to the optimum energy to be applied during the first pass. The trend of the excess pore water pressure, Δu, build-up and dissipation is more difficult to visualize as there are three variables, the energy applied, the time elapsed between blows and the distance between the impact center and the piezometers. Figure 7 shows the recorded Δu versus time for the 2 piezometers at 4.2 m in a more clayey pocket within the natural sand and 9 m, slightly embedded in the underlying clay. Dotted and solid lines gives Δu trend recorded immediately after each blow in the same print. These specific observations were only taken for the first print and for prints #6 and #7 closest to the piezometers. Circles and squares give Δu after completion of each print, say, one minute later. One can understand there may already be a drop in the excess pore water pressure (see points #6 and #7 for instance). It is also interesting to point out that final Δu for points #1 and #5 which are similarly away from the piezometers give almost the same final value at 4.2 m of depth.

One of the major features of the test is the trend of the last readings. For more distant impacts (#8 and #9), Δu decreases in the sandy layer due to some pressure dissipation between tamping periods and increases in the clay layer due to lack of pressure dissipation during tamping intervals.

Finally it must be recongnized that the next morning, at 4.2 m of depth Δu was only 30-millibar and at 9 m Δu = 0. Consequently, if necessary, a second pass could follow first pass within a few days.

The 9-print test showed that:

1) At leat 10 drops can be applied at each print with no distress of the underlaying clay layer. This was later confirmed by S.P.T. tests;

2) There is no heave around prints and between prints when applying 10 drops in prints as long as the spacing varies between 20 and 25-foot; and

3) The excess pore water pressure which may develop in more clayey pockets occurring in

the sand layer dissipates within 36 hours. As a matter of fact, the second coverage was carried out on Monday 15th September with 2 drops at 10 and 12.5 foot centers.

"Quality control" S.P.T. tests were performed the next Monday. Results are shown on Figure 8. Although the average values fulfill the requirements, some individual N values between the 2 and 3 m depths were lower than the acceptance specifications. Consequently, new tests were carried out in mid-November in the pilot test area. These results are also shown on Figure 8. As usual (Mitchell 1984), one can see a large improvement which cannot solely be explained by the fact that this area received additional vibrations during the production job. This leads to the conclusion that acceptance S.P.T. should not be performed earlier than 20 days after completion of the final coverage.

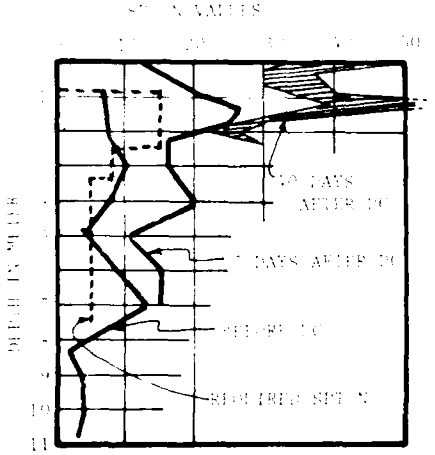

FIGURE 8. SPT N VALUES BEFORE AND AFTER DC., AND TIME-DEPENDENT STRENGTH GAIN (B-9 AREA)

PRODUCTION TAMPING AND SPECIAL CONSIDERATIONS

Subsequent to the verification of the initial design assumptions by the results of pilot test program, production tamping commenced. In general, the operation started from the northern portion of the site and progressed toward the south.

Typically, the thickness of the clayey lenses within the top sand layer ranged from about three to four feet. Such a clayey lens was present under the pilot test area at a depth of about 18 feet below the finished grade. Average SPT at the middle of the lens increased from about three to 11. This indicates that approximately a four-foot thick clayey lens could adequately be densified. In the general area of boring B3-176, a sandy clay layer protruded upward, in a bell shape, into the top sand layer reducing the thickness of the top sand layer to about seven feet instead of 30 feet. In order to provide uniformity with respect to the thickness of the top sand layer, thirty six 16-inch diameter holes were drilled at four feet on center to a depth of about 30 feet, and filled with granular fill materials prior to dynamic compaction. In general, size, spacing and other parameters used for the remedial design were derived from the pilot test program. SPT values after dynamic compaction indicated that

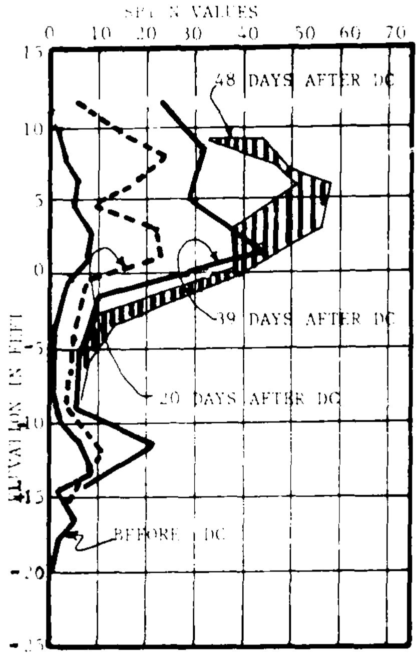

FIGURE 9. SPT N VALUES BEFORE AND AFTER DC., AND TIME-DEPENDENT STRENGTH GAIN (B-3 176)

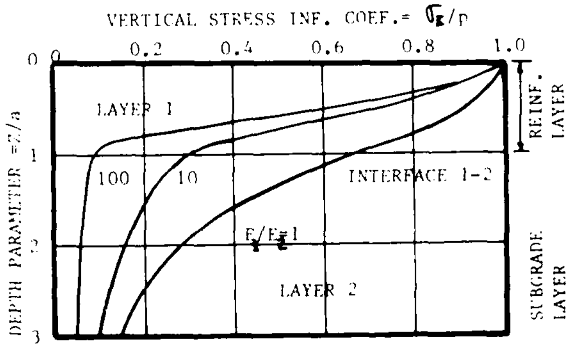

FIGURE 10. BURMISTER TWO-LAYER REINFORCING SYSTEM.

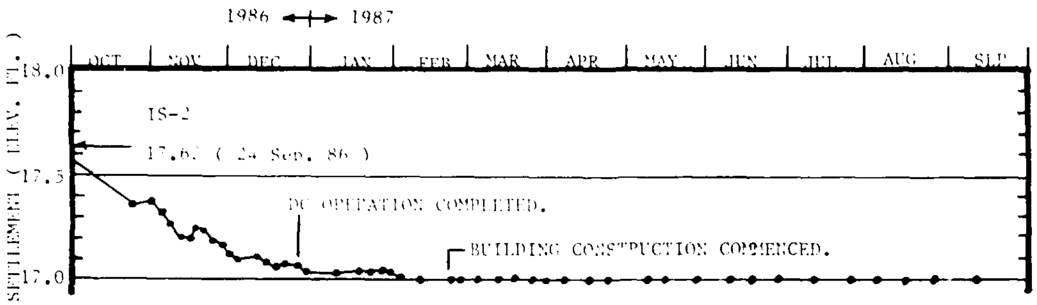

FIGURE 11. TIME SETTLEMENT CURVE

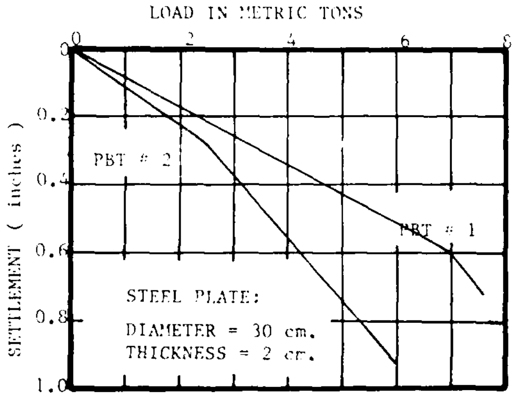

FIGURE 12. PLATE BEARING TEST RESULTS (PILOT TEST AREA)

the improvement obtained satisfied the specification. Increase of SPT N values before and after dynamic compaction is presented on Figure 9. Strength gain with time after the completion of dynamic compaction was observed. However, adequate reasons for the increase were not apparent (Mitchell, 1984).

Figure 10 represents Burmister's two-layer reinforcing system. The higher ratio of E_1/E_2 would produce less stress intensity at the interface 1-2. The modulus ratio of the top sand layer and the soft sandy clay layer is assumed to be on the order of 10, and consequently, a considerable stress reduction at the interface 1-2 would be anticipated. Settlement records indicate that subsidence virtually ceased after the completion of dynamic compaction. Settlement gages were installed in the northeastern, central, and southwestern portion of the site. Each station has two settlement gages at interfaces between the fill material and the top sand layer, and the bottom of the top sand layer and the sandy clay layer. Angular distortion between the settlement stations was on the order of 1/10,000 which is far below the specification requirement. A typical settlement record is presented on Figure 11. Two plate bearing tests were performed and the results are shown on Figure 12.

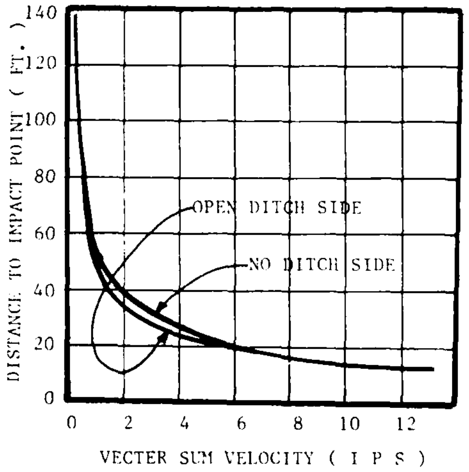

FIGURE 13. VECTOR SUM VELOCITY vs IMPACT DISTANCE

Vibrations induced in the ground by the impact during dynamic compaction were measured in order to establish criteria concerning the peak particle velocity and distance from the impact point. The criteria were to be used in planning for similar future projects in the proximity. The equipment used was SINCO S-6, PEAK VIBRATION MONITOR, MODEL 53136. However, farmers in the proximity complained physically about the vibration produced by the dynamic compaction, and the operation was impeded considerably.

Measurements were made on both sides of an open ditch (widths 5.5' top/3.0' bottom, 5.5' deep, and 70' long) in order to evaluate the existence of an open ditch in reducing the vibration. The results are presented on Figure 13. No major technical problems were encountered during dynamic compaction.

CONCLUSIONS

Approximately 4.5 feet of fill material was placed after removing varying thicknesses of soft rice paddy soils (ML). The fill material was placed primarily to counter the flood (interior drainage hydrology based on 1/500-year rain). However, it also provided a platform to operate the heavy machinery required for dynamic compaction.

The results of dynamic compaction performed at the site indicate that:

1) The design and construction methods adapted produced the results which satisfied the specifications;

2) Although the precise magnitude is unknown at this time, the presence of a stronger layer over a weaker layer contributed considerably in reducing subsequent settlement;

3) Future projects in proximity may be programmed to use dynamic compaction in densifying the top sand instead of relying on pile foundations; and

4) A considerable economy is achieved in both cost and time of foundation construction by the use of dynamic compaction rather than pile foundation with structural slab.

REFERENCES

Mitchell, J.K, and Katti, R.K., (1981), "Soil Improvement, State-of-Art Report", Proc. 10th ICSMFE, Stockholm.

Mitchell, J.K., and Solymar, Z.V., (1984), "Time-Dependent Strength Gain in Freshly Deposited or Densified Sand", ASCE Journal of Geotechnical Engineering, Vol. 110, No. 11.

Proceedings: Second International Conference on Case Histories in Geotechnical Engineering, June 1-5, 1988, St. Louis, Mo., Paper No. 5.17

Use of Reinforcement at Mohicanville Dike No. 2

L.W. Franks
Chief, Materials and Special Studies Section, Huntington District Corps of Engineers, Huntington, West Virginia

J.M. Duncan
W. Thomas Rice Professor of Civil Engineering, Virginia Polytechnic Institute and State University, Blacksburg, Virginia

S.A. Collins
Consultant, Atlanta, Georgia

J. Fowler
Research Civil Engineer, Waterways Experiment Station, Corps of Engineers, Vicksburg, Mississippi

J.F. Peters
Research Civil Engineer, Waterways Experiment Station, Corps of Engineers, Vicksburg, Mississippi

V.R. Schaefer
Research Assistant, Department of Civil Engineering, Virginia Polytechnic Institute and State University, Blacksburg, Virginia

SYNOPSIS: Mohicanville Dike No. 2 is located 60 miles south of Cleveland, Ohio. Initial construction efforts were halted because of persistent foundation failures. The height of the embankment when terminated (1937) was 14 feet, when construction reinitiated (1983) was 8 feet, and when completed (1985) was 27 feet. Conventional limit equilibrium and finite element analyses were performed as part of the studies to raise Dike No. 2 to its design height. Standard approaches for solving design problems of embankments constructed on weak foundations were explored, but none produced the required end of construction factor of safety of 1.3. The use of welded wire fabric as a reinforcement material was selected to provide the additional force required for stability. No significant problems were encountered during construction. Measured reinforcement forces are approximately equal to the finite element predicted values, have peaked, and continue to decline.

INTRODUCTION

The Muskingum River flood control system is located in southeastern Ohio. Between 1934 and 1938, 14 flood control dams were designed and constructed within the Muskingum River basin. Mohicanville Dam is located in the northwestern portion of the basin approximately 60 miles south of Cleveland, Ohio. Mohicanville Dike No. 2 is a 1,600 foot long earth dike located across a low point on the reservoir rim. Initial construction activity in 1936-1937 failed to raise the dike to its intended height because of persistent failures of the foundation and embankment. Between 1983 and 1985 construction activities raised the crest elevation from 965 msl to elevation 984 msl, making the final height 27 feet. This was accomplished by reinforcing the embankment with welded wire fabric.

ORIGINAL CONSTRUCTION ACTIVITY

Construction was initiated at Mohicanville Dike No. 2 in June 1936. Fill placement had progressed to elevation 963 msl (6 feet) by early August of that year when excessive settlement occurred and heavy seepage was observed near both the upstream and downstream embankment toe. Within days, extensive cracking and a large shear failure occurred within the upstream portion of the embankment between Station 8+00 and Station 12+00. This caused suspension of all construction activity until October, when 7-inch "drain wells" were drilled through the failed embankment and peat foundation layer. The wells were then pumped twice daily for three weeks. Construction was not resumed until May 1937. Fill placement progressed at a reduced rate until August when renewed distress was observed and another major shear failure terminated construction at elevation 971 msl. Reconstruction efforts were initiated in 1984.

Several reports have been produced between 1982 and 1986 to document site conditions and design procedures, report on construction activities, and evaluate the structure's performance. This paper presents an overview of the design-construction activities that occurred in raising Mohicanville Dike No. 2 to its design height. The data presented here is dealt with in greater detail in the references listed at the end of this paper.

EMBANKMENT REANALYSIS REPORT

Law Engineering Testing Company of Marietta, Georgia prepared the Embankment Reanalysis Report (ERR) at this project for the Huntington District (Collins et. al, 1982). This report documents the site conditions, subsurface explorations, laboratory testing, and limit equilibrium stability analyses performed for Mohicanville Dike No. 2. The foundation beneath the dike consists of a layer of peat overlying a soft clay deposit. The peat varies in thickness from 20 feet, in the virgin uncompressed state, at both the upstream and downstream toe to approximately 12 feet beneath the embankment centerline. The peat grades from fibrous in texture at the ground surface to amorphous adjacent to the clay. Additionally, explorations within the original failed reach showed the peat as discontinuous. The soft clay deposit beneath the peat varies in thickness from 10 feet near both abutments to almost 60 feet near Station 9+00. Figure 1 presents the typical geological cross section upon which the limit equilibrium analysis was performed.

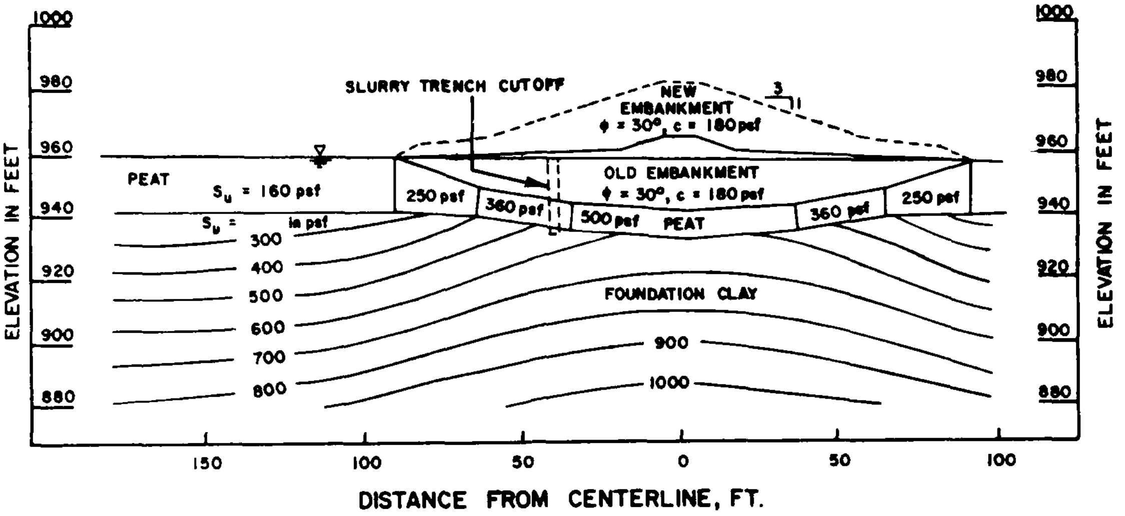
ELEVATION IN FEET
1000
980
960
940
920
900
880
SLURRY TRENCH CUTOFF
NEW
EMBANKMENT
$\phi = 30^\circ$, c = 180psf
3
1
PEAT
S_u = 160 psf
S_u = in psf
250 psf
360 psf
OLD EMBANKMENT
$\phi = 30^\circ$, c = 180psf
500 psf
PEAT
360 psf
250 psf
300
400
500
600
700
800
FOUNDATION CLAY
900
1000
150
100
50
0
50
100
DISTANCE FROM CENTERLINE, FT.

Fig. 1 Cross Section of Mohicanville Dike No. 2 used in ERR (Schaefer et al, 1986)

The weight of the original fill placement in the intervening 50 years since first construction has consolidated the soils beneath the embankment, thereby decreasing their thicknesses and increasing their shear strengths. The soil properties used in this study are presented in Table I.

Standard approaches for the design of an embankment on a weak foundation were pursued. Conventional attempts at obtaining an acceptable limit equilibrium factor of safety (F.S. for End of Construction = 1.3) were unsuccessful for raising the embankment. The factors of safety for all long term stability cases were satisfactory. The long term cases took advantage of the strength gains due to consolidation of the peat and clay and used the higher drained strengths.

At this point it was decided to investigate the use of one or more layers of reinforcement, placed perpendicular to the dike's axis, to raise the embankment to its intended height. It was believed that placing the reinforcement as low as possible would be the most effective location. For this reason the reinforcement was placed at elevation 960 msl, which was just above the groundwater level in the area. To do this required degrading the existing dike from elevation 968 msl to elevation 960 msl before reconstruction was attempted. A tensile force of 16 tons/linear foot of dike was calculated as being required to produce an acceptable factor of safety. This additional factor was assumed to be acting tangentially along the shear surface. There is presently some controversy over the direction that the supplemental force should

TABLE I. Summary of Soil Properties

Soil Property	Foundation Clay	Peat	Embankment Fill
Dry Unit Weight, pcf	OH: 40 to 84 CL-CH: 60 to 91	Pt: 10 to 36	CL: 113 to 120
Water Content, %	OH: 37 to 67 CL-CH: 28 to 65	Pt: 280 to 540	CL: 15 to 18
Liquid Limit	28 to 80	--	27 to 57
Plastic Limit	16 to 37	--	17 to 21
Gradation			
<#4	100	--	73 to 100
<#10	100	--	60 to 95
<#40	96	--	40 to 90
<#200	90 to 95	--	25 to 80
Undrained Shear Strength, psf	400 to 1000	200 to 500	3000 to 6000
Ø', degrees	25 to 29	17 to 32	32
c', psf	0 to 500	200 to 400	200
Permeability, ft/yr	0.1 to 10	0.3 to 66	0.1 to 1

act. Another view is that the force should act in a horizontal direction. The truth probably lies somewhere between and is believed to be a function of the flexibility of the reinforcement. At this project, an assumption that the force would act in a horizontal direction would have doubled the requirement for reinforcement.

Additional studies were considered necessary at this project for a variety of reasons including: the height of this permanent flood control structure, the potential for large deformations in the foundation, the lack of experience in 1982 of designing and constructing a reinforced impervious embankment, the variety in properties of candidate reinforcement materials, and the need to establish predictive parameters for monitoring construction progress using project instrumentation.

FINITE ELEMENT ANALYSIS

To answer the additional questions concerning the use of reinforcement, a second study was undertaken by the Waterways Experiment Station (WES) (Fowler et. al, 1983). Using the limit equilibrium analysis as a guide to determine the amount of reinforcement proved to be a helpful first step because of the uncertainties inherent in using finite element analyses as the sole basis for design. While finite element analyses can be used to calculate movements, pore pressures, and forces. They do not lend themselves to simple evalulation of factors of safety. WES modified the finite element computer program CON2D (Duncan et. al, 1981) to accommodate reinforcing elements. These reinforcing elements were modeled as one dimensional elastic "bars." The properties used to model the soil behavior were strength, stiffness, and permeability. This analysis produced estimates of pore pressures, vertical and horizontal movements, and forces in the reinforcement at various stages of construction. The effect of creep on the structure during construction was not modeled, but it was not believed to be a dominant factor. Predictions were made at locations where instrumentation was to be installed. Table II presents the construction sequence assumed for this model.

TABLE II. Assumed Stages of Construction

Computation Step	Time From Start of Construction Yr.	Final Centerline Elevation, Height Above Reinforcement, Ft.
0	0.0	964 (4)
1	0.08	970 (10)
2	0.16	978 (18)
		Winter Hiatus
3	0.83	978 (18)
4	0.96	983 (23)
5	1.96	"
6	11.96	"

Table III presents the instrumentation program at Mohicanville Dike No. 2 designed to monitor embankment performance during construction.

Soil strength parameters for the finite element model were selected such that vertical movements calculated for an unreinforced embankment would be similar to those anticipated for a structure with a F.S. = 1.0. A vertical displacement of 2.0 feet at the centerline was selected as approximating this condition. To obtain this movement with the finite element model required reducing the shear strength parameters assumed for the limit equilibrium analysis. Analyses were performed using the properties of polyester filter cloths, kevlar products, and welded wire fabric as reinforcement materials.

A significant finding of the finite element study was that to carry the required load determined by the limit equilibrium analysis, without excessive deformations, a stiff material was required. The decision was made to use welded wire fabric. The study indicated that the resistance to horizontal movement was the primary mechanism by which load was transferred to the reinforcement. Steel offered the necessary stiffness (12,000 tons/ft) to carry the design load without excessive lateral spreading. By reinforcing the embankment with welded wire fabric, horizontal deformation at the reinforcement level was reduced from 1.0 foot to 0.1 foot. It was assumed that it was necessary to mobilize as much force in the reinforcement as possible to obtain the overall factor of safety calculated to the limit equilibrium analysis.

A dominate factor in choosing welded wire fabric was that the construction process mobilize the design load within the reinforcement. This would relieve the shear stress in the foundation soils to a level compatible with the overall limit equilibrium factor of safety of 1.3. It has been argued that the only requirement is that sufficient ultimate strength be available, not that the same percentage of each material's strength be mobilized during construction. However, this may result in a factor of safety of 1.0 in the soil and 5.0 or more in the reinforcement. The use of stiff reinforcement worked well at this project. The chosen reinforcement, W12 x W4.5 welded wire fabric, contained the necessary ultimate strength of 24 tons/ft to provide a factor of safety of 1.5 for the 16 tons/ft design load. Using a reinforcement material that would carry the design load in one layer was also desirable because construction activities would be additionally restrained and complicated by each additional layer placed.

The stiffness of the reinforcement had little influence on the amount of settlement. The finite element analysis predicted that vertical deformations under the centerline during construction would be reduced from 1.9 feet to 1.0 foot with the addition of welded wire fabric as the reinforcement. Post construction consolidation settlement (2.0 ft) was expected to be unaffected by the use of reinforcement.

TABLE III. Instrumentation at Mohicanville Dike No. 2

	Station						
Instruments	4+75	6+55	8+00	9+00	11+00	12+20	Total
Piezometers							
Open Tube	1	3		4		1	9
Electric	1	2		3		1	7
Pneumatic	4	8		7		4	23
Inclinometers							
Vertical	1	3		3	1	1	9
Horizontal	1	1		1		1	4
Strain Gages on steel	2	29	2	29 lower 10 upper	2	2	76
Settlement Plates	3	3		3		3	12
Surface Displacement Monuments	5	5	5	5	5		25

A separate condition that was identified in the ERR was the potential for excessive seepage through the peat foundation and transverse cracks in the original embankment material. A large quantity of seepage (500 gpm) was observed in 1969 during a flood event with only 6 feet of head differential existed across the structure. To deal with this condition a slurry trench was excavated through the existing embankment fill and peat foundation layer. The possibility existed for large deformations within the foundation during reconstruction. To ensure continuity of the seepage barrier, a 100 mill thick high density polyethylene geomembrane was placed within the slurry trench before backfilling with soil-bentonite. The trench was located beneath the upstream slope of the dike, approximately 45 feet from the centerline. Further discussion of the slurry trench, is beyond the scope of this paper.

CONSTRUCTION

Construction of Mohicanville Dike No. 2 required two seasons to complete, 1984 and 1985. The work was superintended by Construction Division personnel of the Huntington District using hired labor, equipment rental, and material supply contractual arrangements. This provided the necessary control over the construction activity that the design group believed was required for control on a project where little precedent existed. A simplified construction sequence follows:

1. Degrade the existing dike from elevation 968 msl to 960 msl.

2. Install instrumentation and welded wire fabric on the prepared foundation.

3. Construct embankment to elevation 971 msl by the end of 1984.

4. Completion construction to elevation 984 msl by the end of 1985.

Serving as embankment engineer during the first year's construction activity was Jack Fowler of WES. The dike was excavated to elevation 960 msl with no significant problems. The foundation at that elevation was primarily existing embankment material. Ground water in the area was at elevation 957 msl. A minimal amount of equipment movement was allowed on the unreinforced foundation because of pumping. The soils encountered were moist to wet and typical of the embankment properties shown in Table 1. A minimum of 2% lime was mixed into the 1-foot layer of soil immediately above and below the welded wire fabric. Where trafficability and moisture problems were encountered beneath the wire, as much as 5% lime was added. The addition of lime to the soil surrounding the reinforcement was intended to prevent corrosion damage for the short term. Long term stability, > 10 years, did not require any contribution from the reinforcement for stability. The foundation soils will have gained sufficient strength during that time period, due to consolidation, to be stable without reinforcement.

The four horizontal inclinometers were installed prior to placement of the welded wire fabric. Some of the horizontal inclinometer casing developed precipitates from the lime placed in the surrounding fill. Twelve settlement plates were placed immediately above the reinforcement to check the readings obtained from the horizontal inclinometers. Agreement between the two instruments was very good. The welded wire fabric, W12 x W4.5, was brought to the site in 320 foot rolls, eight feet wide. The wire experienced plastic deformation from being rolled and required mechanical straightening to be used as flat sheets. A portable wire straightening machine was situated proximate to the dike foundation. The wire rolls were placed on a horizontal spindle and binding fasteners released. The fabric was fed through a configuration of three steel rollers and straightened. This method worked very well. The welded wire rolls were then cut into two 160-foot sheets and stockpiled until the foundation had been prepared. The sheets were placed perpendicular to the centerline, forming a continous reinforcement member between the upstream and downstream toes. Seventy-six strain gages were welded to the fabric. Only two of the strain gages failed during construction. They provided a reliable and accurate way of measuring the forces in the welded wire reinforcement.

The embankment material was obtained from two locations on uplands adjacent to the construction site. The fill is a glacial till that is classified as a Gravelly Sandy Clay (CL) with particle sizes extending to 8 inches. Natural water contents were within 2% of optimum. The first layer (12-inch) of embankment fill above the welded wire fabric was compacted using a steel drum roller to prevent damaging the wire. A sheepsfoot roller was used for compaction thereafter. Standard Proctor Compaction testing of the embankment soils produced an average maximum dry density of 120 pcf with an optimum water content of 13%. A total of 58 density tests were performed with dry densities ranging from 115 pcf to 126 pcf. Moisture contents were between 10% and 16%. No effect of the soft existing soils beneath the wire fabric was observed on compaction test results obtained from above the reinforcement. Density tests performed immediately above the wire reinforcement produced values typical of those obtained throughout the remainder of the embankment. Shear strength testing on block samples from the embankment produced higher strengths than assumed for the original fill.

Piezometers and vertical inclinometers were not installed until the reinforcement and two feet of fill were in place. Sections of welded wire fabric were cut and protective pipes welded to the wire to protect the instrumentation as it passed through the reinforcement. One of the electric piezometers never worked properly, but all of the other piezometers and vertical inclinometers functioned satisfactorily throughout construction. The excellent performance record of the instrumentation at this site is believed to have been due to the experienced instrumentation technicians present during all of the installation work and because the construction was handled by hired labor, equipment rental, and materials supply contracts. The normal pressures to relegate instrumentation issues to a position of lesser importance was not felt at this project due to the manner in which construction was administered. Construction in 1984 was halted at elevation 971 msl by bad weather in November.

During the second construction season, Steve Collins, consultant, served as embankment engineer. Construction of the embankment proceeded to completion during the second year with no significant problems. During the second construction season the instrumentation data being collected indicated higher pore pressures in the soft clay foundation at the centerline than predicted. The use of the finite element analysis was the only means available to assess the implications of these high pore pressures on the stability of the dike. Two parameters used in the first finite element model were modified based on additional data obtained during the first construction season. This paper will summarize those results below.

INSTRUMENTATION ANALYSIS

Observations made during the second construction season identified two faulty assumptions in the original finite element model. Exploration data obtained during instrumentation installation indicated that the maximum thickness of soft clay deposit was only 40 feet instead of 60 feet as previously modeled. The effect of this change on the finite element model would be to reduce the reinforcement forces, decrease the foundation movements, and lower the predicted pore pressures. Figure 2 shows the effect of clay thickness on the amount of reinforcement force measured at various centerline locations.

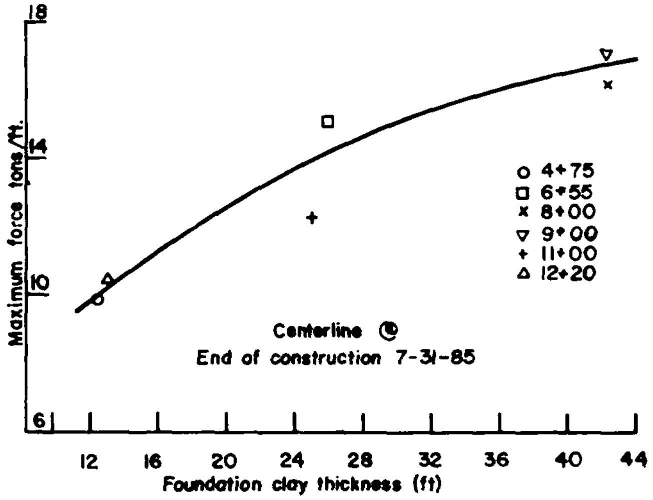

Fig. 2 Reinforcement forces measured for various thickness of soft clay foundation (Collins, 1986)

Secondly, the original model was initialized with the embankment working surface at elevation 964 msl. (Table 2). The actual construction sequence consisted of degrading the existing dike to elevation 960 msl to allow the placement of reinforcement. It was assumed this excavation and replacement to elevation 964 msl would have a neutral effect on the foundation. This was a reasonable assumption along a majority of the dike length. However, initial construction surveys indicated that the amount of fill that actually existed prior to construction at Station 9+00 was significantly less than would exist when reconstruction reached the zero load height of 964 msl. The result of this discrepancy was that the foundation was experiencing more load than anticipated in the analysis at elevation 964 msl. This change caused the original model to underestimate the induced pore pressures. These two assumptions were included in a modified finite element model and a second series of analyses was performed. The second series of analyses was made during construction because of a concern for higher than anticipated piezometric levels in the foundation clay at Station 9+00. These analyses produce piezometric levels closer to those being measured. A comparison of measured and predicted pressures is shown on Figure 3.

The results of the second finite element model and other construction related data and evaluations are discussed in the report by Collins (1986). Figures 3 and 4 present comparative data between the two finite element predictions and instrumentation measurements for piezometric levels and reinforcement forces at Station 9+00. It was concluded that the higher pore pressures and reinforcement forces could be explained by the greater fill loading and would not lead to instability. This use of finite element analysis during construction to resolve unexpected observations was a very beneficial tool at this project and would be prudent for monitoring construction activity of any novel design. It may highlight problems or failure modes that might otherwise be overlooked.

The water levels in piezometers OP-33 and PP-18, located upstream of the slurry trench at Station 9+00, were constant at elevation 957 msl throughout construction. This was the ground water level in the area and suggests that the slurry trench is doing the intended job.

An additional observation from the original finite element model was that when more than one reinforcement layer is used, the stresses would be concentrated in the lower layer of reinforcement. For the welded wire fabric the upper

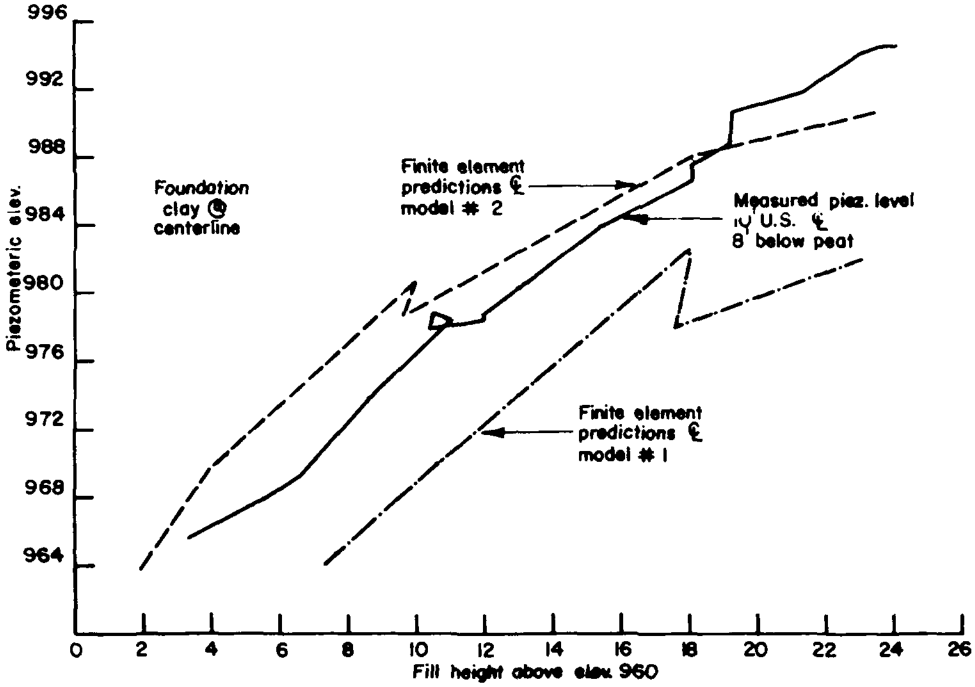

Fig 3. Piezometric levels at Station 9+00 (Collins, 1986)

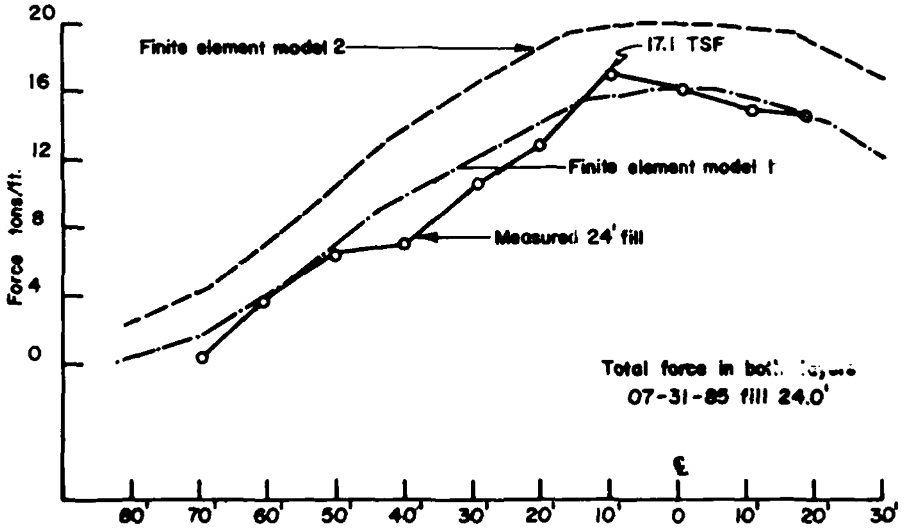

Fig. 4. Forces in the reinforcement at Station 9+00 (Collins, 1986)

layer of reinforcement in a two layer system was predicted to carry 24% as much of the total load as the bottom layer. Two layers of fabric were placed between Station 8+50 and Station 9+50 in an attempt to bridge an area where the previously mentioned slurry trench failed in 1983. This is the same area where construction problems occurred in 1936-1937. Strain gage data at Station 9+00 indicated that at the end of construction the upper layer of reinforcement was carrying only 32% of the total load. This data is presented on Figure 5. The load had continued to shift away from the upper layer of reinforcement since the end of construction and currently that layer carries only 23% of the load. Hindsight indicates that the upper layer of steel mesh placed between Station 8+50 and Station 9+50 was inefficient and unnecessary.

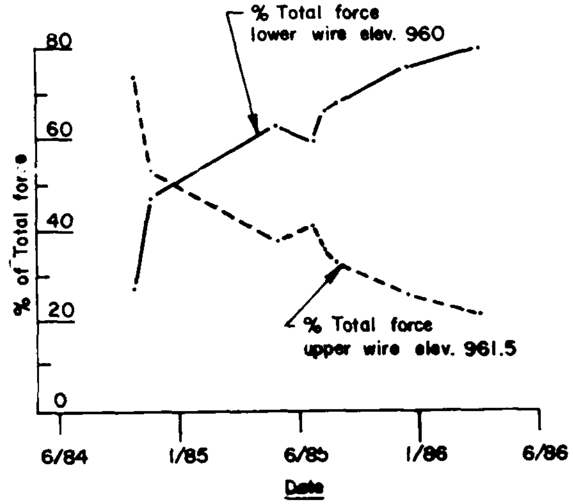

Fig 5. Percent of total load carried by each reinforcement layer at Station 9+00

CONCLUSIONS

Mohicanville Dike No. 2 has now been in place for two years, during which time the reinforcement stresses and pore pressure levels have continued to decrease. The forces monitored in the welded wire fabric were the instrumentation data of most value in controlling construction activities. The pore pressure measurements and horizontal and vertical movements were viewed as having lesser importance. A few of the piezometers and strain gages have ceased to function, but there are still sufficient instrumentation to monitor the structure for the long term. Instrumentation is now being read on a yearly schedule. The use of welded wire fabric as a reinforcing material performed satisfactorily at Mohicanville Dike No. 2.

REFERENCES

Collins, S. A. (1986) "Analysis of Instrumentation and Evaluation of Embankment Performance: Mohicanville Dike No. 2" Report to the Huntington District Corps of Engineers, Huntington, West Virginia, May.

Collins, S. A., Rogers, W. and Sowers, G. F. (1982), "Report of Embankment Reanalysis - Mohicanville Dikes." Report to the Huntington District Corps of Engineers, Huntington, West Virginia, by Law Engineering Testing Company. July.

Duncan, J. M., D'Orazio, T. B., Chang, C. S., Wong, K. S. and Namiq, L. (1981), "CON2D: A Finite Element Computer Program for Analysis of Consolidation." Report No. UCB/GT/81-01, College of Engineering, University of California, Berkeley. March.

Duncan, J. M., Schaefer, V. R., Franks, L. W. and Collins, S. A., (1986), "Design and Performance of a Reinforced Embankment for Mohicanville Dike No. 2 in Ohio." Paper submitted to Transportation Research Board National Research Council. November.

Fowler, J., Leach, R. E., Peters, J. F. and Horz, R. C. (1983), "Mohicanville Reinforced Dike No. 2 - Design Memorandum." Geotechnical Laboratory, U. S. Army Waterways Experiment Station, Vicksburg, Mississippi. September.

Schaefer, V. R. and Duncan, J. M. (1986), "Evaluation of the Behavior of Mohicanville Dike No. 2." Report of Research Conducted for the Huntington District Corps of Engineers, by Department of Civil Engineering, Virginia Polytechnic Institute and State University. November.

Proceedings: Second International Conference on Case Histories in Geotechnical Engineering, June 1-5, 1988, St. Louis, Mo., Paper No. 5.18

Slurry Wall Instrumentation and Monitoring in Taipai

Ching-Tzer Yih
Graduate Student, Department of Civil and Environmental Engineering, New Jersey Institute of Technology, Newark, New Jersey

Raj P. Khera
Professor, Department of Civil and Environmental Engineering, New Jersey Institute of Technology, Newark, New Jersey

SYNOPSIS: An entire city block was excavated to construct a 19-story high building with three basements in downtown Taipai. A monitoring program was implemented to serve as an early warning system. The settlement and lateral displacement continued to occur even after the excavation was completed. Though the excavation was within a silty sand the underlying silty clay resulted in a moderate amount of basal heave. Strut loads exceeded more than 50 percent the estimated values and the largest loads were recorded during the final stages of construction and not at the end of excavation.

This paper is limited to a description of the monitoring program, the soil conditions, and the observed data related to the various phases of construction.

INTRODUCTION

The Central Insurance Building in downtown Taipei is a recent high-rise project which required deep basements extending to a depth of 11.5 m below grade. Due to the critical location of the site, relative to the adjacent structures, streets, and utilities, a comprehensive observation system was designed and implemented to obtain the necessary data for construction control during excavation and foundation installation.

The project site occupies (Figur 1) an area of approximately 35m by 53m in a busy commercial district of Taipei. On the north and south sides are West Chung Shaw Road and First Street, respectively. A 14-story apartment building supported by end-bearing piles, is on the west and 12-story building supported by spread footings is on the east. The foundation types of the older buildings on the south side of First Street are not known.

The observation program began in December 1982 with the installation of field instruments and was terminate in August 1983 with the completion of the underground structure.

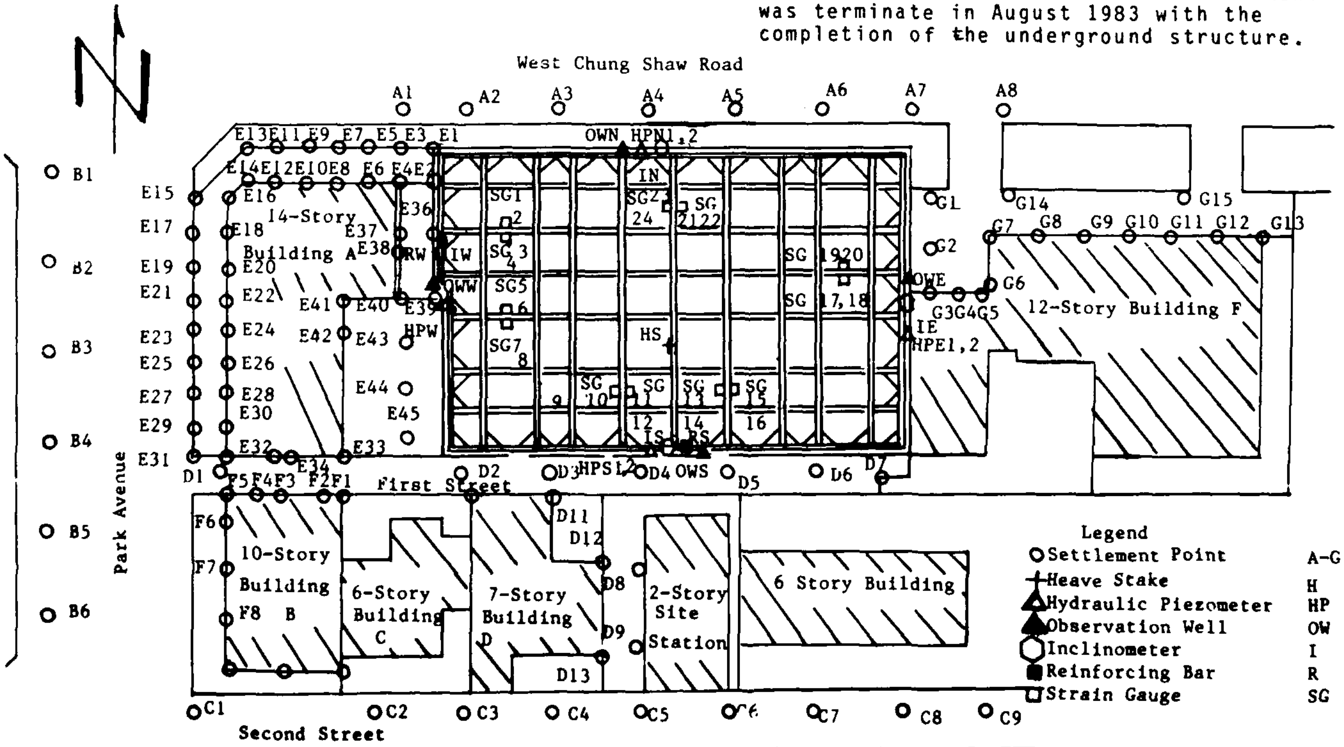
N
West Chung Shaw Road
A1
A2
A3
A4
A5
A6
A7
A8
B1
B2
B3
B4
B5
B6
Park Avenue
14-Story Building A
12-Story Building F
10-Story Building B
6-Story Building C
7-Story Building D
2-Story Site Station
6 Story Building
First Street
Second Street
C1
C2
C3
C4
C5
C6
C7
C8
C9
OWN
HPN1,2
IN
IW
OWW
HPW
RW
OWE
IE
HPE1,2
HS
IS
RS
OWS
HPS1,2
Legend
Settlement Point A-G
Heave Stake H
Hydraulic Piezometer HP
Observation Well OW
Inclinometer I
Reinforcing Bar R
Strain Gauge SG

Fig.1 Site Plan and Layout of Monitoring System

SOIL CONDITIONS

The sub-surface conditions at this site are typical of the downtown Taipei area. The upper soil is a yellow-gray silty clay with a thickness of about 7m. Below the silty clay and extending to an elevation of -17m is a gray silty fine sand which overlies a 7m thick gray silty clay layer. Starting at elevation -31m and extending to -46m is a hard cohesive soil called "hardpan" in the Taipei area. Below the hardpan is a 3m thick layer of fine sand which extended to a very dense layer of gravel. The groundwater level was observed to be at approximately 3m depth.

The diaphragm wall was constructed between November 18 and December 13, 1982. The instrumentation was completed in February 1983. It consisted of settlement points, heave stakes, piezometers, observation wells, inclinometers, instrumented reinforcing bars, and the supporting struts.

EARTH RETENTION SYSTEM AND FOUNDATIONS

A 600 mm thick, 23m deep reinforced concrete slurry wall was selected to bound the project and form a permanent basement wall. The depth of the excavation was 11.4m and the bracing support system consisted of three levels of H 300x300x15mm shape cross-lot struts which were preloaded.

The foundation of this building rested on piles either 1.00m or 1.50m in diameter extending to the dense gravel layer approximately 50m below the ground surface.

SETTLEMENTS

Vertical settlement readings at local spots in the adjacent streets were, in general, less than 15mm. Table 1 shows the largest settlement values for two locations at the end of excavation stage 4 and the casting of the first basement slab.

Table 1. Settlements at Maximum Excavation Depth

	Completion of	
	Excavation	First Basement
14-story building		
point on the road	13	14
	21	24
12-story building	18	20
point on the road	20	23

As shown in Table 1 the 14-story building, which was pile supported, showed settlements about 2/3 those of the adjacent ground. However, the settlement of the 12-story structure, which was supported on spread footings, and the adjacent ground were about the same. Similar behavior was observed for the buildings on the south side indicating that they, too, were resting on shallow footings. As noted earlier the foundation type of the buildings on the south side was not known.

The settlement continued after the completion of the excavation and during the construction. However, no observations were made after the final basement was completed.

The data from various settlement points located at different distances from the excavation and the corresponding depths of excavation are plotted on Peck's (1969) graph and are shown in Figure 2. As may be seen for Figure 2, the data fall within the region of sand (I) and soft clay of limited depth below the base of the excavation (II) and show a workmanship of average quality. Lambe et al., 1972, reported a similar response for a subway excavation in Boston where a slurry wall was used.

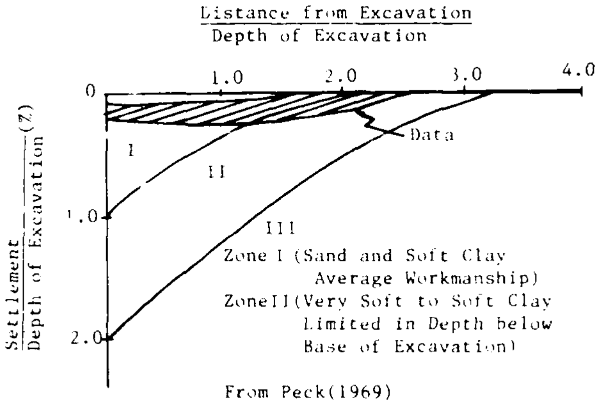

From Peck(1969)

Fig.2 Settlement Adjacent to The Slurry Wall

BASAL HEAVE

The primary reason for heave monitoring was the concern for basal failure during excavation. Two heave stakes were installed at depths of 12.5m. The heave stakes were read daily during the excavation period and twice a week at other times. The larges heave reading during excavation was 42.5mm. After the placement of the foundation mat it had increased to 44.6mm.

The heave is attributed to the swelling of the underlying clay which was of medium consistency. The stress decrease from soil excavation was considerably larger than the stress imposed by the concrete mat. Other contributing factor may have been the seepage forces. As shown in Figure 3 the piezometers show a small drop in the groundwater level outside the excavation even though there was no dewatering.

LATERAL MOVEMENTS

Four inclinometers were installed to monitor the incline and the movements of the slurry wall and the adjoining ground. To check vertical profiles and horizontal deflection of the wall two inclinometers (I-S, I-W) were installed within the slurry wall with their tips at the bottom of the wall. To measure the soil movements below the base the other two slope indicators were I-N and I-E were installed behind the wall (Figure 1) and extended into the hardpan to a depth of 15m below the bottom of the slurry wall.

The data for I-E and I-S are shown in Figure 4 and Figure 5. The data for the external slope indicator show that within the soil the lateral

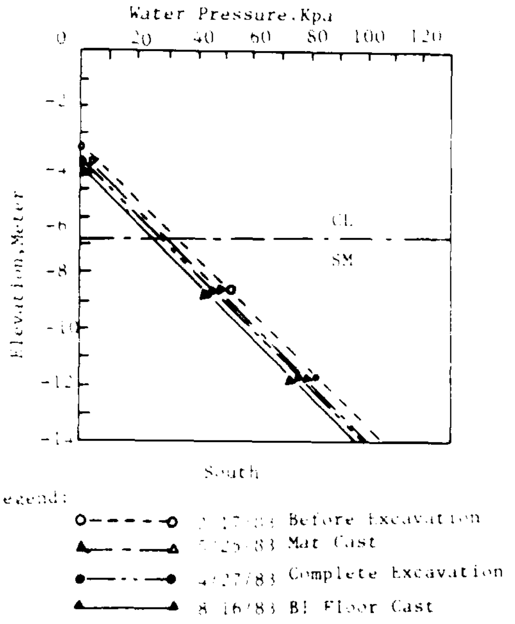

Fig.3 Water Pressure Distribution during Construction

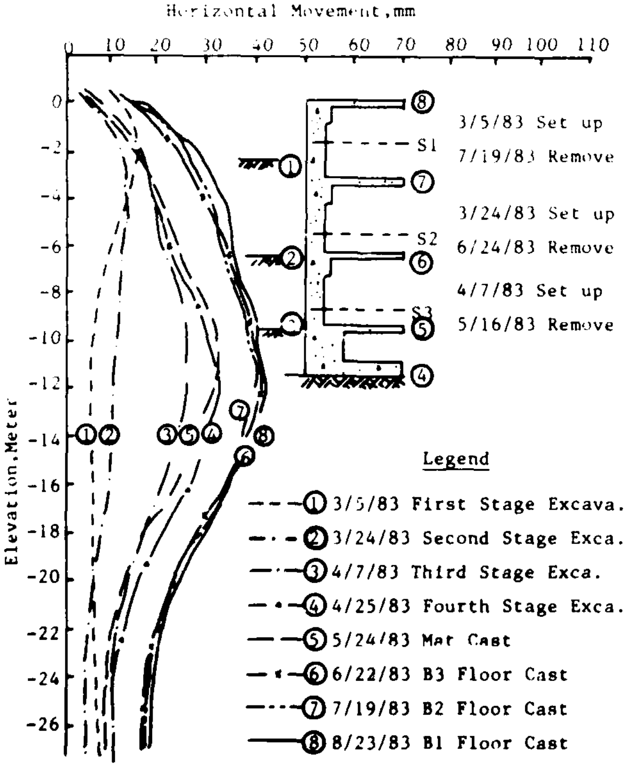

Fig.4 Deflection of External Inclinometer(I-E)

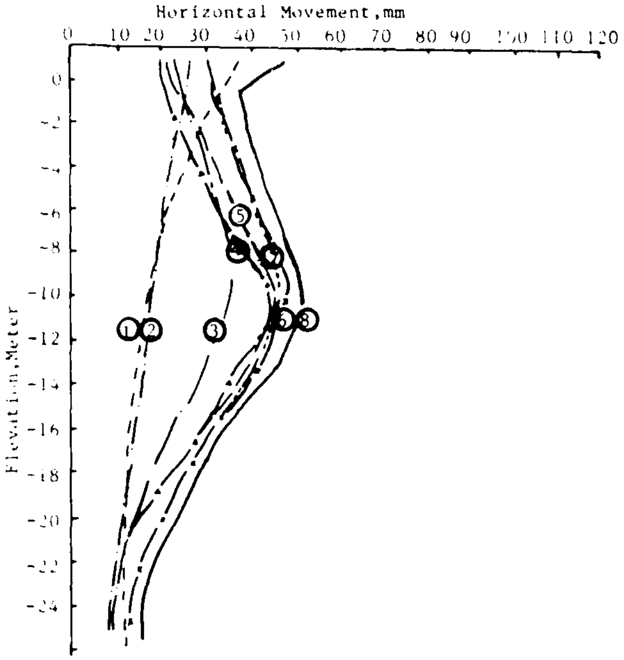

Fig.5 Deflection of Internal Inclinometer(I-S)

movement near the ground surface was less than 15mm and the maximum deflection of 40mm occurred slightly below the bottom of the excavation.

Before the start of third stage of the excavation, the slurry wall only tilted showing the maximum movement at the top. With the progress of the excavation the wall started to bend and had the maximum deformation at the base of the excavation. The wall showed a maximum movement of 20mm to 47mm at the top and 26mm to 51mm at the bottom of the excavation.

When comparing the movement of the ground behind the wall (Figure 4) and the wall itself (Figure 5), the larger displacement exhibited by the wall near the top is attributed to the rigidity of the wall.

STRUT LOADS

The bracing system contained three levels of steel H 300x300x15 mm. Strain gauges were mounted in pairs on each side of the cross-lot strut web at the neutral axis. All the cross-lot struts with post column had the same shape. Bracing sets were installed as the excavation progressed. Excavation depth was held to a limit of 9.50m below a bracing set until the next set was installed and blocked. To minimize soil movements and to ensure tight contacts between the concrete wall and the soil, all the cross-lot struts were preloaded in accordance with the design before the excavation was carried deeper. The maximum allowable design load of the struts was 3675kN. The predicted strut load by Peck's (1969) earth pressure assumption was 1460kN at the first level bracing and 2068kN at the second and third bracings. Thus the design values were twice the estimated values.

Figure 6 shows the actual strut loads for the North-South direction corresponding to various stages of excavation and construction. In general there was reasonable agreement between the predicted and measured strut loads except during the period when the bottom concrete slab was poured and, the bottom set was removed. In the north-south direction the load in the third strut reached 2100kN and in the east-west direction the load in the third strut reached about 2500kN.

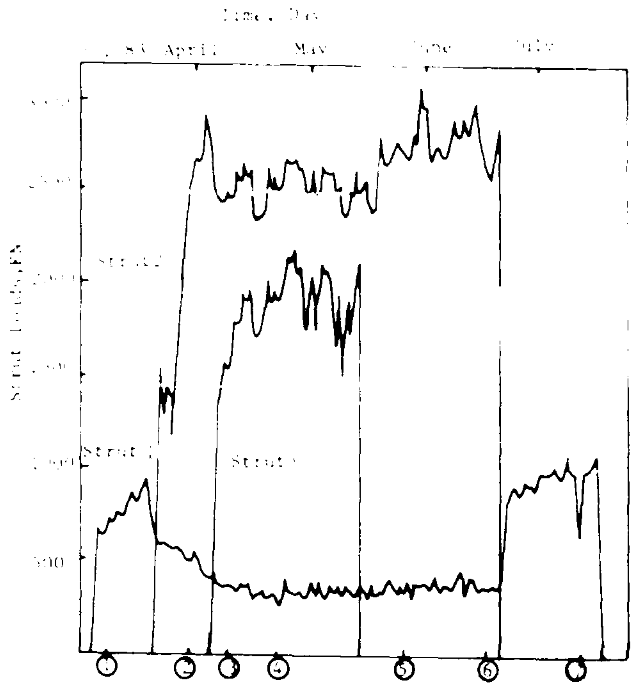

Fig.6 Measured Strut Loads of North-South Bracing

For the second level strut in the north-south direction and the third level strut in the east-west direction most of the readings far exceeded the predicted values of 2068 kN. However, the maximum reading of 3028kN was still within the designer's control and was less than 3675kN.

CONCLUSIONS

Based on the instrumentation data the following conclusions and suggestions can be made:

The settlement data fall within the region of sand and soft clay of limited depth below the base of the excavation when plotted on Peck's graph and show a workmanship of average quality.

The basal heave occurred due to the swelling of the underlying clay and the seepage forces from the lowering of the groundwater.

Excavation sequence was found to influence the wall deflection.

Total horizontal displacements depended upon the time elapsed between the excavation and the installation of the strut.

Strut loads increased even after the completion of the excavation. The largest loads were recorded during the final stages of construction and their magnitude far exceeded the estimated values based on Peck's (1969) diagrams.

Damage occurred to some of the gauges. It is essential that data cross checks are built in the monitoring program to assist in detecting incorrect data and to ensure adequacy of the data.

REFERENCES

Lambe, T. W., L. A. Wolfskill, and W. E. Jaworski (1972), "The Performance of a Subway Excavation", Performance of Earth and Earth-Supported Structures, ASCE, V. 1, Part 2: 1403-1424.

Peck, R. B. (1969), "Deep Excavation and Tunneling in Soft Ground", 7th Int. Conf. on Soil. Mech. and Found. Eng., Mexico City, State-of-the-Art Volume: 225-290.

Proceedings: Second International Conference on Case Histories in Geotechnical Engineering, June 1-5, 1988, St. Louis, Mo., Paper No. 5.19

Deformation Behavior of Wilford Hall Hospital Mat

Lawrence D. Johnson
Research Civil Engineer, U.S. Army Engineer Waterways Experiment Station, Vicksburg, Mississippi

SYNOPSIS. The vertical deformation behavior of the 3.5-ft thick mat supporting an 11-story addition to the Wilford Hall Hospital complex near San Antonio, Texas, was investigated to determine the mode of deformation and to develop a procedure for estimating the effective stiffness of the foundation soil. The observed distortion pattern is dish-shaped and consistent with that of a plate on a semi-infinite elastic foundation. Measured displacements are consistent with displacements calculated by a plate on elastic foundation finite element program using effective elastic soil moduli between 2,945 and 4,000 kips/square foot and poisson's ratio 0.3. An equation was derived for estimating effective elastic soil moduli for soil with elastic modulus increasing linearly with depth.

INTRODUCTION

The behavior of soil foundations, especially in expansive soil areas, is difficult to predict with any reliability. An investigation of mat foundations was therefore initiated to determine a suitable method for evaluating appropriate soil input parameters required for design. A foundation selected for study is the mat addition to the hospital complex located in the northwest portion of Lackland Air Force Base near San Antonio, Texas. This mat was constructed in 1977 and it supports an 11-story tower. This mat is adjacent to and east of the existing hospital complex supported on drilled shafts. The mat is 3.5 ft (feet) thick by 108.33 ft wide by 209.33 ft long and it was placed in an excavation 27 ft below the existing ground surface. Steel reinforcement in the mat constitutes 5 percent of the cross-section and it is located in both top and bottom parts of the mat. The superstructure is built of a

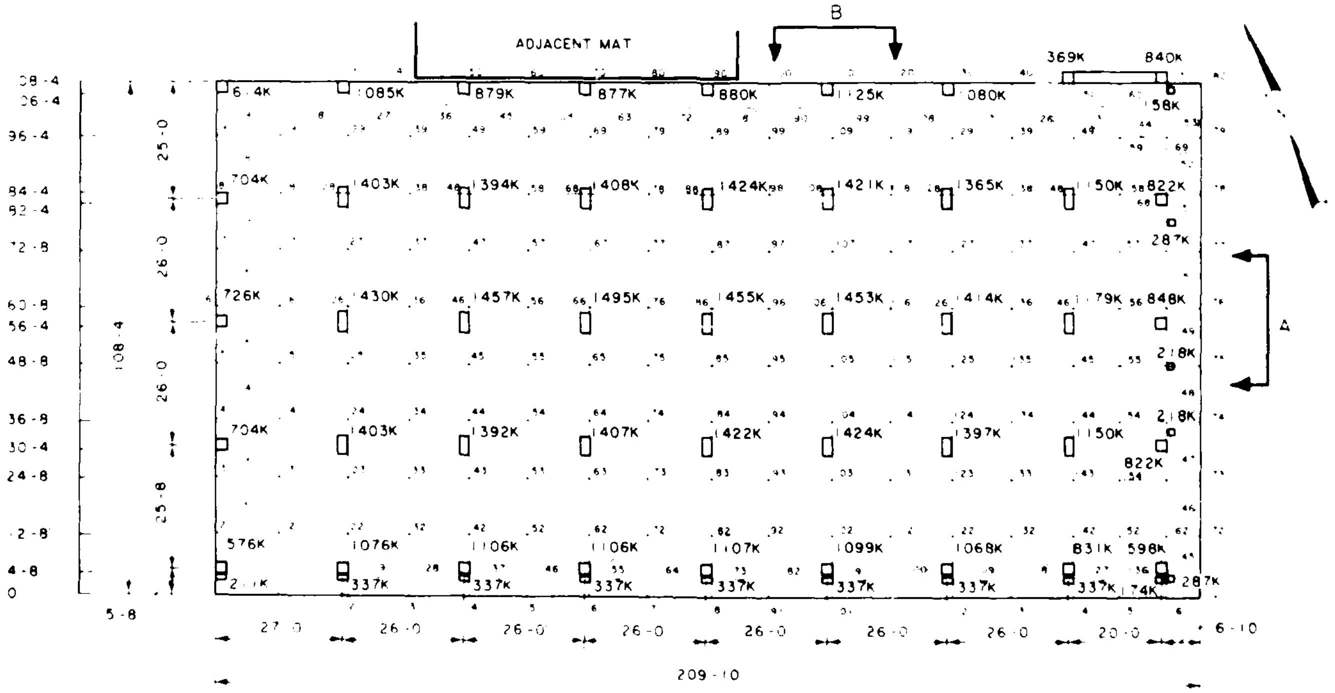
ADJACENT MAT
B
A
369K
840K
108-4
209-10
27-0
26-0
20-0
6-10
5-8
25-0
26-0
25-8
704K
1403K
1394K
1408K
1424K
1421K
1365K
1150K
822K
726K
1430K
1457K
1495K
1455K
1453K
1414K
1179K
848K
1392K
1407K
1422K
1424K
1397K
576K
1076K
1106K
1107K
1099K
1068K
831K
598K
337K
1085K
879K
877K
880K
1125K
1080K
158K
287K
218K

Fig 1. Foundation Plan (Note: Column loads given in kips, dimensions in feet and inches)

structural steel frame supporting a masonry facing.

LOAD PATTERN

Figure 1 shows the plan and column load distribution on the mat. Total dead and live column loads are about 55,000 kips plus 12,000 kips contributed by the mat weight leading to a total building weight of about 67,000 kips. Weight of soil displaced by the building is about 74,000 kips so that there may be a small net loss of weight on the foundation soil beneath the mat. The loads applied to the foundation soil are slightly greater toward the right or east end of the mat, Figure 1. The applied pressures on the foundation soil are less than the maximum past pressures of the soils in the strata.

SOIL PARAMETERS

A soil investigation indicated an expansive plastic CH clay overburden and shale with a perched water table about 23 ft below ground surface, Figure 2. The soil profile consists of overburden, Lower Midway, and Navarro formations with an occasional stratum of clayey gravel in the vicinity of the perched water table. Results of one-dimensional consolidometer swell tests using Method A of ASTM Standard Test Method D 4546 indicate potential for swell in the overburden down to about 17 ft below ground surface and within a 10-ft thickness of soil just beneath the base of the mat.

The Young's elastic modulus determined from results of unconsolidated undrained strength tests on specimen from undisturbed soil samples taken from depths within 50 ft beneath the base of the mat can be approximated as increasing linearly with depth

$$E_s = kz \qquad (1)$$

where: E_s = initial hyperbolic modulus, kips/square foot (ksf)

k = constant relating the elastic modulus with depth, ksf/ft

z = depth, ft

The initial hyperbolic modulus is evaluated after the method of Duncan and Chang (1970). The value k varies within the range of 24 to 32 ksf/ft, Figure 2.

A semi-empirical equation for estimating the effective modulus beneath a mat in a semi-infinite elastic medium with the modulus increasing linearly with depth was derived from a parametric study using the method of Kay and Cavagnaro (1983)

$$E_s^* = \frac{2kR(1 - \mu_s^2)}{0.7 + (2.3 - 4\mu_s^2)\log\left[\frac{R}{D_b}\right]} \qquad (2)$$

where: E_s^* = effective soil modulus, ksf

R = equivalent mat radius $\sqrt{LB/\pi}$, 85.06 ft

L = mat length, 209.83 ft

B = mat width, 108.33 ft

μ_s = Poisson's ratio of soil

D_b = Depth of mat base below ground surface, 27 ft.

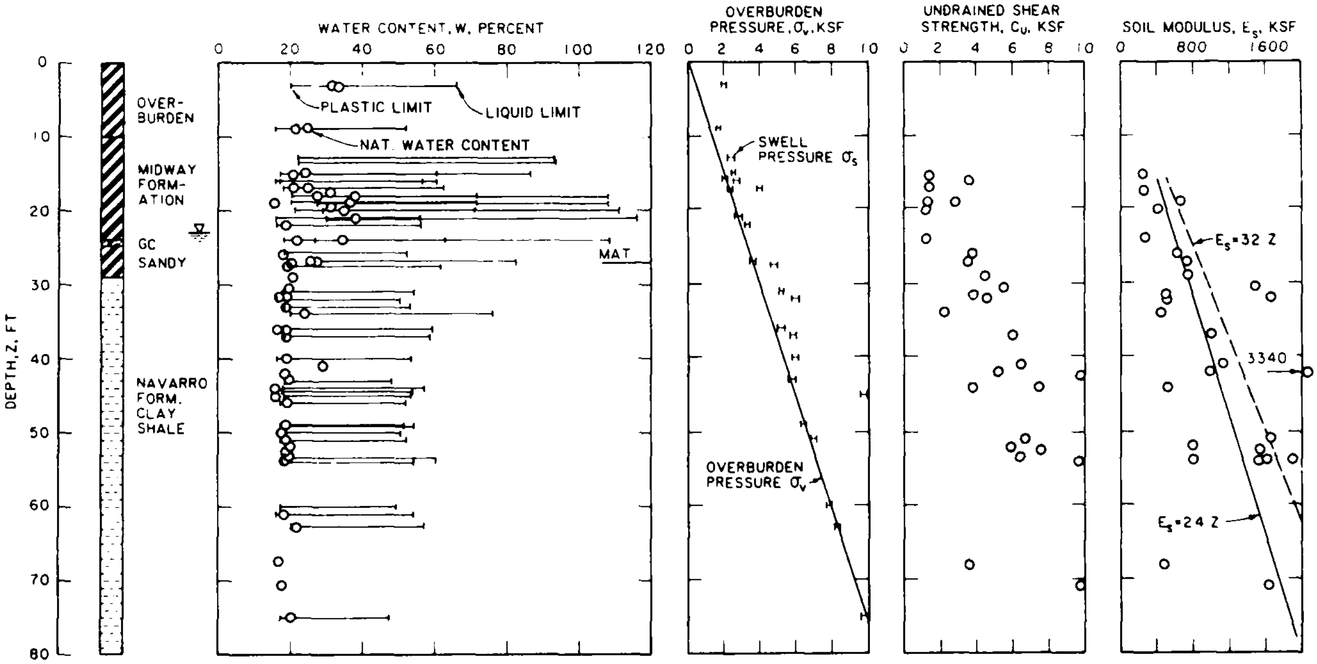

Fig. 2. Soil Parameters

From Equation 2, $E_s^* = 2,976$ ksf if $k = 24$ ksf/ft and 3,968 ksf if $k = 32$ ksf/ft. The Kay and Cavagnaro method (1983) led to a value of $E_s^* = 2,943$ ksf for the lower bound value of k.

ANALYSIS OF SETTLEMENT

Two soil-structure interaction analyses were performed using a slab on a semi-infinite elastic solid finite element computer program SLAB2 modified and applied by Wray (1978). Input load parameters included the column loads shown on Figure 1 and a uniform bearing pressure of 0.5 ksf to simulate weight of the concrete mat. A lower bound value of $E_s^* = 2,943$ ksf and $\mu_s = 0.3$ were used for the soil parameters. Mat parameters assumed a Young's modulus of 432,000 ksf and Poisson's ratio of 0.15. The first analysis used as a mat thickness of 3.5 ft, which assumes no significant stiffness contributed by the superstructure. The second analysis used a much larger mat thickness of 36 ft, which considers a nearly rigid stiffness contributed by the superstructure.

The results of the first analysis using low structural stiffness led to a maximum center settlement of about 1.7 inches and edge settlement of 1.1 inches, Figure 3. The results of the second analysis using the nearly rigid structural stiffness led to a nearly uniform settlement of about 1.3 inches. Substituting a higher bound value of $E_s^* = 4,000$ ksf for the effective soil modulus will decrease these settlements about 33 percent, Figure 3. Settlement points shown from left to right on Figure 3 for Section A, long direction, correspond with nodal points from left to right in Section A on Figure 1 (i.e., nodal points 6, 16, 26, ... 156, 176). Settlement points shown from left to right on Figure 3 for Section B, short direction correspond with nodal points from bottom to top in Section B on Figure 1 (i.e., nodal points 101, 102, ... 109, 110).

LEVEL OBSERVATIONS

Level surveys were initiated immediately after construction of the mat foundation in December 1977 and were performed at 19 locations on the mat surface through May 1985. The reference permanent benchmark is set 65 ft below ground surface. These surveys through May 1985 indicate most settlement of about 1.3 inches near the center decreasing to about 0.8 inches along the east and west edges furthest from the center, Figure 4. Settlement was relatively uniform parallel with the short direction. These settlements do not include settlement of the mat during its construction.

The observed distortion pattern in Figure 4 is dish-shaped and consistent with the calculated distortion pattern shown in Figure 3. The November 1983 survey indicated a slight heave toward the west relative to the August 1978 survey, Figure 4. This heave may be related to the potential for swell of soil within 10 ft beneath the mat base and slightly less column loads toward the west.

Settlements calculated using effective moduli of 4,000 ksf and 2,943 ksf bound the observed

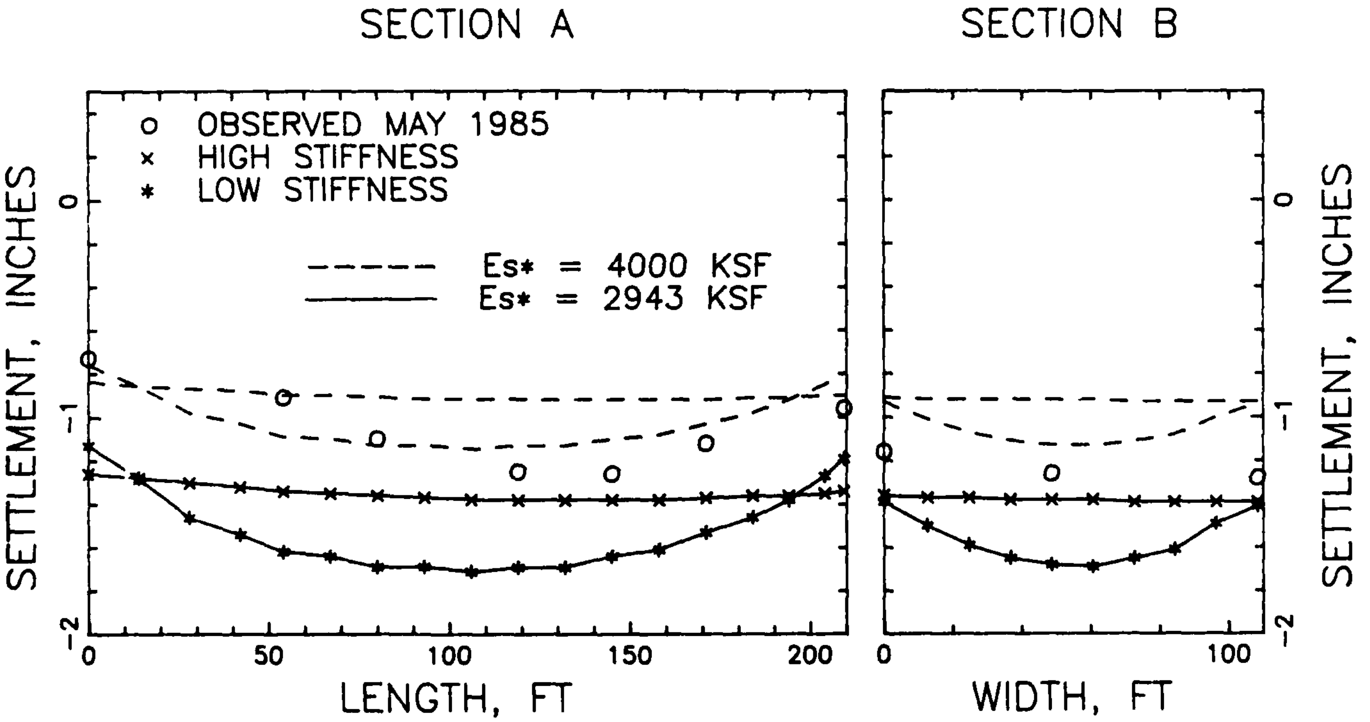

Fig. 3. Settlements

displacements of the mat. Therefore, estimates of the effective elastic modulus using Equation 2 with upper and lower values of k described in Equation 1 and shown in Figure 2 are adequate. Exclusion of the *uniform mat weight* of about 0.5 ksf in the finite element analysis (to be consistent with the observed settlements) will reduce the calculated settlements about 0.1 inch. The mat appears to have a relatively low structural stiffness in the long direction, Section A, with an effective modulus between 4,000 and 2,943 ksf. The mat appears to be relatively stiff in the short direction, Section B. Note that both calculated and observed settlements tend to increase in magnitude from left to right in Figure 3 consistent with the heavier loads toward the right or east end of the mat.

CONCLUSIONS

Comparison of observed with calculated settlements shows that the distortion pattern is consistent with a plate on a semi-infinite elastic medium. An appropriate range of effective elastic soil moduli may be evaluated for evaluation of settlement beneath slabs and the *range depends on* reasonable estimates of the upper and lower bound values of elastic modulus of the soil strata for substantial distances beneath the mat. The assumption of the soil elastic modulus increasing linearly with depth is adequate for this case history. Applied loading pressures must be less than the maximum past pressure of the foundation soil.

ACKNOWLEDGMENT

This study was supported by a grant from the Office, Chief of Engineers, Washington, D.C. The assistance provided by the Foundation and Materials Branch, U.S. Army Engineer District, Fort Worth, toward completion of this study is much appreciated.

REFERENCES

Annual Book of ASTM Standards (1986), "Standard Test Methods for One-Dimensional Swell or Settlement Potential of Cohesive Soils", Soil and Rock; Building Stones, ASTM D 4546-85, 04.08:992-1001, Philadelphia, Pennsylvania.

Duncan, J. M. and Chang, C. Y. (1979), "Nonlinear Analysis of Stress and Strain in Soils", Journal of the Soil Mechanics and Foundations Division, American Society of Civil Engineers, 96:1053-1068.

Kay, J. N. and Cavagnaro, R. L. (1983), "Settlement of Raft Foundations", Journal of Geotechnical Engineering, American Society of Civil Engineers, 109:1367-1382.

Wray, W. K. (1978), "A Design Procedure for Stiffened Slabs Constructed Over Expansive Soils", Ph.D. Thesis, Department of Civil Engineering, Texas A&M University, College Station, Texas.

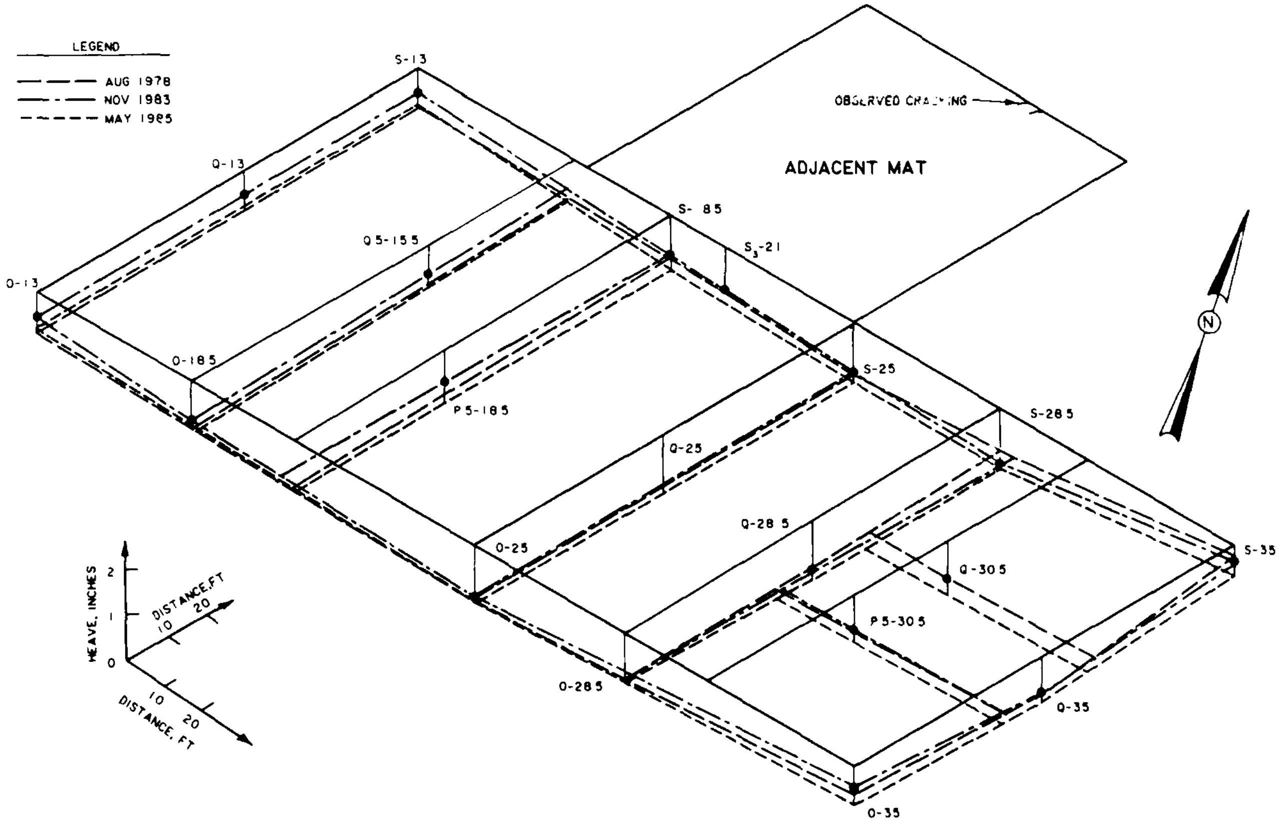

Fig. 4. Level Surveys

Proceedings: Second International Conference on Case Histories in Geotechnical Engineering, June 1-5, 1988, St. Louis, Mo., Paper No. 5.21

Oversteepened Slopes Reinforced with Tensar Geogrid

James E. Laier
Principal Engineer, Southern Earth Sciences, Inc., Mobile, Alabama

Robert M. Mattox
Regional Engineer, The TENSAR Corporation, Atlanta, Georgia

SYNOPSIS: This paper describes geotechnical design concepts used in developing 45-degree and 56-degree embankment slopes to meet strict stability criteria. Typical design sections are presented along with example stability computations to illustrate factors of safety developed under static and rapid drawdown conditions. This paper also discusses pertinent, site specific aspects of construction considered germane to successful, long term performance of oversteepened slopes at this site.

INTRODUCTION

This case history involves the use of TENSAR Geogrid as internal reinforcing for residual soils to permit safe construction of high, oversteepened slopes along the banks of a manmade lake in southwest Jefferson County, Alabama. The site, located in the Alabama Physiographic Province, is characterized by folded, sedimentary bedrock (shale and sandstone) of varying lithology, overlain by residual soils (silty sands and clays), with a differential surface elevation of 98 feet across the site. Originally, site developers proposed to construct a large hotel complex along the crest of a high ridge overlooking the lake. Initial plans incorporated a series of high retaining walls to confine the embankment from the crest of the ridge to the bank of the lake by forming a series of terraces. Cost estimates were prepared on a variety of wall systems including reinforced soil retaining walls. Based on the high cost of these wall systems, project planners decided to investigate the concept of constructing a steep slope reinforced with TENSAR Geogrid. SOUTHERN EARTH SCIENCES, INC., working in conjunction with the slope contractor, United International, Inc., and with The TENSAR Corporation, designed a series of oversteepened, TENSAR reinforced slopes to replace the terraced wall concept along 900+ feet of waterfront on the northern perimeter of the site.

SITE AND SOIL CONDITIONS

The project site is located within the Alabama Valley and Ridge Physiographic Province which consists of a series of alternating northeast striking parallel ridges and valleys. The predominant geologic unit is the Pottsville Formation which consists of alternating beds of shale and sandstone with numerous coal seams and associated beds of underclay overlying sedimentary bedrock. Sandstones near the base of the formation consist predominantly of orthoquartzites with locally occurring beds of quartz pebble conglomerate. Sandstones in the upper part of the formation are generally subdivided into subgraywackes composed of quartz and metamorphic rock fragments. The sandstone of the Pottsville Formation typically weathers to a clayey sand while the shale usually weathers to a clayey soil (1).

Topography at the site is characterized by hills with steep side swales and valleys. Surface elevations typically range from a high of +510 feet (MSL) at the northwest corner of the site, to a low of +412 feet (MSL) along the banks of Chase Lake Creek. Although the sands and sandstones typically absorb small quantities of water, steep surface slopes at the site facilitate rapid water runoff. Consequently, predominant drainage of the area occurs through surface runoff (2). For design purposes the hydrostatic ground water table was assumed to coincide with the normal operating pool level of Chase Lake at approximate elevation +412 feet (MSL).

STEEP SLOPE GEOMETRY AND DESIGN PARAMETERS

Site developers initially proposed to construct a large hotel complex along the crest of a high ridge at the site, overlooking Chase Lake at an average elevation of +460 feet (MSL). Their initial plans incorporated a series of high retaining walls to confine the embankment from the crest of the ridge to the bank of the lake by forming a series of terraces.

Due to economic and construction considerations associated with building high walls along approximately 900+ frontage feet of lakeside, project developers decided to investigate the concept of constructing steep slopes reinforced with TENSAR Geogrid as an alternative design concept for the site. Ultimately, the developers contacted United International, Inc. with the prospect of constructing 45-degree and 56-degree soil reinforced slopes in place of conventional wall systems.

The design concept included analysis and design of three different steep slope sections. Figure 1 shows a typical Plan View of the embankment area, identifying the extent of each section.

(1) Bhate Engineering Corporation Report, 1985, Page 6

(2) Bhate Engineering Corporation Report, 1986, Page 6

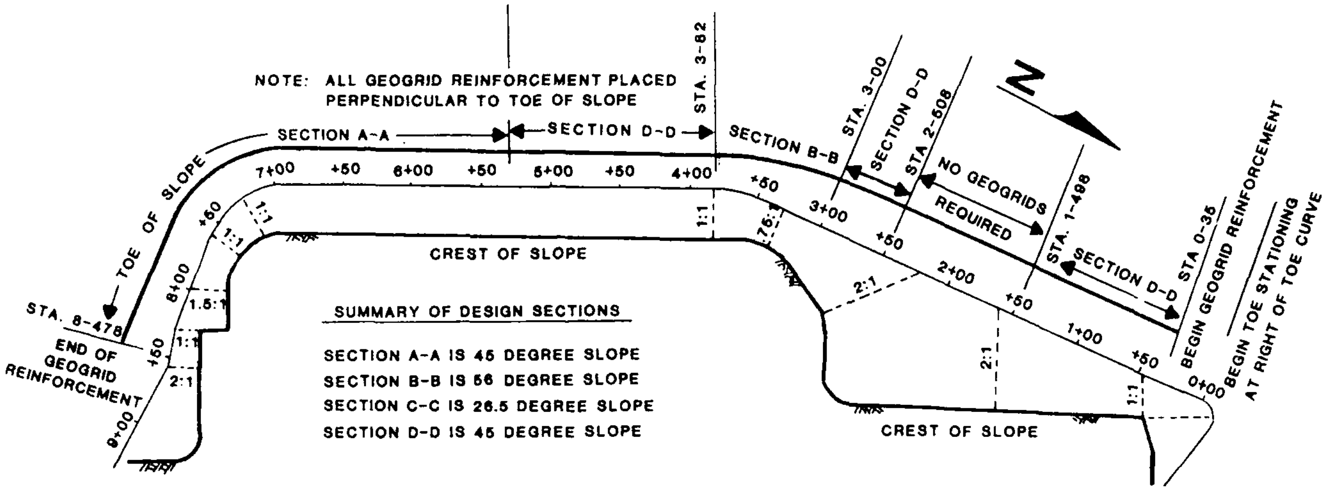
NOTE: ALL GEOGRID REINFORCEMENT PLACED PERPENDICULAR TO TOE OF SLOPE
STA. 3-82
SECTION A-A
SECTION D-D
SECTION B-B
STA. 3-00
SECTION D-D
STA. 2-60B
NO GEOGRIDS REQUIRED
STA. 1-49B
SECTION D-D
STA. 0-35
BEGIN GEOGRID REINFORCEMENT
BEGIN TOE STATIONING AT RIGHT OF TOE CURVE
TOE OF SLOPE
STA. 8-47B
END OF GEOGRID REINFORCEMENT
9+00
+50
8+00
+50
7+00
+50
6+00
+50
5+00
+50
4+00
+50
3+00
+50
2+00
+50
1+00
+50
0+00
1:1
1.5:1
1:1
2:1
1:1
.75:1
2:1
2:1
1:1
CREST OF SLOPE
CREST OF SLOPE
SUMMARY OF DESIGN SECTIONS
SECTION A-A IS 45 DEGREE SLOPE
SECTION B-B IS 56 DEGREE SLOPE
SECTION C-C IS 26.5 DEGREE SLOPE
SECTION D-D IS 45 DEGREE SLOPE

Figure 1

Typical Plan View of Embankment Area

Table 1, below, summarizes specific information about each section:

TABLE 1

Section Designation	Design Slope Angle	Maximum Slope Height	Reinforcement
"A-A"	45.0-Degrees	36-Feet	TENSAR GEOGRID
"B-B"	56.0-Degrees	37-Feet	TENSAR GEOGRID
"C-C"	26.5-Degrees	42-Feet	UNREINFORCED
"D-D"	45.0-Degrees	38-Feet	TENSAR GEOGRID

Soil stratigraphy and design soil parameters were developed from information provided by BHATE ENGINEERING CORPORATION (3). Table 2, below, summarizes soil design parameters used on this project:

TABLE 2

Summary of Design Parameters

Embankment Section	Soil	SOIL DESIGN PARAMETERS pcf	C psf	Ø (Degrees)
"A-A"	1	200	0	0----------Surcharge
	2	120	300	32
	3	120	900	32
	4	120	900	32
	5	135	4000	40
	6	120	150	32
	7	120	900	32
"B-B" "C-C" "D-D"	1	200	0	0----------Surcharge
	2	120	300	32
	3	120	900	32
	4	120	900	32
	5	135	4000	40
	6	120	150	32
	7	120	250	0

(3) Bhate Engineering Corporation Report, 1986, with Addenda

Slope reinforcing materials were provided by the TENSAR CORPORATION and consisted of high tensile strength, high density polyethylene geogrids which are resistant to all chemical substances normally existing in soil. Table 3, below, summarizes pertinent GEOGRID reinforcing information:

TABLE 3

Grid Designation	Geogrid Type	Design Strength (plf)
A	TENSAR UX1100	1000
B	TENSAR UX1200	2000
C	TENSAR BX1100	350

The normal pool elevation of the lake was +412 feet. Hydrographic data, however, showed that the hundred year flood elevation was +425, hence the lower 13 feet of the slope would be subjected to saturation and to possible excess piezometric conditions created by rapid drawdown. The project developer estab'ished a minimum factor of safety of 1.30 for the slopes under rapid drawdown conditions.

METHOD OF ANALYSIS AND DESIGN

All slopes were analyzed and designed using TENSAR guidelines and computer programs capable of incorporating soil reinforcement into stability computations. Circular arc sections were evaluated by the "Method of Slices" using the "Simplified Bishop Equation" (4) and irregular and/or wedge failure surfaces were evaluated using the "Janbu Equation" (5). Generally, a systematic series of wedges and arcs were considered during the analysis process using a trial reinforcement layout to determine the most critical combination of stresses developed in soil reinforcement for a particular combination of soil stratification and slope angle. The analysis and design process continued, iteratively, revising and adjusting GEOGRID layout until a satisfactory solution could be achieved for both normal pool and 100-year flood criteria.

Input data for both methods of analyses are as follows:

1. A surface profile with the location of different soil types.
2. Design soil parameters including densities and effective stress strength values.
3. A profile of ground water conditions.
4. Externally applied loads.
5. Reinforcement type geometry, ultimate tensile strength and allowable tensile stress.
6. Parameters describing the bond between the soil and the GEOGRID reinforcement.
7. Seismic forces.

Once this data has been entered into the computer, a suitable reinforcement layout, providing Safety Factors greater than the specified minimums was rapidly and effectively determined. Graphical output, showing minimum Safety Factors for each trial run were used in conjuction with a detailed printout listing reinforcement forces, margins against reinforcement bond and tensile failures and comparisons with permissible GEOGRID stress levels, to determine the final design type, quantity and layout of GEOGRID reinforcement for a particular slope configuration.

Figures 2 and 3 illustrate typical sections geometry for the 56° slope (section "B-B") showing GEOGRID reinforcement and facing details. In Figure 2, the primary reinforcing was provided by TENSAR UX1200 GEOGRID and the intermediate reinforcing consisted of TENSAR SS-1 GEOGRID. The purpose of the intermediate reinforcing was to handle stresses within the embankment material created for construction process and to facilitate compaction near the edge of the slope for the zones of soil lying between layers of primary reinforcing. The face of the 56° slope was wrapped with SS-1 GEOGRID which contained a layer of straw designed to impede erosion until the vegetative root map had been established (Figure 3). No face wrapping was required for the 45° slopes.

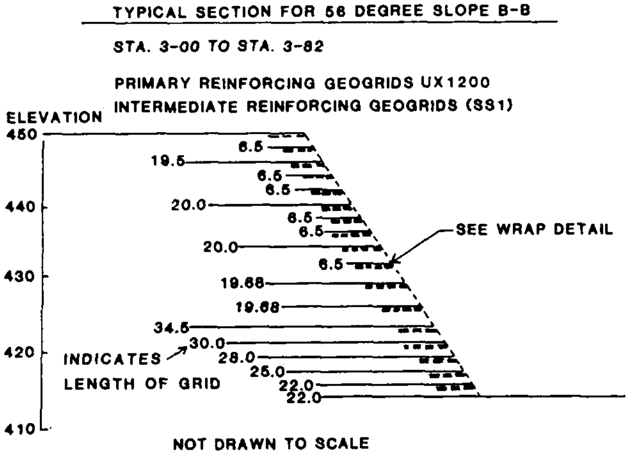
TYPICAL SECTION FOR 56 DEGREE SLOPE B-B
STA. 3-00 TO STA. 3-82
PRIMARY REINFORCING GEOGRIDS UX1200
INTERMEDIATE REINFORCING GEOGRIDS (SS1)
ELEVATION
450
440
430
420
410
6.5
19.5
6.5
6.5
20.0
6.5
6.5
20.0
6.5
19.68
19.68
34.5
30.0
28.0
25.0
22.0
22.0
SEE WRAP DETAIL
INDICATES LENGTH OF GRID
NOT DRAWN TO SCALE

Figure 2

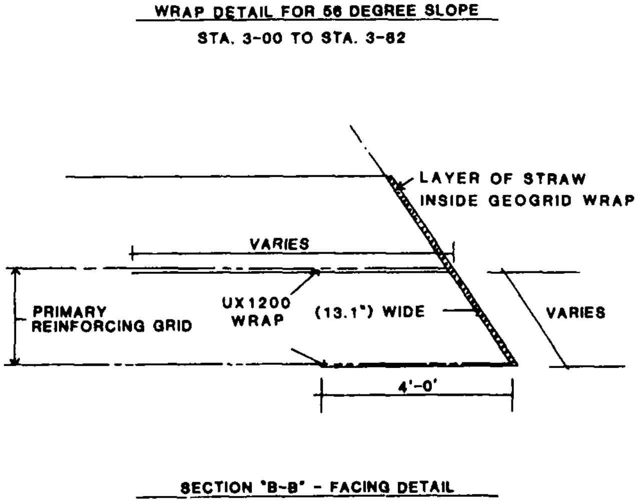
WRAP DETAIL FOR 56 DEGREE SLOPE
STA. 3-00 TO STA. 3-82
LAYER OF STRAW INSIDE GEOGRID WRAP
VARIES
PRIMARY REINFORCING GRID
UX1200 WRAP
(13.1') WIDE
VARIES
4'-0"
SECTION "B-B" - FACING DETAIL

Figure 3

(4) Bishop Geotechnique, 1955

(5) Janbu, European Conference, 1954

Table 4 presents the minimum factor of safety for the final design of slopes on the project for the two conditions studied.

TABLE 4

Minimum Factor of Safety

Section	Normal Pool	Rapid Drawdown
"A-A"	1.64	1.45
"B-B"	1.58	1.45
"C-C"	2.06	1.60
"D-D"	1.63	1.35

Cost estimates revealed that the above designs would require a material cost of $4.25 per square foot of projected slope height. These figures include the cost of both primary and intermediate reinforcing.

CONSTRUCTION

Construction of the project began in July of 1986 with the excavation of soft residual soil in the area of the toe of the slope along the creek leading into the lake. The excavation ranged from three to five feet in depth. While this area was being excavated and backfilled with competent material, the contractor setup a staging area to precut all reinforcing GEOGRIDS to the prescribed lengths. This step facilitated construction of the slope in that all reinforcing grids could be quickly placed at the prescribed elevation without slowing the construction process. D8 bulldozers were used to place fill material over the grids and compaction was achieved with large sheepsfoot and vibratory drum rollers. The contractor, UNITED INTERNATIONAL, INC., reported no problems in achieving compaction to the face of the slope using standard equipment. Rip-rap toe erosion protection was provided along the face of the slope to the hundred year flood elevation and the entire slope was covered with an erosion net to minimize surface erosion until the slope vegetation had been established. The construction of the steeped slope required two months and was completed in September of 1986

CONCLUSION

The difficult site conditions on this project were effectively and economically handled through the use of an oversteeped slope reinforced with TENSAR GEOGRID. The owner reported a savings of approximately one million dollars when compared to their next alternative involving retaining walls. In addition, construction of the oversteeped slope was significantly faster than the projected construction rate for an alternate involving retaining walls. Standard embankment procedures were employed and no delays were encountered in the construction of the slopes. A recent inspection of the parking lot area which extends to the crest of the slopes revealed no cracking or pavement distortion of any type. It is therefore concluded that the use of the TENSAR GEOGRID as slope reinforcing is a viable cost effective alternative to handling differential site conditions and problems associated with instability.

ACKNOWLEDGEMENTS

The authors gratefully acknowledge Mr. George L. Morris, III and Mr. Richard L. Brown of United International, Inc. for their assitance in obtaining project data and their continued support and encouragement during preparation of this paper. Appreciation is also due to the TENSAR Corporation for permitting us to use their technical design information in preparation of this paper. The authors are also grateful to Mr. U.R. Bhate of Bhate Engineering Corporation for his valuable assistance in development of field and laboratory test data. We would also like to express our appreciation to Mr. Stephen Cape for drafting the figures for this paper and to Mrs. Brenda Brantley for typing the manuscript.

REFERENCES

1. Bhate, U.R., Surendra, M., and Tate, D.E., "Final Report of Subsurface Exploration and Geotechnical Engineering Evaluation, Marriott Courtyard Inn, Hoover, Alabama", Bhate Engineering Corporation, October 1985
2. IBID
3. Bhate, U.R. and Surendra, M. "Report of Geotechnical Properties", Marriott Courtyard Inn, Hoover, Alabama", Bhate Engineering Corporation, October 1986
4. Bishop, A.W., "The Use of the Slip Surface in the Stability Analysis of Slopes", Geotechniques, Vol. 5, No. 1, 1955
5. Janbu, N., "Application of Composite Slip Surfaces for Stability Analysis", Proceedings of the European Conference on Stability of Slopes, Vol. 3, 1954

Proceedings: Second International Conference on Case Histories in Geotechnical Engineering, June 1-5, 1988, St. Louis, Mo., Paper No. 5.23

Demonstrating Borehole Drilling Accuracy at the Navajo Dam

Stephen J. Kravits
Mining Engineer, U.S. Department of the Interior, Bureau of Mines, Pittsburgh, Pennsylvania

Hunter C. Harrel
Geologist, U.S. Department of the Interior, Bureau of Reclamation, Denver, Colorado

SYNOPSIS: The U.S. Bureau of Mines recently demonstrated the accurate directional drilling of a near-horizontal borehole with the objective of intercepting a designated target. The project was conducted at the Navajo Dam for the Bureau of Reclamation, U.S. Department of the Interior. The Bureau of Reclamation's objective was to determine the feasibility of accurately drilling long near-horizontal boreholes, from the surface, in lieu of constructing a tunnel under an embankment dam from which shorter boreholes would be accurately drilled to control water seepage.

As a result of the demonstrated drilling accuracy, the Bureau of Reclamation can consider the option of using near-horizontal boreholes drilled from the surface at a cost of $100-200/ft instead of constructing access tunnels at $2,000/ft from which drainage boreholes would be drilled to control water seepage at embankment dams.

DIRECTIONAL DRILLING EXPERIENCE

The Bureau of Mines has researched and demonstrated accurate directional drilling as part of its methane control program (Oyler and Diamond, 1982). In 1979, a directonal surface borehole was drilled using a downhole motor to a measured depth of 1,595 ft, maintaining an arc of 6^0 per 100 ft and coming within 3 ft of horizontally intercepting the Pittsburgh Coalbed 1,012 ft below the surface. 2 Five horizontal methane drainage boreholes, totaling 9,544 ft, were then drilled into the coalbed from the surface borehole.

The Bureau of Mines has also demonstrated drilling accuracy in drilling long horizontal methane drainage boreholes in underground coal mines. Methane drainage boreholes have been drilled to depths greater than 2,000 ft, maintaining vertical borehole trajectory within the coalbed (approximately 6 ft) while controlling horizontal trajectory as desired to prevent interception by future mining (Kravits, Finfinger and Sainato, 1985).

BACKGROUND

Navajo Dam is a zoned embankment structure located in northern New Mexico, 39 miles east of Farmington and about 35 miles southeast of Durango, CO, Figure 1. It is a key structure of the Colorado River Storage Project, regulating the flows of the San Juan River and providing storage for the Navajo Indian Irrigation Project. It also provides a facility for recreation and conservation of fish and wildlife.

Navajo Dam's left and right abutments are experiencing seepage, averaging 1,200 and 600 gal/min, respectively, although seepage is not occurring in the embankment. Open vertical and horizontal joints in the abutments, horizontal bedding planes, and permeable sandstone bedrock provide seepage paths. Investigation by the Bureau of Reclamation has indicated that the current rate of seepage would not be a problem except for the potential piping of erodible material in the core, if open horizontal and vertical joints are in contact with the core (Ehler, 1983). Soletanche is currently constructing a concrete diaphragm cutoff wall on the left abutment to control water seepage, under contract to the Bureau of Reclamation. A similar, but larger, cutoff wall on the right abutment was determined to be too costly. Consequently, the Bureau of Reclamation contracted the construction of a tunnel to Frontier Kemper to provide access to accurately drill 44 drainage boreholes, totaling 15,000 ft, subcontracted to Boyles Bros. Drilling. Accurately drilled drainage boreholes will redirect the seepage away from critical areas of the dam-foundation contact by lowering the phreatic water surface in the right abutment.

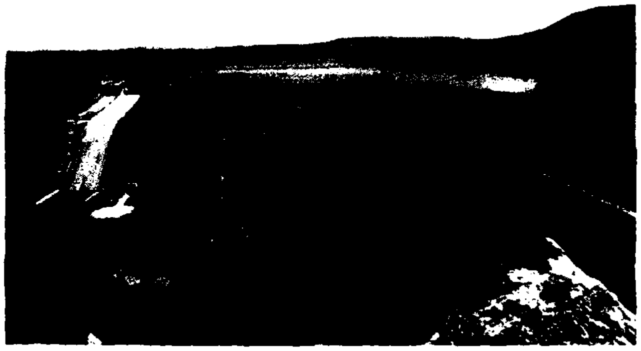
Fig. 1 Navajo Dam, New Mexico

PLANNING THE DEMONSTRATION BOREHOLE

The right abutment of the Navajo Dam was chosen for the location of the demonstration borehole because a relatively long near-horizontal borehole could be drilled with easily accessible starting and endpoint surface locations, Figure 2. Furthermore, information gathered during the drilling of the borehole, including problems encountered and their solutions, could prove valuable to the drilling subcontractor.

The designated "punchout" was to occur by drilling approximately 890 ft of near-horizontal borehole to

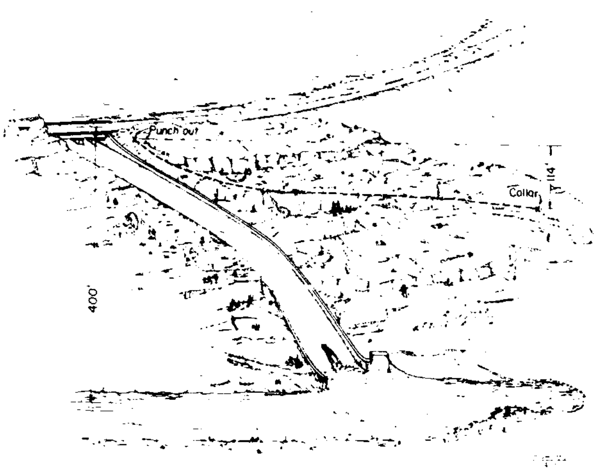
Punch out
Collar
114'
400'

Fig. 2 Navajo Dam Right Abutment

intercept a 5-ft-radius target located near the top of the spillway. The vertical and horizontal trajectories of the borehole were determined after considering the geology of the right abutment and the effects that specific geologic features would impose on the placement of the borehole. The abutment in the vicinity of the borehole consists predominantly of coarse- to medium-grained sandstone with interbedded shale and siltstone, Figure 3. The sandstone is comprised mostly of very angular quartz grains weakly to moderately cemented and having an unconfined compressive strength of less than 6,000 psi (Ehler, 1983).

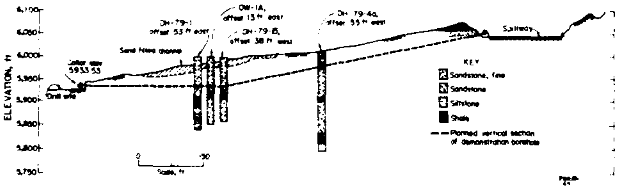
6,100
6,050
6,000
5,950
5,900
5,850
5,800
5,750
ELEVATION, ft
Drill site
Collar elev 5933.53
Sand filled channel
DH-79-1 offset 53 ft east
OW-1A, offset 13 ft east
DH-79-15, offset 38 ft west
DH-79-4a, offset 55 ft west
Spillway
KEY
Sandstone, fine
Sandstone
Siltstone
Shale
Planned vertical section of demonstration borehole
0
50
Scale, ft

Fig. 3 Vertical Cross Section of Planned Demonstration Borehole

Rock outcrops within the right abutment contain both vertical and horizontal joints. Unfortunately, the exact locations of the joints in the subsurface could not be determined; therefore, the borehole trajectory could not be planned to avoid intercepting them. However, the borehole was designed to avoid intercepting the sand-filled channel shown in Figure 3. The elevation at the bottom of the sand-filled channel was estimated to be 5,950 ft, or about 16.5 ft above the collar of the borehole. To prevent drilling into the channel, the first 250 to 300 ft of the borehole were to be drilled near horizontal at about the same elevation as the collar, or 5,933 ft. Borehole elevation would then increase steadily or build at a rate of about 1.8 ft/10 ft drilled, in order to intercept the target elevation. While maintaining desired vertical trajectory as mentioned, an attempt was to be made to maintain departure within 2 ft east or west from the planned straight-line, collar-to-punchout, horizontal trajectory of N 0°-45'-00" E, Figure 4.

DIRECTIONAL DRILLING PROCEDURES

A Diamant Boart[1] DBH 700 hydraulic core drill was used to supply thrust to a diamond drill bit by maintaining hydraulic pressure on the drill rods, Figure 5. A Slimdril 2-7/8-in-OD, high-torque downhole motor was positioned behind the drill bit, Figure 6. The Slimdril is a positive-displacement hydraulic motor that rotates the drill bit without rotating the drill rods. The downhole motor converts the hydraulic horsepower generated by the flow of the drilling fluid, provided under pressure by two triplex piston pumps, into torque and rotational speed, which drives the drill bit.

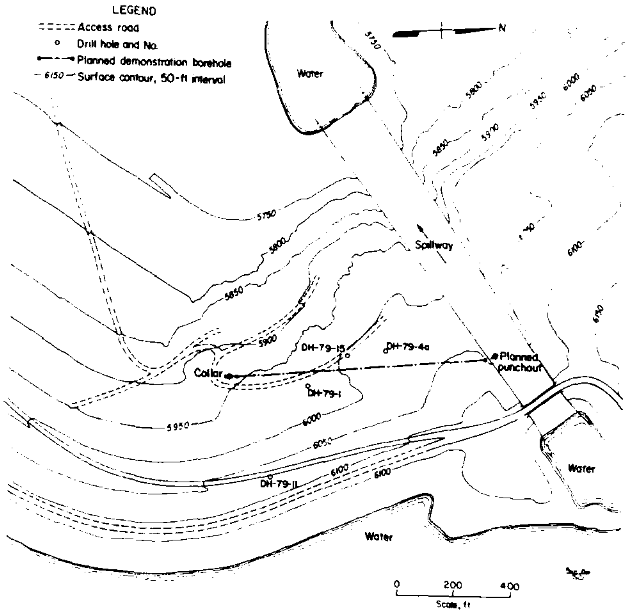
LEGEND
Access road
Drill hole and No.
Planned demonstration borehole
6150 Surface contour, 50-ft interval
N
Water
5750
5800
5850
5900
5950
6000
6050
6100
6150
Spillway
Collar
DH-79-15
DH-79-4a
DH-79-1
DH-79-11
Planned punchout
Water
Water
0
200
400
Scale, ft

Fig. 4 Map View of Planned Demonstration Borehole

Fig. 5 A, Hydraulic Drill; B, Control Panel, Power Unit Not Shown

---

[1] Reference to specific equipment does not imply endorsement by the Bureau of Mines.

The demonstration borehole's horizontal and vertical trajectories were controlled during downhole motor drilling by using several bent housings; the 2° bend was the most effective. While drilling, there is continuous contact between the convex side of the bent housing and the wall of the borehole; this is commonly called side force. The resultant reaction of the side force exerted on the wall of the borehole is a force exerted on the bit in the opposite direction (180°), Figure 6.

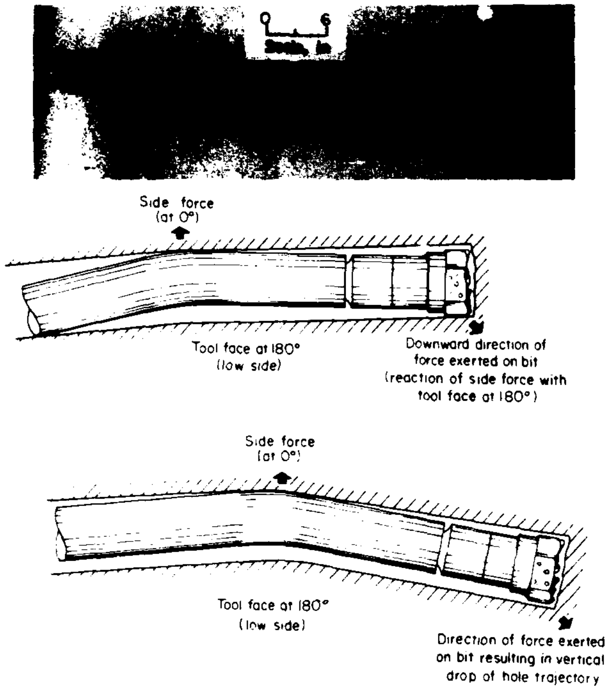

0
6
Scale, in
Side force (at 0°)
Tool face at 180° (low side)
Downward direction of force exerted on bit (reaction of side force with tool face at 180°)
Side force (at 0°)
Tool face at 180° (low side)
Direction of force exerted on bit resulting in vertical drop of hole trajectory

Fig. 6 Side Force Diagram. Downhole Motor (top) and Side Force Schematic (bottom)

The direction of the force exerted on the bit is called tool face direction and is the direction borehole trajectory will follow. Therefore, because the drill rods do not rotate and the downhole motor was used with a bent housing, desired borehole trajectory was achieved by simply aiming or orienting the bent housing in the desired direction, Figure 7. To maintain the desired horizontal and vertical borehole trajectories, borehole inclination, bearing, and tool face direction were monitored using an NL Sperry Sun, Type B 120°, photographic survey instrument, Figure 8.

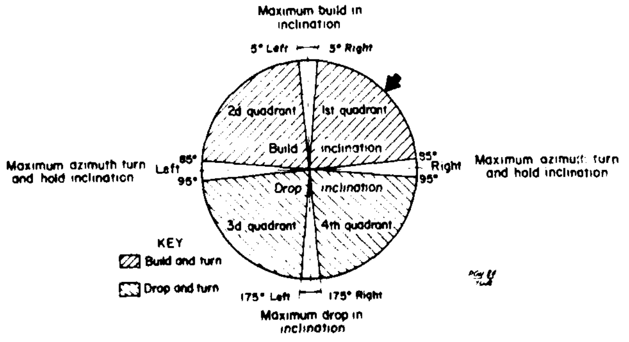

Maximum build in inclination
5° Left ← → 5° Right
2d quadrant
1st quadrant
Build
inclination
Drop
inclination
3d quadrant
4th quadrant
Maximum azimuth turn and hold inclination
Left 85° 95°
85° Right 95°
Maximum azimuth turn and hold inclination
KEY
▨ Build and turn
☐ Drop and turn
175° Left ← → 175° Right
Maximum drop in inclination

Fig. 7 Various Tool Face Settings and Their Effects on Borehole Trajectory

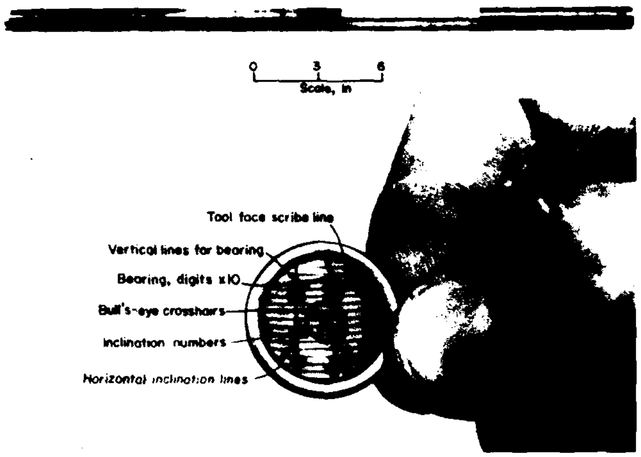

0
3
6
Scale, in
Tool face scribe line
Vertical lines for bearing
Bearing, digits x10
Bull's-eye crosshairs
Inclination numbers
Horizontal inclination lines

Fig. 8 Single-shot Survey Instrument (top) and Reading a Developed Survey Film Disk (bottom)

To conduct a survey, the mechanical timer of the survey instrument is set and the instrument is loaded with a film disk. The loaded survey instrument is placed in its protective casing and inserted in the hollow drill rod, where it is pumped with water to the back end of the downhole motor. The film disk is exposed at a preset time, after which the instrument is retrieved by a wire line attached to the protective casing. The retrieved instrument is removed from its protective casing, and the film disk is removed, developed, and read.

DRILLING ACCURACY

Borehole drilling accuracy is dependent on the inherent accuracy of the survey instrument, magnetic interference from drill rods, downhole motors, drill bits, etc., surveying frequency, and surveying calculation method.

NL Sperry-Sun's specified tolerance in measuring bearing for a recently calibrated Type B 120° compass is ±0.5°. Furthermore, the resolution in reading the photographed compass bearing on the film disk is a random, ±0.5°. Consequently, a potential error of ±1° exists in measuring borehole bearing using the subject survey instrument. Compass units measure magnetic north and require a declination correction to obtain true north. The National Geophysical Data Center in Boulder, CO, provided a declination correction of 12° East for the drill site.

Compass-type surveying instruments sense only the direction of the local magnetic field vector and therefore are subject to interference from drill rods, downhole motors, and drill bits, constructed of magnetic material. A nonmagnetic downhole motor and 100 ft of nonmagnetic stainless steel drill rod were placed directly behind the drill bit. To minimize magnetic interference from the drill bit and the drill rods above the stainless steel rods, the survey instrument was positioned 20 ft from the bit while conducting a survey.

Two additional factors that affect the borehole accuracy are surveying frequency and the surveying calculation method used to determine borehole coordinates and elevation. Borehole surveys were conducted at 10-ft drilling intervals because short survey intervals will generally result in increased borehole accuracy. The radius-of-curvature surveying calculation technique adapted for a handheld calculator was used to determine borehole coordinates and elevation (Oyler, 1983). The radius of curvature method is accepted as one of the most accurate surveying calculation techniques available (American Petroleum Institute, 1985).

DRILLING AND SURVEYING RESULTS

Vertical borehole trajectory was maintained near the collar elevation for the first 300 ft of the borehole as planned, using the downhole motor equipped with a 1/2^{0} bent housing, Figure 9. Drilling continued to a depth of 455 ft without developing the necessary increase in vertical borehole trajectory. At a depth of 455 ft the 1/2^{0} bent housing was replaced with a 1^{0} bent housing. Drilling continued to a depth of 495 ft without experiencing the desired increase in borehole elevation. The weak nature of the sandstone's intergranular material is believed to have negated any potential side force generated by the 1/2^{0} and 1^{0} bent housings. Consequently, the borehole was abandoned in order to start a new borehole from within the initial borehole at a depth of 289 ft. A 2^{0} bent housing was installed on the downhole motor after the new borehole was started. Vertical borehole trajectory was then maintained as desired, with an increase in borehole elevation of about 1.8 ft/10 ft drilled, to borehole completion at 885 ft. According to the borehole surveys, horizontal borehole trajectory for the most part was maintained close to the desired straight-line collar-to-punchout trajectory, Figure 10.

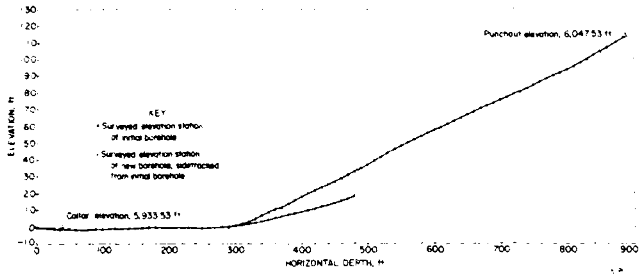

Fig. 9 Vertical Section of Demonstration Borehole

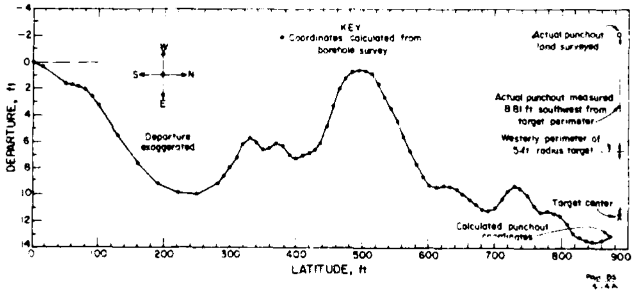

Fig. 10 Plan View of Demonstration Borehole

The demonstration borehole's final near-horizontal depth was 885 ft when punchout occurred near the top of the spillway. According to the departures and latitudes calculated from borehole surveys, the borehole punchout occurred only 1.4 ft east of the target center. Actual punchout, determined by land survey, occurred 13.81 ft west of the center of the target. The error between the actual and calculated punchout departure of 15.21 ft was within the survey instrument's accuracy in measuring bearing to within 1^{0}, Figures 10 and 11.

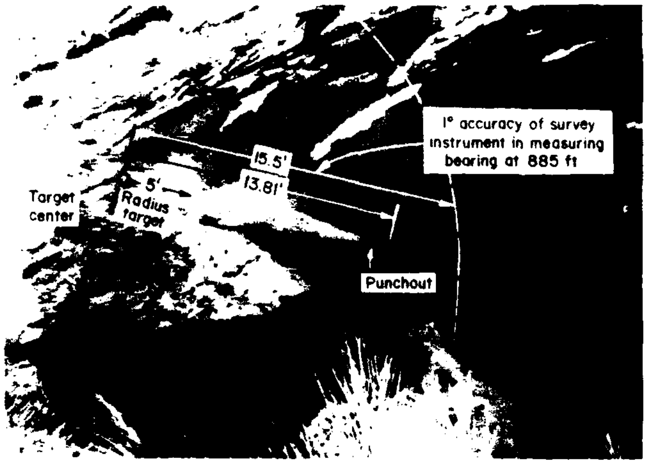

1° accuracy of survey instrument in measuring bearing at 885 ft
15.5'
13.81'
5' Radius target
Target center
Punchout

Fig. 11 Borehole Punchout

The punchout elevation calculated from surveyed inclinations was 6,047.14 ft, which was well within the target elevation of 6,044.03 to 6,054.03 ft and only 0.39 ft from the actual punchout elevation determined by the land survey, Figures 10 and 11. Borehole inclination can be surveyed to within 0.25^{0} using the NL Sperry-Sun, Type B 120^{0} survey instrument.

CONCLUSIONS

The demonstration borehole was accurately drilled to a final near-horizontal depth of 885 ft, where punchout occurred. Final borehole elevation was 1.5 ft from the elevation of the target center, while borehole punchout coordinates were only 8.81 ft southwest of the target's perimeter.

REFERENCES

American Petroleum Institute (1985), "Directional Drilling Survey Calculation Methods and Terminology", Bull. D20.

Ehler, W.C. (1983), "Final Report on Investigations for Seepage Control Navajo Dam", BuReclamation.

Kravits, S.J., G.L. Finfinger, and S. Sainato (1985), "Comparison of Rotary and In-Hole Motor Techniques for Drilling Horizontal Boreholes in Coal", BuMines RI 8933.

Oyler, D. C. (1983), "Program Computes Radius-of-Curvature Coordinates for Straight, Deviated Holes", Oil and Gas J., V. 81, No. 43, 100-108.

Oyler, D.C., and W.P. Diamond (1982), "Drilling a Horizontal Coalbed Methane Drainage System from a Directional Surface Borehole", BuMines RI 8640.

Proceedings: Second International Conference on Case Histories in Geotechnical Engineering, June 1-5, 1988, St. Louis, Mo., Paper No. 5.25

Design and Monitoring of Earth Embankments over Permafrost

S. Dufour
Geocon Inc., Yellowknife, Northwest Territories, Canada (now with IDRC, Ottawa, Canada)

P. Lafleche
Permafrost Research Section, Geological Survey of Canada, Ottawa, Canada

A.S. Judge
Permafrost Research Section, Geological Survey of Canada, Ottawa, Canada

SYNOPSIS: As the northern regions of Canada are developed, there is an increasing need to protect the fragile ecology as well as to maximize usage of local construction materials. The construction of earth dykes to retain liquid wastes is a common requirement in municipal and industrial developments. Frozen core earthfill dykes provide an effective technique to cut off seepage in cold permafrost areas (Sayles, 1984). The seepage of water through an unfrozen overburden or fractured bedrock foundation can occur and accelerate the thermal deterioration of an earth embankment. The development of the active layer during the summer reduces the dam's ability to retain water if the freeboard is inadequate.

Several earthfill dams were built at the Lupin mine near Contwoyto Lake in the Canadian Arctic to form a mine tailings pond. Even though design forecasts indicated 9 m high structures would remain frozen after impoundment of the reservoir, very few case histories were found to support the design. Several earth dams have been monitored since 1982. Initially, ground temperature measurements were taken with thermistor strings in short boreholes. More recently, deep boreholes were instrumented with thermistor strings and the ground probing radar has been used to confirm and locate unfrozen zones within the dams.

Specifically, the performance of three dams is reviewed here. The first dam, the base case, was built over virgin cold permafrost. The complete dam section froze during the first winter after construction. Part of the second dam was built over a 5 m deep talik associated with a seasonal creek and possibly a fault zone. The talik is apparently mostly refrozen and continuing to cool, however, geophysical surveys indicate a possible unfrozen remnant. The third dam was built across the reservoir after impoundment and during the winter. The internal nature of that dam and its thermal behaviour are quite different from the above two.

The thermal regime of the dams and underlying foundation has changed considerably over the five years following construction. The results of the ground temperature and radar profiles are compared for various seasons to reconstruct the transient thermal regime at uninstrumented sections. The findings are significant for the design and monitoring of future water retaining structures in the North.

INTRODUCTION

In today's developing North, there is a recognized need to protect the fragile ecology. As mine and industrial sites are developed and communities grow, the construction of earth dams and dykes to retain liquid wastes is a common requirement. In design of such structures there are economic pressures to maximize use of local construction materials. Frozen core earthfill dams are an effective retainment technique in cold permafrost.

However, before a dam is built the foundation conditions and the ground thermal regime must be sufficiently understood. The development of the active layer during the summer reduces the dam's ability to retain water if the freeboard is inadequate. The seepage of water through an unfrozen overburden or fractured bedrock foundation can occur and induce the thermal deterioration of the frozen earth embankment.

Several earthfill dams were built at the Lupin mine to enclose a small watershed and to form a mine tailings pond. The dams were instrumented with thermistor strings and frequently surveyed with a prototype ground radar. This paper reviews the design and performance of three of these dams. The results of the ground temperature and radar profiles are compared for various seasons to reconstruct the transient thermal regime at uninstrumented sections. This paper also discusses the significance of the findings for design and monitoring of future earthfill structures in the North.

BACKGROUND INFORMATION

Location

The Lupin mine is situated on the shores of Contwoyto Lake, some 380 km northeast of Yellowknife, N.W.T. (Figure 1). The area is characterized by low relief (less than 15 m), a poorly developed drainage pattern, numerous shallow lakes and cold permafrost. The mine is only accessible by aircraft during the summer or by a 400 km ice road during the winter.

The mean annual air temperature is -12.1°C with freezing and thawing indices of 5100 and 680°C-days respectively. Total yearly precipitation is 275 mm. Lake ice reaches a thickness of 2m.

A 614 ha watershed was formed by damming a seasonal creek and five saddles which connected at various elevations with adjoining watersheds (Figure 1). The dams were built during the summer of 1981. Prior to impoundment, the tailings pond area contained 15 lakes up to 15 ha in area and with water 1 to 6 m deep. Since 1985, the tailings area has been divided in two ponds: an upper pond (1) which receives the mill water and allows the solids to settle, and a lower pond (2) which stores the clarified and partially treated water (treatment is carried out while decanting water from the upper to the lower pond) prior to discharge into the natural environment.

The three dams which are the subject of this paper are: Dams 1A, 2 and J shown on Figure 1. Dam 1A was built across the valley of an intermittent creek, the outlet of the enclosed basin. At the time of construction, the talik beneath the bed of the intermittent outlet could not be completely subexcavated because of its saturated state and of the lack of time for completion during the same construction season. Temperature measurements have since shown the talik to extend 5 m below the original ground surface. Dam 2 was built over undisturbed permafrost between two lakes. Finally, Internal Dam J was built across the impounded reservoir. Internal Dam J was built where a shallow lake (up to 3 m deep) used to be and is about 13 m high from toe to crest. The water depth in the tailings basin at the time of construction was about 7 m. The dam has water on both sides.

Subsurface Conditions

The detailed geology and geomorphology at the dams are discussed in Holubec et al. (1982) and Dufour and Holubec (1988). One or two test holes were drilled at each dam site during the winter of 1980-81 for preliminary planning purposes. A go-ahead decision was taken shortly after completion of the preliminary engineering study and further field investigations were not carried out. The site of Internal Dam J was never investigated as it was not part of the initial tailings management plan. The following observations were made at seven test holes within the tailings area. Their results concur with those of nearly 30 holes drilled for the airstrip and the mine facility nearly 3 km.

The overburden is thin and consists of silty sand till 0 to 7 m. The surface is covered by a thin organic layer up to 45 cm thick in wet depressions. The till has from 12 to 42% fine-grained silt and up to 20% cobbles and boulders by weight.

The bedrock is generally competent phyllite with a weathered zone extending 1.5 to 3 m deep. The bedrock is generally highly fractured within the weathered zone. Frost-thrusted blocks (felsenmeer) are common on rock outcrops.

The soil and rock are permanently frozen. The thickness of the active layer varies from 0.6 m in thickly vegetated areas with overburden cover to about 2.5 m in general and up to 7 m occasionally in barren exposed bedrock areas. Ice lensing was observed to be of rare occurrence. The largest ice layer observed was 80 mm thick. Other lenses observed were smaller than 25 mm. The average moisture content is 14%. The undisturbed mean annual ground temperature was measured to be about -9°C. Based upon observations in the mine, the regional permafrost base extends to over 400 m deep.

The silty sand dam foundation and the thin overburden cover on fractured bedrock could pose substantial seepage and stability problems for a water retaining dam on an unfrozen foundation. In view of the cold permafrost regime, it was deemed that seepage could be prevented with a frozen dam core.

Dam Cross-Section

Dams 1A and 2 consist of a summer compacted, sorted silty-sand till (with no cobbles or boulders) core built over the surface stripped of organics. An impermeable membrane was provided on the upstream face and keyed into the permafrost at the upstream toe (Figures 2 and 3). The minimum soil cover on the membrane is 2 m.

Allowing for the thawing of the upper 2 m of overburden, it was predicted that the 6 m high stage I dam would freeze back in three winters at most. The prediction was based upon the review of other case histories and upon one-dimensional heat transfer analysis (Holubec et al., 1982).

Construction and Post-Construction Performance

Dams 1A and 2 were built during the summer of 1981. The construction sequence consisted of first placing the drainage blanket which also served as the access road. This was followed by building the part of the dam downstream of the impermeable liner, excavating the key trench, placing the liner and finally covering the impermeable liner to the crest.

Prior to placing fill the dam base areas were stripped of organics and hummocky soil down to frozen till. Stripping was immediately followed by fill placement to minimize frost degradation of the in-situ till. Construction of the dams was completed to elevation 485 m in early October 1981.

During construction, significant unfrozen soils were encountered at the location of the intermittent basin outlet (north end of Dam 1A). The saturated soils could not all be removed (for lack of adequate equipment and time) and the area was identified for post-construction monitoring. Mill tailings and effluent production began in May 1982 and shortly after thaw in July 1982, seepage was observed at the downstream toe of Dam 1A. A downstream blanket was placed to ballast the dam toe and an upstream silty sand blanket was also built to reduce the seepage. None of the other dams experienced water seepage.

During the winters of 1983-84 and 1984-85, the snow was kept clear of both the upstream and downstream toes of Dam 1A. Snow usually drifted to about 2 m deep on the toes of the dam, thus providing significant insulation.

During the summer of 1984, the pond water level was near minimum freeboard at Dams 1A and 2. The water elevation was higher than the elevation of the base of the active layer on the bedrock hill between the dams. The hydraulic gradient thus created caused escape of water through a heavily fractured area just beyond the south abutment of Dam 2. The seepage stopped upon freezing in the fall.

In August 1984, Dam 1A and 2 were raised to crest elevation 486.5 m by end-dumping unsorted overburden materials on the downstream side of the crest.

The tailings pond was drawn down during the summers of 1985 and 1986 because it had reached minimum freeboard and the water quality was acceptable for discharge into the natural environment.

Internal Dam J (Figure 4) was built in 1985 to divide the existing pond in two basins for water treatment purposes as mentioned earlier. Dam J was built with 150 mm minus mine waste rock (run-of-mill fill) dumped through the ice in the winter. It is estimated, based upon bathymetric soundings taken in 1980, that internal Dam J was built in 7 m of water. The dam was built with few controls and is rather irregular in cross-section due to several failures which resulted from the thawing of ice entrapped in the fill during construction. The waste rock material is relatively permeable and is unable to support a fluid head across the dam. Hence during the summer, dry tailings were borrowed from the existing tailings delta and placed against the upstream side in a thin layer. The following years Internal Dam J was widened on the downstream side in an attempt to take advantage of the cold winter temperatures in building up a frozen core which could further seal the dam.

It is interesting to note that the contaminated water has its freezing point depressed and that the growth of a watertight frozen core cannot be judged on the progress of the 0°C isotherm. In other words, to be watertight, the ground needs to be colder than 0°C. The actual freezing point depression remains undetermined at this time.

THERMAL REGIME

Instrumentation

The first set of thermistor strings was installed by Echo Bay Mines Ltd. in May 1982 to obtain preliminary ground temperature data to a maximum depth of 8 m. In April 1983, new and permanent thermistor strings were installed to formally monitor the dams' thermal regime but again limited to 8 m. Two 15 m deep strings were installed in October 1983. Most instruments were lost while the dams were raised in August 1984. Thermistors were replaced in April 1985 to depths varying between 15 m and 25 m at one section through each of Dams 1A and 2. One thermistor string was installed at Internal Dam J just before this paper was written in August 1987.

Dam 1A

Based on preliminary thermistor readings and seepage observations during the summer of 1982, it is believed that the fill and subjacent active layer froze during the first winter. Only the foundation talik beneath the old creek bed remained unfrozen. The 1983 ground temperature readings on Figure 5 show that the foundation is just below 0°C at the fill/foundation interface and just above 0°C at bedrock. The talik was defined to extend down to elevation 473 m, or 3 m into a bedrock.

All thermistors below the crest of Dam 1A at the creek section (along string D1A-12) show a cooling trend. There is also a net drop in ground temperature after the pond level was drawn down in 1985 and the seepage consequently reduced. The pond level fluctuations are shown in Figure 5. For example, at 18 m deep, the temperature dropped from -1.5°C to -2.2°C.

It is interesting to note that after 1985 the amplitude of seasonal variations increased. This is most likely due to better heat transfer and deepening of the depth of zero seasonal fluctuations following the freeze-back of the underlying soils.

The talik froze back at the instrumented section during the winter of 1984-85, four years after construction. There is little doubt that snow clearing at the dam toes played a large role in the talik freeze-back.

The isotherms in Figure 6 show the thermal regime as at August 1987. The dam section is comfortably below 0°C and well within the depth of large seasonal variations. A bulb colder than -5°C extends from the downstream area into the central core. Readings discussed above show this core is still expanding (cooling).

Dam 2

The fill and thawed part of the foundation soils froze completely during the first winter. This section is representative of all of Dam 2 and of the part of Dam 1A outside the talik area. At mid-summer 1982, thermistors showed a dam core temperature of -1°C (Holubec et al., 1982). By the summer of 1987, the ground temperature at the same location was down to -3°C (Figure 7).

The evolution of the ground temperature is shown on Figure 8. All curves for the deep sensors beneath the dam core show a cooling trend. It is conceivable that the temperatures will eventually approach the mean annual ground temperature of the area. Figure 8 also shows that the depth of zero seasonal variations is about 18 m.

The 1986 pond drawdown appears to have been followed by a 0.4°C temperature drop at 20 m beneath the dam crest (elevation 466 m).

Figure 7 illustrates the isotherms as at August 1987. The foundation beneath the core is colder than -5°C and the dam core itself is clearly within the depth of great seasonal temperature variations. A natural lake some 100 m downstream of the dam probably influences the position of the -4°C isotherm.

Internal Dam J

Ground temperature data collection at internal Dam J commenced at the time of writing and is not yet available. It can be inferred that the complete dam section was probably unfrozen during construction and until the dam was widened.

It is likely that a significant talik existed beneath the former lakes over which part of the dam is built. As for former dry land, it is estimated that there could be up to 5 m of thaw. Hence the thermal regime beneath Internal Dam J is quite complex and varies significantly along its length.

GROUND PROBING RADAR SURVEYS

Ground probing radar (GPR) surveys were undertaken during late June and September of 1986 and April of 1987 along Dams 1A, 2 and J. The purpose of the GPR surveys was to establish if a high resolution geophysical technique, such as ground probing radar, could detect unfrozen zones (taliks) within or below the dams and so reveal a picture of the dam and overburden conditions.

Ground probing radar is a fairly new geophysical tool, the first models being commercially available in the mid nineteen-seventies. GPR is similar in principle to the reflection seismic method in that a pulse of energy is directed into the ground and the arrival times of reflections from subsurface interfaces are recorded. Seismic and ground radar records are very similiar, the most visible difference being in the magnitudes of the vertical time scales. The main difference between the techniques is that radar uses an electromagnetic as opposed to an acoustic energy source. Radar possesses a much more limited depth of penetration than seismic, typically of the order of 50 m or less, but provides a significant increase in resolution. Subsurface resolution is dependant upon the pulse length and, as such, can be as low as 0.5 m. This high spatial resolution can be important in the solution of complex near surface problems.

The depths to specific reflectors are calculated from a knowledge of the subsurface radar velocity distribution. In air, the radar pulse, typically in the MHz or GHz frequency range, travels with the speed of light (0.3 m/ns). In the ground the pulse travels with a velocity which is dependent upon the electrical properties of the material traversed. This velocity will be some appreciable fraction of the speed of light, usually between 10% and 50%. The radar velocity distribution in the ground can be determined, as in the case of seismic surveys, by a common depth point sounding (CDP) (Annan and Davis, 1976). Subsurface velocities to different interfaces are calculated from a plot of antenna separation versus travel time.

Dam surveys

Dams 2 and J were initially surveyed in June of 1986. Internal Dam J was resurveyed in April of 1987. A third site, Dam 1A (Figure 1) was surveyed in late September of 1986 and resurveyed in April of 1987.

The dams were profiled using an A-Cubed Pulse-EKKO III ground probing radar equipped with 50 and 100 MHz antennas. The horizontal axis on the radar profiles represents the distance along the dam, while the vertical axis represents travel time (nanoseconds) to a particular reflection event.

Dam 1A

Dam 1A was surveyed with the object of mapping one or more large unfrozen zones (taliks) which were thought to exist in the dam's foundation. This dam was surveyed using the 100 MHz antennas in September of 1986 in order to provide the best subsurface resolution. The April 1987 survey employed the 50 MHz antennas to achieve maximum penetration in the absence of an active layer. The station interval was 2 m.

Two radar profiles were obtained at this site, one along the crest of the dam and one at a lower elevation along the downstream toe road. The latter profile is shown in Figure 10. Common depth point soundings were taken in both cases. The ground wave velocities at the top of the dam and on the access road are 0.094 and 0.081 m/ns respectively. These are approximately equal to the velocity estimates for Dam 2 discussed later.

The profile along the crest of the dam shows strong reflections from the interface between the original silty-sand fill and the gravelly-sand material used in raising the dams. The interface between the dam fill and the original overburden is also evident. The bedrock/overburden interface is not obvious on this profile. The holes drilled from the top of the dam, D1A-11 and D1A-12, indicate that bedrock is at least 10 m. This corresponds to a minimum of 220 ns in radar travel time.

The 300 m profile along the downstream toe road (Figure 9) shows three strong reflectors (Figure 10). Reflector R1 represents the interface between the gravelly-sand dam fill and the original silty-sand dam fill. Reflector R2 represents the interface between the silty-sand dam fill and the natural overburden. Reflector R3 represents the bedrock interface. Drillhole D1A-10 intersects the bedrock at 5.2m deep. The depth to bedrock at D1A-10 as calculated from the radar profile is 5.1 m. The radar profile shows a pronounced dip in the bedrock topography between locations 130 m and 210 m along the profile. This agrees with the drillhole data which indicates that the bedrock interface is substantially deeper (more than 10 m) at station 166 m.

Generally, returns are recorded to depth along the length of the profile. Two zones showing an absence of deeper reflections are marked on the profile. These are areas of high electromagnetic attenuation which are probably partially to substantially unfrozen. The absorption of electromagnetic energy in the central unfrozen zone has resulted in an extremely weak reflection from the bedrock interface between 170 m and 195 m (as indicated by the dashed line). Furthermore the lower radar pulse velocity associated with this zone has depressed that portion of the bedrock reflector which is visible. The bedrock interface thus appears slightly deeper than it actually is in this region.

The thaw zone between stations 60 and 90 m corresponds with the stream bed leading out of the original watershed, confirming that a talik existed prior to dam construction. The top of the zone lies at a depth of about 5 m. Thawing of the overlying overburden and dam fill has occurred under locations 180 m to 190 m.

Thermistors D1A-10, -12 and -13 are located on the southern edge of this talik which has reduced in extent since the construction of the dam. The talik starts at the top of bedrock beneath frozen overburden. The depth extent of this talik is not indicated by the radar profile.

Dam 2

Dam 2 was surveyed with the object of mapping the sub-dam bedrock and overburden competency. The 1984 seepage was observed to occur around the south abutment of the dam, near station 310 m on the radar profile (Figure 11). The core extracted from a drillhole at location 356 m, beyond the end of the radar profile, showed substantial fracturing through the first 5 m of bedrock.

Dam 2 was profiled from north to south using the 50 MHz antennas. The transmitting and receiving antennas were separated by 4 m and the station spacing was 4 m.

The interpretated stratigraphy is shown on the radar profile in Figure 11. The velocity (0.11 m/ns), determined from CDP soundings, can be used to calculate the depths to reflectors 1, 2 and 3 indicated on Fig. 11 (LaFleche et al., 1987b).

Reflector 1 is at a depth of about 2.0 m appearing to combine the boundary between the new and old dam material and the depth of the active layer. Temperature data from thermistors D2-5 and D2-6 indicate that the latter should reside between 2 and 3 m. Since both interfaces could be roughly coincident at this time of year it would be difficult to resolve them as separate events. It can however be observed that in many places reflector 1 is represented by a broad double pulse indicative of a complex boundary. The new dam fill is coarser sand which should retain much less moisture than the original silty-sand till. Such an interface should provide a good electrical contrast as indicated by reflector 1.

Reflector 2 is at a depth of about 4.2 m and represents the interface of the silty-sand fill with the natural silty sand overburden. The natural overburden should contain considerably more frozen water than the dam fill resulting in a strong electrical contrast. The dam fill material was obtained by drying excavated natural overburden material to substantially reduce its water content.

Reflector 3 varies considerably in depth along the profile. It represents the top of the bedrock. A substantial (5 m) dip in the bedrock topography is observed near the middle of the dam (at distance along the profile of 110 to 222 m). Drillholes D2-6 and D2-7 (Figure 11) indicate bedrock depths of 4.1 and 10.4 m respectively. The depths calculated at D2-6 and D2-7 from the radar profile are 5.9 and 9.5 m respectively. The discrepency arises from an uncertainty of the true velocity profile. Each layer of dam fill possesses its own radar velocity and thickness and these should be taken into account when calculating the true depth to bedrock.

Strong reflections are observed within the bedrock. These most likely represent included ice within the phyllite; the ice could be present either along cleavage planes or in fractures and joints. The bedrock material should possess a higher radar velocity than the natural silty sand overburden; the addition of an increased thickness of lower velocity material stretches out the traces in this area yielding a distorted image of the deep structure.

Internal Dam J

Internal Dam J was surveyed with the object of confirming the prescence of seepage zones and channels through either the dam itself or its foundation. The dam was profiled using the 50 MHz antennas in June 1986 and April 1987. The transmitter-receiver separation and the station spacing were 4 m for the June 1986 survey and 2 m for the 1987 survey respectively. A CDP sounding was taken near the north end of the dam. The radar profiles over the dam are shown in Figures 13 and 14. CDP soundings taken in September 1986 and April 1987 indicate that the top layer velocity is 0.14 m/ns.

In the initial survey (Figure 12) the depth of penetration of the radar is quite limited over the dam itself. This is evidenced by the lack of returns at mid to late times at locations 40 m to 200 m along the profile. The high water content and unfrozen nature of the overburden under Internal Dam J limits the penetration of the radar pulse. Note that the rather clean radar traces directly under Dam J are in direct contrast to the profile presented for Dam 2 (Figure 10) where strong reflections are indicated to depth. The traces at either end of Internal Dam J, that is in the areas not originally submerged, exhibit the latter character.

These initial survey results confirm that several possible seepage paths from Pond 1 to Pond 2 are:

- Through the thin tailings sand liner.
- Through channels left by the melting of lake ice entrapped with the waste mine rock during dam construction.
- Through the unfrozen lake-bottom foundation.

The results of the April 1987 survey (Figure 13), conducted along the newly widened and raised dam, show that radar penetration has increased significantly under the dam itself, suggesting that the dam fill has frozen considerably over the winter of 1986/87. Figure 14 shows, for comparison, the interpreted stratigraphic section for the April 1987 survey. The interface between the old rock fill and the new fill is clearly visible in the radar profile. The base of the dam can now be traced across the old lake bed.

CONCLUSIONS

The experience at the Lupin mine shows that watertight frozen core dams can be economically constructed. The performance of the dams from both an engineering and an environmental point of view has been highly satisfactory. The seepage at Dam 1A was always minor and no significant trace of contaminants was ever detected downstream. The freezeback effectively occured during the first freezing season and has been monitored using a combination of ground instrumentation and geophysical techniques. The ground beneath the former intermittent creek was initially thawed to a depth of 5 m below original ground and has been freezing back since the end of construction.

The case of Internal Dam J will provide in time an interesting study of freezeback of a large water retaining structure constructed over frozen ground and under operating conditions.

The ability of GPR to image the ground allows not only resolution of the dam structures, sub-dam overburden conditions, bedrock topography and depth of thaw, but also unfrozen zones (taliks) within the overburden.

The ground probing radar surveys were able to yield considerable information on the dam thermal (and hence hydrological) performance. This information corresponded well to the known subsurface conditions. The radar was also useful in extending our knowledge of the subsurface to areas where little was previously known. Radar surveys should be a powerful technique for pre-construction site investigation and for monitoring both before and after dam construction. Poor quality of bedrock, such as on the ridge between Dams 1A and 2, can be detected in advance and integrated into the design when necessary. Two probable thaw zones under Dam 1A were identified on the radar profile. These corresponded well with the existing ground temperature data. Likewise the radar was able to detect the unfrozen initial state of Internal Dam J and follow its cooling with time. The major advantage of the radar is that it is able to map the total extent of the thaw zones between drillholes.

Given seasonal ground temperature variations, it would be advantageous to monitor the dam conditions with the radar at several times during the year. This, in conjunction with the on-going temperature monitoring program, would allow determination of any long term changes. A combined geophysical and thermal history of these sites will be an important case study in the consideration of similar developments on this type of permafrost.

ACKNOWLEDGEMENT

Geological Survey of Canada, Contribution No. 37687.

ACKNOWLEDGEMENTS

The authors wish to gratefully acknowledge the cooperation and assistance o all Echo Bay Mines Ltd. staff and particularly Mssrs. H. Wilson and R. Gilroy. The contribution of Dr. I. Holubec, P. Eng. of Geocon Inc. in the design of the dams and in setting up the monitoring programme is also recognized. The work was supported in part by grants from the National Research Council of Canada and Energy, Mines and Resources, Canada. Funding assistance has also been provided by the Northern Environmental Directorate of Indian and Northern Affairs Canada.

REFERENCES

Annan, A.P., and Davis, J.L. (1976). Impulse radar sounding in permafrost. Radio Science, 11, pp. 383-394.

Dufour, S. and I. Holubec (1988), "The Performance of an Earthfill Tailings Dam in the High Arctic", Proc. V. Int. Conf. on Perm., Trondheim, Norway (in press).

Environment Canada, Atmospheric Environment (1975). Canadian Normals, Temperature. Volume 1-SI, 198pp. No. U.S.C. 551-582 (71), Downsview, Ontario.

Futwilder, C.W. (1973). Thermal regime in an Arctic earthfill dam. Proc. 2nd Int. Conf. on Perm., Yakutsk, U.S.S.R., North Am. Cont., U.S. National Academy of Sciences, 622-628.

Holubec, I., Zehir, T., Dufour, S. (1982). Earthfill Dam Design and Construction in Cold Permafrost at Contwoyto Lake, N.W.T. 35th Can. Geot. Conf., Montreal, Quebec, Canada.

LaFleche, P.T., Judge, A.S., and Taylor, A.E. (1987a). Applications of geophysical methods to resource development in northern Canada. CIM Bulletin, 80, p.78-87.

LaFleche, P.T., Judge, A.S., and Pilon, J.A. (1987b). Ground probing radar in the investigation of the competancy of frozen tailings pond dams. Current Research, Part A, Geological Survey of Canada, Paper 87-1A, p.191-197.

Morey, R.M., 1974. Continuous subsurface profiling by impulse radar: Proceedings of the Engineering Foundation Conference on Subsurface Exploration for Underground Excavation and Heavy Construction, American Society of Civil Engineers.

Sayles, F.H. (1984). Design and performance of water-retaining embankments in permafrost. Final Proceedings of the Fourth International Conference on Permafrost, Fairbanks, Alaska, pp. 31-42.

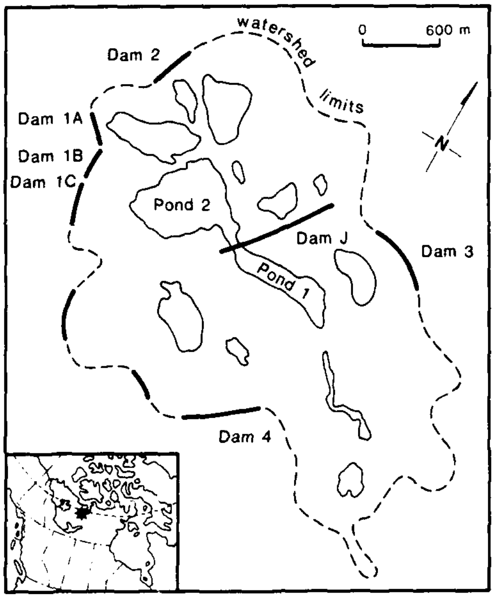
watershed limits
0
600 m
N
Dam 2
Dam 1A
Dam 1B
Dam 1C
Pond 2
Dam J
Pond 1
Dam 3
Dam 4

Figure 1. Location map for the Lupin mine and outline of the tailings facility.

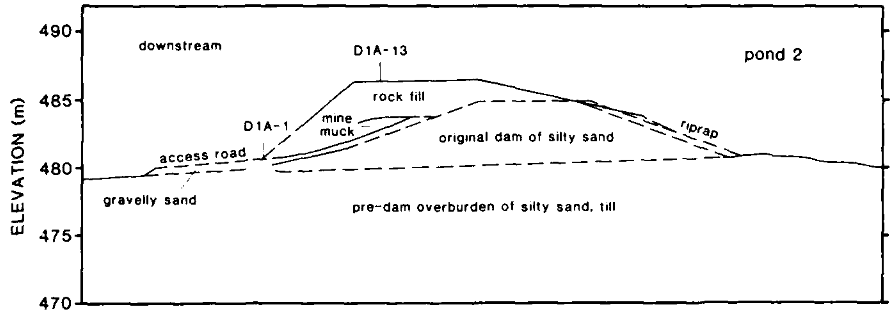
ELEVATION (m)
490
485
480
475
470
downstream
D1A-13
pond 2
rock fill
D1A-1
mine muck
original dam of silty sand
riprap
access road
gravelly sand
pre-dam overburden of silty sand, till

Figure 2. Cross-section of Dam 1A.

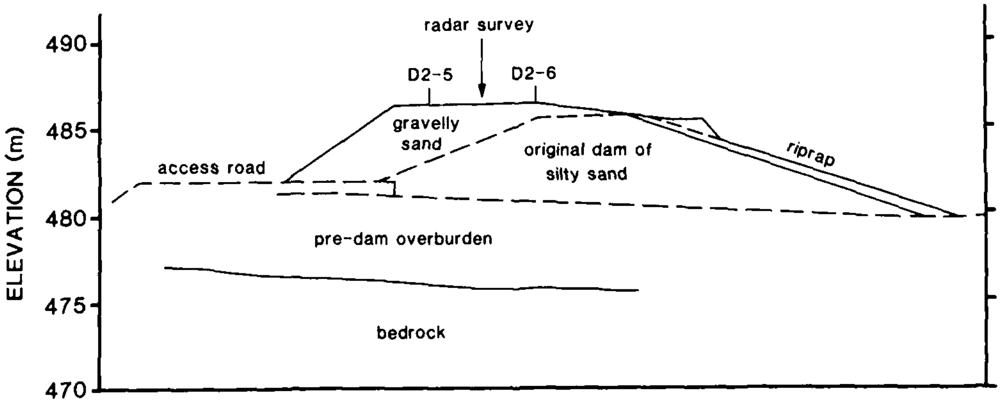
ELEVATION (m)
490
485
480
475
470
radar survey
D2-5
D2-6
gravelly sand
original dam of silty sand
riprap
access road
pre-dam overburden
bedrock

Figure 3. Cross-section of Dam 2.

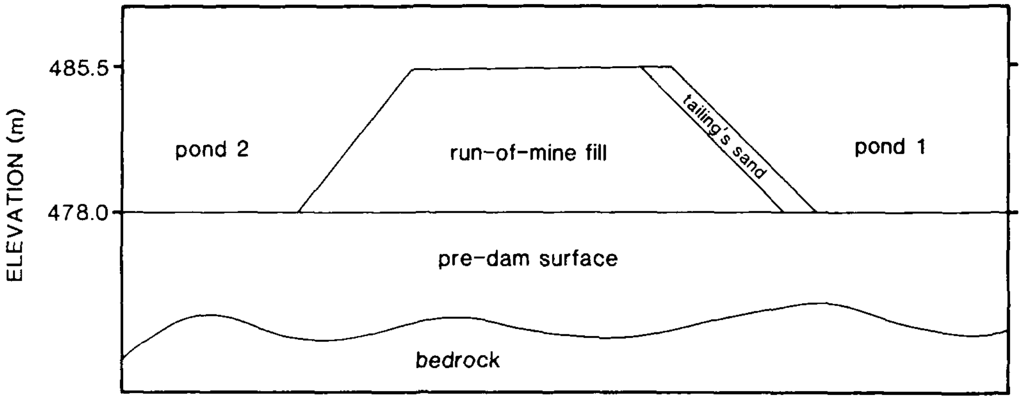
485.5
478.0
ELEVATION (m)
pond 2
run-of-mine fill
tailing's sand
pond 1
pre-dam surface
bedrock

Figure 4. Design cross-section of Dam J.

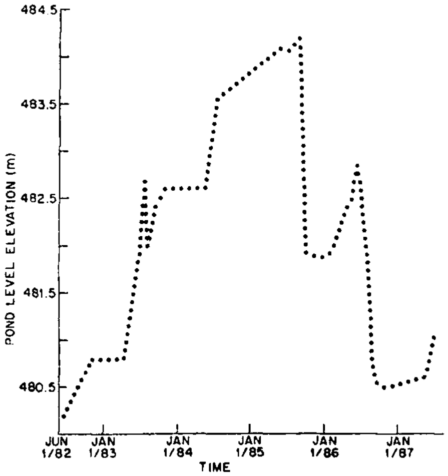

Figure 5. Tailings pond water levels.

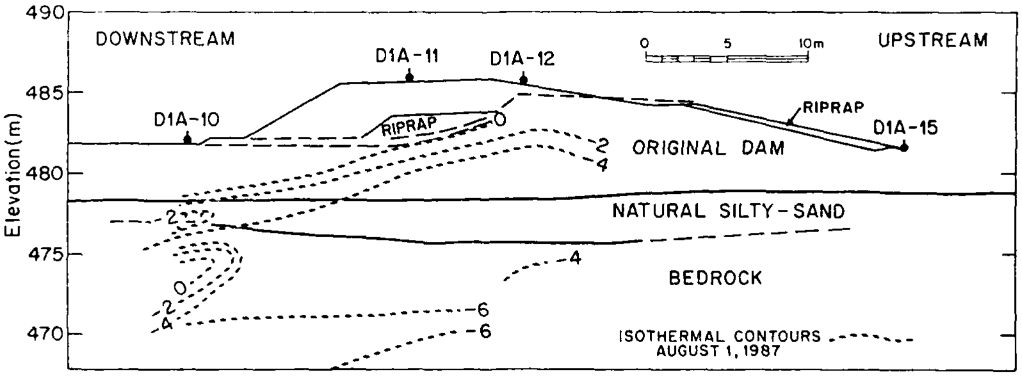
490
485
480
475
470
Elevation (m)
DOWNSTREAM
UPSTREAM
0 5 10m
D1A-10
D1A-11
D1A-12
D1A-15
RIPRAP
RIPRAP
0
2
4
ORIGINAL DAM
NATURAL SILTY-SAND
BEDROCK
-2
0
-2
-4
-4
-6
-6
ISOTHERMAL CONTOURS
AUGUST 1, 1987

Figure 6. Isotherms for Dam 1A, August, 1987.

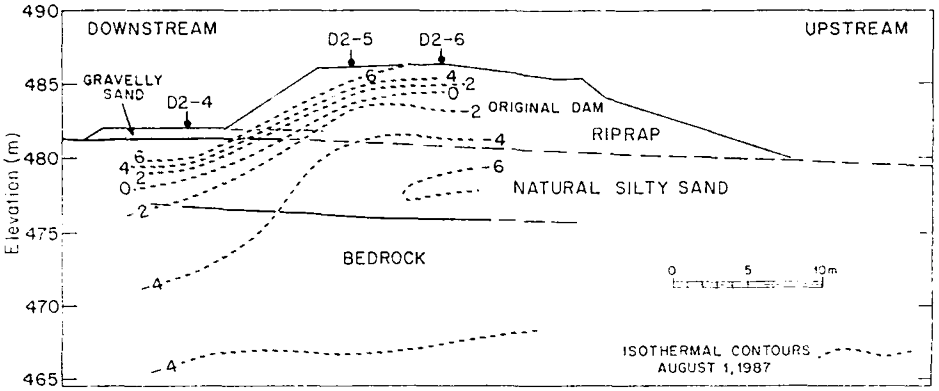
490
485
480
475
470
465
Elevation (m)
DOWNSTREAM
UPSTREAM
D2-5
D2-6
D2-4
GRAVELLY SAND
ORIGINAL DAM
RIPRAP
NATURAL SILTY SAND
BEDROCK
6
4
2
0
-2
-4
-6
0 5 10m
ISOTHERMAL CONTOURS
AUGUST 1, 1987

Figure 7. Isotherms for Dam 2, August, 1987.

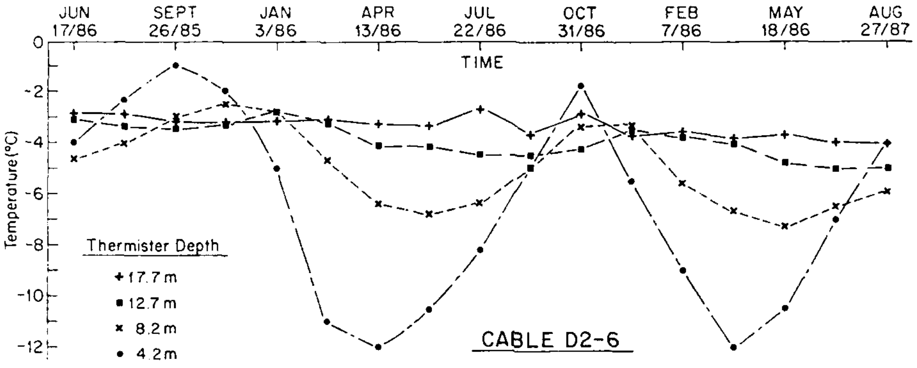

Figure 8. Borehole thermister temperatures for Dam 2.

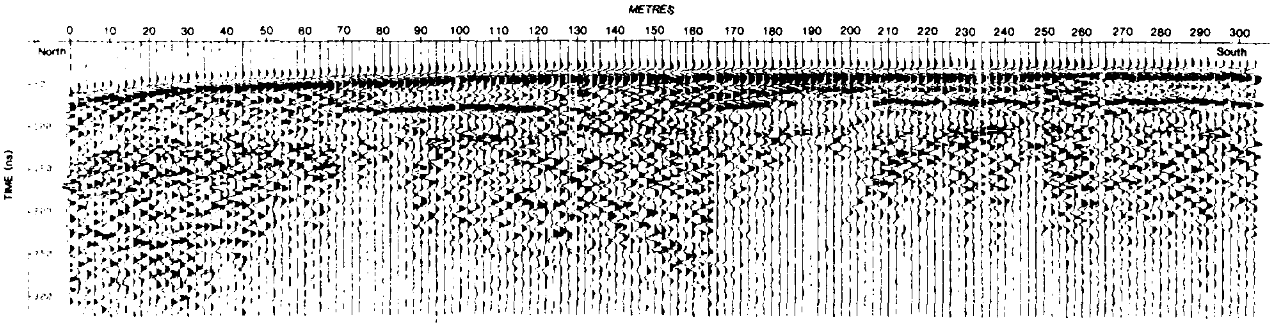

Figure 9. A 100 MHz radar profile along the Dam 1A access road in September of 1986.

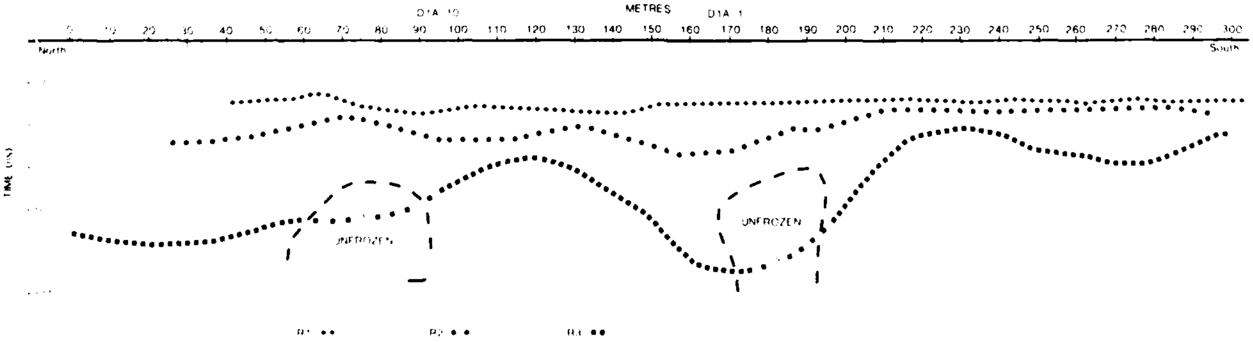
D1A 10
METRES
D1A 1
0
10
20
30
40
50
60
70
80
90
100
110
120
130
140
150
160
170
180
190
200
210
220
230
240
250
260
270
280
290
300
North
South
TIME (ns)
UNFROZEN
UNFROZEN

Figure 10. Interpreted section for the ground radar profile along the Dam 1A access road.

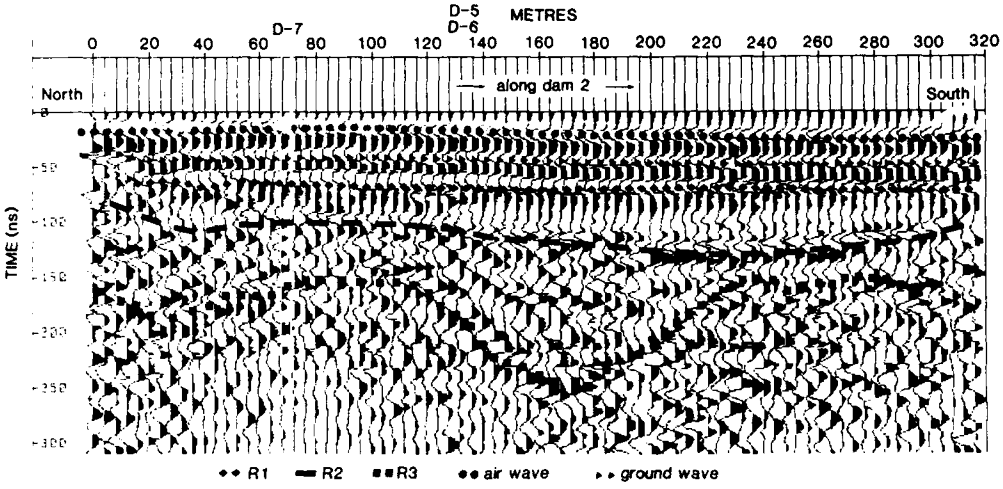

Figure 11. A 50 MHz radar profile along Dam 2 in June of 1986. The interpretation is overlain on the radar profile.

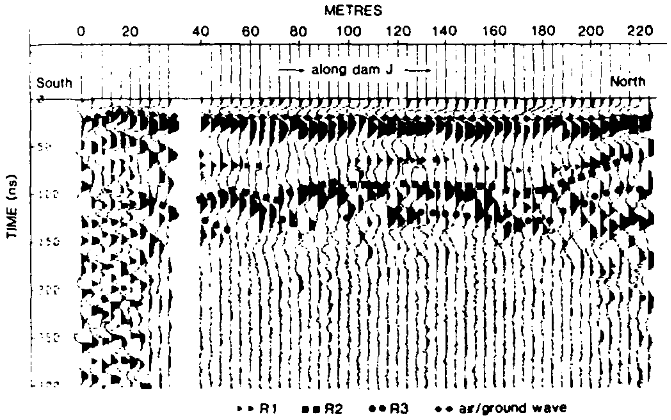

Figure 12. A 50 MHz radar profile along Dam J in June of 1986.

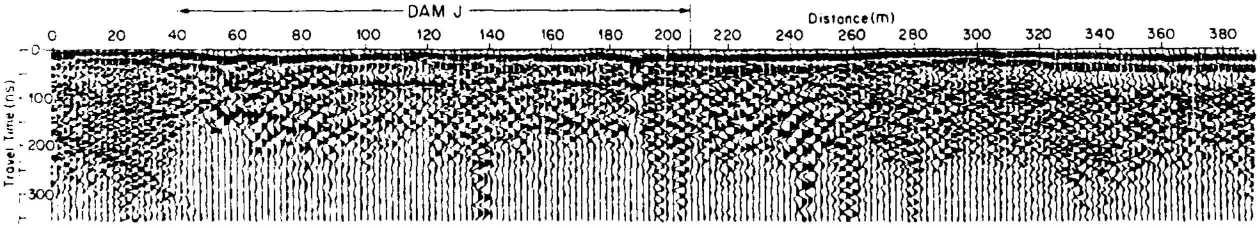

Figure 13. A 50 MHz radar profile along Dam J in April of 1987.

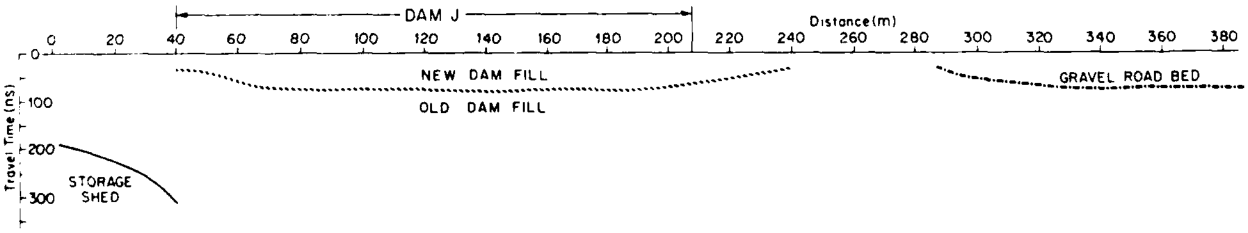

DAM J
Distance(m)
0
20
40
60
80
100
120
140
160
180
200
220
240
260
280
300
320
340
360
380
Travel Time (ns)
0
100
200
300
NEW DAM FILL
OLD DAM FILL
GRAVEL ROAD BED
STORAGE SHED

Figure 14. Interpreted section for the ground radar profile along Dam J.

Proceedings: Second International Conference on Case Histories in Geotechnical Engineering, June 1-5, 1988, St. Louis, Mo., Paper No. 5.27

Soft Ground Tunneling on the Seoul Subway Using NATM

Wulf Schubert
Senior Tunnel Engineer, Geoconsult, Salzburg, Austria

Thomas L. Richardson
Senior Geotechnical Engineer, Law/Geoconsult, Atlanta, Georgia

SYNOPSIS: The New Austrian Tunneling Method (NATM) was used to construct considerable portions of the Seoul (Korea) Subway System in both hard rock and soft ground. This paper presents results from three soft ground sections. The tunneling was performed under adverse conditions including high groundwater, some soft soils, and lack of experienced contractors and equipment. Success in overcoming these adversities resulted from NATM's flexibility, particularly in the way that excavation and ground support can be modified to contend with actual conditions. This paper presents the most important aspects of this NATM application, including comparisons between design calculations and actual results.

INTRODUCTION

From 1979 to 1985 the city of Seoul, Korea constructed over 100 km of subway alignment. The rapid schedule, which was mandated to prepare the city for the 1986 Asian Games, meant that many important decisions had to be made in a short period of time. As difficult as this task would seem in North America or Europe, it was even more difficult in Korea. This was due both to the shortage of experienced engineers for design and construction, and the reluctance of contractors to invest in specialized equipment that might not find reuse after the project completion.

The completed Seoul subway system is shown in Figure 1. Line 1 was constructed using primarily cut-and-cover methods. Line 2 used the same methods, plus steel supported tunneling in the mountainous areas. Lines 3 and 4, under construction from 1981 to 1985, cross in the center of Seoul. While cut-and-cover methods were used for the suburban portions of these lines, those same methods would have imposed a tremendous negative impact on the city. This would have included noise and dust, and extensive disruption of streets and utilities. For this reason tunneling methods were used to construct approximately 15 km of subway alignment within the center of the city.

The geology in Seoul creates a variable depth to rock. Thus, tunneling would encounter both hard rock and soft ground conditions. Traditional steel sets would have required extensive ground improvement in the soft ground sections, while shield driven tunneling could only be used for short stretches and would have required frequent changes in method. In addition, mobilizing a sufficient number of shields would have negatively impacted an already tight schedule.

Early in 1982, the Seoul Metropolitan Subway Corporation (SMSC) decided to use the New Austrian Tunneling Method (NATM) for ten sections in the center of the city. NATM was selected because of its ability to handle both frequent changes in ground quality and tunnel geometries. In addition, the method does not require specialized and sophisticated tunneling equipment. After gaining confidence with NATM, the SMSC selected NATM for an additional seven sections. The senior author's firm was directly involved with seven of the sections. This paper presents the results of soft ground tunneling on three of those sections.

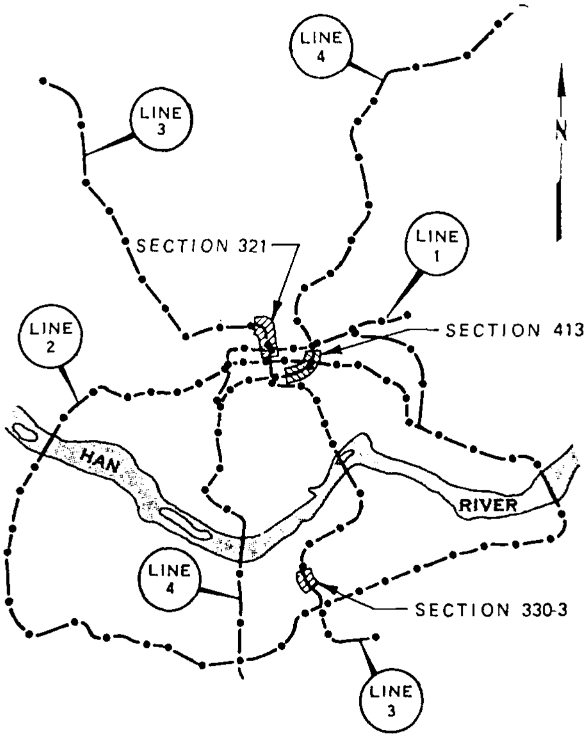

FIGURE 1 - PLAN OF SEOUL SUBWAY SYSTEM.

GEOLOGICAL CONDITIONS

Bedrock in Seoul consists of both granitic and gneissic rock. The rock is erratically weathered to form a residual soil overburden. The depth to rock varies from 0 to 50 meters. The transition to rock can vary significantly over relatively short distances.

The degree of weathering within the residual soil generally decreases with depth. The upper, completely decomposed granite had been subjected to the most intense weathering and had lost most of its (apparent) cohesion. This material was generally classified as a silty sand or silty clay. The lower residual soil, termed the weathered granite, was generally more compact and was classified as a silty sand. Standard penetration resistances varied from 20 to 60. The residual soils retained some of the structural features of the parent rock, including relict joints extending up from the bedrock.

The groundwater table in most locations was approximately 1.5 to 2 meters below the ground surface. This was generally 10 to 13 meters above the tunnel crown.

GENERAL DESIGN AND CONSTRUCTION CONSIDERATIONS

This paper presents important aspects of the New Austrian Tunneling Method as they relate specifically to this project. Readers who require a more fundamental understanding of NATM are directed to papers by Rabcewicz and Golser (1973), Mussger (1982), and Gnilsen and Mussger (1987).

The decision to use NATM was made as shaft sinking was underway for several projects. Thus, the first designs were expedited so as not to adversely impact the construction schedule. These first designs were based on the designer's experience and on some simple calculations. However, it was required that the designs be sufficiently detailed to allow the contractors to prepare the required equipment, and allow fairly adequate quantity take offs for cost estimating.

Finite element method (FEM) computations were made after the basic design was finished, and the concept was sufficiently discussed with the owner. Results of the computations required some minor modifications in the design. Only very limited geomechanical data was available at the time of design, as the investigation and testing were still underway. Thus, input parameters for the computations were more estimated than evaluated. A parametric FEM study was performed to put the design team in a position to later compare actual measurement results with the computed ones, and thus improve accuracy of the input for further computations.

A uniform tunnel shape, optimized for all degrees of ground stiffness, was developed for use in all sections. To account for the anticipated range in geologic conditions, four separate ground types were developed. Of specific interest to this paper are Ground Type III (weathered and heavily jointed rock), and Ground Type IV (soil). The design for Ground Type III involved a 20 cm thick shotcrete lining with a single layer of wiremesh, light steel ribs (depth = 10 cm; weight = 20 kg/m) and rock bolts (length from 3 m to 4 m). The design for Ground Type IV involved a 25 cm shotcrete lining with a double layer of wiremesh and similar steel ribs (no rock bolts). Figure 2 shows the typical single track tunnel shape and Ground Type IV support elements.

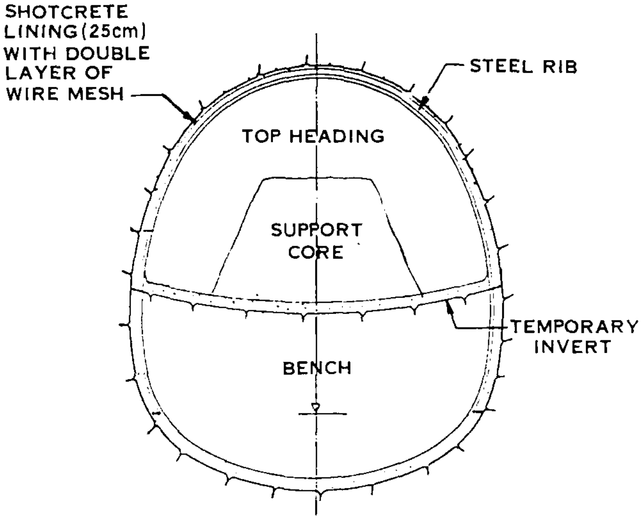

FIGURE 2 - SINGLE-TRACK TUNNEL SHAPE AND GROUND TYPE IV SUPPORT ELEMENTS.

Based on previous experience it was evident that a heading and bench excavation sequence would be required in the soft ground sections (Ground Type IV) to avoid problems with face stability. It was considered that a short bench (that is, approximately 5 to 10 meters) would not yield sufficient stability, particularly considering the lack of experience of local contractors with NATM. In addition, large equipment to excavate the top heading from the tunnel invert (required with a short bench approach) was not readily available. The decision to use a long bench required the installation of a temporary invert in the top heading to assure stability for the required time period (several months). The original concept had been to excavate the entire top heading and then follow with the bench excavation. However, for contractual reasons the contractors more typically elected to stop the top heading several times to excavate a portion of the bench.

The high groundwater table was, of course, a major consideration within the soft ground sections. Adequate dewatering equipment and other ground improvement technology was not readily available within Korea. Thus, the soft ground sections were advanced with a "dewater as you go" approach from inside the tunnel. The methods and success of this approach are presented within the detailed discussions of three individual sections.

Unreinforced cast-in-place concrete was typically used for the single track tunnel final lining. The designers had presented the concept of a completely watertight tunnel without permanent drainage. This concept involved a continous watertight geomembrane all around the tunnel between the initial shotcrete and final concrete liner, with the geomembrane backed by a geotextile to prevent puncture. This concept had been proven on numerous previous NATM projects. After some consideration, the proposal was accepted and utilized by SMSC.

SECTION 321

Section 321 involved two single track tunnels each 850 meters long, plus a station constructed by cut-and-cover methods. As may be seen in Figure 3, geologic conditions in this section were relatively uniform. The tunnel was primarily excavated within the firm to dense residual soil (Ground Type IV) with only one zone of hard rock extending into the alignment. Groundwater levels were approximately 12 m above the tunnel crown.

A roadheader was originally proposed for the excavation. However, the contractor did not want to invest the required capital, and even refused a manufacturer's offer to supply a machine free of charge for three months on a trial basis. As trials with a backhoe indicated slow progress due the locally dense zones, a hydraulic rock breaker was mounted on a small backhoe and used for the initial portions of the job. Some shaping was required utilizing hand operated power spades. Later, blasting was used to increase progress.

As previously discussed, a top heading and bench method was used in Ground Type IV. The topheading excavation utilized advance lengths of 1.2 m. Spiling or forepoling was generally not used except in locally soft areas or when problems delayed initial support installation. The first layer of wire mesh and shotcrete plus the steel ribs were installed after every round. The second wire mesh layer and the remaining shotcrete were installed after every one to three rounds. The design called for the temporary invert to trail the face by no more than 5 m. However, in practice, distances of 20 m were common.

The residual soil generally exhibited stand-up times of several hours. Dewatering in advance of tunneling was not used and water was allowed to seep in at the heading. The generally low permeability of the silty sand (probably around 10-4 cm/sec) kept seepage inflows to minimal levels and did not adversely affect stability. The shotcrete generally adhered to the wet soil and was aided in this process by the presence of the wire mesh.

In the initial stages of construction, lack of equipment and sufficiently experienced laborers considerably slowed the progress. However, due to the generally favorable soil conditions, the tunneling progressed without major difficulties. With increased experience of the mining crews the progress reached a normal advance rate of 2.5 meters per day in each heading.

Tunneling in the city center required that surface settlements be kept to a minimum. When utilizing NATM, control of ground deformations

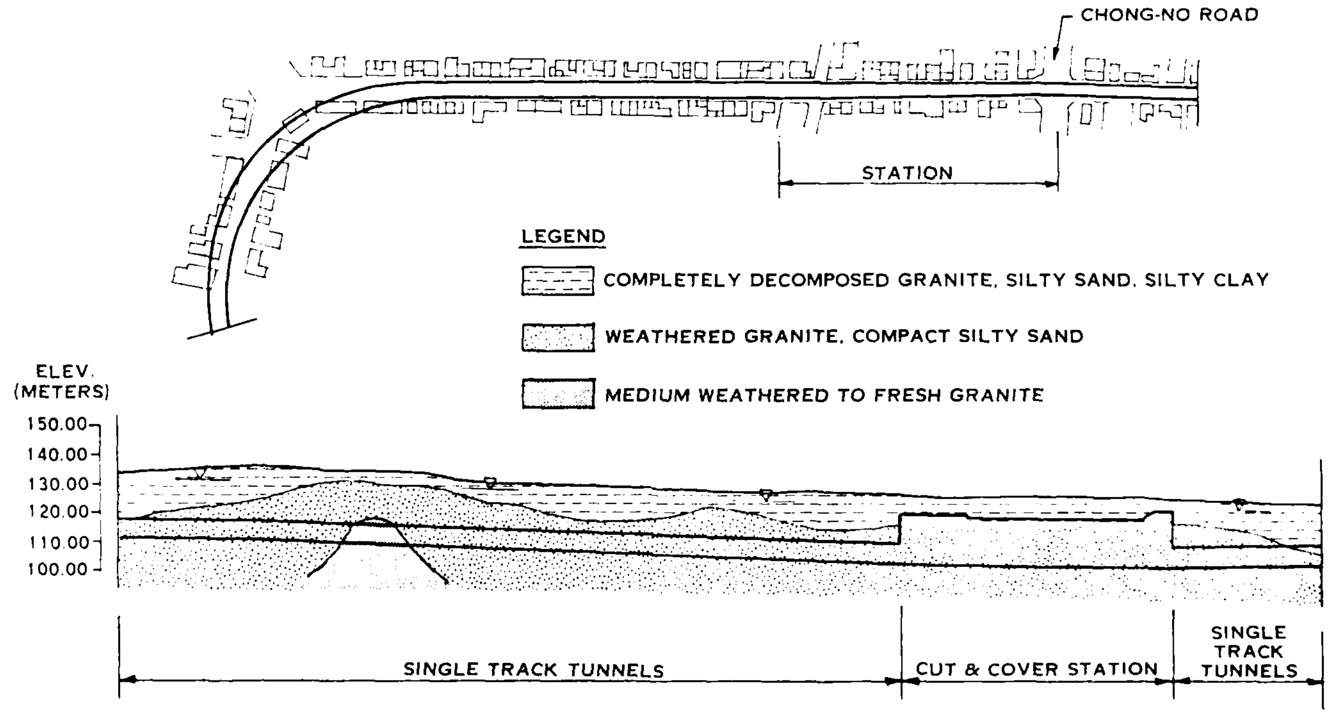

FIGURE 3 - SECTION 321 PLAN AND SUBSURFACE PROFILE

around the tunnel (which lead eventually to surface settlement) are an inherent part of the method. The control is typically achieved, as on this project, by cautious excavation, immediate ground reinforcement or support, and timely installation of the invert, including a temporary invert when a top heading advance is utilized. Within Section 321, the success of the method was shown. Measured surface settlement ranged from 4 to 15 mm and were within acceptable limits. Previous finite element computations had indicated surface settlements of approximately 13 mm. Comparison calculations for support without a temporary invert had indicated approximately 40 percent higher settlements (approximately 18 mm). Because frequent delays in temporary invert placement may have decreased its effectiveness, a realistic estimate of settlements based on the actual construction sequence may be have ranged between 13 mm and 18 mm. Thus, it appears that the calculations accurately estimated maximum settlements, while average settlements were somewhat overestimated. This conservative estmate was probably due to an underestimation of ground stiffness.

It is interesting to back calculate "ground loss" for the project based on the estimated volume of the resulting settlement trough. Although the settlement trough width was not measured, it can be estimated using standard references (Cording et al, 1975) by assuming that the trough extends upward from the tunnel springline at an angle of approximately 25 degrees from the vertical. For an average overburden depth of 16 m this yields an estimated settlement trough width of 24 m. Using this width, the observed settlements, and the tunnel cross section of 42 square meters, a ground loss ranging from 0.1 to 0.4 percent is estimated. These figures, compare favorably with the best results from shield tunnels (Akins and Abramson, 1983), and demonstrate the success of NATM in controlling surface settlement.

Section 321 also included a short stretch (approximately 15 m), where the bed rock reached tunnel level. The transition between the weathered rock and the bed rock required the most attention due to clayfilled joints and considerable water inflow. Face sealing and immediate shotcrete sealing were required to cope with face instability and overbreaks. Those unfavorable conditions also influenced the ground deformation, which reached 30 mm in this area.

Tangential stresses in the shotcrete lining were computed to range between 10 and 25 kg/cm2. Actual measurements using hydraulic pressure cells ranged between 7 and 25 kg/cm2, a very good agreement. Convergence measurements indicated no unusual or unexpected results, and deformations remained in the range of a few millimeters.

SECTION 413

Section 413 was 1200 m in total length and included two 750 m single track tunnels, the cut-and-cover Seoul Stadium Station, 50 m of double track tunnel, and two 50 m station tubes for the Dong Daemun Station. The geology within this contract was similar to Contract 321. However, as may be seen in Figure 4 the rock profile was more erratic and intersected the alignment in several locations. At each transition from soft ground to rock, clay filled joints and large inflows of water were encountered. As in Section 321, dewatering ahead of tunnel was not employed. In comparison with Section 321, a much higher joint frequency was encountered. In addition to the more difficult ground conditions, Contract 413 also passed over under the Seoul Stadium, an underground shopping center, a two level road, and a river.

Excavation was again divided into a top heading/bench operation with a long bench. Water inflows created a very short standup time. As a result, the top heading advances were limited to 1.0 m and forepoling was used to prevent sloughing of the crown. Forepoling consisted of steel pipes (diameter = 3 cm, length = 2.5 m), either pushed into the ground or placed in grouted boreholes.

The transition zones between soil and rock presented a special challenge. The joints filled with soft clay (up to 30 mm thick) created additional ground instability. The particularly heavy water inflows in these areas (up to 15 to 20 liters/second) also required special measures. These included application of straw or fleece to the exposed ground to prevent erosion, and collection of the water in pipes. Sealing shotcrete was then applied over the straw or fleece.

Initial tunneling from the shaft advanced toward the Seoul Stadium. The contractor was generally reluctant to install the specified support in a timely manner. This situation was aggravated by the absence of batching facilities, which led to delays in delivery and poor quality of shotcrete. As the heading approached Stadium I, the ground steadily became weaker causing the surface settlements to increase. The poor quality of work and delayed installation of support did not improve the situation. Fortunately, a main measuring section with extensometers, stress measuring devices, and an increased density of surface leveling points had been installed in this area. This allowed close observation of ground behavior and settlement, and also allowed observation of the efficiency of counter measures.

After a two month period, the settlements finally came to a standstill, reaching approximatel 70 mm in total. The time period involved led to the assumption that a consolidation process was involved. Stadium I suffered a few minor cracks, which was enough to make the contractor reconsider more effective support measures. This led to an improvement in shotcrete quality. More importantly, the work organization improved, which resulted in a more effective and timely installation of supports.

The results of these improved procedures were very impressive: surface settlements decreased to 5 to 14 mm on the remaining tunnel portion. This improved performance allowed an underpassing of Stadium II without any problems.

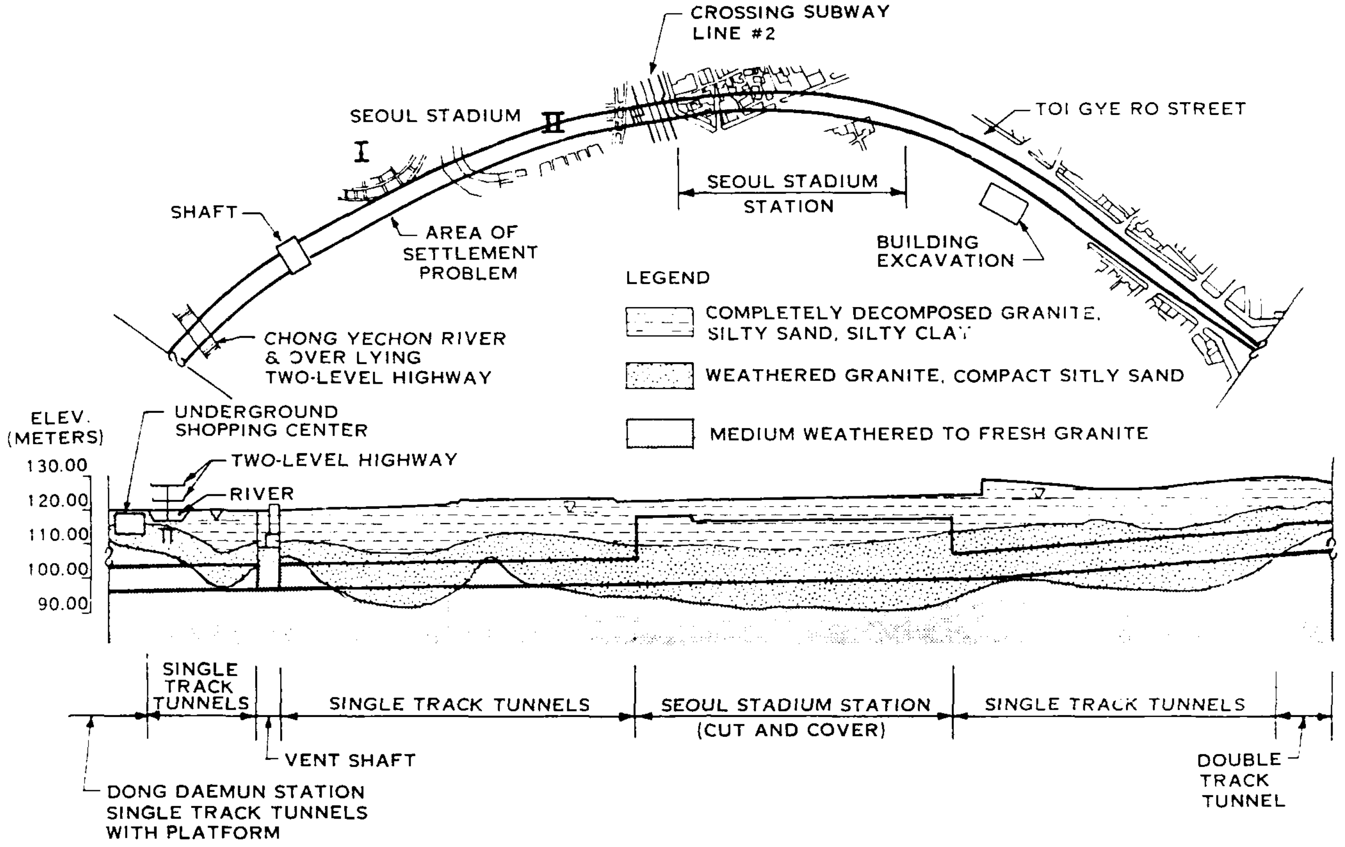
CROSSING SUBWAY LINE #2
SEOUL STADIUM
I
II
TOI GYE RO STREET
SEOUL STADIUM STATION
SHAFT
AREA OF SETTLEMENT PROBLEM
BUILDING EXCAVATION
LEGEND
COMPLETELY DECOMPOSED GRANITE, SILTY SAND, SILTY CLAY
WEATHERED GRANITE, COMPACT SITLY SAND
MEDIUM WEATHERED TO FRESH GRANITE
CHONG YECHON RIVER & OVER LYING TWO-LEVEL HIGHWAY
ELEV. (METERS)
UNDERGROUND SHOPPING CENTER
TWO-LEVEL HIGHWAY
RIVER
130.00
120.00
110.00
100.00
90.00
SINGLE TRACK TUNNELS
SINGLE TRACK TUNNELS
SEOUL STADIUM STATION (CUT AND COVER)
SINGLE TRACK TUNNELS
VENT SHAFT
DONG DAEMUN STATION SINGLE TRACK TUNNELS WITH PLATFORM
DOUBLE TRACK TUNNEL

FIGURE 4 - SECTION 413 PLAN AND SUBSURFACE PROFILE.

Interesting results were obtained from the stress measurements in the main measuring section in the problem area. Axial (tangential) stresses in the shotcrete shell had been computed to be about 25 kg/cm2. However, measured stresses within the top heading were as high as 85 to 95 kg/cm2. In comparison, results from the second main measurement section showed that stresses within the shotcrete lining were very close to previously computed results. This evidence clearly indicated the benefits of timely support and generally good work procedures.

Another unfavorable situation developed within a few hundred meters of the stadium area. A highrise building was under construction adjacent to the tunnel alignment. Excavation of the basement reached a level approximately corresponding to the tunnel invert, and approximately 7 m separated the excavation from the tunnel. The building excavation support consisted of steel soldier piles and timber lagging, which were tied back. The tiebacks extended into one of the tunnel areas. Thus, to prevent an excavation collapse, tunnel excavation had to be delayed until backfilling was partially completed. When the heading finally reached this area it became obvious that the building excavation had not been done with much care and had created a considerable area of loosened ground within the zone of the tunnel. This loosening made the ground much more permeable and created problems with face stability and over excavation. Water infiltrated into the tunnel along joints which had been opened by the ground loosening, and through the loosened material itself. This immediately turned the invert of the top heading into a mud pool, making any activity at the face impossible. Immediate collection of water at the face and the application of temporary shotcrete as close as possible to the face finally helped to control this situation.

Excavation through this area had to be done very carefully. In addition to instability caused by the loosened ground, joints with a strike perpendicular to the tunnel and dipping steeply toward the face caused considerable face instability. For this reason, a support core was left unexcavated at the face. Temporary shotcrete was applied to the support core to contribute the required stability.

The double track tunnel was constructed in a mixed face condition consisting of moderately to highly weathered granite. These conditions were a definite improvement over the remainder of the section, and the mixed face condition was no problem for NATM. A side gallery method was used to advance a top heading (shown in Figure 5). Side galleries were advanced first with a temporary shotcrete lining on the inner drift wall. The center core was then excavated and support completed in the top heading. This was followed by the bench excavation. Support in the double track tunnel consisted of a 15 cm shotcrete liner with a double layer of wire mesh, light steel ribs, and four rock bolts per linear meter (length = 4 m).

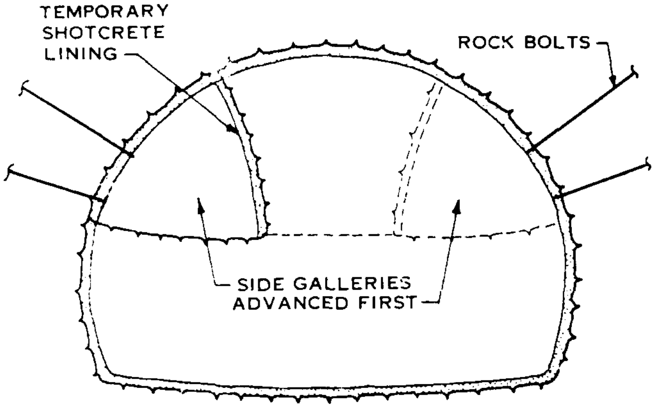
TEMPORARY SHOTCRETE LINING
ROCK BOLTS
SIDE GALLERIES ADVANCED FIRST

FIGURE 5 - DOUBLE TRACK TUNNEL IN MIXED FACE CONDITION.

The Dong Daemun Station tunnels (single track with platform) were advanced in hard rock under the river. These conditions presented no special challenge to NATM.

In spite of the initial settlement problems, section 413 became a full success and was widely used as a demonstration site for other contracts. The importance of a quick acting foreman in poor ground conditions was clearly demonstrated. Each round often had particular problems which required a custom tailored treatment. In addition, it was shown that a design must be flexible enough to allow a good deal of modification during construction.

SECTION 330-3

Section 330-3 was the most interesting of the three soft ground contracts, even though it was only 103 m in length. The tunnel extended through very loose alluvial soils beneath the water table and passed beneath several significant surface facilities including an 8-lane highway, a river, and a sewer channel. Originally cut-and-cover methods were proposed for this section. However, this would have involved diversion of both the river and the sewer channel, and significant reconstruction or underpinning of the highway structure.

As may be seen in Figure 6, the tunnel was primarily advanced through a silt layer above the tunnel springline and a coarse gravel layer in the invert. The unweathered and weathered bedrock appeared at one end of the tunnel but quickly dipped below the alignment. The silt layer contained lenses of clayey silt and cohesionless fine sand. The sand lenses were up to 1 m thick. Standard penetration resistances were approximately 8 to 10 in the silt, as low as 4 in the clayey silt, and as high as 12 in the sand.

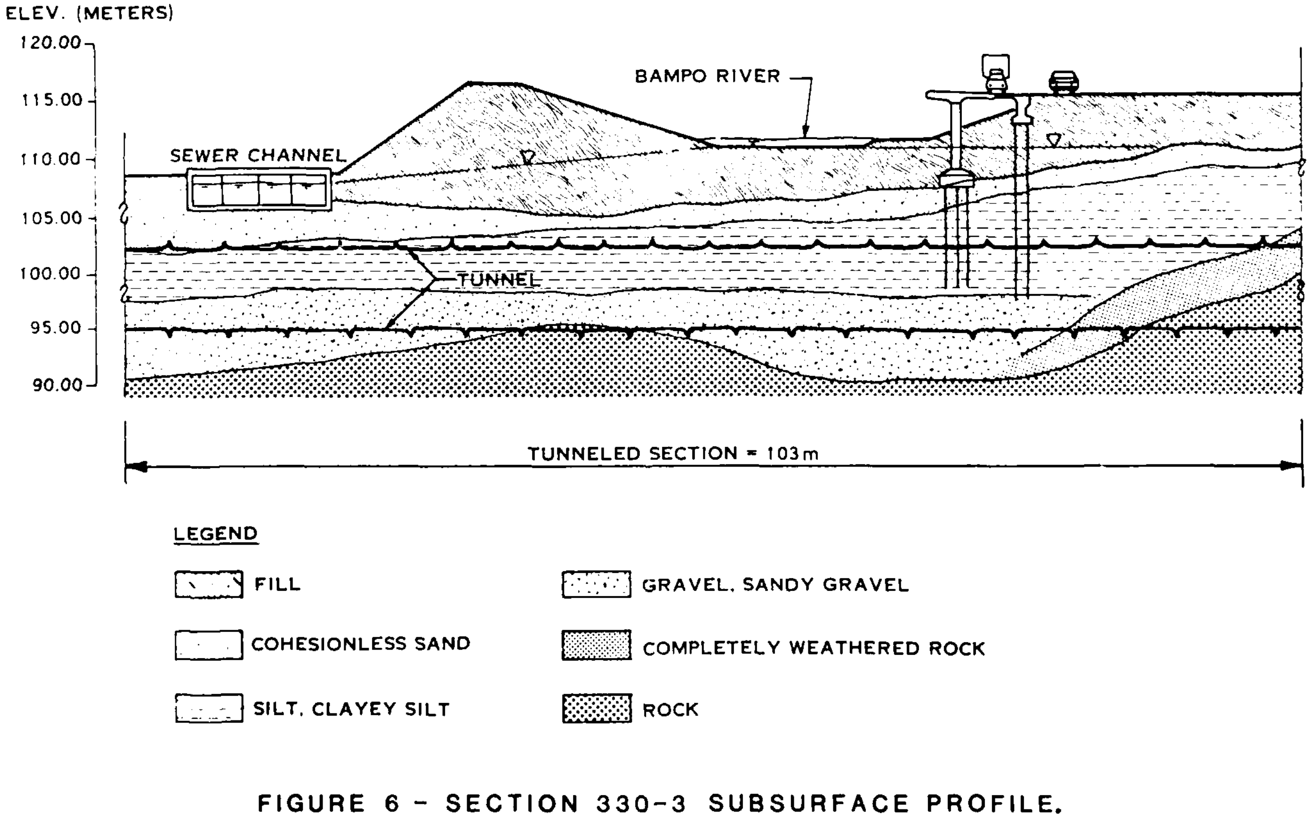
ELEV. (METERS)
120.00
115.00
110.00
105.00
100.00
95.00
90.00
SEWER CHANNEL
BAMPO RIVER
TUNNEL
TUNNELED SECTION = 103m
LEGEND
FILL
COHESIONLESS SAND
SILT, CLAYEY SILT
GRAVEL, SANDY GRAVEL
COMPLETELY WEATHERED ROCK
ROCK

FIGURE 6 - SECTION 330-3 SUBSURFACE PROFILE.

The piles supporting the highway structure extended into the proposed tunnel alignment. Thus, prior to tunnel excavation the bridge was temporarily supported by a steel frame structure. During subsequent tunnel excavation the piles were cut off from within the tunnel.

Groundwater control was a major concern within this contract. Groundwater levels were approximately 8 m above the tunnel crown. The crown would pass 6 m below the river and 1.5 m below the sewer channel. A blow-out in an adjacent excavation bottom within the gravel layer, due to unbalanced hydrostatic heads, heightened the interest level of all concerned. Compressed air was ruled out as an option due to the high initial costs compared to the short tunnel length. Groundwater lowering was deemed infeasible due to the surface obstacles and recharge effects of the river. Finally, chemical grouting was proposed and utilized in an attempt to decrease permeability, particularly in the gravel layer. A test grouting program initially showed promising results, including a reduction of the gravel permeability from 4×10^{-2} cm/sec to 5×10^{-6} cm/sec. The grouting program was carried out, and included grouting from a platform in the river during the low water season. Despite these efforts, when tunneling began it was revealed that the grouting had no positive effect on the ground, primarily because lack of supervision had allowed the grouting contractor to do a low quality job. In fact, the ground quality had actually been worsened because the grout holes had perforated the otherwise relatively watertight silt and clayey silt strata.

The tunnel incorporated both a single track opening and a larger opening to allow transition from a double track into a single track. To limit the size of the advance, a twin-heading method was used (as shown in Figure 7). One heading was advanced and the final lining placed, including a wall which would support the second heading. The second heading was then advanced and tied to the original tunnel.

The initial tunnel lining consisted of a 30 m shotcrete shell with two layers of wire mesh. The top heading had a temporary invert with a 15 cm thickness. Spiling and steel lagging were used to reinforce the crown and limit sloughing which could result in a chimney up to the ground surface. The spiling was used in the cohesive materials and the lagging was used in the sands and gravels. The lagging consisted of steel sections (3 mm x 280 mm x 1600 mm). The sections were pushed into the ground and were always overlapped.

Each heading utilized a top heading and bench excavation sequence. In the more silty and sandy portions, the top heading had to be subdivided to form a "mini" top-heading advance, utilizing a short (3 m) bench. Frequently, cohesionless sand layers with greater water inflows required again subdividing the advance into smaller heading. As may be seen in Figure 8, this involved first advancing a small, short drift in the crown, followed by two additional excavation steps to form the "mini" top-heading. The remaining portion of the top-heading was excavated in three additional steps at a distance of 2 to 3 m behind the "mini" top-heading. Support was installed after each excavation step. The modification of the excavation sequence was rather easy to accomplish as the original design had allowed this option without any modifications to the steel arches or other structural revisions.

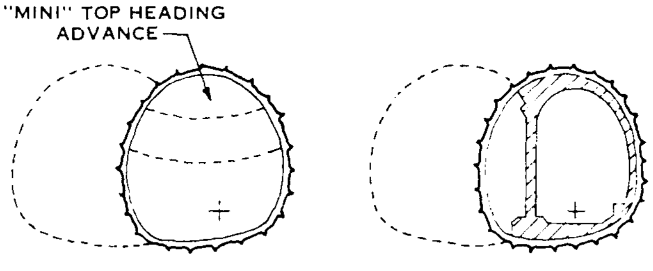

STEP 1 - INITIAL TUNNEL ADVANCE

STEP 2 - PLACE CONCRETE LINING

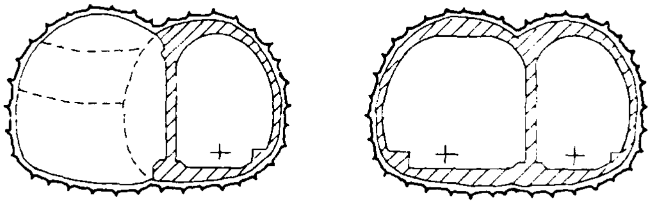

STEP 3 - SECOND TUNNEL ADVANCE

STEP 4 - COMPLETE FINAL LINING

FIGURE 7 - SECTION 330-3 EXCAVATION SEQUENCE.

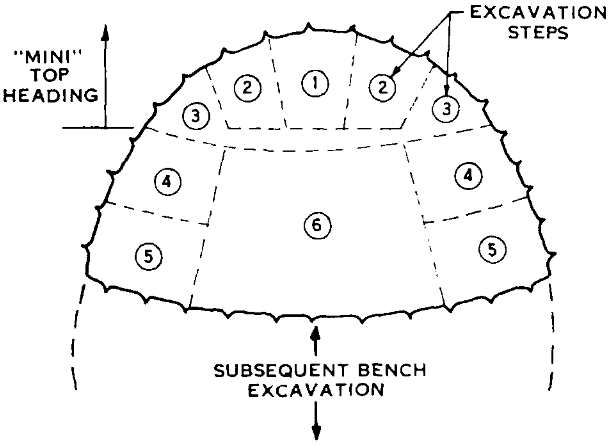

FIGURE 8 - SEGMENTED EXCAVATION SEQUENCE IN TOP HEADING UTILIZED IN VERY POOR GROUND.

Despite the very cautious segmental excavation, the tunneling was probably performed at the edge of the ground's stability. Frequent water inflows through the more pervious soils were commom. These were handled by applying straw or fleece to the soil to prevent erosion and collecting the water in pipes. Sealing shotcrete was then applied. In only one case did a risky situation develop: when a particularly heavy groundwater inflow through a gravel layer washed considerable material into the tunnel.

This example showed the advantage of NATM in dealing with adverse ground conditions. Its flexible approach allows the interruption of excavation and the installation of at least part of the support to stablize the ground. Of course, a good crew is required to react to these situations. In addition, the continuous availability of shotcrete and other supporting materials must be guaranteed.

Surface settlements were continuously monitored during underpassing of the road. Most settlements occured during excavation, with obviously only a low amount of consolidation. Total surface settlements amounted to a maximum of 5 to 7 cm. These values compared very well to the previously computed values. Settlements were not measures in the remaining portion of the section due to inaccessibility. However, visual observations indicated that settlements did not exceed the previously measured values. It was generally considered that limiting the excavation to small amounts, combined with timely ground support, was the reason for keeping settlements within acceptable limits under such adverse conditions.

Deformation measurements of the shotcrete lining showed values of 3 to 4 mm only. Most deformation happened during excavation prior to support installation.

Progress rates in the first tube ranged from 1.5 to ..5 m per day, while in the second tube the rates doubled due to decreased volume and considerable drainage effect of the first tube. Due to frequent delays and a hard winter, the average progress was not as good as it could have been. However, the time schedule was approximately met and the overall program not influenced.

CONCLUSION

Soft ground tunneling on the Seoul subway demonstrated the effectiveness of the New Austrian Tunneling Method in dealing with adverse ground conditions. A key to this success was the flexible nature of the method, particularly in the way that excavation and support could be modified to contend with actual conditions. The importance of timely ground support in limiting both surface settlement and loads imposed on the liner was demonstrated. The method has been shown to be independent of sophisticated equipment. However, the requirements of both an appropriate design and a skilled tunnel foreman cannot be understated. The design should emphasize constructability and provide adequate alternatives to be selected during construction. The importance of cooperation between the owner, designer, and contractor was also demonstrated.

REFERENCES

Akins, K.P. and Abramson, L.W. (1983), "Tunneling in Residual Soil and Rock", Proceedings Rapid Excavation and Tunneling Conference, Chicago.

Cording, E.J. et al (1975), Methods for Geotechnical Observations and Instrumentation in Tunneling, The National Science Foundation.

Gnilsen, R. and Mussger, K. (1987), "Design of Plain Concrete Tunnel Lining in Germany and the United States", Tunnel May, 1987, Cologne.

Mussger, K. (1982), "A Flexible Approach to Tunel Design", ASCE Conference, Shotcrete for Underground Support IV, Columbia.

Rabcewicz, L. and Golser, J. (1973), "Principles of Dimensioning the Supporting System for the New Austrian Tunneling Method", Water Power, March, 1973.

Proceedings: Second International Conference on Case Histories in Geotechnical Engineering, June 1-5, 1988, St. Louis, Mo., Paper No. 5.29

Accelerated Consolidation of Soft Clays Using Wick Drains

J.R. Davie
Engineering Supervisor, Geotechnical Services, Bechtel Civil, Inc.,
Gaithersburg, Maryland

L.W. Young, Jr.
Engineering Supervisor, Geotechnical Services, Bechtel Civil, Inc.,
Gaithersburg, Maryland

M.R. Lewis
Engineering Supervisor, Geotechnical Services, Bechtel Civil, Inc.,
Gaithersburg, Maryland

SYNOPSIS: Construction of the New Istana for the Sultan of Brunei required that fill slopes up to 85 feet high be placed on very soft compressible floodplain soils. Wick drains installed in the soft sediments accelerated their consolidation and reduced long-term settlements. The consolidation also produced a strength increase in the soft soils that allowed the fill to be constructed without danger of a major base slip failure. Instrumentation installed in the floodplain soils provided data on excess porepressures built up during the fill placement, and on the resulting settlements. The measured porepressures and settlements were in good agreement with the predicted values.

INTRODUCTION

The New Istana (Royal Palace) of the Sultan of Brunei is located on high ground above the tidal floodplain of the Brunei River (Figure 1). As part of construction, it was necessary to place fill slopes, some as high as 85 feet, on the floodplain to accommodate the main access road and essential utilities, and to achieve desired architectural effects. Computations made before the fill placement in late 1981 predicted several feet of fill settlement would occur over a period of years from the consolidation of recently deposited sediments beneath the floodplain area. The computations also showed that placement of the fill at the projected construction rate of about 1 foot every 2 days would cause a slip failure through these soft sediments. The tight construction schedule (the New Istana had to be completed before Brunei became independent in July 1983) did not allow for any slowdown in the rate of fill placement, nor could continuing large settlements be tolerated years after project completion. The solution lay in accelerating the consolidation of the floodplain sediments, both to speed up the settlement and to strengthen the soft soils. This paper describes the method employed to accelerate consolidation, the instrumentation installed, and the results of measurements taken before and after fill construction.

SUBSURFACE CONDITIONS

Soils beneath the floodplain (at about El. +5 feet) consisted of muck, peat, silt, and very soft clay and silty clay. These deposits extended as deep as 60 feet under the toe of the new fill, decreasing to about 10 feet beneath the maximum 85-foot height of the 1-V to 3-H slope, as shown in Figure 2. Information on subsurface conditions was obtained from an extensive series of soil borings; the locations of some of the borings are shown in Figure 3.

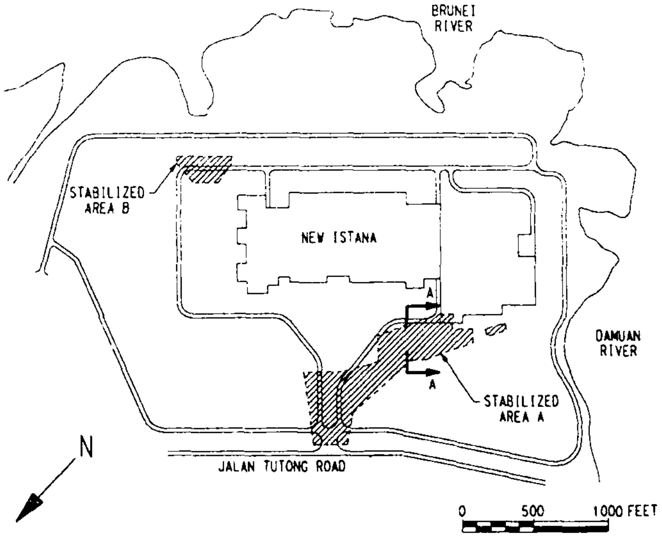

Fig. 1 Plan of New Istana

The very soft clays and silty clays, which made up the majority of the soft floodplain sediments, were generally highly plastic with natural water contents close to the liquid limit. The selected values of the design parameters for this stratum were based on the results of field and laboratory testing. These values are shown on Table 1, along with the values for the other strata described below.

Hard clayey silt extended below the soft floodplain sediments, down to the limit of the borings, i.e., to at least El. -70 feet. The material appeared to be grading into a siltstone with increasing depth, although no structure could be detected from the samples recovered. As shown in Figure 2, a thin layer of stiff residual clay was found above the hard clayey silt in some areas.

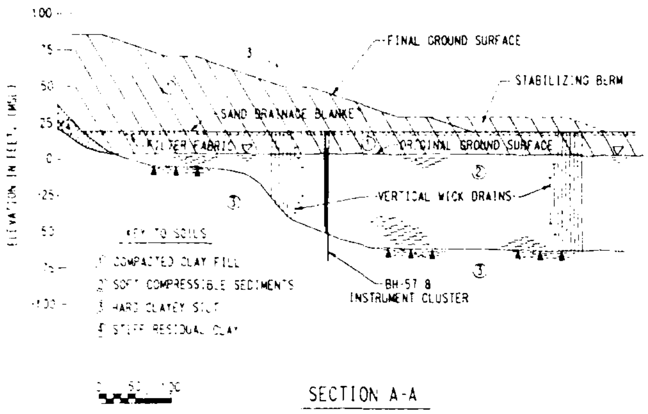
100
75
50
25
0
-25
-50
-75
-100
ELEVATION IN FEET, (MSL)
FINAL GROUND SURFACE
STABILIZING BERM
SAND DRAINAGE BLANKET
FILTER FABRIC
ORIGINAL GROUND SURFACE
VERTICAL WICK DRAINS
KEY TO SOILS
① COMPACTED CLAY FILL
② SOFT COMPRESSIBLE SEDIMENTS
③ HARD CLAYEY SILT
④ STIFF RESIDUAL CLAY
BH-57 & INSTRUMENT CLUSTER
0 50 100
SECTION A-A

Fig. 2 Subsurface Conditions

The fill soil that made up the new embankment was very silty clay that had been excavated during extensive grading operations for the palace on the hill above the floodplain. This clay was placed in maximum 1-foot-thick lifts, and compacted to at least 90 percent of the modified Proctor maximum dry density, at a moisture content ± 2 percent of optimum.

The measured ground water table was, on average, slightly above the water level in the adjacent Brunei River, and essentially at ground surface at about El. +5 feet.

PLAN OF ACTION

As shown in Figure 2, the maximum height of the new fill lay above the thinnest zone of the compressible sediments, while the toe of the fill was above the greatest thickness. This resulted in the predicted primary consolidation settlement of these sediments over the majority of the area being within a fairly narrow range, i.e., 6 to 7 feet. The maximum computed settlement (due to 100 percent primary consolidation) was 8.3 feet, from 45 feet of soft sediments consolidated by 40 feet of fill, while the minimum value was 3.7 feet, from 17 feet of soft sediments being consolidated by 65 feet of fill.

TABLE I. Soil Design Parameters

	Compacted Clay Fill	Soft Floodplain Sediments	Hard Clayey Silt
USCS Symbol	CL/ML	CH to OH	CL/ML to SM/SC
Total Unit Weight, pcf	125	110	130
Natural Moisture Content, %	22	50	11
Liquid Limit	40	53	38
Plasticity Index	16	27	17
Undrained Shear Strength, psf	1600	300	4000
Compression Index	-	0.55	0.12
Coeff. of Consolidation, ft²/year	-	60⁽¹⁾	400
State of Consolidation	-	NC	Highly OC

Notes: (1) This value was assumed to represent both vertical and horizontal coefficients.

(2) The thin layer of stiff residual clay found in some areas above the clayey silt had a unit weight of 120 pcf and an undrained shear strength of 1000 psf.

For the maximum 60-foot thickness of the compressible soil, 50 percent of the settlement was estimated to take 3 years to complete, while 90 percent would take almost 13 years. Slope stability analyses showed factors of safety as low as 0.7 against a slip failure through the soft soils, even with a 15-foot-thick stabilizing berm added at the toe of the slope. Obviously some action was required to accelerate the consolidation rate, and increase the strength of the soft sediments.

The only viable course of action was to install wick drains in the soft floodplain sediments, and to place the fill embankment at a rate that allowed these sediments to consolidate and strengthen sufficiently to avoid a slip failure. Instrumentation was essential to monitor buildup of porewater pressure in the soft soils during the embankment construction, and to determine the settlement of these soils.

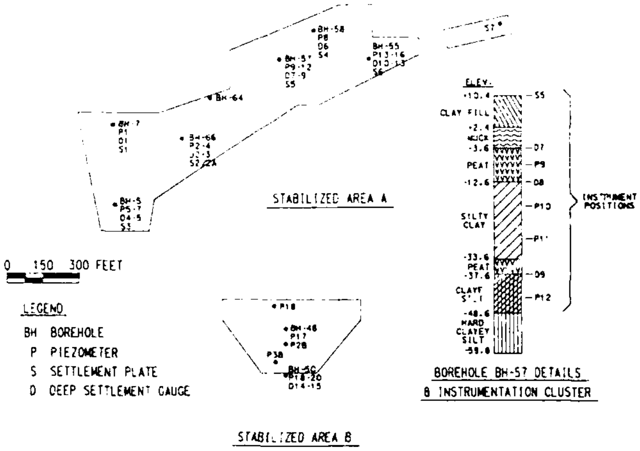
BH-58
P8
D6
S4
BH-55
P13-16
D10-13
S6
S7
BH-57
P9-12
D7-9
S5
BH-64
BH-7
P1
D1
S1
BH-66
P2-4
D2-3
S2, 2A
BH-5
P5-7
D4-5
S3
STABILIZED AREA A
0 150 300 FEET
LEGEND
BH BOREHOLE
P PIEZOMETER
S SETTLEMENT PLATE
D DEEP SETTLEMENT GAUGE
P18
BH-46
P17
P28
P38
BH-50
P18-20
D14-15
STABILIZED AREA B
ELEV.
+10.4
CLAY FILL
+2.4
MUCK
-3.6
PEAT
-12.6
SILTY CLAY
-33.6
PEAT
-37.6
CLAYEY SILT
-48.6
HARD CLAYEY SILT
-59.6
S5
D7
P9
D8
P10
P11
D9
P12
INSTRUMENT POSITIONS
BOREHOLE BH-57 DETAILS
& INSTRUMENTATION CLUSTER

Fig. 3 Boring and Instrumentation Locations

WICK DRAIN DESIGN AND SHEAR STRENGTH INCREASE

Using the soil parameters shown in Table 1, a center-to-center spacing for the wick drains of 5 feet was computed by the method outlined in Hansbo (1979), based on a requirement that 90 percent consolidation of the soft floodplain sediments occur within 6 months. This rate of consolidation was needed to increase the strength of the soft sediments sufficiently to avoid a slope failure. The predicted increase in shear strength of the underlying soft soils during the fill placement was computed using a simplified approach, with the following assumptions.

1) One foot of fill is placed about every 2 days, i.e., 85 1-foot increments in 6 months.

2) At the end of the 6-month placement period, the compressible soils will have consolidated 90 percent due to the first foot of fill placed, and essentially zero due to the 85th foot.

3) For each 1 foot of fill placed between the first and 85th foot, the resulting degree of consolidation U of the soft

soils follows the relationship between U and the radial time factor T for sand drains, as outlined in Leonards (1962). In this relationship, the ratio of wick drain spacing to the wick drain's equivalent radius was calculated as 50.

4) The relationship between consolidation time elapsed and T is based on 90 percent consolidation in 6 months.

5) After 100 percent consolidation under a load equivalent to 1 foot of fill surcharge (about 125 psf), the soft sediments increase in shear strength by 30 psf (i.e., $c/p \simeq 0.25$, based on CIU laboratory tests).

6) Shear strength gain is linearly proportional to the degree of consolidation.

As an example, we can predict the increase in shear strength of the soft soil 6 months (180 days) after the start of fill operations due to the 50th foot of fill being placed, as follows.

- The 50th foot of fill is placed 100 days after the start of fill operations (i.e., 1 foot every 2 days).
- The underlying soft soils consolidate for 180 days - 100 days, i.e., 80 days under this 1 foot increment of surcharge.
- At U = 90% consolidation, time factor T = 0.712 from Leonards (1962), for the ratio of well spacing to wick drain equivalent radius of 50.
- Since time of consolidation
  t = constant x T,
  and t = 180 days at 90% consolidation
  and T = 0.712 at 90% consolidation
  then t = 253 T.
- For t = 80 days, T = 0.316
- From Leonards (1962), for T = 0.316, U = 64%
- Increase in shear strength = 0.64 x 30 = 19 psf, since shear strength gain is assumed to be linearly proportional to the degree of consolidation.

Using the above approach, the shear strength of the soft floodplain sediments 6 months after the beginning of fill operations was computed by summing the strength increases due to each fill increment. For the maximum 85-foot-high embankment, the 6-month undrained shear strength was about 1,700 psf, compared with the initial 300 psf value. At the end of one year after start of fill placement, about 99 percent consolidation would have occurred due to the first foot of fill placed, with about 90 percent consolidation due to the 85th foot. In the long term, assuming 100 percent consolidation, the computed undrained shear strength of the compressible sediments was around 2,600 psf.

The stability analysis of the section shown in Figure 2 indicated a factor of safety against slip failure through the floodplain soils of about 1.2 for the end of construction condition and 1.4 for the long-term condition, using the computed increased strengths due to the wick drain consolidation. This compared with a factor of safety of 0.7 computed for the pre-wick drain condition. It may be noted that the factors of safety increased proportionally far less than the shear strength of the soft sediments. This is because the effects of the shear strength of the clay fill (85 feet thick) and the influence of the stabilizing berm (see Figure 2) were the same in both the before and after analyses.

Although the use of wick drains indicated that primary consolidation settlement would be accelerated by a factor of about 25, the rate of secondary compression was not affected. In fact, the computed amount of secondary compression actually increased slightly because a longer period of secondary compression occurred due to the decreased period of primary consolidation. However, the total predicted secondary compression settlement over 50 years amounted to only about 10 percent of the primary consolidation, and was thus not considered as an important factor in the design. Similarly, settlement of the compacted clay fill above the soft sediments, and the hard clayey silt below these sediments, was considered insignificant in comparison with the settlement of the soft sediments themselves.

WICK DRAIN INSTALLATION AND FILL CONSTRUCTION

The type of wick drain selected was the Alidrain, manufactured by Burcan Industries, Canada. The Alidrain consists of a thin plastic core, approximately 100 mm by 7 mm wrapped in a special filter of cellulosic material. Small closely-spaced plastic studs embossed on the inner surface of the core form channels that allow flow when the sleeve is pressed together.

Because settlements of as much as 8 feet were predicted due to consolidation of the soft floodplain sediments during and after fill placement, 12 feet of fill was placed and compacted on top of the original ground before installation of the wick drains and the instrumentation. A 1-1/2-foot-thick sand drainage blanket was then constructed above the 12 feet of fill. This ensured that the drainage blanket and the top of the wick drains and instrumentation would be above the ground water level throughout the fill construction operations. It also served as a working mat for the heavy equipment needed to install the wick drains.

The Alidrains were installed in the areas shown in Figure 3, by Techniques Louis Menard, S.A. of Singapore. Installation began in mid-July and was completed by mid-October, 1981. In all, 20,075 Alidrains totaling 967,000 linear feet were placed in about 75 working days using three rigs operating on average about 9 hours per day. Drain lengths ranged from 15 to 65 feet, with an average of about 48 feet.

Three cranes specially modified by Menard were used for the drain installation. Two of these were smaller rigs (a Hitachi and a Koehring crawler crane) that installed drains less than about 40 feet deep. A larger Manitowoc 3900 crawler crane was used for the deeper drains. The drains were installed within a 6-inch-diameter mandrel that was pushed into the ground by a vibrator, the whole system being supported by fixed leads attached to the crane. A special shoe on the bottom of the drain anchored it into the ground as the mandrel was withdrawn. After mandrel withdrawal, the drain was cut off leaving about a 3-foot-long pigtail at the top of the sand blanket.

In numerous cases, excess porewater pressures existed in the soil, either due to the fill already placed and/or the installation of the Alidrains themselves, and the outflow of porewater began within minutes of the mandrel withdrawal. The instrumentation to measure porewater pressure and settlement, described in the following section, was installed after the Alidrains but before fill placement started.

Fill placement and compaction above the sand blanket started in mid-September 1981 and was completed by the end of March 1982. In most areas, the rate of filling averaged about 1 foot every 3 days, compared with the 1 foot every 2 days assumed in the wick drain design. However, the rate of fill placement was somewhat uneven, with as much as 8 feet being placed in 5 days at one location.

No stability problems were encountered in the underlying soft floodplain sediments during or after the fill installation. The apparent reasons for this success, namely the rapid drainage, consolidation and consequent increase in strength of the soft sediments, are discussed in a later section. It may be noted, however, that the physical presence of 1 million linear feet of wick drain material within the soft materials probably also helped reinforce and stabilize these soils.

INSTRUMENTATION

Piezometers, surface settlement markers and deep settlement gauges were installed throughout the stabilized area to provide porewater pressure and settlement data before, during and after the fill embankment construction, enabling ongoing evaluation of the wick drain performance. The instruments were installed and monitored by Techniques Louis Menard, S.A. of Singapore. Instrument locations are shown in Figure 3.

Twenty-three Slope Indicator Company porepressure transducers were installed during July through September of 1981. These 1-1/2-inch-diameter instruments had standard Cassagrande-type 6-inch-long porous stone filters, and were installed at depths ranging from 16 to 76 feet below the top of the sand blanket. The instruments were operated by a hydropneumatic balance of forces across a flexible diaphragm, and were read from a remote sensing station, well outside the area of the fill operations, using a portable pneumatic indicator. Readings were taken twice weekly during the fill operations,, and once a week before and after the filling. Only two of the transducers (P-14 and P-16) failed during the 10 to 12-month monitoring period.

Settlement was monitored using 7 surface settlement markers to record total settlement and 15 deep settlement gauges to measure settlement at different depths in the compressible material. The settlement markers, installed during September 1981, consisted simply of a square metal plate (about 2 feet by 2 feet by 1 inch thick) placed on the surface of the sand blanket, with a vertical steel rod attached to the plate. The rod was inside a PVC tube to isolate it from the soil. The rods and PVC tubes were extended vertically in sections as the filling operations proceeded.

The settlement gauges were installed during September 1981 in holes predrilled to a depth 1-1/2 feet short of the desired gauge elevation. Each gauge consisted of a 5-inch diameter screw-type auger, about 1-1/2 feet long, screwed into the undisturbed soil at the bottom of the borehole. The depths of the gauges ranged from 15 to 65 feet. The vertical steel rod attached to the auger extended to the surface through a PVC tube installed to isolate it from the surrounding soil. As with the settlement markers, the rods and the PVC tubes were extended vertically in sections as the filling operation proceeded. Like the porepressure transducers, the settlement instruments were measured weekly except during filling operations when measurements were taken twice weekly. During the fill construction, one settlement marker (S-2A) and one settlement gauge (D-2) were damaged to the extent that they could no longer be read.

As shown in Figures 2 and 3, the instruments were usually installed in clusters at the borehole locations to enable development of a settlement and porewater pressure profile with depth through the soft floodplain sediments. For example, the instrument cluster at borehole BH-57 had porepressure transducers at depths of 24,36,45 and 60 feet below the top of the sand blanket. For settlement measurement, a marker was installed on top of the sand blanket, and gauges were placed at 19,28 and 53-foot depths. These instrument locations are shown in profile in Figure 3. The results from this cluster of instruments are discussed in the following section.

RESULTS OF MEASUREMENTS

Typical results from the porewater pressure and settlement measurements are shown on Figures 4 and 5, respectively, for the instrument cluster at BH-57, near the center of Area A (Figure 3).

Figure 4 shows that excess porepressures built up in the clay sediments (P-10 and P-11) directly reflected the weight of the surcharge fill added. This is well illustrated by the porepressure response from 20 feet of fill placed between mid-December and

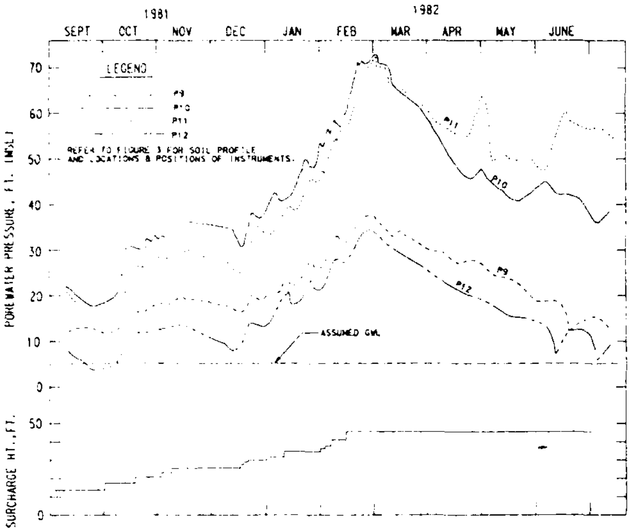

Fig. 4 Piezometer Measurements

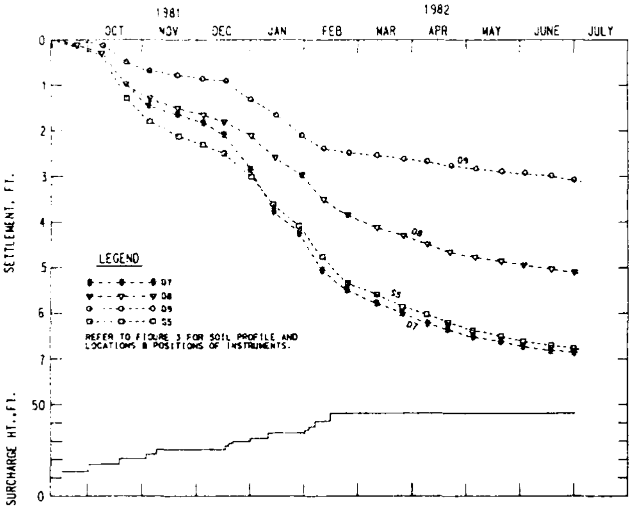

Fig. 5 Settlement Measurements

early February. (There had been no fill placement from early November to mid-December, and porepressure readings had stabilized). The maximum porepressure rise resulting from the 20 feet of fill (at 125 pcf) was equivalent to 40 feet of water (at 62.5 pcf). Porepressures built up in the more permeable peat and silt (P-9 and P-12) dissipated more rapidly with the maximum excess porepressure generated by the 20-foot fill placement being equivalent to only about 15 to 20 feet of water.

Figure 4 shows the excess porepressures dissipating fairly steadily in the peat, silt and clay after completion of the fill placement in early February. Excess porepressures in the peat (P-9) and the silt (P-12) had almost completely dissipated by the last reading in early July; readings in the clay were still moderately high at that time. This porepressure dissipation is reflected also by the changes in settlement shown in the time versus settlement curves for each layer in Figure 6. For example, the settlement of the peat (derived by substracting the D-8 from the D-7 readings) responded rapidly to the change in load, with little settlement being observed much beyond the end of the surcharge addition in mid-February. Recordings in the silt (D-9) showed a distinct reduction in the rate of settlement at the end of the surcharge addition. Settlement of the clay (D-8 minus D-9), on the other hand, indicated little or no rate reduction at that time. Early readings in the muck (D-7 minus S-5) demonstrated a rapid response to loading; the anomalous readings shown between early December and mid-February must be attributed to a temporary malfunction or misreading of deep gauge D-7 or settlement plate D-5 during that period.

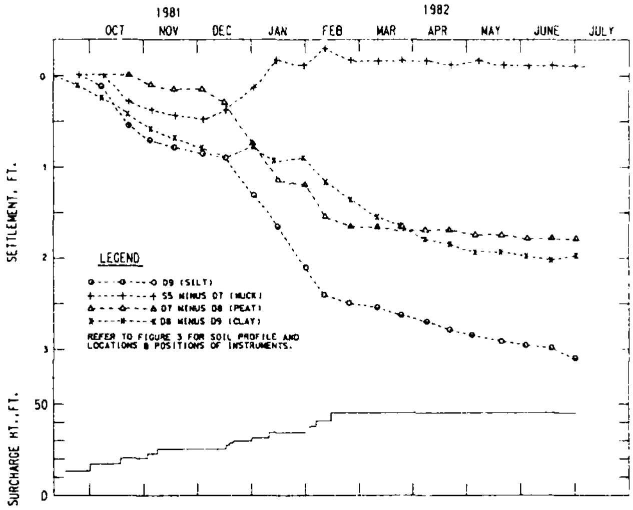

Fig. 6 Settlement Measurements for Each Soil Layer

Figure 5 shows maximum settlement at the BH-57 location to be around 7 feet at the last reading in July. Assuming this represents approximately 90 percent of the primary consolidation (see next paragraph), total primary consolidation settlement will be around 7.8 feet. This compares well with the predicted maximum primary consolidation settlement of 8.3 feet. At the other instrument cluster locations, 100 percent primary consolidation settlement values extrapolated from the July measurements ranged from 3.3 to 7 feet, and were in good agreement with the predicted values.

It is not possible to verify precisely from the porewater pressure and settlement results whether 90 percent of overall primary consolidation settlement was completed in 6 months, since: a) the incremental nature of the fill placement (over a period of 5 months) obscured the rate of porepressure dissipation and settlement, and b) the various sediments behaved differently, in accordance with their different permeabilities. Regardless, from the end of loading increase in mid-February to the last reading taken in early July, (a period of about 5 months), Figures 4 through 6 show that the majority of excess porepressures built up were dissipated (except possibly in the clay), and most of the settlement was completed.

CONCLUSIONS

The installation of almost one million linear feet of wick drains in the soft floodplain sediments enabled construction of the fill embankment on top of these sediments to proceed on schedule. The projected rate of consolidation and the long-term undrained shear strength of the soft sediments were increased by factors of about 25 and 10, respectively. The measured settlements agreed well with the predicted values. The filling operation was completed without any slip failures occurring in the soft sediments, supporting the conclusion that the soft sediments had gained the predicted increase in strength due to consolidation. In short, the wick drains brought about the desired results. The instrumentation installed to measure porepressure changes and settlement during and after fill placement proved to be reliable and robust, as demonstrated by the generally reasonable readings, and very few instrument failures.

REFERENCES

Hansbo, S. (1979), "Consolidation of Clay by Band-Shaped Prefabricated Drains", Ground Engineering, pp 16-25.

Leonards, G.A. (1962), "Engineering Properties of Soils", Chapter 2 in Foundation Engineering, edited by G.A. Leonards, McGraw Hill.

Proceedings: Second International Conference on Case Histories in Geotechnical Engineering, June 1-5, 1988, St. Louis, Mo., Paper No. 5.30

Tunnel Repair Using Cement-Stabilized Flyash

J.C. Neyer
Principal, Neyer, Tiseo & Hindo, Ltd., Farmington Hills, Michigan

H.R. Price
Project Engineer, Neyer, Tiseo & Hindo, Ltd., Detroit, Michigan

K.M. Swaffar
Project Engineer, Neyer, Tiseo & Hindo, Ltd., Detroit, Michigan

SYNOPSIS: A ten-foot diameter water tunnel was restored to service two months after it was found to be badly cracked and deteriorated. To effect the repair, the tunnel was filled with cement-stablized flyash and then cement-flyash grout pumped into the voids around the tunnel. The cement-stablized flyash gained a strength of about 50 psi in 28 days and was readily removed by hand mining techniques once the grouting was completed. It was found that the exterior grouting at pressures up to 150 psi had been very effective in sealing the cracks in the tunnel and preventing further inflow of soil and groundwater. Final tunnel repairs included placement of steel ribs and a shotcrete liner within the damaged section of tunnel.

INTRODUCTION

The Northeast Raw Water Tunnel is a key element in the City of Detroit Water and Sewerage Department (DWSD) water supply system since it supplies water to the northern portion of Detroit and several northeast suburbs. This ten-foot diameter tunnel is approximately 90 feet deep and generally follows street rights of way from Pennsylvania and Forest to Eight Mile and Hoover Roads. It was constructed in 1952 of non-reinforced concrete. Its condition was unknown since it had not been inspected in more than 30 years. However, surface settlement in the vicinity of the tunnel alignment led DWSD to suspect distress in the tunnel itself.

DWSD retained Neyer, Tiseo & Hindo, Ltd. to inspect the tunnel and evaluate its condition. During the inspection, an area of severe structural distress was discovered. Soil was flowing into the tunnel under the pressure of the groundwater 50 feet above the tunnel. Severe cracking and spalling of the concrete lining had occurred over a length of more than 100 feet. As shown in the photo below, the lining had lost much of its ability to carry load in hoop compression.

The tunnel had been shut down for inspection during the winter months but was needed back in service by June 1, 1986 to handle summer water demand. The distress was first found on March 15, 1986, less than 80 days before the scheduled reopening. DWSD authorized Neyer, Tiseo & Hindo, Ltd. to take all necessary steps to repair the tunnel and to restore it to use before June 1.

The tunnel was immediately refilled with water to minimize further inflow of soil. A plan was developed for repairing the tunnel in a cost effective manner. The technique used on other tunnel repairs, pressure grouting from the ground surface, was considered. However, in view of the distressed condition of the tunnel liner, grouting could have caused further liner damage and perhaps total collapse of the tunnel. It was deemed necessary to fill the tunnel with a material which would support the damaged lining during grouting but which could be readily removed once grouting was complete. The material which best met the project requirements was cement-stabilized flyash.

SUBSURFACE CONDITIONS

The tunnel had been driven through glacial drift which varied from very stiff silty clay to very compact fine sand and silt. The groundwater level in this area was approximately 50 feet above the crown of the tunnel. In the area where the distress was found, the soils above tunnel springline were predominantly silty clays and those below springline were sandy silts. The sandy silt had Standard Penetration Test (S T) values of 100 or more in most cases. Grain size test indicated that from 50 to 99% of the soil was generally finer than the No. 200 sieve. A generalized soil profile of the area is shown in Figure 1.

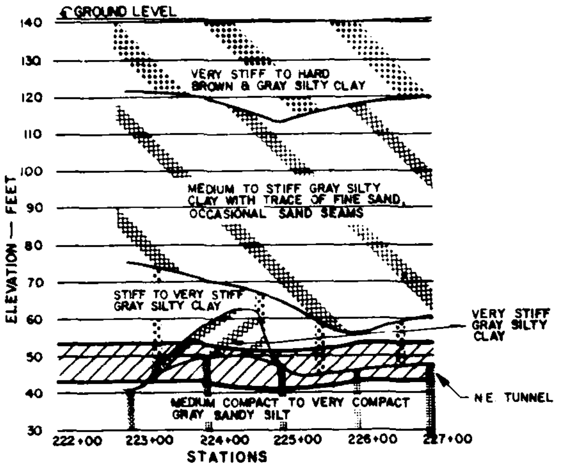
℄ GROUND LEVEL
140
130
120
110
100
90
80
70
60
50
40
30
ELEVATION — FEET
VERY STIFF TO HARD BROWN & GRAY SILTY CLAY
MEDIUM TO STIFF GRAY SILTY CLAY WITH TRACE OF FINE SAND, OCCASIONAL SAND SEAMS
STIFF TO VERY STIFF GRAY SILTY CLAY
VERY STIFF GRAY SILTY CLAY
N.E. TUNNEL
MEDIUM COMPACT TO VERY COMPACT GRAY SANDY SILT
222+00
223+00
224+00
225+00
226+00
227+00
STATIONS

FIGURE 1. GENERALIZED SUBSURFACE PROFILE OF DISTRESSED AREA

FLYASH CHARACTERISTICS

Flyash is a by-product of coal-burning power plants. It is readily available in the mid-western United States. In fact, utility companies have been searching for ways to utilize flyash productively rather than to pay large amounts of money to dispose of it as a waste product.
The flyash used on the project was obtained from Detroit Edison Company and is identified as Type F. Studies by others have defined the range of chemical and physical properties of this type of flyash. The grain-size, as reported by others, is predominately in the range of silt-size particles with 80 to 90 percent of the material falling between 0.074 and 0.002 mm. It is non-plastic and has a maximum dry density in the range of 80 to 90 pounds per cubic foot. Table I (Gray et al) below presents a chemical analysis of a few different Detroit Edison flyash materials.

TABLE 1.

CHEMICAL ANALYSIS OF FLY ASH SOLIDS FROM SOME COAL-FIRED POWER STATIONS IN MICHIGAN

Chemical Composition % by Weight

Fly ash source (1)	SiO (2)	Al O (3)	Fe O (4)	TiO (5)	CaO (6)
D.E.Karn Plant	45.0	28.5	24.3	----	1.0
Marysville Plt	36.5	19.0	33.0	0.6	2.0
St.Clair Plant	36.0	29.0	19.0	1.0	3.8
Trenton Ch.Plt.	46.5	26.5	16.0	1.0	0.9

TABLE 1 - Con't.

	MgO (7)	Na O (8)	K O (9)	SO (10)	Carbon (11)
D.E.Karn Plant	0.5	----	----	Trace	0.7
Marysville Plt	0.8	0.3	1.7	0.66	3.53
St.Clair Plant	0.9	0.4	1.6	0.97	4.75
Trenton Ch.Plt.	0.8	0.4	1.6	0.60	4.32

CEMENT STABLIZED FLYASH

Detroit Edison has conducted extensive research of the feasibility of stabilizing flyash by the addition of Portland cement and water. The stabilized flyash usually contains 5 percent cement (as a percent of dry flyash weight) and sufficient water to impart an 8-inch to 10-inch slump to the mixture. It is designed to develop a strength in the range of 100 pounds per square inch in 28 days.

In addition, Detroit Edison studies have indicated that the stabilized flyash is not dispersive when discharged into standing water and that it is more resistive to erosional forces than traditional granular materials.

For this project, Neyer, Tiseo & Hindo, Ltd. conducted supplementary tests to establish the range of strengths which would develop with different cement contents and different water contents. The results of these studies are presented in Figures 2 and 3.

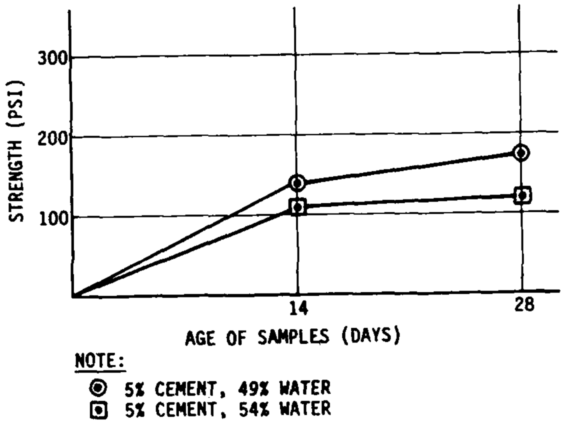

FIGURE 2. 5% CEMENT CONTENT

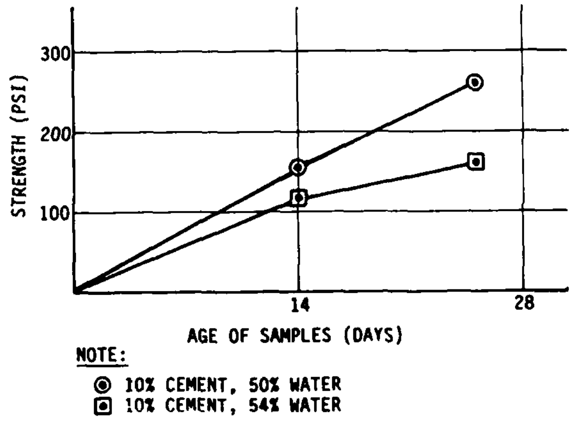

FIGURE 3. 10% CEMENT CONTENT

During the construction of this project, 3 by 6 cylinders were molded in the field and field cured submerged in water. The field cured cylinders were broken periodically to assess the gain in strength over time. The results of the field strength tests as compared to the laboratory results are presented in Figure 4. It can be seen that field strengths were generally less than half of the lab test values for comparable time periods.

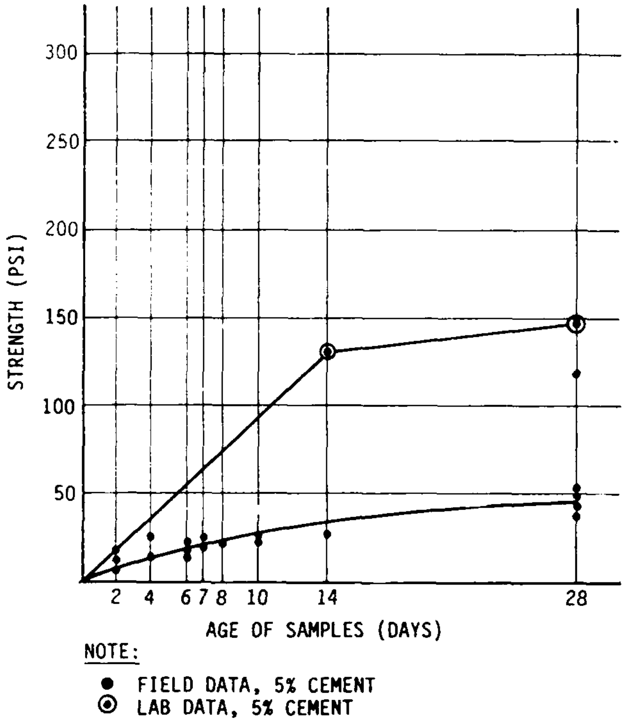

FIGURE 4. FIELD DATA VS. AVERAGE LAB DATA

FLYASH PLACEMENT

In order to place the stabilized flyash in the distressed section of the tunnel, it was necessary to drill a series of drop holes from the ground surface through the crown of the tunnel. Five holes were drilled on approximately 60-foot centers with each hole being 30 inches in diameter. A 24-inch diameter steel casing was grouted in place in each hole prior to coring into the tunnel. The actual tunnel penetrations were 18 inches in diameter.

To prevent the fluid flyash from flowing beyond the distressed area, bulkheads were installed at each end of the damaged section of tunnel. The bulkheads were inflatable polyester fabric bags placed by divers. The 120-inch diameter bags were Test Ball Plugs manufactured by Chere Industries. Water pumped from the ground surface was used to inflate the bulkheads.

Once the bulkheads were in place, stabilized flyash was placed in the tunnel by tremie pipe. The bulkheads, because of their size, could only withstand a differential pressure of 3 pounds per square inch. To maintain the head in equilibrium, it was necessary to pump water from the tunnel at the same rate that flyash was introduced. It was also necessary to place the flyash in three lifts so that each lift could gain partial strength prior to placement of subsequent lifts. A total of approximately 700 cubic yards of cement stabilized flyash were placed over a three-day period.

GROUTING PROCEDURES

Once the distressed areas of the tunnel had been filled with cement stabilized flyash, grouting from the ground surface was undertaken. Grout holes were drilled at a spacing of approximately twenty feet on center on both sides of the tunnel barrel, with the east side grout holes offset 10 feet north of those on the west. Cement-lyash grout was pumped into the grout pipes at pressures of up to 150 psi. The grout mix was three parts of flyash to one part of cement with sufficient water to give the required fluidity.

The intent of the surface grouting was to fill voids left when soil migrated into the tunnel, and to seal cracks in the tunnel to prevent further soil infiltration. During grouting, it was not uncommon for grout to rise in unused grout pipes on the west side of the tunnel while being pumped in on the east side. This phenomenon suggested that voids existed below the tunnel barrel and that the grout was indeed filling the voids.

A total of 55 cubic yards of grout were placed during a one-week grouting period. Much of the grout flowed into the ground under its own weight and grout pressures were only raised after the majority of grout holes had received at least some grout.

REMINING AND RESTORATION

With grouting completed, the water was again pumped out of the tunnel and repair operations initiated. The cement-stabilized flyash was removed by hand mining using pneumatic clay spades. In general, the flyash had the consistency of a stiff clay. Rail mounted muck cars were used to haul the excavated flyash to the shafts for removal.

The external grouting program proved to be very effective in sealing off the infiltration of soil and water into the tunnel. Only a limited amount of internal grouting was required to seal leaking cracks. Steel ribs were placed within the distressed area concurrently with the remining to improve the overall strength of the tunnel barrel and to prevent loose pieces of concrete from falling out of the tunnel lining. The ribs were W4X13 generally placed on approximately 2.5-foot centers.

As a final step in the restoration, a shotcrete liner was placed over the ribs and the damaged concrete. The inside diameter of the new shotcrete lining was eight feet which was considered adequate from a hydraulic viewpoint. The shotcrete contained steel fibers sc that it was not necesssary to install any type of mesh in the tunnel. In order to improve the adhesion of the shotcrete to the interior of the existing tunnel lining, silica fume (microsilica) was added to the mix.

The tunnel was restored to service upon completion of the rib placement and performed satisfactorily during the summer of 1986. The shotcreting was completed in the fall of 1986 and the tunnel completely returned to service in the spring of 1987.

CONCLUSIONS

The use of power-plant flyash in the construction and repair of underground facilities has been shown to be cost-effective. Cement-stabilized flyash as a low-strength, low-cost fill performed well. Cement-flyash grout was effective in filling subsurface voids and in sealing cracks in the tunnel lining. The project was completed in a very short timeframe because the materials were readily available.

REFERENCES

Gray, D. H. and Lin, Y. K. (1972) "Engineering Properties of Compacted Fly Ash" Journal of th Soil Mechanics and Foundations Division, ASCE, Volume 98, No. SM4, p.p. 361-368.

Funston, J. J. and Krell, W. C. (1985) "Need a Dependable Backfill - Try Flowable Fly Ash", Advanced Cementitious Products Fall Convention, ASCE, Detroit, Michigan, Volume I, p.p. 1-13.

Swaffar, K. M. and Price, H. R. (1987) "Investigation and Repair of the Northeast Raw Water Tunnel", Rapid Excavation and Tunneling Conference, New Orleans, LA, Volume I, p.p. 273-291.

Proceedings: Second International Conference on Case Histories in Geotechnical Engineering, June 1-5, 1988, St. Louis, Mo., Paper No. 5.31

Impact of Tunneling on Two Brick-Bearing-Wall Structures

Marco D. Boscardin
Assistant Professor of Civil Engineering, University of Massachusetts,
Amherst, Massachusetts

SYNOPSIS: The responses of a pair of brick-bearing-wall structures to nearby construction of twin, shield driven 21-ft-diameter tunnels in soil are examined. Horizontal and vertical ground displacements are summarized and discussed, as well as, horizontal and vertical displacements, tilting, distortion, and damage sustained by the structures. Transient features of the developing settlement trough and effects on building response are also examined and discussed.

INTRODUCTION

This paper reviews the response of a pair of two-story, brick-bearing-wall structures to excavation of two nearby subway tunnels. The tunnels are part of the Washington, D.C. METRO System, and are 20.8 ft in diameter with a springline depth of 45 ft. The center to center tunnel spacing is 42 ft. Fig. 1 shows the relative positions of the structures and the tunnels in profile. As shown by the site plan, Fig. 2, the longitudinal axes of the buildings are not parallel to the tunnel axes.

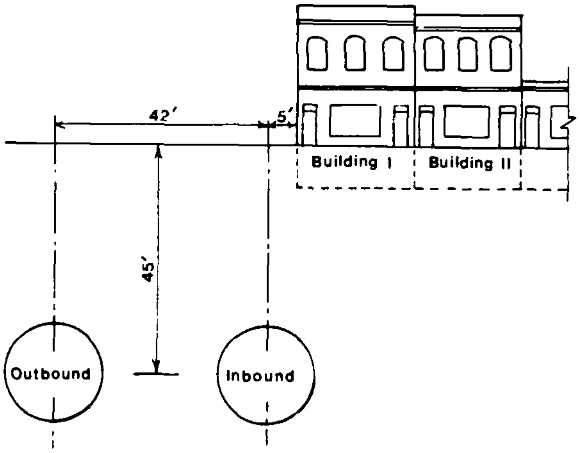
42'
5'
Building I
Building II
45'
Outbound
Inbound

Fig. 1 Profile of Buildings and Tunnels

SUBSURFACE CONDITIONS

The soil profile shown on Fig. 3, indicates that the test section is located near a transition from dense sands and gravels in river flood plain deposits to hard, clayey Cretaceous soils. Observations made at the tunnel heading during excavation beneath the test section indicated that the heading material was a hard red clay with occasional weathered and sandy zones near the tunnel crown. The clay material is hard and fissured with some slickensides present. Deep dewatering wells were used to lower the ground water level during construction. Ground control in the test area was not a problem and ground losses appeared to decrease with passage through the transition zone.

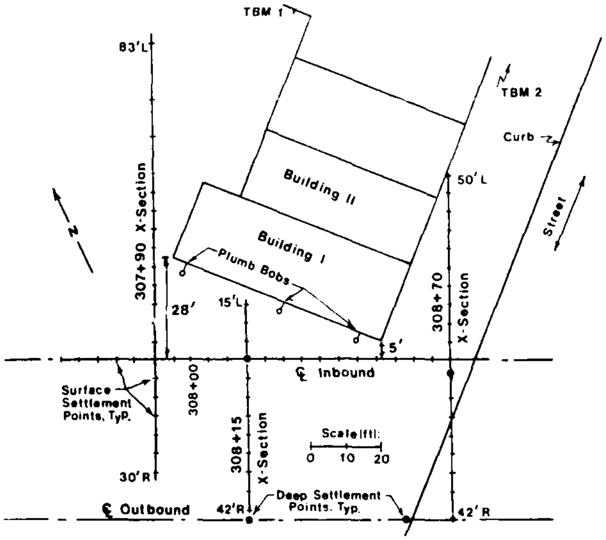
TBM 1
TBM 2
83'L
Curb
50'L
N
Street
Building II
Building I
Plumb Bobs
307+90 X-Section
308+70 X-Section
28'
15'L
5'
℄ Inbound
Surface Settlement Points, Typ.
308+00
308+15 X-Section
Scale(ft):
0 10 20
30'R
℄ Outbound
42'R
Deep Settlement Points, Typ.
42'R

Fig. 2 Plan of Test Site

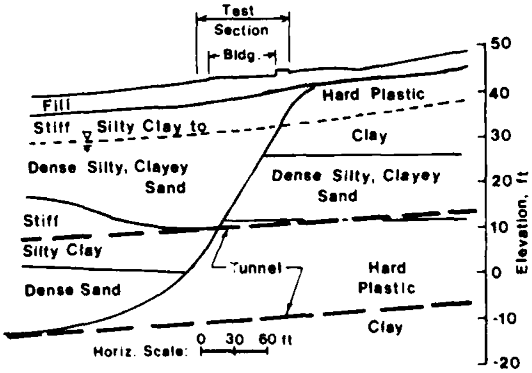
Test Section
Bldg.
Fill
Stiff Silty Clay to
Dense Silty, Clayey Sand
Stiff
Silty Clay
Dense Sand
Hard Plastic
Clay
Dense Silty, Clayey Sand
Tunnel
Hard Plastic
Clay
Horiz. Scale: 0 30 60 ft
50
40
30
20
10
0
-10
-20
Elevation, ft

Fig. 3 Soil Profile

EXCAVATION AND CONSTRUCTION PROCEDURE

The tunnels were excavated using a Robbins articulated shield. The shield was 21.17 ft long at the crown with an outside diameter of 20.53 ft. The shield was equipped with hydraulically operated breasting flaps. The front of the shield included a 4.5 ft long hood with a 1/2 in. overcutter bar all around the leading edge. The shield was composed of three sections, approximately equal in length, with articulation joints connecting the sections. Hydraulic jacks also connected the the front and middle sections and provided control of the attitude of the front section relative to the middle section. The connection between the middle section and the tail section was such that the tail could freely trail the middle section. The tailskin was 1/2 in. thick to minimize ground loss as the temporary support passed out of the tail section.

The excavation cycle consisted of: 1) shoving the shield forward into the soil with hydraulic jacks reacting against the temporary lining, and 2) raking the muck onto a conveyor belt with a hydraulically operated spade. The conveyor then carried the muck from the face into muck cars. A temporary lining consisting of steel ribs and timber lagging was assembled within the tailskin of the shield and then expanded as each rib cleared the tail. The ribs were four-piece W6X25 sections and were spaced about 4 ft center to center. The lagging consisted of 5 in. by 8 in. by 3.75 ft long timbers. The tunnel excavation and support system is described in detail by MacPherson et al., (1978).

STRUCTURES

The two brick masonry structures and their positions relative to the tunnels are illustrated in Figs. 1 and 2. The buildings are two-stories high with full basements. The longitudinal axes of the buildings are oriented approximately 22 degrees from the tunnel axes with the corner of Building I 5 ft from the center line of the inbound tunnel. Because of their proximity to the tunnel excavations these structures were vacated during tunnel construction.

The two buildings are similar in construction. The bearing walls are parallel to the longitudinal axes of the buildings and composed of brick with lime mortar. There is no structural connection between the two buildings. A steel beam supported by the facade walls and three equally spaced interior columns, extends along the length of each building, midway between the bearing walls. The timber floor joists, 2-in. by 10-in. at 16-in. intervals, span between the center beam and the bearing walls. The joist bearing at the masonry pockets was about 4 in. The bearing walls and columns are supported by shallow footings at depths ranging from 4 to 8 ft below the exterior ground level. Information about the exact nature and size of the footings was not available. However, rubble type footings probably support both buildings. Based on type of construction, materials and present condition, the structures are estimated to be 80 to 90 years old. There appears to have been some renovation and restoration of the joists and front facade walls.

The bearing walls are 14 in. thick at basement level and are reduced 1 in. in thickness for each story thereafter. The facade walls are 12-in.-thick brick masonry walls. The front facade walls are faced with one wythe, approximately 4 in., of cement mortar brick masonry backed by 8 in. of lime mortar brick masonry. The exposed lime mortar is generally soft and quite easily scraped from the joints of both the bearing and facade walls. In many instances there are gaps where the lime mortar has been eroded or has fallen from the joints. The exterior of the front facade walls has better mortar and presents a more competent appearance; the joints are tight and very hard with few cracks or gaps. The interior walls of Building I are either exposed brick or plaster over brick. Many cracks were present prior to the tunnel excavation. These cracks may have been related to previous settlement and to cyclic thermal and humidity changes. The interior walls of Building II were either brick or dry wall over brick with cracking prior to tunneling similar to that observed in Building I.

OBSERVATION PROGRAM

Observations may be divided into three categories: Measurements of movement of the ground mass; Distortion measurements of the building; Inspection for visible evidence of building distortion (e.g. cracking, jammed doors, etc.). The observations in each case were made before, after, and periodically during tunnel excavation. The following is a brief description of the observations made. More detailed descriptions of observations may be found in Boscardin (1980).

Observations of movements of the ground mass were predominantly settlement measurements. However, the magnitude of the horizontal strain in the extension zone was estimated through observation and measurement of cracks in the sidewalks and pavement that developed parallel to the tunnel axes. There were three lines of settlement points perpendicular to the tunnel axes at Stas. 307+90, 208+15, and 308+70. A fourth line ran along the centerline of the inbound tunnel from Sta. 307+60 to Sta. 308+70, Fig. 2. Three deep settlement points were also monitored. The anchorages for the deep settlement points are about 4 ft above the crown of the tunnel. Bench marks were located 110 ft and 140 ft from the center of the inbound tunnel. Detailed descriptions of the ground movements may be found in MacPherson et al., (1978).

Building distortion was monitored using five types of observations:

> Interior bay distortion was determined by changes in horizontal and diagonal distances between elements of the bay. Measurements were made using a tape extensometer having a sensitivity of 0.001 in. and a repeatability of 0.004 in.

Building settlement was based upon optical level surveys of exteriors of both buildings and the interior of the basement of Building I. The level-rod system had a repeatability of 0.04 in. and closure errors were on the order of 0.04 in.

Tilt of the south wall of Building I was measured using plumb bobs suspended from the roof. Measurements were repeatable to 0.03 in.

Relative horizontal displacements between Building I and II were determined from changes in distance between pairs of studs attached on either side of the vertical joint forming the interface between buildings. Measurements were made using a caliper with a sensitivity of 0.001 in. Repeatability was on the order of 0.01 in.

Change in bearing of floor joists was determined by displacement of a reference stud on the joist relative to the face of the wall. A caliper with a sensitivity of 0.001 in. was used. The repeatability of the system was 0.01 in.

The third category of observations was inspection for visible evidence of building distortion. Detailed surveys noting the condition of buildings were made. Cracks were mapped and selected cracks were measured before and after tunnel excavation. Building elements which often prove quite sensitive to distortion were also inspected. These included doors, windows, column-beam intersections, and corner areas.

GROUND SURFACE AND BUILDING SETTLEMENTS

The settlements discussed in this section are related only to excavation of the inbound tunnel. Excavation of the outbound tunnel, which was farther from the buildings, occurred first and was monitored by the contractor. Construction records indicate less than 1/8 in. of settlement occurred in Building I in response to outbound tunnel construction and no evidence of building distress due to excavation of the outbound tunnel was observed.

The pattern of ground surface settlement along the centerline of the inbound tunnel is shown in Fig. 4. The five curves illustrate surface settlements associated with various positions of the tunnel heading during excavation. The data indicate that surface settlement decreased as the tunneling passed through the transition zone from sandy Pleistocene terrace deposits to hard Cretaceous clay. Final surface settlements along the centerline range from 1.5 in. (Cretaceous clay) to nearly 3 in. (sandy terrace deposits). Deep settlement monitors in the Cretaceous clay indicated approximately 2 in. of deep settlement above the tunnel crown. Deep settlement also appeared to decrease with passage through the transition zone. Fig. 4 also indicates that the surface settlement preceded the tunnel heading by about 15 ft and 25 ft during tunneling in the Cretaceous clay and sandy terrace deposits, respectively. Ten to fifteen percent of the total surface settlement occurred before the face of the excavation reached a reference point. Forty to sixty percent of the total surface settlement appeared by the time the tail of the shield passed a given point. In addition, the sandy terrace material appeared to settle more than the hard clay material once the tail passed a given point and the ribs and lagging support was in place.

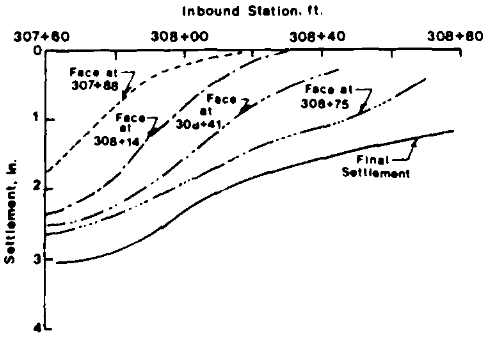

Fig. 4 Centerline Settlement Profile

Surface settlements along a line perpendicular to the tunnel axis at Sta. 308+70 are shown in Fig. 5. Settlement profiles corresponding to several locations of the tunnel face are shown.

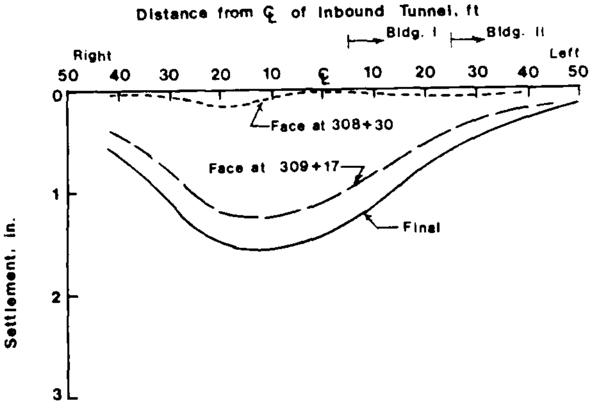

Fig. 5 Settlement Profile at Sta. 308+70

It is apparent that based on the final settlement data portions of the structures lie in the zone of lateral extension while other portions Yma me wca qnea nK YdwaodY unjboaQQmne &oaKao to Fig. 6). However, Fig. 5 also indicates that portions of Building I initially in the zone of lateral extension are later in the zone of lateral compression due to continued development of the settlement profile. Therefore, Building I will be subjected to transient patterns of distortion potentially quite different than the final settlement profile would suggest.

A transient pattern of extension and compression zones is also present when considering lateral ground movements parallel to the tunnel axis. The settlement profile in the vicinity of the tunnel heading exhibits a reversal of curvature and a zone of maximum curvature similar to the transverse settlement profile of the trough. In effect, the buildings are subjected to two components of horizontal

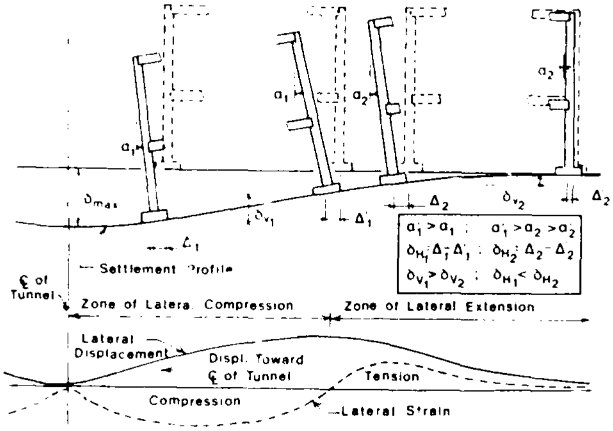
a_1
a_1
a_2
a_2
δ_{max}
δ_{v_1}
Δ_1
Δ_2
δ_{v_2}
Δ_2
Δ_1
$a_1 > a_1$; $a_1 > a_2 > a_2$
$\delta_{H_1} \approx \Delta_1 - \Delta_1$; $\delta_{H_2} \approx \Delta_2 - \Delta_2$
$\delta_{v_1} > \delta_{v_2}$; $\delta_{H_1} < \delta_{H_2}$
Settlement Profile
℄ of Tunnel
Zone of Lateral Compression
Zone of Lateral Extension
Lateral Displacement
Displ. Toward ℄ of Tunnel
Tension
Compression
Lateral Strain

Fig. 6 Effect of Location of Structures in the Settlement Trough

extension and compression, one transverse to the tunnel axis and one parallel to the tunnel axis. Evidence of the horizontal extension transverse to the tunnel axis appeared in the form of several new 0.32-in.-wide cracks, parallel to the tunnel, that formed in the sidewalks 20 to 40 ft from the tunnel centerline. However, the transient condition parallel to the axis of the tunnel is often totally masked when examining the final settlement profile along the centerline of the tunnel.

Settlement surveys of the ground surface and exteriors of the structures indicate that the buildings settled with the ground surface and little bridging occurred. The final settlement of Building I ranged from 1.4 in. to 0.14 in. and the final settlement of Building II ranged from 0.42 in. to less than 0.05 in.

MEASURED BUILDING DISTORTIONS

An exaggerated sketch illustrating the final distorted configuration of Buildings I and II along a transverse cross-section located near Sta. 308+50 is shown in Fig. 7. The sketch along with the settlement contours shown in Fig. 8 summarizes final settlement, tilt, tape extensometer, and crack width data at the cross-section. The dimensions along the diagonals and the horizontals of Fig. 7 are strains along those lines. Extension and compression strains are denoted positive and negative, respectively. Settlements and crack widths are in inches, whereas rotations and slopes are specified as tangents of angles.

The relative positions of Buildings I and II on the ground surface settlement profile should be noted. Building I is nearer the center of the settlement trough and predominantly in the zone of lateral compression. In this zone, vertical settlement dominates and horizontal ground strains are very small. On the other hand, Building II is near the edge of the settlement trough and in the zone of lateral extension. Here, settlements and differential settlements are smaller than those found nearer the center of the settlement trough, and horizontal tensile strains are more significant.

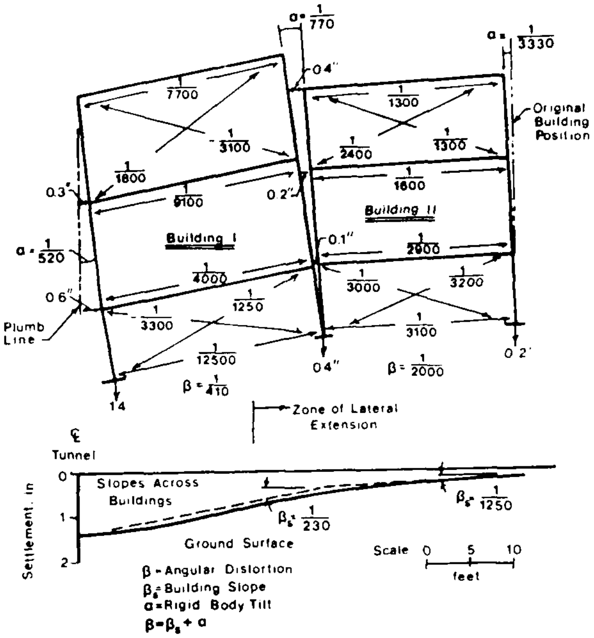
$\alpha = \frac{1}{770}$
$\alpha = \frac{1}{3330}$
0.4"
$\frac{1}{7700}$
$\frac{1}{1300}$
$\frac{1}{3100}$
$\frac{1}{2400}$
$\frac{1}{1300}$
Original Building Position
$\frac{1}{1800}$
$\frac{1}{1600}$
0.3"
$\frac{1}{9100}$
0.2"
Building II
Building I
0.1"
$\frac{1}{2900}$
$\alpha = \frac{1}{520}$
$\frac{1}{4000}$
$\frac{1}{3000}$
$\frac{1}{3200}$
0.6"
$\frac{1}{1250}$
Plumb Line
$\frac{1}{3300}$
$\frac{1}{3100}$
$\frac{1}{12500}$
0.4"
$\beta = \frac{1}{2000}$
0.2"
$\beta = \frac{1}{410}$
1.4
℄ Tunnel
Zone of Lateral Extension
Settlement, in
0
1
2
Slopes Across Buildings
$\beta_s = \frac{1}{230}$
$\beta_s = \frac{1}{1250}$
Ground Surface
Scale 0 5 10 feet
β = Angular Distortion
β_s = Building Slope
α = Rigid Body Tilt
$\beta = \beta_s + \alpha$

Fig. 7 Final Distortions of Buildings

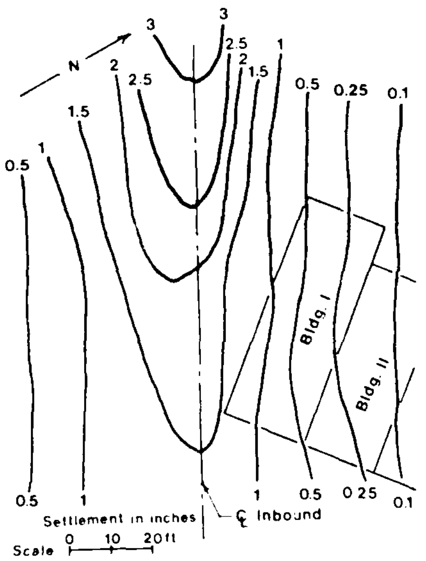
N
3
3
2
2.5
2.5
2
1.5
1
1.5
0.5
0.25
0.1
1
0.5
Bldg. I
Bldg. II
0.5
1
1
0.5
0.25
0.1
Settlement in inches
℄ Inbound
Scale 0 10 20 ft

Fig. 8 Final Settlement Contours

However, final distortion data only tell part of the story. Building I was in the zone of lateral extension during the early stages of development of the settlement trough. When the face of the tunnel was at Sta. 308+50, the total settlement of the bearing wall nearer the tunnel was 0.6 in. with no observable settlement noted at the bearing wall farther away from the tunnel. At this time, the horizontal extension strain at the basement level was 1/3300 and both diagonals were in extension as a result to the lateral extension of the ground (Fig. 9).

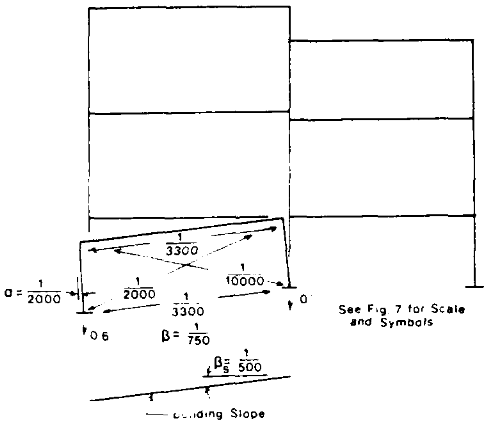

Fig. 9 Building Distortions for Tunnel Face at Sta. 308+50

The shear strains, derived from the differential settlements, caused a greater extension along one diagonal than along the other. The rigid body rotation of the structure was about 1/2000 and the slope of the building settlement profile equaled 1/500. Therefore, angular distortion of the structure (settlement slope across the building minus rigid body tilt) was about 1/750. Thus, during the early stages of the development of the settlement trough, the distortion of the structure had both horizontal and shear strain components, whereas, the final distortion of the structure appears to be dominated by the shear strain caused by differential settlement.

When the face of the tunnel moved to Sta. 308+60, the front door of Building I became tightly jammed. The distortion of the door frame was sufficient to bind the door which had previously opened easily. Later, when the settlement trough was nearly fully developed, the door again worked normally. This one instance illustrates a situation where a portion of the structure experienced more severe angular distortion during the development of the settlement trough than the final measurements indicate. In such cases, predictions of building response based upon estimates of final distortion alone may be misleading.

The final distorted shape of Building I is caused primarily by differential settlements across the structure. The differential settlement between bearing walls is 1 in. and causes a slope of 1/230 across the structure. The final relative horizontal movement between the bearing walls at their base was negligible. The distortion caused by this combination of relative movements has primarily two components: a rigid body tilt and a shear or angular distortion of the building. The rigid body tilt of the structure was apparent from the plumb line measurements and from the opening of the joint between the two structures. The final plumb line measurements lead to a calculated rigid body rotation of 1/710. Shearing distortions are indicated by the strain measured along the diagonal tape extensometer lines. One diagonal of each pair exhibited extension whereas the other exhibited compression as shown in Fig 7.

Due to the orientation of the Building I relative to the tunnel axis, the structure cuts across the settlement contours at an angle and torsion is induced in the structure. This angle of twist was approximately 0.15 degrees over the 60-ft length of the structure. In this case the effect of the torsion of the building was slight. The amount of torsion induced was small and the lack of fixity of the structural connections between the wall and floor systems allowed this structure to tolerate this torsion with negligible deleterious effects. However, a transient torsion can also occur in a structure regardless of orientation relative to the tunnel axis due to the pattern of development of the settlement trough and should be considered in any evaluation of building response.

The final distortions of Building II, shown in Fig. 6, illustrate the behavior of a structure in the zone of lateral extension. The differential settlement between the bearing walls is 0.2 in., causing the building settlement curve to have a slope of 1/1250. The rigid body rotation of Building II is on the order of 1/3300 or less. Thus, the differential settlements and the rigid body rotations of Building II are less than those of Building I. The final angular distortion of Building II is about 1/2000. The horizontal tape extensometer measurements show lateral strains between the bearing walls ranging from 1/3100 in the basement to 1/1300 at the roof. Both diagonals of each set showed extension. The diagonal extension strains range from 1/3000 to 1/1300 for the basement and second story tape extensometer lines, respectively. The greater extension measured along the horizontal and diagonal tape extensometer lines higher up in the structure are caused by a relative rotation of the bearing walls. The bearing wall nearer the center of the settlement trough is on a steeper portion of the ground surface settlement curve and thus rotates more than the farther bearing wall (Fig. 6).

VISIBLE EVIDENCE OF BUILDING DAMAGE

Visual inspections were made before, after, and at intervals during the tunnel excavation under the test site. The initial conditions of both Buildings I and II were quite poor. Extensive cracking was noted on the interiors and exteriors of both structures and the interior plaster walls were cracked and loosened at many locations. The initial state of each building was recorded through photographs, mapping of cracks, measurement of selected cracks, and written descriptions. Additional cracking and the increase in size of pre-existing cracks were noted during and after the tunnel excavation. When viewed in light of the very poor initial condition of both structures any damage caused by the tunnel excavation can only be termed as negligible to very slight. However, if the same structures were in good repair and had been occupied, the same response would probably have been considered to be slight to moderate damage, see Boscardin (1987).

New cracks and an increase in the width of existing cracks were found in Building I during and after tunnel excavation. Areas where the cracking was noticed include a front and rear facade walls, the south bearing wall, and the basement slab. Examples of the cracking at these locations are shown in Fig. 10. The rear facade wall experienced a 1/64 in. increase in the width of several of the existing cracks. An increase in crack size was also noted in the south bearing wall near the front facade wall. Here a diagonal crack from the second-story window down to the facade wall became clearly visible (Fig. 10b). In the front facade wall of Building I, the cracks were concentrated around the doors at the first floor and the windows at the second floor (Fig. 10c).

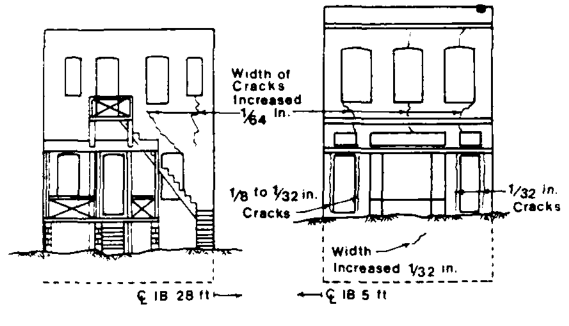
Width of Cracks Increased 1/64 in.
1/8 to 1/32 in. Cracks
1/32 in. Cracks
Width Increased 1/32 in.
℄ IB 28 ft
℄ IB 5 ft

a) Rear Facade Wall

c) Front Facade Wall

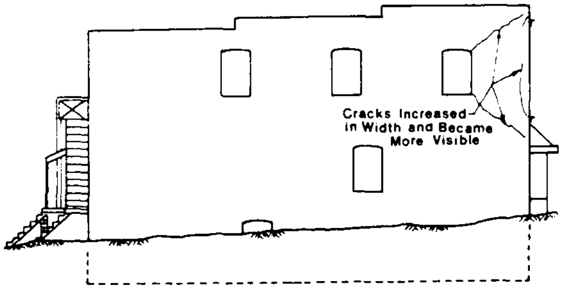
Cracks Increased in Width and Became More Visible

b) South Bearing Wall

Fig. 10 Cracks on Exterior of Building I

Cracks around the door nearest the excavation ranged from 1/32 in. to 1/8 in. wide at the bottom and top of the door, respectively. The door became jammed and difficult to open as a result of the tunnel-induced distortion. The door at the north end of the facade wall was surrounded by cracks about 1/32 in. wide. An increase in the widths of cracks on the front facade wall were also evident at the second floor where vertical cracks below the windows increased about 1/64 in. in width. A new crack also appeared in the basement slab of Building I near the south bearing wall. The crack was nearly 20 ft long and 5/64 in. wide and appeared when the tunnel face was at Sta. 308+30 (Fig. 11). The crack approximated the shape of the contours of settlement for this position of the tunnel face relative to the building. Tape extensometer data matched crack measurement data relatively well.

Cracking in Building II was concentrated at the corner of the south bearing wall and the front facade wall. A pre-existing 1/16-in.-wide vertical crack between the bearing wall and the facade wall opened to 1/8 in. in the basement to 1/4 in. at the second floor. Daylight was visible through the crack at several locations. Another crack at the corner between the ceiling and the front facade wall of the second story was initially 1/8 in. wide and increased to 3/8 in. wide. A pre-existing hairline crack at the corner of the south bearing wall and ceiling of the second story near the front of the building also grew to 1/4 in. wide. The tape extensometer data for Building II show that nearly all of the lateral extension experienced by the structure was concentrated in the the few cracks described above.

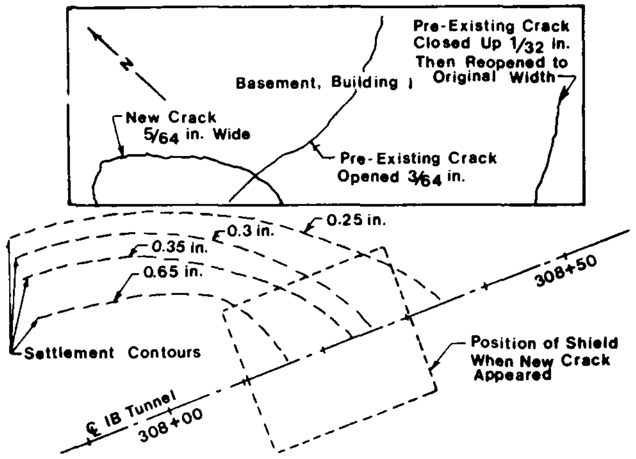
N
Basement, Building I
Pre-Existing Crack Closed Up 1/32 in. Then Reopened to Original Width
New Crack 5/64 in. Wide
Pre-Existing Crack Opened 3/64 in.
0.3 in.
0.25 in.
0.35 in.
0.65 in.
Settlement Contours
308+50
Position of Shield When New Crack Appeared
℄ IB Tunnel
308+00

Fig. 11 Cracks in Basement of Building I

Data from the plumb bob survey are summarized in Fig. 12. The resultant displacements of the top of the wall relative to its bottom at each plumb bob location are shown as vectors for various stages of tunnel progress through the site.

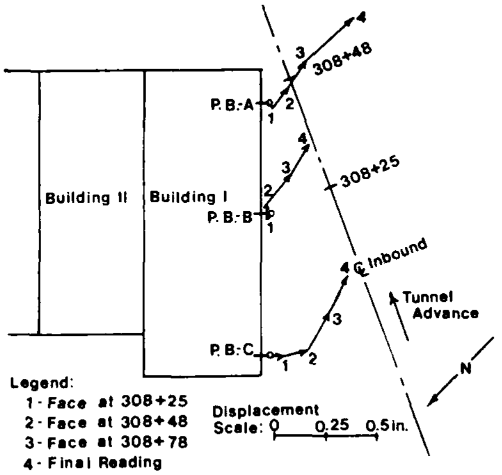

Fig. 12 Plumb Bob Data Summary

Both the distance of the wall from the centerline of the tunnel and the orientation of the wall with respect to the tunnel axis influence the tilt and its pattern of development. In this case the wall is oriented such that it cuts across the settlement trough so that the final tilt occurs both perpendicular to the building wall, toward the tunnel axis, and parallel to the building wall, toward the point where the wall is closest to the tunnel centerline (in this case in the direction of tunnel advance).

Changes in the width of the vertical joint forming the interface between Buildings I and II were monitored. Initially, the joint was approximately 1/8 to 3/16 in. wide. The joint opened an additional 1/8 to 3/8 in. in response to tunnel excavation as shown in Fig. 7. Comparison of joint separation with tape extensometer and plumb bob data indicate the data to be compatible.

DISCUSSION

The building distortion data was also used to study the development of the settlement trough. For example, the plot of the tape extensometer-measured displacements at Sta. 308+50 in Fig. 13 illustrates the behavior of the structure for various locations of the tunnel face.

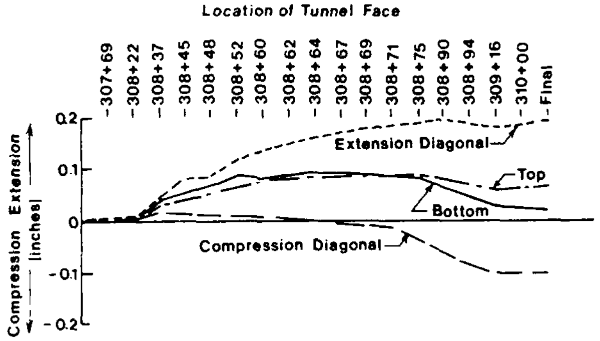

Fig. 13 Tape Extensometer Data Perpendicular to Tunnel Axis

Initially, as the tunnel heading approaches the station of the cross-section being monitored, only the wall nearer the tunnel displaces toward the tunnel to cause an increase in the distance between the bearing walls. During this early phase of the trough development the wall is in the zone of horizontal extension. The wall tilts, moves horizontally towards the tunnel, and settles slightly. As the tunnel heading passes by the station of the cross-section, the settlement trough widens and the wall is no longer in the zone of extension, but in the zone of compression. The horizontal movements are slight, yet the vertical movements are significant resulting in extension of one diagonal and compression of the other. Later, as the tunneling progresses the settlement trough continues to widen and the zone of extension begins to influence the next wall farther out causing it to displace horizontally toward the tunnel. The horizontal distance between the two walls now decreases while the diagonal distances remain constant. The increase in differential settlement between the bearing walls compensates somewhat for the decrease in horizontal distance, and the diagonal distances do not change.

The tape extensometer data for reference points located along the longitudinal axis of Building I, perpendicular to the tape extensometer lines described above, demonstrate the response of the structure to the transient settlement wave in the plane of the tunnel axis. In the vicinity of the tunnel heading, the longitudinal ground surface settlement profile exhibits zones of lateral tension and compression, an inflection point, and a point of maximum curvature similar to the typical surface settlement profile perpendicular to the tunnel axis. As the shield approaches a reference point, the ground moves horizontally toward the shield and the point is in the zone of lateral extension. Once the shield passes the point in question, the absolute horizontal motion is reversed as the ground continues to move toward the shield, but now the reference point is in the zone of lateral compression. Chronologically, the longitudinal span should first tend to extend horizontally, then compress horizontally, and finally extend again if the axis of the building is parallel to the axis of the tunnel. However, the change in a span during passage of the shield will vary somewhat depending upon orientation of the span relative to the tunnel axis and the ground conditions. The case shown in Fig. 14 exhibits this behavior.

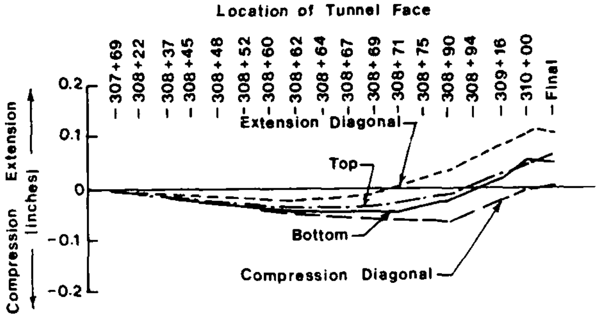

Fig. 14 Tape Extensometer Data Parallel to Tunnel Axis

In this case, the orientation of the building axis relative to the tunnel has negated the initial tendency for the span to sustain horizontal extension however, the latter two phases of horizontal compression and then horizontal extension are apparent. The net result of the horizontal measurements is extension which is at least in part, due to the orientation of the building axis with respect to the tunnel axis and the direction in which the tunnel excavation proceeded.

The resultant vectors of tilt, as shown by the plumb bobs, are toward the source of the ground loss causing the ground movement at that particular time. The tilt parallel to the plane of the wall is approximately the same as the slope of the building settlement profile along the wall. Whereas, the tilt perpendicular to the wall is approximately 1/3 of the slope of the transverse ground settlement profile at the wall. This suggests that the flooring system tends to provide some restraint of the rotation of the wall.

Movement of the first floor joists relative to the bearing surfaces was also monitored. The changes in bearing of the ends of four joists were observed. Overall changes indicated a decrease in bearing approximately corresponding to the lateral extension recorded at each location. However, the decrease in bearing was not the same at each end of a particular joist. Ends of joists bearing in masonry pockets tend to pull out when the span is in a state of extension, but when the span is compressed, the corresponding increase in bearing is restricted to the ends of the joists bearing on the central steel beam. This behavior was probably influenced by: the roughness of the masonry bearing surface relative to the steel-bearing surface and the tendency for debris to collect in the void created between the end of the joist and the back of the masonry pocket, thereby preventing the joist from slipping back into the masonry pocket.

SUMMARY AND CONCLUSIONS

This case study describes observed response of a pair of two-story, brick bearing wall structures above and adjacent to a pair of 21-ft-diameter tunnels in soil. Factors examined include horizontal and vertical ground displacements, horizontal and vertical building displacements, building tilting, building distortion, and building damage as summarized below.

The settlement trough that developed exhibited a typical concave shape, with a zone of lateral compression near the center of the trough and a convex profile (hogging) with lateral extensions in the outer portions of the trough. The longitudinal settlement wave preceding the tunnel excavation was similar in shape and magnitude to one side of the transverse settlement trough. The wave was transient and reversals of curvature of the ground surface settlement profile and horizontal ground movement movement parallel to the tunnel axis occurred.

The structures settled and strained laterally in compliance with the ground movements. The structures did not appear to restrain the ground movements to any significant extent. As a consequence, transient building distortions during development of the settlement trough were larger than the final distortions recorded. Locally, distortions during the development of the settlement trough may have been greater than the final distortions. Reversals of curvature are often induced in buildings as the settlement trough develops, and can cause greater overall distortion than the final measurements would indicate.

The final modes of deformation of the structures are directly related to the position of the structures relative to the settlement trough. Building I, located within the concave or bowl-shaped portion of the settlement trough, sustained primarily shear related deformation. The building width was approximately equal to 1/3 the half width of the settlement trough and so significant rigid body rotation of the building occurred. This resulted in an angular distortion of approximately one-half the average slope of the settlement trough beneath the building The lateral extension sustained by the building is small and most distortion was in the form of angular distortion. Building II is located on the convex portion of the settlement trough where lateral extension is a significant factor in causing building deformation. The convex profile causes a bending mode of distortion which, in turn, produces larger lateral extensions in the upper story.

Cracking and damage to Building I was minor. The cracking and increase in crack widths that did occur was not significant due to the poor initial condition of the structure. The cracking at the front of Building I can be attributed primarily to the angular distortion of the structure. Cracking and damage to Building II was caused primarily by lateral extension and its amplification in the upper story by the independent rigid body rotation of the bearing walls. Nearly all the lateral extension strain across the building was concentrated in one crack.

It is evident that both Building I and Building II experienced some damage in response to the nearby tunnel excavation. However, considering the initial states of these structures, the damage was very slight to slight. If the buildings were initially in good repair, the cracking damage would have been considered slight to moderate.

ACKNOWLEDGMENTS

Collection of these case history and field data was performed by the Department of Civil Engineering of the University of Illinois under sponsorship of the Office of the Secretary, and Urban Mass Transportation Administration, U. S. Department of Transportation (Contract Nos. DOT-OS-70024 and DOT-UT-80039). Support and assistance of WMATA in permitting the field observation program is acknowledged, as is the cooperation of Bechtel Associates, construction manager for Metro, and Traylor Brothers, the contractor.

REFERENCES

Boscardin, M. D. and E. J. Cording (1987). "Building Response to Excavation-Induced Settlement," submitted to Journal of the Geotechnical Division, ASCE.

Boscardin, M. D. (1980). "Building Response to Excavation-Induced Ground Movements," Ph.D. dissertation presented to the University of Illinois at Urbana-Champaign, Illinois.

Boscardin, M. D., E. J. Cording and T. D. O'Rourke (1978). Case Studies of Building Behavior in Response to Adjacent Excavation, Final report prepared by the University of Illinois for the U. S. Dept. of Transportation, Report No. UMTA-IL-06-0043-78-2.

MacPherson, H. H., J. W. Critchfield, S. W. Hong, and E. J. Cording (1978). Settlement Around Tunnels in Soils: Three Case Histories, Final report prepared by the University of Illinois for the U. S. Dept. of Transportation, Report No. UMTA-IL-06-0043-78-1.

Proceedings: Second International Conference on Case Histories in Geotechnical Engineering, June 1-5, 1988, St. Louis, Mo., Paper No. 5.32

Advances in the Construction and Design of Jet Grouting Methods in South America

Giorgio Guatteri
Chairman, Novatecna, Sao Paulo, Brasil

Antonio C. Doria
Project Manager, Novatecna, Sao Paulo, Brasil

Joseph L. Kauschinger
Assistant Professor, Tufts Univesity, Medford, Massachusetts

Edward B. Perry
Research Civil Engineer, U.S. Army Engineer Waterways Experiment Station, Vicksburg, Mississippi

SYNOPSIS: This paper presents a brief historical development of the two most popular jet grouting methods used in South America, namely, the chemical churning pile method (CCP) and jumbo jet grouting. Advantages and limitations of each procedure are cited. A brief discussion follows covering the history of CCP jet grouting in South America. Field trials performed to improve the design methodology and construction of CCP and jumbo jet grouted columns are presented. Finally, three case histories are presented to illustrate the use of jumbo jet grouting where limited head room exists, jet grouting in close proximity to pile supported structures, formation of a diaphragm wall in gravelly soil with boulders. The paper closes with a short discussion of a recent tunnel project in which horizontal jet grouting is used as the temporary tunnel support.

INTRODUCTION:

Jet grouting is a general term describing a construction method which utilizes a high speed fluid to cut, replace, and then mix the native soil with a cementing material. The high velocity jet stream is developed by using high pressure pumps, which eject the fluid through relatively large nozzles or injectors, 2 to 4 mm in diameter. The most important feature of jet grouting, when compared to injection or permeation grouting, is that jetting allows the cementing medium to be uniformly mixed with a wide range of soils, i.e. sands and gravel or even hard clayey soils. Other general advantages of jet grouting include: little ground heave when compared to the volume of soil stabilized; relatively high compressive soilcrete strengths; treatment can begin at most practical depths and can be terminated below the ground surface (Yahiro,1973; Miki 1984).

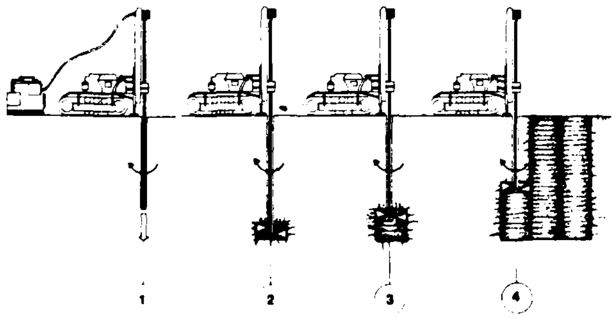

Figure 1 Sequence to Construct a CCP Column
1 - Drilling Guide Hole
2 - CCP Jet Grouting
3 - Lifting and Rotation
4 - Completion and Repetition

At present there are about eight different construction techniques which can be classified as jet grouting methods, with about four or five predominate ones (Miki 1984; Yahiro 1982; Bruce 1987). The diversity in the number of jet grouting methods arises because of the many factors which go into the jet grouting process. Each method has its own advantages and limitations and each should be considered for use in light of their individual characteristics. The two jet grouting methods primarily used in South America, chemical churning pile (CCP) and jumbo grout are discussed more fulling in this paper.

EARLY DEVELOPMENTS OF JET GROUTING:

The chemical churning pile (CCP) method of jet grouting was one of the first forms of jet grouting developed in Japan during the early 1970's by Nakanishi (Miki 1984). The technique utilizes a water-cement grout as the jetting medium which is injected into the soil at high velocities through an injector located at the bottom of a single drill rod. The installation sequence is schematically represented in Figure 1, where it can be seen that: first a guide hole is drilled or jetted; followed by jet grouting which involves both lifting and rotating the single rod while injecting grout. A pile-like, soil-cement (soilcrete) column is formed, which may be interconnected to form a wall.

Most of the early work conducted using CCP jet grouting was performed using chemicals, thus arose the tradename, chemical churning pile (CCP). However, due to environmental concerns, most CCP work today is conducted using a water-cement grout as the cutting and cementing fluid. In 1973, an Italian contractor, Romano Colla, was the first to form CCP columns using ultra-high pressures (5000 psi.) and high flow rates (100 to 250 l./min.) through two rather large injectors (1.8 to 2.4 mm diameter). The CCP technique originally proposed by Nakanishi and later modified by Colla is the CCP jet grouting method presently used in South America by Novatecna.

Experiments conducted in Japan (Yahiro 1973, 1974) indicated that the soil cutting efficiency of a high velocity jet stream could be improved by encapsulating the jet stream within a cone of compressed air, travelling at the speed of sound. Nakanishi modified the CCP method to take advantage of compressed air, and developed jumbo special grout (JSG), which involves simultaneous injection of high speed water-cement grout and compressed air. Injecting two fluids separately into the soil requires a more complex double rod system when compared to CCP jet grouting. In South America JSG is called jumbo jet grouting.

CCP's major advantage over jumbo grout and other jet grouting methods is the simplicity of the single rod system used to jet grout, and therefore, ease with which the single rods can be uncoupled when jet grouting in limited headroom situations. The compressive strength of the soilcrete formed during CCP jet grouting is usually greater than the soilcrete formed during jumbo grouting. The reason is primarily related to the compressed air being trapped within the soilcrete mass formed during jumbo grouting. However, the typical size of a jumbo column is very large, up to 1.9 meters in sands and 1.3 meters in clay, which are at least twice the size of CCP column formed under comparable conditions. Furthermore, the increase in size of the jumbo soilcrete body can be achieved by using lower jetting pressures (3500 - 4500 psi), thus reducing wear to the high pressure pumps. Finally, the cost per unit volume of stabilized soil is generally less expensive when using jumbo jet grouting. The jumbo jet grout method is very popular today in South America and used by Novatecna for a wide range of applications.

JET GROUTING DEVELOPMENTS IN SOUTH AMERICA:

CCP jet grouting was first introduced in South America in 1980 by Novatecna Construction Ltd. of Sao Paulo, Brasil. Jet grouting was rapidly accepted in Brasil because this technique was better suited to grouting the silty and clayey soils of coastal Brasil than conventional methods. Furthermore, the CCP method was initially utilized in Brasil because of the relative simplicity of the rod system used to jet grout.

The first CCP jet grouting job performed in South America was in July 1980 for the Sao Paulo water and sanitation department, (SABESP), and involved the repair of a collapsed tunnel crown for the Sanegran Interceptor Tunnel. The stratigraphy at the site is depicted in Figure 2, and is essentially silty clay in the upper 10 meters, underlain by 4 meters of fine to medium sand with some clay, and then 1.5 meters of fractured gneiss, underlain by sound gneiss. The water table was about 3 meters below the ground surface. The failure surface depicted in this figure developed while blasting rock in a mixed face section (rock/soil) of the tunnel, leading to collapse of the tunnel crown, which caused a 10 meter diameter dish shape depression to form at the surface (Guatteri, et.al. 1986).

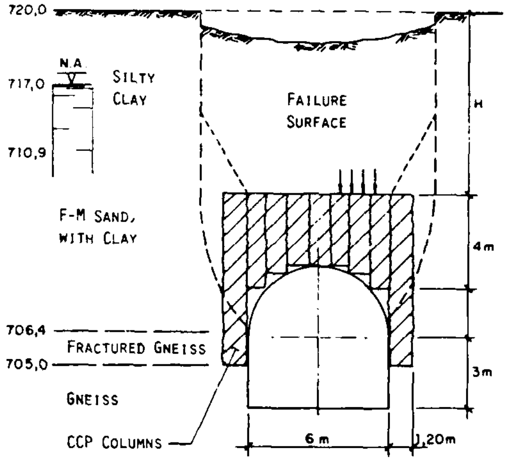

Figure 2 Profile of Sanegran Tunnel Collapse and Typical CCP Repair

The depression was filled with sand and jet grouting initiated. Problems developed when the columns were formed because the loose sand and fill began to slide into the unhardened jet grout columns leading to further lose of soil at the surface and sinking of the jet grout drill rig. A steel support system was erected across the hole and work progressed smoothly. The jetting parameters used to form the 0.75 meter diameter CCP columns listed in Table I, are typical of the jetting parameters used for CCP jet grouting in South America. It took about 60 days to form the 4.5 meter thick soilcrete arch pictured in Figure 2, which consisted of 490 CCP columns.

TABLE I CCP Jet Grouting Parameters For Repair of Sanegran Tunnel

Pressure	(psi)	5300
Rotation Rate	(rpm)	18
Injectors		
diameter	(mm)	1.8
number		2
Lifting Speed	(min/m)	4.2
Grout		
injection rate	(l/min)	63
water : cement ratio		1 to 1
cement consumption	(kg/m)	200
Average Column Size	(m)	0.75

The soil along the 12 km Sanegran Tunnel was variable and susceptible to future collapses. Therefore, SABESP decided to performed additional jet grouting work. During the two years of jet grouting for the Sanegran Tunnel, jet grouting was utilized at 10 problem sections: to repair a second tunnel collapse due to lose of compressed air, and to consolidate soft silty clay fill by forming a soilcrete vault prior to advancing the tunnel shield. Tunnelling progressed smoothly mostly due to using about 70,000 meter of CCP columns to stabilize soft ground prior to advance of the tunnel.

Other early CCP projects performed in South America (Novatecna 1987; Guatteri 1984; Nicolls 1985) include: construction of diaphragm walls and floors for unbraced retaining structures (Mercedes Benz , Dalmine Siderca); deep shafts for a pump station at Capivari reservoir; cutoffs for earth dams (Porto Primavera and Edgard de Souza Dams); underpinning (Sao Paulo iron works); slope stabilization (San Clemente, California). Since the introduction of CCP jet grouting in South America, Novatecna has formed about 130,000 meters of CCP columns.

CCP FIELD TRIALS:

One of the drawbacks of jet grouting is related to the lack of information about the variation of the column diameter while jetting. Now there are no practical methods for measuring the change in the column's diameter with depth. The size of a jet grout column is usually estimated by reliance upon past experience or field trials. In 1982 Novatecna undertook extensive CCP field trials to examine how various drilling parameters interact with different soil types to produce a certain sized column.

The drilling parameters which have the greatest influence upon the formation of CCP columns, include:

- outlet pressure at the nozzle
- size and efficiency of the injector
- number and spacing of injectors
- flow rate of cement grout
- lifting speed of the drill rods
- lifting increment per step
- rpm's of the drill rods

With the exception of soil type, the most important parameter influencing the formation of jet grouted columns is the outlet pressure. If the pressure is not large enough the jet stream will not develop sufficient velocity to cut the soil. Data from the literature (Miki 1984) indicates that for most soils a pump pressure of about 40 MPa (5800 psi) is needed for effective cutting. The size and number of the injectors used is dictated by the capacity of the pump and horsepower of the engine. The injector size, and therefore grout flow rate, are selected so that enough fluid mass is injected to cut the soil and also provide enough cement to satisfy the design compressive strength. It was not the intent of the CCP field study to obtain the optimum combination of the above list of drilling parameters, but rather, understand how a single drilling parameter could be used to control the size and economy of forming CCP columns. Therefore, it was decided to examine what influence the lifting speed had upon the size of CCP columns formed in three soil types. However, since the lifting speed is only an indicator of the amount of time which the jet stream cuts the soil, it was decided for discussion purposes to also use the terms jet impact time and rod revolutions per step. The jet impact time is equal to the product of the lifting speed, lift increment per step, and number of nozzles. The jet impact time has units of time/step. The rod revolutions per step is the product of lifting speed, lift increment per step, and rod revolution rate.

The three soils selected for the CCP field tests were sedimentary soils commonly found in the Sao Paulo area, and included: sands, silty clay, and an organic clay obtained from the Sanegran Tunnel excavation. Three pits 10 X 10 X 5 meters deep were excavated into the bank of the Tiete River above the tide line. All materials were end dumped from a truck into their respective pit and compacted using either a D6 dozer or Cat 966 rubber wheeled front end loader. The highly plastic (LL = 60, PI = 40), soft organic clay was placed at its natural water content in 30 cm. lifts and compacted. The silty clay and sand were compacted in a wet state. The in-place unit weights of the silty clay and sand were 102 and 113 pcf, respectively.

Twenty CCP columns were formed in each pit. All sixty columns were made using the same nozzle pressure, rotation rate, size and number of injectors, water-cement ratio and grout injection rate as specified below in Table II. Within each pit 10 columns were drilled using a lifting speed of 2.9 min./m. and then another 10 were formed using twice that lifting speed, and twice the amount of cement.

Table II Drilling Parameters Used During CCP Field Trials in Sao Paulo

A). Constant Parameters		
Pressure	(psi)	4200
Rotation Rate	(rpm)	18
Injectors		
diameter	(mm)	2.2
number		2
Grout		
water:cement ratio		1 to 1
injection rate	(l/min)	91
B). Variable Parameters		
Lift speed #1	(min/m)	2.9
Rod revolutions/step		2
Jet impact time/step	(sec/step)	14
Cement Consumption	(kg/m)	200
Lift speed #2	(min/m)	5.8
Rod revolutions/step		4
Jet impact time/step	(sec/step)	26
Cement Consumption	(kg/m)	400

The measured size of the CCP columns and average compressive strengths of the soilcrete are summarized below in Table III. The sand compressive strengths reported in Table III are based upon past experience with this material, and were not measured from columns formed during the CCP field trials. However, all other strengths recorded were obtained from soilcrete specimens formed during the field trials.

Table III Results From CCP Field Trials

Soil Type	Lifting Speed min/meter	Column Diameter cm	Average Compressive Strength kg/cm^2
clay	2.9	55 to 60	20
clay	5.8	65 to 70	40
silty clay	2.9	65 to 70	50
silty clay	5.8	75 to 80	70
sand	2.9	75 to 80	80
sand	5.8	85 to 90	120

The data obtained during the CCP field trials supports the following observations:

1). Doubling the jet impact time from 14 to 26 seconds does not have a significant influence upon the size of any CCP column formed. Doubling the jetting time resulted in 15% to 25% increase in the diameter of CCP columns. It appears that most of the cutting action of the water-cement jet is expended during the first two revolutions of the drill pipe.

2). The compressive strength for all soils was significantly increased by doubling the jet impact time, allowing double the weight of cement to be injected per meter of column. The increase in strength was double for the organic clay and about a 50% increase for the silty clay and sand.

3). The soil type played a significant role in determining the size of CCP column formed, and could account for up to 50% of the difference in the sizes of columns. As the amount of clay in the soil increases the columns decrease in size. As shown in Table III, the smallest columns when formed in the organic clay (0.55 to 0.60 m.), intermediate sized in silty clay (0.65 to 70 m.), and largest in sand (0.85 to 0.90 m.).

4). Finally, soilcrete made by mixing 1 to 1 water:cement grout with sand results in compressive strengths (80 kg/cm^2) about four times greater than comparable grout mixes in clay, with the lowest clay strength being about 20 kg/cm^2.

JUMBO GROUT FIELD TRIALS

The diversity of applications of jet grouting produced a need for larger diameter columns than those produced using the CCP process. When constructing a continuous wall a large part of the cost is associated with drilling guide holes prior to jetting. With CCP columns the interaxes spacing between columns is rather close, about 0.50 m, which results in many guide holes to create a wall. Interaxes spacing for jumbo columns is about 1.2 to 1.4 meters, which requires about half the guide holes needed for a comparable CCP wall.

The jumbo grout field trials were conducted in four phases over a period of 9 months, between April to December 1984. The first two phases were performed to understand the role lifting speed played in the formation of jumbo columns in cohesive soils. Phase three consisted of forming jumbo columns in sands, and in the last phase jumbo grout panels were made. At present panel walls represent a provisional method of wall construction, and only the results from the column studies will be discussed in the following sections.

The jumbo grout field trials were conducted in large pits (30 X 6 X 5 meters deep), excavated in the banks of the Tiete River in the vicinity of the original CCP field trials. During phase I and II the same soil type was used, and was typically silty clay, with about 20 to 30% fine sand. The top 1.5 meters of the fill was medium to stiff in consistency and was soft below 1.5 m to the bottom of the pit. The sand used during phase III tests was a fine uniform sand which was placed moist and in a loose state.

All jumbo grout columns were formed using a nozzle pressure of 3000 psi and a single 3.0 mm injector, as listed in Table IV. The double drill rods were rotated at about 18 rpm's, and the air cone was delivered at 4 m^3/min at 100 psi. The 1:1 water:cement grout was injected at about 70 l/min.

Twenty-two jumbo columns were formed during phase I. The only variable changed was the lifting speed, and as indicated in Table IV, the speeds varied between 1.6 and 3 min./m. The fastest lifting speed was selected to insure that at least one full revolution of the drill pipe occurred before moving the jet to a higher elevation. Excavation of all 22 columns revealed nonhomogeneous, poorly cemented cylindrical bodies, with measured diameters between 1.8 and 2.0 meters.

The solution to the nonhomogeneity of the soilcrete body was to either use more than one jet, or jet longer. It was decided to investigate how extremely long jetting times, using one injector, influence the size and strength of jumbo columns. Therefore, during phase II 6 columns were formed using two very long lifting times, 12 and 18 min/m.

The results from the phase II studies showed that no significant size increase resulted in jetting 4 to 6 times longer at a particular elevation; phase II columns were still about the same size as the phase I columns. However, the phase II soilcrete bodies were much stronger and more homogeneous than phase I.

Table IV Drilling Parameters Used During Jumbo Field Trials in Sao Paulo

A). Constant Parameters		
Pressure	(psi)	3000
Rotation Rate	(rpm)	18
Injectors		
diameter	(mm)	3.0
number		1
Grout		
water:cement ratio		1 to 1
injection rate	(l/min)	70
Compressed Air		
pressure	(psi)	100
flow rate	(m^3/min)	4
B) Phase I Clayey Silt		**22 columns**
Lift speed #1	(min/m)	1.6
Rod revolutions/step		1.1
Jet impact time/step	(sec/step)	3.8
Cement Consumption	(kg/m)	90
Lift speed #2	(min/m)	1.8
Rod revolutions/step		1.3
Jet impact time/step	(sec/step)	4.2
Cement Consumption	(kg/m)	100
Lift speed #3	(min/m)	2.0
Rod revolutions/step		1.4
Jet impact time/step	(sec/step)	4.8
Cement Consumption	(kg/m)	115
Lift speed #4	(min/m)	3.0
Rod revolutions/step		2.2
Jet impact time/step	(sec/step)	7.2
Cement Consumption	(kg/m)	175
C). Phase II: Clayey Silt		**6 columns**
Lift speed #1	(min/m)	12
Rod revolutions/step		8.6
Jet impact time/step	(sec/step)	28.8
Cement Consumption	(kg/m)	600
Lift speed #2	(min/m)	18.0
Rod revolutions/step		13.0
Jet impact time/step	(sec/step)	43.2
Cement Consumption	(kg/m)	900
D) Phase III Sand		**2 columns**
Lift speed #1	(min/m)	12
Rod revolutions/step		8.6
Jet impact time/step	(sec/step)	28.8
Cement Consumption	(kg/m)	600

A total of 122 six inch high specimens were cut from the Phase II columns formed using 12 min/meter lifting speed. Samples were cut from the upper, middle, and lower third of the soilcrete body and were allowed to cure for 30 and 60 days. Both unconfined compressive and Brazilian tensile tests were performed. The results are summarized in Table V, where it can be observed that the 30 day compressive strengths vary between 25 kg/cm^2 at the top of the column and decrease to 14.2 kg^2/cm near the bottom of the column. After 60 days of curing the column tends to have a more uniform strength over its length, whereby the lower portion of the column has experienced a 40% increase in compressive strength between 30 and 60 days. The results from the tensile strength tests are inconsistent. The tensile strength in the upper and middle portion of the columns tend to decrease with age, while the tensile strength in the lower third of the columns increase with age. This inconsistency is believed to be due to testing a small number (6 samples) of specimens from each location at 30 days.

Table V Average Compressive and Brazilian Strengths Obtained From Phase II Jumbo Columns

Column Portion Tested	Average Compressive Strength kg/cm^2				Average Brazilian Strength kg/cm^2			
	N*	30 Day	N*	60 Day	N*	30 Day	N*	60 Day
Upper	7	25.0	12	30.9	6	5.6	9	4.5
Middle	12	19.4	8	22.8	6	7.2	20	3.8
Lower	12	14.2	9	20.3	6	3.0	15	4.1

*: N represents number of samples tested

A more comprehensive set of strength data has been reported by Guatteri and Teixeira (1987). The results from their study indicates that the average tensile strength of a jumbo column, formed in a wide variety of soils, increases with time and is about 10 to 15% of the average compressive strength.

Two jumbo columns were made in a loose sand during phase III, as a reference to compare to columns made in cohesive soils. Both columns were drilled using lifting times of 12 min/m. and resulted in extremely uniform (1.9 to 2.0 meter), and slightly larger columns than formed in cohesive soil. However, the sand soilcrete strength was significantly higher than in clay, which is consistent with the results from the CCP field trials.

The results from phase I and II tests indicate that the high speed water-cement jet quickly cuts the soil at a particular elevation, and only takes about 2 revolutions (5 to 7 seconds jet impact time) of the drill pipe to form the column. However, this amount of time does not allow enough cement to be injected, nor is it sufficient time for the jet stream to properly mix the cut soil with the injected cement.

JUMBO GROUT CASE HISTORIES:

One criticism leveled against jet grouting is that due to the relatively low tensile strength of soilcrete, jet grouting is not a cost effective nor technically viable scheme for constructing unbraced earth retaining structures. Although this statement may be true for very deep walls, the use of jumbo grout to form retaining structures for depths up to about 6 meters is not only technically viable, but cost competitive with other construction methods. To illustrate this viability and robustness of jet grouting, three case histories are presented, where jumbo grout was used to construct diaphragm walls for both temporary support of the soil during construction and also as the final wall. Typically, a 15 cm. thick, lightly reinforced concrete wall is placed over the soilcrete wall for protection against the elements and also to create an architecturally pleasing surface. Other important aspects of jet grouting illustrated by the selected case studies included: importance of pre-jetting to eliminate possible high pressures from developing during jetting, applicability of using jumbo grout in limited head room situations, and lastly feasibility of using jumbo grout in soils containing cobbles and large boulders.

RINCAO CHANNEL, SAO PAULO CITY

Sao Paulo City wanted to construct a trapezoidal water channel to convey runoff to the Rio Tiete. A 40 meter long section of the concrete channel had to go beneath a 19 meter wide viaduct at Rincao. The soil beneath the overpass consisted of about 5 meters of soft silty clay, 15 meters of fine to medium sand with some clay, and then a second clay layer. The soil profile for the first 10 meters is shown in Figure 3c, which is about the depth of the jumbo columns used to form the wall, shown in cross section in Figure 3b. The water table was located about 1.5 meters down from the surface. Due to hydraulic considerations for open channel flow, the bottom of the channel had to be one meter within the fine to medium sand layer. Due to the limited overhead clearance under the viaduct and the flexibility of using jet grouting to make both the walls and bottom plug of the channel, city engineers decided to use jet grouting to construct a U shaped channel. The transition between the trapezoidal and U shaped channels was done with a traditional soil bentonite slurry trench which was keyed into the second clay layer located 15 meters below the surface, which was the primary reason for not using a conventional diaphragm wall to construct the walls of the channel.

The jet grouted channel was 40 meters long by 9.50 meters wide, by about 5 meters deep, as illustrated in the general plan view and channel cross section A - A drawn in Figure 3a and 3b. There were a total of 60 columns, each 9 meters long, jet grouted in a single row to make the two walls of the channel. All jumbo columns were about 1.6 meters in diameter and spaced about 1.3 meters apart. The 2 meter thick bottom plug consisted of 207 columns. About 80% of the channel was constructed beneath the 19 meter wide viaduct, shown in the general cross section B - B of Figure 3d, with only 3 meters of headroom.

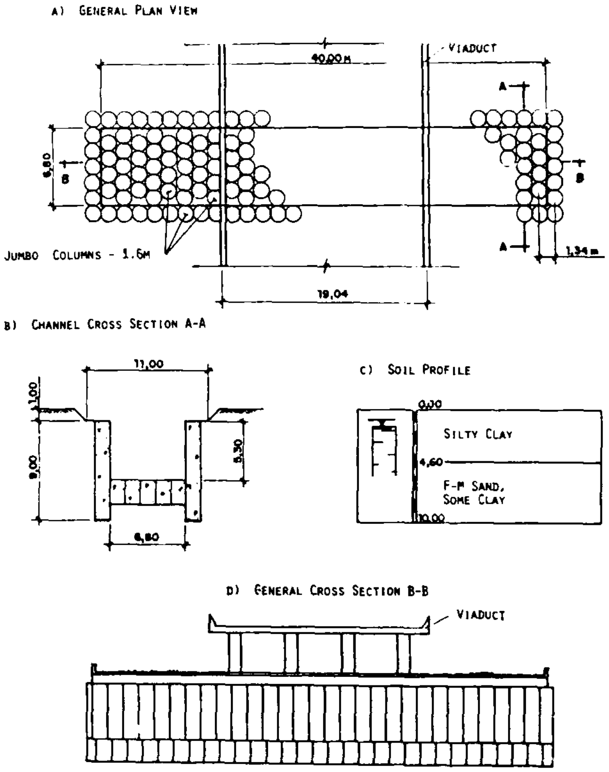

Figure 3 General Cross Section and Profile of Rincao Channel, Sao Paulo City

All columns at Rincao were jetted using 3000 psi pressure with a 1 to 1 water:cement grout, injected through a single 3.0 mm injector, as indicated in Table VI. Half of the wall columns were in sand and half in clay. Two different lifting speeds were used with the slower speed being in the clay so that the wall columns would be able to achieve the design strength of 30 kg/cm^2 in the clay portion of the columns. The plug was located only in sand, and the design strength of 100 kg/cm^2 could be achieved using a lifting speed of 5.5 min/meter.

There were three major concerns expressed by city engineers during construction of the Rincao channel. The first was related to the possibility of causing distress to the viaduct when jetting with high pressures within two meters of the pile foundation supporting the viaduct. Secondly, if the jet grouted wall had windows in the vicinity of the piles, water and sand could flow into the channel, thus undermining the viaduct's foundation. Finally, because the jet grouting work progressed rapidly, the city wanted to excavate the soil from the interior of the channel only after 30 days and not wait for the soilcrete to cure the originally planned 60 days. A low strength jet grout wall near the piles might cause excessive deflection of the viaduct. Due to time constraints it was decided to excavate the soil from inside the jet grout wall after

30 days. Visual observations showed that there were no distressful movements of the viaduct when either jet grouting with high pressures, or wall movements when removing the soil.

TABLE VI Jet Grouting Parameters Used To Form Jumbo Columns at Rincao

Pressure	(psi)	3000
Rotation Rate	(rpm)	18
Injectors		
diameter	(mm)	3.0
number		1
Grout		
injection rate	(l/min)	120
water : cement ratio		1 to 1
Compressed Air		
pressure	(psi)	100
injection rate	(m^3/min)	4
Lifting Speed		
clay	(min/m)	8.8
sand	(min/m)	5.5
Cement Consumption		
clay	(kg/m)	800
sand	(kg/m)	500
Average Column Size	(m)	1.6

The Rincao jet grout wall was not internally reinforced nor was bracing used to support the excavation. For approximately one week the wall was standing free for a height of 5 meters. Furthermore, excavation of the interior soil from the channel revealed a tight, waterproof barrier formed by the jumbo grout columns in the wall and plug of the channel. The channel was then lined with a 15 cm. thick, lightly reinforced concrete covering for erosion protection. The project finished one month ahead of schedule.

GENERAL MOTORS STAMPING MILL PIT:

General Motor of Brazil wanted to expand their manufacturing capabilities by building ten new auto body stamping mills. The mills were to be placed at the bottom of a long, narrow pit (68 X 9.7 X 6.5 meters deep). GM also required that the steel plate stock for the stamped parts be stockpiled along side the pit, which would induce a surcharge loading of about 20 tons/m^2. The lateral force induced by the surcharge would be about twice that imposed by the soil forces. The soil profile at the site is shown in Figure 4c, and consisted of fill in the top 2.5 meters, underlain by alternating layers of silty clay and sand, with the water table about 2 meters below the bottom of the jet grout columns. A diaphragm wall with tie backs was rejected as a solution primarily because the tie backs would have to infringe upon land which GM wanted to conserve for future expansion. Therefore, a single row of unreinforced and unbraced jumbo grout columns was used as the earth retention system. However, toe support of the wall was supplied by 3 meter thick soilcrete struts spaced about 4 meters apart, which are shown in the general plan view of Figure 4a and pit cross section of Figure 4b. The general plan view of the jet grout wall was symmetric about the center line shown in Figure 4a, and only half the general plan view is shown in this figure. The surcharge loads were supported by clusters of columns formed around the perimeter of the pit and arranged as shown in Figure 4a and b.

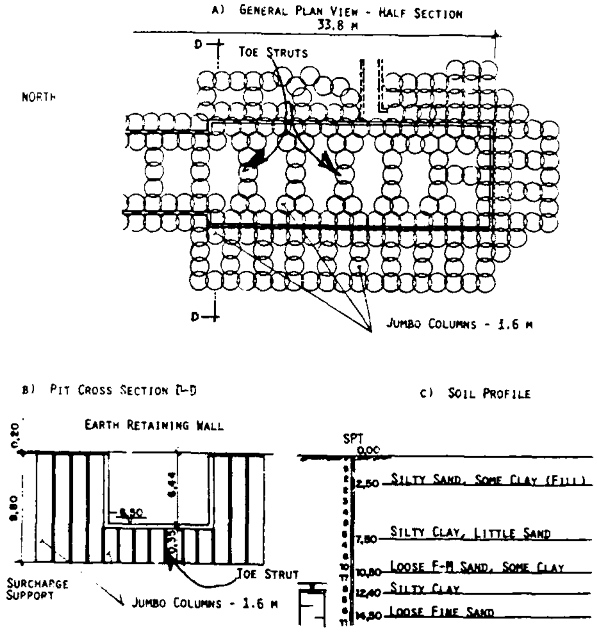

Figure 4 General Plan and Profile of General Motors Stamping Mill Pit

A major concern expressed by GM engineers was related to the effect which the high jetting pressures would have upon the foundation of an existing building, which was only two meters away from the jumbo columns used to support the surcharge along the north side of the pit, upper portion of wall shown in Figure 4a. If sufficient grout flow was not communicated to the surface, then there existed the possibility of building-up very high pore pressures in the sub-soil. The pore pressure build-up could cause distress to the foundation of the adjacent building. Therefore, during this project all the jumbo columns used to support the surcharge along the north side of the excavation were pre-jetted with a special bit so that a 10 inch diameter hole would be created, which would assure pressure relief in the borehole. Furthermore, all surcharge support columns were jetted using relatively low pressures (3500 psi), and rapid lifting speeds (2.2 min/m). Due to the silty nature of the subsoils at the site and need to create large (1.6 meters), strong, soilcrete columns prejetting only water was used to form all columns at the GM pit, as listed in Table VII.

There were three different sets of jetting parameters used to construct the jumbo grout columns in the GM pit. The single row of wall columns were made using the highest nozzle pressures (5200 psi) and slowest lifting speeds during pre-jetting and jetting, 4.4 and 7.2 min/meter, respectively. About 600 kg/meter of cement were injected through the 3.4 mm injector, using a 1:1 water-cement grout. As expected the wall columns were the largest formed, averaging 1.8 meters in diameter. The drilling parameters used for the surcharge support columns and soilcrete struts at the bottom of the excavation were selected to insure a minimum column diameter of 1.6 meters. There were a total of 509 jumbo columns made, totaling 3566 meters. Jetting of all columns was discontinued 0.2 meters below the surface.

TABLE VII Jet Grouting Parameters Used For General Motors Stamping Mill Pit

Pressure (psi)	
wall	5200
toe struts	4000
surcharge support	3500
Rotation Rate	18
Injector	
diameter (mm)	3.4
number	1
Grout	
injection rate (l/min)	
wall	111
toe & surcharge support	103
water : cement ratio	
wall & surcharge support	1 to 1
toe struts	0.8 to 1
Compressed Air	
pressure (psi)	100
injection rate (m^3/min)	4
Cement Consumption (kg/m)	
wall	600
toe struts	400
surcharge support	600
Lifting Speed (min/m)	
wall	
pre-jet water	4.4
jet grout	7.2
toe struts	
pre-jet water	3.3
jet grout	4.4
surcharge support	
pre-jet water	2.2
jet grout	7.7
Average Column Size (m)	
wall columns	1.8
toe & surcharge support	1.6

After the GM pit was excavated down to its full depth of 6.5 meters, a 75 ton Linkbelt crane was used to place a steel frame for the building which housed the pit. A photograph of the fully excavated pit and crane, shown in the background, are pictured in Figure 5. Although the crane moved around the entire excavation, typically only one meter from the edge of the wall, no visual movements of the wall occurred. The jet grout wall system has functioned well, and in July 1987 GM was placing a 15 cm. concrete covering over the wall.

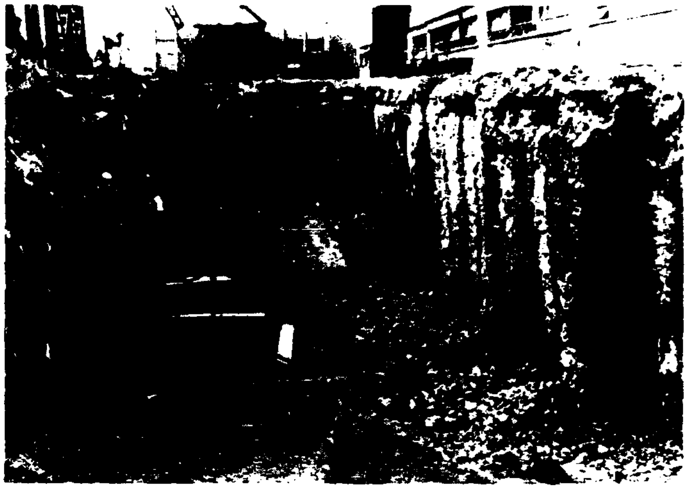

Figure 5 Photograph Showing General View of Excavation For General Motors Pit

PETROBRAS WASTE DISPOSAL PITS

In early 1986, Petrobras, the Brasilian national oil company, wanted to improve their re-cycling and disposal of waste products created during crude oil refinement at their Cubatao installation. The project required soil stabilization beneath a large oil storage silo, along with the excavation for two large waste storage pits (P-3915 and P-3921) and a smaller service pit. Jet grouting was selected because soil stabilization beneath the oil silo and the earth retention system for the pits could be constructed using the same equipment. Furthermore, the site was strewn with boulders and it would have been very difficult to form a diaphragm panel wall. Also the bottom of the excavation needed to be sealed to prevent groundwater intrusion, which was also accomplished using jet grouting.

The soil profile for the largest pit (P-3921) is shown in Figure 6c, and consisted of about 5 meters of silty clay fill, containing several large boulders in the top one meter. Under the fill was three meters of loose, fine gray sand, which formed the bearing stratum for pit P-3921. Beneath the fine gray sand was another sand layer and then over 7 meters of soft, dark organic clay. The ground water table was about 3 meters down from the surface. The soil stratigraphy for the second pit, P-3915, was essentially the same as that just described for pit P-3921. However, in the case of pit P-3915 there were many more boulders in the top 3 meters of fill. The rocks ranged in size from 15 cm. cobbles to 3 meter boulders up to half a meter thick, which can be see in the close-up photograph contained in Figure 7. The wall shown in this photograph is about 3.5 meter deep, and had to be excavated by hand

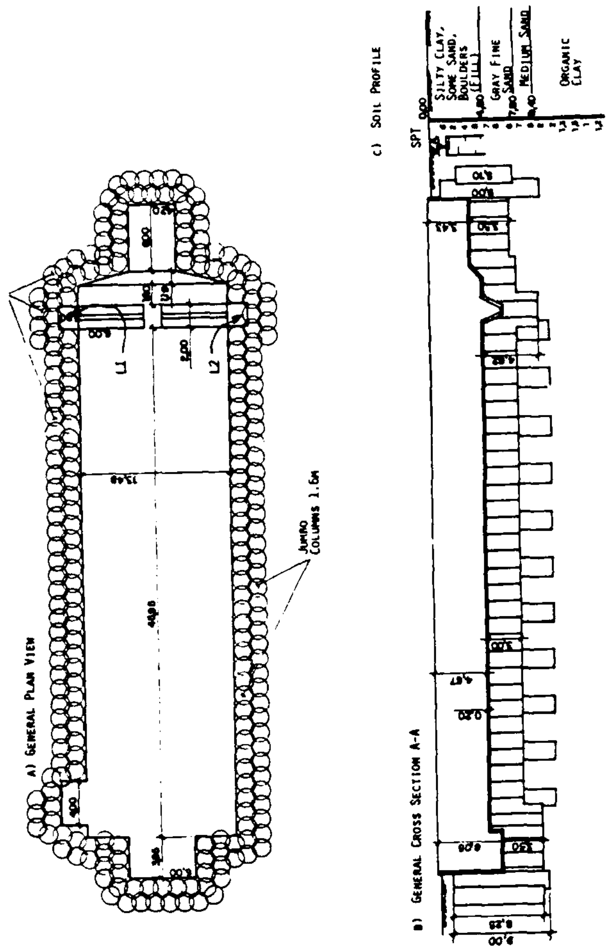

Figure 6 General Plan View and Profile of Petrobras Waste Pit P-3921

Figure 7 Photograph of Large Boulder Jet Grouted Into Wall of Pit P-3915

Jet grouting work commenced in November 1986, utilizing a single Haliburton T10 pump and a Novatecna rotator-extractor drill rig. A large single injector (3.8 mm diameter) was used to create the jumbo grout columns. This is about the largest injector that can be used with a T10 pump and still deliver 140 l/min of grout at 4000 psi, which were the highest flow rates and pressures utilized during the formation of the diaphragm wall for pit P-3921, as listed in Table VIII. Pit P-3921 had the longest free cantilevered length of unreinforced wall (6.1 meters), and therefore, required the greatest compressive and tensile strength. It was decided to inject a relatively large volume of cement (800 kg/meter of column) by injecting grout at 140 l/min and lifting the jet grouting monitor slowly (7.4 min/meter).

TABLE VIII Jet Grouting Parameters For Petrobras Waste Pits

Pressure	(psi)	
Pit P-3915		3500
Pit P-3921		4000
Bottom Plugs		3500
Rotation Rate		18
Injector		
diameter	(mm)	3.8
number		1
Grout		
injection rate	(l/min)	
P-3915		130
P-3921 & Bottom Plug		140
water : cement ratio		
P-3915		0.8 to 1
P-3921		1 to 1
Bottom Plug		1.2 to 1
Compressed Air		
pressure	(psi)	100
injection rate	(m^3/min)	4
Cement Consumption	(kg/m)	
P-3915		700
P-3921		800
Bottom Plugs		550
Lifting Speed	(min/m)	
P-3915		
pre-jet water		3.3
jet grout		6.0
P-3921		
jet grout		7.4
Bottom Plugs		
jet grout		6.0
Average Column Size	(m)	1.6

The bottom plugs for the two pits and walls for pit P-3915 were jetted using the same nozzle pressure (3500 psi) and lifting speed (6 min/m). However, the amount of cement injected for each structure was varied by changing the grout injection rate, with the lowest for the bottom plugs, 130 l/min, which resulted in 550 kg cement per meter of column being injected for a 1.2:1 water cement ratio.

The Petrobras waste pits were the most difficult jet grouting job done by Novatecna up to now because of the relatively high water table and long unsupported length of unreinforced wall. The section modulus of the wall needed to produce an acceptably low tensile stress along the backside of the wall required the formation of a double row of jumbo grout columns, which produced walls about 3 meters in thickness. The largest pit P-3921 was about 46 meters long by 13.5 meters wide, as illustrated in the plan view contained in Figure 6a. The wall for this pit required about 170 jumbo columns, each over 1.6 meters in diameter and spaced 1.3 meters center-to-center. A total of about 330 jumbo columns were used to form the 3 meter thick plug at the bottom of the excavation for pit P-3921, shown in the profile of Figure 6b.

When the soil was excavated from inside pit P-3921 two small leaks developed carrying fine gray sand into the excavation at points L1 and L2 marked on Figure 6a. The relatively high velocity of water inflow made it impossible to seal the leaks using jet grouting. The inflow of water was stopped by building two small brick walls around each leak and then allowing the water to rise inside of the well, thus equalizing the water level inside and outside the excavation. Thereafter, conventional tube-a-machette grouting was used to seal the leak. Several factors could have lead to the leak developing through the plug of pit P-3921. First, the interaxes spacing of 1.3 meters could have been too large, causing small or no overlap of the columns in this area. Secondly, during excavation of the soil inside the pit, the backhoe could have jarred the columns and caused them to separate. Most likely it was a combination of the two effects

The 2198 meters of columns for pit P-3915 were constructed in 41 days, using one rig working 10 hours per day, six days per week. The construction of the largest pit, P-3921, took 50 days working a similar shift. The entire jet grouting project was completed in May 1987, about six months after the start of the project.

CURRENT JET GROUTING WORK IN SOUTH AMERICA

The town of Campinas, approximately 50 km North of Sao Paulo, is presently constructing a twin 16 meter diameter tunnel. The support system for the twin tunnels are being constructed using vertical jumbo columns near the portal of the tunnel for about 50 meters. From 50 meters up to the other end of the tunnel, an additional 200 meters, tunnel support consists of an arch created by horizontal jet grout columns. These horizontal columns are formed using the CCP system. The tunnel is scheduled for completion during Fall 1988.

Access to the portal of the tunnel is permitted by two unbraced, unreinforced, jumbo grout diaphragm walls. The north wall was formed by jetting 5 rows of jumbo columns. Through October 1987, the 17 meter high north wall has not experienced any distressful movements.

CLOSING REMARKS:

We are still in the early stages of the learning curve for understanding jet grouting. Difficulties now exist in measuring in-situ the diameter of the column as it is formed. When jetting very deep columns the problems associated with maintaining verticality becomes critical. However, these technical difficulties can be overcome, and permit improved field quality control. Novatecna is now working on solutions for the above problems.

ACKNOWLEDGEMENTS:

Permission was granted by the United States Army Corp of Engineers, Chief of Engineers, Washington D.C., to publish this information.

REFERENCES:

Yahiro, T., and Yoshida,H., (1973), "Induction Grouting Method Utilizing High Speed Water Jet," Eight International Conference on Soil Mechanics and Foundation Engineering.

Miki, G., and Nakanishi, W., (1984),"Technical Progress of the Jet Grouting Method and Its Newest Type," In-Situ Soil and Rock Reinforcement, Paris.

Yahiro, T., Yoshida, H., and Nishi, K., (1982) "Soil Improvement Method Utilizing a High Speed and Air Jet (Column Jet Grout Method)," Sixth International Symposium on Jet Cutting Technology, Surrey.

Bruce, D., Boley, D. (1987),"New Developments in Ground Reinforcement and Treatment For Tunnelling," Rapid Excavation and Tunneling Conference, New Orleans.

Yahiro, T., and Yoshida, H., (1974),"On the Characteristics of High Speed Water Jet In the Liquid and Its Utilization on Induction Grouting Methods," Second International Symposium on Jet Cutting Technology, Cambridge.

Novatecna (1987)," Jet Grouting: CCP and Jumbo Case Files," Company Brochure.

Guatteri, G., Teixeira, A., and Martins, A., (1986)," Solutions in Stability Problems in Tunnelling by the CCP Method," International Congress on Large Underground Openings," Firenze, Italy.

Guatteri, G., (1984),"Jet Grouting For the Cut-Off Construction of Porto Primavera Cofferdam - CCP Process," International Conference In-Situ Soil and Rock Reinforcement, Paris.

Nicolls, G., (1985),"Landslide Stabilization: High Pressure Cement Slurry Injections, Evaluation of TSSI Columns), Professional Report #2923 - 01, May.

Guatteri,G., and Teixeira, A., (1987),"Improvement of Soft Clay by Jet Grouting Technology," Proceedings Columbia Soil Mechanics and Foundation Engineering, CPMSIF, Carthagena, Columbia.

Proceedings: Second International Conference on Case Histories in Geotechnical Engineering, June 1-5, 1988, St. Louis, Mo., Paper No. 5.33

Ten Years of Dynamic Consolidation in China

Weiyuan Fan
Prof. of Geotechnical Engineering, Taiyuan University of Technology, China

Yihui Qiu
Associate Prof. of Geotechnical Engineering, Taiyuan University of Technology, China

Meiyun Shi
Prof. of Geotechnical Engineering, Taiyuan University of Technology, China

SYNOPSIS: Presented in this paper are the main achievements and results by using Dynamic Consolidation in China during the past ten years for ground treatment. It includes the following aspects. (1) On the basis of field practice and test results in ground improvement by dynamic consolidation for projects located at sites of various types of soil deposits including sand deposits, sandy loam deposits and loess soils, a series of influence factors including contact stress used in the evaluation of effective depths of dynamic consolidation proposed by L.Menard is discussed. Empirical formulae and choice of design parameters are also given separately. (2) The mechanism of dynamic consolidation which includes conventional soil laboratory tests, in situ investigation and scanning electron microscopic (SEM) technique is fully discussed both macroscopically and microscopically. (3) In closure, the authors submit the result of several jobs which are elaborate and took place in recent years.

INTRODUCTION

Since 1978, the process of dynamic consolidation as developed by Louis Menard has been popularly used all over the world for ground treatment. Macroscopically, through the interpretation of a theoretical approach to its mechanism, as stated by Louis Menard, M.P.Gambin, G.A.Leonards, Zheng Qian, X.D.Qian etal, Zhong qi Wang, J.H.Qian, and other researchers, some acceptable theoretical frame may see the light for very specific cases of less complexity. As to the influence factors used in the evaluation of effective depths of dynamic consolidation proposed by L.Menard, there are still no accepted statements for general application. Fan etaL(1986)tried to combine the macroscopic and microscopic approach so as to get a comprehensive explanaton. In this paper, a full review of research results on dynamic consolidation obtained in China during the past decade, especially the performances practised by the authors both at laboratory and in situ investigation along with theoretical analysis is presented. The last part of this paper is contributed as case histories in ground treatment experienced by the authors in recent years with particular emphasis on the microscopic aspect of dynamic consolidation and the choice of parameters.

EFFECTIVE DEPTH OF DYNAMIC CONSOLIDATION

Since the popularization of dynamic consolidation, few work has been done regarding the various influence fatcors used in the evaluation of effective depth of compaction. There are many fatcors which may affect the effective depth of compaction, such as weight of tamper, drop height, base area of tamper, number of passes of tamping, grid spacing, the property of soil, the ground water level, and the stratum condition, etc. According to the analysis of many projects performed by the authors, the main factors are,

- The energy per impact
- Number of passes of tamping
- The impact centers grid
- -- Base area of tamper
- The structural strength of the soil.

The combined effect of the second and the third factor will be the total energy per unit surface area.

Defintion of Effective Depth

The depth of influence given by Menard is

$$D = \sqrt{W\ H\ 10} \qquad (1)$$

Where, D - Depth of influence, M
W - Hammer weight, KN
H = Drop weight, M

It was argued how to correct the depth formula given by Menard to meet the various requirements for different conditions of sites to be treated. The revised effective depth formula advanced after a great deal of practices in our country is

$$D' = K\sqrt{W\ H\ 10} \qquad (2)$$

Where D' is effective depth, K is revision coefficient, and this will be discussed in the later part of this paper.

In practice, we consider that the effective depth is the effective thickness of compaction, and this thickness of compaction should be varied for various requirements of engineering design. Therefore the method of investigation along with criteria should also be varied. For example, for soft soil, the main aim is to raise the bearing capacity and to reduce the settlements. For saturated fine sand and saturated sandy loam, the main purpose is to eliminate liquefaction under a certain magnitude of earthquake. For collapsible loess and newly deposited loess, the principal aims are eliminating collapsibility and raising the bearing capacity. These can be seen in Tab 1.

TABLE 1.

Soft Soil	Raising the BearingCapacity	[R] 150KPa
Saturated Sand	Eliminating Liquefaction $N' = \bar{N}'[1-0.125(d_s-3)-0.05(d_w-2)]$ *	
Collapsible and Newly Deposited Loess	Eliminating Collapsibility and Raising Bearing Capacity	δs 0.015 γd 15KN/M³

* Chinese Code of Earthquake Resistance Design for Industrial and Civil Building Construction. (TJ11-78)

In this table, [R] = Allowable Bearing Capacity
N' = Critical number of S.P.T. forliquefaction under the conditions of ds and dw, where ds is depth of saturated sand beneath the ground surface (M) and dw is the depth of ground water beneath the outdoor ground surface (M)
$\bar{N}'$=Criticalnumber of S.P.T. for liquefaction under the conditions d_s = 3M and d_w = 2M.The number of S.P.T. are 6, 10, and 16, for earthquake intensities of 7, 8, and 9 respectively.
δs = Coefficient of collapsibility.

Empirical Formula for Effective Depth

The following formula for effective depth was gained by the authors in 1980 who had studied and analysed 16 experimental data statistically (cohesive soil and sandy soil).

$$D' = a + bWH + cE \qquad (3)$$

where a = constant, with the dimension of meter and the value of 5.10.
b = coefficient, with the dimension of 1/KN, and the value of 0.00086.
c = coefficient, with the dimension of M^2/KN, and the value of 0.00094.
E = the total energy per unit surface area(KN-M/M²).

An Alternative Approach to Determinethe Effective Depth —— Application of Impact Stress

The dynamic stress under the base of dropping hammer tested in-situ has been used by the authors as a measure to determine the effective depth of eliminating collapsibility forδs<0.015 andγd>15KN/M³.
(1) Firstly, we caculate the stress distribution vertically along the deepness of impact center, by assuming that the dynamic stress tested at the impact surface, Pd, as a quasi-static loading and the ground as a semi-infinite elastic space.

(2) Secondly, we calculate the stress distribution along the deepness (curve Pd) as shown in Fig. 1 and then draw the curve of the yield strength of the press meter test (curve Po), the intersection point of these two curves (point A in Fig.1) can be used to determine the depth of eliminating collapsibility. This depth of point A is 12.2m obtained by the design requirement of δs<0.015 and γd 15 KN/M³. The intersection point B, its depth is 11M and this value is also rather consistent with the value 10.9M *obtained from the laboratory test for the design* requirement ofγd 16 KN/M³. Thus we concluded that the impact stress on ground surface is very important and can be used as a measure to estimate the effective depth. In this project, the deposit is collapsible loess.

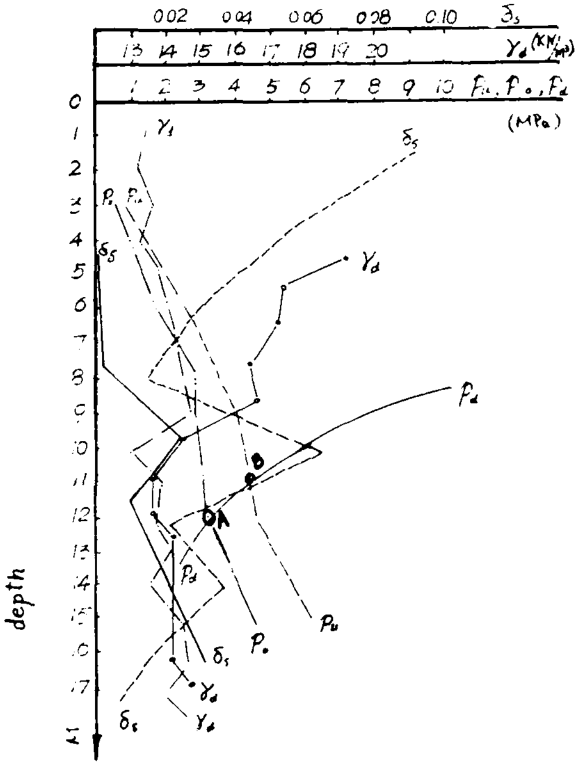

Fig.1

Note, δs-- Coefficient of collapsibility
...... Before tamping, —— After tamping,
γd-- Dry unit weight(KN/M³),
...... Before tamping, —— After tamping,
P_o -- Yield strength of pressmeter test (MPa),
P_u -- Limit loading of press meter test (MPa),
P_d -- Dynamic stress (MPa).

The Measured Dynamic Stress and Its Behavior

The impact stress on ground surface is a main boundary condition. We have measured the impact stress by using self made transducers and the results are shown in Fig.2. The types of impact stresses are of two kinds.

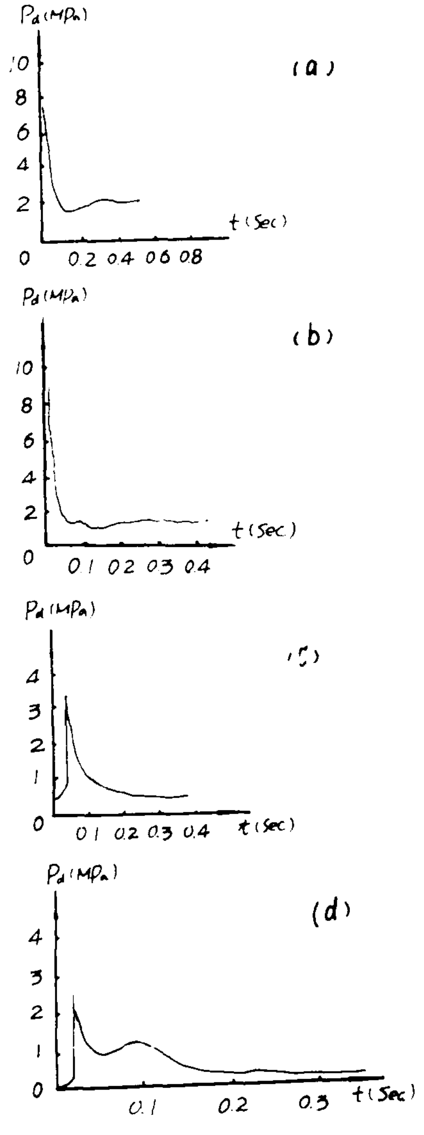

Fig. 2

(1) Fig.2(a) and Fig.2(b) are of the first type. In Fig.2(a), the stratum is rather dry and hard, and the water content is rather low. While in Fig.2(b), the top portion of the strata has shaped a firm layer after repeated tamping and stress wave has a peak value of sharp rise. The time of wave action only lasted 0.04 second.

(2) Fig.2(c) and Fig.2(d) are of the second type. The water *content of those two tamping points are* relatively high, and the wave stress has also peak value of sharp rise. But it damped relatively slowly and the wave action lasted 0.1 second.

In addition neither of the above two types has been registered second peak value of stress wave.

(3) The actually measured dynamic impact stress is related to the degree of hardness of the soil. The range of measured values obtained by the authors is 2.9-9.0 MPa.

(4) According to our experence, the base area of the tamper can be chosen from the thumb rule that the *weight of tamper distributed per unit base area* is 25-40KN/M'.

PARAMETERS FOR DESIGN AND CONSTRUCTION

In order to obtain the ideal effect, it is very importment to choose parameters for design and construction. The main parameters include,

-- The effective depth
-- The total energy per unit surface area
-- Grid spacing
-- *Number of blow per pass*
-- Number of passes of tamping

The Efective Depth

Refering to formula (2), the value of the influence coefficient, K, can be chosen from Tab.2

Table 2

Deposit	Effective Depth (M)
Soft Soil	$D' =(0.45-0.5)\sqrt{W H/10}$
Saturated Sand	$D' =(0.5-0.6)\sqrt{W H/10}$
High Fills	$D'=(0.6-0.8)\sqrt{W H/10}$
Loess and newly Deposited Loess	for $\gamma d>15KN/M'$ $D'=(0.34-0.36)\sqrt{W H/10}$ for $Ss<0.015$ $D'=(0.4-0.5)\sqrt{W H/10}$

The Total Energy Per Unit Surface Area

As to the total energy input, specialist contractors draw up graphs of the improved soil parameters as a function of total energy applied. From the authors' experience, Tab. 3 can be used to bring the final values to a specified level.

Tab. 3

Deposit	Effective Depth Required (M)	Total Energy Per Unit Surface Area (KN M)
Soft ground	5 6	2000 2500
	7 10	3300 3800
Saturated sands (liquefaction potential	5 6	1700 2200
	7 10	2700 3200
Loess	5 6	2200-2700
	7 10	3500 4200

Number of Blows

The number of blows include the total number of blows and the number of blows for each pass.

If the ground is loess, fills or sand, and there is no heaving of ground surface while tamping, the total number of blows can be completed in one pass.

For satuated clayey soils or loess with high water content, the tamping should be performed by passes.

Number of Passes and Rest Period

For sandy soils, generally 1 3 passes will be satisfactory. But for clayey soils, 2-5 passes are required. The rest period, or time of interval can be varied from several minutes for sand to several weeks for clay.

Grid Spacing

The grid spacing may be generally taken as 2-4 d, (d is the diameter of the tamper.). For saturated clayey soil we use the upper limit. For loess and sandy soil we use the lower limit.

The Range of Lateral Strengthening Effect

Shown in Fig. 3 is a chart of γd contour after tamping(6250KN M). From this chart we can see that it takes the shape of a bell and the range of lateral strengthenimy zone is 5 M (for γd 1.5KN M^3) This value is about 1.6 d. The lower boundry of these contours is 1.5 d below the tamping pit. Therefore it will be suitable to choose grid spacing as 2.5 d -3 d.(for loess). In the following first example. We took 5 6 M. (i.e. 2d)

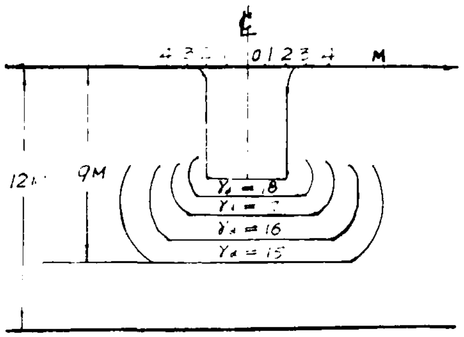

Fig. 3

MECHANISM OF DYNAMIC CONSOLIDATION

Louis Menard proposed a dynamic consolidation model (1976) and thus the soil can be visualized as a stack of "hydropneumatic capacitors". M. P. Gambin (1984) in his paper ''Ten Years of Dynamic Consolidation" gave *the principles and ground for a general theory* and many valuable design guide lines. So did other researchers as stated in the introduction of this paper. But all of those pertain to the category of macroscopic study. As to the microscopic area and there still exists a gap between theory and practice. Accroding to the study of Smart and Dickson (1978), for normally consoldated kaolinite under drained triaxial shear test, the macroscopic void ratio and the microscopic void ratio share their values respectively, but these values will vary with the change of axial deformation of soil. as shown in Fig.

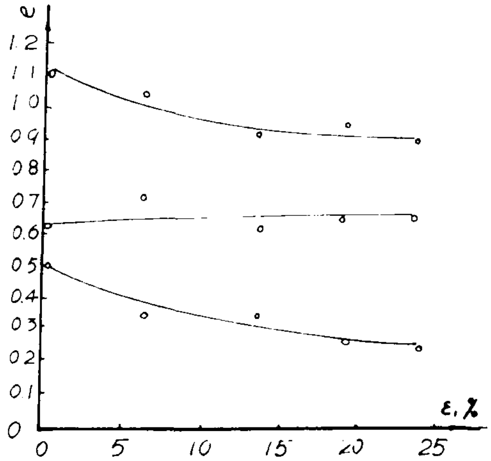

Fig. 4

In addation, the anisotropic ratio of Kaolinite under various consolidation pressures is also shown in Fig.5 After Tovey and Wong

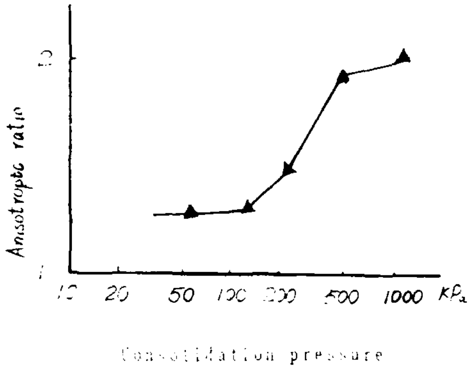

Fig.5

S.Ahmed etal(1974) pointed out that samples with similar total porosity values can have entirely diffrent pore size distribution. He also concluded that pore size distributions can correlate differently with soil behavior than total porosity. Fan etal (1986) stated that heavy tamping changes the macrostructures and microstrures of soil significantly with a certain depth under the tamping pit. They have tabulated the pore size distribution of various types of pores. (Tab.4) and finally concluded that *for loess soil the amount of pores* larger than 5 μM is closely related to the characteristic of engineering properties of the soil. Theoretically, the above statement is consistent with the studies of Ahmed, S.etal, Smart, P.S.etal, and Juang, C.H.etal, and this pore size of 5 μM can be called the threshold value.

By comparison we can see that the microscopic analysis is consistent with the macroscopic effect. Fig.(6) and Fig.(7) are the results of Ss and Es obtained from laboratory tests conducted on loess soil as those of Tab.4. By comparison we can see that

Tab.4

Type of Pore			Extra large Pore >500 μM				Large Pore 500-50 μM				Small Pore 50-5 μM				Micro Pore <5 μM			
Soil Profile			Hor.		Vert.		Hor.		Vert.		Hor.		Vert.		Hor.		Vert.	
Layer	Portion	Depth	B	A	B	A	B	A	B	A	B	A	B	A	B	A	B	A
		1																
Q_4^2	[illegible]	2			6		50		90		625		800		1300		3300	
				0		0		0		0		100		50		1100		10000
		4	5		3		75		60		475		470		2600		2100	
	[illegible]	5		0		0		10		10		300		200		8000		9000
			2		1		40		30		450		400		7300		5000	
Q_4^1		7		5		0		15		13		300		250		10000		8000
		8	2		0		50		25		350		300		5500		6000	
	[illegible]	9		0		5		25		13		300		300		6000		5000
		10	1		2		40		35		300		300		8000		5000	
	4	11		3		5		60		80		350		400		4500		6500
Q_3		12	2		1		45		35		300		400		6500		6000	
		13		1		2		10		45		450		500		4700		6300
		14	2		0		25		20		350		250		3000		3300	
	[illegible]	15		2		0		20		12		400		250		5000		3000
Q_2	[illegible]	16	2				20				200				3500			

Note, B Before tamping
A After tamping

the microscopis analysis is consistent with the macroscopic effect.

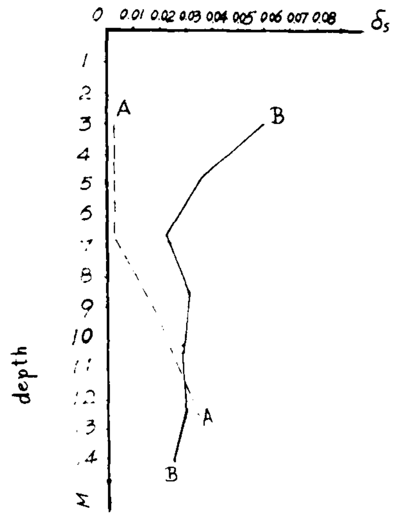

Fig. 6

Note, B --- Before tamping
A After tamping

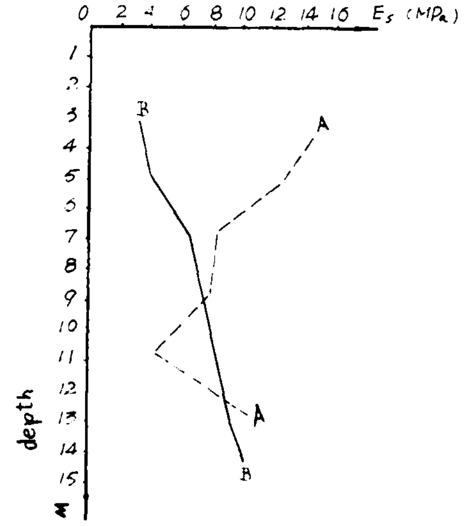

Fig. 7

Note, B --- Before tamping
A --- After tamping

EXAMPLES

The authors take this opportnuity to recall a few features on 2 jobs constructed on loess soil.

1. Chemical Fertilizer Plant

(1). Heavy Compation by Passes

The loess is unsaturated in natural state. people think that loess is apt to be heavily comparted and can be treated only by one pass. This consideration is not complete. Whether or not tamping by passes is necessary depends on the water content of natural loess. along with the bearing capacity and the modulus of compressibility required.

According to the test data obtained from Shanxi Chmical Fertilizer Plant, the tamping energy is 6250 KN-M per blow, being the highest at that time in this country; the water content is 22-25%, the soil becomes saturated during tamping. The inverstigations show that the effective depth and dry unit weight after continuous tamping of 30 blows are nearly the value as those of 8 blows (Fig.8). But when the site is comparted by passes, the values of dry unit weight, the bearing capacity and the modulus of compressibility are all increased significantly as shown in Fig.9 and Tab.5.

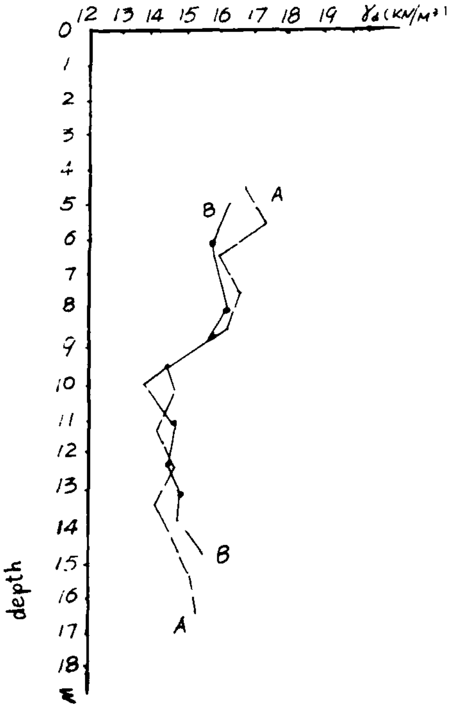

Note, B - Continuous 8 blows
A -- Continuous 30 blows

Fig. 8

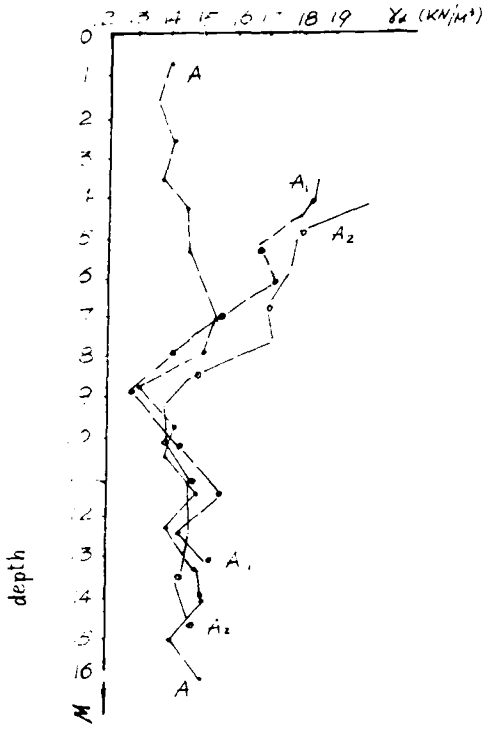

Fig. 9

Note, A — Before tamping
A1--- After 1 pass (11 blows)
A2 — After 2 passes (23 blows)

Table 5.

Item	EnergyLevel Per Blow(KN-M)			
	6250	5000	4000	3000
Depth for Eliminating Collapsibility	12	12	9	7
Effective Depth (M)	9	8	7	6
Es (weighted) (MPa)	12.3	10.6	10.9	10.2
[R] (weighted)(KPa)	285	260	279	272

In the construction site of a certain plant in Taiyuan, the water contant of loess is 14-17%, we used only one pass of dynamic compaction and obtained the required values density and bearing capacity.

(2). The Effective Depth of Dynamic Consolidation.

According to the loess to be improved with the *requirement of dry unit weight* $\gamma d>15KN\ M^3$, the effective depth of dynamic consolidation can be represented by $D' = K\sqrt{WH\ 10}$ as stated above. According to the statistical experence of 18 projects, K= 0.35-0.5, this value is smaller than that for clayey soils and related to the water content of loess and the energy per blow. When the water contant w 15% and the energy per blow is great we use the low value, while the water content w>20% and the energy per blow is small, we use the high value.

The effective depths and depths of eliminating collapsibility investigated in Shanxi Chemical Fertilizer Plant are tabulated for energies from 3000 KN-M to 6250 KN-M per blow, as shown in Tab. 5.

2. A Factory in Taiyuan, China

The authors investigated the effect of vibration caused by dynamic consolidation to neighbouring buildings especially the results of settlement investigations of neighbouring buildings of certain factory on the compaction site.

This factory is situated at a site of self-subsiding collapsible loess of second grade. The thicknessof this soil is 7M. The old neighboring buildings of3 stories built in ninteen fifties including a dwelling and an administration building had cracks. The above two buildings are 2.5 M from nearest tamping point. A two storied laboratory building has no cracks and it is only 1.8 M from the nearest tamping point. The investigations of settlements, cracks and vibrations were performed for all these buildings. The energy per blow was 600 KN-M. The results showed that the settlement of the administration building and the dwelling was only 2.2 MM, and had noadditional settlement at all.And there was no sign of development of the old cracks. As to the laboratory building, the settlement of the point nearest to the tamping pit was 10-12MM, and cracks appeared. This illustrated that in loess deposits, owing to high solidification internal force, the ground subsistence is not apt to be induced, and therefore no addtional cracks could be found, whereas the laboratory is of 1.8M distance from the pounding, and because of the pushing effect of the compacted soil, the settlement arised and the cracks appeared.

CONCLUSION

Evaluation of effective depth of dynamic *consolidation can be made by Menard's formula* with inflence coefficient. But other empirical formula or impact stress can also be used as a measure to estimate the effective depth. Besides factors affecting the coefficient are fully discussed.

The microscopic machanism especially the pore size distribution of soil samples both before and after tamping are discussed, and the authors proposed the idea of threshold of pore size. Its value is 5 UM for loess soil.

Two case histories including the results of settlement investigations of neighbouring buildings on the compaction site are presented finally.

REFERENCE,

Ahmed, S., Lovell, C.W. and Diamond S.(1974)''Pore Sizes and Strength of Compacted Clay'', ASCE, vOL.100, GT4.
Fan, Weiyuan etal.(1986)''Study of Microstructures of Loess Deposit under Dynamic Consolidation'', International Symposium on Environmental Geotechnology. Vol.1. pp.667-679.
Gambin, M.P.(1984)''Ten Years of Dynamic Consolidation'', Proc. of the Eighth Regional Conference for Africa on Soil Mechanics and Foundation Engineering.

Juang, C.H. and Holtz, R.D.(1986)''Fabric, Pore Size Distribution, and Permeability of Sandy Soils'', ASCE. Vol.112, GT9.
Leonards, G.A. etal.(1980)''Dynamic Compaction of Granular Soils'', Proc. ASCE, Vol.106, GT1. pp.35-44.

Menard, L. and Broise. Y.(1976)''Theoretical and *Practical Aspects on Dynamic Consolidation*'', Geotechnique, Vol.25, No.1. pp.3-18.

Qian, J.H.(1987)''Dynamic Consolidation, from Practice to Theory'', Proc. of the Eighth Asian Regional Conference on Soil Mechanics and Foundation Engineering, Vol.1. pp.201-204.

Qian, X.D. etal.(1983)''On Dynamic Consolidation'', Eighth European Conference on Soil Mechanics and Foundation Engineering, Vol.2

Qian, Z.(1985)''Several Soil Improvement Methods in China'', Proc. of 3rd International Geotechnical Seminar, Singapore, pp.237-247.

Qiu, Yihui and Guo, yuling(1984)''The In-situ *Measurementof Dynamic Stress in Soil Mass during* Heavy Tamping by Dynamic Consolidation Method in Ground Improvement'', Journal of Taiyuan Institute of Technology, No.1. pp.45 52.

Smart, P.S. and Tovey, N.K.''Electron Microscopy of Soils and Sediments, Examples'',(1981)

Wang. Z.Q. etal(1984)''Mechanism of Dynamic *Consolidation and Its Evironmental Effect*'', International Conference on Case Histories in Geotechnical Engineering. pp.1459 1465.

Proceedings: Second International Conference on Case Histories in Geotechnical Engineering, June 1-5, 1988, St. Louis, Mo., Paper No. 5.34

Experience in Ground Improvement by Dynamic Compaction and Preloading at Half Moon Bay—Saudi Arabia

N. Ghosh
Senior Engineer, Sir William Halcrow and Partners Ltd., London, England

M.M. Tabba
Director, Saudi Hotels and Resorts Areas Company, Riyadh, Saudi Arabia

SYNOPSIS: Ground improvement techniques were used to meet the design requirements for a beach resort complex at Half Moon Bay on the Arabian Gulf. Extensive site exploration revealed upper layers consisting of loose to medium fine sand, having variable silt content. The original specification called for filling and ground improvement using Dynamic Compaction to achieve 100kN/m^2 surface bearing capacity and 50% relative density at a depth of 10m. Dynamic Compaction (DC) and subsequent field testing, using full scale loading tests as well as CPT and SPT tests, proved that it was possible to achieve these requirements over most areas using dynamic compaction, however it was not suitable in a few other areas where ground response to DC was poor. Those areas contained silty layers and showed signs of rapid pore pressure build up under dynamic compaction, while dissipation was slow and penetration resistance remained poor. Therefore, it was decided to use pre-loading in those areas. Further testing and instrumentation showed that pre-loading was achieving the required ground improvement.

INTRODUCTION

This paper describes the case history of ground improvement at a site in the middle of Half Moon Bay some 50 km south of Al Khobar on the Arabian Gulf (Fig 1). The site covers approximately 3.7 km^2 bounded to the East by Half Moon Bay and to the South by a smaller inner bay.

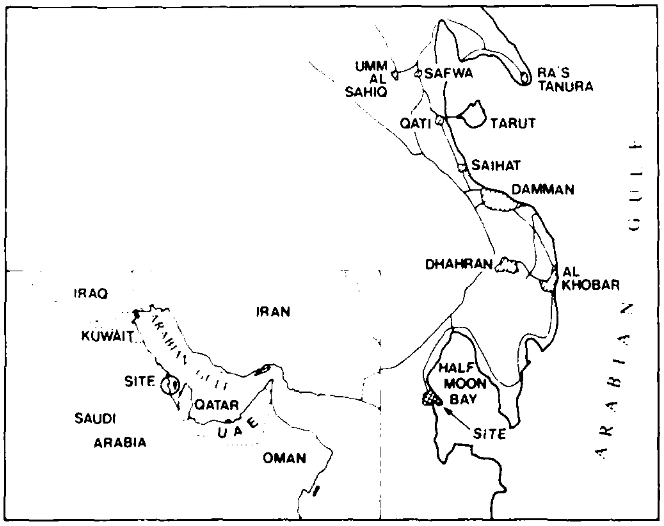
UMM AL SAHIQ
SAFWA
RA'S TANURA
QATIF
TARUT
SAIHAT
DAMMAN
DHAHRAN
AL KHOBAR
IRAQ
IRAN
KUWAIT
SITE
QATAR
U A E
SAUDI ARABIA
OMAN
HALF MOON BAY
SITE
GULF
ARABIAN

Fig 1 Site Location Map - Half Moon Bay.

The development scheme undertaken in Phase I of the Half Moon Bay Beach Resort Project is to consist of two hundred and fifty one chalets surrounding the inner bay together with infrastructure, services and a recreational area in the south eastern peninsula. Various areas of investigation referred to in the following text are shown on Fig 2.

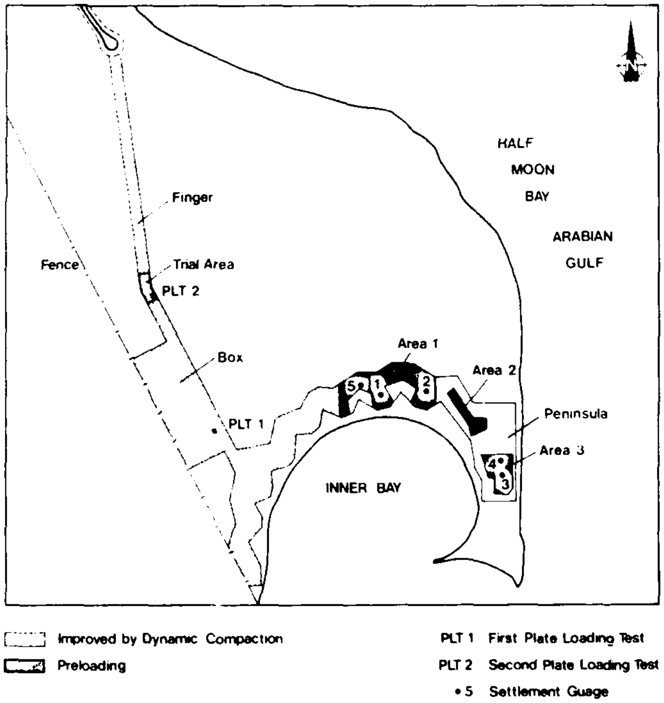
HALF MOON BAY
ARABIAN GULF
Finger
Fence
Trial Area
PLT 2
Box
PLT 1
Area 1
Area 2
Peninsula
Area 3
INNER BAY
5
1
2
4
3
Improved by Dynamic Compaction
Preloading
PLT 1 First Plate Loading Test
PLT 2 Second Plate Loading Test
• 5 Settlement Guage

Fig 2 Layout of Ground Improvement Work.

Regionally, there are Sabkha deposits which cover most of the site, with intermittent caprock consisting of cemented shelly sandstone. These deposits are underlain by marine deposits of Quaternary Age of variable thickness containing non indurated but sometime cemented deposits of silty sand with silty clay bands. The sedimentary bedrock of the Dammam formation of Eocene Age lies at depths greater than 20m. This bedrock typically consists of dolomite and limestone interbedded with marl (calcisiltite) and shale (calcilutite) (Kent, 1976).

A preliminary site exploration was carried out using dynamic probing followed by a full scale investigation which included boreholes, trial pits, standard penetration tests (SPT) and static cone penetration tests (CPT). The in-situ soil conditions confirmed that buildings proposed in the main development area of the site would experience excessive settlement without treatment of the underlying, highly compressible soils. Following this, a ground improvement programme was undertaken using dynamic compaction on a surface reclaimed with dune sand up to 2m thick.

A part of the site, where the in-situ conditions prevented any improvement by dynamic compaction, was preloaded.

SITE CONDITIONS PRIOR TO GROUND TREATMENT

The ground surface originally consisted of Sabkha except in the central part where intermittent caprock was encountered. Underlying the Sabkha, fine to medium sand with traces of silt and a varying amount of shell fragments generally covers the site to a depth of 4m (Fig 3) in the peninsula and this increases to some 9m depth in the western part and in the box (Fig 2) where only traces of shell fragments were found (Fig 4). This stratum is referred to as the upper sand. Below this, extensive deposits of silt and clayey sandy silt some 6 to 7m thick are present in the peninsula (Fig 3) and some 5m were found in the western part (Fig 4). This is referred to as the intermediate silt layer. The SPT and the CPT results indicated that the upper sand and the intermediate silt strata were in a very loose to loose state except in the northern part of the finger and in some locations within the box area (Fig 2) where the upper sand layer was found to be medium dense with increasing depth. Underlying the silt stratum, sand deposits prevail across the site with a transition zone of silty sand generally some 2m thick, and this stratum was normally found to be loose to very dense. This is referred to as the lower sand layer which overlies a hard silty clay generally encountered at 19 to 20m depth.

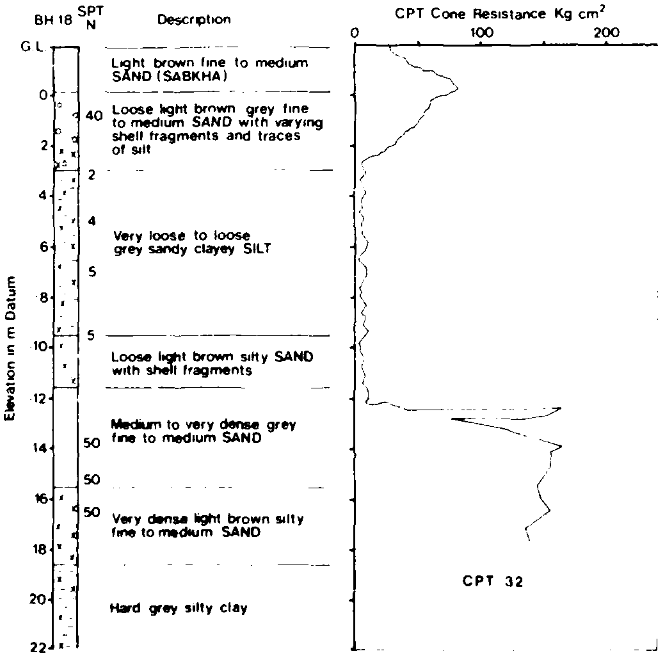

Fig 3 Typical borehole and CPT profile in the Eastern peninsula.

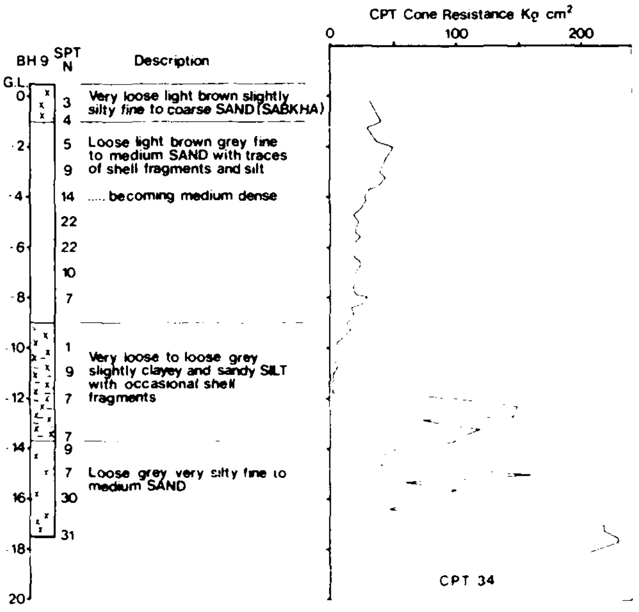

Fig 4 Typical borehole and CPT profile in the Western parts of the site.

Groundwater was found to be within a metre of the ground surface at the northernmost part of the site, but it was within 250mm in the eastern and western parts of the site.

GROUND IMPROVEMENT

The proposed construction site over 44 ha, was initially cleared by removing the Sabkha and reclaimed with a maximum of 2m of dune sand, compacted in layers by vibro compactors, to provide a surface 2m above Datum. The dynamic compaction was applied on this surface with the aim of achieving a safe bearing capacity of 100 kN/m^2 at the surface and densification of the subsoil from the surface downward at least to 10m where the relative density of the soil should not be less than 50 per cent. The CPTs were used to verify the improvement and also to estimate the relative density at 10m depth using Schmertmann (1978), correlation with the cone resistance (q_c) and the effective overburden pressure (p_o).

Dynamic Compaction Trial

An area of the site having relatively poor soil conditions was selected for the dynamic compaction trials (Fig 2). The initial four (Trials 1 to 4) of six trials performed were carried out using a 2 x 2m, 16 tonne pounder dropping freely from a height of 20m using a 120 tonne Manitowac-crawler mounted crane; the last two trials (Trials 5 and 6) were performed with a 25m drop. Normally, 10 blows were applied to each print, except in Trial 5 where 20 blows were applied. In each trial, quality control was performed using piezometers and CPTs. Trial 1 to 4 inclusive were carried out covering grid systems from 5 to 12m either by a single pass or up to 3 passes, whereas in trials 5 and 6 only a 10m grid was used with 2 passes. However, the timing for the passes was not always controlled by the dissipation of pore pressure generated. Three hollow stem auger holes were sunk in the trial area, prior to dynamic compaction. The intermediate silt layer in a very loose state was found at 3m below Datum. The results of the trials confirmed that only the initial 5m, including the compacted fill, improved satisfactorily while responses to dynamic compaction below this level were insignificant.

During the performance of some trials (2,4,5 and 6) it was noticed that the ground water (or in some cases a dark dense odoriferous fluid) overflowed from the standpipes (some 1.5m above the surface), but on some occasions immediate falls of piezometric heads were noticed during the course of tamping. This phenomenon might have been due to local liquefacation of the soil in the intermediate silt stratum. Subsequent monitoring showed that there was little change of these modified piezometric heads in the next six months.

Dynamic Compaction

Following the disappointing results from the trials, the Contractor embarked on the full scale dynamic compaction programme using the same weight, 10 blows per print, 25m drop and 10m centres starting from the north of the finger. Piezometers were installed at 9m below Datum on a 50m grid.

Considerable ground improvement was noticed in many parts of the finger and the box areas, even after the first (north of the trial area), or second passes. However, such improvement in many areas was still insufficient to meet the specified relative density of 50 per cent, to be achieved at 8m below Datum in accordance with the Schmertmann's correlation. A full scale load test was carried out to overcome this situation,and this is described in the following section. The average CPT profile obtained from this test location (Fig 5) was finally used to

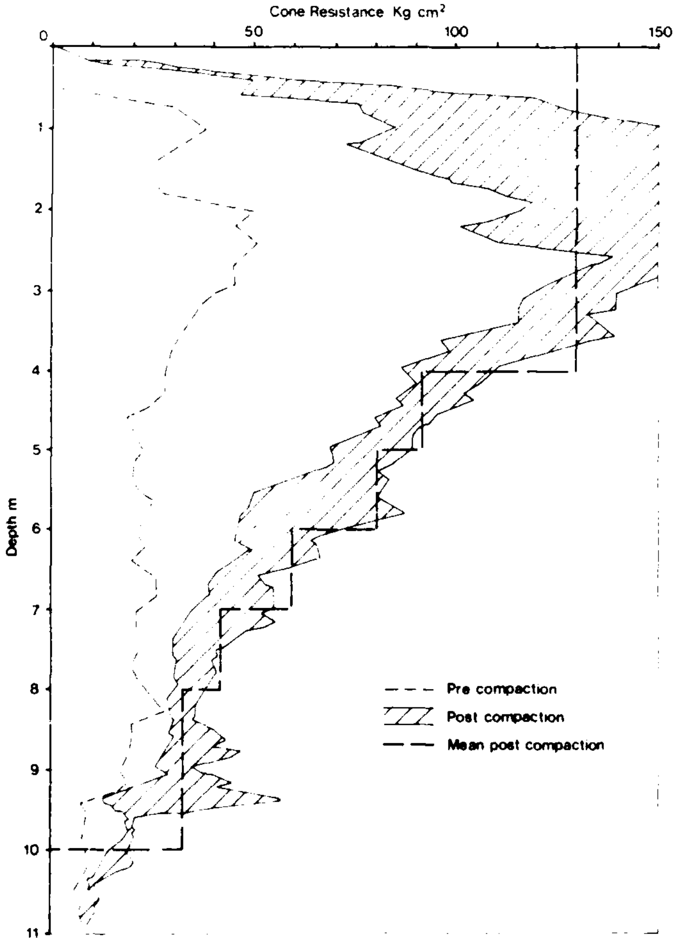

Fig 5 Pre-and-post dynamic compaction CPT results at Load Test 1 location.

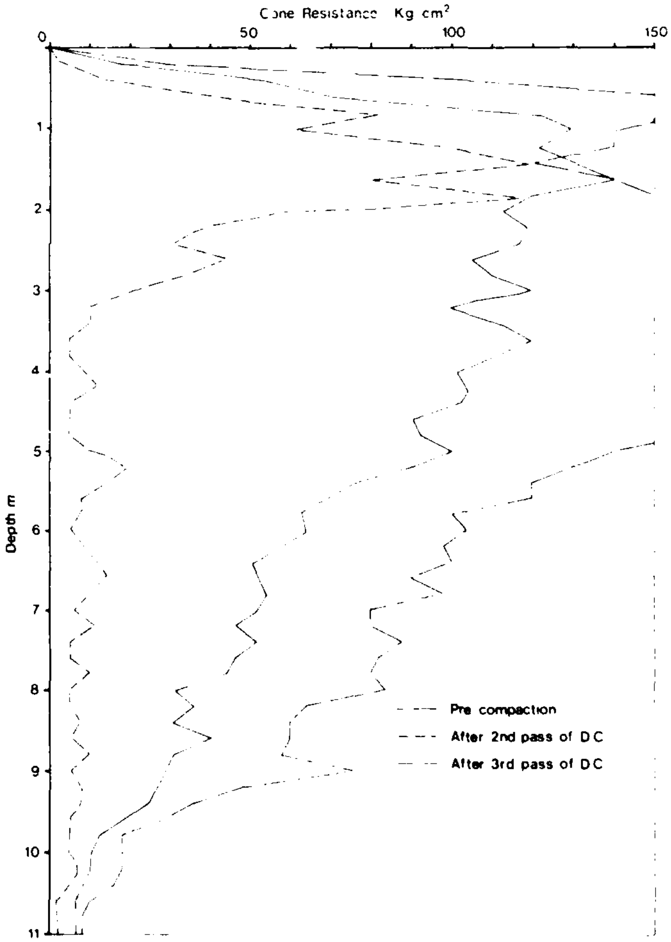

Fig 6 Typical pre-and-post dynamic compaction CPT results from Western parts of the site.

approve the dynamic compaction work at the site.

In areas satisfactorily compacted using two passes of dynamic compaction, pore pressures dissipated within one month, but in those parts treated with upto four passes, where pore pressure dissipated much more slowly. Fig 6 displays typical profiles of both the pre-and post-compaction CPT results. The settlements of the ground after each pass was in the order of 200mm. After the final pass, an "ironing pass" was performed to compact the near surface soils, especially around the craters.

Full scale plate load tests and settlement analysis

The full scale load test referred to above was carried out using a large concrete plate (4 x 4m x 0.4m thick) loaded to 150 kN/m^2 pressure. The location of the first such test (Load Test 1) was chosen in the box area (Fig 2), where two passes of dynamic compaction were given. The load test was carried out at 1.25m above Datum using concrete blocks as Kentledge. Fig 5 displays the results of a few post-compaction CPTs carried out prior to the load test, and a CPT profile from the original site investigation is also included. The load test commenced by placing the full load within the first 24 hour; the total settlement of 5mm took place within 48 hour. The load was maintained for 19 days when no significant movement was recorded.

The plate used acted as a 4 x 4m square footing (B = 4m) and the applied pressure must have influenced the ground at least to a depth of 2B (8m) which was some 7m below Datum.

By comparing the measured settlement with that calculated as suggested in Schmertmann (1978) a value of X = 7 was evaluated ($E = Xq_c$, where "E" is the soil deformation modulus). Schmertmann proposed that the values of X could be taken as 2.5 and 3.5 for square and long footings only with first loading case respectively. But, he quoted that if the sand has been strained by preloading or any other methods, the real settlement will probably be significantly less than predicted using values of X quoted above. Schmertmann, therefore, suggested that in such cases the values of X can be increased by a factor equal to or greater than that would indicate by the resulting increase in q_c. This apparently agrees with the results shown in Fig 5.

A second load test was performed at a location in the trial area (Fig 2) using identical arrangements except that the plate was placed at one metre above Datum. The results of this test was satisfactory, and was used to approve the work which did not meet the criteria of Load Test 1.

Relative Density

Following the encouraging result of Load Test 1, an investigation was made using SPT to assess relative density in areas where dynamic compaction work was approved on the basis of Load Test 1. Three boreholes were drilled using a hollow stem auger and SPTs were carried out at 1.5m intervals using a split spoon sampler. Relative density for a corresponding blow count (N) was evaluated using the analytical expression on given in Giulani & Giulani Nicoll (1982) which incorporates effective overburden pres- sure, and these results are shown on Fig 7. Fig 7 shows that after dynamic compaction, 50 per cent relative density was generally achieved at a depth of 10m. It is interesting to note that some low N values under small overburden pressure are within the medium dense range in the relative density scale, even though this can be classified as loose when the general descriptive terms were used.

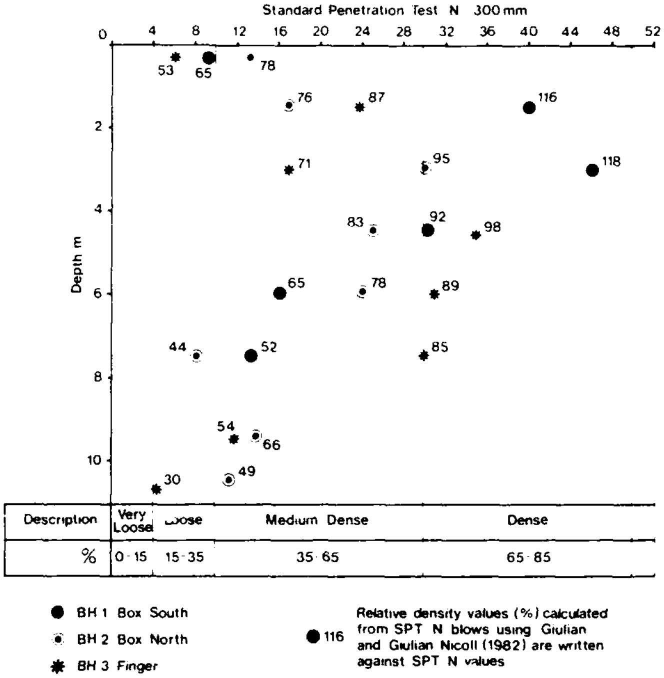

Fig 7 SPT (N) blows profiles with calculated relative density values.

Preloading

Despite the fact that dynamic compaction was successful over most of the site, quite a large part (122 ha) did not respond (Fig 2). The initial site investigation indicated that most of this area contains layer(s) 6 to 7m thick of loose to very loose silt and the groundwater, which is influenced by the tide, was found close to the original ground surface. An additional site investigation consisting of three 25m deep boreholes was carried out, with a view to predicting the time settlement under pre-loading. It was confirmed that no improvement of the intermediate silt layer was apparent after an initial dynamic compaction operation. Fig 8 displays an envelope of particle size distribution of this intermediate silt layer, which shows that the silt content varies between 40 and 80 per cent and the clay content is less than 10 per cent. Fig 8 also includes the grading envelopes of the upper and lower sand strata. The samples from the intermediate silt layer were mostly found to be of low to intermediate plasticity, and some were non-plastic.

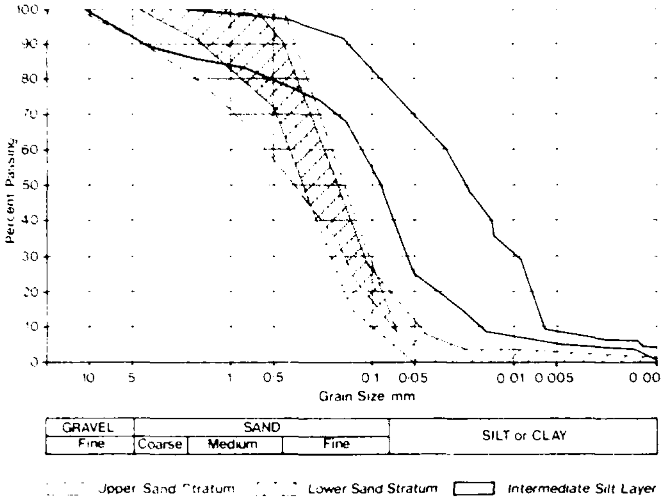

Fig 8 Particle size distribution of upper sand, intermediate silt and lower sand.

Thirteen one-dimensional consolidation tests were performed on undisturbed samples taken from the three boreholes. An attempt was made to assess the pre-consolidation pressure (p_c') and it was found to vary between 140 and 400 kN/m^2. However, the ratios p_c'/p_o' and individual e-log p_o', plots (Halcrow, 1986b) indicated that considerable sampling disturbance may have taken place. The coefficient of consolidation (C_v) values evaluated ranged from 0.7 to 132m^2/year for the corresponding effective pressure range 100 to 200 kN/m^2.

Prior to placing the sand fill for preloading, five settlement gauges were installed at 1.5m above Datum (Fig 2); several piezometers were installed at various depths in the upper three strata. Fig 2 shows the part of the site preloaded with 3.5m of dune sand fill which was end tipped, dozed and compacted using construction traffic.

Settlements under preloading

The predicted settlements at five locations, where the settlement gauges were installed, were calculated using the soil profiles revealed by the nearest boreholes. The settlements of the sand strata (upper and lower sands) were calilated using mean q_c values as appropriate and the method described by Ghosh (1982). This was because the applied load from the preloading was equivalent to an elastic half space, and the method suggested in Schmertmann tends to underestimate the deformation of the sand strata under such load conditions. The settlements of the intermediate silt layer were estimated using m_v values corresponding to appropriate effective pressures, evaluated from the oedometer test results. The total settlement assessed was of the order of 400mm.

The predicted periods for 90 per cent consolidation of the intermediate silt layer were estimated using the coefficient of consolidation (C_v) value of 5, 15 and 55m^2/year were typically 1550, 515 and 140 days respectively. The C_v values of non-plastic and low-plastic silt deposits are of the order of 100m^2/year (Lambe and Whitman 1965), therefore, 140 days for 90 per cent consolidation of the intermediate silt was predicted using a C_v value 55m^2/year and thought to be appropriate. Pore pressures built up in the upper sand during the preloading operation, dissipated within 40 days, and a similar period for the dissipation of excess pressure in the lower sand strata was assumed. Therefore it was considered that the total settlement would be completed by 220 days. Fig 9 shows the total settlement typically for Areas and 3, which were monitored till 25 September 1987.

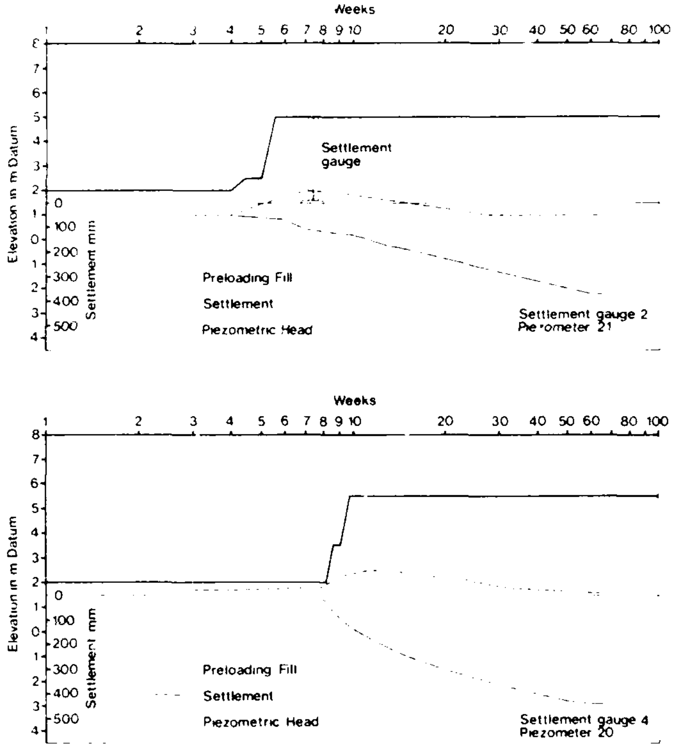

Fig 9 Two typical time settlement curves with piezometric heads under pre-loading.

DISCUSSION

The plots in Fig 9 would seem to indicate that settlements are on the verge of completion, although the excess pore pressure in the lower sand stratum remains high. However, in the intermediate silt stratum the excess pore pressure is only marginally high compared with the ground water level in this area. Table A summarises piezometric heads monitored before, immediately after and a year after the preloading was placed, and the variations of the pressure head within the three strata investigated are noticeable. The excess pore water pressure in the lower sand stratum, as mentioned earlier, apparently remains unchanged in spite of a moderate rise in pressure due to the preload, which suggests, that this layer, overlying the hard silty clay, probably does not drain effectively in a horizontal direction. Piezometers 19 and 20, installed in the upper part of the intermediate silt layer in Area 3, read 1.6m above Datum, whereas, the corresponding pressure head at the centre of the same

AD-A213 199 INTERNATIONAL CONFERENCE ON CASE HISTORIES IN GEOTECHNICAL ENGINEERING (2. (U) MISSOURI UNIV-ROLLA S PRAKASH 30 JUN 89 ARO-25645.2-GS-CF DAAL03-87-G-0129 3/8

UNCLASSIFIED F/G 13/2 NL

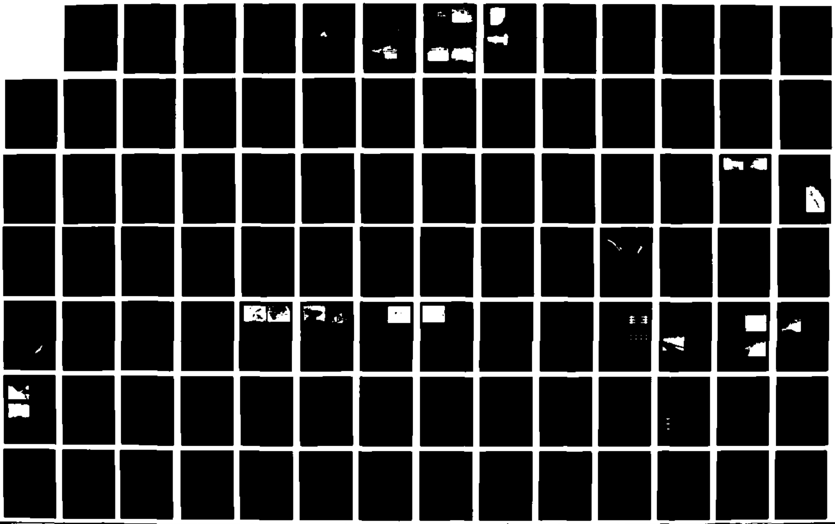

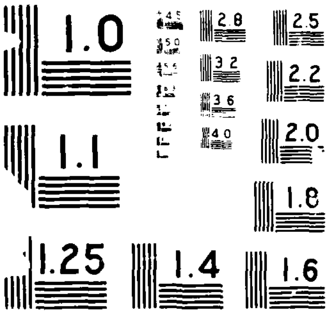
1.0
1.1
1.25
1.4
1.6
1.8
2.0
2.2
2.5
2.8
3.2
3.6
4.0
4.5
5.0
5.6

Stratum Description	Piezometers No.	Level of Installation (m Elv.)	Piezometric Head (M Elv.)		
			After Installation	Maximum After Preload	Recorded on 25/9/87
Upper Sand	22	- 3.0	+0.45	+1.30	+0.65
Upper Sand	*23	- 3.0	+0.65*	+0.95	+0.5
Intermediate Silt	6(GKN)	- 9.0	-	-	+0.76
" "	7(GKN)	- 9.0	+1.0	+1.5	+1.08
" "	18	- 7.5	+0.65	+1.4	+0.95
" "	19	- 5.0	+1.50	+2.0	+1.38
" "	20	- 5.0	+1.70	+2.5	+1.55
" "	21	- 4.0	+0.80	+2.0	+1.05
Lower Sand	16	- 18.0	+0.80	+1.40	+1.66
" "	17	- 14.0	+0.80	+1.60	+1.55

(a) *Fill material was placed near to piezometer 23 before the initial readings were taken.

(b) General groundwater level + 0.45m

TABLE A Piezometer Monitoring Records

layer is about one metre above Datum. Reasons for this variation were not apparent from the site investigations.

The above evidence seems to indicate that the main factors causing failure of dynamic compaction in the eastern part of the site (Fig 4) were the shallow depth of the upper sand above a very loose, waterbound silt stratum together with the complex ground water regime.

CONCLUSIONS

1. It is clearly of prime importance to have a detailed study of the ground water regime before embarking on any ground improvement programme, and especially, when a site tains a thick layer of loose silt.
2. Dynamic compaction is a repid and economic method of ground improvement when it is applied to suitable ground conditions. Results are enhanced considerably by subsequent passes, provided that the excess pore water pressure generated due to the applied energy within the loose subsoil is allowed to dissipate. Ground conditions similar to those encountered in Area 3 are considered unsuitable for dynamic compaction.
3. Full scale load tests designed to meet foundation conditions are considered to be the most appropriate method of verifying ground improvement.
4. Relative density of in-situ silty sand may be assessed effectively using published analytical correlations established with SPT results.
5. The settlement of footings on sand may be assessed reliably using the method due to Schmertmann, but such methods tend to underestimate the deformation of the sand under extended fill loads.

ACKNOWLEDGEMENT

The authors would like to thank the Saudi Hotels and Resort Areas Company (SHARACO), Riyadh, for permission to publish, and Mr N A Trenter, Director, Sir William Halcrow and Partners Ltd for providing valuable comments and facilities to produce this paper.

REFERENCES

Ghosh, N(1982), "Correlation of predicted and measured settlements in full scale loading on sand fill", Proc., 2nd European Symp. on Penetration Testing (ESOPT II), Amsterdam, 567-73.

Giuliani, F and F L Giuliani Nicoll (1982), "New analytical correlation between SPT, overburden pressure and relative density", Proc., Second European Symp. on Penetration Testing (ESOPT II), Amsterdam, 47-50.

Kent, P E (1976), "Middle East - The geological background", Proc., Conf. Engineering Problems Associated with Ground Conditions in the Middle East, the Geological Society, London, Nov., 1-7.

Lambe, T W and R V Whitman (1969), "Soil Mechanics", John Wiley & Sons, Inc, New York.

Schmertmann, J H (1978), "Guidelines for Cone Penetration Test - Performance and Design", Report No FHWA -TS-78-209, US Dept. of Transportation, Washington.

Sir William Halcrow & Partners (1986a), "Half Moon Bay Beach Resort Project, Interim Report on the Performance of the Dynamic Compaction Carried Out at the Site", January, 1986.

Sir William Halcrow & Partners (1986b), "Half Moon Bay Beach Resort Project, Geotechnical Report for the Settlement of Subsoil Under Preloading", October, 1986.

Proceedings: Second International Conference on Case Histories in Geotechnical Engineering, June 1-5, 1988, St. Louis, Mo., Paper No. 5.35

Geogrid Reinforced Soil Retaining Wall on Compressible Soils

R.L. Curtis
Registered Engineer, ATEC Associates, Inc., Marietta, Georgia

V.E. Chouery-Curtis
Geotechnical Engineer, The TENSAR Corporation, Morrow, Georgia

D.A. Miller
Senior Registered Engineer, ATEC Associates, Inc., Marietta, Georgia

SYNOPSIS: A geogrid reinforced soil wall with a wrap-around facing system was successfully constructed on soft, compressible alluvial and residual soils. An originally designed 20-foot (6.1 m) high, reinforced concrete cantilever retaining wall was not constructed because of the expected settlements induced by the wall and backfill. The geogrid reinforced wall was utilized because of its ability to withstand the estimated settlement and because it was considered less expensive than providing deep foundation support of a cantilever wall. This paper discusses the design, construction, and performance of the geogrid reinforced wall.

INTRODUCTION

A 20-foot (6.1 m) high, reinforced concrete cantilever retaining wall was planned adjacent to a proposed clubhouse as part of the site development for a large luxury apartment complex near Atlanta, Georgia. This wall would separate the clubhouse pool area from a small lake to be constructed in a creek channel. During initial grading operations in the proposed retaining wall area, the contractor noticed that the subgrade was very soft. A geotechnical consultant was then retained by the owner to investigate the subsurface conditions in the wall area and to make recommendations concerning design and construction of the wall.

SUBSURFACE INVESTIGATION

Three soil test borings were performed along the proposed curvilinear retaining wall alignment. Standard penetration tests were conducted in the borings at intervals of 2.5 to 5.0 feet (0.8 to 1.5 m). All soil sampling and standard penetration testing were in general accordance with ASTM standard D 1586. The boring data indicated up to 27 feet (8.2 m) of generally soft or loose soils. Alluvial soils were encountered to depths of up to 8 feet (2.4 m) below the existing ground surface. The alluvial soils were deposited by the adjacent creek and typically consisted of fine sandy clay or clayey fine to medium sand (Unified Soils Classification of CL and SC). Residual soils were encountered below the alluvium to boring termination depths. Residual soils are defined as materials formed in-place by the chemical weathering of the parent rock (metamorphic rocks underlying the site include gneiss, amphibolite, and schist). The residual soils were typical of those found in the Piedmont Physiographic Province and generally consisted of micaceous fine sandy silt (ML) and silty fine sand (SM). Standard penetration resistances in the alluvial and residual soils typically varied from 5 to 11 blows per foot in the compressible zone (upper 27 feet of soils). The ground water level was measured at 0 to 6 feet (0 to 1.8 m) below the ground surface in the borings.

Based on the subsurface data obtained and subsequent analyses, it was estimated that total settlements of up to 3 inches (7.6 cm) would occur due to the weight of the required fill behind the wall. Because of varying subsurface conditions and varying wall heights, differential settlements of up to 2 inches (5.1 cm) were estimated. Since it was also estimated that 60 to 70 percent of the total settlement would occur during fill placement, pre-loading was initially considered. However, time constraints set by the owner/developer eliminated pre-loading as a possible alternative. Because of the amount of differential settlement expected and the project time constraints, a conventional spread foundation for the cantilever retaining wall was not feasible.

Two alternatives were then considered for wall construction. First, using the original cantilever retaining wall design, a deep foundation system would be required. Timber piles were considered to be the most economically feasible deep foundation system. The second alternative was to use a flexible wall system that would tolerate the estimated settlement. A polymer geogrid reinforced soil wall with a wrap-around facing was evaluated as the flexible wall system (TENSAR, 1986). The second alternative was chosen by the owner based on economics.

PROJECT REQUIREMENTS

The required retaining wall consisted generally of two semi-circular segments with radii of 16 and 68.5 feet (4.9 and 20.9 m). The smaller radius wall was to be about 8 feet (2.4 m) high while the large radius wall height varied from 2 to 20 feet (0.6 to 6.1 m). Figure 1 shows a plan view of the proposed walls. Since a vertical wall was only required above the proposed lake level, the maximum wall height was changed to 10 feet (3.0 m) supported by a reinforced slope up to 10 feet (3.0 m) high. For architectural reasons, a cast-in-place concrete facing was required for the wall. The concrete facing was designed as a free-standing member subjected to no earth pressure from the geogrid reinforced soil wall. Following construction of the flexible wall and settlement monitoring, the cast-in-place concrete facing would be constructed.

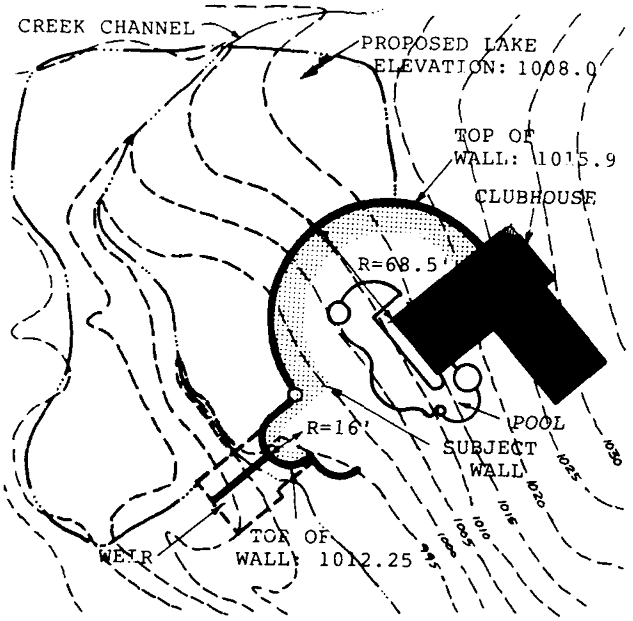

Figure 1. Plan View of Wall

DESIGN

The geogrid reinforced wall was designed using the tie-back wedge method of analysis. It is assumed that active lateral earth pressures are developed for polymer reinforced walls (Jones, 1985). These pressures are then resisted by the tensile force of the reinforcement. The kinematic mechanism of the wall is rotation about a hinged toe and pressures from the backfill retained behind the reinforced mass are also considered in the analysis (Berg, et al, 1986). In addition to internal stability, external stability modes of sliding, overturning, and toe bearing failures were checked using retaining wall analysis techniques.

Overall or global stability of the retaining wall and underlying slope was evaluated using the "Newslope" computer program. This program considers circular failure surfaces and uses the modified Bishop method of slices to determine a factor of safety against failure. The program incorporates geogrid reinforcement by considering the geogrid tensile force as a force that produces additional rotation-resisting moment (Schmertmann, et al, 1986).

Soil strength parameters were determined by the geotechnical consultant based on previous experience with similar soils (ATEC, 1986). The following parameters were used for the wall and slope fill: ϕ' (angle of internal friction) = 28°; c (cohesion) = 50 pounds per square foot (2 kN/m^2); γ (unit weight) = 110 pounds per cubic foot (17 kN/m^3). These parameters are typical for compacted soils in the Piedmont Physiographic Province. For the underlying soft soils, the following parameters were used: $\phi' = 25°$, C = 0 psf, γ = 120 pcf (19 kN/m^3). Ground water was assumed to be at the existing ground surface.

A surcharge equal to 70 psf (3 kN/m^2) was assumed for all cases analyzed to account for pavement and small live loads. The aim of the design was to reach a minimum acceptable factor of safety for global stability of 1.5. For the 10 foot (3.0 m) high wall, 5 layers of TENSAR® SR2 high density polyethylene uniaxial geogrids, with a minimum embedment length of 12 feet (3.7 m) were required to stabilize the soil mass. Polypropylene biaxial geogrids were used for the temporary wrap-around facing system and were placed at a vertical spacing of 1.5 feet. The biaxial geogrids used for the wall face were TENSAR® SS1 geogrids.

Due to the existing soft soil conditions, a layer of biaxial geogrid was included at the top of the existing ground to create a construction working surface. A layer of biaxial geogrid, 24 feet (7.3 m) long was placed 1 foot (0.3 m) below the bottom of the wall to help minimize differential settlement.

For global stability, a layer of uniaxial geogrid was placed 2 to 3 feet (0.6 to 0.9 m) below the bottom of the wall. The embedment length of this layer varied from 18 to 25 feet (5.5 to 7.6 m) based on the slope height. Furthermore, it was necessary to lengthen the two bottom grogrid layers (used for the wall stability) from a minimum length of 15 feet (4.6 m) to a maximum length of 22 feet (6.7 m) depending on the slope height. Figure 2 shows a typical design cross section for the ten foot (3.0 m) high wall underlain by a 10 foot (3.0 m) high slope.

A safe working tensile stress level of 2,000 pounds per linear foot (29 kN/m) was used for the uniaxial geogrid. This value is based on long-term in-isolation creep performance. The ultimate strength of the geogrid is 5,400 (79 kN/m) pounds per lineal foot. A safe working tensile stress (in the cross machine direction) of 270 pounds per lineal foot (4 kN/m) was used for the biaxial geogrid. The peak tensile strength in CMD of this geogrid is 1,400 per lineal foot (20 kN/m).

Drainage for the wall was provided using a continuous drainage net (TENSAR® DN1) with a light weight non-woven geotextile cover placed continuously along the wall face. This drain was tied into a perforated pipe to collect any water and outlet into weep holes in the wall face. Also, a backfill drain was placed behind the reinforced fill to keep the fill from becoming saturated. This drain was placed along the existing slope down to the wall face and tied into the wall drainage system. This drain consisted of a TENSAR® drainage composite DC1200 (a drainage net with a geotextile bonded to both sides). Details of the drainage system are also shown on Figure 2.

CONSTRUCTION

Prior to construction of the slope and wall, the existing soft subgrade was stabilized using a layer of biaxial geogrid. Before the geogrid was placed, the subgrade could not support rubber-tired construction equipment. After the geogrid was placed, a 12- to 18-inch (30 to 46 cm) "bridge" lift of soil was placed using a track-mounted front-end loader. The soil was carefully placed ahead of the loader to keep the tracks from operating directly on the geogrid layer. Following this procedure, the area was stable enough to support rubber-tired scrapers and self-propelled sheepsfoot compaction equipment. The fill slope was constructed using on-site micaceous sandy silts or silty sands. The slope and wall fill was placed in thin lifts (6 to 8 inches loose measure) and compacted to 95% of the standard Proctor maximum dry density (ASTM D 698). Figure 3 shows compaction equipment used in wall construction. A layer of uniaxial geogrid was placed about 2 feet below the wall footing elevation (for global stability) and a layer of biaxial geogrid was placed about 1 foot below the wall footing to minimize differential settlements. When the slope was completed to the bottom elevation of the wall footing, the footing was constructed. Settlement points along the footing were established to determine the extent of settlement as the footing was constructed.

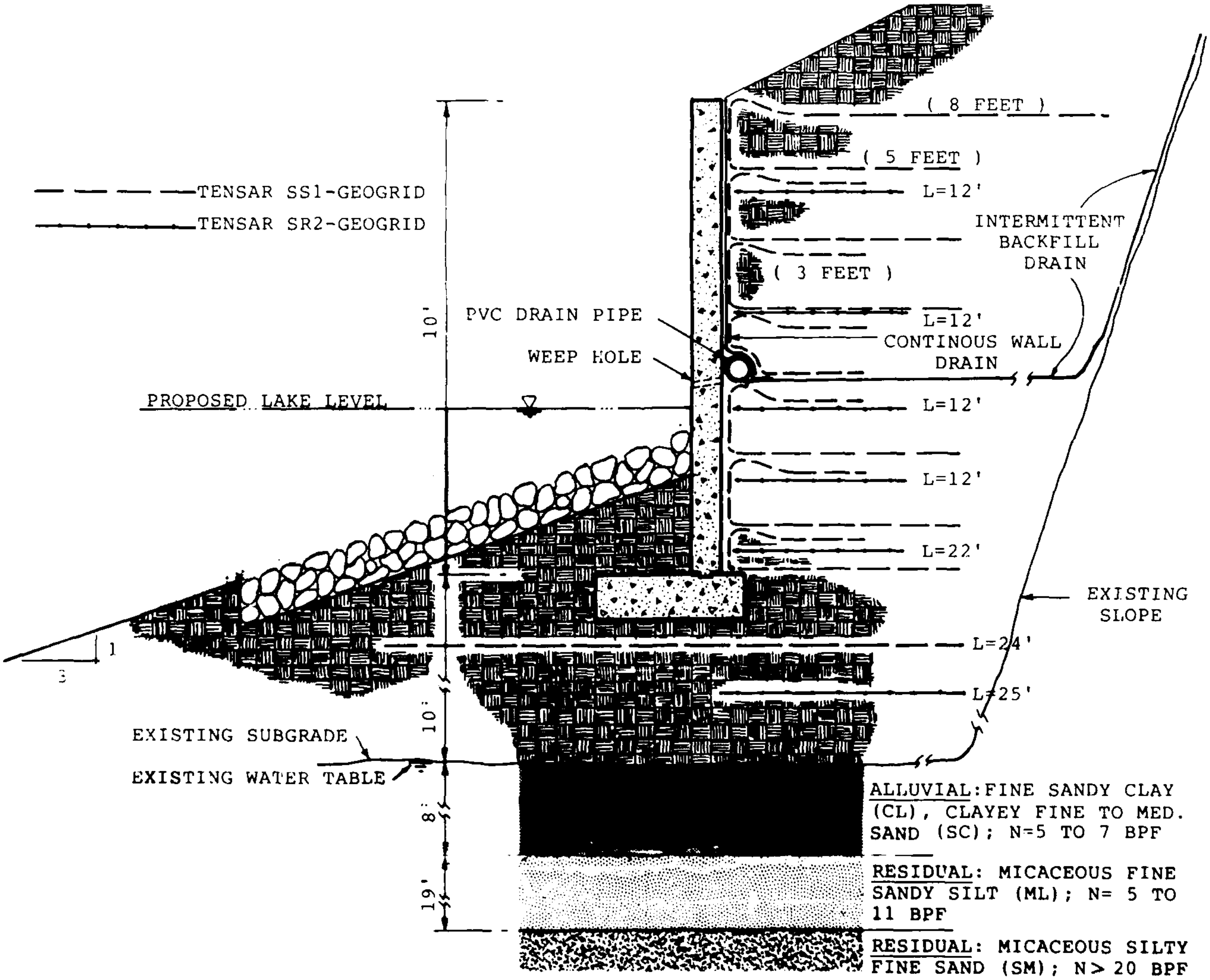
(8 FEET)
(5 FEET)
TENSAR SS1-GEOGRID
TENSAR SR2-GEOGRID
L=12'
INTERMITTENT BACKFILL DRAIN
(3 FEET)
10'
PVC DRAIN PIPE
L=12'
CONTINOUS WALL DRAIN
WEEP HOLE
PROPOSED LAKE LEVEL
L=12'
L=12'
L=22'
EXISTING SLOPE
1
3
L=24'
L=25'
10'
EXISTING SUBGRADE
EXISTING WATER TABLE
8'
ALLUVIAL: FINE SANDY CLAY (CL), CLAYEY FINE TO MED. SAND (SC); N=5 TO 7 BPF
19'
RESIDUAL: MICACEOUS FINE SANDY SILT (ML); N= 5 TO 11 BPF
RESIDUAL: MICACEOUS SILTY FINE SAND (SM); N> 20 BPF

Figure 2. Typical Design Cross Section

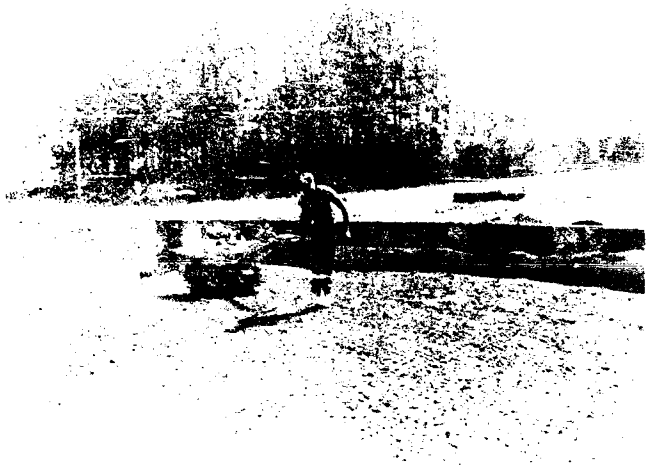

Figure 3. Compaction of Wall Backfill

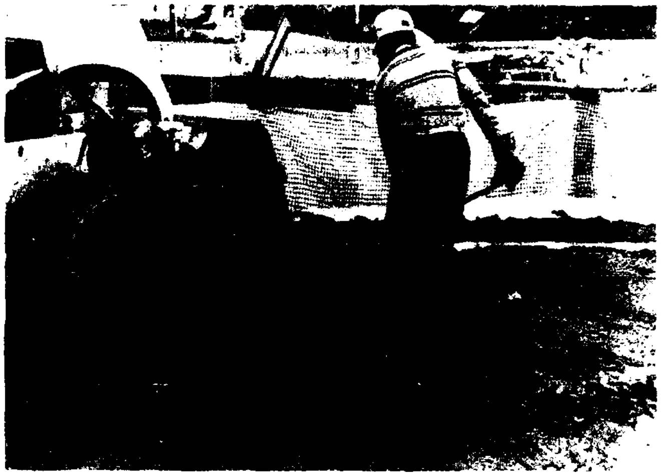

Figure 5. Tensioning of Upper Facing Wrap

Temporary wooden forms were then erected to provide a working face for construction of the geogrid reinforced wall. The wall face was constructed by placing the bottom portion of the wrap on the subgrade and nailing the upper portion of the wrap to the forms. Figure 4 shows the wooden forms with the geogrid and geotextile nailed to the form. After placement and compaction of the required fill depth, the upper portion of the wrap was pulled down and tensioned using pitch forks. Figure 5 shows the upper wrap being tensioned and soil being placed as the wall was continued. At the specified elevations, the main wall reinforcement, TENSAR® SR2 geogrid was placed perpendicular to the wall face. Figure 6 shows the main reinforcement being placed.

The backfill drain and perforated pipe were placed at the specified elevation. The wall drain for the large radius portion of the wall was included inside the facing wraps. For the small radius portion, the wall drain was placed against the geogrid face prior to constructing the concrete face.

PERFORMANCE

When the reinforced wall was completed, settlement measurements were made on the wall footing for approximately one month. Approximately 2 inches of settlement was recorded during the monitoring period. At that time, the settlement was essentially complete and the forms were removed. The geogrid reinforced wall provided a nearly vertical face while the concrete facing was constructed. Figure 7 shows the geogrid reinforced wall with the steel reinforcement for the concrete facing in place.

The concrete facing was completed shortly after the settlement monitoring period. Figure 8 shows the completed wall.

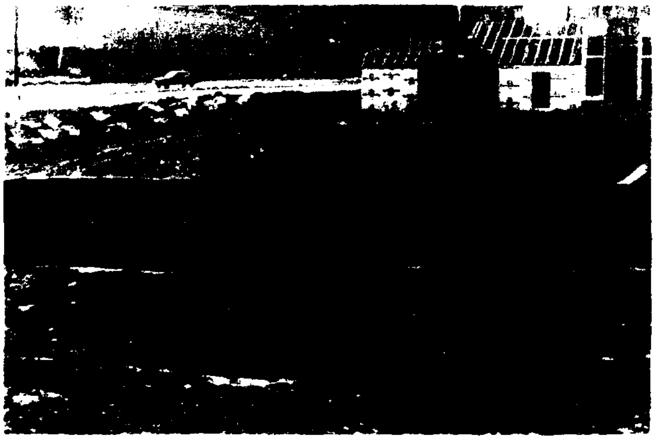

Figure 4. Facing Wrap Attached to Temporary Forms

Figure 6. Placement of Main Reinforcement

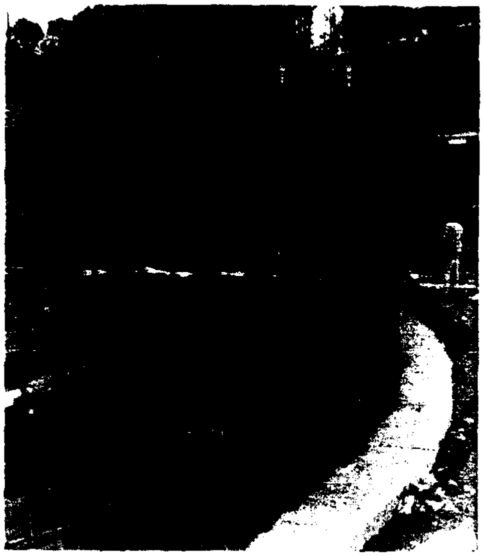

Figure 7. Completed Geogrid Reinforced Wall

Figure 8. Completed Structure

CONCLUSIONS

Because of underlying compressible soils, a conventional concrete cantilever retaining wall was not feasible for this project. Alternatives included a deep foundation system for the cantilever wall or a flexible wall that would tolerate the expected settlements. A geogrid reinforced wall with an underlying reinforced slope was chosen as the most cost-effective solution. Geogrids were used to stabilize the exisitng soft subgrade, reinforce the slope and wall fill, and provide flexible facing elements for the wall. After settlement monitoring of the geogrid reinforced wall, a concrete facing was constructed. The geogrid reinforced wall performed as expected; tolerating the settlement and providing a temporary vertical face.

ACKNOWLEDGEMENTS

The authors thank Harshad Modi of ATEC for his input to this project. Special thanks to Ryan Berg of The TENSAR Corporation for his review of the paper. We also thank Pam McClure and Andy Christian of ATEC for respectively typing the manuscript and drafting the figures.

REFERENCES

ATEC Associates, Inc. (1986), "Subsurface Investigation and Geotechnical Engineering Evaluation - TIMBER TRACE APARTMENTS - Stone Mountain, Georgia" ATEC Project Number 32-63108.

Berg, R.R., Bonaparte, R., Anderson, R.P., and Chouery, V.E. (1986), "Design, Construction, and Performance of Two Geogrid Reinforced Soil Retaining Walls", Proceedings, 3rd International Conference on Geotextiles, Vienna, Austria, Vol. 2, 401-406.

Jones, Colin J.F.P. (1985), Earth Reinforcement and Soil Structures, Butterworth and Co., Ltd.

Schmertmann, G.R., Chouery-Curtis, V.E., Johnson, R.D. and Bonaparte, R. (1987), "Design Charts for Geogrid-Reinforced Soil Slopes", Geo-Synthetics '87 Conference Proceedings, New Orleans, Louisiana, Vol. 1, 108-120.

The TENSAR Corporation (1986), "Guidelines for the Design of TENSAR Geogrid Reinforced Soil Retaining Walls", TENSAR Technical Note RW1.

Proceedings: Second International Conference on Case Histories in Geotechnical Engineering, June 1-5, 1988, St. Louis, Mo., Paper No. 5.36

Performance of Prefabricated Drains in Soft Soils

R. David Charles
Associate, Duffield Associates Consulting Geotechnical Engineers,
Wilmington, Delaware

SYNOPSIS: The use of vertical drains to accelerate the consolidation of soft soils has become a cost effective alternative to the use of pile foundations at many sites. This paper presents a case history of the use of vertical drains to accelerate the consolidation of 20 to 25 feet of low shear strength, highly compressible soils, under embankments of 12 to 25 feet in height. Two separate vertical drain installations at the project site allowed the use of a shallow foundation system for approximately one-half of the foundations. This resulted in a significant savings in foundation costs and allowed an ambitious "fast track" construction schedule to be met.

The purpose of this paper is to present the properties of the site soils and the construction and post-construction observations of the soil response at this site.

INTRODUCTION

The construction of embankments over soft soils typically causes concerns over stability during construction and the subsequent time periods required for settlement to take place. These concerns led to the development of vertical drains to reduce the flow distance and to accelerate drainage, thereby reducing the time for consolidation of the soil. The theory for analyzing consolidation utilizing vertical drains was first developed by Barron. Initially, vertical sand drains were utilized for accelerating the consolidation of soft soils, and the application of Barron's theory to sand drain projects is discussed in a publication by Moran et al.

More recently, because of economic and technical considerations, the use of prefabricated drains has essentially replaced the use of sand drains. These drains are typically "band" shaped corrugated or nubbed plastic cores, wrapped in a geotextile drainage fabric. Barrons' theory is the basis for the analysis of consolidation utilizing prefabricated drains. A discussion of design considerations and methods for prefabricated drain analysis is contained in a recent FHWA report by Rixner et al.

The Northern Solid Waste Facility-1 (NSWF-1), is located along the Delaware River near Wilmington, Delaware and served as the major refuse disposal area for northern Delaware from 1970 until late 1985. Prior to landfilling, the area was utilized for the disposal of dredge spoils by the Corps of Engineers, during the period from 1954 to 1969. The site was a marsh area before its use as a disposal area. A table summarizing the general soil stratigraphy at the site in the early 1980's is presented in Figure 1. The ground surface prior to construction of the landfill was between approximately elevation 17.

Because the NSWF-1 landfill was expected to reach its capacity in 1985, other potential landfill sites were being evaluated in 1982 by the owner, the Delaware Solid Waste Authority (DSWA). A Transfer Station was proposed for the site to accommodate an on-site reclamation facility which recovers metals, glass and other recyclable materials and produces a "Refuse Derived Fuel" (RDF), which can be incinerated to produce energy.

1982 CONSTRUCTION

The transfer station required the creation of a 20 foot grade separation between the upper level tipping floor (El 35) and the lower level "loadout" area (El 15). After evaluating the engineering and cost considerations of various structural and foundation alternatives, it was decided to create the required grade separation by constructing the tipping floor on an 18.5 foot structural fill embankment. It was also decided to construct a 12 foot surcharge embankment on the eastern portion of the site (the "loadout" area), to improve the soils in this area prior to foundation construction, which was scheduled to start in May 1984. The configuration of the embankment is indicated in Figure 2.

Analysis indicated that rapid construction of the embankment to the required heights would result in a potentially unstable condition. Furthermore, consolidation of the subsoils under the design loads would cause an estimated settlement in the range of 1.5 to 2 feet, and under existing conditions would require as much as nine years for 90% consolidation to occur. Therefore, the use of vertical drains to facilitate construction of the embankment and accelerate consolidation to meet the construction requirements was evaluated.

A design value of 0.08 ft^2/day for the horizontal coefficient of consolidation, C_h, was selected for use in the analysis. This value was approximately twice the value of C_v in the

Stratum	Thickness Range	Description	Other Data
1	2.5 ± ft.	Miscellaneous fill	---
2	12 - 13 ± ft.	Medium to high plasticity very soft with some organic material (dredge spoil)	Moisture Content = 40-90% Liquid Limit = 50-57 Plasticity Index = 14-28 Cohesion = 120-400 psf $C_r' = 0.03$, $C_c' = 0.16$ Average Pc' = 1.7 ksf
3	9 - 12 ± ft.	High plasticity silt with some organic material (marsh deposits)	Moisture Content = 60-95% Liquid Limit = 70-78 Plasticity Index = 23-38 Cohesion = 290-650 psf $C_r' = 0.03$, $C_c' = 0.20$ Average Pc' = 1.2 ksf
4	0.5 - 6.5 ± ft.	Peat - fibrous peat in some areas, becoming very silty in others	Moisture Content = 275-475%
5A	---	Medium dense to very dense silty sand (glacial deposits)	
5B	---	Stiff to very stiff medium plasticity silt and clay	Cohesion = 2200 + psf

Note: Ground surface between elevation 17 and 19, groundwater at elevation 12 ±.

FIG. 1 SITE SOIL PROFILE

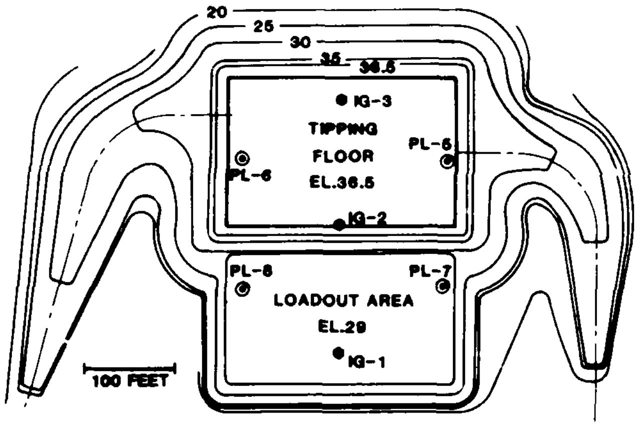

FIG. 2 TRANSFER STATION CONFIGURATION

"virgin" compression range determined from numerous consolidation tests performed on samples of the dredge spoils and marsh deposits in late 1981.

A triangular configuration of drains with an approximate 6 foot spacing was selected for the final design. Prior to construction, three groups of instruments consisting of piezometers and settlement points were installed in the locations indicated in Figure 2. The instruments were installed at the approximate center of the triangle formed by the drains. Approximately 2700 drains, generally ranging in length from 20 to 30 feet, were installed in late September and early October 1982. The earthwork contractor completed the fill placement in approximately 60 days.

During construction, the instruments were read each day to monitor pore pressure and settlement. Typical plots of measured pore pressure and settlement during construction are indicated in Figure 3. Four additional settlement plates were installed 10 days after completion of the embankment in the locations indicated in Figure 2. This data is contained in Figure 3.

Due to a series of events and decisions by the DSWA, the transfer station project was cancelled in 1983. An alternate landfill site approximately 5 miles away had been selected and it was determined that a transfer facility would not be needed. However, monitoring of the instrumentation at the site continued until 1985.

Review of the data obtained indicates that approximately 90 to 100% of the excess pore pressure was dissipated by May 1984 (the proposed start date for foundation construction). The settlement data from IG-1, 2 and 3 indicates that approximately 95 to 97% of the settlement (based on a total settlement as of March 1985) had taken place by May 1984. However, the data obtained from monitoring of settlement plates 5 and 7 on the southern end of the site, indicates that continued settlement was occurring in this area.

1985 CONSTRUCTION

In 1984, the DSWA decided to construct an Energy Generating Facility (EGF) for the purpose of incinerating the RDF to generate steam and electrical energy. The EGF would be constructed at the site of the previous transfer station embankment constructed in 1982. The EGF structure required several grade separations throughout the facility as indicated in Figure 4.

Due to the extremely high equipment loads, and a need to accelerate the construction of the

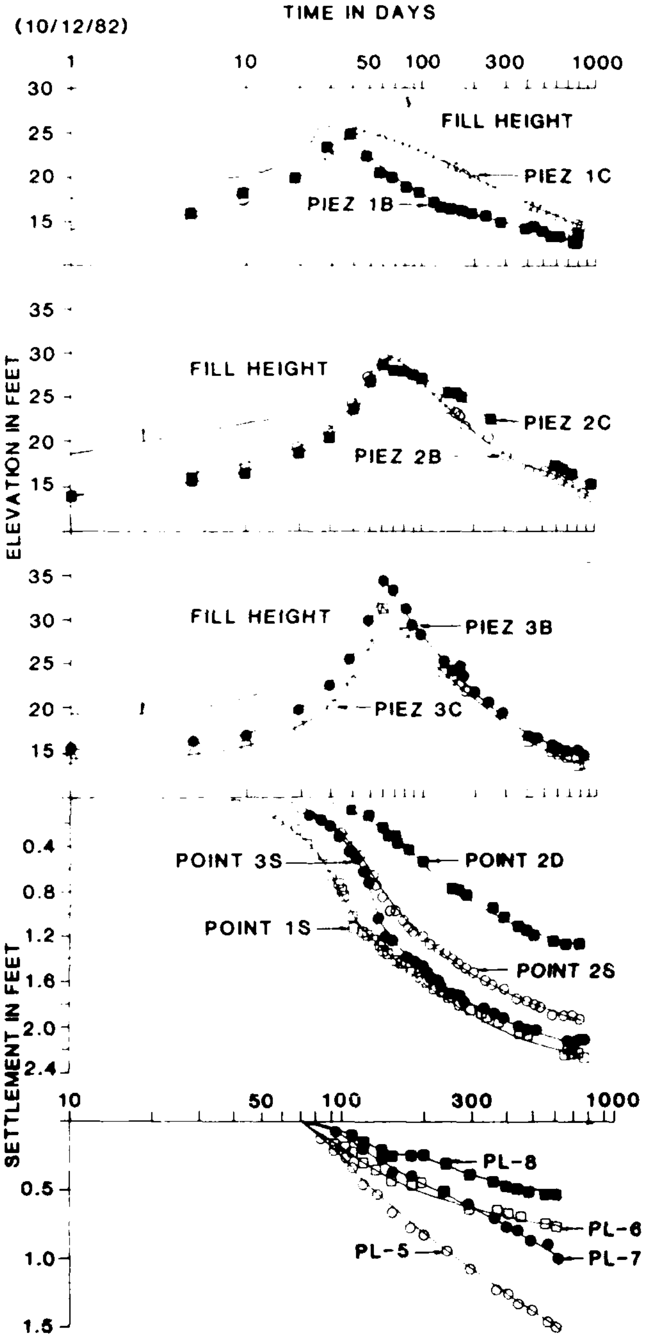

FIG. 3 PIEZOMETER AND SETTLEMENT PLOTS

mechanical installations a portion of the structure and the lower level equipment was pile supported. However, based on the performance of the 1982 drain installation, it was determined that a shallow foundation system could be utilized in the upper level. Because the "footprint" of the EGF structure was much larger than the area previously improved in 1982 Figure 5, additional drain construction was required.

Because of the "fast track" nature of this project, it was determined that only 9 to 10 months was available to construct the embankment fill and obtain the required "precompression" of the subsoils. While the use of shallow foundations was considered possible, there was some concern over the potential for differential settlements between areas which had been previously consolidated by the 1982 embankment, and the adjoining areas which would be loaded by the new embankment. Additionally, the continued settlements which were observed in plates PL-5 and PL-7 also raised some concerns over potential post-construction differential settlements.

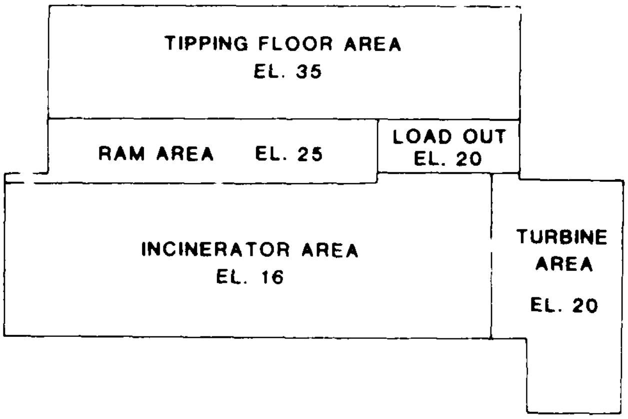

FIG. 4 EGF FINISH FLOOR ELEVATIONS

It was decided to install additional vertical drains on an approximate 3 foot triangular spacing in the areas indicated in Figure 8. Because of the time constraints and differential settlement considerations, the design of the embankment required the construction of 5 and 10 foot surcharges in the upper level building area as indicated in Figure 6.

Prior to the commencement of construction, additional instrumentation was installed at the site at the locations indicated in Figure 6. Several piezometers and settlement points were

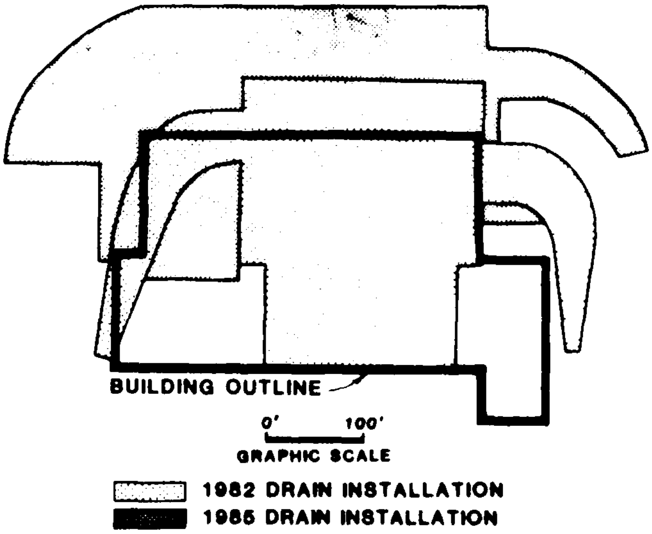

FIG. 5 EXTENT OF VERTICAL DRAINS

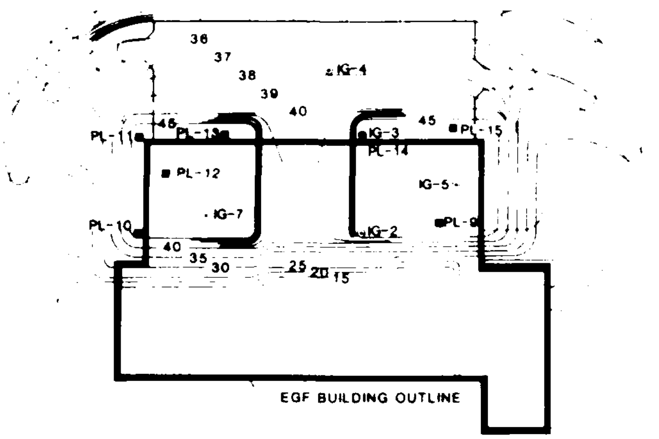

FIG. 6 EGF FILL CONFIGURATION

installed in the area of PL-5 because of the continued settlement observed in this area. Data obtained from piezometer 5B (installed near the base of the compressibles) indicated that an excess pore pressure, apparently resulting from the 1982 embankment construction, existed at the location of this piezometer. A review of the construction records for the 1982 installation indicated that the vertical drains had apparently penetrated below the elevation of piezometer 5B. Therefore, the cause of the excess pore pressure observed before the start of the 1985 construction is not clear.

Approximately 5300 additional drains were installed during the 1985 construction. Construction of the new embankment and surcharge fill took place in approximately 30 days. After completion of the surcharge, settlement plates PL-10 through PL-15 were installed in the areas indicated in Figure 6. Plots of the instrument data obtained during and after construction are indicated in Figures 7 through 10.

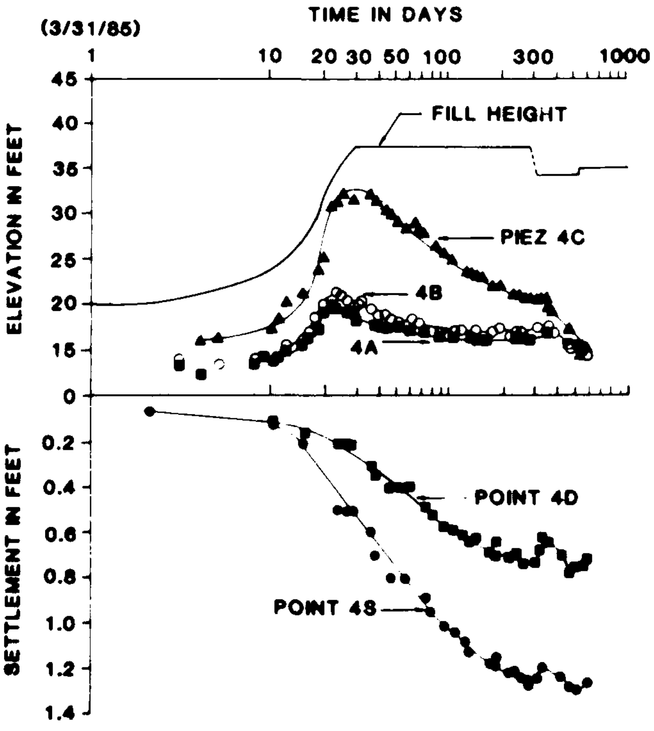

FIG. 7 IG-4 DATA

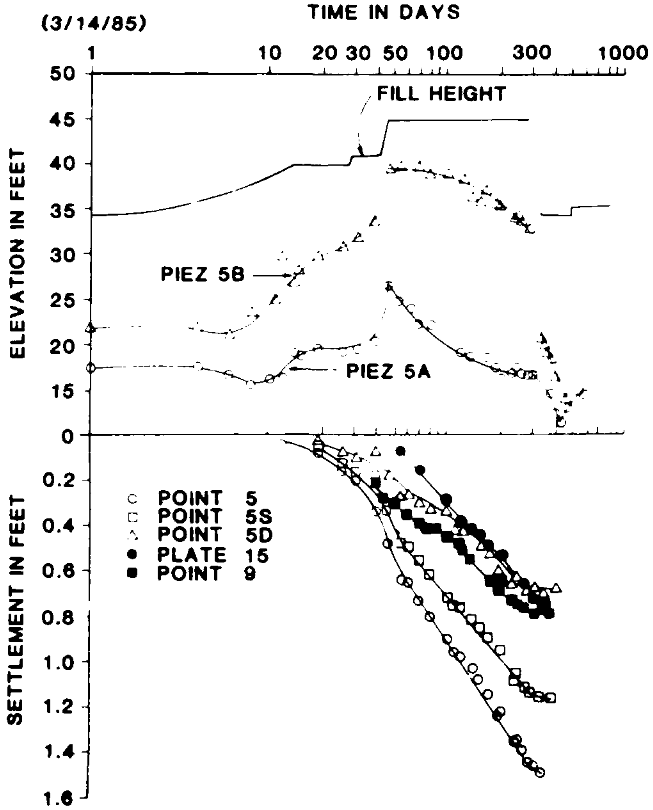

FIG. 8 IG-5 DATA

Settlement data from the various instrument locations was used to monitor the progress of the consolidation and to estimate the magnitudes of settlement and differential settlement. Based upon a review of the data, and the owner's willingness to accept some post-construction differential settlement, it was agreed to remove the surcharge from the northern building area in late 1985 (after an approximate 8 mos. surcharge period) and construct a shallow foundation system. Removal of the remaining surcharge and foundation construction proceeded through February of 1986.

Settlement plates PL-10 through PL-15 were installed in the surface of surcharge and were removed with the surcharge. A majority of the other instrument groups were abandoned due to interference with the construction of the upper level and its structure components. However, instrument groups IG-4 and IG-5 were preserved throughout most of the construction. Recent readings (October 1987) are indicated in the plots for IG-4. However, instrument group IG-5 is now inaccessible. To monitor post-construction settlement, several additional monitoring points were established within the building in early 1986. These points have been monitored periodically through October of 1987. As of

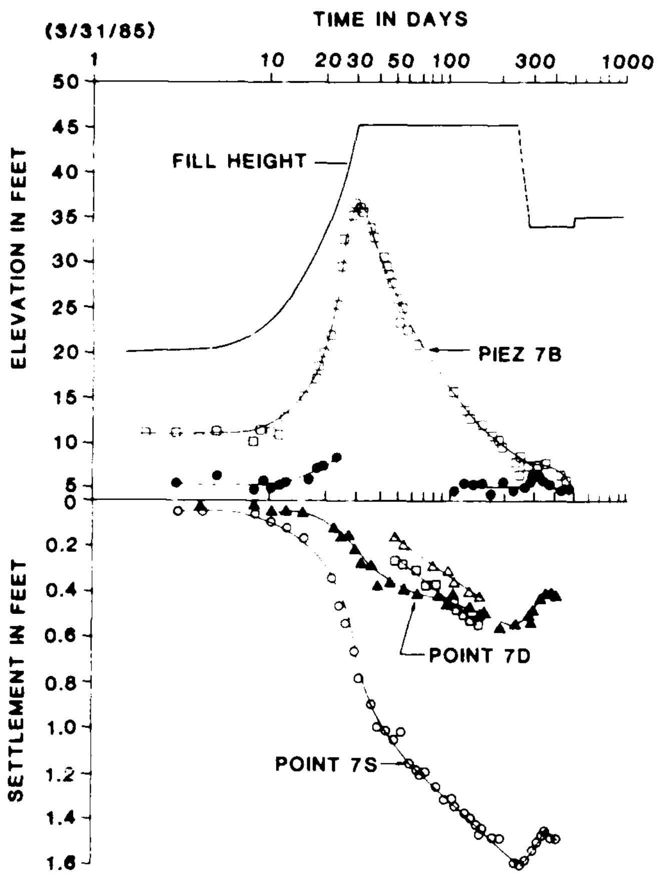

FIG. 9 IG-7 DATA

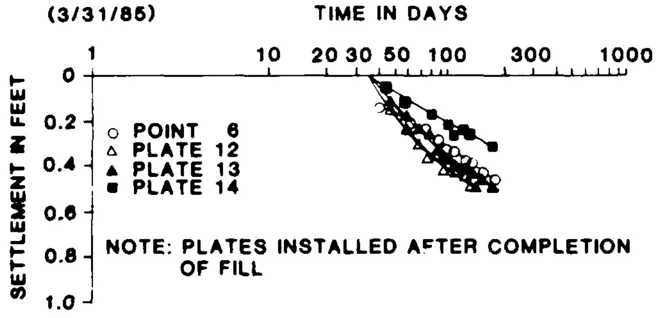

FIG. 10 SETTLEMENT PLATE DATA

that time, the settlements observed are less than one quarter of an inch.

DISCUSSION OF ANALYSIS

The parameters required for the analysis of consolidation are discussed in detail in the publications by Moran et al, and Rixner et al. Briefly, these parameters include:

External Diameter of Influence, d_e - this parameter is a function of the geometry and spacing of the drains. (d_e - 1.05D for a triangular spacing, and 1.13D for a square spacing, where D is the center to center spacing of the drains).

Effective Diameter of the Well, d_w - for sand drains, d_w, is typically the diameter of the sand drain, sometimes reduced for "smear" of the soft soil due to installation disturbance. For analysis of a prefabricated drain system, it is assumed that the "wick" has an "equivalent sand drain diameter" which is analogous to the physical diameter of a sand drain. Several methods of establishing an equivalent drain diameter have been suggested by various practitioners. These include equation (1) below recommended by Hansbo and equation (2) which is discussed in the publication by Rixner et al

$$d_w = \frac{2(b+t)}{\pi} \qquad (1)$$

$$d_w = \frac{b+t}{2} \qquad (2)$$

Where: d_w = equivalent drain diameter
b = long dimension of drain
t = short dimension of drain

Additionally, Fellinius has indicated that larger values than those determined by the above equations might be used, based on consideration of the "free surface area," or the area of the outer fabric which allows water to enter directly into the voids or channels of the drain.

Horizontal Coefficient of Consolidation, C_h - this has been one of the more difficult parameters to estimate for the analysis of vertical drain installations. Several methods of determining C_h have been utilized, which include: determining the ratio of horizontal to vertical permeability in the field or laboratory and using this ratio to convert the coefficient of vertical consolidation, C_v to C_h; and performing laboratory consolidation tests in which the samples are drained radially.

Based on equation 1, the prefabricated drain utilized in both installations at this site (the Alidrain), has an equivalent drain diameter, d_w of 0.22 feet. Using equation 2, the equivalent drain diameter would be reduced to 0.18 feet. In his discussion of vertical drains, Fellenius indicates that based on free surface considerations, the Alidrain may have an equivalent diameter as great as 0.49 feet. The results of recent laboratory testing summarized by Suits et al, indicates that the equivalent sand drain diameter for the Alidrain ranged from 0.11 feet to 0.21 feet for three different types of soils. These tests were performed in a large "wick" drain consolidometer.

The piezometer data obtained at this site were utilized to calculate the effective coefficient of horizontal consolidation, C_h utilizing a method summarized in the publication by Moran et al. The values of C_h were calculated assuming that the piezometers were installed in the geometric center of the triangle formed by the drains, and that only radial draiange took place. Values of C_h were calculated assuming values for d_w of both 0.22 and 0.49 feet. Plots of the values of C_h vs. effective stress are indicated in Figures 11 and 12.

Review of these figures indicates that the smaller value of d_w, results in a larger value of C_h. That is, the values are inversely proportional. Review of these figures also indicates that for an effective diameter of 0.22

feet, the values of C_h are for the most part, typically above the design value of 0.08/ft^2 per day. The plot for an effective drain diameter of 0.49 feet, indicates lower calculated values of C_h.

Review of Figures 11 and 12 indicates that regardless of the drain diameter utilized in the analysis, the coefficient of horizontal consolidation, C_h decreases with effective vertical pressure. This is consistant with observations of other drain installations summarized by Moran et al, and the prefabricated drain installations summarized in the ICE publication.

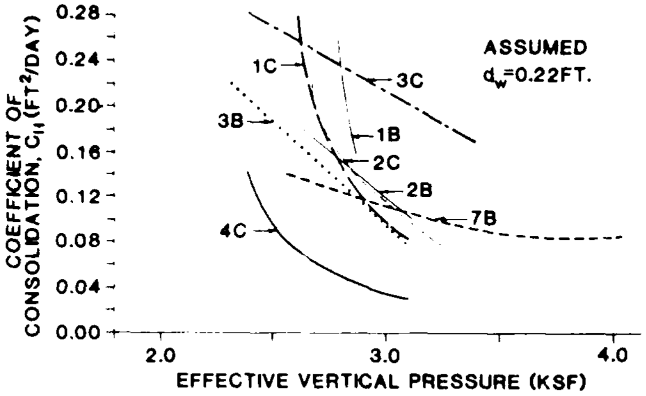

FIG. 11 FIELD C_H (FOR d_w=0.22 FT.)

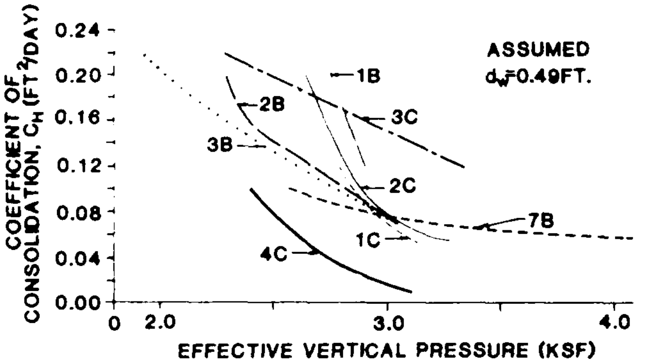

FIG. 12 FIELD C_H (FOR d_w=0.49 FT.)

CONCLUSIONS

Based on the data obtained during our field evaluations and subsequent analysis, we conclude the following:

1. The use of vertical drains was successful in the preconsolidation of the soft subsoils at the site. The use of perfabricated drains resulted in a relatively large savings in construction costs by allowing the use of a shallow foundation system in the eastern half of the building area. The drains were also instrumental in allowing the "fast track" schedule for the building construction to be met.

2. The observed settlements from the 1982 construction ranged between approximately 2 and 2.3 feet which was somewhat greater than that predicted using conventional methods. The observed secondary compression also appears to have occurred at a rate greater than that estimated based on laboratory data. We now believe that variability in the consistency and thickness of the peat layer was primarily responsible for the differences in settlement rate observed across the site.

3. The apparent excess pore pressures observed in the area of instrument group IG-5 prior to the start of the 1985 construction, is not apparent. Review of the 1982 construction records indicate that the drains apparently penetrated below the elevation at which the piezometric data was obtained. It is considered possible that the drains may have been "crimped" due to compression or displacement of the peat resulting from the embankment loading. A conclusive explanation for the observed behavior in this area is not apparent. However, based on the results of the data, the surcharge was effective in accelerating settlement in this area and reducing the potential for post-construction settlement.

REFERENCES

Barron, R.A., "Consolidation of Fine-Grained Soils by Drain Wells," Transactions, ASCE Vol. 113, Paper No. 2346, 1948, p. 718

Fellinius, B.H., "Vertical Drains - The Background and Theory of Vertical Drains with Particular Reference to the Alidrain," (notes for a lecture in Skelleftea, August 24, 1977)

Hansbo, S., "Consolidation of Clay by Band-Shaped Prefabricated Drains," Ground Engineering, Vol. 12, No. 5, 1979.

Institution of Civil Engineers, Vertical Drains, 1982.

Moran, Proctor Mueser & Rutledge, Study of Deep Soil Stabilization by Vertical Sand Drains, Bureau of Yards and Docks, Department of the Navy, June 1958.

Rixner, J.J., Kraemer, S.R., and Smith, A.D., Prefabricated Vertical Drains, Vol I, Engineering Guidelines, prepared for FHWA, September 1986.

Suits, L.D., Gemme, R.L., Masi, J.J. "Effectiveness of Prefabricated Drains on Laboratory Consolidation of Remolded Soils," Consolidation of Soils, ASTM STP 892, 1986.

Proceedings: Second International Conference on Case Histories in Geotechnical Engineering, June 1-5, 1988, St. Louis, Mo., Paper No. 5.37

Case Histories of Foundations with Stone Columns

K.R. Datye
Consulting Engineer, Bombay, India

M.R. Madhav
Professor, Indian Institute of Technology, Kanpur, India

SYNOPSIS : The paper presents case histories of performance of foundations where stone columns were provided, alongwith relevant data regarding structural systems, soil conditions, construction methods and field control criteria. A wide range of applications are included comprising stone columns for area treatment and stone column in small and large groups for isolated footings, pipe pedestals and bridge abutments. In some of the cases design load exceeded the estimated yield load over a part of the stone column length yet collapse did not occur because the soil stress around the stone column increased as more load was passed on to the soil when yield stress was exceeded. There was also the benefit of drainage afforded by the stone columns. Load test data are furnished to substantiate the design approach which takes into consideration the strengthening of the soil annulus around the stone column resulting from compaction and subsequent consolidation.

1.0 INTRODUCTION

1.1 The case histories presented herein report experience of stone column applications for projects of where a total of over 15,000 stone columns were used. The cases include early applications during 1972-76 when theories and design approaches were in the process of evolution. Cases reported include projects where the behaviour matched the postulation, as well as instances when the behaviour was not as expected. The paper begins with a brief review of design approach and theories currently in use. In a further section authors' design approach is summarised and its theoretical basis is explained. This is followed by presentation of case histories with relevant information regarding the soil characteristics, estimated loads and observed performance with regard to settlements and yield loads. A comparison of estimated yield loads and actual loads as well as estimated and observed settlements are furnished for structures which have performed generally as expected. Explanations are furnished of the possible causes of observed deviations from anticipated performance. Salient features of observed behaviour are then summarised in concluding section. Towards the end of the paper, suggestions are made as to further studies and observations needed to clarify some of the unresolved issues and further optimising stone column systems by judicious use of soil reinforcements in the upper 'critical' zones and by providing sand pads with reinforcing fabric layers for minimising differential settlements.

1.2 When the elastic-plastic model and the unit cell approach is used for design of stone columns major uncertainties exist regarding the estimation of yield load. Attempts have been made to estimate the yield loads by adaptation of the cavity expansion theory (Mitchell, 1981), or using the passive earth pressure simulation for a two dimentional case (Van Impe, 1987). A compilation of the results of single column load tests is presented in Section 4.0, and the test results are compared with estimated yield loads. An approximate estimate of the stone column deformation modulus can be made from load test data. Summary of single load test for cyclic loading of 7 day duration are presented to provide an indication of stone column deformation under sustained load.

1.3 The case histories have been grouped to cover various types of applications as detailed below :

- In the first category are included the isolated group of stone columns which are subject to considerable drag loads. There is reason to believe that the stone columns have been during construction or initial surcharge loading, subjected to loads exceeding yield loads calculated according to conventional methods such as Mitchell's adaptation of the cavity expansion theory (Mitchell, 1981). The critical stage of loading for such stone columns is at the end of construction during surcharge loading. It is postulated herein that the additional settlements due to live loads or service loads would be small and would well be within the tolerance of the structure. The case histories substantiate this posulation. Among the cases reported are foundations for steam and ammonia pipelines or large water pipelines. There has been no sign whatsoever of damage by differential settlement in the cases reported, after several years of operation.
- In the second group of cases are included the groups of stone columns supporting rigid structures such as box abutments of major bridges. Here again performance experience of several years and as well observations during recent construction substantiates the design approach.
- In the third group of cases are included embankments and flexible structures subject to area loads and strip loads. The case histories provided an opportunity to verify the design method for a case of soils with significant preconsolidation pressure as well as a pipeline under construction in an area with very soft underconsolidated clays.
- The fourth group of cases covers stone columns in the 'elastic' range such as tank foundations where a conservative basis of design was adopted. The estimated settlement in one case is in fair agreement with the theory of Van Impe, while in another case, the peculiar behaviour of ground treated with 'floating' stone column is discussed to bring out the limitations of the method of analysis used.

2.0 REVEIW OF THEORIES AND DESIGN METHODS

2.1 Theoretical approaches for design of stone columns can be grouped into three categories as described below :

- Analysing the stone column soil system as a 'composite' material where the load shared by the stone column is dependant on the relative values of deformability of the stone column and the surrounding soil. Conventional elastic solution can be used, if care is taken by limiting the load to ensure that the stone column does not yield. The problem then reduces to evaluation of design parameters defining the load deformation behaviour of the stone column and the soil.

In the second method an elastic-plastic stone column behaviour is postulated. The load sharing between soil and stone columns in a unit cell consisting of the stone column and surrounding soil could be based on elastic solutions until yield occurs. Thereafter the stone column load would be limited to the 'yield' value, thereafter the load shared by the soil would be estimated by use of equilibrium relations. Theories such as Vesic's cavity expansion theory may be used to estimate the yield load. Alternatively other modes of failure would be considered and passive pressure theories can be applied by resorting to a two dimensional simulation (Var Impe, 1987).

The third is a semi empirical approach. The stone column system behaviour is postulated in terms of the replacement factor i.e. the ratio of the area of the stone column to the area of the ground treated (α). The relation between the replacement factor, α , and the settlement ratio which is defined as the ratio of settlements of treated and untreated ground β is based on design curves established from past experience on large scale tests.

2.2 The stone column cylindrical element of compacted granular material usually is in a 'high dilatant' condition; high values of angle of internal friction are therefore realised in practice. However, designers often fail to take into consideration the influence of construction methods. It is difficult to model the stone column soil interaction analytically as the soil surrounding the stone column has a complex stress history. It is first subjected to a release of stress while boring. This is followed by recompaction and build up of radial stresses; these stresses could be of a high order depending on the level of compactive effort and consumption of stone and sand. When stone columns are installed through tubes provided with dispensable shoes, the initial release of stress is avoided. An annulus of soil in the immediate vicinity of the stone column-soil interface gains strength as consolidation takes place after installation. The extent of gain varies according to the distance from the soil-stone column interface and is also dependant on the consumption of the stone and the corresponding lateral displacement. There is a radical change in the stress conditions starting from the initial Ko state where the direction of the major principal stress is vertical to a final axisymmetrical state of stress where the maximum principal stress is in a horizontal radial direction. The authors believe that a precise theoretical assessment of the consequences of these stress changes is not feasible. It is also very difficult to verify the theoretical postulations by observation as instrumentation of the zone of interest would be difficult because of the disturbance caused during the installation of the stone columns. One must therefore rely on semi empirical methods and use of load tests to evaluate the parameters used.

2.3 It must also be noted that the stone column behaviour at different elevations would not be the same. In view of the benefit of the increased overburden stress and the availability of comparatively stronger soils at the lower levels, elastic behaviour is often realised in the lower part of stone columns whereas yield generally occurs in the upper layers. Quite often the weak layer immediately below the drying crust or the compacted granular soil pad is 'critical'. It is the authors' contention that, in an optimised design of stone columns, the existence of a zone where yield occurs must be allowed for. The designers must therefore address themselves to be task of analysing the consequences of stone columns 'yield'. In the lower layers where yield does not occur elastic theories can very well be used. Too much refinement in elastic analysis is generally not required since the settlement in the optimised system mainly arises, from the soil stone column deformation in the 'plastic' zone.

2.4 An important aspect of the stone column behaviour in the plastic zone is the contribution made by the stress increase in the soil surrounding the stone column due to the process of load sharing. A conclusion that emerges from an examination of the stone column 'unit cell' behaviour is that there is no hazard of collapse. The stone column progressively gains strength as more load is passed on to the soil. A design which allows for the possibility of 'yield' of stone column in a part of its length is therefore not subject to hazard of collapse and progressive failure, provided that the lateral loads are small. There is however the hazard of stone column failure in sensitive soil. A design approach which relies on the above postulations based on unit cell theory, is not recommended for sensitive clays.

3.0 DESIGN APPROACH ADOPTED IN THE CASES REVIEWED

3.1 The proposed design approach is based on an initial categorisation of the soil zones into elastic and the plastic zones (K.R. Datye, 1982) (Ref. Fig. 1). The stone columns share of load is estimated by using equilibrium methods and a preliminary evaluation is made of the hazard of the stone column yield in different layers considering the in-situ undrained strength and overburden pressure in different layers. This preliminary estimate of 'yield' load is verified by load tests. The realised capacity of the stone column columns (or yield load) has generally been significantly higher than the values estimated according to the parameters suggested by Mitchell (1981). Soil deformation in the elastic zone were estimated by treating the stone column as a compressible pile. The uncertainty in the estimation of stone column settlements in the elastic zone generally arises out of the difficulties in evaluation of the deformation parameters of the soil and the elastic constants for the stone columns. This aspect is discussed further in para 3.5.

3.2 The deformations in the plastic zone are estimated by considering the unit cell wherein the sectional area of the stone column is worked out by examination of the consumption record and it is presumed that the volume of the compacted stone and sand would be about 80% of the total of the loose volumes of sand and stone placed in the stone column.

3.3 Construction Methods : The rammed stone columns were installed in cased bore holes after removing the soil and compacting the stone and sand by ramming as casing was extracted progressively. A gap graded mixture has been used where the maximum size of sand is limited to 5 mm and the minimum size of stone is 25 mm. The sand forms a slurry and works its way into the voids in the stone during compaction when the stone and sand are placed in bore holes full of water. Even if stone and sand was placed in alternate layers thorough mixing has been achieved in practice as verified by inspection of stone columns after excavation and dewatering. Field control was exercised by measuring the consumption and observing the 'set'. The 'set' was defined as the penetration for 25 blows with specified fall of a rammer of specified weight. The installation details are described in Datye & Nagaraju (1981) and the of consequences of installation methods are discussed in Datye & Nagaraju (1984).

3.4 Experience has brought out very clearly the advantages derived from the gain of strength in the soil annulus surrounding the stone column. The maximum vertical stress in the stone column has been generally found to exceed 50 times Cu as against the postulated value of 25 times Cu according to Mitchell (1981).

3.5 Deformation Modulus of the Stone Column : The deformability of the stone column material in situ depends on the material characteristics, gradation and the compactive efforts used in forming the column. If a well graded material is used which is not liable to get crushed at the particle contacts, stone column modulii should match the characteristics of a well compacted rockfill or a dense sand. In the cases reported, highly dilatant and dense material was produced by using a gap graded mixture and observations showed that the voids in the crushed zone were entirely filled by the sand and since a very coarse stone *in the size range from* 25 to 75 mm constituted of hard angular fragments of sound rock was used, remarkably dense stone columns were formed. Particle breakdown, if any, actually contributed to improvement of gradation. In the load test for the first cycle of loading stone column generally reveals very low compressibility corresponding to an elastic modulus of 20,000 to 60,000 t/m^2. After a few cycles of loading and after allowing for consolidation for 7 days at working load, the modulus was reduced and the deformation was increased by factor of about 3. The designs are based on estimated modulus of 8000 t/m^2, which is close to the values suggested by Mitchell. It should be noted that the design values recommended take into consideration the likely increase of the deformation of the stone column due to the consolidation of *the soil* in the radial direction in the soil annulus surrounding the stone column. The actual performance of the stone columns in groups is expected to be better than single column as the opportunity for lateral deformation gets restricted due to increase in the vertical stress in the soil as the stone column deforms in the plastic range and a greater share of load is passed on the soil.

3.6 Soil Modulus : The relevant parameters of the soil constituting the unit cell is the drained oedometric modulus. *It is usually adequate to estimate Pc from shear strength* measurements, on the basis of Cu/pc relations and coefficient of compressibility from laboratory consolidation tests.

3.7 Elastic Analysis : It is the authors' view that conventional methods of analysis for compressible piles or composite material constituting the unit cell are adequate. Too much refinement in the analysis of the elastic settlement is not usually required in practice, since consolidation is very rapid and rectifications or modifications can usually be carried out after a short period of observation.

3.8 Time of Consolidation : The actual time of consolidation of the stone column system has been found to be very short (usually less than 2 weeks). This is due to several factors described below :

- *There appears to be no smear effect presumably due to* remoulding of the soil near the stone column interface and a thorough mixing of the sand and soil.
- There is reason to believe that hydro fracturing occurs due to the high radial stresses developed during compaction *and this would increase the horizontal coefficient of conso*lidation.

4.0 SINGLE STONE COLUMN BEHAVIOUR

4.1 The single stone column behaviour was interpreted on the basis of an elastic-plastic model where a single column load test which is essentially similar to a pile load test was used (See Fig. 2). The load is transferred by means of a cylindrical loading element to the top of the stone *column situated at a depth of* about *1.2 m or more depending* on the soil condition. By using a smooth sided cylinder coated with bitumen the friction is minimised and it is presumed that the entire load in the single *column test is transferred* to the top of the stone column. The test results are interpreted in a conventional way as in pile load tests and the yield stress is worked out by dividing the yield load by the area of the stone column estimated from the consumption data. It is presumed that the stone column cross sectional area corresponds to the average net volume per metre in the zone of interest and the net volume of the compacted sand *mixture is* taken to be 0.8 x the volume of sand plus stone *consumed* during the installation of the stone column as measured in boxes or bins. A parameter F'sc was derived as per following equation.

$$\sigma v \quad Cu \; F'sc$$

where σv = yield stress in the stone column
Cu = undrained cohesion

4.2 Mitchell has proposed, based on the Vesic's cavity expansion theory *a value of 25 for* F'sc. But *in the* cases presented, the F'sc values turned out to be in excess of 40 and were in fact often in the range of 50-60. (See Table I). The data compiled *in table pertain to 1830 mm diameter* piepline, Sion Koliwada; 2345 mm dia pipeline, Kasheli; and stone column installations in Mangalore Chemicals & Fertilisers. Low values are only for very weak soils Cu ~ 0.6 - 0.7 t/m^2.

4.3 'E' value for the stone columns are estimated from individual stone column load test results. The 'E' value for *the first cycle (immediate) loading of the stone column* (undrained modulus) is as high as 50,000-70,000 t/m^2 while for sustained loading (7 days loading) the 'E' value is about *7000* t/m^2. The data are presented in Table *I*. The estimation of 'E' are very approximate and it gives only order of magnitude. The E value has been very much in the range as suggested by Mitchell (1981) i.e. 4000-7000 t/m^2.

4.4 The settlement magnitude for the different foundations are as follows :

Untreated ground	500-100 mm	- 10 m thick layer of clay
Stone column treated ground	50 - 100 mm	- 10 m stone column length

Considering an 'E' value of 8000 t/m^2, strain in the stone column at yield would be 0.6%, which will cause a settlement of 60 mm for a 10 m long stone column. This shows that the settlement of the stone column treated ground would be in the range as mentioned above.

5.0 ISOLATED GROUPS OF STONE COLUMNS

In the cases presented below, the footings bear on stone columns covered by a pad of granular soil 0.6-1.0 m thick. The small groups of stone column thus installed are observed to have performed well. Total load including estimated drag forces were of an order suggested by Broms (1979). The stone columns would have yielded over a part of its length. Even under heavy loads the stone column system did not show any signs of *collapse and the settlement is very small* at the end of construction (of the pipeline/pipe racks).

5.1 Pipe Rack at IFFCO, Kandla (1972)

5.1.1 IFFCO Kandla has constructed pipe racks in 1972. The footings of the *pipe rack were supported on 750 mm* dia 10 m long stone columns.

5.1.2 Subsoil profile and characteristics are presented in Fig. 3.

5.1.3 Stone column design : The stone columns were designed to carry 20 t sustained load and 30 t as short term maximum load. The footings were treated as rigid pile caps, and each footing was supported on 6 stone columns.

Loads on one footing were as follows :

Drag load (upper bound)	120 t
D.L. + L.L.	150 t
Preload (surcharge)	123 t
Total	393 t

With 50% of Drag load (lower bound) total = 333 t.

Drag load was calculated according to Broms guidelines - Broms (1979).

Therefore each stone column was subjected to estimated vertical load of 55t - 65 t (nearly 2.5 times the load given by Mitchell's "25Cu" criteria).

5.1.4 Behaviour of the Stone Column Foundation : The final settlement observed were 15 mm (maximum) to 6 mm (minimum) whereas that of untreated ground would have been of the order of 800 mm. Also the time involved in removing, placing the preload, installation of sand drains etc. would have been considerable. With the piles, the major problem would be the drag caused by settlement of surrounding soil.

5.2 2345 mm diameter Pipeline at Kasheli near Bombay

5.2.1 The pipeline is constructed from Anjru Diping to Majiwade in Thane Dist. The Pipeline alignment is nearly 8 km long and crosses several creeks. The pipeline is divided into 3 sections as follows :

Section 1	Majiwade to RT4 (underground pipeline)
Section 2	RT4 to C-point (piepline above ground)
Section 3	C1-point to G-point (pipeline above ground and over bridge III)

Typical subsoil profiles and soil characteristics are presented in Figure 4.

5.2.2 Stone Column Foundation : The pipeline is supported in concrete pedestals with base area 4.2 m x 2.1 m through which 70 T piepline load is transferred to the ground. Each pedestal bears on 6 rammed stone columns. Nominal diameter of the stone columns is 750 mm. For compaction control first 'set' was taken at a depth of 4 m above tip level and for each 3.5 m additional length one 'set' was taken. The set criteria was for 1.5 T rammer and 1.5 m fall penetration should be less than 20 mm for 25 blows. Approach embankments for the bridges were provided with area treatment with stone columns. Average length of stone columns were as follows :

Section 1	3 - 7 m
Section 2	4 - 8.5 m
Section 3	4 - 7 m

For these sections average diameter of stone column 800 - 1000 mm, Cu of the soil = 1 t/m^2.

5.2.3 Load on each footing was as follows :

Dead load of pipe	13 t	
Pedestal load	21 t	
Drag load	112 t	
Total	146 t*	at the end of construction
Additional water load	45 t	
Final load	191 t**	at the ime of commissioning the pipeline.

* Therefore load/column was 25 t.

** At the time of commissioning the pipeline, load per column was 32 t.

5.2.4 Settlement Monitoring : A few pedestals were selected and provided with magnetic settlement markers, surface settlement markers (plate type) and piezometers to monitor the settlements of clay layers and ground. In almost all the cases, the settlement markers were installed when 50% of the loading (i.e. embankment construction) was over. Settlement recorded was 30 mm. Since Δp is very small, the settlement at the time of commissioning the pipelines would not be of any consequence (Ref. Annexure 1).

5.2.5 Consumption data were analysed considering 80% of the loose volume dumped in. For the stone column gap graded materials were used comprising of stone column of size 25 mm to 75 mm and sand of maximum particle size 5 mm in the ratio of 5:2.

5.2.6 If the stone column would have been designed using Mitchell's '25 Cu' criteria (with F.O.S. = 1) the number of stone columns would have been as large as 16 as against 6 columns provided, which show no sign of yielding.

6.0 LARGE GROUP OF STONE COLUMNS

6.1 Belapur Bridge Abutment (1975)

Stone columns were used for treatment of foundations of the abutment of a major highway bridge near Bombay. The brdige is over a creek and has spans of 50 m, designed to carry a 70 t tracked vehicle. Approach to the bridge is an embankment on ground treated with 40 mm sand drains. The box abutment rests on 37 Nos. of 750 mm diameter rammed stone column with spacing 1.7 m. The design capacity of the stone column is 25 t, the stipulated yield value of 40 t was confirmed by load tests. The bridge deck rests on caisson foundations. Soil characteristics are as exhibited in the figure 5. The load intensity at the base of the abutment is 12 to 14 t/m^2, considering an embankment height of 6.7 m having unit weight of 1.8 t/m^2. The actual load may be higher due to drag forces. Settlement of the virgin soil under this load would be of the order of 1.75 m. Settlement as observed after 7 years of construction is of the order of 8 cm (accuracy ± 5 mm), considering that the deck slab of the bridge and box abutment were constructed to same elevation. This settlement is less than 5% of the settlement of the virgin ground under comparable load. Considering load intensity of 14 t/m^2 and plan area of box abutment 4.5 x 12 m, the estimated load is 756 t and a total drag of 338 t calculated as per Broms' guidelines (Broms, 1979). The load per stone column was almost equal to the design load since 37 stone columns were provided. Alternatives such as piles, preloading were examined and rejected. Piles would have been subject to heavy drag forces and lateral loads due to the deformation of the soil. Preload would have required longer time for stage loading and would have interfered with the construction of the abutment. The structural performance of the abutment is satisfactory except for a minor crack due to an unsatisfactory junction detail. The settlement is stabilised and there is no noticeable settlement in the last 5 years.

6.2 Kasheli Box Abutment

This box abutment was supported on 49 m x No. of 750 mm diameter stone column spaced 1.3 m c/c. The box abutment was designed to carry two pipeline of diameters 2345 mm and 3100 mm on either side and a road in the middle maximum stress intensity at the foundation level is 25 t/m^2. A compacted sand pad of 400 mm thickness is provided between the box abutment footing and stone column top. The soil profile is exhibited in Fig. 4. Over a period of more than 1 year the box abutment has not shown any significant settlement (i.e. observed settlement is less than 50 mm).

7.0 AREA TREATMENT WITH STONE COLUMNS

As against the individual footing i.e. small group of stone columns, the large group of stone column is capable of reaching much more load because each unit cell of stone column bears more load due to, radial confinement of stone columns. In large group the loads also turned out to be very small. The cases falling under this category are reported below.

7.1 Large Scale Test Plot at Bhandup near Bombay (1982)

7.1.1 Construction of lagoons for treatment of sewage is contemplated near Bhandup, a north-east suburb of Bombay. Use of stone columns is foreseen for improvement of the ground for the embankment of the lagoon and foundations of various structures. An instrumented test embankment was constructed to verify the design approach and specifically the following aspects :-

- Use of single column load test data for evaluating the yield load parameters for large stone column groups.
- Estimates of increase in stone column capacity for stone columns in large groups subjected to area loads.
- Use of equilibrium methods for estimating the stress in the soil in stone column treated ground and corresponding values of settlement.
- Verification of the efficacy of stone columns as load relievers for ensuring overall stability of embankments on soft clay.

7.1.2 The subsurface profile and soil characteristics are exhibited in Fig. 6. The relevant data are summarised bleow :

Cu 0.7 t/m^2 $Cc/1+eo$ = 0.23
Depth of clay 4.8 m

7.1.3 The stone column layout was selected to provide a factor of safety of 1.4 with respect to overall stability. *At the designed height of embankment, the yield capacity* of stone column was exceeded so that a considerable part of the applied load was shared by the soil. Shear deformations were expected along with significant lateral movements near the toe of the embankment.

7.1.4 Following Instruments where provided for monitoring

- Overflow type as well as magnetic type buried settlement markers.
- Casagrande piezometers placed below the centre of the embankment.
- Lateral displacement markers installed near the toe of *the fill to indicate horizontal movements.*

The scheme of instrumentation is exhibited in Fig. 7.

7.1.5 Single column load test results for the rammed stone columns show that the column did not yield even when the vertical stress intensity in the column had reached 45 Cu.

7.1.6 Several settlement markers were installed, many of liquid level markers did not function due to damage of the tubing by rodents. However, 5 markers functioned satisfactorily. Maximum observed settlement varied from 90 mm to 125 mm giving an average settlement of 112 mm at the centre of the loaded area. The observed settlements in an adjoining sand drain test plot were analysed to verify the design values of parameter $Cc/1+eo$ & Pc. Based on these verified parameters the settlement of untreated ground at the load imposed on the stone column test plot was estimated as 450 mm. A ratio of settlement of stone column treated ground to settlement of untreated soil was 0.25. The stone columns arrangement below the embankment has an area replacement ratio ($1/\alpha$) of 4.4.

7.1.7 The relation between $1/\alpha$ and β are computed by the equilibrium method allowing for the stone column yield. Curves accounting for the effect of preconsolidation pressure are also shown in Datye & Nagaraju (1984). Observed settlements are quite close to values estimated by equilibrium theory even after making some allowance for the probable error in estimation of the tributary are for the stone column groups and the corresponding imposed load on the unit cells.

7.1.8 Lateral displacements were monitored by rigid stakes. The top stiff descicated clay and compacted general fill was isolated by installing the marker in 60 cm diameter RCC pipe. Horizontal movements of the marker were measured *by a theodolite and the tilt was read by placing a tilt*meter on top of the marker. Lateral displacements were computed from tilt readings and theodolite readings.

Even for 6 m height of fill were small which confirmed that factor of safety against shear failure was sufficiently large. Movements were accentuated *only after excavating* for a depth of 1.5 m below ground level near the toe even then the lateral movements were smaller than an adjoining plot with 5 m fill load on untreated ground.

7.2 Stone Column for 1830 mm dia Pipeline, Sion-Koliwada, Bombay

7.2.1 The water pipeline at Sion Koliwada is supported on the ground treated with an arrangement of stone columns consisting *of two rows at a spacing of 4 m along the rows* and 2 m between the rows and a line of stone column in the centre at spacing of 4 m c/c.

7.2.2 Very soft underconsolidated clays deposits (4 m thick), having a Cu of 0.6 t/m^2, was encountered here through which stone columns were installed bearing on dense murrum strata. *Final compaction 'set' criteria were followed for the stone* column installation as discussed earlier.

7.2.3 Settlement monitoring data are not available at the time of writing this paper. However, when the data are available, they will provide good basis for the stone column design approach discussed earlier.

8.0 STONE COLUMNS IN ELASTIC RANGE

For critical structures such as storage tanks storing hazardous liquids where large settlements could not be tolerated, the large groups of stone columns were designed conservatively. In these cases a 2.0 m thick compacted sand pad has been provided for load dispersion.

8.1 Phosphoric Acid Tanks at Mangalore Chemicals & Fertilisers, Mangalore

8.1.1 Subsoil profile is presented in the Fig. 8.

8.1.2 Tank Data :

No. of tanks = 2
Dia. of the tanks = 23 m
Storage height = 13 m
Design load intensity at the tank bottom = 22 t/m^2

8.1.3 Stone Column Foundation :

Type of stone column = Vibro-float
Nominal dia. of stone column = 750 mm
Total No. of stone columns = 780 (for the two tanks)
Spacing of stone column = 1.3 m c/c in triangular grid
Load intensity at the top of stone column = 14.43 t/m^2
Load on the unit cell = 19.3 t

While the individual stone columns were subjected to load test, settlement under 35 t load was 6-15 mm.

8.1.4 When the tanks were subjected to hydrotest they have shown settlements of 39 mm and 55 mm.

8.1.5 Considering an average sectional area of 0.785 m^2 and Cu value of 1 t/m^2 the stone column capacity would be 20 t according to Mitchell (1981) and with a factor of safety of 3 times the number stone columns would be required.

8.1.6 Settlement calculations are presented in Annexure 2.

8.2 Phos Acid Tanks at IFFCO, Kandla

8.2.1 Tank Data :

No. of tanks = 2
Dia. of tanks = 28 m
Storage height = 10 m
Design load intensity at the bottom of the tank = 20 t/m^2

8.2.2 The subsoil characteristics are same as presented in Fig. 3.

	Initial values	Values after preloading
Sand fill	= 2.0 m	
Soft clay (3.0 m thick) Cu	- 1 t/m^2	3.2 t/m^2
Clayey sand (5.0 m thick) Cu	- 3 t/m^2	4.5 t/m^2

Dense sand layer below clayey sand layers.

8.2.3 Area Treatment : Sand drains were provided in the entire area and the area was preloaded upto half the maximum design stress. 1 m of the top soft clay was removed and filled with compacted sand and thereafter 750 mm rammed stone columns were installed. The tank was constructed on a sand pad of total 3 m thickness.

8.2.4 Testing of the Tanks : The tanks were tested by filling water and then with acids. The settlement recorded are as follows :

	Water load (10 t/m^2)		Phos acid load 18 t/m^2		Total	
	Max (mm)	Min (mm)	Max (mm)	Min (mm)	Max (mm)	Min (mm)
North tank	60	48	142	74	202	122
South tank	49	42	118	80	167	122

8.3 Settlements observed versus computed

8.3.1 Results of computations are summarised in Annexure 2.

8.3.2 For M.C.F. computed settlements are close to the values computed by Van Impe method.

8.3.3 In Kandla settlement would be very small as by equilibrium method considering that the soil was preloaded prior to stone column installation and stone column yield value was 30 t. The large actual settlement can be attributed to settlement of compressible soil layers below stone column tip. The stone columns tend to concentrate the load increasing the intensity on the soil layer below the tip. The effective preload intensity in the lower layers is singificantly less than the applied load on the surface. These two factors seem to have contributed settlement beyond the estimated values.

9.0 CONCLUSIONS

9.1 The case histories bring out clearly the advantages of using a simple theory based on a one dimensional analysis where the soil-stone column interaction is simulated by unit cell consisting of a cylindrical element of compacted granular soil placed within a soil annulus. A simple linear elastic model of stone column behaviour and equilibrium relations have been used successfully to predict behaviour of ground improved with stone columns.

9.2 Precise modelling of the soil-stone column interaction is not feasible in view of the complications arising from a complex stress path followed by soil elements around the stone column, involving relaxation from an initial Ko state to a stress condition with high radial horizontal stresses. Rotation of the direction of major principal stress, variation of stress conditions with distance from the soil stone column interface further complicates the analysis. The benefit of axial symmetry could be taken by adopting the unit cell simulation. The reliability of prediction very much depends on accuracy in estimation of the odeometric modulus of the soil, determination of sectional area of the compacted stone column insitu and estimation of the yield load as well as deformation modulus of the stone columns. If the stone column section is determined from consumption records and elastic modulae in the range of values suggested by Mitchell are used, conventional elastic solution provide an adequate basis for estimation of settlements for stone column systems working in the elastic range.

9.3 A major element of uncertainty lies in the estimation of the yield stress for the stone column. This parameter is strongly influenced by construction methods. For the cases reported it has been found that the actual stone column capacities realised are about twice the values estimated according to Mitchell's parameters based on cavity expansion theory (Mitchell, 1981).

9.4 The case histories substantiate the author's postulation that the stone column in a unit cell would not collapse as the increased load transferred to the soil after local yield occurs, improves the capacity of the stone column. The case histories substantiate the author's view that factor of safety in the range of 4-3 is not necessary. Number of stone columns required can very well be determined by taking the unit cell capacity to be equal to yield loads measured in single column load test.

9.5 The case history demonstrates conclusively that there is no hazard of long term increase in the deformation by progressive enlargement of the stone column as the surrounding soil consolidates. The long term or the sustained load modulii are in the range of values proposed by Mitchell (1981) eventhough the loads for each unit cell are 2 to 3 times the capacities based on Mitchell's parameters. Several years of post construction performance observations over a range of soil condition bring out clearly the merit of an observation based design approach where the design parameters were evaluated by conducting single column load tests. Suggested elastic-plastic model provides a good assessment of the settlements when yield occurs over a significant part of the stone column length when replacement ratio is high. However, when stone column behaviour is in elastic range as for cases when replacement ratio is in excess of 0.4 the Van Impe model would provide a better prediction.

9.6 As the stone columns also function as a drain and the consolidation of the surrounding soil takes place in a very short period, adverse consequences of deviation from the postulated behaviour can be taken care of by controlled stage loading and use of surchage loads. In initial stages of loading observations of settlements and pore pressures by magnetic plate settlement markers and porous tube piezometers located at various elevation could be adequate for verification of stone column behaviour. By choice of suitable structural system, structural damage can be avoided and therefore too great a refinement in estimation of settlement is not necessary. The case studies have brought out the importance of the influence of construction method. Successful application of the suggested design approach is dependant on establishing field procedure and compaction control criteria in the initial stages of work by observing consumption of stone followed by use of load tests to verify the estimates of yield loads and deformation modulii.

9.7 Suggestions for Further Research

There is a need to take up systematic investigations of unit cell behaviour by laboratory large scale odeometer tests and mathematical modelling to verify the postulation made herein regarding the absence of hazard of collapse of stone columns subjected to loads exceeding the estimated yield loads. More systematic investigation is also needed of the gain in strength of the soil annulus surrounding the stone column and the corresponding increase in the yield load. This could best be done by studying the soil behaviour in large odeometers tests and establishing the relationship between the post consolidation water contents and the state of stress in the soil annulus for given initial void ratio Pc and Cc values. The field observation of moisture content in similar soil after installation of stone column and the reduction in the moisture condition as compared to initial conditions will help to substantiate the postulated unit cell behaviour.

More observations from large loaded area and as well as small groups with magnetic settlement markers porous tube piezometers and soil moisture content measurement before and after consolidation will help to verify the zone categorisation and postulated load settlement behaviour.

There is a need to standardise the load test procedure. Use of load cells would help to establish the actual stress developed in the stone column and by using loading elements of various lengths the yield load at various levels can be determined.

By use of soil reinforcement for the granular fill the hazard of premature collapse of the stone column in the critical zone can be minimised, thereby increasing the capacity of stone column. There is also the prospect of using sand mats reinforced with geotextiles which would minimise differential settlement. In many practical applications stage loading could then be used in the place of preloading to take care of differential settlement.

ACKNOWLEDGEMENTS

The authors would express their appreciation of the co-operation of Indian Farmers Fertiliser Co-op. Ltd. & Municipal Corporation of Greater Bombay in load testing observation and in accepting an observation based approach especially in the earlier stages of the development of the stone columns. Discussions with Prof. Van Impe and Prof. Juran have been helpful in clarifying the issues. The encouraging observations of Prof. Broms on authors papers during early stages of the development have been a great value in optimising stone column designs.

REFERENCES

Barksdale, R.K., Bachus, R.C. (1981) : Report on 'Site Improvement using Stone columns', prepared for U.S. Department of Transportation Federal Highway Administration.

Broms, B (1979) : 'Negative Skin Friction', State of the art report, Proc. of the 6th Asian Regional Conference, Singapore.

Datye, K.R., Nagaraju, S.S. (1981) : 'Design Approach and Field Control for Stone column', X ICSMFE, Stockholm.

Datye, K.R. (1982) : 'Settlement and Bearing Capacity of Foundation System with stone columns', Proc. of the International Symposium at AIT, Bangkok.

Datye, K.R., Nagaraju, S.S. (1984): 'Optimisation of Stone column design', Proc. of International symposium on geotechnical aspects of mass and material transportation, Bangkok.

Mitchell, J.K., Katti, R.K. (1981) : 'Soil Improvement', General report, X ICSMFE, Stockholm.

Van Impe, W, De Beer, E., (1983) : 'Improvement of Settlement behaviour of soft clays by means of stone columns', Improvement of ground, VIII ICSMFE, Helsinki.

Van Impe, W.F. (1987) : 'Soil Improvement by means of stone columns', Lecture delivered in Bombay, July 1987.

Table - 1 : SINGLE STONE COLUMN BEHAVIOUR

Site	Stone Column No.	Column Length (m)	Consumption (%)	Average Diameter (m)	Max. Load (t)	Total settlement under max. load immediate (mm)	Total settlement under max. load at 24 hrs. (mm)	Cu t/m^2	E (t/m^2)		σv/Cu = F'sc	Remarks
									24 hrs.	7 days		
2345 mm pipeline, Kasheli, Bombay	SC-1	4.53	186	1.060	40	15.885	36.060	1	17560	3850	45.33	Stone column not yielded
	SC-5	8.10	196	1.090	40	12.590	20.970	1	26455	11306	42.87	Stone column not yielded
	RT2-C/ TB-208	7.25	120	0.822	40.51	9.100	16.100	1	62099	21681	76.33	Stone column not yielded
	SC-4	3.18	215	1.140	40	8.630	14.280	1	17803	6231	39.2	Stone column not yielded
	SC-2	4.00	174	1.030	40	6.290	7.540	1	38405	18974	48.03	Stone column not yielded
						24 hrs. settlement	7 days settlement					
1830 mm Pipeline, Bombay	1554-C	3.325	259	1.062	30	65	105	0.6	1732	1073	33.88	Stone column yielded
	1066-C	8.540	237	1.016	30	73	$75^{\S}$	0.6	4329	2809	37.02	Stone column yielded
	564-E	4.480	156	0.824	20.13	48	$61^{\P}$	0.6	3523	2028	37.77	Stone column yielded
	1698-C	4.700	215	1.100	30.2	70	79^{*}	0.6	2135	1291	31.79	Stone column yielded
MCF Acid Tanks	996	9.25	124	1.00	35.5	15.0	-	1	32000	$12800^{\yen}$	63	Stone column not yielded
	810	8.5	118	0.99	35.5	12.2	-	1	31500	$12600^{\yen}$	66	Stone column not yielded
	881	9.0	127	1.02	35	9.1	-	1	44050	$17620^{\yen}$	62	Stone column not yielded
	682	7.75	134	1.04	36	5.9	-	1	36500	$14600^{\yen}$	59	Stone column not yielded

§ Measured under 20 t
¶ Measured under 14.73 t
* Measured under load of 20.62 t
¥ Assuming $E_{2\text{ hrs.}}/E_{7\text{ days}} = 2.5$

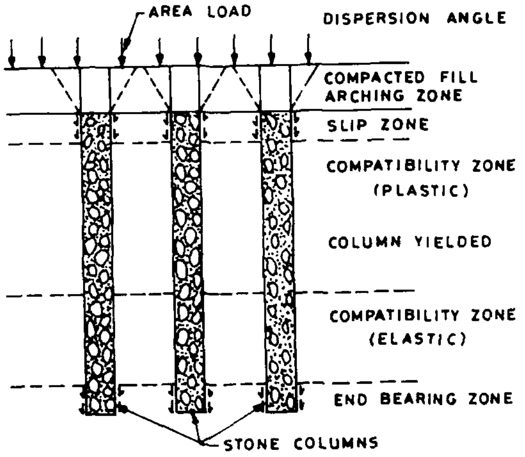
AREA LOAD
DISPERSION ANGLE
COMPACTED FILL
ARCHING ZONE
SLIP ZONE
COMPATIBILITY ZONE (PLASTIC)
COLUMN YIELDED
COMPATIBILITY ZONE (ELASTIC)
END BEARING ZONE
STONE COLUMNS

Fig. 1 : ZONE CATEGORIZATION

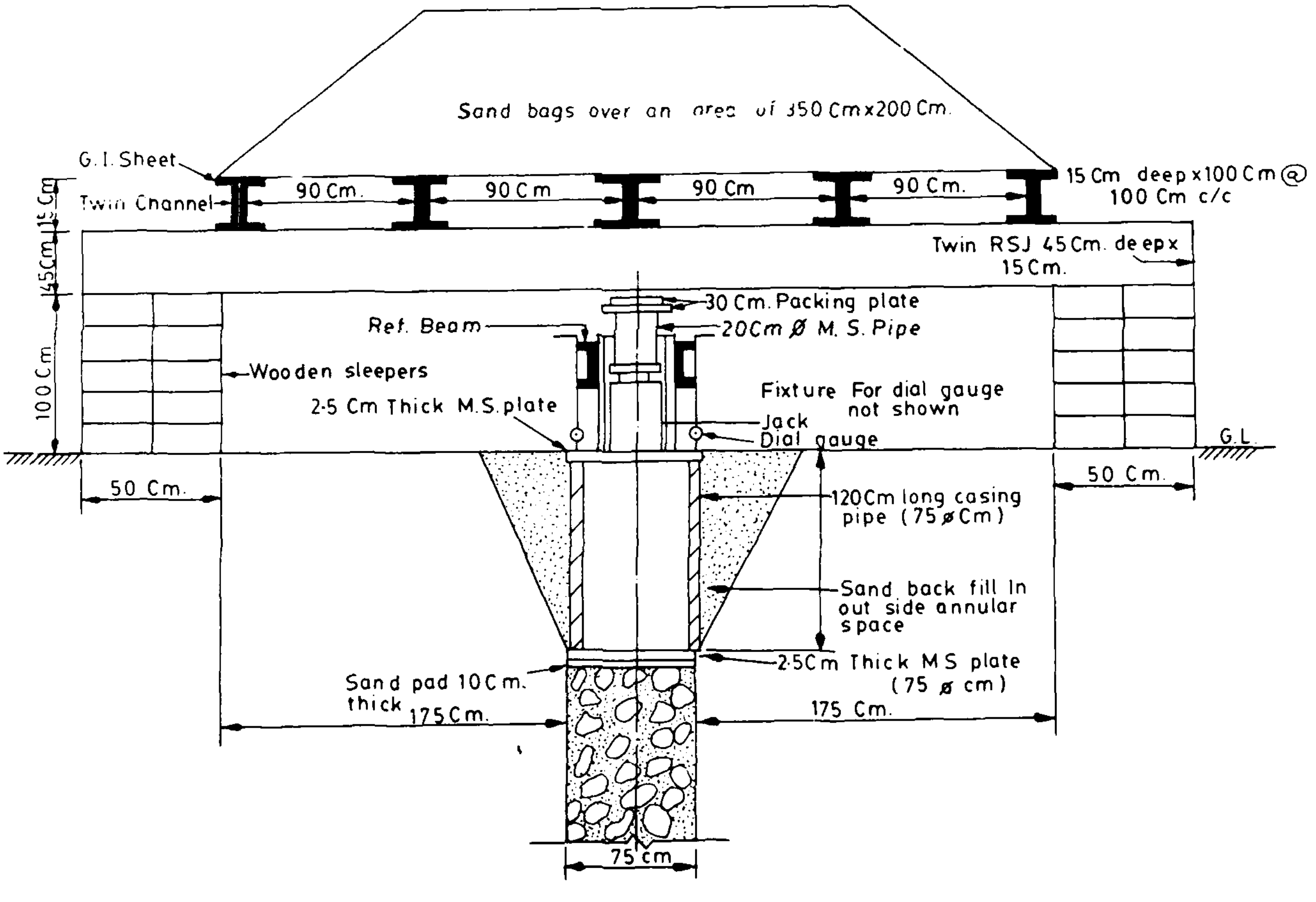
Sand bags over an area of 350 Cm x 200 Cm.
G.I. Sheet
Twin Channel
90 Cm.
90 Cm
90 Cm
90 Cm.
15 Cm deep x 100 Cm @ 100 Cm c/c
Twin RSJ 45 Cm. deep x 15 Cm.
15 Cm
45 Cm
100 Cm
30 Cm. Packing plate
Ref. Beam
20 Cm Ø M. S. Pipe
Wooden sleepers
Fixture For dial gauge not shown
2·5 Cm Thick M.S. plate
Jack
Dial gauge
G.L.
50 Cm.
50 Cm.
120 Cm long casing pipe (75 ø Cm)
Sand back fill In out side annular space
2·5 Cm Thick M S plate (75 ø cm)
Sand pad 10 Cm. thick
175 Cm.
175 Cm.
75 cm

Fig. 2 : SINGLE STONE COLUMN LOAD TEST ARRANGEMENT

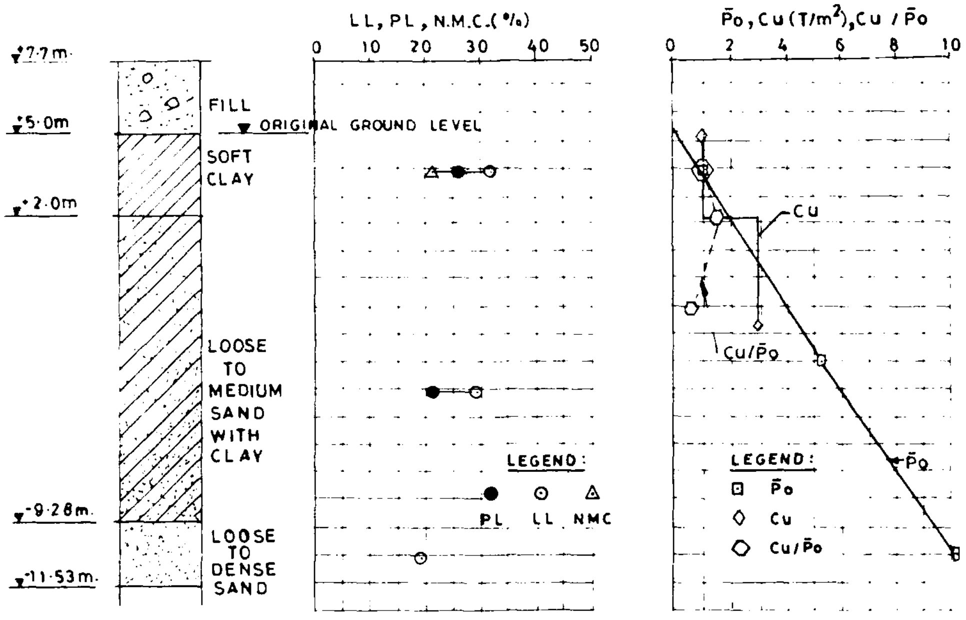

Fig. 3 : SUBSOIL CONDITIONS AT KANDLA

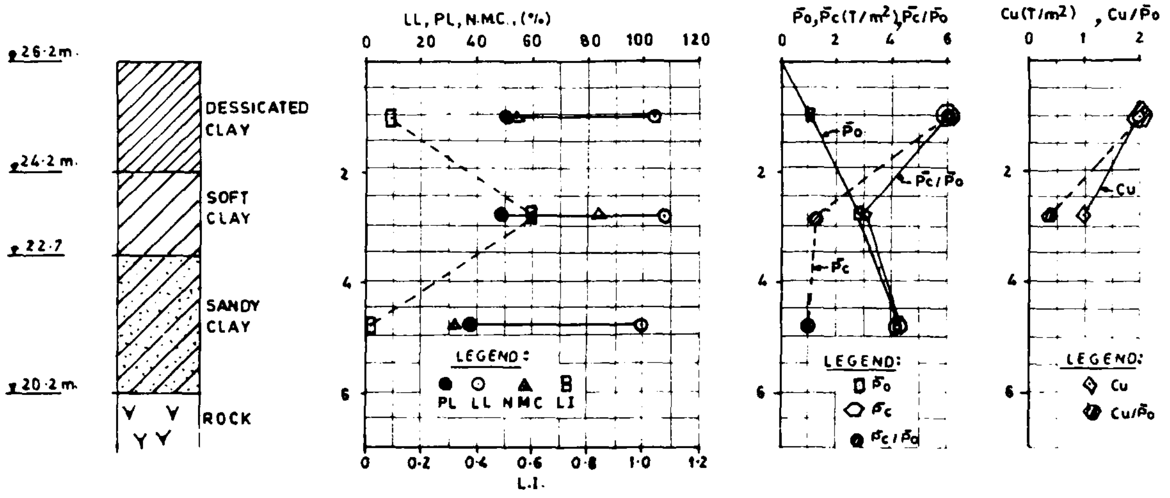

Fig. 4 : SUBSOIL CONDITIONS AT KASHELI

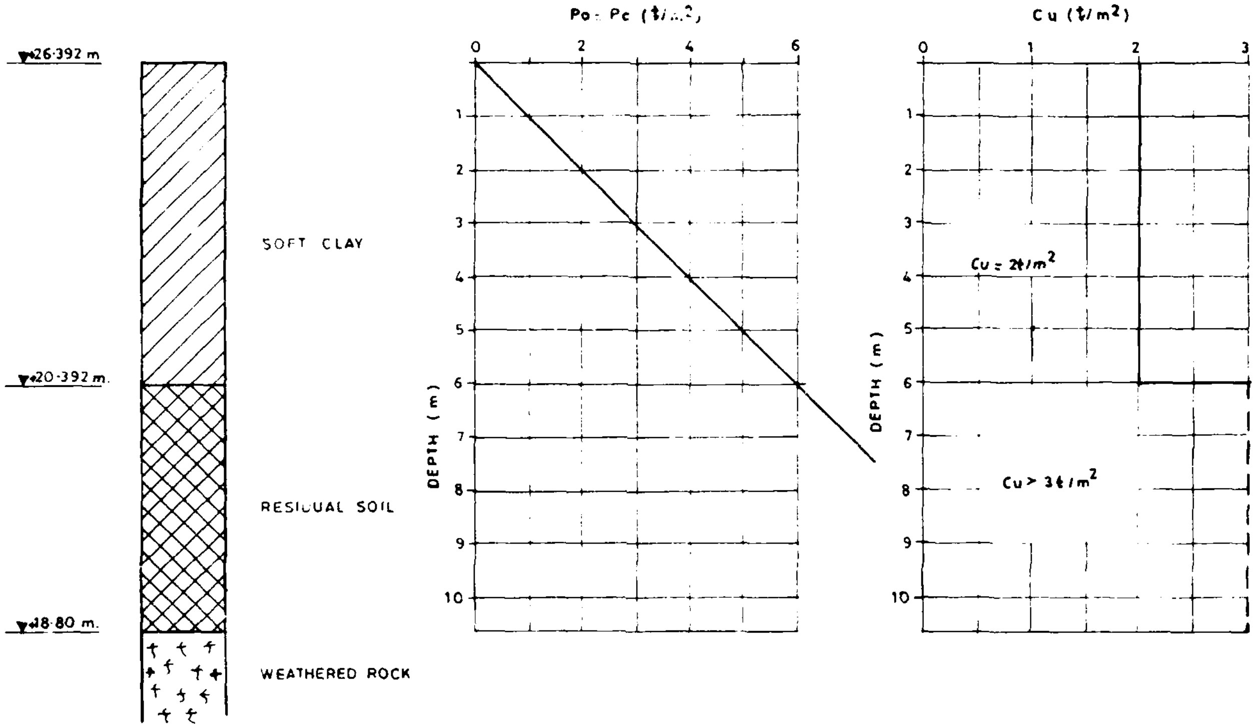

Fig. 5 : SUBSOIL PROFILE FOR BELAPUR ABUTMENT SIDE

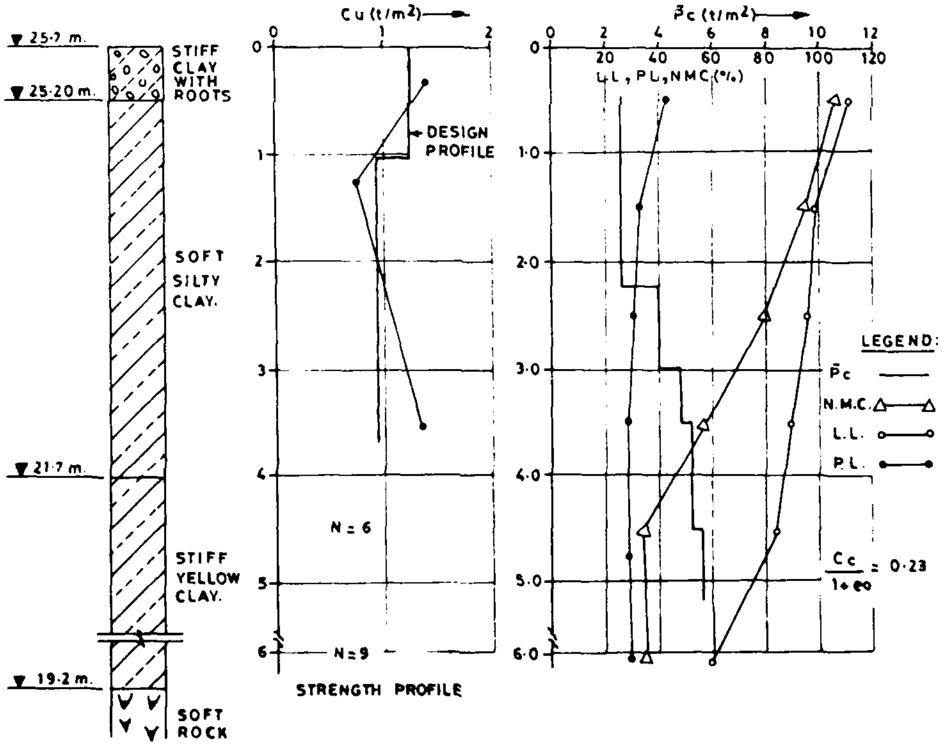

Fig. 6 : SUBSOIL CONDITIONS AT BHANDUP TEST PLOT

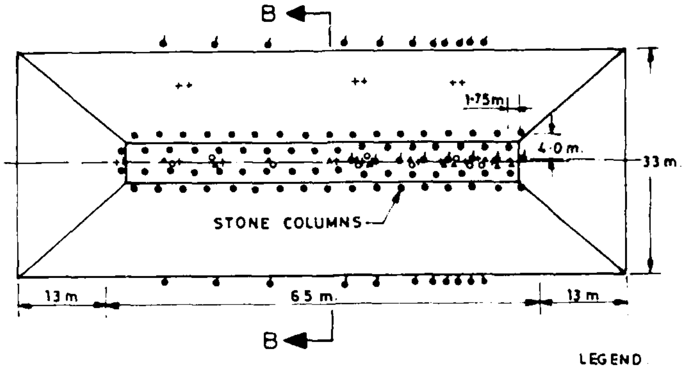
B
B
1·75m
4·0m
33m
STONE COLUMNS
13m
65m
13m

LAYOUT FOR TEST EMBANKMENT

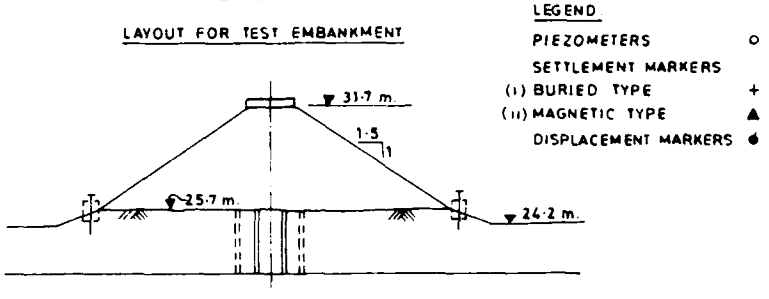
LEGEND
PIEZOMETERS ○
SETTLEMENT MARKERS
(i) BURIED TYPE +
(ii) MAGNETIC TYPE ▲
DISPLACEMENT MARKERS ●
31·7 m
1·5
1
25·7 m
24·2 m

SECTION AT B-B

Fig. 7 : EMBANKMENT & INSTRUMENTATION DETAILS AT BHANDUP TEST PLOT

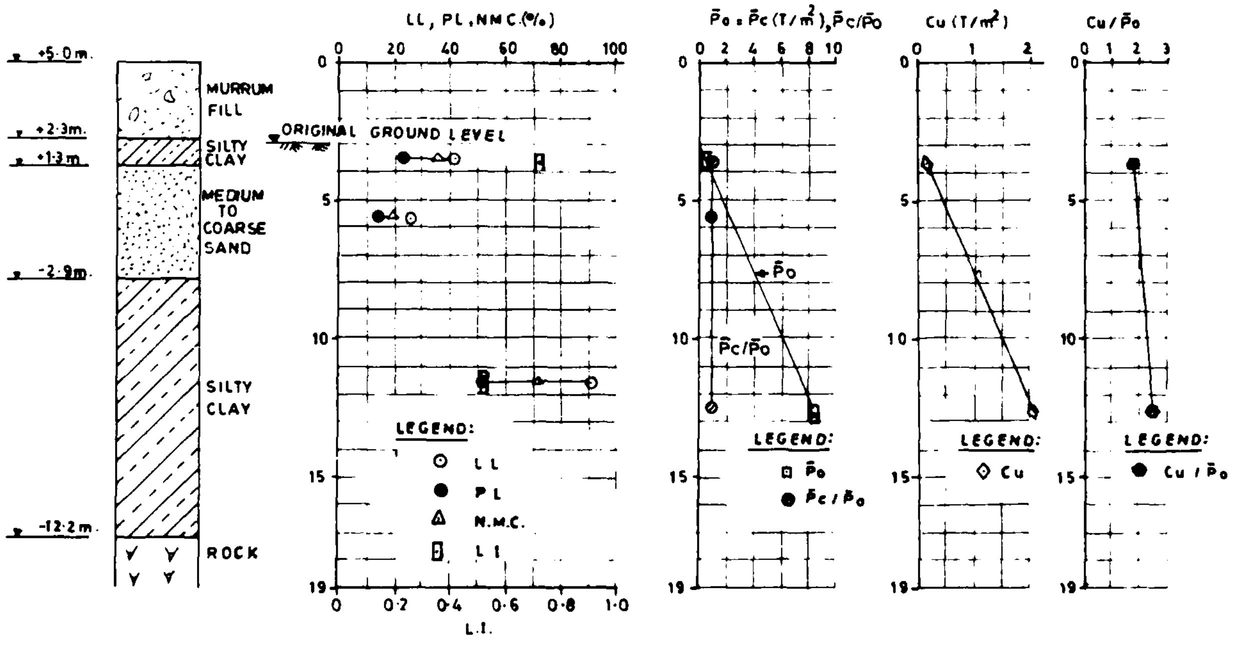

Fig. 8 : SUBSOIL CONDITIONS AT M.C.F. MANGALORE PORT AREA

Annexure - 1 : SETTLEMENT CALCULATIONS FOR KASHELI PIPELINE

Layer	Thickness (mm)	Cu t/m²	$\frac{Cc}{1+eo}$	P_c t/m²	P_o t/m²	Settlement calculation of untreated ground				Settlement calculation using Van Impe's model	
						Δp_1* t/m²	Settlement (mm)	Δp_2** t/m²	Settlement (mm)	Under Δp_1*	Under Δp_2**
Desiccated Clay	2000	2	0.3	6.0	1.00	7.66	142	10.0	157		
Soft clay	1500	1	0.23	3.0	2.75	7.03	177	9.2	207		
Sandy clay	2500	-	-	4.25	4.25	5.29	222	6.9	261		
Total Settlement							541		625	325	375

* due to Dead load of pipe + pedestal load + drag load.

** due to Dead load of pipe + pedestal load + drag load + water load

NOTE : 1) As per Van Impe's model 50 mm of settlement will occur after placing water load. It may be noted that in actual practice Cu of the soil will increase after first stage of loading after consolidation (since sufficient time was available between two stages during construction) resulting in increase in Pc value. Therefore settlement would be far less than the calculated ones.

2) Observed settlement during last half of the first stage loading was 30 mm.

Annexure - 2 : SETTLEMENT CALCULATIONS FOR MCF, MANGALORE

Tank diameter	23 m	Stress at the tank bottom	22 t/m²
Storage height	13 m	Stress at the stone column top level	16 t/m²

(There is a compacted sand fill below tank bottom and above stone column top)

Layer	Thickness (mm)	Settlement calculation of untreated ground						Settlement with stone column (Van Impe's model) (mm)
		$\frac{Cc}{1+eo}$	Cu (t/m²)	P_c (t/m²)	P_o (t/m²)	Δp (t/m²)	Settlement (mm)	
Silty clay	1000	0.10	0.10	0.5	0.5	15.951	137	12
Medium to coarse sand	4200	Settlement not taken into account due to *negligible contribution*						
Silty clay	9300	0.10	2.1	8.17	8.17	14.20	407	42
Total Settlement (mm)							544	54

NOTE : Observed settlement 55 m under maximum acid load

Proceedings: Second International Conference on Case Histories in Geotechnical Engineering, June 1-5, 1988, St. Louis, Mo., Paper No. 5.40

The Rehabilitation of Terminal 2—A Case History

D.J. Hardin
Principal, Geotechnical Resources, Inc., Portland, Oregon

S.V. Mills
Project Engineer, L.R. Squier Associates, Portland, Oregon

M.L. Byington
Manager of Construction Port of Portland, Oregon

SYNOPSIS

The Port of Portland, Oregon recently completed the rehabilitation of the downstream portion of Terminal 2. The project included the placement of more than 1 million cy of dredged hydraulic sand fill and the construction of a 1,400-ft-long pile-supported wharf. Up to 60 ft of sand fill was placed over soft, submerged sediments. The silt along the toe of the slope was removed prior to placing the fill. No shear failures or mudwaves were detected during filling. The fill induced settlements of up to 63 in., which agreed well with the predicted maximum settlement of about 60 in. Underwater sand fill slopes were placed at about 2.5H:1V and subsequently trimmed to 2.25H:1V. The slope was subsequently densified and steepened to 1.75H:1V with fragmental quarry rock. After slope construction, 840 vertical, 24-in. octagonal prestressed concrete piles were driven for the wharf.

INTRODUCTION

In 1982, the Port of Portland, Oregon, began design studies for the expansion and rehabilitation of the downstream portion of Terminal 2. The project team consisted of the Port; the wharf consultant, Swan Wooster Engineering, Inc. of Portland; the geotechnical consultant, the Portland office of Dames & Moore; and the dredging consultant, Ogden Beeman and Associates of Portland.

The terminal is a general cargo facility located along the west bank of the Willamette River in the Portland harbor area. The original Terminal 2 facility was built in the 1920s and consisted of wood construction with wharfs supported by timber piles. All of the original wood construction was demolished for the latest rehabilitation. The upstream portion of the terminal was upgraded in the 1960s and consists of a pile-supported concrete wharf constructed on the riverward side of a sheet-pile bulkhead. The major elements of the recent modernization included a new 1,400-ft-long wharf structure, the in-water filling of existing slips with over 1 million cy of fill to create about 20 acres of new terminal area, building construction, and new cargo handling equipment. The final grade of most of the wharf and filled area is elevation +26 ft. The downstream portion of the new wharf is for roll-on roll-off (RO/RO) use with the top of the wharf at elevation +20 ft. The new wharf structure extends the existing concrete wharf structure downstream 1,100 ft. The design dredge line along the face of the wharf is elevation -45 ft.

SITE CONDITIONS

The mudline elevation in the fill areas varied from about -30 to -38 ft in the upstream slip, -10 to -25 ft in the downstream slip, and -30 to -35 ft along the face of the proposed wharf. The existing wharf is of reinforced concrete and is supported by 20-in.-square, prestressed-concrete piles. A sheet-pile bulkhead is located behind the wharf.

SUBSURFACE CONDITIONS

The subsurface investigation included 22 borings and two cone penetration test probes to explore subsurface conditions in the fill and wharf areas; 21 borings were made to evaluate potential dredge sand borrow sources in nearby reaches of the Willamette River. The subsurface conditions at the terminal can be characterized as shown on Figure 1.

In general, a layer of soft, gray silt with an average thickness of about 15 ft occurs at the mudline; the silt is underlain by loose to medium dense sand which extends to an underlying stratum of sandy gravel at about elevation -85 ft. A review of past dredging records indicated that most of the proposed fill areas had been dredged to about elevation -35 to -40 ft. As a result, the soft silty soils occurring above these elevations were relatively recent sediments. The sand formation consists of generally medium dense, gray, fine- to

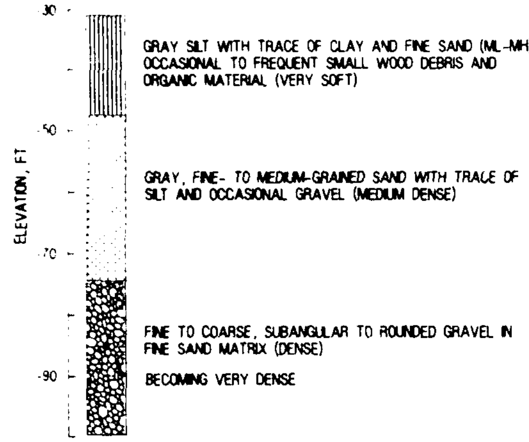
-30
GRAY SILT WITH TRACE OF CLAY AND FINE SAND (ML-MH); OCCASIONAL TO FREQUENT SMALL WOOD DEBRIS AND ORGANIC MATERIAL (VERY SOFT)
-50
ELEVATION, FT
GRAY, FINE- TO MEDIUM-GRAINED SAND WITH TRACE OF SILT AND OCCASIONAL GRAVEL (MEDIUM DENSE)
-70
FINE TO COARSE, SUBANGULAR TO ROUNDED GRAVEL IN FINE SAND MATRIX (DENSE)
-90
BECOMING VERY DENSE

Fig. 1 Typical Boring Log

medium-grained sand with a trace of silt. The top of the underlying gravel occurs between elevation -75 to -95 ft. The gravel consists of relatively well-graded, rounded to subrounded gravel in a matrix of sand with a trace of silt. The borings revealed that the gravel was generally medium dense to dense and is not cemented.

The borings within the proposed dredge borrow areas generally encountered a layer of silt or silty sand at the mudline which was underlain by clean, gray, fine- to medium-grained sand. The mudline at the boring locations generally ranged from about elevation -40 to -60 ft. Based on a review of past dredging near the project, and the results of the subsurface explorations, two potential areas near the site were identified as sand borrow sources. The gradation of the borrow-area sand is summarized on Figure 2.

SOIL PROPERTIES

Based on an extensive laboratory testing program and a detailed review of geotechnical data obtained from nearby sites in the Portland harbor area, the following soil properties were used in the geotechnical studies.

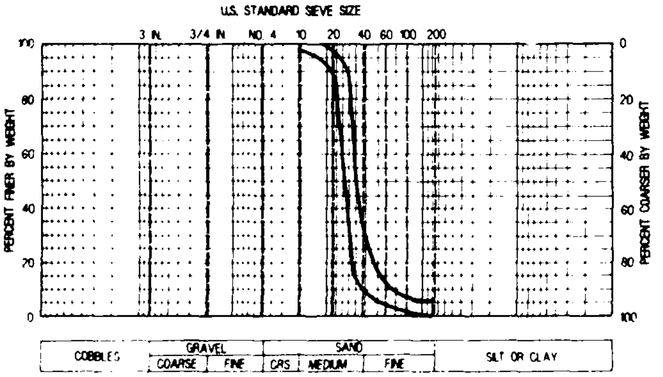

Fig. 2 Gradation of Sand Fill

Shear Strength

Angle of internal friction (Ø)	
New sand fill (SP) above water	$34^{\circ}-35^{\circ}$
New sand fill (SP) below water	$32^{\circ}-35^{\circ}$
In situ sand (SP)	35°
In situ silty sand (SM)	$30^{\circ}-32^{\circ}$
Undrained shear strength of soft, silty mudline soils (ML-MH)	50 psf
Angle of internal friction (Ø)	16°

Consolidation

Coefficient of compressibility of soft silt (ML-MH), $\frac{C_c}{1+e_o}$	0.19
Coefficient of consolidation for soft silt, (ML-MH), C_v	1.0 ft^2/day
Coefficient of compressibility, silty sand (SM), $\frac{C_c}{1+e_o}$	0.05

Unit Weight

Soft silt (ML-MH)	
Saturated unit weight	84 pcf
Submerged unit weight	22 pcf
Sand (SP)	
Total unit weight of fill	115 pcf
Saturated unit weight	120 pcf
Submerged unit weight	58 pcf
Silty sand (SM)	
Saturated unit weight	115 pcf
Submerged unit weight	53 pcf

DESIGN PROCESS

While the geotechnical investigation was in progress, the wharf consultant developed preliminary design concepts that fulfilled the Port's performance criteria, appeared practical to construct, and considered the subsurface conditions. The following types of structures were selected for further evaluation.

- open pile-supported wharf
- pile-supported wharf with sheet-pile bulkhead
- cellular sheet-pile structure

The open pile-supported wharf with a cast-in-place concrete deck was selected for the final design. The selection of this type of structure was based on cost comparisons, technical considerations, and scheduling constraints. This wharf design used only vertical piles of one type and size. The wharf deck was of a uniform thickness, with no distinct pile caps. These features were adopted to contribute to more straightforward construction.

The cellular sheet-pile structure was cost-competitive; however, the required configuration of the cells would have imposed critical tolerances for construction. In particular, the fender line of the wharf and the new crane rails had to match the existing upstream structure. Based on past experience, it was agreed by the design team that the actual riverward projection of the cells following filling could be plus or minus 1 ft of the desired line. This uncertainty was considered undesirable and imposed constraints upon the type of fender system that could be used.

Since the project would involve the placement up to 60 ft of sand fill above and below water, a detailed study was performed to evaluate the liquefaction potential of the fill. The studies indicated that unless the fill was installed to adequate relative densities or had sufficient confinement, liquefaction under stresses induced by the design earthquake would be a potential problem near the slope. The results of the studies for the riverward slope indicated that a relative density of 60% would be necessary to obtain a factor of safety slightly more than 1 against liquefaction or lateral deformation during the design earthquake. For this reason, it was necessary to densify the sand fill beneath the wharf structure. To provide sufficient confinement for the surface sand fill materials during densification, the design included a 10-ft-thick blanket of coarse granular material over the slope. Rounded sandy gravel and cobbles were considered the most appropriate materials for the confinement layer, since it could be easily penetrated by vibratory probes that would be used for densification. The adopted slope configuration based on the geotechnical studies is shown on Figure 3.

A pile-supported wharf with sheet-pile bulkhead would be comparable to the existing upstream structure. This design was initially considered the most appropriate for the project. However, the Port determined that the wharf must accommodate container cranes with 100-ft rail spacing. Since the pile-supported wharf would be about 74 ft wide, the rear crane rail would be landward of the sheetpile bulkhead and require a separate foundation. It was recognized that the foundation would probably interfere with the tie-back system used to restrain the bulkhead.

Based on the project team's selection of the open pile-supported wharf as the preferred alternative, Dames & Moore proceeded with final design studies for site filling and wharf support.

For cost purposes, it was necessary to minimize the width of the pile-supported wharf; this, in turn, required that the fill slopes be constructed as steep as possible. The soft silty sediments occurring at the mudline were the primary consideration in the construction of steep, stable slopes. To provide sufficiently steep slopes constructed of hydraulic sand fill, it would be necessary to make a toe trench excavation to remove the soft silty soils at the toe of the slopes. Computer-assisted slope stability studies were performed to aid in the development of practical design criteria for the slopes along the wharf. The studies indicated that stable sand fill slopes having an adequate factor of safety could be constructed at inclinations of up to 2.5H:1V to 2.25H:1V, depending on the configuration of the toe trench excavation. The slopes could be further steepened to 1.75H:1V by filling over the sand slope with well-graded angular rock.

Based on past experience by Dames & Moore, it was considered feasible to place the hydraulic sand fill over the very soft silt sediments present at the mudline by using carefully controlled construction methods that would minimize or avoid shear failures and formation of mudwaves. Mudwaves could produce pockets of compressible silty soils which could result in irregular settlement of the fill surface and, if formed near the slope, could reduce the stability of the fill slopes. It was recognized that the placement of the initial underwater fill was the most critical aspect of

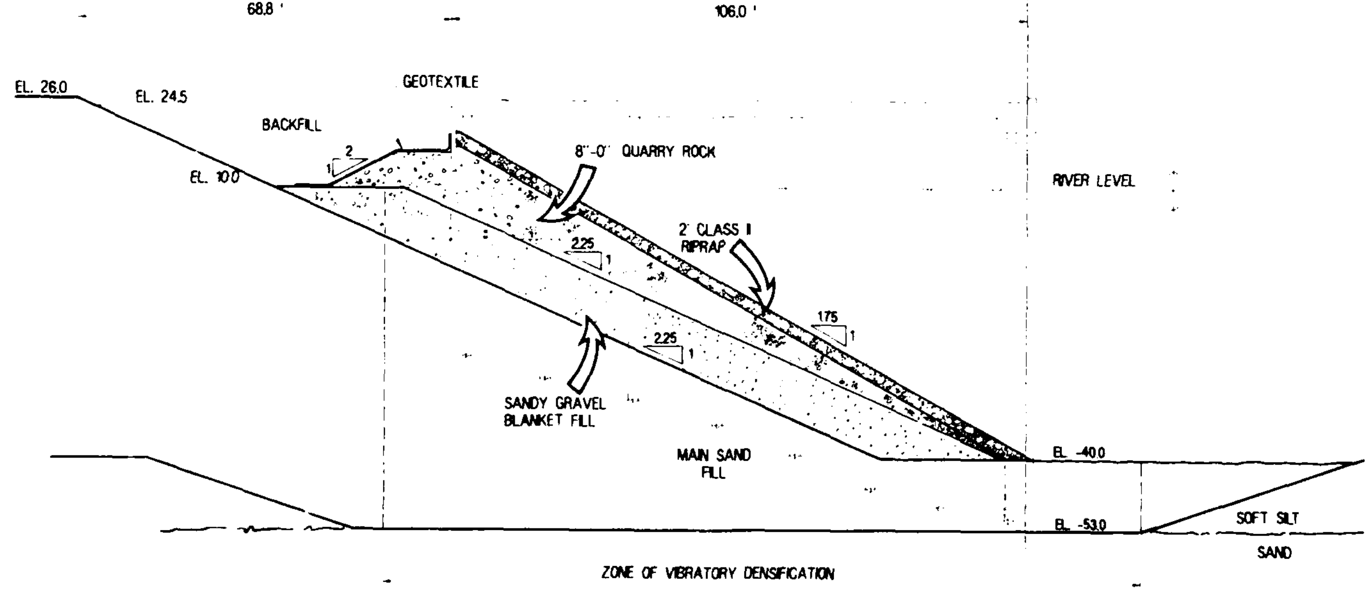

Fig. 3 Slope Section

the fill plan. The installation of each of the initial four lifts was to begin and end at the same locations to provide the maximum time period for consolidation of the soft silts prior to placing the following lift. The initial lift would have a nominal thickness of 3 ft, or less, which would require frequent or continuous repositioning of the dredge discharge. The subsequent three lifts could each be placed at a maximum thickness of 5 ft. The remaining fill could be placed in maximum 10-ft-thick lifts. Fill placed above the river level would be placed so that the resulting minimum dry density was on the order of 90%, as determined by ASTM D 1557. This degree of compaction is usually obtained by normal hydraulic filling operations.

Since the borrow sand fill was relatively clean, it was anticipated that the underwater sand fill could be placed as an open, unconfined fill. It was anticipated that the underwater slopes could be filled as steep as 2.5H:1V and would require subsequent trimming to the specified slope of 2.25H:1V.

The preliminary studies indicated that foundation support for the wharf would be provided by high-capacity vertical piles driven into the underlying gravel strata. A capacity of 225 tons was recommended for 24-in. octagonal prestressed concrete piles and 24-in.-diameter open-end steel pipe piles. The capacities pertain to real loads and were based on soil support considerations and included an estimated factor of safety of at least 2. The capacities were estimated by static analytical methods and were supplemented by dynamic analyses (wave equation studies) and the review of pile load tests performed at comparable sites and during the previous rehabilitation of the upstream portion of Terminal 2. It was anticipated that concrete and steel piles would penetrate 4 to 8 ft and 10 to 15 ft, respectively, into the gravel strata.

SETTLEMENT

During design, studies were conducted to estimate the total settlement and rate of settlement associated with the installation of dredged fill over the soft river sediments. The results were used to evaluate the effect of long-term settlement on the construction schedule, and differential settlement on proposed facilities within the filled area. The studies considered the consolidation of the highly compressible river sediments that occurred at the mudline and had an average thickness of about 15 ft. Conventional one-dimensional consolidation theory was used in the analysis. The stress distribution along the edge of the dredged fill area was evaluated using a linear elastic analysis. Settlement of the 50-ft-thick sequence of sand was evaluated using elastic analysis. The medium dense to dense, sandy gravel that lies below the sand at approximately elevation -85 ft is considered to be essentially incompressible. A conventional ramp-loading approximation was used to simulate the filling sequence. Settlement was dependent on the thickness of the underlying compressible soils and the thickness and configuration of the dredged fills. The analyses predicted that up to 60 in. of total primary settlement would occur, 80% of which would occur by the end of filling. The studies suggested the potential for significant post-construction differential settlements across the filled area. The design team recommended a 15-ft-thick surcharge fill within the building areas to limit post-construction differential settlement. The paved areas were overfilled to compensate for post-filling settlement.

SETTLEMENT MONITORING PROGRAM

Considering the relatively large anticipated settlements and the potential impact of the rate of settlement on the construction schedule, a monitoring program was considered necessary to evaluate settlement progress. Pneumatic settlement transducers and pneumatic piezometers were selected since they would be unobtrusive to the contractor during the filling operation. The performance requirements for the monitoring system were specified in the bid documents. The general contractor, Riedel International, Inc., retained a subcontractor to design and install the system. The system consisted of 12 pneumatic settlement sensors, five pneumatic pore pressure transducers, and two pneumatic readout boxes. The pneumatic settlement sensors and pneumatic pore pressure transducers were installed at the mudline and the middle of the compressible silt layer, respectively, prior to fill placement.

During the monitoring period which extended from the beginning of the filling operation, over a period of approximately 7 months, a total of 10 settlement sensors and four piezometers failed. Behavior of the failed instruments suggested the tubes had been pinched or severed. Many of the failed settlement sensors were replaced with surface settlement plates after the fill was above the river level.

Information obtained from undamaged instruments and the surface settlement plates was used to predict the post-filling settlements to determine the overfill quantities. In addition, several instruments survived long enough to permit comparison of predicted time-rate and magnitude of settlement versus actual field performance. In general, the actual time-rate of settlement occurred faster than the consolidation test results had indicated. A comparison between estimated time-rate of settlement curves with actual results from field monitoring, is shown on Figure 4. A maximum settlement of about 60 in. was estimated based on the settlement studies; the actual maximum settlement measured by the monitoring system was 63 in.

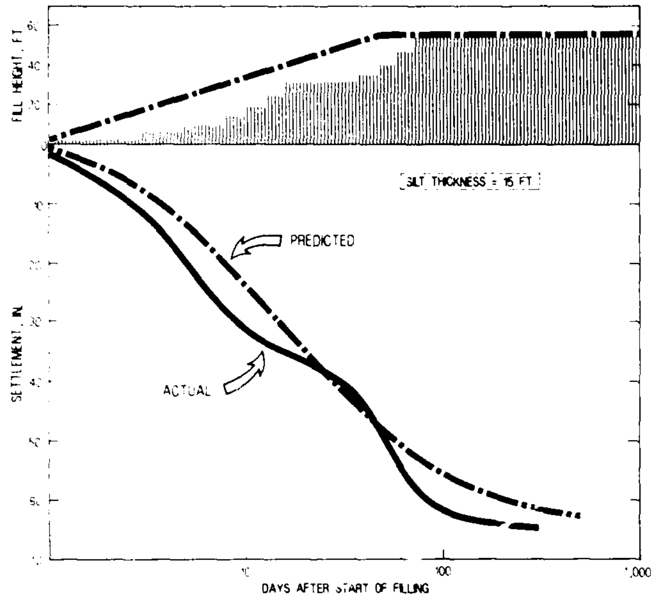

Fig. 4 Predicted versus Actual Maximum Settlement

SITE FILLING AND SLOPE CONSTRUCTION

Initially, a 150-ft-wide trench was excavated along the toe of the slope to remove the soft silt. The toe-trench excavation was made using a 26-in. hydraulic suction dredge equipped with a cutterhead. The suction dredge generally left 12 in. or less of silt in the bottom of the toe trench. The final cleaning was made with a barge-mounted crane and clamshell.

The general sand fill and the fill slopes were made with the hydraulic suction dredge. The dredge ladder was extended to permit dredging to depths of about 100 ft, and the cutterhead was removed and replaced with jets. The borrow sources were near the middle of the river with a maximum pumping distance of about 4,500 ft. To place the fill, the dredge pipe discharged into a vertical 8-ft-diameter pipe that was suspended from a barge. The bottom of the pipe was usually maintained about 13 ft below the water surface and could be raised and lowered to control turbidity and optimize fill placement.

Following completion of the toe trench, the sand fill slopes were constructed by the installation of a toe dike along the alignment of the toe trench. The toe dike was placed in two lifts ultimately to elevation -15 ft. The fill material consisted of excellent quality gray sand containing significant gravel and few fines. Alignment of the discharge barge was maintained with on-shore lasers. Bathymetric surveys conducted after installation of the toe dike indicated average slopes of 2.5H:1V and generally good control of slope lines and positions.

Following installation of the initial toe trench fill, the main dredge fill was installed within the limits of the toe dike. The general fill was placed over the soft river sediments using the discharge barge. The initial two lifts were 3 ft thick, the next two were 3 to 5 ft thick, and the remaining lifts to the water surface were 7 to 10 ft thick. During filling, the instrumentation was closely monitored and bathymetric surveys were made after each lift to monitor unusual river bottom bulging which would indicate the occurrence of a mudwave. Bathymetric surveys were also used to monitor the quality of the installation procedure and check lift thicknesses below the river level. In general, the fill placement was satisfactory and no mudwaves were detected.

The above-river filling was conducted by constructing a dike along the river slopes to contain the dredge fill. Dredge water was directed riverward through a temporary spillway structure. The dredged fill was placed in approximately horizontal lifts by movement of the discharge pipe and spreading with a dozer. The placement procedures resulted in an in-place density of the fill placed above the river level comparable to 88 to 91% of the maximum density determined by ASTM D 1557.

Following installation of the slopes and the general site fill, the sand slopes were trimmed to the specified slope of 2.25H:1V. The contractor used a dozer to trim the slope above the river level and a barge-mounted crane operating a 5 cy clamshell bucket to trim the underwater slope. The contractor initially attempted to trim the fill slopes using the suction dredge; however, control of the cutter head was difficult and several gouges and minor slope failures occurred during the attempt. The contractor completed the remainder of the trim excavation using the barge and clamshell operation.

The slope trimming operation was followed by the placement of the 10-ft-thick granular confining blanket. The material was barged to the site and unloaded with a barge-mounted crane operating a clamshell bucket. The sandy gravel fill consisted of rounded, well-graded gravel and cobbles with a clean sand matrix. Care was taken to lower the bucket below the surface of the water to minimize fill segregation during installation.

Following installation of the sandy gravel blanket, the river slopes were densified using a barge-mounted vibratory probe. The probe consisted of a 36-in.-diameter open-end pipe which was slowly inserted to and withdrawn from the bottom of the fill to approximately elevation -40 to -53 ft while being vibrated with a 25,000 ft-lb Toyamenka 6000 vibratory hammer. The generalized zone of vibratory densification is shown on Figure 3.

Standard penetration tests (SPTs) were used to verify densification requirements and to provide information for selecting the appropriate probe spacing. A truck-mounted drill rig operating from a barge performed the SPTs in borings drilled at regular intervals along the wharf fill slopes. Overdensified slopes were a concern because of the potential for difficult driving of the wharf piles. Initial tests indicated that probing on a 5- by 5-ft grid resulted in overdensification. A 7- by 7-ft grid pattern was eventually adopted since it generally produced the specified density throughout the depth of sand fill.

Following densification, the river slopes were steepened to 1.75H:1V by placement of a wedge of 8-in.-minus fragmental quarry rock. The quarry rock was barged to the site and installed on the slope from the toe upward by a barge-mounted crane a 4 cy skip bucket.

The sand fill was placed during October through December 1985, when the level of the Willamette River was in the range of elevation +2 to +5 ft. During early 1986, high river levels up to elevation +18 ft resulted in the deposition of 3 to 7 ft of silt at the toe of the slope. The silt was removed prior to placement of the sandy gravel blanket and fragmental rock fill. Slope construction was completed after driving of the wharf piles by the placement of the riprap protection.

PILE INSTALLATION

Support for the wharf structure is provided by driven, 24-in.-octagonal prestressed, solid concrete piles having a design capacity of 225 tons. The piles were driven into the underlying gravel, and pile lengths varied from 108 to 120 ft. Alternating piles along the rear cutoff wall were designed for lateral loads only and were driven to tip elevations of -60 ft. The pile driving plant consisted of a large barge-mounted crane equipped with leads and a hydraulic spotter. Most of the piles were driven with a Delmag D46-32 diesel hammer delivering a maximum rated energy of 107,000 ft-lbs. In an attempt to increase production, several piles were driven with a Delmag D62-00.

Prior to and during production driving, 10 indicator test piles were driven along the wharf alignment to determine pile length requirements and identify potential problems in advance of the production driving. Most of the test piles were monitored during driving by the Pile Dynamic Analyzer (PDA) provided and operated by Goble-Rausche-Likens (GRL), of Boulder, Colorado. Information obtained from the program was used to develop terminal driving criteria and select appropriate pile lengths that would require minimum cutoff and preferably no splicing. In addition, the monitoring provided information regarding pile capacity, driving-induced stresses, and hammer and cushion performance.

Production piles were installed over a 7-month period during 1986, with relatively few problems. A localized occurrence of piles damaged during driving required special study and additional dynamic testing. The monitoring results indicated that the hammer had an increased efficiency which resulted in excessive tensile stresses during initial driving. Pile quality control problems were also considered to be a contributing factor to pile damage. Based on the monitoring and the results of wave equation analyses, the contractor increased the thickness of the wooden pile cushion from 11.5 to 16 in. Most of the piles were driven 5 to 10 ft into the underlying gravel stratum with a terminal driving resistance of 50 to 65 blows/ft.

Some difficulty was encountered maintaining pile position and alignment during initial driving on the relatively steep slopes (1.75H:1V) and through the quarry rock. A substantial number of piles were out of position and alignment following completion of driving. Fortunately, the uniform thickness of the wharf deck allowed considerable flexibility using misaligned and out-of-position piles.

CONCLUSIONS

The Terminal 2 project was successfully constructed on schedule and within budget. Essentially no conditions were encountered during construction that were not anticipated in the design and could not be accommodated or resolved by the original fill and construction plan. The project involved a knowledgeable client, a design team with extensive waterfront experience, a thorough geotechnical investigation, and a qualified contractor who understood and appreciated the technical considerations of the project. The primary factors contributing to the design and construction of the project included the following:

1) Thick fill can be placed over soft, submerged sediments, provided the fill is placed in a carefully controlled manner so that fill-induced stresses are essentially uniform at all times. This requires placement of at least the initial thicknesses of the fill in uniform thin lifts.

2) Relatively steep (2.25H:1V) underwater sand fill slopes were constructed using careful construction procedures. However, slopes must be constructed from the bottom to the top.

3) Underwater sand fill was placed by hydraulic methods as steep as 2.5H:1V. The inclination of the underwater sand fill depends on the method of placement and the quality of the dredged sand.

4) The relative density of the submerged sand fill was increased from less than 50% to more than 60% by densifying with vibratory pipe-pile probes.

5) High-capacity, 24-in. octagonal concrete piles were successfully driven through the relatively steep, rock-filled slope. However, it was difficult to control the final position of the pile top to small tolerances. These deviations were anticipated and accommodated in the wharf design by the uniform thickness of the wharf deck.

6) Actual settlement of the sand fill agreed well with the predicted settlements. However, the instrumentation used to monitor the rate and magnitude of the fill settlement suffered a high rate of failure. The ability of pneumatic sensors to withstand long tubing runs and large settlements is not well developed at this time.

7) During pile driving, the pile dynamic analyzer (PDA) was a valuable tool for aiding the evaluation of pile hammer performance, driving-induced stresses, and estimated pile capacity.

Proceedings: Second International Conference on Case Histories in Geotechnical Engineering, June 1-5, 1988, St. Louis, Mo., Paper No. 5.42

A Geotextile Reinforced Embankment for a Four Lane Divided Highway—U.S. Hwy. 45, West Bend, Wisconsin

B.R. Christopher
Principal Engineer, STS Consultants, Ltd., Northbrook, Illinois

A.B. Wagner
Regional Vice President, STS Consultants, Ltd., Milwaukee, Wisconsin

SYNOPSIS: Geotextile reinforcement was used to construct an embankment for a four lane divided highway over up to 22 feet of low strength peat. The embankment had heights up to 7 feet. Special field testing and conventional laboratory tests were performed to measure the shear strength and compressibility. Stability analysis indicated that geotextile reinforcement could be used to construct a stable embankment on the peat deposit, provided the geotextile had sufficient strength to prevent rotational shear failure and to limit lateral deformation of the embankment. Construction of the embankment was begun in late summer of 1984. The highway opened for traffic in late 1985. Performance of the embankment was monitored during and after construction. The design, construction procedures, and results of the settlement monitoring program are presented.

BACKGROUND

The existing U.S. Highway 45, located south of West Bend, Wisconsin, had experienced a poor safety record. The Wisconsin Department of Transportation (WDOT) planned to construct a four lane divided by-pass around the city. The new alignment crossed the edge of Mud Lake, a filled glacial lake. The lake contained significant peat deposits.

Traditionally, the peat soils would have been displaced or excavated and replaced with granular fill. However, the following constraints precluded the conventional approach: 1) No disposal sites were available for the organic soils; 2) Since the area was considered a wetlands, there were environmental concerns related to excavating the organic soils; 3) The large volumes of soils involved would have resulted in large costs; 4) To allow direct observation of the foundation, expensive dewatering would have been required.

As a result of the constraints, the design engineers, J.C. Zimmerman Engineering Corporation, contacted their geotechnical engineering consultants, STS Consultants, Ltd., concerning the feasibility of constructing the embankment over the organic soils.

SOIL CONDITIONS

Borings performed by WDOT showed that the organic soils occurred over a span of 2300 feet. The peat occurred in two "basins" that were nearly separated by a ridge of inorganic soil. In the south basin the peats were up to 22 feet thick and in the north basin were up to 18 feet thick. Since the embankment crossed the west edge of the lake, the ground surface declined to the east and the organic soils became thicker to the east.

Three distinctive organic layers were encountered. The upper layer was a root mat having a thickness of zero to 2 feet. The second layer was a relatively decomposed fibrous peat ranging in thickness from 4 to 18 feet. The fibrous peat, which occurred at all locations that were explored, had losses on ignition ranging from 60 to 90% and water contents typically ranging from 100 to 1000%. The third layer, which was primarily encountered in the south basin, was an amorphous type sedimentary peat found below the fibrous peat. The sedimentary peat had ignition losses of less than 10% and water content ranging from 40 to approximately 250%.

The organic soils were underlain by inorganic silty and sandy soils that were generally in a loose to medium dense condition.

The strength of the organic soils was initially measured in the WDOT laboratory by means of numerous unconfined compression tests and by a single direct shear test.

In order to provide better definition of the shear strength of the organic soil, the geotechnical engineer undertook a program of field testing. This included both conventional vane shear tests and a new small-diameter plate bearing device. This device consisted of a 3 inch diameter disc that was connected to a smaller diameter push rod by means of a load cell. Due to the small diameter plate and the weak soils, it was possible to manually push the rod into the soil. By virtue of its location, the load cell ignored the effect of friction on the rod. The shear strength of the organic soil was calculated using the bearing capacity equation for "deep foundations".

Typical strength results from laboratory and field tests are shown on Figure No. 1. The data shown is from the south basin and represents all three organic layers. As shown on the figure, the strengths ranged from 30 to

520 psf, with the lower strengths measured in the amorphous peat layer.

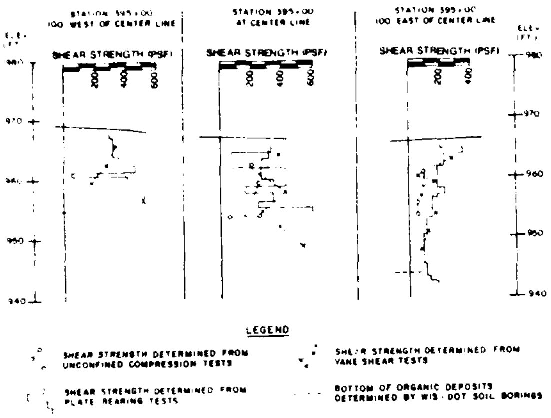

Figure 1 Comparison of Strength Tests

In the authors' opinion, the in-situ test results appeared to provide the most reliable shear strength for the organic material.

To evaluate embankment settlement numerous standard consolidation tests were performed in the WDOT laboratory. These tests indicated compression indices ranging from 0.1 to 5.0. The tests performed on fibrous peat had compression indices greater than 1.7. Tests on sedimentary peat indicated compression indices of 1.0 or less.

Additionally, several long term consolidation tests were performed to measure the secondary compression coefficient. The tests indicated secondary compression coefficients ranging from 0.009 to 0.029. The lowest coefficient was measured for sedimentary peat, while the higher values were measured on fibrous peat. The 1/3 order of magnitude variation in secondary compression coefficient between the two types of peat, indicated relatively uniform secondary compression behavior.

SOIL MODEL FOR STABILITY ANALYSES

A soil model was developed for each of the zones so that slope stability analyses could be performed.

For the purposes of this paper, only the analysis of the most critical zone will be reviewed. The soil model for this zone, illustrated on Figure No. 2, included fibrous peat occurring in a layer extending from 4 to 15 feet below the surface. This layer was thickest at the western end of the cross-section and the thickness decreased toward the east. On the basis of field testing, this layer was assigned a shear strength of 250 psf.

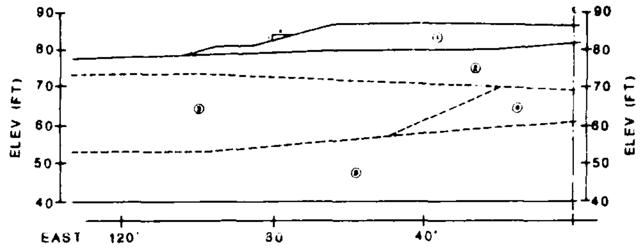

LAYER	GENERAL SOIL TYPE	ϕ	C (psf)	δ_t (psf)
1	EMBANKMENT FILL	35°	0	138
2	FIBROUS PEAT	0	250	65
3	SED PEAT WITH SILT	0	100	95
4	SED PEAT WITH SAND	0	400	95
5	SANDY SILT	26°	0	

Figure 2 Soil Model

At the east end of the cross-section, the fibrous peat was underlain by sedimentary peat having a thickness of 15 feet near the extreme east end of the section. The thickness of this layer decreased to the west and the layer tapered out completely about 20 feet east of the embankment centerline. This sedimentary peat layer was assigned a shear strength of 100 psf based on the field test results.

The fibrous and sedimentary peats were underlain by a localized sandy sedimentary peat deposit that extended about 20 to 30 feet on either side of the embankment centerline. This layer was assigned a shear strength of 400 psf.

The organic soils were underlain by inorganic silts and sands which were assigned a friction angle of 26 degrees.

DESIGN REQUIREMENTS

An embankment having a maximum height of 7 feet was necessary to meet final, after settlement, grade requirements.

For the normal long term situation a factor of safety of 1.5 was required. Although somewhat conservative, it was felt that this factor of safety would result in a better long-term performance of the embankment. However, for a short term condition, such as initial fill placement, or the placement of surcharge fill, a factor of safety of 1.3 was considered adequate.

STABILITY ANALYSIS

The stability of the unreinforced embankment was first analyzed for bearing capacity and rotational shear stability using conventional geotechnical techniques. The slope stability analyses were made using the computer program STABL developed by Purdue University. This program calculates the factor of safety by the method of slices. The analyses employed the modified Bishop method which is applicable to circular failure surfaces and the simplified Janbu method applicable to failure surfaces of general shape.

The STABL program features unique random techniques for the generation of potentional failure surfaces for subsequent determination of the more critical factors of safety. Typically, 50 to 100 potential failure surfaces were analyzed for each case. Both circular arc and sliding block surfaces were considered in the analyses.

For normal weight fill, factors of safety ranged from 0.72 for 4:1 embankment side slopes, to 0.87 for 8:1 side slopes. Both values are well below the desired factor of safety. The critical result of the slope stability analysis was checked manually using the method of slices. The manually calculated factors agreed within 0.1, which was considered good agreement.

For the analysis, it was apparent that the embankment could not be constructed without some form of subgrade or embankment modification. Since excavation and replacement was not a viable alternative, other methods including the use of wick drains, stone columns, light weight fill, piles, as well as soil reinforcement were considered. After a comparison of the methods with respect to feasibility, performance and cost, it was apparent that the use of geosynthetics was the most effective alternative. The use of metallic reinforcement was excluded due to the high corrosion potential in the acidic organic soils and relatively high cost.

EMBANKMENT REINFORCEMENT

By placing high tensile strength reinforcement at the base of the embankment, the stability of the embankment could be improved through increased shear resistance offered by the reinforcement. In addition, the reinforcement theoretically provided additional stiffness to the base of the embankment, allowing for a more uniform distribution of embankment loads. As the reinforcement should also reduce shear stresses at the embankment subgrade interface, it aided in reducing the potential for lateral spreading of the embankment over the weak subgrade.

Other reasons for using geosynthetic reinforcement included:

1. Allowing for initial support of vehicles out over the soft soil deposits, so that fill could be placed.
2. Providing for more controlled construction, less disturbance, and less displacement of the organic soil during construction.
3. Preventing the embankment from penetrating downward into the soft subgrade.
4. Maintaining the integrity and uniformity of the embankment construction. The reinforcement was not anticipated to reduce settlement of the embankment but was assumed to provide for a more uniform settlement. As such, the geosynthetic was anticipated to reduce differential settlement at points of transition in organic soil thickness.

REINFORCEMENT REQUIREMENTS

Analyses were carried out in order to determine the strength of the reinforcement necessary to enable the proposed embankment to be constructed to its full height. The calculation method utilized the critical failure surface from the slope stability analysis of the unreinforced section to determine the resisting moments required to raise the factor of safety above 1.3 at the end of construction. This additional resisting moment was then assumed to be developed by the reinforcing element. The strength required of the reinforcing and its location was then determined analytically. The long-term factor of safety was met through post-construction (consolidation) shear strength gains in the subgrade.

Several methods of analyzing the required strength of the geosynthetic were used as summarized in the FHWA Geotextile Engineering Manual, (Christopher and Holtz, 1985). The methods included those proposed by Fowler, 1980 and Wager, 1981. The Fowler method assumes that the reinforcement is placed in tension by alignment tangent to the failure surface such that the resisting moment provided by the geotextile is equal to the radius of the circle times the allowable strength in the reinforcement. Please refer to Figure No. 3. The increase in resisting force is defined by the following equation:

$$M_r = T R \qquad (1)$$

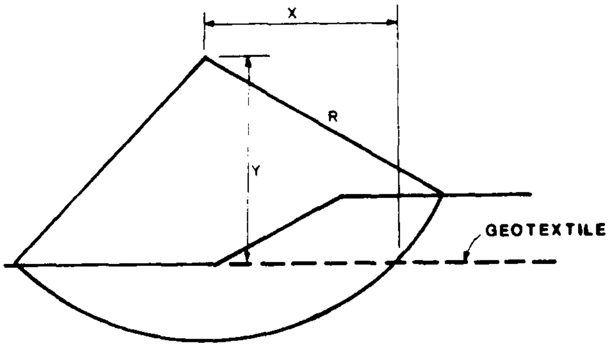

Figure 3 Geotextile Reinforcement Model

The Wager method uses a vector approach which accounts for soil-fabric interaction plus the strength of the textile. The Wager method allows for the soil-fabric friction by adding the geotextile tensile strength (T) times the height (Y) of the radius point of the slip circle above the fabric, to the textile strength times the horizontal component of the radius (X) times the tangent of the embankment fill friction angle (ϕ). See Figure No. 3. Therefore, the increase in resisting moment (M_r) provided by the geosynthetic is defined by the following equation:

$$M_r = T\,Y + T\,X \tan \phi \qquad (2)$$

For highly deformable soils such as peat, it was our opinion that the Wager method provided a realistic model and was used for the final selection. For other less deformable soil conditions, the Fowler and Wager methods may be non-conservative (Bonaparte and Christopher, 1987).

The geosynthetic reinforcement analysis indicated that at the most critical location, a total reinforcement tensile strength on the order of 1500 lb/in would be required. Even though this is a relatively high geosynthetic strength requirement, it could be easily be met by commercially available products if several layers of geosynthetic were used. By considering several layers, other efficiencies could be gained as strength requirements were neither uniform across the site nor along the alignment.

Several items were required to assure compatibility of the multiple layers. Firstly, the reinforcement layers were separated by a minimum of one foot of granular soil such that maximum soil-fabric friction could be achieved by each layer. Secondly, similar stress-strain characteristics were required of each layer such that strength requirements were achieved at compatible strains. Finally, a re-analysis was made to verify the strength requirements for each successive layer.

The reinforcing requirements were also evaluated with respect to the ability of the reinforcement to limit lateral movement of the embankment. An analysis was made to determine the factor of safety against the embankment fill sliding laterally on top of the reinforcing material. A soil-fabric friction angle of 25° was required. An analysis was then made to determine the strength of the reinforcing required to resist substantial lateral movement. The force to be resisted was assumed to be the force resulting from the active lateral pressure at the base of the embankment with an applied factor of safety of 1.5.

As substantial movement was anticipated along the alignment of the embankment during construction, the above lateral spreading analysis was also used to determine the required geotextile strength in that direction.

A limiting design strain was then established to control the lateral and longitudinal movement at the design strength requirements. A limiting strain of less than 10% was selected to reduce the potential for tension cracking in the embankment following construction (5% induced strain was assumed during construction). Geotextile requirements will be detailed in a later section.

TOE BERM REQUIREMENTS

The reinforced embankment was then checked for overall bearing capacity failure. Since the reinforcement was designed to prevent local shear failure, the stress at the base of the embankment could then be assumed to be distributed more over the full width of the embankment. A classical (Prandtl) analysis averaging the strength of all soils within the classical failure zone indicated a factor of safety in excess of 1.5. However, it is unlikely that an embankment that is wide relative to the thickness of the underlying soft layer would fail in this mode. A more probable mode of failure would involve the lateral squeezing of soils from beneath the embankment. An elastic shear stress versus shear strength analysis (Jurgenson: Boston Society of Civil Engineers, 1934) at the edge of the embankment indicated an unsafe condition in the lower strength subgrade area (factor of safety approximately 1). Passive pressure and shear resistance analysis indicated higher factors of safety. Due to the possibility of low factors of safety in these areas. Special construction procedures were recommended to increase stability, including the use of a berm at the toe of the embankment in those sections to provide additional lateral resistance and the construction of a berm prior to to construction of the embankment to contain soil and prevent it from squeezing laterally. These construction techniques are typically referred to as mud wave construction techniques and will be reviewed further in the construction details section.

EMBANKMENT SETTLEMENT

The settlement of the embankment was calculated two ways using the results of the laboratory consolidation tests. The first way involved a conventional consolidation theory using the compression index measured by the conventional laboratory consolidation tests. Using this method, extremely large settlements were predicted. In most cases, the predicted settlement exceeded the height of the embankment. While it is certainly possible for the settlement to exceed the height of fill placed, this was not judged to be likely based upon past experience.

The second method of predicting settlement was more simplistic. This method used the results of the long-term consolidation tests that were performed in the laboratory. In this method, the predicted settlement was equated to the compression measured in the laboratory under a similar pressure times the ratio of the thickness of the compressing soil in the field to the laboratory sample thickness. The results of three long-term consolidation tests performed at a constant load increment of 1000 psf, the maximum pressure expected to result from embankment construction, were used for this analysis. The pertinent compression was taken to be that occurring at the completion of full primary consolidation.

Based upon this analysis the calculated primary settlement, under an embankment load of 1000 psf and assuming a 20 foot peat thickness, ranged from 8 inches to 28 inches.

In addition to the primary consolidation discussed above, secondary compression of the peat was anticipated. The secondary compression was computed, based upon the coefficient of secondary compression determined from the long-term consolidation tests.

The predicted total settlement including the primary consolidation and the secondary compression is summarized on Figure No. 4. The wide band of settlement resulted from variations in laboratory consolidation test results.

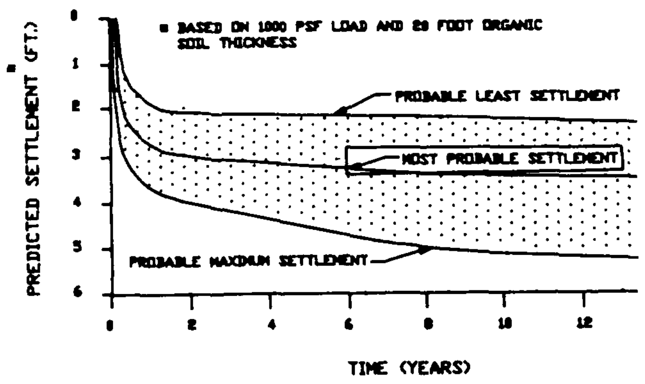

Figure 4 Predicted Settlement

The noted settlement was for the conditions of 20 feet of compressing soil and an embankment load corresponding to 1000 psf. Where the embankment was lower or where the thickness of the organic soil was less, proportionately less total settlement was anticipated.

GEOTEXTILE SPECIFICATIONS

The specifications that were prepared for the project are summarized on Table No. 1 which follows:

Each fabric roll was required to be marked showing the type of fabric upon delivery to the field. Two (2) copies of the mill certificates for the geotextile were required to be provided with each shipment of the fabric.

Testing by an independent agency was specified to confirm the design parameters. A complete design parameter test series was required for the first shipment to the site. Additonal sets of strength and modulus parameters were required for each additional 10,000 square yards used on the project.

TABLE No. 1

GEOTEXTILE SPECIFICATIONS

PARAMETER	METHOD*	FABRIC DESIGNATION	MINIMUM VALUE	DIRECTION
1. Tensile Strength	ASTM D4595-Wide Width Method	500 lb/in 1000 lb/in	500 lb/in 350 lb/in	Machine Cross
		1000 lb/in	1000 lb/in 350 lb/in	Machine Cross
2. Modulus	ASTM D4595-@ 10% Strain	500 lb/in	2500 lb/in 2000 lb/in	Machine Cross
		1000 lb/in	2500 lb/in 2000 lb/in	Machine Cross
3. Elongation at Required Strength	ASTM D4595	All Fabric	20% Maximum	--
4. Soil-Fabric Friction Angle	Direct Shear Method	All Fabric	25°	--
5. Puncture Strength	ASTM D3787-5/16" Hemispherical Tipped Rod	All Fabric	100 lb	--
6. Trapezoidal Tear	ASTM D4533	All Fabric	100 lb	--
7. Mullen Burst	ASTM D3786	All Fabric	500 psi	--
8. Apparent Opening Size	Corps of Engineers CW 02215	All Fabric	30-100**	--
9. Permeability	ASTM D4491	All Fabric	0.01 cm/sec	--
10. Percent Open Area	Corps of Engineers AD-745-085	All Fabric	1	--

* Updated to current methods
** Refers to lower layer of fabric. Upper layer could have up to 1/2 inch A.O.S.

Since the geotextile contributed significantly to the strength of the embankment, seams were allowed only in the transverse direction, the direction in which the shearing stresses were lower. The seams were required to develop the specified strength of the geotextile in the cross direction. The seams were required to be sewn with thread having equal or greater strength and durability as the material of the geotextile. The seams were specified to be double sewn with parallel stitching approximately 1/2 inch apart. Chain-lock seams were required to reduce the potential for unraveling. The sewn-fold was required to be placed on the upper surface of the geotextile to facilitate observation of the seams.

CONSTRUCTION DETAILS

The following items briefly highlight major construction procedures:

- A well-graded granular fill was specified to facilitate placement and compaction. It was also felt that granular fill would be more tolerant of the anticipated settlement.
- The bottom 1.5 feet of fill was specified to contain less than 5% fines in order to function as a drainage layer.
- Side slopes were specified to be 4 (horizontal) : 1 (vertical) or flatter. A 10 foot wide toe berm was required for embankment heights greater than 10 feet.
- The lower geotextile reinforcement layer extended across the full embankment width. The upper geotextile extended 10 feet beyond the embankment crests.
- The east half of the embankment was filled only to half height during the first construction season. Thus, it served as a temporary berm for the higher western half of the embankment.
- The temporary berm allowed a surcharge to be placed on the western half of the embankment to accelerate settlement.

- A minimum of 3 feet of separation between the peat and the pavement subgrade was required.

- Felled trees were left in place to create a "corduroy road", which aided trafficing on the subgrade and provided slight additional reinforcement. The length of trees was oriented perpendicular to the embankment alignment.

- The contractor opted to place a low strength "sacrificial" geotextile directly above the felled trees. Drainage fill was placed on the "sacrificial" fabric to provide a working platform.

- The first layer of geotextile reinforcement was smoothly rolled out on the working platform. The fabric was pulled as taut as possible to remove wrinkles and then sewn as specified.

- The placement of subsequent fill was initiated at the toe of the embankment and proceeded toward the center. The settlement occurring at the toes further tensioned the fabric.

- No turning of the fill placement vehicles was allowed on the first lifts of fill.

- The height of fill piles was restricted to 3 feet before blading. No fill piles were allowed to remain overnight. Side slopes were not allowed to become steeper than 4:1 at any time.

EMBANKMENT PERFORMANCE

Monitoring of the construction operations and the performance of the embankment was provided by WDOT.

The instrumentation that was installed included settlement plates, pore pressure piezometers and inclinometers. The majority of the instrumentation was concentrated where the organic soils were weakest and thickest. The primary data related to settlement of the embankment is discussed in the following paragraphs.

The during construction and immediate post-construction performance of the embankment, as determined by monitoring the settlement plates, was as predicted. In most areas, the settlement which had occurred at the time of pavement construction was in the range of 2 to 4 feet. The one exception was in the localized area where overfilling caused shear displacement that resulted in 6 feet of apparent settlement.

It is believed that early during construction, a localized seam failure occurred in the sacrificial fabric at this location. The failure likely resulted from the unintentional placement of excessive fill in this area, which overstressed the seam. Several feet of excess fill was placed in this area before the failure was detected. The large movement observed at the east side at Station 395+00 appeared to result from shear displacement-not consolidation settlement.

The area was repaired by filling the depression with light weight fill (branches and twigs) up to the surrounding fill surface. The area was then covered with an additional sacrificial geotextile layer, which overlapped a minimum of 5 feet over the stable surrounding fill. Conventional procedures then resumed, including placement of the two high strength geotextile reinforcing layers.

The post-paving performance of the embankment has been as good or slightly better than predicted. Survey markers installed on the pavement, shortly after placement, experienced from zero to 5 inches of settlement during the subsequent year and a quarter. Since post-paving differential settlement has occurred over a long span, the distortion is minimal and rideability of the section is considered good.

CONCLUSIONS

1. Geosynthetic reinforcement can be engineered, using procedures discussed herein, to allow the support of embankments over weak foundations.

2. Geosynthetic reinforcement is a cost-effective method. It is conservatively estimated that $400,000 was saved on the Highway 45 project, when compared to more conventional alternatives.

3. The settlement of embankments can be predicted using methods discussed herein.

4. The geotextile reinforced embankment can be tolerant of significant settlement.

5. The post-pavement construction settlement has been slight and the rideability of the highway is excellent.

6. Close construction monitoring is important and should be considered an extension of the design process.

ACKNOWLEDGEMENTS

The authors express their appreciation to the J.C. Zimmerman Engineering Corporation, and in particular Mr. John Penshorn for the opportunity to become involved in the project. Appreciation is also extended to the Wisconsin Department of Transportation for the information that they shared concerning the performance of the embankment.

REFERENCES

Christopher B.C. and Holtz, R.D. (1985), "Geotextile Engineering Manual", Federal Highway Administration, Washington, D.C.

Fowler, J. and Hailburton, T.A. (1980), "Design and Construction of Fabric Reinforced Embankments", The Use of Geotextiles for Soil Improvements, Preprint 80-177, ASCE Convention, Portland, Oregon, pp. 89-118.

Wager, O. (1981), "Building of a Site Road Over a Bog at Kilanda, Alvasborg County, Sweden", Report to the Swedish State Power Board, Boras, Sweden, 16 p.

Proceedings: Second International Conference on Case Histories in Geotechnical Engineering, June 1-5, 1988, St. Louis, Mo., Paper No. 5.43

Field Measurement on a Slope Cutting with Tensile Inclusions

Tamotsu Matsui
Professor, Osaka University, Japan

Ka Ching San
Graduate Student, Osaka University, Japan

Terumasa Amano
Assistant Chief, Osaka Prefectural Government, Japan

Yoshinori Otani
Engineer, Hirose and Co. Ltd., Japan

SYNOPSIS In a road widening project, tensile inclusions were used to stabilize some parts of cut slope works. The site condition and the construction of reinforced slope cutting are presented. A full scale field test on a reinforced cut slope was performed being incorporated with this road widening project. The field test consisted of a field loading test and a field excavation test. Details of the field test, field measurements and site observation are presented. Finite element analysis of the field test is performed. Based on the field measurements together with the analytical results, the reinforcement mechanism of a reinforced cut slope under a surcharge load and that under an effect of excavation are discussed.

INTRODUCTION

Natural slope stabilization by means of tensile inclusions, that is, root piles or soil nailing, has attracted special interests recently. Reticulated root piles which is an in-situ soil reinforcing technique were employed to stabilize some parts of cut slope works in a road widening project, in Osaka, Japan. The reinforcement mechanism and its estimation in practical projects, however, have not been elucidated yet. Therefore, a full scale field test was performed being incorporated with this road widening project. The field test consisted of a field loading test and a field excavation test. Long term site observation program continued to monitor the performance of the reinforced cut slope.

In this paper, first the general ground condition of the site of the road widening project and the construction of the reinforced slope cutting are described. Then the detail of the field test, field measurements and the site observation are presented. Finite element analysis of the field test is carried out. Finally, based on the field measurements together with the analytical results, the reinforcement mechanism of the reinforced slope cutting under a surcharge load and that under the effect of excavation are discussed.

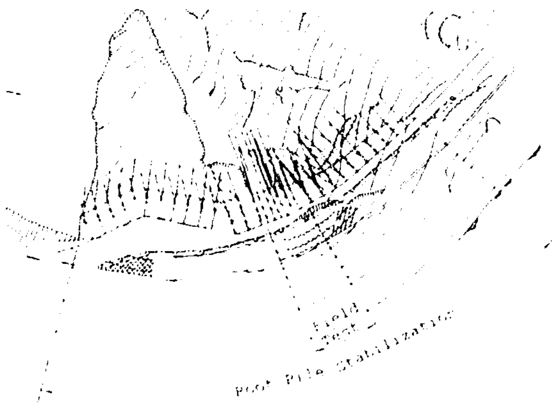

Fig. 1 Plan of the Reinforced Slope Cutting

ROAD WIDENING PROJECT

Site condition

The site is located on a mountainous region in the suburbs of Osaka, Japan. The site consists dominantly of gneiss-granite deposit. The existed road is at the mid-level of slope with the elevation of about 300m above sea level. The slope consists of an inclined soft rock stratum overburdened by a completely decomposed granite residual soil layer of several meters with a dip of 20°-35°. In the nearby area a slope failure happened previously during the cutting in the road widening works.

Construction of the reinforced cutting

In order to ensure the long term slope stability of the cut slope and the safety of the cutting during construction, slope stabilization by root piles was used in some part of cutting in the road widening project. The proposed plan and section of the reinforced slope cutting are shown in Figs.1 and 2, respectively.

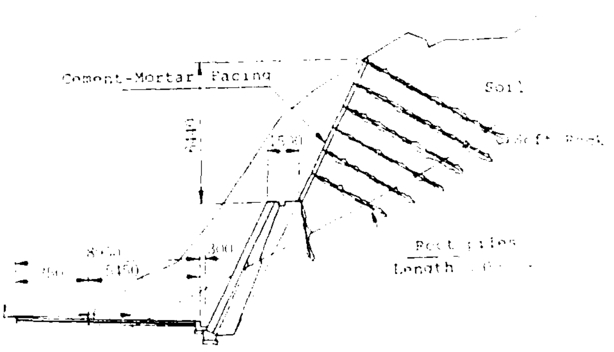

Fig. 2 Section of the Reinforced Slope Cutting

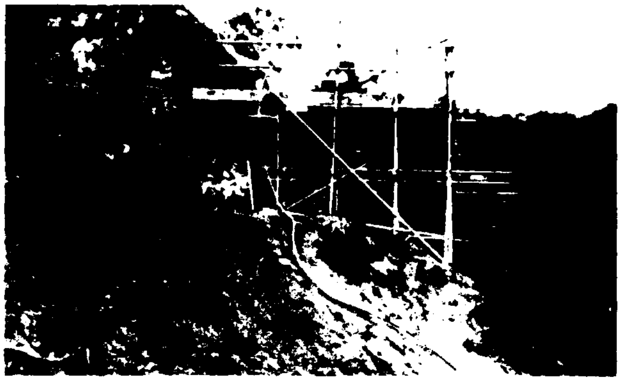

Photo 1 Construction of the Reinforced Slope Cutting in Progress

The extent of the reinforced slope cutting works is 46.75m long and the proposed reinforced cutting is in a gradient of 1:0.5. The excavation is carried out by steps with a pitch of 2.5m. After the completion of each step of excavation, drilling hole of diameter of 116mm is formed by a rotary drill (see Photo 1). The reinforcement of root pile is a small steel pipe with 36mm diameter and 6mm thickness. The root pile is formed by grouting the steel pipe with expansive mortar. In order to increase the bond between the mortar and reinforcement, a special ring is fixed in the steel pipe at 500mm interval. The head of the root pile is fixed with a bearing plate and a nut, as shown in Fig.3. The surface of the cutting is protected by 30mm thick mortar with a steel mesh (see Photo 2). The sequence of construction of root pile is illustrated in Fig.4.

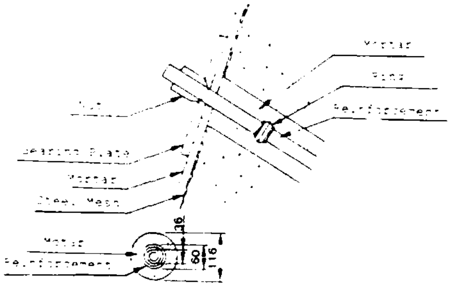
Mortar
Ring
Reinforcement
Nut
Bearing Plate
Mortar
Steel Mesh
Mortar
Reinforcement
36
60
116

Fig. 3 Section of the Root Pile

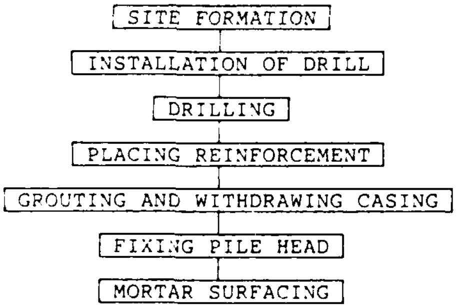
SITE FORMATION
INSTALLATION OF DRILL
DRILLING
PLACING REINFORCEMENT
GROUTING AND WITHDRAWING CASING
FIXING PILE HEAD
MORTAR SURFACING

Fig. 4 Construction Sequence of Root Pile

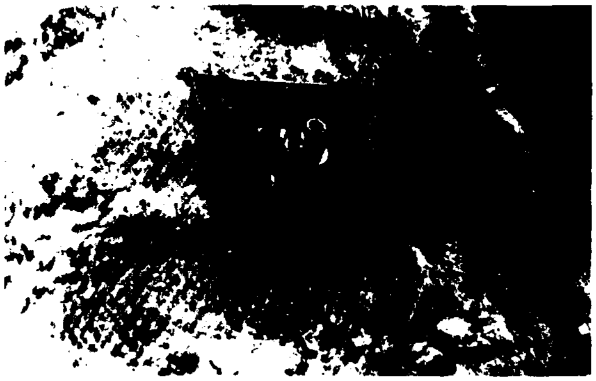

Photo 2 General View of the Root Pile Head

Design of reinforced slope cutting

Codes or Standards on the slope stabilization by tensile inclusions have not been established yet. In this project the reinforced cutting is designed by empirical method. The unreinforced cut slope is first analyzed by limit equilibrium slope stability method. Then the tensile force of reinforcement to obtain a required factor of safety of the cutting is estimated. From the required tensile force of the reinforcements, length, arrangement and inclination of the reinforcements are determined by considering the ultimate allowable stress of the section of the reinforcement and the ultimate allowable bond stress between the reinforcement and the soil.

The general design approach for the slope stability analysis on a slope cutting stabilized by tensile inclusions is illustrated in Fig.5. The analysis of the reinforced cutting, the equilibrium of forces and the strain compatibility between the reinforcement and the soil should be satisfied. In the limit equilibrium analysis the strain compatibility condition is not satisfied. It seems that the deformation analysis by finite element method could be a better solution for the reinforced cutting analysis. An appropriate design method of a reinforced slope cutting cannot be developed if the mechanism is not

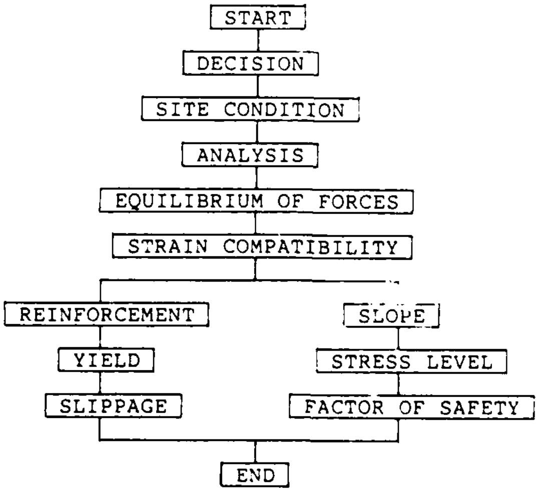
START
DECISION
SITE CONDITION
ANALYSIS
EQUILIBRIUM OF FORCES
STRAIN COMPATIBILITY
REINFORCEMENT
SLOPE
YIELD
STRESS LEVEL
SLIPPAGE
FACTOR OF SAFETY
END

Fig. 5 Design Approach of Reinforced Slope Cutting

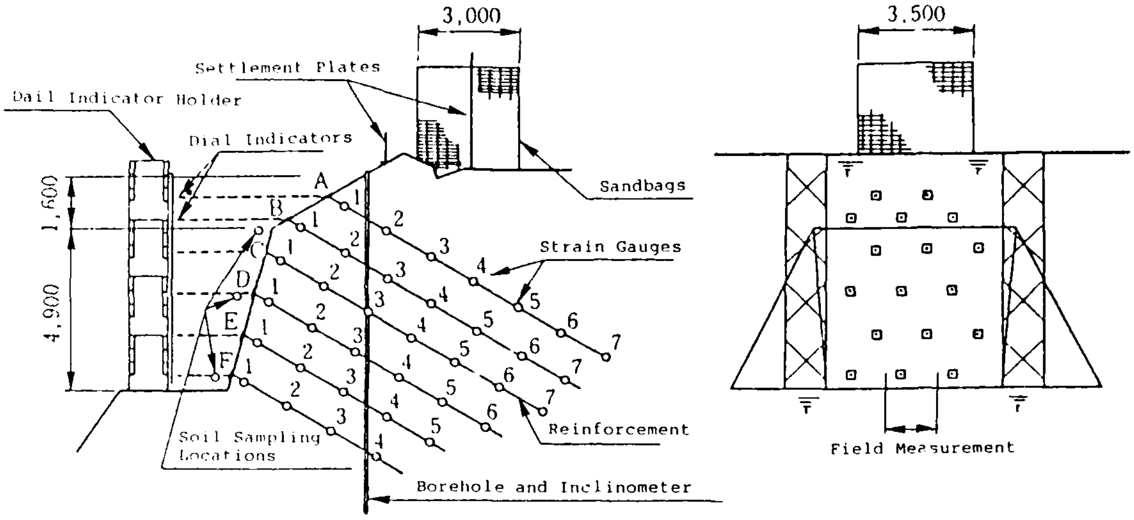
3,000
Settlement Plates
Dail Indicator Holder
Dial Indicators
1,600
4,900
A
B
C
D
E
F
1
2
3
4
5
6
7
Sandbags
Strain Gauges
Reinforcement
Soil Sampling Locations
Borehole and Inclinometer
3,500
Field Measurement

a) SECTION b) ELEVATION

Fig. 6 Section and Elevation of the Reinforced Slope for the Field Test

clarified. Therefore a full scale field test is performed in the middle section of the reinforced cutting works to examine the mechanism of reinforced slope cutting.

FIELD TEST

Test site

In order to monitor the safety of the reinforced cutting, to ensure the effect of reinforcement and to examine the reinforcement mechanism, a field loading test and a field excavation test were performed (see Photo 3). Fig.6 show the section and the elevation of the reinforced slope for the field test. The gradient of the slope cutting is 1:0.3 The soil profile at the borehole location is shown in Fig.7. The thickness of the decomposed granite layer is about 7m from the top of slope. The physical properties of the decomposed granite are given in Table 1.

The reinforced slope cutting was constructed by three steps as shown in Fig.8. In the first step, before first excavation the reinforcements A and B were constructed. In the second step, the upper portion of excavation was conducted, then the reinforcements C, D and E were installed. In the third step, the last reinforcement F was installed after the lower portion of excavation was completed.

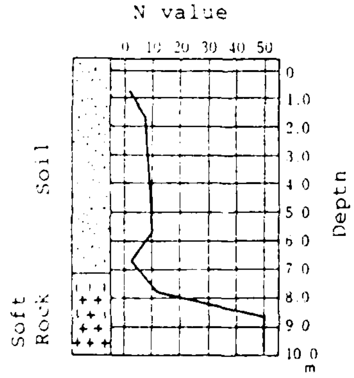

Fig. 7 Soil Profile at the Borehole Location

Photo 3 General View of the Field Test

Table 1 Test Results of Decomposed Granite

Test Items	Locations of Sample		
	C	D	F
Unit Weight (gf/cm^3)	1.97	1.96	1.90
Water Content (%)	8.3	5.7	14.0
Void Ratio	0.55	0.55	0.56
Ignition Loss (%)	3.7	3.5	6.1

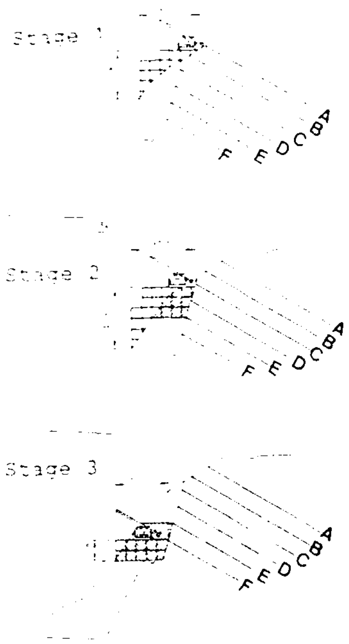
Stage 1
Stage 2
Stage 3
A
B
C
D
E
F

Fig. 8 Construction Sequence of Reinforced Slope Cutting

Instrumentation

The instrumentation consisted of numbers of strain gauges on the reinforcement, six dial indicators on the surface of the cutting, an inclinometer in the borehole and two settlement plates on the top of cut slope, as shown in Fig.6.

Limit equilibrium analysis

The limit equilibrium analysis was performed using the method of slices by assuming a circular slip surface. The material properties were estimated from the N values obtained from the borehole and the back analysis of the previous landslide. The parameters of the soil and the soft rock used in the slope stability analysis are summarized in Table 2.

Figs.9 and 10 show the results of slope analysis of the unreinforced slope under the surcharge load and the effect of excavation, respectively. The minimum of factors of safety obtained from the limit equilibrium analysis are summarized in Table 3.

Table 2 Parameters of Soil and Soft Rock

Parameters	Soil	Soft Rock
c (tf/m^2)	1.0	1.0
ϕ (degree)	19.0	45.0
Unit Weight (tf/m^3)	1.80	2.00

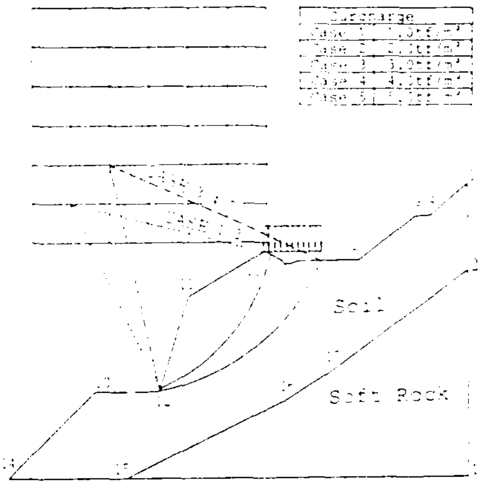
Surcharge
Case 1
Case 2
Case 3
Case 4
Case 5
3.0tf/m²
4.0tf/m²
CASE
CASE
Soil
Soft Rock

Fig. 9 Slope Stability Analysis of a Slope under a Surcharge Load

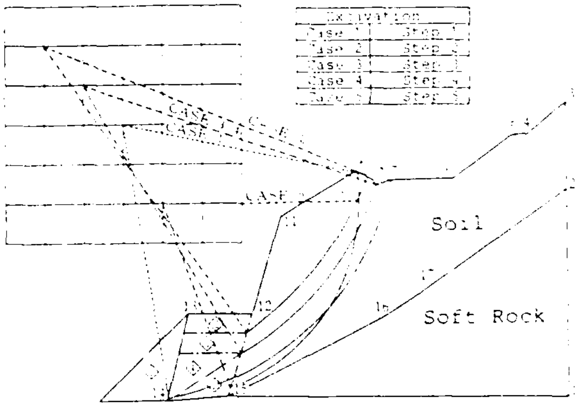
Excavation
Case 1
Case 2
Case 3
Case 4
Case 5
Step 1
Step 2
Step 3
Step 4
Step 5
CASE
CASE
CASE
Soil
Soft Rock

Fig. 10 Slope Stability Analysis of a Slope under an Effect of Excavation

Table 3 Factors of Safety of the Unreinforced Cut Slope

Cases	Factor of Safety	
	Load Test	Excavation Test
Case 1	0.835	0.763
Case 2	0.799	0.735
Case 3	0.745	0.666
Case 4	0.697	0.666
Case 5	0.655	0.615

Field loading test and field excavation test

In order to apply a uniformly distributed load, the loading test was carried out by piling up sandbags on the top of slope as shown in Fig.6. The sandbags were placed at a controlled loading speed of 0.59tf/m²/h. The loading curve is shown in Fig.11. For the purpose to check whether the instruments work properly, a preloading test was performed in the first day. The typical measured maximum tensile forces developed in the reinforcements, such as reinforcement A and C, are given in Fig.12.

The field excavation test was carried out after the sandbags were removed by excavating the lower part of slope up to about 5m depth. It was necessary to remove the dial indicator holder to carry out excavation, therefore the surface horizontal displacement could not be measured. The excavation was carried out by steps. Typical measured maximum tensile forces developed in the reinforcements, such as A and C, versus the elapsed time after excavation is shown in Fig.13.

From Figs.12 and 13 it can be seen that the tensile force developed in the reinforcement under an effect of surcharge reached a stable state immediately after the surcharge loading was applied and the tensile force slightly reduced after the surcharge loading was removed. However it took about two weeks for the tensile force developed in the reinforcement to reach a stable stage under an effect of excavation. This delayed response of the development of tensile force in the reinforcement may be due to the effect of the relic joint in the decomposed granite. When a surcharge loading is applied, the relic joint is compressed immediately and permanently. So the tensile force developed in the reinforcement immediately after the surcharge load is applied and such a tensile force reduces in a very small amount after the surcharge load is removed. On the other hand, stress relief produced by excavation may cause the relic joint to expand. Such swelling process is slow, because water absorption needs time for the water to penetrate. The field measurement shows that such a process takes about two weeks to reach a stable stage.

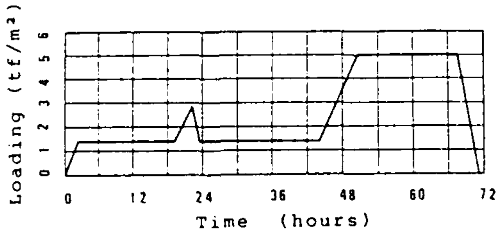

Fig. 11 Applied Surcharge Load versus Time

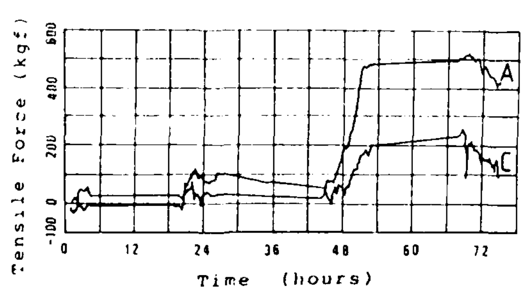

Fig. 12 Measured Tensile Force versus Time

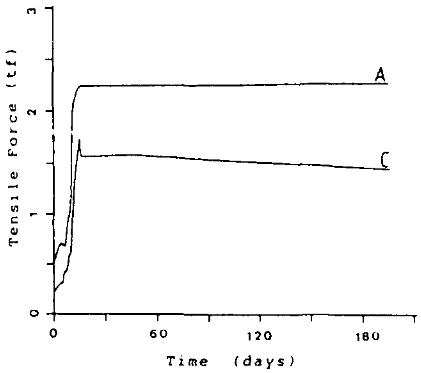

Fig. 13 Measured Tensile Force versus Days after Excavation

Field measurement

Fig.14 shows the measured horizontal displacement of slope surface for the loading test. Fig.15 shows the horizontal displacement at the borehole location for both loading test and excavation test. Field measurement shows that the upper portion of the slope moved forward while with negligible movement at the lower

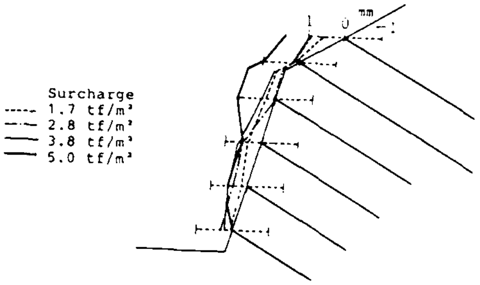

Fig. 14 Measured Horizontal Displacement at the Surface of the Slope

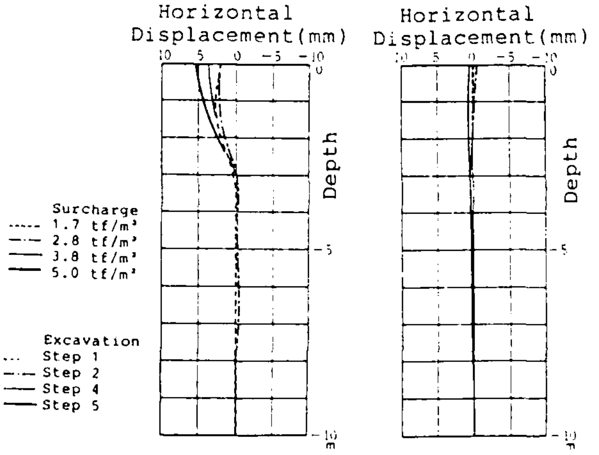

a)Surcharge b)Excavation

Fig. 15 Measured Horizontal Displacement at the Borehole Location

portion.

Figs.16 and 17 show the measured axial forces developed in the reinforcements for the loading test and the excavation test, respectively. Field measurement shows that the axial forces developed in the reinforcement are not all in tension in case of surcharge and that are mainly in tension in case of excavation.

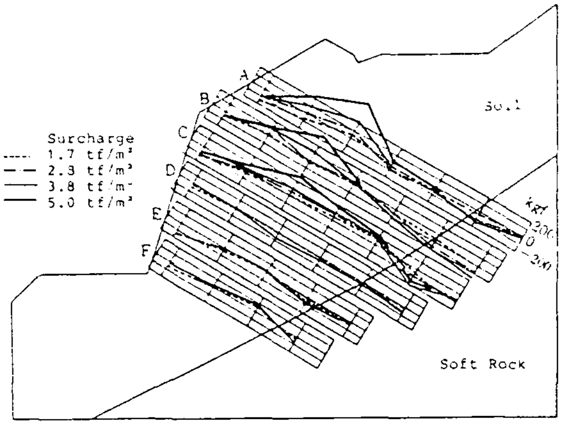

Fig. 16 Measured Axial Force Distribution of Reinforcement(1tf/m²-5tf/m²)

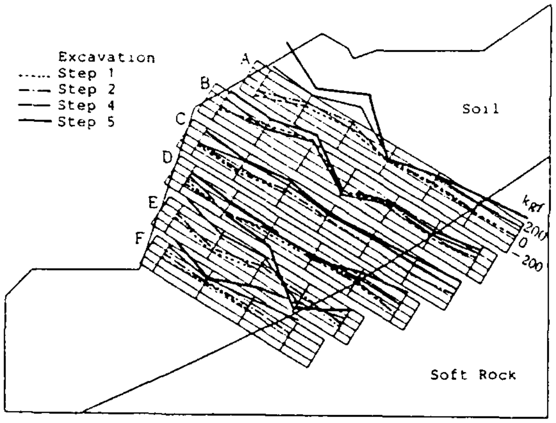

Fig. 17 Measured Axial Force Distribution of Reinforcement (At the End of Excavation Step)

COMPARISONS OF MEASURED AND ANALYTICAL RESULTS AND ITS CONSIDERATIONS

General remarks

Finite element analyses of the field test have been performed (Matsui and San, 1987). In the analyses, the soil is assumed to be nonlinear elastic with a hyperbolic tangent modulus (Duncan and Chang, 1970) and the soft rock linear elastic. The slippage between the reinforcement and the surround medium and between the soil and the rock is modeled by a elasto-plastic joint element (Matsui, Abe and San, 1986, Matsui and San, 1988). The reinforcement is considered as one dimensional bar element. The material properties used in the present analysis are summarized in Table 4.

Deformation of the slope and axial forces developed in the reinforcements

The deformation of the slope under 5tf/m² of surcharge loading obtained from finite element analysis is shown in Fig.18. By comparing Fig.18 with Figs.14 and 15(a), it can be seen that both analytical and measured results show that the top of slope surface moved forward, while with a small movement at the toe and that the horizontal displacement within the slope is large at the upper portion while with negligible movement at the lower portion.

Fig.19 shows the analytical axial force distribution of reinforcements for the case of

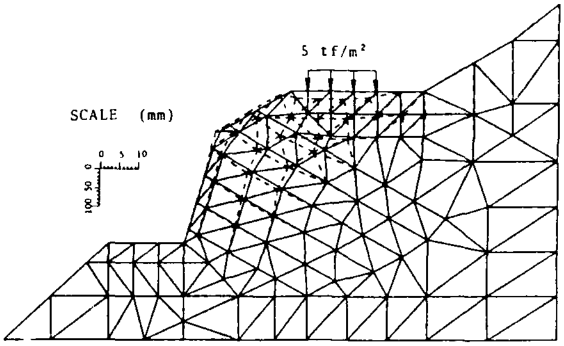

Fig. 18 Analytical Deformation of the Reinforced Cut Slope under 5tf/m²Loading

Table 4 Material Properties

	Decomposed granite	Soft rock	Reinforcement
Elastic modulus E (tf/m²)	2.2×10^3	1.4×10^5	2.1×10^7
Unit weight γ (tf/m³)	1.8	2.0	-
Poisson's ratio ν	0.3	0.3	0.3
Friction angle ϕ (degree)	19	45	-
Cohesion c (tf/m²)	1.0	1.0	-
Coefficient of earth pressure at rest K_0	0.67	0.67	-
Hyperbolic constant K	210	-	-
Hyperbolic constant K_{ur}	420	-	-
Hyperbolic constant n	1.02	-	-
Failure ratio R_f	0.69	-	-
Cross section area A (m²)	-	-	5.2×10^{-4}

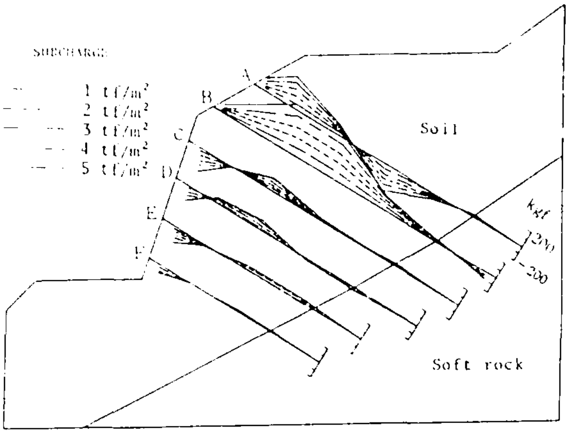

Fig. 19 Analytical Axial Force Distribution of Reinforcement (1tf/m²-5tf/m²)

field loading test. From Figs.16 and 19, it can be seen that both analytical and measured results show that the axial forces developed in the reinforcement are not all in tension, and that the tensile force developed in the upper reinforcements are significantly larger than the lower.

Shear strength of reinforced soil mass

Figs.20 and 21 show the distribution of total principal stress in the reinforced and unreinforced slopes under the loading of 5tf/m², respectively. It can be seen that the orientation of principal stress of the soil is slightly changed, while the minor principal stress is significantly increased in the reinforced soil mass. It is very clear that the increase in the minor stress contributes to increase the shear strength of the reinforced soil mass without any change of c,ϕ values.

CONCLUSIONS

A full scale field test on a reinforced cut slope incorporated with a road widening project has been presented. Finite element analyses of the field loading test have been also presented. The agreement between analytical results and field measurements is satisfactory. From the comparisons between measured and analytical results of the field loading test, the success of the slope stabilization by tensile inclusions, such as root piles, has been demonstrated. Both site observations and analytical results show that the upper part of the surface of the slope significantly moves away with small movement at the toe under the surharge. The analytical results indicate that the orientation of principal stress of soil is slightly changed, while the minor principal stress is significantly increased under the effects of reinforcement. The increase in the minor principal stress contributes to increase in the shear strength of soil without any change in c, ϕ values. Moreover, the reinforcement mechanism of a reinforced cut slope under an effect of excavation is different with that of surcharge. By comparing the reinforcement mechanism of a reinforced cut slope under a surcharge load and an effect of excavation, some distinguished aspects are summarized as follows:

(1) The axial forces developed in the reinforcement are not all in tension under surcharge loading. Such axial forces develop immediately as the surcharge is applied, and decreased in a small amount after the surcharge is removed.

(2) The axial forces developed in the reinforcement are mainly in tension under an effect of excavation with a maximum near the surface just after excavation is completed. Such axial forces increase with elapsed time and reach a stable condition after two weeks.

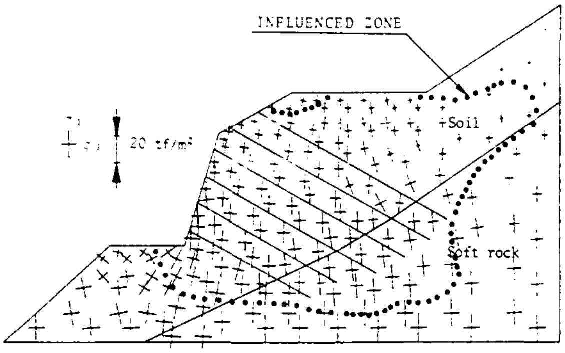

Fig. 20 Principal Stress Distribution of the Reinforced Cut Slope under 5tf/m² Loading

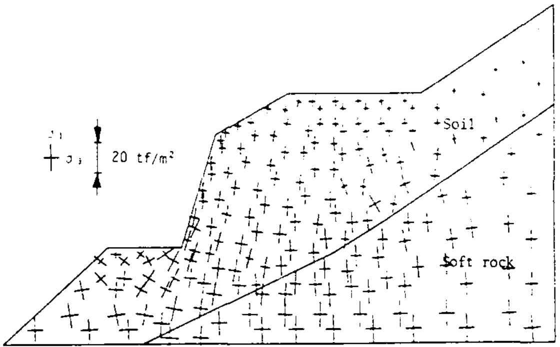

Fig. 21 Principal Stress Distribution of the Unreinforced Cut Slope under 5tf/m² Loading

REFERENCES

Duncan, J.M., and Chang, C.Y. (1970), "Nonlinear Analysis of Stress and Strain in Soils", J. Soil Mech. and Found. Engg. Div., ASCE, SM5, Vol.96:1629-1653.

Matsui, T., Abe, N., and San, K.C. (1986), "A Simple Mechanistic Model for Slippage with Application to Reinforced Soils", Proc. of 21st National Conf. JSSMFE: 1093-1096.

Matsui, T., and San, K.C. (1987), "Reinforcement Mechanism of Cut Slope with Tensile Inclusions", Proc. 8th Asian Reg. Conf. SMFE., Kyoto Vol.1:185-188.

Matsui, T., and San, K.C. (1988), "A Model for interface Slippage with Application to Reinforced Soils", Soils and Foundations. (to be published)

Proceedings: Second International Conference on Case Histories in Geotechnical Engineering, June 1-5, 1988, St. Louis, Mo., Paper No. 5.44

The Performance Behaviour of a Grain Silo Foundation in Jeddah Supported on Stone Columns

D.L. Jones
L.G. Mouchel & Partners, West Byfleet, Surrey, United Kingdom

M.H. Golder
L.G. Mouchel & Partners, West Byfleet, Surrey, United Kingdom

G.J. Macdonald
L.G. Mouchel & Partners, West Byfleet, Surrey, United Kingdom

SYNOPSIS: This paper describes the ground treatment carried out and the subsequent load settlement behaviour of a grain silo in Jeddah, Saudi Arabia. Predicted performance based on the results of both SPT and cone penetration tests are compared with actual behaviour. The prediction based on the SPT results is poor, with the cone penetration analyses giving a significant improvement. A knowledge of cone resistance and hence modulus values for the full depth of influence of the silo would have further refined the prediction.

INTRODUCTION

This paper details the settlement behaviour of a port silo of 20,000 tonne capacity constructed at Jeddah Port (Saudi Arabia) for imported cereals and expellers. (See Fig 1).

The silo installation at the port acts in the capacity of transit storage, permitting vessels of up to 65,000 tonnes to be discharged at 600 tonnes per hour, and the cereals transferred to inland feedmill storage silos by road vehicles. This case history relates to Phase I of the silo construction contract.

The silo structure comprises a block of 12, 10.5 metre square steel bins, constructed from deep profile corrugated steel sheet supported by hollow section concrete filled posts and diagonal tie bars.

The silo structure is founded on a reinforced concrete cellular raft 32.5m x 42.5m imposing an average stress of 250 kN/m² and a maximum of 300 kN/m² when 8 out of the 12 bins are loaded towards the end of the silo.

GEOLOGY AND GROUND CONDITIONS

The coastal plain around Jeddah Port consists of Quarternary/Recent deposits of gravel, sand, coral limestone and silt underlain at depth by Quarternary Volcanics or Pre Cambrian basement rocks.

The ground investigation for the silo complex consisted of cable percussion boreholes and static cone penetrometer tests. The investigation revealed that the site which is partly in an area of reclaimed land, is underlain by very loose marine shelly sands and silts with layers or lenses of clay and gravel and coral limestone. Graded bed sequences with gravel at the base, fining upwards, were evident as was the local concentrations of heavy minerals due to wave action at former beach levels.

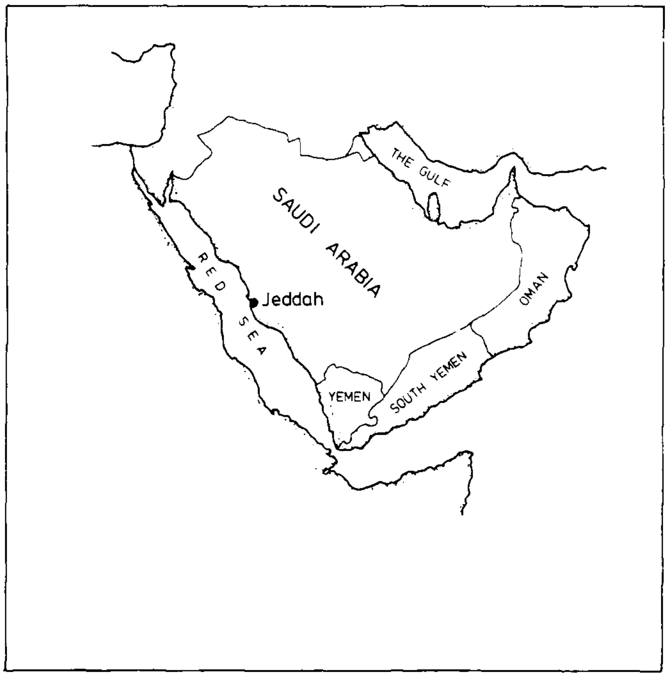

Fig. 1 Location Plan

The sequence contained thin laterally discontinuous bands of coral limestone up to 6m thick concentrated between depths of 2m to 9m and 18m to 32m respectively. The limestone is a breccioconglomeratic calcirudite composed of coral and limestone fragments with shell debris in a sandy matrix. Voids of between 20mm to 60mm were identified within the limestone layers. A further porous shelly limestone layer with dissolution cavities partially filled with sand gravel and clay was encountered from 49.0m to 59.5m depth but it is not known whether this is laterally persistent as only one borehole was taken to this depth, the others terminating between 40m and 50m. A typical section is shown in Fig 2.

Groundwater was encountered at some 1.5m below ground level, that is approximately at the founding level of the silo raft, a design criteria.

The Standard Penetration Test profiles recorded within the boreholes were generally similar with SPT 'N' values of between 2 to 20 to a depth of 16m reducing to between 0 and 12 to a depth of approximately 26m. (See Fig 2). Below this level SPT 'N' values increased significantly to between 25 and 50 with refusal being recorded after a short penetration into the limestone lenses. A number of cone penetration tests were subsequently carried out to further investigation the zone of low SPT results to a depth of 26m.

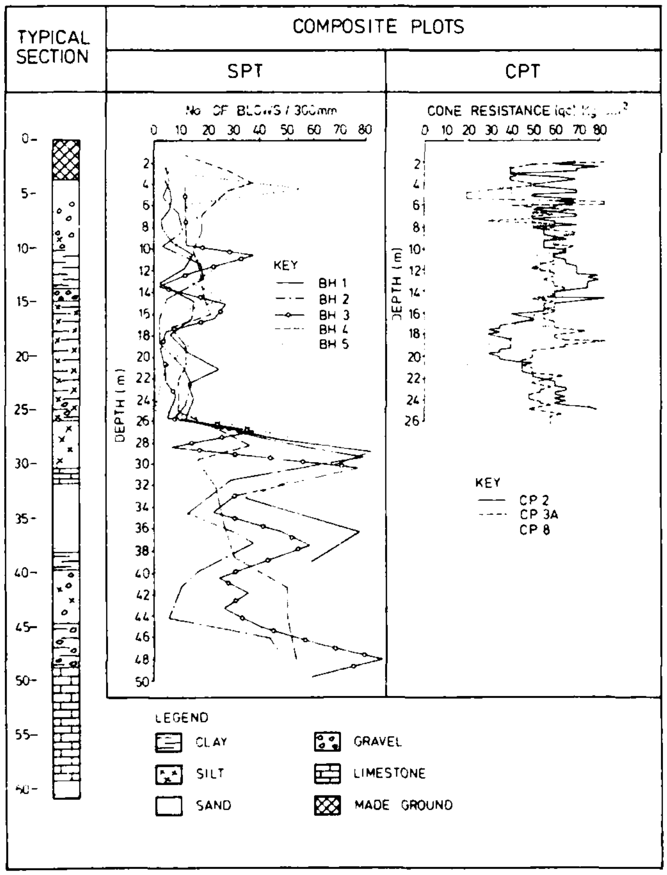

Fig 2 Typical Section and Penetration Test Results

FOUNDATIONS

In view of the low cone readings and low SPT 'N' values measured to a depth of 26m the possibility existed that a bearing capacity failure could occur under adverse silo loading conditions. The decision was therefore taken to adopt ground treatment to reduce adverse differential settlements and minimise the risk of bearing failure.

Options investigated included the formation of jet grouted columns, piling, dynamic compaction and vibro-replacement the latter being considered the most appropriate on the basis of financial and technical considerations.

The varying silt content within the ground suggested that vibro-replacement rather than vibro-compaction would be most effective. In view of the increasing friction ratio with depth, identified from the static cone testing, it was considered that a treatment depth of between 10m to 12m would represent the practical maximum depth throughout which useful treatment could be achieved. With friction ratios from the static cone penetrometer tests generally exceeding 3% within the zone to be treated by vibro-compaction, the treatment process becomes one of installing relatively stiff columns into the ground which itself shows little increase in relative density.

The ground treatment for the Phase I silo comprised the installation of some 500 stone columns to depths of 12m with a grid spacing varying from 2.0m to 2.5m.

PERFORMANCE BEHAVIOUR - PREDICTED

Settlement calculations were undertaken using the results of the SPT 'N' values and the static cone penetrometer tests. The SPT 'N' values exhibited a wide range which reflected the interbedded and lenticular nature of the deposits rendering a settlement analysis based on the results of average SPT 'N' values inappropriate. Typical settlements under an applied loading 250 kN/m² calculated by varing methods are 30mm and 40mm using Meyerhof (1965) and Schultze and Sherif (1973) respectively, and up to 70mm by Parry (1971). The more recent analysis by Burland and Burbridge (1985) produces a calculated settlement of 80mm.

Analysis based upon SPT testing would therefore suggest that the predicted settlements are within a range that could be accommodated by a silo raft where controlled loadings apply. However it is understood that severe settlement had been experienced on an adjacent silo site. A method of analysis based upon static cone penetrometer tests which provide a continuous profile of resistance with depth was therefore preferred. The results were analysed using Schertmann's (1970) procedure which assumes a triangular strain distribution up to a depth of twice the foundation width, that is some 65m. Although boreholes had been sunk to this depth the static cone testing met with refusal around a depth of 26m. Reference to the borehole records also indicated high SPT values below this level in dense sand and gravel with lenses of limestone.

A comparison of the measured penetration results with a chart for the interpretation of penetration tests in chalk by Searle (1979) suggest that the soils compare with a medium dense to dense structureless chalk and that the carbonate silts and sands are weakly cemented. An assumption was therefore made that the presence of high modulus materials below a depth of 26m would modify the stress distribution below the raft such that the majority of settlement occurred above this level.

A modulus value of 100 MN/m^2 was arbitarily ascribed to the materials below 26m depth. The effect of this assumption was to limit the predicted settlment to 25mm within the zone from 26m to 65m.

Based upon the above assumptions a calculated total settlement for the silo raft of 220mm was obtained which is significantly greater than that obtained using SPT results.

In assessing the reduction in settlement caused by the installation of stone columns reference was made to the method proposed by Priebe (1976). With the column spacings adopted, a settlement reduction factor of 2 could be applied. This is equivalent to doubling the modulus in the treated ground compared with the untreated ground. The effect on installing stone columns is thus limited to halving the settlement within the treated layer and is insignificant when compared with the overall anticipated settlement, the majority of which occurs below the treated zone. The reduction in settlement was calculated as being around 25mm. However, it was believed that the stone columns would significantly increase bearing capacity and by forming a layer of uniform stiffness would minimise differential movement.

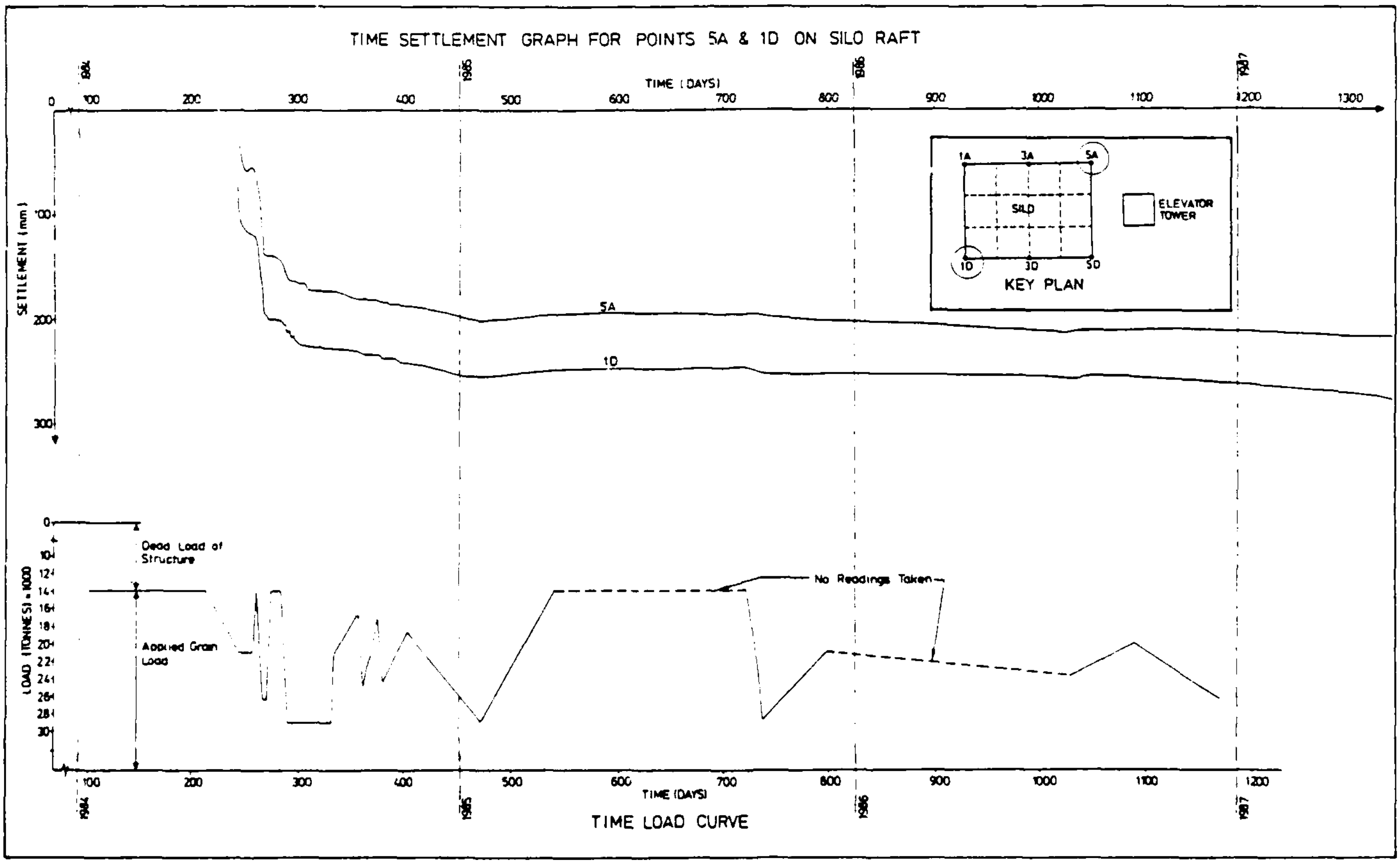

Fig 3 Load Settlement Behaviour

PERFORMANCE BEHAVIOUR - OBSERVED

Following completion of the silo raft in September 1983 steel targets were cast into corners and mid points of the long axis of the raft. Readings which were taken prior to the construction of the silo bins acted as datum for subsequent settlement measurements. The dead weight of the raft is 14000 tonnes giving an imposed bearing pressure of 100 kN/m². From the observations of subsequent load settlement behaviour it can be assumed that settlement of the raft was concurrent with construction.

The loading of the silos was carefully controlled by redistribution of grain to ensure uniform ground pressures and settlement. Reference to the load/settlement behaviour for two of the targets (Fig 3) indicates that settlement is virtually immediate upon application of load followed by a relatively minor time related settlement which lasts of the order of two to three weeks. The operational demands of the silo were such that full consolidation for a given load could not always be reached. As would be expected with subsequent unloading and reloading further settlement only occurred when the previous highest loading had been exceeded or where full consolidation has not been reached under previous loadings. As the full silo condition was approached only relatively small settlement increases occurred compared with those experienced during initial loadings. The magnitude of any elastic recovery during unloading was insignificant.

The design of the silo raft has allowed substantial redistribution of stresses to occur and can be thought of as approaching a rigid raft condition with regards to its settlement performance. Although the settlement of the centre of the raft was not monitored the performance of the silo suggests that there has been no adverse dishing at the centre. Relatively planar settlements can therefore be assumed.

The headhouse tilted towards the silo due to the influence of the silo loading on the settlement of the headhouse raft. This caused no structural or operational problems, but the access platforms between the headhouse and silo were adjusted to prevent damage by contact.

DISCUSSION

The observed settlements are large and exceeded that predicted. It should be noted that settlement readings were only taken after construction of the raft had been completed which accounts for approximately 40% of the load under a full silo condition. From the settlement observations, settlement under primary loading has been shown to be virtually concurrent with loading, followed by a minor consolidation period lasting 2 to 3 weeks. From this it can be assumed that settlement of the raft would have been essentially complete at the time of installing the steel targets. On a pro-rata basis the settlement of the raft alone could have been around 150mm.

For the carbonate deposits encountered, the ratio of observed to predicted settlement based on the results of SPT tests was high. Calculations using the cone penetrometer results superficially gave good agreement between predicted and observed, but if an allowance is made for settlement of the raft, this approach also underestimated total settlement. It is considered that the disparity is predominantly due to an overestimate of the modulus value below a depth of 26m.

The stone columns have provide very effective in reducing differential settlement and eliminating any bearing failure. The actual amount of total settlement has had little effect on the operational performance of the silos.

CONCLUSION

The load/settlement behaviour of the silos could not be adequately predicted using SPT based methods. The use of a static cone penetrometer enabled a better prediction to be made. However, as cone penetrometer tests were only able to penetrate to a depth less than half that influenced by the silo, a suitable estimate of the variation in modulus with depth could not be obtained. The use of a relatively high modulus at depth led to an underestimate of settlement.

The use of stone columns has prevented bearing failure and limited differential settlement. The silo has been fully operational since construction and has been unaffected by the settlement. The load/settlement behaviour of the silos shows that settlement has essentially ceased.

ACKNOWLEDGEMENTS

The writers wish to acknowledge Shiek A Fakieh of Fakieh Poultry Farms, Makkah, Saudi Arabia for permission to publish this paper. The civil contractors for the

development were Icori Estero SA and Berga Impianti Cereali SFS of Italy. The ground treatment was carried out by Cementation and Foundation Engineering Ltd, Great Britain and the ground investigations by Alhoty Stanger Ltd and Foundation Engineering Ltd, Saudi Arabia.

REFERENCES

Burland, J.B. and Burbidge, M.C. (1985) - "Settlement of Foundations on Sand and Gravel." Proc. Inst. Civ. Eng., Part 1, 78, Dec., pp 1325-1381.

Clarke and Walker (1977) - "A Proposed Scheme for the Classification and Nomenclature for Use in the Engineering Description of Middle Eastern Sedimentary Rocks." Geotechnique, Vol. XXVII, No. 1, pp 93-99.

Meyerhof, G.G. (1965) - "Shallow Foundations." ASCE, JSMFD, Vol. 91, SM2, pp 21-31.

Parry, R.G.H. (1971) - "A Direct Method of Estimating Settlements in Sands from SPT Valuves." Proc. Symp. Inter. Struct. Found. Mid. Soc. SMFE, Birmingham, pp 29-37.

Schmertmann, J.H. (1970) - "Static Cone to Compute Static Settlement over Sand." ASCE, JSMFD, Vol. 96, SM3, pp 1011-1043.

Schultze, E. and Sherif G. (1973) - "Prediction of Settlements From Evaluated Settlement Observations for Sand." Proc. 8th Int. Conf. Soil Mech. Fdn. Engng., Moscow, Vol. 1.3, pp 225-30.

Searle, I.W. (1979) - "The Interpretation of Begemann Friction Jacket Cone Results to give Soil Types and Design Parameters." Proc. 7th European Conf. Soil Mech. Fdn. Engng., Brighton, Vol. 2, pp 265-270.

Proceedings: Second International Conference on Case Histories in Geotechnical Engineering, June 1-5, 1988, St. Louis, Mo., Paper No. 5.45

Designing Geotextile Support for Submarine Power Cables

K.Y.C. Chung
Consultant of Geotechnical Services, Gilbert/Commonwealth,
Jackson, Michigan

SYNOPSIS: Six 36cm diameter submarine pipe-cables were buried in a 1.2 km long, fabric-lined trench in the soft river mud under 17m average water head across the Hudson River about 4.8km north of the Newburgh Bridge, New York. This paper describes the design considerations based on geotechnical point of view of using geotextile to support submarine power cables.

INTRODUCTION

Field and laboratory test results indicate that the upper river sediment is extremely soft and is thermally unstable (G/C, 1984). Thermal sand was required as backfill because its heat dissipating qualities prevent the conductors from over-heating.

Three alternatives to improve the stability of the trench were considered during design stage:

- Increase the trench depth to 2.44m and maintain the thickness of thermal sand at 1.83m.
- Maintain the 1.83m trench depth, and backfill with lightweight aggregate instead of the originally proposed thermal sand.
- Maintain the 1.83m trench depth, and place filter cloth in the trench prior to the placement of the thermal sand and pipes.

Environmental concerns prohibited river or ocean disposal of the dredged waste. A deep trench disposal plan was cancelled because of the volume and cost limitations of the upland disposal site. Cost comparisons indicated that using lightweight aggregate to replace the thermal sand was more expensive and less reliable than the fabric alternative. The filter fabric was therefore selected to line the trench, to help stabilize the trench bottom, and to prevent the river muck from mixing with the sand backfill.

SEDIMENT CHARACTERISTICS

Borings, samplings, in-situ vane shear tests, and laboratory tests such as classification, strength, sensitivity, consolidation, thermal resistivity and chemical tests were performed to study the engineering properties of the soft river sediments. The results were evaluated. Drilling in the river was conducted from a 18.3 by 7.6m barge. A special submersible platform which supported the drilling casing and the Geonor vane shear device was provided by the contractor to isolate the testing from the operation of the barge. In order to obtain relatively undisturbed soil samples for laboratory testing, Osterberg samples were recovered at certain elevations at some borings.

The Hudson River sediments consist of gray soft plastic clay occasionally interbedded with silt layers. Shell fragments were also noted. The organic content of the sediments decreases as depth increases. The thickness of this clay varies from zero to 6m at the shorelines and 29m in the middle of the channel. Underlying the clay is a layer of very dense silty sand. Project location and the subsurface profile along the submarine river crossing are presented in Figure 1. Figures 2 and 3 present the soil classification based on Unified Classification System and the gradation range for the sediment, respectively. Field and laboratory shear strength data, Atterberg limits, maximum past pressure, and consolidation data for the sediment with respect to depth are presented in Figure 4.

The undrained shear strength (Su) of the sediments varies from about 2.4 kn/m^2 near the river bottom to 38 kn/m^2 at depths of 19.8 to 21.3m below the river mudline. The 3m sediment is gray organic plastic clay and the natural water content ranges from 70 to 100%, which is higher than the liquid limit of the soil. The average liquid limit is about 60 percent. With natural moisture contents near and higher than the liquid limit, these clays are sensitive with a sensitivity value of 2 for the top 1.83m to 6 for a greater depth. Sensitivity is defined as the ratio of the undisturbed and the remolded shear strengths. The clays are slightly overconsolidated with the overconsolidation ratio (OCR) of 1.5 to 2 in the upper 9.1m and of 1.1 to 1.3 below 9.1m. Test data indicate that the submerged unit weight of the river sediment ranges from 0.45 to 0.51 g/cm^3.

In order to select an adequate shear strength value for design of the foundation system, the field and laboratory strength data were evaluated and compared with typical values from available literature (Bjerrum, 1972; Duncan, 1973; Ladd, 1977; & Osterman, 1959).

For a normally consolidated marine clay, the ratio of undrained shear strength of the effective overburden pressure ($Su/\sigma'vo$) is directly proportional to the plasticity index of the clay (Osterman, 1959). In this case, the ratio ($Su/\sigma'vo$) for the normal consolidated soil is 0.22. Since the upper clay was found constantly disturbed by tidal action and currents and slightly overconsolidated, the shear stress ratio was adjusted based on the stress history (or overconsolidation ratio, OCR) according to the work of Ladd (1977). A normalized shear stress ratio curve incorporated with the stress history is also drawn in Figure 4. The shear stress ratios based on the field vane shear test results are

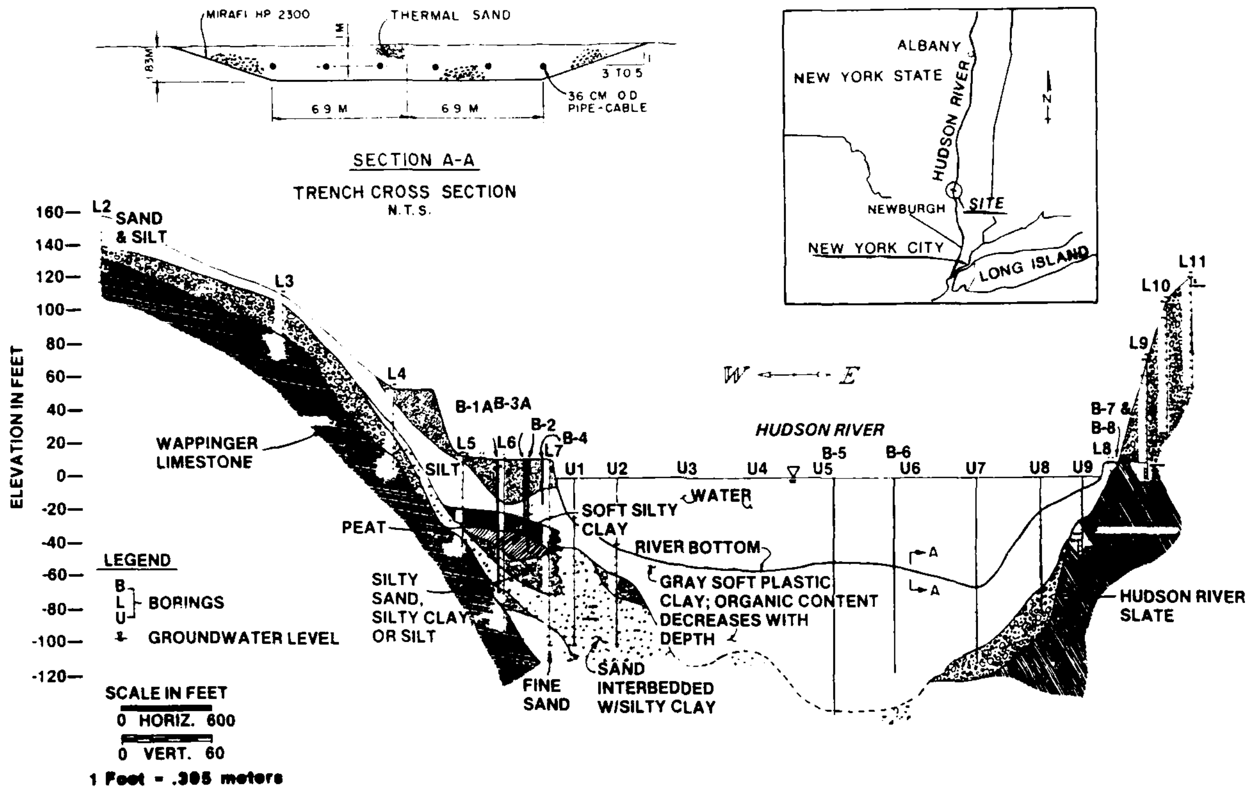
MIRAFI HP 2300
THERMAL SAND
1.83M
3 TO 5
1
6.9 M
6.9 M
36 CM OD PIPE-CABLE
SECTION A-A
TRENCH CROSS SECTION
N.T.S.
ALBANY
NEW YORK STATE
HUDSON RIVER
N
NEWBURGH
SITE
NEW YORK CITY
LONG ISLAND
ELEVATION IN FEET
160—
140—
120—
100—
80—
60—
40—
20—
0—
-20—
-40—
-60—
-80—
-100—
-120—
L2
SAND & SILT
L3
L4
B-1A B-3A
B-2
B-4
L5
L6
L7
SILT
WAPPINGER LIMESTONE
PEAT
U1
U2
U3
U4
U5
U6
U7
U8
U9
B-5
B-6
HUDSON RIVER
W E
SOFT SILTY CLAY
WATER
RIVER BOTTOM
GRAY SOFT PLASTIC CLAY; ORGANIC CONTENT DECREASES WITH DEPTH
SILTY SAND, SILTY CLAY OR SILT
SAND INTERBEDDED W/SILTY CLAY
FINE SAND
A
A
B-7 &
B-8
L8
L9
L10
L11
HUDSON RIVER SLATE
LEGEND
B
L
U
BORINGS
GROUNDWATER LEVEL
SCALE IN FEET
0 HORIZ. 600
0 VERT. 60
1 Foot = .305 meters

Fig. 1 Geologic Cross Section, Hudson River Submarine Crossing

also computed as shown on the same figure. A reduction factor of 0.9 on the vane shear test results to account for disturbance, rate of test, time delay during test, and vane size effects was applied in calculations (Bjerrum, 1972). Based on comparisons, a shear stress ratio (Su/σ'vo) of 0.32 for the top 3m sediment was selected for design.

STABILITY OF TRENCH BOTTOM

The stability of the trench bottom is governed by the shear strength of the river sediments and the weight of the backfill material. During placement of the backfill, the ultimate bearing capacity, Qult, underneath the granular fill can be expressed by the bearing capacity equation:

$$Q_{ult} = N_c S_u + \gamma'_s D_s$$

in which Su = Undrained shear strength of the sediment in psf

γ'_s = Average submerged unit weight of the sediment in pcf (1 g/cm^3 = 62.4 pcf)

Ds = Depth of excavation in ft (1 ft = 30.48 cm)

Nc = Bearing capacity factor for clay: 5.7 based on Terzaghi and 5.14 based on Prandtl, (Moorhouse, 1972).

The applied pressure (Q) due to placement of the backfill is:

$$Q = \gamma'_f D_f$$

in which γ'_f = Average submerged unit weight of the granular backfill in pcf

Df = Depth of the backfill in ft

Let FS be the safety factor against the bearing capacity failure at the bottom of backfill. Then

$$FS = Q_{ult}/Q$$

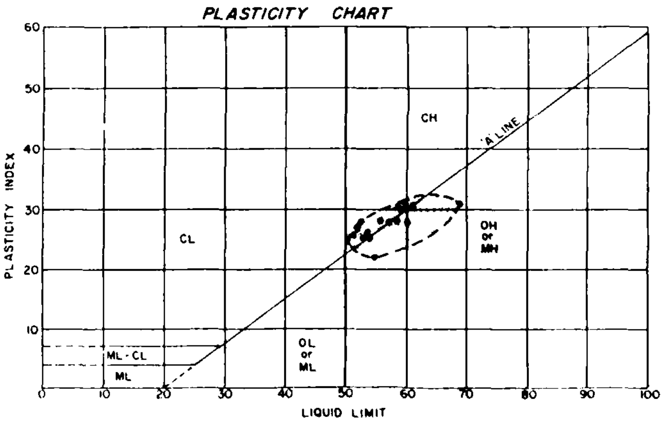

Fig. 2 Soil Classification for Hudson River Sediment

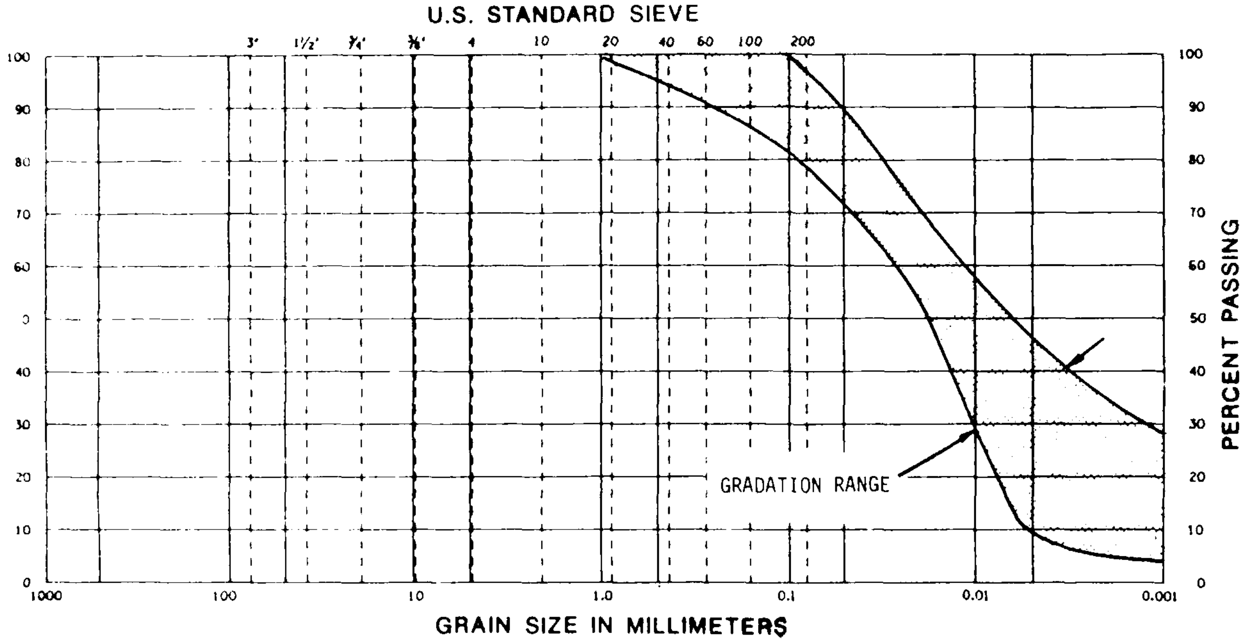

Fig. 3 Gradation Range for Hudson River Sediment

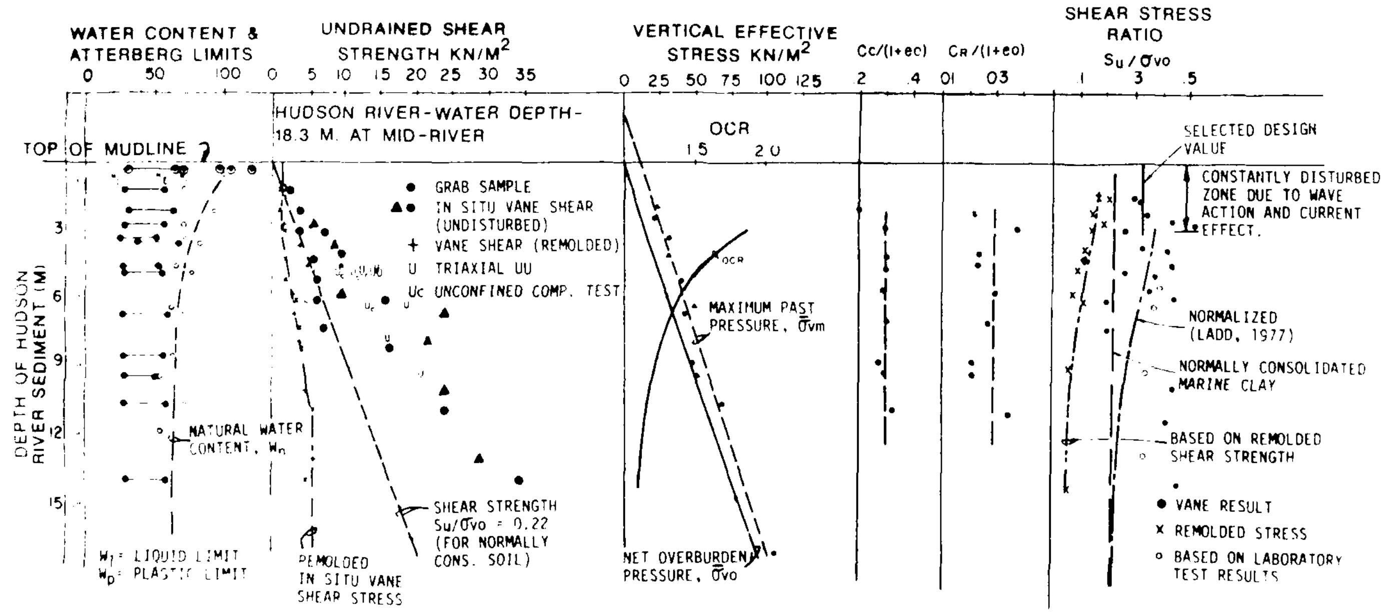

Fig. 4 Soil Properties. Hudson River Sediment (1 psf = .048 kn/m^2; 1 ft - .305 m)

Using submerged unit weights of the granular backfill and the existing top sediment of 65 pcf (1.04 g/cm^3 and 30 pcf (0.48 g/cm^3, respectively, and substituting the design undrained shear strengths and the effective overburden pressure (σ'_{vo}), the factors of safety for the stability of the trench bottom at the end of construction vary from 1.2 to 1.3. The result is based on the assumption that no variation of the backfill thickness during construction would occur. Should the shear strength of the sediment decrease for any reason such as disturbance during excavation to the remolded strength, the factor of safety against the bearing capacity failure of the trench bottom would become 0.87.

Due to uncertainties associated with the construction operation (nonconformity of the backfill thickness), the effect of currents and wave action, and the unknown soil strength of the top 0.61m of sediment, this upper bound safety factor (1.30) is considered to be too low. The rate of the secondary compression (creep), C' ($=\Delta H/H/\Delta \log_{10} t$), has been found higher than 0.03 for the top 3m sediments. At low factor of safety, creep to failure is possible for this soft marine clay. Furthermore, if the remolded strength is used, the factor of safety is less than one. The most likely bearing capacity failure mode for soft soil at top and stiffer soil at bottom would be lateral plastic flow. Therefore, should the trench slope and bottom fail, some granular cover will be lost laterally. The pipe-cable will be covered by river sediment instead of sand backfill.

Filter cloth to line the trench was selected and installed. Analysis indicated that the filter cloth could protect the thermal sand, increase the bearing capacity of the sediment, and increase the stability of the overall system.

Settlement analysis for the combined pipe-backfill system was performed. The maximum total settlement consist of 47cm of consolidation settlement and 25.4cm of secondary settlement (creep). The differential settlement between two points 30.5m apart along the cable alignment could then be estimated to be less than 30.5cm. The maximum amount of settlement was not expected to impact the pipe cables. The stress in the pipe induced by these total and differential settlements was verified by conventional analysis using beam on elastic foundation approach and was negligible.

INSTALLATION

A woven polyester (Mirafi's 2300 HP fabric) with excellent resistance to stress relaxation was selected. It was favored over polyethylene because of its heavy weight (1kg per square meter and a specific gravity of 1.3) and the fact that it could be designed to 40 percent of its ultimate tensile strength instead of 25 percent for polyethylene. Other critical properties of the 2300 HP fabric are: grab tensile strength of 6.8 MN/m^2; wide strip tensile strength of 6 MN/m^2; burst strength of 10.2MN/m^2; soil to fabric friction of 28°; puncture strength of 159 kg; grab elongation of 15%; and equivalent opening size of 0.42mm.

In order not to disturb a fish spawning season in the Hudson River, the dredging operation, using a barge-mounted crane with watertight clamshell bucket and fabric placement, had to be completed between July 15 and October 15, 1986. Approximately 36,810 square meters of fabrics were produced for the project and shipped in fabricated panels of 21.3 by 30.5m.

To get the fabric in position, a lead roller was run along the river bottom in front of the roll containing the fabric in order to push down the bottom mud in the trench. 6.1m of fabric overlapped at the end of each roll to provide a continuous stretch of geotextile across the river. As each roll was installed, divers inspected the fabric to make sure it was correctly positioned. Because of cross currents of as much as four feet per second, the fabric was unrolled at a slight angle and a 0.45m layer of thermal sand was placed on top of the fabric for every 6.1m that was unrolled. The edges of each fabric at some locations were also held down to the mud using 2m+ long by 2.2cm diameter pins at 1.5m spacing. The thermal sand was placed through a combination of direct clamshelling and a tremie hopper system. Six 36cm OD conduits were assembled on the west side of the river and then pulled with a winch across the river. The conduit was kept as a neutral buoyancy, which let it float a slight distance above the layer of thermal sand over the geotextile. A special sled device at the nose of the conduit kept them from plowing down into the sand and the filter fabric. Once the conduit was in position on the river bottom, it was covered with 1.37m sand to complete the thermal sand environment. The conduit was evacuated to a high vacuum and the conductor cable was then pulled through the conduit from the east side to the west.

During installation, the contractor provided an offshore surveying and monitoring crew to confirm all the work he performed. The crew was equipped with a Cubic "Autotape" model DM-40 Two-Range Precise Navigation system, which was capable of 0.5m accuracy in range measurement. For vertical measurement, the crew was equipped with a Raytheon DE-719 Survey Depth Sounder and a Klein model 400 Side Scan Sonar. Prior to the dredging operation and after the final work, bathymetric surveys at an interval of 6.1m and a minimum width of 61m along the whole cable alignment were performed.

An underwater sediment profile using a Bottom/Subbottom Video Profiler with sonar remote sensing capability was also recorded by Video Recorder during dredging operations to confirm sediment condition.

CONCLUSION

Use of the geotextile enabled the owner to successfully place the pipe-cables underwater despite the unstable river bottom. The decision to use the geotextile resulted in approximately a third less dredging and a considerable savings in time and labor.

ACKNOWLEDGMENTS

The author wishes to acknowledge the continued support of the New York Power Authority (NYPA) on this Submarine Cable Crossing project. In particular, the efforts of the following NYPA managers are recognized: W. W. Crouch, Senior Project Manager; S. A. Dave, J. D. Schrenkel, A. W. Hagstrom, and E. I. Hahn, Project Manager and Project Engineers, respectively. In addition, the author wishes to thank Dr. M. I. Esrig of Woodward-Clyde Consultants and all Gilbert/Commonwealth Construction management and geotechnical groups for their valuable contributions. The author particularly thanks R. J. Broad and J. A. Nelson, G/C Overall Transmission Manager and Project Manager of the submarine cable crossing project respectively for their valuable review and suggestions regarding this geotechnical program.

REFERENCES

Bjerrum, L. (1972), "Embankments on Soft Ground," State-of-the-Art Report, Proc. ASCE Special Conference on Performance of Earth and Earth-Supported Structures, June 11-14, Purdue Univ.

Duncan, J. M. and A. L. Buchigani, (1973), "Failure of Underwater Slope in San Francisco Bay," ASCE, Journal of SMFD, SM-9, Sept.

Gilbert/Commonwealth (G/C,) (1984), "Design Study of the Hudson River Submarine Crossing - Offshore Geotechnical Investigation." Study No. DS-19. Jackson Michigan.

Ladd, C. C., et al., (1977), "Stress-Deformation and Strength Characteristics." Proc. 9th ICSMFE, Japan, Vol. 2, pp. 421-494.

Moorhouse, D. C., (1972), "Shallow Foundations." ASCE, Proc. of the Specialty Conference on Performance of Earth and Earth-Supported Structures, June 11-14, Purdue Univ.

Osterman, J., (1959), "Notes on the Shearing Resistance of Soft Clays," Acta Polytechnical Scandiavica, No. 263.

Proceedings: Second International Conference on Case Histories in Geotechnical Engineering, June 1-5, 1988, St. Louis, Mo., Paper No. 5.46

Foundations on Stone Columns Resting on Coralline Limestone

K.S.A. Rahim
Associate Professor, Civil Engineering Department, King Saud University, Riyadh, Saudi Arabia

A.W. Dhowian
Associate Professor, Civil Engineering Department, King Saud University, Riyadh, Saudi Arabia

SYNOPSIS: The subsoil conditions along the Red Sea coast in Saudi Arabia are complex due to existance of very thick beds of coralline limestone of recent geological origin. These coral beds are soft, porous and nonhomogeneous. They are often interspaced with large cavaties and soft sandwitched layers of finer particles. Analysis of the subsoil conditions to a fifty meter depth based on data from deep boreholes, Standard Penetration Tests (SPT), Quasi Static Cone Tests (DCT) and large size Plate Load Tests is presented. The strength and compressibility characteristics of the strata and the correlation factors for the SPT and DCT in coralline limestone are evaluated. The results from the plate load tests conducted on natural soil and on soil compacted with stone columns are included. An evaluation of the performance of the foundation for the heavy turbines resting on soil compacted with vibro-compaction replacement method with stone columns was made.

INTRODUCTION

Saudi Arabia is a vast country with several geologic environments. The western coastal area is a flat narrow plain bounded by the Red Sea in the west and by the Al Hiyaz mountain ranges in the east. It is underlain by the Arabian Shield. The Precambrian Basement Complex of the Arabian Shield are mainly igneous and metamorphic and form a dome shaped topography, Saad and Zolt (1978). The main geological features and climatic conditions in Saudi Arabia are discussed by Oweis and Bowman (1981). Due to favourable marine and climatic conditions coral cultures grew along the Red Sea coast forming terraces of coralline limestone. The reef conditions caused continuous changes in coralline limestone beds. The high porosity of the soft coral beds and the destruction caused by the boring organisms permitted flowing of water and sedimentation of sand and silt particles between coral layers. Sometimes the sediments and soft coral formations were washed away creating cavaties.

This case study involves a large project located on the Red Sea coast about 140 kilometers south of Jeddah. This multi-million dollar Power and Desalination Plant is spread over an area of approximately 10 hectors and it has five foundations pads of 100 square meters (SQM) for each of the five turbines. Only the heavy foundations with loads of 15 mega newtons (MN) each for the five turbines are discussed in this case study.

SUBSOUL INVESTIGATIONS

The shed housing the turbines and the boilers covers an area of 300 meters (M) by 150 M. To investigate the subsoil conditions, a 50 M deep borehole was drilled in the center of the area and six more boreholes up to 25 M depth were sunk within the area. Forty five Quasi Static Cone penetration tests (Dutch Cone Test (DCT)) up to 25 M depth were conducted within the area. The DCT results along with the borehole log data representing the average subsoil conditions in the area is given in Figure 1. The DCT was conducted in the immediate vicinity of the borehole and Standard Penetration Tests (SPT) were performed during drilling of boreholes. Two plate load tests at a depth of one meter below ground level were also conducted. The details for all the boreholes, the DCTs, the plate load tests and the laboratory tests are given by Keller (1984).

SUBSOIL CONDITIONS

The water table *lies between* 1.25 *to* 2.5 M below ground level (G.L). The overburden is 5 to 7 M thick. It is composed of a mixture of silt (up to 60 percent (%)), fine sand (up to 25%) and clay (up to 20%). A generalised grain distribution plot is given in Figure 2. The silts are soft to medium soft in consistency and are classified as Silts of Low Plasticity (ML). The SPTs indicate low penetration resistance with blow count (N) ranging between 5 to 15 N with an average of N=11 for the 12 tests. The N values show that the stratum is loose to medium loose with q_{ad} (allowable bearing pressure) is less than one bar, Terzaghi and Peck (1948). In conformity with SPTs, the DCTs gave the cone resistance (q_c) ranging between 10 to 20 bars with an average of 14 bars and a friction ratio ranging between 4 to 6% for the 45 DCTs conducted for the full depth of the overburden. Thus q_{ad} for the stratum is one bar for raft foundation, Terzaghi and Peck (1948). The correlation factor, $n = q_c/N$, relating the SPT blow count N to DCT cone resistance q_c ranges between 2 to 4 for all the tests in the overburden. The correlation factor is in conformity with the published results for loose silts, Schmertmann (1970), and Sanglerat (1972). The plate load test conducted on a 5 SQM concrete slab indicated a bearing pressure of 0.75 bars with a settlement of 2.58 millimeters (mm). The laboratory test results are given in Table 1.

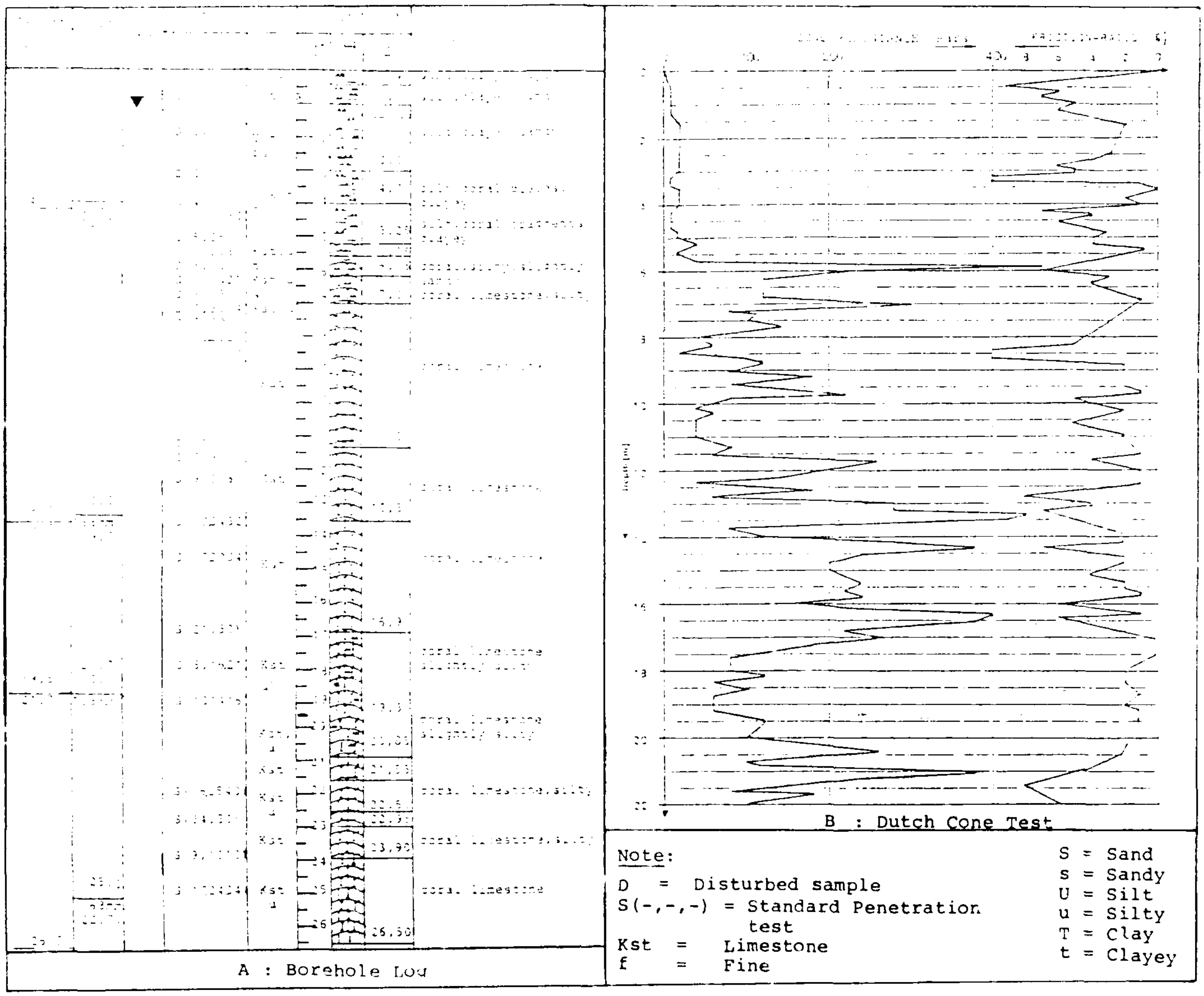

Fig. 1 Subsoil Conditions

Below the overburden lies the coral limestone extending to deeper depths (more than 50 M below ground level). Due to its natural growth the coralline limestone is soft, nonhomogeneous and porous. The density, porosity, and strength characteristics of the coral formation vary erractically. The core recovery ranged between 10 to 70 % with an average of 40 % that confirms the erractic and weak characteristics of the coral formations.

Data from 50 to 60 M deep boreholes (Borehole log for a 50 M deep borehole was not included due to space limitation) show that thin sandy silty layers are sandwitched between thick coralline limestone layers at deeper depths. It also shows that there are cavaties (up to 5 M thick) at depths of 35 to 45 M below ground level followed by a 1.5 to 2.0 M thick gravel beds. It was possible to penetrate the coral

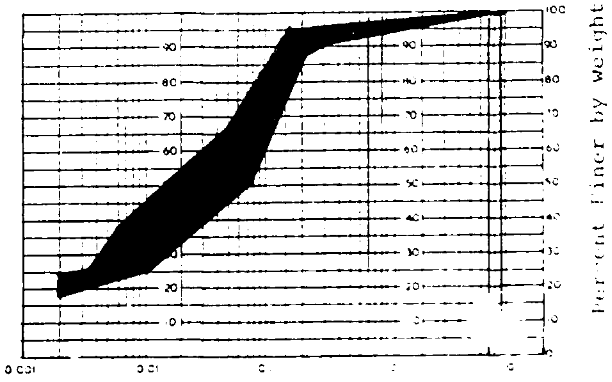

Fig. 2 Grain Distribution Curves

formation and a few SPT and DCT tests were conducted. SPT tests indicate medium resistance of 15 to 35 N and the q_c in DCT tests ranged between 20 to 70 bars in the porous and weaker grey coralline limestone containing sandwitched layers of silt and fine sand. Compact coralline limestone is white to brown in color with a tight but porous structure. The SPT ranged between 25 to 60 N and q_c in DCT tests ranged between 80 to 200 bars. The N values indicate that q_{ad} ranges between 1 to 3 bars for the weaker grey coralline limestone and it varies between 2 to 5 bars for the compact white coralline limestone. Similarly the q_c from DCTS show that q_{ad} varies between 0.5 to 2 bars for the grey layers and it ranges between 2 to 5 bars for the compact white stratum. Hence, a value for q_c of 2 to 3 bars can be assigned for the entire coralline limestone strata. The correlation factor (n) for the weaker grey layers ranges between 2 and 3 and it varies between 3 and 4 for the compact white layers. The unconfined compressive strength of intact cores from the white layers ranged between 6.2 to 22.6 bars with unit weight ranging between 10.4 to 18.8 kilo-newtons per cubic meter.

TABLE 1. Laboratory Test Results

A. Undisturbed Samples From Overburden

Borehole No.	Sample No.	Depth (meters)	Water Content (percent)	Dry unit weight (KN/M3)	Liquid limit (percent)	Plasticity Index	Direct shear Test: Cohesion (bar)	Direct shear Test: Angle of internal friction (degrees)
[illegible]	[illegible]	3.5	28.3	15.0	40	15	0.08	14
12	[illegible]	2.[illegible]	26.4	14.2	-	N.P	0.25	11
	[illegible]	3.3	33.2	13.9	45	16	0.20	11
14	[illegible]	2.[illegible]	36.5	13.4	41	14	0.07	12
	[illegible]	3.5	-	-	40	12	0.06	16
	[illegible]	4.5	21.6	16.3	39	12	0.04	12
18	[illegible]	3.7	2[illegible].9	14.8	47	17	0.30	6
[illegible]	[illegible]	3.[illegible]	3[illegible].3	-	35	8	0.46*	0
[illegible]	[illegible]	2.[illegible]	29.3	14.7	30	6	0.44*	0
	[illegible]	3.3	33.7	-	36	1[illegible]	0.38*	0

Note: * = Triaxial Test - Unconsolidated Undrained [illegible]

B : Intact Core Samples From Coralline Limestone

Borehole No.	Sample No.	Depth (meters)	Moist unit weight (KN/M3)	Absorption (percent)	Compressive strength (bars)	Remarks
[illegible]	[illegible]	[illegible]	-	-	13.42	
[illegible]	[illegible]	[illegible]	[illegible]	15.9	8.12	Soft, white, highly porous
	S-2	12.[illegible]	[illegible]	12.8	6.23	Light, soft, highly porous
	S-3	15.5	17.5	10.3	16.07	Hard, white, compact
	S-4	30.5	19.8	8.5	12.78	Hard, white, compac
[illegible]	S-1	7.2	-	-	10.98	
	S-2	[illegible]	-	-	6.71	
	S-3	[illegible]	-	-	22.57	
[illegible]	S-1	9.7	16.[illegible]	-	13.00	
	S-2	17.9	14.8	-	10.00	
	S-3	15.9	15.6	-	12.00	

THE PROBLEM AND THE SOLUTION

The upper stratum of 5 to 7 M thick is mostly silts mixed with sand and clay size particles. It is nonhomogeneous, compressible and of low bearing cpacity of 0.75 to 1.0 bar. The coralline limestone formations underneath are of recent geological origin. The density and strength characteristics vary erracticaly. Thin layers of silts and sands are sandwitched between thick layers of coralline limestone. The coralline limestone possesus medium strength with q_{ad} = 2 to 3 bars and is unsuitable for bearing piles.

Any solution to the foundations must ensure the load distribution within the upper stratum of 5 to 7 M in order to avoid load concentration on coralline limestone underneath. It should also meet the settlement criteria. The other factors are the time element and the cost. Thus the improvement of the upper stratum by compaction techniques is one of the best economical solutions to be considered.

Dynamic Compaction

The subsoil condition are not ideally suited for application of dynamic compaction. The compaction of a 7 M thick stratum with high water table and a large content of fines would make dynamic compaction ineffective. Also, the shock waves generated during dynamic compaction could loosen the structural boundaries of the coralline limestone.

Preloading - Surcharge Method

The required massive surcharge loads and the drainage system necessary to compact the 7 M thick stratum below the water table would require a long duration and would be uneconomical.

Vibro-Compaction with Stone Columns

For the subsoil conditions the Vibro-compaction Replacement Method with stone columns for compacting the 7 M thick upper stratum was an effective and economical solution requiring a minimum of time. The method improves the subsoil with reduction in voids and compaction of weak material due to formulation of densely compacted stone column tightly interlocked with the surrounding soils.

Plate load tests were conducted to accertain the effectiveness of the vibro-compaction method. The load-settlement curves for two plate load tests are given in Figure 3. Test No. 1 was performed on natural soil deposit (without any treatment) and Test No. 2 was conducted on soil compacted with stone columns. The stone columns were one meter in diameter and were placed at 1.2 M center to center embeded 7 M in the compacted overburden and penetrating one meter into the coralline limestone. Both tests were conducted with a concrete test slab; 600 mm thick with a base area of 5 SQM. Loads were applied in increments through a hydraulic jack located below the loading platform. The settlements were monitored at four points with dial gauges reading to 0.01 mm and the average settlement was recorded for each load increment which was held constant for six hours. Test No. 1 in Figure 3 shows that settlements increased excessively for loads exceeding 375 kilonewtons (KN) indicating general shear failure, Terzaghi and Peck (1948). Test No. 2 does not indicate any shear

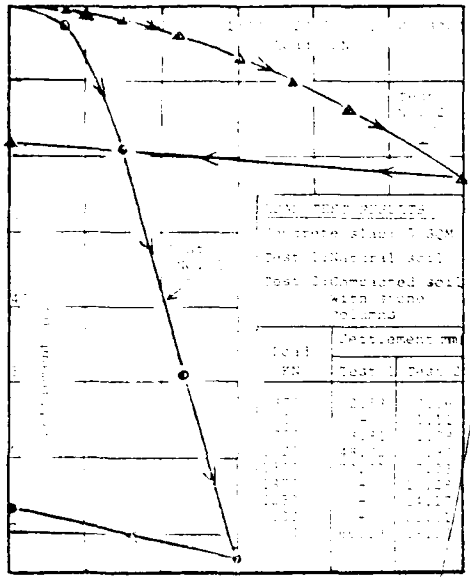

Fig. 3 Plate Load Tests

failure for loads up to 3000 KN with a total settlement of 23.21 mm. At the design foundation pressure of 1.5 bars (load of 1500 KN on a 5 SQM slab), the total settlements was 7.03 mm. An analysis of these curves gave the Elastic Modulus for natural soil (Test No. 1), E = 6700 kilonewtons per meter square (KN/M^2) and the Elastic Modulus for compacted soil with stone columns (Test No. 2), E = 64000 KN/M^2. Using the deep borehole log data and DCT results the Elastic Modulus for different layers of coralline limestone varied between 40,000 KN/M^2 to 120,000 KN/M^2 for the 44 M thick strata in a 50 M deep borehole. The allowable bearing pressure on weaker layers of coralline limestone with q_c less than 70 bar is 2 to 3 bars, Sanglerat (1972). Thus the improvement of overburden with vibro-compaction with stone columns has in effect improved the characteristics of the overburden to be in conformity with the characteristics of the coralline limestone with respect to bearing pressure, settlements and other mechanical properties.

THE SOLUTION

The solution to the foundation problem was to grout the cavaties with a rich mixture of cement and sand under pressure and to compact the overburden with vibro-compaction with stone columns. The stone columns were 6 M to 8 M in length (penetrating one meter into coralline limestone) and 0.9 M to 1.0 M in diameter constructed on a triangular grid of 1.2 M center to center. All stone columns were constructed with clean gravel of size 10 mm to 75 mm using at least 0.75 cubic meters (M^3) of gravel per meter length of the column. The stone columns were vibrated and compacted with heavy machine hammers and the resistance offered to the hammer was electronically recorded on strip charts. Also, precautions were taken to limit washing out of fines during construction and compaction of the stone columns and the quality and quantity of gravel used was closely monitored. On completion of all the columns for each turbine foundation, the top one half meter was scraped as the soil was disturbed and the stone columns contained excessive fines in the upper most one half meter layer. A structural fill of 0.5 M with selected aggregate was constructed over the entire area and the turbine foundation pads were placed on the structural fill. An analysis with a uniform pressure of 1.5 bars on 100 SQM foundation pad for the turbine indicated a total settlement of 47.30 mm and a differential settlement of 5.8 mm for the elastic compression of the 50 M thick strata.

CONCLUSIONS

The data from each of the three different types of field tests, the STPs, the DCTs and the Plate Load Tests seem to correlate the results well as almost similar values were obtained for the allowable bearing capacity for the silty overburden and the coralline limestone. The correlation factor (n) for the SPTs and DCT appears to be 2 for the soft, grey and porous coralline limestone and n seem to range between 3 to 4 for the white, compact and hard coralline limestone.

The vibro-compaction replacement method with stone columns is an effective and speedier method to compact and improve thick layers of silty soils below the water table. The compaction of the overburden with stone columns has improved the bearing capacity and compressibility characteristics significantly (ultimate bearing capacity from 75 KN/M^2 to 600 KN/M^2 and elastic modulus from 6700 KN/M^2 to 64000 KN/M^2. The project is on a completion stage and presently it is on a trial run. The turbine foundations are performing satisfactorily.

REFERENCES

Keller, GKN, (1984), "Power and Desalination Plant - Site Investigation Report", Report prepared by GKN Keller Arabia Ltd., Riyadh, Saudi Arabia.

Oweis, I. and Bowman, J., (1981), "Geotechnical Considerations for Construction in Saudi Arabia", ASCE Proceedings, Vol. 107, No. GT3.

Saad, S.A. and Zotl, J.G., (1978), Quatenary Period in Saudi Arabia, Springer-Verlag, New York, N.Y., U.S.A.

Sanglerat, G., (1979), The Penetrometer and Soil Exploration, Elsevier Scientific Publishing Co., Amsterdam, The Netherlands, 2nd Edition.

Schemertman, J.H., (1970), "Static Cone to Compute Static Settlement Over Sand", Proc. ASCE, J. Soil Mech. Found. Div. 1970.

Terzaghi, K. and Peck, R.B., (1948), Soil Mechanics in Engineering Practice, John Wiley & Sons, New York, N.Y., 2nd Edition.

Proceedings: Second International Conference on Case Histories in Geotechnical Engineering, June 1-5, 1988, St. Louis, Mo., Paper No. 5.48

Special Tunnelling Methods for Settlement Control: Infilaggi and Premilling

D.A. Bruce
NICON, Pittsburgh, Pennsylvania

F. Gallavresi
Giovanni, Rodio & Co., Milano, Italy

SYNOPSIS

This paper provides an introduction to two tunneling methods specially developed to optimize settlement control. This is particularly relevant in urban environments.

The concept of neither method may be regarded as novel: infilaggi is a development of the principles of forepoling, whilst the premilling idea has been considered for some years. However, recent trends in the nature of the tunnel market, and major advances in the equipment and systems involved have fostered a rapid growth in Western Europe. A description is provided of the major points of each method, and case history data are cited to illustrate their excellent performance.

1 INTRODUCTION

When tunneling in urban environments often at relatively shallow depths and in variable ground conditions, the development of surface settlements is an attendant reality. Depending on the local circumstances, such settlements may be deemed too small to be of significance. Alternatively some form of settlement mitigation or correction may be necessary, for example grouting (Bruce, 1987) or insitu reinforcement (Bruce et al., 1987). Such methods, and others, will also aid the progress and safety of the tunneling contractor and his personnel (Mongilardi and Tornaghi, 1986).

On the other hand it may be more practical or economic to attack the problem at source--to isolate the impact of the excavation method from the surrounding ground, which would thereby retain its virgin status, and not affect overlying structures.

This paper describes two particular techniques, infilaggi and premilling, which have been developed to minimize ground movements above tunnels. Although entirely different in execution, they share many common features, principally:

- they are executed from the face in advance of excavation, thereby minimizing subsequent decompression.
- they are not new ideas--infilaggi has been known as forepoling or spiling in the U.S. for decades, whilst the premilling system has taken some time to refine to its current status; however,
- given current trends of shallow tunneling in urban areas both have a revived potential rapidly being realized in Western Europe in particular
- recent developments in equipment technology have broadened that potential with respect to speed, reliability and cost effectiveness

Each technique is described below, illustrated by reference to recent applications by Ing. Giovanni Rodio & Co., in Italy

2 INFILAGGI

The use of forepoling or spiling has long been common as a supplemental support method in U.S. tunneling practice. For example, Clough (1981) described how the array of steel rebars driven suprahorizontally around the crown forms an umbrella of reinforced ground above the subsequent excavation. However, within the last few years in Western Europe, the concept has been expanded upon, to the extent that horizontal insitu reinforcement or retention of this type (infilaggi) has become a primary tunnelling method. This has arisen for three main reasons:

- Demand - there is a vibrant phase of tunnel construction in certain countries in Western Europe--especially Italy, France, Germany and Austria--for new or upgraded transport networks. Much of the construction is in ground which can be classified as soil or rock of inferior mechanical characteristics.
- Equipment - recent advances in specialized drilling equipment (e.g., RODIO SR500 [Photograph 1] and SR510 diesel hydraulic machines) can allow up to 20m of protection to be installed in one pass, with very high productivities and with minimal demands on the facilities or assistance of the excavation contractor.
- Contractual - the contractual atmosphere fosters innovation and the principles of risk sharing. Thus individual companies, or groups of companies are encouraged to evolve new concepts to improve cost effectiveness and productivity. Equally, these ideas may allow contractors to minimize initial capital expenditure, by virtue of using or modifying existing equipment.

The length of each pass of infilaggi varies according to the ground conditions and the balance between the various aspects of the tunnel construction processes necessary to ensure efficient utilization of all resources by all parties. In certain instances, the steel pipes forming the reinforcement may also be used for grouting the surrounding ground, and the use of sleeved ports for example permits a range of cements and chemicals to be used, depending on ground conditions and the support requirements.

CASE HISTORY: LIMINA TUNNEL, MAMMOLA, ITALY

The Limina motorway tunnel is located in the south of Italy, near Mammola, approximately 20 Km northeast of Reggio di Calabria. Typically, the 12m diameter tunnel has the profile of Figure 1, but at 250m intervals it opens out by 4m for a 40m

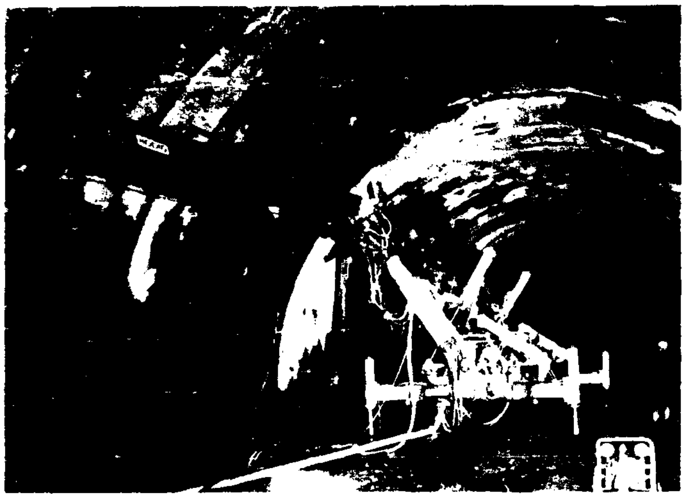

Photograph 1 [illegible] diesel hydraulic tunnel drilling [illegible] [illegible] mm dia [illegible]

Photograph 2 Drilling for installation of infilaggi (seen stored on drilling rig). Earlier phases of infilaggi ribbing and shotcreting seen above the rig. Lamina Motorway Tunnel, Mammola, Italy.

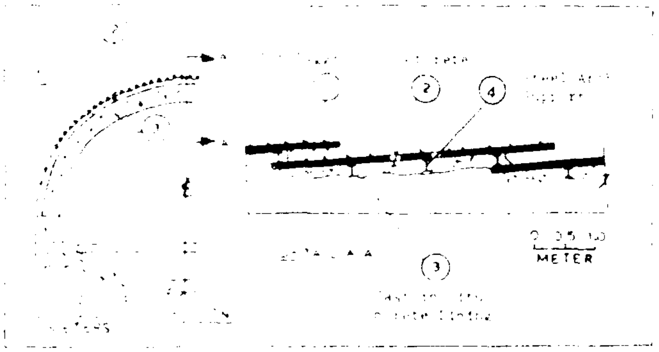

[illegible] and attached in the [illegible] infilaggi, Lamina Motorway [illegible] Mammola, Italy.

[illegible] points. The tunnel runs east west and [illegible]

[illegible] is an extremely variable hornblende biotite [illegible] fractured and weathered irregularly. It trends oblique [illegible] the tunnel and each face can exhibit both good [illegible]. Bedrock water is tapped by groups of four or five [illegible] 12m long drilled up from interim face [illegible]

[illegible] short infilaggi proved to be the safest and [illegible] and a maximum installed length of [illegible] determined (5.5m in enlargements). With the steel [illegible] placed at 1.25m centers this gave the option of [illegible] from 1.25m (poorest ground) to 3.75m (best [illegible] Figure 2) depending on the rock conditions. [illegible] date the average has been 3.64m/drive.

[illegible] 850 [illegible] rigs were not therefore [illegible] truck mounted diesel hydraulic rig [illegible] (Photograph 2). This drilled holes of 120mm diameter using foam flush (to minimize water flush requirements) through a hydraulic roto percussive top hammer. The 45mm drill rods were sleeved to 90mm o.d. to ensure hole straightness.

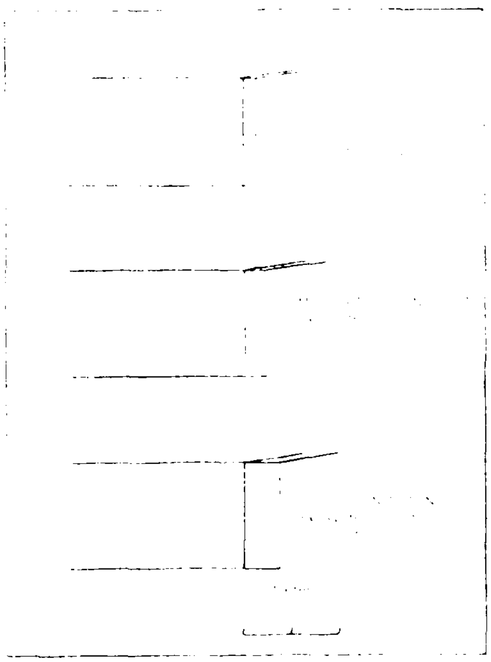

Figure 2 Simplified elevation showing variation in excavation length under infilaggi related to rock quality. Lamina Motorway Tunnel, Mammola, Italy.

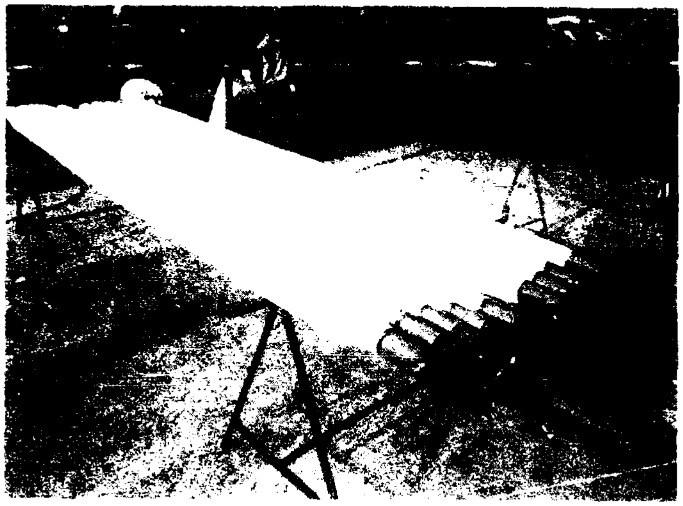

[illegible]

[illegible] a specialized tunnelling [illegible] have appeared [illegible] in the [illegible]

[illegible] comprises a track mounted frame [illegible] Figure 5 [illegible] in front is a large hand [illegible] about 5 m long [illegible] Photograph 5 [illegible] This [illegible] the frame to cut a slot about 20 [illegible] the ground around the volume to be excavated. In [illegible] the slot is left open to optimize the subsequent [illegible] and performance. In soft ground the slot is [illegible] with high strength fast setting concrete [illegible] decompression effects during [illegible]

[illegible] in response to the need to [illegible] in urban areas [illegible] the surface underground [illegible] conditions even the [illegible] standard New Austrian [illegible] examples [illegible]

[illegible] with [illegible] Figure 6 [illegible] provides the [illegible]

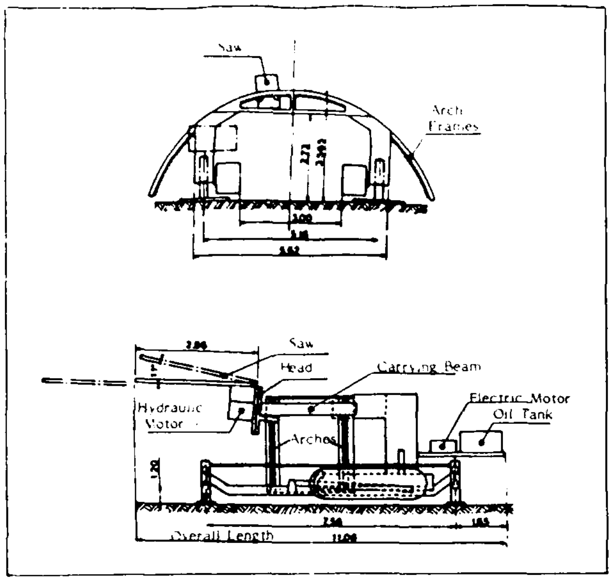

Figure 3 - General layout of typical premilling machine (Hydraulic arm for shotcreting not shown).

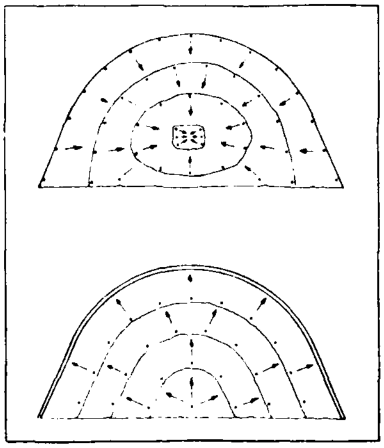

Figure 4 - Round blasting concepts - classical (upper) and with premilled slot (lower).

- less explosives (and blast holes) are required, rendering the entire blasting operation safer, faster and environmentally more acceptable.
- no fissuring or decompression occurs in the surrounding rock mass, thus preserving its virgin properties, and so reducing the demand for subsequent reinforcement, e.g., with bolts.
- there is no overbreak, and therefore associated cost savings in time, effort and materials.
- the smooth profile makes the placing and performance of arches more efficient.
- less contact or consolidation grouting is needed behind the final tunnel lining.
- following blasting there is a greatly reduced danger from rock falls due to chimneys of fractured ground developing above the excavation.

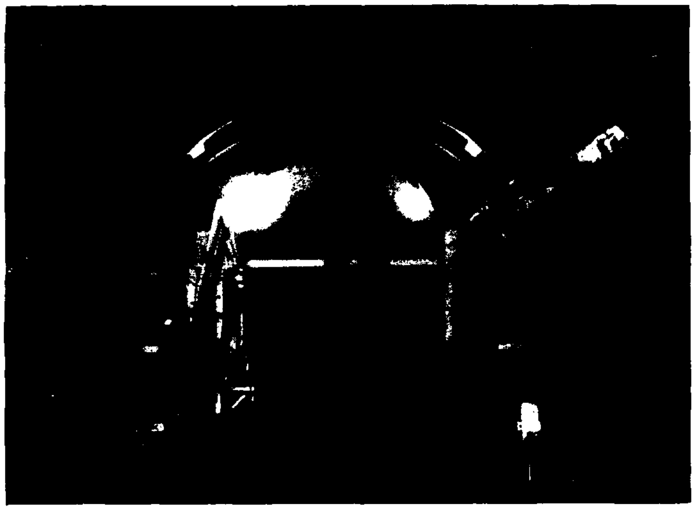

Photograph 5 - Premilling machine, seen from the front and showing premilling saw (upper right) and hydraulic arm (left) for shotcreting operations.

- the magnitude of vibrations transmitted upwards towards nearby surface structures is greatly attenuated.

Developments of the technique continue, for example, in special diamond tools, high pressure water jetting, and increased cutting power, to permit its use in harder rock formations, faster, and with increased safety.

In soft ground, as noted above, the major difference is that *the cut slot is filled with a special concrete mix* as early as possible. The advantages are as identified above for the rock premill, although the prime target is the elimination of surface settlements induced by the tunnelling.

Each cover, up to 3.5m long, depending on the soil, is inclined slightly outwards and overlaps the preceding one by 300 to 500mm (Photograph 6). The cone is cut in discrete segments so that the concrete can be placed in each segment, as early as possible and without having to wait for the whole arch profile to be first completed. Cutting times for a typical 3m long segment may be as low as one minute.

The concrete may be placed by dry or wet shotcrete methods. A typical mix reported by Bougard et al (1979) comprises, per cubic meter of mix:

Cement	450Kg
Sand	560Kg
Fine gravel	650Kg
Coarse gravel	650Kg
Accelerator (Sigunite)	27Kg
Water, as appropriate, typically w/c = 0.25-0.30	

This gives a strength of up to 100 bar at eight hours. Replacement of the normal cement with 350Kg of cement fondu gives *the minimum target strength of 80 bars in 4-5 hours.* In addition, spraying the mix into the premilled slot ensures that none of the fine aggregate is lost, as is the case in conventional NATM applications of shotcrete on open faces. The concrete in place is, therefore, of superior quality, further enhancing the performance of the system.

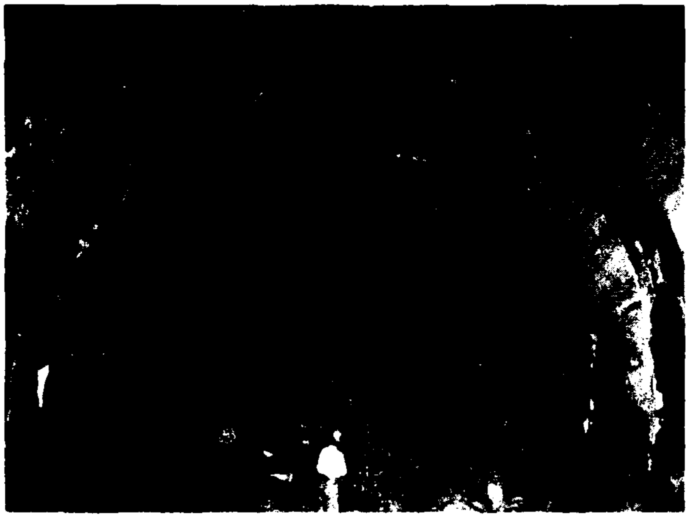

Photograph 6 - Tunnel excavated under the premilled in situ arch, showing overlap of each cut, and placement of supporting steel ribs.

In comparison with the NATM, there are certain similarities, notably the overall concept of the support, and the common construction elements such as shotcrete, bolts, and arches. However, the major dissimilarity is that with premilling the primary lining is placed up to 3m ahead of the face before excavation, whereas in NATM the lining follows 1 or 2m behind the excavated face. This greatly impacts the generation and scale of tunnel deformations, and so the effect on overlying structures (Figure 5). Goër (1982) described a monitored case history of the relative performance of the two methods in the same material--Argenteuil marl (Figure 6). Typical properties of this material were listed as:

Density = 2
Effective φ = 20°
Effective cohesion = 0.5 - 1.0bar
Undrained cohesion = 1.5 bar
Deformation modulus = 500 bar

Three times less settlement was achieved in the tunnel protected by premilling.

Most of the earlier applications have been carried out with the conservative "divided section" profile. However, excellent results with the "full section" profile (i.e., cutting a 270° arc,and excavation in one pass) in a shallow circular collector tunnel 3.50m diameter (Département de la Seine-Saint-Denis, France), in very difficult ground, encouraged its use in Lot 7 of the Lille Metro, Belgium. As evident in Figure 7 the performance of the full section profile was superior, with surface settlements no more than 1mm. Prefabricated base slabs were connected structurally to the premill cover by shotcrete, and the steel ribs then placed, bearing on the slabs. This system also proved faster than the divided section approach.

CASE HISTORY: RAILWAY TUNNELS, FROM MONGRASSANO TO SAN MARCO ARGENTANO, NEAR ROGGIANO, ITALY

During 1986 and 1987, three tunnels totalling 2000m in length were formed by premilling. The soil was generally lightly indurated and variable sediments, typified by waterbearing silty claystones with fine sand lenses. The profile of the tunnel is shown in Figure 8, the 140mm wide slot extending 21m around the shape and 3.5m beyond the face. Each cover overlapped the earlier by 500mm, enabling the excavation to proceed full section in 3m drives, at an average rate of one advance per 24 hours, viz:

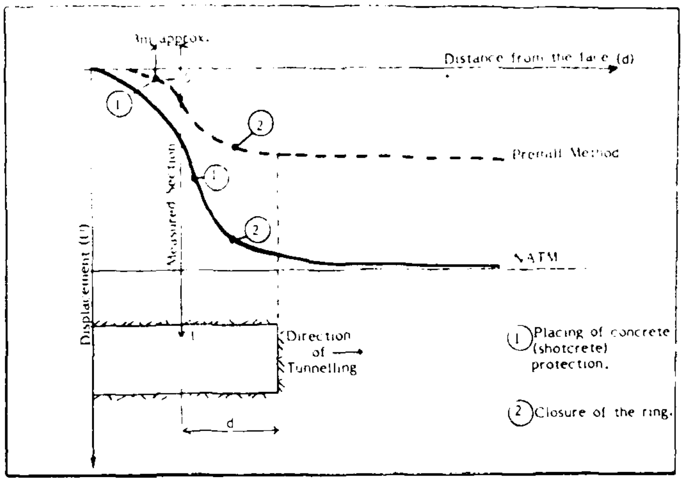
3m approx.
Distance from the face (d)
①
②
Premill Method
Measured Section
①
②
NATM
Displacement (U)
Direction of → Tunnelling
d
① Placing of concrete (shotcrete) protection.
② Closure of the ring.

Figure 5 - Qualitative comparison of development of tunnel movements with Premill and NATM. (LeGoër, 1982).

• Premill and shotcrete	8 hours
• Shotcrete stiffening period	6-8 hours
• Excavation and placing ribs	8-10 hours

The three faces were advanced simultaneously and laser guides used to ensure precise tunnel orientation.

The special dry shotcrete mix designed for this contract also incorporated steel fiber (about 30Kg/m^3) to aid performance, and the mix reached 100 bar at 8 hours. Segments of 2-4m length were successively cut and filled.

During premilling in particularly poor conditions, the face (previously lightly shotcreted) was temporarily supported by simple mechanical props. Under these conditions, the spacing of the steel arches was halved. The final lining followed not more than 50m from the face.

4. SUMMARY AND CONCLUSIONS

The potential for the cost-effective use of infilaggi for soil and poor rock tunnelling has been greatly expanded by recent developments in drilling and grouting technologies. It is now realistic to anticipate single drives of over 15m, fully protected by the insitu reinforcement, and with or without complementary ground injection, using the new generation of purpose built drilling rigs.

In cases where surface settlements must be absolutely minimized then the premilling technique has been proved an excellent method, markedly superior in performance to the standard NATM. It can be carried out in both rock and soil.

The successful application of each technique, however, demands close and harmonious cooperation between the support specialist and the excavation/lining contractor. Once such links are forged in the U.S., the demands of the urban shallow tunnelling market will be more efficiently served.

ACKNOWLEDGEMENTS

The authors have pleasure in acknowledging the assistance of their colleagues at NiCON Corporation, Pittsburgh, PA., and at Ing. Giovanni Rodio & Co., Milano, Italy.

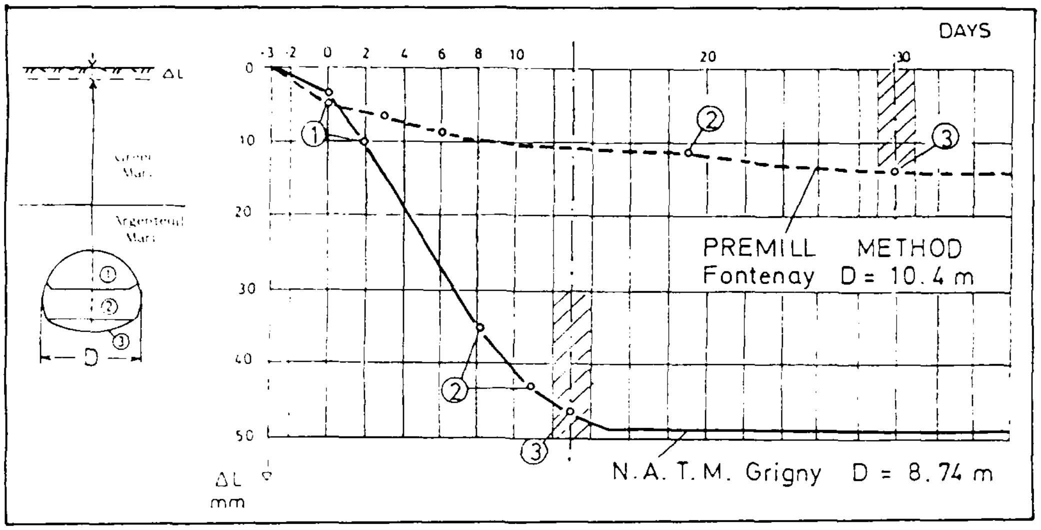

Figure 6 - Comparison of settlements generated with time in identical geological conditions, by Premill and NATM. (LeGoër, 1982).

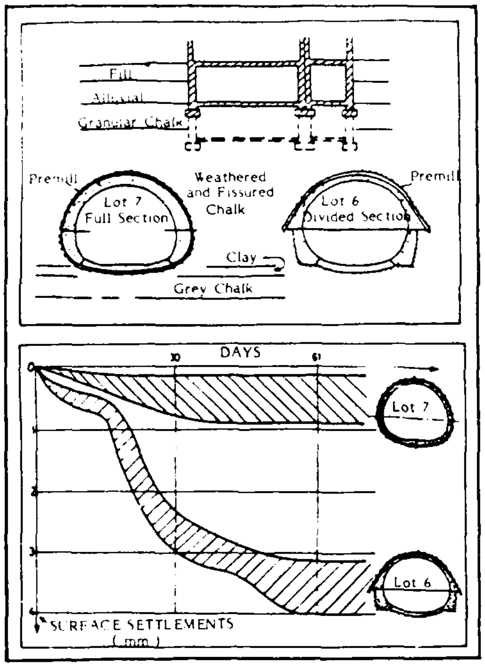

Figure 7 - Comparison of settlements generated by Premilling in Divided Section and Full Section, Lille, Belgium (LeGoër, 1982).

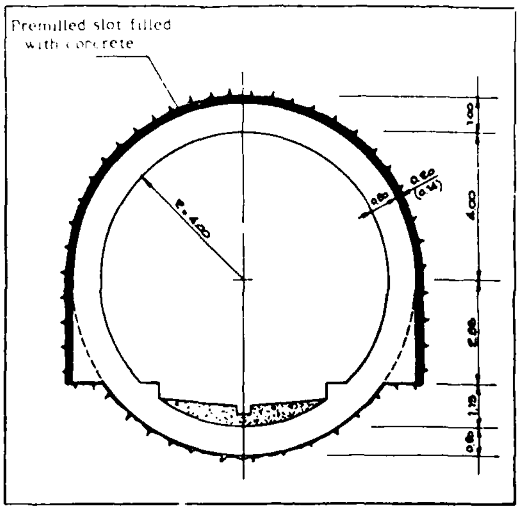

Figure 8 - Geometry of Roggiano Railway Tunnel, Italy, showing premilled protective arch.

REFERENCES

Bougard, J.F., Francois, P., and Longelin, R. (1979), Le prédécoupage mécanique: un procédé nouveau pour le creusement des tunnels. Tunnels et Ouvrages Souterrains, 22 (July-August), pp 174-180, 23 (Sept.-Oct.), pp 202-210, 24 (Nov.-Dec.), pp 264-272.

Bruce, D.A. (1987), Tunnel grouting - an illustrated review of recent developments in ground treatment. Proc. Int. Conf. on Foundations and Tunnels, London, March 24-26, pp 156-173.

Bruce, D.A., Boley, D.L. and Gallavresi, F. (1987), New developments in ground reinforcement and treatment for tunnelling. Proc. Rapid Excavation and Tunneling Conference, New Orleans, June 14-17, Vol. 2, pp 811-835.

Clough, G.W. (1981), Innovations in tunnel construction and support techniques. Bull. Assoc. Engrg. Geol., 18 (2), pp 151-167.

LeGoër, Y. (1982), *Le creusement des tunnels en site urbain par prédécoupage mécanique*. Travaux, December, pp 74-79.

Mongilardi, E. and Tornaghi, R. (1986), Construction of large underground openings and use of grouts. Proc. Int. Conf. on Deep Foundations, Beijing, September, 19 pp.

Proceedings: Second International Conference on Case Histories in Geotechnical Engineering, June 1-5, 1988, St. Louis, Mo., Paper No. 5.51

Reinforced Soil in the Repair of Embankment and Cutting Slip Failures

James Paul
Sales & Marketing Director, Civil Engineering, Netlon Limited,
United Kingdom

SYNOPSIS: The paper considers the causes of slips in embankments and cuttings and examines the traditional methods of repair and reinstatement. Reinforced soil solutions are examined and compared with the more traditional systems.

Following consideration of the structure and properties of a polymer geogrid for use in reinforced soil applications, two case histories are presented. The first involves the repair of a cutting slip in overconsolidated clay in S.E. England. Both the design method and construction system are examined along with indications of relative costs. The second example is a slip in a highway embankment in Sweden where a reinforced soil solution was adopted at a cost of only 25% of the standard solution.

INTRODUCTION

In many parts of the world slip failures are relatively common in embankments and cutting slopes. Failures range from slippage of topsoil due to erosion, shallow translational/rotational slips, through to deep seated rotational slips which are often caused by insufficient bearing capacity of the embankment foundation.

The most common type of failure is the relatively shallow slip where the failure surface is one to three metres from the surface. Reinforced soil techniques have proved to be extremely efficient and cost-effective in the repair of such slips.

CAUSES OF FAILURE

In the South East of England many major highways cross areas of over-consolidated clays. Cuttings constructed through these stiff clays and embankments constructed from them have a history of failure several years after construction. On release of overburden pressure near the face of a cutting or when taken from a deep borrow pit and placed near the face of an embankment, the clay swells as the negative pore pressures reduce and water is drawn into the soil. This process often continues until the once stiff clay becomes soft and even on relatively flat slopes of 1:3 a shallow slip is initiated.

In other parts of the world the cause of instability may be a rapid change in moisture content due to severe climatic conditions. In Northern Europe wet autumn weather followed by long periods of sub-zero temperatures and heavy snowfall creates a major problem when spring arrives and a rapid thaw releases large volumes of water into surface layers of soil.

In tropical climates the culprit is the monsoon-type storm which can produce rainfall intensities of around 100mm/hour and in exceptional cases daily rainfall in excess of 600mm.

TRADITIONAL REPAIR OPTIONS

The most obvious repair option is to reduce the gradient of the slope either by placing additional fill at the toe or by removing material from the crest. In many cases, however, this solution is not possible due to restrictions on the availability or cost of additional land or due to the presence of existing structures.

In urban situations the importation or removal of large volumes of soil may be environmentally unacceptable even if economically feasible.

Other repair techniques include the construction of a gabion wall, replacement of the failed cohesive material with a free draining granular fill, lime treatment of the failed clay and a reinforced soil repair using either strip materials together with a facing unit or polymer grid reinforcement which interlocks with the fill and requires no facing.

A study has been carried out using these five systems to repair a section of 7 metre high embankment constructed from Gault clay in Cambridgeshire, England and is reported by Johnson (1985).

In the study the first reinforced soil system used a polymer strip material looped around used car tyres to form the facing. Other tyres used as anchor points were placed in trenches within the stable portion of the embankment.

The second system used polymer geogrid reinforcement (designation 'Tensar' SS1) which was wrapped up at the face and returned below succeeding layers to fully encapsulate the fill at the face.

Table 1 shows the associated costs and time taken for the repair of a 20m length of embankment for each of the five systems.

Table 1. Embankment treatment repair costs.

Reinstatement Technique	Time Taken (Days)	Total Cost (£)
Gabion wall	18	8,360
Granular replacement	5	5,020
Anchored tyre wall	8	4,760
Lime stabilisation	7	4,730
Geogrid reinforcement	6	3,430

(after Johnson 1985)

Of the five repair systems the gabion wall and anchored tyre wall involved the construction of a 3 metre high toe wall then flattening the slope to 1:3, whilst the other techniques retained the original 1:2 slope.

The lime stabilisation and geogrid reinforcement systems re-used the failed material while the other systems involved off site disposal of soft clay and importation of substitute granular fill.

Of the five systems investigated the reinforced soil repair using polymer geogrids was one of the fastest solutions and was considerably less expensive than all others.

STRUCTURE AND DURABILITY OF POLYMER GEOGRID REINFORCEMENT

The range of 'Tensar' polymer geogrids are produced by punching a carefully spaced array of holes in a sheet of polymer and then stretching the sheet at carefully controlled temperature and strain rate. The sheet is stretched in one direction to produce uniaxial grids (Fig 1), and for some products, stretched in the orthogonal direction to produce biaxially oriented grids (Fig 2). The stretching process takes place at a relatively low temperature and causes the long chain molecules of the polymer to become oriented in the direction of stretch; dramatically increasing the tensile strength and modulus of the grid. This unique process produces grids with integral junctions which are extremely efficient in transferring stresses from the soil into the reinforcing grid. Products with welded joints, as opposed to integral junctions, have potential weak points.

Tensar grids are eminently suitable for use in the repair of slips since they will interlock efficiently with soft clay materials even close to the face where overburden pressures are low.

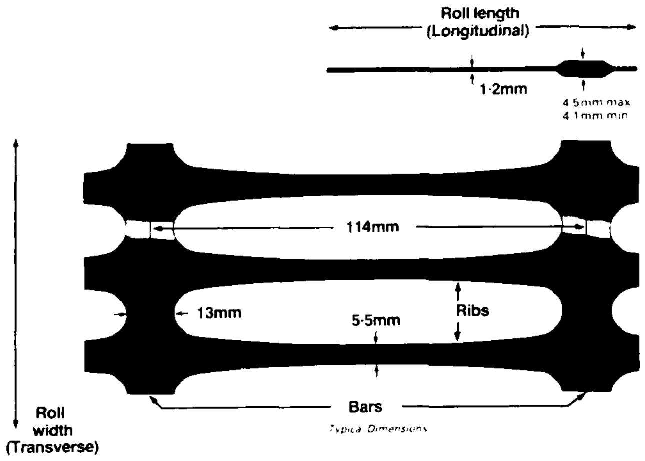

Figure 1 - Tensar SR2 geogrid - a typical uniaxial grid.

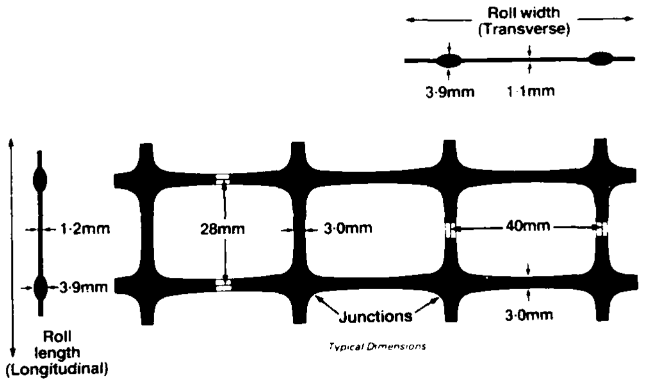

Figure 2 - Tensar SS2 geogrid - a typical biaxial grid.

The polymers used in the production of the grids are high density polyethylene and polypropylene, both of which are known to be inert to the chemicals normally found in soils and to almost all chemicals which could conceivably drain into soils as a result of a road accident.

If the repair involves construction of a toe wall or embankment at a slope in excess of 45° then the higher strength uniaxial grids would be used with wrap-around face containment. Shelton and Wrigley (1987) have shown that these grids will retain 90% of their tensile strength after approximately 50 years exposure to ultra-violet attack. Protection is achieved by incorporation of carefully calculated quantities of finely divided carbon black.

In the field however, the normal cover of vegetation provides permanent protection by shielding the grid from sunlight. Obviously the buried sections of grid, which carry the major loads, do not suffer any deterioration since they are not exposed to sunlight.

CASE HISTORIES

Many slips have been repaired using polymer grid reinforced soil due to the simple construction techniques and consistently low project costs. Several projects have been reported and will not be considered further in this paper e.g. Busbridge (1984), Oliver (1985), Bonaparte and Margason (1984), Bell et al (1984) and Toh et al (1986).

1. Repair of a Cutting Slip on the A406, London, England

The A406 forms the North Circular Road close to the centre of London. Several years after its construction in 1968, slip failures began to occur in a cutting near Waterworks Corner where the A406 runs through Epping Forest (Fig 3). The 500 metre long cutting is up to 9 metres in depth through London clay and was constructed with side slopes of 1:2. Although the cutting was stable for the first seven years after construction, slips began to occur with increasing regularity causing damage to fence lines and spillage onto the carriageway.

Figure 3

Several remedial measures were considered, including granular replacement and toe retention with crib walling or sheet piling combined with flatter slopes. These options were prohibitively expensive. Lime stabilisation was ruled out mainly due to doubts on the viability of achieving uniform mixing on site and uncertainty about long term performance.

A reinforced soil solution was selected on the basis of cost, ease of construction and confidence in the design, which involved reinstatement of the failed London clay, reinforced with horizontal layers of 'Tensar' geogrids. Drainage was also provided.

Investigation showed the slip to be a shallow failure and the reinforced soil repair was designed using a method developed by Murray (1984). The method simplifies the analysis by approximating the failure surface to a bilineal slip plane and good agreement has been found between the results of the simplified and the more conventional circular or non-circular slip surfaces.

Design charts have been developed to select the geogrid reinforcment requirements for a range of slope conditions. The reinforcement is designed to intersect potential failure planes. It must possess proven long term tensile strength characteristics, and sufficient interaction with the soil to resist direct shearing of soil over the reinforcement and also to provide pull out resistance using a relatively short anchorage length.

The design charts are used to determine a factor of safety based on the following parameters,

Tperm = Permissible long term tension which may be applied to the geogrid reinforcement

Sv = Vertical spacing of the reinforcement (assumed to be constant)

H = Height from lowest to the highest point on the anticipated slip surface (often taken as slope height)

ru = Pore water pressure ratio

γ = Density of soil

β = Slope angle

ϕ' = Effective angle of internal friction of the remoulded soil (c' assumed = 0)

At Waterworks Corner the soil parameters were taken as

$\phi' = 20°$

$c' = 0$

$\gamma = 20\ kN/m^3$

It was found from the design charts that the required factor of safety was obtained when using horizontal layers of 'Tensar' SR2 geogrid reinforcement at 1.5 metres vertical spacing.

Since the slope angle was less than 45°, no face wrap-around was specified. However, due to the large vertical spacing of the primary layers of reinforcement, short horizontal layers of lightweight Tensar SS1 biaxial grid were specified as secondary reinforcement. These were placed at 0.5 metres vertical spacing to stabilise the slope surface against potential sloughing between layers of the primary reinforcement.

The length of each layer of primary reinforcement is determined by extending the grid a sufficient distance behind potential failure surfaces to ensure safety against pull-out. Using a full junction strength grid reduces this length to a minimum. As is normal in such repair systems, a layer of free draining granular material is laid at the rear of the excavation (Fig 4).

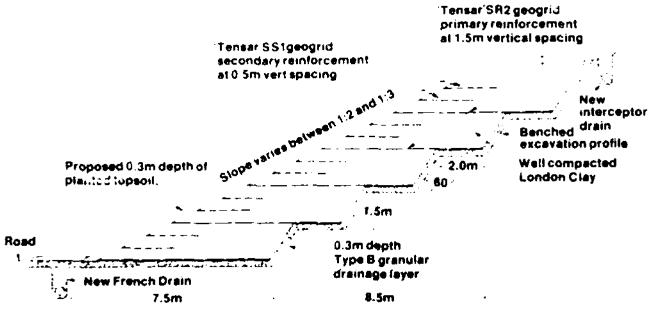
Tensar'SR2 geogrid
primary reinforcement
at 1.5m vertical spacing
Tensar SS1geogrid
secondary reinforcement
at 0 5m vert spacing
Slope varies between 1:2 and 1:3
New
interceptor
drain
Benched
excavation profile
Well compacted
London Clay
Proposed 0.3m depth of
planted topsoil.
2.0m
60
1.5m
Road
1
0.3m depth
Type B granular
drainage layer
New French Drain
7.5m
8.5m

Typical section of reinstated slope (North side), A406 North Circular Road, London.

Figure 4

Work was begun in September 1985 using a standard earthworks team of one Cat 215 tracked excavator, one Volvo four wheel drive dumptruck and one Cat 951 dozer with a four-in-one bucket and a towed vibrating roller. Manual operations were carried out by two labourers.

Use of the reinforced soil system reduced traffic management measures to a minimum since there was minimal removal of spoil and no importation of granular fill which would have involved large numbers of trucks reversing on to and off the carriageway.

Main earthworks began with the excavation and removal from site of a 35m long strip of slipped soil. Excavation extended beyond the failure plane with benched steps cut into the undisturbed clay (Fig 5). The general sequence then adopted was to reinstate the first strip using fill excavated from an adjacent second strip, to minimise double handling. The second strip was then reinstated using fill excavated from a third strip and so on.

Figure 5

Fill was tipped from the Volvo, placed using the Cat 951(Fig 6), and compacted to a maximum layer depth of 200mm using the vibrating roller towed by the Cat 951. The 2.0m widths of 'Tensar' SS1 secondary reinforcement were obtained by cutting the standard 4.0m wide rolls in half on site with a disc cutter.

Figure 6

'Tensar' SR2 rolls were cut to the required length and laid perpendicular to the slope face. Adjacent rolls were butt jointed (Fig 7). The slope face was over filled and trimmed in the conventional manner.

Along part of the slope where additional land was available the gradient was reduced to 1:3.

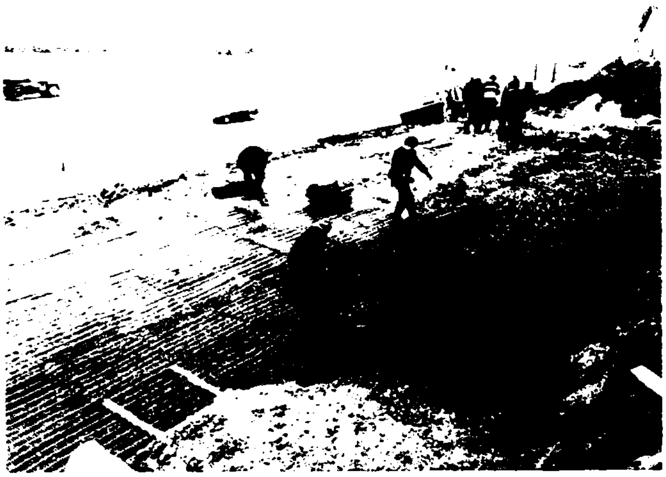

Figure 7

Approximate quantities involved in the 500 metre long repair were:

Excavation	23,000 m³
Refilling	12,600 m³
Gravel drainage layer	5,400 m³
'Tensar' SR2 primary reinforcement	17,000 m²
'Tensar' SS1 secondary reinforcement	8,000 m²

In spring 1986 approximately 500 cubic metres of topsoil were placed on the reconstructed slope for subsequent planting.

In the South East of England the more traditional repair involving removal of the slipped material and replacement with granular fill typically costs around £25/m³. The reinforced soil technique using Tensar geogrids has been shown to cost between £7 and £12/m³ i.e. savings of between 50% and 70%.

2. Slip in Road Embankment, Sweden

Near the town of Sundsvall, 400km north of Stockholm, a slip occurred in autumn 1984 on road number 331 involving part of the road pavement.

The road was cut into the side of a steep hillside with the outer edge constructed on an embankment using material from the cut section. The downhill face slope was 1:1.7 and the soil in the structure was a silty moraine with very little stone material. During the spring thaw movement was noted at the edge of the embankment but this soon stabilised. In autumn a period of heavy rainfall extending over several days caused saturation of the moraine materials and the creation of very high pore water pressures in silt layers near the top of the embankment. Movement was again detected with first the metal fence becoming suspended in mid air and then a 50 metre length of carriageway edge cracking and moving downhill. As the road is in a forested area much of the traffic consists of 60 tonne timber loaded lorries which impose high loading on the road pavement.

The initial repair solution was to reduce the downhill slope angle by placing additional fill. Unfortunately the height of the slope was 15 metres and at the base was a thick deposit of peat.The proposal was to place blasted rock into the peat to form a toe wall and then build up a new slope face at a gradient of 1:2.5.

As the estimated cost of this repair was found to be extremely high a more innovative, lower cost solution was sought.

Using the uniaxial 'Tensar' SR2 grid reinforcement it was found that stability could be achieved by incorporating 3 horizontal layers of reinforcement in the top 3 metres of the embankment using the original fill material and a single drainage layer. Each layer of reinforcement extended 6 metres from the face and in this way the shoulder was stiffened and the layers of grid intercepted deeper potential slip surfaces. At the same time the opportunity was taken to steepen the face of the slope over the 3 metre high repair to 1:1 using a biaxial grid wrap-around to contain the face. Thus an additional 2 metres of shoulder width was obtained.

Construction was carried out using standard earthworks equipment and techniques (Figs 8 & 9) with minimum disruption to traffic and at a cost of only 25% of the original proposed solution.

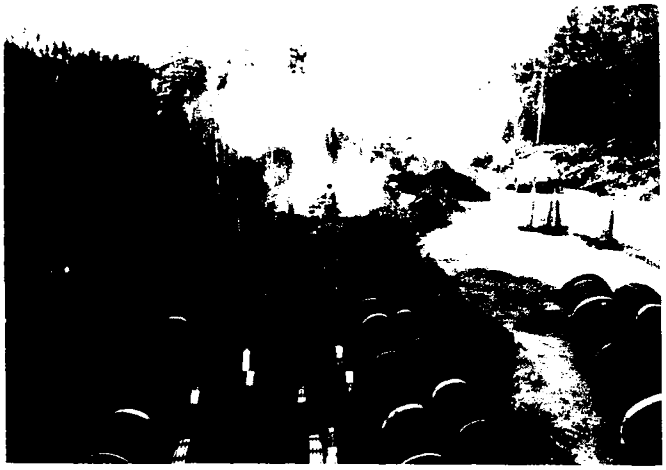

Figure 8

Figure 9

CONCLUSIONS

There is now extensive experience relating to the use of polymer grids in reinforced soil repairs to slip failures.

Such techniques have been used in many parts of the world and in many different soil types including clays, silts, moraines and laterite soils.

The use of a grid reinforcement with full strength junctions is extremely important as this means that the required pull-out resistance can be achieved with the minimum of excavation behind the failure plane.

In addition, the grid structure will efficiently transfer stresses from the fine grained and often wet fill material.

Tensar grid reinforced soil repair techniques re-use failed soils, minimise traffic disruption and delay and, most importantly reduce costs.

REFERENCES

Bell, J.R., Szymoniak, T. and Thommen, G.R. 1984. Construction of a Steep Sided Geogrid Retaining Wall for an Oregon Coastal Highway. Proc. Symp. on Polymer Grid Reinforcement in Civil Engineering, London, pp 198-202

Bonaparte, R. and Margason, E. 1984. Repair of Landslides in the San Francisco Bay Area. Proc. Symp. on Polymer Grid Reinforcement in Civil Engineering, London, March '84 pp 64-68.

Busbridge, J.R. 1984. Stabilisation of Canadian Pacific Railway slip at Waterdown, Ontario, using 'Tensar' grid. Polymer Grid Reinforcement: 58-63, Thomas Telford, London.

Johnson, P.E. 1985. Maintenance and repair of highway embankments: studies of seven methods of treatment. Department of Transport, T.R.R.L. Research Report 30, Crowthorne.

Murray, R.T. 1984. Reinforcement techniques in repairing slope failures. Polymer Grid Reinforcement: 47-53, Thomas Telford, London.

Oliver, T.L.H. 1985. Reinforced soil technique for the reinstatement of failed slopes using geogrids. Proc. Symp. on Failures in Earthworks: 417-419, Thomas Telford, London.

Shelton, W.S. and Wrigley, N.E. 1987. Long-term durability of geosynthetic soil reinforcement. Geosynthetics '87 Conference, New Orleans, L.A.: 442-455.

Toh, C.T., Chee, S.K. and Ting, W.H. 1986. Design construction and performance of a geogrid reinforced high slope and unreinforced fill slopes. I.E.M. - JSSMFE Joint Symposium on Geotechnical Problems: 90-111, Kuala Lumpur, Malaysia.

Proceedings: Second International Conference on Case Histories in Geotechnical Engineering, June 1-5, 1988, St. Louis, Mo., Paper No. 5.53

Distribution of Contact Pressure and Stresses under Skirted Footings

M.L. Ohri
M.B.M. Engineering College, University of Jodhpur, Jodhpur, India

G.R. Chowdhary
M.B.M. Engineering College, University of Jodhpur, Jodhpur, India

A. Singh
M.B.M. Engineering College, University of Jodhpur, Jodhpur, India

SYNOPSIS : Skirted footings posses many novel characteristics which render them eminently suitable for construction of structures in situations involving heavy loads and poor soil conditions with promise of economy. The results of the present investigations will help considerably to understand a detailed picture of the complex phenomenon of contact pressure distribution and vertical stress distribution in soil under skirted footings.

INTRODUCTION

A skirt may be constructed as an integral part of the footing along its periphery or independently adjacent to it. These footings have staged their entry into foundation engineering in the early eighties by their use in some important projects located in the Thar desert of India (Singh, Punmia and Ohri, 1981). They may be found efficient for strengthening the buildings under distress due to excessive total or differential settlement. A model skirted footing provided with integral skirt at 45° with vertical and having skirt depth equal to 0.5 times the top width is capable to take 30% more pressure intensity than its equivalent flat footing in dune sand. Rao and Sharma (1980) have brought out the beneficial effects of non-integral vertical skirts around a footing in increasing bearing capacity and reducing settlement characteristics. Skirted granular piles also improved the load carrying capacity significantly (Rao and Bhandari, 1979).

For the realistic design of a skirted footing, the nature of pressure distribution at the footing-soil interace and also within the soil mass should be known. Regardless the hypothesis by which these may be calculated the desirability of their determination by actual measurements is always keenly felt. Apart from the present experimental studies, the attempts to measure contact pressures and stress distribution in soil under skirted footings are non-existent. These were investigated under the perfect case of rigidity, using cast iron skirted footing models which settle uniformly at all points on the footing. It ensured not only perfect rigidity but also retention of shape at all stages of loadings.

SOIL

The uniformly graded dune sand used in the test programme had fine sand fraction (425 micron to 75 micron)=98%, coefficient of uniformity = 1.28, coefficient of curvature = 0.94, mean diameter = 0.11 mm, effective size =0.084 mm, specific gravity = 2.66, maximum dry density = 1.43 g/cc, ultimate friction angle is 29° under all conditions of moisture and loading. The peak angle of internal friction in dry state lies in the range of 32° to 35° at the rate of 3° per 10% change in voids ratio.

DESCRIPTION OF MODEL PROGRAMME

Footings

The model footings used in the investigations were made as strip footings of 80 mm x 500 mm provided with skirt at 0°, 20°, 30°, 40°, 45°, 50°, 60° and 90° with the vertical (θ). The depth of the skirt was kept as 0.7 B (B=width of footing), for contact pressure measurements and that of 0.5 B for vertical stress measurements studies. All the footings of each set had the same contact area. Twenty four grooves of 20 mm diameter and 4 mm deep were machined in the footings to receive the boundary earth pressure cells. They were snug fitted and set flush with the base of the footing.

Placement of Sand and Test Equipment

A tank measuring 1.25 m x 0.50 m in plan and 0.90 m in depth was used in the test programme. The sand was allowed to fall freely from a sieve having perforations of 2mm diameter at 25.4 mm c/c from a height of 0.60 m in lifts of 50 mm to achieve a density of 1.60 g/cm^3 The sand was vibrated to achieve a density of 1.65 g/cm^3 Dead load system with a lever arrangement was used to apply the load to the footing. It ensured the constant application and transfer of the applied load from the footing to the soil in each test observations. The dead load system is especially suitable when such sensitive observations as contact pressure and pressure distribution measurements are made. Density measurements were made in each test and probe penetrometer soundings were also performed for density control.

Experimental Procedure

Correct positioning and placement of a model skirted footing required considerable care and effort. The method of its placement on dune sand was perfected after several trials. The stainless steel pressure cells of 20 mm and 30 mm diameter (D) with integral diaphragm, designed and fabricated with considerable care and effort were used for contact pressure and stress distribution measurements respectively.

TABLE 1. Charateristics of Pressure Cells

Cell	Capacity (kN/m²)	Inner dia.(d) mm	Outer dia.(D) (mm)	$(\frac{d^2}{D^2})$	Aspect ratio	Thickness of Cell (mm)	Thickness of Diaphragm(mm)
Contact pressure Cell	0-300	14	20	0.49	0.20	4.0	0.40 + 0.03
Embedded Pressure Cell	0-100	20	30	0.45	0.20	6.0	0.45 + 0.03

The characteristics of the cells are given in Table 1. The pressure cells were calibrated by using compressed air in triaxial cell and also by applying pressure from a column of mercury manometer designed for purpose. Both the methods gave parallel results. An integral skirted footing containing 24 pressure cells was placed in its position on the sand bed. For the determination of stresses inside the sand medium, twenty four pressure cells were embedded at a time. To have large number of stress points,the position of pressure cells were changed in the second stage of the test on the same footing. Two dial gauges of 0.01 mm least count were set on the footing. A seating pressure of 100 g/cm^2 was applied and released before the start of the test. The wire leads of each pressure cell were connected to the multi-channel input. The output terminal was then connected to the digital strain indicator. By operating the multichannel selector switch, the desired pressure cell was connected to the strain indicator and its initial reading was recorded. The loads corresponding to 20%, 33% and 50% of the ultimate load were applied in steps to the footing (soil deposited at 1.65 g/cm^3) for contact pressure measurements and tat of 30 kN/m^2 (soil deposited at 1.60 g/cm^3) for stress distribution studies. The reading of the strain indicator of each pressure cell was recorded when the settlement of the footing had ceased. The difference between the initial and final readings of the strain indicator gave the magnitude of the strain that each pressure cell had undergone. Each test was repeated atleast three times to check the reproducibility of the test results. The defective cells, if any, were replaced in the subsequent observations.

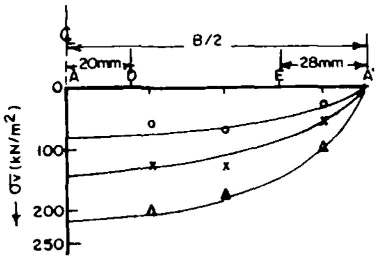

1 (a).

TEST RESULTS AND DISCUSSIONS

Contact Pressure under Footings.

Fig 1(a) shows that the contact pressure distribution under a flat footing which is maximum at the centre and minimum near the edges. The contact pressure increases with the increase of the applied pressure. The observed contact pressure for the footings having skirts at 20°, 30°, 40°, 45°, 50° and 60° are plotted on the projected plan width (Bp) of each footing and that of 0° on the geometry of the footing (Fig 1(b) to 1 (h)). The contact pressure below the skirt tends to reduce significantly when the angle of skirt (θ)is more than 45°. The contact pressure distribution is nearly constant when the angle of skirt is 60°. When the skirt of a footing is at 0° with the vertical, the contact pressure is maximum at the centre and relatively non-existent along the length of the skirt. With the increase of angle of skirt from 0° to 50°, there is but a gradual decrease in the cotact pressure at the centre of the footing and significant increase in it along the depth of the skirt. When the angle of skirt is 40°, the contact pressure at the centre of the footing is very nearly the same as that of the skirted footing having the same as that of the skirted footing having θ=45°. However, the same at the edge of the skirt for θ = 45° is 14.5% more than that of θ=40°. The concentration of stresses in general is less at centre and more at edges of the skirted footings when θ ≥30. This trend is reversed for footings having θ≤ 20. The

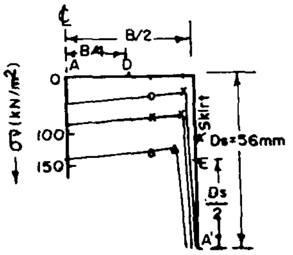

1 (b).

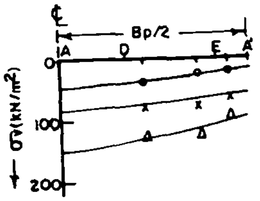

1 (c).

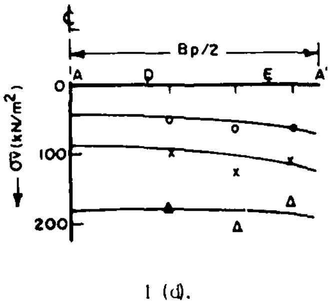

1 (d).

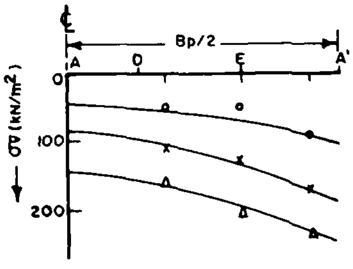

1 (e)

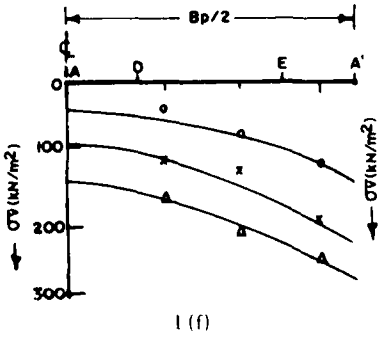

1 (f)

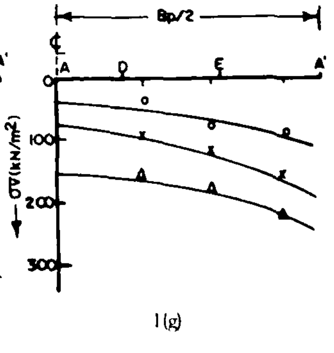

1(g)

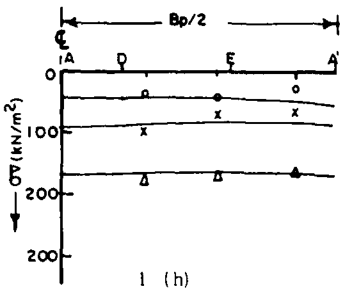

1 (h)

Fig. 1. Contact Pressure Distribution under Skirted Footings.

maximum amount of contact pressure at a given pressure intensity at the bottom edge of the skirt has been observed when the angle of skirt (θ) is 45° with the vertical.

Vertical Stress Contours under Skirted Footings.

Fig.2 (a) to 2(d) show the vertical stress contours for skirted footings provided with skirt at 0°, 20°, 30°, 40°, 45°, 50°, 60° and 90° with vertical at the pressure intensity of 30 kN/m^2. The depth Z/Bp (Z= Depth of soil, Bp = plan width of footing

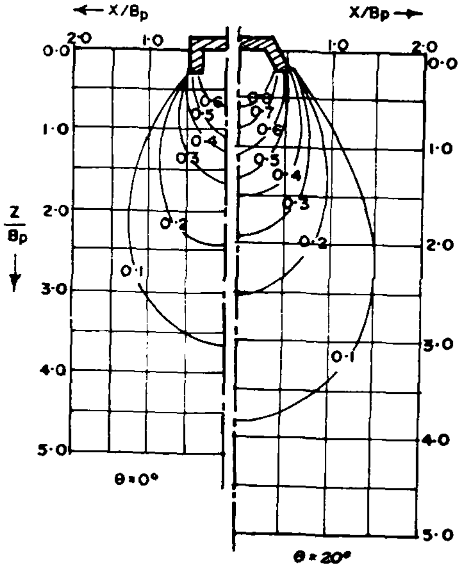

2 (a)

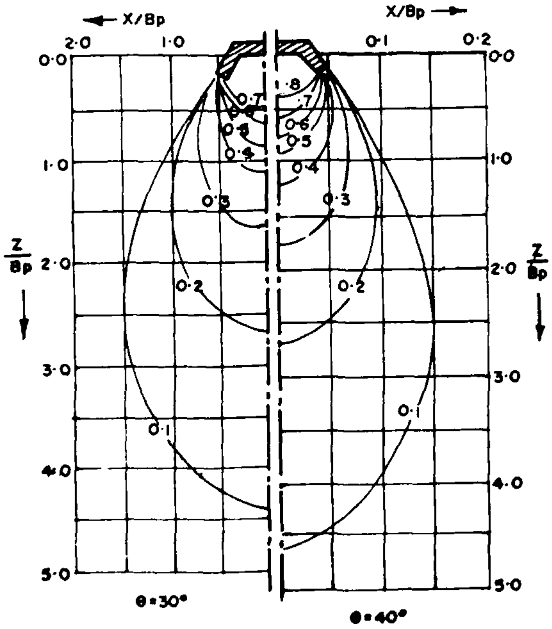

2 (b)

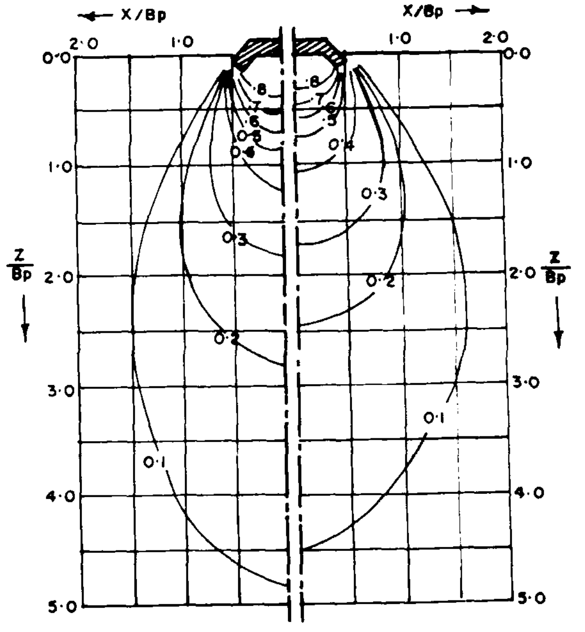

2 (c)

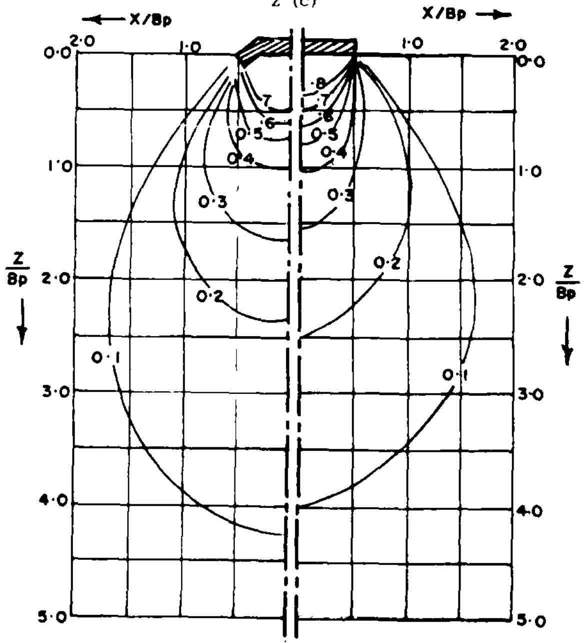

2(d)

Fig.2. Vertical Pressure Distribution under Skirted Footings.

at the centre of skirted footingof the stress contour of 0.1q intensity due to the applied pressure on a skirted footing having $\theta = 0^\circ, 20^\circ, 30^\circ, 40^\circ, 45^\circ, 50^\circ, 60^\circ$ and 90° is 3.65, 3.80, 4.4, 4.5, 4.8, 4.4, 4.25 and 4.25 times the plan width of footing respectively. It may be observed from the figures that region of distribution of a vertical stress of a given pressure intensity increases laterally with increase of angle of skirt from 0° to 60°. The actual stress measured at a given depth below the flat strip footing ($\theta=90^\circ$) is lower than that obtained by Boussinesq. This may be due to the non-linear behaviour of soil. The more the confinement of sand in the skirt zone, the higher is the magnitude of vertical stress at a given depth. The confinement of sand is maximum when angle of skirt is 45°.

CONCLUSIONS

On the basis of a series of laboratory tests on rigid skirted footings bearing on dune sand the nature of contact pressure distribution as well as vertical pressure distribution in soil have been studied and found to be mainly dependent on the angle of skirt. A perfect picture regarding the distribution of contact pressure emerges from the tests. The contact pressure show a definite tendency for edge concentration for $30^\circ \leq \theta \leq 50^\circ$. The contact pressures also exhibit a tendency to shift of concentration towards the central regions of these foundations when the applied load is at a factor of safelty of 2. The pressure bulbs of vertical pressure distribution under skirted footings have been developed and presented which were not so far available in literature. The reported study comprehensively attempts to present the behaviour of skirted footings on dune sand and throws light into the manner in which the loads are transferred from the footings to the soil.

REFERENCES

Barden, L. 1962. An approximate solution for finite beams *resting on elastic soils, Civil Eng.Pub.Works, Rev.Vol.57*

Boussinesq, J. 1885. Application Des potentiels a L'Etude de L' Equilibre et du Mouvement Des Solids Elastiques, Gauthier Villars, Paris, France.

Chowdhary,G.R. 1987. Behaviour of skirted footings on Dune sand. Ph.D. thesis, Univ. of Jodhpur,India.

Ohri,M.L., A.Singh and G.R.Chowdhary, 1987. Bearing capacity of skirted footings in sand. Proc. International Conference on foundation. and tunnels, London.

Rao,B.G. and A.K.Sharma, 1980. Skirted granular pile foundations for seismic and flood-prone zones. ICEPND, Asian Instt. ofTech. Bangkok.

Rao, B.G. and R.K.Bhandari, 1980. Skirting - a new concept in the design of heavy storage tank foundation. Proc. 6th SEACSE, Taipei.

Singh,A. B.C.Punmia and M.L.Ohri.1985. Regional Deposits Desert soils. *A state of the art report*, Indian Commemorate Volume released by IGS on XI ICSMFE,44-53.

Vardarajan,A. 1983. FEM and its use in soil-structure-inter action studies, International Workshop on soil structure Interaction, Roorkee, India.

Proceedings: Second International Conference on Case Histories in Geotechnical Engineering, June 1-5, 1988, St. Louis, Mo., Paper No. 5.55

Behaviour of a Geogrid Reinforced Embankment over Waste Material

P. Rimoldi
Italy

A. Pagotto
Italy

D. Cazzuffi
Italy

SYNOPSIS: The paper deals with the monitoring of a geogrid reinforced embankment, 5.0 m high and 600 m long, built to contain additional waste material in the municipal landfill in Modena (Northern Italy).
The embankment was founded directly over the waste already placed in the landfill, consisting of compressible and dishomogeneus material, varying from solid urban waste to muddy industrial material. The geotechnical parameters assumed to characterize the fill soil and the waste material of the foundation soil are described.
The settlements of the embankment and the forces and strains in the geogrids were monitored from the beginning of the construction until some months later. The instrumentation used in order to perform this control is described.
The actual results are compared with those obtained from the design model and with other field tests concerning geogrid reinforced structures.

FOREWORD

The works presented in this paper are related to the construction and to the monitoring of an earth embankment for the urban waste disposal facility in Modena (Northern Italy).
In successive times, a series of dikes, starting from the filled level of the existing landfill, was and will be built, in order to contain additional waste material up to a total height of about 15 m.
The embankments, 5 m high, have a constant shape in their longitudinal development and for the 3 successive levels: until now, only the first embankment was built.
This embankment was founded directly over the urban waste of the landfill, consisting of compressible and dishomogeneus material; only a little part of the embankment was founded on industrial wastes, consisting of inert muddy materials.

The embankment was reinforced with horizontal layers of high density polyethilene uniaxially oriented geogrids, and was designed with a sort of "foundation beam", constituted by a layer of soil totally wrapped in a geogrid. The geogrids used were Tenax TT1 manufactured in Italy by RDB Plastotecnica.
The use of geogrids as reinforcement allowed to improve the geotechnical characteristics of the fill: the factor of safety against rotational failure, for a 1:1 slope as the instrumented one, calculated according to the Fellenius modified method, was 0.9 without reinforcement and 2.5 with geogrid reinforcement (Pagotto - Rimoldi, 1987).

DESIGN

Geotechnical characteristics

The geotechnical characteristics of the foundation material and of the fill soil for the embankment were measured by means of tests, carried out both on site and in laboratory. The main results obtained are as following:

-foundation material: the plate loading tests were carried out in a certain number of points on the waste disposal area. The average of the values, obtained for the urban solid waste, compared to the results obtained by Cancelli and Cossu (1985) on the same type of material, have given results similar to those typical of organic soils:

- unit weight γ_f = 10 kN/mc
- cohesion c'_f = 30 kPa
- internal friction angle ϕ'_f = 22 degrees
- primary compression index C_c = 0.6
- secondary compression index C_α = 0.1

-fill soil for the embankment: grain size analysis, Atterberg limits, consolidation tests, triaxial tests (U.U. and C.D.) and permeability tests (by oedometer) were carried out, obtaining the following results:

- unit weight γ_e = 18 kN/mc
- liquid limit W_L = 65%
- plastic limit W_p = 24%
- cohesion c'_e = 25 kPa
- internal friction angle ϕ'_e = 25 degrees
- permeability coefficient k = 3 x 10 E-11 m/s

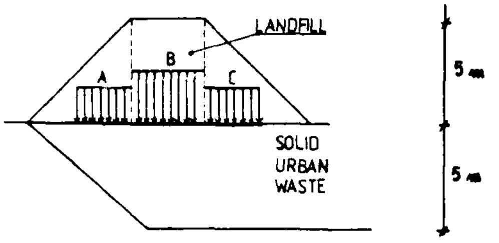

Fig. 1 : Scheme of the load distribution for the settlement evaluation without geogrid reinforcement.

Evaluation of the settlements without geogrids

The embankment standard cross-section was divided into sectors of unitary thickness in order to calculate the settlements: three different loads have been defined, as presented in Figure 1.
The settlements were estimated using the oedometric theory by means of the formula:

$$S = H \cdot \frac{C_c}{(1+e)} \cdot \log \frac{\sigma_o + \Delta\sigma}{\sigma_o} \qquad (1)$$

The results obtained for the section founded on urban solid waste were as follows:

$S_A = 0.32$ m $S_B = 0.40$ m $S_C = 0.35$ m $S_{average} = 0.36$ m

For the section founded on muddy wastes the settlement, calculated according to the same method, gave an average value of 1.05 m.

Design parameters for the reinforced embankment

The design of the embankment was carried out on the base of the following parameters:

- height $H = 5$ m
- slope angle max $\beta = 55$ degrees
- surcharge $q = 10$ kPa
- maximum tensile strength of geogrid $\alpha_f = 66$ kN/m

The factors of safety were assumed as following:

- FS global = 1.1
  (well known geotechnical parameters);
- FS time = 1.35
  (medium difficulty and duration of the work);
- FS construction = 1.35
  (soil used not suitable as fill material);

- FS grid = FS global x FS time x FS construction = 2.00

The design parameters were assumed as follows:

- reduced friction angle $\phi'^* = \mathrm{arctg}(\mathrm{tg}\phi'_s/\mathrm{FSglobal}) = 23°$;
- allowable tensile strength $\alpha_a = \alpha_f$ /FS grid = 33 kN/m.

The final configuration of the embankment cross-section, according to the design method presented by Jewell et al. (1984) and revised by Rimoldi (1987), is shown in Fig. 2a.

Design model

Since the reinforced embankment was built on a compressible foundation, settlements in the waste disposal area were important, so that the geogrid placed at the base of the embankment was expected to be bent and tensioned.
In order to calculate the embankment settlements and the distribution of tensile forces in the base geogrid a model based on a Winkler scheme was developed. In fact the lower layer of soil, totally wrapped in the base geogrid, acts as a beam on a Winkler soil characterized by the modulus of subgrade reaction k_s, as shown in Figure 2b.
Therefore the beam length is assumed equal to the embankment width and the beam width equal to 1 m corresponding to the geogrid transversal dimension; a possible plate structural behaviour was not considered, in favour of safety. The beam has an height of 0.9 m and is loaded with a trapezoidal surcharge given by the shape of the embankment cross-section.
The modulus of subgrade reaction k_s is a parameter which takes into account the average compressibility of the waste layer which forms the embankment base. Consequently, the modulus was calculated as follows:

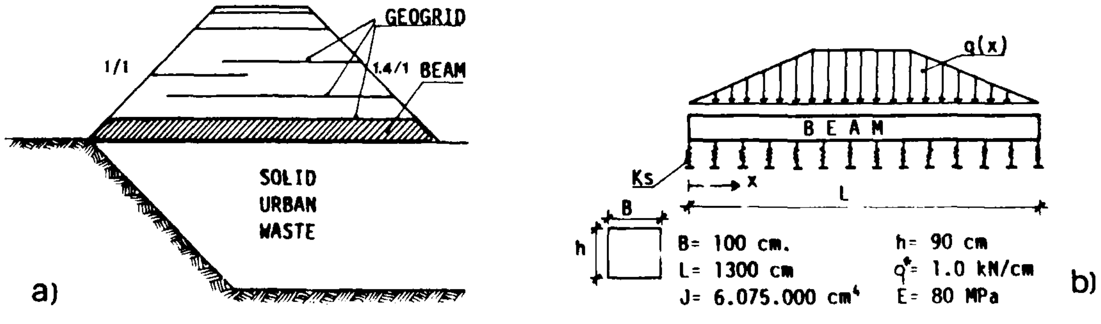

Fig. 2 : a) Cross-section of the embankment reinforced with geogrids.
b) Scheme adopted for the Winkler model.

$$k_s = \frac{q^*}{S} \cdot P_g = 0.1 \div 0.3 \quad N/cm^3 \qquad (2)$$

where: q^* = maximum pressure on the waste disposal

S = average settlement (see Eq. 1)

P_g = factor which takes into account the presence of the base geogrid.

The value of P_g, equal to 1.08÷1.13, was determined with loading tests on plates to evaluate the elastic response of the soil formed by the actual compacted waste under the load.

The minimum value of k_s (0,1 N/cmc) was obtained in presence of the muddy material, while the highest value of k_s (0,3 N/cmc) was recorded for solid urban waste, normally compacted.

Assuming the values presented in Figure 2b, and taking into account an elastic modulus E of the clay equal to 80 MPa, the settlements and the moments along the beam axle were calculated, using a standard computer program for beams on Winkler soil.

The tensile stress σ_g in correspondence of the base geogrid was given by:

$$\sigma_g(x) = \frac{M(x) \times 0.9h}{J} \qquad (3)$$

and the tensile force in the geogrid was obtained by the equation:

$$\alpha_g(x) = \sigma_g(x) \times T_g \qquad (4)$$

where: T_g = average thickness of the geogrid (2 mm)

The above formulas allowed to obtain the values of the forces $F_g(x)$ and the settlements S(x) in two situationsof foundation, as plotted in Figure 3. Site 1 is referred to the urban solid waste foundation material, while Site 2 is related to the muddy foundation material.

Until now no evidence of significative deformations of the embankment body has occurred, so it seems that the "foundation beam" and the geogrid reinforcement allow the embankment to withstand also important settlements.

INSTRUMENTATION

The parameters directly measured with instruments placed in the body of the embankment were the settlements of the base, the tensile forces and the strains in the geogrids.

The settlements of the base of the embankment were measured in 4 points by means of the most simple instrument: a steel plate, having a diameter of 60 cm, directly laid on the base geogrid; the plate presented a steel tube welded on it in vertical position, which was incremented with elements, 1.0 m long, as the embankment construction went on. The steel tube was inserted in a plastic tube, to avoid lateral friction. The tubes came out of the embankment just on the inner edge of the crest, in order to avoid any disturbance due to the passage of trucks.

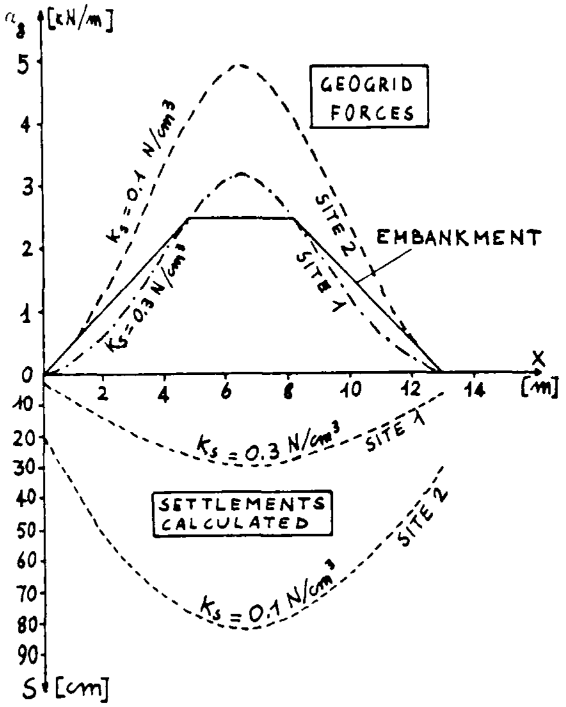

Fig. 3 : Distribution of the forces in the base geogrid and of the embankment settlements resulting from the calculations based on the Winkler model.

After the end of construction the vertical position of the portion of steel tube over the crest was measured periodically with topographic methods.

Both tensile forces and strains were measured in the geogrids, also in order to control if significant creep phenonema occur.

The tensile forces in the geogrids were measured by load cells: the geogrid was cut transversally and the two edges were fixed in steel clamps specially manufactured and firmly connected to the load cells, as shown schematically in Figure 4.

The forces in the load cells were read with a small digital dynamometer, instantly connected to the signal wires with a jack, giving directly the values of tensile forces.

The strains were measured on single longitudinal ribs in the center of the geogrids, by means of two extensometers for each position, one on and one under the strand in order to have a compensation for flexure (Bathurst et al., 1987). The extensometers used were SHOWA (Y11-FA-5-120), which can support a maximum deformation of about 20%. The signal wires were collected into a concrete box together with the load cells ones. The strain values were measured periodically, connecting each signal wire to the appropriate reading unit.

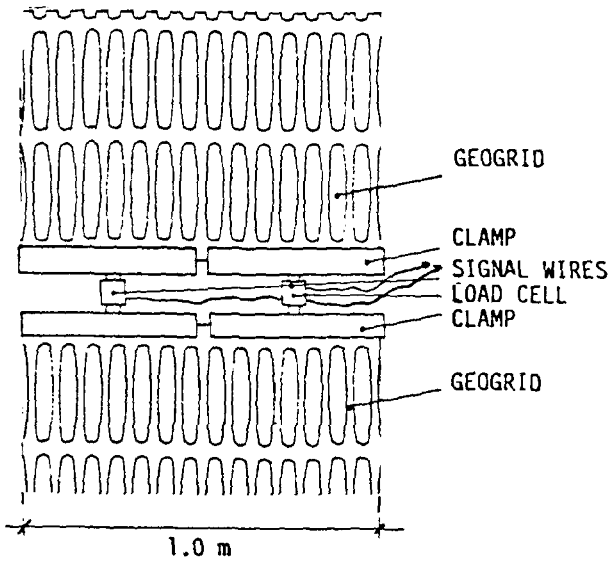

Fig. 4 : Scheme of the device used for the measurement of the tensile forces in the geogrid.

All the load cells and the extensometers were concentrated in a length of 3 meters along the embankment, in order to have all measurements related to the same effective situation.

The selected measuring section was placed on a zone of highly compacted waste, in order to have only small settlements, which actually were about 5 cm: in this way the measured values are directly comparable to other field tests having a solid base under the geogrids reinforced block.

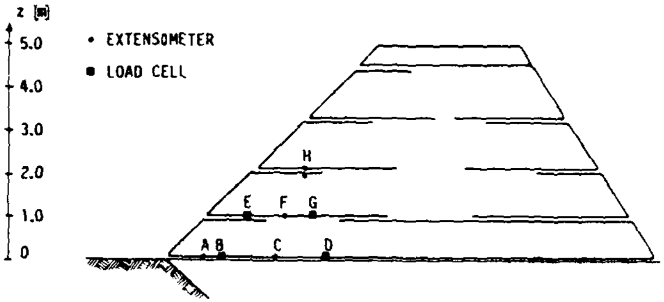

INSTRUMENT	A	B	C	D	E	F	G	H
DISTANCE FROM SLOPE [m]	0.80	1.20	2.50	3.70	1.00	1.80	2.50	1.00

Fig. 5 : Instrumented cross-section.

Figure 5 shows the measuring cross-section with the position of instruments.

Due to the presence of waste material, it was not possible to place instruments in the internal part of the embankment, that is near the steepest slope (55 degrees = 1,4:1). Anyway, the external slope of 1:1 allows to achieve some interesting information on the behaviour of a steep reinforced slope made with a cohesive soil.

RESULTS OF MEASUREMENTS

Due to the particular situation of the test site, there were some problems during the period of stress-strain measurements. The main one was vandalism: two weeks after the installation of instruments, during the night, some vandals destroyed the offices of the waste disposal facility and cut the signal wires in the concrete box. It was possible to repair only few instruments, so some measures are incomplete. Anyway the behaviour exhibited in the first two weeks seems to be very important, because at the moment of vandalism the situation was about asymptotic. After this vandalism act, only settlements were measured without problems, thanks to the simplicity of the device.

The results of these measurements, shown in Figure 6, range from an average settlement of about 30 cm, in Site 1, to an average settlement of about 85 cm, in Site 2. Sites 3 and 4 are composed of mixed wastes.

The values of the settlements calculated in the two different foundation situations were similar to the actual settlements occurred after the embankment construction. The points, for the actual measurement of settlements, were placed in correspondence to 4 different waste material:

- Site 1: urban solid wastes (k_s = 9.3 N/cmc)
- Site 2: muddy material (k_s = 0.1 N/cmc)
- Sites 3 and 4: mixed waste (with k_s varying between the above values).

The results of measurements with load cells and extensometers are shown in Fig. 7, Fig. 8 and Fig. 9. It's interesting to note that the maximum tensile forces in the geogrids occur during the compaction of the layer of soil directly placed on the geogrid (first layer). The soil was in fact compacted in a single layer, 45 cm thick.

Figure 10 shows an extrapolation of force and strain measured values, in order to obtain the diagram of tensile forces along geogrids: the qualitative behaviour was in good agreement with the theory presented by Jewell et al. (1984) and with other field tests carried out in similar conditions (Yamanouchi et al., 1986). Like in other tests, the values of tensile forces are very small, far from the peak tensile strength of geogrids.

Taking into account the greater settlements obtained from the design model, it seems that the Winkler model has given good predictions of the forces in the base geogrids.

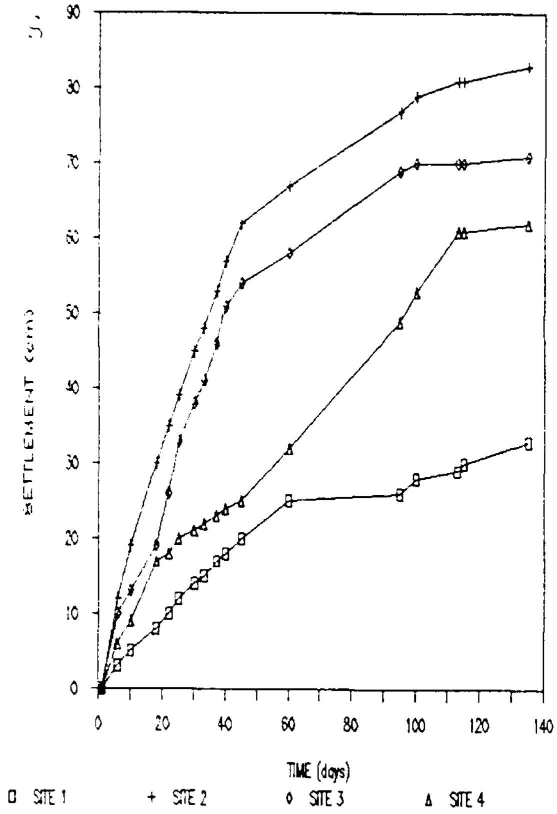

Fig. 6 : Settlements vs. time.

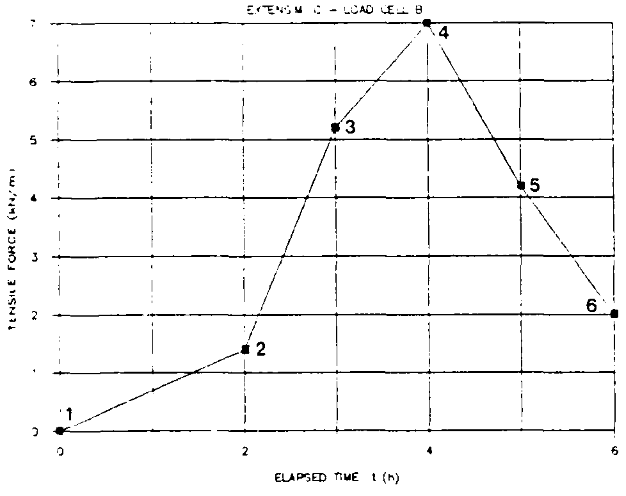

Fig. 7 : Tensile forces in the base geogrid during the construction of the embankment.

1. Start of construction
2. Placement of fill soil: first phase
3. Placement of fill soil: second phase
4. Compaction of the first layer of soil
5. Compaction of the second layer of soil
6. End of construction

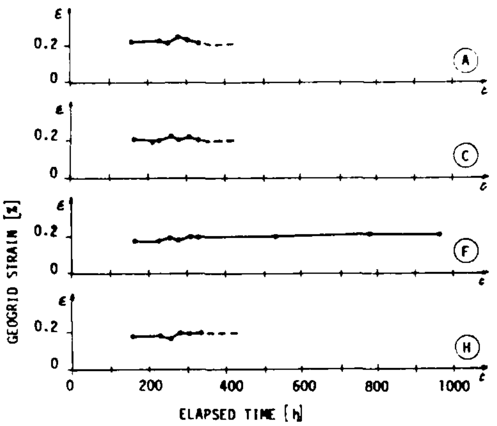

Fig. 8 : Readings from the extensometers A, C, F, H.

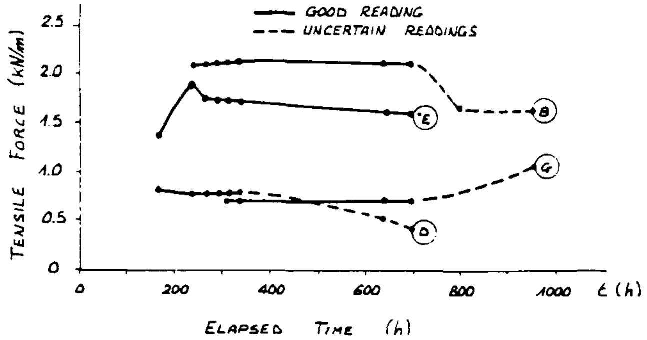

Fig. 9 : Readings from the load cells B, D, E, G.

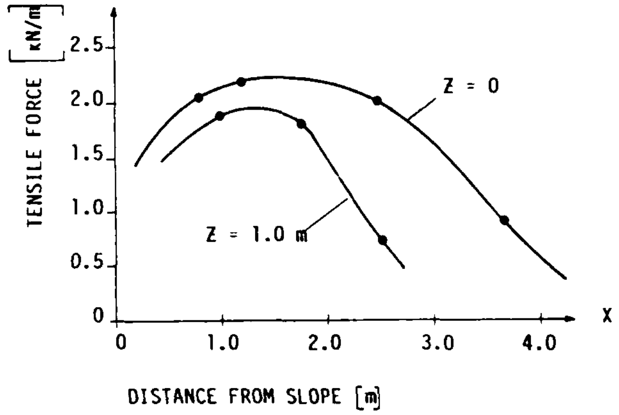

Fig. 10: Distribution of tensile forces for the base geogrid (z = 0 m) and for the upper geogrid (z = 1 m) resulting from extensometers and load cells readings.

Table 1 shows a comparison of the actual results obtained in Modena with other field tests concerning geogrid reinforced structures.
Three different conditions were considered:

- Design condition (D): design values of the parameters were used to evaluate stresses and strains in the geogrids;
- Calculation condition (C): values of the parameters were used to obtain calculated effective values of stresses and strains in geogrids;
- Measured condition (M): the actual situation.

Indicating with H the height of the slope, with N_{TOT} the total number of reinforcing geogrid layers, and with the subscripts C,D,M the conditions above mentioned, the formulas used to obtain the values described in Table 1 are the following:

- Pore pressure parameter: $R_u = u / \gamma_e H$
- Fictitious height : $H^* = H + q/\gamma_e$
- Soil pressure parameter: $k^* = f(\phi'_e, \beta, R_u)$ measured from design charts (Jewell et al., 1984)
- Required total tensile force: $T_C = 1/2 \cdot k^*_C \cdot \gamma_{eC} \cdot H^{*2}_C$
  $T_D = 1/2 \cdot k^*_D \cdot \gamma_{eD} \cdot H^{*2}_D$
- Average tensile force per unit width in the geogrids:
  $\alpha_C = T_C/N_{TOT}$
  $\alpha_D = T_D/N_{TOT}$
- Average strain in the geogrids:
  $\varepsilon_C = f(\alpha_C)$
  $\varepsilon_D = f(\alpha_D)$
  measured from the stress-strain curve of the geogrids
  ε_M: measured
  α_M: measured or from the geogrid stress-strain curve

The following factors of safety were introduced:

RFS = α_C / α_M : Real factor of safety
DFS = α_D / α_C : Design factor of safety
TFS = α_D / α_M : Total factor of safety
PFS = α_F / α_M : Peak tensile strength factor of safety
AFS = α_a / α_M : Allowable tensile strength factor of safety

From the values contained in Table 1 the following considerations can be drawn:

- the tensile forces measured in the geogrids are smaller than that ones calculated according to design conditions, allowing very high factors of safety both on the peak (PFS = 11÷30) and the allowable tensile strength (AFS = 4÷13);
- the calculation condition gives results in substantial agreement with the actual values of forces and strains, if the fill soil has a negligible cohesion;
- the high cohesion of the fill soil used in Modena embankment is probably responsible of the difference between calculation and measured conditions, regarding the evaluation of forces and strains in geogrids;
- a research is needed to have a better understanding of the mechanism of reinforcement for high cohesion soils.

TABLE 1: Comparison of different field tests for geogrid reinforced structures

REFERENCE	PAGOTTO-RIMOLDI (1987)			YAMANOUCHI ET AL. (1986)			BATHURST ET AL. (1987)			CARROLL-RICHARDSON (1986)		
TEST SITE	MODENA (ITALY)			KAGOSHIMA (JAPAN)			KINGSTON (ONTARIO)			TUCSON (ARIZONA)		
GEOGRID USED	TENAX TT1			TENSAR SR2			TENSAR SR2			TENSAR SR2		
	C	D	M	C	D	M	C	D	M	C	D	M
H (m)	5.00	5.00	5.00	7.00	6.60	7.00	4.00	4.00	4.00	4.65	4.65	4.65
β (degrees)	45	45	45	78	78	78	90	90	90	90	90	90
q (kN/m^2)	0	10	0	10	10	10	12	12	12	12	12	12
γ_e (kN/m^3)	17.2	20.0	17.2	14.6	17.7	14.6	17.6	17.6	17.6	19.6	19.6	19.6
FS global (-)	0	1.10	-	0	1.70	-	0	?	-	0	1.12	-
ϕ'_e (degrees)	25	23	25	45	30	45	43	?	43	37	34	37
c'_e (kN/m^2)	0	0	25.0	0	0	2.45	0	0	0	0	0	0
R_u (-)	0.0	0.25	0.0	0.0	0.0	0.0	0.0	0.0	0.0	0.0	0.0	0.0
α_f (kN/m)	-	60.0	-	-	78.5	-	-	80.0	-	-	80.0	-
α_a (kN/m)	-	30.0	-	-	31.4	-	-	29.0	-	-	29.0	-
k^* (-)	0.15	0.38	-	0.11	0.27	-	0.18	?	-	0.24	0.28	-
ε (%)	1.2	3.7	0.2	~0.3	~2.0	~0.3	~0.5	?	0.4	~0.3	~0.4	~0.2÷0.6
α (kN/m)	6.4	23.0	2.2	6.6	17.5	2.9÷6.9	8.7	?	~6.0	6.5	7.6	~2.5÷7.0
RFS (-)	2.9			0.9÷2.3			1.4			0.9÷3.2		
DFS (-)	3.6			2.7			?			1.2		
TFS (-)	10.9			2.5÷6.1			?			1.2		
PFS (-)	27.2			11.3÷27.0			13.3			11.5÷32.0		
AFS (-)	13.6			4.5÷10.8			4.8			4.2÷11.6		

LABORATORY TESTS

A series of tensile tests was carried out at the ENEL-CRIS Special Materials Laboratory in Milano, in order to control the behaviour during the time of the geogrid reinforcements.
A geogrid sample, placed in the embankment, was extracted after more than one year of soil burial; another sample of brand new geogrid, manufactured by the same company, was used for comparative test.
The tensile tests were conducted on a tensile testing machine, under controlled laboratory conditions of 20°C and 65% Relative Umidity, with a constant rate of extension of 50 mm/minute.
Test specimens were cut from the samples three ribs wide and two ribs long and they were prepared for testing by cutting the outer longitudinal ribs, in order to test actually only one integral longitudinal rib (Fig. 11).
The obtained results, summarized in Table 2, are reported to the unit width of the geogrid (Fig. 12).

TABLE 2: Results obtained from tensile tests on geogrids (average values on 5 specimens)

	Peak tensile strength (kN/m)	Strain at yield (%)
New geogrid	44.70	15,7
Buried geogrid	43.96	17,7

The loss of strength after one year of exposure to environment seems to be very negligible; on the contrary, there are some signs of relaxation, in terms of strain at yield.

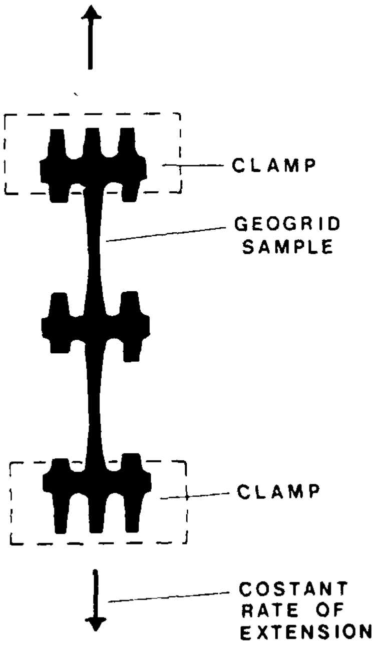

Fig. 11: Scheme of the grogrid tensile test adopted at ENEL-CRIS Laboratory.

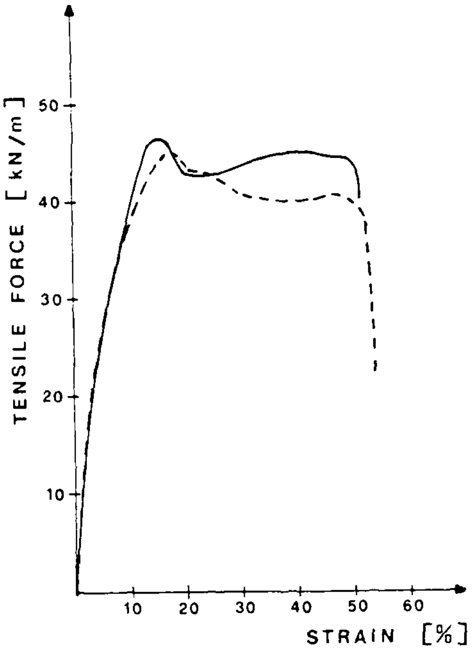

Fig. 12: Tensile test results on Tenax TT1 geogrid:
—— new sample
- - - buried sample

CONCLUSIONS

Considering the results obtained from the measurements of forces and strains in the geogrids placed in the Modena embankment, it seems that creep phenomena in geogrid materials are negligible, principally due to the very low tensile forces which actually occur in the reinforcement elements.

The settlements of the embankment and the tensile forces in the base geogrid, calculated according to a Winkler model, are in good agreement with the measured ones: the model seems to be satisfactory for design needs.

The "foundation beam" and the geogrid reinforcement allows the increasing of embankment stability, also in presence of remarkable settlements of the foundation material.

The design method actually used for geogrid reinforcement of steep slopes, as presented by Jewell et al. (1984) and revised by Rimoldi (1987), seems to be conservative according to the results of measures in different field tests: therefore with this method it's possible to design "with confidence".

Mechanical tensile properties of geogrids seem to be little affected by a one-year period of soil burial.

REFERENCES

Bassett, R.A. (1986), "The instrumentation of the trial embankment", Proc. Reinforced Embankment Prediction Symposium, London, U.K.

Bathurst, R.J., Wawrychuk, W.F., Jarret, P.M. (1987), "Laboratory investigation of two large scale geogrid reinforced earth wall", Proc. NATO Advanced Research Workshop on Application of Polymeric Reinforcement in Soil Retaining Structures, Royal Military College of Canada, Kingston, Ontario, Canada.

Berg, R.R., Bonaparte, R., Anderson, R.P., Chouey, V.E. (1986), "Design, construction and performance of two geogrid reinforced soil retaining walls", Proc. Third International Conference on Geotextile Vienna, Austria.

Cancelli, A., Cossu, R. (1985), "Problemi di stabilità degli scarichi controllati: aspetti geotecnici e degradazioni biochimiche", Atti del XXX Corso di Aggiornamento in Ingegneria Sanitaria, Politecnico di Milano, Italy.

Carroll, R.G., Richardson, G.N. (1986), "Geosynthetic reinforced retaining walls", Proc. Third International Conference on Geotextiles, Vienna, Austria.

Jewell, R.Q., Paine, N., Woods, R.I. (1984), "Design methods for steep reinforced embankments", Proc. Symp. Polymer Grid Reinforcement in Civil Engineering, London, U.K.

Pagotto, A., Rimoldi, P. (1987), "Design and construction of a geogrid reinforced embankment over waste material", Proc. Geosynthetic '87 Conference, New Orleans, USA.

Rimoldi, P. (1987), "The design of steep reinforced slopes", RDB Technical Memorandum-1, RDB Plastotecnica, Viganò, Italy.

Yamanouchi, T., Fukuda, N. Ikegami, M. (1986), "Design and techniques of steep reinforced embankments without edge supporting", Proc.Third International Conference on Geotextiles, Vienna, Austria.

LIST OF SYMBOLS

The following symbols are used in the paper:

γ_f (kN/m^3)	unit weight of foundation material
c'_f (kPa)	effective cohesion of foundation material
ϕ'_f (deg)	effective angle of internal friction of foundation material
C_c (-)	primary compression index of foundation material
C_α (-)	secondary compression index of foundation material
γ_e (kN/m^3)	unit weight of fill soil
w_L (%)	liquid limit of fill soil
w_P (%)	plastic limit of fill soil
c'_e (kPa)	effective cohesion of fill soil
ϕ'_e (deg)	effective angle of internal friction of fill soil
k (m/s)	permeability coefficient of fill soil
S (m)	embankment settlement
H (m)	embankment height
e (-)	void ratio of foundation material
σ_0 (kPa)	vertical stress in foundation material
σ (kPa)	increment of stress due to the surcharge in foundation material
β (deg)	embankment slope
q (kPa)	surcharge
α_f (kN/m)	peak tensile strength of geogrid
ϕ'^* (deg)	reduced angle of internal friction of fill
α_a (kN/m)	allowable tensile strength of geogrid
k_s (N/cm^3)	modulus of subgrade reaction
P_g (-)	factor which takes into account the base geogrid
q* (kPa)	maximum surcharge
E (kPa)	deformation modulus of fill soil
σ_g (kPa)	tensile stress in the base geogrid
M (kN·m/m)	moment in the "foundation beam"
h (m)	height of "foundation beam"
J (m^4)	moment of inertia of "foundation beam"
L (m)	length of "foundation beam"
B (m)	width of "foundation beam"
α_g (kN/m)	tensile force in the base geogrid
T_g (m)	average thickness of geogrid
z (m)	embankment elevation above base level
x (m)	distance of instruments from slope
N_{tot} (-)	total number of geogrids
u (kPa)	pore pressure in fill soil
R_u (-)	pore pressure parameter
H* (m)	embankment fictitious height
k* (-)	soil pressure parameter of fill soil
T (kN/m)	required total tensile force in fill soil
α(kN/m)	average tensile force per unit width in geogrid
ε (%)	average strain in geogrid

Proceedings: Second International Conference on Case Histories in Geotechnical Engineering, June 1-5, 1988, St. Louis, Mo., Paper No. 5.56

Performance of LPG Storage Tanks on Ground Improved by Stone Columns

E.R. Farrell
Trinity College, Dublin, Ireland

T.L.L. Orr
Trinity College, Dublin, Ireland

T. O'Donovan
E.G. Pettit & Co., Dublin, Ireland

SYNOPSIS: This paper describes the construction of four large tanks on poor soil conditions consisting of hydraulic fill placed over estuarine silt in Dublin port. The limited differential settlement that could be tolerated by the tanks required that they could not be placed on the existing ground. The optimum solution was found to be ground treatment using vibro-replacement with the formation of stone columns and compaction of the fill. The paper describes the design method used and the control tests. The predicted settlements are compared with settlement readings of the tanks following construction. These show that the chosen solution has performed well and satisfied the design requirements.

INTRODUCTION

The storage capacity of a Liquid Petroleum Gas storage depot [illegible] km from the city centre of Dublin, Ireland was to be expanded. Aesthetics and safety considerations precluded the use of overground large tanks. Other storage methods were investigated, including deep underground caverns. The site was on land reclaimed from the estuary of the River Liffey and because of this the soil conditions were relatively poor. A cost analysis of the various storage options indicated that the optimum solution comprised the construction of cylindrical steel tanks placed on the surface of the existing ground with their longitudinal axes horizontal and covered with earth. The manufacturers of the tanks laid down very strict tolerances for the allowable differential settlement of these tanks. Various methods of support for these tanks such as piles and preloading were considered before it was decided that ground treatment by vibro-replacement offered the optimum solution.

This paper sets out the methods used to estimate the short and long term settlements and the site control tests carried out during the work. These estimates are compared with the settlement readings taken on the tanks since their construction.

DETAILS OF STRUCTURE

The proposed structure comprised four LPG bullet storage tanks. These were 50m long by 5.5m diameter, placed on a 1m thick granular bed and covered with granular fill to give 0.5m cover to the tanks. The area covered by the tanks and fill was about 45m by 60m. Details of the arrangement are shown in Figure 1. A further four tanks may be placed adjacent to these tanks at a later date. The approximate average bearing pressure on the surface of the existing ground with the tanks full of LPG is 110kN/m².

The tanks were designed to withstand a 50mm differential deflection over half their length (25m) and were to be water tested prior to filling with LPG.

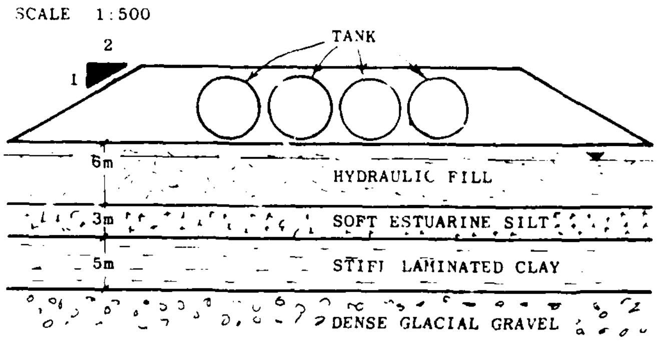

FIG 1 TANK ARRANGEMENT AND STRATIFICATION

GROUND CONDITIONS

The subsoil comprised about 6m of hydraulically placed fill over 3m of loose estuarine silt over 3m of gravel, over 5m of stiff laminated clay over dense glacial gravels. This stratification is indicated in Figure [illegible]. The hydraulic fill and the soft estuarine silts had the greatest potential for settlement and are discussed in further detail below.

The hydraulic fill was essentially a loose silty sand with pockets of very silty material at the lower levels. A plot of the N values versus depth are shown in Figure 2 and typical grading curves are given in Figure 3. It can [illegible] that the N values dropped to zero [illegible] the [illegible] depths that were generally within the [illegible]

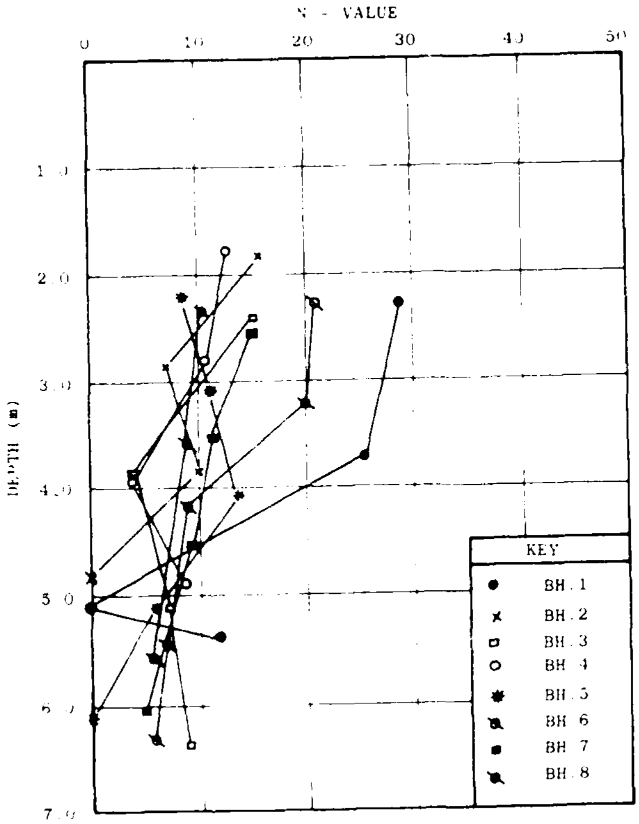

FIG 2 N VALUE versus DEPTH

The estuarine silt was [illegible] silt and slightly [illegible]. The undrained shear strength measured by in situ vane tests and quick undrained triaxial tests on 38mm and 100mm diameter specimens from piston samples recorded Cu values of between 11kN/m2 and [illegible]kN/m2 with a sensitivity of [illegible]. Laboratory consolidation tests indicated that the appropriate Mv value was between [illegible]m2/MN and [illegible]m2/MN, the low values being associated with the sandy zones. The preconsolidation pressure for these soils obtained from the e-log p curves using the Casagrande method agreed with the existing overburden pressure. The silt layer was therefore essentially normally consolidated. The silt had a liquid limit of between 34% and [illegible] with a plasticity index of about [illegible]. This material generally plotted as an inorganic clay of medium plasticity on the plasticity chart. A typical grading is shown in Figure 3. Although the index tests classified this soil as a clay, its grading and visual behaviour was more that of a silt. Because of this the term silt is used to describe this soil. Laboratory consolidation tests gave Cv values of between 1m2/yr and [illegible]m2/yr while in situ permeability tests carried out in piezometers inserted into the silt gave permeability values which indicated Cv values of about 4[illegible] m2/yr.

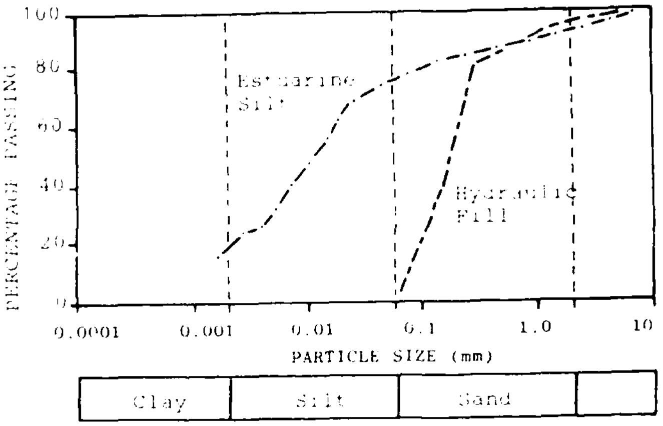

FIG. 3 GRADING CURVES FOR SILT AND FILL

The water level in the hydraulic fill varied with the tide. The minimum recorded level was 1.[illegible]m below ground level at the time of the investigation.

GROUND IMPROVEMENT METHOD

Using a conventional analysis it was estimated that the settlement of the existing fill and the estuarine silt due to the loading of 110kN/m2 from the tanks and the earth embankment would be about 1[illegible]mm. About 80% of this settlement, 140mm, is due to consolidation of the silt layer. Settlements of this order were unacceptable for the LPG tanks and therefore it was necessary to find some method to reduce these settlements.

Various options were considered including preloading, piled foundations and vibro replacement. Preloading was ruled out because of the extreme time constraints imposed on the project. Piling was more expensive than ground treatment and was considered to be less compatible with the flexible type of structure proposed. Ground compaction replacement with water flush was considered to be the most appropriate method. The ground treatment was taken through the hydraulic fill and the estuarine silt layers into the underlying gravels. The average depth of treatment was 1[illegible]m. This process essentially formed stone columns for the entire depth and also compacted the permeable hydraulic fill. Thus a stiff upper layer was formed under the tanks.

In line with normal construction practice in this country for this type of specialist work, specialist contractors were required to submit their design construct proposals for the ground treatment and to indemnify the client against non performance. The specification set out the settlement criteria, the type of gravel or stone to be used in the columns, the environmental conditions relating to the disposal of outwash water and the number and type of site control tests to be carried out. The proposals submitted by the contractors were assessed by E.G. Pettit and Co. The joint proposal submitted by Irish Geotechnical Consulting Services Ltd and Cementation Co. (Ire) Ltd was accepted for the work. This proposal provided for stone columns at [illegible]m centres in a triangular grid pattern with a minimum diameter of [illegible]mm and a maximum diameter of [illegible]mm. The vibroflot was [illegible]mm diameter. The design proposal included extra columns at the outer edges to prevent lateral squeezing out of the soil by plastic yielding.

The work commenced on [illegible] January 1985 and was completed on 4th March of the same year. A total of [illegible] stone columns were formed. The volume of gravel used far exceeded the initial estimates. This was considered to be due to erosion of the estuarine silt layer by the water flush.

SETTLEMENT PREDICTION

The settlement of the tanks on the improved ground was estimated principally by using the reduction factors proposed by Priebe (1976). These showed that, for the triangular pattern of stone columns adopted and assuming a φ' = 45 for the angular stone used in the columns, the settlements in the estuarine silt layer would be half those determined from the conventional analysis for the untreated ground under the same load. This implies that the consolidation settlement would be about 35mm. The settlement due to compression of the hydraulic fill would be of the order of 15mm. The total settlement was therefore estimated to be about 50mm with an estimated differential settlement of 40mm. This was within the design tolerance.

Because of the high values of the coefficient of consolidation, the consolidation settlements were estimated to take about 6 months.

CONTROL TESTS

It was appreciated that it would be difficult to carry out a site test capable of applying a representative load to the section of the stone column in the estuarine silt. The effectiveness of the ground treatment was assessed using three different types of load test, each designed to test different volumes of soil. These comprised 0.6m diameter circular plate tests, a 2.5m by 2.5m pad test located centrally over a column with a load of 0 to 140 tonnes and a water test of the tanks themselves.

The plate loading tests were carried out both on top of the columns and in between, the latter to see if the hydraulic fill itself was compacted. The results of these tests demonstrated that the vibro flot successfully compacted the hydraulic fill. The estimated Young's modulus (E) values at both locations assuming a Poisson's ratio of 0.2, were 45 MN/m^2 and 78 MN/m^2, respectively. These values were confirmed by the pad test which gave an approximate E value for the hydraulic fill of 70MN/m^2.

The water test of each of the tanks applied a pressure of about 120 kN/m^2 over a relatively large area. The earth surround was not at full height for these tests and each tank was tested separately. The settlements under these tests were less than 25mm.

MEASURED SETTLEMENTS

Since completion of construction, the settlement of all four tanks has been monitored by recording regularly the levels at four points on the top of each tank. These readings were first taken after the tanks had been constructed and covered with soil. They have been filled with LPG for most of the time since the readings began. As mentioned previously, the consolidation settlements were estimated to take about 6 months. The tanks have been in place for over 3 yrs, consequently movement would be expected to have essentially ceased.

The level readings for the four tanks have been plotted in Figure 4. These show that the

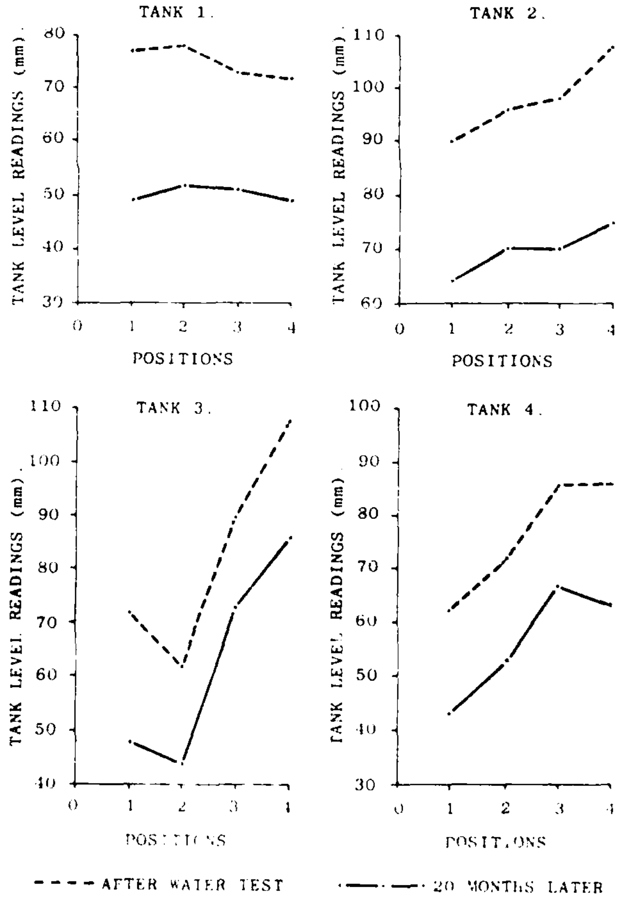

Fig 4   LEVEL READINGS ON TANKS

tanks are settling uniformly and that the differential settlement has not increased beyond the initial differential settlement which occurred on the first filling of the tank.
The settlement for a point on tank 16 has been plotted against log t in Figure 5. This plot shows that settlement is continuing at a steady rate and is likely to continue. Assuming that this represents secondary consolidation a C_α value of 8x10-3 would be interpreted. This of the order of magnitude to be expected from an organic silt with an initial water content of about 60%. However the total settlement to date is still less than that estimated from the field and laboratory tests and the differential settlement is well within the design tolerances

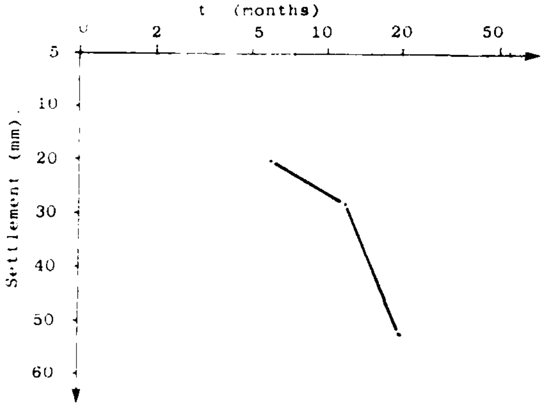

FIG 5 SETTLEMENT versus TIME

CONCLUSIONS

1 Ground treatment by vibrocompaction-replacement with the formation of stone columns and compaction of the fill was used successfully to improve the ground to enable the construction of long 'bullet' LPG storage tanks constructed on loose hydraulic fill over soft estuarine silt.

2 The total and differential settlements are considerably less than those estimated from field and laboratory tests. There is a small but on-going settlement of the tanks which is possibly due to secondary consolidation. However this further movement is occurring uniformly along the length of the tanks and is not giving rise to increased differential settlements.

REFERENCES

Priebe, H. (1976) 'Abschätzung des Setzungsverhaltens eines durch Stopfverdichtung verbesserten Baugrundes' Die Bautechnik, 53, 5.

Proceedings: Second International Conference on Case Histories in Geotechnical Engineering, June 1-5, 1988, St. Louis, Mo., Paper No. 5.61

The Use of Synthetic Liner and/or Soil-Bentonite Liner for Groundwater Protection

Hari D. Sharma
Principal Engineer/Technical Specialist, Fluor Canada, Calgary, Alberta

Paul Kozicki
President Ground Engineering Ltd., Regina, Saskatchewan, Canada

SYNOPSIS

This paper briefly reviews the various liner materials, their properties and applications to prevent contaminate spread into the groundwater. Following this, two cases have been described that cite the use of two liner types for this purpose. One case provides the details of designing the reinforced CPE liner and its under-drainage system to store the fluids at a new petrochemical plant. The second case provides the details of designing and constructing a soil-bentonite liner for aerated lagoon facilities.

INTRODUCTION

Liners to control liquid seepage have been used for a long time e.g. bitumen-lined sewer drains were used in Mesopotamia over 3000 years ago. In recent years concrete, asphalt, soil-cement, clay and other types of liners have widely been used for canals, reservoirs and waste disposal ponds and lagoons. The use of liners for pollution control to impound different types of wastes has, recently, been increasing to meet various pollution control regulations.

Pollution control liners are mainly required to prevent contaminate migration to the surrounding environment due to excessive leakage. Table 1 lists various liner materials.

TABLE 1 - LINER MATERIALS (FOLKES, 1982)

CLASS	TYPICAL MATERIALS	REMARKS
Compacted fine-grained	Local clayey soil	Porous, discontinuous liner, economical, typically 0.3-1.2m thick.
Admixes	Bentonite Soil cement Hyraulic asphalt concrete (HAC)	Low permeability binder mixed in with native soil typically 5-10cm thick layer
Polymeric membranes		
Thermoplastics	Polyvinyl chloride (PVC) Chlorinated polyethylene (CPE) Chlorosulfonated polyethylene (CSPE) (Hypalon)* Elasticized polyolefin (ELPO)	Continuous liner, discontinuous where damaged, relativelv expensive, typically 0.5-2.6mm thick, may be reinforced with polyester scrim
Vulcanized elastomers	Butyl rubber Neoprene (CR) Ethylene propylene diene monomer (EPDM)	
Crystalline thermoplastics	Low density polyethylene (LDPE) High density polyehtylene (HDPE)	
Spray-ons	Catalytically blown asphalt Emulsified asphalt	Continuous liner, discontinuous at pinholes, cracks, typically 4-8mm thick
Sealants	Polyacrylamide Liquid viny polymer	Sprayed, dusted or ponded, may result in nonuniform coverage
Chemisorptives		Function is to absorb contaminants, experiments

* Hyplon is DuPont's Registered Trademark for its Synthetic Rubber

The two main properties that should be considered in liner design are that (i) the liner permeability and (ii) the liner and stored fluid compatibility. Figure 1 summarizes typical ranges of laboratory and field hydraulic conductivity (permeability) of various liner materials.

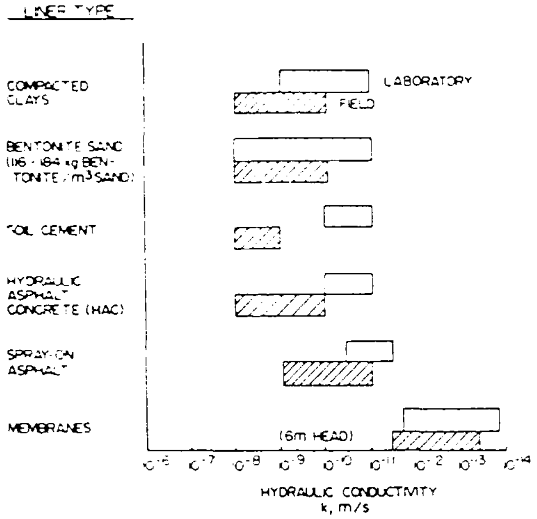

FIGURE 1 - Typical Ranges of Laboratory and Field Hydraulic Conductivity of Various Liner Materials (Folkes, 1982)

Folkes (1982) indicates that for a meaningful comparison of liner materials seepage velocities should be considered along with liner thicknesses. This is shown in Table 2 where seepage velocities for 1m total head on usual liner thicknesses is summarized.

TABLE 2 - SEEPAGE RATES FOR TYPICAL LINER THICKNESS

LINER MATERIAL (TYPICAL THICKNESS)	FIELD SEEPAGE RATE FOR 1M TOTAL HEAD DIFFERENTIAL, m/s
Compacted Clays (600mm - 1200mm)	3×10^{-8} to 8×10^{-11}
Bentonite - Sand (50mm - 150mm)	2×10^{-7} to 7×10^{-10}
Soil Cement (100mm - 150mm)	10^{-7} to 8×10^{-9}
Hydraulic Asphalt Concrete (50mm - 100mm)	2×10^{-7} to 9×10^{-10}
Spray-On Asphalt (4mm - 8mm)	2×10^{-8} to 3×10^{-9}
Polymeric Membranes (0.5mm - 1.0mm)	9×10^{-9} to 6×10^{-11}

LINER AND STORED FLUID COMPATIBILITY

The liner material may be chemically affected by the contained fluid. This may either result in a liner breakdown and/or cause increased liner permeability. Table 3 provides some data on the effects of industrial wastes on soil and admix liners while Table 4 summarizes information on liner-industrial wastes compatibilities. There is a lack of information on the long term liner and the stored fluid compatibility data. Such work should therefore be carried out on specific projects.

This paper presents cases for two liner types. In one case a reinforced chlorinated polyethlene (CPE) liner was used to protect groundwater at a petrochemical plant and in the second case, a soil-bentonite underseal was used as a seepage control barrier for aerated lagoon facilities.

CASE 1 - REINFORCED CPE FLEXIBLE LINER TO PROTECT GROUNDWATER AT A PETROCHEMICAL PROJECT SITE

At Union Carbide's ethylene glycol plant site in Central Alberta, Canada, the land form is that of a ground moraine, with glacial deposits generally overlain by a thin veneer of clays, silts and sands. The bedrock underlying the till stratum consists mainly of soft weathered sandstones and siltstones interbedded with clay shales. The groundwater movement takes place through pervious members of the till and bedrock formation. The water is confined by the till resulting in artesian condition. The surficial soil thickness varies from 4m to 12m. Site specific details are further provided by Sharma (1983) and Pritchard et al (1983).

The near surface artesian groundwater is a source of water for cattle in the area. It therefore, became essential to protect this water from any undesirable seepage from the stored fluid within the plant boundary. Among many liquid storage ponds, the waste water pond was of concern for the groundwater protection. The chemical composition of the fluids stored in the pond was diluted sulphuric acid about 10%, caustic chemicals about 5%, glycol about 5% and small amounts of diluted ethylene oxide. The environmental requirements set for these ponds was that no fluid was allowed to seep into the groundwater. It was therefore decided to provide a liner in the pond and to establish a long-term groundwater monitoring system at the site.

TABLE 3 - EFFECT OF INDUSTRIAL WASTES ON SOIL AND ADMIX LINERS*

Liner material	Acidic waste (HNO_3, HF, HOAC)	Alkaline waste (spent caustic)	Lead (low lead gas washing)	Oily waste		Pesticide (weed killer)
				Aromatic oil	Oil pond 104	
Compacted fine-grained soil 305 mm thick	Not tested	Measurable rate of seepageage $v_s=10^{-10}-10^{-9}$m/s, waste penetrated 3-5 cm after 30 months (a)		$k=1.8x10^{-10}$ $k=2.4x10^{-10}$ $k=2.6x10^{-10}$ (tests on soil after 30 months)	+	+
Soil cement 100 mm thick	Not tested			No measureable seepage after 30 months		
Modified bentonite and sand (2 types) 127 mm thick	Not tested	Measureable seepage after 30 months, channelling of waste into bentonite(b)			Failed (waste seepage through liner)	+
Hydraulic asphalt concrete (6 mm tick	Failed	Satisfactory	Waste stains below liner asphalt mushy	Not tested	Not tested	Satisfactory
Spray-on asphalt and fabric 8 mm thick	Not tested	Satisfactory	Waste stains below liner	Not tested	Not tested	Satisfactory

+Same as (a)

+Same as (b)

*Summarized by Folkes (1982) from data originally presented by Haxo (1981)

TABLE 4 - LINER - INDUSTRIAL WASTES COMPATIBILITIES*

Liner Material	Caustic petroleum sludge	Acidic steel-pickling waste	Electro-plating sludge	Toxic pesticide formulations	Oily refinery sludge	Toxic pharma-ceutical waste	Rubber and plastic
Polyvinyl Chloride (oil resistant)	G	F	F	G	G	G	G
Polyetheylene	G	F	F	G	F	G	G
Polypropylene	G	G	G	G	G	G	G
Butyl Rubber	G	G	G	F	P	F	G
Chlorinated Polyethylene	G	F	F	F	P	F	G
Ethylene propylene rubber	G	G	G	F	P	F	G
Hypalon+	G	G	G	F	P	F	G
Asphalt concrete	F	F	F	F	P	F	G
Soil cement	F	P	P	G	G	G	G
Soil asphalt	F	P	P	F	P	F	G
Asphalt membranes	F	F	F	F	P	F	G
Soil bentonite (saline seal)	P	P	P	G	G	G	G
Compacted clays	P	P	P	G	G	G	G

+P = poor, F = fair, G = good
+Registered trademark of DuPont
Registered trademark of American Colloid Company

*Stewart (1978) as Cited by Penttinen (1984)
+ Hypalon is DuPont's Registered Trademark for its Synthetic Rubber

POND LINER

The selection of liner material was based on the requirement that (i) the liner should have low permeability and (ii) should be resistant to chemical attack from stored fluid and (iii) should be resistant to ultraviolet radiation over 20 years design life. A review of Figure 1, Tables 2, 3 and 4 indicated that based on performance and economics chlorinated polyethelene was found to be the most suitable liner for the ponds. Furthermore, there existed a potential for uplift pressure at the base of liner due to the hydrostatic pressure. Therefore, it was decided to use reinforced feature in the liner. Thus, the reinforced chlorinated polyethylene liner was selected for the project.

Figure 2 shows the details of the liner installation system. Below this liner a 300mm sand bedding was placed both on the sides and at the bottom of the pond. A gravel-filled trench was also placed at the pond bottom along its centerline. A 150mm perforated drain pipe wrapped in woven filter fabric was placed at the bottom of the trench. This perforated-drain pipe was sloped towards the pond center and connected to a 200mm sump through a pipe. This under-drainage system was installed to serve two purposes: The first purpose was to relieve about 4m of groundwater pressure at the pond base below the liner. This became important because the pond was required to be operated often at low levels. Thus the groundwater pressures could be relieved by pumping from the sump before lowering the water level in the pond. The second purpose of this under-drainage system was to periodically collect water samples for laboratory testing to detect any contaminant leakage from the process waste water pond.

GROUNDWATER MONITORING

Groundwater monitoring stations were installed across the site. These stations were located on four sides of the pond and at some distances away from the pond to measure the upgradient and downgradient underground water quality due to the presence of the pond. Figure 3 shows the typical details of the groundwater monitoring station. This consisted of two or three piezometers located at different groundwater sources. These groundwater monitoring stations were installed approximately one year prior to plant startup. Groundwater levels and water samples have since been taken and analyzed periodically. The overall system has been operating successfully for approximately the past five years.

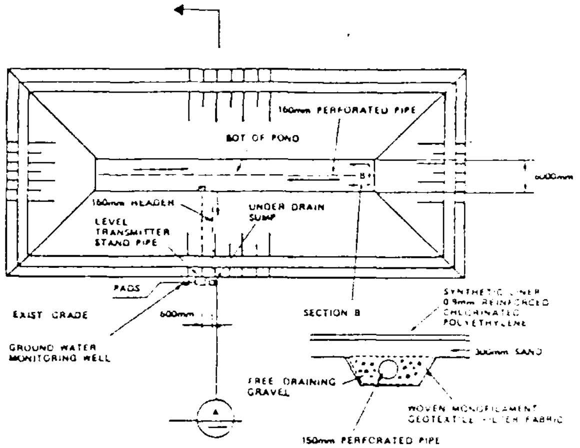
160mm PERFORATED PIPE
BOT OF POND
6000mm
B
160mm HEADER
UNDER DRAIN SUMP
LEVEL TRANSMITTER STAND PIPE
PADS
EXIST GRADE
600mm
SECTION B
GROUND WATER MONITORING WELL
SYNTHETIC LINER 0.9mm REINFORCED CHLORINATED POLYETHYLENE
300mm SAND
FREE DRAINING GRAVEL
WOVEN MONOFILAMENT GEOTEXTILE FILTER FABRIC
150mm PERFORATED PIPE

(a) Plan of Process Waste Holding Pond

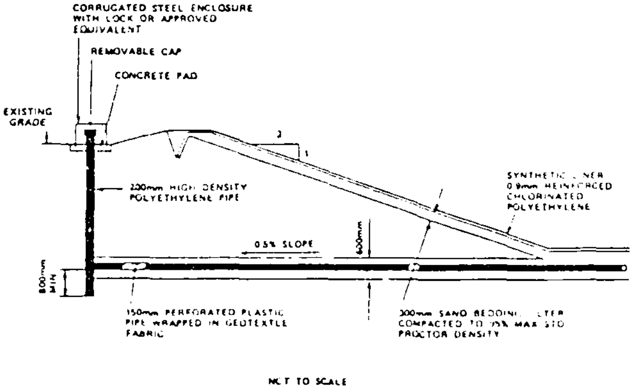
CORRUGATED STEEL ENCLOSURE WITH LOCK OR APPROVED EQUIVALENT
REMOVABLE CAP
CONCRETE PAD
EXISTING GRADE
2
1
200mm HIGH DENSITY POLYETHYLENE PIPE
SYNTHETIC LINER 0.9mm REINFORCED CHLORINATED POLYETHYLENE
0.5% SLOPE
600mm
800mm MIN
150mm PERFORATED PLASTIC PIPE WRAPPED IN GEOTEXTLE FABRIC
300mm SAND BEDDING AFTER COMPACTED TO 95% MAX STD PROCTOR DENSITY
NOT TO SCALE

(b) Section AA to Represent Under-Drainage System

FIGURE 2 - Details of Pond Liner and Under-Drainage System

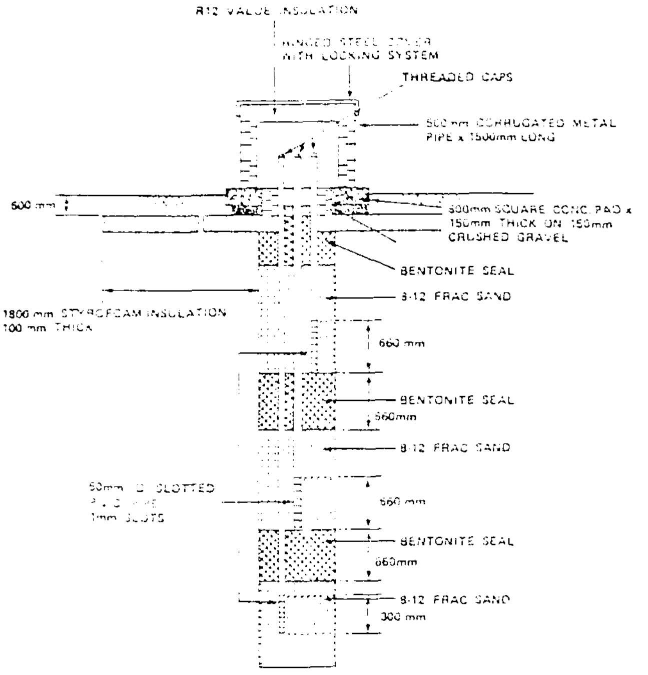
R12 VALUE INSULATION
HINGED STEEL COVER WITH LOCKING SYSTEM
THREADED CAPS
500 mm CORRUGATED METAL PIPE x 1500mm LONG
500 mm
600mm SQUARE CONC. PAD x 150mm THICK ON 150mm CRUSHED GRAVEL
BENTONITE SEAL
8-12 FRAC SAND
1800 mm STYROFOAM INSULATION 100 mm THICK
660 mm
BENTONITE SEAL
660mm
8-12 FRAC SAND
50mm ID SLOTTED PVC PIPE 1mm SLOTS
660 mm
BENTONITE SEAL
660mm
8-12 FRAC SAND
300 mm

FIGURE 3 - Typical Groundwater Monitoring Station Design

CASE 2 - SOIL-BENTONITE LINER FOR AN AERATED SEWAGE LAGOON FACILITY

The second case history is that of a soil bentonite underseal seepage control barrier installed in aerated lagoon facilities constructed at Wawa, Ontario. The predominant soils at the site of the lagoon facilities consist of highly permeable coarse sands and gravels. The insitu permeability of the natural sands and gravels was estimated to be in the range of 10^{-1} cm/sec and therefore can be considered permeable. The existing adjacent lagoon system has had reported leakage problems and it was proposed to construct the new cells with a high density polyethylene liner. However, a soil-bentonite liner was selected on the basis of economics.

GROUNDWATER TABLE

The soil and groundwater conditions at the site of the aerated sewage lagoons were reported by Trow Inc. in a report dated May 1, 1986. The water table at the time of the geotechnical investigation was approximately 1.0 metres below natural ground surface and approximately 1.0 metres above the proposed cell base. The groundwater table was permanently lowered about 1 metre below the bottom elevation of the sewage lagoons by constructing a perimeter drainage ditch along the east and north sides.

LABORATORY TESTING

Grain size analysis tests indicated that the coarse sand and gravel contained about 50 percent gravel up to 75mm diameter, 45 percent sand, and less than 5 percent clay and silt size particles. The stripping material contained 30 percent gravel up to 30mm diameter, 43 percent sand and 27 percent silt and clay size particles. The stripping material also contained organic material. However, the amount of organics in the sample was not considered a problem insofar as imparing the performance of the soil bentonite liner.

Two (2) laboratory permeability tests were conducted on blended mixtures of gravel and stripping with four (4) and six (6) percent sodium bentonite. Soil-bentonite mixtures were brought to the desired moisture content and then compacted in a 100mm diameter constant volume permeameter at Standard Proctor effort. The mixtures were then saturated and permeability tests conducted using the constant head method.

Since the pH of the stored fluid in sewage lagoons ranges from 6.0 to 8.0, a soil-bentonite liner will not be chemically affected by the stored fluids. In this case, laboratory testing was not considered necessary to confirm liner and stored fluid compatibility.

DESIGN OF SOIL-BENTONITE LINER

The design of the soil-bentonite liner was based on the results of permeability tests performed on different soil mixtures. The permeability testing summarized in Table 5 indicated that a low laboratory hydraulic conductivity could be attained by admixing bentonite and stripping material with the coarse sand and gravel. However, for this to translate into an effective soil-bentonite liner with a low field permeability, attention had to be given to design and construction methods. The design had to consider the thickness of the liner and cover materials, while construction had to consider such factors as spreading of bentonite, degree of mixing, amount and type of compaction and molding moisture content.

The design thickness of the soil-bentonite

TABLE 5 - SUMMARY OF PERMEABILITY TESTING

Permeability Test	Sample Description		Saturated Laboratory Hydraulic Conductivity (cm/sec)
A	Gravel: Stripping: Sodium Bentonite:	70.5% 23.5% 6.0%	$2.5x10^{-9}$
B	Gravel: Stripping: Sodium Bentonite:	72.0% 24.0% 4.0%	$3x10^{-9}$

NOTE: Cobblestones greater than 38mm diameter were removed prior to proportioning

TABLE 6 - CALCULATED SEEPAGE RATES

MIXTURE	ANTICIPATED FIELD PERMEABILITY (cm/sec)	LINER THICKNESS (mm)	SEEPAGE RATE* (m^3/yr/square metre)
A	$1.3x10^{-8}$	200	0.13
		300	0.09
B	$1.5x10^{-8}$	200	0.15
		300	0.10

liner was generally based upon the predicted seepage rates through the liner and the comparison of this rate to the allowable. The seepage rate through the liner is a function of liner thickness, permeability and the head of water contained. The seepage rates shown in Table 6 have been calculated based upon anticipated field permeabilities, liner thicknesses between 200 and 300mm and an assumed height of water in the lagoon above the top of liner of 6 metres. The field permeability of the two (2) mixtures have been anticipated to be one half of an order of magnitude higher than that shown in Table 5. Table 6 indicates that for a seepage rate as high as $0.15m^3/yr/m^2$ to be acceptable, then the soil liner could be designed to be 200mm thick and containing four (4) percent bentonite. The required maximum hydraulic comductivity for the liner was specified at $5x10^{-8}$ cm/sec.

The selected liner thickness for the aerated lagoon facilities at Wawa was 200mm and the bentonite application rate of 5 percent by weight of soil. A 200mm thick surface cover consisting of locally available granular material was placed on top of the soil-bentonite liner. Figure 4 shows the Plan and Section View of the Final Liner Design.

QUALITY CONTROL

Construction of a soil-bentonite liner is not a routine construction operation. It requires a good knowledge of characteristics of the material and an

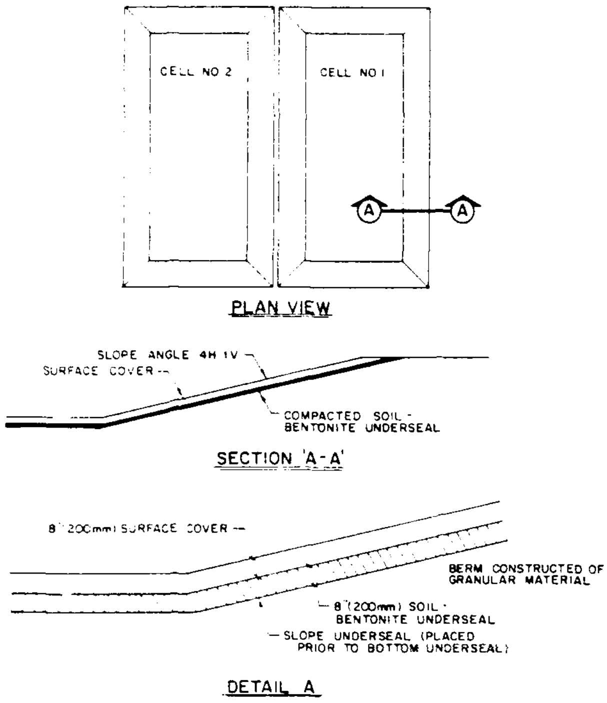
CELL NO 2
CELL NO 1
A
A
PLAN VIEW
SLOPE ANGLE 4H 1V
SURFACE COVER
COMPACTED SOIL - BENTONITE UNDERSEAL
SECTION 'A-A'
8" (200mm) SURFACE COVER
BERM CONSTRUCTED OF GRANULAR MATERIAL
8" (200mm) SOIL - BENTONITE UNDERSEAL
SLOPE UNDERSEAL (PLACED PRIOR TO BOTTOM UNDERSEAL)
DETAIL A

FIGURE 4 - PLAN AND SECTION VIEW OF FINAL LINER DESIGN

understanding of the importance of careful adherence to the specifications.

Regular compaction testing of completed sections of the liner was performed using a nuclear test gauge on backscatter mode to determine the compacted dry densities and molding moisture contents. The results of this testing is summarized in Figure 5 to 9, inclusive. The greatest variability in the compaction of the liner was for the east berm of Cell #1, which was the first section of liner completed. This section of liner was completed with densities as low as 85 percent of Modified Proctor Maximum Dry Density and molding moisture contents well dry of optimum. Even with these lower dry densities and molding moisture contents, the liner on the east berm of Cell #1 still met the specified permeability requirements of $5x10^{-8}$ cm/sec. The construction control on all other sections of liner was considerably improved with densities generally along the Line of Optimums.

A series of laboratory permeability tests were conducted on soil samples from the site. The samples were remixed in the laboratory and then compacted into the permeameter at moisture contents and densities simulating construction values. The results of this testing is also shown in Figures 5 to 9.

From a theoretical view point, the hydraulic conductivity of a compacted soil-bentonite (at the moisture contents and densities considered here) should decrease when either the moisture content or dry density increase. Therefore, any compaction test result shown in Figures 5 to 9 with a higher dry density or higher moisture content than any permeability test, should have the same or lower hydraulic conductivity. It was because of this theory that all permeability tests were conducted at the lowest densities and/or moisture contents typically achieved in the field.

All permeability tests conducted on soil samples from the actual soil-bentonite liner met or exceeded the maximum hydraulic

FIGURE - 5

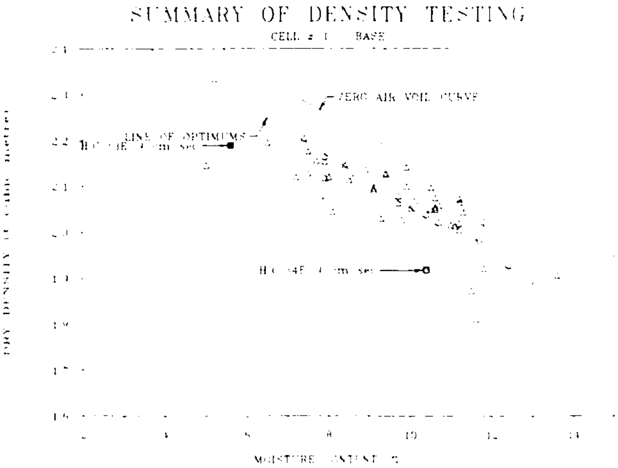

FIGURE - 6

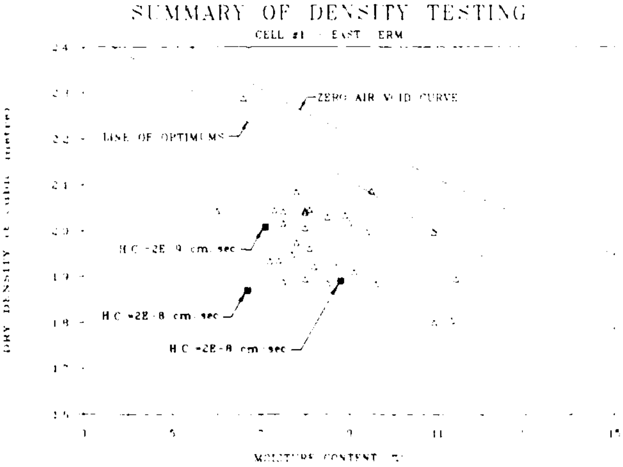

FIGURE - 7

SUMMARY OF DENSITY TESTING

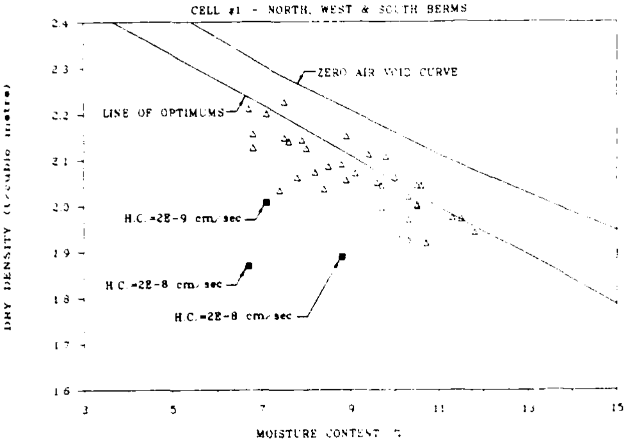

FIGURE - 8

SUMMARY OF DENSITY TESTING

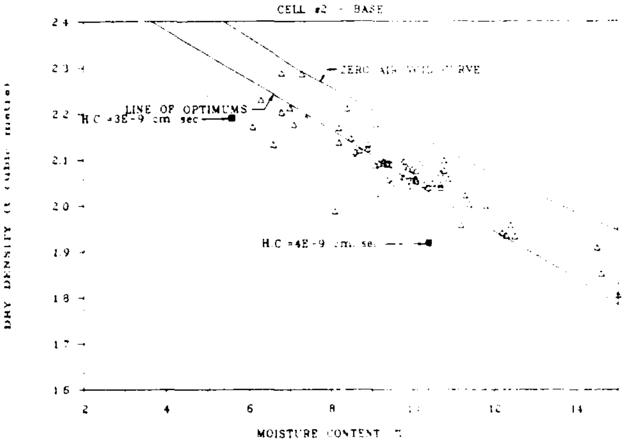

FIGURE - 9

SUMMARY OF DENSITY TESTING

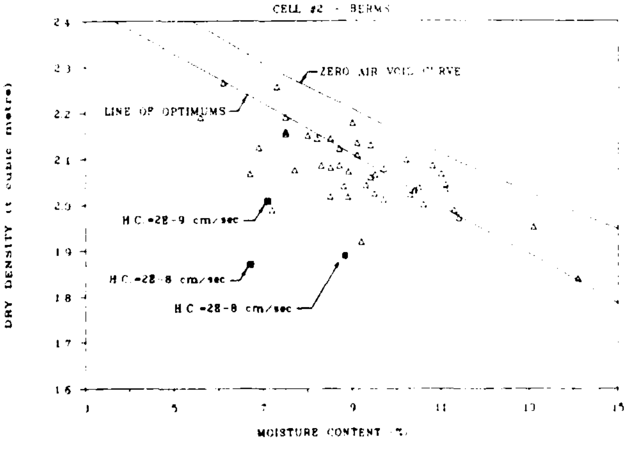

conductivity for the liner of 5 x 10^{-8} cm/sec. As well, most field compaction test results were at moisture contents or densities greater than those used for the permeability tests. Therefore, it is considered that all portions of the soil-bentonite liner along the berms and base of the sewage lagoons met or exceeded the specified permeability requirements.

CONCLUSIONS AND RECOMMENDATIONS

Based on the two case studies cited here the following can be concluded:

.1) A reinforced synthetic (CPE) liner complete with an under-drainage system to solve uplift pressures was successfully installed at a new petrochemical site to protect the surrounding drinking water.

.2) Field monitoring of the piezometers, for about 5 years indicates that the liner and the under-drainage system has been performing effectively and have contained the stored fluid.

.3) A soil-bentonite type liner is an effective alternate method of constructing an economical liner to prevent contaminate spread into groundwater. This technique provides an economical solution to prevent contaminate spread into the groundwater.

.4) A soil-bentonite type of liner should not be constructed without adequate testing. This testing should include permeability testing with equipment capable of accurately measuring both flow in and out of the sample, and to determine liner and stored fluid compatability

.5) In addition to adequate testing, special care is also required in the construction of this type of liner. Thus, it is recommended that, where possible, contractors with experience in liner construction be employed to construct or assist in the construction of these liners.

REFERENCES:

Buettner, W. (1985), "Permeability Testing of Soil with Low Hydraulic Conductivity", unpublished M.Sc. Thesis (in Print).

Buettner, W. and Haug, M. (1983), "Permeability Testing of Fine Grained Soils", First International Symposium on Potash, Saskatoon.

Day, M.E. (1970), "Brine Disposal Pond Manual", Research and Development Progress Report No. 588, United States, Department of the Interior, Washington, D.C.

Folkes. D.J. (1982), "Fifth Canadian Geotechnical Colloqium-Control of Contaminant Migratrion by the Use of Liners", Canadian Geotechnical Journal, Vol. 19, Pages 320 - 344.

Haxo, H.E., Jr. (1981), "Durability of Liner Materials for Hazardous Waste Disposal Facilities", In Landfill Disposal Hazardous Waste. Proeceedings, 7th Annual Research Symposium, U.S. Environmental Protection Agency, Philadelphia, Pages 140 - 156.

Pritchards, R.B., Sharma, H.D., and Kollemeyer, M.J. (1983), "Groundwater Protection and Monitoring for a Petrochemical Plant", 33rd Chemical Engineering Conference, Toronto, October, Pages 140 - 156.

Penttinen, S.E. (1984), "Flexible Synthetic Liners and Their Use in Liquid Waste Impoundments", Alberta Environment, Page 78.

Sharma, H.D. (1983), "Groundwater Monitoring and Liners for Ponds at a Petrochemical Plant Site", Fluor Canada Ltd., Page 30.

Stewart, W.S. (1978), "State-of-the-Art Study of Land Impoundment Techniques",Exxon Research and Engineering Company, Prepared for U.S. Environmental Protection Agency, Report No. EPA-600/2-78-196, Cincinnati, Ohio, Page 76.

Trow Ontario Ltd., "Subsoil Conditions Proposed Aerated Lagoon Facilities TWP. of Michipicoten Sewage Works Program M.O.E. Project 3-035B-Wawa, Ontario. - Report dated May 1, 1986.

Proceedings: Second International Conference on Case Histories in Geotechnical Engineering, June 1-5, 1988, St. Louis, Mo., Paper No. 5.64

Long Term Building Performance over an Injected Subgrade

Ronald F. Reed
Senior Vice President, Rone Engineers, Dallas, Texas

Paul Wright
President, Woodbine Corporation, Fort Worth, Texas

SYNOPSIS

Several foundation designs and stabilization methods are used with varying degrees of success to cope with the problem of expansive clays. Many of these methods are very expensive, therefore alternate technology that is both cost and performance effective has been developed. This paper presents a case history with pre- and post- stabilization test data for a 4-building project where pressure injection of lime and water was used to preswell weathered clay-shale to a depth of 10 feet. Use of pressure injection technology economically reduced post construction movements to 0.5 inches to 1.8 inches over a 7 year monitoring period. Movements observed have been upward, with no settlement or shrinkage related movements related over the observed period.

INTRODUCTION

Numerous methods are employed for design and construction of buildings over expansive soils. Within the Dallas-Fort Worth (D/FW) area, methods include; suspension of the structure over the soils, with foundations placed below the active zone; composite buildings where the structural elements are founded within stable materials, and the floor is "independent" of the structure i.e. "floating"; and shallow, ground supported reinforced foundations. Movement of a ground supported floor slab must be within acceptable limits, or a non-functional building results. Likewise, movement of a shallow foundation must be limited or distress within the superstructure becomes unacceptable. Acceptable movement is owner and user defined, but in the D/FW area it is generally taken to be less than 1 inch for "floating" floor slabs and 2 to 3 inches for shallow foundations. Reduction of potential soil movements to within "acceptable" limits requires modification of the supporting soil. Some of the more common methods used in the D/FW area are listed in Table I. Costs associated with the techniques are also shown.

This paper addresses the procedures used, and results obtained on one, four-building complex within the Eagle Ford Formation. The method used consisted of preswelling the soils using a combination of lime slurry and water injection.

Initial site preparation occured in early 1981, with completion of the structures in the fall of the same year. Measured movements of the site during preswelling as well as periodic post construction floor movements are provided.

PROJECT DESCRIPTION

The project consists of a four building office/warehouse complex located in Irving, Texas, a suburb to the west of Dallas. The complex was speculative, i.e. user undefined.

Design constraints imposed by the developer included; tilt-wall construction; low rental fees; and a ground supported floor with maximum allowable movements of the floor in office areas of 1 inch, and in warehouse areas of 2 inches. Warehouse and offices in the immediate area had experienced floor movements in excess of 10 inches. (Reed, 1985) The method used for stabilization typically consisted of over-excavation and replacement with inert fill. Modifications to this method included providing a lime stabilized 6 to 12 inch layer below the inert fill.

Initial site topography required cut and fill earthwork to achieve desired finished grades.

TABLE I

Summary of Techniques used for "stabilizing" near surface soils

Techniques	Applicable Depth (feet)	Cost/ft^2	Comments
Excavate existing soils, mix with lime and recompact	3 to 5	\$1.60 – \$1.90 (3') \$2.50 – \$2.90 (5')	
Overexcavate and replace with inert, non-expansive soil	3 to 7	\$1.25 – \$1.40 (3') \$2.90 – \$3.20 (7')	If inert materials are permeable, can result in ponded conditions below grade.
Pressure Injection	10 to 15	\$0.72 (2 Lime & 2 Water) \$0.45 (1 Lime, 3 Water)	Requires more rigid engineering control during earthwork. Greater depths are possible. Slower then overexcavating and replacement.

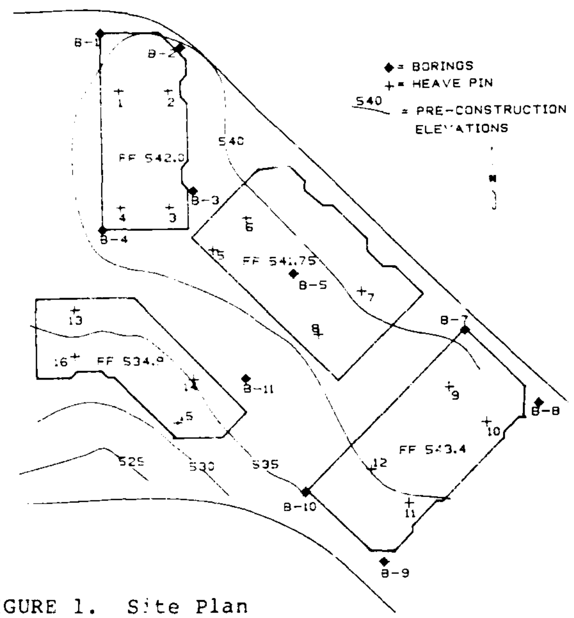

FIGURE 1. Site Plan

associated with stress reduction, cut within building areas was limited to one of the four structures. Initial site contours and finished floor elevations are shown in Figure 1.

The initial design for the project encorporated the use of 3-1/2 feet of inert fill over six inches of lime stabilized clay. This technique was rejected by the owner because of poor performance related to excessive floor movement on projects in the general vicinity.

The use of pressure injection was considered as an alternative, however it's use was initially rejected because of a "feeling" by various consultants that the soils were too hard and dry to effectively inject. Due to the historical performance of other proposed modification techniques, however, the owner elected to pursue injection. A monitoring program to evaluate the effectiveness of both the injection operations and post-construction floor performance was therefore established.

In order to reduce the risk of movement at entrances to the office areas, a suspended floor system was used. Other design modifications included use of one site clays for backfilling trenches and utilities in place of sandier, more permeable soils.

GEOLOGY

The site is underlain by soils and shale of the Eagle Ford Group, a marine, montmorillonitic clay shale of Upper Cretaceous age. The shale is thinly laminated, gray to bluish-gray in color and weathers to tan to olive tan and gray with ironstaining along joints and fissures. Depth of weathering across the site varies from 29 to 40 feet. Ground water was not encountered during the initial geotechnical investigation, although intermittent perched water is anticipated to be occasionally present along the weathered/unweathered interface during rainy seasons.

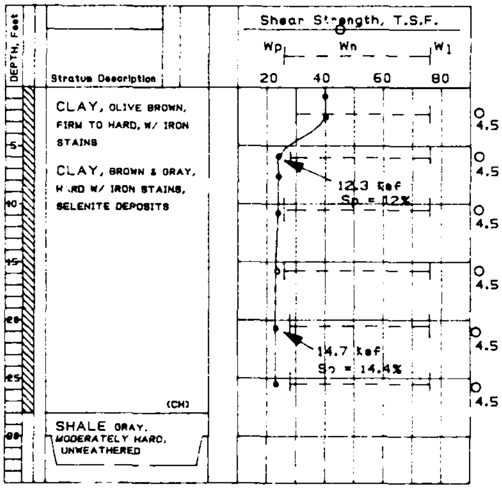

FIGURE 2. Typical Stratigraphy & Soil Moisture Profile

Weathering of the clay-shale results in a tan to olive-tan and gray residual clay. The clay retains the shales' laminated fabric, and is jointed and fissured on spacings of 2 to 8 inches. The joints and fissures are commonly ironstained and occasionally silt lined.

The upper 3 to 9 feet of clay soil is subjected to variations in seasonal soil moisture, but these values are less than the average for the Dallas metroplex which is generally estimated to be on the order of 12 to 15 feet. The reduced seasonally active zone is considered to be primarily a result of the sloping site topography, the relative low permeability of the clay soils, and the jointed structure.

TABLE 2
SUMMARY OF SOIL PROPERTIES

PROPERTY	UNITS	POPULATION	RANGE	MEAN	DEVIATION
Liquid Limit, w_l	--	16	48 - 86	69.8	8.51
Plastic Limit, w_p	--	16	22 - 38	32.2	4.61
Plasticity Index, I_p	--	16	26 - 56	37.6	7.43
Dry Unit Weight, d	pcf	27	84 - 108	99.6	6.83
Wet Unit Weight, w	pcf	27	110 - 133	124.2	5.92
Specific Gravity, G_s	- -	3	2.79 - 2.93	2.85	0.03
Saturation, S	%	12	87 - 97	92.0	0.03

AD-A213 199 INTERNATIONAL CONFERENCE ON CASE HISTORIES IN 4/8
GEOTECHNICAL ENGINEERING (2. (U) MISSOURI UNIV-ROLLA
S PRAKASH 30 JUN 89 ARO-25645.2-GS-CF DAAL03-87-G-0129
UNCLASSIFIED F/G 13/2 NL

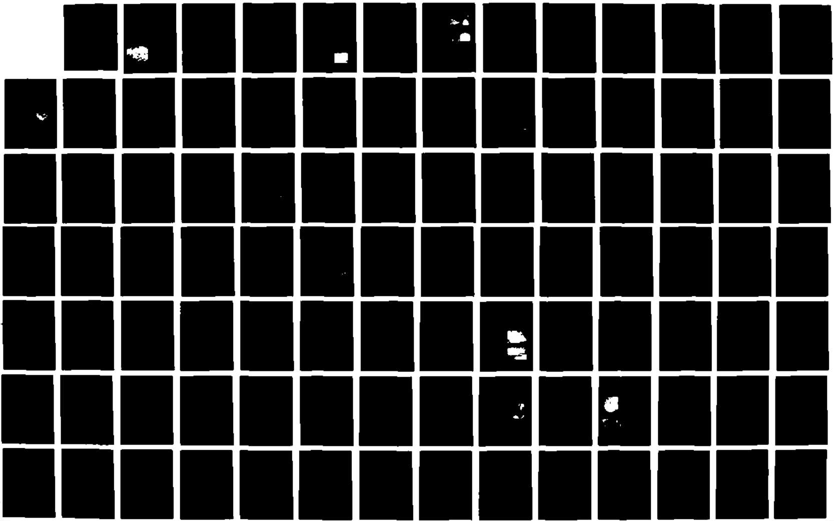

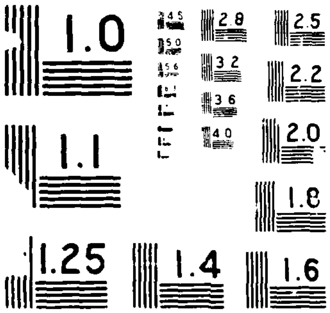
1.0
4.5
5.0
5.6
2.8
3.2
3.6
4.0
2.5
2.2
2.0
1.1
1.8
1.25
1.4
1.6

The natural moisture content of the clays below the seasonal influence is 4 to 7 percentage points below their plastic limit. The moisture content generally decreases with depth, as is common in weathered shales. An example of a typical Log of Boring is shown in Figure 2. This figure illustrates moistures above the plastic limit to a depth of about 5 feet, and soil moisture below the plastic limit below this depth. Also shown in figure is the maximum pressure (Ps) and the percent swell at overburden, (Sp), from the result of two Constant Volume Swell tests.

The weathered shale classifies as a CH soil, in accordance with the Unified Soil Classification System. The consistency varies in the zone of seasonal moisture, becoming hard below this zone. A summary of some of the pertinent soil properties is provided in Table 2.

CONSTRUCTION SEQUENCE

Finished floor subgrade elevations, minus 5 inches, were initially established in January 1981 utilizing on-site clays as fill. The subgrade was left 5 inches below desired subgrade to account for the desired pre-swelling of the upper soils.

Materials were compacted in approximate 10-inch lifts to a density of between 90 and 95 percent of ASTM D-698, at a moisture wet of optimum. Four heave pins were then installed on each building pad with the base of the pin 18 to 22 inches below grade. Heave monitoring pin locations are shown in Figure 1. Pin elevations were obtained and tied to a bench mark founded at a depth of 25 feet below grade. The bench mark was sleeved throughout the upper soils to reduce uplift.

Pads were then double lime slurry-pressure injected, followed by 2 water injections, to a depth of 10 feet on building pads A thru C, and 3 water injections on building pad D. Continuous undisturbed Shelby tube samples for moisture content tests were obtained to a depth of ten feet after each water injection. Heave monitoring pins were surveyed after each injection.

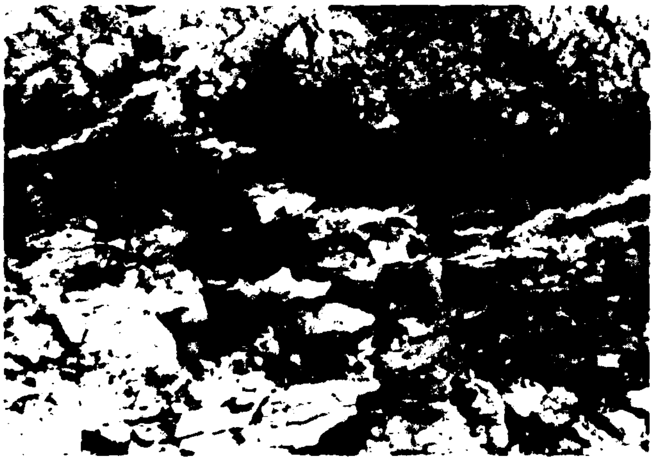

FIGURE 3. Exposed lime seams in face of excavation.

Upon completion of the injection operations, the near surface soil were blended with the surficial lime, compacted, and brought to grade. Utilities were then installed. Construction then proceeded in a normal manner.

RESULTS

Injection procedures progressed normally throughout the project. Adequate dispersal of lime was observed. Some of the exposed seams of lime are shown in Figure 3.

The change in measured soil moisture and the measured heave during injection on two of the four buildings are presented in Figures 4 and 5, and 6 and 7, respectively. Test results are typical for all four buildings.

Measured heave below the survey pins varied from approximately 0.75 inches to 3.50 inches. Actual heave is anticipated to be on the order of 5 to 6 inches because approximately 1 to 2 inches of soil had to be cut from the pads at the completion of injection operations to achieve desired subgrade. As previously

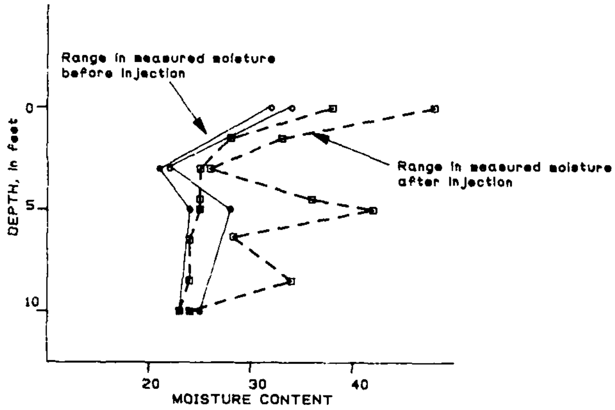

FIGURE 4. Rise in moisture after 2 lime and 2 water injections, Building A

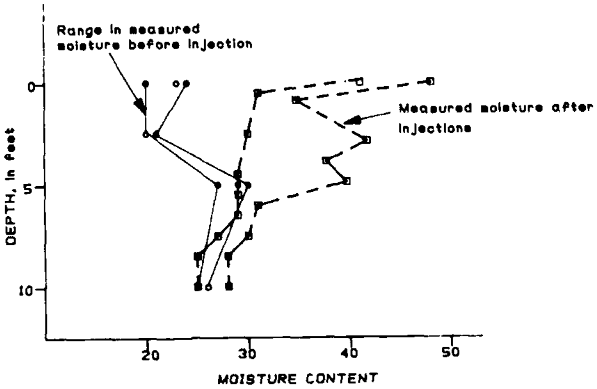

FIGURE 5. Rise in moisture after 2 lime and 3 water injections, Building C.

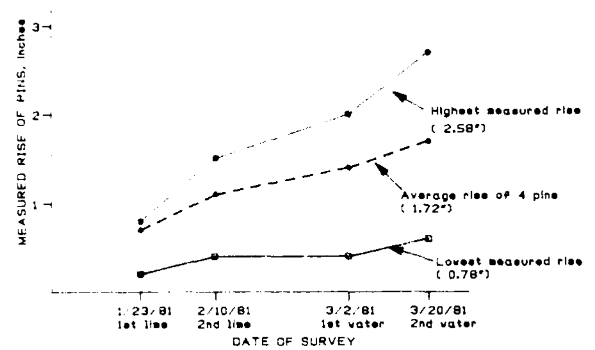

FIGURE 6. Measured rise in elevation of Pad Survey Pins during construction, Building A.

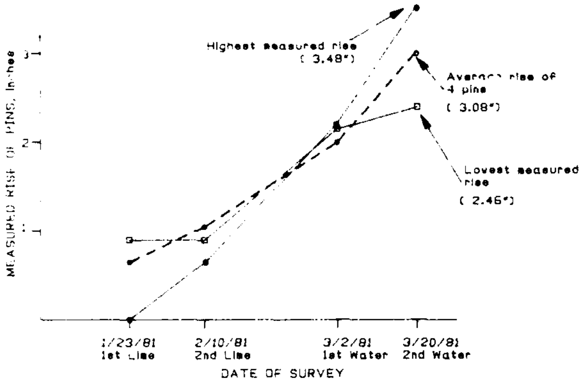

FIGURE 7. Measured rise in elevations of Pad Survey Pins during construction, Building D.

mentioned, subgrade before injection was left 5 inches below desired finished grade to account for heave.

Post construction floor movements have been within acceptable limits, with measured heave through September of 1983 varying from about 0.5 inches to 1.8 inches. Measured heave in building A is shown in Figure 8. Based on visual observations, much of the measured heave is attributed to survey error, and/or movement of the bench mark.

To confirm the visual results, 21 profiles of the floor in buildings A and B perpendicular to the walls were monitored from June 1982 through September 1983. Typical results for one station are plotted in Figure 9. The profiles indicate equal differential movements across the floor. Since it is extremely unlikely that movements would be uniform, the difference in elevation over the period surveyed was attributed to survey error. Corrected movements for building "A" are shown in Figure 10. The monitoring through 1983 indicated no appreciable movement, and was therefore discontinued.

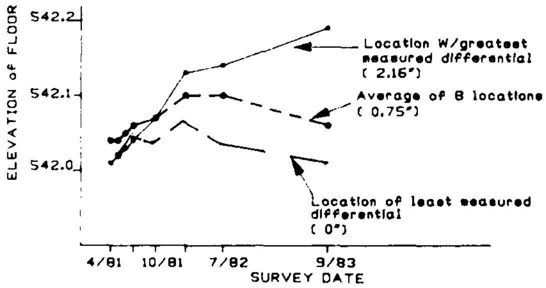

FIGURE 8. Measured post construction floor movement, Building A.

Periodic site visits have been performed since completion of the monitoring program. No distress or differential floor movement has been detected or reported.

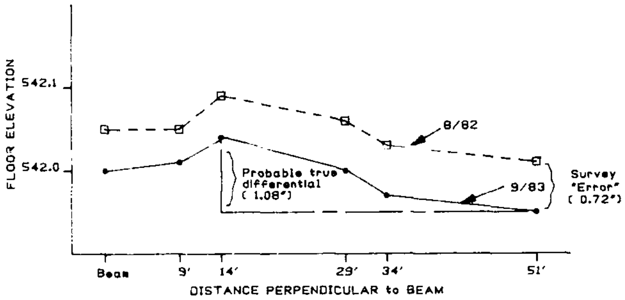

FIGURE 9. Measured movements perpendicular to perimeter wall, Building A at location 4.

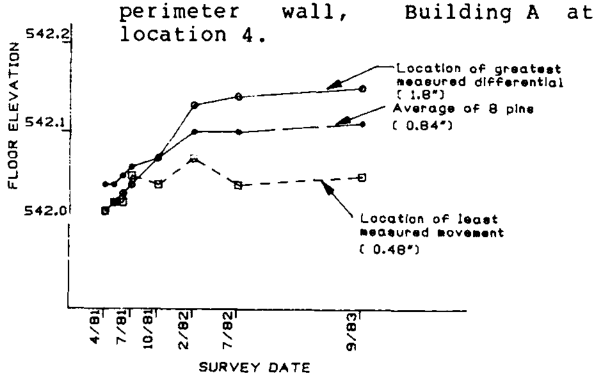

FIGURE 10. Floor movement, Building A, Corrected for survey error between 7/82 and 9/83.

CONCLUSIONS

1. Effective reduction of the potential vertical movement of the upper soils of the Eagle Ford formation was obtained by using a combination of lime-slurry and water pressure injection.
2. Construction monitoring of the subgrade indicated heave as a result of injection operations on the order of 2 to 4 inches.
3. Post construction monitoring of the floor slabs over a seven year period indicates movements of 0.5 to 1.8 inches, which are within design tolerances. No post construction settlement or shrinkage has been experienced.

4. Costs for the injection modification were approximately one-half compared to costs associated with other techniques used in the D/FW area. Performance of the injected project has been superior to that experienced on projects in the immediate area.

REFERENCES

Reed, F.R., (1985), "Foundation Performance in an Expansive Clay", Proc., 38th Canadian Geotechnical Conference, Theory and Practice in Foundation Engineering, Edmonton, Alberta, pg. 305-313.

Proceedings: Second International Conference on Case Histories in Geotechnical Engineering, June 1-5, 1988, St. Louis, Mo., Paper No. 5.66

Epoxy Resin Grout System for Solutions to Traditional Geotechnical Problems

A.V. Shroff
Professor, Applied Mechanics Department, M.S. University, Baroda, India

D.L. Shah
Research Fellow, M.S. University, Baroda, India

D.P. Amin
Research Student, University, Baroda, India

SYNOPSIS: Use of chemicals for foundation treatment and sealing of crack is of recent origin. The aim of this paper is to find time-viscosity and time-strength relationships of epoxy grout system for proper flow mechanism and strength interaction with rock collected from dam sites of India. The bonding mechanism of gel in the injected mass is explained with the help of Scanning electron microscopy and Infra-red spectroscopy. After trial field grouting the stratascopy has revealed better bonds of moist surface with flexibility to accomodate movement before bond or shear failure occurred and had lower volumetric shrinkage during curing.

INTRODUCTION

Cement grouting is well recognised method available to the Civil engineering practice. Epoxy resin have often used for various problems in civil engineering works in India, during the last decades. The sealing of cracks (Koyna, 1968; Konar, 1971; Hirakund, 1976) in concrete structures, plugging of leaks in hydraulic structures and bonding of fresh concrete to hardened concrete are the main applications which are quite wide spread. The main traditional Geotechnical problem for foundations in jointed and fractured rocks is the low bearing power against the structural stresses. The recently innovated application of epoxy grouting of jointed and fractured rock for reducing mass permeability and increasing compressive and tensile strength of bed rock (Norad dam, 1968). For the last application, the corelation of initial rheology of epoxy grout and the interacted strength of set grout at joints are very essential.

This paper developes epoxy gel by interacting chemical compound derived from bis-phenol A with epichlorohydrin and catalyst or hardener consisting of amines and polyamides by conceptual approach along with conventional frame work approach. The aim is to find a suitable time-viscosity relationship of an injection mix which facilitates proper flow mechanism into rock joints or fissures or cracks of the fractured rocks. The microscopic examination helps putforth the interaction and bonding mechanism of grout in an injected mass. Rock strengthening of samples collected from the site near to Panam dam and Karjan dam site and one construction site near Chhuchapura of Gujarat, India, were accomplisned by laboratory injection of epoxy grout which has provided greater strength and better penetration than could have been obtained with the use of portland cement grout. This advantage justifies the use of epoxy grout as against the use of cement grout.

GEL FORMATION AND ITS MECHANISM

When catalyst or hardener is mixed with base resin, the formation of gel occures in three sequential steps: (1) Formation of primary micro gel, (2) Formation of secondary micro gel, and (3) Formation of macro gel.

The reactivities of primary and secondary amine groups of hardener give a linear structure in the alkaline media due to a combination of exothermic heat of reaction, the temperature will rise in the vicinity of the resin molecules, resulting into reaction of secondary amine group, causing the increase of vacant places between the molecules reflecting increase of fluidity. The growth of nuclei continue until the reactive polymer molecules can diffuse to the reactive sites of the nuclei. During this process several new nuclei are also developed resembling the crystallization process.

The primary micro gel and growing nuclei begine to interact each other and give rise to new nuclei for the secondary micro gel increasing viscosity of the system.

At a critical solid concentration the secondary micro gel pack together very suddenly and the experimental gel point is observed (Fig.1).

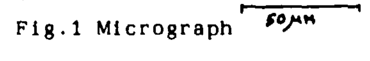

Fig.1 Micrograph

The higher cross linked density reflects in better coherence by bonding with dry and wet surfaces of mass to be interacted.

Infra-red spectroscopy of a unit cell of set mass gives chracteristics bonds of methyle or methylene, and phenyl groups at 1440 and 1505 cm^{-1} bends.

DEVELOPMENT OF GROUT MIX

As per the requirement of resultant gellified mass, either rigid, elastic or elastoplastic, the unit cell is cultivated employing conceptual frame work approach by proportionating resin, hardener and water components. From the unit cell a repeatable unit in the polymer structure is developed.

Gel time increases upto resin: hardener ratio of two, thereafter it drops. The addition of water effectively reduces the gel time (Fig.2)

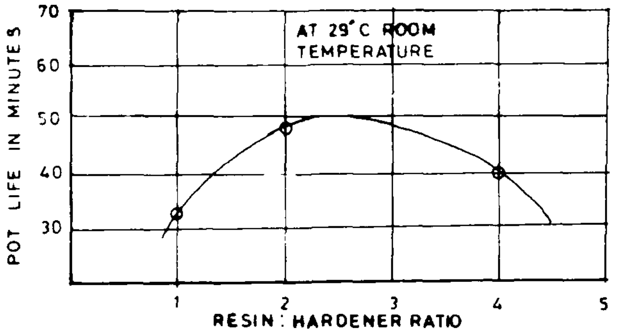

Fig.2 Variation of pot life

Strength of raw gel is controlled by resin to hardener ratio, while trace amount of water optimizes the viscosity of the grout system in addition to lowering the heat of reaction. While interacting with rock, it acts as a wetting, lubricating and spreading agent of grout.

RHEOLOGICAL ASPECTS

Rheological analysis of developed grout system are carried out by time-viscosity study employing Brookfield synchroletric viscometer, U.S.A., and newly developed Orifice type glass cone viscometer. It seems from time-viscosity curve (Fig.3), that initial viscosity drops to 50 per cent upto 12 minutes, thereafter increases to semi-viscous limiting injection stage transforming suddenly to gel stage at about 35 minutes. The time-viscosity plot suggest the proper injection time of 12 minutes and limiting injection time of 24 minutes after mixing. Shear modulus data as obtained from the wave velocity pattern of pulse transmission through gellified mass interprets that gel mass which was visco-elastic before gel time transforms to elastic at gel time.

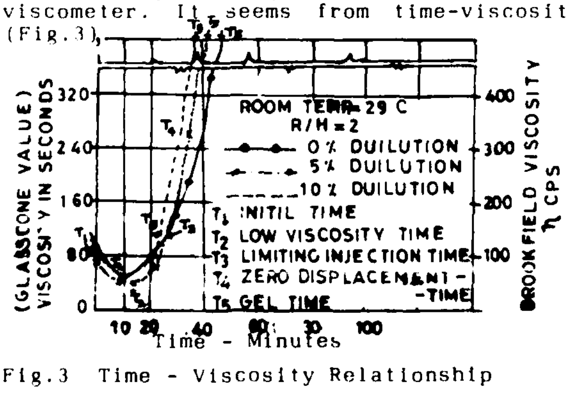

Fig.3 Time - Viscosity Relationship

STRENGTH ASPECTS

Triaxial, unconfined compressive strength and tensile strength at 1 hour, 14 days and 21 days are increased upto resin: hardener ratio two, which tends to decrease thereafter. Unconfined compressive strength as measured on 200 T capacity 'VEB-Wekstofforuf maschinen', for resin: hardener ratio of two, gives 662.8 kg/cm^2, 775.36 kg/cm^2, 800.12 kg/cm^2 at 1 hour, 14 days and 21 days curing time (Fig.4).

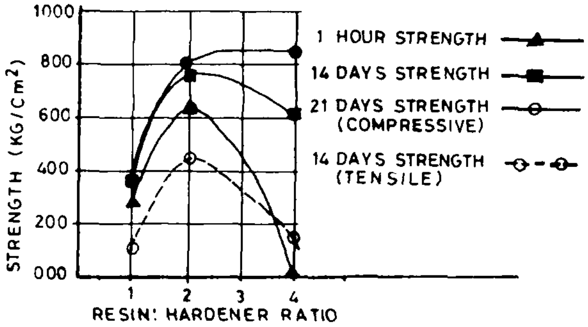

Fig. 4 Compressive and Tensile strength.

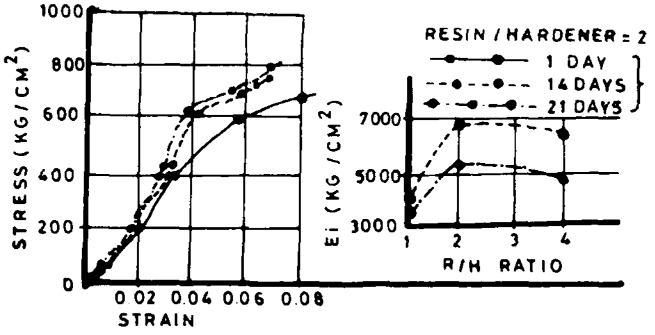

Fig.5 Stress-strain - Time relation of raw gel

Stress-strain curve (Fig.5) indicates that peak stress increases with increase of curing time reverting strength-time relationship of epoxy set mass as strongly time dependent. Two categories basically identified, mainly time dependent linear elastic and time dependent non-linear elesto-plastic leading to brittle failure. Increase of resin: hardener ratio increases the brittleness in the system. As resin: hardener ratio increases to two, initial tangent modulus drops. Per cent failure strain decreases initially with increase of curing period upto 14 days and tends to remain constant thereafter. Trace amount of water in resin-hardener system makes the set mass elesto-plastic rather than brittle plastic exhibiting bulging at failures. Stress-strain curve of raw grout portrayed during tensile test conforms to set mass simillar to St.Venant material. Initial tangent modulus, failure strain and creep strain of tensile stress-strain curves are optimum at resin: hardener ratio of two. High pressure triaxial test give cohesion value of 450 kg cm^2.

GROUTED ROCK MASS

Considering the above time viscosity and strength behaviour the grout is selected for injection purpose consists of optimum ratio of resin: hardener two, along with five per cent dilution.

The rocks collected from various sites as mentioned earlier possess the following magascopic and microscopic characters:

(A) (i) Porphyretic Basalt (collected from the site near Panam dam) - Minute fractures in horizontal direction and moderate weathering.
  (ii) Agglomerate Igneous (collected from the site near to Karjan dam) - trap, rock pieces are seen enclosed in the ground mass which is hetrogenous. Hetrogenity is more in horizontal direction, prominent fracturing, moderate weathering.

(B) (i) Metamorphic, Criss-cross ion veinlets bearing (collected from construction site nearer to Chhuchapura) - bends are observed in horizontal direction, veinlets are noticed in horizontal direction, common fracturing and moderate weathering.
  (ii) Serpentile bearing metamorphic (collected from construction site nearer to Chhuchapura) - Greenish white bends observed in horizontal direction, while minute fracture seen in vertical direction, prominent fracturing and moderate weathering.

Samples of 10cmX10cmX10cm with cut configuration at various orientation are produced and are placed in a square grouting box. Two drill holes from top surface of the above specimen are made upto the location cut to intersect maximum discontinueties. A suitable injection gun is developed for grouting (Fig.6).

A grouting operation is normally carried out to the lowest point to the highest. After filling the gun with epoxy grout, it is connected with tubing to an air compressor. A pressure of 4 to 7 kg/cm^2 is used for the injection. A polyethylene nozzle of the gun is inserted into the drill hole of the rock specimen. Injection is continued till the resin begins to ozzes from the another drill hole. The process is continued until the cracks are completely sealed.

1.Brass top cover fixed with clamps.
2.Inlet for compressed air
3.Outlet
4.Compressed air
5.Polyethylene piston
6.Resin mix
7.Brass casing
8.High density polyethylene syrings
9.Polyethylene nozzle.

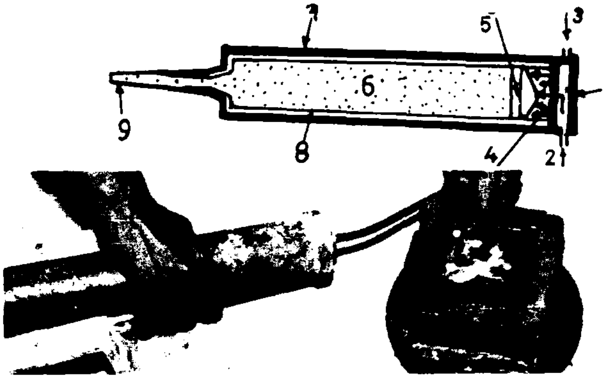

Fig. 6 Injection Gun.

STRENGTH OF GROUTED MASS

For these two groups of rock, adhesion over discontinuties and cracks by epoxy grout always exceed the strength of the rock (Fig.7).

Fig.7 Rock specimen after failure.

Rupture always occures through rock and never through the bonded crack surface. The strength of grouted rock specimens either in horizontal or vertical direction keeping the plane of cut perpendicular to the discontinuety, veinlets and structural hetrogeneity give compressive strength higher than intact rock. The test results on wet surfaces also show that significant strength could be developed across the discontinueties by bonding them with this epoxy resin grout (Fig.8 and 9).

After this laboratory grouting test, a trial injection was made with the above resin grout mix at the above mentioned sites. It is found that, it provides better bonds to moist rock and had more flexibility than other chemical grouts to accomodate movement before bond or shear failure occured, and had shown lower volumetric shrinkage during curing. The strascopic inspection at the site have indicated that larger cracks and smaller cracks are appeared to be filled up and interacted properly with epoxy grout.

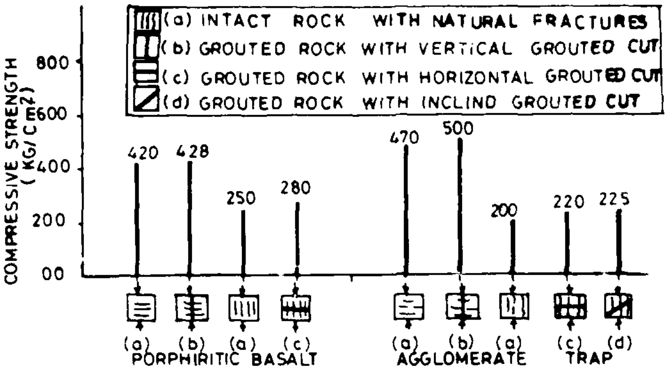

Fig.8 Compressive strength : Igneous rock.

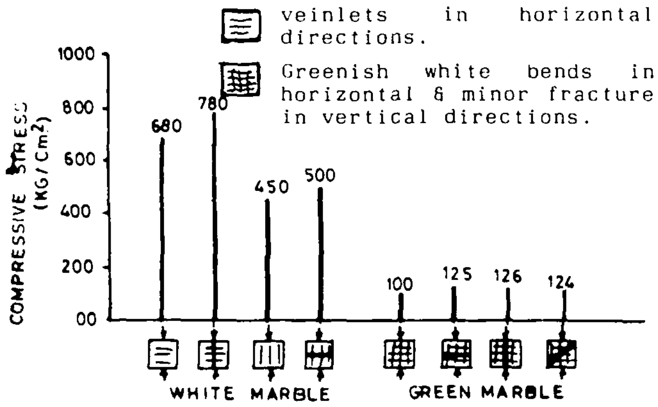

Fig.9 Compressive strength intact & grouted metamorphic rock.

CONCLUSIONS

(i) Epoxy grout system has controlled gellification time, insoluble gel in water, high gel strength, and high long term compressive and tensile strength.

(ii) This grout system identifies following rheological changes during sol to gel : decrease of viscosity from original viscosity due to inherent temperature, increasing further to semi viscous, non-Newtonian converting suddenly to elasto-viscous gellified orange mass.

(iii) Strength time relationship of set mass is strongly time dependent. For evaluation of deformation two categories basically identified : mainly time dependent linear elastic and time dependent nonlinear elasto-plastic leading to brittle failure. Trace amount of water and resin hardener system makes the set mass elastoplastic rather than brittle plastic exhibiting bulging at failure. During tensile strength stress strain behaviour conforms to St. Venant material.

(iv) For igneous and metamorphic group of rocks, adhesion over discontinuties and cracks by epoxy grout always exceed the strength of the rock. Rupture always occures through rock and never through bonded crack.

(v) After trial field grouting, the stratascopic study has revealed better bonds of moist surface with flexibility to accomodate movement before bond or shear failure occurred alongwith lower volumetric shrinkage.

ACKNOWLEDGEMENT

This research wo.k is performed at Geotechnical Engineering Division, Applied Mechanics Dept. M.S.University of Baroda, Gujarat, India.

REFERENCES

(i) Choudhary, M.M. etal (1984) "Epoxy grouting of cracks in concrete", Indian concrete journal, Jan., 1984 pp 4 - 10.

(ii) Choudhari, M.M. etal (1987), "Epoxy grouting technique", Indian concrete journal Jan., 1987, pp 9 - 16.

(iii) Pande, G.M. & Sharma, V.M. (1983),"Epoxy grouting of cracks in dams, does it really help?", Indian concrete journal, Apr. 1983 pp 165 - 166.

(iv) Erickson, H.B. (1968), "Strengthening of rock by injection of chemical grout", Proc. ASCE, Jr. of SMFE Div. Jan. pp 159-173.

(v) Shah, D.L. & Shroff, A.V. (1985), "Resin grout system for rock treatment", Indian Geotechnical conf. (I.G.C. - 85), Roorkee, Dec. 1985, Vol.I, pp 203 - 208.

(vi) Shah, D.L. (1986), "Time viscosity relationship and strength of Newtonian and **Binghamian grouts", Doctoral** thesis submitted to M.S.University of Baroda.

(vii) D.P. Amin (1987), "Characteristics of Epoxy grout system", M.E. Dissertation submitted to M.S.University of Baroda.

Session VI

“Case Histories of Soil Structure Interaction”

Proceedings: Second International Conference on Case Histories in Geotechnical Engineering, June 1-5, 1988, St. Louis, Mo., Paper No. 6.02

Partial Underpinning a Five-Storey Building

Phung Duc Long
Civ. Eng., Institute for Building Science & Technology, Vietnam

Nguyen Van Quang
Doctor, State Committee of Science & Technology, Vietnam

Bo Berggren
Doctor, Swedish Geotechnical Institute, Sweden

SYNOPSIS: Partial underpinning is often not accepted because of dangerous damage that may be caused by the redistribution of stresses in the superstructure. A five-storey building was partially underpinned successfully. To give stability to the building only a small number of piles, about 70% fewer than with the conventional method, were used. The results observed have proved the success of the partial underpinning.

INTRODUCTION

Underpinning is an increasing need in the construction field. Underpinning with piles must be performed if a major part of the settlements of a building is due to consolidation of soft soil, a frequent cause of damage to buildings. In Vietnam, the thickness of the soft soil layer underlying the dry crust is commonly 15-20 m in Hanoi, and up to 30-40 m in Hai Phong and Ho Chi Minh City. The conventional underpinning method aims at totally avoiding any further settlement. Therefore, not only the damaged part but also the rest of the building is often underpinned, a safe but expensive solution. It should then be discussed whether it might be possible to underpin only a part of the building to reduce the rate of settlement to an acceptable level and to prevent further damage due to differential settlements. In many cases, especially when there is a certain non-homogeneity of either the soil or the superstructure, this method may be successful. The partial underpinning method would be much cheaper than the conventional method, possibly 30 to 50%. However, it is evident that partial underpinning is very dangerous. Partial underpinning with piles means introducing more rigid supports under a part of the existing shallow foundation. By redistributing stresses in the superstructure, further damage may be caused, e.g. by shear stresses, especially between the underpinned part and the rest. Partial underpinning needs more careful soil investigation and design, taking into account the interaction between the soil and the building structure.

In this paper, the partial underpinning of a five-storey brick masonry building, La Thanh Hotel in Hanoi, which has seriously settled and tilted at a rather high rate, will be presented. A simplified design method will also be introduced. The method has proved to be successful since the settlement, distortion and tilting of the building so far have been stopped with no further damage.

DESCRIPTION OF BUILDING AND SOIL CONDITIONS

Building. La Thanh Hotel is located six kilometres west of the centre of Hanoi. The building that required underpinning is a five-storey building of 8.4 m width and 50 m length in two sections separated by a gap. Construction of the building started at the end of 1977 and was completed in October 1978. The building is a brick masonry building with cross-walls, assembled panel floors and reinforced concrete frames along the corridors. The foundation consists of strip footings beneath the walls and isolated footings beneath the columns of the corridor frames. The strip footings are generally 1.20 m below the zero level of the building.

Settlement observations

Just after the building was completed, serious settlements were discovered, especially in the west section. Settlement observations at 25 points started just after the completion of construction and the result is shown in Fig. 1. The values of the maximum settlement and the maximum differential settlement are both much larger than the allowable values according to the Vietnamese Building Code. In July 1985, just before underpinning was started, the maximum settlement was about 500 mm (point H15, see Fig. 1a), while the maximum differential settlement of the west section was about 350 mm. The maximum rate of settlement, also at point H15, was still rather high, about 6 mm or even more per month.

In view of the existing soil conditions, the use of shallow foundations for the five-storey brick building was inconvenient. The large settlements are due to relatively large shear stresses and to consolidation of the weak soil layer, the organic soil and the mud. The two upper layers, the dry crust and the upper clay, can be considered to be relatively stiff. Between axes 14 and 15, where the total thickness of the two layers is smallest and the foundation depth is lowest, the soil may locally yield. This is the main reason for the large differential settlement of the building.

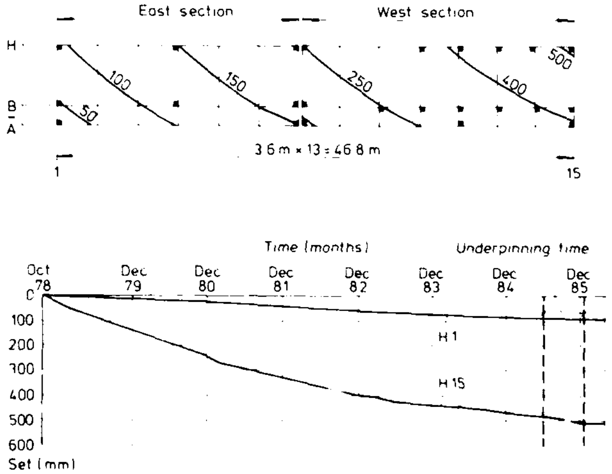

Fig. 1a Settlement curves (Dec. 1985).
1b Time-settlement curve.

Soil conditions

In March 1983, in order to find out the causes of the large settlements, an additional soil investigation was made, including 6 penetration tests and soil sampling in two boreholes. The soil layers can be described schematically as follows:

1) Dry crust: the thickness varies from 1.5 to 2.5, sandy clay with large quantities of broken brick, point penetration resistance q_c = 1.0 MPa, void ratio e = = 0.71, angle of internal friction ø = 22°, cohesion c = 10 kPa.
2) Upper clay: medium stiff. The thickness varies from 1.0 to 2.5 m, q_c = 1.5-2.0 MPa, e = 1.30, ø = 10°, c = 50 kPa.
3) Organic soil: plastic with a high organic content. The thickness varies from 2.0 to 3.5 m, total penetration resistance is about 2.0 to 4.0-5.0 MPa, $q_c \leq$ 1.0 MPa, e = 1.43, ø = 10°, c = 30 kPa. In this layer there is a thin layer of peat of about half a metre. The peat is very wet and porous and contains rotting tree leaves.
4) Mud: underlies the organic soil layers, reaching to a depth of 13 to 17 m. The mud contains much organic matter, $q_c \leq$ 1.0 MPa, e = 1.65, ø = 8°, c = 25 kPa.
5) Lower clay: below a depth of 13 to 17 m, stiff clay. The total penetration resistance is more than 10.0 MPa, while the point resistance is about 5.0 MPa.

The water table is found at a depth of 0.5 to 1.0 m. In Fig. 2 two soil cross-sections are shown.

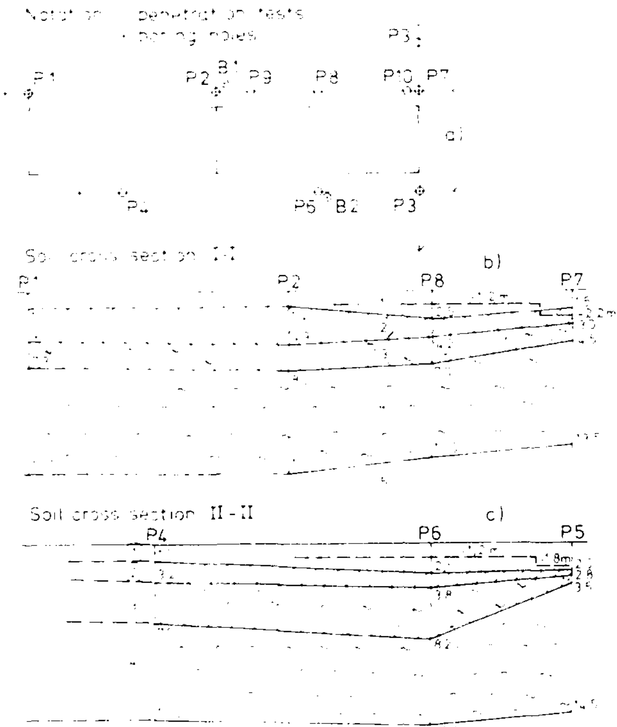

Fig. 2 Soil conditions.

PARTIAL UNDERPINNING

Jacked concrete piles were chosen in order to give stability to the building. It was decided that only the west section of the building and furthermore only the most seriously settled part of the section should be underpinned. In this way, the expansion of the differential settlement could at least be reduced. It is evident that partial underpinning is very dangerous. By redistributing stresses in the superstructure, further damage may be caused by shear stresses, especially between the underpinned part and the rest. However, the rigidity of the superstructure foundation system is fairly high, which may be the main reason why there are only a few small cracks. For safety purposes, strengthening beams were installed along the building.

In order to avoid any danger, the following underpinning steps were suggested, see Fig. 3.

- Underpinning with Mega piles only in the part between axes 13 and 15;
- observing regularly the development of settlements and cracks;
- jacking down additional piles if further damage is found in the superstructure. In this case, the partial underpinning becomes a complete underpinning with a varying density of piles.

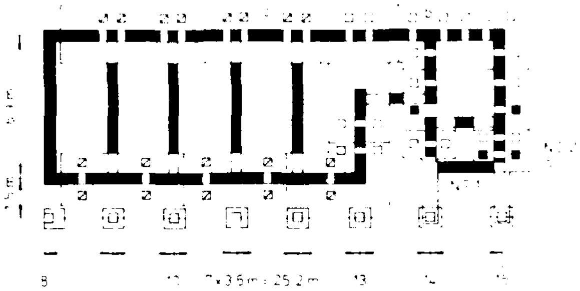

Fig. 3 Partial underpinning
a. Test piles
b. Piles already jacked
c. Piles will be jacked if necessary

METHOD OF DESIGN

Partial underpinning is reliable if the soil-structure interaction is taken into account in design. Although many advances have been made in soilstructure interaction analysis, e.g. Poulos (1981), it is rather difficult to apply them to underpinning design. This is because partial underpinning is a time-dependent problem. Moreover, causes of damage to buildings are often very complicated. In many cases, damage may be caused by creep settlements or settlements due to local yielding that have not been very well understood so far. For these reasons, a simplified method of design was suggested and applied in this case. The building foundation system is considered as a beam on a deformed foundation. When rigid supports, i.e. underpinning piles, are placed only partially under the beam, it must be strong enough to withstand the redistributed stresses, especially the shear stress Q, at the cross-section between the underpinned part and the rest of the beam. Q can be determined by the following expression:

$$Q = P - G \qquad (1)$$

where P = the load transferred to all piles.
G = the weight of the underpinned part, see Fig. 4

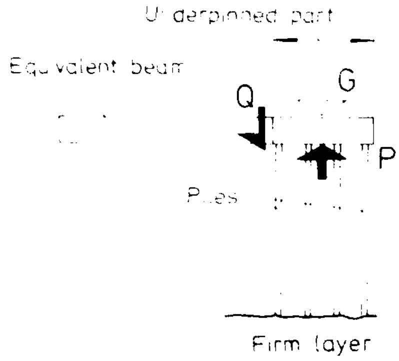

Fig. 4 Scheme of simplified calculation.

There will be three possible cases after the partial underpinning:

a the non-underpinned part has no more settlement. In this case P = G, thus Q = 0. No strengthening beam will be needed.

b the non-underpinned part has further settlement. Thus P > G, and Q > 0. Strengthening may be needed.

c the non-underpinned part continues to settle considerably. In the extreme case

$$Q_{max} = n \cdot P_u \qquad (2)$$

where n = number of underpinning piles
P_u = ultimate bearing capacity of each pile

Thus,

$$Q_{max} = n \cdot P_u - G \qquad (3)$$

To be safe, the equivalent shear resistance of the building-foundation-strengthening beam system, Q_e, must be larger than the shear stress

$$Q_e \geq Q_{max} \qquad (4)$$

For a cross-wall structure, the shear resistance at a cross-section may be taken as the aggregate resistance of all the elements of the section, including brick walls, reinforced concrete beams or slabs, foundation beams and strengthening beams. The latter need to be designed. Because the shear strength of a brick is very small, it can be neglected in the analysis.

For the given case, the total area of concrete at the section between the underpinned part and the rest is about 7,530 cm^2 with a total steel area of 102 cm^2. If the shear strength of the concrete is about 0.3 kN/cm^2 and the shear strength of the steel is 17 kN/cm^2, the equivalent shear resistance of the beam, Q_e will be:

$$Q_e = 0.3 \times 75{,}400 + 17 \times 102 = 4{,}000 \text{ kN}$$

At the site, 23 piles were used with an average ultimate capacity of each pile of about 450 kN, see the static load test results. The estimated weight of the underpinned part is about 4,000 kN. Thus Q_{max} = 23 x 450-4,000 = 6,350 kN. Because $Q_{max} > Q_e$, a strengthening beam is needed.

It was decided to place four strengthening beams, each having a cross-section of 65 cm x 50 cm with a steel reinforcement area of 11 cm^2, along the axes B and H of the building, on both sides of the walls. These beams will also be used as load transfer beams, if additional piles are needed.

Taking the same shear strength of concrete and steel as above, Q_e = 6,650 kN > Q_{max}. The design would have a high enough safety factor even in the most dangerous case.

The above calculations would overestimate the maximum shear stress, but they help to create a realistic attitude to partial underpinning work. Similar analysis can be performed for bending behaviour. For masonry walls, the overall stiffness along the length of the walls may be obtained from Thorburn et al (1977).

SITE EXPERIENCE

At the construction site, with some exceptions, piles are jacked down in pairs on both sides of the walls, outside the old foundation and from the ground surface, see Fig. 5. Compared with jacking piles from the bottom of the existing foundation, this method has the following advantages:

- the working space for handling the rather heavy pile segments is large and makes the work easier,
- installation is not affected by ground water whose level is rather high at the site, and it can therefore be performed even during the rainy season,
- the necessary excavation is reduced to a minimum.

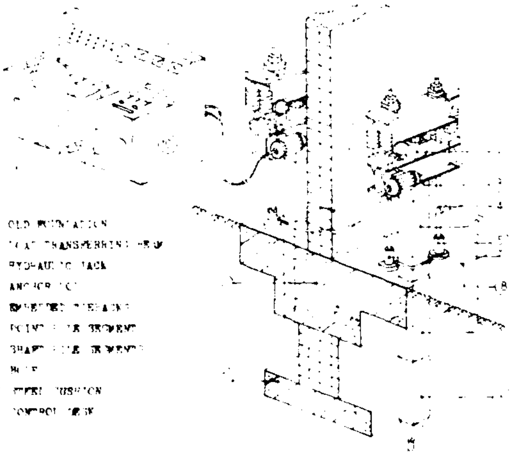

Fig. 5 Installation of jacked concrete piles.

Pile segments with a cross-section of 200 mm x 200 mm and a length of 600 mm, which are easy to handle and quick to join, were chosen. The segments are joined by a 30 mm diameter steel rod in the centre and two 12 mm diameter steel locks at each joint. The central rods are 600 mm long, see Fig. 6.

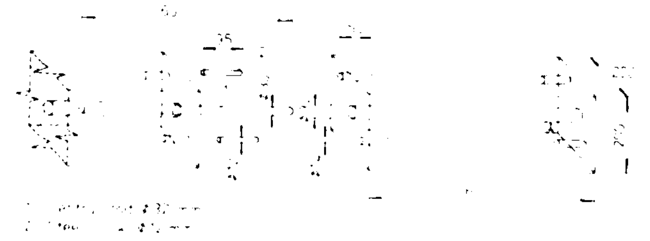

Fig. 6 Pile segment and pile joint.

The hydraulic jacks used for the underpinning work originally belonged to equipment for installing buildings of the lift slab type. The load-transfer system consists of ladder-shaped reinforced concrete beams which stretch along both sides of the walls and lie across the walls where piles are located, Fig. 3.

At the site, the load transfer system was first concreted section by section. The jack system was then installed by joining the anchor rods with the embedded tiebacks in the load transfer beams, see Fig. 5. Piles were jacked down into the soil segment by segment through the prefabricated holes in the beams until the jacking force reached a predicted value. An average of four piles were jacked down at the same time. After all piles had been jacked down, they were simultaneously fixed to the load transfer system without any prestressing.

In June 1984, the first two piles were installed as test piles. After construction of the load transfer system, from October to December 1985, the next 21 piles with a total length of about 400 m were installed. The length of the piles ranges from 13.2 to 15 m. The jacking force used during the installation varied from 360 to 410 kN. The time for jacking each pile was about 24 hours on average, including breaks. The rate of settlement had not decreased by the time the piles were fixed. So far, the settlement and tilting of the building have been stopped and no more cracks have appeared. No additional piles were needed and the partial underpinning has proved to be successful.

STATIC LOAD TESTING

Static load tests were carried out on two piles using the quick maintained load test, the ML method. In this method of testing, the load is increased every fifteen minutes by a constant amount, approx. 5% of the estimated ultimate load. Dial gauges are read 3, 6, 9, 12 and 15 mins. after application of a new load increment. In Fig. 7 the test results are shown for piles Nos. 1 and 2. For pile No. 1, failure was reached at a load of 480 kN. The creep load evaluated by the creep load curves with reading between 9-15 mins. is about 450 kN. For pile No. 2, the ultimate load is 420 kN, while the creep load is about 390 kN.

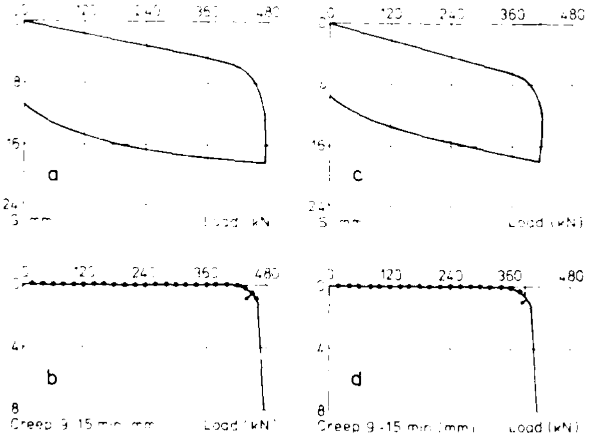

Fig. 7 Results from static load test using the ML-method.
a, b Pile No.1
c, d Pile No.2

Discussion

- o The ultimate bearing capacity of a pile predicted from CPT-tests is in good agreement with the value received from a static load test. Based on CPT tests, the length of the pile can be predicted with fairly high accuracy.
- o Using the jacking force-depth curves plotted during installation, the base resistance of the pile can be evaluated as the difference between the maximum jacking force and the force just before reaching the hard clay layer.
- o There is a certain relation between the ultimate load and the maximum jacking force used during installation. Using a number of typical load tests, this ratio can be determined reasonably exactly and the ultimate load can therefore be predicted for each pile with good accuracy.
- o The ratio between the creep load and the ultimate load is slightly more than 0.9. According to the Swedish Building Code, this ratio is normally about 0.9.

CONCLUSIONS

1. Partial underpinning is a method that allows a cost saving of 30 to 50% in comparison with the conventional method, in the given case, about 50%. To avoid any danger due to the redistribution of stresses, especially shear stresses in the superstructure, strengthening beams should be used.
2. Partial underpinning would be successful in buildings damaged by local subsidence that may be caused by differential clay shrinkage, removal of lateral support from the ground beneath the foundation, or differential consolidation where the basements provide deep foundations under part of a building. This method can also be applied to preventive work.
3. The simplified calculation method suggested above can be used if design is to be on the safe side. The partial underpinning method is reliable if the soil-structure interaction is taken into account in the design. Furthermore, piles should be designed as "settlement reducers". This will further reduce the number of piles.

REFERENCES

Phung Duc Long (1982). Underpinning Buildings Damaged by Foundation Causes. SGI Report No 101, Linköping.

Phung Duc Long, Berggren, B (1987). Underpinning a Five-storey Building with Jacked Concrete Piles. Proc. 9th Southeast Asian Goetechnical Conference, Bangkok.

Poulos H.G. (1981). Soil-structure Interaction - General Report. Proc. 10th ICSMFE, Stockholm.

Thorburn, E., edt (1977). Soil-Structure Interaction - A State-of-the-Art Report, Inst. Struc. Engrs. London.

Proceedings: Second International Conference on Case Histories in Geotechnical Engineering, June 1-5, 1988, St. Louis, Mo., Paper No. 6.05

Damage to Masonry Structures in the Historic Center of Arezzo (Tuscany, Italy) Following the Excavation of a Sewer Tunnel

A. Ghinelli
Department of Civil Engineering, University of Florence, Italy

G. Vannucchi
Department of Civil Engineering, University of Florence, Italy

ABSTRACT: The work carried out in the 1983-84 period for the building of a sewer line at a shallow depth in the historic center of Arezzo (Tuscany - Italy) caused serious damage to many of the masonry structures.
For a depth of 6-7 m., the foundation underground is made of a thick deposit of eterogeneous soils, mainly clayey silt of medium or soft consistency, including elements of gravel, boulders and organic sediment.
The tunnel has a circular section, its external diameter being 1.90 m, cover 3.40-5.20 m, and the work was carried out using a shield. The method of excavation and the subsequent operation of the tunnel brought about a prolonged disturbance and resettling of the ground in contact with the casing and thus, where fairly large boulders came into contact with the outside edge, gaps formed which were not injected with plastic concrete.
On the basis of the geotechnical data available, the surface subsidence has subsequently been calculated and has been compared with what is allowable without damaging the overhead structures.

Introduction

Arezzo is a town in Tuscany about 60 Km south-east of Florence.

The original layout is from the Etruscan-Roman period (4th. century B.C.), and the present urban configuration is the *result of an uninterrupted and millenary building* and urbanistic transformation. The historic center is enclosed within the pentagonal ring of the Medicean city walls, and is crossed in a SE-NW direction by the Castro creek. In Roman times, once it had reached the city, the Castro most probably pursued its straight and artificial course, wich it already had, for a kilometer and a half (Fatucchi, 1969). It made its way from east to west, passing to the south of the amphitheatre and, immediately afterwards, bending towards the northwest (Figure 1).

The creek was covered over in different times for its entire city lenght: already in the 13th. century, the bed was covered in the section included between the present Corso Italia and Via Madonna del Prato, in corrispondence with the ancient "Ospedale di S. Maria del Ponte"; around 1870, the stretch included between Via Madonna del Prato and Via Guido Monaco; in the second post-war period, the remaining urban sections were covered over.

The most important building operation which involved the historic center of Arezzo was consequent on the building of the Florence-Arezzo-Perugia-Roma railway line, inaugurated in 1866.

In the immediate subsequent years, within the sphere of a vast program of expansion and re-ordering of the old building plan, were realized the large circular Piazza Guido Monaco, the widening of streets and squares (with the demolition of numerous buildings, among which in part the 15th-century "Convento dei Minoriti"), the opening of new passages in the city walls, and the covering over of the bed of the Castro creek with a large barrel vault, for a distance of about 80 m.

In the years 1983-84 at Arezzo, the fourth section of a large sewer line was built which, at shallow depth of few meters for several hundreds of meters, brushes the historic center of the city (figure 2), travelling along Via Garibaldi in the vicinity of the covered over bed of the Castro.

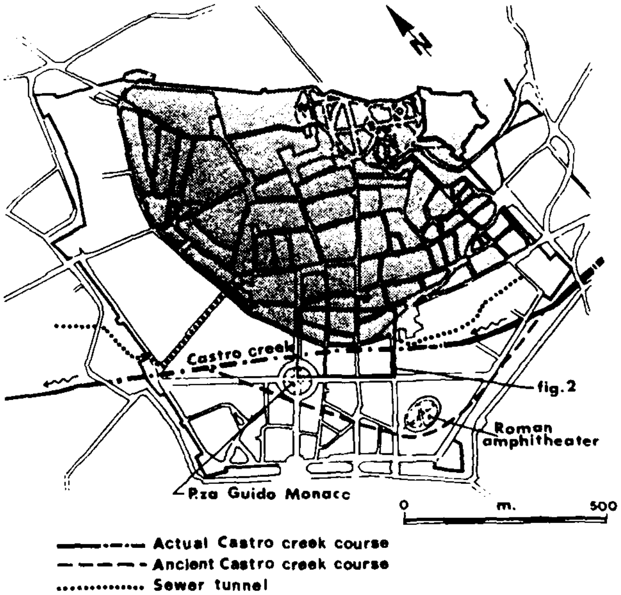

Fig. 1: Plan of historic center of Arezzo

During the excavation of the tunnel, several buildings in the historic center suffered damages of varying extents.

The walled city is divided into two clearly distinct zones, from Via Sacra, now Via Garibaldi, which has semicircular layout (figure 1). The Castro, whose course in the city segment seems to coincide with a bedding fault, is very close to Via Garibaldi in the section included between Via Madonna del Prato and Corso Italia.

- NW of the creek and of the bedding fault, Via Garibaldi encloses the oldest nucleus of the historic center, otherwise defined by the Medicean city walls. The topographic conformation of this zone of the city is on a steep slope with acclivity included between 5% and 25%. The geological map indicates stony rocks of the Tuscan Series ("Macigno del Mugello"), made up of sandstones alternated with marls and shales; over this rock formation are present, for a thickness varying between 4 and 6 meters, heterogeneous soils of a silty-clayey character containing elements of gravel, pebbles and organic sediment, heavily anthropized, fill materials and remains of ancient pre-existences.

- SW of the creek and of the bedding fault and more in general of Via Garibaldi, the topographic conformation of the city is almost flat. The geological map indicates alluvial-fluvial deposits of clay, sand and pebbles. Due to the more recent building development of the zone, the foundation soils are less anthropized.

1. THE LAYOUT AND EXCAVATION TECHNIQUES

The layout of the sewer line to the right of the Castro is indicated in figure 1. It is developed in line with Via Garibaldi, and does not pass under any building although, due to the small covering and the narrowness and curving of the street, in several points, it is dangerously close to the foundations of the buildings located on the sides. In fact, Via Garibaldi has a variable width, average 8 m, but in some sections it narrows to 4.5 m.

The sewer line was designed with the thought in mind of making an open-cast excavation, by previous construction of reinforced concrete retaining diaphragms; but for the historic center, the solution of the mini tunnel, to be made with the following excavation technique, was afterwards preferred:

1) Construction of a main thrust pit in Piazza del Popolo: 4.75 m deep, the shape of which would permit the housing of the thrust machinery in two directions. The structure was made with bored concrete piles, diameters 80 and 40 cm, connected by a slab at the base of the excavation and by reinforced concrete walls in the upper part.

2) Construction of intermediate jacking stations for the recovery of the thrust by means of a series of hydraulic jacks set along the perimeter of the lining.

3) Making of a circular hole, diameter 1.90 m, by means of the sinking of a shield and subsequent removal and carrying away of the soil from the cavity. As the shield advanced, the cavity was lined with precast reinforced concrete cylindrical pipes, 22 cm thick and 3 m long. Since the thrust was exerted by means of hydraulic jacks, which operated in the thrust pits (main and intermediate), the section of tunnel lining already realized, was made to shift ahead, as the excavation proceeded.

The excavation was carried out by means of milling cutter mounted on a trolley and manoeuvered by a workman on the face of excavation. The material loosened by the bits was removed on a conveyor belt, deposited in a container at the main pit then picked up and carried away completely from the workyard.

The excavation technique and installation of the tunnel involved a remolding and prolonged in time re-arrangement of the soil in contact with the lining, as well as the creation of voids where rocky elements of considerable dimensions were encountered along the contours.

After the first disorders were manifested in the masonry buildings underpassed by tunnel, the excavation technique was perfected: a mixture of fine sand, bentonite and cement was systematically and radially injected, to fill up the void left by the cutting edge. This device, at time combined with protective or underpinning works for the buildings underpassed or located very closely to the tunnel, avoided further damages to the masonry structures.

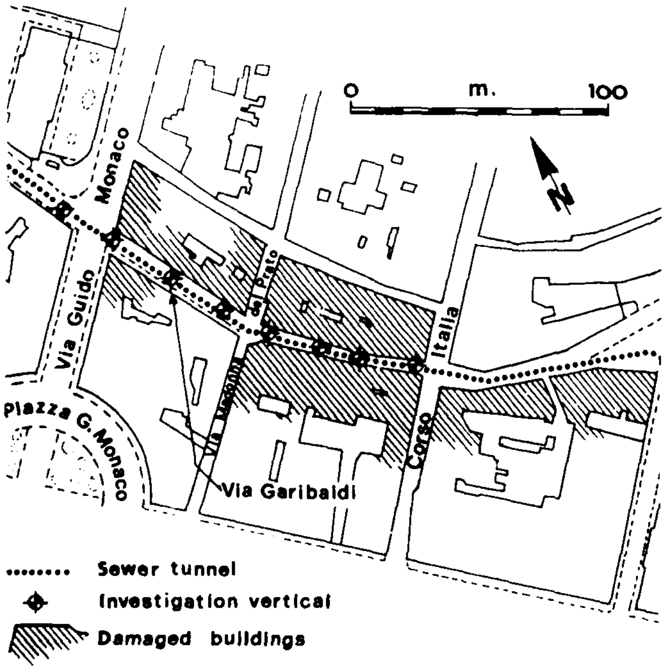

Fig. 2: Close-up to damaged area

2. GEOTECHNICAL DESCRIPTION

The stratigraphy of the soil involved in the sewer line in the historic center of Arezzo can be briefly described as follows:

- from street level to a depth of 4.0 ÷ 6.0 m:
  sandy and silty clays, from soft to medium consistency, at times with pebbles and fragments of bricks, often with organic sediments;

- below a depth of 4.0 ÷ 6.0 m:
  marls alterated and/or silty shales, sometimes in the high part, in the form of layer portions in a silty and clayey matrix.

The bottom of the tunnel is located at a level of 4.2 ÷ 5.5 m from street level. Since the finished work has an outside diameter of 1.9 m and thickness of 22 cm, a large part of the excavation took place in the silty and sandy clay surface formation (figure 3).

The origin of the surface layer must be related to three distinct and partly connected phenomena:

- the deposit of Castro creek;
- the accumulation of surface erosion debris of materials constituting the hill on which the historic center of Arezzo rises; and
- the backfill due to organization.

At present the Castro flows in a contact foot hill zone between the fluvial deposits of the plain and stony rocks which constitute the principal relief of Aretine urban territory. This location does seem, moreover, to be the original one (Fatucchi, 1969), and it can be hypothesized that the Castro, canalized into new foot hill bed, has eroded not yet completely consolidated materials,

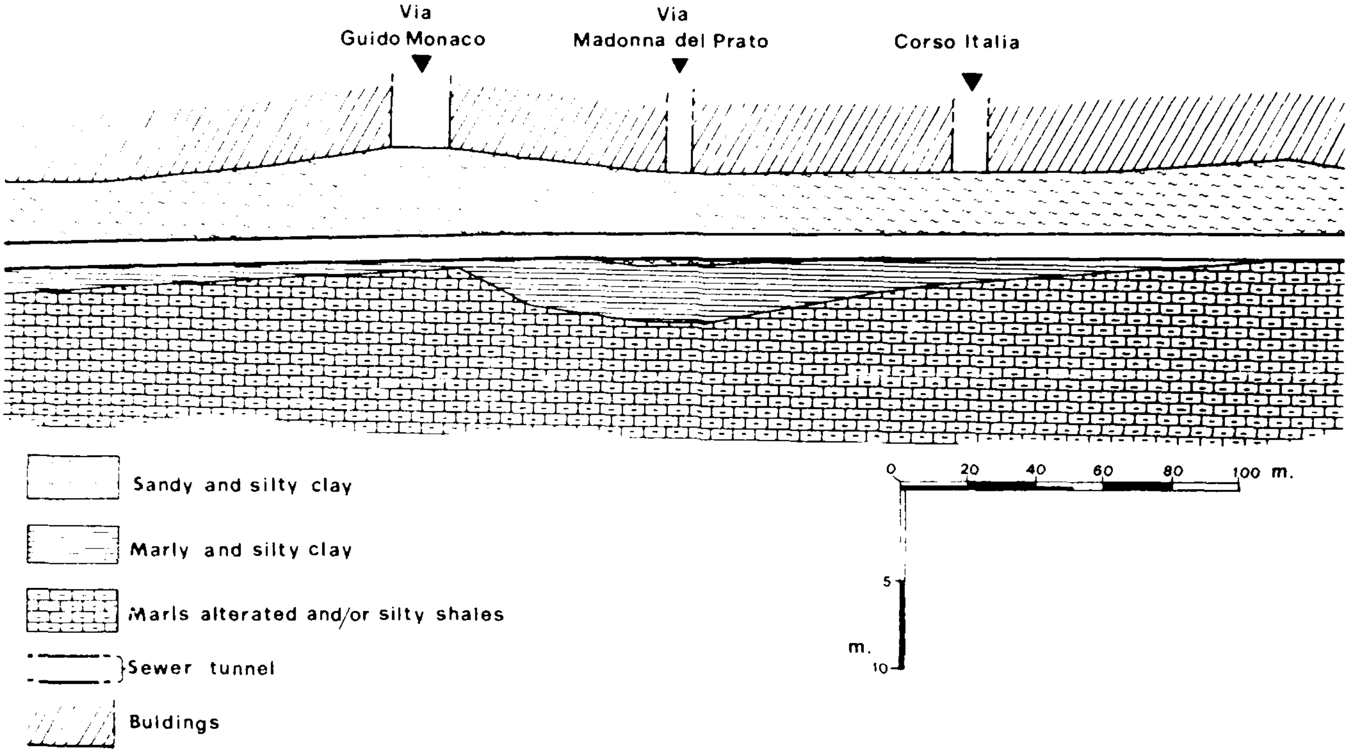

Fig. 3. Geotechnical section of the tunnel in the damaged area

subsequently causing the caving in of the surface rubble overhead.

The geotechnical properties of the surface layer vary gradually, passing from the foot hill zone to the hill zone of the city. In the plasticity chart (figure 4), the representative points of the surface soils in the hill zone, marlish in origin, fall within the highest part of the chart, while the representative points of the surface soils in the foot hill zone, fluvial in origin fall within the lower part of the chart, they have a larger silt/sand component and, therefore, lesser plasticity.

In the zone involved with the sewer tunnel construction, where the most serious damages to the buildings on the sides occurred, the geotechnical properties of the surface layer, taken from the documentary material which it has been possible to gather from geotechnical surveys made at different time and with different aim, are the following:

- Liquid limit — Wl = 29÷37%
- Plastic limit — Wp = 17÷19%
- Plasticity index — Ip = 12÷18%
- Activity — A = 0.3÷0.6
- U.S.C.S. classification — CL

- Unit weight — τ = 1.92÷1.95 gr/cmc
- Moisture content — W = 24÷26%
- Degree of saturation — Sr = 88÷93%
- Relative consistency — Ic = 0.3÷0.6

- Specific gravity — Gs = 2.68÷2.72 gr/cmc
- Void ratio — e = 0.73÷0.76
- Compression index — Cc = 0.15÷0.20
- Confined compression modulus — E' = 30÷80 Kg/cm²
  (in the pressure interval, p = 1.5-3.0 Kg/cm²)

- Cohesion — Ccu = 0.0 Kg/cm²
- Angle of internal friction — Φcu = 26°÷29°

- N. of blows in S.P.T. — Nspt = 7÷9

The granulometric zone of the upper soil in the section considered is represented in figure 5.

Unfortunately, it must be reported that an adequate number of laboratory tests does not correspond to the number of verticals examined (30 stratigraphic columns of depths of between 6.0 m and 23.0 m from street level; 6 static penetrometric tests; 6 dynamic penetrometric tests).

A typical CPT profile, in which the general stratigraphic outline is recognizable, is represented in figure 6.

The more superficial water table has been measured at depths varying between 4.0÷5.0 m from street level.

During the excavation of the tunnel, rocky blocks of even considerable dimensions were encountered, as well as the remains of ancient masonry, walls with 4.0 m interaxis, on which perhaps in part the foundations of existing buildings rested.

3. DAMAGES TO BUILDINGS

The buildings damaged in consequence of the excavation of the sewer tunnel in the historic center of Arezzo rise on both sides of Via Garibaldi, in a section of about 250 m. between Via Guido Monaco and Via Margaritone (figure 2).

The supporting structures are of brick and/or stones masonry; the floors are of wood or of iron and shelves of brickwork; the foundations are superficial and continuous. The period of construction differ greatly. Several

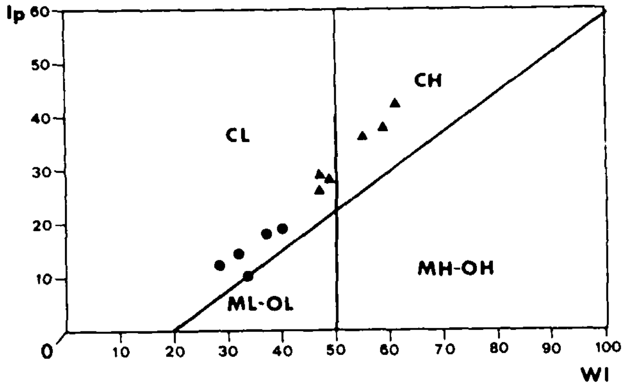

Fig. 4: Plasticity chart

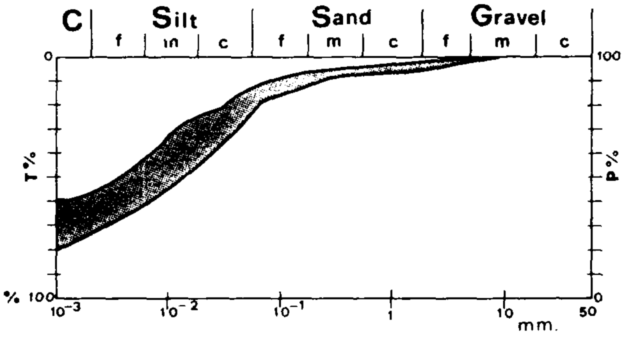

Fig. 5: Granulometric zone of the upper soil

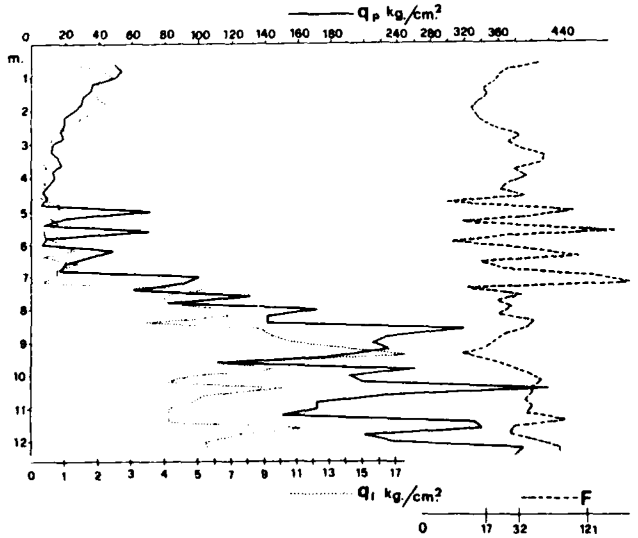

Fig. 6: Tipical CPT profile

buildings have suffered in time successive modifications and even structural remakes: some recent and documented; others, older and difficult to identify. The design drawings of the structures in elevation and in foundation were not available. In particular, the depth of foundation plan was not known.

It was not possible to establish exactly the evolution in time of the disturbance phenomena and their correlation with the progress of the excavation front, since the instrumentation of the buildings was planned only after evident and serious cracks on the masonries appeared togheter with the impossibility of opening and closing doors and windows. Nevertheless, there is reason to believe that such damages manifested themselves, for every building, during and immediately after the passing of the excavation front.

In fact, for example, from the workyard daybook containing the description and chronology of the work carried out, it can be gathered that on 22nd November 1983 the excavation front was at the crossroad with Corso Italia.

The notification of serious damages to one of the buildings on the corner between Via Garibaldi and Corso Italia is dated 4 December 1983.

Since the measurement instruments, installed on 14th March 1984, and consisting of extensometers and inclinometers only reported very small and not monotonic movements, it must be considered that the phenomenon lasted for a brief period and wore itself out in a short time.

4. Stability of the excavation front and calculation of the settlements.

The stability conditions of the excavation front of a circular tunnel in cohesive soil can be evaluated through the stability ratio, defined in the following manner:

$$N = [(\sigma s - \sigma t + \tau \cdot (C + D/2)]/Cu$$

where:

C is the cover
D is the diameter of the tunnel
Cu is the undrained shear strength of soil, constant with depth
σt is the fluid pressure in the tunnel
σs is the uniform pressure applied to the ground surface
τ is the soil unit weigth

In the case in point, approximately, taking into account the uncertainty of several data, N results between 4 ÷ 3, to which corresponds the safety factor SF = 0.55 ÷ 0.75 (Davis et al., 1980). The excavation front was therefore stable, although with a not very high safety margin.

The building of a tunnel always produces strains in the surrounding soil, which fact is reflected in settlement of the ground level. As is well known (Peck, 1969), the surface subsidence has a normal or Gaussian error curve profile:

$$S = Smax\ exp(-X/2i)$$

where

X is the current abscissa measured by the center-line of error curve profile: that is, the distance from the tunnel's vertical axis;
Smax is the maximum ground settlement over the tunnel center-line;
S is the ground settlement in correspondence with the current abscissa X;
i is the X abscissa of the inversion point of the curve.

Because of movements of the ground, both radial and normal at the excavation front, as well as subsidences in the lining, the volume of soil removed is always larger than the final volume occupied by the tunnel: the difference between these two volumes is called ground loss per unit length of tunnel, Vs. In undrained conditions the cohesive saturated soils strain in costant volume, and therefore the ground loss per unit length of tunnel is equal to the area of the settlement trough.

If the latter is described by an error curve profile, we have

$$Vs = 2.5 \cdot i \cdot Smax$$

Although there is uncertainty and variability in several data, in the case in point we can reasonably estimate $i = 2.5$ m (Peck, 1969) and $Vs = 6.5\%$ (Mair et al. 1981). With reference to the more critical geometric conditions, the maximum settlement of the street level can be computed as follows:

$$Smax = 1.04 \text{ cm}$$

At the depth of the foundation level, which for several damaged buildings has been ascertained between 1.5 m and 2.7 m from street level, $i = 1.10 \div 1.70$ m and $Smax = 1.5 \div 2.4$ cm.

The angular distorsion is, therefore:

$$[Smax - S(i)]/i = 0.009 \div 0.008$$

values not allowable with the structural integrity of multi storey buildings of masonry. By way of orientation, the U.S.S.R. building code adjudges (Mikhejev & al., 1961; and Poslhin & Tokar, 1957) as acceptable for multi storey buildings of masonry and settlements which wear themselves out rapidly in time, distortion values of 0.003, three times lower than those which were presumably verified for the buildings on the sides of Via Garibaldi in the most critical section. Bjerrum (1963) considers that, for angular distorsion greater than 1/150 = 0.007, considerable cracks are foreseeable in courtain and bearing walls of brickwork, as well as structural damages to the buildings.

5. MEASURES ADOPTED IN ORDER TO AVOID FURTHER DAMAGES

Because of the damage suffered by the buildings in the vicinity of the sewer tunnel in the period November 1983 January 1984, excavation work of tunnel was suspended until March 1986.

For completion of the tunnel, the following measures, which have avoided, or at least greatly limited, the damages to the structures, were adopted:

- behind the cutting edge of the shield and to fill in the void left by it, injections of plastic mixture of bentonite, fine sand and cement were made

- the foundations of the buildings nearest to the tunnel were protected by a discontinuous bulkhead of drilled micropiles 8÷10 m long, reinforced with a steel pipe and connected at the top by a reinforced concrete beam. In order to realize a structure of considerable stiffness, the micropiles were bored fan-shaped with different inclinations; and to avoid the creation of grout curtains (watertight diaphragms), they were sherted with a geotextile braiding (figure 7).

CONCLUSIONS

In the planning of civil engineering works, we often resort to structural and geotechnical idealizations which do not always correspond adequately to actual local conditions. This is especially true when one is operating in an environment which, for historical as well as natural reasons, is very complex and difficult to become acquainted in advance. At times the consequences can be very "unpleasant": the realization of the sewer tunnel in the historical center of Arezzo is an example of this.

The objective and "unbiased" analysis of the causes of unsuccess and of the efficacy of the remedies adopted can furnish very useful informations for future design. Unfortunately, and this is understandable, only very rarely the failures are made public. In planning geotechnical investigations for the realization of a civil engineering work, one must take into consideration both a costs benefit analysis and an evaluation of the potential (not only economic) damage in the case of failure.

It is essential to provide controls in the course of the work in order to verify the suitability of the design hypothesis for the actual local conditions, and to use realization techniques which can, in part and without excessive burdens, be possibly modified during the work so as to adapt themselves to local conditions which are different from the ones considered most probable during the primary planning stage.

In the case of sewer line in Arezzo, where the geotechnical conditions were particularly difficult and not completely foreseeable on the basis of the investigations made before starting the work (in others not very distant zones in the city, the foundation soils in fact were found to be more consistent), the damage would have been more limited if an efficient control system both of the soils encountered during excavation and of surface movement, had been planned in advance. Furthermore, these same measures for avoiding or limiting damages, which were adopted with success after more than two years of interrupted work, could have been adopted immediately after the manifestation of the first serious disturbances.

Acknowledgements

We wish to thank the Municipal Administration of Arezzo, Department of Technical Services, for the documentary material and for having given the permission to publish the present paper.

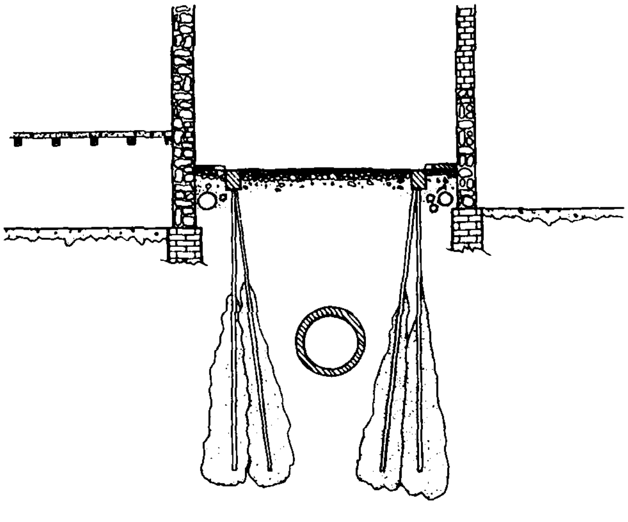

Fig. 7: Sketch of buildings' protection

REFERENCES

BJERRUM, L. (1963). "Allowable settlement of structures". Proc. European Conference on Soil Mechanics and Foundation Engineering, Weisbaden, Germany, Vol. III: 135 - 137.

BOSELLI, L.; FRANCINI, G. & SBRAGI, E. (1985), "Suolo e Ambiente - Quaderni di Arezzo 3", Revisione del Piano Regolatore Generale, Arezzo.

COMUNE DI AREZZO (1972-1986), materiale documentario relativo al progetto ed alla realizzazione del IV° Stralcio Esecutivo del Collettore in Destra Castro.

COMUNE DI AREZZO (1987), "Variante Generale del Piano Regolatore 1987 - Cartografia Geologica. Relazione Generale" Arezzo.

DAVIS, E.H.; GUNN, M.J.; MAIR, R.J. & SENEVIRANE, H.N. (1980), "The stability of shallow tunnels and underground openings in cohesive materials", Geotechnique, 30, 397-416.

FATUCCHI, A. (1969). "I primi mille anni della vicanda urbanistica di Arezzo", Atti e Memorie dell' Accademia Petrarca, Vol.XXXIX, Nuova Serie, Anni 1968-69, Arezzo, 284-321.

GHINELLI, A. & VANNUCCHI, G. (1980), "L' attraversamento in sotterraneo del centro storico di Firenze: previsione dei cedimenti", Atti del 14° Convegno Nazionale di Geotecnica, Firenze, Vol. I, 205-214.

MAIR, R.J.; GUNN, M.J. & O'REILLY, M.P. (1981), "Ground movements around shallow tunnels in soft clay", Proc. 11th. International Conference on Soil Machanics, Stockholm, Vol. I, 323-328.

MERLA, G. & ABBATE, E. (1967), "Note illustrative della Carta Geologica d' Italia, Fogio 114, Arezzo", Servizio Geologico d' Italia, Ministero dell Industria, del Commercio e dell' Artigianato.

MIKHEJEV, V.V. & al. (1961), "Foundation Design in the USSR", Proc. 5th. International Conference on Soil Mechanics, Paris, Vol. I, 753-757.

PECK, R.B. (1969), "Deep excavations and tunnelling in soft ground", Proc. 7th. International Conference on Soil Mechanics, Mexico City, State of the Art Volume, 225-290.

POLSHIN, D.E. & TOKAR, R.A. (1957), "Maximum allowable non-uniform settlement of structures", Proc. 4th. International Conference on Soil Mechanics, London, Vol. I, 402-405.

RISTORI, G.B. (1871), "Nuova guida della Citta' di Arezzo", Firenze.

ROSSI, F. (1985), "Il piano regolatore del 1867", Notiziario Turistico, Anno X, nn. 103-104-107, Arezzo.

TAFI, A. (1978), "Immagine di Arezzo, Guida storico artistica", Arezzo, Banca Popolare dell' Etruria.

Proceedings: Second International Conference on Case Histories in Geotechnical Engineering, June 1-5, 1988, St. Louis, Mo., Paper No. 6.06

Structural Damage Arrested by Stabilization of Landfill

Arthur H. Wu
Senior Geotechnical Engineering Specialist, Naval Facilities Engineering Command, USA

SYNOPSIS: This paper presents a case of landfill movement and the stabilization methods employed, including: a description of the causes of the landfill instability; the soil displacement monitoring methods used and their results; the damage to the structure caused by ground settlement and displacement; the slope stability and pile distress analysis made to evaluate the extent of the problem; the remedial work undertaken to correct the landfill instability; the settlement problems which still exist, along with the current maintenance requirements.

INTRODUCTION

The project involved converting 3.5 acres of creek bed into usable land. Oyster shell, a locally available lightweight fill, was selected to cover a 55 ft depth of soft organic clay in order to minimize settlement. In some areas the fill had to be placed as high as 30 feet. Before placing the fill, vertical sand drains were installed in the clay soil. Then a waiting period was established to allow for the anticipated initial large settlement. However, a faster and much greater settlement occured than that which consolidation theory predicted.

The library, constructed on piles in the landfill area, suffered structural damage. Lateral soil movement had resulted in excess earth pressure on the piles, causing cracking in the pile caps. The slope in the fill had become unstable due to uneven settlement, presenting the possibility of a large general slide, which would cause extensive damage to the multimillion dollar library and adjacent facilities.

To address this danger, landfill stabilization was implemented in 1977, employing careful design techniques and a well controlled construction sequence and monitoring system. As a result, the progressive lateral movement of the fill toward the creek has been minimized. Still, even today, land settlement is occurring at a rate larger than anticipated. Therefore, periodic additions of fill in some areas are necessary if traffic and parking are not to be impeded.

SITE CONDITIONS AND INITIAL CONSTRUCTION

In 1970, the U.S. Naval Academy in Annapolis, Md, created about 3.5 acres of land in the Dorsey Creek to provide a site for the Nimitz Library and parking facilities for Rickover Hall. The original ground elevation ranged from El. -3 to El. -20. The soil consists of a soft organic clay layer averaging about 55 ft in depth followed by a compact sand stratum. The soft clay has an average natural water content of 110 percent, an average liquid limit of 75 percent, and an average plastic limit of 42 percent, which indicates that the clay is highly plastic and sensitive to remolding, and is highly compressible. The undrained shear strength of the soft clay ranges from 150 psf to 350 psf. The in situ vane shear tests shows that the undisturbed shear strength ranges from 400 psf to 1350 psf, and the remolded strength ranges from 120 psf to 600 psf.

By filling an on site creek and adjacent areas with lightweight oyster shell, the buildings were supported and parking areas provided. The natural density of the oyster shell was about 88 pcf saturated and 66 pcf dry. The effective angle of internal friction of the oyster shell, determined by using the direct shear test, averaged about 38 degrees. The density of the compact sand stratum was approximately 125 pcf. The effective angle of internal friction of the compact sand was evaluated at 36 degrees.

To accelerate consolidation of the soft clay deposit, vertical sand drains were installed. The construction of the 3.5 acre landfill, begun in the summer of 1970, was completed in September 1971. The Nimitz Library was partially constructed in the landfill in 1972 and 1973, and was founded on cast-in-place concrete piles. The piles were cased in steel pipes of 16 inch outside diameter and 15-1/4 inches inside diameter. The length of the piles varied between 90 ft and 105 ft, extending from the top of the oyster shell fill to a depth of 20 to 25 ft into the compact sand stratum. Rickover Hall, which is adjacent to the landfill area, was constructed during the years 1973 to 1975.

PROBLEMS DEVELOPED

Upon completion of the Nimitz Library, the ground surface in the landfill area showed large subsidence. Additional soil borings made in the landfill revealed that some of the vertical sand drains installed previously were not made deep enough to expedite the consolidation of the soft clay. Subsequent investigations further revealed that the excessive fill movements were aggravated by overloading of the upland area during construction of Nimitz Library and Rickover Hall. It was discovered that large quantities of construction material, stockpiled on the landfill, had caused an increase in the speed of settlement. The settled area was filled with gravel to raise the ground surface. The new heavy fill eventually triggered a slide of the entire filled area toward the adjacent creek.

The lateral soil movement of the landfill resulted in additional earth pressure on the piles, thus inducing structural damage to the library building. A close inspection of the building structure revealed that cracks had developed in some of the pile caps and girders. Emergency removal of 3 to 5 ft fill was made to prevent further structural damage and landfill instability. This urgent measure slowed the subsidence, but measureable lateral movement continued. And now a new problem presented itself: because of the lowered fill grade, the area became flooded whenever a high tide in the creek occurred, and vehicle access was lost.

It was obvious that unless stopped, the lateral movements and subsidence of the fill would cause potentially serious structural damage to the existing building and make future development of the landfill area impossible.

Remedial measures were immediately undertaken to arrest the lateral soil movement and prevent further subsiding of the ground surface.

FIELD INSTRUMENTATION AND SLOPE STABILITY ANALYSIS

In 1973, to monitor the rate of landfill settlement and lateral displacement, 15 settlement platforms and 9 inclinometers were installed in the fill area as shown in Fig. 1. Settlement was found to be occuring at the rate of approximately 1.2 inch per month, about three times greater than predicted by theoretical analysis.

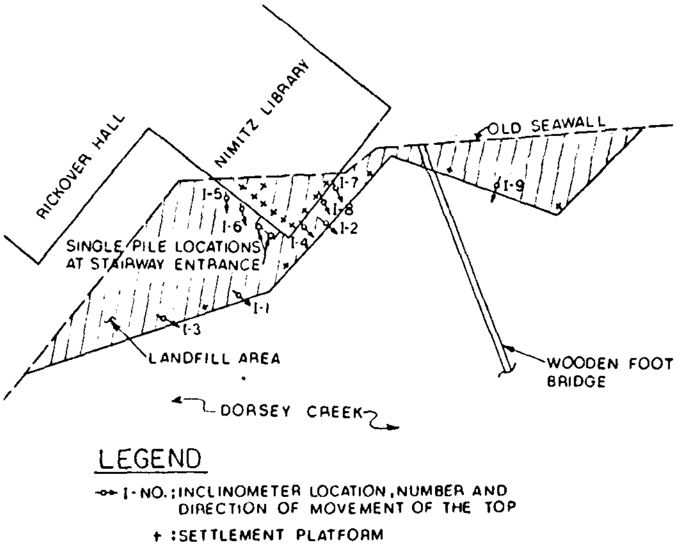
RICKOVER HALL
NIMITZ LIBRARY
OLD SEAWALL
I-5
I-6
I-7
I-8
I-2
I-4
I-9
I-1
I-3
SINGLE PILE LOCATIONS AT STAIRWAY ENTRANCE
LANDFILL AREA
WOODEN FOOT BRIDGE
DORSEY CREEK
LEGEND
I-NO.: INCLINOMETER LOCATION, NUMBER AND DIRECTION OF MOVEMENT OF THE TOP
+ : SETTLEMENT PLATFORM

Fig. 1 Inclinometers and Settlement Platform Locations

The inclinometer data indicated that the zone of movement extended throught the entire clay stratum, in the general direction of Dorsey Creek. Fig. 1 also shows the direction of movement of the top of each inclinometer as designated by arrows. The lateral deformation profiles determined from inclinometers Nos. 6 through 8 during a 7 month period are given in Fig. 2.

A cross section of the soil in front of Nimitz Library was used for analysis of the stability of the entire soil mass, including the landfill and the soft clay.

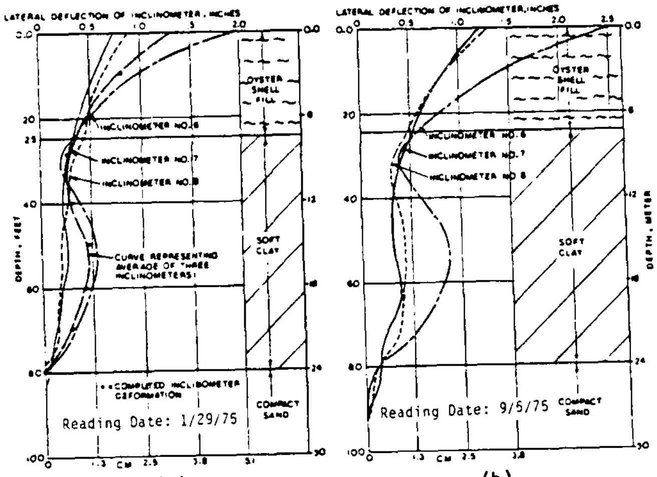

(a) (b)

Fig. 2 Inclinometer Readings

Stability was determined by total stress analysis, using the low value of an undrained shear strength of 150 psf for the soft clay. Using a computer program based upon the Bishop method of analysis, the factors of safety for various possible sliding circles shown in Fig. 3 were computed. Results of the analysis give factors of safety of 1.10, 1.04, and 0.99 for sliding circles A, B, and C, respectively. These findings indicate that the most critical mode of possible failure is the one involving sliding of the soft clay toward the deepest part of Dorsey Creek some 100 ft to 200 ft away from the water edge of the fill, i.e., sliding circle C.

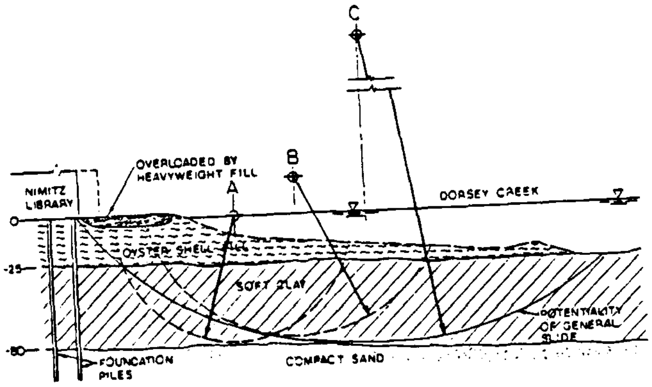
C
B
A
OVERLOADED BY HEAVYWEIGHT FILL
NIMITZ LIBRARY
DORSEY CREEK
0
-25
-80
OYSTER SHELL FILL
SOFT CLAY
POTENTIALITY OF GENERAL SLIDE
FOUNDATION PILES
COMPACT SAND

Fig. 3 Typical Landfill Section Potentiality of Instability

STRESS AND DEFORMATION IN PILES

The deformation and stress distribution for a single pile, due to lateral movement of the surrounding soil, was analyzed. Cracking of this pile's cap was first noticed in January 1975, the average value of lateral soil movement being computed from inclnometers Nos. 6, 7, and 8. The soil pressures required to cause this lateral soil movement were estimated. It is generally accepted that, for soils having increasing shear strength with depth, the soil modulus values increase linearly with increasing depth. Using the determined values of moduli of subgrade reaction and the average lateral soil momvements measured from inclinomiters Nos. 6. 7, and 8, the lateral soil pressures were computed.

The moduli of subgrade reaction are given below, and the computed lateral soil pressure is shown in Fig. 4, lateral soil pressure diagram.

Oyster Shell	K=4.4 Z
Soft Clay	K=0.6
Compacted Sand	K=1.5 Z

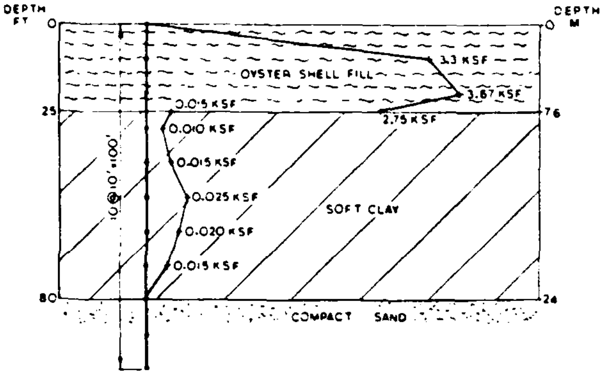
DEPTH FT
0
25
80
DEPTH M
0
7.6
24
3.3 KSF
OYSTER SHELL FILL
3.67 KSF
0.05 KSF
2.75 KSF
0.010 KSF
0.015 KSF
0.025 KSF
SOFT CLAY
0.020 KSF
0.015 KSF
10@10'=100'
COMPACT SAND

Fig. 4 Lateral Soil Pressure Diagram

where K is the modulus of subgrade reaction in kip/ft3, and Z in feet is the depth measured from the top of the landfill. Under the action of the lateral soil pressure, the behavior of the single pile was analyzed using the finite elemenmt computer program.

Results of the finite element analysis give pile deformation, shear, and moment diagrams as shown in Fig. 5, pile deformation, shear, and moment diagram. The horizontal reaction and resisting moment at the top of the pile were then used to check the structural integrity of the pile cap.

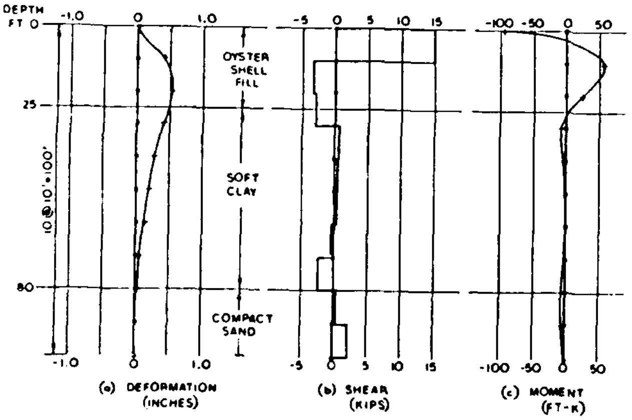

Fig. 5 Pile Deformation, Shear, and Moment Diagram

REMEDIAL CONSTRUCTION

The basic object of the design was to provide for a three to four foot settlement of the fill area on which the new facilities (seawall, utility services, pavements, landscaping, etc.) were to be built, while maintaining their structural and functional adequacy. Field investigations and design analyses resulted in the adoption of rededial measures involving a combination of steps.

In February, 1976, remedial construction on the landfill took place. The stabilization methods included application of several techniques:

(1) A counterweight was placed at the toe of the fill slope and the slope flattened to confine the entire fill area. Also a stone berm was constructed in the creek, restoring the slope to 1 verticle to 10 horizontal. It was estimated that stability of landfill increased about 70% against sliding.

(2) A pile-supported seawall at the perimeter of the landfill was constructed. Stability of the landfill was estimated to have been increased by about 120% as a result of carrying the embankment weight to a compact sand layer at a deep elevation.

(3) The wieght on the upland was reduced by removing the heavyweight fill from the area and replacing it with lightweight slag fill. Stability of the landfill was estimated to have been increased by about 110% as a result.

Other features of remedial construction included application of a controlled construction sequence and monitoring system to minimize disturbance of the landfill and to observe any fill movements during construction. The following sequences of construction were specified and implemented:

(a) Install tell-tale tripods in Dorsey Creek for monitoring to avoid a mud wave during stone berm filling.
(b) Place stone berm at the toe and on the slope of the embankment evenly.
(c) Drive steel bearing piles for seawall support according to a specified order and avoid excessive vibration to the adjacent Nimitz Library.
(d) Construct pile caps and place precast concrete panels to form seawall.
(e) Replace heavyweight fill on the upland area with lightweight slag.
(f) Place flexible pavers and dry wells for drainage on the parking areas.

Fig. 6 shows the remedial construction used to stabilize the landfill movement. These measures stopped the lateral movements, but there was no economically feasible way to prevent further subsidence. Drainage was controlled by construction of a grid of independent dry-well catch basins. Adjacent to the library building, tilt slabs were placed between the pile supported beams and on grade to provide a transition zone and allow for future settlement. Provision was made for future releveling of the tilt slabs by mudjacking.

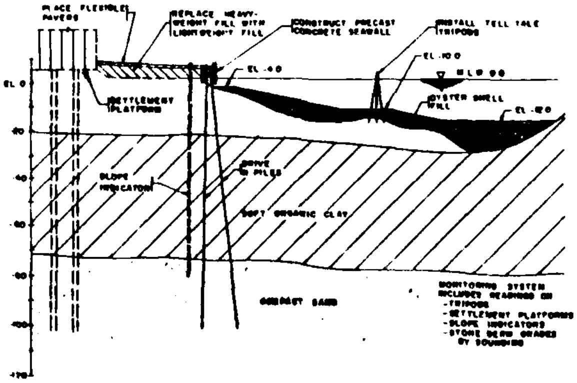
PLACE FLEXIBLE PAVERS
REPLACE HEAVY-WEIGHT FILL WITH LIGHTWEIGHT FILL
CONSTRUCT PRECAST CONCRETE SEAWALL
INSTALL TELL TALE TRIPODS
EL 0
EL -4.0
EL -10.0
MLW 0.0
SETTLEMENT PLATFORM
OYSTER SHELL FILL
EL -12.0
DRIVE H PILES
SLOPE INDICATOR
SOFT ORGANIC CLAY
COMPACT SAND
MONITORING SYSTEM INCLUDES READINGS ON
-TRIPODS
-SETTLEMENT PLATFORMS
-SLOPE INDICATORS
-STONE BERM GRADES BY SOUNDING

Fig. 6 Section of Remedial Construction

The use of flexible designs and details provided the basis for a successful design. For example, a pile supported seawall, jointed at short invervals to accommodate predicatable future settlements, enclosed the settling area, thus maintaining a level bulkhead line. Unit block pavers, used in lieu of standard pavement, will allow for differential settlement. As settled areas are regraded, pavers can be removed and replaced.

These remedial construction procedures aided in the restoration of areas disturbed during construction of the buildings, and provided stable landfill.

STABILITY OF SEAWALLS AND SETTLEMENT PROBLEMS

Initial design considered the use of either a floating concrete box seawall or a pile-supported precast concrete seawall to retain an oyster shell landfill. Floating concrete box seawalls sitting on an oyster shell fill would ultimately settle and then tilt, resulting in misalignment. Pile-supported precast concrete seawalls would be more expensive, and pile-driving through the oyster shell fill and thick soft clay to the dense sand layer might involve pile installation difficulties.

A detailed soil engineering analysis, along with the available landfill settlement records, indicated that the area would continue to settle at a rate greater than had been previously predicted. While the concrete box seawall could prevent erosion of the backfill, it would be very costly to correct its misalignment once it started to settle and tilt. A pile-supported precast concrete seawall would provide a stable seawall, but it could not prevent backfill erosion, and the initial construction cost would be higher.
The pile-supported precast concrete seawall was finally chosen, with steel bearing piles being used to overcome driving difficulties. After completion of the project, a large soil settlement was observed behind the seawall. An investigation revealed that the fill behind the seawall was being undermined by the erosion caused by wave action acting under the seawall. Erosion under the seawall was causing rapid settlement of the grade, a condition requiring constant maintenance. An end to the erosion was eventually achieved by installing timber sheeting against the backface of the seawalls.

Fig. 7 show the design of seawall systems and the timber sheeting installed to prevent erosion of the landfill.

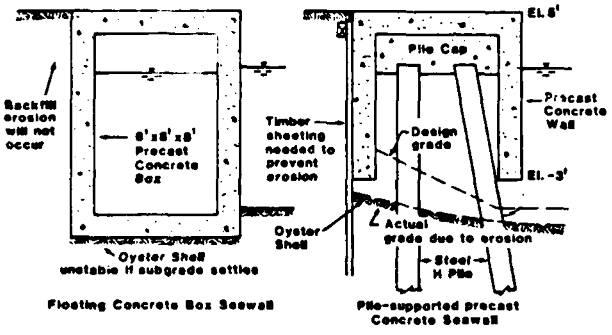
EL 8'
Pile Cap
Backfill erosion will not occur
8'x8'x8' Precast Concrete Box
Timber sheeting needed to prevent erosion
Design grade
Precast Concrete Wall
EL -3'
Oyster Shell
Actual grade due to erosion
Oyster Shell unstable if subgrade settles
Steel H Pile
Floating Concrete Box Seawall
Pile-supported precast Concrete Seawall

Fig. 7 Design of Seawall System

MAINTENANCE REQUIREMENTS

Today, 10 years after completion of the remedial construction, there is still noticeable settlement in the parking area. Even greater settlement is occurring in the drive way where trafic is more frequent. Along the old bulkhead line there has been continuous differentiall settlement between the old fill and the new landfill. Frequent leveling is required if the parking area is to be used without interruption. Settlement has been paticularly severe in the areas where tilt slabs were constructed. The tilt slabs were lifted and mudjacked 5 years after completion of redemical construction, but relevel of the fill surface will still be needed in the near future. All of these settlement problems impose the requirement of regular maintenance.

SUMMARY AND CONCLUSIONS

A case history of structural damage caused by lateral movement of the soil and the landfill stabilization methods used to arrest the damage were presented. Landfill created on a soft clay soil can not avoid large settlement but lateral movement can be lessened if landfill stability is assured. In this case lateral soil movement was induced by an unexpected overloading of the landfill causing a shear failure in the soft clay soil. Landfill stability can be greatly increased during and after construction through careful monitoring and the use of proper design methods.

The foundation piles embedded in the landfill were stressed by the lateral movement of soil, thus developing cracks in the pile caps and girders. The behavior of piles subjected to lateral soil movement can be predicted by employing the finite element computer program, in which appropriate properties of the surrounding soil and the pile material, and the proper magnitude of lateral soil movement are used. For any possibility of lateral movement of the surrounding soil, the stress and deformation of the piles induced by the lateral earth pressures can be analyzed.

The landfill stabilization method employed in the project has proved to be successful. However, settlement still can not be avoided, and a regular maintenance programn is needed in order to use the area as intended.

REFERENCES

Wu, A. H., "Landfill Prevents Riverside Subsidence From Endangering Academy's Nimits Hall," Navy Civil Engineer, Fall 1977, pp 41-42.

Wngs, M. C., Wu, A. H., and Schessele, D. J., "Stress and Deformation in Single Piles Due to Lateral Movement ot Surrounding Soils," Behavior of Deep Foundations, ASTM STP 670, Raymond Lundgren, Ed., American Society of Testing and Materials, 1979, pp. 578-591.

Wu, A. H., Yachnis, Michael, "Documenting Lessons Learned: A NAVFAC Consulting Engineer's Goal," Navy Civil Engineer, Winter 1986, pp 10-12.

Proceedings: Second International Conference on Case Histories in Geotechnical Engineering, *June 1-5*, 1988, St. Louis, Mo., Paper No. 6.10

Compaction-Induced Distress of a Long-Span Culvert Overpass Structure

Raymond B. Seed
Berkeley, California

Chang-Yu Ou
Berkeley, California

SYNOPSIS: Compaction of backfill produces soil stresses and earth pressures which are not amenable to analysis by conventional methods. These compaction-induced earth pressures can produce stresses and deformations in flexible buried culvert structures which may significantly affect the stability and performance of these structures. This paper presents the results of a study in which deformations of a long-span flexible metal culvert were measured during carefully monitored backfill operations. These field measurements were then compared with the results of finite element analyses in order to investigate (a) the influence of compaction effects on culvert stresses and deformations, and (b) the ability of recently developed finite element analysis procedures to accurately model these compaction effects. The structure being monitored suffered excessive and unacceptable deformations which were shown to be primarily the result of compaction effects; these were well modelled by the analyses performed.

INTRODUCTION

This paper presents the results of a study in which deformations of a large-span flexible metal culvert structure were measured during backfill operations. Detailed records were maintained of backfill placement procedures and deflections were monitored at various stages of backfill placement. This case study was similar to an earlier study of a similar long-span culvert overpass structure (Seed & Ou, 1987) except that compaction procedures for the earlier study were carefully controlled in order to minimize the influence of compaction on structural deformations, whereas in this current study compaction procedures were not strictly controlled and poor backfill placement procedures led to large and unacceptable structural deformations.

Two types of finite element analyses were performed to model field conditions: (a) conventional analyses which are well able to model incremental placement of backfill in layers but which cannot model compaction-induced stresses and deformations, and (b) analyses incorporating recently developed models and analytical procedures which do permit modelling of compaction effects (Seed & Duncan, 1986). Comparison of the results of these two types of analyses with each other, as well as with the field measurements, provides a basis for assessing: (a) the potential importance of considering compaction effects in analyzing culvert stresses and deformations, and (b) the accuracy and usefulness of the new analytical methods for modelling compaction effects.

THE VISTA CULVERT STRUCTURE

The Vista culvert structure is located in Vista City, California, and is designed to perform as a two lane bridge over a small river. Figure 1(a) shows a cross-section through the structure. The culvert is a low-profile arch with a span of 38 feet 5 inches, a rise of 15 feet 9 inches and a length of approximately 90 feet, founded on 3-foot high reinforced concrete stem walls with a reinforced concrete base slab. The culvert consists of 9 x 2-1/2-inch corrugated aluminum

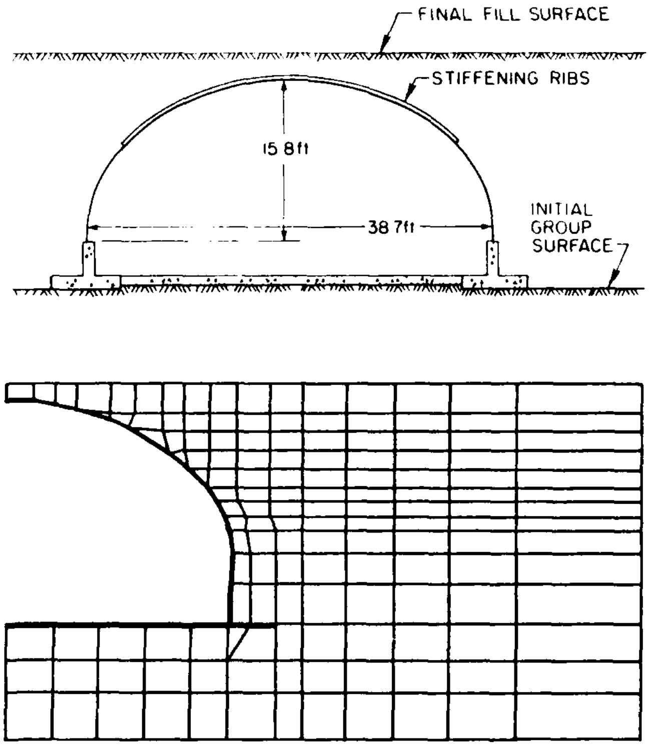

Fig. 1 The Vista Culvert Structure

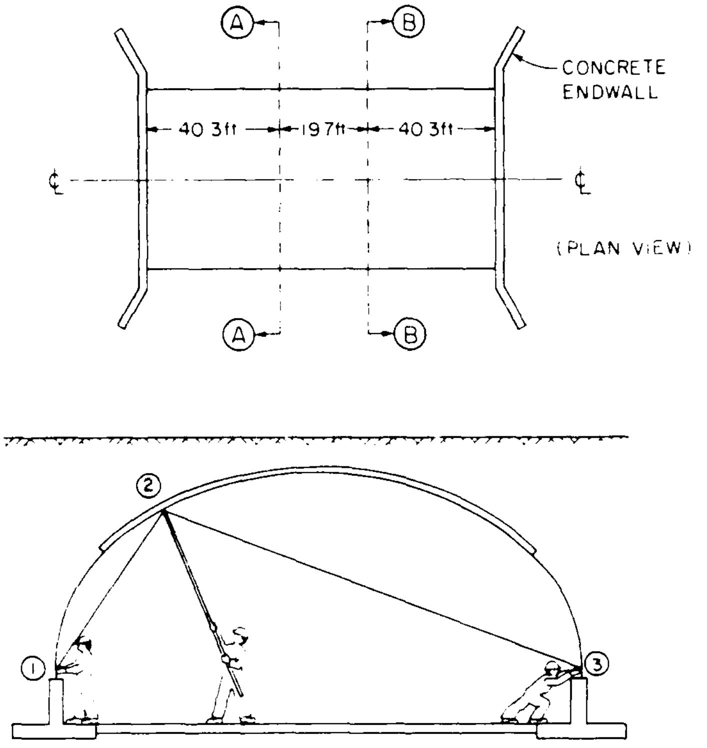

Fig. 2 Measurement of Culvert Deformations

structural plate 0.2 inches thick, and the crown section is reinforced with Type IV aluminum bulb angle stiffener ribs which occur at a spacing of 18 inches. The culvert haunches are grouted into a slot at the top of the stem walls, providing a rigid connection for moment transfer at this point.

The existing foundation soil at the site was a non-plastic silty sand (SM). The existing silty sand was used as backfill and was compacted to a minimum of 95% of the maximum dry density determined by a Standard Proctor Compaction Test (ASTM 698-D). Backfill placement and compaction procedures will be discussed later in detail. The final depth of soil cover over the crown of the structure was approximately 2 feet.

FIELD MEASUREMENTS OF DEFORMATIONS DURING BACKFILLING

Culvert deformations were monitored at two culvert sections during backfill placement and compaction. As shown in Figure 2(a), these sections (A-A and B-B) were separated by approximately 20 feet and were both located approximately 40 feet from the ends of the culvert to avoid any influence of restraint provided by the two reinforced concrete endwalls. At both cross sections, the displacements of 13 measurement points were monitored relative to a pair of reference points at the base of the culvert haunches, as illustrated in Figure 2(b). The change in span between the two reference points was also measured, and all relative displacements were corrected accordingly. Monitoring the relative displacements of these fifteen points permitted determination of the deformed shape of each of the full cross sections at any given stage of backfill operations.

The distances between the measuring points and each of the two reference points at each section were measured using lightweight steel tapes. The measuring points were permanently established by means of marker bolts, and the ends of the steel tapes were held to the ends of these bolts by means of a fixture at the end of a pole which was designed to mate consistently with the measuring points. Tape tension was kept constant, and no correction was made for thermal expansion or contraction of the tape because the estimated maximum correction was less than 1/16 inch under the least favorable conditions encountered. Numerous practice measurements were taken before backfill operations began until it was demonstrated that all measurements could be repeated consistently within ± 3/32-in. At the end of each day of construction operations a number of the most recent measurements were repeated at random to verify that this level of measurement accuracy was maintained.

No special steps were taken to control backfill operations, but it was found that measured deformations of Sections A-A and B-B were very similar at all backfill stages, as illustrated by Figure 3 which shows the final deformed culvert shapes at both measured sections upon completion of backfill placement and compaction. Throughout the remainder of this paper, all "measured" deformations reported will represent averaged deformations for the two measured sections.

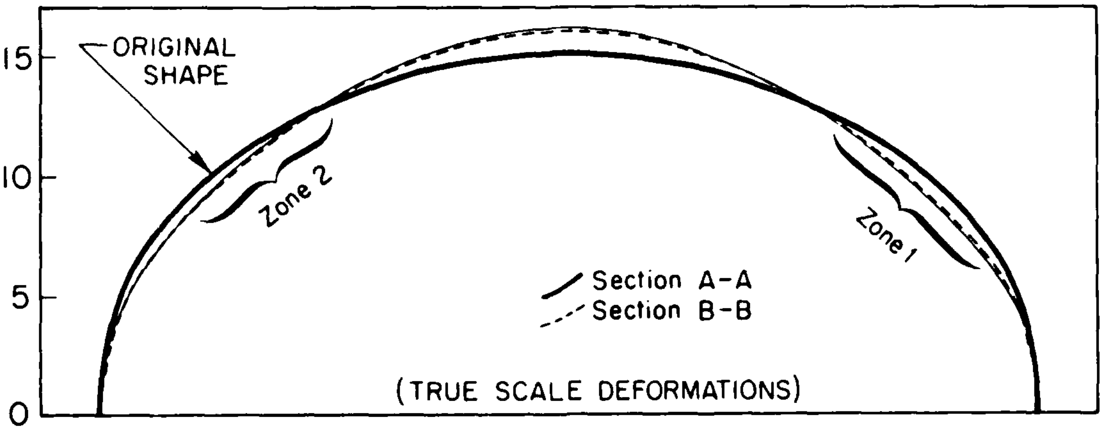

Fig. 3 Final Deformations of the Vista Culvert at Measurement Sections A-A and B-B

The large inward radial deflections at the upper quarter point regions shown in Figure 3 were considered excessive and unacceptable, as they represented "flattening" and even minor reversal of curvature in these key regions. This, in turn, led to concerns regarding long-term stability. Accordingly, the last five feet of backfill were removed, allowing the culvert to "rebound". The upper backfill was the replaced and compacted using light compaction equipment in order to minimize deformations. This resulted in an acceptable final culvert configuration.

Figure 4 shows measured deformations at three backfill stages: (a) backfill midway up the haunches, (b) backfill approximately 1.5 feet below the crown, and (c) the final soil cover depth of 2.0 feet. In Figure 4, deformations are exaggerated by a factor of 5 for clarity. The general pattern of culvert deformations consisted of decreasing span and inward flexure of the quarter points at the juncture of the haunch and crown sections with increasing fill height, accompanied by an upward movement of the crown ("peaking"). The backfill elevation was carefully maintained at nearly the same level on both sides of the culvert at all fill stages, and placement and compaction operations were sufficiently similar on both sides of the culvert at any given fill stage that deformations of both sides of the culvert were largely symmetric as shown in Figure 4. Maximum peaking of the crowns of both measured culvert sections was approximately 12.5 inches, and the maximum inward radial deflection at the upper haunches was approximately 9 inches.

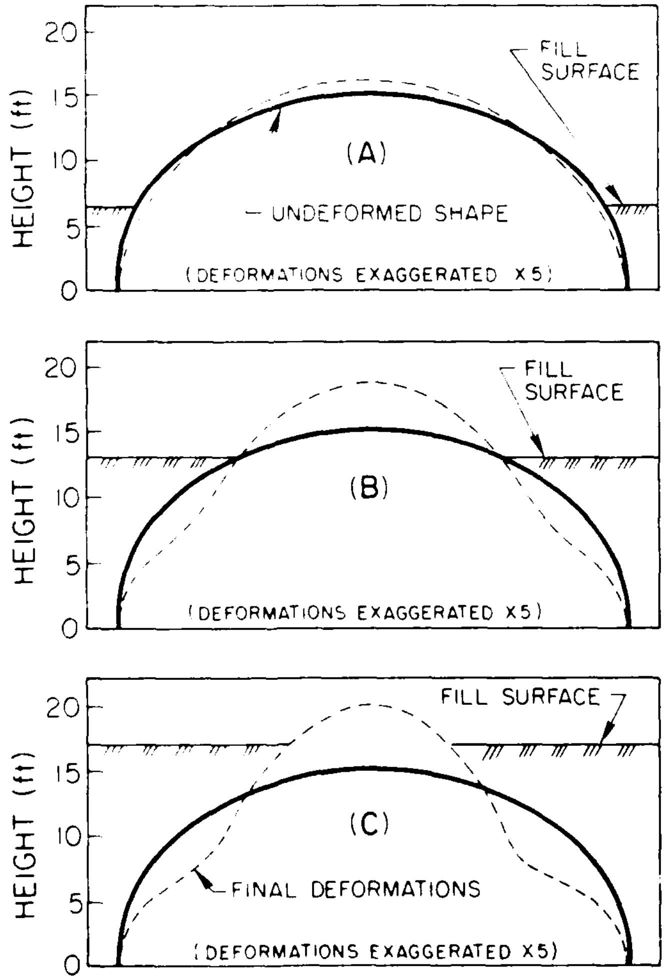

Fig. 4 Measured Deformation at Three Stages

The measured culvert deformations can be well characterized by monitoring the vertical deflection of the crown point and the radial deformation of the quarter point, as shown in Figures 4 and 5. In Figure 5, which shows crown and quarter point deflections as a function of backfill level, it can be seen that as backfill was placed above the crown of the structure, peaking reversed and the crown began to descend slightly under the weight of the new crown cover fill.

OBSERVATIONS DURING BACKFILL PLACEMENT

The most important factors affecting the magnitude of compaction-induced earth pressures around the perimeter of the culvert are the contact pressure, footprint geometry and closest proximity to the point of interest achieved by any given compaction (or other construction) vehicle at any stage of backfill placement (Seed & Duncan, 1986). In order to properly model compaction-induced earth pressures acting against the culvert, it was thus necessary to continuously monitor the closest proximity to the culvert achieved by each construction vehicle at each stage of backfill placement and compaction, and field observers maintained a detailed and continuous record of this.

Six types of construction equipment were used during backfill operations: (a) a CAT D8H tracked dozer, (b) a CAT 824B rubber-tired dozer, (c) a CK780 backhoe/blade with four rubber wheels, (d) a 4,500-gallon water truck, (e) a two-drum vibratory hand roller, and (f) a single-drum vibratory roller pulled by a small Bobcat tractor. Fill was brought to the site in dump trucks, but these trucks never passed near to the structure.

Long-span "flexible" culverts are known to be susceptible to compaction induced deformations. Accordingly, it is common practice to require that only light hand compaction equipment operate in close proximity to the structure, while larger vehicles operate at some larger distance from the structure. Unfortunately, these requirements are sometimes poorly enforced and/or poorly understood by the contractor placing the fill. This was the case for this project.

Initially, as fill was placed at the lower haunches, only the small hand compactor operated within four feet of the structure, and the dump trucks and large water truck were kept at least 8 feet from the structure, even when operating as compactors. The zone 3 to 8 feet from the structure was compacted with the medium-sized rubber-tired vehicles.

At later backfill stages, however, as the fill reached the upper quarter point region, the contractor began to increasingly encroach on the structure with larger vehicles. This, in turn, led to a significant increase in compaction-induced earth pressures against the culvert and compaction-induced culvert deformations. At a fill stage of approximately 2 feet below the crown, the large water truck passed to within very close proximity of the culvert (about 3-foot separation) along both sides of the structure. This produced readily noticeable plastic deformations which can be clearly seen in Figure 5. The contractor was promptly warned at this point, and no further instances of extremely large vehicle loads passing in close proximity to the structure occurred. Relatively large vehicles, including the CAT 824B and the CK780 did, however, continue to be used to compact inadvisedly close to the structure (to within 2 to 3 feet of the structural plate) in this upper quarter-point fill region.

The degree of compaction achieved has only a minor effect on the magnitude of soil stresses induced by compaction but has a significant influence on the stiffness of the backfill. For this reason it was also necessary to closely monitor the degree of compaction achieved at all points in order to properly model backfill stress-deformation behavior in the finite element analyses performed. Based on constant observation of field operations, as well as 14 in-situ density tests, it was judged that the average density achieved was approximately 96% of the Standard Proctor maximum dry density at an average water content of approximately 7%. Density and water content variations were judged to be small.

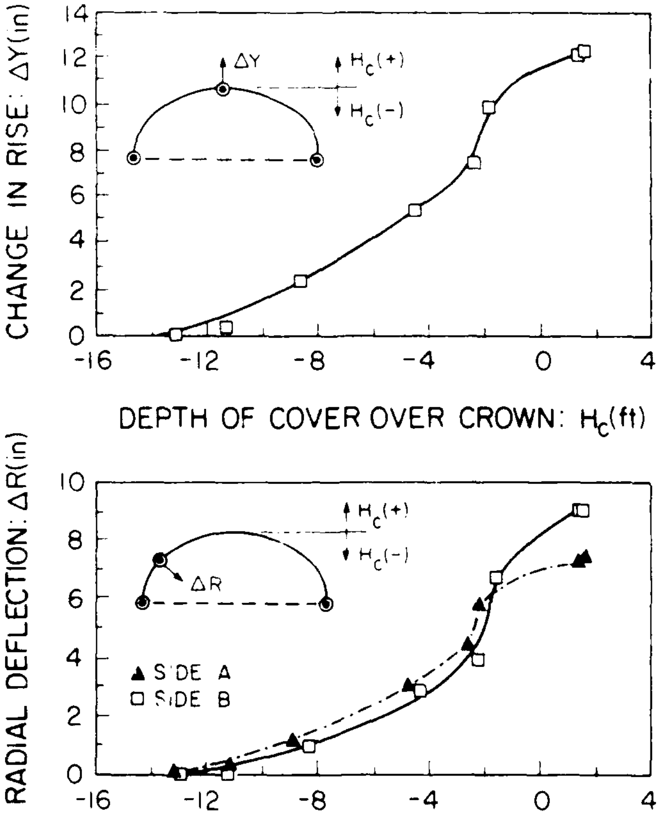

Fig. 5 Measured Deformations vs. Fill Height

FINITE ELEMENT ANALYSES PERFORMED WITHOUT MODELLING COMPACTION-INDUCED STRESSES

Two types of finite element analyses were performed in order to evaluate the significance of compaction effects on culvert deformations and stresses: (a) conventional analyses without any capacity for consideration of compaction-induced stresses, and (b) analyses incorporating recently developed finite element models and algorithms allowing consideration of compaction-induced soil stresses and associated deformations.

Both types of analysis used the hyperbolic formulation proposed by Duncan et al. (1980) as modified by Seed and Duncan (1983) to model nonlinear stress-strain and volumetric strain behavior of the soils involved, varying the values of Young's modulus and bulk modulus in each soil element as a function on the stress state within that element at any given stage of the analysis.

The conventional analyses, without compaction effects, consisted of modelling placement of fill in successive layers or increments. A two-iteration solution process was used for each increment to establish appropriate soil moduli in each element in order to model nonlinear soil behavior. These analyses were performed using the computer program SSCOMP (Seed & Duncan, 1984), a two-dimensional plane strain finite element code.

Figure 1(b) shows the finite element mesh used for these analyses. Only one-half of the culvert and backfill was modelled because of the symmetric nature of both the backfill operations and the measured deformations. Soil elements were modelled with four-node isoparametric elements and the culvert structure and underlying concrete members were modelled with piecewise-linear beam elements. Nodal points at the right- and left-hand boundaries of the mesh were free to translate vertically, but were rigidly fixed against rotation or lateral translation providing full moment transfer at the culvert crown and the centerline of the concrete base slab.

The program SSCOMP models all structural elements as deforming in linear elastic fashion, and this was appropraite as calculated structural stresses remained within the linear elastic range. Structural properties used to model the various components of the culvert structure were based on large-scale flexural test data, and are listed in Table 1.

TABLE 1. Structural Properties Modelled

Structural Component	E (kips/ft^2)	I (x10^4) (ft^4/ft)	Area (ft^2/ft
Concrete Sections	464,000	0.75	352.0
Haunches (No Ribs)	1,468,000	0.0194	0.774
Crown (Rib)	1,468,000	0.0282	3.98

A series of isotropically consolidated, drained triaxial tests with volume change measurements were performed on samples of the backfill soil. Samples were compacted to approximately 95% of the Standard Proctor maximum dry density, taken as representative of field conditions, and were tested at effective confining stresses of between 7.6 and 21.8 psi. Figure 6 shows the results of these tests, as well as the modelled soil behavior based on the following hyperbolic soil model parameters: $\gamma = 126$ pcf, $c = 0$, $\phi = 38.6°$, $\Delta\phi = 7.2°$, $K = 730$, $n = 0.3$, $R_f = 0.85$, $K_b = 200$, $m = -0.1$, and $K_{ur} = 1100$. Modelled stress-strain behavior is in excellent agreement with the test results. Modelled volumetric strain behavior agrees well with the test data at low stress levels, but diverges at higher stress levels because the hyperbolic soil model used cannot model dilatency.

The open squares in Figure 7 illustrate the results of incrementally modelling fill placement without compaction-induced stresses using the program SSCOMP. As shown in this figure, calculated culvert displacements at the crown point are only approximately 40 percent of the measured values at all fill stages, and the maximum calculated radial deflection of the quarter point is less than one-fifth of that measured in the field. It is unlikely that this magnitude of discrepancy between deformations calculated without consideration of compaction effects and the actual field measurements is due to poor modelling of soil or structural stiffnesses, as these are all based on reliable test data, and it thus appears likely that compaction-induced earth pressures significantly influenced the measured field deformations.

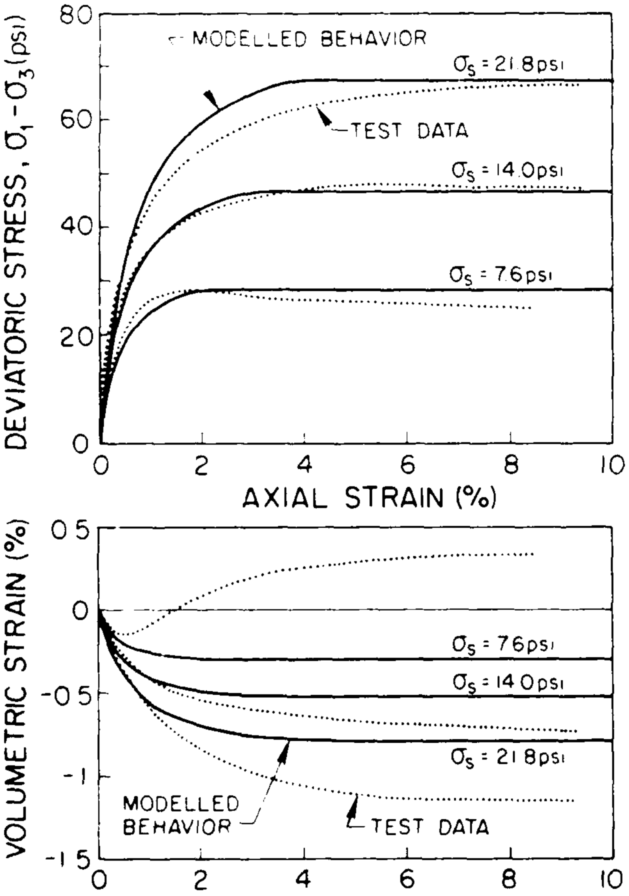

Fig. 6 Modelled vs. Measured Soil Behavior

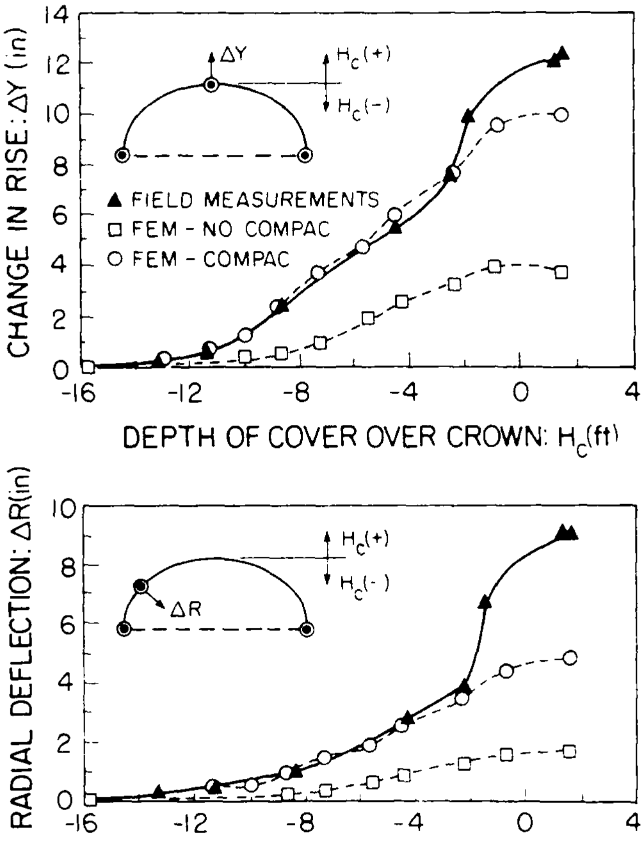

Fig. 7 Measured Culvert Deformations vs. Values *Calculated With and Without Compaction*

FINITE ELEMENT ANALYSES WITH MODELLING OF COMPACTION EFFECTS

A second set of finite element analyses were performed, this time using the program SSCOMPN (Ou, 1987), to model the effects of compaction-induced earth pressures. These analyses again incrementally modelled the placement of backfill in layers, but after each backfill placement increment an additional two-iteration solution increment was used to model the effects of compaction operations at the surface of the new backfill layer. The models and analytical procedures used to simulate compaction effects are described in detail by Seed and Duncan (1987), and a slightly modified hysteretic stress-path model developed by Ou (1987) was incorporated in these analyses. As these are unfortunately rather complex, only a brief general description follows.

Two soil behavior models are employed in these analyses. Nonlinear stress-strain and volumetric strain behavior is again modelled with the hyperbolic formulation used for the conventional analyses without compaction. The second soil behavior model is a model for stresses generated by hysteretic loading and unloading of soil. This hysteretic model performs two roles during analyses: (a) it provides a basis for the controlled introduction of compaction-induced soil stresses at the beginning of each compaction increment, and (b) it acts as a "filter," controlling and modifying the compaction-induced fraction of soil stresses during all stages of analysis.

Horizontal stresses within a given soil element are considered to consist of two types of fractions defined as: (a) geostatic lateral stresses ($\sigma_{x,o}$), which include all stresses arising due to increased overburden loads and deformations which results in lateral stress increases, and (b) compaction-induced lateral stresses ($\sigma_{x,c}$), which are the additional lateral stresses arising at the beginning of each compaction increment as a result of transient compaction loading. The overall lateral soil stress (σ_x) at any point is then the sum of the geostatic and compaction-induced stresses.

Compaction-induced lateral stresses are introduced into an analysis during "compaction" increments. Both the peak and residual compaction-induced lateral stresses at any point are modelled based on the peak, virgin compaction-induced horizontal stress increase ($\Delta\sigma_{x,vc,p}$) which is defined as the maximum (temporary) increase in horizontal stress which would occur at any given point as a result of the most critical positioning of any surficial compaction plant loading actually occurring if the soil mass was previously uncompacted (virgin soil). This use of $\Delta\sigma_{x,vc,p}$ allows consideration of compaction vehicle loading as a set of transient surficial loads of finite lateral extent which pass one or more times over specified portions of the fill surface, properly modelling the three-dimensional nature of this transient concentrated surface loading within the framework of the two-dimensional anlayses performed. The need to model the most critical positioning actually achieved by each compaction vehicle relative to each soil element at each backfill stage necessitated the constant monitoring of vehicle movements during backfill operations.

$\Delta\sigma_{x,vc,p}$, which is independent of previous hysteretic stress history effects, can be evaluated using 3-D linear elastic analyses, and is directly input for each soil element at the beginning of each compaction increment. The hysteretic soil behavior model then accounts for previous hysteretic loading/unloading cycles (e.g., previous compaction increments) and calculates both the actual peak and residual lateral stress increases on planes of all orientations within a soil element (residual vertical stress remains constant) based on $\Delta\sigma_{x,vc,p}$ and the previous hysteretic stress history of the soil element.

In addition to establishing the magnitudes of residual compaction-induced lateral stresses introduced at the beginning of each compaction increment (prior to nodal displacements and associated stress redistribution), the hysteretic soil behavior model also acts as a "filter," controlling and modifying the compaction-induced component of stress in soil elements at all stages of analysis. All calculated increases in σ_x at any stage during an analysis are considered to represent an increase in geostatic lateral stress and represent hysteretic "reloading" if a compaction-induced stress component is present. Subsequent to the solution of the global stiffness and displacement equations for any increment, therefore, the resulting calculated increases in σ_x are used as a basis for calculating an associated decrease in the compaction-induced fraction of lateral stress ($\sigma_{x,c}$). This progressive erasure or "overwriting" of compaction-induced lateral stresses by increased geostatic lateral stresses results in an overall increase of σ_x less than the calculated increase in $\sigma_{x,o}$ for soil with some previously "locked-in" compaction-induced lateral stress component, and corresponds to hysteretic "reloading." When solution of the global stiffness and displacement equations results in a calculated decrease in σ_x, it is assumed that this decrease is borne by both the geostatic and compaction-induced fractions of the pre-existing lateral stress in direct proportion to their contributions to the overall lateral effective stress.

Compaction-induced lateral stress increases in a soil mass can exert increased pressure against adjacent structures, resulting in structural deflections which may in turn partially alleviate the increased lateral stresses. Multiple passes of a surficial compaction plant, however, continually re-introduce the lateral stresses relaxed by deflections and result in progressvie rearrangement of soil particles at shallow depths. In order to approximate this process with a single solution increment, both compaction-induced lateral stresses and the corresponding nodal point forces for a given compaction increment are assumed to represent "following" loading from the current ground surface down to the depth at which $\sigma_{x,c}$ exceeds $\sigma_{x,o}$. All soil elements above this depth are assigned neglible moduli, resulting in calculations of displacements at all locations as a result of compaction-induced lateral forces, but (a) no changes in soil stresses result from displacements in soil elements above the specified depth of "following" compaction loading, and (b) compaction-induced nodal forces in this upper region are also undiminished by deflections.

Four additional soil parameters are needed for the hysteretic model controlling compaction-induced soil stresses, and these may be evaluated by correlation with the soil strength parameters c and ϕ (Seed & Duncan, 1986; Ou, 1987). The model parameters used for this analysis were: $K_o = 0.38$, $c_B = 0.0$, $K_{1,\phi,B} = 4.32$ and $\alpha = 0.57$.

Calculation of the peak, virgin compaction-induced lateral stress ($\Delta\sigma_{x,vc,p}$) to be input into each soil element at the beginning of each compaction increment is a time-consuming process. In the "free field" away from the culvert, three-dimensional linear elastic analyses were performed using Boussinesq closed-form solutions to calculate the peak lateral stresses induced at any given depth by each piece of construction equipment. These vlaues were then enveloped to produce a single profile of $\Delta\sigma_{x,vc,p}$ vs. depth which was used for all soil elements occurring at a distance of more than 6 or 7 feet from the culvert at all fill stages.

For soil elements near the culvert it was necessary to carefully review the recorded field observations in order to model peak stresses arising as a result of the most critical positioning (closest proximity) achieved by each piece of compaction equipment at each fill level. Initially, at fill levels up to the top of the haunches, the small hand compactor controlled peak compaction-induced stresses ($\Delta\sigma_{x,vc,p}$) adjacent to the culvert. At fill levels above the haunches, however, larger vehicles began to exert increasing influence on values of $\Delta\sigma_{x,vc,p}$ for soil elements in the region of the quarter point midway between the haunch and crown.

The analyses performed with SSCOMPN used a nonlinear structural behavioral model which modelled the same behavior in the elastic range as was used for the previous analyses without compaction modelling, but which modelled nonlinear deformation behavior in the inelastic stress ranges. Parameters were again based on larg-scale flexural test data.

The open circles in Figure 7 show the results of incrementally modelling both backfill placement and compaction. Modelling of compaction effects has resulted in significantly improved agreement between calculated and measured culvert deflections at all backfill stages, as compared to the earlier analyses without compaction. The calculated maximum crown rise (peaking) of 10 inches represents an increase of 150% over the maximum peaking of 4 inches calculated by conventional analyses without consideration of compaction effects, and is only about 20% less than the value actually measured. Modelling compaction effects also more than doubled the maximum calculated radial displacement of the quarter point to more than 5 inches. This new value is still considerably less than the value actually measured, but this is due in large part to the large inelastic inward radial deflections caused by the close approach of the large water truck to the structure at a fill stage of approximately 2 feet below the crown, as discussed previously. Until this point, agreement between calculated and measured deflections was nearly perfect.

Figure 8 shows culvert bending moments and axial thrust around the culvert perimeter following completion of backfill operations as calculated in both sets of finite element analyses performed (with and without compaction). In Figure 8(a) it can be seen that modelling compaction effects resulted in increased bending moments in both the crown and haunch regions. The increased positive crown moment results in a factor of safety of only 1.45, which is less than that allowed for design. This is not of serious concern for design purposes, however, as it is still below the level required for the onset of plastic yield and represents an increase in the ability of the crown section to withstand subsequent negative moments which will arise due to live traffic loads.

The increased bending moments at the top and base of the unreinforced haunch region are considerably more serious. Without compaction effects the calculated minimum factor of safety with regard to exceeding the plastic moment capacity in the haunch region was more than 2.5, apparently representing conservative design. Modelling compaction effects reduced this factor of safety to slightly less than 1.0 (FS = 0.93) at the top of the haunch region and FS = 1.8 at the base, and both of these moments correspond to flexure in directions representing potential failure modes. These moments, together with the resulting unacceptable deformed shapes of the upper haunch and quarter point regions, led to the decision to excavate the last five feet of fill. This permitted the structure to rebound, and the backfill was then replaced using only light hand compaction equipment to minimize compaction-induced stresses and deformations. This resulted in an acceptable final structural configuration.

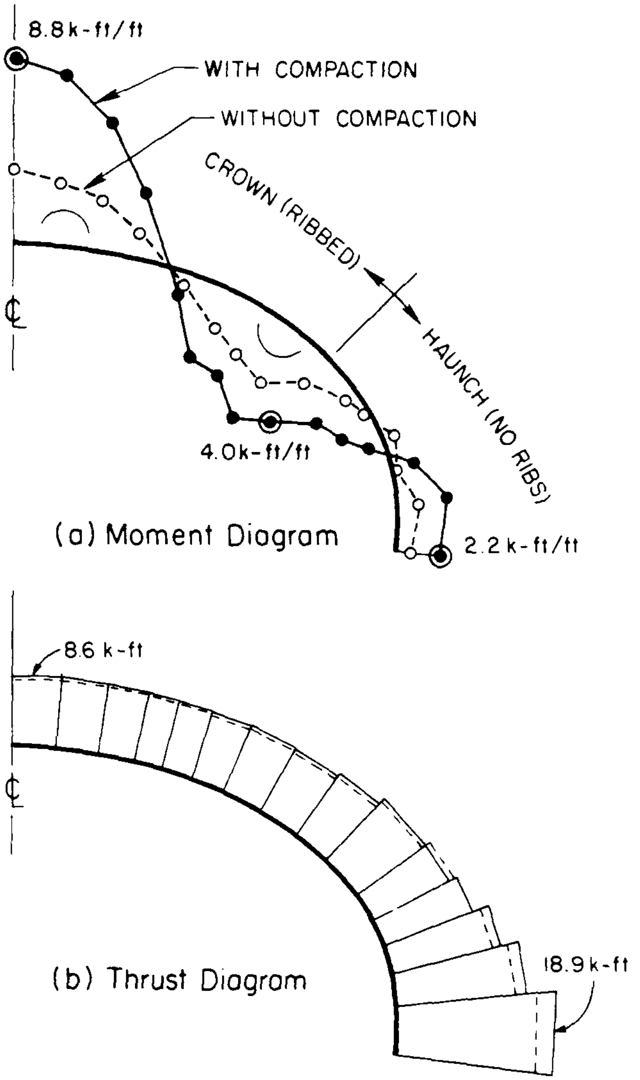

Fig. 8 Calculated Culvert Bending Moments and Thrusts With and Without Compaction

In Figure 8(b) it can be seen that modelling compaction-induced earth pressures resulted in calculation of only minor increases in thrust around the perimeter of the culvert. These increases, which were between zero and 15% around the culvert perimeter, were much less pronounced than was the effect of modelling compaction on calculated culvert bending moments.

SUMMARY AND CONCLUSIONS

Two types of finite element analyses were performed as part of these studies: (a) conventional analyses which were well able to model incremental placement of backfill in layers, but which cannot model compaction-induced stresses and deformations, and (b) analyses incorporating recently developed behavioral models and analytical procedures which do permit modelling of compaction effects. The results of these analyses were compared with the field measurements of culvert behavior, and these comparisons showed that compaction-induced earth pressures resulting from poor backfill compaction procedures were the principal cuase of the unsatisfactory structural behavior observed. This conclusion was well-supported by the satisfactory culvert performance following excavation (and rebound) and careful recompaction of the upper backfill zone. In addition, these studies provided good support for the accuracy and effectiveness of the new behavioral models and finite element analysis procedures used to model the effects of soil compaction.

ACKNOWLEDGEMENTS

Support for this research was provided by Kaiser Aluminum and Chemical Corporation as well as by the National Science Foundation under Grant No. NSF-11637, and this support is gratefully acknowledged. The authors also wish to extend their thanks to Mr. Mony Antoun of Kaiser Aluminum and Chemical Corporation for his valuable assistance during the field operations involved in this project.

REFERENCES

Duncan, J.M., Byrne, P., Wong, K.S. and Mabry, P. (1980). "Strength, Stress, Strain and Bulk Modulus Parameters for Finite Element Analyses of Stresses and Movements in Soil Masses, Geotechnical Engineering Research Report No. UCB/GT/80-01, University of California, Berkeley.

Seed, R.B. and Duncan, J.M. (1983). "Soil-Structure Interaction Effects of Compaction-Induced Stresses and Deflections," Geotechnical Engineering Research Report No. UCB/GT/83-06, University of California, Berkeley.

Seed, R.B. and Duncan, J.M. (1984). "SSCOMP: A Finite Element Program for Evaluation of Soil-Structure Interaction and Compaction Effects," Geotechnical Engineering Research Report No. UCB/GT/84-02, University of California, Berkeley.

Seed, R.B. and Duncan, J.M. (1986). "Compaction-Induced Stresses and Deformations for Yielding Structures," Journal of the Geotechnical Engineering Division, ASCE, Vol. 112, No. 1, January.

Seed, R.B. and Ou, C.Y. (1987). "Measurement and Analysis of Compaction Effects on a Long-Span Culvert," Transportation Research Record, No. 1087, pp. 37-45, January.

Ou, C.Y. (1987). "Finite Element Analysis of Compaction-Induced Stresses and Deformations," Ph.D. Thesis, Stanford University, November.

Proceedings: Second International Conference on Case Histories in Geotechnical Engineering, June 1-5, 1988, St. Louis, Mo., Paper No. 6.11

Three Examples of Innovative Retaining Wall Construction

Lee W. Abramson
Senior Geotechnical Engineer, Parsons Brinckerhoff Quade & Douglas, Inc., San Francisco, California

William H. Hansmire
Senior Professional Associate, Parsons Brinckerhoff Quade & Douglas, Inc., Honolulu, Hawaii

SYNOPSIS: The performance of three recently constructed retaining walls are compared. The first case involves a precast concrete panel element wall for the ventilation building of the 9-mile-long Rogers Pass railroad tunnel in British Columbia. In the second case, the widening of Interstate 75 near the Georgia Institute of Technology campus required widening of the Fifth Street bridge and high adjacent retaining walls. Tieback construction with soldier piles and wood lagging was used for temporary excavation support and then combined with a cast-in-place concrete facing for the permanent retaining wall structure. The third case involves slope cuts for access to the portal of the pilot tunnel for the Cumberland Gap highway tunnel project. The use of soil nails and shotcrete minimized the cut and allowed a fairly steep slope in soil which best conformed to the look of the natural countryside. Load measurement and wall deflection monitoring were performed for all three projects and are compared herein. The cases highlight the ability of reinforcement to knit the soil together, the validity of Terzaghi and Peck's apparent earth pressure diagrams for design, load transfer characteristics of soil reinforcement, the effect of wall system stiffness on horizontal deflections, and the importance of adequate drainage behind the walls.

INTRODUCTION

The past decade has brought with it several new and innovative methods for retaining the sides of cuts and excavations. Top-down support and incorporation of temporary support structures with permanent ones are two important changes in the way design and construction are now approached. Cost effectiveness and effects on adjacent structures are more important than ever. The purpose of this paper is to discuss three case histories that exemplify some of the new excavation retaining methods being used today. Performance of these walls is assessed and compared to other published case histories.

ROGERS PASS VENTILATION BUILDING ELEMENT WALL

The Rogers Pass Tunnel is a 9-mile-long railroad tunnel in British Columbia, Canada. Because of its unusually long length (longest rail tunnel in North America), a special system for ventilation was used. Part of this system consists of a mid-tunnel 1000-ft-deep shaft connecting the tunnel to the ground surface where most of the ventilation equipment is located. A 25.5-ft-deep excavation for the building housing this equipment above the shaft had to be made at a remote and rugged hillside location. (Figure 1).

Thick overburden at the site consists of bouldery colluvium making constructibility of a typical soldier pile and wood lagging wall questionable. After considering various alternative solutions, a precast concrete panel "element wall" was selected. The element wall relies on permanent soil tiebacks for lateral stability and the concrete panels, or "elements" provide support between the tiebacks. An early use of this method is shown in Ground Engineering (1976). A savings was derived by using this particular method because the element wall became part of the permanent building structure acting as the back wall.

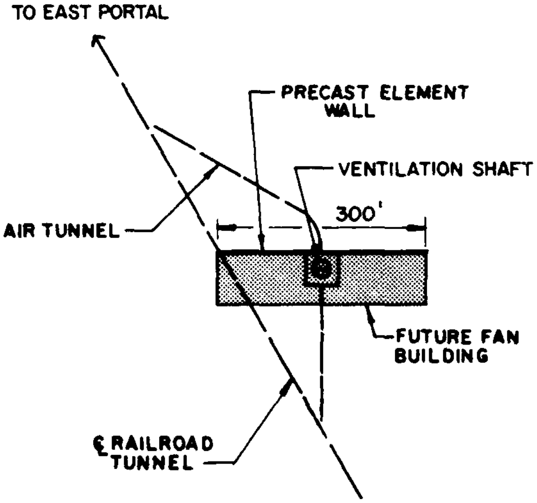

FIGURE I. ELEMENT WALL GENERAL SITE PLAN, ROGERS PASS

Element Wall Design

Parsons Brinckerhoff designed the element wall for the owner, CP Rail. The soil was generally described as dense, poorly graded, gravelly sand with some cobbles and boulders. The angle of internal friction was estimated to vary between 35 and 40 degrees. No cohesion was considered. Short-term lateral earth pressures assumed for the wall design were calculated based on Terzaghi and Peck (1967) apparent earth pressure envelope for braced cuts in sand. This short-term pressure envelope is equivalent to 65 percent of the active earth pressure at the wall base but is distributed uniformly along the height of the wall. The resultant total force is 1.3 times the theoretical active force. Because the wall also became part of the final structure, a long-term earth pressure loading was used (Schnabel, 1978). The long-term envelope is more conservatively based on the average of the active and at-rest earth pressures and was about 1.6 times the theoretical active case.

Tiebacks were spaced and sized based on the more conservative long-term loadings. The wall was not designed for water pressure because the permanent water table is far below wall level and drainage was provided behind the wall. However, the site is annually covered by snow during the winter and a surcharge snow load of 340 pounds per square foot was assumed.

Three rows of corrosion protected Dywidag bars, 1¼-inch diameter, were specified with horizontal and vertical spacing of 10 and 8 feet, respectively. A typical elevation and cross-section are shown in Figures 2 and 3. Tieback design loads were 76.5 kips for the top two rows and 112.5 kips for the bottom row. The upper cantilever wall and concrete element panels were designed for the combined earth pressure and tieback loading, as well as handling stresses for the precast units. Both panels and tiebacks were sized taking into consideration that the tiebacks would be proof tested to 133 percent of design load and locked off at 80 percent of design load. Tieback free lengths ranged from 16 to 36 feet and design bond lengths were 8 and 12 feet for the 76.5 and 112.5 kip design loads, respectively.

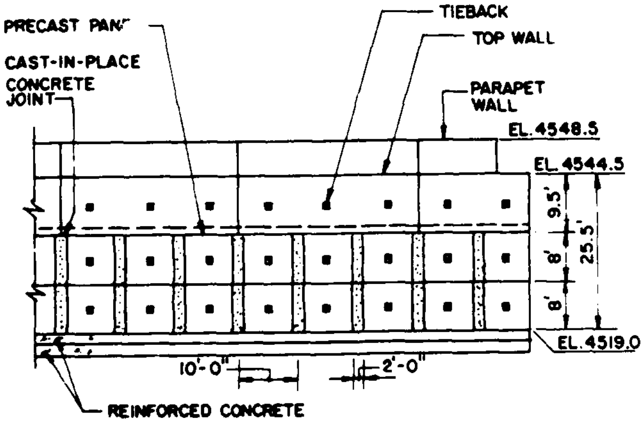

FIGURE 2. TYPICAL ELEMENT WALL SECTION, ROGERS PASS

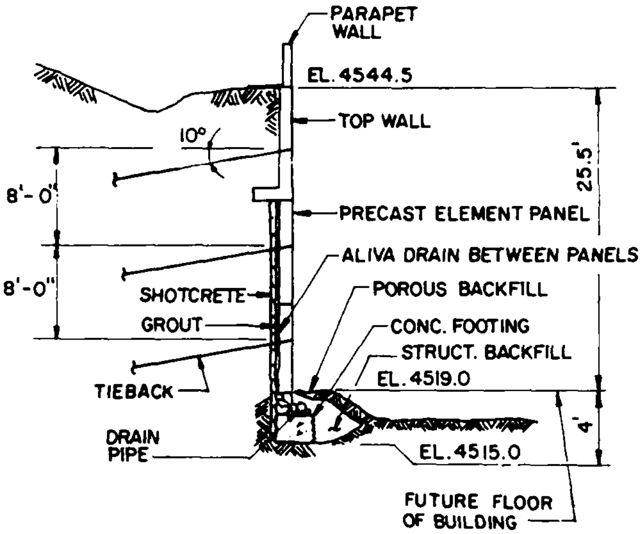

FIGURE 3. ELEMENT WALL CROSS SECTION, ROGERS PASS

Element Wall Construction

The top cantilever wall was constructed in the sequence of excavating, placing the cast-in-place concrete wall, installing the tieback, backfilling, and finally tensioning the tieback. The rest of the wall used precast panels installed in the sequence of excavating, shotcreting the soil face, placing the panels, installing and tensioning the tieback. A 2-ft-wide vertical space was left between panels and was later filled with cast-in-place concrete after installation of behind-the-wall drains.

On the whole, construction proceeded roughly in the manner specified and the structure was successfully built. However, design changes are frequently made in the field with structures such as these and was the case on this project. The soils were siltier than predicted on the basis of a few borings and several tiebacks failed proof testing. Bond lengths were consequently increased to 18 feet and from 28 to 33 feet for the 76.5 and 112.5 kip design loads. Failed tiebacks were replaced with longer ones.

Additionally, installing panels in the sequence specified was difficult for the contractor and was modified to suit his concept and equipment. Aliva drains proved to be difficult to install under these conditions and short PVC pipes pushed into the ground were substituted. Lastly, ground temperatures were lower than anticipated by the contractor and special methods were required to get proper tieback grout set-up and strength.

Element Wall Performance

Wall performance was assessed by means of lift-off tests, inclinometer readings, water seepage measurement, and visual observation. Lift-off tests were performed at 7, 15, 19, and 30 months. Schedule and completeness of lift-off testing varied with the on-going shaft excavation and lining schedule. Also, tieback loads were apparently affected by spring run-off and winter freezing of trapped water behind the wall.

Twenty-four-hour lift-off tests were performed on all tiebacks. A 5-percent load gain or loss in 24 hours (95 to 105 percent lock-off load) is commonly considered to be normal for tieback wall systems. The 24-hour readings indicated that nearly 60 percent of the tiebacks were within this range while about 35 percent of the tiebacks were holding less than 95 percent of the lock-off load, and about 5 percent were holding more than 105 percent of lock-off (Figure 4).

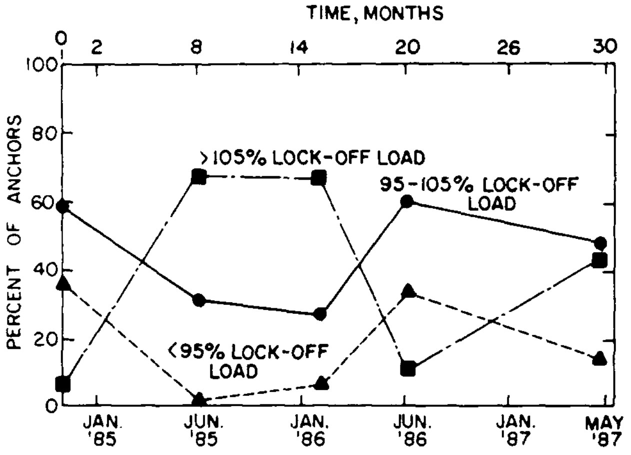

FIGURE 4. ELEMENT WALL ANCHOR LOAD VARIATION, ROGERS PASS

Usually tieback loads would be expected to stabilize within a few months of construction, but this was not the case at Rogers Pass. At 30 months, about 15 percent of the tiebacks held less than 95 percent lock-off, 40 percent held between 95 and 105 percent lock-off, and 45 percent held more than 105 percent lock-off. There appeared to be a tendency, particularly during springtime, for the tiebacks to gain load. However, by and large the tiebacks were stable in that most tiebacks above lock-off at 24 hours were above lock-off at 30 months. Likewise, tiebacks at 95 to 105 percent lock-off and ones less than lock-off tended to remain in the same categories over time. Continuous monitoring over a period of at least a year of a statistically significant population of tiebacks would have been required for a better understanding of the relationship of tieback load variation to changing environmental conditions.

Three inclinometers were installed 10 feet behind the wall. Inclinometer readings were taken at similar intervals as lift-off tests. At 30 months, maximum wall deflections ranged between 1/16 and 1/4 inches or, expressed another way, between 0.02 and 0.07 percent of the wall height (0.0002H to 0.0007H). According to Goldberg, Jaworski and Gordon (1976), soldier pile and lagging walls with tiebacks in similar soils usually do not deflect more than 0.25 percent of the wall height (0.0025H).

In spring of 1985, the first spring after construction, the wall became noticeably wet during snow melt. Water seeped between concrete panels and out of tieback bearing plates. The presence of water was first noticed at the low portions of the wall and rose higher presumably as water built up behind the wall. As the snow melt subsided, so did the signs of water behind the wall. Seepage was immediately perceived as a potential problem which indicated that the drainage system behind the wall was not functioning satisfactorily. Water flow around the tiebacks also posed a potentially serious long-term corrosion problem. Water seepage from the tieback heads was subsequently monitored during the following two snow melt (spring) seasons of 1986 and 1987. About two-thirds of the tiebacks were observed to have water seepage. Several tiebacks had relatively high seepage rates and seepage water carrying soil fines. As in 1985, seepage tended to increase with depth and occurred predominantly along the bottom row of tiebacks. Total seepage through the wall averaged between 3 and 8 gallons per minute during the spring of 1986 and was fairly constant during spring of 1987 at 5 gallons per minute.

In conclusion regarding the element wall at Rogers Pass, there was consensus among project personnel that the wall structurally was performing satisfactorily. Water seepage was not an imminent threat to stability, can probably be eventually reduced or eliminated, and in the interim can be accommodated by drainage from within the future building. Tieback loads exhibited variation with time, but trends of excessive loss or gain in load were not indicated. The horizontal movements were small in comparison to other experience. Braced cuts might be expected to have a maximum movement of 0.0025H or about 3/4 inch for H of 24.5 ft (Goldberg et al., 1976). This wall moved a maximum of 0.0007H (1/4 inch). Low lateral movements are attributed to the stiff soils and the construction procedure. By shotcreting the soil face immediately upon exposure and placing the concrete panels in a timely manner, a minimum amount of time was allowed for the soil to ravel and deform. Tieback prestress forces were sufficiently high to minimize further movement as excavation for lower rows of tiebacks took place.

INTERSTATE 75 PERMANENT TIEBACK WALL

At the time of this project (1983), earth anchored tieback walls had previously been used in Georgia for temporary earth retaining systems but had never been used as permanent retaining walls. Widening the I-75 highway required the construction of a retaining wall (Figure 5). The right-of-way limitations and potential effects of construction on the adjacent structures limited the type of retaining wall that could be built at this location. The traditional approach would be to construct a temporary earth anchored tieback wall and then to construct a permanent cantilevered retaining wall in front of the temporary system. However, with the approval from the Federal Highway Administration, the Georgia Department of Transportation chose to construct one of Georgia's first permanent earth anchored tieback walls at this location. This wall combined the temporary tieback wall and the permanent retaining wall and resulted in significant cost savings. Since the use of the permanent tiebacks was relatively new, the FHWA chose the wall as a demonstration project. The wall was instrumented to determine the long-term performance of such a system.

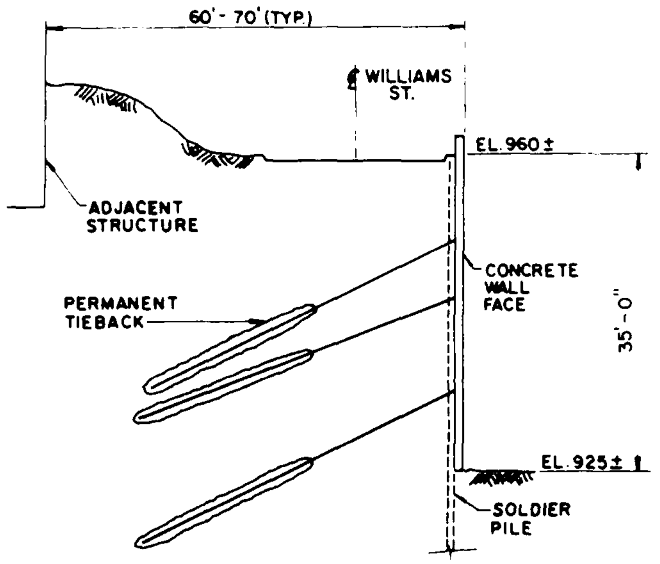

FIGURE 5. PERMANENT TIEBACK WALL CROSS SECTION, I-75
(MODIFIED FROM LAW/GEOCONSULT, 1985)

Tieback Wall Design

The soils immediately affecting the wall at this site are medium dense to very dense micaceous sandy silts and silty sands typical of Piedmont Province residual soils. Standard Penetration Test resistances range from 11 blows per foot to refusal (60 blows with no penetration). Soil density generally increases with depth but hard and soft layers occur frequently. Large slickensided surfaces were observed in the field. Groundwater was encountered approximately 40 feet below the ground surface. The depth to hard rock varies from 45 to 65 feet.

Design loading on the wall included active earth pressure, and impact and surcharge loads, which were included due to the close proximity of traffic on the adjacent Williams Street. These loads were to be resisted by pile embedment (passive earth pressure) and tieback loads. Active earth pressure loading was assumed to be a uniform distribution acting on the soldier piles and wood lagging above excavation level. This distribution was assumed to be 65 percent of the computed active earth pressure load at the excavation level, as described by Terzaghi and Peck (1967). Full active earth pressure was assumed to act on the soldier piles below excavation levels. Passive earth pressure resistance was assumed in front of the piles below excavation levels. No water pressure loading was assumed to act on the retaining wall since groundwater levels were deeper than excavation levels. Also, drainage fabric was installed behind the concrete facing to carry away any groundwater that might collect behind the wall.

Tieback loads were calculated using a structural computer program and were checked by hand calculations. Both methods consisted of summing forces and moments and checking for equilibrium. One level of tiebacks was included in a lower height portion of the wall, while the remaining portion of the wall included two levels. Design tieback loads ranged from 57 kips (in the lowest portion of the wall) to 138 kips. In cases where the design load in a tieback was not achieved during field proof testing, the requirement for an additional tieback was also calculated by summing moments and forces.

Tieback Wall Construction

Tieback wall construction involved several steps. First, the soldier piles were placed in augered holes extending from the top of the wall to a designated point below the bottom of the wall. Soldier piles ranged from 1-W18 x 50 steel beam at the lowest portion of the wall to 2-W18 x 46 at the highest portion. Concrete was poured in place around the piles from the bottom of the hole to the future ground line. Timber lagging was installed between the piling as the earth in front of the wall was excavated. At designated levels, holes were drilled through the piling into the earth behind the wall, at calculated lengths and angles. The 7 wire - 5 strand (0.6 inch diameter) tendons were then installed and grout was pressure injected at 2 pounds per square inch per foot of overburden.

After curing, the tiebacks were load tested and post tensioned to a predetermined load. The process of lagging installation and tieback installation was repeated until the excavation in front of the wall was complete. The final step was to install strips of drainage fabric over the lagging and to pour a cast-in-place concrete facing over the entire wall. The concrete was attached to the soldier piles by a series of studs embedded in the concrete.

The predetermined lock-off load for the tiebacks was normally 80 percent of the "design load". Occasionally conditions in the field were different from that assumed in design and the tieback would not hold the design load. When this happened, the "design load" was reduced to reflect actual capacity of the tendon and the designers assessed what effect the change in tieback load might have on the whole retaining system. With a redistribution of load, other tiebacks and toe embedment were found to be sufficient.

Tieback Wall Instrumentation

The instrumentation program was undertaken by Law/Geoconsult International for Georgia DOT and was intended to measure deflection of the wall face and soil behind the wall and to measure load variations in the tiebacks within the unbonded and bonded zones. Results of the instrumentation program are summarized below and in the report titled "Report of Field Performance - Permanent Tieback Wall" by Law/Geoconsult (1985).

Instrumentation consisted of many different monitoring devices. The performance of the wall was monitored with ten tiebacks that were instrumented with some combination of rod telltales, wire telltales, and permanent load cells. Conventional strain gages could not be used with the 7 wire - 5 strand tiebacks because of the inherent difficulty of mounting the gages to the tendons. Telltales were chosen as an alternative with a custom fitted fixation to the strand. The external movement of the wall system and adjacent structures was monitored with slope inclinometers and optical survey points.

Two monitoring stations, spaced approximately 135 feet apart, were used to monitor the wall performance at the highest portions of the wall. At each monitoring station, primary instrumentation was on both tiebacks on a soldier pile. Secondarily instrumented tiebacks were on adjacent soldier piles.

Instrumentation for the primary instrumented tiebacks (Figure 6) consisted of one rod telltale fixed to one of the strands of the 5-strand tieback at the interface of the unbonded and bonded zones. Also to this strand, five wire telltales were fixed within the bonded zone. It was assumed that all 5 strands in the tiebacks behaved the same and instrumentation of one strand would predict the behavior of the entire tieback. A second rod telltale was fixed to one of the remaining four strands at the end of the bonded zone. When the tieback was installed, a permanent load cell was mounted at the tieback lock-off point. The secondary instrumented tiebacks had only one rod telltale fixed to one of the 5 strands at the unbonded/bonded zone interface. No permanent load cell was used.

Tieback Wall Performance

Maximum horizontal wall deflection measured with inclinometers was 0.8 inches or 0.2 percent of the wall height (0.002H). Visual survey markers indicated somewhat higher deflections but less than 1.2 inches or 0.3 percent of the wall height (0.003H).

Goldberg, Jaworski and Gordon (1976) reported a range of horizontal movements of 0.1 percent and 0.6 percent of wall height (0.001H to 0.006H) for tieback walls in sand and gravel. Experience in the Atlanta area indicates that development of the active earth pressure case requires a horizontal wall movement of approximately 0.3 to 0.6 percent of wall height (0.003H to 0.006H). Movements of the permanent tieback wall are in the range of those generally associated with the active earth pressure condition for soils in the Atlanta area.

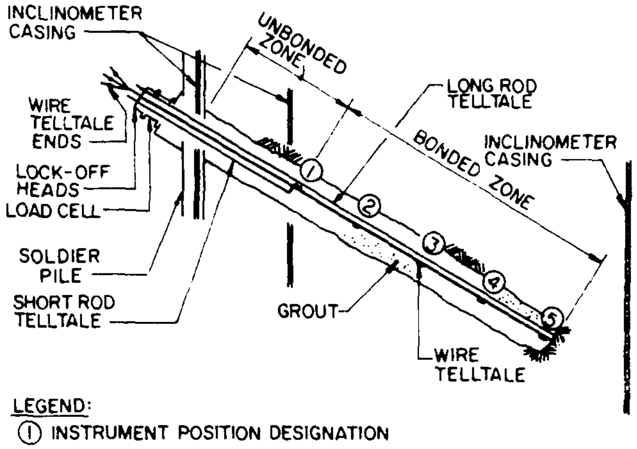

FIGURE 6. SCHEMATIC OF PRIMARY INSTRUMENTED TIEBACK, I-75
(LAW/GEOCONSULT, 1985)

Of most importance regarding tieback load variation are: tieback load loss or gain with time, and load transfer characteristics of the bonded zone. Of the ten tiebacks monitored, seven were holding between 95 and 105 percent of lock-off after 8 months. One tieback held less than 95 percent lock-off at 8 months and two held more than 105 percent. Readings since 1985 have indicated that the tieback loads remained relatively stable after 8 months with similar percent lock-off variations. The inherent flexibility of the retaining system (soldier piles, lagging, tiebacks, and concrete facade) allows for some variation in tieback loads and load readjustment to take place. Therefore, variation from lock-off is usually observed and should be expected within nominal bounds of ±5 percent of initial lock-off.

Because of the necessity to use telltales on the strands to measure load, accuracy was not expected to be as high as, say, electrical resistance or vibrating wire strain gages on steel bars (historically the more common way to instrument tiebacks). A comparison of load measurement accuracy for different types of instrumentation is given in Abramson and Greene (1985). Load in the strand can theoretically be calculated by taking the difference of displacement between two telltales (assuming uniform strain) and applying Hooke's Law to convert elongation to load. Although the goals of load transfer measurement were more or less realized, slippage of some of the telltales relative to the strand may have occurred adding to the uncertainty and inaccuracy of measurements.

The dependency of load transfer on bond zone elongation is shown in Figure 7 for three of the tiebacks at maximum loading (150 kips). With the stated caveats above, test data indicated that at low tieback loads, only a small portion of the bonded zone became loaded. As the tieback load was increased, the length of stressed bonded zone also increased. This increase apparently took place when the load transfer (slope of load distribution line) reached some limiting level which most likely was related to the shear strength characteristics of the soil. As the tieback load was increased, load transfer between the first and second wire telltales generally increased to some peak level and then decreased to a residual level. When this peak level between wire telltales 1 and 2 was reached, load transfer between wire telltales 2 and 3 began to increase at a faster rate. If tieback loading had continued, load transfer between wire telltales 2 and 3 probably would have peaked and a greater load transfer would have occurred between wire telltales 3 and 4. This apparent behavior was first reported by Abramson (1983) at the 34th Annual Highway Geology Symposium in Atlanta.

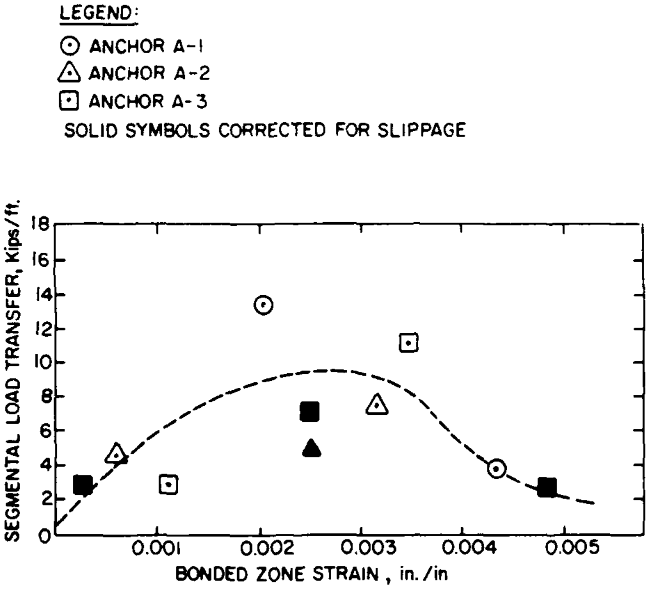

FIGURE 7. LOAD TRANSFER VERSUS BOND ZONE ELONGATION, I-75

Average load transfer distribution based on measurements from the four primary instrumented tiebacks is shown in Figure 8 for the maximum load condition of 150 kips. The average load transfer over the entire 6-inch diameter bonded zones (between 32 and 35 feet long) ranged between about 4 and 5 kips per foot of bond length. This is the range of values one would expect for SM-classified soils in Atlanta recognizing the fact that the relatively high mica contents tend to reduce shear strength somewhat. Load transfer between telltales exceeded the average of 4 to 5 kips per foot and reached a maximum of as much as about 8 kips per foot.

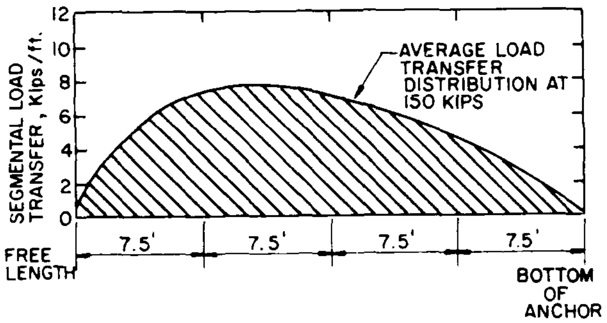

FIGURE 8. LOAD TRANSFER ALONG BONDED ZONE, I-75

The measurements described above are based on tieback loads measured with load cells. Tieback proof testing is commonly conducted using a jack pressure gage for the load indicator. It is commonly thought that the pressure gage is not a reliable indicator of tieback load in the unloading mode. A load cell was used to proof test every instrumented anchor. A comparison of jack pressure gage load to load cell reading was made. The results indicated that the jack gage overestimated load during loading and underestimated load during unloading. Load as measured by the jack had an apparent accuracy of ±5 to 10 percent.

CUMBERLAND GAP SOIL NAIL WALL

Twin highway tunnels will be constructed south of Cumberland Gap National Park along U.S. 25E to replace the 3-mile long, two-lane bottle-neck which presently exists. The Federal Highway Administration is managing the project for the National Park Service. Most of the route is four lanes wide and connects Interstate 81 at Morristown, Tennessee with Interstate 75 at Corbin, Kentucky.

A pilot tunnel was built during 1984 and 1985 to explore the complex geology at the site. Slope cuts were made at the Kentucky portal where pilot tunneling began. Most of the slope cut was within bedrock. However, the rock was overlain in places by as much as 40 to 45 feet of soil overburden and weathered rock. The site is within a national park and minimum disturbance to the environment is a high priority. To avoid damage to the natural slope and vegetation above the cut and to minimize the extent or flatness of the slope, soil nailing was chosen to reinforce the rather steep overburden cut. FHWA funded this work since future economics were foreseen from the use of this new technology. This project has been described by Nicholson (1986) and Juran and Elias (1987) previously and is only reviewed here for comparison to the other two case histories.

Soil Nailing Design

The wall was designed and built by Nicholson Construction. Peter Nicholson (1986) states that the general theory of soil nailing is "to build a gravity mass that is tied together and will act as a unit or coherent mass. As such, the structure must be analyzed for both external and internal stability." External stability includes sufficient safety factors against sliding, overturning, bearing capacity, and external slip circles. These factors are common to all gravity retaining structures and are not unique to soil nailing. No further explanation is warranted herein.

Internal stability relates to the length and spacing of nails necessary to insure that the soil acts as a mass. Nail spacing must be close enough so that the zones of influence overlap, generally between 5 and 15 times the nail diameter for fine and coarse grained soils, respectively. Each zone of influence is governed by the nail diameter and type of soil. Cumberland Gap overburden consists mainly of colluvial and residual soils that have resulted from the differential weathering of the underlying sandstone, siltstone, shale, and coal interbeds. The length of the nail is determined by the size of the active zone, generally 0.3H, and the load transfer capacity of the nail beyond the active zone.

For Cumberland Gap Project, Shen's (1981) method of design was used resulting in a triangular pressure distribution with the highest nail loads near the bottom of the wall. For the 40-foot high section of the wall, 20 to 30-foot-long nails were used on a 5-foot square grid pattern. The upper 3 or 4 rows of nails consisted of #8 Grade 60 reinforcing bars and #11 bars were used for lower rows.

Soil Nail Construction

The excavation through overburden was made at a slope of 1H:4V in 5 to 6-foot lifts. As the soil was exposed, drainage fabric strips were placed against the soil in 15-foot horizontal intervals and covered with a 3-inch thick layer of wet-mix shotcrete. Holes for the nails were then drilled perpendicular to the slope (about 15 degrees below horizontal) and between 4 and 4½ inches in diameter. The reinforcing bars were placed in the hole and tremie grouted into place with neat cement. Wire mesh, walers, and bearing plates were installed on each nail and the nails were stressed to 5 and 10 kips for the #8 and #11 bars, respectively, in order to insure intimate contact with the initial layer of shotcrete. After the bars were prestressed and cut off, a second 3-inch-thick layer of shotcrete was applied. As each row of nails was completed, excavation of the next lift commenced until sound bedrock was encountered. A drainage ditch was provided at the top of the wall and weeps were connected to the drainage fabric behind the shotcrete at the base of the wall. The completed cross section of the wall is shown in Figure 9.

Soil Nail Performance

Testing of the nails consisted of pull-out tests as well as production testing of bars during construction to 90 percent of bar yield. These tests yielded pullout strengths between 5 and 10 kips per foot for embedment lengths varying between 11 and 25 feet. This fit with predicted values assuming average overburden, an internal friction angle of 38 degrees, but a 7-inch-diameter drill hole.

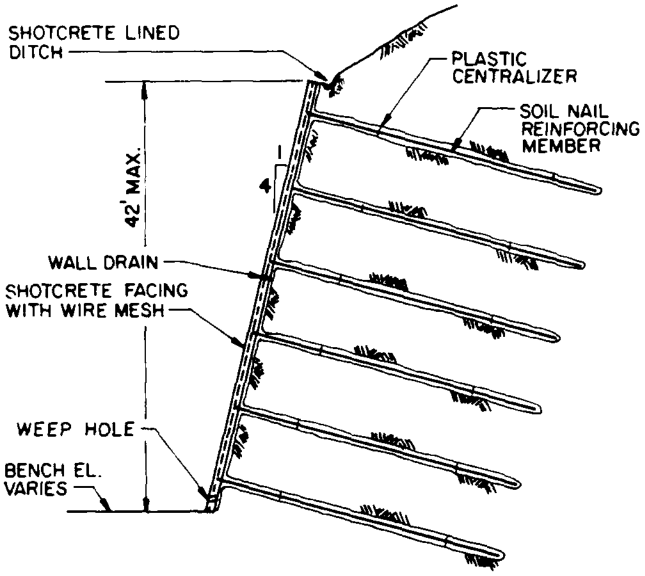

FIGURE 9. SOIL NAIL WALL SECTION, CUMBERLAND GAP
(NICHOLSON, 1986)

Inclinometers and survey markers were used to measure outward wall movement which was between 1/4 and 3/8 inches, or less than 0.2 to 0.3 percent of the wall height (0.002H to 0.003H).

Strain gages were installed on 16 of about 300 soil nails. Analysis of this data led Juran and Elias (1987) to the conclusion that "the measured variations of maximum tension forces with depth observed in the soil nailed structures are similar to empirical diagrams of earth pressure distribution......for the design of braced open cut supports." This is not consistent with the triangular pressure distribution used for design. Furthermore, water apparently did not drain freely from behind the shotcrete leading to freezing during the winter and additional tensile load on the nails (Figure 10). Nicholson (1986) recommended more frequent drain fabric strips to improve drainage on future projects.

COMPARISON OF THE THREE CASE HISTORIES

The three case histories presented were constructed in similar SM-SC soils. Despite different geologic origins, engineering properties of the soils were somewhat similar. The cuts were of similar heights between about 25 and 40 feet (Table 1). Tiebacks or "active" soil reinforcement were used on two of the walls, Rogers Pass and I-75, and had relatively high prestress loads. The other wall, Cumberland Gap, used soil nails or "passive" reinforcement with nominal prestressing to insure good contact with the surface reinforcement. Tieback and nail dimensions (diameter and length) were similar for all three cases.

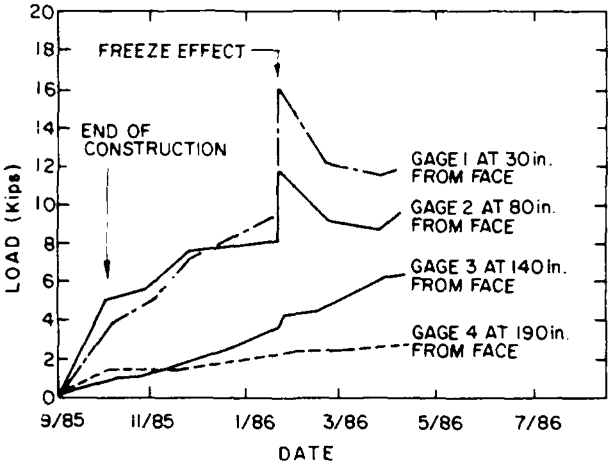

FIGURE 10. POST CONSTRUCTION MEASUREMENT OF NAIL FORCES AND FREEZE EFFECTS-CUMBERLAND GAP
(MODIFIED FROM JURAN AND ELIAS, 1987)

Design Approach

Three different critical factors related to design and function of the respective structures were exhibited by these three case histories. In the first case, the designers were strongly motivated to produce a conservative design for the wall of the ventilation building at Rogers Pass. Repair of the wall would be difficult once the ventilation equipment was installed. Failure of the wall would also result in costly interruption of rail service through the long tunnel. The design lateral loading was therefore selected to be significantly above active (1.6 times theoretical active), with the intent of avoiding long-term problems with the wall. The design earth pressure envelopes and the actual capacity of the anchors are shown in Figure 11a.

In the second case at I-75 in Atlanta, an adjacent street and buildings were of high concern to the designers. However, this case is not considered to be as critical as the first one where the wall was a specific element of the building structure. Use of total lateral earth pressure of 1.3 times theoretical active was considered appropriate for the I-75 case (Figure 11b).

In the third case at Cumberland Gap, no adjacent permanent structures were involved, and some movements could be tolerated. Using an enlightened approach for the time, soil nails

TABLE 1

COMPARISON OF WALL PERFORMANCE

Case	Type	Maximum Wall Height (H) ft.	Vertical Tieback Spacing (L) ft.	Wall Facade Stiffness (EI) kip-ft.^{2}	Estimated Wall System Stiffness (EI/L^4) ksf	Maximum Horizontal Deflection in. (%H)	Estimated Soil Stiffness $\frac{\gamma z(1-\sin\phi)}{c\cos\phi}$
Rogers Pass Vent. Building	Precast concrete panels and tiebacks	25.5	8	28,000*	7.2	1/4 (0.1)	1.5
I-75 and Fifth St., Atlanta	Soldier piles and lagging, tiebacks, and concrete face	34	8 to 9	32,000	5.6	1-1/4 (0.3)	2.5
Cumberland Gap Pilot Tunnel Portal	Shotcrete and soil nails	42	5	4,500 to 6,000	8.6	3/8 (0.1)	1.5

*for monolithic section

were used. In a coarse way, the design capacity was on the order of 1.0 times theoretical active, the lowest of all three case histories (Figure 11c). In addition, the soil nails were only lightly pre-tensioned, which was considerably different from the high proof loading and lock-off to 80 percent of design capacity that the tiebacks in the other two cases underwent. However, as stated below, the soil nailed wall performed as well, or better than, the other two cases.

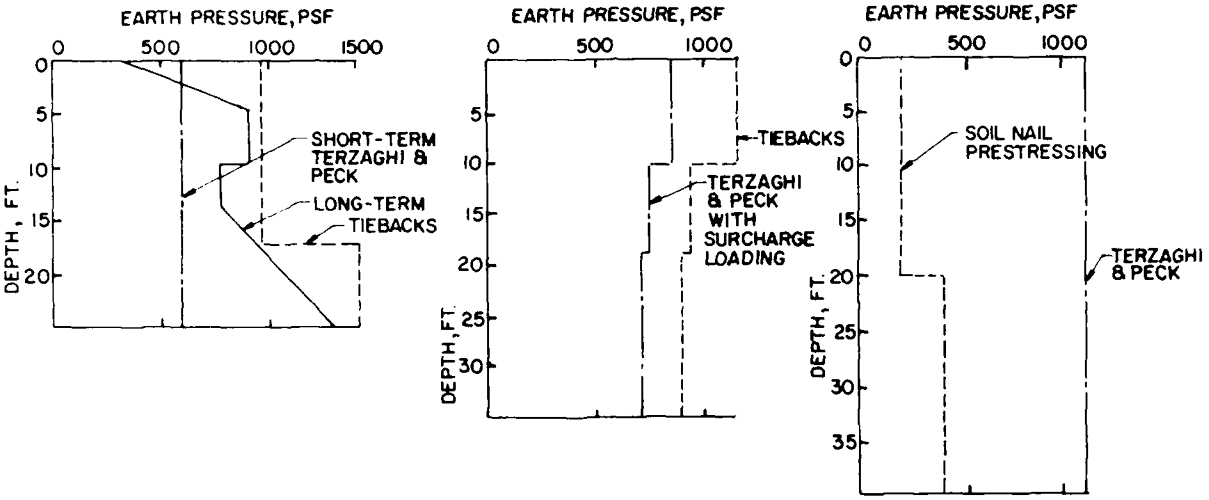

(a) ROGERS PASS VENTILATION BUILDING

(b) I-75 PERMANENT TIEBACK WALL

(c) CUMBERLAND GAP PORTAL

FIGURE 11. COMPARISION OF TYPICAL EARTH PRESSURES AND REINFORCEMENT PRESSURES

Performance

The most outstanding feature of all three cases was the performance of the wall built with soil nailing at Cumberland Gap. The conventional thinking in much of the world until the 1980's was that ground reinforcement for excavations in soils had to be pre-tensioned. The first two case histories, at Rogers Pass and I-75, exemplify such thinking. With numerically more elements of ground reinforcing, the soil nailed wall performed as well as the other two cases which were much more highly engineered and had high prestress forces.

All three walls performed satisfactorily for their purposes. Small ground movement in the range of 0.001H to 0.003H were observed. The largest movements were associated with the least stiff wall which was constructed in the weakest soil relative to wall height. Table 1 shows the stiffness of the I-75 wall to be about 2/3 that of the others, and the relative soil stiffness (stability ratio) to be over 1.5 times greater.

General Observations

The following observations have been made from these case histories:

1. Soil reinforcement tends to knit the soil together so that the reinforced soil acts as a gravity mass. This was so whether tiebacks (active reinforcement) or nails (passive reinforcement) were used. This concept of getting the soil to support itself rather than building a structure to resist maximum possible earth loads is analogous to current tunneling practice where rock bolts and shotcrete are used to create a reinforced rock arch.

2. The use of apparent earth pressure diagrams for braced cuts by Terzaghi and Peck (1967) remains an acceptable approach for the design of retaining structures which use tiebacks. On the basis of limited field evidence, it also appears to be acceptable for design of soil nail reinforcement.

3. The precise characteristics of anchor load transfer are still not known. However, the load transfer values commonly used in design are averages which automatically account for the variation in load transfer rates along the bonded zone. In places, peak load transfer may be two or three times the average value.

4. Horizontal wall deflections are a function of soil and wall stiffness. The strength of the soil certainly is an important factor. However, once that is known, the designer has significant lattitude in developing a wall system that will limit horizontal deflections when properly constructed (Figure 12). The cross sectional stiffness of the wall facing can be balanced with the vertical spacing of tiebacks or nails to obtain a compatible system which gets the soil to support itself.

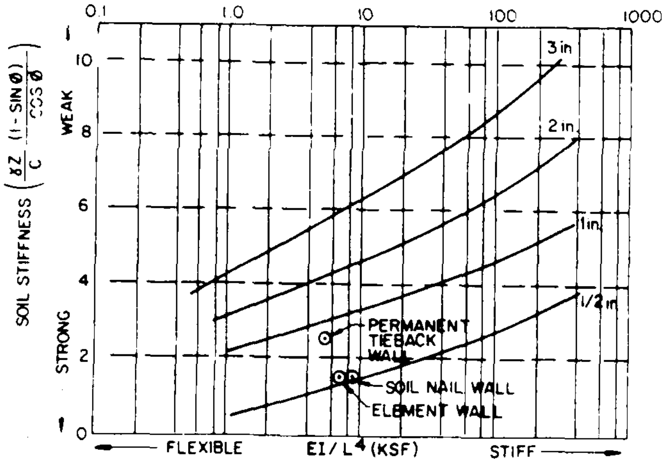

FIGURE 12. EFFECT OF WALL STIFFNESS AND SOIL STRENGTH ON LATERAL WALL DEFLECTIONS
(MODIFIED FROM GOLDBERG ET AL, 1976)

5. Walls which utilize tiebacks or soil nails are just as sensitive to water as any structure built with or with earthen materials. Flowing water (seepage) can cause accelerated corrosion of steel members as well as hydrostatic loadings for which the structure was not designed. If the water can be trapped behind the wall due to the absence of or faulty drainage and this water can be subjected to freezing temperatures, high ice jacking loads will result and can occur cyclically season after season. With the addition of a variety of very useful geotextile fabrics to the geotechnical industry, it has never been easier to design more than adequate yet economic drainage systems for retaining walls.

ACKNOWLEDGMENTS

The authors wish to acknowledge Mr. Ron Tanaka of CP Rail for permission to publish the case history on the Rogers Pass Ventilation Building Element Wall. Also we are grateful to Messrs. Tennock, Penner, and Hamilton who supplied field observations and records on which much of this case history is based. Mr. John Dunnicliffe was the instrumentation consultant for the I-75 tieback wall. Mr. Robert Leary of the FHWA managed the instrumentation efforts on both the permanent tieback and soil nail walls.

REFERENCES

Abramson, L. (1983), "Geotechnical Instrumentation of Modern Retaining Wall Designs in an Urban Setting", Proceedings of the 34th Annual Highway Geology Symposium, Atlanta, Georgia, May, pp. 87-127.

Abramson, L. and Green, G. (1985), "Reliability of Strain Gages and Load Cells for Geotechnical Engineering Applications", 64th Annual Transportation Research Board Meeting Symposium on Reliability of Geotechnical Instrumentation, Washington, D.C., January, TRB Publication No. 1004, pp. 13-19.

Goldberg, D., Jaworski, W., and Gordon, M. (1976), "Lateral Support Systems and Underpinning - Vol. II. Design Fundamentals", Federal Highway Administration Report No. FHWA-RD-75-129, April, pp. 13, 20, 23.

Ground Engineering (1976), "Germany's First Element Wall Installed in Stuttgart", by W.M.B., March, pp. 14-18.

Juran, I. and Elias, V. (1987), "Soil Nailed Retaining Structures: Analysis of Case Histories", American Society of Civil Engineers, Geotechnical Special Publication No. 12, New York, pp. 232-244.

Law/Geoconsult International (1985), "Report of Field Performance - Permanent Tieback Wall - Final Report", Georgia Department of Transportation Project PEI-75-2(41) Fulton County, May, 29 pp.

Nicholson, P. (1986), "Insitu Earth Reinforcement at Cumberland Gap, US25E", Penn DOT Conference, Harrisburg, Pennsylvania, April, 23 pp.

Schnabel Foundation Company (1978), "Permanent Tieback Manual", Engineering Criteria, Bethesda, Maryland, Figure 13.

Shen, C., Herrman, L., Rostadetal, K. et al, (1981), "In Situ Earth Reinforcement Lateral Support System", University of California - Davis, National Science Foundation Report No. NSF/CEE-81059.

Terzaghi, K. and Peck, R. (1967), Soil Mechanics in Engineering Practice, John Wiley and Sons, New York, Art. 48, pp. 394-413.

Proceedings: Second International Conference on Case Histories in Geotechnical Engineering, June 1-5, 1988, St. Louis, Mo., Paper No. 6.13

Anchored Bulkhead Failure on the Arabian Gulf

Jonathan J. Grosch
Supervisor, Geotechnical Unit, Arabian American Oil Company,
Dhahran, Saudi Arabia

Khalifa S. Al-Yahyai
Geotechnical Engineer, Arabian American Oil Company, Dhahran,
Saudi Arabia

SYNOPSIS: A 1500-m long anchored bulkhead with a height of 20 m exhibited a localized failure in the form of broken and overstressed anchors several months after construction. The wall had not yet been subjected to its full design loadings. The soil conditions in the failure area differ from those occurring along the rest of the quay wall by the presence of a very soft silt/clay layer, and during construction the wall had been strengthened in this area. Post-failure analysis of the anchored bulkhead indicated that the primary cause of the failure was overly optimistic design assumptions for the strength of the silt/clay layer and mobilization of passive pressure. The effects of certain construction methods employed and the settlement of the silt/clay were contributing factors in the failure. A relieving platform constructed one year after the failure was designed for the original undrained strength of the silt/clay, without taking into account the effects of soil consolidation and strength gains which had occurred.

INTRODUCTION

A large quay wall was planned as the central part of a new harbor and marine development in the northern Arabian Gulf. Three separate geotechnical investigations of the harbor area were conducted in the early 1980's, two of which concentrated on the planned quay wall. Taken collectively, these investigations provided sufficient data for the design of the wall; however, certain design/construction techniques (i.e., staged construction) would have required additional data. The soils occurring over most of the 1500-m length of the wall were competent sands and stiff clays, but a thick layer of very soft silt/clay existed over the last 250 m of the wall.

The original design of the wall consisted of circular sheetpile cells (cofferdam), a conservative (and expensive) approach to the problem of weak soils. However, the contract for construction of the wall was awarded based on an anchored sheetpile bulkhead alternate design submitted by the successful bidder. During installation of the sheetpiles, it became apparent that the final 115 m of the wall required strengthening and a fourth geotechnical investigation was conducted. The design was then modified in this area by adding H-piles driven on the inside of the sheetpiles and enlarging the anchor wall.

Approximately three months after achieving final fill elevation, but before the bulkhead was subjected to the design surcharge and berthing forces, a localized failure occurred approximately 75 m from the end of the wall as indicated on Figure 1. Upon investigation, five tie rods, including three in a row, were found broken. Following an additional geotechnical investigation and load tests of the anchor system, the wall was repaired by constructing a pile-supported relieving platform over the final 184 m one year after failure.

SITE STRATIGRAPHY AND SOIL PROPERTIES

Three geotechnical investigations conducted in the harbor area from June, 1981 to June, 1982 included six borings in the final 350 m of the planned quay wall: four borings spaced at 100-m intervals along the face of the quay wall and two borings 75 and 110 m behind the wall face. A fourth investigation was conducted in September, 1983, immediately following driving of the sheetpiles, and consisted of three borings and five Dutch cone penetrometer tests. The borings were drilled from jack-up barges to depths of 15 to 30 m below the seafloor (elevation -6 ±). The investigations revealed a very soft silt/clay layer along the final 250 m of the quay wall, extending from the seafloor to elevation -11.9 to -12.4 m ISLW, trending slightly deeper towards the end of the wall, as shown in Figure 2. This layer

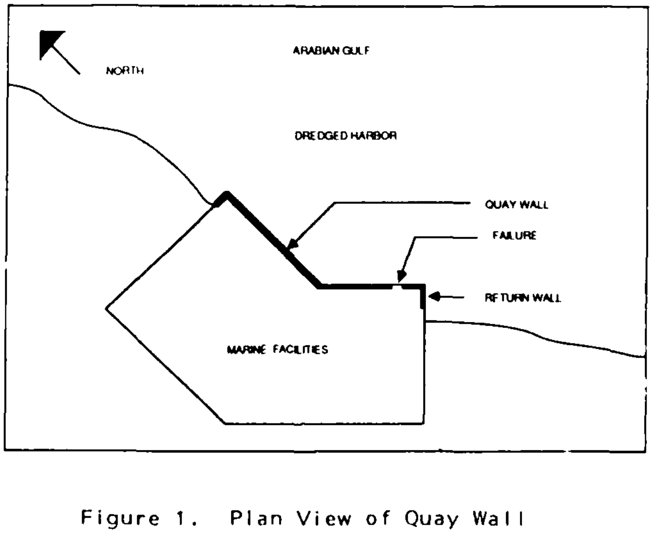

Figure 1. Plan View of Quay Wall

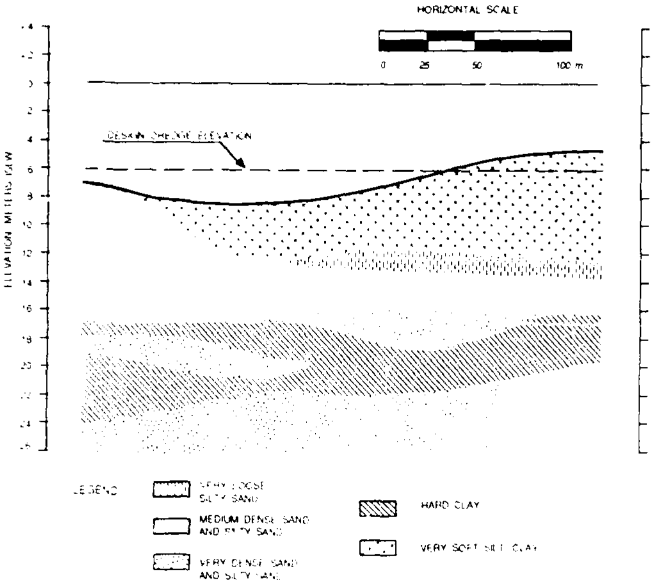

Figure 2. Soil Profile of Final 350 m

is of particular importance to the stability of the wall.

The soil layer was described in the four geotechnical reports as both a silt and a clay with sand pockets and shells. Based on Liquid and Plastic Limits, the soil appears to be a borderline soil, classified as either a silt or lean clay (ML or CL) in the Unified Soil Classification System. The soil exhibited carbonate contents of 25 to 65% and water contents well in excess of the Liquid Limit (Liquidity Index of 2 to 4.8), suggesting that the soil may be sensitive (Wu, 1976).

Results of the laboratory miniature vane and Torvane strength tests and laboratory unconsolidated-undrained triaxial compression tests for the silt/clay layer are plotted as a function of depth on Figure 3. The undrained strength increases from 4 to 5 kPa at the top of the of the layer to 16 kPa at elevation -12 m. These low shear strengths are consistent with field observations that the boreholes were advanced the first 1 to 3 m by the weight of the drill rods, and that during the 1983 investigation the legs of the jack-up barge were pushed into the seabed rather than lifting the barge's deck out of the water. The shear strength is 4 kPa at the surface, increasing with depth corresponding to a c/p ratio of about 0.30, indicating slight, constant preconsolidation.

The soil layers underlying the silt/clay layer are sand and silty sand of increasing density from elevation -12 to -18.6 m; hard (overconsolidated) clay to elevation -21.5 m; and very dense silty sand to the maximum depths explored.

BULKHEAD DESIGN

The quay wall was designed as an anchored bulkhead with a coping beam and facia panel. Two methods for analyzing anchored bulkheads are commonly employed, with the difference being the assumption of the support of the bottom of the sheetpile. The free earth support method assumes that the bottom is simply supported, free to rotate but not translate. The fixed earth support method assumes a fixed support, with no rotation nor translation (Terzaghi, 1943; Tschebotarioff, 1973). Anchored bulkhead failure usually falls into one or more of four types: anchor or tie rod failure, flexural failure of the sheetpiles, toe failure, or a general (slope) failure (Daniel and Olson, 1982).

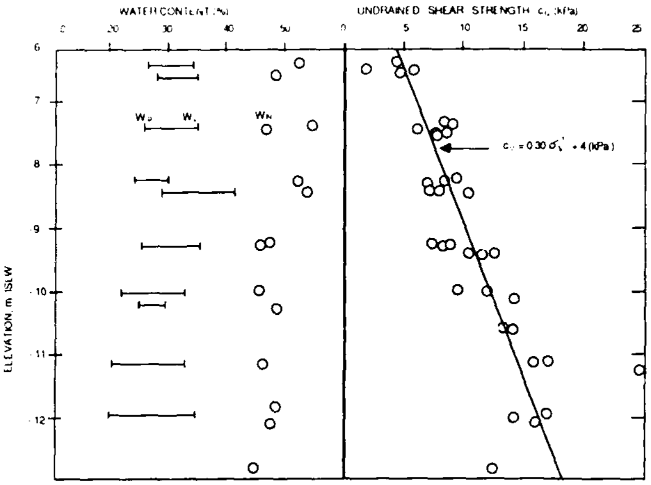

Figure 3. Silt/Clay Properties (After Ladd, et al, 1985)

The design documents indicate that the analysis of the sheetpile wall was conducted using the fixed-earth support method and generally concurring to European industry recommendations (EAU, 1980). The type and depth of sheetpile varied along the length of the wall, governed by the soil conditions. The design loadings included a surcharge of 10 kN/m^2; a mooring load (bollard pull) of 200 kN at ±30° every 16 m; and berthing forces of a 1000 DWT vessel at a speed of 0.3 m/s. Parameters used in the analysis included the harbor bottom at elevation -6.2 m with no consideration for scour or overdredge; low tide at elevation -0.12 m; and the water level behind the wall at elevation +0.84 m. The allowable stress in the steel was 60 percent of the yield strength for both the anchor rods and the sheetpiles.

The design soil profiles for most of the 1500-m bulkhead were in good agreement with the stratigraphy evident from the geotechnical investigations, and the properties chosen for the sands and stiff to hard clay layers were conservative. The performance of the bulkhead was satisfactory except for the final 200 m. The remainder of this paper will concentrate on anchor failure and flexural failure of this portion of the wall.

Original Design

The design soil profile and soil properties for the last 250 m of the bulkhead is shown in Figure 4. The analyses yielded a required sheetpile penetration to elevation -16.26 m to achieve the fixed earth condition, an anchor force of 238 kN/m of wall, and a maximum bending moment of 688 kN-m/m of wall. For anchor rod spacing of 2.55 m, the computed force per anchor rod was 62.9 tons and the Factor of Safety against tie rod failure was 1.82. The Factor of Safety against flexural failure was 1.80.

Modified Design

Following installation of the sheetpiles and the 1983 geotechnical investigation, the design soil profile was changed by extending the depth of the silt/clay layer for the last 75 m of the wall. Reanalysis yielded required tip penetration to elevation -17 to -18 m, indicating that the installed sheetpiles had insufficient penetration to achieve the fixed earth support assumption. The Factor of Safety against flexural failure was reduced to 1.52, less than the required 1.67 safety factory for steel members. The Factor of Safety against tie rod failure of 1.70 was considered adequate.

The design was modified over the final 75 m to include H-piles driven on the inside of the sheetpiles to elevation -20.0 m. It was assumed in design that the H-piles would extend the effective length of the sheetpiles, providing the required fixation, and would carry 21 percent of the bending moment. The Factor of Safety against flexural failure for the sheetpiles was recomputed as 1.82. The Factor of Safety for the H-piles was 1.40, but was recorded as greater than 2.5 due to a calculation error.

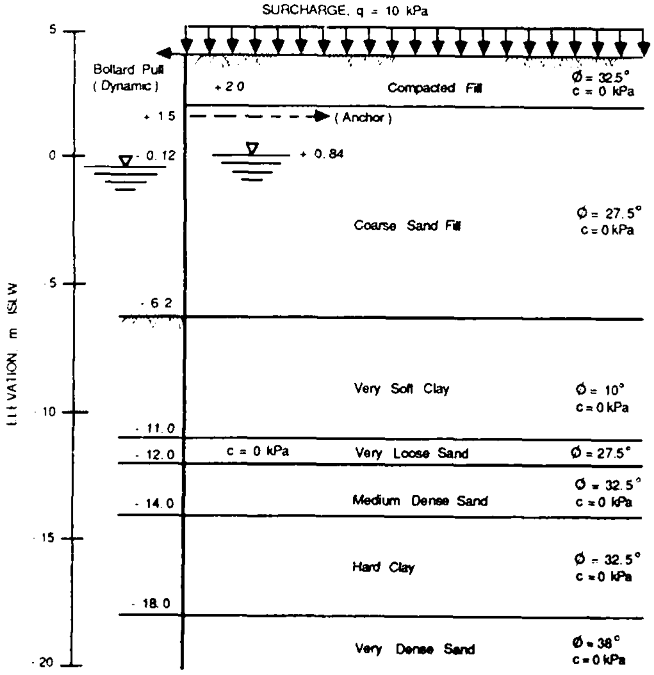
SURCHARGE, q = 10 kPa
Bollard Pull (Dynamic)
+2.0
Compacted Fill
Ø = 32.5°
c = 0 kPa
+1.5
(Anchor)
-0.12
+0.84
Coarse Sand Fill
Ø = 27.5°
c = 0 kPa
-6.2
Very Soft Clay
Ø = 10°
c = 0 kPa
-11.0
-12.0
c = 0 kPa
Very Loose Sand
Ø = 27.5°
-14.0
Medium Dense Sand
Ø = 32.5°
c = 0 kPa
Hard Clay
Ø = 32.5°
c = 0 kPa
-18.0
Very Dense Sand
Ø = 38°
c = 0 kPa
5
0
-5
-10
-15
-20
ELEVATION m MSLW

Figure 4. Original Design Soil Profile

QUAY WALL CONSTRUCTION

The harbor had been dredged to elevation -6.2 m, and 20.25-m long British Frodingham FR-5-DR sheetpiles, BS4360 Modified Grade 50B, were vibrated and driven to a tip elevation of -16.25 m. Concurrent with the sheetpile installation, a sand fill (Stage 1) was placed to elevation +1.0 m some 20 m behind the wall, sloping to within 1 m of the dredged bottom as it neared the sheetpile, as shown in Figure 5. A sheetpile anchor wall was installed in this Stage 1 fill, and the anchor rods placed. H-piles were driven between the sheetpiles and the wale beam (on the inside of the sheetpiles) to elevations -19.0 and -20.0 m. Due to material availability constraints, two types of H-piles were used: 254x254x71 piles installed on 0.85-m centers for the first 25 m and W 10x89 piles installed on 1.70-m centers for the remaining 50 m. Additional hydraulic fill (Stage 2) was then placed to elevation +2.25 m, with the remaining sand fill (Stage 3) to elevation +3.8 m compacted by vibratory rollers. Precast concrete mats to elevation +4.0 m provided the final working surface of the quay wall.

The 63-mm diameter steel anchor rods (yield strength of 38.3 kN/m^2) were installed at elevation +1.5 m at every third sheetpile, a spacing of 2.55 m. The anchor wall, 34 m behind the main sheetpile wall, consisted of 3.15-m long FR-2N-DR sheetpiles of Grade 43A steel driven to alternating tip elevations of +0.1 m and -0.9. Because the Stage 1 fill sloped downward, the anchor rods had a free suspension of 15 to 20 m and were allowed to sag. The built-in sag varied from anchor to anchor, but was of the magnitude of about 0.5 m.

At the end of the quay, a return wall was constructed perpendicular to the main sheetpile wall. This return wall was tied back to an anchor wall 34 m away. Thus, the 34-m by 34-m corner of the quay wall was crisscrossed by two anchor systems (walls and rods). The main wall sheetpiles were installed in August, 1983, followed by Stage 1 filling in Sept.,

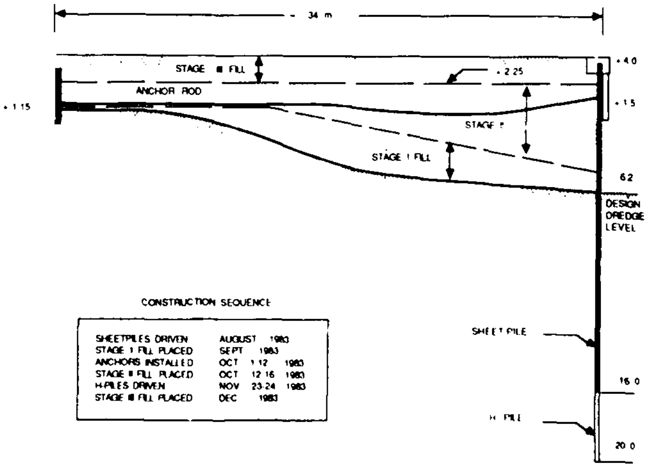
34 m
STAGE III FILL
+2.25
ANCHOR ROD
+1.15
+4.0
+1.5
STAGE II
STAGE I FILL
6.2
DESIGN DREDGE LEVEL
CONSTRUCTION SEQUENCE
SHEETPILES DRIVEN AUGUST 1983
STAGE I FILL PLACED SEPT 1983
ANCHORS INSTALLED OCT 1-12 1983
STAGE II FILL PLACED OCT 12-16 1983
H-PILES DRIVEN NOV 23-24 1983
STAGE III FILL PLACED DEC 1983
SHEET PILE
16.0
H PILE
20.0

Figure 5. Profile of As-Built Bulkhead

1983. The anchor wall and anchor rods were installed October 1 to 12, 1983. Stage 2 hydraulic fill was placed October 12 to 16, 1983, and some Stage 3 fill was placed October 28 to 31, 1983. The H-piles were driven November 23 to 24, 1983, and placement of fill and concrete mats was completed in late December, 1983.

FAILURE AND INVESTIGATION

On March 3, 1984, before the wall had been subjected to surcharge or berthing forces, a localized failure occurred 75 m from the end of the wall. The concrete pads behind the sheetpile wall dropped approximately 10 cm, and the top of the bulkhead moved outward 50 to 70 mm along a 25-m length of the wall. Project records are incomplete regarding the extent and timing of the settlement of the concrete mats, but it appears that the settlement was confined to the area of failure and coincided with the outward movement of the wall.

Excavation to the anchor rod level revealed that three anchors in a row had failed at the connection to the main sheetpile wall, a result of one of the connection ring plates fracturing in each instance. Ring plate connections of other anchors nearby appeared to be rotated and eccentrically loaded (Wiltsie, 1985). Further investigation revealed that two other anchors had failed at the ring plate connection.

Full-Scale Laboratory Tests

To test the overall anchor capacity, the tie rod/ring plate connection system was duplicated in the laboratory using the same type of materials used in the field. The tested plates came from three sources: new plates, new plates from the site stock, and used plates obtained from the quay wall. The anchor rods were loaded in tension to failure. Four different loading conditions were used on the ring plates such that the anchor rods were either aligned, eccentric, rotated, or catenary. The results of the tests are shown in Table 1 and indicate that the loading conditions had no effect on the yield load but did reduce the ultimate capacity of the anchor system.

Table 1. Full-Scale Anchor Rod/Ring Plate Connection Tests

TEST NO.	PLATE ORIGIN	ALIGNMENT	YIELD LOAD, KN	FAILURE LOAD, KN	FAILED ELEMENT
1	M	ALIGNED	1310	1867	ROD
2	S	ALIGNED	1213	1744	ROD
3	Q	ALIGNED	1310	1647	ROD
4	M	ECCENTRIC	1228	1802	ROD
5	S	ECCENTRIC	1309	1586	ROD
6	Q	ECCENTRIC	1224	1529	CONNECTION
7	M	CATENARY	1340	1860	CONNECTION
8	S	CATENARY	1300	1571	CONNECTION
9	Q	CATENARY	1288	1644	CONNECTION
10	M	ROTATED	-	2006	CONNECTION
11	S	ROTATED	-	1782	CONNECTION
12	Q	ROTATED	-	1599	CONNECTION

M - MANUFACTURER S - SITE STOCKPILE Q = QUAY WALL

In-Situ Measurements of Anchor Rod Forces

Two months after failure, the forces in the anchor rods were measured by means of hydraulic jacking behind the anchor wall. Forces in the 800 to 1000 kN range were recorded at several locations in the final 100 m of the wall, well in excess of the design anchor force. However, as these measurements occurred after system relief (outward wall movement, excavations and tie rod replacements) occurred, the authors believe that the anchor rod forces at failure were probably higher than the measured forces, and that these tests are significnat only in that forces much higher than the design level were measured.

Further Geotechnical Investigation

A fifth geotechnical investigation was conducted in August, 1984 consisting of 5 borings, 12 Dutch cone penetration tests, and 11 Piezocone penetration tests. The results show generally increased strength (maximum of 38 kPa) and decreased water contents in the silt/clay layer. Laboratory consolidation and permeability tests indicated a permeability (k) of 3×10^{-8} cm/sec and a coefficient of consolidation (Cv) of 3×10^{-3} to 8×10^{-4} cm²/sec.

FAILURE ANALYSIS

Although the Factors of Safety for the wall appeared to be adequate, the design of the wall was based on optimistic assumptions regarding the properties of the silt/clay layer, the development of passive pressures, and the effectiveness of the H-piles.

Properties of the Silt/Clay

The initial strength parameters selected for the silt/clay during design were cohesion (c) of 15 kPa and an angle of internal friction (ϕ) of 10°. Settlement or compression of this layer was apparently not considered in design.

The soil properties in Figure 3 indicate that the soil is cohesive, with $k = 10^{-6}$ to 10^{-8} cm/sec (Abbs, 1985) or Cv = approximately 4×10^{-3} cm²/sec (Ladd, et al, 1985). The layer would be expected to exhibit an undrained (ϕ = 0) response to loading with initial shear strength (cohesion) of 7 to 10 kPa. The inclusion of a frictional component overestimated the intial strength of the layer by a factor of 5.

Passive Pressures

Earth pressures appear to have been calculated using the Coulomb equations, and included wall friction on both the active and passive sides of the sheetpile. (The inclusion of wall friction increases the passive pressures and decreases the active pressures.) If the angle of wall friction (δ) is greater than $\phi/3$, Coulomb's equations may significantly overestimate the passive pressures (Terzaghi and Peck, 1967). The values for δ used in design ranged from 40 to 62 percent of ϕ.

Development of passive pressure requires outward movement of the wall. To develop full passive pressure in the dense sands near the toe of the wall would require outward movements of 20 to 25 cm, 2 percent of the embedment length (U.S. Navy, 1982; Lambe and Whitman, 1969). However, the fixed earth support method used in design assumes toe fixation with virtually no outward movement. Thus, a factor of safety is commonly applied to the passive forces. The design computations used full passive pressures throughout the effective embedment length. Combined with the inclusion of wall friction, the design used an unconservative estimate for passive pressures (Luscher, et al, 1985).

H-Pile Effectiveness

The modified design assumed the addition of H-piles would extend the effective length of the sheetpiles and resist some of the bending moment. The H-piles were driven on the inside of the sheetpile and had a greater section modulus and penetration depth. Because the H-pile is stiffer than the sheetpile it provides fixation only if on the outside of the sheetpile; otherwise (as in this case), the sheetpile will move away from the H-pile and the fixed earth support assumption will not be achieved (Ladd, et al, 1985).

The H-piles are effective in resisting bending moment by reducing the soil forces acting on the sheetpile at the location of the H-pile. Thus the amount of bending moment reduction is a function of the H-pile spacing and width rather than a ratio of section moduli as assumed in design.

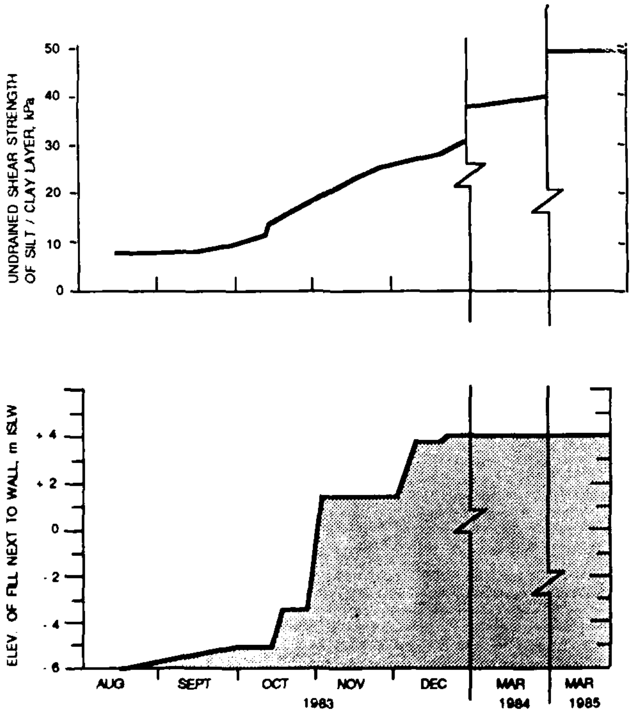

Figure 6. Strength of Silt/Clay Layer versus Time

Table 2. Effect of Strength and Passive Pressure Assumptions

CASE	DESCRIPTION	FS VS ANCHOR FAILURE	FS VS BEND. MOM. FAILURE
1	ORIGINAL DESIGN	1.81	1.76
2	MODIFIED DESIGN	1.69	1.80
3	CASE 2, STRENGTH CORRECTION	1.29	1.07
4	CASE 2, PASSIVE PRESSURE CORR.	0.81	1.23
5	CASE 2, BOTH CORRECTIONS	0.58	0.67

Design Evaluation

The original and modified designs were reanalyzed by the authors using an IBM-PC version of BMCOL (A Program for Finite-Element Solution of Beam Columns with Nonlinear Supports) (Matlock and Haliburton, 1964). The H-pile and the sheetpile were modeled as separate entities whose deflections had to match at certain points.

The designs were analyzed using the original design assumptions and yielded results similar to those in the design calculations. The effects of the strength of the silt/clay and passive pressure/fixed earth support assumptions were also analyzed. The mobilization of passive pressure was modeled by iterative soil-structure interation using Q-W (load-deflection) curves. The results, shown in Table 2, indicate that the wall was underdesigned and would be expected to fail.

Failure Model

Fill was placed behind the quay wall from September to December, 1982, and the strength of the silt/clay layer increased with consolidation, as illustrated in Figure 6. This period is the most critical in determining the anchor rod forces: although the silt/clay continued to increase in strength after filling was complete, the wall deflections

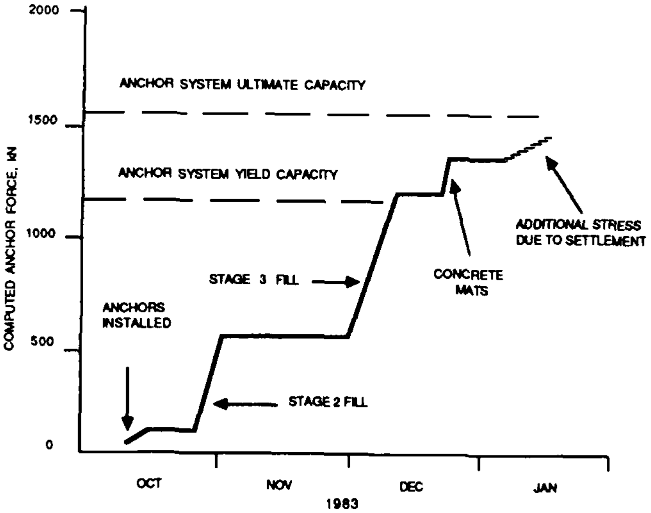

Figure 7. Computed Anchor Rod Forces versus Time

(and thus the anchor rod extensions and forces) could not be reduced due to the sand fill. Figure 7 illustrates the increase in anchor forces as a function of time, taking into account filling levels and strength gains.

The initial tension in the tie rods varied due to construction techniques. The driving of the H-piles which forced the sheetpile wall outward and the initial sag of the tie rods prior to fill placement introduced the greatest degree of variability. Subsequent tightening of rods 190 to 210 after fill placement introduced additional stresses on those rods (the failed rods were 201, 206, 207, 208, 213). Misalignment of the anchor rod connections resulted in variability of the ultimate force each rod could withstand. As opposed to design assumptions, soil properties are not uniform, and therefore pressures on the wall varied as well. As settlement occurred with time, the downward force added additional stress on the rods which were already near their failure threshold, and five broke.

As the wall moved forward, additional passive pressures were mobilized, and pressures acting on the active side of the wall were reduced. The H-piles contributed to stabilizing the wall as they were attached to the sheetpile by the wale beam. However, it was extremely fortunate that a progressive failure did not occur.

RELIEVING PLATFORM

A relieving platform was selected for repair of the wall, with design beginning in January, 1985, and construction from March to August, 1985. The original failure was believed to be primarily due to overestimation of the strength of the silt/clay layer, and therefore, conservative estimates of the initial undrained strength of the clay (c = 7.2 kPa, ϕ = 0°) were used for the relieving platform. The resulting design called for a 184-m long pile-supported structural deck, 15 to 18 m in width, as shown in Figure 8.

This approach failed to recognize the strength increases in the silt/clay due to consolidation under the fill. The shear strength of this layer is estimated to be c = 45 to 50 kPa, ϕ = 0° one year after the fill had been in place. The overall relieving platform was thus overdesigned, but the structural deck, designed for normal working loads, precluded using this portion of the quay wall for heavier than normal loads.

CONCLUSION

A 1500-m long anchored bulkhead experienced localized anchor rod failures several months after construction. The failure was due to overly optimistic design assumptions regarding the strength of a thick very soft silt/clay layer and the mobilization of passive pressures. Other factors, such as sheetpile toe fixation, driving of H-piles to strengthen wall, and settlement of clay layers were contributing factors. The wall was repaired by constructing a relieving platform one year after failure. The platform was designed for the original undrained strength of the clay layer without taking into account the effects of soil consolidation and strength gains which had occurred.

ACKNOWLEDGEMENTS

The authors gratefully acknowledge the work of Dr. Charles C. Ladd and Dr. John T. Germaine of the Massachusetts Institute of Technology in characterization of the properties of the silt/clay layer. Appreciation is also given to the Saudi Arabian Ministry of Petroleum and Mineral Resources and to the Arabian American Oil Company for permission to publish this paper.

REFERENCES

Abbs, A. F. (1985) "*Tanajib Quay Wall - Review of Soil Parameters and Design Method for the Sheetpile Wall and its Remedial Works*," Dames and Moore International Report to Delta Marine Consultants, London.

Daniel, D. E., and R.E. Olson (1982), "Failure of an Anchored Bulkhead," ASCE Journal of the Geotechnical Engineering Division, Vol. 108, No. GT10.

EAU (1980), Recommendations of the Committee for Waterfront Structures, Wilhelm Ernst & Sons, 4th English Edition, Berlin.

Ladd, C.C., A.S. Azzouz, M.M. Baligh, and J.T. Germaine (1985), "Evaluation of Anchored Steel Sheetpile Quay Wall, Southeast Section, Ras Tanajib Marine Facility, Saudi Arabia," Ladd and Associates Report to Daniel Construction Company International, Concord, MA.

Lambe, T. W. and R. V. Whitman (1969), Soil Mechanics, John Wiley and Sons, Inc., New York, N.Y.

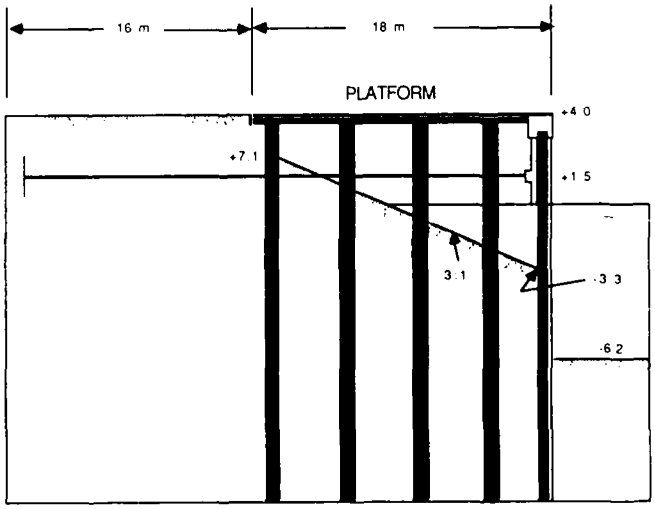

Figure 8. Profile of As-Built Relieving Platform

Luscher, U., R. A. Millet, G. Lawton, and S. Klien (1985), "Anchored Bulkhead Evaluation - Tanajib Marine Facility Quay Wall, Saudi Arabia," Woodward Clyde Consultants Report to Daniel Construction Company International, Walnut Creek, CA.

Matlock, H. and T. A. Haliburton (1964), "A Program for Finite-Element Solution of Beam Columns on Nonlinear Supports," The Universsity of Texas at Austin, Austin, TX.

Terzaghi, K. (1943), Theoretical Soil Mechanics, John Wiley and Sons, Inc., New York, N.Y.

Terzaghi, K. (1954), "Anchored Bulkheads", ASCE Transactions, Vol. 119.

Terzaghi, K. and R. B. Peck (1967), Soil Mechanics in Engineering Practice, John Wiley and Sons, Inc., New York, N.Y.

Tschebotarioff, G. P., Foundations, Retaining and Earth Structures, McGraw-Hill Book Co., Inc., 2nd Edition, New York, N.Y.

U. S. Navy (1982), Foundations and Earth Structures, Design Manual 7.2, Naval Facilities Engineering Command, Washington, D.C.

Wiltsie, E. A. (1985), "Ras Tanajib Quay Wall Failure Analysis", Internal Report of the Arabian American Oil Company, Dhahran, Saudi Arabia.

Wu, T. (1976), Soil Mechanics, Allyn and Bacon, Inc., Boston, MA.

Proceedings: Second International Conference on Case Histories in Geotechnical Engineering, June 1-5, 1988, St. Louis, Mo., Paper No. 6.16

The Influence of Thin Clay Layers on the Design and Performance of a Flexible Cantilever Retaining Wall

R. Cameron
Geotechnical Engineer, Syncrude Canada Ltd., Canada

C.A. Carr
Senior Geotechnical Engineer, Syncrude Canada Ltd., Canada

SYNOPSIS

This case study presents the methods that were used successfully to redesign and monitor the performance of a flexible cantilever retaining wall, incorporating an in situ support berm, at a site where thin, weak clay layers were detected in the foundation during construction. A potential mode of failure termed "berm-block sliding", where the retaining wall pushes out the entire support berm as a block along the clay layers, governed the design analysis. Evidence of presheared planes within the clay layers required that the design shear strength parameters be based on residual values. The clay had a significant cohesion component which was utilized in the design along with an observational method towards construction and post-construction behavior. The observational approach included a comprehensive instrumentation and monitoring program and the development of a remedial stabilization contingency plan to be implemented if necessary. This design methodology resulted in significant cost savings.

INTRODUCTION

This paper presents a case history of the design and performance of a flexible cantilever retaining wall constructed at the Syncrude Canada Limited open pit oilsand mine near Fort McMurray, Alberta, Canada. In particular the influence of thin clay layers is discussed.

Syncrude Canada Ltd. operates a mine and processing plant in which bitumen is extracted from the mined oilsand and upgraded to produce approximately 130,000 barrels of synthetic crude oil daily. The synthetic crude oil is pumped to Canadian refineries for further processing through a pipeline which passes close to the crest of the overburden slope along the northern edge of the mine. Overburden, in the context of this paper, is the material overlying feed-grade oilsand. Another pipeline, which supplies natural gas to the plant, is located within the same pipeline corridor.

In the northwest quadrant of the mine limited space between the pipeline corridor and the planned location of the in-pit mine conveyor system made excavation of a stable unsupported overburden slope impossible and necessitated the construction of a retaining wall which is the subject of this paper. It was very important that the wall provide sufficient support to the retained soil and ensure that differential movement of the piplines would be maintained within tolerable limits for a scheduled service life of 12 to 18 months. A cantilever-type retaining wall comprising soldier piles with precast concrete lagging and incorporating an in situ support berm was selected.

Thin clay layers were discovered in the foundation immediately below the proposed support berm during the retaining wall construction. This required that the retaining wall be redesigned. The methods used to analyze a potential "berm-block sliding" mode of failure for this situation and the selection of the clay shear strength parameters is outlined. Details of the original and final retaining wall designs are discussed. Construction costs could have more than doubled if it had not been possible to construct the retaining wall with a wider support berm and implement an observational method towards construction and post-construction behavior. This included an instrumentation program and the development of a contingency plan for remedial stabilization.

Performance of the wall has been monitored during and after construction by instrumentation which includes slope inclinometers, survey prisms and piezometers. The instrumentation results were analyzed to ensure the reliability of the retaining wall structure. The information from the instrumentation monitoring provides valuable details on horizontal deformation of the retaining wall and ground deformation behind and in front of the wall over a period of more than twelve months since construction. An indication of existing and allowable pile bending stresses was obtained by computer modelling in which pile deformation was provided by an attached slope inclinometer.

The discussion in this paper is confined to the eastern portion of the retaining wall which incorporates the final design support berm. Along the western portion of the retaining wall the support berm was fully supported by unexcavated overburden material.

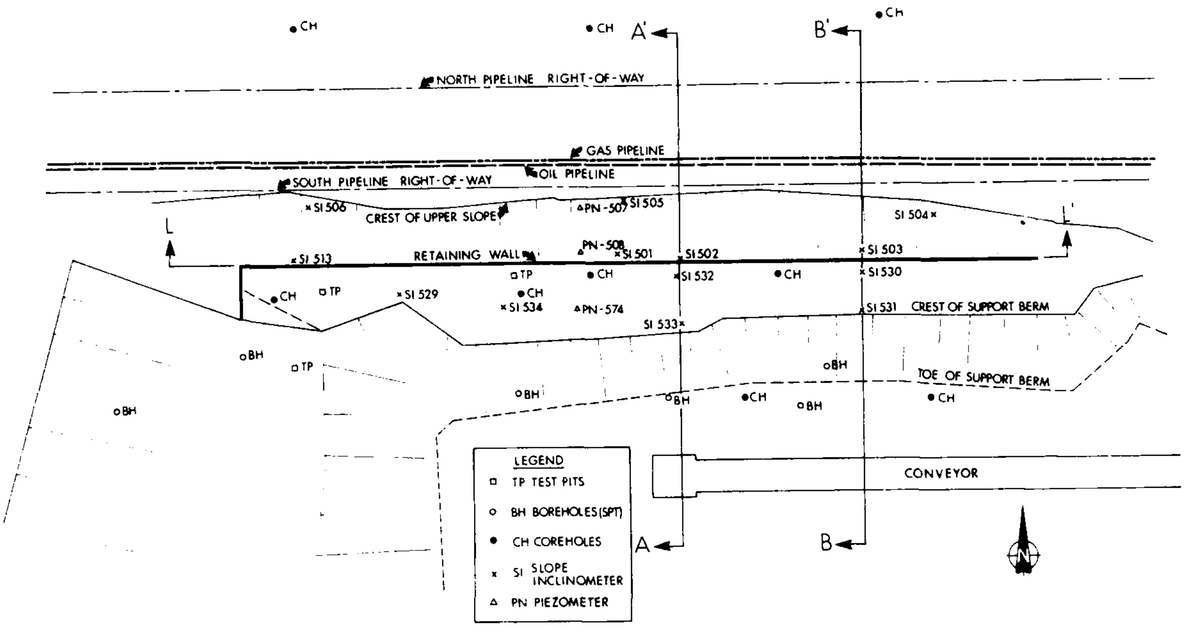
CH
CH
A'
B'
CH
NORTH PIPELINE RIGHT-OF-WAY
GAS PIPELINE
OIL PIPELINE
SOUTH PIPELINE RIGHT-OF-WAY
SI 506
CREST OF UPPER SLOPE
PN-507
SI 505
SI 504
L
L'
SI 513
RETAINING WALL
PN-508
SI 501
SI 502
SI 503
TP
CH
SI 532
CH
SI 530
CH
TP
SI 529
CH
SI 534
PN-574
SI 531
CREST OF SUPPORT BERM
SI 533
BH
TP
BH
BH
TOE OF SUPPORT BERM
BH
BH
CH
BH
CH
LEGEND
TP TEST PITS
BH BOREHOLES (SPT)
CH COREHOLES
SI SLOPE INCLINOMETER
PN PIEZOMETER
CONVEYOR
A
B
N

Fig. 1 Site Plan and Instrument Locations

SITE DESCRIPTION

The general topography of the project area prior to overburden removal and retaining wall construction consisted of gently undulating terrain with muskeg and tree cover crossed by several small creeks and tributaries.

Surface details of the site, after wall construction and subsequent overburden removal, are shown on the site plan in Figure 1. The retaining wall was constructed along the northern mine boundary, within the overburden slope, and is 138 m in length with a short wing wall at the western end. A typical cross-section through the wall and overburden slope is shown in Figure 2. Overburden comprises all the material above the mine bench elevation. In front of the wall is a support berm approximately 5 m in height with a bench width of 9 to 12 m. The mine conveyor system is located to the south of the support berm. The retaining wall supports the overburden soils to the north by means of a 3 m high cantilever section comprising reinforced concrete lagging panels and steel I-section soldier piles placed at 3 m centres. The ground slopes upward to the north to a maximum height of about 4.5 m above the concrete lagging panels, where it reaches the southern edge of a 10 m wide pipeline corridor. Two pipelines are located within the corridor at a depth of about 3 m below ground surface; a 0.51 m diameter pipeline which carries synthetic crude oil from the plantsite to Edmonton and a 0.41 m diameter pipeline which supplies the plant with natural gas.

To the east of the retaining wall the overburden height decreases considerably and is sloped at about 2.5(H):1(V) to a toe ditch north of the conveyor access road. Approximately 35 m of the western portion of the retaining wall is partially buttressed by a stable composite slope of 6(H):1(V) reducing to 3(H):1(V) towards a toe ditch on the mine bench.

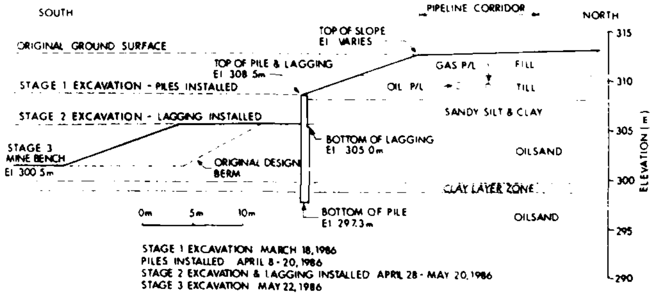
SOUTH
PIPELINE CORRIDOR
NORTH
TOP OF SLOPE
El VARIES
ORIGINAL GROUND SURFACE
TOP OF PILE & LAGGING
El 308 5m
GAS P/L
FILL
STAGE 1 EXCAVATION - PILES INSTALLED
OIL P/L
TILL
STAGE 2 EXCAVATION - LAGGING INSTALLED
SANDY SILT & CLAY
STAGE 3
MINE BENCH
El 300 5m
BOTTOM OF LAGGING
El 305 0m
ORIGINAL DESIGN BERM
OILSAND
CLAY LAYER ZONE
0m
5m
10m
BOTTOM OF PILE
El 297.3m
OILSAND
STAGE 1 EXCAVATION MARCH 18, 1986
PILES INSTALLED APRIL 8 - 20, 1986
STAGE 2 EXCAVATION & LAGGING INSTALLED APRIL 28 - MAY 20, 1986
STAGE 3 EXCAVATION MAY 22, 1986
315
310
305
300
295
290
ELEVATION (m)

Fig. 2 Typical Cross-Section Through the Retaining Wall and Overburden Slope

SITE INVESTIGATION

The geological conditions at the site were interpreted from boreholes and test pits. Details of the geology are shown on the longitudinal section in Figure 3 .

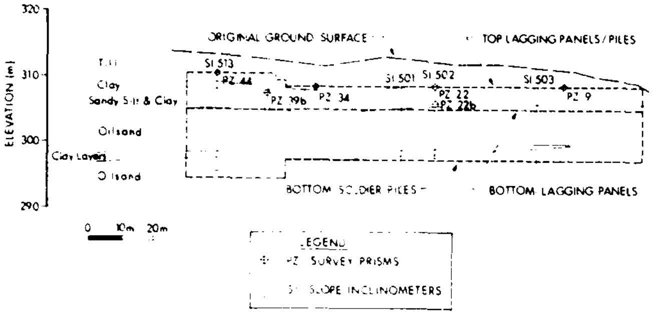

Fig. 3 Geology Longitudinal Section L-L'

The initial information on the subsurface ground conditions was provided by four auger-drilled boreholes with Standard Penetration Testing and sampling. Based on this information the stratigraphy was found to comprise very dense oilsand which is a bituminous silty sand, the upper part of which has a bitumen content of less than 8%. The oilsand is overlain unconformably by 2.8 to 3.5 m of dense glauconitic sandy silt and clay, including a 300 mm thick siltstone layer. Glaciation has eroded the original bedrock surface and deposited 2 to 5 m of stiff clay till and medium dense to dense gravelly sand till which are covered in places by recent fill consisting of a mixture of loose to medium dense silty sand with rock fragments.

After installation of the piles had been completed additional information was obtained from a further subsurface investigation in the retaining wall area. This investigation was carried out after site investigation results from another part of the mine indicated that thin weak clay layers may be present within the upper part of the relatively high strength oilsand. The drilling of four coreholes, excavation of two test pits and detailed geological logging, followed by laboratory testing of samples, confirmed that thin silty clay layers were present within a relatively thin zone of less than 1 m thickness, that could influence the stability of the proposed retaining wall. Individual clay layers were found to be generally less than 100 mm thick, soft to firm and characteristically bioturbated with silt and sand inclusions. Evidence of pre-sheared planes within the clay layers was observed in one test pit and was confirmed by direct shear testing performed along these planes. Laboratory tests indicate the clay has a representative natural moisture content of 22%, a liquid limit of 50% and a plastic limit of 25%. Particle size distribution is varied with a representative gradation of 63% silt and 37% clay.

The groundwater conditions at the site were monitored by several pneumatic piezometers installed at various depths. Piezometer data indicated piezometric levels about 4 to 5 m below the original ground surface.

ORIGINAL WALL DESIGN

The basic wall design considered in both the original and final design consists of reinforced concrete lagging panels installed down to elevation 305.0 m. The lagging panels fit between steel I-section soldier piles concreted up to elevation 305.0 m in 0.9 m diameter prebored auger holes which are spaced at 3 m centres. The I-section used for the piles was a W610 x 179 which has a depth of 0.61 m and a width of 0.3 m. The retaining wall design details are shown on the cross-section in Figure 2 with the original berm design shown by a dashed line.

Soil Pressure Distribution

The soil and net water pressure distributions associated with the original design are provided in Figure 4. The net water pressure is the water pressure remaining after cancellation of equivalent water pressures acting on each side of the wall. For ease of presentation the active soil pressure distribution has been corrected by cosine 21° corresponding to the slope of the ground behind the retaining wall to align forces in the horizontal direction and the passive soil pressure distribution has also been corrected by cosine 20° corresponding to the Coulomb friction assumed. Lateral pressures which include active and passive soil pressures and water pressures acting from 308.5 m down to 305.0 m were considered to act over a 3.0 m width per soldier pile except for the passive resistance of the soil from elevation 305.5 m to 305.0 m. Lateral pressures and water pressures below elevation 305.0 m were considered to act over a 1.17 m width per soldier pile, which is 0.9 m times 1.3, an empirical factor modified from that recommended by Golder and Seychuk (1967). The passive soil resistance between elevations 305.5 and 305.0 m was considered to act over a 1.17 m width per soldier pile. The assumed area of influence for the lateral pressures acting on the piles, as given in Figure 5 case (a), is included in pressure distributions shown in Figure 4.

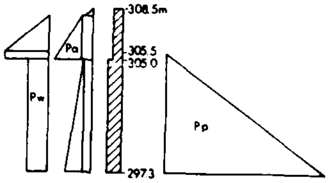

Fig. 4 Soil and Net Water Pressure Distribution for the Original Retaining Wall Design

Design Parameters and Analysis

The original design parameters used for the

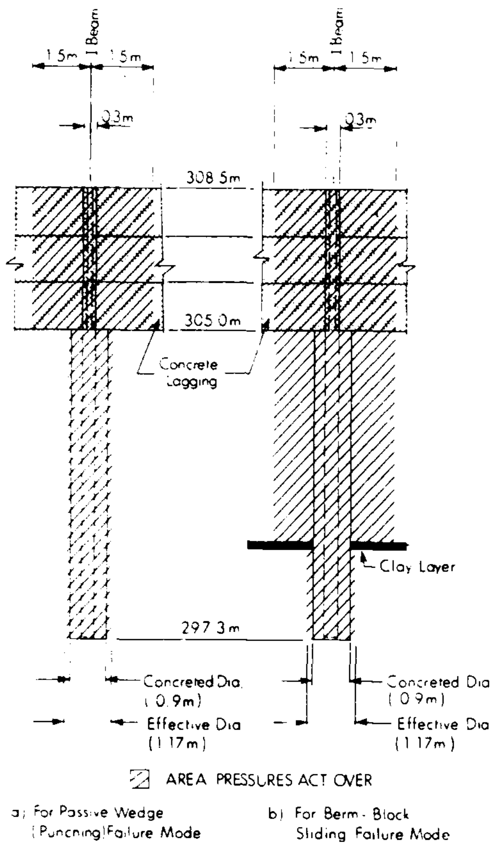
I Beam
1.5m
1.5m
0.3m
308.5m
305.0m
Concrete Lagging
Clay Layer
297.3m
Concreted Dia. (0.9m)
Effective Dia (1.17m)
▨ AREA PRESSURES ACT OVER
a) For Passive Wedge (Punching) Failure Mode
b) For Berm-Block Sliding Failure Mode

Fig. 5 Assumed Area of Influence for Lateral Pressures Acting on Piles for Modes of Failure Considered

various soil types are provided in Table 1. The at-rest earth pressure coefficient (Ko) prior to wall construction for the glauconitic sandy silt and clay and the oilsand is in the order of 2.0 to 5.0 as indicated by previous studies at the mine site. Active earth pressure conditions are, however, expected to be mobilized for a cantilevered retaining wall. It was considered that the oilsand immediately behind the retaining wall would stress relieve resulting in an effective friction angle (Ø') of 44° which, with a slope surcharge (ß) of 21°, gives an active earth pressure coefficient (Ka) of 0.21, for Rankine assumptions. For design purposes a Ka value of 0.3 was adopted for oilsand. The passive earth pressure coefficient(Kp) of oilsand was not required as the Culmann Graphical Method, as it applies to support berms, was used to determine the passive resistance. (Navfac Manual, 1982) This method was used due to the difficulty of determining a passive earth pressure coefficient for a berm geometry.

The calculated factors of safety are provided in Table 2 for the failure conditions considered. The factors of safety against overturning are based on net water pressures.

A guideline for the maximum allowable pipeline movement was established by Lamb McManus Associates Ltd. Based on a formula provided by them differential movement along the length of the pipeline was to be less than 175 mm for a 10 m section.

Table 1: Design Parameters Used in Original Design

Soil Type	Effective Shear Strength Ø'	Bulk Density (kN/m³)	Ka (ß = 21°)
Fill	32°	19.7	–
Till	32°	21.2	0.38
Sandy Silt and Clay	25°	19.7	0.57
Oilsand			
a) in situ	50°	21.2	0.30
b) in situ but stress relieved	44°	21.2	0.30

Table 2: Factors of Safety Against Failure for Original Design

Failure Condition	Required Factor of Safety	Minimum Calculated Factor of Safety
Retaining wall overturning	1.5	1.62
Overall slope stability (under soldier piles)	1.5	2.35
Upper slope stability for failure involving the pipelines	1.5	2.01
Upper slope stability for failure not involving the pipelines	1.3	1.39
Lower slope stability(support berm slope)	1.5	1.48

FINAL WALL DESIGN

Design Changes

The detection of thin clay layers of low strength, within and directly under the proposed in situ oilsand berm, substantially reduced the lateral support the berm would have provided to the retaining wall. A redesign of the retaining wall was therefore required to ensure an adequate factor of safety against overturning. The clay layers, which occur in a thin zone of about 1 m thickness, also extended behind the retaining wall structure so all modes of failure previously considered in the original design had to be rechecked. Since excavation of the in situ support berm had not started enlarging the proposed support berm was an economical and quick solution which would allow mining activities to continue on schedule but with reduced access for conveyor maintenance and cleaning.

A typical cross-section of the cantilever retaining wall that was constructed based on the design changes is shown in Figure 2. The only changes from the original design is the width of the support berm.

Methods of Analysis

With the discovery of the clay layers a new mode of failure involving overturning had to be considered. The failure mode can best be described as berm-block sliding in which the retaining wall pushes on the support berm, causing it to move out as an entire block sliding on the clay. This means that all the water pressure and the active soil pressures behind the soldier piles down to the clay layer elevation had to be included in the driving forces as shown in Figure 5 case (b). It has been assumed that the very dense and high strength oilsand would arch between the piles.

The forces resisting overturning consist of the shear resistance mobilized along the clay layer, any passive resistance developed in the oilsand at the toe of the sliding block where clay layers are below the final ground elevation, the passive soil resistance in front of the soldier piles for the portion of the pile embedded below the clay layer zone and the partially balancing water forces. The actual support provided is dependent on the elevation of the clay layer zone in relation to the elevations of the toe of the berm and the base of the soldier piles.

Selection of Clay Layer Shear Strength Parameters

The selection of the clay shear strength parameters used in the analyses of overturning and stability were based on the results of direct shear tests. Evidence of pre-shearing in some clay samples required that residual shear strength parameters be used in the analyses. The residual strength as shown in Figure 6 demonstrated a significant (apparent) effective cohesion component (c_r') of 10kPa. Lupini (1981) refers to it as an apparent cohesion intercept and uses a secant angle of shearing resistance (ϕ_{rs}') equal to $\tan^{-1}$ (shear resistance divided by normal stress), which is normal stress dependent, for the shear strength in his work. Williams (1980) suggests there is some doubt as to whether the cohesion intercept can be viewed as true cohesion but postulates that the ploughing effect of a sand fraction on the shear planes displaces softer clay and it is this carving of the sand grain into the clay that produces the cohesion intercept. Skempton (1985) gives the residual strength versus the normal effective pressure for most clays as a non-linear relationship and expresses the residual strength as the secant angle of shearing resistance. He also suggests that for design purposes it is often useful to take a "best-fit" linear envelope over the range of pressures involved, using both the effective cohesion and effective angle of shearing resistance.

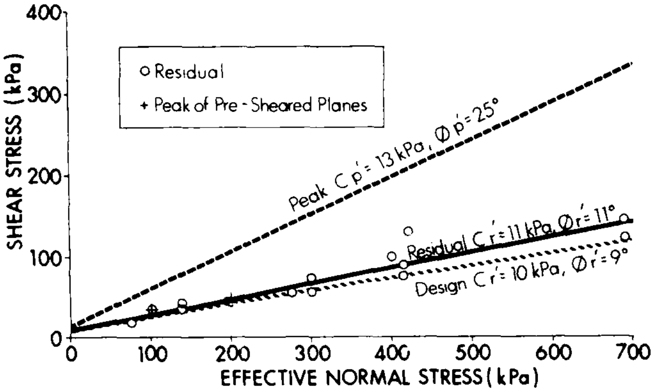

Fig. 6 Clay Layer Shear Strength Parameters

By establishing an instrumentation program and remedial stabilization plan the selection of a less conservative design was implemented in which full cohesion is used from the measured residual shear strength parameters for the clay of $c_r' = 10$ kPa, $\phi_r' = 9°$. This represents the lower bound linear envelope for the residual shear strength of the clay. The use of all the cohesion for the clay layers in front of the retaining wall for long term design was a concern due to the sensitivity of the design to the cohesion value used and the possibility of further reductions in cohesion in low stress areas, which is difficult to test in the laboratory. Significant stress relief of the oilsand and clay layers in front of the wall is expected due to excavation and for long term design a reduction in effective cohesion to $c_r'=0$ was considered.

No loss of cohesion is assumed behind the retaining due to the dowelling effect of the soldier piles through the clay layers and minimal stress relief due to the minor excavation of the supported slope. Hubbard, et al (1984) also used both effective cohesion and the effective angle of shearing resistance for short term retaining wall design considerations.

Low calculated factors of safety for the short term and factors of safety below 1.0 for long term analyses made it imperative to have a contingency plan for remedial stabilization ready to implement if required. Since any loss of cohesion due to stress relief of the clay layers in front of the retaining wall was expected to occur over a period of time, and would not be instantaneous, proper evaluation and interpretation of the monitoring results would provide adequate time to implement the contingency plan. The contingency plan consisted of a semi-continuous cast-in-place reinforced concrete pile shear wall to be installed through the support berm in front of the retaining wall, if required.

Soil Pressure Distribution

The soil and net water pressure distributions, for a clay layer at an elevation of 299.5 m, are provided in Figure 7. For the block of soil above the clay layer in front of the wall no Coulomb friction was used on the back of the block. The passive soil resistance developed in the oilsand at the toe of the sliding block from elevation 300.5 to 299.5 m is included in the block resistance since its action is to support the block which in turn supports the retaining wall. From elevation 308.5 m down to the clay layer at 299.5 m all lateral pressures are considered to act over a 3.0 m width per soldier pile. Below the clay layer the lateral pressures are considered to act over a 1.17 m width per soldier pile.

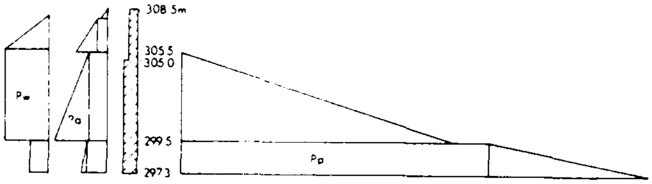

Fig. 7 Soil and Net Water Pressure Distribution for the Final Retaining Wall Design for the Clay Layer at 299.5 m

Design Parameters and Analysis

The soil parameters used in the final design are provided in Table 3. The Ka values given in Table 3 are based on a surcharge slope angle (β) of 21°. The Kp value for oilsand is required to calculate passive resistance provided by the oilsand at the toe of the sliding block where the clay layer zone is below the final grade and for calculating passive resistance in front of the soldier piles for pile embedments below the clay. For design purposes a Kp value of 10 was adopted. This value was obtained by Coulomb's method using an effective friction angle of 44° for stress relieved oilsand and an angle of wall friction (δ)of 20° with a factor of safety of 1.5 applied. Earth pressure coefficients are not applicable for the relatively thin clay layer zone. For the effect of a potential berm-block sliding failure mode due to the presence of clay layers the analysis is dependent on the shear strength parameters selected for the clay layers.

Table 4 gives factors of safety for the clay layers at elevation 299.5 m, 300.5 m and 297.3 m in which calculations are based on Ka values corresponding to respective surcharge slope angles of 21°, 16° and 14°. The factors of safety for the original design support berm geometry, based on the clay layer at an elevation of 299.5 m , is also provided for comparison. The calculations of the factors of safety against overturning were performed using the net water pressure.

Table 3: Design Parameters Used in Final Design

Soil Type	Effective Shear Strength		Bulk Density	Ka $\delta = 0$	Kp $\delta = 20°$
	c' (kPa)	ϕ'	kN/m^3	$\beta = 21°$	$\beta = 0°$
Fill	0	32°	19.7	–	–
Till	0	32°	21.2	0.38	–
Sandy Silt and Clay	0	25°	19.7	0.57	–
Oilsand					
a) in situ	0	50°	21.2	0.30	
b) in situ but stress relieved	0	44°	21.2	0.30	10
Clay Layers					
a) behind wall	10	9°	19.7	–	–
b) in front of wall					
i) short term	10	9°	19.7	–	–
ii) long term term	0	9°	19.7	–	–

INSTRUMENTATION PROGRAM

The location of the instrumentation is shown on the site plan in Figure 1 and on the longitudinal section in Figure 3.

Slope inclinometers (SI) 501 and 503 were installed approximately 1.5 m behind the retaining wall to check any movement due to deep instability below the pile embedment and to monitor the soil movement directly behind the retaining wall lagging. SI 502 and 513 were attached to the inside-edge of the back flange of the pile I-sections to provide the shape of deflection including the point(s) of inflection of the piles. SI 504, 505 and 506 were primarily installed to monitor soil movements in front of the pipelines. SI 530, 531, 532 and 533 were installed five days after final excavation of the support berm to monitor movements of the support berm along the thin clay layers. SI 529 and 534 were installed 33 and 27 days after the final excavation of the support berm to provide more coverage to the west.

Optical survey prisms (PZ) 9, 22, 34 and 44 were bolted to brackets welded 0.3 m below the top of selected piles. They were installed prior to the removal of any soil in front of the retaining wall, with the exception of PZ 9, and were used to check horizontal deflection of the top of the piles. PZ 22B and

Table 4: Factors of Safety Against Failure Conditions Considered in Analysing Final Design

Failure Condition	Factors of safety for original berm with the clay layer at 299.5 m		Factors of safety for final design for the clay layer at 299.5 m		Factors of safety for final design for the clay layer at 300.5 m		Factors of safety for final design for the clay layer at 297.3 m	
	Short Term	Long Term	Short Term	Long Term	Short Term	Long Term	Short Term	Long Term
Retaining wall overturning	0.70	0.40	1.26	0.76	1.48	0.99	1.45	1.14
Overall slope stability (under soldier piles)	2.4		> 1.3		> 1.3		1.3	
Upper slope stability for failure involving the pipeline	> 2.0		> 2.0		> 2.0		2.0	
Upper slope stability for failure not involving the pipeline	> 1.4		> 1.4		> 1.4		1.4	
	Short Term	Long Term	Short Term	Long Term	Short Term	Long Term	Short Term	Long Term
Lower slope stability (support berm slope)	1.30	0.72	1.6	0.8	1.7	0.6	2.1	1.9

Notes: (a) Short term uses the clay layer shear strength of $c_r'=10$ kPa and $\phi_r'=9°$.
(b) Long term uses the clay layer shear strength of $c_r'=0$ kPa and $\phi_r'=9°$ for clay layers in front of the wall and $c_r'= 10$ kPa and $\phi_r'=9°$ for clay layers behind the retaining wall.

39B were installed 0.3 m above the support berm approximately 6 days after the soil was removed from in front of the wall. These prisms were installed to check the deflection of the lower exposed section of the piles.

Pneumatic piezometers (PN) 507 and 508 were installed during construction to confirm design piezometric levels behind the retaining wall. PN 574 was installed in the support berm to provide information on pore pressure dissipation in the oilsand.

Instrumentation Results

The slope inclinometers were read on average every 10 days. Readings were taken at 0.6 m intervals for the entire depth except SI 502 and 513 which were read at 0.3 m intervals. Incremental and cumulative displacement plots were regularly updated for each SI. Incremental displacement represents the lateral differential movement occurring at each interval measured. Cumulative displacements are the sum of the incremental displacements starting from the bottom of the slope inclinometer. The cumulative displacements determined for any elevation will represent the total lateral ground movement occurring at that point. This assumes the slope inclinometer has been anchored sufficiently deep that no lateral displacement is occurring in the ground below. The slope inclinometers are generally read to 1.2 m below the top of the SI casing due to equipment restrictions. Figure 8 and Figure 9 show the cumulative displacements for the slope inclinometers installed along cross-sections A-A' and B-B' as shown on the site plan in Figure 1.

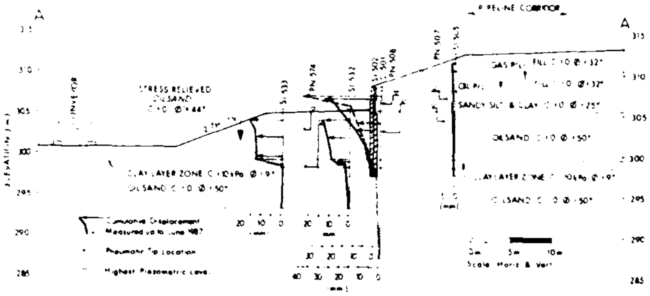
A
A'
PIPELINE CORRIDOR
STRESS RELIEVED OILSAND C'=0 Ø'=44°
PN 574
SI 532
SI 502
PN 508
PN 507
GAS P/L
OIL P/L
FILL C'=0 Ø'=32°
SANDY SILT & CLAY C'=0 Ø'=25°
OILSAND C'=0 Ø'=50°
CLAY LAYER ZONE C'=10kPa Ø'=9°
ELEVATION (m)
315
310
305
300
295
290
285
Cumulative Displacement Measured up to June 1987
Pneumatic Tip Location
Highest Piezometric Level
20 10 0
(mm)
40 30 20 10 0
0m 5m 10m
Scale Horiz & Vert

Fig. 8 Cross-Section A-A' Instrumentation Results

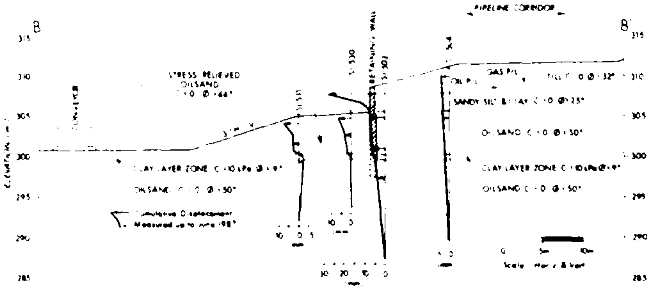
B
B'
PIPELINE CORRIDOR
RETAINING WALL
STRESS RELIEVED OILSAND C'=0 Ø'=44°
SI 530
SI 503
GAS P/L
OIL P/L
FILL C'=0 Ø'=32°
SANDY SILT & CLAY C'=0 Ø'=25°
OILSAND C'=0 Ø'=50°
CLAY LAYER ZONE C'=10kPa Ø'=9°
ELEVATION (m)
315
310
305
300
295
290
285
Cumulative Displacement Measured up to June 1987
10 0 5
10 0
30 20 10 0
mm
0 5m 10m
Scale Horiz & Vert

Fig. 9 Cross-Section B-B' Instrumentation Results

Slope inclinometer readings indicated movement occurring on discrete planes, within a zone less than 0.6 m thick, corresponding to the location of the clay layer zone. At these critical depths incremental displacement was monitored closely with particular checks made of movement velocity. Figure 10 shows the change in incremental displacement with time for SI 530, 531, 532 and 533 for the critical depths. The velocity is the slope of the lines connecting the readings and the change in velocity is given by the change in slope of the lines.

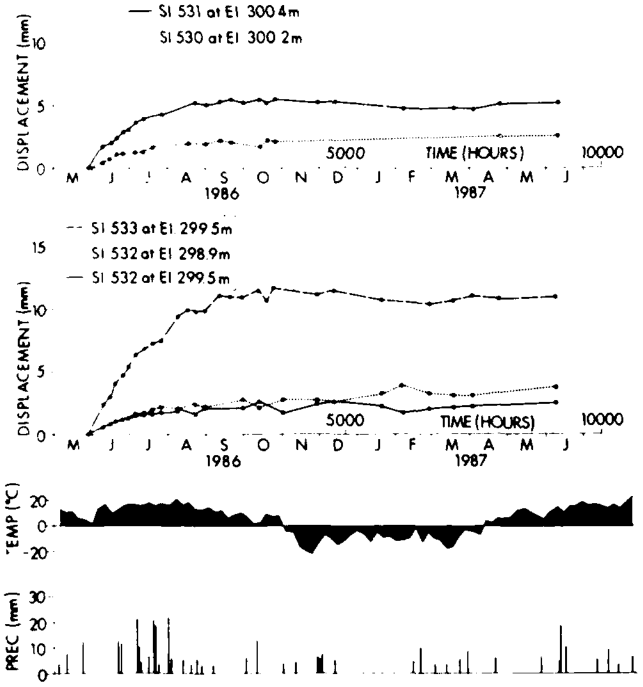

Fig. 10 Incremental Displacement Along Critical Movement Planes Measured by Slope Inclinometers

Figure 11 gives an indication of the outward movement of the soil immediately behind the top of the retaining wall shown by SI 501 and 503 and deflection of the top of the wall is shown by SI 502.

Figure 12 shows the cumulative displacement profile of SI 502 and the associated prism deflection. This is compared to the allowable deflection, calculated by computer modelling of the observed pile deflection discussed in the following section.

Individual prism deflection readings are shown in Figure 13 which also shows the deflection of the top of the retaining wall indicated by prisms PZ 9, 22 and 34.

Piezometer readings for the piezometers installed behind and in front of the wall are provided in Figure 14.

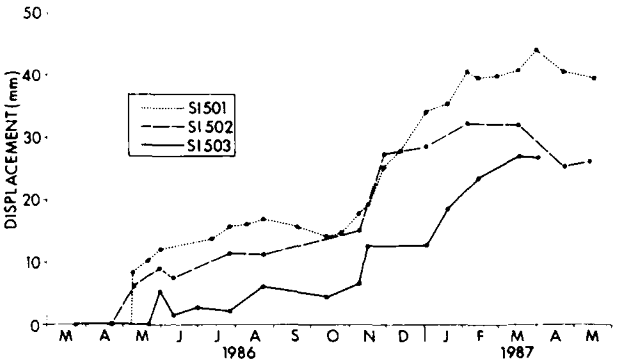

Fig. 11 Cumulative Displacement 1.2 Meters Below the Top of the Retaining Wall Measured by Slope Inclinometers

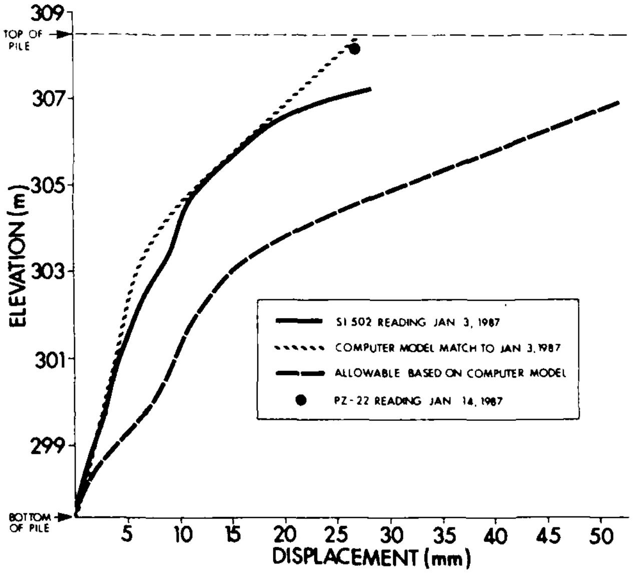

Fig. 12 Profile of Allowable Pile Deflection Based on SI 502 and PZ 22 Field Measurements and Computer Modelling

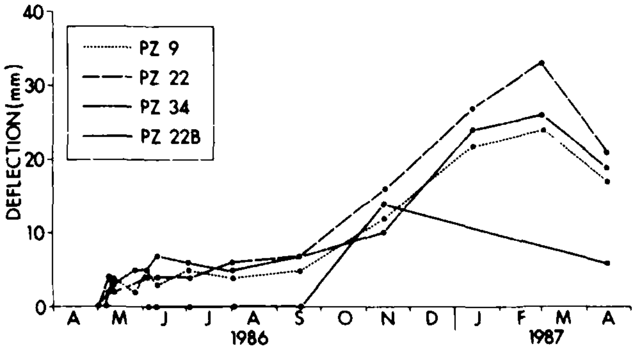

Fig. 13 Deflection of Top of Piles Measured by Prisms

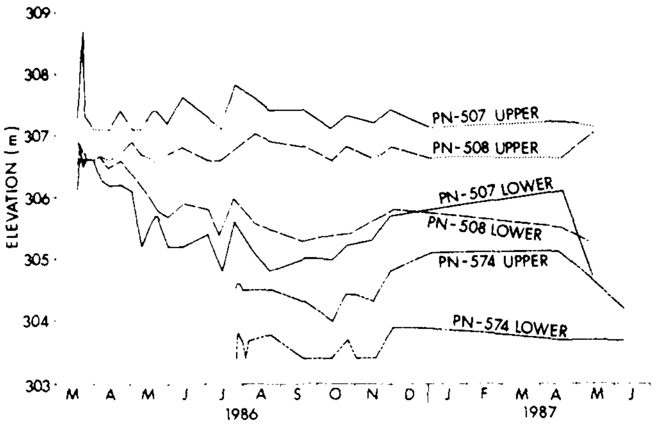

Fig. 14 Piezometric Levels

Discussion of Instrumentation Results

A comprehensive instrumentation program should provide data necessary for an effective observational method towards construction and post-construction behavior in which lower factors of safety are accepted in design so long as an established contingency plan for remedial stabilization can be implemented before failure. In this case two weeks advanced warning would have been required to implement remedial stabilization. The observational approach consisted of (i) monitoring changes in slope inclinometer movement velocity at the critical movement depths and (ii) evaluating the stress conditions of monitored piles when significant movements were experienced. Criteria were established which, if exceeded, would trigger thorough examination of the situation and if necessary the implementation of the contingency plan.

The movement velocity criteria required that detailed assessment would be required if the velocity for any movement depth increased above the original recorded velocity and the incremental displacement exceeded a total of 15 mm. The results of the time displacement plots in Figure 10 show that the velocity at the critical movement depths decreased more slowly for SI 531 and 533 which are located furthest from the wall and closer to the stress-free surface of the support berm face. Movement velocities stabilized after 50 days and 117 days respectively. The movement did not correlate to rainfall or temperature. The maximum velocity recorded was 0.3 mm/day in SI 533 and the greatest displacement was 11 mm. Total displacement may have been slightly more because the slope inclinometers were not installed until several days after excavation. Extrapolating back (assuming initial recorded velocity) to the time of excavation indicated that additional displacement ranging from 12 to 19% of the total incremental displacement could have occurred. Considerable expertise in the installation and monitoring of slope inclinometers has been developed in the course of their extensive use within the mine at Syncrude Canada Ltd. The accuracies of the incremental displacement readings presented in Figure 10 are better than plus or minus 0.6 mm.

Although movement velocities had stopped by November, 1986 there was a concern that movement may be re-initiated in the spring due to the freeze/thaw effects reducing the shear strength and increasing pore water pressures of the clay layers under the support berm. It was also considered possible that an increase in loading onto the back of the retaining wall may occur in the winter due to frost heave and in the spring due to freeze/ thaw effects helping to break down the retained soil and increasing the pore water pressures. This was postulated since there were indications that the maximum load was not acting on the wall as shown by the results of computer modelling discussed below.

No significant movement which may indicate buckling of the pile was observed in SI 502 on the inside flange of the pile at the depth of the clay movement planes, although the deflection profile in Figure 12 indicates a berm-block sliding influence as opposed to solely passive resistance influence. This is suggested by a slight bend near the clay layer zone.

For the pile length and size used in the wall construction it was estimated that the piles could deflect between 25 mm to 50 mm at the top although retaining wall deflections are difficult to determine because of the difficulty in predicting soil/structure interaction and the influence of construction methods and timing. It was decided that if deflection of the top of the pile exceeded 25 mm the pile would be stress analysed. When this occurred a computer program was used that could determine the shear forces, shear stresses, bending stresses, bending moments and deflection of a beam with given section properties along its length, under a given loading condition. Using the P-Frame computer program and a "trial and error approach" different load combinations were applied to the simulated pile until the deflection profile generated by the load combinations matched the deflection profile measured in the field by SI 502 and PZ 22. The existing stresses in the pile could then be determined from the modelled deflection profile. It was calculated that the allowable bending moments in the steel and concrete section of the pile would be reached at 2.5 times the modelled deflection profile. Any significant change in the deflection profile measured in the field would require a revised computer analysis. The existing calculated stress versus allowable stress conditions are given in Table 5.

The maximum stress condition occurred on or about March 18, 1987 and although the bending moments were not rigidly calculated for this date extrapolation of the Jan. 3, 1987 reading gives the critical bending moment at slightly more than 40% of the allowable. There was a partial reversal in the deflection profile of the piles after the winter as shown in Figure 11 and Figure 13. This was most likely due to elastic rebound of the piles following the removal of frost heave effects. The largest measured deflection of the retaining wall was 33 mm.

Table 5: Calculated Stress Conditions for Pile Monitored by SI 502 and IZ 22

Date of Reading	Steel only Section Existing/Allowable (%)	
	Maximum Shear Stress	Maximum Bending Stress
Jan 03/87	26	21
Mar 18/87	30	25

Date of Reading	Steel and Concrete Section Existing/Allowable (%)	
	Maximum Shear Force	Maximum Bending Moment
Jan 03/87	16	37
Mar 18/87	-	-

The piezometer readings for PN 507 and 508 have shown that the design piezometric levels may have been 0.5 m to 1 m too high. PN 574, which was installed 63 days after the support berm was excavated, showed very slow dissipation of the pore water pressures in the in situ oilsand and quick recharge back to the elevation of the top of the support berm following rainfall which confirms the original design assumption.

Although movement occurred along the clay layers within the support berm no failures or surface cracking occurred. The majority of the movement is considered to be due to stress relief from the excavation, with only minor effects from the retaining wall loading. The pile deflection profile suggested a berm-block sliding influence in the deflection curvature. No major deformation of the retaining wall or individual piles occurred and stress conditions in the piles appeared to be slightly more than 40% of the allowable, based on measurements taken on one pile. No upper slope or overall slope stability problems were observed in the field or measured by the instrumentation. Ground movements in the vicinity of the synthetic crude oil and natural gas pipelines were less than 5 mm, well below the maximum movement tolerances.

CONCLUSIONS

The presence of clay layers can have a significant impact on the design of retaining wall structures if not detected at the initial design stage. This case study shows that a thorough subsurface investigation that includes continuous coring or similar methods of sampling capable of detecting thin clay layers, is very important.

The discovery of clay layers during the construction stage required that the retaining wall design be reanalyzed with the following considerations; (i) potential mode of failure of the support berm underlain by weak clay layers and (ii) selection of design parameters for the clay based on evidence of pre-sheared planes.

The overturning stability of the retaining wall and redesign of the support berm has been analysed by considering that the entire berm could be pushed out by the retaining wall in what has been termed a berm-block sliding mode of failure. Based on the lower bound linear envelope from direct shear box tests on the clay, effective residual shear strength parameters were chosen which included a significant cohesion component. Although full residual cohesion and angle of shearing resistance were used in the analyses and a larger support berm selected in the redesign, factors of safety for overturning were lower than considered necessary for short term design. Without the cohesion component the factors of safety would be further reduced.

To safely and reliably allow for a less conservative design approach an observational method towards construction and post construction behavior was used to supplement the design. This included frequently monitored and analyzed instrumentation and the establishment of a ready-to-install contingency plan for remedial stabilization. This approach was successful and the contingency plan did not have to be implemented. If it had not been possible to construct a larger support berm and infringe on the conveyor maintenance accessway this approach could not have been used and the construction cost would have more than doubled since a more elaborate method of supporting the retaining wall would have been required.

ACKNOWLEDGEMENTS

The authors acknowledge the helpful advice of their colleagues and the Syncrude Geotechnical Review Board during the project. In particular the authors wish to acknowledge the contribution of M. Afzal Khan, P.Eng during project design and construction. The authors are also grateful to Syncrude Canada Ltd. for permission to publish this paper.

REFERENCES

Golder, H.Q., and J.L. Seychuk (1967), "Soil Problems in Subway Construction", Proceedings of Third Panamerican Conference on Soil Mechanics and Foundation Engineering, Caracas, Volume II, 203-241.
Hubbard, H.W., D.M. Potts, D. Miller and J.B. Burland (1984), "Design of the Retaining Walls for the M25 Cut and Cover Tunnel at Bell Common",Geotechnique 34, No. 4, 495-512.
Lamb, McManus Associates Ltd., Calgary, Alberta Correspondence concerning pipeline movement tolerance, 1986.
Lupini, J.F., A.E. Skinner and P.R. Vaughan (1981), "The Drained Residual Strength of Cohesive Soils", Geotechnique 31, No. 2, 181-213.
Navfac Manual (1982), "Foundations and Earth Structures", Design Manual 7.2
Skempton, A.W. (1985), "Residual Strength of Clays in Landslides, Folded Strata and the Laboratory", Geotechnique 35, No. 1, 3-18.
Williams, A.A.B (1980), "Shear Testing of some Fissured Clays", Seventh Regional Conference for Africa on Soil Mechanics and Foundations Engineering, Accra, 133-139

Proceedings: Second International Conference on Case Histories in Geotechnical Engineering, June 1-5, 1988, St. Louis, Mo., Paper No. 6.20

Some Case Histories in Urban and Rural Geotechnical Engineering

S.I. Tsien
Professor, Institute of Mechanics, Chinese Academy of Sciences,
Beijing, China

SYNOPSIS: This paper presents several aspects of engineering performances including satisfactory,unsatisfactory but later remedied, and failure experiences in the fields of building foundation,underground construction, and slope stability problems. These projects were completed in China in the past decade. Five case records of performance are used as illustrative examples. Further research work are finally suggested.

INTRODUCTION

During the past decade, a great deal of construction works involving all phases of geotechnical engineering have been completed in China. Most of them proceeded satisfactorily, some encounterproblems but were later remedied, and few failed with evident causes. In general, successes were attributed to well-planned site exploration and soil investigation, careful consideration of topographical, hydrological and geological conditions in design, and close monitoring and control of field phenomena during construction. On the other hand, poor soil data, incorrect design assumptions and crude supervision of construction are mainly responsible for unsatisfactory performances.

It is recognized that specific techniques and experiences must be carefully exercised to suit needs of each engineering project. For illustrative purpose, a few case histories in urban and rural geotechnical engineering are herein presented.

BUILDING FOUNDATION

For ordinary buildings, foundation failures in general, are not due to inadequate soil bearing capacity, and, instead, are caused by excessive deformation. However, plastic flow beneath footing sometimes occurred because of too optimistic bearing value assigned. The degree of consistency between computed and observed deformations depends, of course, on computation method, but more importantly, on proper selections of soil modulus, thickness of compressible layer, and interaction between foundation soil and superstructure. Non-linear constitutive relationship and compatible study between deformation and strength of foundation soil should not be overlooked. Satisfactory building foundation performance may be achieved by using soil modulus value back-figured from deformation records of existing building in project area, pressure-settlement curves derived from plate-loading test, and earlier settlement data for predicting ultimate values. Consideration of rigidity of structural foundation in design is also a key factor leading to success.

In case of pile foundation, large-dimension with a maximum diameter of 3 m cast-in-place piles have been used with increasing popularity in China. The problems remained to be solved are: hole-forming technique, end-bearing capacity of large-size cast-in-place pile for various thicknesses of overlying soil layers, pile-soil interaction and settlement computation method, detection of broken pile in place, and minimization of disturbance to near-by structure during pile driving.

Non-uniform settlement and tolerance value of large-size oil storage tanks built on soft foundation in coastal areas have long been problems of serious concern to designers. The former often causes two important types of failures, i.e. excessive torsional deformation of tank wall and failure emerged between wall and floor slab. To eliminate or reduce differential settlement, the method of water-preloading with carefully controlled loading rate is generally adopted in China, with reinforced concrete ring footing to safeguard against lateral deformation. There are three principal modes of deformations beneath steel cylindrical oil storage tanks, viz, plane tilting of tank body as a unit, non-planar settlement, i.e. differential settlement along circumference of tank, and sag of bottom slab. It is unreasonable to assume that failure of tank wall is solely due to plane tilting. Non-planar settlement causes radial torsional deformation, and/or develops secondary stress in tank wall, in addition to that due to shear deformation occurred in foundation soils.

Among the 60 cylindrical oil storage tanks built in the China's coastal areas (Jia,1984), 60-80% of the ultimate settlement took place during water-preloading stage. The bearing value of the foundation soils was as high as 240 kPa.
The circumferential settlements were 20-170 cm with tilting of the tank body ranged from 2-13×10^{-3}. The statistical analyses showed that these tanks functioned satisfactorily when tilt was less than 6×10^{-3}, leas satisfactorily when $6\text{-}9\times10^{-3}$, and unacceptible when greater than 10 $\times10^{-3}$. Fig.1 shows the statistical relationship

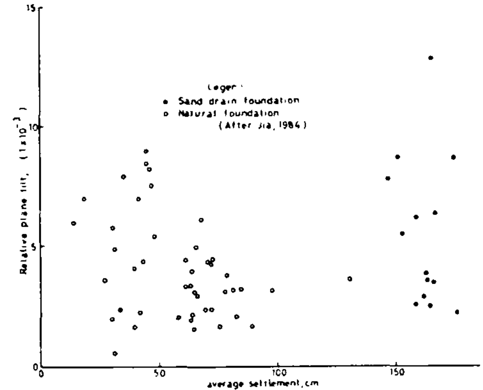

Fig 1 Statistical relationship between average settlement and relative plane tilt of cylindrical oil tanks

between average settlement and relative plane tilt of the 60 oil tanks, ranging from 1000 to 30,000 m^3 in capacity, built on natural and sand drain stabilized foundations.

The statistical data of the 60 floating-top and fixed arch-roof oil tanks also indicate that tilt and sag of floor slab correlate well with H/D (ratio of height and diameter of tank) and ultimate settlement. To drain off residual oil toward tank periphery and avoid excessive tensile stress in floor slab, it is important to estimate closely the maximum sag at the center of floor slab. The recommended sag tolerance is D/90-D/100 Empirical formulae were developed for each case.

The merit of using box foundation for multi-story building on clayey soil was investigated in detail considering rebound and recompression of bottom of foundation pit, settlements in various subsoil layers, subgrade reaction and internal stresses in foundation slab, etc. (Wang & Sun, 1984). The building investigated was a 10-story above ground and $1\frac{1}{2}$-story basement, with reinforced precast concrete floor slab and cast-in-place concrete walls. Its total height including foundation is 34.7 m. The 12.3 m wide by 96.6 m long box foundation was constructed on natural subgrade comprising of alternate layers of sandy clay and silty sand. The bearing value of the subgrade is 220 kPa. The foundation embedded depth is about 4.5 m and a floor slab thickness of 50 cm. The measured rebound of the pit ranged from 0.6 to 0.8 cm, about 60% of the total settlement upon completion of entire structure. The settlement records of various underlying soil layers were taken by installing six observation datum points within a depth of 5 to 17 m below foundation base level. It was interesting to find that the settlement of top 10 m depth amounted to 25 to 40% of the total. The measured effective compression depth was close to the estimated depth at superimposed pressure not greater than 20% of the initial overburden pressure. The rebound and recompression curves follow basically along a atraight line as shown in Fig.2a. The longitudinal tilt was 0.2×10^{-4}.

Vibrating-wire earth pressure cells were installed, with emphasis on the peripheral areas. The measured distributions of subgrade reaction (Fig. 2b) were fairly uniform when imposed load was less than the relief load and then, gradually increased in the peripheral regions to about 20-40% larger than the average measured values. The pattern of subgrade reaction resembled a parabolic curve and their degree of non-uniformity is not so large as that computed from elastic theory. Recheck was made ten years after completion. The cells had performed satisfactorily and the pattern of stress distribution remained about same as before, except a slight shift of pressure concentration from the peripheral toward the interior areas.

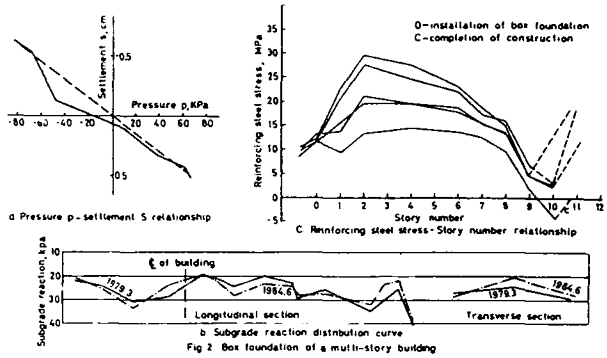

a Pressure p-settlement S relationship

C. Reinforcing steel stress-Story number relationship

b Subgrade reaction distribution curve

Fig 2 Box foundation of a multi-story building

Reinforcing steel stress gages were used to measure internal stress in the foundation concrete slabs. The measured values were generally very small with a maximum of only 30.3 MPa in the slab. Stresses in the reinforcing steel increased with the heights of the building (Fig.2c). But, when ratio H/L = 0.3 (H:constructed height of the building including foundation, L: length of the building), the steel stress reached its maximum value. Then, it gradually decreased and increased again upon completion of the building. In stress gage measurements, it was observed that shrinkage and heat of hydration evolved during concrete setting produced adverse effect on the measured values. Structural load, however, still played the major role in affecting the stress changes.

UNDERGROUND CONSTRUCTION

In recent years underground constructions in China for tunnels, subways, and mining adits in soil and rock strata, etc. have been completed with various degrees of success. Deformation and failure mechanism together with related phenomena were observed by precise measurements during different stages of construction. Remedial measures, if necessary, were then taken. For example, due to inadequate investigation on soft saturated clay especially concerning its rheologic, thixotropic and expansive characteristics, and improper design of floor slab by assigning uplift soil pressure less than that at roof, an excessive heave at bottom of a stone-lined subway took place, an inverted arch had to be reconstructed.

It has been observed that vertical roof load of high fill acting on a relatively rigid structure often exceeds overburden pressure by 20-50%, because of the arching in soils, whereas vertical pressure on the sides of the structure gradually increases outward and equals to overburden weight at approximately three outside span distance.

In mining construction, collapsible deformation of openings in soft or decomposed rock were often a serious hazard. Material evidences showed the superiority of open-type support system over the closed-type, because of the relievement of some deformation in ambient rock stratum. Clear understanding of rock behavior is, therefore, a prerequisite to a good design.

Anchoring type and technique in weak rock is regarded as another important item to be considered in design. Combination of shotcrete-anchoring on wire screen net has proved a good practice for underground opening support both on safety and economy.

In construction of a large subaqueous highway tunnel of total length 2760.72 m, shield method was adopted with success. The circular section of the tunnel is 1322 m long, 8.8 m I.D. and 10 m O.D., built in soft soil under the Huang Pu River, Shanghai, China (Sun et al, 1984). It is a reinforced concrete fabricated lining structure. The subsoil at a depth of 28 to 38 m below adjacent ground surface, where the central portion of the circular tunnel under the river is located, is mainly comprised of silty clay with natural water content about 34%, unit weight of 18.0 KN/m^3, cohesion 7 kPa and angle of internal friction 22^o. The soil layers where the remaining portion of the shield tunnel penetrated through are predominantly silty clay and silty sand.

To accomodate the geological conditions encountered along the length of the tunnel, various methods for stabilizing the surrounding soil were investigated. These included desiccation by lowering water-table, partial or full front face excavation, compressed air to holdupthe frontface and then, semi-shoving (50% soil squeezed inside the diaphragm), or complete closed-breast shoving through very weak soil layers. The total design thrust was 8000 tons. But, the actual force required to shove ahead was much larger in sandy soils. Thus, opened-breast excavation by manpower was the only solution. In case of clayey soils, the front resistance was largely increased through desiccation of soil by water-table lowering or by compressed air, and only semi-shoving was possible.

During the advance of the shield, great concern was concentrated on disturbance of the surrounding soil and the ground surface movement. Although weight of the excavated soil was much greater than that of the lining structure and vehicles, longitudinal axis of the tunnel settled as much as 35 cm after its completion and the differential settlement was noticeable. This phenomenon was closely related to the method of construction The best result was obtained in sandy soils by using compressed air for the section under the river and by adopting well points on the shore.

It was observed that the advancing resistance was greatly increased by full closed-breast shoving methodin the silty clay layer beneath the river bed. Severe disturbance occurred in the neighboring soil, and the overburden was pushed upwards causing 3 m heave of the river bed. The ensuing subsidence was large even after its completion. This is the results of reconsolidation of the underlying disturbed clay and rebound of the compressed clay in front of the shield during retreat of hydraulic jacks to facilitate lining fabrication. To overcome the upward movement of the head of the shield, more than 5% declination was required in maintaining the design orientation of the tunnel's longitudinal axis. In so doing, additional disturbance was resulted and torsional deformation produced in the shield shell.

The external and internal stress conditions of the shield tunnel were carefully checked both during and after construction. Fig.3 shows the external load distribution of a ring erected by semi-closed-breast shoving (area opening 2% and incoming soil volume 40-50%), as compared with the value predicted by theory based on full front face excavation. The smaller measured vertical pressure was clearly due to upward movement of the soil on top of the tunnel, and the greater lateral pressure was the result of partial or full closed-breast shoving. The figure also shows the distribution curves of predicted and measured moments and internal rib stress of the same ring.

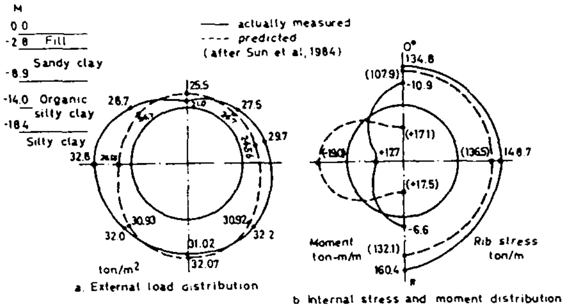

a. External load distribution

b Internal stress and moment distribution

Fig.3 Moment and stress distribution around a ring of a subaqueous tunnel

The soil pressure gages indicated that vertical pressure acting on top of the tunnel was approximately equal to 85% of the overburden weight and the coefficient of lateral soil pressure was about 1.4 under partial shoving operation.

The longitudinal deformation of the tunnel had changed from time to time during and after construction, because of variable soil conditions encountered and methods of shoving used. Particular attention was paid at the junctions of the shield tunnel and the shafts with different modes of deformation.

Leakage at the longitudinal and transverse cracks was one of the critical problems to be dealt with in this project. Epoxy resin failed as a sealing material at the cracks due to its poor crack-resistant behavior. Elastic rubber or bentonite were more suitable for this purpose. As an additional precautionary measure, empty space left behind advance of shield shell was immediately filled up by pressure grouting.

SLOPE STABILITY PROBLEMS

The slope stability problems are closely related to change in groundwater condition, evolutionary history of river channel, soil and rock condition and other hydrologicaland engineering geological environments, etc. in project areas. Many slope failures were caused by water percolation and inadequate provision of drainage facilities especially during heavy rainy seasons. Collapsible loess (Tsien & Liu, 1987) and stiff jointed clay often undergo considerable seasonal variations in their water contents, and thus, become a potential stimulating factor of slope instability. Chemical and structural changes due to weathering, leaching, etc. also have manifold practical consequences. Likewise, high and weathered rock slopes having bedding planes dipping toward river are highly susceptible to failures. The attributing factors are: artificial filling on top, cutting at toe, surface water accumulation, leakage of buried pipe, and vibrations induced by nearby explosion, traffic, pile driving, etc. Infiltration of rainfall into fissures of rock is frequently liable to cause instability. Thus, strict control of surface as well as groundwater by effective drainage systems is considered to be one of the key factors leading to success in engineering practice. Study of slope stability problems by centrifugal model testing is advisable and is presently undertaken in China.

A slide occurred in a gravity type wharf area (Chen, 1984). The wharf is 600 m long with design water depths ranging from 3 to 5 m. After its completion, the owner requested deeper excavation along the adjacent navigation channel and dredging to 1 m below the original seabed elevation. Unfortunately, the dredger had already over-excavated a depth of 0.4 to 1.4 m. This negligence lead to a sloughing of the bank wall into sea over a length of 48 m and its adjoining wall section of 20 m, with an affected width of about 12 m. After a heavy rainfall, the load of accumulated water on the wharf platform was about 10 kPa. As a result, the entire structure leaned backward with 17°-30° inclination. The toe moved outward 6.2 m and the heel subsided about 3-4 m (Fig.4).

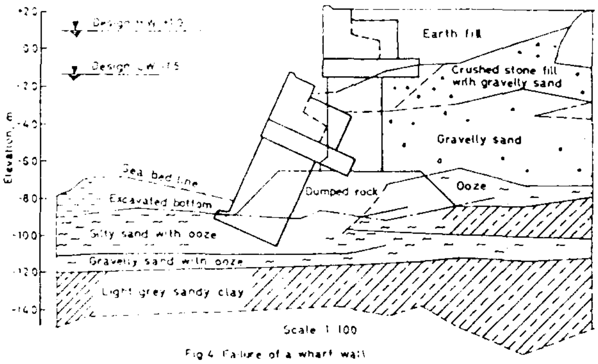

Fig.4 Failure of a wharf wall

After this incident, a large-scale investigation was carried out with 28 borings spaced about 2 m apart. The boring logs showed a soft layer comprising of 1-3 m thick light grey sandy clay (C_u= 14 kPa, $\varnothing_u$= 9°), silty sand or gravelly sand intermingled with ooze, possessing undrained shear strength parameters, C_u = 9 kPa and $\varnothing_u$ = 5°.

To analyze the causes of sloughing, centrifugal model testing was undertaken, along with conventional circular arc analyses. The effective radius of the centrifuge machine is 2.4 m, and the maximum centrifugal acceleration, 100 g. It was found that the mass sloughing and sliding was mainly due to low strength of the foundation soil. The computed factor of safety against sliding was about 0.75. This slope failure was apparently attributed to over-dredging immediately adjacent to the wall. It should be noted that the wharf structure was just in a critical state of equilibrium with a horizontal displacement of 9.5 cm and a settlement of 12.5 cm upon its completion. Once over-dredging started, its overall stability further reduced, finally leading to a mass slide.

Another exemplication of stability problem is slides often occurring in collapsible loess foundation (Hu & Zhang, 1984). A workshop with double transverse spans of 24 m each and 108 m in length and an adjacent open crane ground of 2,3000 m^2 were built on self-weight collapse loess for illustration. The loess has a water content = 18%, unit weight = 16 $kN/_{m^3}$, e = 1.0, W_L = 29% and W_P = 18%. A steep cut, south of the shop, was protected by a retaining wall of 3 m in height. The original design was based on an assumed non-self-weight collapse foundation soil and the adoption of an explosion-enlarged pile foundation. This scheme was later abandoned due to difficulty of controlling the dimension of the enlarged base and the subsidence of the adjacent ground. In the revised design, enlarged footing areas and lime-soil cushion were provided to keep the base pressure less than the initial soil bearing value. One day, large amount of rain-water and waste water seeped into a part of the foundation soil after a 300 mm dia. sewage pipe was broken by travelling trucks. The pillars tilted and struts between the pillars badly deformed. Since then, sloughing and slides occurred alternately (Fig.5).

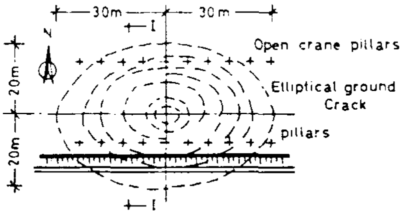

a. Plan

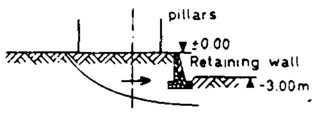

b. Section I-I

Fig.5. Collapse of a loess foundation

The accumulated self-weight collapse settlement ranged from 15 to 19 cm. The causes of failure are:

1. Increase of consumption of industrial and household water, and inadequate drainage facilities for rainwater, resulting in a noticeably high water content in the soil.
2. Surface infiltration of natural water including flood.
3. The foundation soil of recent origin collapsed under its own weight in the presence of water.

As soon as the immersed loess collapsed and subsided, a slide was incipient toward the cut area beneath the retaining wall.

Successful remedial measures were then taken which include strict control of water sources by provision of drainage ditches and wells, change of location of flood discharge outlets. In the mean time, the collapsible foundation loess was stabilized by driving cast-in-place piles and a monolithic structure through connecting all the pillars with large beams. No more trouble happened ever since.

DISCUSSIONS AND CONCLUSIONS

The aforementioned and similar examples clearly indicate that the main causes of foundation failure during and after construction are: inadequate site exploration and soil investigation, improper design assumptions either on environmental and geological conditions, or on soil parameters. Naturally, inadvertent selection of construction method and soil stabilization scheme, poor supervision of construction, and careless man-made operation after completion in adjacent areas are also responsible. Obviously, satisfactory performances as described above are sufficient to embody these considerations. Remedial measures based on soil and rock mechanics principles are often quite useful in overcoming damages already happened. Once damage is done, cost of repairs and renovations usually far exceeds initial cost of engineering projects. To insure promptness of remedial action, constant monitorings and observations are imperative during construction. Besides, detrimental effect to adjacent structure should be constantly watched. Collection of enough information of survey and measured data of existing structures together with successful and failure experiences involved in same project site are utterly important for a satisfactory design and construction. There is no unique method of design and construction that can be used indiscriminately for all projects. Broad comparisons of possible alternatives should always be made before adopting the one which fits best the specific project both from economy and technical feasibility point of view.

It is suggested that the following items be included in the future research work:

1. Engineering behavior of soil and soft rock including appropriate methods of testing.
2. Effect of rigidity of structural foundation on bearing soil response.
3. Quality control and in-situ monitoring technique in foundation construction.
4. Time-effect stress distribution of lining in underground construction.
5. Water-control systems particularly for collapsible soils and fissured soft rocks.

ACKNOWLEDGEMENTS

The materials reviewed herein are mostly selected from the "Symposium on Case Histories in Urban and Rural Geotechnical Engineering" held in December 1984, Shanghai, China. The writer would like to express his sincere thanks to those authors whose materials are freely quoted in this paper and will assume the full responsibility if they are misquoted.

REFERENCES

Bell, R. A., and J. Iwakiri (1980). "Settlement Comparison Used in Tank-Failure Study", Journal of the Geotechnical Division, ASCE, Vol. 106, No. GT2, Feb.

Chen, X. L. (1984). "Test on Failure Mechanism of a Gravity Type Wharf", (in Chinese).

Green, P. A., and D. W. Hight (1974). "The Failure of Two Storage Tanks Caused by Differential Settlement". Proc. of the Conference on Settlement of Structures , Cambridge University, British Geotechnical Society, John Wiley & Sons, New York.

Hu, L. W., and Y. P. Zhang (1984). "An Analytical Check and Treatment of Collapse-Slide of a Collapsible Loess Foundation". (in Chinese).

Jia, Q. S. (1984). "Recommended Control Standards for Analysis of Measured Deformation and Allowable Tilt Value of Large Oil Tanks". (in Chinese).

Krynine, D. P., and W. R. Judd (1957). Principles of Engineering Geology and Geotechnics, McGraw-Hill Book Co., Inc. New York.

Sun, G. S., J. H. Liu., and Z. J. Jin (1984). "Geotechnical Problems in Constructing the First Sub-aqueous Tunnel under the Huang Pu River, Shanghai, China". (in Chinese).

Terzaghi, K., and R. B. Peck (1948). Soil Mechanics in Engineering Practice, John Wiley and Sons, New York.

Tsien, S. I., and Y. Liu (1987). " Engineering Behavior of Lanzhou Loess". to be presented in "International Conference on Engineering Problems in Regional Soils". Aug. 1988, Beijing.

Wang, S. Q., and J. L. Sun (1984). "Engineering Case Histories of Box Foundations of Tall Buildings in Beijing". (in Chinese).

Proceedings: Second International Conference on Case Histories in Geotechnical Engineering, June 1-5, 1988, St. Louis, Mo., Paper No. 6.24

Treatment of KARST Subgrade by Deep Drilled Pile Foundations

Wang Yiji
Chief Engineer, Wuhan Foundation Engineering Centre, China

SYNOPSIS: A record of geotenical engineering in the Karst region is provided in this paper.The drilled piles method was adopted in the engineering for building foundations in order to guarantee the safety and usage of buildings. This is a new exploration in contrast with conventional grouting method.

Five five-storey apartment buildings(Fig.1.)constructed at the residential area of DaYe Steel Works are located in the Karst region. At the east side about 1 km away,pumping is frequenty taken during a small scale coal mining operations. From the year 1984,local ground sinkings are observed in this residential area. Half height of one restaurant house of these buildings are settled into the ground.(Fig.2.)This has endanger the normal usage of this buildings and security of lives and properties of people,therefore,a great concern of safety has induced. Through the exploration by engineering geologists,it was discovered that the geological structure below the ground has formed mainly by Quaternary(Q) stratigraphic layer Da-Ye group limestone of Trias and Ta-Ron formation(P2d) limestone of Permian. The earth cavern with the max. height up to 4.8m has been found in soil layer. The rocks in the strata are extensively fractured with rich cracks and fissures. Crossing and overlapping distribution of the caverns of Karst nature are frequently noticed. In certain area this overlapping of caverns in five different layer has been found. The height of the cavern in fifth layer is 9.05 m. The top layer thickness of the part Karst cavern is less than design value.(Fig.3.4.5, The distribution of ground water is very comlicate and the flow motion of water is also very active. Those five residential buildings are located within the dangerous cave in area. If these buildings are rested and relocated,it will cost five million dollars.

The Wuhan Foundation Engineering Centre took up the work of treatment for this engineering projects. The treatment measures were designed based on the charactenistic nature of the project. Reinforced concrete drilled piles of 600 mm in diameter were installed in the open space around the caverns and down to the stable rocks with a depth of 1 m,beneath the caverns. The length of pile is varied according to the cavern location with max.

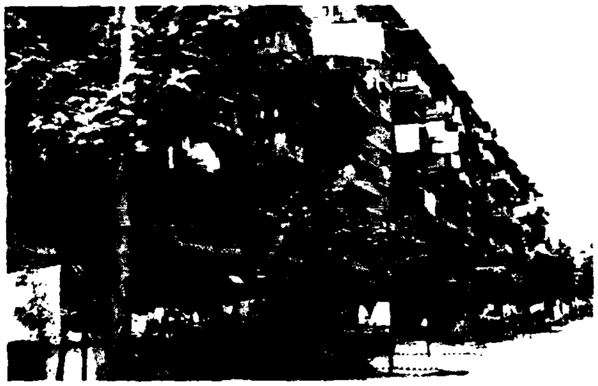

Fig.1. Five five-storey apartment buildings

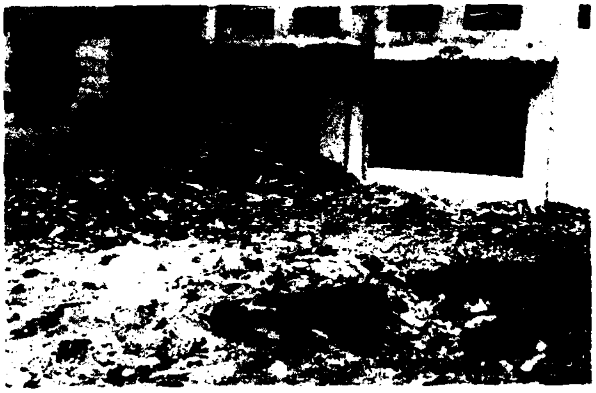

Fig.2. Half house is settled into the ground

pile length up to 50 m. The small diameter of 120 mm drilled piles were used at indoor ground with bottom bearing plates. In the mean time, the piles and cap platform of bottom bearing plates were firmly integrated with the original beam foundation as a single body, therefore, the loadings from the upper structures can be transmitted directly to the stable rock base(Fig.6.7).

The load carrying pattern of this treatment method is more reasonable as compared with the conventional grouting method. The final effect is remarkable and good quality is also assured.The design work for this engineering treatment project was complected in June 1985 and construction work is get ready currently.

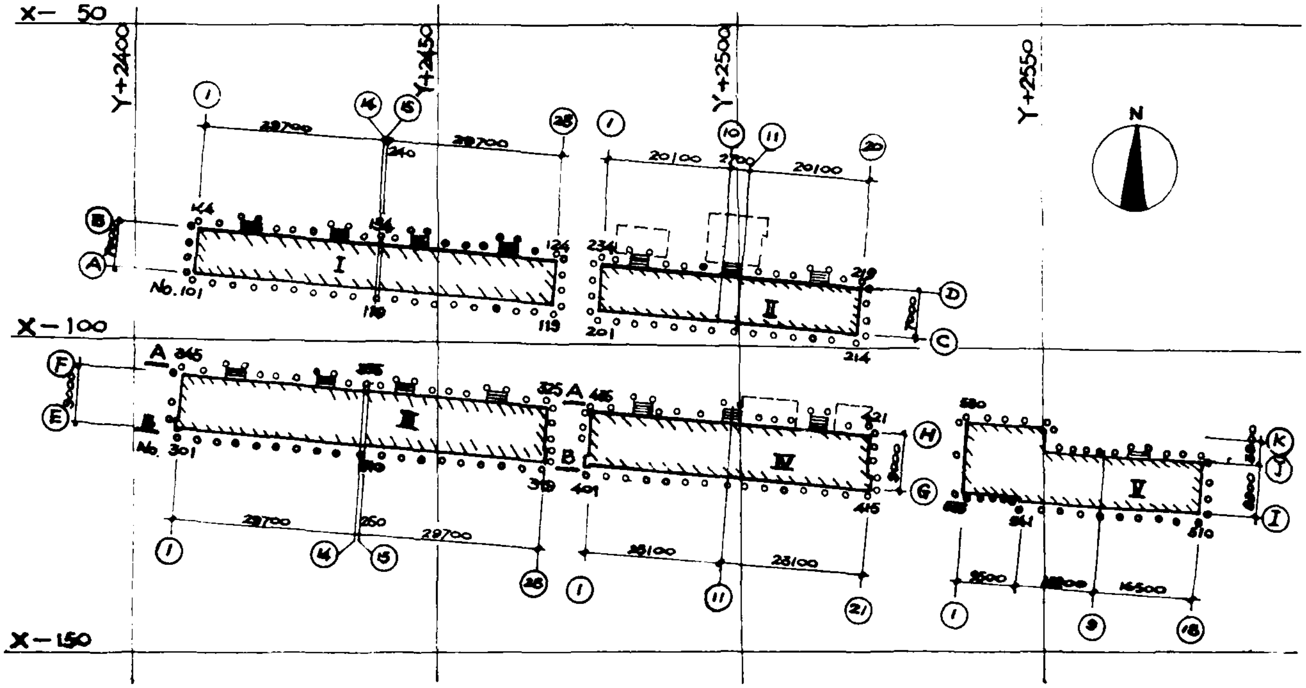
X-50
X-100
X-150
Y+2400
Y+2450
Y+2500
Y+2550
N
I
II
III
IV
V
No.101
No.301
29700
20100
28100
16500
A
B
C
D
E
F
G
H
I
J
K

Fig.3 Plane of five apartment buildings and drilled piles

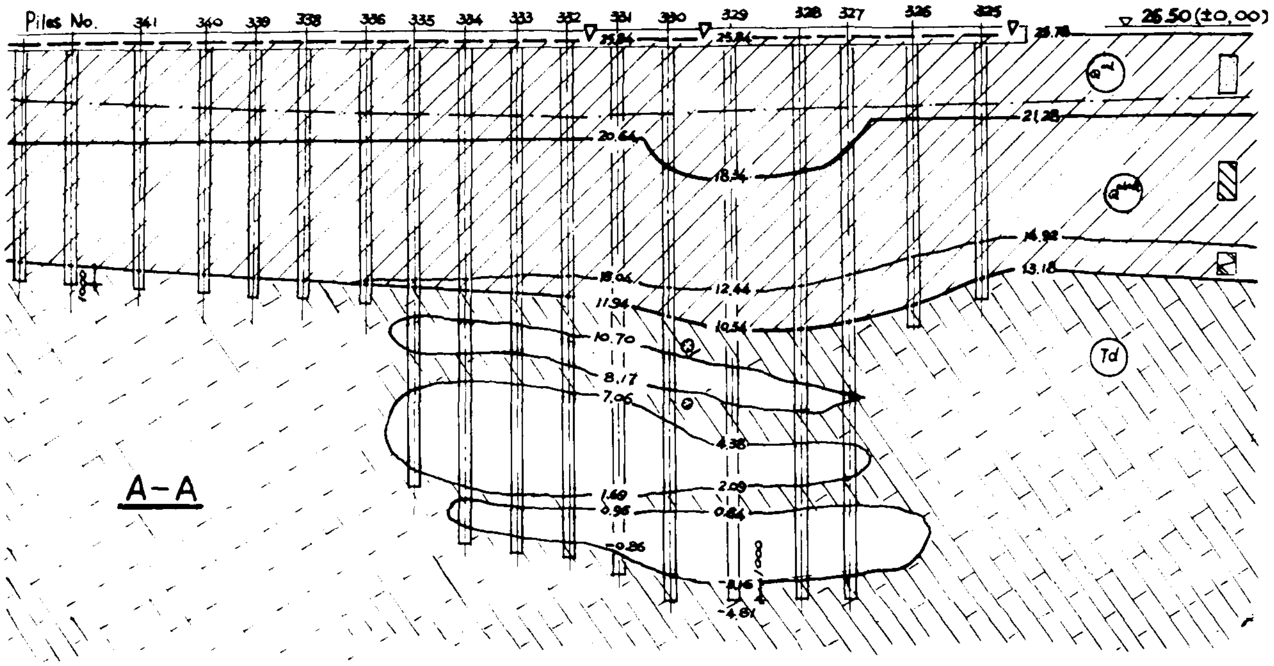
Piles No.
341
340
339
338
336
335
334
333
332
331
330
329
328
327
326
325
25.84
25.84
25.78
26.50(±0.00)
21.28
20.64
18.54
14.92
13.18
18.06
12.44
11.94
10.54
10.70
8.17
7.06
4.38
1.69
2.09
0.96
0.84
-0.86
-4.16
-4.81
Td
A-A

Fig.4. Section A of Engineering Geology

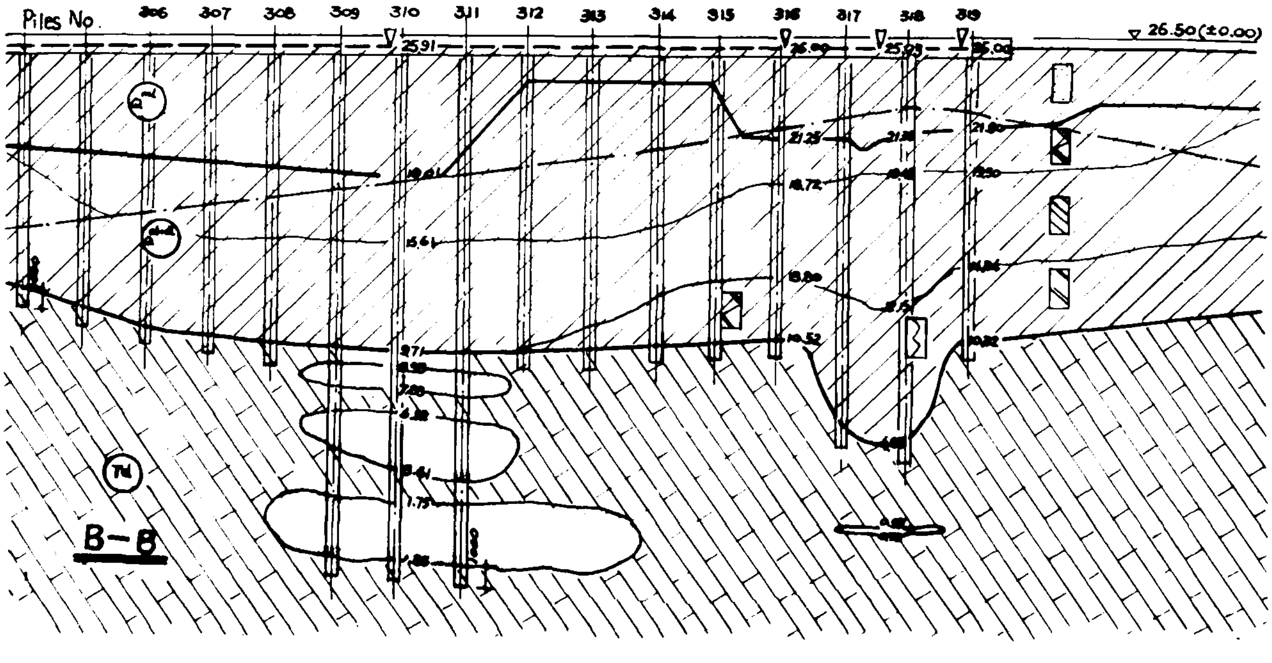
Piles No.
306
307
308
309
310
311
312
313
314
315
316
317
318
319
25.91
26.00
25.93
26.00
26.50(±0.00)
21.25
21.38
21.80
19.01
18.72
19.48
19.50
15.61
13.80
14.86
12.51
10.52
10.82
9.71
7.80
6.38
3.41
1.75
Td
B-B

Fig.5. Section B of Engineering Geology

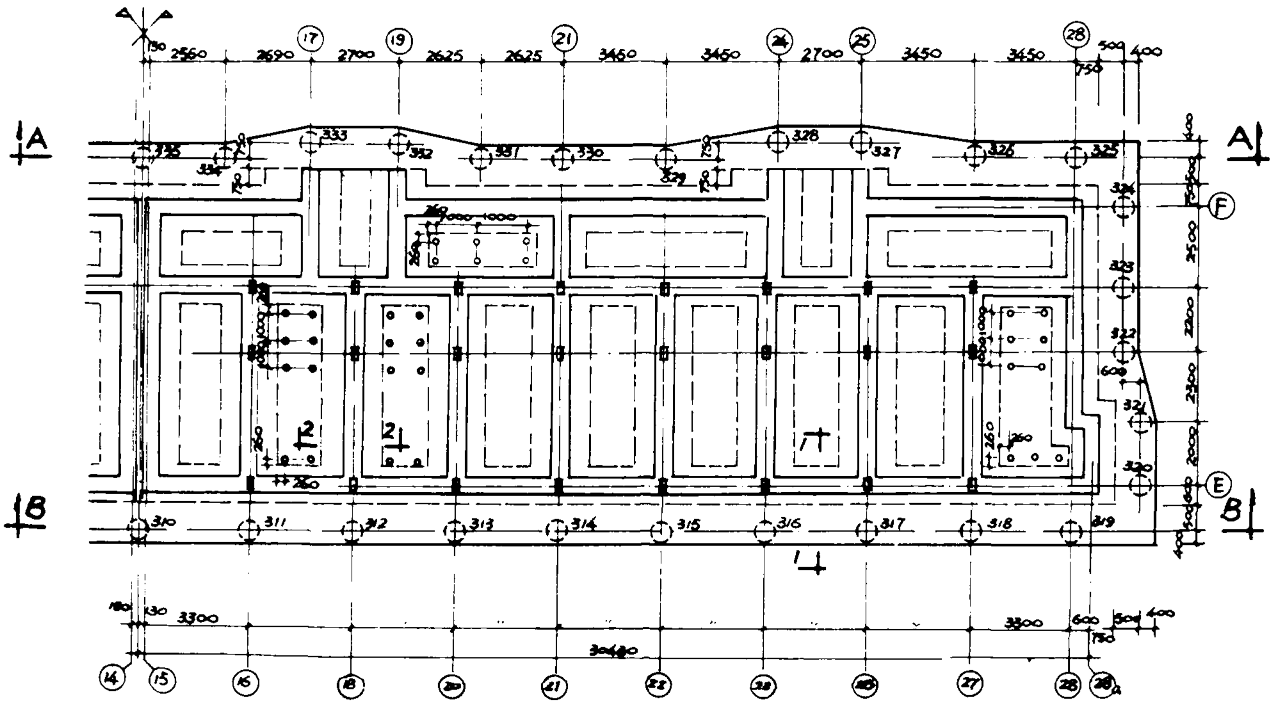
A
A
B
B
E
F
2560
2690
2700
2625
2625
3450
3450
2700
3450
3450
500
400
750
3300
3300
600
500
400
750
30480
2500
2200
2300
2000
333
332
331
330
328
327
326
325
324
323
322
321
320
310
311
312
313
314
315
316
317
318
319
1000
1000
260
14
15
16
17
18
19
20
21
22
24
25
27
28
1-1
2-2

Fig.6. Plane of No.3 apartment building and drilled pile

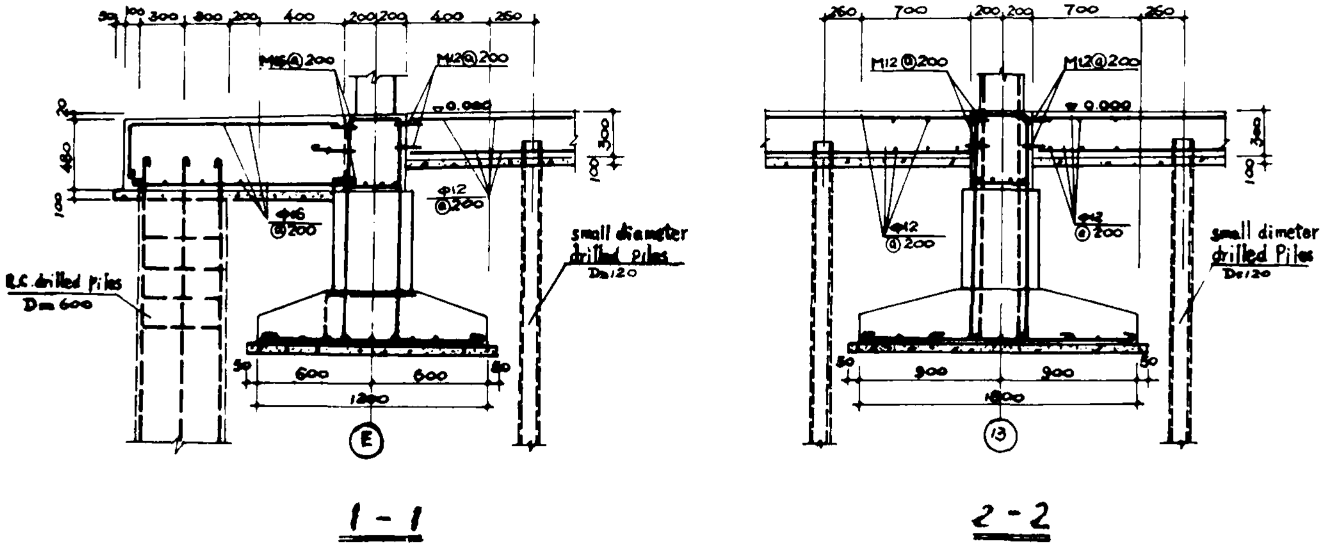
50
100
300
800
200
400
200
200
400
260
M16@200
M12@200
±0.000
300
100
480
100
Φ6 @200
Φ12 @200
R.C. drilled Piles D=600
small diameter drilled piles D=120
50
600
600
50
1200
E
260
700
200
200
700
260
M12@200
M12@200
±0.000
300
100
Φ12 @200
Φ12 @200
small dimeter drilled Piles D=120
50
900
900
50
1800
13

1 - 1

2 - 2

Fig.7. Section 1 and 2 of Foundations

Proceedings: Second International Conference on Case Histories in Geotechnical Engineering, June 1-5, 1988, St. Louis, Mo., Paper No. 6.25

Diagnosis of Structural Damage and Movement Due to More Than One Cause

G.E. Barnes
Senior Lecturer in Civil Engineering, Bolton Institute of Higher Education, Bolton, England

SYNOPSIS: A structural and ground investigation was carried out on a domestic property at Leigh, Lancashire, England. The settlement of the property was measured and showed a complex pattern of movement which was separated into: (i) an overall tilt towards the east; (ii) an outward tilt of the northern and southern ends; and (iii) severe tilting and cracking at the northern end. Following detailed investigation separate causes were assigned to each of these movements as: (i) preferential longwall mining to the east of the site; (ii) eccentric loading at the northern and southern ends; and (iii) moisture removal from the stiff clay beneath the northern end by the roots of a nearby tree. Details of the settlement of the property, soil conditions and mining situation are presented together with appraisal and analysis of the separated movements.

INTRODUCTION

The property, Nos. 38 and 40, was constructed in 1945/46. It comprises a traditional 2-storey loadbearing brickwork semi-detached building with a solid ground floor. No known serious damage was suffered until 1976 when because of severe cracking of the brickwork and distortion of the upper floors No. 38 had to be evacuated. No. 40 did not suffer any serious damage and was still occupied.

FOUNDATION AND GROUND CONDITIONS

Pits excavated around the outside and inside No. 38 showed the building to be supported on a simple concrete slab type foundation, about 0.1 - 0.15m thick with a thickened portion, 0.2m thick and 2.6m wide along the gable end. This thickened portion was probably provided because of the large amount of brickwork both downstairs and upstairs, see Figure 1, and presumably also exists along the gable end of No. 40. The underside of the slab was at about 0.4 - 0.5m below ground level.

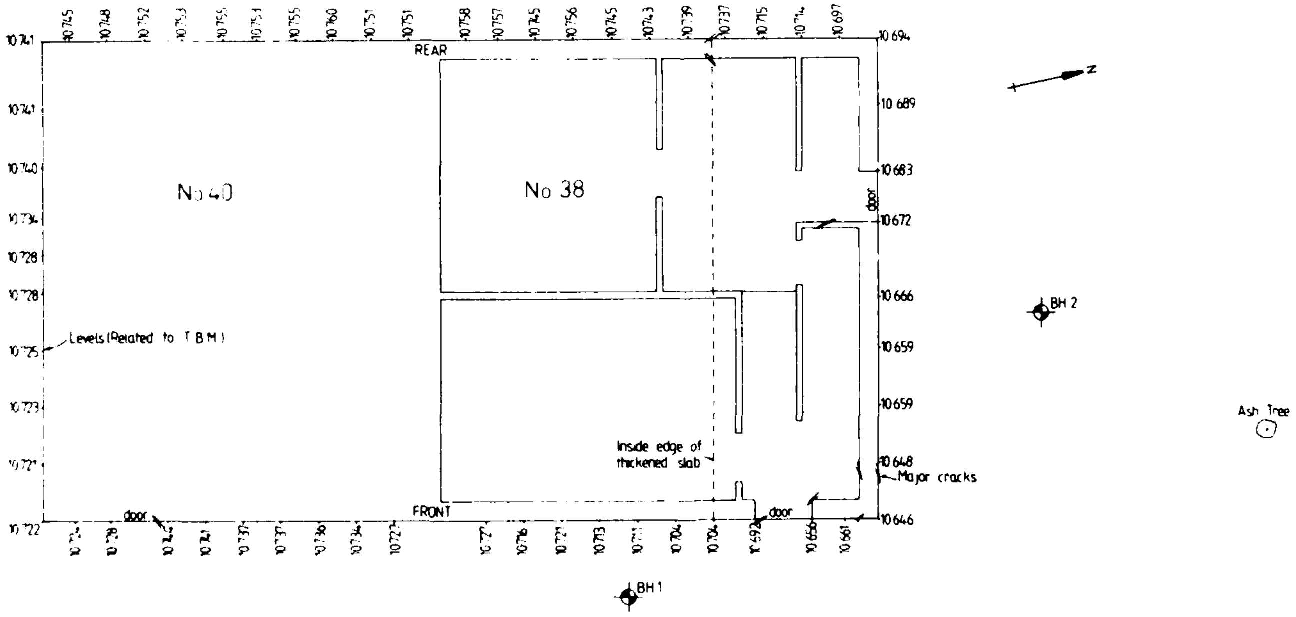
REAR
FRONT
No 40
No 38
N
BH 1
BH 2
Ash Tree
door
door
door
Levels (Related to T B M)
Inside edge of thickened slab
Major cracks
10 741
10 694
10 689
10 683
10 672
10 666
10 659
10 659
10 648
10 646
10 722
10 745
10 748
10 752
10 760
10 758
10 757
10 756
10 737
10 715
10 697
10 736
10 734
10 722
10 704
10 656
10 661

FIGURE 1 : Site Layout

The ground conditions proved below foundation level comprised three distinct layers of glacial clay, see Table 1 for their properties. Beneath these was a thick layer (8m) of very dense sand, gravel and cobbles which overlay the Bunter Sandstone bedrock. The water table existed within the sand and gravel at about 4m below ground level.

TABLE 1 : Soil Properties

Layer	Description	Thickness m	Liquid Limit %	Plastic Limit %	Mean Moisture Content %		Estimated change in Thickness mm
					BH.1	BH.2	
1	Silty clay with gleyed fissures	1.8	61-72 66	22-24 23	22.1	21.1	30
2	Laminated Clay	2.7	50-65 57	21-23 22	28.5	24.1	50
3	Sandy clay with gravel inclusions	2.0	29-38 33	14-17 15	13.0	12.8	8

OBSERVED DAMAGE

No. 40 - some relatively minor cracking existed both externally and internally over the front doorway and the staircase had a detectable tilt. The remainder of this dwelling had suffered no damage.

No. 38 - significant cracking had occurred in the brickwork, mainly within a strip about 2.5 - 3m away from the gable end with the largest movements at the front of this property.

SETTLEMENTS

By levelling along a brickwork course the differential shape of the property could be ascertained. From an inspection of surrounding houses it appears reasonable to assume this property was built horizontally and the measurements obtained reflect differential settlements. Obviously total settlement measurements were not available but these would be estimated to be small, apart, of course, from the mining subsidence. The measurements are given on Figure 1 and the profile along the front and rear are plotted on Figure 2. From these profiles it was considered that there were three quite distinct types of movement, namely

(i) an overall tilt of about 20mm across the building towards the east, about 1 in 400,

(ii) a local tilt or rotation parallel to the gable end of No. 40 (southern end) of about 15 - 20mm over the 2.6m wide thickened raft portion (and presumably also at the northern end), about 1 in 150, and

(iii) a differential settlement in a northerly direction across No. 38 of about 60mm at the rear and about 90mm at the front and from an examination of the structure, ground conditions and surroundings these movements could reasonably be assigned to three different causes, namely :

(i) preferential coal mining beneath

(ii) eccentric loading of the thickened raft portion along the ends of the building

(iii) removal of moisture from the clay beneath by the roots of a nearby ash tree.

MINING SITUATION

Coal extraction has been carried out beneath this area from the nineteenth century but since 1945 when the property was built most of the coal mining within the support area of the site took place by longwall working between 1953 and 1965 so a considerable amount of vertical subsidence would have occurred but movements would have virtually ceased by 1976. However, the most significant factor affecting these workings is the presence of a major geological fault, the Pennington Fault, which runs in a NNW-SSE direction, outcropping about 250m west of the site. This fault plane dips steeply at about 1 : 3 (horizontal : vertical) in an easterly direction with a fairly large throw on the eastern side of the fault. The records show that some workings were taken up to the fault but several were terminated east of the site, see Figure 3.

From the above it would be reasonable to expect that the property would retain an easterly tilt after mining ceased, and this was assigned to be the cause of the tilt observed. However, it should not be forgotten that the small differential level measured may not be a tilt but simply the out of level laying of the brickwork originally.

ECCENTRIC LOADING

It is estimated that the load from the gable wall is about 40% of the total load on the 2.6m wide thickened portion of the slab and since it lies at the edge (with little or no projection of the slab outside the brickwork) a significant moment is applied.

The rotation of a rigid strip subjected to moment loading can be calculated from equation 1, given by Muskhelishvili (after Poulos and Davis, 1974) :

$$\text{Rotation } \emptyset = \frac{16M\,(1-\nu'^2)}{\pi\,E'\,B^2} \qquad (1)$$

M = moment applied

ν' = poisson's ratio

E' = soil modulus

B = width of strip

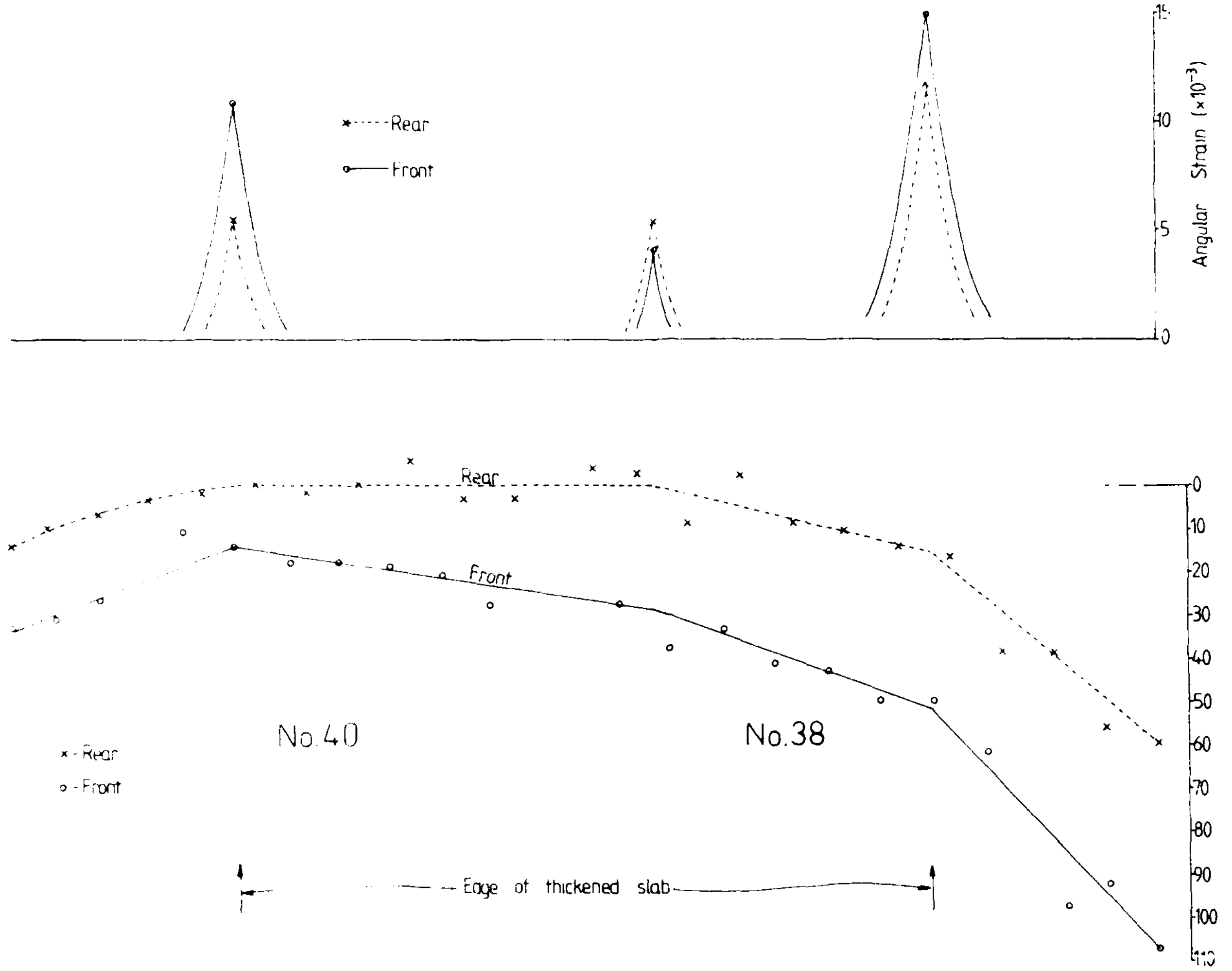

FIGURE 2 Differential Shape and Angular Strain

Assuming 'elastic' conditions to pertain and using drained parameters, ' and E', the total rotation can be calculated. The soil modulus has been obtained from the results of oedometer tests using equation 2 (from Burland, Broms and de Mello, 1978).

$$E' = \frac{0.9}{M_v} \qquad (2)$$

M_v = coefficient of volume compressibility, m^2/MN

With an average value for soil layers 1 and 2 of $0.25m^2/MN$ a rotation of about 0.005 is obtained which compares reasonably well with the measured rotation of 0.006. Eccentric loading is, therefore, considered to be the cause of the rotation at the gable end of No. 40 and consequently must be part of the rotation at No. 38.

It is feasible that part of this rotation could be due to seasonal moisture variation in the underlying clay, particularly as the slab foundation is very shallow. However, there was no evidence along the front and rear of the property to support this view.

MOISTURE REMOVAL BY TREE

A single fairly mature tree of the Ash family existed about 6m to the north of the front corner of the gable end of No. 38. Pits excavated at the gable end proved thick fresh roots (up to 15mm diameter) and numerous fine roots within the silty clay underneath the foundation. Open fissures in the clay were also observed. Tree roots or open fissures were not observed in pits excavated at the front and rear of the property. Thus the lateral extent of the tree root system was limited to the gable end and no further.

Evidence of the removal of moisture from the clay strata was obtained from comparison of the moisture contents from Boreholes 1 and 2 sunk outside and within the tree root extent, see Figure 1. Average moisture contents are given in Table 1 and show lower values near the tree. It can be seen that the differences are small and could be within the variation to be expected for a natural soil, especially one of glacial origin. Nevertheless, it is also shown that if these are to be considered reductions in moisture content then the change in (vertical) thickness of each layer

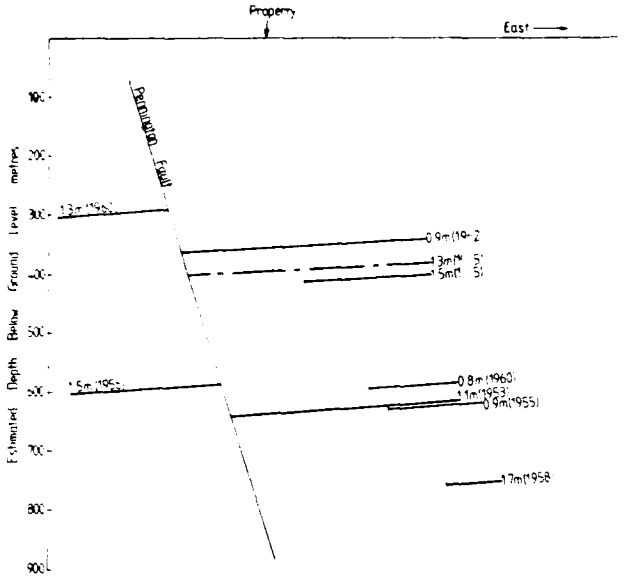

FIGURE 3 Coal Extraction After 1945

calculated simply from the loss of moisture (and assuming no effects from plasticity, suction, horizontal movements etc.) is significant, see Table 1. The total change in thickness is also comparable to the observed settlement at the front of the gable end of No. 38 when the movements due to other causes are removed.

During the summer of 1976, exceptional drought conditions were experienced in the U.K. which obviously aggravated this situation.

STRUCTURAL DISTORTION

Criteria for the onset of visible cracking have been given for loadbearing brickwork structures (Burland et al, 1978) and it has been shown that the hogging mode of deformation is the most critical. These authors give a critical hogging ratio,

Δ/L, of 2×10^{-4} where

Δ = central deflection

L = length of structure

The overall hogging ratio at the rear and front of the property (No. 38) is calculated as 30 and 34 ($\times 10^{-4}$), respectively, which is far in excess of the critical value and obviously represents very severe cracking, as found. Ignoring the effect of the tree, i.e. solely due to eccentric load rotation, the overall hogging ratio would be 11×10^{-4}, still above critical and compatible with the observed settlement and cracking at the southern end of No. 40.

Where the settlements are non-uniform, as in this case, their effects can be better depicted by plotting the angular strain, see Figure 2. The locations of high angular strain relate well to the zones of more severe cracking.

CONCLUSIONS

The author considers there are two main conclusions from the above

1. Ground movements and associated structural distortions are not always attributable to one cause, which provides the geotechnical engineer with the difficult task of separating the causes and their effects and attributing responsibility,

2. the effects of moisture removal by tree root systems and to a lesser extent eccentric loading provide the most serious consequences for brickwork structures since they produce the more critical hogging mode of deformation.

ACKNOWLEDGEMENTS

The author wishes to thank the Estates Department of British Coal for their kind permission to publish the details in this paper. The views expressed are those of the author alone.

REFERENCES

Burland J.B., Broms B.B. and de Mello V.F.B. (1978), "Behavour of Foundations and Structures" CP51/78, Building Research Establishment, Garston, Watford, England.

Poulos H.G. and Davis E.H. (1974), "Elastic Solutions for Soil and Rock Mechanics", John Wiley and Sons, New York.

Proceedings: Second International Conference on Case Histories in Geotechnical Engineering, June 1-5, 1988, St. Louis, Mo., Paper No. 6.26

Pressure-Injected Footings—A Case History

M.R. Lewis
Engineering Supervisor, Bechtel Civil, Inc., Gaithersburg, Maryland

M.M. Blendy
Chief Engineer, Spencer, White and Prentis, Rochelle Park, New Jersey

SYNPOSIS: A specialty contractor installed high-capacity pressure-injected footings (PIFs) for foundations in a congested area of an existing coal-fired power plant. Some concrete cylinders broke at strengths significantly lower than the minimum specified strength. Initial coring of some of the PIFs uncovered voids and deleterious matter at the junction of the shaft and the end-bearing base of the PIFs. Subsequent load tests and additional coring substantiated the load-transfer problem. A field testing program was initiated to verify the load-carrying capacity of all the completed PIFs. Wave equation analyses optimized the testing program, established the field testing criteria, and predicted ultimate capacities close to the measured capacities determined from load tests. Load tests also verified the design equation used to control installation of the foundation units. Field testing increased the overall average factor of safety with respect to ultimate capacity.

INTRODUCTION

An existing, coal-burning power plant required a stack-gas, emission-control system addition. Noise and vibration restrictions, space limitations, and economic considerations resulted in the selection of pressure-injected footings (PIFs) for foundation support. The entire foundation system consisted of 128 PIFs, placed in groups of three or four. Subsurface conditions in the area consisted of 40 feet of sand and clay fill, 30 feet of dense sand, underlain by hard silt and clay, with the ground water level about 20 feet below the existing ground surface.

A PIF is an end-bearing foundation unit consisting of an enlarged concrete base at the bottom of a concrete shaft. The base is formed in the soil bearing stratum by using a high-energy drop hammer to drive concrete out through the bottom of a drive tube to form a "bulb" of concrete. The function of the "bulb" of concrete or base is to deliver the load to the compacted soil; the shaft delivers the load to the base. The shaft is compacted concrete poured in-place, either in contact with the soil, or encased in a corrugated, metal shell.

This case history describes and discusses an unanticipated problem encountered during PIF installation, its solution, and the results.

SUBSURFACE CONDITIONS

A subsurface exploration program was carried out at the location of the facility. Standard penetration test (SPT) borings were drilled to depths up to 120 feet below ground surface. The results verified earlier investigations performed for the existing structures. A generalized soil profile is shown on Figure 1.

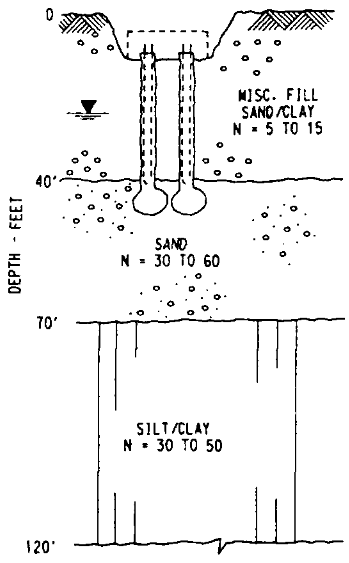

Fig.1 Typical Installation And Subsurface Conditions

The subsurface conditions in the vicinity of the facility consist of approximately 40 feet of miscellaneous fill, with SPT N-values ranging from 5 to 15 blows/foot. Underlying the fill is a layer of medium dense to very dense, medium to coarse sand about 30 feet thick, with SPT N-values ranging from 30 to 60 blows/foot. Below the sand is a layer of very stiff to hard silty clay about 50 feet thick, with SPT N-values ranging from 30 to 50 blows/foot. The ground water level is 20 feet below the existing ground surface.

PRE-PRODUCTION LOAD TESTS

After solicitation of bids and award of the contract, PIF installation began. After several production PIFs were installed at random locations around the site, one was selected for load testing. Since PIF-111 required the fewest number of hammer blows to expel the last 5 cubic feet of zero-slump concrete to form the base, it was selected for the load test.

The load test was carried to twice the 170-ton design load, or 340 tons. A single hydraulic jack, placed between the top of PIF and the bottom of a reaction beam, applied the load. Four PIFs on each side of the reaction beam served as the anchor. Load increments of approximately 40 tons were applied and held for one hour each until the maximum test load of 340 tons was reached. At this point, the test load was held for 24 hours and the settlement was monitored. The measured gross settlement under the test load was 1.2 inches. Since the structures could tolerate this amount of settlement, the 340-ton test load was considered the ultimate load capacity for PIF-111. The load-deflection curve for PIF-111 is shown on Figure 2.

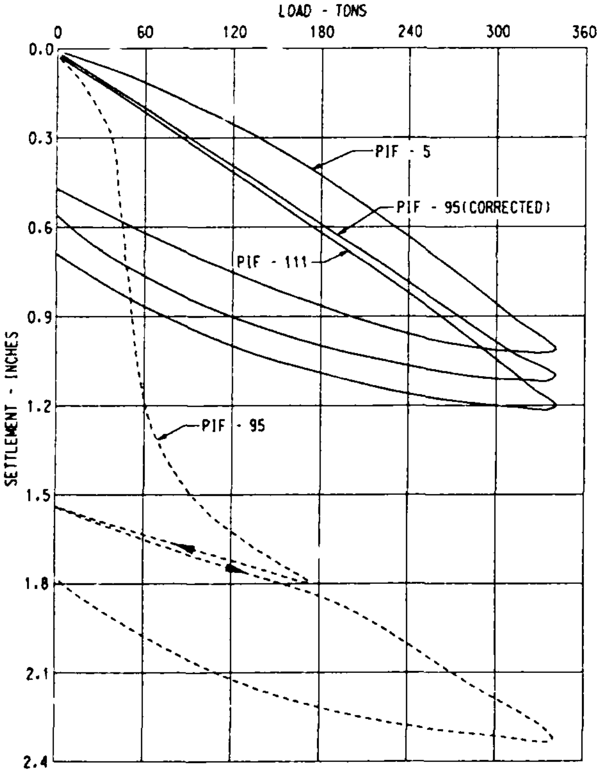

Fig.2 Load Test Curves

The results verified both the adequacy of the bearing stratum and the analytical equation for PIF capacity developed by R. L. Nordlund, (1970) i.e., the ultimate capacity of the base is directly proportional to the number of blows of the hammer ram to inject the last cubic foot of zero-slump concrete into the base, and proportional to the energy per blow of the ram.

$$L_u = \frac{B \times W \times H \times V^{2/3}}{K} \qquad (1)$$

where: L_u = Ultimate capacity, in tons

B = Number of blows required to inject the last five cubic feet of zero-slump concrete into the base

W = Weight of drop hammer used to form base, in pounds

H = Fall of drop hammer to form base in feet

V = Total volume of zero-slump concrete to form the base, in cubic feet

K = Constant of proportionability for design equation = 60

The resulting ultimate capacity equation for PIFs in granular soil is shown on Figure 3.

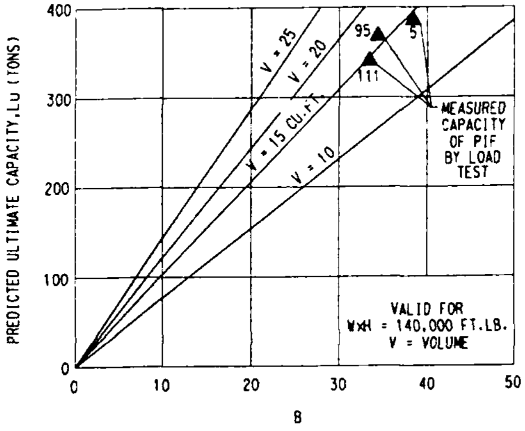

Fig.3 PIF Design Equation

Following load test completion, the contractor then proceeded to install the remaining PIFs, using the same procedures as those used for PIF-111, namely, a drop-hammer energy of 140,000 foot-pounds, and a minimum of 34 hammer blows to expel the last 5 cubic feet of zero-slump, base concrete.

CONSTRUCTION PROBLEMS AND ADDITIONAL TESTING

During PIF installation, an independent testing firm was retained to perform quality control testing. As part of the contract, the firm monitored the PIF installation and prepared concrete cylinders for routine compressive strength tests. During construction, some of the 28-day compressive strength breaks were significantly lower than the specified strength of 4,500 psi. Upon reviewing the testing firm's procedures, it was determined water was being added to the concrete just prior to making the cylinders, thus casting doubt on the results. At this point, it was concluded the only way to accurately determine the strength of the already placed concrete would be to core the concrete of the completed PIFs and perform compressive strength tests on the recovered concrete cores.

The coring program uncovered several apparent voids and foreign material, such as mud and brick fragments in the stem area above the base. Further, compressive strength results were as low as 1,000 psi. The combination of potential voids, segregrated concrete, foreign material, and low compressive strength indicated a potential problem of load transfer through the steam area. With PIF installation essentially complete at this time, additional core sampling and load tests were recommended and conducted on additional complete PIFs.

A double-tube core barrel, which produced 4-inch diameter samples, was used for the additional coring. These large-diameter core samples were tested to determine the unconfined compressive strengths and unit weight. The minimum compressive strengths recorded for the additional cores were 2,400 psi from the stem area and 1,700 psi from the base, with the unit weight being approximately 148 pcf.

Additional load tests were performed on completed PIFs 95 and 5. During initial loading of PIF-95, a rapid settlement of about 1.5 inches occurred between the loads of 40 and 80 tons, as seen on Figure 2. The load test was continued to 170 tons, and subsequently reduced to zero to determine the net settlement. The load test was then cycled back to 170 tons, and continued to 340 tons. The curve was corrected for this rapid movement by extending the portion of the curve between 170 and 340 tons back to zero load and then shifting the entire curve to the origin. The corrected curve for PIF-95 and the curve from the test conducted on PIF-5 compared quite closely to PIF-111 as shown on Figure 2.

These two load tests also verified the adequacy of the sand bearing stratum to support the load imposed by the base, and the analytical equation for PIF capacity as shown on Figure 3. However, the sudden movement in PIF-95 indicated a potential weak link in the load transfer mechanism between the shaft and the base, a condition unsatisfactory for the as-built PIF. As a result, all of the untested PIFs were considered suspect, and thus a method was needed to test the as-built condition of these PIFs.

WAVE EQUATION ANALYSIS

After evaluation of cost and time factors, a dynamic testing program was selected to verify or achieve the required capacity for each as-built PIF. This program consisted of driving the concrete piles to high end-bearing resistance on the base. Typical PIF installation and simulation are shown on Figure 4. The basic assumption was that there was a void or weak zone at the junction of the shaft and base. The wave equation program (Goble and Rausch, 1976 and Lowery, 1970) was used to evaluate pile capacity and associated stresses caused by driving. Details of the wave equation theory will not be given here, but are well documented elsewhere (Goble and Rausche, 1976, Lowery, et al. 1969, and Smith, 1960).

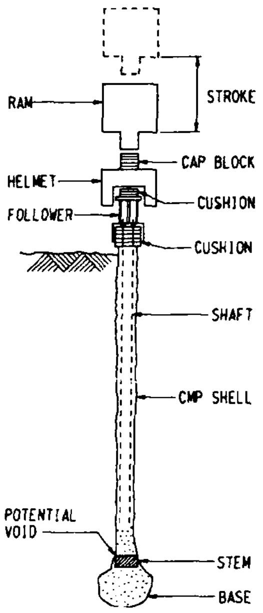

Fig.4 Dynamic Testing Problem Simulation

The solution consists of idealizing the actual pile-driving system as a series of concentrated weights and springs as shown on Figure 5. Idealization includes simulation of the soil medium as well as the pile driver and pile.

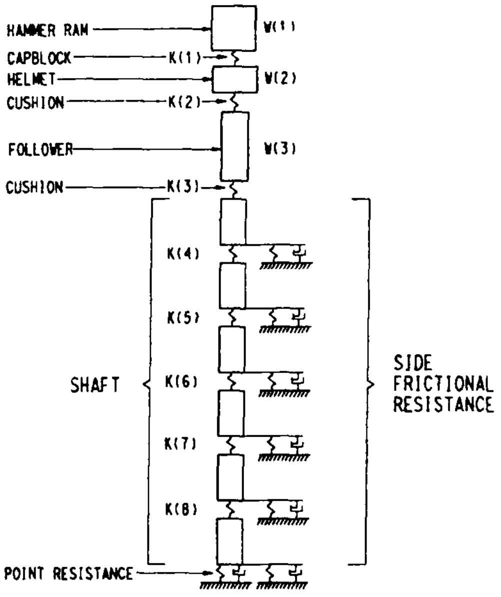

Fig.5 Model For Wave Equation Analysis

TABLE I. Wave Equation Input Data

Hammer Model	Pile (PIF) Model	Soil Model
a. Vulcan 014 single acting air/steam hammer b. Ram Weight - 14,000 pounds c. Rated Energy - 42,000 d. Capblock Material - Alternating disks of aluminum/micarta, 20 inches high, 17 inches in diameter, with an elastic modulus of 700 kips/square inch and a coefficient of restitution of 0.8 e. Cushion - Fir plywood, with an elastic modulus of 35 kips/square inch and a coefficient of restitution of 0.4	a. Length - 33 feet b. Diameter - 17 inches c. Concrete unconfined compressive strength of 5,000 pounds/square inch d. Concrete elastic modulus of 4,200 kips/square inch e. Concrete unit weight of 148 pounds/cubic foot	a. Distribution - Triangular b. Amount of skin friction - 10% c. Amount of end bearing - 90% d. Side Quake - 0.1 inch e. Tip Quake - 0.1 inch f. Side damping (Smith type) - 0.05 second/feet g. Tip damping (Smith type) - 0.15 second/feet

The results of the analysis are used to construct a bearing graph that relates ultimate resistance and stress to the set or blow count. Details of the input used in the analysis are given on Table 1.

Initial ultimate capacity of each as-built PIF was not known, but it was reasonable to estimate a combined frictional- and end-bearing capacity of 50 tons if a void was assumed in the concrete at the base of the shaft. This was based on the performance of PIF-95, which was load tested and began to settle in the range of 40 to 80 tons. Soil resistance distribution was assumed to be about 90 percent end bearing because the method of installation resulted in minimum friction friction along the shaft. Three cases were analyzed, details of which are given in Table 2. Case 1 provided a soft ram impact, kept the compressive stresses low for the first few hammer blows, and built up some resistance while cases 2 and 3 provided an increasingly harder impact, higher compressive stresses, and higher resistances.

TABLE II. Wave Equation Cases

Case	Hammer Stroke In Inches	Cusion on Follower In Inches	Cushion on PIF In Inches
1	24	3	12
2	24	0	10.5[(1)]
3	30	0	9[(1)]

(1) Compressed due to driving

The results of the wave equation analyses are shown on Figure 6. Case 1 condition resulted in a maximum tensile stress of 400 psi in overcoming a minimum ultimate resistance of 50 tons. The corresponding compressive stress was approximately 2,000 psi. This condition occurred at a set of 1 inch per blow. As shown in Figure 6, as long as an initial set of 0.5 inches or less is measured under the first hammer blow, tensile stresses are not critical. Higher compressive stresses and ultimate capacities were developed with Case 2 because of the harder impact and Case 3 resulted in even higher ultimate resistances and compressive stresses because of the longer stroke and minimal cushioning.

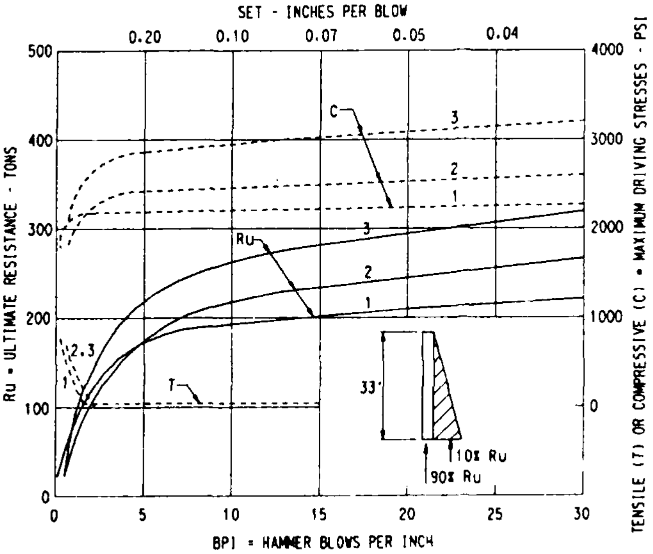

NOTE: NUMBER ADJACENT TO CURVES ARE CASE NOS. ANALYZED.

Fig.6 Wave Equation Analysis

The following example is based on Case 2 with reference to Figure 6. If, in the field, the final hammer blow produced a permanent set of 0.1 inch, then the ultimate, load-bearing capacity immediately after driving should be about 220 tons, and the maximum compressive stress induced in the shaft should be about 2,400 psi. This ultimate resistance is the total soil resistance overcome during driving.

DRIVING CRITERIA

The wave equation analysis for Case 3 (full ram stroke and approximately 9 inches of plywood cushion) and the results of PIF-95 established the field-driving criteria to be used for dynamic testing. For Case 3, a final set of 0.15 inch predicted an ultimate resistance of 240 tons and a maximum compressive stress of 2,900 psi in the shaft. Since the design load of 170 tons correspond to an approximate stress of 1,500 psi, this criteria provided a minimum factor of safety equal to 1.4, with respect to load carrying capacity, and 1.9, with respect to compression driving stress. As all the PIFs would be tested, these factors of safety were considered acceptable. The load-test curve for PIF-95, which settled excessively during the 40 to 80 ton increment, was reviewed. The break on Figure 2 indicates that the resistance built up after the shaft penetrated approximately 1.5 inches. Therefore, the field-driving criteria selected was a final set for Case 3 of 0.15 inch or less for the last hammer blow, and a total penetration of less than or equal to 1.5 inches. Case 1 and Case 2 driving criteria were arbitrarily selected to be a final set of 0.25 inch or less, and 0.2 inch or less, respectively.

FIELD TESTING

All 128 PIFs were tested dynamically within ten working days, with one crew working a standard eight-hour day. The testing was performed in the following manner. A graduated scale was attached to the side of the shaft, and the horizontal cross hair of a transit was used as a reference to measure the set under each hammer blow. The top of the shaft was leveled with some sand, and 12 inches of plywood pile cushion, with holes cut to pass the reinforcing, was then set on the top of the shaft. Next, a follower was placed over the cushion and reinforcing, and an additional 3 inches of plywood cushion was placed on top of the follower. The hammer was then set in place on the follower. Figure 4 shows the dynamic testing set up. One hammer blow was delivered using the short stroke, and the set of the pile was measured. Additional hammer blows were delivered until a set of 0.25 inch or less was obtained (Case 1). The hammer was lifted off the follower and the 3 inches of plywood was removed. The hammer was set back in place, and additional hammer blows were delivered, using the short stroke, until a set of 0.20 inch or less was obtained (Case 2). Finally, a full ram stroke was used and additional hammer blows delivered until a set of 0.15 inch or less was obtained (Case 3).

The three PIFs which had been load tested previously were retapped to compare the wave equation predicted capacity, R_u, with the measured load test capacity. The wave equation predicted the ultimate capacity within 15 percent of the measured values as shown on Figure 7. As a result, the predicted stresses were considered to be within this same range of accuracy.

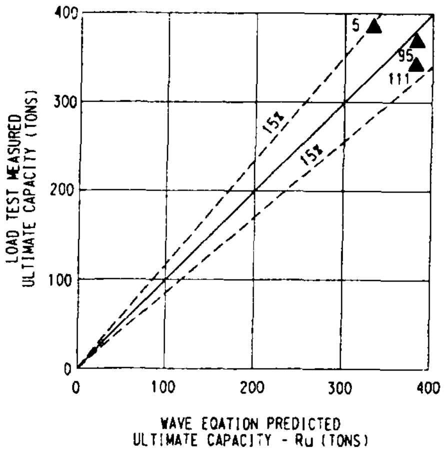

Fig.7 Wave Equation And Load Test Comparison

RESULTS AND EVALUATIONS

The reasonable accuracy of the wave equation to predict the ultimate capacity of the PIFs permitted comparing the initial capacity and the final capacity. The set measured under the first hammer blow was converted to the ultimate capacity (Figure 6), and is considered the initial as-built capacity. The PIF was then driven and the final set was converted again to ultimate capacity (Figure 6). Table 3 is a summary of this comparison.

TABLE III. Wave Equation Results

FINAL ULTIMATE CAPACITY - TONS	INITIAL ULTIMATE CAPACITY - TONS 170	200	230	260	290	320	350	380	TOTALS
170	1(1)								1
200									0
230									0
260	2	1	1						4
290	6	4	5	1					16
320	1	9	12	3	1				26
350	1	5	15	8	4		4		37
380		1	21	3	4			15	44
TOTALS	11	20	54	15	9	0	4	15	128

(1) PIF - 37 INITIAL CAPACITY 100 TONS AND FINAL CAPACITY 120 TONS

The initial, or as-built, capacity ranges are across the top and the final capacity ranges are down the side. Figures in the table represent the number of PIFs with the particular initial and corresponding final capacities. Totals for each capacity range are shown also. For example, there were 15 PIFs with an initial and final ultimate capacity in the range of 350 to 380 tons. Table 3 clearly shows that at least 11 PIFs had an initial ultimate capacity less than the design load of 170 tons.

The field data were analyzed to determine the initial and final factors of safety with respect to load carrying capacity. Factor of safety is defined as the ratio of the initial or final ultimate soil bearing capacity to the design load of 170 tons. Initial factors of safety ranged from a minimum of 0.5 to a maximum of 2.2,, and the average was 1.4. After dynamic testing, the resulting final factors of safety ranged from a minimum of 1.4 to a maximum of 2.2, and the average was 1.9. PIFs-32, 27, and 94 were not included in computing the final factor of safety because they did not meet the driving criteria, and were subsequently replaced with PIFs installed adjacent to the unacceptable PIFs.

SUMMARY AND CONCLUSIONS

Load tests and coring of as-built PIFs confirmed a potential problem of load transfer between the shaft and the base of some of the 128 PIFs, which had a design load of 170 tons. The wave equation was used to estimate the bearing capacity and stresses resulting from driving the PIFs to a high, bearing resistance against the base.

The wave equation predicted ultimate capacities within 15 percent of measured capacities, determine from load tests, and these load tests also verified the design equation which was used to control PIF installation.

All of the PIFs except three met the driving criteria; the three were replaced. Dynamic testing estimated the initial, ultimate load-carrying capacity of each PIF, and identified at least 11 which were found to have initial, ultimate capacities less than the design load of 170 tons. Dynamic testing permitted driving each PIF to a higher, ultimate capacity, and resulted in increasing the overall average factor of safety from 1.4 to 1.9. The completed structure has performed satisfactorily.

REFERENCES

Goble, G.G., and Rausche, F., (1976) "Wave Equation Analysis of Pile Driving - WEAP Programs," Prepared for the U.S. Department of Transportation, Federal Highway Administration, Implementation Division, Office of Research and Development.

Lowery, L.L., Hirsch, T. J. Edwards, T. L., Coyle, H.M., and Samson, C.H., (1969) "Pile Driving Analysis-State of the Art," Research Report No. 33-13, Texas Transportation Institute.

Lowery, L.L., (1970) "User's Manual for the Computer Program - Pile Driving Analysis by the Wave Equation".

Nordlund, R.L., (1970) "Pressure Injected Footings," Design and Installation of Pile Foundations and Cellular Structures, Lehigh University.

Smith, E.A.L., (1960) "Pile Driving Analysis by the Wave Equation," Journal of the Soil Mechanics and Foundation Division, Proceedings of the American Society of Civil Engineers, Proc. Paper 2574, SM4.

Proceedings: Second International Conference on Case Histories in Geotechnical Engineering, June 1-5, 1988, St. Louis, Mo., Paper No. 6.27

Anchor Failures at a Deep Excavation

Vinod K. Garga
Associate Professor, Department of Civil Engineering, University of Ottawa, Ottawa, Ontario, Canada

SYNOPSIS: The Paper describes failures of some high tensile strength steel tensioned rock anchors at a deep excavation. The failures are attributed to stress corrosion to which the high tensile strength steel is particularly susceptible. The method which was used to estimate the life of remaining anchors on the project is described. The need for ensuring a high level of care during transportation, storage and installation of such high tensile strength steel bars is emphasised.

INTRODUCTION

The use of ground anchors to provide lateral support for excavations is now a common practice. These anchors can be designed with an adequate margin of safety by using current design methods in combination with well documented data from previous projects, and by exercising adequate quality and testing control during the installation process. In particular the adoption of current methods of design and construction have greatly reduced the possibility of failure of the anchors along the grout-ground, and grout-tendon interfaces. However one aspect of anchor design where great caution still needs to be exercised, relates to the corrosion failure of tensioned steel tendons or the steel anchor head assembly. These failures are seldom reported in literature, although most designers are aware of cases where such instances have occurred in the field.

A detailed case history has been presented by Jurell (1985) who described an anchor failure at an underground machine hall in Sweden. A total of 118 Dywidag 80/105 prestressing bars, 26 mm. in diameter, and with an average length of 12 mm, were stressed to a load of 300kN during 1955. In the spring of 1981, one of the bars failed 2.5 m from the anchor head with such a force that it flew out and landed 8 m away on the floor. Such sudden release of energy apears to be typical of stress corrosion failures. Subsequent investigation revealed that the failure had been triggered by a 5 mm deep primary crack originating from the bottom of a large corrosion pit having a maximum depth of only 0.8 mm. A section of the bar at the corrosion pit where the fracture initiated is shown in Fig. 1.

This paper presents a case history of a deep excavation in downtown Vancouver, B.C. Canada, where several anchors failed during construction despite the fact that corrosion protection for the temporary use of these anchors had been provided. Subsequent investigation on these failures, and the method to estimate the remaining life of anchors to complete the project are also discussed.

The Site

The site, approximately 75 m x 43 m in plan, and 20 m deep was located at a busy intersection. In view of the very close proximity of sensitive structures and major underground utility services including two small tunnels, a vertical excavation was selected. It was further stipulated that the excavation would be maintained at essentially "at rest" (K_0) condition so that the elaxtic deformations could be kept to a minimum.

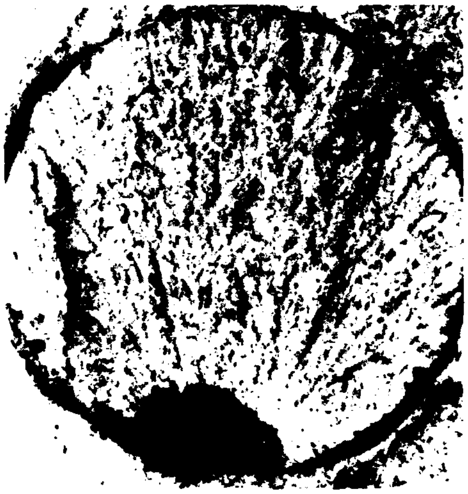

Fig. 1. Fracture surface at corrosion pit (Jurell, 1985)

The subsurface conditions at the site were evaluated from results of 14 drill holes, 10 auger holes, and a number of laboratory tests. Typically, the surficial soils consist of loose silty sands and sand and gravel fill overlying dense sand to an average depth of 3 m. The dense sand is a residual soil derived from weathering of sandstone bedrock. The contact between the dense sand the bedrock is therefore transitionary. The overburden is underlain by sandstone that is generally gradational from fine grained at the top to coarse grained at a depth of approximately 12 m. A 2 m thick mudstone layer underlies the coarse-grained sandstoone at an average depth of 14 m. The sandstone had a typical rock hardness index of R2 (classification after Piteau et al. 1979) The regional groundwater table at the site lies below the excavation floor; however, perched water tables are encountered at several higher elevations especially above mudstone contacts.

Excavation Support System

A method of excavation support using a combination of soldier piles and lagging in the overburden and tensioned temporary soil or rock anchors was judged to be most suitable for the site conditions (Fig 2). All anchors were to be destressed at the end of construction. Current jurisprudence in British Columbia does not permit the use of anchors for permanent support if the bond length intrudes on adjacent property. The permanent lateral support is provided by the heavily reinforced substation walls and floor slabs. A 75 mm thick shotcrete layer was applied on all exposed bedrock surfaces to minimimize rock weathering and to reduce the risk of local rockfall.

The specifications for the three types of tensioned grouted anchors proposed by the contractor are given in Table 1. It is important to note that despite their temporary nature, the anchors were provided with a corrosion protection. All metal component were coated with corrosion inhibitor and the free length of the bar was enclosed in a grease-filled polyethylene sheath, which was sealed to the bar at the bottom of the free length to prevent ingress of grout in the annular space. Despite low regional groundwater, a perimeter drainage system was designed to relieve pressure from perched groundwater tables. Groundwater around the excavation was controlled by 30 cm diameter vertical perimeter collector drains. A total of 37 drains, at a nominal spacing of 6 m, was installed to the full depth of the excavation. The upper end of the drains, was sealed to prevent entry of additional water from the pervious overburden. At each collector drain, a series of "inclined" seepage drains at a vertical spacing of 3 m were drilled in the bedrock. These drains were cased with 38 mm diameter pre-slotted PVC pipe, and their lengths were varied to drain bedrock at the fixed lengths of the anchors.

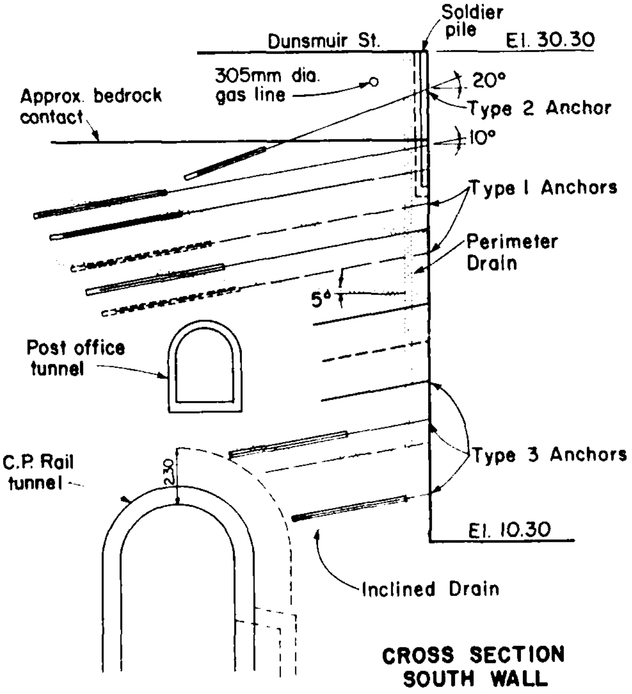

Fig. 2. Excavation support system.

The overburden support was provided by timber lagging retained by bedrock-anchored soldier piles and tiebacks. The support system was optimized using anchors with a maximum working load of 403kN (type II anchors) for the upper tiebacks and anchors with a working load of 659kN (type I anchors) for the two lower tiebacks, for an average horizontal spacing of 2 m. The type I anchors also constituted part of the bedrock support system. Anchor holes were drilled to a diameter of 89 mm for types I and II anchors, and 75 mm for type III anchors. The anchors were designed at a typical grid spacing of 2 m x 2 m to provide an average stress of $150kN/m^2$ on the walls. Based on earlier anchor pullout tests, the bond lengths were determined on the basis of working shear resistance of 0.7 MPa at the rock-grout contact. Typical bond lengths for type I and type II anchors were 5 m and 3 m, respectively. Reference should be made to Garga et.al. (1984) for further details on design and construction of the excavation support system for this project.

All anchors were required to be destressed when the horizontal earth pressure could be supported by the rigid perimeter walls and floor slabs of the underground reinforced concrete structure.

Type I Rock Failure Anchors

After all anchors were installed, and during the construction of the perimeter walls and floor slabs, a total of seven randomly distributed sudden failures, occurred in the stressed type I rock anchors. The first tendon to fail under the design load fractured at the interface of the free and bond lengths, aproximately 10.5 m from the face of the excavation. The unbonded portion of the rod was protected against corrosion by a grease-filled polyvinyl sleeve that was taped at both ends. The elastic strain energy stressed in the bar was of such magnitude that it launched the failed portion of the bar 20 m across the site. Fortunately, no injuries or other damage occurred.

Failure Investigation

The failed anchor rod had performed satisfactorily for 13 months with no apparent increase in tension. It was therefore assumed that a delayed cracking mechanism was responsible for the failure. A detailed study of the anchor rod fracture surface using various metallurgical techniques indicated the following:

(i) The fast brittle fracture was initiated by a small elliptical surface crack that was covered with a black magnetite corrosion product (Fe_3O_4). The crack originated in a surface corrosion pit which induced stress and chemical concentration effects. Radial fracture lines covered 98% of the fracture surface and clearly lead back to the fracture origin.

(ii) The defect that initiated brittle fracture was intergranular in nature, and had a maximum depth of 0.86 mm and a maximum length of 3.02 mm (Fig. 3). The striking resemblance to Fig. 1 is obvious.

TABLE 1. High Tensile Steel Anchor Specifications

Type	Use	Dia. mm	Yield Stress N/mm^2	Specified Working Load, Pw kN	Minimum Yield Load, Py (=1.5 Pw) kN	Minimum ultimate capacity, P_{cf} (=1.25Py) kN
Type I	Rock support	36	1080	659	989	1236
Type II	Overburden support	32	835	403	605	756
Type III	Local rock support in front tunnels	25	835	103	195	244

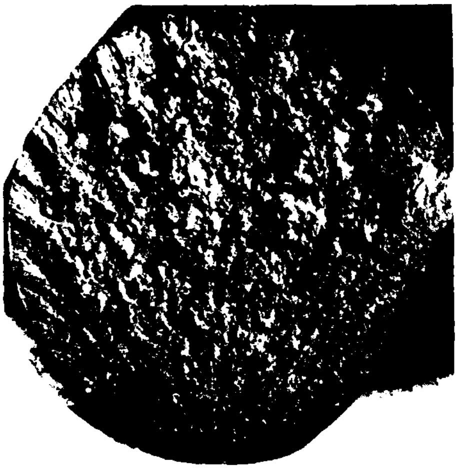

Fig. 3. Fracture surface from first anchor failure. Arrow indicates originating defect. Magnification x 2.5

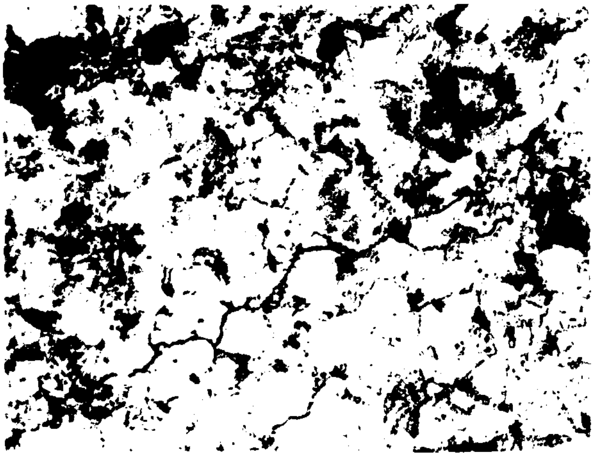

Fig. 4. Micrograph showing intergranular nature of crack. Magnification x 200.

(iii) A small intergranular crack was found immediately above the rod fracture face. This crack also originated in a surface corrosion pit and had a maximum depth of 0.5 mm (Fig. 4). The general condition of the bar was good, with no evidence of gross surface pitting.

The evidence indicated that the fracture-originating defect was probably caused by a form of stress corrosion cracking. Samples of construction materials and ground-water were analyzed but the corrosive medium that caused the cracking could not be identified.

Material Evaluation

Mill certificates supplied by the steel manufacturer indicated that the rock anchor steel was a high carbon, high silicon type with a vanadium addition (type ST 1080/1230). Metallographic examination of the steel revealed a microstructure of nearly 100% pearlite. The yield strength of the rod material was 1100 MPa, which is 40% above the apparent stress in the rod when the failure occurred. Fracture toughness testing was therefore initiated to determine the material performance in the presence of surface defects.

Fracture toughness testing was completed on test samples of the steel bar cut from areas adjacent to the fracture surface. All testing was performed in air at room temperature (20°C). These tests showed that the fracture toughness value (K_{Ic}) for the rock anchor material was aproximately 30 MPa $\sqrt{m}$ in air.

The first broken anchor rod performed satisfactorily for a period of 13 months. At failure, the defect had a maximum depth of 0.86 mm and a circumferential length of 3.02 mm. No other data relating to the rate of crack growth is available. A defect analysis was next performed using the three-dimensional case of semielliptical surface defects in finite plates (Paris and Sih 1965). The maximum normal working stress of 690 MPa was used for the purpose of calculating the K_{Ic} value which corresponded to the measured critical defect size. For the measured critical flaw size in the field environment, the following equation applies:

$$K_{Ic} = [1 + 0.12(1-a_c b)] . \frac{\sigma(\pi a_c)^{1/2}}{\Phi} . \left| \frac{(2t)}{\pi a_c} \tan \frac{(\pi a_c)}{2t} \right|^{1/2} \qquad [1]$$

where a_c = critical defect depth = 0.86 mm; b = 1/2 defect length = 1.52 mm; σ = working stress = 690 MPa; t = bar diameter = 36 mm; Φ = elliptic integral = 1.37. The value of K_{Ic} = *from eq* [1] is calculated to be 3.65 MPa $\sqrt{m}$.

A comparison of the K_{Ic} value determined in the laboratory by testing in air and that back-calculated for the site environment from the measured defect size on failed anchor rod thus showed an order of magnitude difference.

Remaining Life Estimates

The velocity of the growth of stress corrosion cracks depends on the environment, the stress intensity, and the material properties. Both the environment and the stress intensity could vary thoroughout the life of the bar. The nature of the cracking found immediately below the fracture face indicated that the cracks were growing in a stable fashion. Stress corrosion cracks of this type develop in three stages. Crack initiation is usually followed by a rapid growth over a very short period of time (stage I), followed by cracking at a steady crack growth velocity (stage II). The final stage comprises of unstable crack growth at a very rapid rate. The best estimate of crack growth velocity i.e. assuming that the defect grew at a constant rate, may be obtained from:

$$v = \delta\ell / \delta t \quad [2].$$

For t = 13 months; ℓ = 0.86 mm (initial defect depth), a crack velocity $v = 2.71 \times 10^{-8}$ mm/s is obtained. The value of K remains constant in a given environment. The critical crack size which would permit unstable fast fracture to occur can therefore be calculated for a variety of stress conditions, by using Eq.(1). To estimate the minimum remaining life, of the anchors the bars in the excavation can be proof loaded to a higher load after which they can be "locked off" again at the original working load. The survival of the bars during the proof loading process provides a direct confirmation that the defect did not yet attain the critical depth. It should be noted that the higher proof stress results in a smaller critical depth (Equation 1). The critical defect size at the working load is known from examination of the fracture surface. The difference between the measured value of defect size at the normal working load of 690 kN and the calculated value of the defect size at some higher proof stress can be transformed into time by dividing by the estimated stable crack velocity. As an example, for a working stress of 690 MPa, a critical defect size, a_c, of 0.86 mm was mesured in the field. If the stress during proof loading is increased by, say, 20%, then a new critical defect size can be back calculated for Eq.[1]. In this case, for the higher stress of 828 MPa, a defect size, a_c, equal to 0.66 mm is calculated. The difference in critical crack size is therefore 0.20 mm. Assuming that the rate of crack propogation remains constant at 2.71×10^{-8} mm/s as determined from Eq.[2], the additional time gained by proof loading to 827 MPa is given by 85 days ($0.20\text{mm}/1.71 \times 10^{-8}$ mm/s). The same argument can, of course, also be aplied to a decrease in stress level in the bar. A lower stress value will result in a larger critical defect size. The difference between this value and the measured critical defect size at the normal working load can also be transformed into a minimum time to failure.

At the time of the first anchor failure the stress level in the anchor rods could not be reduced since the floor slabs were not yet fully constructed, and were therefore not capable of resisting the ensuing increase in lateral stress. It was therefore decided that a statistically significant number of anchor rods should again be proof stressed above the normal working stress. As explained int he preceeding paragraphs, fracture toughness data was used to generate a proof load versus time gained curve as shown in Fig. 5. This curve was based on the average load of 700 kN initially reported for the rock anchor system. A total of 125 type I anchors were proof-loaded to 850 kN to obtain a minimum theoretical remaining life of 110 days. The work was resumed at the site with this knowledge.

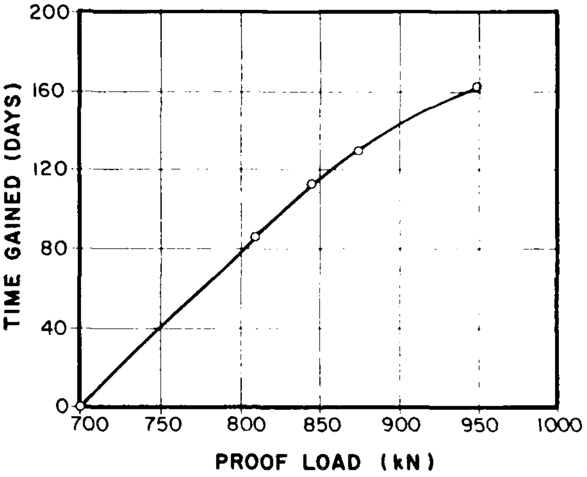

Fig. 5. Proof load versus time gained.

Approximately 70 days after proof loading was completed, a second rock anchor in the south wall failed suddenly. The fracture features were identical to those found on the first anchor failure. This anchor failed at the taped interface between the corrosion protection sleeve and the unprotected end of the rod immediately below the anchor plate. At the time the second failure occurred, it was learned that the type I anchor rods in the system were tensioned at loads varying between 620 and 838 kN (average value 700 kN). Since further failures appeared likely, it was decided to partially destress all type I rock anchors because some lateral load could now be carried by the lower floor slab and perimeter walls. The strength of the installed concrete substation walls allowed destressing to an equivalent load of 620 kN on all type I anchors. New calculations were made to estimate the time to be gained by both proof loading to 850 kN, and unloading to 620 kN immediately thereafter. Table 2 shows the calculated values of time gained versus the original recorded load in the bar. These results are shown graphically in Fig. 6.

Table 2. Remaining life estimates

Initial Load in bar (kN)	Critical Defect depth a_c (mm)	Proof Loading to 850 kN (1)		Unloading to 620 kN (2)		Total time gained (1) + (2) (days)
		a_c (mm)	Time gained (days)	a_c (mm)	Time gained (days)	
600	1.14	0.56	234	---	0	234
620	1.07	0.48	205	---	0	205
650	0.97	0.38	162	0.10	43	205
680	0.89	0.30	129	0.18	76	205
700	0.84	0.25	108	0.23	97	205
750	0.71	0.13	54	0.36	151	205
800	0.64	0.05	22	0.43	184	205
850	0.56		0	0.51	216	216
900	0.51		0	0.56	233	233

Two additional type I rock anchors failed during proof loading to 850 kN. Proof loading was an effective means of identifying anchor rods containing defects approaching the critical defect size. The combined total time gained by proof loading and partially unloading the type I anchor bars provided a minimum of 205 days of safe working time at the Cathedral Square site. No further rock anchor failures occurred during construction after partial unloading was completed. During final destressing of the rock anchors after all the concrete was placed, three tendons failed just below the anchor nut as the tensile load was being applied to the anchor for "lift-off."

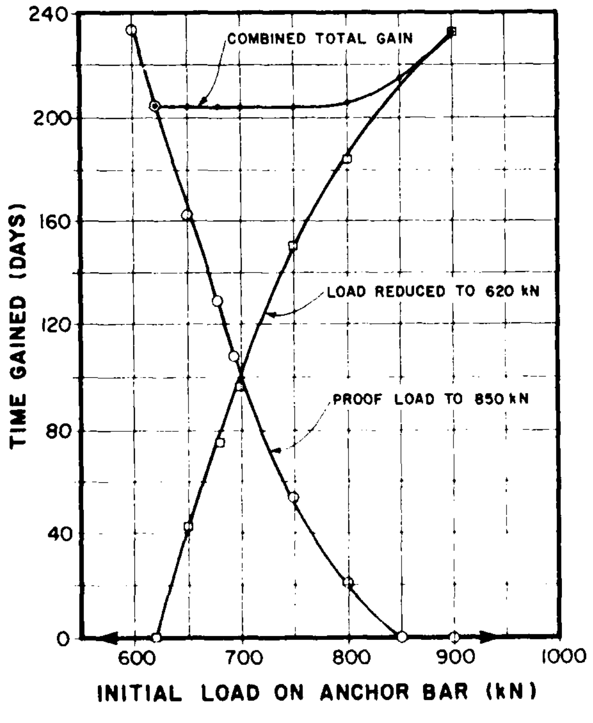

Fig. 6. Time gained by proof loading and load reduction.

Discussion

High tensile strength steels of the type used in this project are produced with a pearlite microstructure These steels have been developed to maximize tensile strength, but at the expense of toughness. As witnessed at this site, surface defects of seemingly insignificant depth can initiate catastrophic brittle failure in bars that are stressed to normal working stress levels. The bars at the site were provided with corrosion protection consistent with their temporary use, and yet failures occurred aproximately 13 months after installation.

It is important to emphasise, since it is not commonly appreciated, that high tensile strength post-tensing bars and accessories require an extraordinary care during transportation, storage and installation. Often the level of care demanded cannot be guaranteed even on well managed construction sites. For example, the specifications for such steels often contain requirements to the following:

-Steel must be transported dry.
-Any damage to the surface such as notches, abrasions, etc. must be absolutely avoided.
-Steel bars must not be thrown or dumped from a truck.
-The steel must be stored in a dry place, and sufficient ventilation must be provided to avoid condensation of water. In other words, direct contact of plastic sheet with steel is not permitted.
-The steel bars must not come in contact with the ground during storage.
-Hot welding sparks may initiate failure.

It is difficult to contemplate the enforcement of the above requirements, on an average construction project in North America.

Conclusion

1. After experiencing anchor failure, proof loading of anchors coupled with a careful examination of the fractured anchor bars was an effective means of determining the remaining life of the anchors.

2. The high strength steel of the type used in this project develops a high tensile strength at the expense of toughness. Hence, even minor defects on the surface of the bar can initiate catastrophic failure. Such steels require an exceptionally high level of attention during all phases of transportation, storage and installation. The Engineer must satisfy himself whether such level of care can be guaranteed on the project.

REFERENCES

Garga, V.K., Carey, E.I. and Milne R.W. (1984), "The Cathedral Square Substation Anchored Excavation, Vancouver, British Columbia". Canadian Geotechnical Journal, Vol. 21, No. 4, pp. 621-633.

Jureil, G. (1985), "Investigation into the Failure of a Prestressed Rock Anchor," Water Power and Dam Construction, February, pp. 45-47.

Paris, P.C. and Sih, G.C. (1965), "Stress Analysis of Cracks". Fracture Toughness Testing and its Applicatons, ASTM, Special Technical Publication,. STP 381, pp. 30-83.

Piteau, D.R. et al. (1979), "Rock Slope Engineering Reference Manual". Federal Highways Administration, Washington, D.C., Report No. FHWA-TS-79-208.

Proceedings: Second International Conference on Case Histories in Geotechnical Engineering, June 1-5, 1988, St. Louis, Mo., Paper No. 6.28

The Failure of Oil Storage Tanks and Their Control

Stanislav Dovnarovitch
Doctor of Science, Engineering, Research Institute of Bases and Underground Structures, Moscow, USSR

Yurij Ivanov
Doctor of Science, Engineering, Research Institute of Bases and Underground Structures, Moscow, USSR

SYNOPSIS: The paper discusses of some results of flexible footings and their models behaviour in the case of loading-unloading cycles applied to them. The revealed effects have been used to explain the causes of some tanks failures. It has been shown that one of the possible causes is the difference between the displacements of the tank bottom and soil under it following unloading and subsequent loading. A simple technique has been proposed to prevent the failures that can be easily applied when constructing the tanks. The application of the technique both eliminates the causes of the failures and greatly reduces the deflections of the tank's bottom thus making it possible to avoid materials and labour intensive footings.

INTRODUCTION

When designing and constructing tanks simplified assumptions on tank-soilbase interaction are introduced. Existing models can not give the adequate description of flexible plate interaction with soilbase. The experiment is the only tool to fully investigate the complicated processes of this interaction. This circumstance made NIIOSP to stage a long-term research program. Some of the relevant results and the discussion are due below.

THE FLEXIBLE PLATES LOADING TESTS

To get a better understanding of the results and conclusions let us consider at first laboratory loading-unloading tests performed on circular flexible plate models on a sandbase. The sandbase was filled in a 4 x 4 x 4 m.test-box without compaction by dropping sand with a grapple from a fixed height. The dencity of the sand was 1.62 t/m^3. The sand was medium-grained (0.5-1.0 mm. fractions amounted to 67%). The 5000 sq.sm plate models were manufactured from steel 5 mm thick as well as from a transparent material 12 mm thick. In the latter case possibility of visual observation of the effect going on in the model-sand contact surface was provided. Jacks were used to apply loads to the central part of the model through a rubber substrate. Each loading stage was retaind till the settlement stabilize. Maximum loads limited by the values that corresponded to the deflections close to the allowed values for flexible footings of structures, e.g. storage tanks. Vertical displacements of the models were measured along their three radii same as displacements of the sandbase surface both under the models and outside them. Evolution of cracks was registered on the sand surface.

DISCUSSION OF RESULTS

Consider Fig. 1 depicting a model and the sand surface displacements in the model center following the primary loading-unloading cycle. In the course of loading the model and the sand displacements coincide.

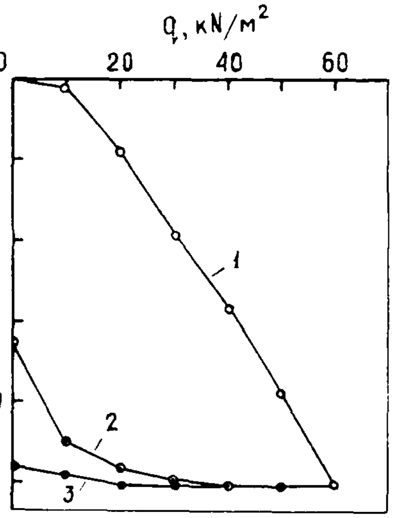

Fig. 1 Displacements of the Model Center and the Sand Surface under It
1, 2- model center 3- sand surface

During unloading the model rises elastically while the sand rebound largely lags behind. This results in formation of a gap between the sand surface and the model during unloading. This gap is shown on Fig. 2. Formation of the gap was registered while testing 2.1x2.1x2.1 m reinforced concrete slabs as well (Palatnikov, E.A. and all, 1978).
Evidently, the gap between the unloaded plate and the soil affects the contact pressure distribution in the course of the subsequent loading making it different from that of the continuous contact between the plate and soilbase. At the beginning of the repetitive loading of the plate contact pressures appears only over a

narrow peripheral ring being rather high so that they may thrust the sand upward inside and outside this ring.

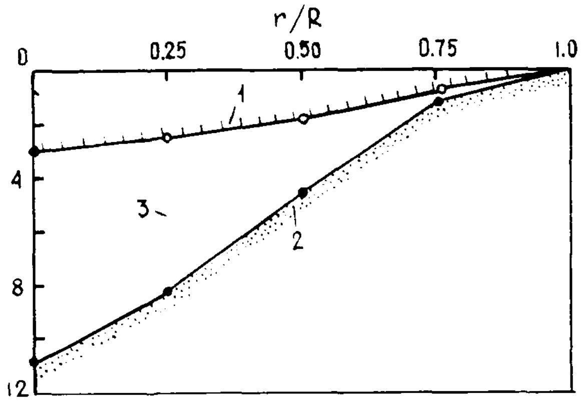

Fig. 2 Position of the Model and the Sand Surface after the First Loading-Unloading cycle

1- model 2- sand surface 3- gap

Such high contact pressures over the periphery of centrally loaded plates caused by repetitive loading was registered in large-scale tests. The data of (Dovnarovitch S.V. and all, 1987) show that plates that successfully endured the primary load may fail under the subsequent load due to the gap between the plate and the soil. Consider Fig. 3 (Bell R.A. and all, 1980) displaying of tanks bottom position of the actual structures after failure: tanks T-270 and T-39 with diameter 52 m. and 46 m. respectively.

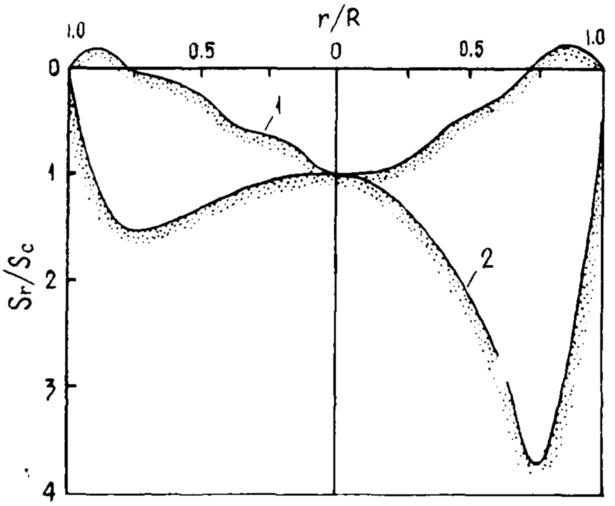

Fig. 3 Differential Settlement of Tanks Bottom after the Accidents

The accident of T-270 happened when it was filled with oil during the service while its water test did not provoke any failure. Such position may be explained as the result of large soil movements under the edges of the tanks where high pressures are caused by repetitive loading. Besides, the effects described above appear both if the tanks rest on soil and on piles. Fig. 4 show vertical displacements of the circular model plate center mentioned above and those of the tank bottom supported by piles (Mohan D. and all, 1978) following first loading, unloading and second loading after remedial underpinning of this foundation.

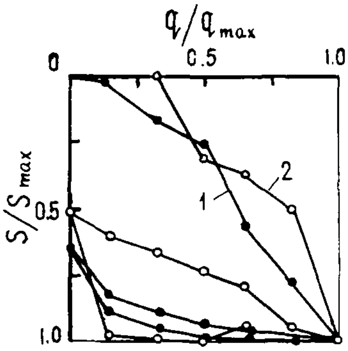

Fig. 4 Relative Vertical Displacements of the Model and Tank Bottom

1- model 2- tank bottom

Rapid settlement growth is observed at the beginning of second loading both in the case of the model and of the tank bottom. It may be explained by the emergence of the soil-footing interaction discussed above.

PROPOSED TECHNIQUE

These and many other results obtained by respective investigations and review of the known data encourage us to develop a new technique for constructing storage capacity principally different from the conventional ones to prevent accidents and greatly reduce as the differential settlement of structures well as the cost of construction. The technique envisages formation of the tank bottom-soilbase gap and filling said gap with a hardening material. This filling is to be completed during construction operations and water tests before commissioning the storage capacity.

Evidently, the primary load that precedes formation of the gap should be less than the maximum operation load. In the course of the study the proposed technique was elaborated to form and to fill the gap depending on the properties of the soils, the tank size, loads, time-schedule, etc.

The feasibility of the construction technique from the standpoint of the soilbase-structure stability is quite clear. Consider another no less important effect of technique. Look at Fig. 5 showing the deflection of the familiar circular plate model with empty and filled gap. It can be seen that deflections reduce more than twofold if the gap is filled in due time. This makes piles, that would be indispensible for conventional construction tichniques, unnecessary if the described technique is applied. Notably, the proposed technique does not practically involve any extra cost and is applied without employing sophisticated mashinary and highly skilled specialists.

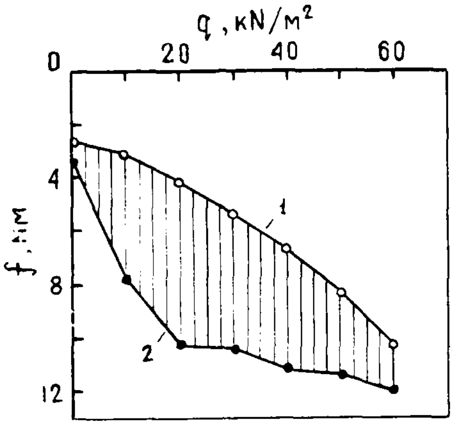

Fig. 5 Deflections of the Models under Second Loading
1- filled gap 2- empty gap

We have touched upon and schematically presented just some of flexible plate-soil interaction features. The problem in question is much more complicated. It is acute in the case of primary loading either. When the plate is loaded centrally, its edges rise above the ground and the contact area reduces while contact pressures grow as compared to the mean pressure with all respective implications, Fig. 6.

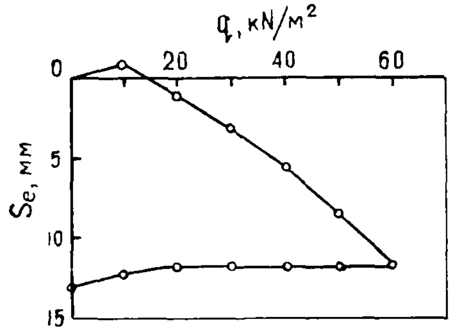

Fig. 6 Displacements of the Model Edge

When the primary load is being reduced the plate edges first do not rise as may be expected, but rather lower. All these and other specific effects might be expected in some cases and sometimes they are even taken into account still they are not only theoretically important and, therefore, the whole problem of interaction of flexible footing with the soilbase needs further thorough investigation.

CONCLUSIONS

The results of tests and field study show that interaction of soilbase and flexible footings of structures, e.g. storage tanks bottom that apply repetitive loads to soilbase may produce specific phenomena that interfere with normal operation of structures. These phenomena, that are not conventionally taken in account, may generate considerable extra deformations and even lead to failures of tanks after the subsequent loading while this very load could be safe in the course of the primary cycle.
The risk of repetitive loading is due to the difference in deformation properties of footing and soil that takes place till the gap between the structure and the soil is formed up when the structure is unloaded. A construction technique is recommended that makes it possible to control formation of the gap between the tank bottom and the soilbase and fill it with a material further on.
The filling increases both stability of the storage tank-soilbase system and reduces more than twofold the deflections of the tank bottom and, respectively, lowers labour and material consumption for erecting the tank footing.

REFERENCES

Bell, R.A. and J.Iwakiri, (1980),"Settlement Comparison Used in Tank-Failure Study," Proc. ASCE, Journal of the Geotechnical Engineering Division, vol. 106, no. GT2, 153-169.

Dovnarovitch, S.V. and A.A.Teplyakov, (1987), "Streses under Rigid and Flexible Footings at the Repeating Loads", Soil Mechanics and Foundation Engineering, no. 1, 29-31,(in Russian).

Mohan D., G.R.S.Jain, R.K.Bhandari, (1978),"Remedial Underpinning of Still Tank Foundation", Proc., ASCE, Journal of the Geotechnical Engineering Division, vol. 104, no. GT5,639-655.

Palatnikov E.A., A.A.Teplyakov, D.S.Baranov, S.V.Dovnarovitch, D.E.Polshin, V.F.Sidorchuk, (1978), "Experimental Investigation of the Flexible Reinforced Concrete Plates on the Sandbase", Proc., GiproNIIaviaprom, vol. 17, 7-21, (in Russian).

Proceedings: Second International Conference on Case Histories in Geotechnical Engineering, June 1-5, 1988, St. Louis, Mo., Paper No. 6.29

GBS Platform Evaluation Using Field Instrumentation

Joseph M. Keaveny
Senior Engineer, Norwegian Geotechnical Institute, Oslo, Norway

Farrokh Nadim
Senior Engineer, Norwegian Geotechnical Institute, Oslo, Norway

Per Magne Aas
Senior Engineer, Norwegian Geotechnical Institute, Oslo, Norway

SYNOPSIS: A case history of the foundation behaviour of an offshore gravity base structure (GBS) is presented. The platform rests on an overconsolidated fissured clay, bounded, top and bottom, by pervious sand layers. Sixteen piezometers have been placed within this 30 m layer. Based on one-dimensional consolidation theory, independent analyses using both settlement and pore pressure measurements indicated a high degree of consolidation had occurred much sooner than was estimated in the initial design phase. These analyses indicated that laboratory oedometer tests underpredicted the coefficient of consolidation by one to two orders of magnitude. Updated settlements and stability analyses yielded 50% of the initially anticipated settlement and a 20% increase in the available safety factor. In addition, the certainty that the theory relating pore pressure to settlements was appropriate, led to confidence in the piezometer performance, and in turn the procedure used to install them.

INTRODUCTION

Following the installation of Gullfaks A platform in May 1986, the Norwegian State Oil Company (Statoil) asked the Norwegian Geotechnical Institute (NGI) to perform a verification of the initial design based on accrued measurements after installation. The design verification was performed in cooperation with Norwegian Contractors (NC). This paper presents partial results of that work.

Analysis of measured pore pressures and settlements at the Gullfaks A platform were performed in order to verify the initial design settlement and stability analyses. The platform is a concrete gravity base structure (GBS) located in the North Sea. A schematic diagram of the platform is shown on Fig. 1, and key data concerning it are given in Table 1. The soil conditions and piezometer locations are summarized on Fig. 2.

Table 1. Key figures concerning platform

Foundation area, m²	11 000
Embedment, m	1
Depth of water at site, m	134
Submerged weight, MN	3 600
Horizontal force at mudline, MN	865
Overturning moment at mudline, MNm	35 930
Load coefficient to be applied	1.3

The upper 3 to 4 m consists of a layer of very dense gravel and sand with clay overlying very stiff fissured clay to a depth of approximately 13 m. Below 13 m exists a very stiff clay. Of special note is the soil at a depth of approximately 34 m which is clay exhibiting pockets and seams of fine sand. This layer was found at all the boring locations at the site. The clay layer bracketed by the two drainage layers at 3 and 34 m is the layer in which the piezometers are embedded. Because of the large width of the platform relative to the thickness of this layer, one-dimensional consolidation theory (Terzaghi, 1943) and extensions of it (Taylor, 1948; Scott, 1963) were used in evaluating the measured settlements and piezometer pore pressure response due to platform loading.

EQUIPMENT DESCRIPTION AND INSTALLATION PROCEDURE

Two piezometer strings are installed in the soil beneath the Gullfaks A platform (Fig. 2). One is a plain piezometer string installation (PP1) with two vibrating wire transducers implanted at five different levels. The other installation is a combination of a piezometer assembly, similar to the first one (PP2), and a long term settlement measuring equipment for measurement of platform settlement relative to a fixed point 75 m below seabed.

Both installations have been made in predrilled and stabilized boreholes. The boreholes were sealed after installation with a cement-tixoton grout.

EVALUATION OF DEGREE OF CONSOLIDATION

The method used to evaluate the average degree of consolidation in the clay layers beneath the platform can be summarized as follows:

1. Determine the consolidation settlement as a function of time for the load time history, by plotting measurements and subtracting out the initial (immediate) deformations.

2. Construct an equivalent consolidation settlement as a function of time curve for instantaneous loading using a method first described by Taylor (1948).

3. Estimate the coefficient of consolidation, C_v, and the average degree of consolidation at any time using above constructed curve and one-dimensional consolidation theory.

4. Estimate the average degree of consolidation at any time using measured pore pressures and one-dimensional consolidation theory.

5. Compare values determined in Items 3. and 4. The average degree of consolidation in both cases should be similar to each other.

Consolidation settlement-time relationship

The load-time curve is shown on Fig. 3. Full ballasting occurred within the period 25-30 May 1986. Total settlement as a function of time up to 7 Sept. 1986 is shown on Fig. 4. During periods of loading relatively large settlements occurred that can be directly attributed to initial settlement. Using the settlement data from Fig. 4 and subtracting the initial settlement (about 100 mm) an actual consolidation settlement versus log-time curve was constructed and is shown on Fig. 5. This consolidation-time relationship is a function of an approximately linearly increasing load with time during the period from 11 May to 29 May 1986. By a graphical technique first proposed by Taylor (1948), an equivalent instantaneous loading consolidation settlement-time curve can for 11 May be constructed (Fig. 6).

An empirical value of the coefficient of consolidation, C_v, was determined using the log time and square root of time methods (Lambe, 1951) on the consolidation settlement-time data derived for instantaneous loading.

From this value a value of the time factor, T, was estimated using the one-dimensional consolidation theory, where

$$T = \frac{C_v\ t}{H^2} \qquad (1)$$

and t = time after instantaneous loading (taken from 11 May 1986)
H = drainage height ≈ 15.5 m
C_v = coefficient of consolidation.

Pore pressure-time relationship

A second way of estimating the time factor, T, was to use the measured pore pressures to determine the consolidation ratio $U_z = 1-\Delta u/\Delta u_i$, where Δu is the excess pore pressure at a given depth and time and Δu_i is the initial excess pore pressure due to the platform weight (Fig. 7, for 8 June 1986). From this plot, the time factor, T, was estimated directly.

Results and discussion concerning degree of consolidation

Once T is known, an estimate of the average degree of consolidation, U, can be made using Fig. 8. A summary of the estimated C_v, T and U values using the various methods is given on Table 2.

Table 2. Coefficient of consolidation, C_v, time factor, T, and average degree of consolidaiton, U, determined from settlement and pore pressure readings.

Method	Coefficient of consolidation (m^2/year)	Time factor T	Average degree of consolidation U, %	Comment
Settlement-log time	Unable to determine	-	-	Instantaneous load settlement curve.
Settlement-square root of time	4236	1.36	>90	Instantaneous load-settlement curve. T and U taken at 8 June 1986.
Measured pore pressures	1184	0.38	68	- From 11 May to 8 June 1986 - Taking lower bound U_z values
Measured pore pressures	150	0.35	65	- From 11 May to 2 December - Taking lower bound U_z values
Measured pore pressures	1846	0.59	81	- From 11 May to 8 June 1986 - Taking average U_z values
Measured pore pressures	2512	0.81	90	- From 11 May to 8 June 1986 - Taking upper bound U_z values.

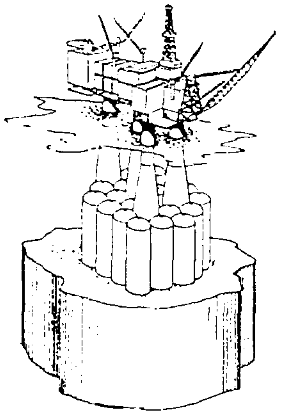

Fig. 1 General View of the Gullfaks A Structure.

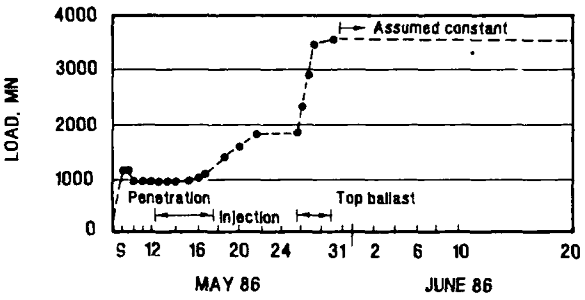

Fig. 3 Load-time Relationship

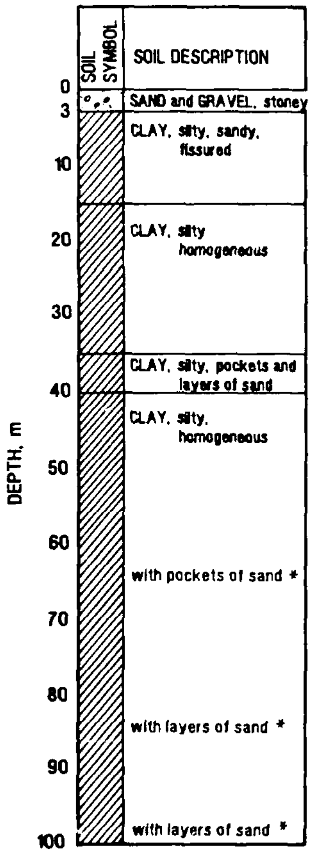

SOIL SYMBOL
SOIL DESCRIPTION
DEPTH, m
0
3
10
20
30
40
50
60
70
80
90
100
SAND and GRAVEL, stoney
CLAY, silty, sandy, fissured
CLAY, silty homogeneous
CLAY, silty, pockets and layers of sand
CLAY, silty, homogeneous
with pockets of sand *
with layers of sand *
with layers of sand *

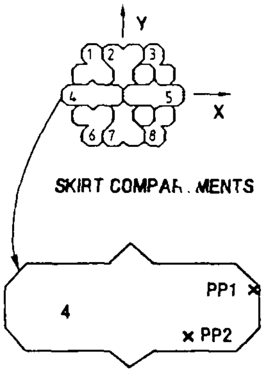

Y
X
1
2
3
4
5
6
7
8
SKIRT COMPARTMENTS
4
PP1
PP2

	PIEZOMETER		STRING	
	PP1		PP2	
DEPTH, m	HYD.	ELEC.	HYD.	ELEC.
3	H11	PP11A	H21	PP21A
6	H12	PP12A	H22	PP22A
9	H13	PP13A	H23	PP23A
12	H14	PP14A	H24	PP24A
16	H15	PP15A	H25	PP25A

* Based on one test boring

Fig. 2 Simplified Soil Profile and Piezometer Locations.

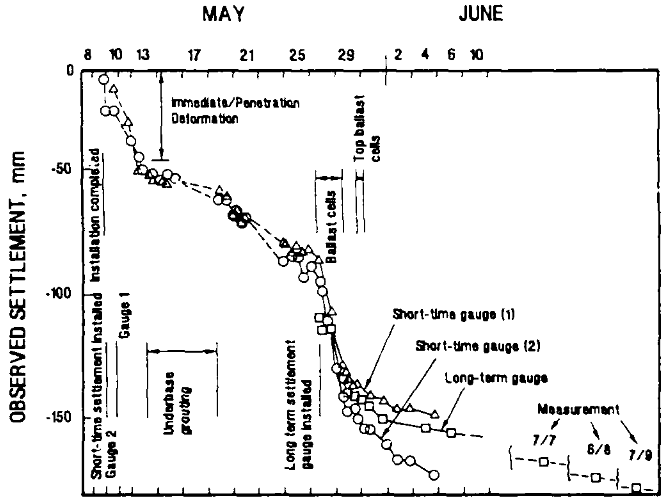

Fig. 4 Measured Settlement versus Time.

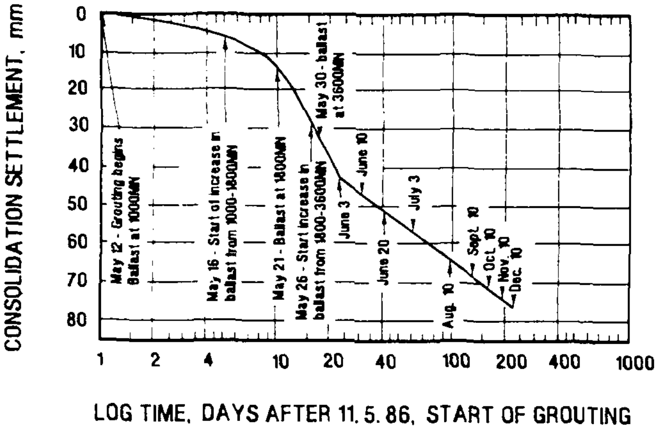

Fig. 5 Consolidation Settlement versus Log-time.

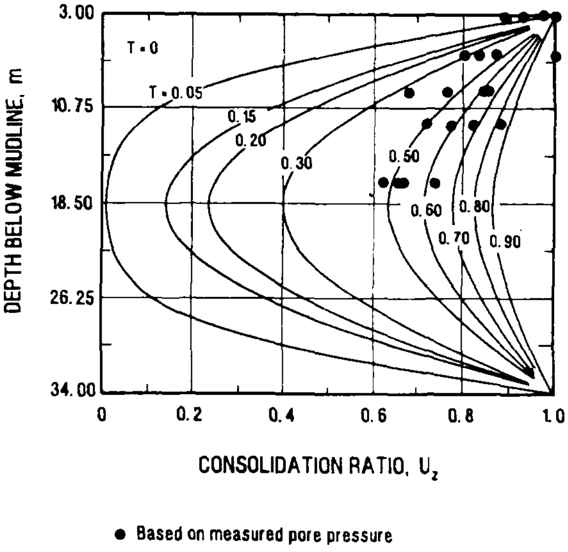

Fig. 7 Consolidation Ratio, U_z, Based on Measured Pore Pressure Values on June 8, 1986.

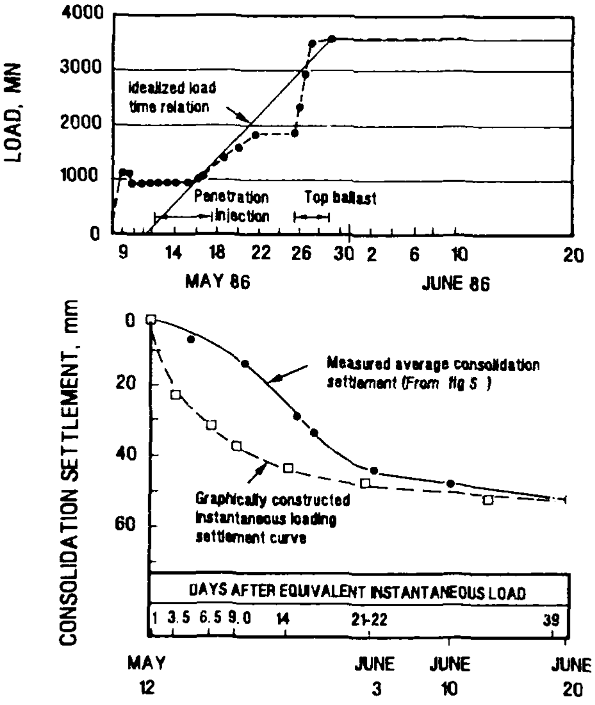

Fig. 6 Instantaneous Loading consolidation Settlement versus Time using Taylor (1948) Method.

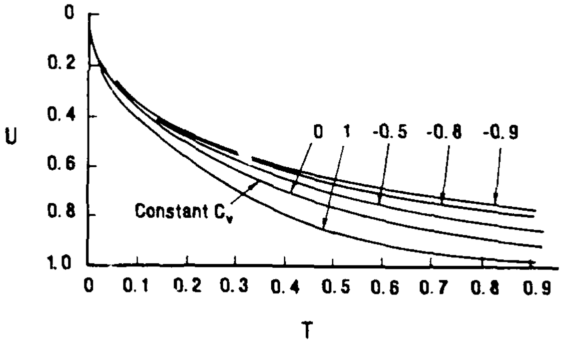

NOTE: C_v varies linearly with effective stress

$C_v = C_{vo}(1 + aU)$ values of 'a' shown on curves.

Fig. 8 Average Consolidation, U, with Varying Coefficient of Consolidation Obtained by Numerical Analysis (Scott, 1963)

In general the values of C_v appear to range between one and two orders of magnitude greater than the value of 30 m^2/year used for the initial design of the platform. Reasons for this discrepancy can be explained as follows. The initial design value was based on lower bound laboratory oedometer results that ranged up to 150 m^2/year. In a fissured clay the in situ permeability can easily be one to two orders of magnitude higher since the soil sample tested in the laboratory will be relatively intact compared to the overall fabric beneath the platform. Since

$$C_v = \frac{k\ M}{\gamma_w} \tag{2}$$

where

k = permeability
M = constrained modulus
γ_w = unit weight of water

then, a two order increase in k would directly influence C_v. In addition, based on settlement measurements, the actual constrained modulus in the field appears to be a factor of approximately 4 greater than the laboratory determined value. This again would have the effect of increasing the actual value of C_v.

It could be argued that an overestimate of the drainage height, H, has led to excessively high field estimates of C_v, using Eq. (1) and measured pore pressure determined T values. The drainage height would have to be a factor of 10 less in order to have field and laboratory C_v values coincide, and this is not indicated by the field test borings.

One important note is that both the settlement readings and the pore pressure readings indicate a high degree of consolidation had taken place by as early as 8 June 1986. Further testament to the fact that a high degree of consolidation has taken place is that the slope of the vertical strain-log time plot, called the coefficient of secondary compression, C_α, compares favourably with measured values for similar soils. This is shown on Table 3.

Table 3. Coefficients of secondary compression.

Method	C_α (%)
• Backcalculated from settlement measurements assuming layer thickness = 100 m	0.1
• Predicted from empirical relationships	
- water content as basis (Navdocks, DM-7, 1961)	0.2-0.4
- void ratio as basis (Kapp et al., 1966)	0.2-0.5
- typical values recommended by Lambe and Whitman, 1969, for clays with OCR > 2	<0.1

This relatively slow rate of compression implies that either primary consolidation has completed or that the rate of excess pore pressure dissipation in the later stages of consolidation is very slow.

EVALUATION OF PIEZOMETER PERFORMANCE

Since pore pressure measurements were used in one of the methods for determining the degree of consolidation, an analysis of piezometer performance at Gullfaks A was performed by comparing predicted pore pressure response with those actually measured by piezometers below the platform. One-dimensional consolidation theory assuming a layer from depth 3 m - 34 m with double drainage was used as the prediction model. The following conclusions can be made:

1. The high degree of consolidation as determined by piezometer-measured pore pressures and one-dimensional consolidation theory agrees well with the degree of consolidation as determined by settlement readings alone, or in conjunction with one-dimensional consolidation theory. A high degree of consolidation is also indicated by the current slope of the measured vertical strain versus log time plot.

2. One half year after the end of loading (December 1986) the pore pressures indicate that the layer from 3 m - 34 m has reached approximately 80% consolidation. The pore pressures have not dissipated appreciably since June 1986. This can be explained in the following way. As the layer consolidates the coefficient of consolidation decreases. This is indicated by comparing the values of C_v in laboratory oedometer tests at in situ stresses and at stresses associated with full consolidation. By computing the parameter a

$$a = \frac{\left(\frac{C_v}{C_{vo}} - 1\right)}{U} \tag{3}$$

where C_v = coefficient of consolidation at effective stress associated with an average consolidation ratio, U.
C_{vo} = coefficient of consolidation at in situ vertical effective stress prior to platform loading (Note: Values associated with the reload cycle were used).
U = 75%.

The average value for the clay layer was a = -0.6. This decreasing C_v with increasing vertical effective stress causes the U-T curve to shift upward (Fig. 8). Thus the more consolidated the layer becomes the longer it takes to dissipate the remaining excess pore pressures. As can be seen, theoretically for values of T of approximately 0.9 (i.e. about the value predicted after June) the average consolidation ratio approaches a value of about 80%. The pore pressures measured during the last half of 1986 indicate a value of U $\approx$ 80%.

3. Using the extended one-dimensional consolidation theory (Scott, 1963) for varying C_v, and an initial coefficient of consolidation as determined by the settlement - square root of time method using the instantaneous load-settlement curve (i.e., C_v = 4236 m²/year) yields predicted pore pressure as a function of time values similar to those measured (Fig. 9) and in particular after 1 June 1986. There is, however, a general overprediction in peak response during the brief period of topside loading. The ratio of measured to predicted excess pore pressures during this time ranges from 0.3 at 3 m depth to 0.7 at a depth of 16 m. This indicates a possible decrease in permeability of the grout seal with depth, and a partial hydraulic connection between, at least, the upper piezometer and top sand layer. In addition, just before the measured pore pressure response starts increasing (point A', Fig. 9), the pore pressures are decreasing. Point A' corresponds in time to the end of the grouting operation. This indicates that the grout might temporarily be causing the initial low response.

4. The time it takes to reach the peak measured response (horizontal distance between Points A' and B') corresponds to the time it took to load the platform from 1800 to 3600 MN (Fig. 6). Theoretically, substantial pore pressure dissipation can occur in that amount of time (vertical distance between Points B and D on Fig. 9). In light of this, comparing the vertical distance between A and D on the predicted curves and A' and B' on the measured curves yields a favourable result.

On 5 August 1986 the water pressure in skirt compartment 4 was reduced by 30 kPa. It was assumed that the boundary conditions change only at the top of the clay layer (3.0 m depth). This is to say that the piezometric level in the sand layer above the clay is lowered by 30 kPa, while the piezometric level at depth 34 m remains unchanged. This condition sets up a triangular negative excess pore pressure. Again using one-dimensional consolidation theory, Fig. 10 shows the theoretical relationship between consolidation ratio U_z versus depth relationship as a function of time factor, T. The magnitude of the decrease in pore pressure at any depth or time is estimated by multiplying ΔU_z, at an appropriate depth and time factor, by 30 kPa. For a $C_v \approx 2000$ m²/year (since by 5 August the C_v has decreased due to increased consolidation) and a time t of 0.01 years (5 August to 9 August) the computed time factor T is 0.085. Table 4 compares predicted versus measured responses. The measured response is in general greater than predicted at greater depths indicating a higher coefficient of consolidation than assumed.

Table 4. Comparison of predicted versus measured pore pressure response due to skirt compartment suction pressure

Depth (m)	Average measured decrease in pore pressure (kPa)	Predicted decrease in pore pressure (kPa)
3	28	30
6	23	19
9	25	9
12	17	5
16	12	2

In conclusion it appears that the piezometers at Gullfaks A are functioning properly, but that some may have partial hydraulic connection with the upper sand layer.

EVALUATION OF PLATFORM STABILITY

Based on the analysis presented, it was conservatively assumed that at 2 December 1986 the clay layer between the depths of 3 m and 34 m below seabed exhibited an average degree of consolidation, U = 65%. This value of U corresponds to an approximate lower bound value based on empirical methods of determining the coefficient of consolidation and subsequent value of U outlined above. Assuming a low value of U is conservative in that the undrained strength of the clay layer increases with increased U. Assuming that the platform load occurred instantaneously around 11 May 1986, then an average coefficient of consolidation, C_v, of about 150 m²/year is indicated.

This value of C_v, which is approximately equal to the upper bound of laboratory measured values (but still an order of magnitude less than what is in the field), was used to calculate the degree of consolidation at various times after installation.

Strength increase due to consolidation

In situ undrained shear strength as would be measured in a laboratory triaxial compression test, CU_A, as a function of time and depth is shown on Fig. 11. Similar relationships for triaxial extension and direct simple shear undrained shear strengths were also developed in that the bearing capacity method used (Lauritzsen and Schjetne, 1976; Kvitrud, To and Lauritzsen, 1985) utilize a weighted average of these strengths depending on the depth and shape of the assumed failure surface. In situ stresses beneath the platform, as a function of depth and time, increase due to the consolidation process. In situ strength, as a function of depth and time, can be established by relating it to the laboratory strength determined under the same effective confining stresses.

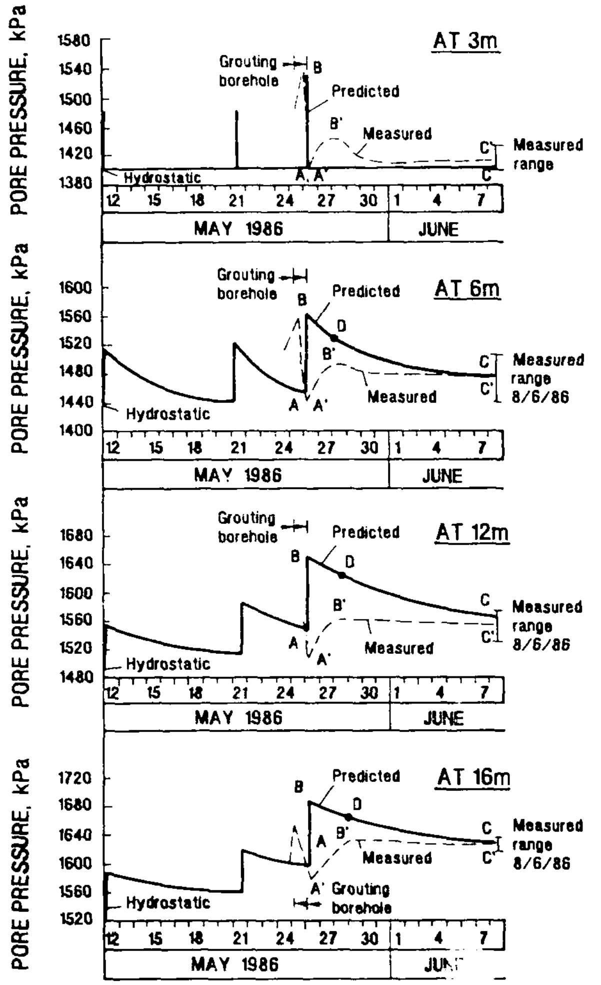

Fig. 9 Predicted Versus Measured Pore Pressure Response - Three Load Pulse Assumption. C_v Varies from 4236 m^2/Year (May 11) to 2329 m^2/Year (June 8) According to Increase in Consolidation.

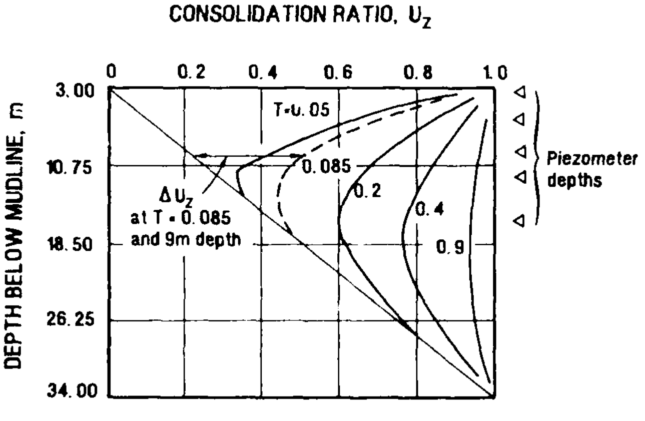

Fig. 10 Consolidation Ratio, U_z, as a Function of Depth and Time Factor, T, due to Application of Skirt Water Pressure at Depth 3 m.

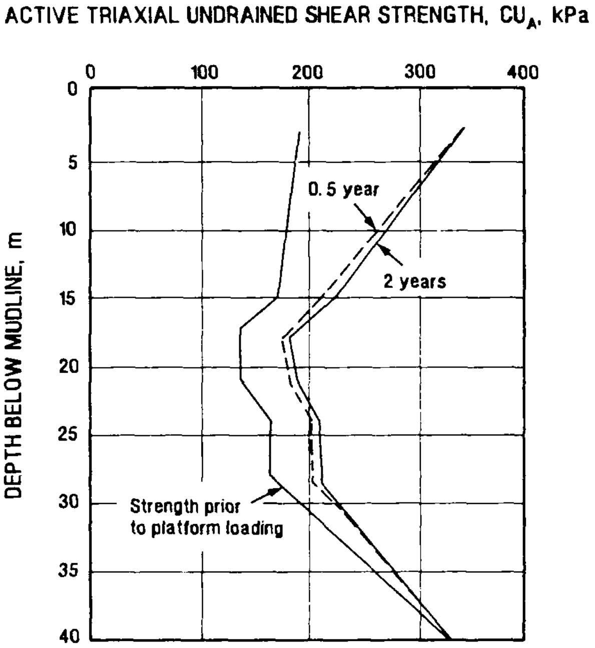

Fig. 11 Active Triaxial Undrained Shear Strength Profile as a Function of Time after Installation.

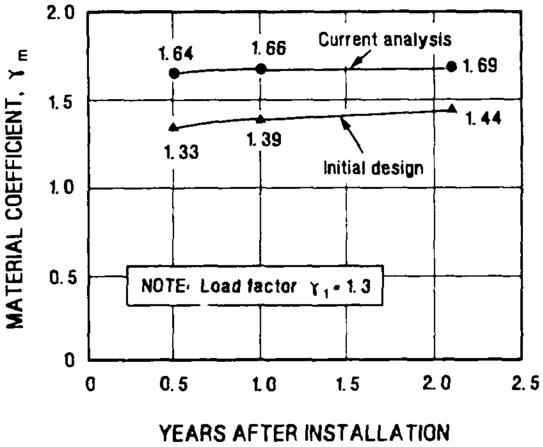

Fig. 12 Increase in Material Coefficient as a Function of Time after Installation.

Results of stability analysis

The strength profiles at various times were used in a bearing capacity analysis using the slip surface method developed at NGI (Lauritzsen and Schjetne, 1976; Kvitrud, To and Lauritzsen, 1985). Environmental loads are multiplied by a load coefficient in accordance with the regulations given by the Norwegian Petroleum Directorate (1985). Horizontal force equilibrium is evaluated with the ratio of the overall horizontal component of soil resistance to the overall horizontal component of the factored loads being the material coefficient, γ_m. The material coefficient as a function of years after installation is shown on Fig. 12. As can be seen, for a load coefficient, $\gamma_L = 1.3$, the material coefficient ranges from 1.64 to 1.69 within a two year period after installation. This compares favourably to the range of 1.35 to 1.44 estimated in the design phase.

CONCLUSIONS

The main conclusions of the study are:

1. Both settlement and pore pressure measurements indicate that the layer down to a depth of 34 m beneath the platform has been subjected to a high degree of consolidation. This implies that the coefficient of consolidation, C_v, is approximately two orders of magnitude higher than assumed in the design phase.

2. There is strong indication that the piezometers are giving reliable readings.

3. Based on the new consolidation parameters determined from measurements made in the field, an updated settlement and stability analysis was performed yielding approximately 50% of the initially anticipated settlements and a 20% increase in the available material coefficient at any given time after platform installation.

ACKNOWLEDGEMENT

The authors would like to thank Mr. Graham Bach of Statoil for his enthusiastic support. Permission of Statoil for publication of the data presented in this paper is gratefully acknowledged.

REFERENCES

Kapp, M.S., D.L. York, A. Aronowitz and H. Sitomer (1966), "Construction on marshland deposits: Treatments and results", Highway research board, Record No. 113, pp. 1-22.

Kvitrud, A., P. To and R. Lauritzsen (1985), "User manual for the computer program CAP" Internal Report 52406-47, October.

Lambe, T.W. (1951), "Soil testing for engineers" John Wiley and Sons, New York.

Lambe, T.W. and R.V. Whitman (1969), "Soil mechanics", John Wiley and Sons, New York.

Lauritzsen, R.A. and K. Schjetne (1976), "Stability calculations for offshore gravity structures", Offshore Technology Conference 8, Houston, Texas, Proceedings, Vol. 1, pp. 75-61.

Navdocks, DM-7 (1961), "Soil mechancis, foundations and earth structures", Design manual. Department of the Navy, bureau of Yards and Docks, Washington.

Norwegian Petroleum Directorate (1985), "Regulations for structural design of load bearing structures intended for exploration of petroleum resources"

Scott, R.F. (1963), "Principles of soil meachanics", Addison-Wesley Publishing Co., Reading, MA.

Taylor, D.W. (1948), "Fundamentals of soil mechanics", John Wiley and Sons, New York.

Terzaghi, K. (1943), Theoretical soil mechanics, John Wiley and Sons, New York.

Proceedings: Second International Conference on Case Histories in Geotechnical Engineering, June 1-5, 1988, St. Louis, Mo., Paper No. 6.31

Underpinning of an 11-Storey Building in Boston: A Case Study

Thomas K. Liu
President, Haley & Aldrich, Inc., USA

Mark P. Mitsch
Staff Engineer, Haley & Aldrich, Inc., USA

Cetin Soydemir
Senior Engineer, Haley & Aldrich, Inc., USA

SYNOPSIS: A 113-ft. long exterior wall of an 11-story building with one basement level in Boston, Massachusetts was underpinned to allow a 40-ft. deep excavation for construction of three below-grade levels for an adjacent development. The existing building, subsurface conditions and underpinning system are described. Vertical and horizontal building movement data obtained during construction are presented.

INTRODUCTION

Construction of three below-grade parking levels for the new 28-story 150 Federal Street building required a 40 ft. deep vertical excavation along one side of the existing 11-story 211 Congress Street building in downtown Boston, Massachusetts. The exterior column and wall footings required underpinning since the excavation was to extend between 16 and 22 ft. below footing bearing levels. Figure 1 shows the 211 Congress Street building in plan relative to the excavation and surrounding streets.

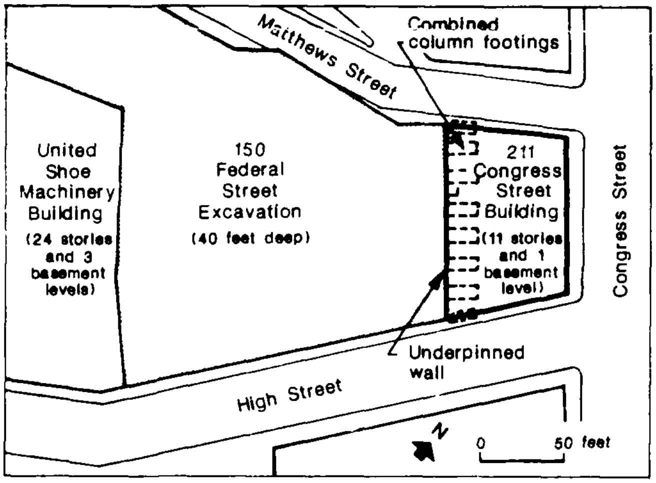
Matthews Street
Combined column footings
United Shoe Machinery Building
(24 stories and 3 basement levels)
150 Federal Street Excavation
(40 feet deep)
211 Congress Street Building
(11 stories and 1 basement level)
Congress Street
Underpinned wall
High Street
N
0
50 feet

Figure 1. Plan view of 211 Congress Street building and 150 Federal Street excavation.

The underpinning system consisted of hand excavated underpinning piers and post-tensioned concrete beams. Elevation reference points were installed on the underpinned footings to monitor performance of the building during underpinning and subsequent excavation and construction of the 150 Federal St. building foundations.

UNDERPINNED STRUCTURE

The 211 Congress Street building was built in the early 1920's and has one basement level. The structure has a steel frame and covers an area of approximately 7,300 sq. ft. The three sides of the building along Congress, Matthews, and High Streets have ornate terra cotta facades considered susceptible to cracking if differential settlements become excessive. The fourth side is the 113-ft. long brick wall along the common property line with the new development, which was underpinned.

The foundation units along the brick wall are reinforced concrete spread footings. There are nine column footings which are typically 6 to 9 ft. wide by about 21 ft. long and 3 to 5 ft. deep. These footings act as combined footings to support the exterior columns, part of the 11-story brick wall and the first bay of interior columns. The brick wall is supported by concrete wall footings about 3 ft. thick between column footings. The underpinned wall and footings are shown schematically in elevation and section on Figure 2.

SUBSURFACE CONDITIONS

The footings of the 211 Congress St. building bear on a lightly overconsolidated marine silty clay between 18 and 24 ft. below street grade. The medium stiff silty clay is underlain by a hard transitional glacio-marine clay layer several feet thick, which overlies glacial till. The glacial till varies from hard silty clay to dense silty fine sand, with varying amounts of gravel, sand, and cobbles. Fill overlies the marine clay from bottom of footings to ground surface. Groundwater was typically near the top of column footings in the fill prior to the start of construction. Figure 2 includes generalized soil and groundwater conditions in the vicinity of the underpinned wall.

UNDERPINNING SYSTEM

The underpinning system included 17 concrete underpinning piers to support the nine column footings. Generally, each footing was underpinned by a pair of piers side by side. Wall

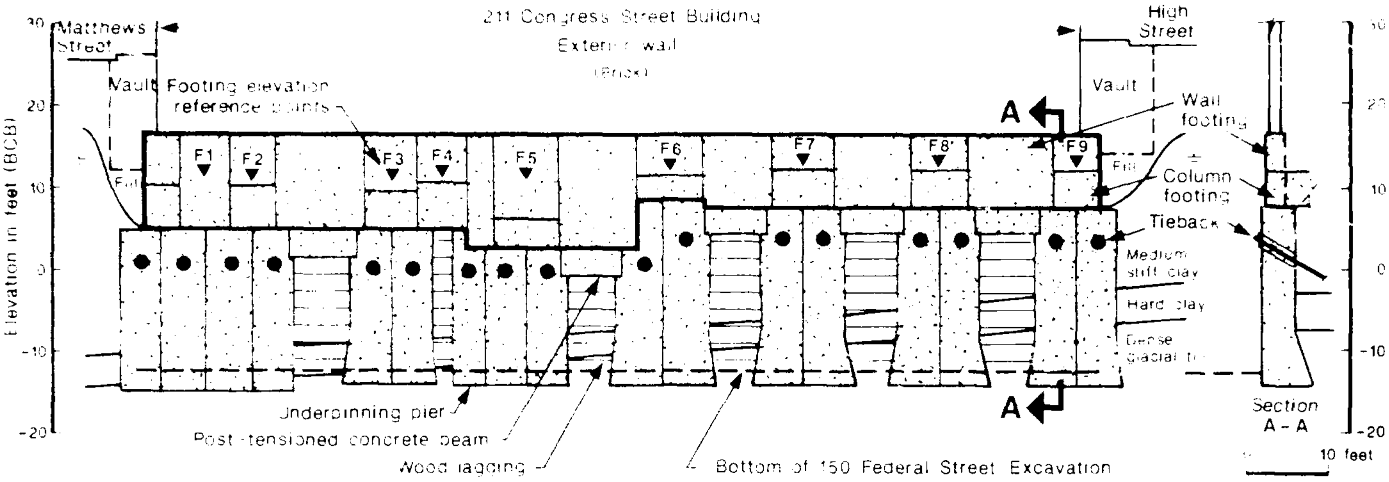

Figure 2. Elevation and section view of underpinned wall and underpinning system.

Footings were either supported by post-tensioned concrete beams spanning between piers or by the piers themselves.

Each underpinning pier was restrained from movement toward the excavation by a tieback near the top of the pier. Tiebacks were anchored in the glacial till and tensioned to the computed design anchor load after installation. Wood lagging supported the vertically cut clay between piers and below beams. The underpinning system is shown schematically on Figure 2.

Excavations for piers and beams were made by hand utilizing power shovels. Excavation width was limited to 5 ft. to control the unsupported length of the footings during the work. The minimum distance between excavations conducted simultaneously was limited to 12 ft. for beams and 18 ft. for piers.

Underpinning began with construction of the five post-tensioned concrete underpinning beams shown on Figure 2. The beams were typically 3 ft. high and 5 ft. wide and between 6 and 8 ft. long. Each beam was excavated and concreted one half at a time. Two PVC sleeves were cast into the beams for later installation and tensioning of two 1-3/8-inch diameter high strength steel bars. Beams were concreted up to about 2 in. below the footing to be supported. The resulting space was later "drypacked" using a dry sand-cement mix to provide support for the footing.

Pier construction began when both halves of the adjacent beam were concreted and drypacked. The underpinning piers were typically 3 ft. by 5 ft. at the top, then were belled at the base to as large as 6 ft. by 6 ft. Belling was required to maintain pier bearing pressures below an allowable bearing pressure of 6 tsf in the glacial till. Bells were formed at the back and sides of the excavations as indicated on Figure 2. The front of the piers could not be belled due to the location of a future foundation mat for the 150 Federal St. building. The piers were between 18 and 23 ft. deep, extending a minimum of 1 ft. and up to about 3 ft. below the proposed bottom of the 150 Federal St. excavation as required to reach glacial till.

Sides of pier excavations were supported with wood lagging boards to provide lateral support for the excavations. Soil and straw was placed behind the lagging boards as required so that the lagging was in firm contact with the soil. Individual pier excavations were dewatered by open pumping as required.

Problems with loss of ground behind lagging boards were encountered in several of the pier excavations when sandy zones of soil were encountered below the water table. The boards were generally backfilled again with soil and straw or with lean concrete where necessary. Because of a recurring loss of ground problem in one excavation, the entire excavation was backfilled with lean concrete then re-excavated later.

Each pier was concreted after the excavation was made to the required depth and the bearing surface was prepared adequately. Piers were initially concreted and drypacked up to adjacent beams and then up to the column footings. Post-tensioning bars were installed in a beam after the first adjacent pier was concreted and drypacked to the bottom of the beam. The bars were tensioned after the second pier was drypacked up to the bottom of the beam.

CONSTRUCTION SEQUENCE

A generalized time graph of the construction sequence is included on both Figures 3 and 4. Underpinning operations began on 3 September 1985 and were completed on 30 October 1985, followed by tieback installation, foundation excavation, and construction of a 6-ft. thick structural mat in front of the underpinning piers. The structural mat extended 45 ft. out from the underpinning piers to support a portion of the new building. The mat was also designed to provide stability to the underpinning system.

Tieback installation was completed on [illegible] November 1985. Excavation and construction

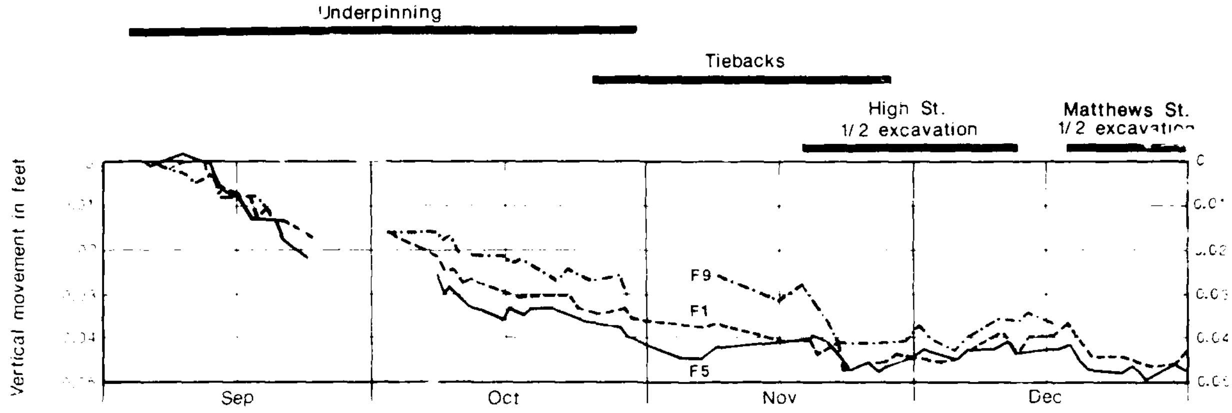

Note: Gap in data curve indicates reference point inaccessible.

Figure 3. Vertical movements of footing reference points F1, F5, and F9 versus time.

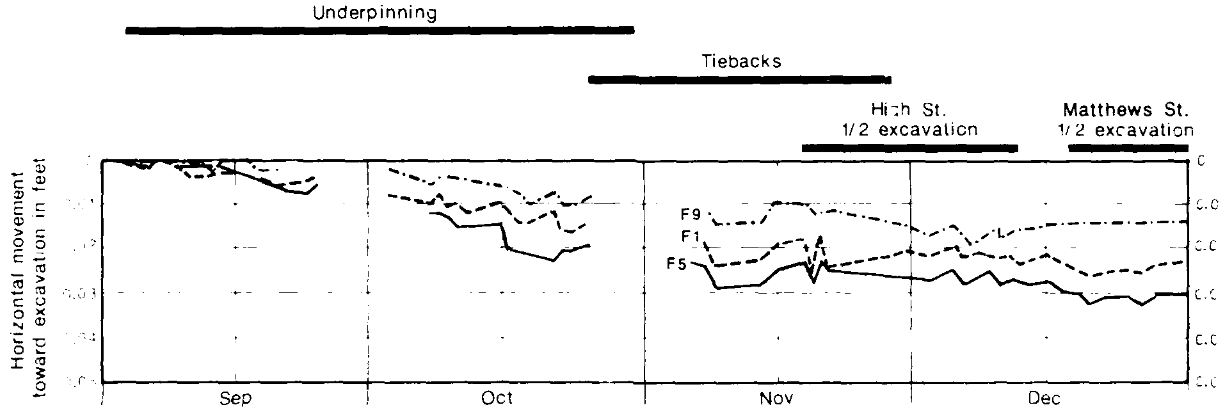

Note: Gap in data curve indicates reference point inaccessible

Figure 4. Horizontal movements of footing reference points F1, F5, and F9 versus time.

of the foundation mat was completed on 31 December 1985 with the exception of a small section along Matthews Street.

Excavation for the mat was completed approximately one half at a time so that changes in in-situ stresses due to excavation below the underpinned footings would be as gradual as possible. Excavation began at the High Street end in mid-November and proceeded toward Matthews Street. The High Street half of the mat was concreted in two sections, the first on 3 December and the second on 12 December. The excavation began for the remainder of the mat after the High Street half was completed. The Matthews Street half of the mat was concreted on 31 December 1985.

INSTRUMENTATION

Underpinning and foundation construction activities were monitored on a full-time basis by the project geotechnical engineer. Elevation reference points were installed on the underpinned footings to monitor vertical and horizontal movements of the building during construction. The locations of reference points F1 through F9 are indicated on Figure 2.

Elevations and offsets of the reference points were monitored daily using optical survey instruments from beginning of underpinning to concreting the structural mat. The observed vertical and horizontal movement data are plotted versus time in Figures 3 and 4, respectively, for reference points F1, F5 and F9.

The performance data indicate that the major portion of the vertical movements generally occurred during the two months of underpinning. The rate of movement typically decreased after foundation loads were transferred to the underpinning system. Horizontal movements were of lesser magnitude and occurred more gradually than vertical movements.

Vertical and horizontal survey data obtained at completion of both underpinning and the structural mat for each of the nine footing reference points are summarized on Figures 5 and 6, respectively. Figures 5 and 6 indicate that the settlement and horizontal offset patterns are relatively uniform. Surveyed reference point settlements differed by less than 0.2 in. across the brick wall, ranging from 0.44 in. to 0.60 in. (0.037 ft. to 0.050 ft.). Horizontal offset of the points

AD-A213 199 INTERNATIONAL CONFERENCE ON CASE HISTORIES IN 5/8
GEOTECHNICAL ENGINEERING (2.. (U) MISSOURI UNIV-ROLLA
S PRAKASH 30 JUN 89 ARO-25645.2-GS-CF DAAL03-87-G-0129
UNCLASSIFIED F/G 13/2 NL

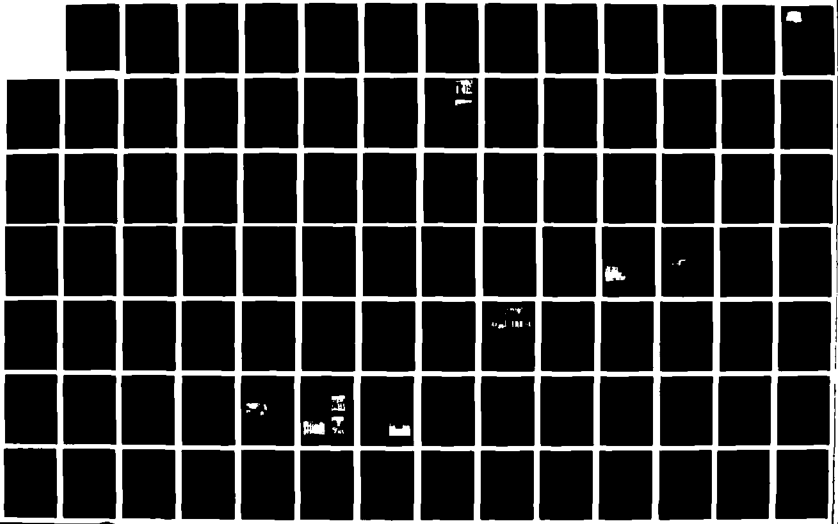

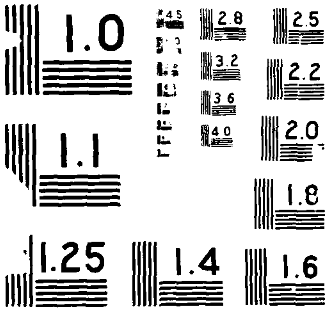
1.0
4.5
2.8
2.5
3.2
2.2
3.6
4.0
2.0
1.1
1.8
1.25
1.4
1.6

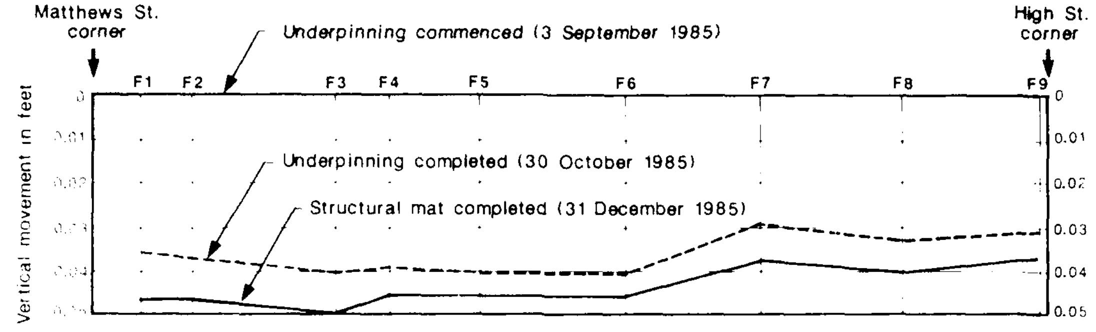

Figure 5. Vertical movement of footing reference points for selected dates.

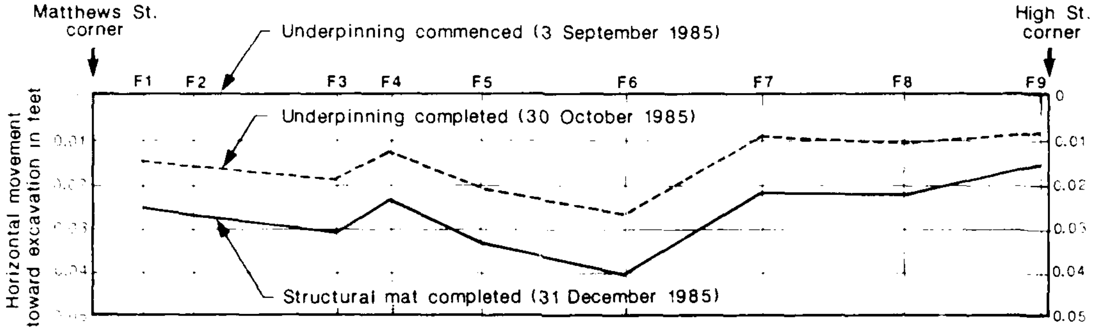

Figure 6. Horizontal movement of footing reference points for selected dates.

differed by 0.3 in. maximum, ranging from 0.18 in. to 0.48 in. (0.015 ft. to 0.04 ft.). The maximum angular distortion for vertical movements was approximately 1:1200 between adjacent reference points at the time of completion of the foundation mat.

The footing reference points became inaccessible almost immediately after completion of the foundation mat due to construction of the 150 Federal Street foundation wall. However, in addition to the footing reference points, reference points SP1 through SP7 were installed at ground floor level around the outside of the 211 Congress St. building. Locations for SP1 through SP7 are indicated on Figure 7.

These points were surveyed from before the start of underpinning through erection of the 150 Federal Street superstructure. Total vertical movements from September 1985 through April 1987 are given on Figure 7. As indicated, the maximum angular distortion between adjacent reference points during the period of monitoring was 1:1240.

CONCLUSION

The 113-ft. long exterior brick wall of the 11-story 211 Congress St. building was satisfactorily underpinned using the methods described herein. Maximum measured building settlement was 0.6 in. The maximum angular distortion between reference points was about 1:1200.

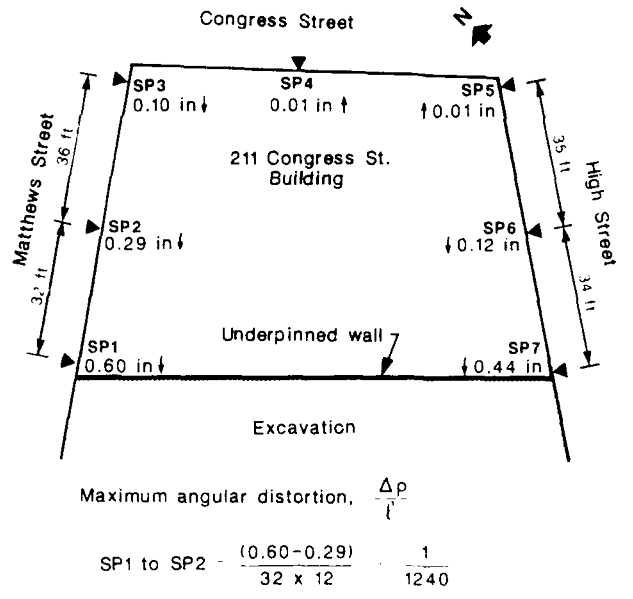
Congress Street
N
SP3
0.10 in↓
SP4
0.01 in↑
SP5
↑0.01 in
211 Congress St. Building
Matthews Street
36 ft
32 ft
High Street
35 ft
34 ft
SP2
0.29 in↓
SP6
↓0.12 in
SP1
0.60 in↓
Underpinned wall
SP7
↓0.44 in
Excavation
Maximum angular distortion, $\frac{\Delta\rho}{\ell}$
SP1 to SP2 = $\frac{(0.60-0.29)}{32 \times 12} = \frac{1}{1240}$

Figure 7. Perimeter elevation reference point vertical movements from beginning of underpinning in September 1985 through April 1987.

ACKNOWLEDGEMENT

The developer of the 150 Federal Street project is Meredith & Group, Inc., and the 211 Congress Street building is owned by the Codman Co., Inc., both of Boston, Massachusetts. The general contractor for the project was Turner Construction Co. The underpinning work was undertaken by Schnabel Foundation Co.

Proceedings: *Second International Conference on Case Histories in Geotechnical Engineering*, June 1-5, 1988, St. Louis, Mo., Paper No. 6.32

Design, Construction, and Performance of a Deep Excavation in Soft Clay

Richard Riker
Geotechnical Engineer, CH2M HILL, Corvallis, Oregon

David Dailer
Geotechnical Engineer, CH2M HILL, Corvallis, Oregon

SYNOPSIS: A deep internally braced excavation in soft clay was performed for a pump station at a sewage treatment plant in Milwaukee, Wisconsin. The design was influenced by the limited site area; potential for bearing capacity failure and/or hydrostatic blowout in the bottom of the excavation; and the necessity to limit ground deformation outside the excavation to protect existing structures and utilities. A performance specification and design was prepared by the owner's engineer. The design included minimum earth and hydrostatic lateral loading conditions to be used by the contractor, a minimum depth of penetration for the earth support system, and a maximum allowable horizontal deflection. The final earth support system design was prepared by the contractor and reviewed by the owner's engineer. Construction monitoring included slope inclinometers (to measure horizontal deflection of the earth support system) and piezometers to measure hydrostatic pressure in a confined aquifer. Measured horizontal deformation of the excavation support system exceeded the predicted deformations. The influence of the contractor's methods and sequence of excavation and earth support system installation on the actual-versus-predicted deformations are also discussed.

INTRODUCTION

The new influent pump station and preliminary treatment facility for the Jones Island Wastewater Treatment Plant is part of the Milwaukee Metropolitan Sewerage District's (MMSD) $1.6-billion rehabilitation and expansion program. The new pump station and preliminary treatment facility is on Jones Island, next to existing treatment plant facilities and new plant facilities under construction, and directly west of a major bridge over the Milwaukee Harbor entrance. The new treatment facility, which receives the main plant influent, is a pile-supported structure. The deepest part of the excavation for the facility was directly adjacent and parallel to the only road entering the plant site. The main plant water, gas, sewage, and storm sewers run adjacent to the excavation, parallel to the main road.

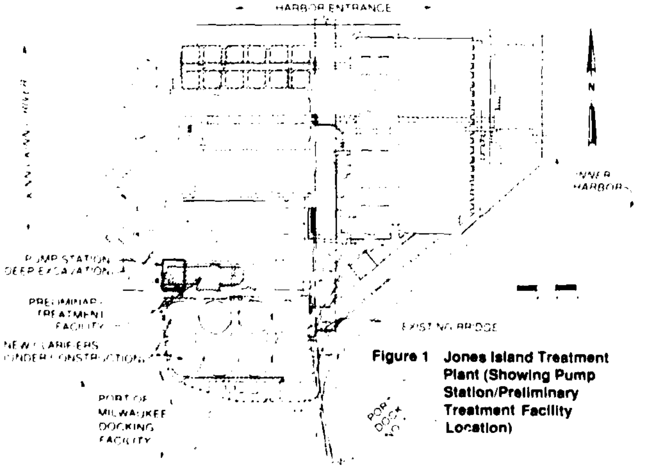
HARBOR ENTRANCE
N
INNER HARBOR
PUMP STATION DEEP EXCAVATION
PRELIMINARY TREATMENT FACILITY
NEW CLARIFIERS (UNDER CONSTRUCTION)
EXISTING BRIDGE
PORT OF MILWAUKEE DOCKING FACILITY
PORT DOCK

Figure 1 Jones Island Treatment Plant (Showing Pump Station/Preliminary Treatment Facility Location)

Figure 1 shows the location of the pump station/preliminary treatment facility relative to the existing plant facilities, existing bridge, and new structures under construction. An incineration structure, which had occupied part of the site, was demolished as part of MMSD's program. As part of the demolition, the incinerator building's pile foundation (consisting of 40- to 50-foot-long timber piles) was extracted.

GEOTECHNICAL PROFILE

A field investigation was conducted before design to determine subsurface conditions. The field investigation consisted of soil borings, in situ vane shear testing and laboratory testing of samples obtained from the borings. Additional field investigations were performed during construction. The field investigation revealed a general soil profile consisting of 35 feet of loose to dense granular fill, underlain by 40 feet of estuarine deposited soils consisting of 7 feet of medium stiff organic silty clay, underlain by 15 feet of soft to medium silty clay, underlain by 18 feet of stiff, organic, silty clay. Below the estuarine deposits are 95 to 105 feet of glacial drift, consisting of clay, silt, sand, and gravel. The glacial drift overlies bedrock. Laboratory consolidation tests show that the organic silty clay layers in the estuarine deposits are normally consolidated and highly compressible. The general soil profile of the site and the associated field and laboratory strength tests are shown in Figure 2.

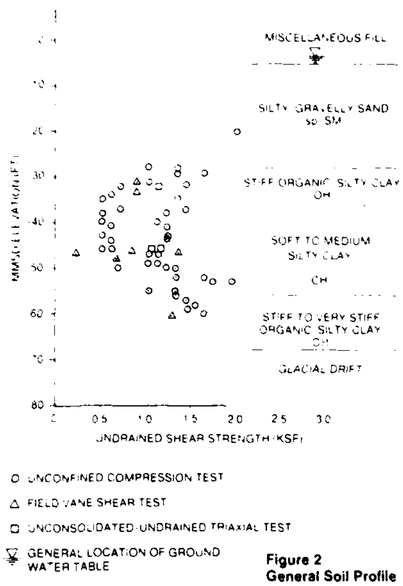

Figure 2
General Soil Profile and Strength Test Results

Figure 2 also shows the general groundwater level determined from observation well installed in select borings on the site prior to and during construction. A surface aquifer and a confined aquifer in the glacial drift, isolated by silty clay layers, were also identified in the field investigation.

The construction of the pump station required an excavation approximately 160 feet by 60 feet in plan dimension and approximately 42 feet deep. The design identified the following concerns:

- The existing sewage treatment plant facilities are founded on short timber piles that terminate in the compressible silty clay layer. Lowering the groundwater table could cause settlement of the timber piles and supported structures. Also, lowering the groundwater table could expose the tops of the timber piles and cause drying and deterioration of the tops of the untreated timber piles.

- The confined aquifer in the glacial drift has a hydrostatic pressure equal to Elevation -1.4 feet (MMSD datum). With the excavation 42 feet deep (approximate Elevation -35), the magnitude of the hydrostatic boundary force at the bottom of the silty clay layer (confining layer) exceeds the total weight of the silty clay layers below the bottom of the excavation. The uplift pressure was calculated as 4.2 kips per square foot; the pressure from the weight of the silty clay soil within the excavation above the glacial soil was calculated as 3.4 kips per square foot.

  In addition, the demolition of the incinerator building and the extraction of the timber piles left zones that may have been loosened and weakened, which could allow upward flow and result in piping and boiling in the bottom of the excavation.

- The soft- to medium-stiff clay layer at the excavation bottom appeared susceptible to failure due to bottom heave. Estimates of the factor of safety (F.S.) against bottom heave ranged from slightly less than 1.0 to 1.2. Using Terzaghi's model (Terzaghi and Peck, 1967), and assuming that the average shear strength below the excavation bottom is 850 pounds per square foot, gives the following:

$$\text{F.S.} = N_c \frac{S}{\gamma D + q} \qquad (1)$$

Where:

N_c = 6.3 (bearing capacity factor, from Bjerrum and Eide, 1956)

S_{AVE} = 0.85 ksf

γD = 4.9 kips per square foot (ksf)

q = 0.6 ksf (assumed surcharge)

$$\text{F.S.} = (6.3) \frac{0.85 \text{ ksf}}{4.9 \text{ ksf} + 0.6 \text{ ksf}}$$

$$\text{F.S.} = 0.97$$

- The immediately adjacent treatment plant utilities had to remain in service during construction, and thus the design had to accommodate that need.

DESIGN APPROACH

Primary factors in the approach to the design of the excavation were:

- The location of the excavation and the critical nature of the adjacent utilities, transportation facilities, and existing plant facilities

- The tight schedule of the construction project and the impact that any delay would have on this and subsequent projects

- Use of standard construction methods and techniques

It was determined that delay in construction or interruption of service due to a construction failure was an unacceptable risk. The excavation design, therefore, intruded into the contractor's traditional area of design of temporary earthwork facilities. The excavation design approach that was adopted had the following objectives:

- Reduce the risk of temporary excavation failure through performance criteria

- Use prescriptive criteria to remove some of the contractor's judgement and risk-taking ability

- Adopt a construction monitoring program to measure compliance with the contract documents and assess the effectiveness of the contractor's methods

To achieve these objectives, the contract documents contained the following provisions:

- A 2-inch lateral-movement limit on the excavation support system. The limit was based on Peck (1969) and Hansen and Clough (1978). Two inches was intended to be a "warning" limit and was estimated as approximately one-half to one-third of the maximum movement, based on empirical data presented by Hansen and Clough (1978) for braced excavation with prestressed bracing.

- A requirement for depressurizing the lower aquifer within the excavation to a level within 10 feet of the bottom of the excavation when the excavation was below Elevation -27. This requirement was set to prevent bottom blowout or boiling due to hydrostatic pressure.

- A requirement that the contractor extend the temporary earth support system to the glacial drift layer (Elevation -68) to address the bottom heave problem.

The contract documents also contained a geotechnical report that addressed the issues of constructability and design of the excavation for the pump station.

The geotechnical report contained lateral earth pressures to be used by the contractor during design of the excavation. The lateral earth pressures above the excavation bottom were based on apparent earth pressures developed by Terzaghi and Peck (1967). For the embedded portion of the excavation support, it was recognized that an unbalanced earth pressure may develop. Earth pressures were calculated with Rankine earth pressure theories, using undrained strength values. For design, it was assumed that the excavation wall was pinned at the bottom support, and fixed at the bottom of the steel sheets (Elevation -68).

The contractor was also required to preload each brace to between 35 and 50 percent of the estimated design loads.

EARTH SUPPORT SYSTEM

The layout of the earth support system and the location of slope inclinometers are shown on Figure 3. Final locations for the inclinometers were chosen after the contractor's final excavation design was approved. Two slope inclinometers were installed on the west side of the excavation. Seven piezometers were also installed next to the excavation to monitor hydrostatic pressures in the lower aquifer. From Elevation +7 (ground surface) to Elevation -5, the contractor chose to open excavate the east side, and install soldier piles (HP 10 42 at 7-foot centers) and wood lagging on the north, south, and west sides of the excavation. Foundation piling were driven from Elevation -5. Sheetpile were used to enclose the excavation on all sides below Elevation -5. The sheetpile used was Hoesch 175 (S_x=48.4 inches^3/lf) on the west side, and PZ 32 (S_x = 38.3 inches^3/lf) on the east side. A transition piece was installed consisting of a PZ 32 interlock split lengthwise and welded to an H-175 sheet.

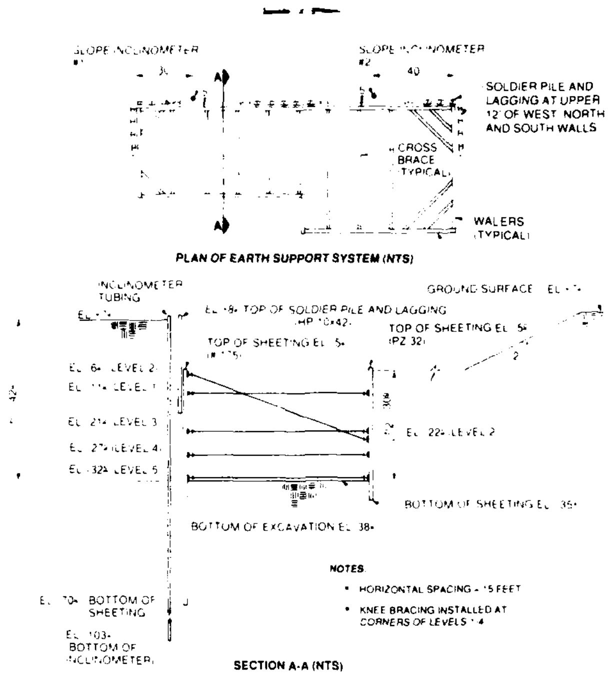
SLOPE INCLINOMETER #1
SLOPE INCLINOMETER #2
30
40
A
SOLDIER PILE AND LAGGING AT UPPER 12' OF WEST NORTH AND SOUTH WALLS
CROSS BRACE (TYPICAL)
WALERS (TYPICAL)
PLAN OF EARTH SUPPORT SYSTEM (NTS)
INCLINOMETER TUBING
GROUND SURFACE EL +7
EL +8 TOP OF SOLDIER PILE AND LAGGING (HP 10x42)
TOP OF SHEETING EL -5 (PZ 32)
TOP OF SHEETING EL -5 (H 175)
EL -6 LEVEL 2
EL -11 LEVEL 1
EL -21 LEVEL 3
EL -27 LEVEL 4
EL -32 LEVEL 5
EL -22 LEVEL 2
2
1
BOTTOM OF SHEETING EL -35
BOTTOM OF EXCAVATION EL -38
NOTES
• HORIZONTAL SPACING - 15 FEET
• KNEE BRACING INSTALLED AT CORNERS OF LEVELS 1-4
EL -70 BOTTOM OF SHEETING
EL -103 BOTTOM OF INCLINOMETER
SECTION A-A (NTS)

Figure 3
Earth Support System Design and Inclinometer Location

The schedule for the walers and bracing is shown in Table 1. Braces on the north end of the excavation were larger members because the span was longer. Sheeting on the west side extended to Elevation -65, and on the east side to Elevation -38.

Depressurizing in the lower aquifer was accomplished with two 3-inch submersible pumps. The flowrate during construction was steady and approximately 200 gpm. Table 2 shows piezometer levels prior to and during construction dewatering. The tips of the piezometers are in a sand layer in the glacial drift at approximately Elevation -70. Surface dewatering for the remainder of the site was accomplished by pumping from shallow wells inside a slurry wall. The slurry wall was constructed around the site and intersected the sheeting.

Table 1
MEMBER SIZES

Level	Walers	Struts	Strut Length (ft)	Strut Stiffness k = AE/L (kips/in)
1	W33x118	N = 22"Φ x.312	58.5	935
		S = 18"Φ x.312	44.0	1,020
2[a]	W30x108	N = 20"Φ x.312	61.0	816
		S = 17"Φ x.312	47.0	955
3	W36x150	N = 22"Φ x.312	58.5	935
		S = 20"Φ x.312	44.0	1,130
4	W33x118	N = 22"Φ x.375	58.5	1,125
		S = 20"Φ x.312	44.0	1,130
5	W30x108	N = 22"Φ x.375	58.5	1,125
		S = 20"Φ x.375	44.0	1,365

NOTES:

[a] Inclined.
N = North side.
S = South side.

RESULTS

Depressurizing the Lower Aquifer

Table 2 shows the drawdown in the piezometer installed in the lower aquifer.

Table 2
PIEZOMETER DRAWDOWN

Piezometer	Level Before Pumping	15 Days After Pumping Start	30 Days After	60 Days After
1	-1.4	-10.1	-16.4	-18.2
2	-1.3	-13.0	-19.9	-21.6
10	-1.4	-11.1	-15.8	-18.1
11	-1.4	-9.1	--[a]	-16.8
12	--[b]	--[b]	-19.5	-20.9
13	--[b]	-9.2	-17.3	-19.5

[a] Not read.
[b] Not installed.

NOTE: Groundwater levels are elevations (MMSD datum).

Measured Deflections

Figures 4 and 5 show measurements from slope inclinometers SI-1 and SI-2, which were on the west side of the excavation. Also shown on Figures 4 and 5 are the excavation sequence and brace installation sequence, noted in days after the excavation started.

The slope inclinometer data shows that a great deal of movement occurred at the soldier pile and lagging support while it was cantilevered, and again before Brace No. 2 (the inclined brace) was installed. Additional movement continued at each brace level after the braces were installed.

Although not shown on Figures 4 and 5, there was additional deflection between the end of September and the end of December, several months after all braces had been

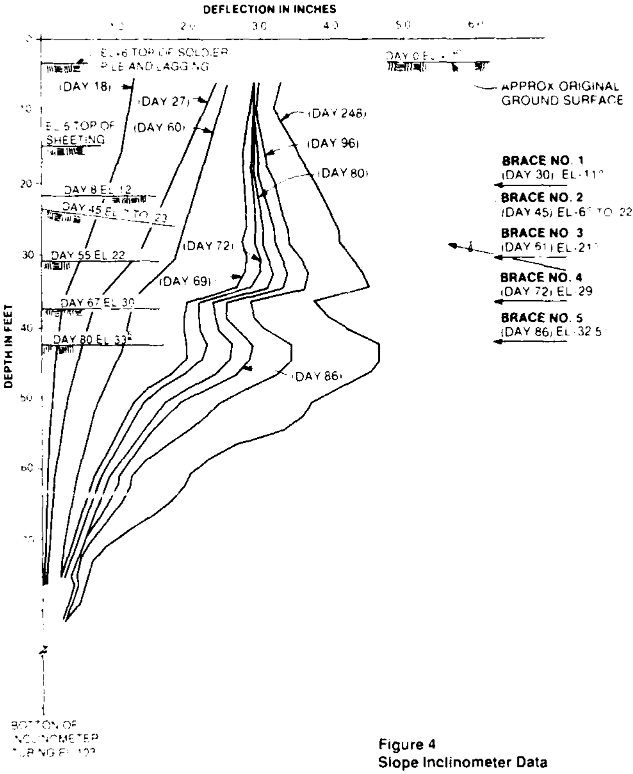

Figure 4
Slope Inclinometer Data
(Wall Deflection vs Depth)

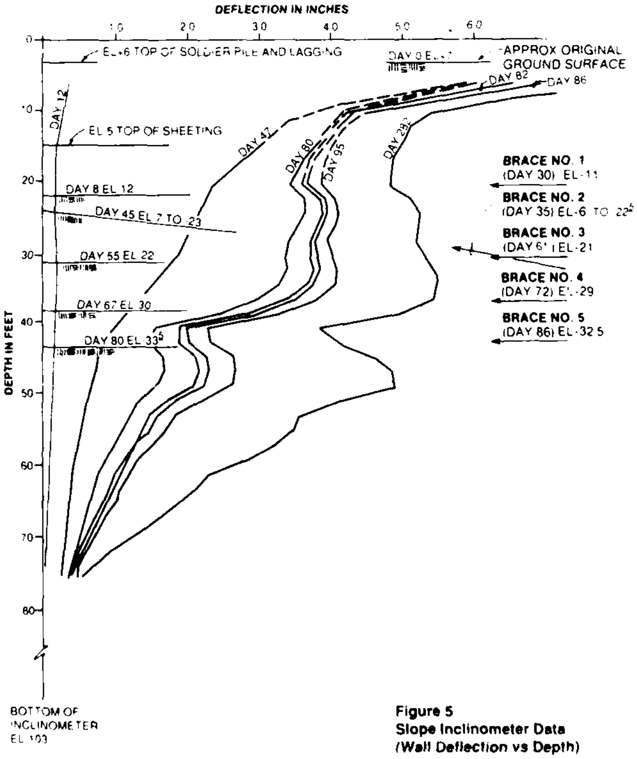

Figure 5
Slope Inclinometer Data
(Wall Deflection vs Depth)

installed. This additional deflection may have resulted from thermal shrinkage of the braces. The south end moved approximately 1/2 inch, while the north end moved approximately 3/4 inch.

Deep movement at the toe of the sheetpile on the west side (Elevation -65) reached approximately 1/2 inch. The toes of the inclinometers were deep (Elevation -103) and no movement was detected.

Measured Loads

An attempt was made to measure actual loads at selected struts by installing strain gauges around the strut, at each end of the strut. The strain gauges in each case did not provide reliable data, and therefore actual loads could not be determined from the measurements.

DISCUSSION

Sheet Pile Wall Deflections

The most significant features of deflection behavior as shown on Figures 4 and 5 are the movement before installation of the upper level braces, and the continued movement during, and even after, all levels of bracing were installed.

As shown on Figures 4 and 5, the first level of excavation was reached at Day 8 and the first level bracing was not installed until Day 30. As shown on Figure 5, the deflection at Day 12 (2 days after the excavation to Level 1 was completed) was less than 1/2 inch. This was the case at both the top of the earth support system and at Elevation -11, the elevation at which the first level bracing was to be installed.

Figure 4 shows that by Day 27 significant deflection (approximately 2-1/2 inches) had occurred at the top of the sheet piling. Further, Figure 5 shows that between Day 12 and Day 47, 2 days after the Level 2 bracing was installed, the deflection at the top of the sheeting was approaching 6 inches. The deflection at Elevation -11 exceeded 2 inches at both inclinometer locations before the installation for the first level bracing. The upper 18 feet of earth support system (soldier pile and lagging and upper sheet piling) were allowed to cantilever for approximately 30 days. If the first level of bracing had been installed within just a few days after the completion of the first level excavation and the cantilever condition had existed only for a very short duration, the deflections of the wall would have been reduced significantly. The duration and sequence of critical construction phases (in this case, installation of the upper level braces) had a significant influence on the behavior and performance of the earth support system.

Approximately 1 inch of movement also occurred at each brace level after the braces were installed. Each brace was preloaded by calibrated jack as it was installed, and shimmed with the jack in place. Upon investigation, however, it was found that some of the walers had separated from the sheeting (in other words, that there was a gap between the walers and the sheeting in some brace locations). Some of the walers used in the construction were cambered wide-flange sections salvaged from a bridge demolition project. Some of the gaps between walers and sheeting were 6 inches wide. Once found, the gaps were shimmed (starting on Day 65), and subsequent movement was relatively less. Table 3 indicates the estimated maximum load at each strut (based on the loads given in the geotechnical report), the relative stiffness of each strut, the ideal elastic deflection at each strut, and the actual deflection at each strut level after strut installation through the time the base slab was cast.

Table 3
IDEAL VS. ACTUAL STRUT DEFLECTIONS

Level	Estimated Maximum Strut Loads (kips)	Strut Stiffness $k = AE/L$ (kips/in)	Ideal Elastic Deflection $\delta = P/k$ (in)	Actual Deflection (in)
1	255	N = 935	.27	1.6
		S = 1,020	.25	2.1
2	200	N = 816	.25	1.1
		S = 955	.21	1.2
3	302	N = 935	.32	1.7
		S = 1,130	.27	1.5
4	612	N = 1,125	.54	1.5
		S = 1,130	.54	1.8
5	503	N = 1,125	.45	1.4
		S = 1,365	.37	1.2

NOTES:

N = North side.
S = South side.

It can be seen that the actual deflections exceed the theoretical deflections by a factor of 3 to 8. The imposed preload in the struts was 100 kips, which should also have reduced the theoretical deflections. O'Rourke (1981) discussed preloading practices and the effect that preloading has on the effective stiffness of the excavation support system. It appears that the preloading was ineffective and that most of the preload may have been taken in the camber of the walers. It further seems that the excavation support system was actually much more flexible than its theoretical stiffness.

The continued movement of the earth support system, even after all levels of bracing were installed, is not well understood. It is believed that this continued movement occurred in part as a result of thermal contraction (the temperature was approximately 120°). Another factor may have been a general trend of the entire system to move eastward as the theoretical earth pressures on the west side of the excavation exceeded those on the east side. The entire east side for several hundred feet was excavated to Elevation -5, approximately 12 feet lower than the west side.

Base Heave

No instrumentation was installed to monitor or measure base heave, but it did not appear that base heave was a problem. In fact, it appears that extending the sheet pile wall into the dense and/or stiff glacial soils provided an effective means of controlling base heave.

As discussed previously, the potential for base heave was identified early in the design phase. The analysis of the base heave problem indicated a marginal to unacceptable factor of safety, ranging from 1.2 to less than 1.0. Although base heave did not appear to be a problem, the potential for base heave was evidenced during construction by significant measured movement of the buried portions of the sheet pile wall at locations where heaving potential was suspect (approximate depth of 50 feet). The deflection at depth 50 feet approached 4 inches. This movement is shown in Figures 4 and 5.

The movement measured in the buried portion of the sheets also suggests that the earth pressures on the buried portion of sheeting should be considered in the design of the earth support system. In this case, the buried section was considered as fixed at the top of the glacial soils and pinned at the lower level brace. The earth pressure was based on Rankine active earth pressure theory. This approach provided adequate design of the earth support system.

Hydrostatic Blowout

Maintaining the hydrostatic pressure in the lower aquifer to less than 10 feet above the bottom of the excavation provided adequate protection against blow out and/or boiling.

Design Approach

The design approach for this project was unusual in that areas of traditional contractor design (temporary earthwork and excavation support facilities) were specifically addressed in the design and construction contract documents in terms of prescriptive and performance criteria. Specifically, the contractor was given:

- The minimum earth pressures to be used in design of the earth support system, along with maximum deflection criteria
- The minimum depth of the bottom of the earth support system (in this case, the minimum tip elevation of the steel sheet piles)
- Criteria regarding groundwater and hydrostatic pressure levels

This design approach was adopted because it allowed the contractor to design the details of the earth support system and incorporate these details with his chosen method of construction. At the same time, this approach removed some of the contractor's judgement and risk-taking ability in the design of temporary construction works. That removal was deemed necessary to minimize the potential for construction delays or interruption of service of existing utilities and facilities.

The criteria for the final design of the temporary support works was modified from the criteria in the contract documents as a result of geotechnical investigation performed during construction by the contractor. The design approach in this case prompted the following positive results:

- The contractor retained the services of a geotechnical engineer to further investigate appropriate criteria for the design of the earth support system.
- The contractor participated in instrumentation beyond that required by the contract documents.
- The project was completed on time without serious interruptions or inconveniences to the owner. The only failure experienced was a broken 10-inch water line during backfilling and removal of the sheeting.

CONCLUSIONS AND SUMMARY

A deep excavation was made in soft- to medium-stiff clays for an influent pump station and preliminary treatment facility for the Jones Island Wastewater Treatment Plant in Milwaukee, Wisconsin. The excavation used a unusual design approach in that the contract documents contained performance and prescriptive criteria to address traditional contractor design areas. Lateral deflections were measured as the excavation proceeded and the earth support system bracings were installed.

Significant deflections in the earth support system occurred early in the project and continued movement occurred after all levels of bracing were installed. The duration and sequence of critical construction phases, particularly the timing of the bracing installation, have a significant influence on the deflection behavior of earth support systems. Careful preloading and ensuring preload transfer also have a significant influence on deflections.

Conventional methods of controlling base heave and hydrostatic blow out provided adequate performance. Extending the sheet piles below the layer with heaving potential into denser materials provides adequate performance, provided the earth pressures on buried portions of the sheeting are considered in the design of the earth support system.

The unusual approach to the design of the excavation support system encouraged positive input from the contractor and resulted in a successful project.

ACKNOWLEDGEMENTS

The geotechnical investigation for this project was one element of the overall design of the Jones Island Wastewater Treatment Plant expansion conducted for the Milwaukee Metropolitan Sewerage District (MMSD). Permission of the MMSD is gratefully acknowledged.
CVR150/036

REFERENCES

Bjerrum, L. and O. Eide, 1956, "Stability of Strutted Excavations in Clay," Geotechnique, Vol. 6, No. 1, pp. 32-47, Norwegian Geotechnical Institute, Publ. 19.

Hansen, L.A. and G.W. Clough, (1978), "Design Aids for Estimating Movements of Excavation Support Systems," unpublished research report, Civil Engineering Department, Stanford University.

O'Rourke, T.D. (1981), "Ground Movements Caused by Braced Excavations," Journal of the Geotechnical Engineering Division, ASCE, Vol. 107, No. GT9, pp. 1159-1178.

Peck, R B. (1969), "Deep Excavations and Tunneling in Soft Ground," Proceedings, 7th International Conference on Soil Mechanics and Foundation Engineering, State-of-the-Art Volume, pp. 225-290.

Terzaghi, K. and R. Peck (1967), "Soil Mechanics in Engineering Practice." John Wiley and Sons, Inc., 2nd edition.

Proceedings: Second International Conference on Case Histories in Geotechnical Engineering, June 1-5, 1988, St. Louis, Mo., Paper No. 6.33

Failure of an Oil Storage Tank

A. Verghese Chummar
Managing Director, F.S. Engineers Pvt. Ltd., Madras, India

SYNOPSIS: One of the three oil storage tanks constructed failed while being test loaded by filling with water. A detailed study of soil characteristics and the causes for the failure of only one of the three oil storage tanks is analysed in detail in the paper. A method of stabilising the weak soil for the re-construction of the tank at the same location is recommended based on laboratory studies made.

INTRODUCTION

One of the three 25 M diameter 15 M high petroleum product storage tanks constructed at Visakhapatnam in Andhra State, India, failed during the test loading. A detailed study of the soil characteristics revealed the causes for the failure of only one of the tanks. Stabilisation of the weak soil by sand-lime piles for the reconstruction of the tank is also analysed.

SOiL PROFILE

The Soil Exploration done in this arca indicates a general soil profile as given in Fig. 1.

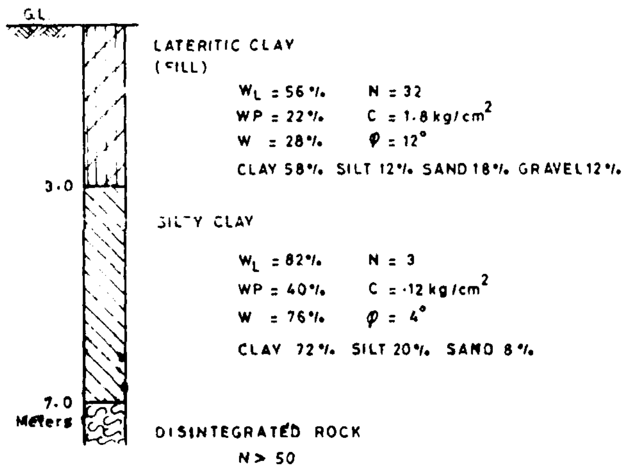

FIG.1. GENERALISED SOIL PROFILE

Visakhapatnam comprises of low-lying areas with hillocks in between. The low-lying areas are connected to the back waters and has got marine silty clay deposits. While raising the level of the low lying areas for the purpose of constructions, soil from the hillocks which comprises essentially of lateritic clay was used. The soil profile given in Fig. 1 gives a typical profile of such formation. The top 2 M of soil is lateritic clay. The underling layer of 4 M thickness is marine silty clay. The layer following is the original sea bed formation comprising of disintegrated rock. The water table is at a depth of about 3 M below ground level.

The properties of the soil layers are indicated in Fig. 1. The lateritic clay layer has got a value of cohesion in its natural state of about 1.8 Kg per Sq.Cm. and friction angle of 12°. The underlying silty clay has got a value of cohesion of only 0.12 Kg per Sq.Cm. with a friction angle of 4°. The limit values, natural moisture content and consolidation curves of the marine clay indicate that the layer is only normally consolidated.

CONSTRUCTION TECHNIQUE OF TANKS

The tanks in this area are constructed by removing the top 15 Cms of soil mixed with vegetation forming the tank pad with lateritic clay of 1 M height. Tanks existing in this area are of 12 M high and the new tanks constructed are 15 M high and 25 M dia.

ANALYSIS OF BEARING CAPACITY

The bearing capacity under a system as indicated in Fig. 2 could be analysed considering the layered system analysis, using the curves given in Fig. 3.

For a C_2/C_1 ratio of 0.07 and D/B of 0.25, N_c value of 1 could be adopted for computation of the bearing capacity. Thus the ultimate bearing capacity,

$$Q_a = 1.8 \times 1 \ \text{Kg/Cm}^2$$
$$= 1.8 \ \text{Kg/Cm}^2$$

The tank loaded upto 15 M with water would give a loading rate of 1.6 Kg per Sq.Cm. Thus a factor of safety of just 1.12 is available.

MECHANICS OF TEST LOADING

The tanks after construction are loaded gradually by pumping in water. One metre height of water is sustained for

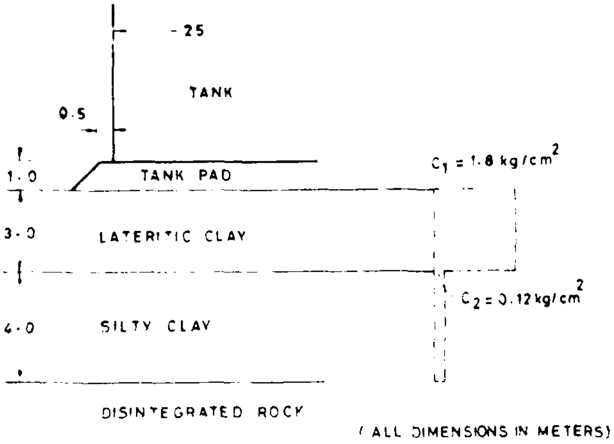

FIG 2. TANK CONSTRUCTION

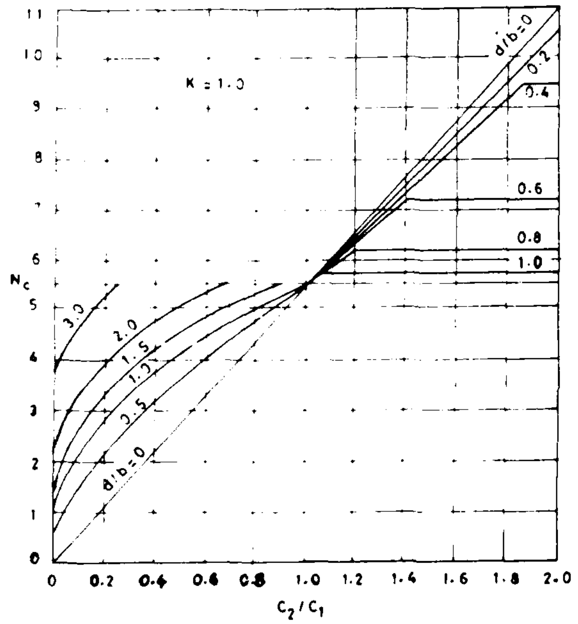

FIG 3. BEARING CAPACITY OF LAYERED SYSTEM

a period of nearly seven days allowing the settlement to take place. In this process certain amount of consolidation of the underlying layer is achieved, increasing its value of cohesion and thus gradually increasing the bearing capacity. Two tanks were tested in this form successfully.

FAILURE OF THE TANK

The third tank while being loaded, when water level was being raised from 11 to 11.5 M, there was heavy downpour inundating the area. Bearing capacity failure of the tank as indicated in Figs.4 & 6 occured, the tank sinking by 1.5 M on one side and 1 M on the opposite side over a period of five minutes. Failure wedge bulged out all around.

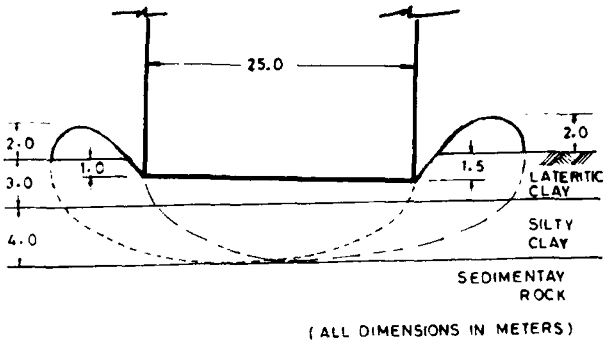

FIG.4. FAILURE OF TANK

CAUSES FOR THE FAILURE

The probable cause for the failure is the reduction in the value of cohesion of the top laterite soil due to inundation. Value of cohesion of such lateritic clay reduces drastically when saturated. The samples from the area after the failure took place were tested which indicated a value of cohesion of 1 Kg per Sq.Cm. with a friction angle of 10°. Under this value of cohesion, the ultimate bearing capacity, Q_u is 1 Kg per Sq.Cm which explains the reason for the failure of the tank when the load was increased from 11 to 11.5 M.

REMEADIAL MEASURES

An inspection of the tank which tilted by failure indicated that no damage is caused to the tank shell. It is hence possible to unload the water in the tank, jack up the shell and re-erect the tank. However, this could be done only after stabilising the soil. Stabilisation of the soil by sand--lime piles was therefore recommended. Laboratory tests were conducted by forming a test tank using the marine silty clay and providing 2 Cms diameter sand-lime piles with 25% quick lime and 75% sand at a spacing of 20 Cms. The soil samples collected from the space in between the piles after a period of two weeks indicate that the shear strength increases from 0.12 Kg per Sq.Cm. before treatment to nearly 0.6 Kg per Sq.Cm. after treatment. This clearly indicated that the surrounding soil to the extent to which the failure wedge formed could be stabilised by provision of sand-lime piles. The system of sand-lime piles as indicated in Fig. 5 was therefore recommended to increase the shear strength allround the tank. The system is under implementation.

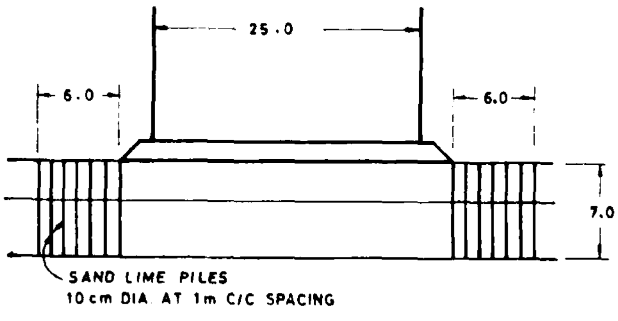

(ALL DIMENSIONS IN METERS)

FIG.5. STABILISATION BY SAND LIME PILES

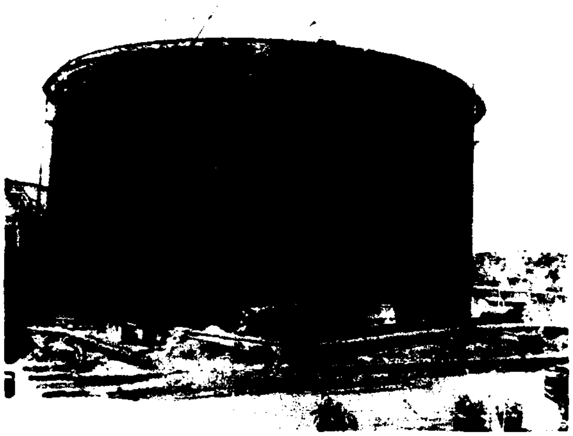

FIG. 6 FAILED TANK

CONCLUSIONS

The failure of the tank took place because of reduction in shear strength of the top crust of lateritic clay due to inundation by rain fall. The existing tanks are found to be stable, the test loading being conducted during dry season with the underlying layer having achieved increase in shear strength by consolidation. For future constructions and re-erection of the failed tank stabilisation of the soil by sand-lime piles is recommended.

REFERENCES

Bowels J.E. Foundation Analysis and Design - McGraw-Hill Kogakusha Ltd. 1977 - pp 127 to 131

Bengt B. Broms and P. Boman (1979), - Lime Columns - A New Foundation Method - Journal of Geotechnical Engg. Division, American Society of Civil Engineers. Vol. 105, pp 539 - 596

Verghese Chummar, A. - Soil Exploration Report No. 930 - Construction of Oil Storage Tanks at Visakhapatnam

Proceedings: Second International Conference on Case Histories in Geotechnical Engineering, June 1-5, 1988, St. Louis, Mo., Paper No. 6.35

The Effects of Mining Subsidence on a Motorway Bridge

C.J.F.P. Jones
Professor of Geotechnical Engineering, University of Newcastle
Upon Tyne, England

SYNOPSIS: Mining subsidence causes ground movements which are imposed on any structure in the area of influence. Bridges are particularly susceptible to subsidence, which frequently causes damage and occasionally collapse. Special bridge designs have been developed to cater for mining subsidence. This paper provides details of the performance of such a structure subjected to significant ground strain.

INTRODUCTION

Mining subsidence is ground movement caused by mineral extraction. In many cases, the movement extends to the surface and is three dimensional in character. Any affected point within the zone of influence having components of displacement along all axes of a Cartesian coordinate system. These displacements are imposed on any structure in the affected zone and may cause damage or distress unless adequate safeguards are taken. Bridges are particularly susceptible to mining subsidence damage leading to the need to impose load restrictions or even causing total collapse.

In the past, buildings and structures were sufficiently small or flexible that the effects of mining subsidence could be tolerated or avoided by the sterilisation of appropriate areas from mining activity. Modern mining methods which use highly mechanised systems of extraction and which demand major capital investment, make sterilisation of coal under a particular area or bridge prohibitively expensive and inefficient. As a result it is necessary for bridge structures to be capable of withstanding ground strains resulting from the moving mining wave.

This paper provides a case history of a modern motorway bridge which has been subjected to severe mining subsidence. Details are given of the design of the bridge and of the mining together with the resulting ground strains and the performance of the structure. The management of the bridge during the mining phase is described and details of the remedial works and costs provided.

DESIGN OF BRIDGES IN AREAS OF MINING SUBSIDENCE

The majority of bridges built in the United Kingdom were constructed before the introduction of modern mining methods and no structural precautions were taken to cater for large differential ground movements. Little is known about the tolerance of bridges to movement. What is known is that certain structural forms are more susceptible to ground strain than others. Arch bridges are particularly at risk.

A valuable contribution to tolerance movement criteria in bridges has been provided by Moulton et al (1982) in a study undertaken on behalf of FHWA. Based upon a large number of observations, Moulton et al were able to establish tolerance limits for a number of movements including:

i. Angular distortion (differential settlement/ span length)
    Continuous steel structures - 0.004
    Simply supported steel bridges - 0.005

ii. Horizontal movements of Abutments < 34mm

iii. Differential vertical settlement
    Simply supported bridges - no limit (within the range tested)
    Continuous bridges - total negative stress over supports < AASHTO (1975) Limiting stress criteria

The findings of Moulton et al confirm the observations in the United Kingdom that mining subsidence movements, in which settlements in excess of 1 metre and ground strains of upto 0.5 per cent are frequent, would normally result in overstress and damage to a conventional highway bridge.

The problem of mining subsidence was recognised in the United Kingdom at the start of the motorway building programme in the 1960's when the M1 London Yorkshire motorway was detailed to pass across the Derbyshire and Yorkshire coalfields.

Two main approaches to the design of bridges were developed to provide safeguards against the effects of subsidence. The bridges could be designed to be statically determinate, with stiff decks resting on a three point support system (similar to a three legged stool) or, alternatively made flexible being built up of a series of articulated parts and having low torsion decks capable of accommodating large angular rotations.

In the first design concept the bridge rides the subsidence wave and differential horizontal movements are accommodated with the use of anticlastic bearings. In the latter design technique the bridge is made capable of absorbing the mining movements as they occur without loss of load carrying capacity. Experience of the Yorkshire coalfield in the United Kingdom has shown that an average highway bridge of between one to four spans could be subjected to the following mining movements:

a. Differential longitudinal horizontal displacement ± 150-225mm
b. Differential transverse displacement ± 150mm
c. Differential vertical displacement 0.6-0.9m
d. Longitudinal angular distortion 1 in 80
e. Transverse angular distortion 1 in 150
f. Differential rotation in plan 0.3°

No bridge would be subjected to the full range of movements detailed above, but a major complication in design is that predicting which movements would occur is dependent on the geometry of the mining relative to the bridge. At the time of design this is unknown.

In the majority of cases in the Yorkshire coalfield, the flexible design approach was adopted. Minor damage to the structures was deemed acceptable and inevitable but the full use of the motorway had to be retained, except during post mining repairs. In addition it was important that the cost of bridges built to cater for mining subsidence should not be greater than the cost of a conventional bridge. In the systems developed in Yorkshire this latter condition was exceeded in that the low torsion decks developed for mining was adopted for general use even when mining was not expected, the reason being that the low torsion decks proved to be less costly than the conventional decks.

SHILLINGHILL BRIDGE

Shillinghill Bridge carries the M62 Lancashire Yorkshire motorway M62 over the A645 Pontefract-Knottingley road. The M62 crosses a railway embankment 200 metres to the north of the A645 and the difference in carriageway levels is in the order of 12 metres. The A645 has a carriageway width of 13 metres with two 2 metre footpaths. For both economic and asthetic reasons the bridge was designed as two identical parallel 3 span structures, one supporting the eastbound carriageway, the other the westbound.

Each deck consists of 12 standard prestressed concrete beams (type 75/D) 21 metres long and a 175mm reinforced concrete deck slab. The bridge skew is approximately 11°. The deck was analysed using load distribution methods with an allowance for edge beam stiffening.

The piers are reinforced concrete and were designed to take into account small but significant mining movements and a steeply sloping foundation. At the time of the design of the bridge in 1970, mining movements were predicted to be in the order of 1.5mm/metre but is was not known when these movements would occur. The piers were designed using a computer program, Sims, Jones and Bellamy (1972). It was assumed that the movements would be taken up in the laminated rubber bearings and the shear forces produced were included in the design of the piers and bank seats.

The expansion joints were provided with a movement capacity sufficient to accommodate the anticipated mining strain of 90mm over the length of the bridge. The rock strata on which the bridge was founded slopes steeply from south to north and the northern piers are approximately 7 metres higher than the southern ones. Further technical details associated with the design of the bridge are given in Table 1. The bridge was constructed during 1972-1973.

TABLE 1. Technical Details of Shillinghill Bridge

Deck Details

Number of lanes	4 Eastbound	4 Westbound
Width of deck	17.4m	17.4m
Thickness of deck slab	175mm	175mm
Span	20.1m	20.1m
Number of spans	3	3
Dead weight of deck	266.5 KN/m	265.5 KN/m
Number of beams/span (75/d)	12	12
Shear rating of bearings	2.35KN/mm	2.35KN/mm
Thickness of bearings	75mm	75mm

Pier Details

Height (average)	18.5m	18.5m
Width (top)	17.3m	17.3m
Base width	5.5m	5.5m
Base breadth	13.8m	13.8m
Base thickness	1m	1m
Permissible bearing stress	536.25KN/m^2	536.25KN/m^2

NOTE 25 per cent over stress permitted during HB loading

MINING SUBSIDENCE

Shillinghill Bridge was mined under in 1981. Details of the mining are shown in Table 2. Figures 1,2 and 3 give details of the panel layout relative to the bridge and also provide details of the predicted surface contours for the longitudinal and transverse strain and the subsidence, based upon the use of the empirical prediction method developed by the National Coal Board (1975).

TABLE 2. Details of Mining Subsidence at Shillinghill Bridge

Colliery: Prince of Wales, Pontefract			
Seam	Depth	Width of Panels	Extraction
Castleford 4 foot	245m	240m	1.45m
Subsidence		Panel 44's	Panel 45's
Vertical		0.15m	0.2m
Longitudinal strain		Negligible	Negligible
Transverse strain		+ 4mm/m	+ 4mm/m

The position of the bridge relative to panels 44's and 45's was not advantageous and the bridge was subjected to significant movements. The mining caused the east and west bound carriageways to move apart at the western end of the bridge by upto 100mm. The bridge settled differentially and the decks rotated in plan causing disruption of the expansion joints and resulting in the combined parapet and crash barrier to fail in tension. An illustration of the degree and complexity of the movement suffered by the bridge is shown in Figure 4. The movements included an angular distortion of one deck in excess of 1 in 70. Although the mining caused severe disruption to the vertical alignment of the motorway supported by the bridge which required the imposition of speed limits, at no time was the carrying capacity of the bridge reduced.

The allowable shear strain of the rubber bearings was exceeded during the mining phase. Maintenance procedures were undertaken to relieve and reposition the bearings during the mining. This was achieved by the use of hydraulically linked flat jacks positioned between the bearings which were used to raise the deck a nominal amount (2mm) sufficient to permit the distorted rubber bearings to jump back into position. These works were undertaken by West Yorkshire Bridge Engineers working on Sunday mornings when the bridge traffic was light. Repositioning of the bearings was undertaken on a number of occasions.

REMEDIAL WORKS

The damage to the motorway caused by the mining subsidence was substantial. In accordance with the Coal Mining (Subsidence) Act of Parliament 1957, the National Coal Board are required to meet the cost of the remedial works considered necessary to restore the highway to a condition fit for use. In the case of the motorway at Shillinghill Bridge, remedial works cost in excess of £1.0 m. The National Coal Board contribution to the repair of the bridge was £110,000.

The remedial works which were undertaken when the motorway alignment and drainage was reconstructed consisted in jacking the bridge decks to conform with the revised vertical alignment and to remove the angular distortion. Included in the works was the partial reconstruction of the bridge bank seats raising them to the new alignment, renewing all bearing plinths and replacing all bearings and expansion joints.

No problems were encountered in the remedial works other than that the force needed to jack the deck well clear of the bearings proved to be in excess of the dead weight of the deck. This was caused by the presence of polystyrene foam used to create the expansion joint between the ends of the deck and the bank seat. Although this material is weak in compression, polystyrene proved to be very strong in shear.

CONCLUSIONS

Shillinghill Bridge was one of the first motorway bridges which had been specifically designed to cater for mining subsidence to actually be subjected to mining. The movements caused by the mining demonstrated the three dimensional nature of subsidence and also illustrated the difficulties of predicting movements at the design stage. The movements far exceeded and were different in nature to those anticipated in 1970.

The bridge behaved very well during the subsidence and demonstrated the validity of the design concept developed to cater for bridges in mining areas. The success of the design was further strengthened by the fact that three adjacent arch bridges had to be demolished and totally rebuilt because of the mining subsidence. In addition, a nearby overhead sign gantry had to be dismantled during the mining, and three miles to the east of Shillinghill Bridge the decks of a bridge spanning the M62 motorway had to be removed and shortened by diamond saw. To the north the cantilever span of a small footbridge had to be raised out of position while the mining wave passed through the area.

Figure 1

Contours of Transverse Strain (mm/m)

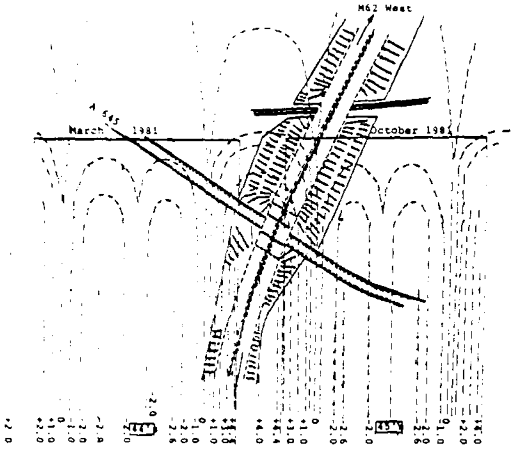
M62 West
A 645
March 1981
October 1981

Figure 2

Contours of Vertical Settlement (Metres)

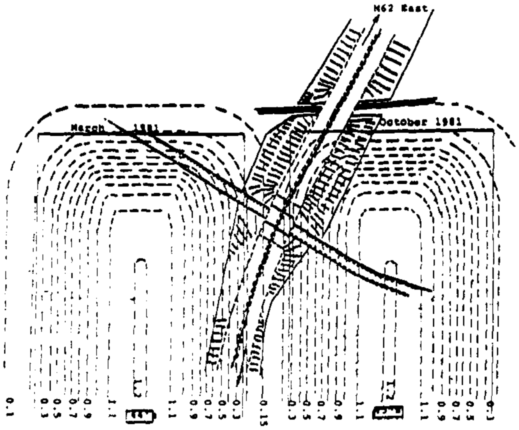
M62 East
March 1981
October 1981

Figure 3

Contours of Longitudinal Strain (mm/m)

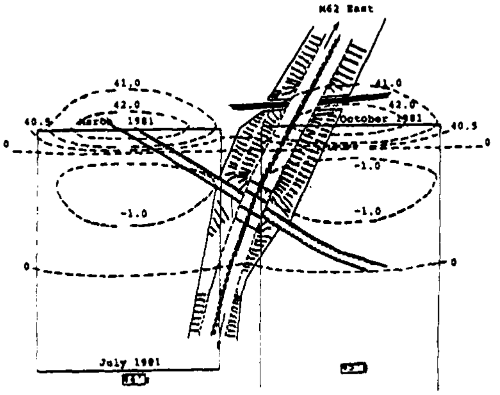
M62 East
41.0
42.0
40.5
March 1981
October 1981
41.0
42.0
40.5
0
-1.0
-1.0
-1.0
0
0
July 1981

Figure 4

Shillinghill Bridge M62 Motorway

Mining Movements (mm) May 1981 - March 1982

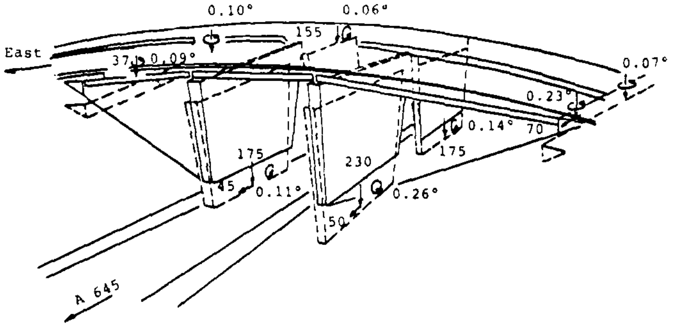
0.10°
0.06°
East
155
37
0.09°
0.07°
0.23°
0.14°
70
175
230
175
45
0.11°
50
0.26°
A 645

REFERENCES

Moulton, L.K., Ganga Rao and Halvorsen, G.T., (1982), "Tolerable movement criteria for Highway Bridges", Volume 1, Report No FHWA/RD - 81/162, United States Department of Transportation.

American Association of State Highway and Transportation Officials, (1977), "Standard Specifications of Highway Bridges", 12th Edition.

National Coal Board, (1975), Subsidence Engineers Handbook.

Sims, F.A., Jones, C.J.F.P. and Bellamy, J.B., (1972), "Computers and Bridges - A computer design suite for standard bridges", Concrete, Volume 6, No 4.

ACKNOWLEDGEMENTS

Shillinghill Bridge was designed by the North Eastern Road Construction Unit under the authors direction. The structure was monitored, maintained and repaired by the West Yorkshire Metropolitan County. The assistance of Mr. J. Frankland, Chief Mining Engineer in West Yorkshire, in supplying mining data is gratefully acknowledged.

Proceedings: Second International Conference on Case Histories in Geotechnical Engineering, June 1-5, 1988, St. Louis, Mo., Paper No. 6.36

Correlation between the Actual and Predicted Settlements of Structures at Nsukka, Nigeria

H.O. Chukweze
Department of Civil Engineering, University of Nigeria, Nsukka, Nigeria

SUMMARY: The paper compares the measured and calculated settlements of two buildings and one concrete water tank founded on the red-weathered soils of Nsukka, Nigeria. Prior to actual construction of the structures the three sites were investigated, soil samples were collected and tested in the laboratory and the data collected were used to predict the total and differential settlements of the structures.

Then permanent concrete slabs were establshed as bases at each of the three sites for obsering other points. The theodolite was used at each of the sites to monitor the movements of each of the structures, starting from the time when the base concrete slab or footings were laid to the end of major or active construction operations.

It was found that excepting the water tank which continued to settle albert slowly and uniformly, the buildings showed insignificant vertical settlement after about five years later and that the correlations between the measured and predicted settlements were relatively poor, generally less than 40 percent. The results suggested that the field or actual settlements were always larger than the predicted ones. The poor correlation was adduced to primarily the several and serious assumptions made in the establishment of the analytical equations for the determination of settlements analytically and also to the paucity of field data which could help to improve on the relevant consolidation equations using the field results.

INTRODUCTION

This paper is an attempt to evaluate the validity of the one dimensional consolidation equation due to Terzaghi (1943) and of the elastic law of soil deformation (Janbu, 1971) in predicting the total settlements of the structures founded on the tropical soil formation. One of the major setbacks in the confident prediction of the settlements of structures in the country is the fact that there is hardly any feedback in the form of settlements measured directly from structures in service so that the earlier analytical predictions could be evaluated. The few available records are confusing because they seem to strike a balance between over- and under-estimation of the actual or field settlements (Lee, 1968; Tavenas & Leroueil, 1980).

In addition the soils of this country, especially in the hintherlands contain pseudeoparticles and encrustations (Chukweze, 1976; GBRI, 1971). These pseudo particles break readily under moderate pressure producing more fine-grained soil particles. On the other hand the encrusted particles can impart a false high bearing strength on the soil. The analytical predictions involving the use of small soil samples could thus be in error. Another important factor of note is that the soil formation in this region is unsaturated throughout the year. Yet the laboratory testing procedures recommend the use of saturated soil samples for the prediction of settlements analytically. These two differing conditions could influence the results.

THEORY

The long-term or consolidation settlement of the structure on a real soil is calculated from the one dimensional consolidation equation for saturated soils (Terzaghi, 1943). In practice the soil is assumed to be fully settled after 24 hours of loading. Consequently the secondary consolidation (creep) is not considered but the primary and secondary settlements together can be evaluated from the recent modified one dimensional consolidation equation due to Mesri & Godlewski (1977). Thus

$$S_c = \frac{HK}{1 + e_o}$$

where

S_c = consolidation settlement

e_o = initial void ratio of soil

H = compressible soil layer **thickness**

K = $C_c A + C_\alpha B$

C_c = compression index of soil

A = $\log \frac{\sigma_o^1 + \Delta\sigma^1}{\sigma_o^1}$

σ_o^1 = effective overburden

$\Delta\sigma^1$ = increase in stress

C_α = (0.045 ± 0.01) Cc

$S = C_\alpha \log t$

t = design life of structure

Unfortunately some degree of undrained distortion accompanies the normal consolidation of the soil and this has been neglected by the above mathematical model (Tavenas & Leroueil, 1980). There is also the behaviour of the construction pore pressure which has not been fully accounted for as yet (Skempton, 1954; Hentel, 1960; Tavenas and Leroneil, 1980).

However it is now possible to account for any lateral shifts as this has been related to the vertical movements undergone by the structure (Tavenas et al, 1979).

Thus

$$\Delta h = (0.16 \pm 0.02)S$$

where

Δh = lateral displacement

S = settlement of the structure

Although the above equation (eq. 2) is related to the conditions prevalent in clays, it is interesting to note the serious attempts being made to improve on the analytical methods of predicting settlements in the long term.

In order to predict the immediate settlements reliance continues to be placed on the elastic theory (Janbu, Bjerrum and (Kjaernsli, 1956). Thus

$$S_i = \frac{u_1 u_o q_n B_i}{E}$$

where

S_i = immediate settlement

u_1 and u_o = constants

q_n = normal pressure on the soil

B_i = width of the loaded area

E = modulus of elasticity of the soil

The attraction of eq. 3 is that no corrections are required. Also the Poisson's ratio is assumed to be 0.5 consistent with the undrained condition assumed in determining the parameter, E_u (eq. 3).

Although there has been some objections to the method the total settlement is in practice taken to be the sum of the immediate and the consolidation settlements (Skempton & Bjerrum, 1957; Berre & Iversen, 1972).

Methods of field measurements of settlements have not been standardised. Additionally there is no information on the influence of particle crushing on the settlements of structures.

EXPERIMENTAL WORK

The structures examined in this study are all located in the University of Nigeria, Nsukka, campus. The area is located in the map shown in fig. 1. The actual sites are found in the localities shown in figs. 2 & 3.

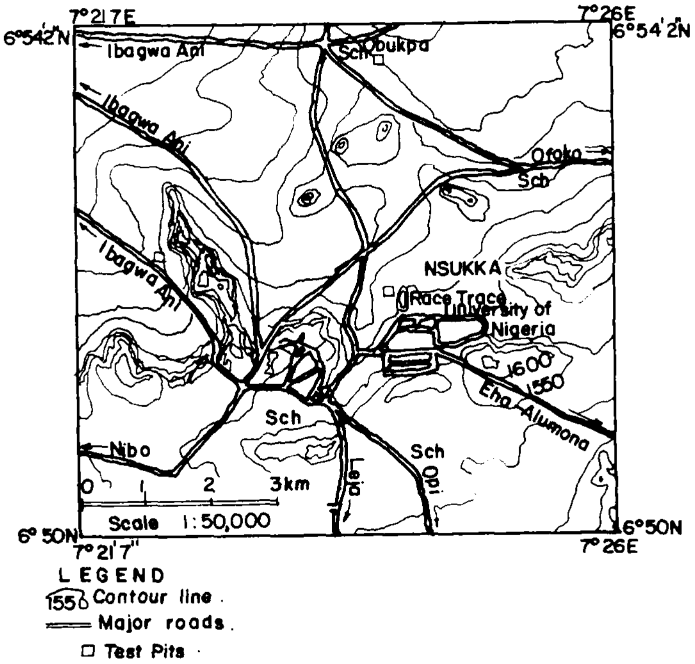
7°21 7E
7°26E
6°54'2N
6°54'2N
Ibagwa Ani
Sch
Obukpa
Ibagwa Ani
Ofoka
Sch
Ibagwa Ani
NSUKKA
Race Track
University of Nigeria
1600
1550
Eha Alumona
Sch
Nibo
Sch
Opi
0 1 2 3km
Scale 1:50,000
6° 50N
7°21'7"
6°50N
7°26E
LEGEND
1550 Contour line
Major roads
□ Test Pits

Fig. 1

Two aspects of the experimental work described below are the field and laboratory studies.

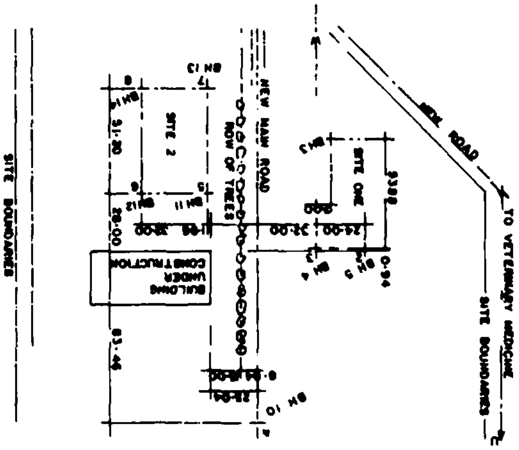
NEW MAIN ROAD
ROW OF TREES
SITE 2
SITE ONE
SITE BOUNDARIES
BUILDING UNDER CONSTRUCTION
NEW ROAD
TO VETERINARY MEDICINE
SITE BOUNDARIES

Fig. 2. Site for two general purpose buildings.

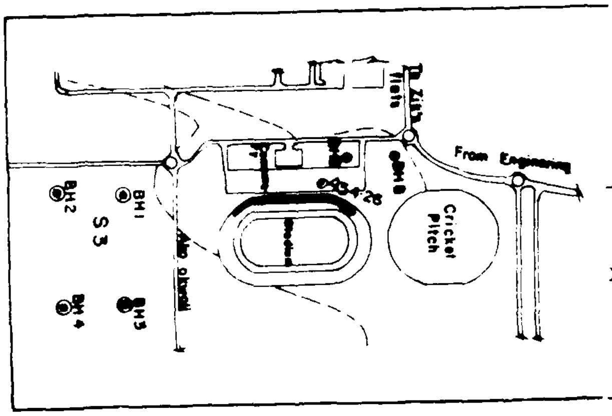

Fig 3 Site for the concrete water tank.

FIELD WORK

The three sites for the proposal structures were carefully examined. Both the disturbed and undisturbed soil samples were collected using the percussion drilling rig. Borings were made for up to 15m deep. The undisturbed soil samples were required for the oedometer tests and the disturbed soil samples for the classification and index test determinations.

To measure the settlements special devices typical of the one shown in fig. 4 were constructed at each of the four corners of each building and three of them round the concrete water tank. The device consisted of a steel rod carrying a dial guage protruding from the base of the structure. The vertical and lateral displacements of this rod due to the movements of the structure are measured by means of another rod placed vertically and in contact with the dial guage.

Additionally a concrete base was established at each site so that the tips of the horizontal rods could be observed routinely using the theodolite. As a result accurate measurements of the foundation movements were assured. These measured movements constituted the observed settlements. Measurements lasted from January 1978 to August, 1979 and then at 4 yearly intervals.

LABORATORY WORK

The distrubed soil samples were used to classify the soils of each site and also to determine the soils' index properties. The undisturbed soil samples were used to conduct the oedometer and the undrained preconsolidated triaxial tests and to determine the unit weight of the soils in-situ. All the tests were carried out by the standard labcratory methods. eg. BS 1377, 1975.

In order to use eg. 1 to calculate the consolidation settlement the thickness of the compressible stratum, H was taken as the depth of significant stress in that the soil formation was found to be unstratified throughout the depth investigated. The width, B_1 and the pressure on the soil, q_n for use in eg. 3 were extracted from the structural map supplied by

Table 1: Classification parameters for the soils.
(Standard error generally less than 5%)

Locality	Maximum sample depth (m)	Average values of the Atterberg limits (%)*				Average values of the particle content			
		LL	PL	PI	SL	Clay	Silt	Sand	Gravel
1	10	36	20	16	7	19	30	40	11
2	15	31	18	23	8	22	31	42	5
3	13.5	38	19	19	7	20	32	46	2

* LL = Liquid limit; PL = Plastic limit;

PI = plasticity index; Sl = shrinkage limit

Table 2: The Compression parameters of soils

Locality	Natural moisture content (%)	Undrained Young's modulus (kN/m^2)	Compression Index, C_c	Void Ratio e_o	Specific gravity G_s	Bulk unit weight kN/m^3	Permeability, m/sec x 10^{-10}
1	9	9,000	0.061	0.48	2.72	18.1	3.53
2	8	6,500	0.070	0.52	2.66	18.5	3.95
3	10	5,500	0.065	0.45	2.69	18.8	3.44

Table 3: Calculated settlements of structures*

Locality	Compressible soil layer (m)	Width of loaded area (m)	Footing pressure kN/m^2	Settlements(mm)		
				Immediate	Long-term	Total
1	11	1.1	1430	39	223	262
2	11.2	1.1	1630	47	313	360
3	7	7	13,160	42	304	346

* Depth of footing from ground surface = 1.3m

the contractors. The undrained Young's modulus was obtained from strain-controlled undrained triaxial tests noting that the results could be affected by the strain rate, stress path and stress level (ladd, 1964).

All the field and laboratory results have been compiled and summarised in tables and graphs now discussed below.

RESULTS AND DISCUSSIONS

Table 1 shows the results of the classification tests. It is seen that the soils investigated are generally clayey sand and silt with fines of intermediate compressibility. The positions of the soil samples on the Casagrande's plasticity chart (Casagrande, 1948) are above the A-line. Such soils exhibit high bearing strengths when dry and this can be deceptive unless care is observed to insure that the relevant tests are conducted with soil samples whose water contents correspond with those of the service conditions. It is **important to note that serious** accidents of failures have occurred in this country because the contractors base their results on erroneous soil moisture content data.

Table 2 shows the other index and strength properties of the soils studied. The undrained modulus, E_u is seen to range from 5,500 kPa to 7000 kPa. This range clearly exposes the dry nature of the soils. It additionally demonstrates the in-admissibility of some of the empirical values for clay soils like 1200 kPa (D'Appolonia et al, 1971) for these types of soils.

The consolidation parameters also shown in table 2 have been obtained for the saturated conditions specified by *the testing methods* Thus, although the soils in-situ are far from being saturated, the data presented in table 2 are admissible for use in eq. 1 for the calculation of the long-term or consolidation settlements.

The immediate, oedometer (consolidation) and the total settlements of all three structures are presented in table 3. Remarkedly it is seen that the immediate settlement for all the structures is less than fifteen percent of the total calculated settlement. Thus most of the calculated settlements emanutes from long-term loading effects, or consolidation. This results may be expected considering that the parameters used in the determination of the immediate settlement may be nearer the actual states of unsaturation of the soils and in this state the soil has bearing resistances apparently greater than when they are saturated and can more readily collapse (consolidate) when loaded. Thus the consolidation settlement ranges from 221mm to 313mm. Whilst the total settlements range from 250mm to 340mm. These settlements are significantly high and may be associated with between 125mm and 170mm of differential settlements.

The actual settlements were observed initially from the laying of the footing slab to the end of major construction activities (fig. 5.0). Thereafter readings were taken every 4 years.

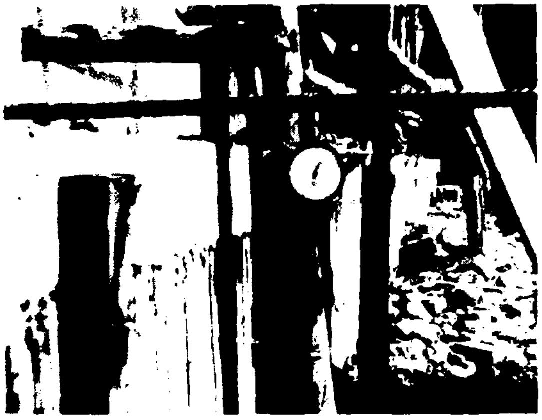

Fig. 4

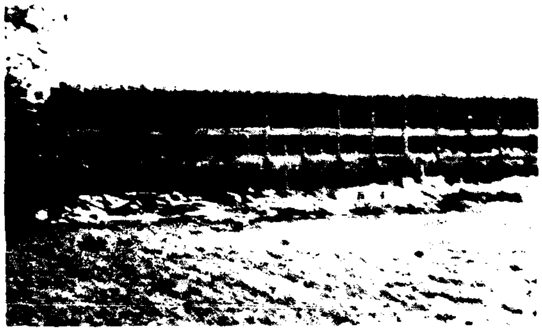

Fig. 5

The vertical settlements and horizontal shifts for the structures recorded for the first continuous period of up to 80 weeks January, 1978 to August, 1979) are shown in figs 6 & 7 respectively. The two readings taken at 4 years intervals (1983 and 1987) are included in table 4.

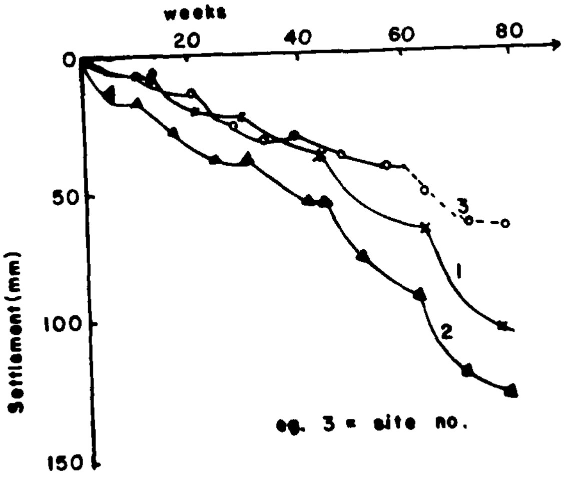

Fig. 6 Observed settlements.

It is seen from fig. 6 and table 4 that

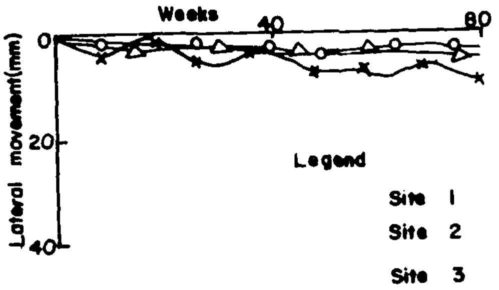

Fig. 7. **The lateral movements of the structures.**

some measureable settlements are still observed after nearly eight years of cessessation of actual construction works. These additional settlements may be accounted for, in part, by the added finishings and partly by the live loads in that the structures have been put into active service. This may be especially true for the concrete water tank which has suffered an additional settlement of 106mm compared to those of the buildings of only 42mm (site 1) and 34mm (site 2) respectively.

Table 4. Observed settlements of the structures.

Period	Settlements (mm) for sites		
	1	2	3
1978-1979	99	127	55
1979-1983	27	23	64
1983 - 1987	15	9	42

Table 5: Observed lateral shifts of the structures for periods 1978 to 1987

Period	Displacements (mm) for sites		
	1	2	3
1978-1979	9	3	2
1979-1983	2	2	3
1983-1987	2	2	2

From table 5 it is seen that all the structures have suffered from some lateral movements. The range of values observed are from 7mm to 13mm which differ radically from the values which are obtainable using eq. 2.

By comparing also the results of the calculated settlements (table 3) and those observed from actual field records (table 4) it is seen immediately that the calculated values are much larger, ranging from 262mm to 360mm compared to the field range of 141mm to 161mm. Thus for the three sites studied the ratio, calculated to observed settlements are 1.85, 2.26, and 2.14 respectively. The laboratory methods thus overestimate the actual settlements by more than one hundred percent judging from the current results. Only a few previous results have been as precise as those reported herein.

It is seen from table 4 and 5 that measureable but small settlements continue more than six years after the cessation of construction. Thus it may require several more years before the structure settles permanently. It is considered that when this condition is reached then the settlement ratio may reduce a bit, to 1.5 say.

For the tropical soil foundations this ratio of 1.5 is considered favourable. It means that structures to be founded on such soils are designed for settlements far in excess of those that can occur in service. A magin of safety is thus automatically incorporated into the design by virture of the nature of the soils as pointed out earlier in this paper.

CONCLUSIONS

The soils around Nsukka, Nigeria are typical for the tropics being concretionary or preudo-particulate and so readily collapse under relatively high pressure especially when wet.

For such soils the laboratory methods of settlement determinations over-estimate the total actual settlements of the soils under vertical loading.

The vertical settlements are generally accompanied by lateral movements which are best estimated by actual field measurements in that the analytical equations currently available do not agree with the actual field records.

The laboratory methods of settlement determinations are advantageous when used for the tropical soils because some safety factor is then automatically incorporated into the design of the structure.

ACKNOWLEDGEMENT

The author is grateful to the laboratory technical staff of the Department of Civil Engineering, University of Nigeria, Nsukka, who assisted in establishing the observation posts for the present study.

REFERENCES

Berre, T. & Iversen, K (1972), "Oedometer tests with different specimen heights on a clay exhibiting large secondary compression", Geotechnique, 22(1), pp. 53-70.

Casagrande, A. (1948), "Classification and identification of soils", Trans. ASCE., Vol. 113, pp 901 - 991.

Chukweze, H.O. (1976), "Some principal engineering-geological properties of typical Nigerian Laterites", M.Sc Thesis, Univ. of Ife, Nigeria, P. 105.

D' Appolonia, D.J., Panlos, H.G. and Ladd, C.C. (1971), "Initial settlement of structures on clay", ASCE. Journal of the S.M & F.E. Div., 97 (sm10), pp. 1359-1377.

Building & Road Research Institute, Ghana (1971), "Laterite and lateritic Soils (and other problem soils) of Africa", Agency for Int. Dev., BRR1, pp. 5-29.

Henkel, D.J. (1960), "The shear strength of saturated remoulded clay", Proceedings, ASCE, Specialty conference on Shear strength of Cohesive Soils, Boulder, Colorado, pp 533 - 554.

Janbu, N. (1967), "Settlement calculations based on the tangent modulus concept", Institutt Geoteknikk og Fundamenteringslaere, Technical University of Norway, Trondheim, Bulletin 2.

Janbu, N., Bjerrum, L. & Kjaernsli, B. (1956), "Veiledning Vedlosning avfundamentering soppgarer", Publ. No 16, Norwegion Geotechnical Institute.

Ladd, C.C. (1964), "Stress-Strain modulus of clay in undrained shear", ASCE Journal of the SMZFE. Div., 90 (SM5), pp 103-132.

Lee, I.K. (1968), "Soil Mechanics: Selected topics", Elsevier Publ. Co. Ltd, N.Y. Chap. 1 - 4.

Mesri, G. & Godlewski, P. (1977), "Time and stress compressibility interrelationships", ASCE Journ. of the Geotechnical Engrg. Div. 103 (GT5), pp. 417 - 430.

Skempton, A.W. (1954), "The pore pressure coefficients A and B", Geotechnique, 4 (4), pp. 143 - 147.

Skempton, A.W. & Bjerrum, L. (1957) "A contribution to the settlementanalysis of foundation on clay", Geotechnique, 7, 168-178.

Tavenas, F. & Leroneil, S. (1980), "The behaviour of embankments on clay foundation", Canadian Geotechnical Journal Vol. 17, pp 236 - 260.

Tavenas, F., Mieussens, C. and Bourges F. (1979), "Lateral displacements in clay foundation under embankments", Canadian Geotechnial Journal, 16, pp. 532-550.

Terzaghi, K. (1943), "Theoretical soil Mechanics", John-Wiley Publication, N.Y. P. 425.

Proceedings: Second International Conference on Case Histories in Geotechnical Engineering, June 1-5, 1988, St. Louis, Mo., Paper No. 6.37

Bearing Capacity of Pile Foundations

Xie Sheng-sun
Engineer of Geotechnical Engineering, Beijing Electrical Power
Design Institute, Beijing, China

SYNOPSIS: This paper deals with the case histories about the bearing capacity of piles in an off shore thermal power plant, it includes:(1) The exploring of the site and the setting of the data in pile foundation design. (2) Static load test of inclined piles with deviations ranging from 3 to 10 degrees from vertical.

INTRODUCTION

The geotechnical engineering exploration of the site of the thermal power plant was carried out before construction to make certain of the bearing stratum of pile points and the length, the cross section area and the ultimate bearing capacity of the pile. As the tilting of the piles was caused by poorly driving and by excavation of adjacents soils during construction, thus static load tests were conducted to determine the influence of tilting on the pile capacity. The results are presented herein.

EXPLORATION AND DESIGN OF PILE FOUNDATION

The site was explored by drilling, static and dynamic penetration and laboratory tests of undisturbed samples. The typical results of static cone penetration tests measured at different places where the boiler, chimney, coal silo and cooling tower will be built are shown in Fig.1. Laboratory test results are shown in Table 1. Based mainly on the data of static load tests conducted in 126 holes it was decided to select the bearing stratum of point bearing piles at about 20 m under ground surface. The bearing stratum was sandy loam with thickness of 2.2 to 4.9 m, below which was sandy clay. The length of the pile ranges from 16.5 to 18.5m, the cross section area of the square pile was 1600 cm2, and the ultimate bearing capacity computed by the formula (1) for various structures was listed in Table 2. Based on Table 2 and the result of static loading tests of vertical piles shown in Fig. 2, the designed ultimate bearing capacity of pile was determined to be 1600 kN, and the allowable bearing capacity of pile was 800 kN.

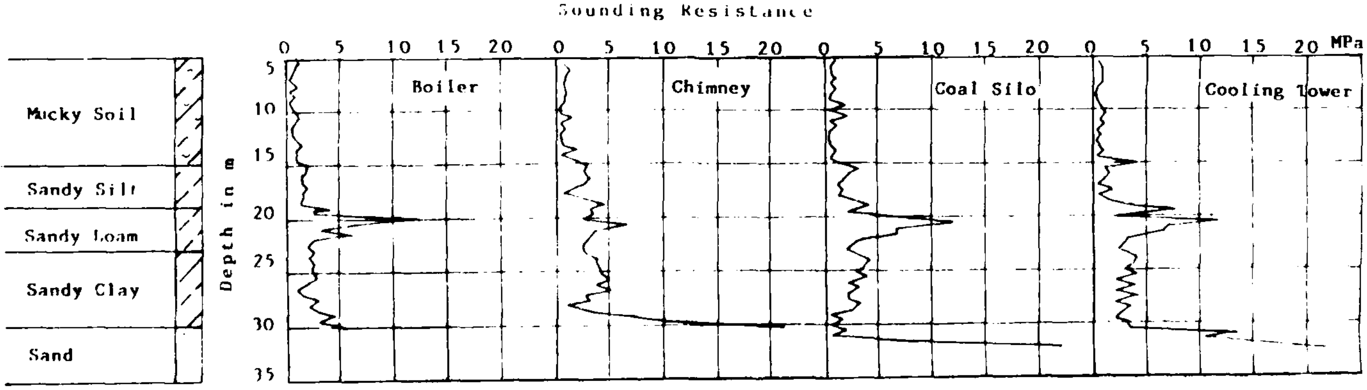

Fig. 1. Results of Static Cone Penetration Test

$$P_u = \alpha_i q_c A_c + U \sum \beta_{si} f_{si} h_i \quad (1)$$

Where: P_u Ultimate bearing capacity of pile

q_c = Average sounding resistance

f_{si} Average skin friction

A_c Cross section area of the square pile

U = Perimeter of pile

h_i Depth

α_i = Correction factor of sounding resistance

β_{si} = Correction factor of skin friction

The correction factor α_i and β_{si} listed shown in Table 3 and Table 4 respectively were given by Xie (Xie, 1984)

TABLE 1. Laboratory and Field Test Results of Soils

Number of Stratum	Soil	Thickness of Stratum H m	Sounding Resistance q_c MPa	Water Content W %	Bulk Unit Weight of Soil γ kN/m^3	Void Ratio e	Plasticity Index I_p	Liquidity Index I_L	Coefficient of Compressibility a_{1-2} MPa^{-1}
1	Mucky Soil	4.0–14.4	0.3–0.7	38.5–48.9	17.9–18.4	0.92–1.19	10.7–15.8	0.96–1.80	0.44–0.78
2	Sandy Silt	1.4–8.2	1.7–2.5	14.8–26.4	19.7–21.7	0.44–0.76	4.5–9.4	0.50–1.34	0.12–0.27
3	Sandy Loam	2.2–4.9	4.4–6.0	18.5–24.5	20.3–21.7	0.51–0.69	6.7–8.7	0.74–1.15	0.12–0.26
4	Sandy Clay	3.2–10.4	2.5–3.3	19.0–32.4	19.6–20.7	0.59–0.82	10.5–16.9	0.05–1.11	0.13–0.29
5	Sand	–	18.0–38.0	–					

TABLE 2. Test and Computed Results

Buildings or Structures	Depth of Pile Point in m	Sounding Resistance, q_c, in MPa				Number of Experiments	Point Bearing Capacity in kN	Skin Friction in kN	Ultimate Bearing Capacity, in kN
		Mucky Soil	Sandy Silt	Sandy Loam	Sandy Clay				
Boiler	16.5	0.6	1.7	5.7	3.3	74	450	1170	1620
Chimney	18.5	0.5	1.8	4.4	3.0	11	370	1280	1650
Coal Silo	18.0	0.6	1.7	6.0	3.2	14	450	1250	1700
Cooling Tower	16.5	0.5	1.9	5.6	3.1	17	340	1080	1420
Ash Handling	18.0	0.7	1.7	5.2	2.6	18	410	1210	1620
(Loading Test)	16.3	0.6	1.0	7.2	3.5	1	490	1150	1640

TABLE 3. Correction Factor α_i

Sounding Resistance q_c, in MPa	α_i
< 1	> 1.1
1 - 2	1.1- 0.8
2 - 5	0.8- 0.6
5 - 10	0.6- 0.4
> 10	< 0.4

TABLE 4. Correction Factor β_{si}

Skin Friction f_{si}, in MPa	β_{si}
< 0.02	> 1.5
0.02 - 0.04	1.5 - 1.0
0.04 - 0.10	1.0 - 0.5
0.1 - 0.25	0.5- 0.4
> 0.25	< 0.4

LOAD TEST OF PILE CAPACITY FOR INCLINED PILE

During construction of the project it was found that among 1200 piles of the boiler foundation, the piles with deviation from vertical less than 3 degrees accounted for 80%, those from 3 to 7 degrees accounted for 15.5%, those from 7 to 9 degrees accounted for 4.0%, and those about 10 degrees accounted for 0.5%. In order to determine the decrease of pile capacity due to inclination of the pile, static load tests were carried out for the selected four piles. The results are shown in Fig.2, Fig.3 and Fig.4.

a. The deviation of 3 degree from vertical

The results for the concrete pile No.1 are shown in *Fig.2,Fig.3 and Fig.4. When the load* was increased to 800 kN, the vertical settlement and the horizontal displacement of pile cap were small, but under the load of 1600 kN, the vertical settlement reached 21.5 mm and *the horizontal displacement 6 mm. From these* results the requirements of the design were met.

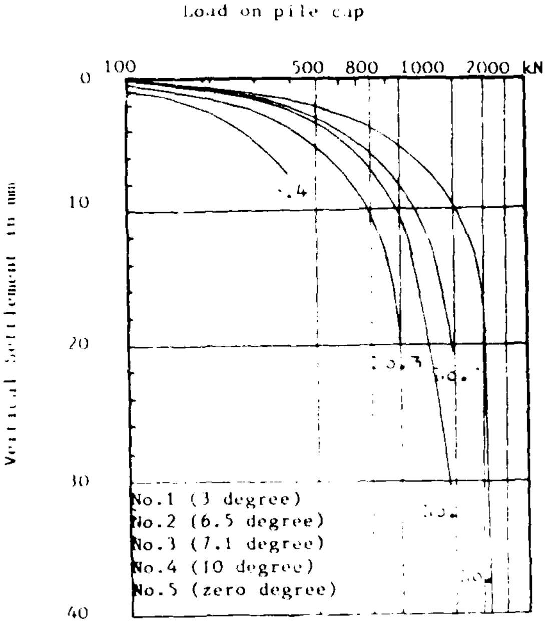

Fig.2. Load - Settlement Curves of Piles

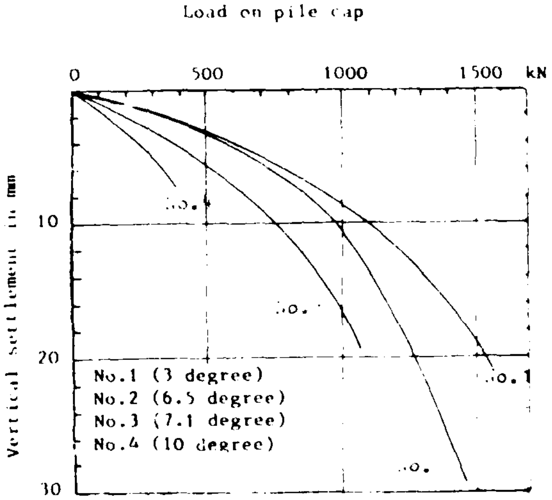

Fig.3. Load - Settlement Curve of Piles

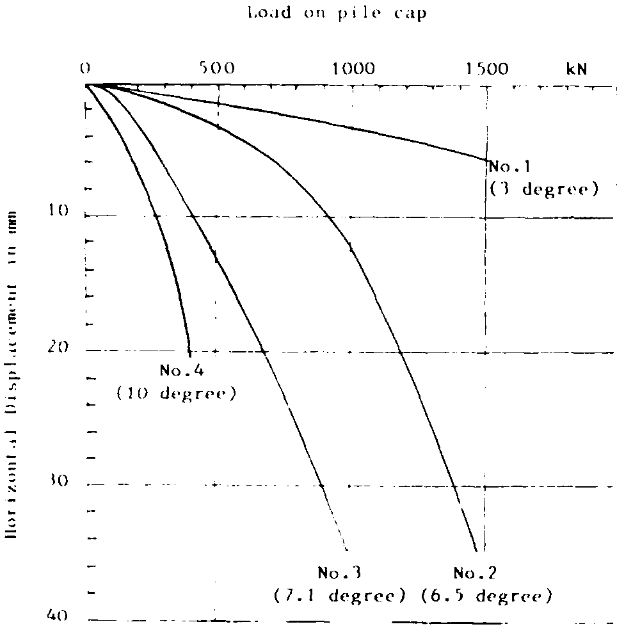

Fig.4. Load - Horizontal Displacement Curve of Piles

b.The deviation of 6.5 degree from vertical

See the concrete pile No. 2 in Fig.2, Fig.3 and Fig.4 . Under the load of 800 kN, the vertical settlement and horizontal displacement of pile cap were small, but under the load of 1500 kN the vertical settlement and horizontal displacement increase obviously. Compared with the ultimate bearing capacity determined for the vertical pile, the pile capacity decreased by about 10%.

c. The deviation of 7.1 degree from vertical

Under the load of about 1100 kN the vertical settlement of the concrete pile No.2 reached 19.3 mm and the horizontaldisplacement reached as large as 41.7 mm. Compared with the ultimate bearing capacity determined of the vertical pile, the pile capacity decreased by about 30%.

d. The deviation of 10 degree from vertical

For the concrete pile No.4, when the load was about 400 kN the vertical settlement was only 6.8 mm, but the horizontal displacement reached 20.2 mm. Then the test was stopped and the capacity of the pile No.4 decreased by about 80%.

CONCLUSIONS

The following conclusions were obtained from the static load tests. For the piles with deviation less than 3 degree from vertical, the requirements of the design were met. The deviation of 6.5 to 7.1 degree from vertical decreased the capacity be about 10 - 30%. The deviation of 10 degree from vertical decreased the capacity by about 80%.

The results of static load test prove up to the hilt that static cone penetration tests could be used successfully to select the bearing stratum for piles and to determine the length and the cross section area of the square piles and the ultimate bearing capacity of pile.

ACKNOWLEDGMENTS

The Static Loading Test was performed by the Navigational Engineering Investigation Institute, the Ministry of Communications of China.

REFERENCE

XIE Sheng-sun (1984): "Application of Static Cone Penetration Testing in Pile Foundation Engineering", Proc. Selected Papers of the Second Geotechnical Investigation and Surveying Symposium Sponsored by the Commission of Geotechnical Investigation and Surveying, the Architectural Society of China, pp.138-144, in Chinese.

Proceedings: Second International Conference on Case Histories in Geotechnical Engineering, June 1-5, 1988, St. Louis, Mo., Paper No. 6.39

Stress Analysis of Gravity Dam Founded on Rock Mass Having Horizontal Seam (A Case Study of Bargi Dam in Madhya Pradesh, India)

J.K. Jain
Assistant Professor of Applied Mechanics, Maulana Azad College of Technology, Bhopal, India

R.K. Khare
M. Tech. Student of Applied Mechanics, Maulana Azad College of Technology, Bhopal, India

SYNOPSIS: Under certain situations where horizontal seams of weaker material are detected below a depth of relatively competent rock and if it is decided to found the base of the dam on the rock below weak seam, the current practice of extending the triangular profile right down to base proves to be uneconomical both in terms of cost of excavation and quantity of concrete. In such situations for realistic assessments it becomes imperative to study the effect of foundation block having seam, on the behaviour of entire dam structure. With a view to assist the design of such dams, results of plane strain elastic finite element stress analysis for a typical Bargi dam in Madhya Pradesh, India, where a horizontal seam of weaker material expected in the foundation block are presented in this paper considering gravity load hydrostatic pressure.

INTRODUCTION

Conventional design of gravity dams is based on the assumption that a gravity dam acts like a rigid triangular cantilever resting on the foundation and held in equilibrium under its own weight and the reservoir loading. The uplift forces are also taken into accounts. The distribution of vertical reaction at the base being assumed to be linear, the maximum stresses occur at the toe of the dam under reservoir full conditions. In some of the dams a situation often arises when seams of weaker material are detected at some depth below the dam base. If it is decided to excavate this soft rock and take base of the dam to the sound rock below weak seam, a vital question arises whether the base of the dam has to be extended. Many designers insists on increasing the base width so that a triangular profile is maintained. However, this procedure which leads to increase in excavation is not only uneconomical but at times also hazardous if further excavation tends to undermine valley slope with consequent possibility of slides.

Such a situation arises in many dams constructed in hilly areas. In these cases, it becomes imperative to consider the foundation block consisting of strong rock mass having seam of weaker material. Thus the analysis shall cater the effect of composite foundation block on the behaviour of entire dam structure. From the geological investigations this type of situation is also assessed in case of Bargi dam in Madhya Pradesh, India, where a horizontal seam of relatively weaker material is expected at a competent depth below the foundation level of the dam. This gravity dam is founded on strong basaltic rock. The present study deals with stress analysis of this dam using plane strain elastic finite element technique considering gravity load and hydrostatic pressure.

DETAILS OF PROBLEM

The 5380 metre long Bargi dam (1983) is constructed across the river Narmada in Vindhya mountain ranges of state of Madhya Pradesh, India. The 69 metre high and 870 metre long masonry section of dam is constructed betweeen two earthen sections of total 4510 metre length. The masonry section has 386 metre long and 49.5 metre high spillway portion equiped with twenty one radial gates of 13.7 m x 15.25 m size. The area around dam site possess dense, dark basaltic rock varying from 10 metre to 30 metre in depth. A thin layer of tuffaceous clay of about 0.5 m thickness is assessed at about 10 to 15 metre below the foundation level of the dam. The salient features of the non-overflow and overflow sections of the dam are shown in figures 1 and 2.

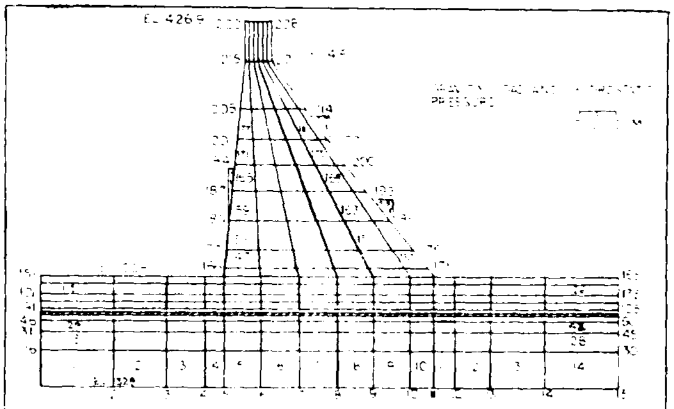

FIG. DETAILS AND DISCRETISATION OF NON OVERFLOW SECTION OF BARGI DAM

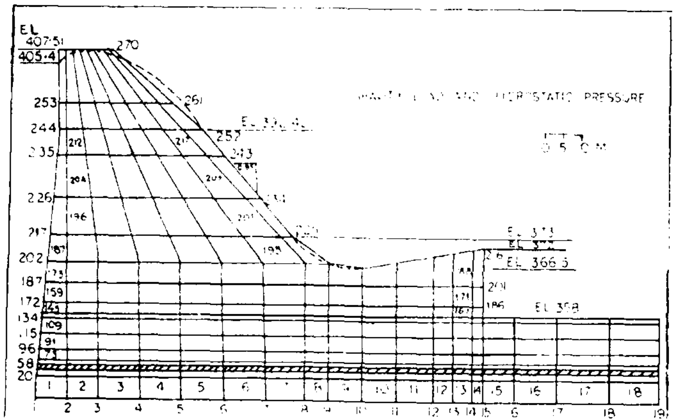

FIG 2 DETAILS AND DISCRETISATION OF OVERFLOW SECTION OF BARGI DAM

METHOD OF ANALYSIS

Though there are several methods of analysis of such class of problems but the finite element method possesses certain characterstics that takes advantage of special facilities offered by high speed computers. In particular the method can be systematically programmed to accomodate such complex and difficult problems as nonhomogeneous materials, nonlinear stress strain behaviour, arbitrary loadings and complicated boundary conditions. Thus for the analysis of such problems the finite element method proves to be a valuable technique.

In the present study the stress analysis has been carried out for both non-overflow and overflow sections by discretising them into two dimensional four nodal quadrilateral elements. In case of Plain strain analysis,each node will have two degrees of freedom thus total eight unknown deflections per node are to be determined. Hence the displacement functions are to be chosen with eight coefficients as

$$U = \alpha_1 + \alpha_2 X + \alpha_3 XY + \alpha_4 Y \qquad (1)$$

$$V = \alpha_5 + \alpha_6 X + \alpha_7 XY + \alpha_8 Y \qquad (2)$$

The finite element method principally involves the determination of stiffness of each element and then over all stiffness of the continuum for yielding unknown deformations. Thus the stiffness determination plays significant role in this method. In the present case the stiffness of each element [Ke] is derived using the displacement coefficients given in equation (1) and (2) by conventional energy approach as

$$[Ke] = \int_V [B]^T \; [D] \; [B] \, dvol. \qquad (3)$$

where [B] represents matrix of coefficients relating strain and displacements

and [D] represents the elasticity matrix interms of modulus of elasticity E and poisson's ratio and has the form

$$[D] = \frac{E(1-\nu)}{(1-\nu)(1-2\nu)} \begin{bmatrix} 1 & \frac{\nu}{(1-\nu)} & 0 \\ \frac{\nu}{(1-\nu)} & 1 & 0 \\ 0 & 0 & \frac{(1-2\nu)}{2(1-\nu)} \end{bmatrix} \qquad (4)$$

The computation algorithm suggested by Desai (1977) is used to calculate [B],[D] and subsequently the element stiffness matrix [Ke] for given material properties, applied forces and boundary conditions. The overall stiffness of the structure is assembled which yields the nodal displacements. Stresses at the centroidal points of each element are calculated by using these nobal displacements.

Discretisation

The two masonry sections of Bargi dam are analysed for assessed horizontal seam of 50 cm thickness, 10 metre below the foundation level of the dam. The non-overflow section has been discretised into 234 four nodal quadrilateral elements while the overflow section has 194 elements with 270 and 228 nodes respectively. Smaller elements near the seam are considered for assessing the behaviour of seam. The discretisation of non-overflow and overflow sections are also shown in figures 1 and 2.

Loads

Dam weight i.e. gravity load and water pressure in full reservoir condition are considered in stress analysis on dam. The uplift pressure is duly accounted by readjusting the gravity load. While analysing the overflow section, an expected vertical crack at the upstream heel is also considered up to the seam level for representation of ideal situation.

Material Properties

As suggested by Pant (1980), the material properties of the masonry and hard rock mass on which dam is founded are assumed to be same. The values of various material constants for rock and seam material are taken as

	Masonry/Rock	Seam Material
Young's modulus	2.1×10^6 t/m^2	2.8×10^5 t/m^2
Poisson's ratio	0.2	0.15
Unit weight	2.3 t/m3	1.65 t/m3

Boundary Conditions

In conventional design procedures the base of the dam is assumed fixed i.e. the displacements in the two

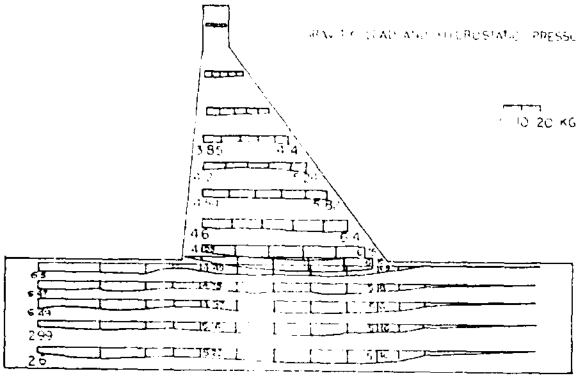
GRAVITY LOAD AND HYDROSTATIC PRESSURE
0 10 20 KG/CM^2
3.85
4.6
6.3
5.37
6.44
2.99
2.6

FIG 3 DISTRIBUTION OF NORMAL STRESSES IN NON-OVERFLOW SECTION
(FOUNDATION WITHOUT SEAM)

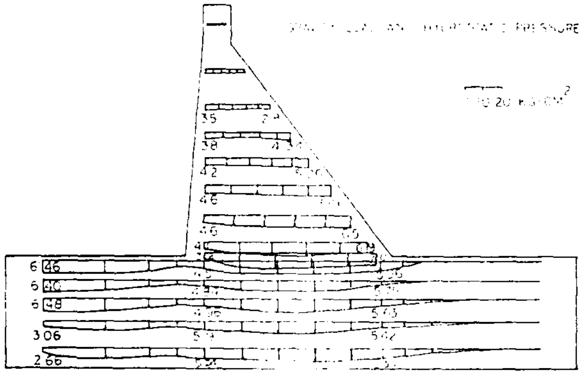
GRAVITY LOAD AND HYDROSTATIC PRESSURE
0 10 20 KG/CM^2
3.5
3.8
4.2
4.6
6.46
6.40
6.48
3.06
2.66
5.63
5.62

FIG 4 DISTRIBUTION OF NORMAL STRESSES IN NON OVERFLOW SECTION
(FOUNDATION WITH SEAM)

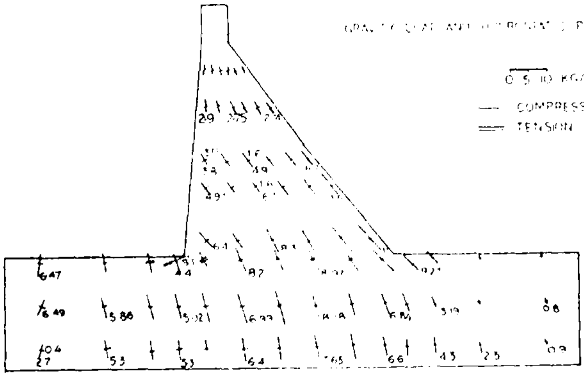
GRAVITY LOAD AND HYDROSTATIC PRESSURE
0 5 10 KG/CM^2
COMPRESSION
TENSION
2.9
6.47
6.49
5.86
5.02
6.33
0.8
0.4
2.7
5.3
5.3
6.4
6.5
6.6
4.3
2.5
0.9

FIG 5 DISTRIBUTION OF PRINCIPAL STRESSES IN NON OVERFLOW SECTION
(FOUNDATION WITH SEAM)

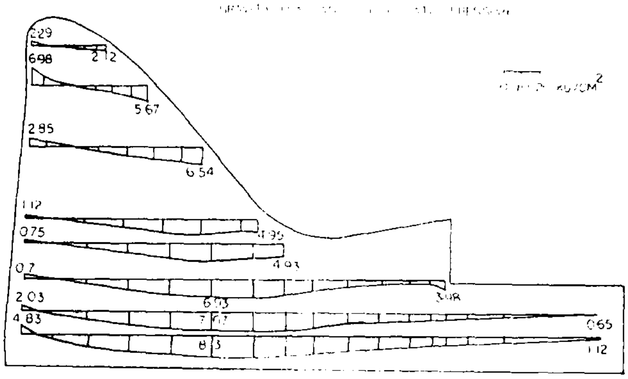
GRAVITY LOAD AND HYDROSTATIC PRESSURE
KG/CM^2
2.29
6.98
2.12
5.67
2.85
6.54
1.12
0.75
1.95
4.03
0.7
2.03
6.93
3.98
4.83
7.07
0.65
8.3
1.12

FIG 6 DISTRIBUTION OF NORMAL STRESSES IN OVERFLOW SECTION
(FOUNDATION WITH SEAM)

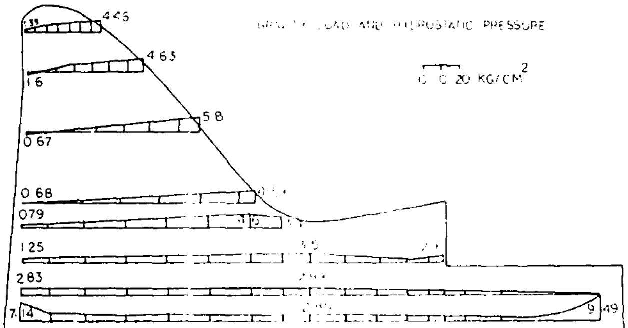
GRAVITY LOAD AND HYDROSTATIC PRESSURE
0 10 20 KG/CM^2
4.46
4.63
1.6
5.8
0.67
0.68
0.79
1.25
2.83
7.14
9.49

FIG 7 DISTRIBUTION OF SHEAR STRESSES IN OVERFLOW SECTION
(FOUNDATION WITH SEAM)

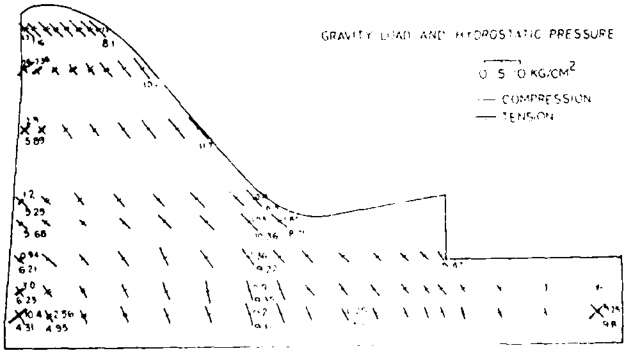
GRAVITY LOAD AND HYDROSTATIC PRESSURE
0 5 10 KG/CM^2
COMPRESSION
TENSION
8.1
5.89
3.25
3.68
6.21
6.25
4.31
4.95
2.56
10.36

FIG 8 DISTRIBUTION OF PRINCIPAL STRESSES IN OVERFLOW SECTION (FOUNDATION WITH SEAM)

directions are assumed to be zero. But practically complete fixity at the base can not be achieved and hence in the present analysis the base above the seam level is assumed flexible and below as fixed till 30 metre depth. The fixity is also assumed at 50 metre up and down-stream lengths of the base.

RESULT AND DISCUSSIONS

Though the present study is mainly focused towards studying the behaviour of gravity dam founded on hard rock mass with horizontal seam of weaker material in the foundation block, it also depicts the behaviour and stress variations of gravity dams in general. Apart from the consideration of gravity load and hydrostastic pressure, the analysis has also been done for extreme condition of empty reservoir, the chances of which are very remote. The normal vertical stresses, shear stresses and consequently the two principal stresses are calculated at centroidal points of various elements and some typical results are shown in figures 3 to 8 whereas, detailed results are discussed by Khare (1987) in his M.Tech. Thesis.

Upon studying various stress distributions, following points are observed:

1. In the analysis of non-overflow section with gravity load only, it is observed that the stress distribution in the dam at higher levels is linear but it becomes nonlinear near the interface of the masonry base and the rock. The vertical stress near the heel reaches as high a value as 14.15 Kg/cm^2 when analysed without seam and 14,32 kg/cm^2 whem analysed with seam. It is also seen that the distributions are nearly the same, except few local changes due to provision of seam. Similarly the effect of seam in case of shear and principal stresses is also negligible. The shear stress touches the peak value of 5.0 kg/cm^2 whereas, the major principal stress reaches the value of 15.4 kg/cm2 .

2. In analysing the non-overflow section with gravity load and hydrostatic pressure, it is observed that the maximum values of vertical stress and principal stress are reduced by about 50% and 20% respectively whereas, the maximum shear stress is increased by about 10%, indicating negligible variations due to provision of seam.

3. While analysising the overflow section for gravity load and hydrostatic pressure, the higher values of normal stresses are observed along the seam with maximum value to the tune of 8.3 kg/cm^2 . The maximum shear stress value of 9.5 kg/cm^2 at toe and some tension at the heel section is also reported which can be easily taken care of.

CONCLUSIONS

Based on the observations made in the stress analysis of Bagri dam following conclusions can clearly be drawn:

1. The effect of 50 cm. thick seam of tuffaceous material 10 metre below the foundation level of the dam and sandwiched between two layers of basaltic rock is negligible on the behaviour of the entire dam structure except development of few higher values of shear stresses at toe and tensions at the heel section which are generally taken care by provision of heavy reinforcement and shear keys.

2. The finite element method could be successfully used in solving such difficult design problems which are not easily amenable to conventional methods of analysis.

ACKNOWLEDEMENT

The authors are grateful to Shri J.K.Tiwari Deputy Director, Bureau of Design of Hydel Irrigation Projects, Irrigation Department, Govt. of Madhya Pradesh, Bhopal, for providing necessary information and rendering help time to time in preparation of this research project. Thanks are also due to Shri O.N. Thaper, Director, Bureau of Design of Hydel Irrigation Projects, Irrigation Department, Govt. of Madhya Pradesh, Bhopal, for his valuable suggestions.

REFERENCES

Bargi Multipurpose Project Head Works (1983), Vol. 1 and 3, Irrigation Department, Govt. of Madhya Pradesh, Bhopal.

Desai, C.S. and J.F. Abel (1977), Introduction to Finite Element Method, East West Publication, New Delhi.

Khare, R.K. (1987), Some Design Aspects of Gravity Dam (An Analysis by Finite Element Method), M.Tech. Thesis, Bhopal University, Bhopal.

Pant, B., D.K. Vaid, B. Thomas and S.K. Choudhary (1978), An Innovation in Gravity Dam Profile to Suit Local Foundation Conditions, Proceedings of 47th R and D Session of Central Bureau of Irrigation and Power, India.

Pant, B. and D.K. Vaid (1980), Some Aspects of Analysis and Design of Gravity Dam Founded on Rock Ridge, Proceedings of 50th R and D Session of Bureau of Irrigation and Power,

Proceedings: Second International Conference on Case Histories in Geotechnical Engineering, June 1-5, 1988, St. Louis, Mo., Paper No. 6.42

A Foundation Failure in Philadelphia

W.B. Fergusson
Associate Professor of Civil Engineering, Villanova University,
Villanova, Pennsylvania

E.F. Glynn
Assistant Professor of Civil Engineering, Villanova University,
Villanova, Pennsylvania

SYNOPSIS: The foundation failure of the 22 story, steel framed, federal courthouse in Philadelphia occurred because of an inadequate geotechnical assessment of a complex geological condition. The founding elevations for caissons were improperly determined on materials that could not sustain the design load. This condition was further complicated by the presence of groundwater and poor concrete construction practices. These conditions resulted in an extensive and costly remedial measures which included a grouting program and the replacement of 14 faulty caissons.

INTRODUCTION

This paper examines the foundation problems that developed during the construction of the James A. Byrne Federal Courthouse, a 22-story steel framed building in center city Philadelphia. The courthouse and accompanying federal office building occupy a 650 ft by 375 ft block between Sixth and Seventh Streets and bounded by Arch Street on the north and Market Street on the south.

The courthouse tower rises above a 240 ft by 270 ft 4-story podium on the southern portion of the block. The 10-story concrete office building occupies the northern portion of the block. The two structures share a common basement with an area of 320 ft by 630 ft at an elevation (above mean sea level) of about 14.0. The basement is approximately 15 ft below street level.

Both of these structures are supported by belled caissons. In particular, the courthouse tower is supported by 46 caissons which carry column loads ranging from 1200 tons to 2300 tons. The caissons were to be seated on sound bedrock (mica schist) with a bearing pressure of 40 TSF (tons per square foot). Lightly loaded columns on the periphery of the structure were to be supported on caissons with 8 TSF bearing pressures.

The original foundation report issued in 1965 recommended that steel H-piles be used to support the building. Caissons (and pressure injected footings) were listed as alternative foundations in the bid documents for subsurface work. The proposed founding grades for the caissons were based on limited core recovery data; however, the specifications detailed a procedure for verifying the adequacy of the founding material. In fact, the 40 TSF caissons were all founded at higher elevations than the proposed grades while the 8 TSF caissons were founded at lower elevations.

Settlement observations on 26 columns began in July 1970 when the first column sections were erected. Thirteen more columns were included in the program once the structural framing was completed in April, 1973. Readings on the remaining 7 columns began in January, 1974.

By late July, 1974 ten of the columns had settled at least 0.50 inches including one at 2.42 inches and another at 1.07 inches. Some cracking had occurred in the building and the structural design firm was concerned about secondary stresses developing from differential settlements.

The foundation required extensive repairs. The remedial measures, included the construction of replacement caissons, the grouting of caissons to repair defective concrete and underpinning caissons through grouting. The cost of the repairs (including damages) approached 6 million dollars (LePatner and Johnson, 1982).

SUBSURFACE CONDITIONS

Wissahickon Formation

The bedrock formation beneath the city is the Wissahickon Formation of Cambrian and Ordovician Age. The bedrock is a complex of schist and gneiss locally crosscut by granitic bodies. The schists are mica rich and are strongly foliated and fissile. Locally the schists are quartz and feldspar rich and are referred to as the "Wissahickon Gneiss" - a coarser grained rock, low in mica and thus less shistose and fissile than the typical mica-rich schists.

The Wissahickon Formation is characterized by extremely variable physical characteristics dependent upon the orientation of the steeply dipping rock beds which are crosscut by closely spaced, steeply dipping and open joints. This geometrical complexity is further complicated by the degree and nature of the weathering of the upper surface of the Wissahickon Formation. Unweathered sound Wissahickon may have an unconfined compressive strength of 200 TSF whereas highly weathered soft Wissahickon has a strength of 10 TSF or less.

The distinction between sound and unsound rock appears to have been originally based on the percentage of rock core recovered during drilling; sound rock had an average core recovery of over 90% while unsound rock ranged between 0 and 89% recovery. The borings were taken prior to the general use of rock quality designation (RQD).

This upper weathered surface has a secondary porosity and permeability (ranging up to 3 ft per day) through the weathered open joints and rock cleavage. This forms a groundwater reservoir capable of yielding a median flow of 20 gallons per minute (GPM) (**Geyer and Wilshusen**, 1982).

The surface of the Wissahickon Formation at the site lies at elevation between -62 and -83, the average elevation is -70. This upper rock surface has a tendency to disintegrate when exposed to moisture over a short period of time.

The Wissahickon Formation grades upward from sound rock, to slightly weathered medium-hard rock, to highly weathered soft rock into entirely decomposed rock (saprolite).

Wissahickon Formation - Saprolite

Overlying the severely weathered and eroded rock surface of the Wissahickon Formation is a layer of saprolite, usually referred to as "decomposed mica schist." The saprolite was formed in place by severe chemical weathering on the exposed Wissahickon Formation surface both prior to (by circulating groundwater) and after the deposition of the overlying Cretaceous rocks.

The saprolite beneath the site is a soft, friable, silty, sandy, thoroughly decomposed mica schist characterized by the preservation of the geologic structures and texture of the unweathered Wissahickon Formation. The saprolite beneath center city Philadelphia ranges in thickness between <10 and 70 ft. The saprolite at this site is encountered at an average elevation of -31 and ranges in thickness between 20 and 65 ft with an average of 40 ft.

The standard penetration resistance of the saprolite averages 125 blows per foot. The saprolite is less dense and more moist than the parent rock. The average saprolite moisture content is 17.5%, with a dry density of 115 PCF (pounds per cubic foot). Sound mica schist has a moisture content of 1.5%, and a dry density of 165 PCF.

Potomac-Raritan-Magothy Sequence

The Wissahickon Formation and its overlying saprolite are covered unconformably by the unconsolidated alluvial deposits of the Potomac-Raritan-Magothy rock sequence of Cretaceous Age. These stream channel and flood plain deposits consist of interbedded clays, silts, sands and gravels. At the site this sequence is found beneath the southern half of the site (beneath the courthouse) where it ranges in thickness between 4 and 17 ft, with its upper surface between -20 and -33 in elevation. The deposit consists of a lower dense to very dense gravelly sand bed (with an average standard penetration resistance of 123 blows per foot) and an upper medium dense silty sand bed. The Potomac-Raritan-Magothy sands and gravels form artesian aquifers beneath center city. The yield of this aquifer in the vicinity of the courthouse seldom exceeds 400 GPM (Greenman, et al., 1961).

Trenton Gravel

The surface of downtown Philadelphia is formed by the Trenton Gravel which completely masks the underlying alluvial deposits, saprolite and bedrock. The Trenton Gravel is composed of highly weathered gray to brown dense gravelly sands and sandy gravels with interbeds of cross bedded loose sand and silt and occasional boulders. These beds attain an average thickness of approximately 30 ft at the site.

The porosity and permeability of the Trenton Gravel deposits are both very high and may yield groundwater at rates over 1000 GPM. The water table lies within these deposits between elevations of -2 and -10.

FOUNDATION CONDITIONS

Construction Procedures

The 40 TSF caissons had shaft diameters ranging from 30 inches to 90 inches. The caissons had 60° bells so that the diameter of the bearing area ranged from 36 inches to 120 inches. The caissons were supposed to have permanent steel liners extending from the top of the bell to the top of the shaft. In many cases the liner could not be advanced to its design depth and ended as much as 20 ft above the top of the bell. The design strength of the concrete was 4000 pounds per square inch. The concrete was poured through a tremie pipe so that the free fall was limited to 10 ft. Water inflow was controlled by pumps until concrete placement. The CE noted that during the concrete placement some caissons had water rising to the top of, and flowing out of, the concrete. The caissons were essentially unreinforced - 6 ft long cages were used to tie the shafts to the caps.

Settlement

Early in 1973 engineers noted that many. columns in the courthouse were settling. By 1974 settlement measurements ranged from 0.09 to 2.42 inches.

The caisson (G-9) beneath the column that had subsided 2.42 inches was jacked up and shimmed with steel plates while the surrounding rock around the caisson was grouted.

Susbsequent studies involved the drilling of 112 test borings 39 borings adjacent to the caissons, 30 borings in the center of each four column bay, and 43 borings through the caissons. These test borings indicated that the caissons were poorly constructed and not founded on sound rock (Table I).

TABLE I. Material Beneath Caissons

MATERIAL FOUNDED ON	NUMBER OF CAISSONS
Saprolite to soft rock	31
Soft to medium hard rock	15
Sound rock	0

The caisson concrete was found to contain many voids and water bubbles and in rather poor general condition. Table II summarizes the concrete defects found in borings cored through 38 of the courthouse caissons.

TABLE II. Physical Condition of Caissons

CAISSON CONDITION		NUMBER OF CAISSONS
Honeycombed		8
Mortar segregated		4
Cold joints		2
Poor concrete		18
Aggregate segregation	(<6")	3
	(>6")	4
Mica schist inclusions		10
No recovery		7

A plan of action was outlined in early 1975 (Table III).

TABLE III. Caisson Remedial Action

RECOMMENDED ACTION	NUMBER OF CAISSONS COURTHOUSE
No action - except monitoring	14
Repair concrete	15
Relevel columns	10
Replace caissons	16

Fourteen of the courthouse caissons were replaced by the installation of a pair of 24 inch diameter caissons on either side (2 feet from) of the existing caisson into sound rock - an average of 18 ft below the original caisson. The length to diameter ratio of the rock sockets is over 10.

CONDITIONS AND CAUSES OF FAILURE

Specifications for the Determination of Caisson Elevations

The construction contract detailed a procedure for verifying the adequacy of the founding material for the 40 TSF caissons and the 8 TSF caissons. The courthouse/office complex had a total of 186 40 TSF and 124 8 TSF caissons. The direction of the testing, and approval of the tests was assigned to the Construction Engineer (CE).

Forty TSF Caissons: The use of 40 TSF bearing capacity for sound mica schist has become common practice in Philadelphia. The specifications at the site used an unconfined compressive strength of 160 TSF as the criterion for distinguishing sound rock. The specifications did not, however, require a laboratory test at each each caisson. They required the contractor to take rock samples from the bottom of 10 caissons selected by the CE. The samples could be either cored (2 inch diameter by 4 inch long) or cut (2 inch square by 4 inch long). The samples were to be properly oriented geologically and tested in unconfined compression. The strength of each sample was compared to the penetration rate of 1 inch diameter, 90 pound pneumatic drill at the same caisson. The purpose of the program was to establish a maximum penetration rate for 160 TSF material. The maximum penetration rate, i.e., minimum time to drill 5 ft, served as a criterion to evaluate the founding grade of caissons which had no strength tests.

Eight TSF Caissons: The specifications required that the founding stratum for 8 TSF caissons have a standard penetration resistance of at least 150 blows per foot. These caissons were generally founded in dense gravelly sands.

Test Borings

The difficulties at Caisson G-9 appear to define the entire problem and resulting failure. One of the original 47 test borings (38-B) was taken at the site of G-9. Although the G-9 was supposed to be founded on sound rock at an elevation of about -70 ft, boring 33-B was completed at an elevation of -40.9 ft. In fact only 17 of the original 47 test borings encountered rock. Therefore the caisson foundations had to be tested.

Twenty seven of the original borings were bottomed at depths of exactly 70, 71, or 71.5 ft - well above the rock and in two cases above the saprolite. The remainder of the borings were between 100 and 115 ft in depth - with two exceptions one to 97 and the other to 123 ft.

Two old test borings adjacent to the site are reported in the literature (Greenman, et. al., 1961) one to a depth of 71 ft at Sixth and Market the other to 72 ft at 5th and Market. Both report 'mica rock' at an elevation of -50 (actually saprolite). This may be the precedent for the depth of the borings.

The depths of the test borings, and the pattern of drill sites appear to be geotechnically illogical. An additional 112 test borings were necessary to correct the lack of information provided by the original borings.

Determination of Caisson Elevations

Obviously the cause of settlement of the courthouse was the failure to found the caissons on sound rock.

Admittedly the mica schist of the Wissahickon Formation is problematical because of the highly irregular contact between it and the overlying saprolite (from -62 to -82 elevation on the site). The very irregular vertical gradation in this 20 foot interval from completely weathered mica schist (saprolite) through varying degrees of rock weathering (high-moderate-slight) and rock durability (sound-hard- medium hard-soft) further complicates the problem.

The rock itself changes rapidly in geological character and hence in engineering character both vertically and laterally. An increase in quartz content in mica schists increases rock strength and durability - while an increase in mica decreases the rock strength and forms inclined weakness planes within the rock mass. This micaceous foliation constantly changes its orientation - changing the orientation of weakness planes and thus changing the rock strength and relative stiffness.

Many of these rock characteristics can be determined and evaluated by careful visual inspection of rock cores - particularly if the RQD is used in their evaluation. The RQD was not developed in 1965 when the original test borings were taken. The rock quality was roughly estimated by the percentage of core recovery. In general the higher the percentage of rock recovery and the longer and more intact the pieces of core recovered the higher the quality of the rock.

The system used at the courthouse to evaluate the soundness of rock by drilling time rates is theoretically useful. If the laboratory tests performed on the samples from the 10 selected caissons are accurate and representative of the rock mass as a whole and the rock mass is reasonably uniform and the drilling time rates are accurately measured the evaluation system is relatively useful. None of these premises are met.

Later legal investigations indicate that the laboratory tests were performed on 2 inch cubes rather than specimens 2 inch square 4 inches deep. This of course gave false readings of rock strength because as the aspect ratio (length/diameter) decreases the apparent compressive strength increases. Furthermore, it appears that very little attention if any was paid to the proper orientation of the foliation in the test samples. Construction records indicate that the penetration rates used to verify sound rock were remarkably similar - a rather interesting outcome considering the variability of the founding material (Table I).

Because the top weathered surface of the mica schist and the overlying saprolite slake rapidly when wet and because they lie beneath the water table and an artesian aquifer the presence of water in the caisson excavations probably caused serious deterioration of the mica schist. In fact the CE admitted there was difficulty keeping the excavations dry and that 166 of the caissons were filled with concrete before testing information was delivered to him. The basis for pouring the caissons was the drilling time rates. Additionally the caisson inspector only inspected about 25% of the caissons because he was busy conducting and recording the drilling time rates.

CONCLUSIONS

The original subsurface investigation appears not to have thoroughly tested or interpreted the geology and engineering characteristics beneath the site. The important factors that should have been verified were;

1. the presence, amount and affect of groundwater
2. the elevation of the top surface of sound rock.

The plan for establishing drilling time rates to determine the unconfined compressive strength to establish sound rock was not workable.

The slaking effect of groundwater on the soft, friable saprolite and highly weathered mica schist was not appreciated.

The caissons were poured hastily to avoid groundwater problems and in the process poor concrete conditions contributed to the settlement.

Decisions were not made on the basis of sound geotechnical information by persons with little or no geotechnical education or experience.

REFERENCES

Dames and Moore, (September, 1974), "Studies and Investigations of Existing Caisson Foundations and grouting and Soil Stabilization of Caisson Foundation G-9 Federal Courthouse and Office Building, Philadelphia, Pa.".

Dames and Moore, (May, 1975), "Report on Caisson Foundation Evaluations Federal Courthouse and Office Building, Philadelphia, Pa.".

Dames and Moore, (June, 1975), "Report on Subsurface and Bearing Capacity Characteristics Beneath Caissons Federal Courthouse and Office Building, Philadelphia, Pa.".

Dames and Moore, (November, 1975), "Report on Evaluation of Concrete Caisson Foundations Federal Courthouse and Office Building, Philadelphia, Pa.".

Geyer, A.L., Wilshusen, J.P. (1982), "Engineering Characteristics of the Rocks of Pennsylvania", Commonwealth of Pennsylvania, Bureau of Topographic and Geologic Survey, Harrisburg, Pa.

Greenman, D. W., Rima, D. R., Lockwood, W. N., Meisler, H., (1961), "Ground-Water Resources of the Coastal Plain Area of Southeastern Pennsylvania", Commonwealth of Pennsylvania, Bureau of Topographic and Geologic Survey, Harrisburg, Pa.

Koutsoftas, D.C. (1981), "Caissons Socketed in Sound Mica Schist", ASCE Journal of the Geotechnical Engineering Division, vol. 107, GT6.

LePatner, B.B., Johnson, S.M. (1982), "Structural and Foundation Failures: A Casebook for Architects, Engineers, and Lawyers", McGraw-Hill, New York, N.Y.

Proceedings: Second International Conference on Case Histories in Geotechnical Engineering, June 1-5, 1988, St. Louis, Mo., Paper No. 6.43

Ground Response to Sheet Pile Installation in Clay

Richard J. Finno
Asst. Prof. of Civil Engineering, Northwestern University, Evanston, Illinois

Steven M. Nerby
Graduate Student, Department of Civil Engineering, Northwestern University, Evanston, Illinois

Dimitrios K. Atmatzidis
Prof. of Civil Engineering, University of Patras, Greece

SYNOPSIS: The effects of sheet pile installation on an adjacent cohesive soil mass are described herein. Observations indicate that driving sheet pile caused pore pressures to double at some locations. These pore pressures extended further than reported in previous studies concerning driven piles. Initially pore pressures rapidly dropped, but dissipation slowed after this initial adjustment. Inclinometer and extensometer data indicate that the clay was laterally displaced up and away from the sheeting causing the ground surface to heave. The impact of this behavior on subsequent stress changes during excavation is discussed.

INTRODUCTION

The effects of sheet pile installation on an adjacent soil mass are not considered in either the design of braced excavations or predictions of wall movements and surface settlements. As a result, potential deleterious effects of high pore water pressures in cohesive soils on subsequent geotechnical construction are not considered. A literature search revealed scant data on measured ground response to sheet pile installation. However, data have been reported as single piles are driven into the ground.

Ground and bracing system response have been monitored during construction of a 40-ft-deep subway excavation through compressible clays in Chicago. As part of this monitoring program, vertical and horizontal displacements and pore water pressures were measured in adjacent soil as two rows of steel sheet piles were driven. This paper presents a summary of these observations. Because these responses occur prior to excavation and support of a braced cut, they alter the "initial" conditions that are commonly assumed when analyzing braced cut behavior. Possible effects of this prestressing of the soil adjacent to the cut on subsequent response are discussed.

SUBSURFACE CONDITIONS

The subsurface conditions at the test section location consists of 13 ft of rubble fill underlain by a 60-ft-thick sequence of saturated glacial clays, the consistency of which increases with depth from soft to very stiff and hard (Fig. 1). Beneath the clays a 5-ft-thick deposit of sand and gravel overlies limestone bedrock. The water table is located near the bottom of the rubble fill and a downward gradient of flow exists in the lower clays. Finno, et al. (1988) describe these subsurface conditions in more detail and present engineering characteristics of the clays. Note that the Blodgett and Deerfield tills make up the compressible Chicago clays commonly refered to in literature (Peck and Reed, 1954). The subway cut is made entirely within these soft to medium clays, while the sheet piles extend through the very stiff to hard Park Ridge till.

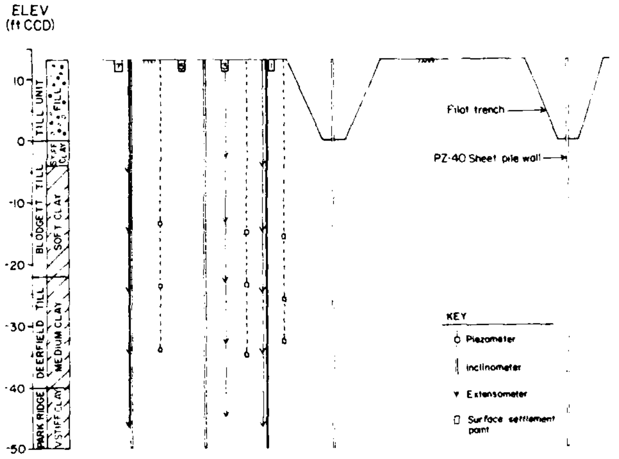

Fig. 1. Elevation at Test Section

CONSTRUCTION PROCEDURES

Two rows of sheet piles were driven to provide temporary support for the excavation (Fig. 1). Prior to driving each row of sheet piles, a 13-ft-deep pilot trench was excavated through the rubble fill because of the presence of large obstructions which would hinder pile driving operations. The construction sequence is summarized in Table 1. The PZ-40 sheet pile wall was installed in two passes. In the first pass along each wall, the contractor drove the sheeting to el.-28 ft Chicago City Datum (CCD); subsequently the contractor drove the sheeting to its design grade of el.-50 ft CCD.

Table 1. Construction Sequence

Day No.	Construction Activity at at Test Section
1	Excavate east pilot trench
3-4	Drive sheeting to el.-28 ft along east wall
7-8	Drive sheeting to el.-50 ft along east wall
15 and 16	Excavate west pilot trench
52 to 54	Drive sheeting to el.-28 ft along west wall
64 and 65	Vibrate and drive sheeting to el.-50 along west wall
101	Begin excavation at section

Notes: Elevations refer to ft Chicago City Datum. Day 1 was December 15, 1986.

INSTRUMENTATION

Ground instrumentation consists of (a) 3 primary instrument clusters placed on a line perpendicular to the sheeting; each cluster contains 3 piezometers at different depths in the clays, one 65-ft-deep slope inclinometer casing, and one 5-point, mechanical extensometer with hydraulic anchors at different depths in the clay; (b) 3 inclinometers and one 5-point extensometer offset from the primary line to provide redundancy in the data, and (c) a surface survey net consisting of 7 reference points (Fig. 2).

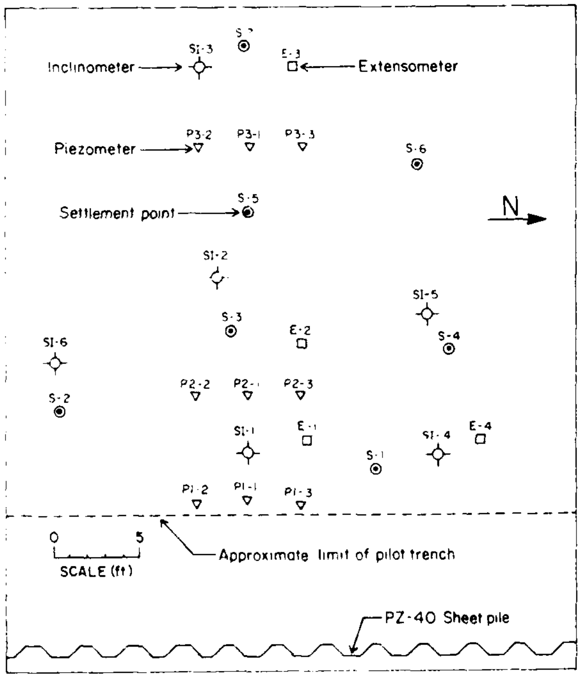

Fig. 2. Instrumentation Plan

Readings were collected during the two months prior to the start of construction at the test section; thus overall accuracy of the installed instrumentation was established. In tne period between instrument installation and excavation of the east pilot trench, three sets of SINCO Model 200B slope inclinometer data were obtained. Readings were obtained in orthogonal directions. The angle that the orientation of the inclinometer casing grooves made with a perpendicular line from the sheeting was measured; all data were corrected so that horizontal displacements, both perpendicular and parallel to the sheeting alignment, were obtained. These data indicated that the repeatability of the readings was approximately ± 0.05 in. Manufacturer's specifications indicate that the 200B indicator has a sensitivity of 1 part per thousand. Extensometer data were obtained with a micrometer that read to 0.001 in.; the accuracy of these data were limited to 0.12 in. by survey measurements of the elevation of the top of the reference plate. Manufacturer's specifications indicate that the triple-tube pneumatic piezometers, SINCO Model 514178, are accurate to within 0.30 ± .05 psi. Field tests prior to sheet pile driving indicate that repeatability of the readings was approximately ± 0.05 psi; response of each of these transducers was checked during field installation by comparing observed pressures with those calculated from the height of water in the borehole prior to sealing and backfilling each borehole.

RESULTS OF FIELD OBSERVATIONS

Based on observed response, driving operations along the east wall caused no significant soil deformations or pore pressure changes at the test section location. All significant observations resulted from driving the west wall. The general trends of the observed soil behavior wall are described in terms of displacements that occurred perpendicular to the sheet pile alignment (herein called transverse), displacements that occurred within a horizontal plane, pore pressures, and vertical displacements at both the ground surface and top of the clay strata.

Transverse displacements are shown in Fig. 3. These displacement vectors are plotted for construction days 54 and 66, that correspond to completion of the first and second pass, respectively, along the west side of the test section. The vectors consist of a combination of extensometer data and inclinometer data obtained at elevations of the extensometer points. Maximum incremental displacements were on the order of 0.5 in. Upon initial driving, soil at elevations above the bottom of the penetration displaced laterally and vertically as much as 0.4 in. After final seating of the sheet piles, the soil at lower elevations displaced away from the sheeting, but this time with a more marked horizontal component. A rather large inward component of movement was observed at shallow elevations near the sheeting. While the pattern of movements could be interpreted in terms of a flow around a penetrating object, part of the magnitude of these inward movements near the surface are thought to have been caused by an increase in temperature during this time. The temperature rise would have thawed the frozen rubble fill at the edges of the pilot trench; the fill was observed to be substantially weaker in the thawed state and movements toward the sheeting undoubtedly occurred in the fill as a result.

Note that the magnitude of the outward movements

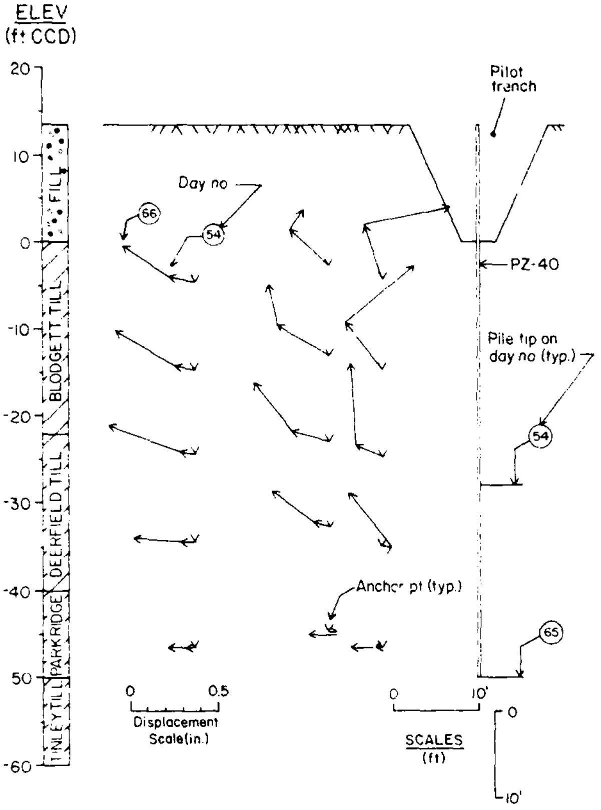
ELEV (ft CCD)
20
10
0
-10
-20
-30
-40
50
-60
FILL
BLODGETT TILL
DEERFIELD TILL
PARKRIDGE
TINLEY TILL
Pilot trench
Day no
66
54
PZ-40
Pile tip on day no (typ.)
54
65
Anchor pt (typ.)
0
0.5
Displacement Scale (in.)
0
10'
0
10'
SCALES (ft)

Fig. 3. Transverse Displacements During Driving

could have been expected. Within the saturated clays, an estimate of the lateral displacement can be made by assuming that a quantity of soil equal to the volume of the section must be displaced. The PZ-40 section displaces an equivalent of 1 in. of soil per foot of section. By assuming that equal amounts displace in each direction, 0.5 in. (13 mm) lateral movement can be expected.

Displacements in the horizontal plane at two elevations within the clay are shown in Fig. 4. Although the trend of the movements is essentially perpendicular to the sheeting, significant northward components of movements were recorded at the locations of inclinometers SI-1 and SI-5. These corresponded to the direction of the pile driving.

Pore pressures during pile driving operations are shown in Fig. 5. The leads to piezometers P1-1 and P1-2 were cut while excavating the west pilot trench. The remaining piezometers show that pore pressures rose rapidly in response to each pass of the sheet pile driving. The largest increases were recorded after the second pass was completed on day 65. After the peak values were observed immediately after driving, the pore pressures dissipated rapidly at first, then decreased at a slower rate.

Sheet pile driving caused time-dependent movements of the ground surface (Fig. 6). Movements at the ground surface were tracked with standard leveling equipment with an estimated accuracy of ± .12 in. To illustrate the relation among

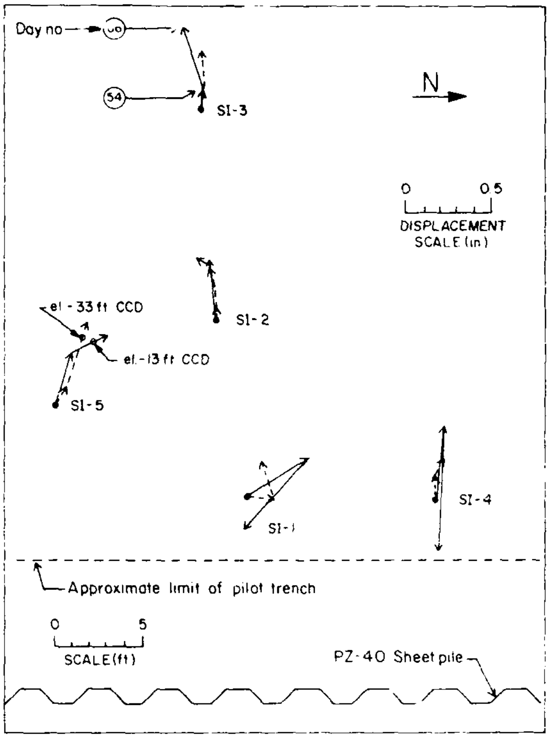
Day no
65
54
SI-3
N
0
0.5
DISPLACEMENT SCALE (in)
el -33 ft CCD
el. -13 ft CCD
SI-2
SI-5
SI-1
SI-4
Approximate limit of pilot trench
0
5
SCALE (ft)
PZ-40 Sheet pile

Fig. 4. Horizontal Displacements During Driving

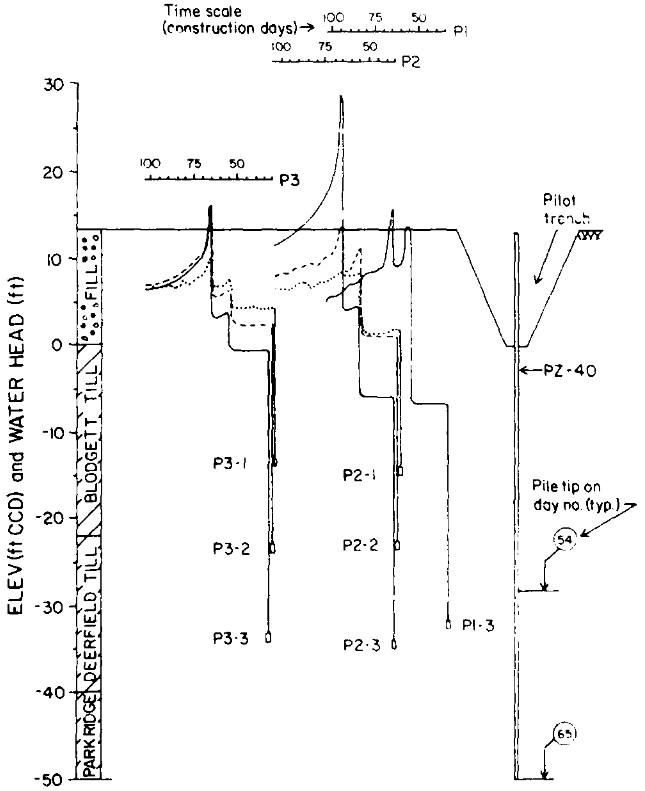

Fig. 5. Pore Pressures During Construction

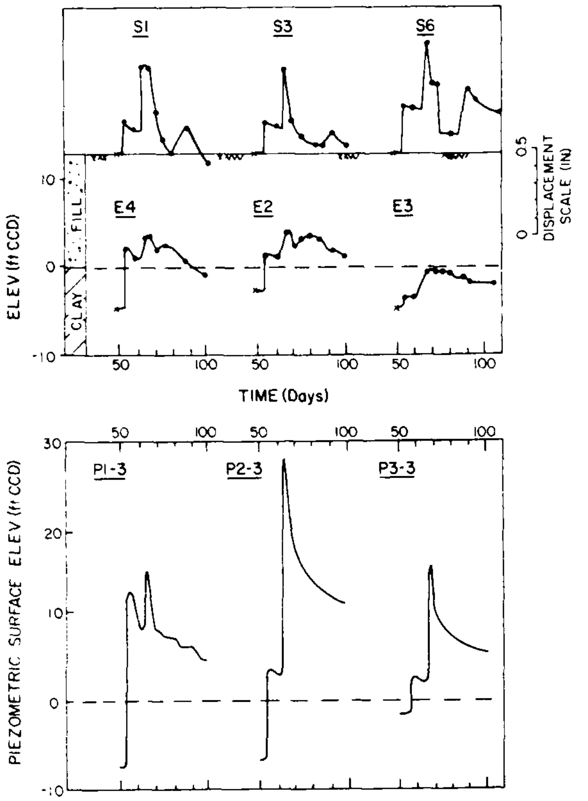

Fig. 6. Vertical Displacements During Construction

movements, pore pressures and pile driving, vertical displacements at the ground surface and the top of the clay and pore water pressures are plotted versus time for this construction period. The sudden increases in pore pressure correspond to sheet pile driving; the ground surface clearly heaved as a result of installing the sheeting. As pore pressures dissipate, consolidation occurs within the clay, and both the ground surface and top of the clay subsides.

DISCUSSION

The most striking features of the observed response were the pore pressures. Pore pressures during pile driving have been reported by several investigators (e.g., Lambe and Horn, 1965; Orrje and Broms, 1967; Hagerty and Garlinger, 1972; and Flaate, 1972). Their effects on subsequent pile response is well-documented. However, very limited data (i.e., Karlsrud, 1986) are available concerning pore pressures associated with sheetpile driving and their effects on subsequent excavation behavior.

Figure 7 shows the maximum ratios of excess pore pressure/effective overburden pressure plotted versus normalized distance from the sheet pile. Also shown is a band that reflects normalized excess pore pressures caused by driving single piles as reported by Hagerty and Garlinger (1972). The band reflects data from six reported case studies. Note that an equivalent diameter of 1.34 ft, equal to the depth of the PZ-40 section, was used to compute normalized distance. The data indicate that the extent of

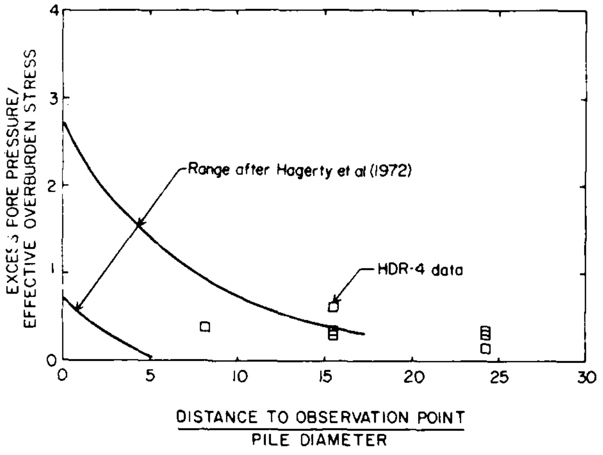

Fig. 7. Comparison Between Pore Pressures For Single Piles and HDR-4 Data

excess pore pressures can be larger when driving sheet piles than when installing piles. The pore pressures adjacent to the sheet piles could not be measured because of the presence of the pilot trench; however, the magnitudes are expected to follow the same trends as piles. The wider zone of influence for the sheet piles can perhaps be attributed to the differences caused by plane strain conditions associated with sheet piles and axisymmetric conditions associated with piles.

It should be emphasized that these pore pressures are associated with sheet pile driving and are not significantly affected by construction equipment loadings. This is clearly shown in Fig. 6. The transient stress increases caused by the cranes would not significantly stress the soil below the bottom of the rubble fill. In addition, the pore pressures generally were largest adjacent to the sheeting and decreased with distance from sheeting.

The effects of the sheet pile driving on subsequent response during construction can be evaluated by examining the postulated stress path for two soil elements adjacent the wall at the locations of piezometers P2-2 and P2-3 (Fig. 8). Refer to Fig. 5 for locations of P2-2 and P2-3. The stress paths were plotted assuming that sheet pile driving increases the total horizontal stress, while maintaining the vertical stress constant. Total stress changes were computed using an A parameter of 1.0 and the measured pore pressure values. This A value is based on preliminary results of K_0-consolidated, triaxial extension tests.

Stress conditions at 5 different times during construction are presented. After completion of the second pass on day 65, note that the effect of the operation is to preload the soil adjacent to the excavation. Shear stresses are reduced, and normal stresses subsequently increase as consol-idation occurs. These changes create a benefi-cial effect that ameliorates the effects of sub-sequent lateral stress reduction as excavation occurs. In this case, stresses are built into the system to counteract subsequent detrimental stress changes.

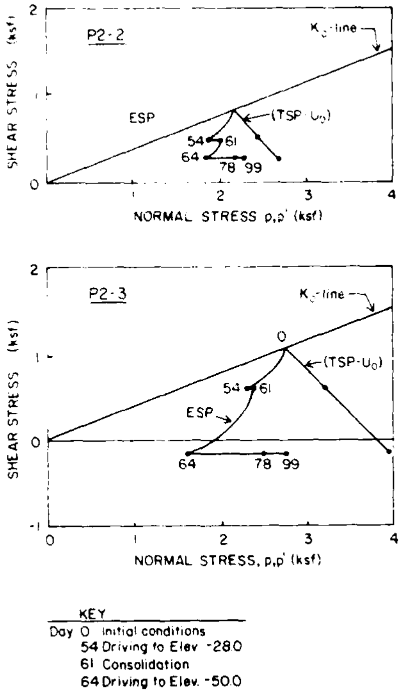

Fig. 8. Estimated Stress Paths During Construction

On the other hand, for soil located between the sheet pile walls below the excavated grade, these stress changes may create a detrimental effect. In this case, as excavation proceeds, vertical stress is reduced to failure. The amount of additional shear stress that can be sustained by the soil is less than that which would exist if pile driving had no effect. This would both reduce the available passive resistance that could be developed by an embedded sheet pile and decrease the amount of movement necessary to generate the full passive resistance.

It should be noted that these paths are based on rather simplified assumptions. A better approximation of the stress paths on both the active and passive sides of the sheeting would be developed on the basis of finite element simulations of the entire construction sequence. These studies will be undertaken in the near future.

CONCLUSIONS

Based on the observed performance data presented in this paper, the following conclusions can be drawn:

1. Driving sheet piles through saturated clay for temporary support of a braced excavation can lead to the development of soil movements away from the sheet piles on the same order of magnitude as the amount of soil displaced by the sheeting. These movements and the associated excess pore pressures are not generally considered in the analysis or design of such works.

2. The excess pore pressures generated by the sheet pile driving operation appear to be on the same order of magnitude as those associated with pile driving, but their lateral extent appears to be wider. This phenomenon may be caused by the difference between the plane strain conditions representative of a sheetpile wall and the axisymmetric conditions representative of piles.

3. The somewhat unexpected response of the soil to the sheet pile installation emphasizes the fact that the profession still can learn much from field observations derived from complete instrumentation schemes.

ACKNOWLEDGEMENTS

The authors wish to thank Messrs. Thomas Wagner and James Patterson of Kenny Construction Co. for their cooperation and efforts in keeping the test section instrumentation intact. Thatcher Engineering Company drove the sheeting under a subcontract to Kenny Construction Co. The care that they used when driving the sheet pile near the test section is much appreciated. Also special thanks are due Mr. Ted Maynard, Head of the Soils Section of the Dept. of Public Works of the City of Chicago for providing the inclinometer and piezometer readout devices and for his encouragement throughout the project. Messrs. Scott Perkins and Yori Sofrin of Northwestern University aided in the construction monitoring effort.

This material is based upon work supported by the National Science Foundation under Grant No. MSM-8796169.

REFERENCES

Finno, R. J., S. M. Nerby, and S. B. Perkins (1988), "Soil Parameters Implied by Braced Cut Observations," to be published in the Proceedings, Symposium on Soil Properties Evaluation from Centrifugal and Field Performance, ASCE, Nashville.

Flaate, K. (1972), "Effect of Pile Driving in Clays," Canadian Geotechnical Journal, vol. 9, no. 1, 81-88.

Hagerty, D. J., and J. E. Garlinger (1972), "Consolidation Effects Around Driven Piles," Proceedings, ASCE Specialty Conference on Performance of Earth and Earth-Supported Structures, Purdue University, vol. I, part II, 1207-1222.

Karlsrud, K. (1986), "Performance Monitoring of Deep Supported Excavations in Soft Clay," Fourth International Geotechnical Seminar, Field Instrumentation and In-Situ Measurements, Nanyang Technological Institute, Singapore, 187-202.

Lambe, T. W., and H. M. Horn (1965), "The Influence on an Adjacent Building of Pile Driving for the MIT Materials Center," Proceedings, VI International Conference on Soil Mechanics and Founation Engineering, vol. 2, 280-284.

Orrje, O., and B. B. Broms (1967), "Effects of Pile Driving on Soil Properties," Journal of the Soil Mechanics and Foundations Division, ASCE, vol. 93, no. SM5, part 1, 59-73.

Peck, R. B., and W. C. Reed (1954), "Engineering Properties of Chicago Subsoils," Engineering Experiment Station Bulletin no. 423, University of Illinois, 61 pp.

Proceedings: Second International Conference on Case Histories in Geotechnical Engineering, June 1-5, 1988, St. Louis, Mo., Paper No. 6.44

Full-Scale Load Test of Caisson on Chicago Hardpan

Stephen A. Bucher
Project Engineer, STS Consultants, Ltd., Northbrook, Illinois

Raymond J. Krizek
Professor and Chairman, Department of Civil Engineering,
Northwestern University, Evanston, Illinois

Dimitrios K. Atmatzidis
Professor, Department of Civil Engineering, University of Patras,
Patras, Greece

SYNOPSIS: The results of a full-scale load test on a belled caisson bearing on hardpan in the downtown Chicago area are presented herein and are discussed in terms of current design practice and the results of other pertinent full-scale tests and a small-scale model test. Current specifications for allowable bearing pressures are shown to be conservative, and previously established settlement limits required to mobilize side resistance are reconfirmed. The settlement measured during the test is in good agreement with that predicted by use of pressuremeter test data. The confinement of the bell in a hard clay layer appears to be beneficial in that it serves to limit the development of major cracking at the base.

INTRODUCTION

Drilled piers or caissons bearing on very dense glacial till (hardpan) are a common type of foundation for high rise structures in the Chicago area. The local building code specifies a maximum bearing pressure of 12 ksf, but higher pressures are allowed if adequate testing and supporting data are provided. As a result of accumulated experience and increased confidence in the use of in-situ testing, such as the pressuremeter test, design bearing pressures of 20 ksf to 25 ksf are now used commonly. Although full-scale caisson load tests can provide valuable information to validate or improve the bearing capacity and settlement theories used in design, actual load tests are rarely conducted because of the required high reaction loads and the associated expense and inconvenience. Results from two full-scale load tests on caissons in the Chicago area have been reported; one series of tests was conducted during the construction of the Chicago Union Station (D'Esposito, 1924), while the other was completed during foundation construction for the Cummings Biological Research Center at the University of Chicago (Holtz and Baker, 1972).

Presented and discussed herein is information obtained from a full-scale load test on a caisson bearing on hardpan in the downtown Chicago area. The caisson had a shaft diameter of 2.5 feet, a bell diameter of 6.33 feet, and a total length of 60.65 feet; it was instrumented with load cells and strain gauges and tested to a maximum load of 1100 tons, which approached the estimated ultimate bearing capacity. The anticipated performance of this caisson during the load test was determined on the basis of current design practice in terms of settlement, bearing capacity, and side resistance or skin friction. The observed performance of the caisson is presented and discussed both in terms of current design practice and in comparison with available results from full-scale tests in similar soils.

SOIL CONDITIONS

The subsurface conditions at the project site are representative of the typical downtown Chicago soil profile, which has been presented in detail by Bretz (1939) and Peck and Reed (1954). Surficial deposits of fill materials are typically encountered over layers of beach sands. Underlying these soils are glacial deposits (consisting of lacustrine clay and stratified clayey till sheets of varying strengths and water contents) of the Wisconsin Glacial era; these deposits vary with depth from soft to hard silty clays and extremely dense silt, sandy silt, or gravel zones overlying the bedrock.

At the site of the full-scale load test, soft to medium silty clays were encountered to an elevation of approximately -48 feet CCD (Chicago City Datum). Below these soils, very stiff to hard silty clays were encountered to an elevation of -63 CCD. Then, alternate layers of hard sandy and silty clay (hardpan) and extremely dense silt or sandy silt were encountered to the top of bedrock at elevation -105 CCD. Information about the typical subsurface profile and soil properties at the test site is presented in Figure 1. Pressuremeter tests were conducted between elevations -66 CCD and -81 CCD, and the values of the parameters obtained are summarized in Table 1. The soils tested exhibited pressuremeter parameter values that are comparable to a large number of available values for soils in the same general area of Chicago (Lucas and deBussy, 1976).

Table 1. Pressuremeter Parameters

Elevation(CCD) (feet)	Pressure (tsf)			Modulus E_d (tsf)
	Horizontal At Rest P_0	Creep P_f	Limit P_p	
-66.0 to -68.5	4.0	15	29	156
-68.5 to -71.0	4.0	10	20	111
-71.0 to -73.5	5.0	16	32	198
-73.5 to -76.0	4.5	20	40	297
-76.0 to -78.5	4.5	15	29	267
-78.5 to -81.0	8.0	-	-	1043

TEST CAISSON

The test caisson had a shaft diameter of 2.50 feet and a bell diameter of 6.33 feet; it was constructed by using the typical procedures employed for production caissons, although it was not part of the load-carrying grid of caissons for the new structure. The shaft was auger-drilled at a diameter slightly larger than designed to a

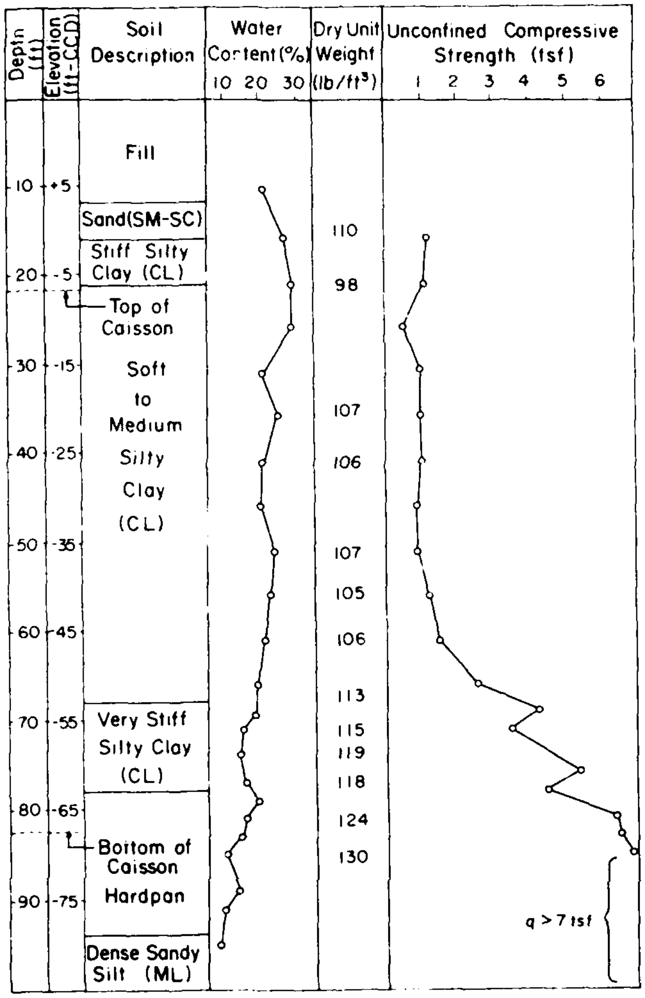

Figure 1. Soil Profile

depth of about 15 feet below existing grade, and a temporary steel casing was inserted through the fill and sand into the underlying silty clay. The shaft was then advanced by augering at the design diameter to a depth of 73 feet (-67.4 CCD), where a suitable hardpan layer was encountered.

The base of the shaft was enlarged at this level by means of a 60° belling bucket. The bell angle was then reduced to about 50° by hand excavation to obtain a geometry similar to that used by Reese and Farr (1980) so that results could be compared in terms of the development of cracks at the base of the bell. The thickness at the perimeter and at the center of the base pad of the bell was 1 foot and 2 feet, respectively. The dimensions of the test caisson, as measured in the field, are shown in Figure 2.

ANTICIPATED PERFORMANCE OF TEST CAISSON

The test caisson was designed to transfer load to the foundation soils primarily through end bearing, but some amount of side resistance or skin friction was also expected to develop. During testing, the top of the caisson was expected to settle by an amount equal to the sum of the elastic compression of the shaft and the settlement at the base. Accordingly, estimates of bearing capacity, skin friction, base settlement, and elastic compression were made on the basis of available data. The ultimate end bearing capacity, Q_b, of deep circular foundations in cohesive soils can be computed according to Skempton (1959) as

$$Q_b + W = A_b(Nc_b + \gamma H) \qquad (1)$$

where W is the weight of the caisson, A_b is the cross-sectional area of the base, N is a bearing capacity factor, c_b is the average shear strength of the soils within a depth of two-thirds the base diameter from the base, and γ is the average total unit weight of the soil for the total length, H, of the caisson. If it is assumed that $W = A_b \gamma H$ and N is set equal to 9 for saturated cohesive soils (Skempton, 1951), Equation (1) can be reduced to

$$Q_b = 9c_b A_b \qquad (2)$$

The undrained shear strength of cohesive soils can be calculated from pressuremeter data according to the

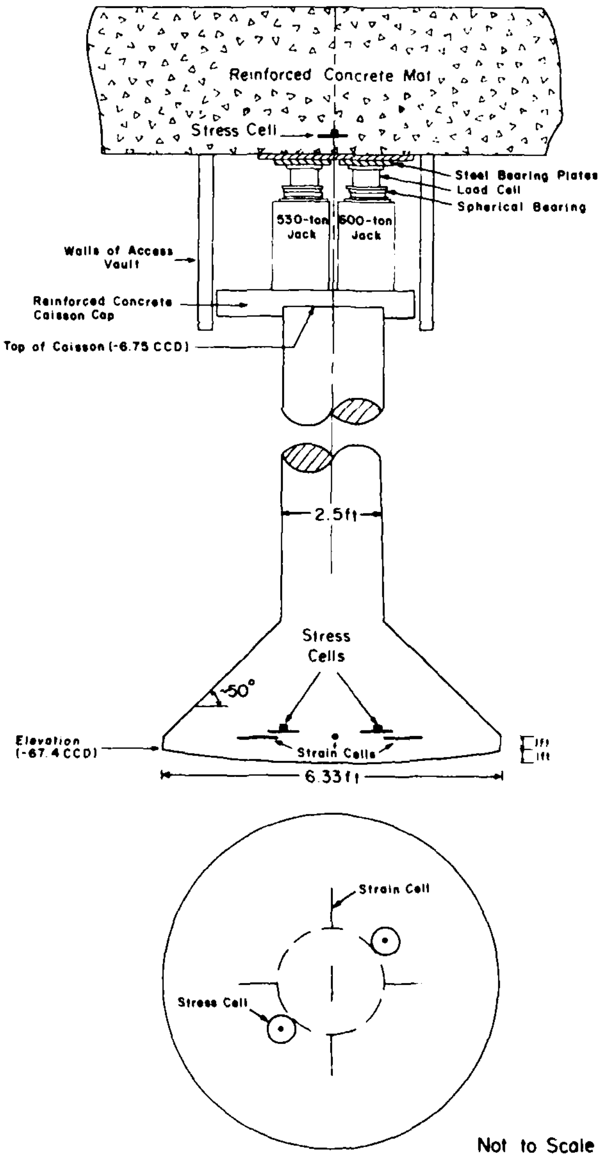
Reinforced Concrete Mat
Stress Cell
Steel Bearing Plates
Load Cell
Spherical Bearing
530-ton Jack
600-ton Jack
Walls of Access Vault
Reinforced Concrete Caisson Cap
Top of Caisson (-6.75 CCD)
2.5ft
Stress Cells
~50°
Elevation (-67.4 CCD)
Strain Cells
1ft
1ft
6.33ft
Strain Cell
Stress Cell
Not to Scale

Figure 2. Details of Instrumented Caisson

following relationship advanced by Menard (1965, 1975):

$$c = \frac{p_\ell - p_o}{2K_b} \qquad (3)$$

where c is the cohesion, P_ℓ and P_o are the limit pressure and horizontal earth pressure at rest, respectively, at the pressuremeter test level, and K_b is a coefficient which, for typical Chicago area soils, has a value of about 2.7 (Lucas and deBussy, 1976). Using average values (obtained from Table 1) of 27 tsf and 4.3 tsf, for p_ℓ and p_o, respectively, Equation (3) yields a cohesion of about 4.2 tsf. The available unconfined compression data shown in Figure 1 indicate a minimum cohesion value for the soils under the base of the caisson of about 3.5 tsf. Accordingly, the net end bearing capacity of the caisson was computed to be about 1100 tons. The appropriateness of using Equation (1) to compute the end bearing capacity of caissons on Chicago hardpan has been confirmed by Holtz and Baker (1972).

The side resistance or "skin friction" of the test caisson was estimated on the basis of the available undrained shear strength values for the various soil layers. To facilitate the computations, the bell was neglected and the shaft of the caisson was separated into two parts with lengths L_1 = 41.25 feet (-6.75 CCD to -48 CCD) and L_2 = 17 feet (-48 CCD to -65 CCD). The average cohesion, c_1 and c_2, for each section was estimated to be 0.48 tsf and 2.05 tsf, respectively. To obtain estimates of the adhesion between the soil and the caisson, these cohesion values were multiplied by 0.8 and 0.4, respectively (Department of the Navy, 1982), to give:

$$Q_S = \pi D(0.8\ L_1\ c_1 + 0.4\ L_2\ c_2) \qquad (4)$$

where D is the diameter of the caisson shaft. Accordingly, the total skin friction was found to be about 230 tons.

A method for using pressuremeter data to estimate the settlement, w, at the base of foundations has been presented by Menard (1965, 1975); a general form of the resulting equation (Lucas and deBussy, 1976) is

$$w = \frac{1+\nu}{3E_d}\ PR_o\left(\lambda_2 \frac{r}{R_o}\right)^{\alpha} + \frac{\alpha\lambda_3}{4.5\ E_d}\ pr \qquad (5)$$

where E_d is the pressuremeter or deviatoric modulus, ν is Poisson's ratio and is set equal to 0.33 because the value of E_d is computed from pressuremeter data on the hypothesis that ν = 0.33, R_o is an empirical coefficient equal to 30 cm, r is the radius (expressed in cm) at the base of the foundation, p is the uniform pressure on the foundation, λ_2 and λ_3 are empirical coefficients that are functions of the shape of the foundation, and α is an empirical coefficient depending on the type and structure of the soil. By setting $\lambda_2 = \lambda_3 = 1$, $\alpha = 2/3$, p = 35 tsf, and E_d equal to 200 tsf for a depth equal to the foundation radius below the base of the foundation and 270 tsf for larger depths, the anticipated settlement was computed according to Equation (5) to be about 2.4 inches for the maximum applied load of 35 tsf.

The theoretical elastic compression, ΔL, of the test caisson was computed according to the relationship

$$\Delta L = \frac{PL}{AE} \qquad (6)$$

where P is the axial load, L is the length of the caisson, A is the cross-sectional area of the caisson, and E is the elastic modulus of the concrete used to construct the caisson. Samples of the test caisson concrete were obtained by coring the top of the caisson to a depth of approximately 5 feet two weeks after the load test was completed. This limited portion of the shaft was assumed to be representative of the entire caisson and yielded values of 3.4×10^6 psi for the elastic modulus and 0.28 for Poisson's ratio. Because typical values of Poisson's ratio for normal strength concrete are on the order of 0.15 to 0.20, a value of 0.25 was selected for further computations.

INSTRUMENTATION AND TESTING

The instrumentation for the test caisson consisted of five strain cells and two stress cells installed at the base and a single stress cell mounted directly over the caisson within the reinforced concrete mat. All cells were stock items manufactured by the Carlson Instrument Company in Campbell, California. The locations of the instruments within the caisson are indicated in Figure 2. The strain cells were mounted horizontally at the base of the caisson and were intended to monitor lateral strains at the base of the bell. All instruments at the base of the bell were carefully embedded in fresh concrete and their positions were fixed by allowing the concrete to harden overnight. Placement of the remaining caisson concrete was completed the following day.

In conjunction with the construction of the heavily reinforced concrete foundation mat, a concrete vault was built below the mat to provide access to the top of the test caisson once construction of the high rise structure had proceeded above the foundation level. Foil strain gauges were bonded to the upper and lower surfaces of the mat to monitor strains during the load test. Gauges on the lower mat surface were damaged during the set-up of the jacking system and water seepage later rendered them useless. However, the top gauges functioned throughout the test.

The theoretical failure load of the test caisson was estimated to be 1100 tons, but a single hydraulic jack with that capacity was not available. Therefore, a special reinforced concrete caisson cap was constructed to accomodate two smaller jacks which would provide this capacity. The concrete mat, together with about 10 stories of the newly constructed concrete structure, provided a sufficiently large reaction to perform the load test, which was conducted according to the Standard Method of Load Testing for Piles under Axial Compressive Load as desribed in ASTM Specification D-1143-74. Two dial gauges were mounted at diametrically opposite locations over the top of the caisson to measure the settlement during loading. However, the length of time that each load was maintained on the caisson was different from that specified by ASTM so that the test could be completed within a reasonable time. Loading the caisson incrementally to the maximum capacity of the jacks was the primary criterion, since loading to failure would not likely be possible with the equipment available. The actual loading sequence used during the test is shown in Figure 3.

Although no cycling of the load test was originally planned, a temporary malfunction in one of the jacks necessitated an unloading to just below 500 tons. The caisson was then reloaded from this point to the maximum load of 1100 tons. Each load increment was maintained for at least one hour. A maximum load of 1060 tons was applied for a period of 6 hours. This load was increased to 1100 tons by taking both jacks to their full capacity. Due to difficulties in controlling the release of the hydraulic pressure, the unloading proceeded directly to zero load without intermediate steps.

Prior to unloading the caisson, specially fabricated steel shims were placed between the caisson cap and the concrete mat to transfer as much of the jack load as possible to the caisson. Since the load cell readings indicated that very little load had been transferred, the test caisson was reloaded several days later to a maximum of 1040 tons and additional shims were placed. Each of the instruments was monitored during these procedures, as well as over the following 15 month period.

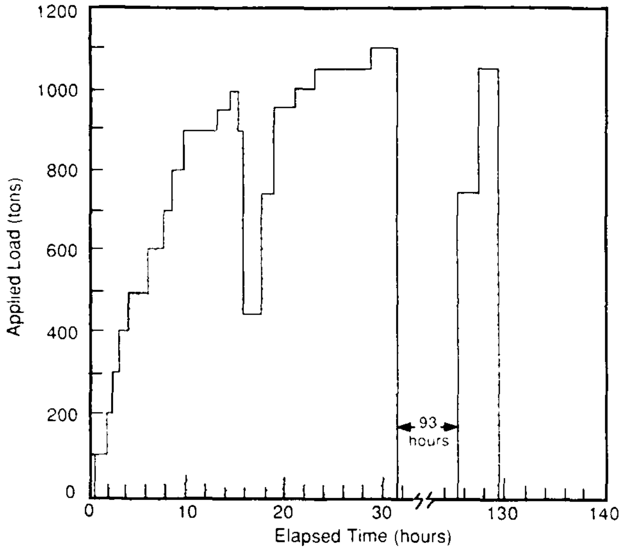

Figure 3. Summary of Test Load Sequence

RESULTS AND OBSERVATIONS

The measured settlement at the top of the caisson as a function of the applied load is shown in Figure 4, together with two lines indicating the computed elastic compression of the test caisson. The elastic compression represented by the lower line was computed by assuming that the entire difference between the applied load at the top of the caisson and the load reaching the bottom is carried in the concrete shaft with no load dissipation along the shaft and no settlement of the base of the caisson. The upper elastic line is obtained by assuming a linear dissipation of the actual load in the shaft (that is, the difference between the applied load and the load reaching the bottom) beginning at the top of the shaft and continuing to the base. The latter line seems more realistic, since it is apparent that some load is carried in side friction and considerable settlement of the base has occurred.

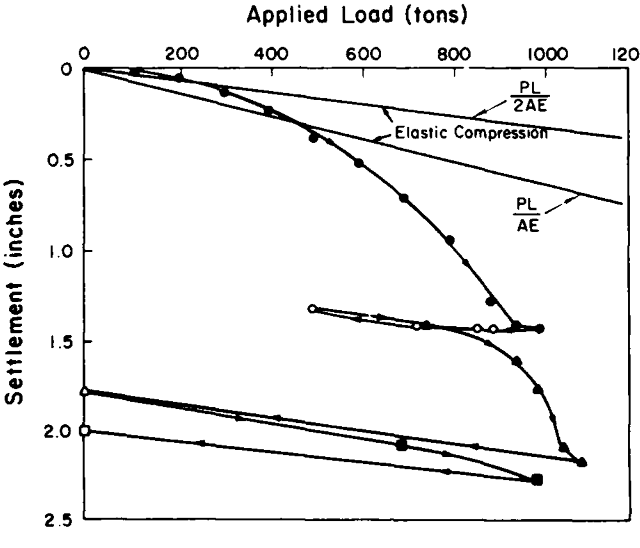

Figure 4. Measured Settlement of Top of Caisson as a Function of Applied Load

According to previous investigators (Burland et al, 1966; Whitaker and Cooke, 1966; Holtz and Baker, 1972; and Reese et al, 1976), a movement of up to 0.5% to 1.0% of the shaft diameter, or a maximum of 0.25 inch, is required to mobilize the full side resistance. The upper elastic compression line and the load test curve intersect at a settlement of about 0.1 inch or 0.33% of the shaft diameter and indicate a maximum side resistance of about 245 tons, which is in very good agreement with the value of 230 tons computed by using conventional procedures.

The average adhesion factor calculated according to the indicated side resistance of the test caisson is on the order of 0.65 to 0.70 and corresponds well with the range of 0.5 to 0.8 reported by Holtz and Baker (1972) for friction caissons in typical Chicago clayey soils. However, when compared with adhesion factors in the range of 0.4 to 0.7 for overconsolidated Texas plastic clays (Reese and O'Neill, 1969) and London clay (Skempton, 1959), the factors obtained are somewhat high. This could be attributed to the lower plasticity and lower sensitivity of the Chicago silty clays.

If the elastic compression of the shaft is subtracted from the settlement measured at the top of the caisson, the settlement of the bottom can be obtained. Accordingly, it can be observed that the bottom of the caisson settled by about 1.85 inches under the maximum applied load of about 35 tsf. According to Equation (5) and for a load at the base equal to about 26 tsf (maximum applied load adjusted for load supported by side resistance), the anticipated settlement at the base, computed according to pressuremeter data, is about 1.90 inches, which is in very good agreement with the measured settlement. Caissons bearing on hardpan were loaded during the Chicago Union Station tests (D'Esposito, 1924) and settled by 0.9 inches and 2.0 inches under maximum applied loads of 18.4 tsf and 87.5 tsf, respectively. The hardpan bearing caisson loaded during the University of Chicago tests (Holtz and Baker, 1972) settled about 2.5 inches under a maximum load of 53 tsf. Accordingly, the settlement at the bottom, as a percent of the diameter of the loaded area, was about 1% to 4% for the Union Station caissons, about 1% for the University of Chicago test caisson, and about 2.6% for the test reported herein. Whitaker and Cooke (1966) found that full mobilization of the base resistance in London clay did not occur until settlments were between 10% and 20% of the base diameter. The load-settlement curve shown in Figure 4, as well as those reported by Holtz and Baker (1972), do not show a sharp break, and it is therefore not clear if these caissons were actually loaded to their maximum capacity. This observation is further reinforced for the case reported herein if it is considered that the maximum applied load was about equal to the computed ultimate bearing capacity, but about 20% of that load was supported by side resistance.

Finally, the unloading curves shown in Figure 4 indicate that most of the measured settlement is nonrecoverable. Tests in London clay (Whitaker and Cooke, 1966; Ellison et al, 1971) have also indicated that most of the vertical movement, which occurs after the ultimate adhesion between the shaft and the surrounding soil is reached, is nonrecoverable and that significant rebound should not be anticipated. Although the conditions of the load test reported herein are different from those of the test conducted in the London clay (primarily an end bearing caisson on hardpan compared to primarily a friction pier in stiff fissured clay), slippage along the shaft is still nonrecoverable and any elastic rebound from the base of the caisson greater than about 0.1 inch would be resisted by negative friction along the shaft of the caisson. This observation is in good agreement with information reported by D'Esposito (1924) for the Union

Station tests and Holtz and Baker (1972) for the University of Chicago tests where, upon unloading, the rebound of caissons bearing on Chicago hardpan was not more than 0.1 inch after accounting for the elastic rebound of the concrete shaft.

Based on the load test curve shown in Figure 4 and the foregoing observations, it can safely be concluded that a large portion of the final applied load (about 820 tons) would reach the bottom of the caisson and would be transferred to the soil through the base of the bell. Unfortunately, computations of the load at the base of the bell, made on the basis of the stresses measured by the two stress cells installed at the base of the bell, yielded only a small fraction of this anticipated load. The average computed load, based on stress measurements, was only about 200 tons for an applied load of about 1060 tons and should not be considered indicative of the actual load transferred to the base of the caisson. It is likely that some "honeycombing" of the concrete below the cells may have been caused during installation and, consequently, relatively softer zones of concrete may have existed below the cells. This would have the effect of significantly reducing the modulus of elasticity of the concrete below the cells and could account for the low measured stresses. Furthermore, arching in the concrete above the cells may have occurred upon initial deflection of the cell face and additional stresses may not have been directly transferred to the cell. Finally, stress cell calibration may change due to a number of reasons, which include the development of stress concentrations and/or relief zones during installation procedures.

Alternatively, stresses and loads at the base of the caisson were computed on the basis of strains measured by the five horizontally oriented strain gauges, together with the assumption that, in the absence of applied horizontal stresses, the measured horizontal strains are attributable primarily to the Poisson effect. By assuming elastic behavior for the concrete and using laboratory test values of 3.4 x 10^6 psi and 0.25 for Young's modulus, E, and Poisson's ratio, ν, respectively, the vertical stress, σ_v, was computed in terms of the measured lateral (horizontal) strain, ε_h, as

$$\sigma_v = E \frac{\varepsilon_h}{\nu} \qquad (7)$$

Using an average value for the computed vertical stress, the load transferred to the base was computed and the results are shown in Figure 5. Also shown in Figure 5 is a line indicating the anticipated relationship between the applied load and the load transferred to the base. This line was obtained by considering that about 230 tons of the applied load are supported by side resistance. It can be observed that the results of the strain cell measurements are in very good agreement with predictions based on conventional procedures, as well as with the actual load test curve presented in Figure 4 for an applied load of up to about 900 tons. For higher loads, the measured strains increased disproportionately with the increases in load.

It can also be observed that, upon unloading, a large percentage of the stress or load remained "locked in", as indicated in Figure 5 by the significant shift of the data above the theoretical line. This apparent "locked in" stress may very well indicate the development of minor cracks at the base of the bell. Furthermore, the computed stress is observed to increase with time under the maximum load of 1060 tons, which was held constant for six hours, and this may be due to the propagation of microcracks or creep under constant load. Lateral strains in excess of 30 x 10^{-6} inches per inch were measured by four of the five strain cells, while strains of up to 50 x 10^{-6} inches per inch were recorded by two strain cells. These levels of lateral strain are significant enough to suspect the development of microcracks at the base of the bell. Reese and Farr (1980) performed unconfined compression tests on small-scale model caissons which were constructed with a variety of bell angles. It was observed that caissons with bell angles of less than 60° to the horizontal would fail by the formation of a tension crack in the bell and that a 45° bell would fail at significantly smaller loads than a 60° bell with the same base area. It appears that the 50° bell of the test caisson described herein performed better than would have been anticipated on the basis of the conclusions reached by Reese and Farr (1980). Although small lateral strains developed at the base of the bell, it can be stated that the confinement of the bell within the hardpan layer provided an additional factor of safety against failure by major cracking at the base of the caisson.

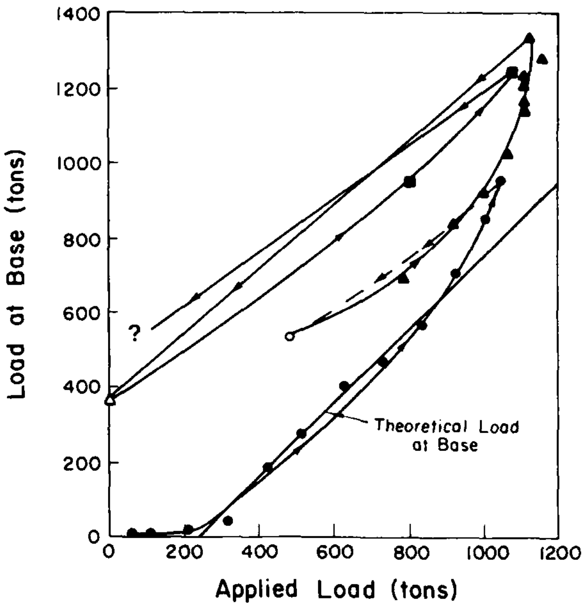

Figure 5. Load Transferred to Base of Caisson as a Function of Applied Load

Monitoring of the instrumentation was continued for a period of 15 months after the end of the test and the final shimming. At the end of this period survey measurements indicated that the finished structure had settled approximately 0.62 inches. Since the settlement which resulted during the load test was on the order of 2 inches, the building settlement may have not been enough to result in complete load transfer through the shims to the test caisson. The average increase in strain cell readings was on the order of 20 x 10^{-6} inches per inch, indicating that about 850 tons of structural load was being transferred to the caisson through the shims and the natural building settlement. However, it could also indicate that there had been an equivalent amount of creep under a much smaller load because of the suspected past microcracking. The cumulative lateral strain measured at the base of the caisson from the start of the load test through the last readings was less than 70 x 10^{-6} inches per inch, and this could indicate that the caisson bell remained essentially intact, aided perhaps by confinement in the very stiff clay and hardpan soils which surrounded it.

CONCLUSIONS

Based on the results of the full-scale load test and the observations and discussion presented herein, the following conclusions, which are primarily applicable to the soil profile encountered in the Chicago area, can be advanced.

1. The high bearing capacity of Chicago hardpan and the accuracy of settlement predictions based on pressuremeter data have been reinforced. The base of the caisson was loaded to about 26 tsf without approaching the bearing capacity of the hardpan and the resulting settlement was about 1.85 inches. Accordingly, increased allowable bearing pressures can be established for caissons on Chicago hardpan, when the anticipated settlements are tolerable.
2. Previously established limits of movement for the mobilization of side resistance are confirmed; movements on the order of 0.5% to 1% of the shaft diameter or up to 0.25 inches are more than adequate to mobilize the full side resistance of caissons in Chicago silty clays.
3. The generated side resistance is found to be in close agreement (about 5% difference) with that computed according to conventional methods. The corresponding average adhesion coefficient of about 0.65 to 0.70 is within the limits established for similar soil profiles.
4. Very small, but nonrecoverable, strains were measured at the base of the caisson bell, indicating probable microcrack development during loading. The confinement of the bell in a hard soil layer is considered beneficial and, although not considered in current practice, it provides a measure of additional safety to current design procedures. The current requirement for 60° bells should be maintained for high bearing pressure caissons.

ACKNOWLEDGEMENT

The advice and guidance of Jorj Osterberg of Northwestern University and Clyde Baker of STS Consultants throughout the conduct of this study are gratefully appreciated.

REFERENCES

Bretz, J. H. (1939), "Geology of the Chicago Region", Illinois State Geological Survey, Bulletin Number 65, Part 1.

Burland, J. B., Butler, F. G., and Dunican, P. (1966), "The Behavior and Design of Large Diameter Bored Piles in Stiff Clay", Proceedings of the Symposium on Large Bored Piles, Institution of Civil Engineers, London, England, pp. 51-71.

D'Esposito, J. (1924), "Foundation Tests by Chicago Union Station Company", Journal of the Western Society of Engineers, Volume XXIX, Number 2, pp. 33-40.

Department of the Navy (1982), "Foundations and Earth Structures", Design Manual NAVFAC DM-7.2, Alexandria, Virginia.

Ellison, R. D., D'Appolonia, E., and Thiers, G. R. (1971), "Load-Deformation Mechanism for Bored Piles", Journal of the Soil Mechanics and Foundations Division, American Society of Civil Engineeers, Volume 97, Number SM4, pp. 661-678.

Holtz, R. D., and Baker, C. N. (1972), "Some Load Transfer Data on Caissons in Hard Chicago Clay," Proceedings of the Specialty Conference on the Performance of Earth and Earth Supported Structures, American Society of Civil Engineers, Lafayette, Indiana, pp. 1223-1242.

Lukas, R. G., and deBussy, B. (1976), "Pressuremeter and Laboratory Test Correlations for Clays", Journal of the Geotechnical Engineering Division, American Society of Civil Engineers, Volume 102, Number GT9, pp. 945-962.

Menard, L. (1965), "Rules for the Calculation and Design of Foundation Elements on the Basis of Pressuremeter Investigations in the Ground", Proceedings of the Sixth International Conference on Soil Mechanics and Foundation Engineering, Volume II, pp. 265-271.

Menard, L. (1975), "Interpretation and Application of Pressuremeter Test Results", Sols-Soils, Volume 26, pp. 1-43.

Peck, R. B., and Reed, W. C. (1954), "Engineering Properties of Chicago Subsoils", University of Illinois Engineering Experiment Station, Bulletin Number 423, Urbana, Illinois.

Reese, L. C., and Farr, J. S. (1980), "Plain Concrete Underreams for Drilled Shafts", Journal of the Structural Division, American Society of Civil Engineers, Volume 106, Number ST6, pp. 1329-1341.

Reese, L. C., and O'Neill, M. W. (1964), "Field Tests of Bored Piles in Beaumont Clay", Paper presented at the Annual Meeting, American Society of Civil Engineers, Chicago, Illinois.

Reese, L. C., Touma, F. T., and O'Neill, M. W. (1976), "Behavior of Drilled Piers Under Axial Loading", Journal of Geotechnical Engineering Division, American Society of Civil Engineers, Volume 102, Number GT5, pp. 493-510.

Skempton, A. W. (1951), "The Bearing Capacity of Clays", Proceedings of the Building Research Congress, London, England, Volume 1, pp. 180-189.

Skempton, A. W. (1959), "Cast In-Situ Bored Piles in London Clay", Geotechnique, Volume 9, pp. 153-173.

Whitaker, T., and Cooke, R. W. (1966), "An Investigation of the Shaft and Base Resistances of Large Bored Piles in London Clay", Proceedings of the Symposium on Large Bored Piles, Institution of Civil Engineers, London, England, pp. 7-49.

Proceedings: Second International Conference on Case Histories in Geotechnical Engineering, June 1-5, 1988, St. Louis, Mo., Paper No. 6.45

Settlement of Two Tall Chimney Foundations

J.R. Davie
Engineering Supervisor, Geotechnical Services, Bechtel Civil, Inc.,
Gaithersburg, Maryland

M.R. Lewis
Engineering Supervisor, Geotechnical Services, Bechtel Civil, Inc.,
Gaithersburg, Maryland

SYNPOSIS: The foundation of tall chimneys on shallow mats is of particular interest, not only because of the importance of minimizing differential settlement, but because the axisymmetric loading and the simple relationship between the chimney height and this loading can provide an accurate correlation between load and settlement, not often available with other structure types. This paper presents settlement case histories of two tall chimneys, one on overconsolidated clay and the other on sands and gravels. The computed values of the elastic soil properties, backcalculated from the load versus settlement relationship, are discussed and compared with values found in the literature.

INTRODUCTION

Heavily overconsolidated clays are usually assumed to behave in an elastic or at least pseudo-elastic manner when loaded at a level well below their preconsolidation pressure. Medium dense to dense sands and gravels are assumed to behave in a similar fashion. Unfortunately, for many large structures, verification of this elastic behavior and subsequent backcalculation of the appropriate elastic parameters are often not completely successful, even where settlement is carefully monitored. This is because of various factors such as an unknown amount of heave during foundation excavation (particularly for deep structures), uneven load distribution across the structure, unclear correlation of construction progress and foundation loading, or a complex soil profile. This paper presents the results of settlement monitoring of two tall chimney foundations where there was negligible excavation heave, axi-symmetric loading, accurate correlation of construction progress and foundation loading, and a reasonably homogeneous soil profile. The linear nature of the load versus settlement relationship is demonstrated, and the computed elastic properties of the foundation soils are presented.

CHIMNEY AND FOUNDATION SOIL DETAILS

Case 1: Chimney on Clay

The 475-foot-high brick-lined concrete chimney has a total weight, including the pedestal and base, of almost 14,000 kips, resulting in a gross static bearing pressure of 3.2 kips per square foot (ksf). Details of the chimney dimensions and loads are shown in Table 1.

The chimney is constructed on an octagonal mat founded 8 feet below original grade on overconsolidated highly plastic clay known as the Beaumont Clay Formation. These clays, deposited during the early Wisconsin glacial stage, are part of the Pleistocene age terrace that extends from the Rio Grande to the deltaic plain of the Mississippi River. As a result of exposure to weathering later in the glacial stage, when the sea level was approximately 400 feet lower than it is today, the clay is overconsolidated due to desiccation. The minimum preconsolidation pressure estimated from consolidation tests on the site soils was 6 ksf.

A log of the foundation soils at the plant site together with a profile showing various soil parameters is shown in Fig. 1. The initial 20 feet of clay beneath the foundation mat contained several thin non-continuous sand layers. Undrained shear strength readings based on pocket penetrometer tests made on clay samples extruded in the field averaged 2.5 ksf to a depth of about 30 feet below the foundation. There was a large scatter in the results, reflecting both the method of strength measurement and the crustal nature of the upper material. Many of the soil samples from this zone that were subjected to unconfined compression testing in the laboratory exhibited a slicken-

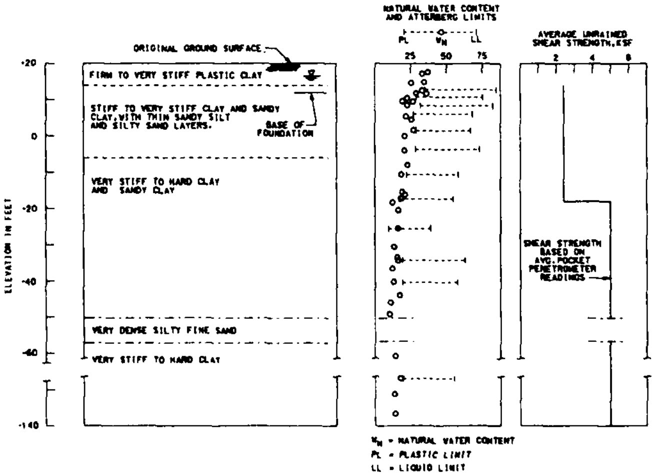

Fig 1. Typical Profile - Case 1

sided structure, and gave somewhat lower recorded strengths. On a sitewide basis, the average undrained shear strength computed from unconfined compression tests was only about 60 percent of that estimated with the pocket penetrometer. The material below the upper zone was fairly homogeneous, very stiff to hard plastic clay, with an average undrained shear strength of about 5 ksf estimated from pocket penetrometer readings. Groundwater was very close to the surface.

Case 2: Chimney on Sand

The 350-foot-high concrete chimney has three steel flues. The total weight, including the foundation, is almost 7,000 kips resulting in a gross static bearing pressure of 2.4 ksf. Details of the chimney dimensions and loads are shown in Table 1.

TABLE I. Chimney Dimensions and Loads

		Case 1	Case 2
Base Mat and Pedestal Dimensions	Base elevation, feet	12.5	69.5
	Final grade, feet	23.0	75.0
	Original grade, feet	20.4	70.0
	Thickness of base mat, feet	5.5	6.5
	Thickness of pedestal, feet	5.0	0.0
	Width of base mat, feet	72.0(1)	54.0(2)
	Area of base mat, sq. feet	4290	2916
	Equivalent base mat diameter, feet	73.9	61.0
Concrete Shell Dimensions	Height of chimney, feet	475	350
	Outside diameter at base, feet	39.25	29.6
	Thickness at base, inches	18.0	20.0
	Outside diameter at top, feet	22.3	25.6
	Thickness at top, inches	8.0	8.0
Liner(3) Dimensions	Outside diameter at base, feet	21.6	7.5
	Thickness at base, inches	13.0	0.31
	Outside diameter at top, feet	15.7	7.5
	Thickness at top, inches	6.0	0.31
Loads and Pressures	Deadweight of base, pedestal and chimney, kips	13,810	6,940
	Gross static bearing pressure, ksf	3.2	2.4
	Deadweight of chimney (shell & liner), kips	9,220	4,100
	Static bearing pressure from chimney, ksf	2.15	1.4
	Wind shear at chimney base, kips	486	256
	Wind moment at chimney base, kip-feet	110,275	48,000

(1) Case 1 has octagonal mat; width is distance between flats.
(2) Case 2 has square mat.
(3) Case 1 has single brick liner; Case 2 has 3 separate steel flues.

The chimney is constructed on a square mat founded about 7 feet below the ground surface on medium dense sands and gravels. These materials are of glacial derivation, deposited predominantly as a result of glaciation during the late Pleistocene epoch. Bedrock beneath the soils is part of the Southeastern New England Platform Geologic Province, and consists of the Dedham granodiorite of late-Precambran age.

A log of the foundation soils at the chimney location with pertinent soil parameters is shown on Figure 2. Essentially, the medium to dense fine to coarse sand and gravel can be assumed to form a continuous layer, with occasional thin silt layers and numerous cobbles and boulders. The original ground surface was at about elevation 70 feet, msl, and the top of rock was about El. 42 feet, msl, ie about 28 feet of sand and gravel. Neglecting the upper 5 feet of in-situ soil (it was recompacted during construction) the SPT N-values range from 8 to over 50 blows per foot with an an average value of about 30. Groundwater was located at El. 68 feet, msl.

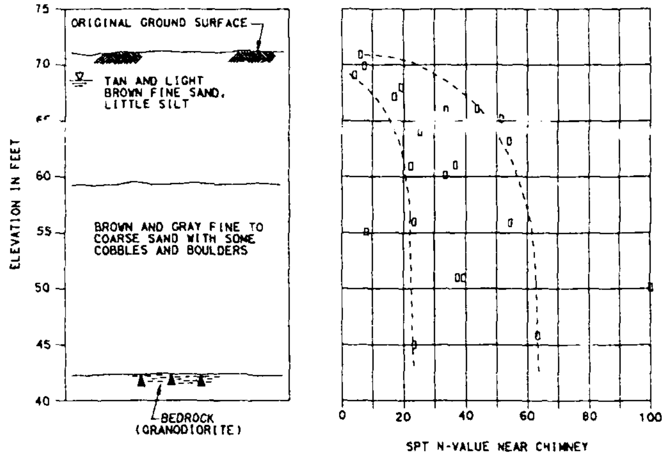

Fig. 2 Typical Profile - Case 2

SETTLEMENT ESTIMATE

The purpose of estimating foundation settlement is to determine if the structure under consideration will be stable and perform its intended function within the predicted range of deformation. This is particularly important for tall chimneys where even a small differential movement at the base can result in significant lateral movement at the top.

One standard procedure used to determine elastic settlement is to estimate the elastic modulus, E, of the foundation material and then utilize any one of several elastic equations available for settlement computation. Alternatively, we can rely on charts, based on past experience, relating SPT N-values to observed settlements (Peck, Hanson and Thornburn, 1974). Both methods are widely used and accepted. The only major unknown in the evaluation is the stiffness or the elastic modulus.

The elastic modulus can be measured or estimated in several ways. For clays, it is common to relate E to the undrained shear strength, s_u. A large range of E/s_u ratios has been reported in the literature, from as low as 50 (Skempton, 1951) to as high as 2500 (D'Appolonia et. al., 1971). The ratio depends on the plasticity, loading history, type of clay and the type of laboratory or field test used to determine E and s_u. For sands E is frequently related to the results of field tests such as the SPT, cone penetration tests (CPT), pressuremeter tests, dilatometer tests, or plate bearing tests. The authors have had good results relating E to SPT N-values. The advantages of the SPT are that it is simple and widely used. The well-documented disadvantages are that the results are not reproducible due to inevitable variations in equipment, the drilling crew and the soil being sampled.

For the original estimate of the elastic settlement, it was assumed the foundation soils at both sites were homogeneous within the zone of influence, H = 5B for Case 1 and

H = the thickness of sand over rock for Case 2. Although other elastic equations were used in the original analyses, very similar results were obtained using the following recently published equation (Bowles, 1987):

$$s = 4qB' \frac{(1-\mu^2)}{E} I_s I_f \qquad (1)$$

where s = Settlement at the center of the foundation

q = Net applied static bearing pressure

B′ = B/2 = Half the width of the foundation mat

μ = Poisson′s ratio

E = Modulus of elasticity

I_s = Influence factor depending on the shape of the foundation

I_f = Influence factor depending on the foundation embedment

The actual values used in the analyses for Cases 1 and 2 are summarized in Table 2. The results show that the chimney in Case 1 would settle about 0.9 inches and the chimney in Case 2 would settle about 0.2 inches.

SETTLEMENT MONITORING RESULTS

Case 1: Chimney on Clay

Settlement markers were installed on the north, south, east and west edges of the chimney pedestal before the chimney construction started. The net pressure exerted by the octagonal mat foundation and the pedestal was about 0.35 ksf, enough to recompress any heave due to the foundation excavation, but not sufficient to cause more than about 1/8 inch of net settlement. Thus, we can assume that no significant net settlement took place prior to the start of settlement monitoring or chimney construction and that the weight of the mat foundation and pedestal can be neglected when considering correlation between measured load and settlement.

TABLE II. Parameters for Settlement Computation

Parameter	Case 1	Case 2
q, ksf	2.15	1.40
B′, feet	32.75 (equivalent square)	27
μ	0.35	0.30
E, ksf	1500	1260
I_s	0.50	0.22
I_f	0.97	0.73

The chimney was constructed in two stages. The concrete shell was poured to a height of 472.5 feet, and then the inner brick liner was placed up to 475 feet height. Using the chimney designer′s quantities, a correlation between chimney height and static bearing pressure was produced. This correlation was used to develop plots of chimney settlement and load versus time, and chimney load versus settlement, as shown on Figures 3 and 4. Settlement was measured optically, generally

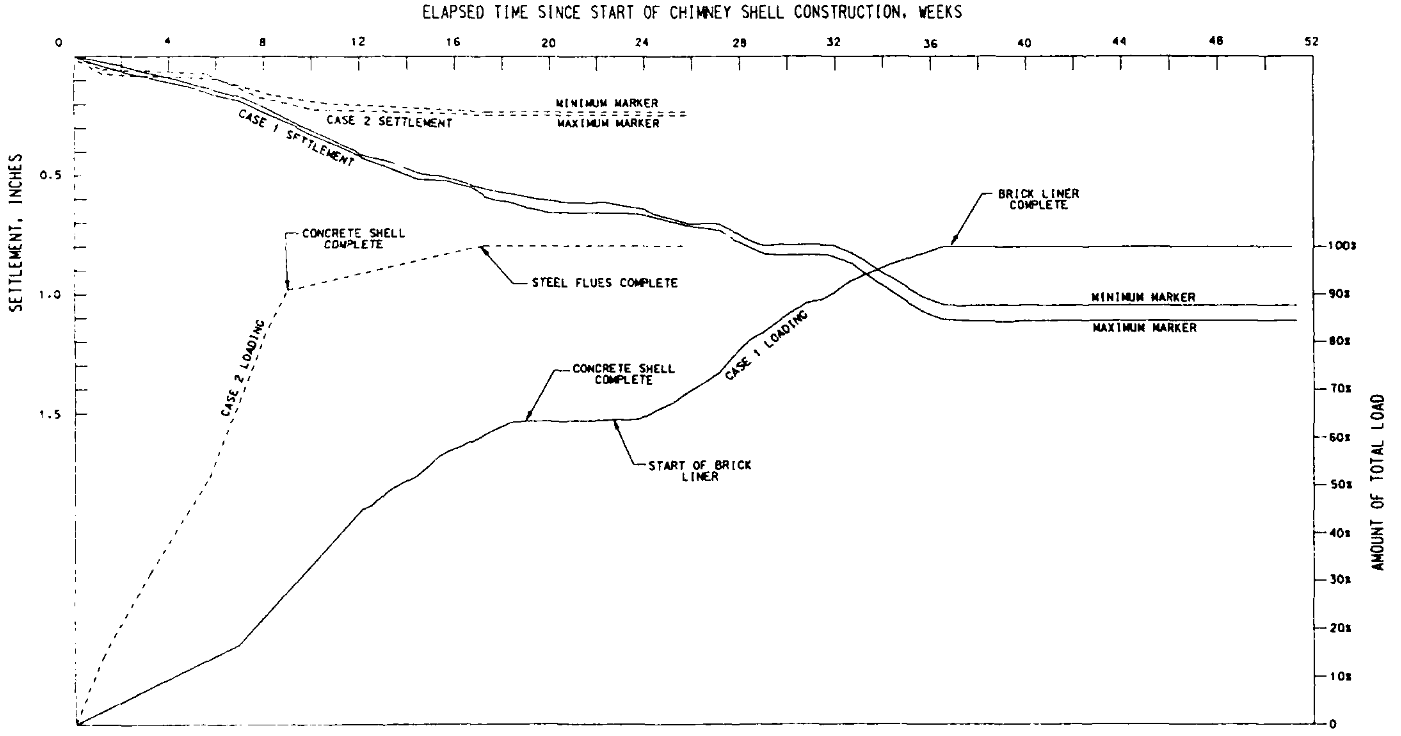

Fig. 3 Chimney Settlement and Load Versus Time

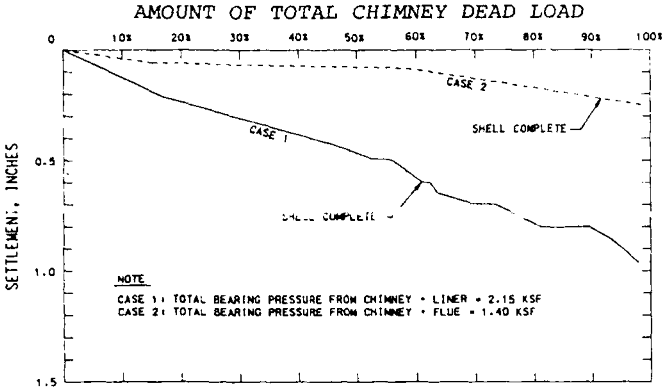

Fig. 4 Chimney Load Versus Settlement

once per week after the shell height had reached about 75 feet.

Case 2: Chimney on Sand

Three settlement markers were installed on the top of the base mat, each 120 degrees apart. The net pressure of 1 ksf exerted by the mat foundation is essentially the same as the gross pressure since the bottom of the mat is within one foot of the original ground surface. The markers were cast in the foundation base mat. However, the initial survey was not made until 3 weeks after the base mat was buried. Thus, if the sands and gravels behave elastically, we can assume that settlement due to the base mat was not measured, and the weight of the mat should be neglected when considering the measured load versus settlement values.

The chimney was constructed in two stages. The concrete shell was placed to a height of 350 feet, followed by each of the three steel liners. Using loading provided by the chimney designer, a relationship between chimney height and static bearing pressure was developed. This was used in the plots of chimney settlement and load versus time and chimney load versus settlement, as shown on Figures 3 and 4.

Settlement was measured optically, generally every two weeks during chimney construction and at one month intervals during liner installation.

ANALYSIS OF MEASURED SETTLEMENT

The results of the settlement monitoring are shown on Figures 3 and 4. Five observations can be made from these figures.

- o the load versus settlement curve is almost linear,
- o there was little differential settlement,
- o there was an immediate response of settlement to load increase,
- o settlement ceased as soon as loading was completed, and
- o long term creep-type settlement was not observed in the period following chimney completion.

These results confirm that the foundation soils at both sites behaved in an almost elastic manner within the loading range applied, i.e., strain in the soil was almost proportional to the applied stress. Consequently, the elastic modulus of the foundation soil can be backcalculated from these results and compared with the values used in the original settlement estimate and other published values.

Case 1: Chimney on Clay

The value of elastic modulus backcalculated using equation (1) and the maximum measured settlement of 0.95 inches is 1390 ksf. This value is based on the assumption that the Beaumont Clay has a constant elastic modulus value with depth, at least to a depth of 5 times the width of the mat. However, as noted earlier and shown in Figure 1, although the foundation soils are fairly homogeneous within the zone of influence of the chimney foundation, the 30 feet of soil immediately below the foundation mat has, on average, only about one half the strength of the underlying clays. It can therefore be reasonably assumed that the elastic modulus of the upper soils will be about half of that of the lower soils. To estimate these values of elastic modulus, the following basic stress-strain equation can be used.

$$s = \sum_{i=1}^{n} \frac{p_i h_i}{E_i} \qquad (2)$$

where n = Number of layers considered beneath the foundation
h = Thickness of each layer
p = Average applied stress in each layer.

To obtain p, three stress distribution curves below the foundation were computed, namely the stresses under the center and edge of a rigid circular footing, and the average stress beneath a circular flexible foundation (Muki 1961, Ahlvin and Ulery 1962). Since the chimney foundation incorporates all of these cases to some degree, the assumed average stress distribution was obtained by averaging the three curves. The layer thickness H was chosen as B/4. The stress at the center of each layer was computed as a percentage of the applied static bearing pressure in successive layers below the foundation to a depth of 2B (approximately 150 ft) below the foundation; at that depth, the stress level was less than 10% of the foundation pressure and it was assumed that the settlement due to soil below 2B was 10% of the total settlement. The value of elastic modulus computed using equation (2) was 900 ksf for the upper 30 ft of clay beneath the foundation, and 1800 ksf for the underlying clay. If equation (2) is used assuming the foundation soil to be homogeneous, the computed average elastic modulus is about 1300 ksf, in good agreement with the values computed using equation (1).

It is apparent that the average values of elastic modulus E of 1300 to 1400 ksf backcalculated from the settlement readings using the elastic settlement equation are close to the E value of 1500 ksf assumed in the settlement prediction analysis. This is not surprising since E = 1500 ksf was based on an average interpreted E/s_u ratio computed from numerous case histories of mat foundations on Beaumont Clay by Williams and Focht (1982). The Williams and Focht E/s_u ratios were derived mainly from unconsolidated-undrained triaxial and unconfined compression test results. Using the unconfined compression strength of the clay measured in the present case (about 60 percent of the strength estimated from pocket penetrometer readings) we obtain an E/s_u ratio based on E back-calculated from equation (2) of about 600.

Case 2: Chimney on Sand

The value of elastic modulus backcalculated using equation (1) and the maximum measured settlement of 0.25 inches is about 1066 ksf which compares favorably with the assumed value of 1260 ksf. Several authors (D'Appolonia, et. al. 1970, Parry 1971, Yoshida and Yoshinaka 1972, Bowles 1987) have related E to SPT N-values, and Schmertman (1970, 1978) has related E to CPT and CPT to N-value. The results are shown in Table 3.

TABLE III. Summary of Various Estimates of Modulus Elastic

Reference	Relationship	Notes
D'Appolonia, et. al., 1970	E = 432 + 21.2N (ksf)	For normally loaded sands from case histories
Parry, 1971	E = 100N (ksf)	From plate bearing tests
Yoshida and Yoshinaka, 1972	E = 42N (ksf)	Based on plate load tests and lateral pile load tests
Bowles, 1987	E = 10 (N+15) (ksf)	
Schmertman, 1970 and 1978	E = 30N to 50N (ksf)	For gravelly sand q_c/N = 6 to 10 and $E = 2.5q_c$

Using a representative N-value of 30 for the soil column beneath the chimney, we estimate the elastic modulus E to be about 36N ksf based on actual settlement measurements. This compares well with the relationships proposed by D'Appolonia 1970, Yoshida and Yoshinaka 1972, and Schmertman 1970, 1978.

CONCLUSIONS

The total settlements recorded for the two chimneys were close to the predicted values. Maximum differential settlements in both cases were very small. Settlements during construction were almost linearly related to the applied loads, thus verifying the approximately elastic behavior of the medium dense to dense sands and gravels, and the Beaumont Clay at loading levels well below the preconsolidation pressure. The cases presented confirmed ratios of E/s_u and E/N found in the literature. For the Beaumont Clay, the E/s_u ratio backcalculated from the measured settlements was 600, while for the sands and gravels, the backcalculated E/N ratio was 36.

REFERENCES

Ahlvin, R. G., and Ulery, H. H., (1962) "Tabulated Values for Determining the Complete Pattern of Stresses, Strains, and Deflections beneath a Uniform Load on a Homogeneous Half Space," Highway Research Board, Bulletin 342, pp. 1-13.

Bowles, J. E. (1987), "Elastic Foundation Settlements on Sand Deposits," Journal of Geotechnical Engineering, ASCE, Vol. 113, GT 8.

D'Appolonia, D. J., D'Appolonia, E., and Brissette, R. F. (1970), "Settlement of Spread Footings on Sand," Closure, Journal of the Soil Mechanics and Foundations Division, ASCE, Vol. 96, SM 2.

D'Appolonia, D. J., Poulos, H. G., and Ladd, C. C. (1971), "Initial Settlement of Structures on Clay," Journal of the Soil Mechanics and Foundations Division, ASCE, Vol. 97, SM 10.

Muki, R., (1961) "Asymmetric Problems of the Theory of Elasticity for a Semi-Infinite Solid and Thick Plate," Progress in Solid Mechanics, Vol. 1, North Holland Publishing Company, Amsterdam.

Parry, R. H. G., (1971), "A Direct Method of Estimating Settlements in Sands from SPT Values," Proc. Symp. Interaction of Structures and Foundations, Midlands Soil Mech. and Found. Eng. Soc., Birmingham, pp 29-37.

Schmertman, J. H. (1970), "Static Cone to Compute Static Settlement Over Sand," Journal of the Soil Mechanics and Foundations Division, ASCE, Vol. 96, SM 3.

Schmertman, J. H., Hartmann, J. P., and Brown, P. R. (1978), "Improved Strain Influence Factor Diagrams," Journal of the Geotechnical Engineering Division, ASCE, Vol. 104, GT 8.

Skempton, A. W., (1951) "The Bearing Capacity of Clays," Building Research Congress, pp. 180-189.

Williams, C. E., and Focht, J. A., (1982) "Initial Response of Foundations on Stiff Clay" ASCE Convention, New Orleans, Louisiana.

Yoshida, I., and Yoshinaka, R. (1972), "A Method to Estimate Modulus of Horizontal Subgrade Reaction for a Pile," Soils and Foundations, the Japanese Society of Soil Mechanics and Foundation Engineering, Vol. 12, No. 3.

Proceedings: Second International Conference on Case Histories in Geotechnical Engineering, June 1-5, 1988, St. Louis, Mo., Paper No. 6.49

Distress to Structures on Loose Ash and Cinder Fills

Moustafa A. Gouda
Chief Geotechnical Engineer, Lippincott Engineering Associates, USA

D. Raghu
Civil and Environmental Engineer, New Jersey Institute of Technology, USA

I. Wayne Lippincott
P.P., President, Lippincott Engineering Associates, USA

ABSTRACT

The Logan Section of the City of Philadelphia, that encompasses 17 city blocks and includes 997 "row type" dwellings, was constructed in the early 1900s. It is reported that settlement of these structures has continued since their construction. In 1986, a Geotechnical Investigation, commissioned by the City of Philadelphia, revealed that a total of two to three feet of settlement, with as much as one to two feet of differential settlement, has taken place. Recent measurements indicated that settlement is still in progress. This settlement has resulted in severe structural damage and, in some cases, collapse of the buildings. One hundred (100) homes have been declared imminently dangerous, 110 homes have been declared dangerous, and the remaining homes are considered moderately damaged. This paper discusses the probable causes of settlement, and evaluates the geotechnical characteristics and properties of the ash and cinders. These characteristics are considered the prime cause of the problem at the Logan Section.

INTRODUCTION

Lippincott Engineering Associates (LEA) was retained by the City of Philadelphia, in the Spring of 1986, to investigate the settlement problems of the Logan Section of Philadelphia. The purposes of the investigation were to determine the causes of settlement, to make recommendations to arrest the settlement, and to provide remedial measures to rehabilitate the structural distress. (Figure 1 indicates type of differential settlement)

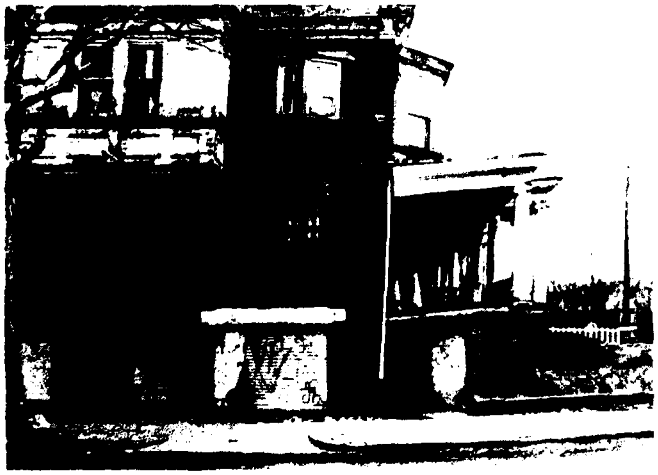

Figure 1 - House located at 920 Wyoming Avenue

SITE HISTORY

A study of historic maps indicated that the site is a reclaimed valley of the old Wingohocking Creek, which crossed the area in the early 1900s. As part of the Logan Section Development, the stream was contained in a 17 foot diameter brick storm sewer and the valley was filled with approximately 40 feet of loose ash and cinders. The dwellings were supported within the loose, uncontrolled, unengineered fill on shallow foundations. Construction of all dwellings was completed by 1920. There appears to be no evidence at this time indicating that the stream is flowing.

GEOLOGIC SETTING

The site, which is located on Roosevelt Boulevard in northeast Philadelphia, is underlain by metamorphic bedrock of the Wissahickon Schist formation. In general, the natural soil overlying the bedrock consists of residual soil and decomposed mica schist.

SUBSURFACE CONDITIONS AT THE SITE

A total of 38 test borings were advanced at the site. The SPT's was performed continuously through the fill. All borings were extended to or into the surface of bedrock. The boring results indicated that the site is covered with as much as 40 feet of loose ash and cinders overlying residual soil and decomposed mica schist. Based on test boring results, the following describes the on-site materials.

Fill (F)

A layer of grey-black ash and cinders cover the entire site and extends from zero, at the edge of the old creek valley, to 40 feet at the at the center of the old valley. The ash and cinders fill were found to be in an extremely loose condition, with blow counts of less than six per foot and in-situ densities of 55 to 60 pounds per cubic feet, being typical of conditions found.

Recent Alluvial Layer (RA)

A recent alluvial layer was occasionally encountered along the alignment of the old stream. The layer was two to five feet thick and consisted of sand, gravel and silty clay.

Residual Soil (RS)

Micaceous medium-stiff clay layers, formed by weathering of the mica schist bedrock, underlie the fill. The layers ranged in thickness from 10 to 15 feet.

Decomposed Rock and Bedrock (DR&R)

These were the last formations encountered in the borings. RQD of mica schist bedrock ranged from 7 to 30% in the areas where rock cores were recovered. (Figure 2 presents a general geologic section across the valley)

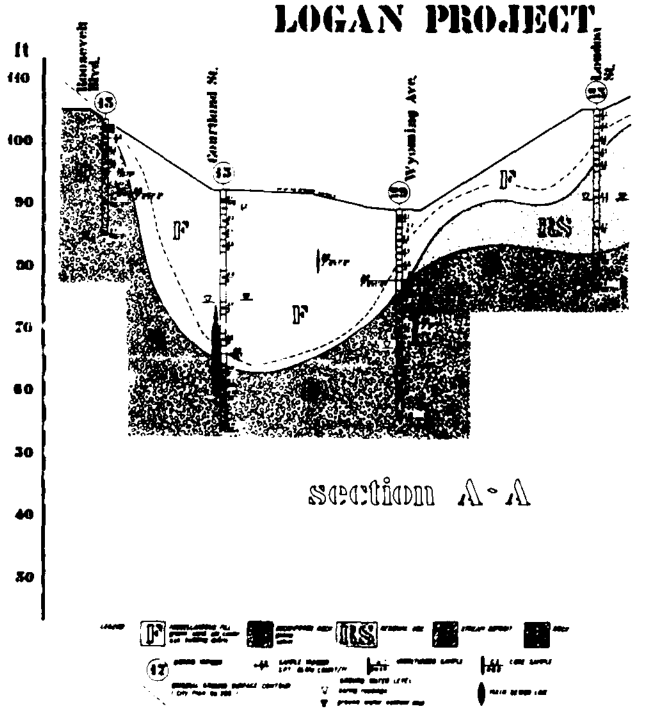

Figure 2 - Geologic Section

REVIEW OF LITERATURE

In order to determine the probable causes and mechanisms for structural distress, the engineering properties of ash and cinders have to be determined. A review of literature indicated that some work has been done in this area. It was noted that the engineering properties of these materials were influenced by the chemical components which varied from source to source. Hence, it was dicided to conduct laboratory and field tests on the on-site materials.

TESTS CONDUCTED

In order to determine the relevant engineering characteristics of the fill materials, the following types of tests were conducted:

1 - Laboratory Tests
2 - Laboratory Model Tests
3 - Field Tests

Laboratory Tests

This phase of testing consisted of Conventional Index and Mechanical Properties Tests, X-Ray Defraction, Chemical Testing, and Pin Hole Test (to study piping potential).

Evaluation of the laboratory test results revealed the following were characteristics of ash and cinders fill:

1 - The grain-size of ash and cinders resemble well graded sand and gravel with 17 to 30% fines. (See Figure 3.)

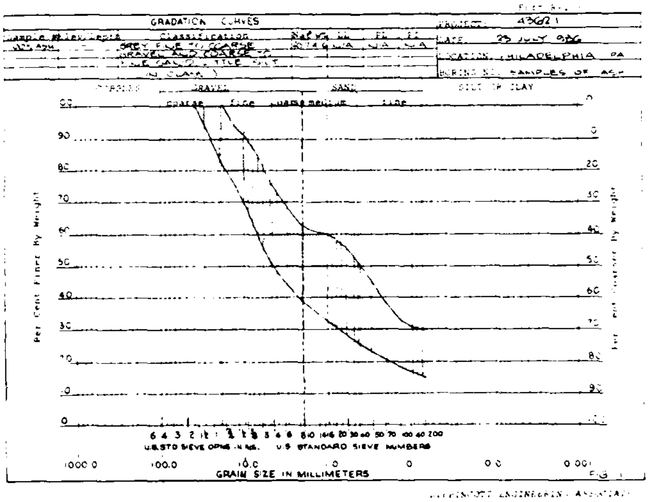

Figure 3 - Envelope of gradation analysis on Ash and Cinders

2 - The shear strength of loose ash and cinders is similar to that of loose granular materials. However; a greater, noticeable, drastic reduction of shear strength can be caused by flowing water.

3 - The maximum dry density is 88 PCF; the minimum density is 55 PCF.

4 - The specific gravity is 2.4.

5 - The consolidation characteristics are the same as granular soil coefficient of consolidation of one square foot per day was obtained. (See Figure 4)

6 - Ash and cinders are non-plastic materials.

7 - Loose ash and cinders are highly dispersive; compacted ash and cinders are not dispersive.

8 - The X-ray defraction indicated the primary constituent elements of the ash and

cinders are Al, Ca, Fe, and Si. Thirty-four percent of the sample was soluble in strong acid; 4% was soluble in tap water; however, 10% was soluble in weak acidic solution. (pH of 4)

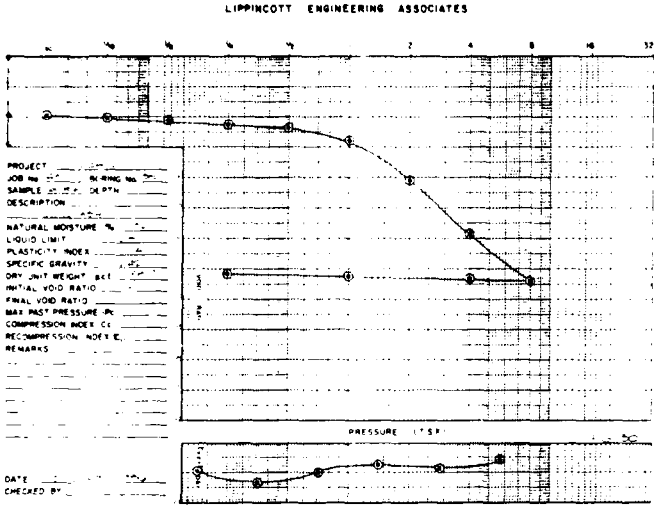

Figure 4 - Typical consolidation curve on Ash and Cinders near minimum density.

Laboratory Model Test

Based on the laboratory test results, it was felt that greater loss by piping, rather than consolidation, is the cause of the continuous settlement. To study this, a laboratory model was built and consisted of a 3 x 3 x 3 foot tank. A foot high layer of loose ash and cinders was placed in the bottom of the tank. The tank, then, was flooded several times with about one foot head of water. After the first flood, a reduction of 29% in volume was noticed. No further reduction was noted with further flooding. A second experiment was performed to study the piping potential of ash and cinders. In this experiment, a two inch diameter PVC pipe was buried in the middle of a two foot layer of ash and cinders. The pipe was perforated with 3/8 inch holes at six inch intervals, for the entire length of the pipe. Water was allowed to flow within the ash and cinder material. After one hour, the buried pipe was about half full of ash and cinders.

Field Plate Load Bearing Tests

To study the shear strength of the ash and cinders and the effect of water on shear strength, a plate load test was performed on ash and cinders in a test pit excavated to a typical foundation level. Standard plate load test procedures were followed with bearing pressure increased to 2000 PSF (estimate building bearing pressure). After one hour at 2000 PSF, a total settlement of approximately one inch was measured. To study the effect of water on the ash and cinders fill, the plate load test pit was flooded with a foot head of water, while the maximum bearing pressure was maintained on the plate; instantaneously as water was introduced into the test pit, the plate sunk four inches in the ash and cinders. A complete "loss of foundation supporting capability" was noted.

DISCUSSION OF TEST RESULTS

Based on the field and laboratory testing, these major observations were made:

1 - Primary consolidation of the loose ash and cinders probably resulted in four to twelve inches of settlement; however, settlement was completed within 12 to 24 months.

2 - Despite two to three feet of measured settlement, ash and cinders remain in a very loose state.

These two facts led us to rule out consolidation as a reason for continuous settlement. This, coupled with the result of the model testing and the pin hole test, led us to believe that ground loss by piping is the primary cause of the continuous settlement.

Our further investigation, which included house utility and city sewer line inspections ascertained that ash and cinders are piped through underground house utilities into the city sewer lines located in the city streets. This was confirmed by visual and television camera surveys of house utilities and city sewers and by the discovery of large quantities of ash and cinders within the city sewer system.

SEQUENCE OF EVENTS LEADING TO THE STRUCTURAL DISTRESS

Based on the discussion of the test results, the following is the probable sequence of events leading to structural distress in the dwellings:

1 - Initial settlement of four to twelve inches was experienced under the weight of the structures.

2 - This settlement resulted in breakage and opening of the joints in the underground cast iron and terra cotta utility pipes.

3 - Leakage of water from damaged pipes lead to continuous loss of shear strength of ash and cinders, leading to further breakage and opening of utilities.

4 - Ultimately, openings were large enough to allow piping to take place.

We expect the subsidence to continue indefinitely until repair work is done and all routes for piping are eliminated.

BUILDING DAMAGE

The two to three feet of total settlement and the one to two feet of differential settlement in the Logan Section has lead to severe damage to properties and has rendered some of the dwellings unsafe for occupancy. Three major types of distress resulted from the severe differential settlement; functional, structural, and architectural.

Functional Distress

This type of distress rendered several elements of the buildings unfit for their intended use. It is believed that most of the houses' underground utilities have suffered functional distress. Clogged or backed-up sewer lines are daily occurrences. In many homes, waste and waste matter drain directly into the fill below the houses and do not reach the sewer lines. Dye testing was performed by dropping dye in selected house toilets. Our observation indicated that the dye-marked water never reached the city sewers.

Severe differential settlement made living in the homes very difficult. This type of distress can be corrected.

Structural Distress

Based on the structural damage evaluation of the Logan Section dwellings, 100 homes were declared imminently dangerous. These homes were evacuated by the city. One hundred and ten (110) homes were declared dangerous. It was recommended that these homes be rehabilitated or demolished before reaching the imminently dangerous stage. The remainder of the homes were moderately dangerous and in need of rehabilitation before they progressed from dangerous to imminently dangerous.

Architectural Distress

The homes in the area visually exhibited the severe distress which the structures had endured. Most of the homes are leaning and tilting dramatically toward each other. Recent technological advances can be implemented to arrest further deterioration and possibly eliminate further movement; however, because of the age of the properties and the way in which the homes were constructed, there are no methods by which these homes can be made level. No matter how much money is spent on rehabilitation, the esthetics of the area will remain as is

CONCLUSION AND RECOMMENDATIONS

From an economical standpoint, the cost of rehabilitation of the homes will probably outweigh the present value of the structures; however, as Engineers, we feel that the following steps, if adapted, will arrest further deterioration and settlement of the homes.

It is our opinion that ground loss and migration of ash and cinders by piping can be reduced drastically by rehabilitating the underground utilities for all structures in the area. Rehabilitation of the city sewers and an increase in the number of drain inlets in the streets would reduce the potential for flooding and greatly reduce runoff infiltration. However, due to the increase in seismic activities in the Philadelphia area in the recent past, and due to unforseeable weather conditions, recommendations were given to underpin all the houses that will be rehabilitated using pinpiles extending to bedrock surface.

ACKNOWLEDGMENT

This study was paid for by the Department of Licenses and Inspections (DL/I) of the City of Philadelphia. The assistance of the city department heads and particularly, of Mr. David L. Wismer, Deputy Commissioner of DL/I, is greatly appreciated. The writers also appreciate the valuable comments by Mr. Charles Sutphen of Lippincott Engineering Associates. Special thanks also to Mr. Dusan Jovanovic and Mary Ann Kozachenko, and Carol Adams, all of Lippincott Engineering Associates for their assistance on this paper.

REFERENCES

There is very little literature written about the use of ash and cinders as controlled fill or about the geotechnical characteristics of ash and cinders; however, several papers on flyash were reviewed during the preparation of this report.

Chae, Yong S., and Snyder, James L., "Vibratory Compaction of Flyash".

Cunningham, June A., et al., "Impoundment of Flyash and Slag".

Collins, Robert J., "Highway Construction Use of Incinerator Residue".

Seal, Roger K., et al., "In-Situ Testing of Compacted Flyash".

All the above papers were presented in the "Geotechnical Practice for Disposal of Solid Waste Materials", June 13-15, 1977, University of Michigan, Ann Arbor.

Proceedings: Second International Conference on Case Histories in Geotechnical Engineering, June 1-5, 1988, St. Louis, Mo., Paper No. 6.50

Design and Field Monitoring of 70-Foot High Tied Anchor Retaining Wall

Nolasco P. Angeles
Structural Consultant, Smith, Hinchman & Grylle Associates, Inc., USA

Ulrich W. Stoll
Consultant, Soil and Materials Engineers, Inc., USA

SYNOPSIS: Temporary tied anchor retaining walls have been used extensively where deep excavations are required. However, permanent tied anchor retaining walls to provide lateral support along one side of a multi-story building are seldom utilized. The wall was monitored for deflection and tie load changes during and after construction. A partial detensioning program was instituted in order to maintain the design stresses.

INTRODUCTION

To meet site conditions and to provide for economical and flexible interior space, lateral support for a seven-story office building was provided by an integral, tied anchor retaining wall along one side. Figure 1(a) indicates the building outline in its relation to the adjacent sloping topography which necessitated permanently shoring an excavation about 800 feet in length and to a maximum depth of 70 feet. The general concept envisioned first excavating and shoring to the base elevation over the building site, constructing the building foundations, over a scheduled 6-month period, and then constructing the final exterior wall incorporating the shoring and with the tied anchor system providing the permanent lateral support of long-term earth pressures. Because of the critical, dual function of the shoring scheme, a specifically designed load cell and slope indicator installation and observation program was incorporated into the construction contract, rigorously adhered to, with data concurrently analyzed and findings acted upon.

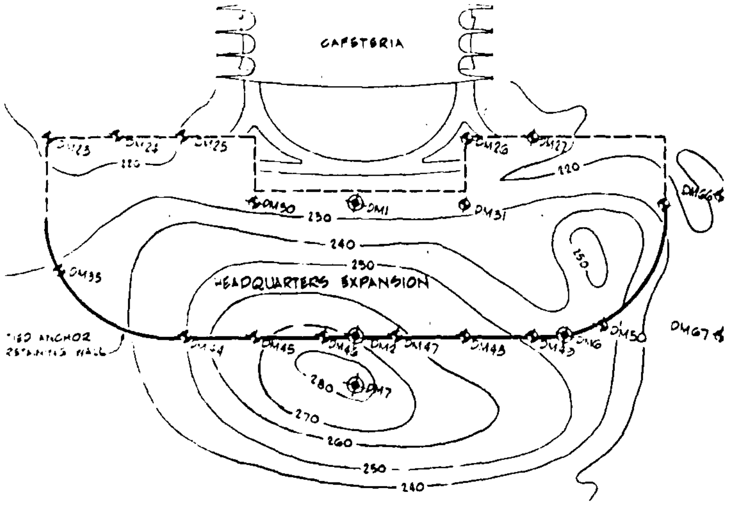

Fig. 1(a) Building Site Plan

This paper describes salient details of the subsoil conditions, the structural design and the monitoring scheme, and summarizes observations and adjustments made during construction.

SUBSOIL CONDITIONS

The building is located in the Virginia Piedmont, characterized by bedrock primarily of igneous and metamorphic origin. These are comprised of granite, shist, metasedimentary, metaigneous and metavolcanic rock types. Bedrock surface is somewhat irregular and usually covered by weathered residual material, called saprolite. Bedrock map of the site indicates gneiss and granofels, with a mineral composition of quartz, feldspars, mica and chlorites. It commonly has two steeply inclined foliations, locally faulted and sheared, with steeply dipping intersecting joints spaced 3 feet or more apart.

The specific site investigation involved drilling and recovering and evaluating samples from soil and rock borings, located as indicated on Figure 1(a).

A typical soil profile log is that for Boring DM-46, shown as Figure 2. We note soil overburden of saprolite, with texture ranging from clayey silt in the fully weathered upper stratum to the partially weathered gravelly sandy silt with increasing amounts of interbedded, moderately weathered gneissic rock as one approaches bedrock at a 75-foot depth at this location. Standard penetration blow counts N are in excess of 100 blows per 6 inches below about 30 feet from the surface, in association with the partially weathered stratum. The bedrock was cored, indicating moderately fractured granite gneiss, with about 97 percent recovery. Although the upper clayey stratum was moist, there was no free water encountered in the boring and the boring was dry upon completion.

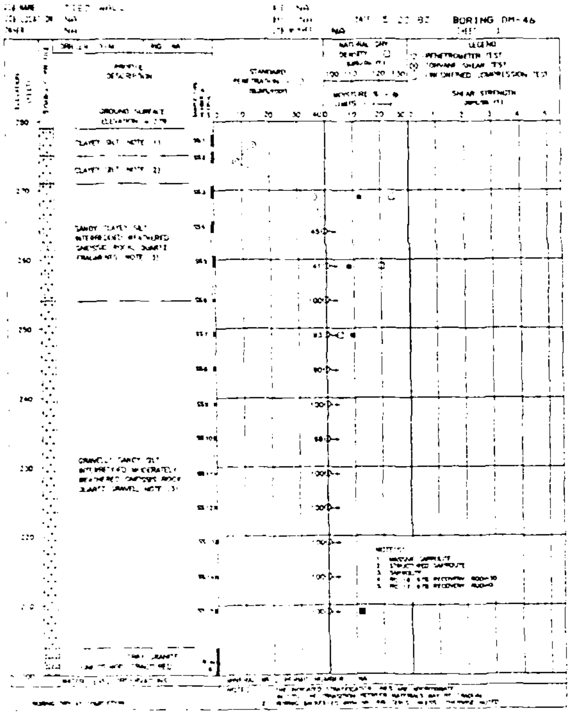

Fig. 2 Typical Soil Profile Log
Boring DM-46

A generalized soil profile is indicated on Figure 3 based on the other borings along or adjacent to the proposed location of the shored wall. The soil strata have been designated on the basis of similar, salient characteristics as follows:

Zone A - Massive saprolite, with unclear evidence of primary structural features of the parent rock. At the site it ranges only a few feet in thickness.

Zone B - Structured saprolite, with clear evidence of primary structural features of the parent rock (i.e., foliation, jointing, crystal structure). At the site it ranges generally from 20 to 30 feet thick.

Zone C - Saprolite, a transitional zone, grading from the structured, substantially fully weathered Zone B to the relatively intact bedrock (i.e., Zone D). At the site it ranges from about 40 feet in thickness at the middle half of the wall alignment to perhaps 10 to 15 feet at the ends.

It is noted that the proposed subgrade of the building roughly coincides with the bedrock surface along the wall alignment, but bedrock surface rising as much as 5 feet above subgrade Elevation 205 at some locations. This fact was recognized and accounted for in the shoring design and contract documents.

DESIGN OF PERMANENT TIE BACK SHORING AND BUILDING WALL

In view of the dual function of the tie back wall, the design lateral forces were predicated on assuring "at rest" earth reactions. The assigned pressure coefficients ranged from Ko = 0.45 (i.e., N < 60) in Zone A and upper Zone B, to a minimum 0.30 in Zone C (i.e., N > 100/6"). It was recognized that these coefficients lead to relatively conservative loadings, appreciably above those ordinarily appropriate for temporary excavation shoring. But in view of the critical nature of the structure and absence of documented observations of long-term performance of tied walls in similar circumstances, it was deemed prudent not only to assign the design lateral loads to account for the varying soil resistance, but to also incorporate a load and deflection monitoring system into specific wall elements and monitor and evaluate measurements during construction.

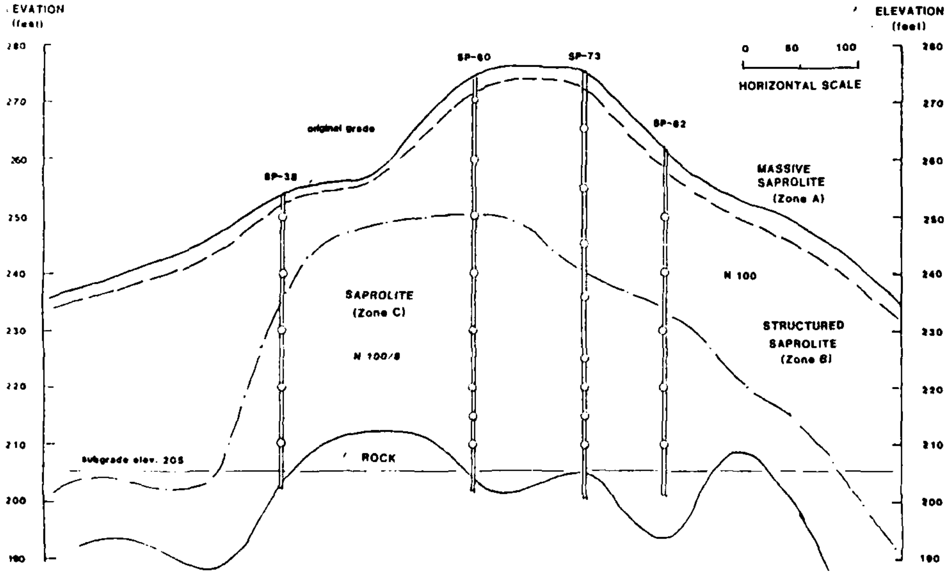

Fig. 3 Generalized Soil Profile
Location of Slope Indicators and Tied Anchor Load Cells

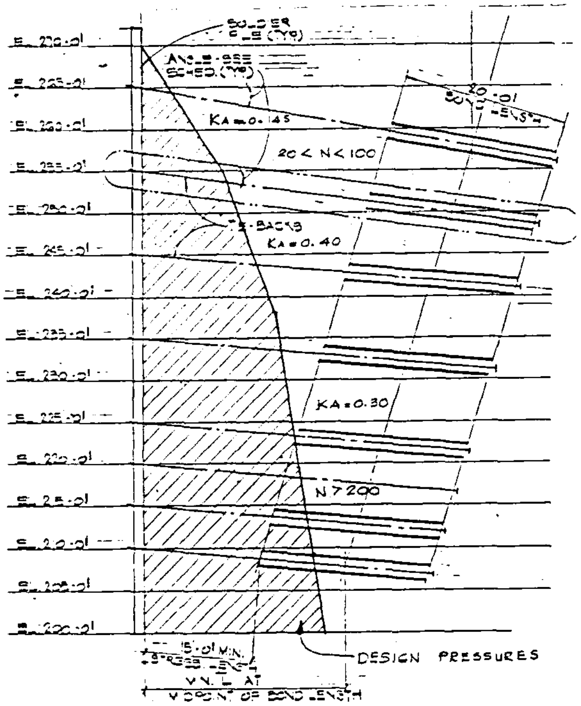
SOLDIER PILE (TYP)
KA=0.45
20 < N < 100
KA=0.40
KA=0.30
N > 200
DESIGN PRESSURES
15'-0' MIN.

Fig. 1(b) Section thru Tied Anchor Wall including Design Pressures

Figure 1(b) shows a section through the deepest portion of the tie wall, indicating the design pressures and attendant vertical tie spacing and embedded lengths of pressure grouted anchor rods, based on soldier piles at lateral spacing of 7.5 feet to permit use of conventional wood lagging. Typical details of the soldier piles, tie anchors, and wood lagging of the temporary shoring are included in Figures 4(a) and 4(b). Details of the finished structural wall incorporating the temporary shoring and interposed bentonite panel waterproofing are shown in Figure 4(c).

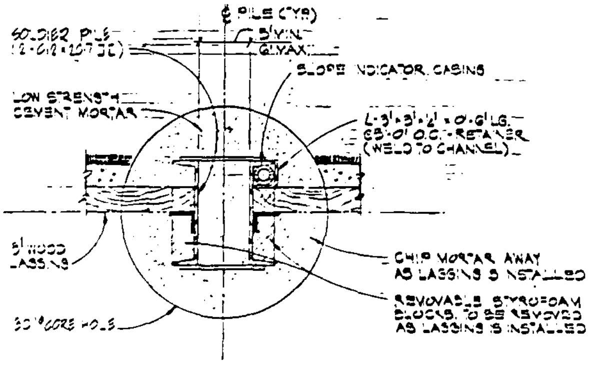
SOLDIER PILE
℄ PILE (TYP)
LOW STRENGTH CEMENT MORTAR
SLOPE INDICATOR CASING
3' WOOD LAGGING
CHIP MORTAR AWAY AS LAGGING IS INSTALLED
REMOVABLE STYROFOAM BLOCKS, TO BE REMOVED AS LAGGING IS INSTALLED
30"⌀ CORE HOLE

Fig. 4(a) Detail - Soldier Pile and Wood Lagging

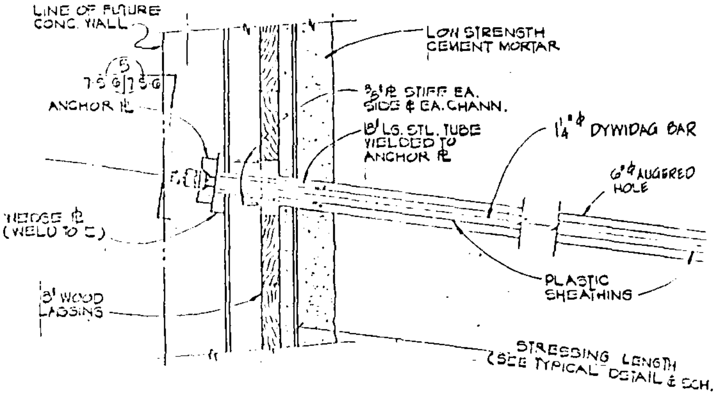
LINE OF FUTURE CONC. WALL
LOW STRENGTH CEMENT MORTAR
ANCHOR ℄
18' LG. STL. TUBE WELDED TO ANCHOR ℄
1¼"⌀ DYWIDAG BAR
6"⌀ AUGERED HOLE
WEDGE ℄ (WELD TO C)
3' WOOD LAGGING
PLASTIC SHEATHING
STRESSING LENGTH (SEE TYPICAL DETAIL & SCH.)

Fig. 4(b) Detail - Anchor Tie

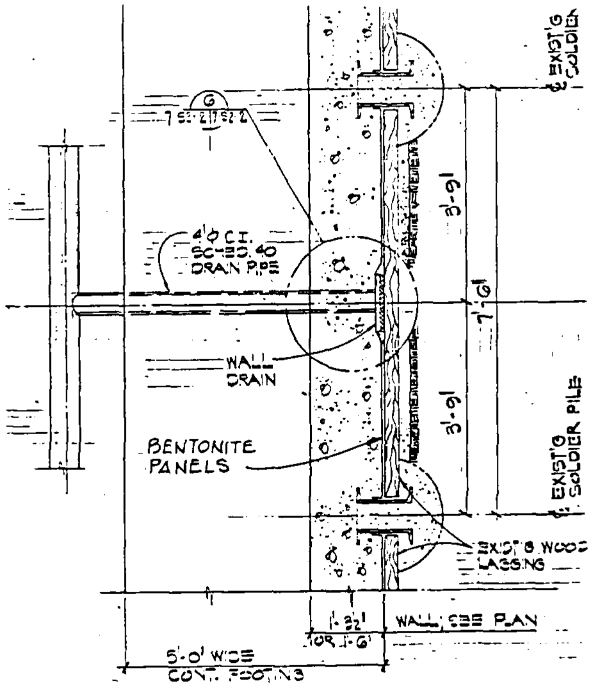
EXIST'G SOLDIER PILE
4'⌀ C.I. SCHED. 40 DRAIN PIPE
WALL DRAIN
BENTONITE PANELS
EXIST'G WOOD LAGGING
3'-9"
7'-6"
WALL; SEE PLAN
5'-0' WIDE CONT. FOOTING

Fig. 4(c) Typical Detail - Finished Structural Wall

The tied anchor wall, 800 feet long, consisted of 119 steel soldier piles spaced at 7'-6" o.c., 3-inch wood lagging, 555 - 1-1/4 inch diameter Dywidag steel threadbar rods, and 15-1/2 to 18 inch reinforced concrete wall. The steel soldier piles, made up of two 12-inch channels assembled back to back, vary in height from 25 feet at the ends of the wall to 70 feet at the center. The number of tiebacks vary from two at the 25-foot minimum wall height to eight at the 70-foot maximum height. The tiebacks were spaced at 10'-0" to 5'-0" o.c. and staggered.

Design load on a tieback is 56 tons, except for the upper which included several at 36 tons. Each of the 555 tiebacks was load tested up to

115 percent of design load, except that 10 percent selected ties were tested to 134 percent of design load or 75 tons.

Load cells and slope indicators were installed at four selected soldier piles in order to monitor the behavior of the tied anchor wall during construction and approximately 180 days after completion (see Figures 3 and 4(a)).

Vertical wall drains between soldier piles were provided and Volclay Type C bentonite waterproof panels were fastened to the wood lagging prior to placing a reinforced concrete wall, 15-1/2 to 18 inches thick (see Figure 4(c)). The concrete wall was designed to span between soldier piles.

Figure 3 shows the location of four slope indicator tubes incorporated with the designated soldier piles. A total of 27 load cells were installed at these soldier piles, attached to the ends of the tie anchors as these were drilled and tensioned in the course of excavation. All were monitored at regular intervals during and subsequent to excavation and shoring. The remainder of this paper focuses on the findings and the response and/or conclusions in light of those findings.

LOAD CELL AND SLOPE INDICATOR OBSERVATIONS - DURING AND SUBSEQUENT TO EXCAVATION

The general shoring sequence involved installing all the soldier piles into 30-inch diameter, predrilled holes and backfilling with cement stabilized sand. Excavation proceeded in 5- to 10-foot increments, extending about 2 feet below the designated elevation of anchor ties in each increment. The ties were installed by drilling and grouting via a 6-inch diameter hollow stem auger and were tensioned generally three to four days thereafter. Subsequent to completion of each excavation increment but prior to tie tensioning, all the slope indicators and installed load cells were monitored. During the initial stages of excavation, slope indicators and load cells were also monitored after tie tensioning, prior to proceeding with additional excavation, but it became evident that tensioning the lower tier had insignificant influence on the loads on the previously installed ties at higher elevation.

The general interrelation between depth of excavation and changes in slope indicator profile and associated load cell readings are illustrated in Figure 5, at soldier piles SP-60. The following is particularly noteworthy:

1) The maximum lateral deflection was about 24 millimeters (i.e., 1 inch) and occurred in the course of excavating in Zone C, saprolite.

2) Discrete increments of lateral movements developed while excavating successive depth increments Zone C.

3) Lateral movements caused a significant increase in the tension forces in the adjacent tie anchor(s). Note in Figure 5, load on tie anchor at Elevation 240 increased from 57.2 tons immediately after installation, up to 62.9 tons when excavation reached nominal Elevation 230 and to 67.0 tons with excavation at 220. Also, tie load at Elevation 230 increased from 58.2 tons to 65.1 tons with excavation at 220. Similar response was noted at all the instrumented soldier piles in the course of excavating in Zone C (saprolite).

These movements had not been originally anticipated and corresponding tie load increases were of a magnitude to require corrective action. A review of the slope indicator profile did not suggest that the lateral movements were deep seated nor extending beyond the tied anchors. Also, there was no indication of moisture movement to cause swelling of the exposed face of the freshly excavated soil. On the other hand, the freshly exposed saprolite was steeply jointed and comprised of relatively hard chunks of weathered rock, with the fractured surfaces only weakly adhering to each other. One could observe during the smoothing of the exposed face preparatory to placing the wood lagging that soil readily broke off along the steep joints, particularly in Zone C. These circumstances were discussed with Professor George Sowers of Georgia Tech University and he advised of similar response he had observed when excavating in deeply weathered rock and residual soils in the Atlanta area and Piedmont in general. He speculated that deflections were due to mechanical rearrangement of the fractured materials and would stabilize after a relatively short period. He concurred with proceeding with a tie detensioning program and on-going tie load monitoring.

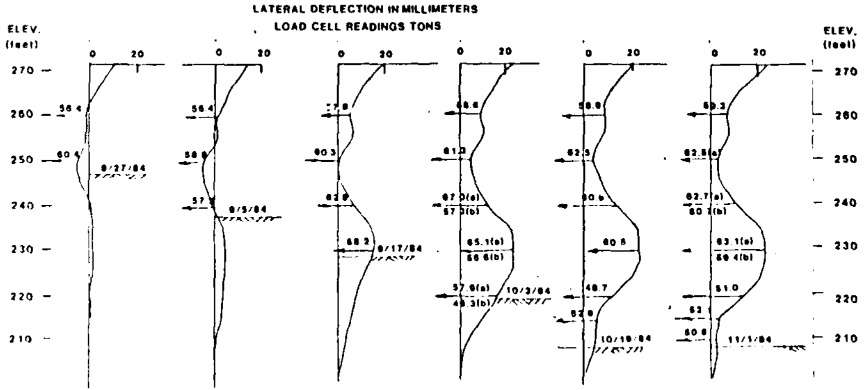

Fig. 5 Tie Loads - Lateral Deflection at SP-60

The scheme was as follows:

a) Commencing from a load cell indicating greater than 63 tons, the tensioning jack was reset at an adjacent tie and tension loaded until unseating the anchor nut, noting the force required. If force exceeded 63 tons, tie was detensioned to design load (i.e., 56 tons).

b) If a specific tie anchor was unseated by load greater than 63 tons, all adjoining ties were unseated and detensioned as per a) above.

c) If specific tie anchor was unseated by load less than 63 tons, further detensioning ties at that tier elevation were discontinued moving outward from the starting point in this test sequence.

Figure 6 indicates the location and number of times that specific tie anchors were unseated and detensioned in accordance with the above protocol. Of a total of 555 ties installed, 185 were detensioned either before or shortly after completion of excavation. It is clearly evident that the detensioned ties were concentrated in the Zone C saprolite strata as interpolated from the original soil investigation, Figure 3. Further, only 32 ties were detentioned twice, and these are clustered in the thickest portion of Zone C, between SP-40 and 75.

Although the reported initial unseating loads exceeded 75 tons in three instances, these are questionable since the jacking assembly registered unseating loads up to 6 tons greater than for corresponding load cell readings. The specific unseating and detensioning scheme was aimed at assuring a safe structure and jacking loads were too crude to define trends in load changes accurately subsequent to completion of excavation. However, Figure 7 indicates load cell readings for critical ties over about a 6-month period subsequent to completion of excavation and initial detensioning. The following is noteworthy:

a) The logarithmic time plot indicates a decelerating increase in tie loads over the observation period.

b) The load increase observed over 6 months ranges from 2,5 to 4.5 tons.

c) There is evidence that tie loads had reached equilibrium after 6 months.

d) Load cell readings were appreciably affected by environmental factors, particularly during the winter and spring observation period with indicated loads fluctuating up to 1 ton from the trend lines.

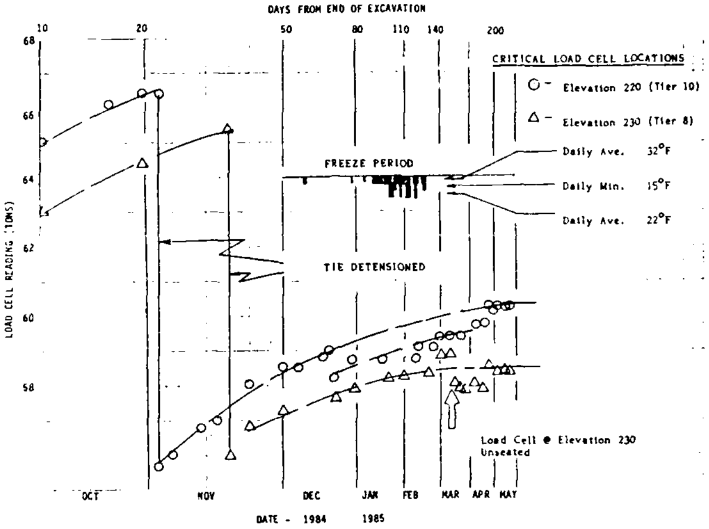

Fig. 7 Load Cell Readings After Excavation Completed - SP-82

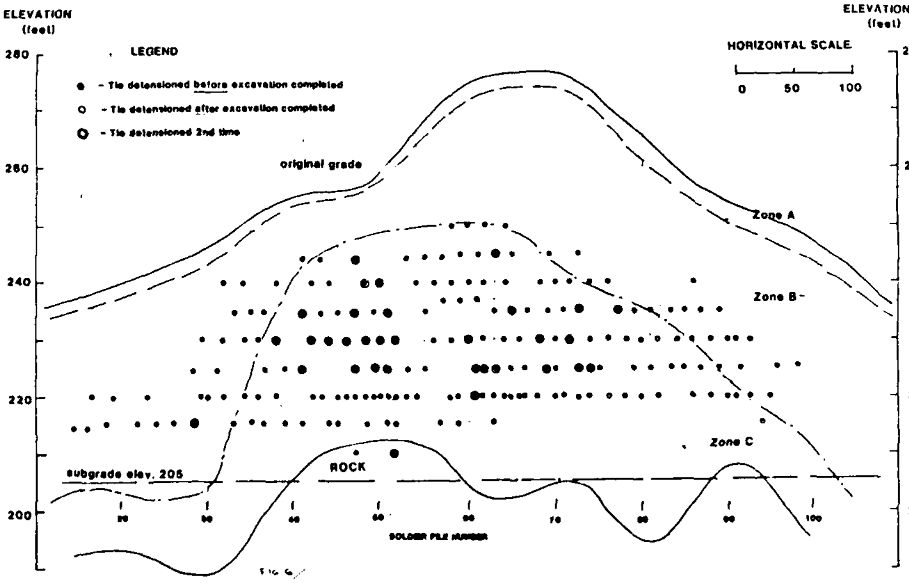
ELEVATION (feet)
280
260
240
220
200
LEGEND
● - Tie detensioned before excavation completed
○ - Tie detensioned after excavation completed
O - Tie detensioned 2nd time
original grade
HORIZONTAL SCALE
0
50
100
ELEVATION (feet)
280
260
240
220
200
Zone A
Zone B
Zone C
ROCK
subgrade elev. 205
20
30
40
50
60
70
80
90
100
SOLDIER PILE NUMBER

Fig. 6 Summary of Tied Anchor Detensioning

The observations as a whole indicate that lateral expansion in the course of excavation in Zone C can reach 1 inch and cause the tie loads to increase about 10 to 15 tons from installed values (i.e., from 56 tons to over 70 tons). Of that increase, from 2.5 to 4.5 tons was attributable to long-term expansion of Zone C, essentially completed in about 6 months at this site.

ANALYSIS OF EFFECT OF BENTONITE PANELS IN PERMANENT WALL

As indicated in Figure 4(c), the finished structural wall incorporated the temporary shoring, with bentonite waterproofing panels sandwiched between the wood lagging and the poured concrete wall. There had been a general concern that should the bentonite panel swell subsequent to the hardening of the concrete in the wall, tie loads in the affected areas might increase. Selected load cells were prepared to permit monitoring during the initial wall pours. Concurrently, load-swelling information was obtained from the panel supplier and load-compression relationship of the granular backfill behind the wood lagging determined.

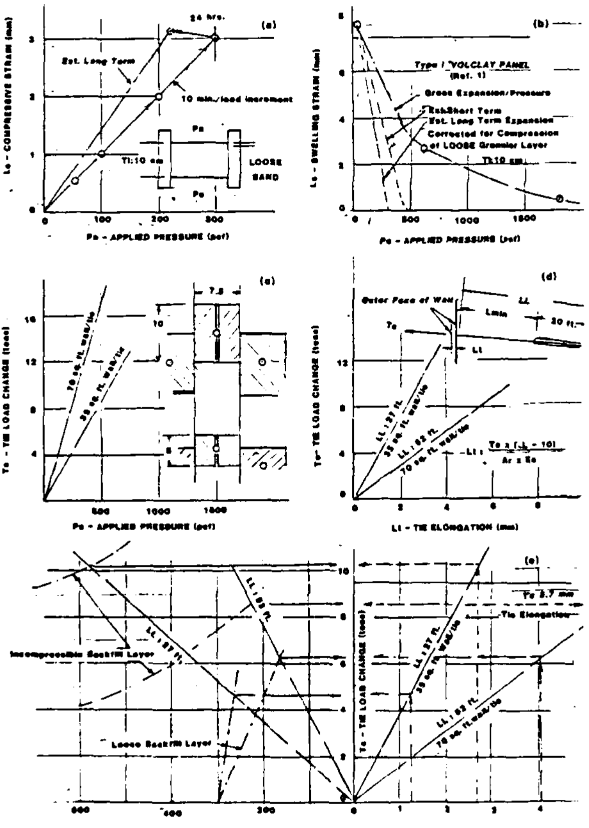

Fig. 8 Effect of Bentonite Panel Expansion On Tie Anchor Loads

Figure 8 indicates the essential factors and the corresponding parameters used to estimate the tie load increases attributable to swelling of the bentonite panels. Figure 8(a) shows relation between compressive strain and applied pressure for loose granular soil deemed representative of backfill as placed. Figure 8(b) plots the ultimate swelling strain versus applied confining pressure for the bentonite panel. As indicated in Figure 4(c) the strain corresponds to inward movement of the concrete wall relative to the inner surface of the wood lagging. This relation is corrected as indicated for the estimated short- and long-term outward strain of the wood lagging as it compresses the backfill at the same and corresponding applied pressure. Figures 8(c) and (d) show interrelation between changes in net swelling pressures and corresponding changes in tied anchor loads and strains for the applicable wall areas of influence. Finally, Figure 8(e) interrelates the tie load changes and rod length changes and associated swelling pressures and attendant wall movements, corrected for assumed extremes of compressibility of backfill. It is noted that for the range of effective lengths of tie rods (i.e., 27 to 52 feet) and associated areas of wall supported (i.e., 70 to 35 square feet, respectively), the calculated tie load increases ranged from 4.5 to 6 tons up to an outer limit of 8.5 to 10 tons, depending on the compressibility of the backfill retained by the wood lagging.

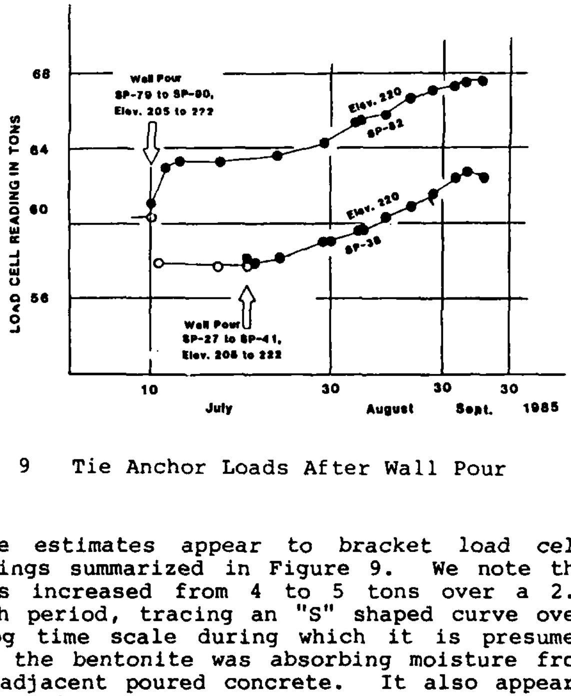

Fig. 9 Tie Anchor Loads After Wall Pour

These estimates appear to bracket load cell readings summarized in Figure 9. We note the loads increased from 4 to 5 tons over a 2.5 month period, tracing an "S" shaped curve over a log time scale during which it is presumed that the bentonite was absorbing moisture from the adjacent poured concrete. It also appears that swelling was completed in about 2 months in these circumstances. To the writers' knowledge there has been no visual manifestation of additional swelling or tie load increase during the succeeding two years.

SUMMARY

Observations of a tied anchor retaining wall, ranging up to a 70-foot height in variable residual soil and weathered rock indicated unanticipated variable lateral movements up to 1 inch due to a rapid and limited expansion of the partially weathered rock (i.e., saprolite) during excavation. This was evidently due to localized mechanical rearrangement as the heavily jointed and fractured stratum was first exposed. Attendant anchor loads increased from a design load of 56 tons to over 70 tons during and immediately subsequent to excavation. Affected tie anchors were subsequently unseated and partially detensioned one or more times where necessary to re-establish design load values. Tie loads were observed to increase at a sharply reduced rate over about 6 months after completion of excavation, limited to 4.5 tons above the original 56 tons.

Analysis indicated that bentonite waterproofing panels incorporated behind the structural wall could swell sufficiently to appreciably increase the affected tie anchors. Load cell readings increased over a 2-month period, leveling out at a maximum 4-ton increase. Depending on the compressibility of fill behind the wood lagging, analysis suggests increases might reach 8 tons in particular circumstances.

ACKNOWLEDGEMENTS

The original geotechnical investigation and geological analysis for the project was performed by Dames and Moore, John Kittridge, Project Manager. Woodward Clyde Associates supervised installation and monitored the load cells and slope indicators.

Proceedings: Second International Conference on Case Histories in Geotechnical Engineering, June 1-5, 1988, St. Louis, Mo., Paper No. 6.51

Performance of Foundations and Retaining Structures

Daniel P. Gado
Associate, Langan Engineering Associates, Inc., Elmwood Park, New Jersey

John J. McElroy
Assistant Project Engineer, Langan Engineering Associates, Inc., Elmwood Park, New Jersey

George P. Kelley
Vice President, Langan Engineering Associates, Inc., Elmwood Park, New Jersey

SYNOPSIS: The design, construction, and performance of several building foundations and temporary earth retaining structures located in the downtown area of White Plains, New York are presented in this paper. High rise structures were supported on shallow mat or spread foundations bearing on erratic saturated alluvial silt and sand deposits. Additionally, the construction of two and three level underground parking structures required the use of cantilevered and braced excavation support systems to retain the adjacent streets and utilities. Several assumptions were required to design and predict the performance of the building foundations and retaining structures. The accuracy of these assumptions was verified through the use of precise field measurements during and after construction. The results of these field measurements and comparison with predicted values are presented and discussed.

INTRODUCTION

Foundation problems had impacted the growth of the White Plains core area since the founding of the City. Located in prestigious Westchester County, just 12 miles north of New York City, the City of White Plains had experienced prosperity in certain areas while others were depressed and economically unproductive. While the east side flourished and major structures were constructed on competent bearing materials, the west side remained under-utilized and was occupied by substandard small buildings.

During the 1970's, the structures in the western portion were totally demolished during the early stages of the urban renewal program but only the surface problems were cleared; the complex subsurface soil strata remained to be dealt with by future redevelopment. The difficult subsurface conditions and asssociated high cost of foundations continued to hamper the redevelopment effort and the land remained vacant for many years.

Market forces demanded high rise, high quality structures and underground parking structures were required to satisfy zoning ordinances. The subsurface soil conditions with erratic layers of sensitive "bull's liver" silt, pockets of loose and variable density sands, a deep bedrock stratum, and a shallow groundwater table unfavorably impacted this type of construction and created numerous design challenges.

The authors became involved with the first building of the reconstruction effort in 1974 and subsequently for an additional 20 structures within the White Plains core area. The extreme subsurface variations coupled with the fact that conventional soil sampling was unreliable, complicated the design of cost effective foundation and excavation support systems. Since numerous design assumptions were required, it was necessary to confirm these during construction through precise monitoring under actual fully loaded conditions.

As performance results became available, more confidence in various design procedures resulted, and it was possible to perform refinements or "fine tune" designs to achieve additional efficiency and related savings in construction costs for shallow foundations and support systems for excavations. A series of case histories are presented which illustrate the design and analysis procedures utilized on some of the projects. Performance results are provided for these projects as well as other projects not specifically discussed in detail. A site location map showing the project areas to be discussed is presented in Figure 1.

SUBSURFACE CONDITIONS

The downtown area is generally underlain by fill material, river alluvium, glacial till and gneiss bedrock. The fill consists of building materials mixed with soils and has been placed within the past 200 years. The river alluvium consists of sand and discontinuous silt deposits and is of the Holocene or the late Pleistocene (glacial) epoch. The glacial till of the Pleistocene epoch is composed of a heterogenous mixture of silt, sand and gravel soil with occasional boulders. The Fordham gneiss formation of the Precambrian period is predominantly granitic with occasional schistose and quartzose zones.

The stratigraphy beneath the Westchester Financial Center and the Gateway Project sites is consistent with the general subsurface conditions presented above with the exception of the absence of a continuous alluvial silt deposit beneath the Gateway sites. The general subsurface conditions beneath the downtown area and the location of the subject buildings are presented in Figure 2.

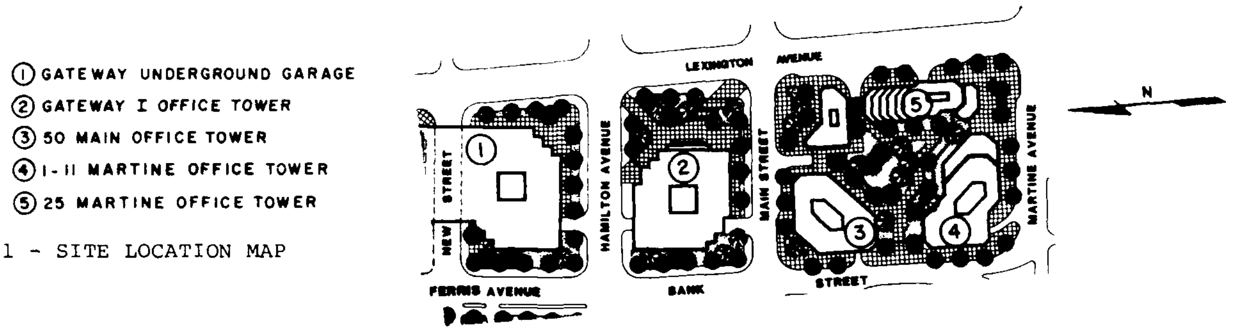
① GATEWAY UNDERGROUND GARAGE
② GATEWAY I OFFICE TOWER
③ 50 MAIN OFFICE TOWER
④ 1-11 MARTINE OFFICE TOWER
⑤ 25 MARTINE OFFICE TOWER
LEXINGTON AVENUE
N
NEW STREET
HAMILTON AVENUE
MAIN STREET
MARTINE AVENUE
FERRIS AVENUE
BANK
STREET

FIG. 1 - SITE LOCATION MAP

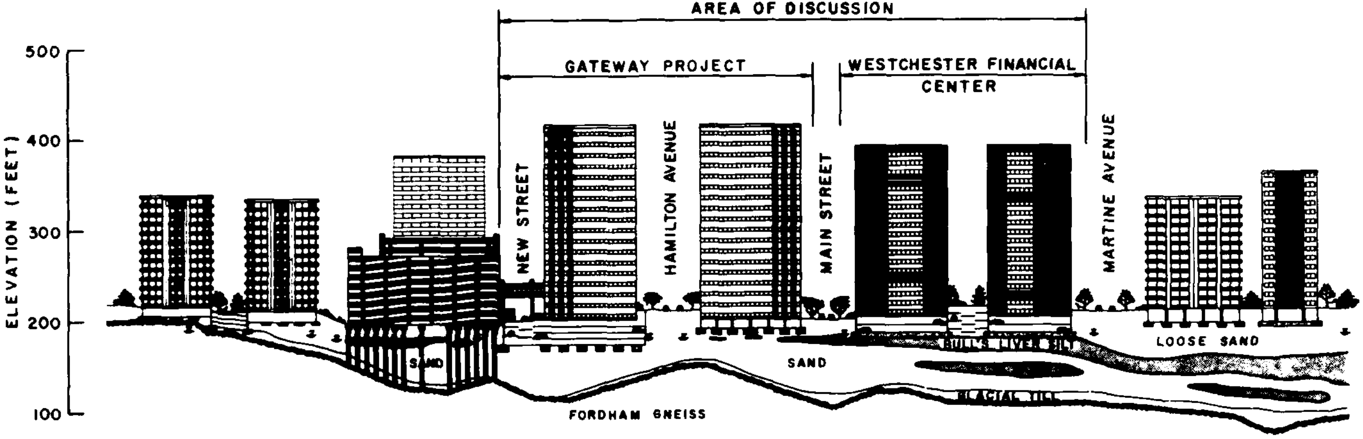
AREA OF DISCUSSION
GATEWAY PROJECT
WESTCHESTER FINANCIAL CENTER
500
400
300
200
100
ELEVATION (FEET)
NEW STREET
HAMILTON AVENUE
MAIN STREET
MARTINE AVENUE
SAND
LOOSE SAND
BULL'S LIVER SILT
GLACIAL TILL
FORDHAM GNEISS

FIG. 2 - GENERAL SUBSURFACE PROFILE

The Westchester Financial Center is underlain by saturated alluvial silt and sand deposits. The silt deposit exhibits extreme dilative characteristics and is locally known as "bull's liver" due to its shiny appearance. The silt is generally encountered at or below the groundwater level and possesses a high sensitivity to construction disturbance. The alluvial sand is composed of an upper and lower deposit which are separated by the silt stratum. The thin glacial till layer overlies the rock which is at a depth of approximately 100 feet (ft) from the ground surface.

The Gateway sites are underlain by a continuous alluvial sand deposit which extends to the glacial till or rock surface. The sand contains occasional thin silt lenses located near the groundwater level. The depth to rock varies from 50 to 80 ft below the ground surface.

FOUNDATION DESIGN AND PERFORMANCE

Details concerning foundation design, construction, and performance of specific case histories will be discussed.

Westchester Financial Center

50 Main Office Tower/1-11 Martine Office Tower

These office towers are both 15 story cast in-place concrete structures with post tensioned concrete floors and architectural facades composed of stone and glass panels. A 2 level underground garage structure is common to both buildings. The footprint area of the towers are 28,000 square feet (sf) for 50 Main and 20,000 sf for 1-11 Martine. The lowest garage floor is located at elevation (el) 185 ft and the foundation subgrade is located at el 180, approximately 20 ft below street grade. The design loads vary from 1500 to 4000 kips per column.

Subsurface Conditions

The subsurface conditions beneath the building areas are similar. The dilative silt or silty fine sand deposit was encountered at foundation subgrade and the groundwater level was at 1 to 3 ft above the bottom of the foundations. The non-plastic silt is varved with fine sand seams and was in a loose to medium dense condition. The water contents range from 22 to 40 percent, the liquid limit and plastic index are approximately 29 and 6, and the virgin compression ratio is approximately 0.06. The thickness of the silt varies from 0 to 25 ft. The lower sand deposit underlying the silt layer is in a medium dense to dense condition. The design and subsurface conditions are shown on Figures 3a and 4a.

Foundation Construction

Soil improvement procedures in conjunction with 4 to 5 ft thick reinforced concrete mat foundations were used to transfer the heavy column loads to the subsoils. A majority of the foundation subgrade consisted of the saturated silt or silty fine sand soils which varied in thickness and density. The denser lower sand deposit also formed a portion of the subgrade. A mat foundation was used to span the variable subgrade and to limit differential settlement that would have occurred for a conventional spread footing system.

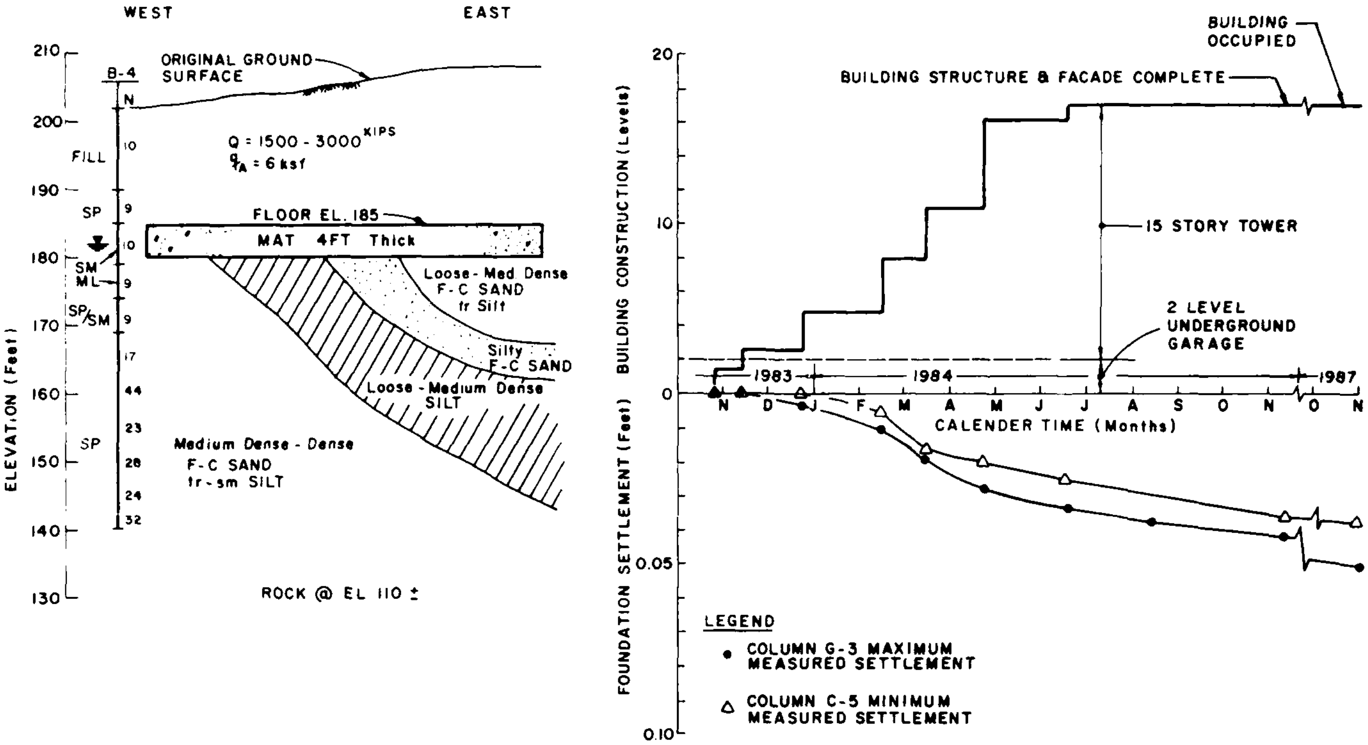

a. Design Conditions

b. Mat Foundation Settlement Versus Construction

FIG. 3 - 50 MAIN OFFICE TOWER

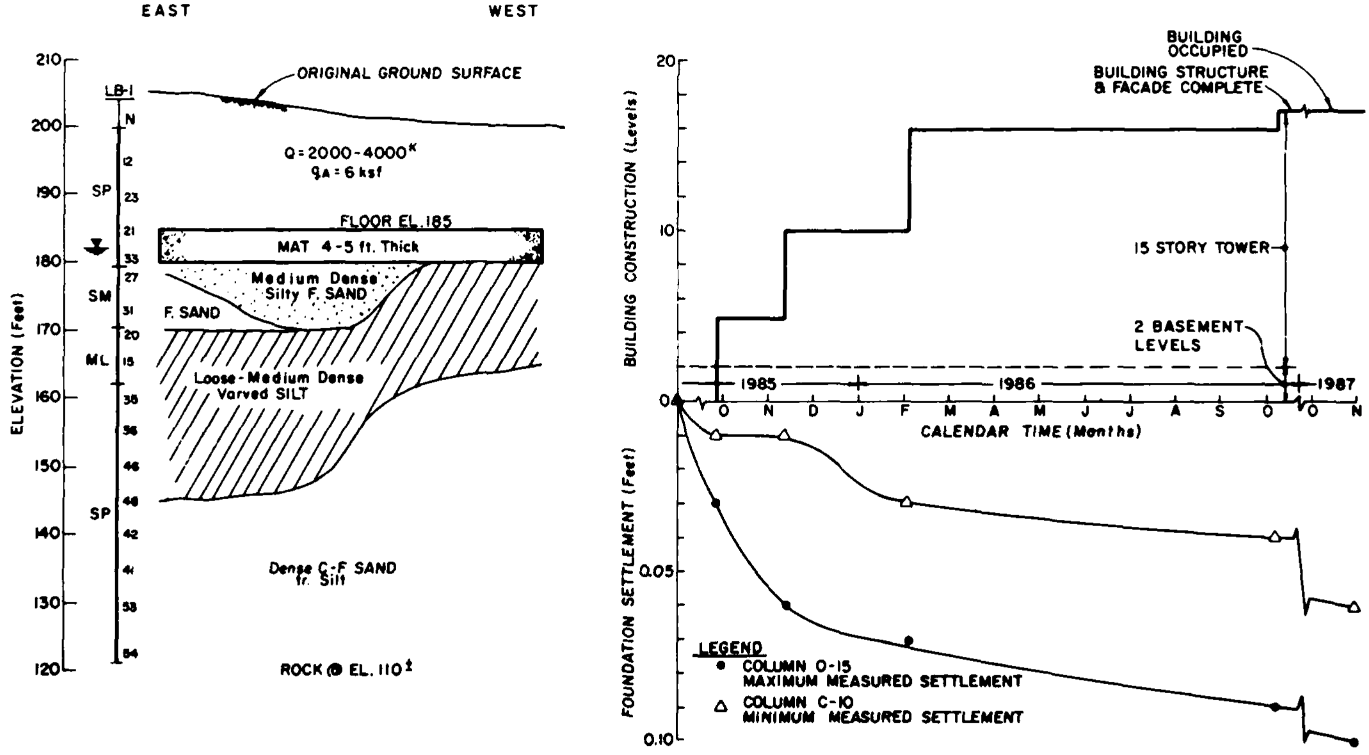

a. Design Conditions

b. Mat Foundation Settlement Versus Construction

FIG. 4 - 1-11 MARTINE OFFICE TOWER

Prior to the construction of the mat foundations, the following soil improvement procedures were accomplished to control groundwater seepage and to stabilize and confine the silt subgrade soils.

1. Overexcavation of the silt to a depth of 2 ft below the foundations.
2. Placement of a geotextile on top of the silt subgrade.
3. Placement of compacted 3/4 inch stone backfill to foundation subgrade.

A mold blade backhoe bucket was used to excavate the silt soil below foundations to minimize the disturbance of this sensitive soil. Groundwater seepage from the silt was controlled using the stone backfill and conventional pumps. Following the placement of the stone backfill, a 2 inch thick concrete "mud mat" was poured to provide a working surface for construction of the mat foundations.

Foundation Design

The foundations were designed as flexible mat foundations using the Portland Cement Association MATS computer analysis. An allowable soil bearing pressure of 6 ksf and a modulus of subgrade reaction (K) of 100 kips per cubic foot (kcf) were selected for the design of the 50 Main mat. Since the 50 Main structure was completed prior to the design of the 1-11 Martine building, the performance results from the completed building were used to refine the analysis for the design of the later structure.

Predictions

The two methods of analyses selected to estimate the settlement of the mat foundations were the D'Appolonia (1968) and the Schmertmann (1970) analyses. Both methods are applicable for layered granular soils. Since the silt exhibited non-plastic behavior it was analyzed as a cohesionless soil. The D'Appolonia approach was used with a weighted average elastic modulus for the layered soil profile. An estimation of elastic moduli of the soil layers was based on a correlation with Standard Penetration Test (SPT) N values. The Schmertmann approach uses a layered soil profile, cone penetrometer resistance, and a graphical plot of strain influence values as a function of depth to footing width. The cone penetrometer resistance was estimated using a correlation with SPT N values as a function of grain size. The predicted settlements for the 50 Main and 1-11 Martine mat foundations are presented on Table 1.

TABLE 1: Predicted Settlements - 50 Main and 1-11 Martine Mat Foundations

	D'Appolonia (1968)	Schmertmann (1970)
Total Settlement (ft) 50 Main Mat	0.20	0.09
Total Settlement (ft) 1-11 Martine Mat	0.23	0.11

Performance

Following the construction of the second level basement floor, settlement monitoring points were established on the columns. Settlement monitoring was accomplished with a high precision survey level and readings were recorded to the nearest 0.005 ft. Monitoring was accomplished through November 1987. The buildings were occupied prior to the completion of the monitoring program. Therefore, the dead and live loads were transmitted to the mat foundations. The measured foundation settlements versus building construction are presented on Figures 3b and 4b.

The measured settlement for the 50 Main foundation was 0.035 ft for exterior columns to 0.05 ft for interior columns. The ratio of average predicted total settlement to the maximum measured settlement is 3.0. The measured settlement range for the 1-11 Martine foundation was 0.06 ft for exterior columns to 0.10 ft for interior columns. The ratio of average predicted total settlement to the maximum measured settlement is 1.7. The measured results indicated that the flexible mat foundations limited the amount of differential settlement to approximately 40 percent (%) of the total measured settlement.

The average subgrade modulus computed from the measured settlements was 140 kcf for 50 Main and 75 kcf for 1-11 Martine. The selected design value was 100 kcf.

Gateway Project

Gateway I Office Tower

This office structure is an 18-story cast in-place concrete building with post tensioned floors and a glass panel facade. A one level deep basement for mechanical equipment is located below the office tower. The building has a footprint area of approximately 15,000 sf and its basement floor is at el 192. The foundation subgrade is located at el 186, approximately 20 ft below street grade. The design loads range from 1200 to 2500 kips per column.

Subsurface Conditions

The basement level is underlain by a sand deposit with occasional silt seams. The medium dense to dense sand deposit consists of fine to coarse sand with trace silt. The silt seams are approximately 3 to 12 inches thick and interspersed with fine sand lenses. Groundwater was encountered approximately 4 ft below foundations at el 182. The design and subsurface conditions are presented in Figure 5a.

Foundation Design and Construction

Soil improvement densification procedures and shallow spread foundations were used to support the office tower structure. The footings were designed for an allowable contact pressure of 6 ksf. The sand footing subgrade was densified using a 5 ton static drum weight vibratory roller.

Predictions

The Schmertmann method and a layered solution by DeBeer and Martens (1957, 1965) modified by Meyerhof (1965) were used to estimate the settlement of the spread foundations. The Meyerhof method also uses cone penetrometer resistance to estimate elastic moduli for the soil layers. The predicted settlement is presented in Table 3.

TABLE 3: Predicted Settlements - Gateway I Spread Foundations

	Meyerhof (1965)	Schmertmann (1970)
Total Settlement (ft)	0.11	0.13
Differential Settlement (ft)	0.03	0.01

Performance

Settlement points were established on the 1st floor columns and monitoring was accomplished through March 1985. Monitoring was terminated following the completion of the architectural facade at which time approximately 90 percent of the total load was transferred to the building foundations. The measured foundation settlement versus building construction is presented on Figure 5b.

The measured settlement for the office tower footings ranged from 0.055 ft for exterior columns to 0.075 ft for interior columns. The ratio of predicted total settlement to the maximum measured settlement is 1.6. The measured differential settlement was approximately equal to the predicted values.

Discussion

A summary of the predicted and measured foundation settlements for the previously discussed case histories and for other building sites in the downtown area are presented in Table 4.

The maximum measured settlement occurred at the 1-11 Martine mat foundation where 0.10 ft of settlement was recorded.

The differential settlement between adjacent columns for this mat and the 50 Main mat was less than 0.04 ft for 28 ft column spacing. This amount of differential movement is considered acceptable for concrete structures. The total settlement for the remaining structures supported on shallow foundations did not exceed 0.08 ft and the differential movement between adjacent columns was equal to approximately 0.02 ft.
The predicted settlement values, based on the methods discussed in the case histories, exceeded the measured settlements by 50 to 200%. The use of SPT N values to estimate cone resistance may have led to the high predicted settlements.

The Schmertmann method appeared to provide the best estimate for the settlement of the mat foundations with a predicted to measured ratio of 1.1 to 1.8. The Meyerhof approach provided the closest approximation for estimating the settlement for the buildings supported on spread foundations with a predicted to measured ratio of 1.4 to 1.6.

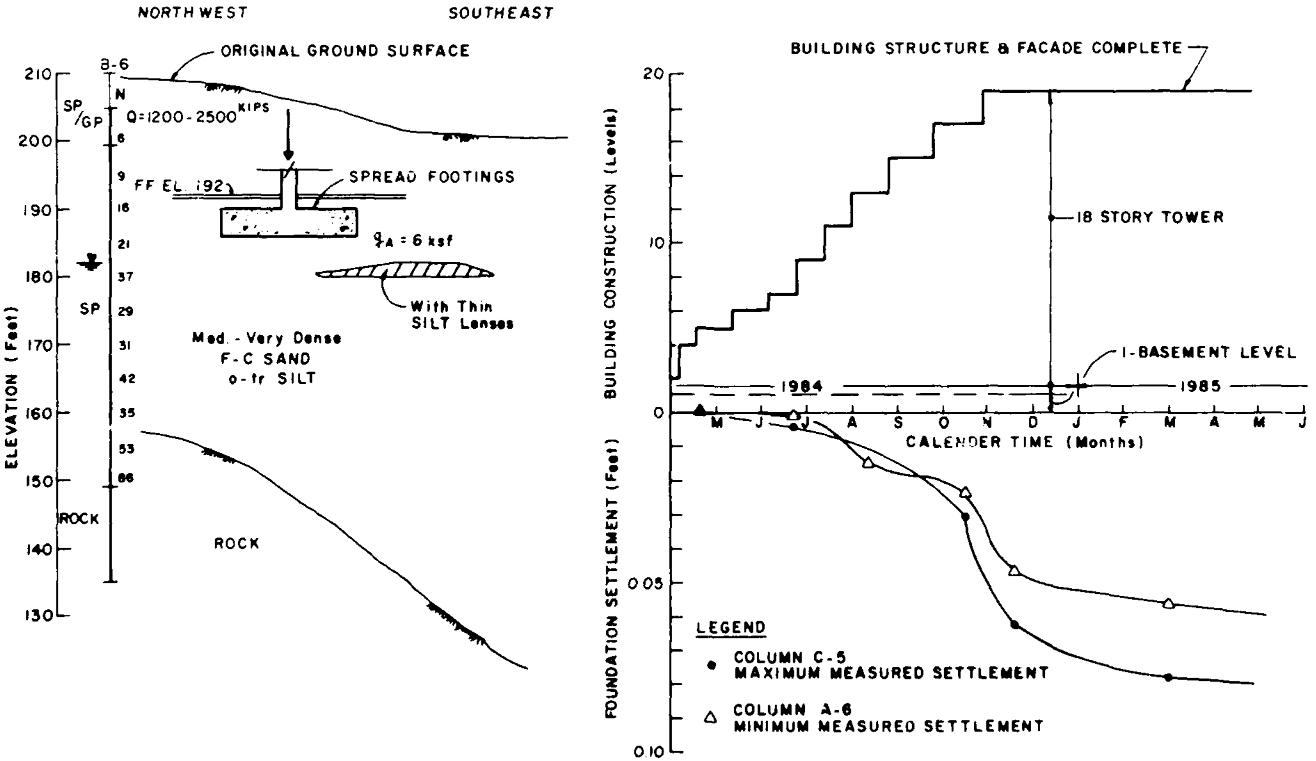

a. Design Conditions
b. Spread Foundation Settlement Versus Construction

FIG. 5 - GATEWAY I OFFICE TOWER

TABLE 4: Summary of Foundation Settlement Results

Project	Building[1] Height (levels)	Foundation Type	Contact Pressure (ksf)	Predicted[2] Settlement (ft)	Measured[3] Settlement (ft)	Predicted / Measured
50 Main	17	Mat	6	0.15	0.05	3.0
1-11 Martine	17	Mat	6	0.17	0.10	1.7
Gateway I	19	Spread	6	0.12	0.08	1.5
25 Martine	14	Spread	6	0.10	0.06	1.7

[1] Includes below grade levels
[2] Average predicted settlement using Schmertmann (1970), D'Appolonia (1968) or Meyerhof (1965) methods of analysis
[3] Maximum measured settlement

EXCAVATION DESIGN AND PERFORMANCE

Details for the design, construction and performance of temporary excavation support systems will be discussed.

Westchester Financial Center

50 Main Excavation

An excavation depth of approximately 20 ft below street grade was required to construct foundations for the 2 level underground parking structure which is common to the Westchester Center site. The soil supporting the adjacent streets and utility services needed to be retained throughout the period for construction of foundations and the underground structure. A temporary flexible retaining structure was constructed in conjunction with open cut excavation slopes to achieve the foundation subgrade. Cantilevered soldier pile and timber lagging walls were designed and constructed for exposed heights up to 13 ft. The design and subsurface conditions for the excavation adjacent to Bank Street are presented in Figure 6a.

Design and Construction

The soil parameters used for the design of the cantilevered structure are shown on the figure. A conventional earth pressure analysis (U.S. Steel, 1984) was used to determine the soil pile size and depth of embedment. A factor of safety of 2 was used for the passive soil resistance at the toe of the soldier pile wall.

The HP 14 X 73 soldier piles were driven to the depths shown on the figure with a Vulcan 010 air hammer. The piles were spaced at 6 ft on center. As the excavation proceeded in stages, 3 inch thick by 10 inch wide timber lagging was installed behind the front face of the pile flanges to retain the soil. In areas where running sand was encountered, backpacking behind the lagging was accomplished with sand and straw hay, and the depth of unsupported excavation was reduced to one board height.

Predictions

An elastic approach assuming the soldier pile wall acts as a fixed cantilevered beam was used to estimate the maximum lateral deflection at the top of the retaining wall. The active earth pressure loading was applied in a triangular distribution assuming that the computed resultant load would be applied to a beam length equal to the exposed height of the excavation plus one half the embedment depth of the pile (U.S. Steel, 1984). The predicted elastic lateral movement at the top of the wall was 0.12 ft.

Performance

Following the installation of the soldier piles, monitoring points were established at the top of selected piles. Lateral movements were monitored throughout the excavation to foundation subgrade with optical survey equipment. Movements were recorded to the nearest 0.01 ft. The measured lateral movements versus excavation elevation are presented on Figure 6b. The measured lateral movement ranged from 0.04 to 0.17 ft. The ratio of the predicted elastic movement to the maximum measured movement is 0.71.

Gateway Project

Gateway I Excavation

An excavation depth of 20 ft below Hamilton Avenue was required to construct foundations for the deep basement beneath the Gateway I office tower. The contractor designed and constructed a temporary cantilevered soldier pile wall to retain the sand soil supporting the adjacent utilities and street. The exposed height of the wall was 18 ft. The design and subsurface conditions are presented in Figure 7a.

Construction

The HP 14 X 73 soldier piles were spaced at 6 ft centers and driven with a Vulcan 010 air hammer. Timber lagging was placed between the soldier piles. The excavation proceeded in stages from the top of the piles at el 206 to foundation subgrade at el 188. After the final excavation had been achieved, the cantilevered wall began to move toward the excavation at an accelerated rate. Therefore, the contractor decided to install raker braces at 12 ft centers to control the lateral movement.

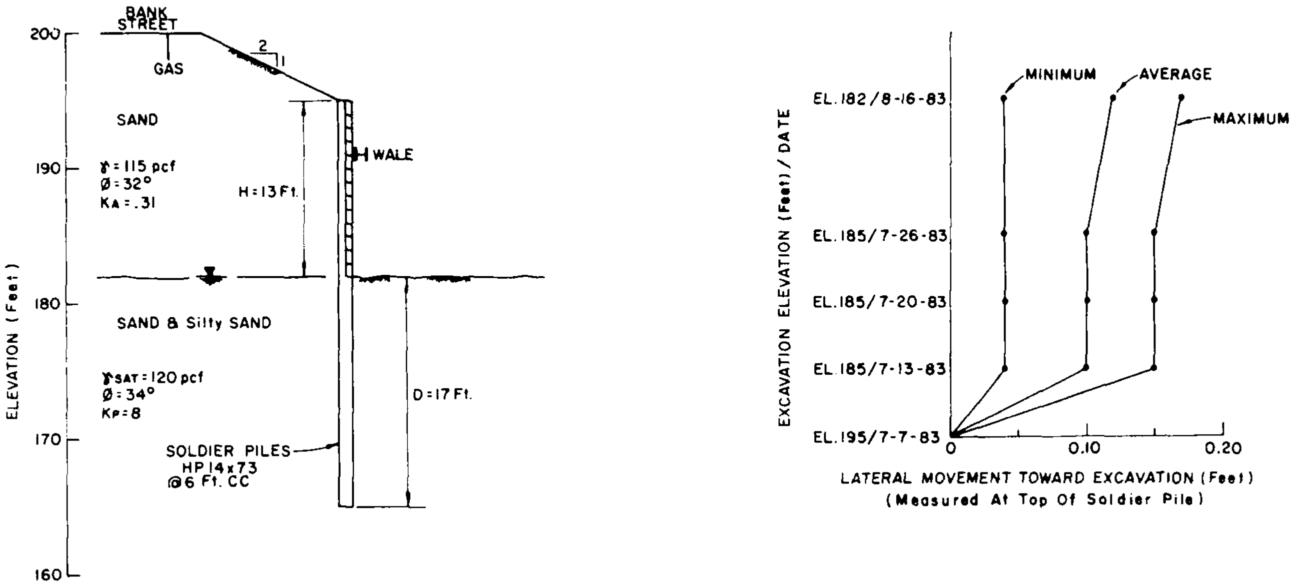

a. Design Conditions

b. Lateral Movement Versus Excavation Depth

FIG. 6 - CANTILEVERED SOLDIER PILE WALL - 50 MAIN EXCAVATION

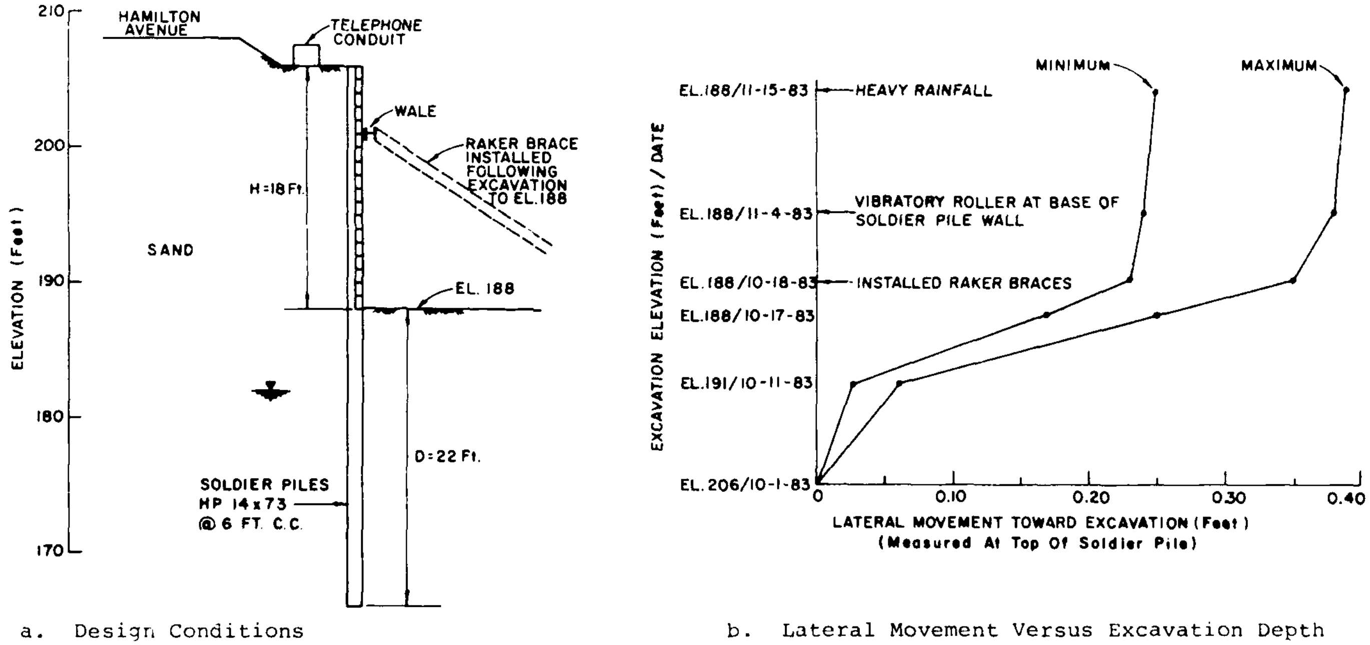

a. Design Conditions

b. Lateral Movement Versus Excavation Depth

FIG. 7 - CANTILEVERED/BRACED SOLDIER PILE WALL - GATEWAY I EXCAVATION

Predictions

The fixed elastic beam approach (as previously discussed) was used to estimate the maximum lateral movement at the top of the pile wall. A predicted elastic lateral deflection of 0.43 ft was calculated for the 18 ft high cantilevered soldier pile wall.

Performance

The contractor established monitoring points on top of the piles and recorded lateral movements as the excavation proceeded. In addition, monitoring points were established at the curb line to measure the lateral movement of the cracks in the street pavement that occurred during the excavation. The pavement cracks were located parallel to and approximately 12 ft away from the soldier pile wall. The measured lateral movements versus excavation elevation are presented in Figure 7b.

The total measured lateral movement varied from 0.25 to 0.39 ft. The ratio of predicted elastic movement for the cantilevered wall to the measured movement was 1.10. However, the installation of the raker braces limited the total lateral movement of the temporary cantilevered wall.

Gateway Project

Gateway Underground Garage Excavation

This 3 level below ground cast in-place concrete structure is located below New Street in the north area of the Gateway Project. An excavation depth of approximately 30 ft below Ferris Avenue was required to construct the garage foundations at el 165. A temporary earth retention system was required to retain the soil supporting the sidewalk, street, and utilities. The deep excavation was supported using a soil anchored soldier pile wall. The design and subsurface conditions are presented in Figure 8a.

Design and Construction

The 25 ft high soil anchored soldier pile wall was designed for a two stage construction excavation. During the first stage of excavation to the level of the wale and soil anchor, the wall was analyzed for conventional active earth pressure loading. For the second stage excavation, following the installation of the soil anchors, the wall was analyzed for approximately 2/3 of the apparent earth pressure loading. The soil anchors were designed for the full apparent earth pressure.

The HP 10X42 soldier piles were spaced at 7.5 ft centers and driven with an ICE vibratory hammer. Conventional timber lagging was placed behind the pile flanges, and straw hay was placed between and behind the lagging boards. The soil anchors were installed at 15 ft centers using pressure injected techniques. A 4 inch hole was drilled, cased, and washed using rotary equipment. The anchor reinforcement (four 270 ksi steel strands) was grouted in the hole using low pressure primary and high pressure secondary grout applications. A regrout tube was installed with the anchor reinforcement. The 10 ft stressing length of the anchor reinforcement was sheathed with plastic and the bond length of the anchor was approximately 25 ft. All of the anchors were prooftested to 125% of their design load and locked-off at 75% of the load.

Predictions

Since the soldier pile wall was subjected to both active soil pressure loading and concentrated point loads associated with the soil anchors, elastic superposition methods were used to estimate the lateral deflection of the wall. The predicted maximum lateral deflection at the top of the wall was 0.15 ft.

Performance

Following the installation of the piles, monitoring points were established at the top of selected piles. Monitoring was accomplished through the staged excavation sequence. Lateral movements versus excavation elevation for the Ferris Avenue wall are

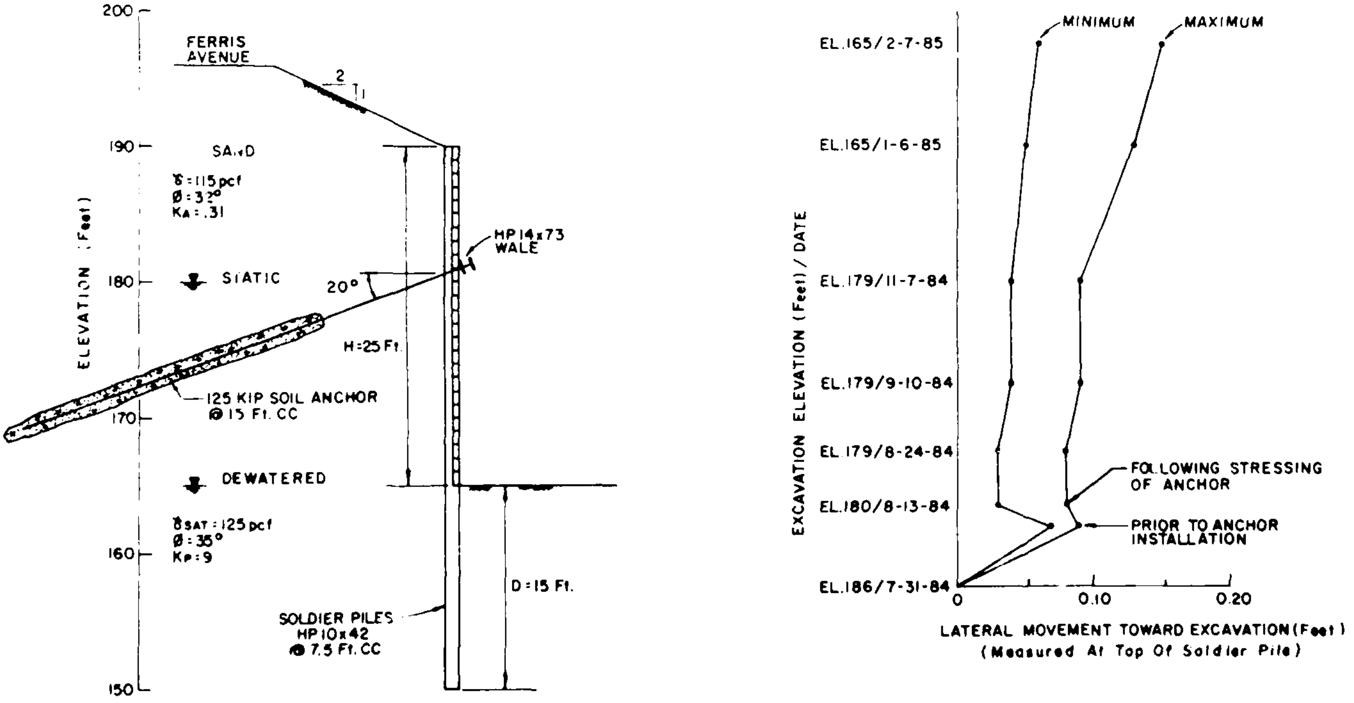

a. Design Conditions

b. Lateral Movement Versus Excavation Depth

FIG. 8 - SOIL ANCHORED SOLDIER PILE WALL - GATEWAY UNDERGROUND GARAGE EXCAVATION

TABLE 5: Summary of Excavation Support Movements

Project	Retaining Structure[1]	Height[2] (ft)	Predicted Movement (ft)	Measured[3] Movement (ft)	$\frac{\text{Measured}}{\text{Predicted}}$
50 Main	Cantilevered SP	15	0.12	0.17	1.4
50 Main	Cantilevered SP	14	0.08	0.12	1.5
25 Martine	Cantilevered SP	14	0.09	0.23	2.6
Gateway I	Cantilevered/Braced SP	20	0.43	0.39	0.9
Gateway Underground	SP w/1 level of anchors	21	--	0.11	--
Gateway Underground	SP w/1 level of anchors	28	0.15	0.15	1.0
Gateway Underground	SP w/2 level of anchors	30	--	0.08	--

[1] SP = Soldier pile and timber lagged wall.

[2] Height = Equivalent height wall with a level ground surface at the top and bottom of the retaining wall. This equivalent height accounts for backslopes and toe berms.

[3] Maximum lateral movement measured at top of retaining structure.

presented in Figure 8b. The measured lateral movement ranged from 0.06 to 0.15 ft. The ratio of predicted lateral movement to the maximum measured movement is 1.0.

Performance tests were accomplished on two soil anchors to determine the residual or permanent movement of the grouted anchor. An incremental series of load and unload cycles were performed up to 150% of the anchor design load for an 86 kip three strand anchor with a bond length of 20 ft and a 125 kip four strand anchor with a bond length of 28 ft. At 100% of their design load, the permanent (non-elastic) anchor movement was measured to be 0.026 ft for the 86 kip anchor and 0.032 ft for the 125 kip anchor. The permanent anchor movement at 100% of the design load was equal to 0.12% of the bond length of the anchor.

Discussion

A summary of the predicted and measured lateral movements for the previously discussed retaining structures and for other excavation retention systems in the downtown vicinity are presented in Table 5.

The maximum measured movement occurred at the Gateway I excavation, where 0.39 ft of lateral deflection was recorded for the cantilevered/braced 20 ft equivalent height wall. Additional lateral movement may have occurred at this site if the originally constructed cantilevered wall had not been internally braced. The 14 to 15 ft equivalent height cantilevered walls experienced movements up to 0.23 ft and the 21 to 30 ft equivalent height soil anchored walls moved up to 0.15 ft toward the excavation.

The measurements from these case histories indicate that for conventional HP soldier pile sections, the maximum equivalent cantilevered wall height is approximately 15 ft. Beyond this height, lateral movements can become excessive.

The predicted elastic movements for the cantilevered soldier pile walls were less than the maximum measured lateral movement by 40 to 160%. Construction methods and surrounding ambient conditions have led to lateral movements in excess of the estimated elastic deflection. The presence of running cohesionless sand during the lagging installation may have left voids behind the soldier pile wall. These voids sometimes extend behind the back flange of the soldier piles, thereby, significantly reducing the arching or self supporting effect of the soil between the piles. Backpacking and attempting to backfill from the top of the soldier pile wall does not usually succeed in reestablishing the natural arching capacity of the soil. In time, vibrations caused by heavy street traffic and intense rainfalls caused the voids behind the lagging to become filled with loose soil. The loose soil does not have the arching capacity of the natural dense soil. Therefore, additional soil pressures are transmitted to the soldier piles and greater than predicted lateral movements occur.

Limiting lateral movements for lagged soldier pile walls in running sand can be accomplished by the use of contact lagging attached to the front face of the soldier piles. This procedure limits the disturbance of the natural arching of the in-situ sand between the piles.

CONCLUSIONS

Through the use of field measurements, it was possible to analyze and evaluate the performance of completed building foundations and temporary earth retaining structures. Original design assumptions and methods of predicting their performance could be checked and evaluated to assist in the design and analysis of future structures.

As indicated in the discussions:

- The maximum measured total and differential settlement, 0.10 ft and 0.04 ft, respectively , was recorded at the 1-11 Martine mat foundation. This magnitude of settlement is considered to be acceptable for the concrete structures discussed.
- Measured differential settlements were observed to be less than 40% of the total measured settlement.
- The predicted settlements exceeded the maximum measured settlement by 50 to 200%.

- The Schmertmann analysis provided the best estimate for the settlement of the mat foundations and the Meyerhof method yielded the closest approximation for the settlement of spread foundations.
- The predicted elastic movements for the cantilevered soldier pile walls were less than the maximum measured lateral movements by 40 to 160%.
- Construction difficulties during the lagging installation caused by running sand conditions may have led to the increased lateral movements.
- The use of contact lagging installed on the front face of the pile flange could limit disturbance of the arching effect of the in-situ sand, thus, decreasing the potential for lateral movement of the soldier pile walls.
- For conventional HP soldier pile sections the maximum cantilevered equivalent wall height is approximately 15 ft. Beyond this height, lateral movements can become excessive.

APPENDIX I - REFERENCES

D'Appolonia, D.J., E. D'Appolonia, and R.F. Brissette, (1968) "Settlement of Spread Footings on Sand", JSMFD, ASCE, Vol. 94, No. SM3, May, pp 735-760. Discussions in Vol. 95, No. SM3, pp 900-916 and Vol. 96, No. SM2, pp 754-762.

DeBeer, E. and A. Martens, (1957) "Methods of Computation of an Upper Limit for the Infuence of Heterogeneity of Sand Layers on the Settlement of Bridges", Proceedings, 4th ICSMFE, London, Vol. 1, p 275.

DeBeer, E. (1965) "Bearing Capacity and Settlement of Shallow Foundations on Sand", Proc. Sym. Bearing Capacity and Settlement of Foundations, Duke University, pp 15-33.

Meyerhof, G.G. (1965), "Shallow Foundations", JSMFD, ASCE, Vol. 91, No. SM2, March, pp 21-31.

Schmertmann, J.H. (1970) "Static Cone to Compute Static Settlement over Sand", JSMFD ASCE, Vol. 96, No. SM3, May, pp 1011-1043.

United Stated Steel, Steel Sheet Piling Design Manual, Updated and reprinted by US DOT/FHWA, July 1984.

APPENDIX II - NOTATION

The following symbols are used in this report:

D = Depth of embedment
H = Exposed height of wall
K = Modulus of subgrade reaction
K_a = Coefficient of active earth pressure
K_p = Coefficient of passive earth pressure
N = Standard penetration test N-value in blows per foot
Q = Column load
q_a = Allowable bearing pressure
ϕ = Angle of internal friction
γ = Total unit weight
γ_{sat} = Saturated unit weight

APPENDIX III - CONVERSION OF UNITS

The following english units can be converted to the International System (SI) units:

1 foot (ft) = 0.3048 meters (m)
1 inch (in) = 25.4 millimeters (mm)
1 kilopound = 1000 lbf = 0.50 tons
1 kilopound (kip) = 4.448 kilonewtons
1 kilopound per square feet (ksf) = 47.88 kilo pascal (kPa)
1 pound per cubic foot (pcf) = 16.02 kilograms per cubic meter (kg/m^3)

Proceedings: Second International Conference on Case Histories in Geotechnical Engineering, June 1-5, 1988, St. Louis, Mo., Paper No. 6.54

Common-Sense Foundation Design

Sven Hansbo
Professor of Geotechnical Engineering, Chalmers University of Technology, Gothenburg, Sweden

SYNOPSIS: In this paper, two case records are presented as an illustration of the advantages of using what one might call "common sense" foundation design.

The first case is an illustrative example of the detrimental effects on older buildings that can be caused by traditional piling in non-cohesive soil. The possibilities of avoiding damage by application of a less rigid foundation design method are discussed. Thus, having access to more sophisticated soil investigation methods than those originally used, it can be shown that a mixed foundation, partly on settlement reducing piles and partly on shallow footings would have been possible. The concept of settlement reducing piles means that the length and number of piles in the pile groups are chosen with a view to eliminating settlement differences between piled and unpiled foundations. Using this solution, the part of the new building nearest to the older ones would have been founded on shallow footings, which would have meant both a considerable reduction of damage to the older buildings and considerable savings in foundation costs.

The second case record is presented in support of the design method suggested. The subsoil conditions under the building in this case are very similar to those in the first case. Here, on the basis of more developed soil investigations methods, it was decided to found the building partly on settlement reducing piles and partly on shallow footings. To keep a check on the result, the building was monitored with settlement gauges. The results of the settlement observations showed excellent agreement between prediction and performance.

INTRODUCTION

In urban renewal work new buildings often have to be founded at a much deeper level than older buildings in their immediate vicinity. These older buildings may be considered to be valuable for historical or other reasons and must therefore be protected against damage in the best possible way during the construction of new buildings. This can create difficult foundation problems which may require unconventional solutions. This is undoubtedly true in cases where the choice of foundation method has a great influence on the preservation of the nearby buildings.

Old buildings are usually founded at shallow depth and are therefore very sensitive to any kind of construction work causing disturbance at great depth in the subsoil. However, in order to make sure that the new buildings will not suffer damage by differential settlement, or by future building activity, the designer often decides on pile foundations irrespective of whether this is required or not. If piles are required in one part of the building, then the whole building will be placed on piles. It would appear that there is a belief that the safety of a building against damage is hazarded if part of the building is founded on piles while the other part is founded on shallow footings.

This attitude is of course based on the difficulties experienced in settlement prediction. The soil investigations carried out may not form a reliable basis for settlement prediction. This is particularly true in cases where the subsoil consists of non-cohesive soil. In these cases, soil investigations generally only consist of different kinds of sounding, such as SPT, CPT, or the like, and (but not always), the taking of disturbed samples for soil identification. Unless the geotechnical characteristics of the soil can be directly evaluated from the sounding resistance, on the basis of well-documented local experience, then the uncertainties involved are so great that the choice of pile foundations is only natural.

Since pile driving, as pointed out, often does very considerable damage to nearby buildings it should therefore be avoided whenever possible. How then is this goal to be achieved? The traditional design of pile foundations whereby the total load of the building is assumed to be carried by the piles alone is undoubtedly the foremost obstacle that has to be overcome. In this type of design the piles are assumed to act as columns, and, to avoid settlement, a high safety factor against pile failure is applied. This, of course, entails hard pile driving to great depths. Moreover, since the settlement of pile foundations is believed to be negligible, a combination of piled and unpiled foundations is not considered to be safe and sound.

The insight which has been gained into modern foundation design somehow seems obviously to be forgotten as soon as piling comes into the picture. Much could be gained if only the principles of geotechnical engineering applied in other connections, e.g. in the design of shallow foundations, were also applied in connection with piling. Some examples of this were demonstrated by Hansbo (1984), Burland (1986), Kasali et al. (1987) and Peaker et al. (1987).

In the following, an example of the damage caused by pile driving in non-cohesive soil will be given. The possibility of using shallow foundations in combination with deep foundations (on piles), will be discussed – a combination which is less harmful to the surrounding buildings. In support, another case record will be presented where the subsoil conditions are quite similar. In this latter case pile foundations and shallow foundations were used in combination. Settlement prediction and performance were in good agreement.

CONVENTIONAL PILED FOUNDATIONS

Buildings in the Överkikaren block

A number of new buildings, Fig. 1, were to be erected in the Överkikaren block, which is situated in the centre of Stockholm on the southern embankment of Lake Mälaren. The buildings considered in this report are designated B and C, Figs 1-2.

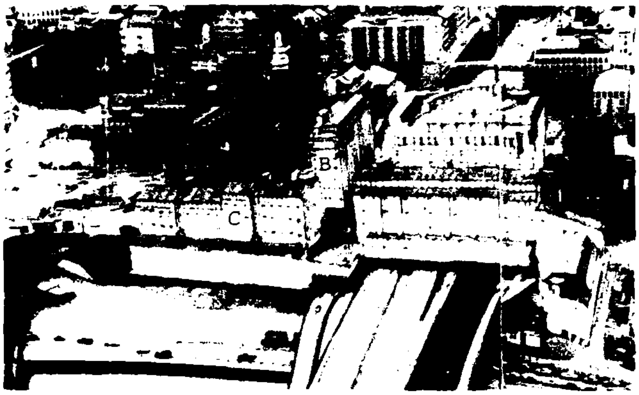

Fig. 1. Architectural layout of the new buildings in the Överkikaren block.

The buildings are situated on the esker which passes through the central parts of Stockholm. The esker material at the site consists of sand and gravel of varying relative density and stratification. Its surface level is indicated in Fig. 2. In connection with previous building activity it had been filled up with different kinds of material, partly organic, and unsuitable for building purposes. The bedrock level is given in Fig. 2. The groundwater level is subjected to annual variations from around -0.8 to +0.5.

Building B

The ground level before excavation varied between maximum +20 m in the south and minimum +10.5 m in the north. Around 60% of the building area was at level +19.9 m. The foundation level of the building (basement floor level +3.0) is below bed-rock surface in its southernmost part while in its northernmost part the depth to bed-rock is around 22 m.

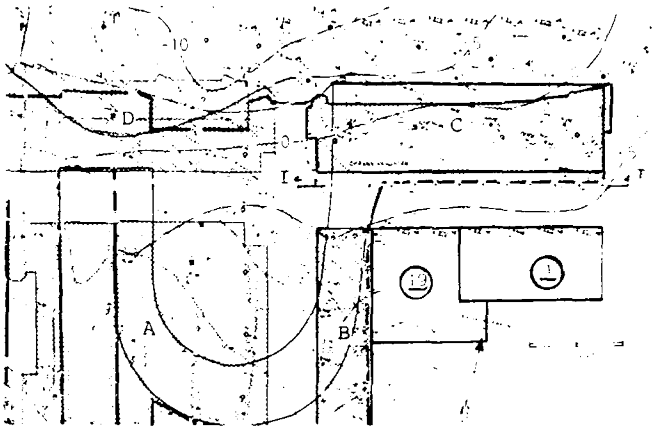

Fig. 2. Site plan of the new buildings. Broken lines indicate bed-rock level, broken and dotted lines indicate level of upper surface of natural esker material.

The soil investigation for Building B consisted of Swedish weight sounding and ram sounding. Because of strong variations in sounding resistance, the consultant decided that foundation on piles should be used in the part of the building underlain by esker material, and that the pile tips should be carried down to bed-rock.

Building C

The ground level before excavation varied between maximum +12.6 in the south and minimum +5.5 in the north. Within the main part of the building, the ground level was between +10.0 and +12.6.

The soil investigation for Building C consisted of weight sounding (5 boreholes), ram sounding (14 boreholes) and CPT (5 boreholes). Disturbed soil samples were taken in 7 boreholes for soil identification. After excavation the first soil investigation was supplemented by another set of weight and ram soundings and soil sampling for soil identification. The main purpose of the soil sampling was to identify the interface between fill and natural esker material.

As in the case of Building B, there were large variations in sounding resistance, indicating great differences in the relative density of the soil. The lowest resistance was obtained just below the groundwater table. An example of the results of the soil investigation (Section I-I, Fig. 2) is given in Fig. 3. The results of the CPT, which perhaps best reflect the firmness of the soil, also show great variation in penetration resistance. The lowest point resistance, obtained in two boreholes in the sand layers just below the groundwater table, is 2-4 MPa (the lower value probably due to nearby driving of two casings).

With the chosen basement floor level (+3.0), approximately 20% of the basement area in the northernmost part of the building was underlain by fill material. In this area foundation on piles was undoubtedly required. For the remaining part, a settlement analysis carried out by the consultant on the basis of empirical correlations between compression moduli and sounding resistance (Bergdahl and Eriksson, 1983), gave an estimated settlement of shallow footings of 12-13 cm. Since such a large settlement would lead to unacceptable distortion between the part of the building on piles and the part on shallow footings, it was decided that the whole building should be founded on conventional driven piles. As a result, 382 precast concrete piles were driven to an average depth of 24.5 m.

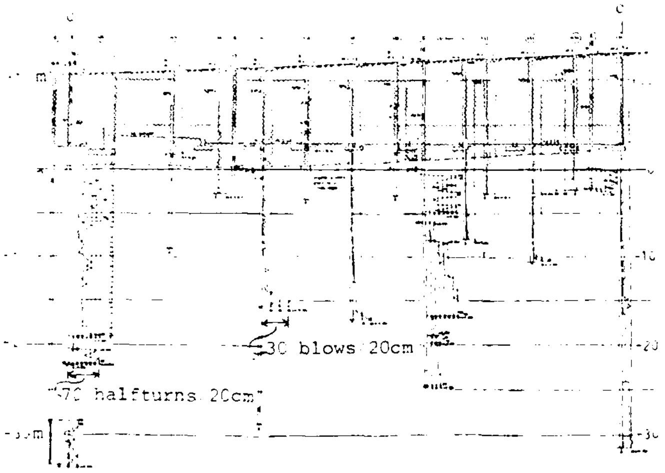

Fig. 3. Results of soil investigation (ram sounding and weight sounding) along Section I-I, see Fig. 2. Shaded area represents fill material.

Damage caused by piling

In the immediate vicinity of Buildings B and C there were two existing houses of great historical and architectural interest. They were founded on shallow footings and their basement floor levels were +7.1 (House 19, Fig. 2) and +10.0 (House 1, Fig. 2). Due to the installation of a sheet-pile wall south of Building C, and installation of bored piles west of Building B (Fig. 4) prior to and during excavation, certain settlement of the old houses took place. However, the most serious trouble was met with due to the pile installation. House 1 tilted to the north, towards Building C, and House 19 to the north-west. Wide cracks opened up, Fig. 5, and a column in House 19 was sheared off which led to the collapse of the concrete roof, Fig. 6, just after the end of a meeting in the room in question. Settlement observations showed that the northwest corner of House 19 had settled about 13 cm vertically and had moved about 3 cm horizontally in an outward direction, Fig. 7. Most of the settlement was obviously caused as a result of reorientation of grains into a denser state (compaction of loose esker material) by vibrations and soil displacement during pile driving.

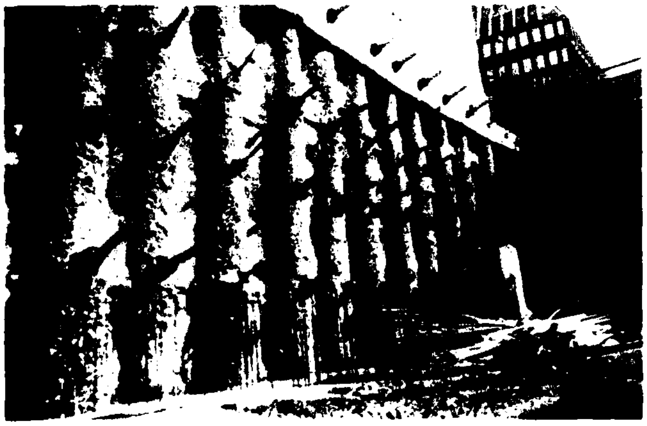

Fig. 4. View of supporting bored pile wall against House 19, west of Building B.

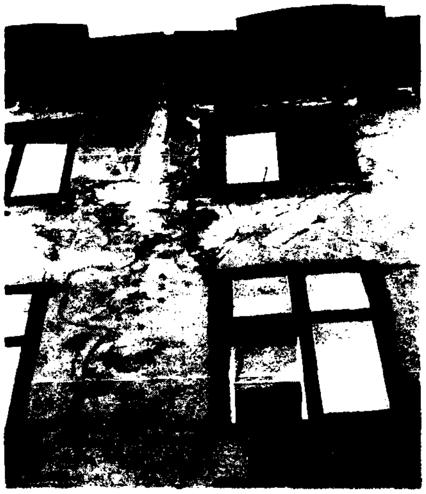

Fig. 5. Cracks in the western façade of House 19 caused by settlements due to piling.

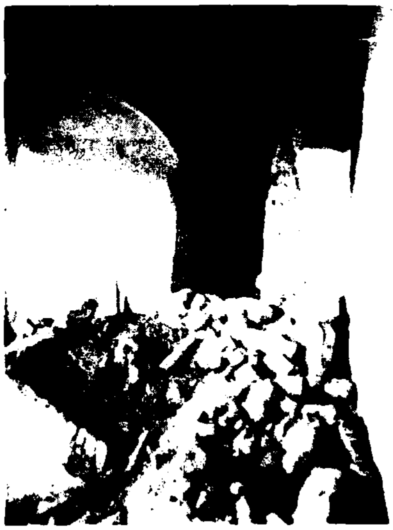

Fig. 6. Remainders of concrete roof which collapsed after a supporting column had been sheared off.

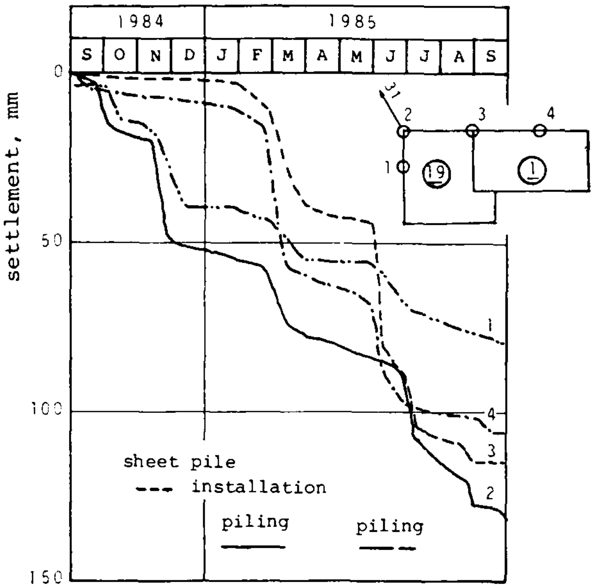

Fig. 7. Settlements of Houses 1 and 19 during foundation work for Buildings B and C.

COMMON SENSE FOUNDATION

Buildings in the Överkikaren block

Knowing the result, one is forced to ask oneself if the choice of foundation method was well-founded. Above all, no investigation of the deformation properties of the natural esker material had been carried out and, consequently, a very conservative settlement analysis was made on an empirical basis. Moreover, no regard was paid to the positive influence on settlement of unloading due to excavation. As shown by Jamiolkowski et al. (1985), the correlation between sounding resistance and deformation moduli in sand is very much dependent on the overconsolidation ratio.

For Building B unloading due to excavation caused a stress release of between 0.20 and 0.35 MPa. There is therefore no doubt that foundation of Building B on shallow footings would have been possible. To minimize differential settlement, overblasting of the bed-rock in the part of the foundation area with exposed bed-rock surface could have been carried out as an extra safety measure.

More interesting, however, is the question as to what possibilities existed for using another type of foundation for Building C which would have been less dangerous for the adjacent buildings. To investigate this, pressuremeter tests were later carried out in two boreholes, one immediately east and the other immediately west of Building C. In order to be able to correlate the pressuremeter values with the sounding resistance in the original investigation, weight sounding was also carried out in the immediate vicinity of the pressuremeter holes. The weight sounding results in these new boreholes were very similar to those previously obtained, and therefore, the pressuremeter values can be considered as being representative of the original soil conditions.

Now, a settlement analysis based on the results of the pressuremeter tests (cf. Baguelin et al., 1978) shows that a mixed foundation partly on shallow footings and partly on piled footings would have been possible. Piled footings would only have been required where the foundation level was in fill. Choosing the foundation level ±0, and a permissible average ground pressure for the footings of 0.3 MPa, settlements were calculated to vary between 0.02 and 0.03 m. In the settlement calculation, the pressuremeter moduli at stresses below the preconsolidation pressure (re-bound values) were assumed to be 3 times the measured "virgin" values and α values applicable to overconsolidated soil were chosen. To minimize differential settlements between unpiled and piled footings, the piles, according to settlement analysis based on the pressuremeter results (cf. Sellgren, 1985), should not be driven deeper into the esker material than 15 m. By choosing this foundation method a total settlement of maximum 4 cm and a maximum differential settlement of less than 2 cm could be expected. These settlements would have been quite acceptable. As a result, the compaction effects on the esker material underneath Houses 1 and 19 would have been considerably reduced. Moreover, apart from the lesser risk of damage to the adjacent buildings, the mixed foundation suggested would have resulted in considerable saving in foundation costs.

Sollentuna hospital

The mixed type of foundation suggested above for Building C in Överkikaren had already been carried out in a previous project, the Sollentuna hospital, Fig. 8. The subsoil conditions on the site of this hospital are very similar to those prevailing at the site of Building C, with the exception that in part of the building area the esker material is covered by clay instead of fill, Fig. 9. The maximum thickness of the clay layer wedging into the building area from the south is 5-8 m. Its undrained shear strength varies between 10 and 30 kPa. The esker material consists mainly of sand. Typical results obtained outside and inside the clay area are given in Fig. 10.

With the chosen basement floor level +23.5 it was no doubt necessary to found the part of the hospital underlain by clay on piles. Then, from

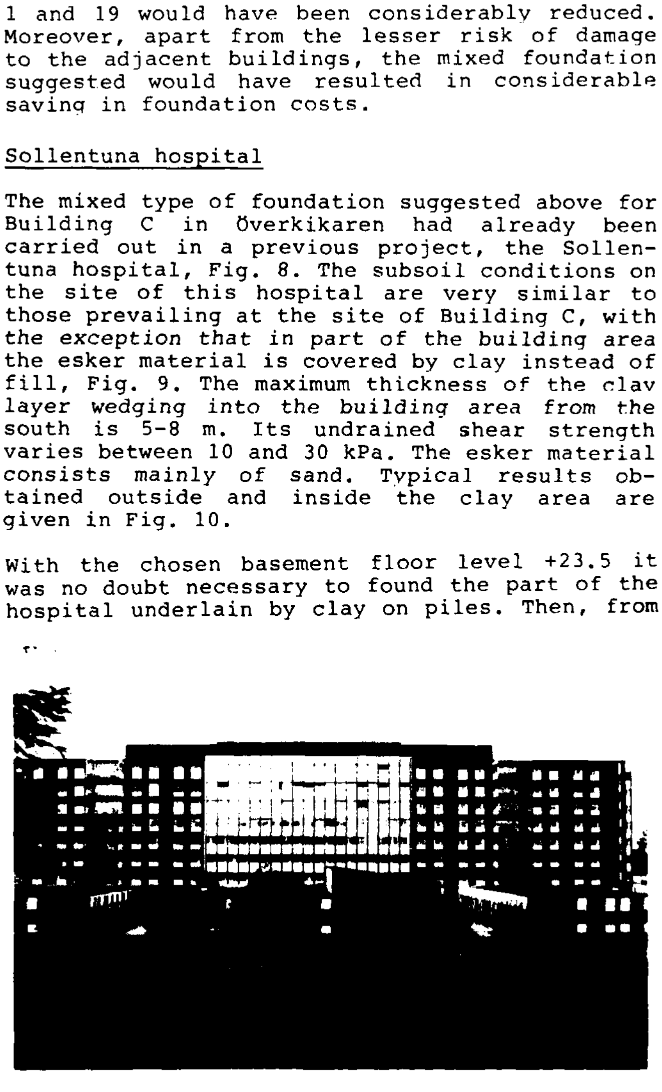

Fig. 8. The Sollentuna Hospital

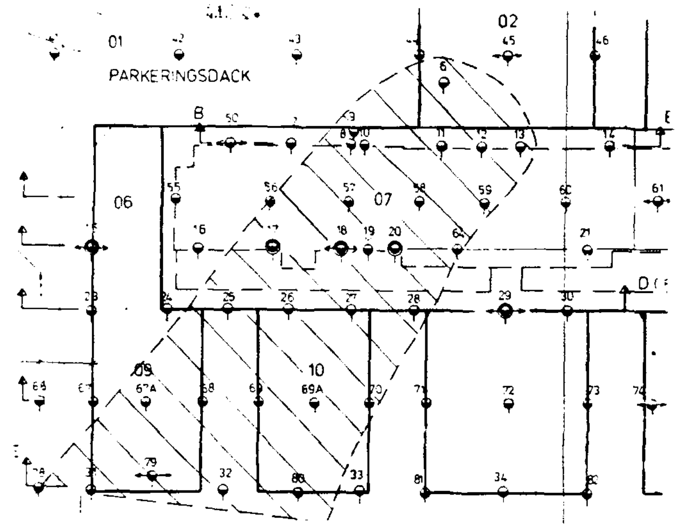

Fig. 9. Location of boreholes and site plan of the Sollentuna Hospital. Dashed area shows the clay layer wedging into the hospital site.

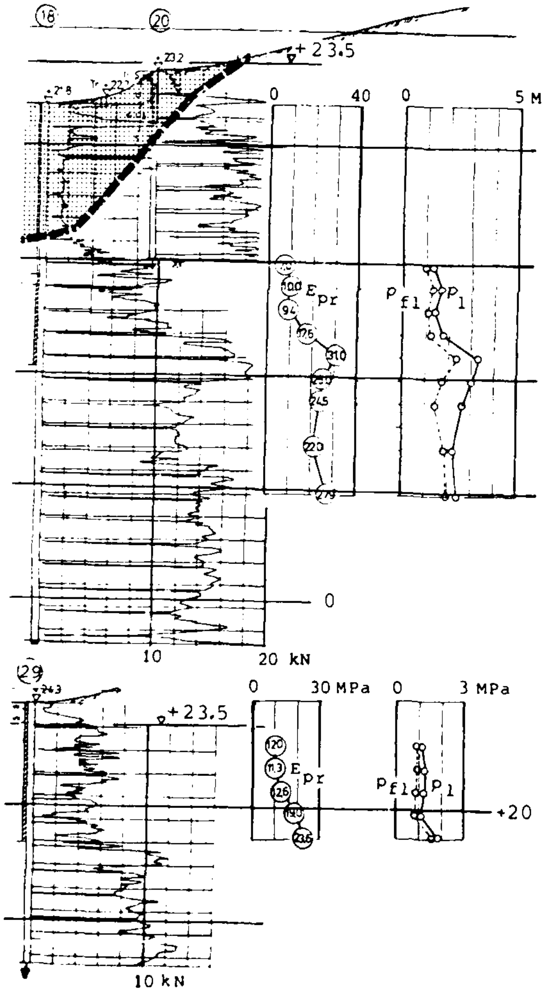

Fig. 10. Typical results of CPT soundings (total of point resistance and skin friction) and Ménard pressuremeter tests.

the traditional point of view, due to fear of detrimental differential settlement, piled foundations would have been considered as being the most natural choice for the whole building, including the part resting on non-cohesive soil. However, a settlement analysis based on the pressuremeter results showed that it was possible to use a mixed foundation, partly on shallow footings and partly on piled footings. With the aim of minimizing the differential settlements between piled and unpiled footings a limit was set to the depth of pile driving into the sandy esker material.

For example, using the results of the pressuremeter tests shown in Fig. 10, we find for a driven pile with a cross-sectional area of 0.275x0.275 m^2 driven 5 m into the esker, a failure load of (cf. Sellgren, 1985)

$$P_f = 5x4x0.275x0.080 + 2.7x2.2x0.275^2 = 0.9 \text{ MN}$$

The settlement of the pile head can be estimated from the relation (Sellgren, 1985)

$$s = a\frac{P}{1-P/P_f}$$

where

$$a = \frac{1}{b}\,\frac{1+(\beta/\theta E_p b)\tanh(\theta l)}{\beta+(\theta E_p b)\tanh(\theta l)}$$

$$\beta = 18E_{pr}/(1+\nu_s)$$

Inserting E_p = elastic modulus of pile =
= 30.000 MPa
b = width of pile = 0.275 m
l = length of pile in gravel = 5 m
E_{pr} = pressuremeter modulus = 17 MPa
ν_s = Poisson's ratio of soil = 0.3
we find a = 0.007 mm/MN

Consequently, the settlement under a load of 450 kN can be estimated at 6 mm.

For a square footing with 2.5 m width, founded at 1 m depth, the settlement can be calculated from the relation (Baguelin et al., 1978).

$$s = 1.12\,\frac{q}{9}\left\{\frac{1.2(1.1x2.5/0.6)^{\frac{1}{3}}}{E_{pr,d}} + \frac{1.1x2.5}{3E_{pr,i}}\right\} \text{ m}$$

Inserting $E_{pr,d}$ = pressuremeter modulus in zone governed by deviatoric stress condition = 15 MPa
$E_{pr,i}$ = pressuremeter modulus in zone governed by isotropic stress condition = 12 MPa
we find for an average ground pressure of 0.5 MPa (safety against failure around 3) a settlement of 11 mm.

For the suggested foundation and the actual loading conditions, a maximum differential settlement of 10 mm and a maximum total settlement of 15 mm was predicted. 70% of the settlement was assumed to take place during the construction period.

In order to persuade the client to accept what he thought would be an unsafe and untried type of foundation, the building was carefully monitored with settlement gauges. If some large deviations from prediction should arise, then these could be blamed on the consultant. The settlements were followed up during the construction of the building and also for a subsequent period of 2 years. At the end of that time, settlement seemed to have terminated. The final settlements are given in Fig. 11. The results of settlement observations show very good agreement with prediction. From the end of the construction period until 2 years later the average relative increase of settlement was about 38% (from about 20% to about 80%).

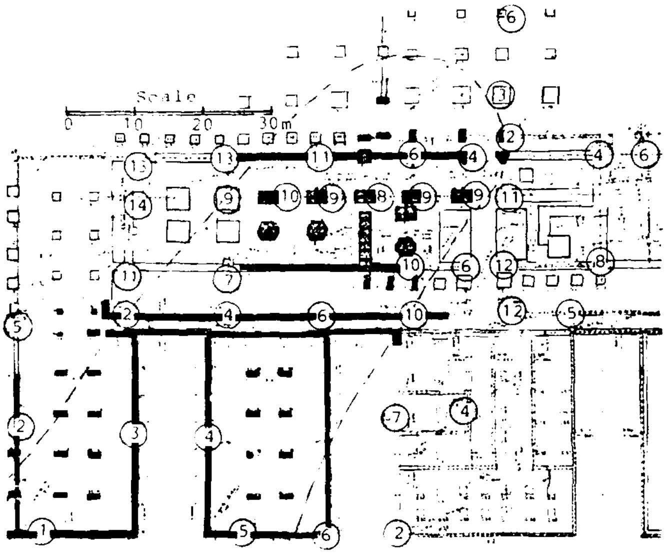

Fig. 11. Settlements (in mm), measured 2 years after the completion of the building. *The footings shown black are placed on* piles. Maximum differential settlement around 1:800.

CONCLUSION

The first case record presented in this paper shows the detrimental effects on nearby buildings that can be caused by pile driving. It also shows that most probably a foundation which was both more economical and less likely to cause damage to nearby buildings would have been possible — had more sophisticated soil investigations been carried out in order to determine the deformation characteristics of the soil.

The second case record is an example of a successful application of a mixed foundation, partly on shallow footings and partly on pile footings where the piles were designed in such a way so as to minimize differential settlement. It also shows that acceptable agreement between prediction and actual behaviour can be obtained provided that the in-situ deformation characteristics of the subsoil have been satisfactorily investigated.

The moral: Continue to use your geotechnical know-how and common sense even when piling comes into the picture.

REFERENCES

Baguelin, F., Jézéquel, J. F. and Shields, D.H. (1978), The Pressuremeter and Foundation Engineering, Trans Tech Publications, Clausthal, Germany

Bergdahl, U. and Eriksson, U. (1983), "Bestämning av jordegenskaper med sondering - en litteraturstudie (Determination of Soil Characteristics by Sounding - A Literature Study)", Swedish Geotechnical Institute, Report No 22.

Burland, J. (1986), "The Value of Field Measurements in the Design and Construction of Deep Foundations", *Proc. International Conference* on Deep Foundations, Beijing, 2:177-187.

Hansbo, S. (1984), "Foundations on Friction Creep Piles in Soft Clays", Proc. International Conference on Case Histories in Geotechnical Engineering, St. Louis, II:913-922.

Jamiolkowski, M., Ladd, C.C., Germaine, J.T. and Lancelotta, R. (1985), "New Developments in Field and Laboratory Testings of Soils". Theme lecture, Proc. XI: International Conference on Soil Mechanics and Foundation Engineering, San Francisco, 1:118-120.

Kasali, G., Burton, C. and Rutherford, J.B. (1987), "Settlement Prediction Using Lightweight Fill - Prediction and Performance", Proc. International Symposium on Geotechnical Engineering of Soft Soils, Mexico City, 1:347-352.

Peaker, K.R., Ahmad, S.A. and Gore, J.W. (1987), "Sensenbrenner Hospital Construction on Weak Clays", Proc. International Symposium on Geotechnical Engineering of Soft Clays, Mexico City, 1:353-358.

Sellgren, E. (1985), "Prediction of the Behaviour of Friction Piles in Non-Cohesive Soils", Proc. International Conference on Soil Mechanics *and Foundation Engineering*, San Francisco, 4:1463-1468.

Proceedings: Second International Conference on Case Histories in Geotechnical Engineering, June 1-5, 1988, St. Louis, Mo., Paper No. 6.55

Dynamic Testing Versus Static Load Tests: Five Case Histories

Stephen S.M. Cheng
Manager, Pile Technology Division, Trow Geotechnical Ltd., Canada

Shaheen A. Ahman
Manager, Geotechnical Division, Trow Geotechnical Ltd., Canada

SYNOPSIS: Five case histories, where the ultimate bearing capacity of the piles was evaluated by both dynamic measurements and static load tests in Southern Ontario, Canada, are presented. The ultimate bearing capacity of the piles obtained by both methods are compared and found that the ultimate bearing capacities evaluated by dynamic measurements are within 1 to 15 percent of the static load test results analysed by the Offset Limit Load Criterion. In four of the six piles evaluated, the dynamic analysis results are within 10 percent of the static load test results. The correlations have shown that dynamic analysis of pile capacity by dynamic measurements is an excellent alternative to static load test.

INTRODUCTION

Since pile driving causes failure of the soil, it is therefore logical to use dynamic measurements made during pile driving to estimate the ultimate bearing capacity of the pile. The use of dynamic measurements to predict pile capacity was put in use in the early 1970's, and since then the use of dynamic measurements to predict pile capacity has been gaining wide acceptance by practicing civil engineers. In the field, the ultimate static bearing capacity of the piles was evaluated from the strain and acceleration measurements by the case method. The ultimate static bearing capacity was also estimated in the laboratory by the CAPWAP analysis. In the CAPWAP analysis, the hammer-pile-soil, and resistance distribution on a pile was modeled and compared with the strain and acceleration measurements obtained in the field.

Ontario is a province located in the mid-eastern portion of Canada. The southern part of Ontario has close to 80 percent of the population of Ontario. The area was covered by ice sheets a million years ago and the subsoil generally consists of glacial tills. The glacial tills are generally competent to support a building by the conventional type of shallow foundation. However, there are areas with deep deposits of fill, softer clay, loose silt or sand, where deep foundations are required. In these instances, driven piles or augered in-place caissons are used to support the proposed structures.

The estimation of the ultimate static bearing capacity of a driven pile is highly theoretical. Some engineers use basic soil mechanic analysis to estimate the frictional and end bearing resistances of a driven pile. Others used various kinds of dynamic formulae to estimate the ultimate bearing capacity of piles when the driving system, pile type and size are known. When E.A.L. Smith (1) introduced wave propagation theory in the 1930's to be applied to a pile during driving, a new chapter had opened in the analysis of the ultimate bearing capacity evaluation. With the evolution of the digital computers and various instruments for the measurements of strain and acceleration during pile driving, the dynamic monitoring of piles was put into use in the early 70's. This paper presents the results of the dynamic analysis of piles at five sites where static load tests were also undertaken.

THEORETICAL BASIS

The dynamic evaluation of pile capacity using Smith's wave propagation theory has been reported by Rausche, Goble and Likins (1975). In the driving of a pile, the strain and acceleration of the pile induced by the pile driver are measured. From the strain measurement, the force at the pile top can be obtained once the pile material and cross sectional area is known. From the acceleration measurement, the velocity of the pile being driven into the ground can be integrated. From the force and velocity obtained at the pile top, the static capacity of the pile can be estimated by the case method:

$$RSP = (F1 + F2)/2 + MC/2L\ (V1 - V2) - J$$

Where: RSP = Ultimate Static Bearing Capacity
F1 = Force at Impact
F2 = Force at Time 2L/C
M = Mass of Pile
C = Wave Speed
L = Length of Pile
V1 = Velocity at Impact
V2 = Velocity at Time 2L/C
J = Damping

The ultimate static bearing capacity of the pile can also be evaluated by another method in the laboratory called CAPWAP analysis. In this analysis, the measured force at the pile top is used as input into the program. Values for the soil parameters, resistance distribution on each pile elements are assumed and a dynamic analysis is performed to obtain the required force at the point of measurement to generate the imposed acceleration. The various parameters are changed in an effort to match the computed top force to the measured top force as close as possible. When the computed top force is matched to the measured top force, the field condition is simulated and the ultimate static bearing capacity of the pile can be obtained.

TEST METHOD

The dynamic measurements were carried out by using two sets of gauges and a portable computer called a Pile Driving Analyser. The gauges consisted of:

The instrumentation for the Pile Driving Analyser was attached near the top of the pile. This consisted of two reusable strain gauges and two accelerometers securely bolted near the top of the pile. For each hammer blow, electrical signals were fed into the preprogrammed Pile Driving Analyser and the basic measurements of strain and acceleration were converted into force and velocity parameters as a function of time. From these parameters the ultimate (mobilized) bearing capacities were automatically computed. In addition, the maximum forces, the developed energies and the hammer blow rate, etc., are some of the output from the Analyser. The force and velocity wave traces were continually observed in the field and their analog signals were recorded on magnetic tape by an FM instrumentation tape recorder.

After the dynamic measurements were completed, the piles were subjected to static load test. The static load test was generally carried out in accordance with the ASTM D1143-81 procedures. With the exception of Site A and Site E, all tests were carried out with the standard loading procedures of the ASTM D-1143-81 standard. At Site A and E, the quick load test option outlined in the ASTM procedures was used. The load on the pile was placed incrementally with a hydraulic jack to twice the design load or to failure. A load cell was used in addition to the pressure gauge to monitor the load imposed on the pile. In cases where the pile held twice the design load, the load was maintained for a period of 24 hours prior to unloading.

SITE A

A single storey parking structure was constructed at a site located in North York, Ontario. The contractor elected to use three different pile sizes to suit the various column loads in order to minimize the number of piles to be used. The contractor proposed a driving criteria for the various pile types using a 35 Kn drop hammer falling a distance of 1.2 to 1.5 m to drive the three types of piles.

The piles used at this site consisted of:

Pile Type	Pile Size O.D. mm	Wall Thickness mm	Design Load kN
Steel Pipe	194	8.3	55
Steel Pipe	244	8.9	1000
Steel Pipe	298	8.5	1140

The subsoil at this site consisted of a fill of variable thickness overlying a compact to very dense sand. The fill consisted of clayey silt, sand, rubble and organics and extended to a depth of 10 to 11 m depth. The wet sand extended to a depth of 22 to 26 m where the boreholes were terminated. All test piles were terminated in the sand. The soil conditions are shown in Figure 1, Borehole Log A.

The dynamic results for the load test pile are presented in Table 1. The laboratory CAPWAP analysis results are shown in Table 2. The pile was driven to a final driving resistance of 19 blows per 25 mm under 54 KJ of driving energy. However, the pile top was slightly damaged when the blow counts were taken. The following day, after the pile top was trimmed to sound steel, the pile was restruck and the penetration resistance was measured at 11 blows per 25 mm. An input energy of 75 kJ was used during the restrike.

The ultimate bearing capacity of the load test pile evaluated by the dynamic analysis was 2180 kN. The pile was statically load tested to a maximum load of 2240 kN. The load test was carried out in accordance with the quick load test option of the ASTM D-1143-81 procedures. At the maximum load, the pile top settled a distance of 24.71 mm. The offset limit load criterion for this pile was reached at a load of 2170 kN. It appeared, from the load test curve, that the pile would plunge to failure beyond the maximum load of 2240 kN. The results of the load test for the pile at this site are plotted in Figure 2.

SUMMARY OF RESULTS FOR CASE A

In situations where different pile sizes are used, dynamic monitoring can be used to correlate the capacities of different pile sections once a correlation with at least one static load test is established. The static load test result can be used to establish the soil damping factor to be used in the case method analysis. Provided that the remaining piles are founded in similar soil, the capacity of the remaining piles can be evaluated with reasonable confidence. The ultimate bearing capacity evaluated by CAPWAP analysis to the Offset Limit Load Criterion (Davisson) was within one percent.

Figure 1

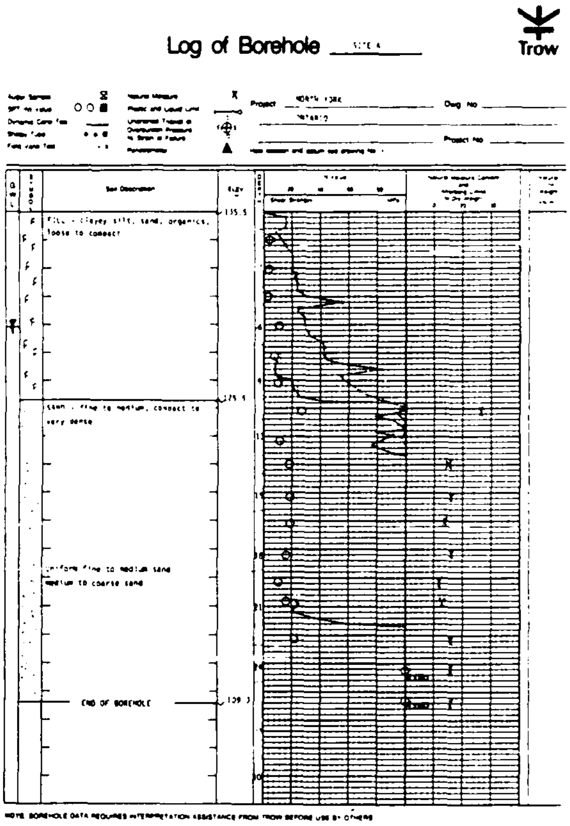

Table 1

TABLE 1 - SUMMARY OF PILE DRIVING ANALYSER TEST RESULTS

				DRIVING RESISTANCE		ENERGY		FORCE		ULTIMATE CAPACITY (kN)		
Pile I.D.	Event	Emb. Depth (m)	Hammer	Measured blows per mm	Equivalent Blows per 25 mm	Mean (kJ)	Ratio %	Impact (Max.) (kN)	Max. Stress (MPa)	Case Method	CAPWAP	Load* Test
SITE A												
A5	B.O.1.R.	19.25	35 kN at 1.5 m Drop	2/2	25	40	62	1670 (1800)	191 (233)	1840	1825	
	B.O.2.R.	20.0	69 kN at 1.5 m Drop	5/11	11	57	69	1360 (2010)	177 (261)	1985	2185	2170
SITE B												
37	B.O.2.R.	9.05	B300	5.0	5.0	8.5	19	1130	165	1260	785	
21	B.O.1.R.	9.35	B300	8.0	11	11.7	21	1360	190	900	660	
13*	B.O.2.R.	9.15	B300	3.0	8.5	9.1	20	1490	165	1175	880	1020
16	B.O.1.R.	9.10	B300	7.0	5.6	11.7	25	1290	180	1065	1015	
SITE C												
TP1	B.O.R.	49.96	B400	40/25	40	20.2	33	1910	192	2300	2375	2600
TP2	B.O.R	33.33	B400	7/13	14	18.1	29	1720	178	1685	1522	1630
SITE D												
24	E.O.I.D	11.75	D12	13/25	13	10.5	34	870 (1130)	235	815		
	B.O.R.	11.75	D12	10/5	50	7.4	24	980 (980)	210	990	921	1080
SITE E												
C 60	B.O.R	16.83	D30 15	05/12.5	10	67.6	67	1985	211	2860	2910	2935

Notes:
B.O.I.R. - Beginning of first and second restrike
Beginning of restrike results based on the first good blow with substantial penetration
E.O.I.D. - End of Initial Driving
B.O.R. - Beginning of Restrike
* Load Test failure load defined by Off set Limit Load Criterion (Davisson) [illegible] (4+B/D) x 10^{-3}, where [illegible] elastic deformation of pile, D = pile diameter.

Table 2

TABLE 2 - SUMMARY OF CAPWAP RESULTS

Pile	Event	Embed. Depth (m)	Permanent Toe Displacement Calc. (mm)	Permanent Toe Displacement Meas. (mm)	Quake (mm) Skin	Quake (mm) Toe	Damping Case Skin	Damping Case Toe	Damping Smith sec/m Skin	Damping Smith sec/m Toe	Ultimate Static Capacity (kN) Side	Ultimate Static Capacity (kN) Tip	Ultimate Static Capacity (kN) Total
SITE A													
A5	B.O.2.R	20.0	0.9	2.2	0.55	0.83	0.236	0.650	0.078	0.115	[illegible]	1240	2181
SITE B													
11	B.O.2.R.	9.1	5.2	1	2.5	3.0	0.25	0.40	0.51	0.22	79	701	880
22	B.O.3.R.	9.1	5.5	9.0	2.5	5.5	0.15	0.25	0.52	0.16	105	627	732
28	B.O.1.R	9.1	5.1	7.0	2.5	6.5	0.44	0.57	0.88	0.26	144	673	817
SITE C													
TP1	E.O.I.D	46.9	0.69	1.27	1.50	1.50	0.750	0.500	0.271	0.291	1128	701	1819
TP3	B.O.R	46.9	0.00	0.61	1.2	1.2	1.005	0.400	0.265	0.291	1672	558	2230
TP2	B.O.R	55.5	2.31	1.81	2.50	2.50	0.449	0.575	0.266	0.317	788	739	1527
SITE D													
26	B.O.R	11.75	0.15	0.50	1.9	4.5	0.117	0.700	0.2351	0.370	549	372	921
SITE E													
L-60	B.O.R	16.65	1.12	2.5	7.0	9.0	0.800	0.355	0.165	0.158	1856	852	2710

Notes:
E.O.I.D - End of Initial Driving
B.O.R Beginning of Restrike

the fill and the penetration resistance increased abruptly to 10 blows per 8 mm or less on or slightly into the shale bedrock. The maximum design load for the piles was 800 kN with majority of the piles carried a load of 500 kN or less.

At the early stages of the project, four piles were driven around the site so that a load test pile could be selected. During the restrike, however, it was apparent that relaxation (a decrease in bearing capacity between the end of driving and restrike) of the piles on the shale bedrock occurred. The magnitude of the relaxation of the piles however, varied from pile to pile, even after three to four restrikes. Dynamic monitoring was therefore suggested to evaluate the capacity of the piles under the relaxation conditions.

Based on the 10 piles dynamically tested during restriking, the estimated ultimate bearing capacity ranged from 640 to 1015 kN. The penetration resistance of the piles upon restriking ranged from 3 to 8 blows per 25 mm, whereas the piles were all driven to a final resistance of greater than an equivalent of 30 blows per 25 mm.

Figure 2

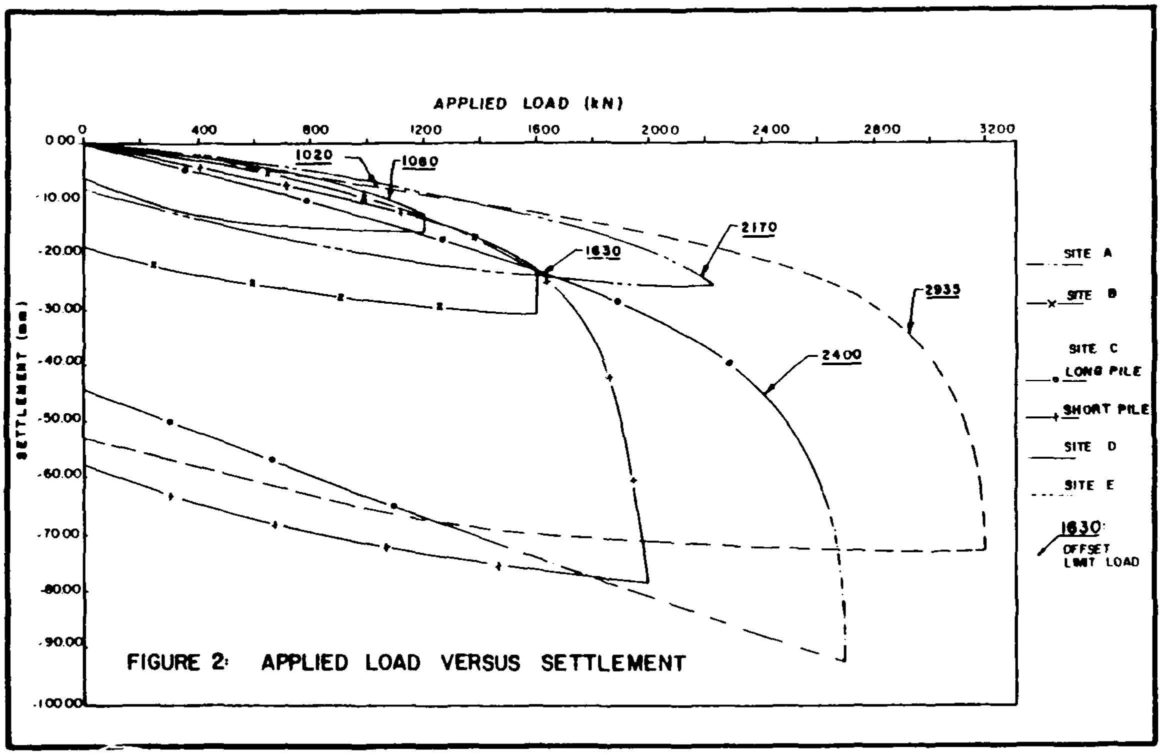

FIGURE 2: APPLIED LOAD VERSUS SETTLEMENT

SITE B

A 1 1/2 storey industrial type building was constructed at a site in Mississauga, Ontario. The subsoil at this site consisted of flyash fill overlying a Georgian Bay shale. The building was to be supported by steel pipe driven through the fill and founded on or slightly into the shale bedrock. The fill depth ranged in thickness from 9 to 11 m in thickness. The soil conditions are presented in Figure 3, Borehole Log B.

The piles were 244 mm O.D. with 12 mm wall thickness closed-ended steel pipes. The piles were driven with a berminghammer B-300 single acting open-ended diesel hammer. The hammer has a rated energy of 46 KJ. The pile was driven easily through

The load test pile achieved an equivalent penetration resistance of 8 blows per 25 mm. Upon restriking, the ultimate bearing capacity as evaluated by CAPWAP analysis on the first hammer blow was 880 kN.

The static load test was carried out in accordance with the standard loading procedures of the ASTM D-1143-81 standard. A maximum load of 1600 kN, equal to twice the maximum design load, was jacked onto the pile. The maximum load was held for a period of 24 hours. Under this load, the pile top had settled a distance of 30.65 mm. The net settlement of the pile top was 17.60 mm after the load was removed. During the loading, the pile did not achieve a settlement rate of 0.25 mm per hour or less beyond a load of 800 kN. The Davisson criterion for this pile was reached at a load of 1020 kN.

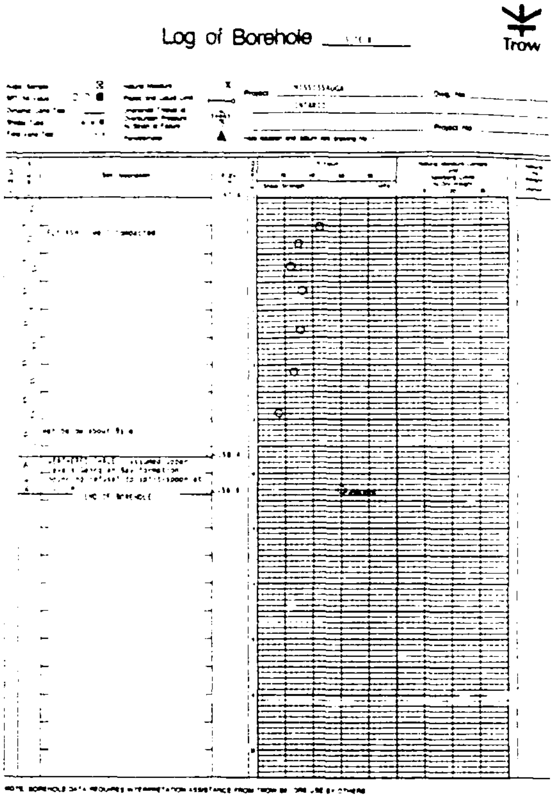

Figure 3

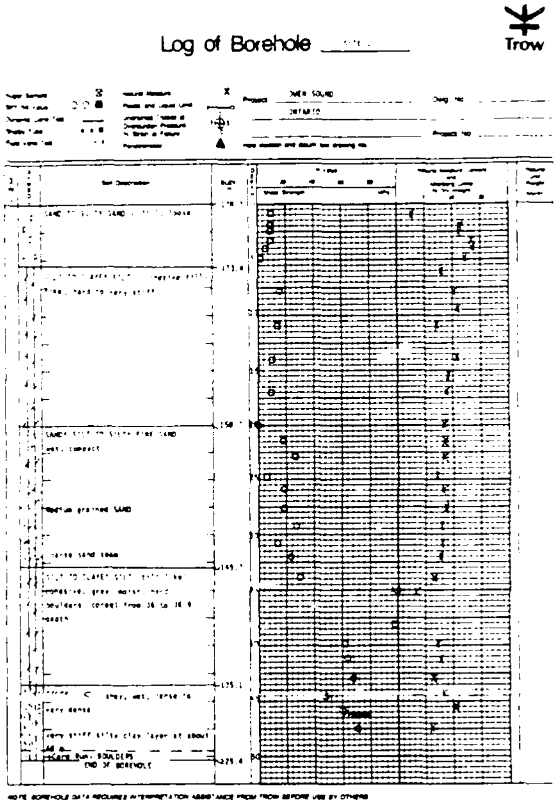

Figure 4

SUMMARY OF RESULTS FOR CASE B

In situations where there is relaxation, dynamic monitoring can be used to compare the ultimate bearing capacity of piles under different relaxation conditions. The capacity evaluated by the dynamic monitoring in this case was low by approximately 14 percent. This could be attributed to the fact that in pile relaxation conditions, each restrike may improve the capacity of the pile. Consequently, the capacity of the pile evaluated from the dynamic analysis was low when compared with the load test result.

SITE C

A test program was undertaken at a site in Owen Sound, Ontario, to evaluate the allowable bearing capacity of piles founded in two slightly different soil strata. The subsoil at this site consisted of 4 to 5 metres of sandy fill overlying a thick stratum of clayey to sandy silt to a depth of 44 metres. This silt is generally compact with a very dense zone near 32 to 34 m depth. Beneath this silt stratum is a very dense bouldery till. The soil condition is shown in Figure 4, Borehole Log C.

The two test piles were 244 mm O.D. with 13.8 mm wall thickness closed-ended steel pipe piles. The piles were driven with a Berminghammer B-400 single acting diesel hammer with a rated energy of 62 kJ. The two test piles were dynamically monitored to the end of the driving as well as during the restrike on the following day.

The long pile was driven to a depth of 46.96 m where it achieved a penetration resistance of 20 blows per 25 mm. The short test pile was driven to a depth of 33.5 m where a penetration resistance of 8 blows per 25 mm was achieved. During the restrike, the penetration resistance of the two test piles was measured to be 40 and 14 blows per 25 mm for the long and short piles respectively.

The ultimate bearing capacity of the two test piles as evaluated by CAPWAP analyses was 2375 and 1525 kN for the long and short piles respectively.

The static load tests were carried out in accordance with the standard loading procedures of the ASTM D-1143-81 standard. Both piles were load tested to plunging failure. For the long pile, a maximum load of 2950 kN was jacked onto the pile. A maximum load of 2000 kN was jacked onto the short pile. The Offset Limit Load Criterion was reached at 2400 kN for the long pile and 1630 kN for the short pile.

SUMMARY OF RESULTS FOR CASE C

The ultimate bearing capacity of the two test piles was successfully estimated by dynamic testing method at this site. During the dynamic monitoring of the first pile, it was evident that the estimated ultimate bearing capacity of the pile at the higher level would be substantially less than the 2600 kN for which the designer had hoped. As a result, a second pile was driven to a lower depth.

The results obtained from the dynamic monitoring of the two test piles when compared with the static load test results were within 1 percent for the long pile and 7 percent for the short pile. The test program proved to be an advantageous exercise since the capacity of the short pile expected by the designer did not materialize. Had the production piling been carried out with the high design load, significant redesigning and extra cost for the piling and delay to the other subtrades would have occurred. This would be not only costly to the owner but would have also caused delay to the contruction.

SITE D

A two-storey building was to be constructed in the island area in Lake Ontario in Toronto, Ontario. The subsoil consisted of

11 to 12 metres of hydraulic fill overlying shale bedrock. The hydraulic fill consisted of loose to dense fine to medium sand. The subsoil conditions are presented in Figure 5, Borehole Log D.

Figure 5

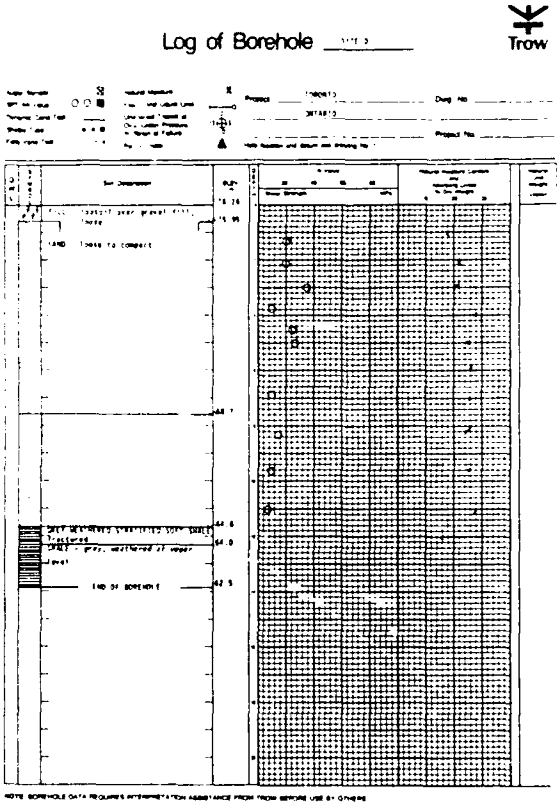

The piles consisted of 324 mm O.D. with 4.8 mm wall thickness, closed-ended steel pipe piles. The piles were to be driven to the shale bedrock to carry a design load of 600 kN. The shale bedrock in this area is known to have relaxation problems for small diameter pipe piles and H-piles. (Thompson and Thompson, 1985; Likins and Hussein, 1984). Initially, the contractor used a MKT 9B3 air hammer to drive the piles. However, the hammer proved to be too small for the 324 mm piles and the subsoil condition at this site as the penetration resistance was in excess of 50 blows per 25 mm at shallow depths. Subsequently, a Delmag D-12 single acting diesel hammer was used to drive the piles. A total of seven piles were monitored at this site; a group of four piles, a group of two piles and a single pile.

Based on the dynamic test on CAPWAP Analysis results, presented in Table 1 and 2, the single pile was selected for static load test. This pile was found to have the lowest ultimate bearing capacity, primarily due to the fact that the shaft resistance was lower for the single pile, as the sand did not densify from the pile driving in the same magnitude as the pile groups. The final penetration resistance for this pile at the end of driving was 15 blows per 25 mm. Upon restriking, the penetration resistance increased to an equivalent of 50 blows per 25 mm. The ultimate bearing capacity estimated by the dynamic analysis for this pile was 920 kN. The Offset Limit Load criterion was met at a load of 1080 kN. Comparatively, the result was 15 percent low. The static load test curve is shown in Figure 2.

SUMMARY OF RESULTS FOR CASE D

The ultimate bearing capacity of the pile predicted by the dynamic analysis was expected to be low in this situation. The main reason for the low capacity was the fact that the pile did not move under the hammer blows; i.e., very high penetration resistance. Similar to a static load test where the failure loads was not jacked into a pile, the ultimate bearing capacity of a pile could not be assessed in such cases. Another point of interest at this site was that relaxation was not experienced by the 324 mm diameter pipe piles driven to the shale bedrock. This could be an indication that relaxation of piles on shale bedrock is localized and that relaxation problems for layer diameter pipe piles are either non-existent or not as severe as small diameter pipe piles.

SITE E

A major steel plant was expanding the steel making facilities in Hamilton, Ontario. More than 5000 piles were required to support the proposed structure. Up to six pile drivers were used at the site at any one day and some pile drivers were working double shifts in order to increase the piling production. The quality control for the piling included inspection of piles, static load tests and periodic dynamic testing of randomly selected piles.

The subsoil at the site consisted of 13 metres of fill overlying a layer of very stiff to hard silty clay and very dense sandy silt till to a depth of 18 metres. The piles were terminated in a very dense silt till below 18 metres. The subsoil conditions are summarized in Figure 6, Borehole Log E.

Figure 6

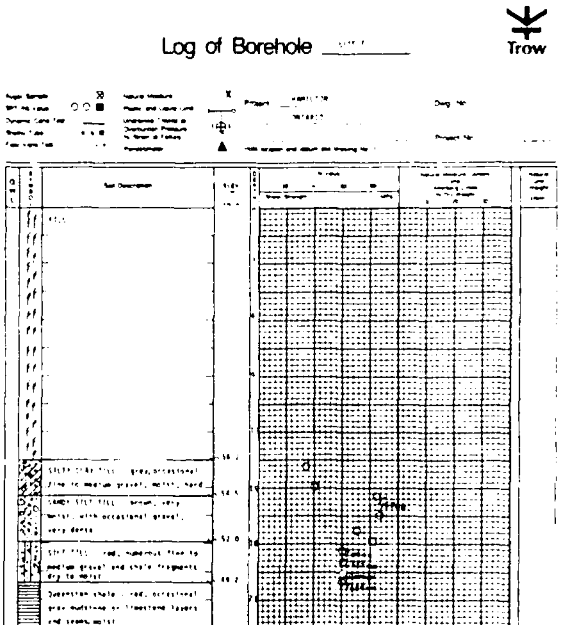

The piles installed at this site were 324 mm O.D. with 9.5 mm wall thickness closed-ended pipe piles designed for an allowable load of 1780 kN. The piles were driven to the founding level with three Delmag D30-13 or D30-23 single acting diesel hammers. The ultimate bearing capacity of the piles was confirmed in a test program consisting of dynamic testing and static load test prior to the production piling. A second static load test was also carried out at the beginning of the production piling to confirm the ultimate bearing capacity of the piles. From the test program, it was established that the piles would have to be driven to refusal (20 blows per 25 mm), in the silt till stratum with a minimum developed stress level during the final driving of 230 MPa.

During a routine dynamic testing on some randomly selected piles, the penetration resistance of some of the piles was found to be less than the specified 20 blows per 25 mm upon restriking. The evaluated capacity of the piles was also less than the average experienced at this site. More dynamic testing was therefore carried out and the results indicated that the Delmag D30 hammers were pre-igniting during installation of the piles and consequently a false penetration resistance was observed. A static load test was requested by the owner on a pile driven with a pre-igniting hammer in order to confirm the findings in the dynamic testing.

The result of the dynamic testing are presented in Table 1. The corresponding CAPWAP analysis of the load test pile is shown in Table 2. The static load test curve is shown in Figure 2. The estimated ultimate bearing capacity of the piles based on the dynamic analysis was 2715 kN. The Offset Limit Load Criterion for the pile was met at 2935 kN. The ultimate bearing capacity of the piles evaluated by dynamic analysis was 7 percent low.

SUMMARY OF RESULTS FOR CASE E

The static load test of the pile at this site confirmed that under pre-igniting conditions of a diesel hammer, the ultimate bearing capacity of the pile was significantly reduced. From a routine visual inspection point of view, there was nothing unusual about the pile since the specified piston rise and the penetration resistance was met for all the pile driven with the pre-igniting hammer. Dynamic measurement, however, revealed the pre-ignition and found that the energy and force delivered to the pile was considerably reduced, primarily due to the cushioning effect on the piston due to the fuel was pre-igniting in the combustion chamber.

The ultimate bearing capacity estimated by the dynamic analysis was found to be 7 percent lower than the Offset Limit Load Criterion. However, in this case, the Offset Limit Load Criterion was not conservative as the pile plunged to failure shortly after this load. The information obtained at this site further reinforced the need for dynamic testing so that the hammer performance could be evaluated.

CONCLUSIONS

The dynamic testing and the static load test at the five sites resulted in the following conclusions:

1. Dynamic testing is an excellent alternative for estimating the ultimate bearing capacity of a driven pile.
2. In order to evaluate the ultimate bearing capacity of a driven pile by dynamic method, the hammer blow analysed must produce a permanent displacement of the pile into the soil in the order of 2 mm per blow. If the permanent displacement due to the hammer blow is low, dynamic analysis would under-estimate the ultimate bearing capacity of the pile unless further analyses were made.
3. Dynamic analysis can be utilized in situations where different pile sizes were used to carry different design load. By performing a static load test on one pile size, the ultimate bearing capacity of the other pile sizes can be evaluated dynamically with a similar degree of confidence.
4. In situations where there is relaxation, the ultimate bearing capacity of the piles can best be evaluated by dynamic method of analysis for the various degree of relaxation.
5. Dynamic testing can be used to evaluate hammer performance and to identify problem hammers.
6. Dynamic testing can be used to test many piles in one day, whereas the conventional method of static load test can obtain information for only one pile after a test period of 1 to 2 days.
7. By monitoring the piles for the end of initial driving and restriking, real or apparent relaxation can be differentiated.
8. Relaxation of pipe piles on shale bedrock tends to be localized and may be dependent on the pile diameter.

REFERENCES

AHMAD, Shaheen, A., and CHENG, S.M., December 16 - 19, 1987. Indian Geotechnical Conference, Bangalore, India.

GOBLE, G.G., LIKINS, G.E., and RAUSCHE, F., 1975. Bearing capacity of piles from dynamic measurements: final report for Ohio Department of Transport. Department of Civil Engineers, Case Western Reserve University.

RAUSCHE, F., 1970. Soil response from dynamic analysis and measurements on piles. Case Western Reserve University, Ph.D. Thesis.

RAUSCHE, R., GOBLE, G.G., and LIKINS, G.E., 1985. Dynamic detection of pile capacity. Journal of Geotechnical Engineering, American Society for Civil Engineers, Vol. 111, No. 3.

SMITH, E.A.L., 1960. Pile driving analysis by the wave equation. Proceedings of American Society for Civil Engineers, Vol. 86, No. SM4, pp 35-61.

THOMPSON, C.D. and THOMPSON, D.E., 1985. Real and apparent relaxation of driven piles. Journal of Geotechnical Engineering, Vol. III, No. 2.

THOMPSON, C.D. and DEVATA M., 1980. Evaluation of ultimate bearing capacity of different piles by wave equation analysis. Proceedings of the International Seminar on Application of Stress Wave Theory on Piles, Stockholm, Sweden.

TROW, W.A. and THOMPSON, C.D., 1980. Control of pile driving using the pile driving analyser. Proceedings of Annual Conference, New Zealand, Institute for Civil Engineers, Dunedin, New Zealand.

Proceedings: Second International Conference on Case Histories in Geotechnical Engineering, June 1-5, 1988, St. Louis, Mo., Paper No. 6.56

Settlement and Repairs to Cement Plant in Central Utah

R.C. Hepworth
President, Chen & Associates, Inc., Denver, Colorado

J. Langfelder
Director, Harbor Branch Oceanographic Institution, Inc., Fort Pierce, Florida

SYNOPSIS

The plant site is located on a terrace of ancient Lake Bonneville. The underlying soils consist of collapsible clays and silts, low-density dune sands and coarse-grained colluvial/alluvial deposits with an abundant fines matrix. Most of the structures were originally founded on footings and mats. After a number of wetting incidences, settlements, both rapid and gradual, occurred. Most of the structures have been underpinned since 1982 by means of piles, hand-dug caissons, and compaction grouting. Most of the underpinning took place while the plant was in operation. Performance and operation have been satisfactory since remedial work was completed.

INTRODUCTION

The cement plant is located about five miles east of Leamington, Utah on Highway 132. Most of the construction was completed during 1981, and the plant was placed in operation in early 1982. Settlement of some structures has been evident since their individual completion. Other structures have shown no signs of movement or distress.

The facility consists of a number of structural units including storage silos, high steel towers, conveyors, mill, rotary kiln and other ancillary buildings. Several of these units, raw materials silos, conveyor bents and finish cement silos, were founded on pipe piles at the time of original construction. Most of the remaining structures were founded on spread footings or mats. At one structure, the mobile equipment repair shop, overexcavation and compaction of the natural soils was accomplished.

In March 1981, the first of a number of wetting incidences occurred. A fairly direct relationship can be followed through the history of the plant site with subsequent wetting incidences. These have occurred as a result of natural phenomenon, mechanical leaks, and operation. Settlements causing concern have ranged from as little as 1 inch to as much as 32 inches in the past five years. Settlements have occurred as a result of rapid consolidation of collapsing soils as well as slower and lower magnitude settlements of coarse-grained soils. There appears to be a direct relationship between the type of wetting, type of soil and magnitude of settlement

Some of the structures have undergone distress which required complete removal and reconstruction, whereas others have been underpinned while remaining in operation and others have undergone almost no distress. Several methods have been used to underpin the structures, and the subsequent performance has generally been good. Negative skin friction is a factor that needs to be fully appreciated for such conditions. Instrumentation has been placed in some of the new foundation elements to try to gain a better understanding of negative skin friction and the transmission of stress to the foundation. These have not been completely successful. The cost of the remedial measures has totaled about $20 million to date. A very positive point is the plant has remained in operation throughout most of the time since construction was complete.

SITE GEOLOGY

The site is located on a northwest-facing terrace feature south of the Sevier River. The plant site elevation is just below the 4900-foot contour, and the topographic feature probably corresponds to an old shoreline or near-shoreline of the Provo stage of ancient Lake Bonneville. The site is situated at the mouth of a drainage. A higher terrace, Bonneville level, is prominent around the site. The lake level fluctuated during climatic changes. The sediments resulting from the changing environment of deposition are extremely complex and heterogeneous. They vary from lacustrine sediments to near-shore dune sands to colluvial/alluvial granular soils. The water table occurs at a depth close to the elevation of the Sevier River at about 4790 feet.

To provide construction pads, the site has been graded into two major levels. The upper level at elevation 4895 contains raw material silos, raw mill, blending silos, kiln and other structures. The lower level, which varies from elevation 4880 to 4885, contains the substation, machine shop, finish mill, control room and storage silos. The levels have been created by a combination of cut on the south side and shallow fill on the north side. Surface drainage has been provided by means of interception ditches on the south, culverts and general site grading. The latter is the means of discharging surface water through the two main levels of the plant. Figure 1 shows the location of the various structures.

SUBSOIL CONDITIONS

Several different series of test holes have been drilled at the site by various geotechnical consultants. The test holes have been advanced with rotary methods, solid auger, hollow stem auger and percussion drilling. Dry sampling with auger or using air rotary were the methods employed in the studies for remedial work.

The soil conditions are extremely erratic. As a general characterization, the upper soils can be described as fine-grained on the west side and coarse-grained on the east side. An approximate line showing this generalization is shown on Fig. 1. The locations of test holes and survey points discussed are also shown on Fig. 1. Figure 2 shows the logs of three holes which typically represent the areas across the site.

low-density clays and sands received considerable attention in the early reports. The consolidation characteristics of the upper coarse-grained soils on the east side of the site received less attention. High penetration resistance and the coarse-grained nature of the soils led the investigators to believe that it was a competent material. Measured settlement of structures founded on the coarse-grained soils led to a suspicion that they were also moisture-sensitive.

Several types of laboratory tests were performed on undisturbed samples of fine-grained soils and remolded samples of the coarse-grained soils. On Fig. 3 is a plot of the results of consolidation tests for two samples of the fine-grained soils. They show two different characteristics for a similar type soil. Test Hole C-19 was drilled in an area that had not been wetted and represents close to the pre-construction conditions. The soil can be termed a collapsing one, since it consolidated about 7% upon wetting. The sample from Test Hole C-21 was in an area that was affected by a waterline break and shows that the soil has a high moisture content from the wetting incident, does not collapse but does consolidate to a high degree upon loading. In fact, the net consolidation is the same for both samples. These soils were laminated and appeared to be of lacustrine origin. The same consolidation characteristics can be expected of the upper clay and sand which occurs on the west side of the site.

Although the upper granular soils on the east side of the site appear to be very dense, the low moisture

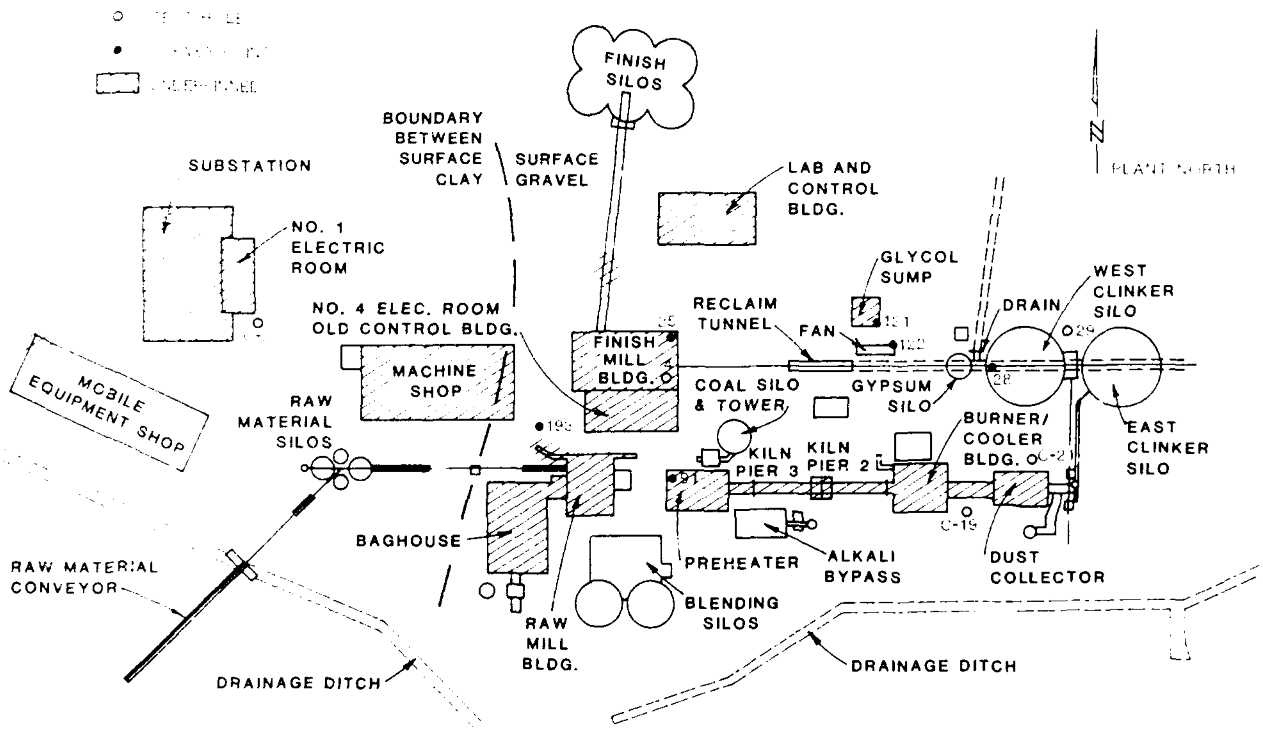
FINISH SILOS
BOUNDARY BETWEEN SURFACE CLAY
SURFACE GRAVEL
SUBSTATION
LAB AND CONTROL BLDG.
PLANT NORTH
N
NO. 1 ELECTRIC ROOM
GLYCOL SUMP
WEST CLINKER SILO
NO. 4 ELEC. ROOM
OLD CONTROL BLDG.
RECLAIM TUNNEL
FAN
DRAIN
FINISH MILL BLDG.
MACHINE SHOP
MOBILE EQUIPMENT SHOP
COAL SILO & TOWER
GYPSUM SILO
RAW MATERIAL SILOS
BURNER/ COOLER BLDG.
EAST CLINKER SILO
KILN PIER 3
KILN PIER 2
C-21
C-19
BAGHOUSE
PREHEATER
ALKALI BYPASS
DUST COLLECTOR
RAW MATERIAL CONVEYOR
BLENDING SILOS
RAW MILL BLDG.
DRAINAGE DITCH
DRAINAGE DITCH

Fig. 1 Site Plan

The soils on the west side of tne site can be generalized as an upper layer of stiff clay and silt with interlayered medium dense, fine sand overlying very dense sand and gravel below depth 55 feet. The soils on the west side of the site, which consists of the majority of the structures, consist of about 45 feet of dense to very dense sand and gravel with some cobbles overlying an intermediate stiff clay with sand lenses which in turn overlies a very dense gravel and cobble stratum below depth 100 feet. The water table is generally at this depth also. On the extreme eastern side of the site, the upper soils are much the same as just described, but the fine-grained soils extend to a much greater depth. The coarse-grained cobble-gravel stratum was not found at depth 160 feet in Test Hole K-29.

The upper fine-grained soils on the west side of the site have been recognized since the first studies to be moisture-sensitive. The collapse potential of the

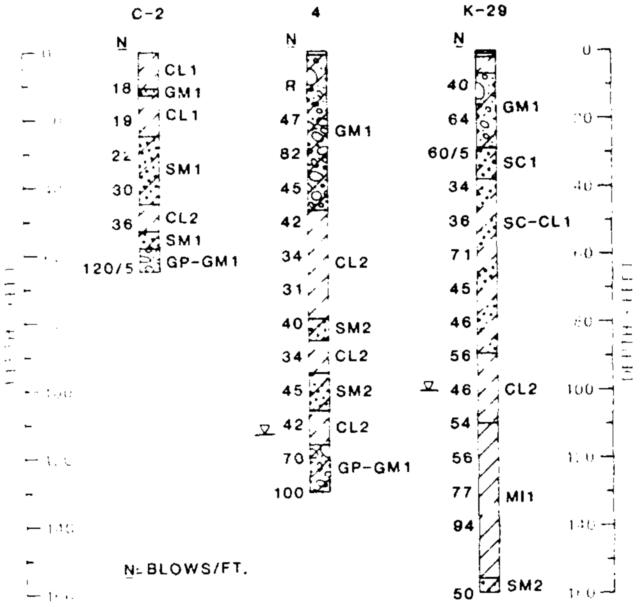

Fig. 2 Logs of Typical Test Holes

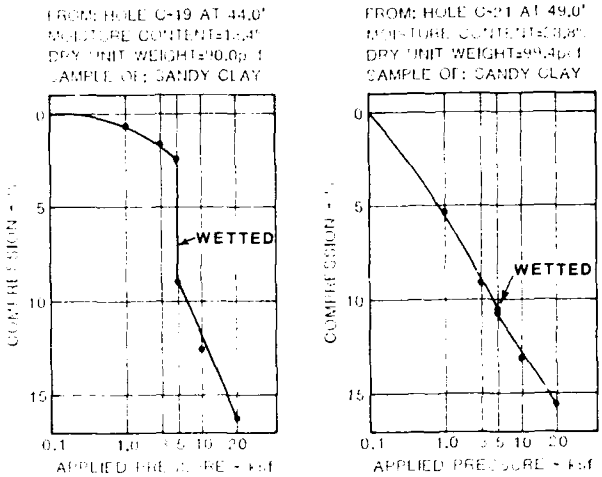

Fig. 3 Consolidation Test Results

content and relatively high fines content suggest they may have been deposited more under the influence of gravity than by water. Samples of the upper granular soils were compacted into a 6-inch diameter mold and loaded to 5,000 psf and then wetted. Initial moisture content was 3%, and the dry density was 124 pcf. When wetted, the sample consolidated 1 1/2%. At the same time, the effects of vibration were also observed, but they were small compared to the settlement observed for wetting.

The standard properties of the soils are shown on Table I. These samples are specific from the test holes shown on Fig. 2, and there was a wider range of property values than indicated by the specific tests. The generalization is that pre-construction condition consisted of dry soils with a high strength and penetration resistance. After wetting, the fine-grained soils become soft and consolidate, whereas the coarser-grained soils still are relatively dense but consolidate slightly.

ANALYSIS

The reaction of the soil to wetting had been tested as discussed above, and the next question was the source of wetting. There were several readily identified wetting incidences that allow good correlation to immediate settlement events. There was also a more subtle settlement, particularly in the coarse-grained soils where specific sources could not be identified but a general migration of the wetting front from another area occurred. This type of settlement occurred inside the mill building, at the preheater and bag house.

Correlating the various structures, subsoils and the wetting, two generalizations were evident.

(1) Where a point discharge of water occurs, there is a rapid settlement. The fine-grained soils show a large magnitude on the order of several inches, whereas the coarse-grained soils show a lower magnitude, on the order of 1 to 2 inches.

(2) Where an advancing front of moisture occurs, the settlements are gradual and long-term. The magnitude is greater in the fine-grained soils than in the coarse-grained soils.

Examples of the first generalization occurred at the southeast corner of the machine shop where a fireline broke and approximately 18 inches of settlement occurred immediately. Examples of the second generalization occur in the ground surface area between the mill building and machine shop.

REMEDIAL MEASURES

Design Considerations

Early in the remedial study, several options were considered to provide a fix to the structures. Since only a few structural elements were showing signs of settlement, a fix on an as needed basis was considered. Deep foundations appeared to be the best solution, but there was an initial concern about driving piles through the upper dense sands and gravels. This proved to be relatively easy, and no pile refusal was encountered in that stratum. H-piles were selected as the best means of achieving small displacement and high bearing capacity. HP 8x36 and HP 12x53 piles were used initially. As underpinning progressed, a heavier section, HP 12x74, was used.

The pile design capacity was determined both statically and dynamically. It was planned that each pile would be driven to its ultimate capacity based on dynamic measurements in the field. Static design

TABLE I. Properties of Typical Soil Groups

Soil Group	Sample Hole/Depth	Blow Count	Moist. %	Dry Dens. pcf	Gravel %	Sand %	Silt Clay %	LL	PI	Remarks
CL-1	C2/10	18	8	90		28	72	26	13	Consolidated 6% on wetting
CL-2	4/60	34	11	105		22	78	32	16	Consolidated 2% on wetting
ML	K29/110	54	25	95		14	86	30	10	
SC-CL	K29/70	45	5	100	Tr.	61	39	NP		
SM-1	C2/30	22	2	89		71	29	21	4	Consolidated 7% on wetting
SM-2	4/100	45	12	116			17			
GM	K29/15	50	7		45	27	28	22	7	SPT sample, some cobbles present
GP-GM	4/130	100	7		35	49	16	NP		SPT sample, cobbles present

considered the working load, a safety factor of 2, negative skin friction and a freeze effect. HP 8x36 sections were driven to 100 tons, HP 12x53 sections were driven to 200 tons and HP 12x74 were driven to 250 tons. Negative skin friction was taken as about 35% of the ultimate pile capacity. This was based on the type of soil, its thickness and estimated depths of wetting. Working loads varied from 45 to 80 tons. The freeze effect was found to be at least 10% of the ultimate pile capacity. This was obtained by allowing the pile to set up and restriking with the dynamic analyzer attached. The field dynamic tests were compared to WEAP analysis performed in the office, and a curve was developed giving blows per foot vs. ultimate capacity.

Construction Considerations

Driving the piles throughout the project required judgment and careful consideration of the tip elevation and driving stress. Hammers consisted of Vulcan 010 and 014, Raymond 3/0 and Kobe 35. Hammer energy on the order of 40,000 ft./lbs. was needed to drive the piles to their desired capacities. Protective tips were used on all piles. It was desired to drive the piles through the upper granular layers and into the lower dense sand-gravel-cobble stratum at or below the water table. Although considerable information had been developed on the subsoil conditions, erratic lengths of piles occurred in the short distances. As an example, at Kiln Pier 2 pile lengths varied from 88 feet to 173 feet, in a horizontal distance of 20 feet. At the beginning of each series of pile driving, the Case-Goble analyzer was used to correlate blow count and capacity. Using this method, it was possible to assess pile damage and separate out the driving resistance due to the soils, the actual bearing capacity of the pile and the freeze effect. During driving, consideration for overdriving and damaging the pile was made as well as the tip elevation of the pile, which was desired to be near the water table.

The underpinned structures included: Substation, No. 1 electrical room, lab and control building, glycol sump, machine shop, finish mill building and mill, bag house, raw mill, preheater, kiln and burner/cooler baghouse.

Negative Skin Friction

Although the underpinning is deemed successful and the buildings and equipment are functional, there has been some small settlement since underpinning. This is attributed to the real effect of negative skin friction which, with the subsiding ground, is still creating stress. A notable failure occurred at the northeast corner of the finish mill building. That corner had been underpinned with two piles in February 1983. The piles were driven to a depth of about 98 feet. Settlement had been very minor until October 1984. After that time, approximately 3 inches of settlement occurred over the next two months. There had been a spill of water in a mixing room at that location about the same time. During November, survey readings showed the settlement to increase, and distress was appearing in the pavement at this corner. In November, a hole was cut through the pavement and a void beneath the pavement of 6 inches was measured. In January 1985, this same void increased to 12 inches. The original pile design was for a 200-ton ultimate capacity with about a 60-ton working load. Considering freeze-up, approximately 100 tons would have been available for negative skin friction. In January, the pile cap was excavated, and it was found the easterly pile had separated from the pile cap and there was an 8-inch gap between the two. The pile cap, where the survey point was located, was in effect cantilevered on the west pile. This pile and the cap were still intact. A test hole was drilled adjacent to the east pile and indicated wetting to almost the water table, depth 100 feet.

It was concluded that the spill from the mixing room had flowed into the soil around the east pile, creating a local area of negative skin friction. The pile was pulled out of the pile cap by the downward settlement of the soil. Shimming and jacking were used to support the pile cap for the next several months. In May 1985, three HP 12x74 piles were driven to support this corner of the building. Prior to driving the piles, the top 50 feet of the subsoils were predrilled and cased with a 20-inch diameter steel casing. A bentonite slurry consisting of one pound of bentonite per gallon of water was placed in the annulus between the casing and the pile. Lime was added to the mixture to raise the pH value to at least 8. Since underpinning, this corner has shown only 1/2-inch of initial settlement and then nil for the last year.

Before underpinning was complete, a test was made of the failed pile. Two of the newly driven piles, which had a length of about 150 feet, were used for reaction. A hole was cut in the pile cap and an extension welded to the failed pile, and the extension in turn welded to an H-beam between the two reaction piles. A one hundred ton jack at each reaction pile applied a tensile load to the failed pile. A load of 182 tons had been applied for 32 minutes with a displacement of 0.4-inch. At this time, the splice weld broke and testing was discontinued. This test showed that the pile was probably intact and that the skin resistance was in excess of 182 tons. It was concluded the pile failed in tip bearing and penetration due to negative skin friction.

West Mill Pier

One of the most challenging pile underpinnings was the west finish mill pier, which was underpinned in July 1982. The mill, 14 feet diameter by 40 feet long and weighing 150 tons, was rolled onto a separate carriage that could be moved out of the way. Motor and drive assemblies were dismantled and removed. The reinforced concrete pier was then removed by controlled explosive demolition. Because of the overhead restriction, piles were driven in 8-foot sections that were butt-spliced together. The pile lengths were about 95 feet. Two of the piles were instrumented with strain gauges; however, by the time the driving was complete, the strain gauges were inoperative. It was suspected that the many splices and working around the clock had an effect on the quality of the electrical connections.

Control Room

The control room had been moved in the fall of 1982 and was founded on piles driven into the upper gravel stratum with lengths on the order of 35 feet. In November 1984, settlement began occurring at the southwest corner of this structure. The building was underpinned in early 1986. Support included piles driven along the building perimeter and steel beams placed in tunnels under the building. Because of the high working load of the piles, 100 tons, the upper 40 feet of the pile was protected with a casing and the annulus between the pile and the casing was backfilled with bentonite slurry. During the remedial work a drain connection was found to be faulty, and during drilling of the casing extremely wet conditions were found in the southwest corner.

Hand-Dug Caissons

Movement of about 1 1/2 inches with a differential of 1 inch had occurred at the preheater tower. This is a 200-foot high steel frame structure. Column loads are on the order of 1,500 kips. The kiln and its supporting three piers extend to the east of the structure. There was a concern with this movement that both the tilting of the preheater tower and misalignment of the kiln piers would occur in time. Studies were made by Kaiser Engineers to determine the best method of underpinning of these structures as well as the raw mill. Pile driving was the preferred method because it was felt that a certain confidence factor can be obtained by driving piles to high resistance. However, with the overhead obstruction, complete shut down and expensive dismantling would be required. Caisson support would be satisfactory if the desired bearing stratum could be identified. Spencer, White & Prentis was engaged to help with the design. They developed a scheme of hand-dug caissons which would allow the plant to remain in operation during the remedial work. An extensive exploration program was initiated to provide more positive information on the bearing elevation and the nature of the soils below that depth. Drilling was undertaken at locations as close to the specific caissons as possible. The holes were advanced with hollow stem augers and by air rotary, and testing was performed as the holes advanced. Near the bearing elevation, pressuremeter tests as well as penetration tests were taken both before and after wetting. The bearing stratum at a depth of about 100 feet was identified as being satisfactory to support the caissons. A bearing capacity of 20 ksf was assigned to the gravel-cobble stratum.

Construction of the caissons went very smoothly. Two dewatering wells were installed where the bearing elevation was at 110 feet, about 10 feet below the water table. Excavation for the caissons consisted of an access pit at the edge of the mat, a tunnel to the centerline of the column, and vertical 4'x4' excavation to the bearing elevation. Lagging was used as the caisson was extended. In some cases, fine sand ran into the shaft but improved mining techniques overcame this difficulty. Once the caissons reached their proposed bearing elevation, the soils were inspected and probed. At that time, a 12x2 bell was constructed. After the bearing stratum was approved, dowels were placed in the bottom of the mat and a reinforcement cage approximately 35 feet long was installed in the shaft. The shaft and bell were then backfilled with concrete to within a few inches of the bottom of the mat foundation. This space was then dry packed with grout. Construction of the caissons continued on a one by one basis for each structural unit. Approximately three weeks were required by two 4-men crews to complete the caissons. A total of twenty-two caissons were installed in this manner. In two of the caissons, instrumentation was placed to measure strain and calculate stress. Although extreme care was used in placing the gauges and securing them, only about 50% survived the concrete placement. Readings of these gauges are continuing. The cost of a caisson was about $200,000.

INSTRUMENTATION

Very complete long-term settlement measurements have been made at the site. These readings extend from May 1982 through the present. Figure 4 shows six plots that are selected for discussion. The locations of these survey points are shown on Fig. 1.

Point 25 is the northeast corner of the finish mill building that has been previously discussed. A total of less than an inch of settlement occurred at this point until October 1984. From October 1984 to February 1985, approximately 3 inches of additional settlement occurred. Underpinning was completed in June 1985, and settlement has been nil since that time.

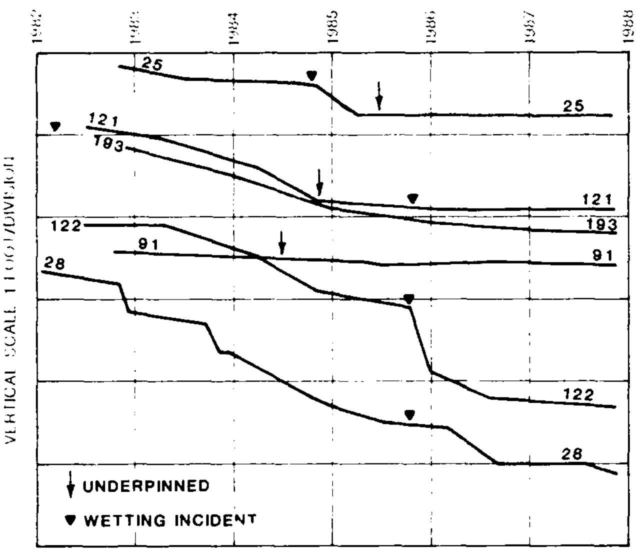

Fig. 4 Settlement Plots

Points 121 and 122 show settlement of the glycol area. This area had become wetted early in the remedial work during a heavy rainstorm when surface drainage had not been completed. A considerable amount of water flowed toward this area. The resulting wetting of the granular soils caused gradual settlement of the sump and fan. Point 121 shows result of an advancing wetting front in the granular soils. Approximately 10 inches of settlement occurred from mid-1982 to the fall of 1984. About the same magnitude of settlement occurred at the fan. In December 1984, the glycol sump was underpinned with six piles. Settlement since that time has been very small. The fan, on the other hand, is founded on a footing and was not underpinned. In November 1985, rapid settlement of this point began to occur. It was also discovered several weeks later that a line in the glycol sump had broken and a several thousand gallon spill occurred. The settlement curve for Point 122 represents the reaction of the wetting which extended through the upper granular soils to the lower fine-grained soils. A large magnitude rapid settlement occurred at the time of the spill. Approximately 12 inches of settlement occurred over the next six months. The rate of settlement is gradually decreasing.

Point 28 represents the west side of the west clinker silo. This structure was first loaded in November 1982. Settlement of about 8 inches had been predicted for the two silos. The silos have a 12-inch thick reinforced concrete wall, and are 80 feet diameter and 140 feet high. Each silo can hold 25K tons of clinker. The sharp increase in settlement on each loading can be seen through 1984. It is believed that some of the early settlement noted here is the result of wetting from the waterline break near Test Hole C-21 and poor surface drainage. There is gradual settlement but at a decreasing rate until late 1985. Detailed examination of the settlement readings shows there is a slight elastic rebound when the silos are unloaded, but the general trend is downward. Again in late 1985, as a result of the glycol spill, there was an increased settlement which occurred with each loading. Total settlement at this point is about 32 inches on the west side and 12 inches on the east side. This curve also indicates deep wetting of the fine-grained soils which was proved by subsequent drilling and sampling. It is estimated that another 12 inches of settlement is possible here without further wetting, and an unpredictable amount of settlement could occur if further wetting takes place. The silos have been instrumented with strain gauges which have not indicated any excessive hoop stress. The tops of the silos were reinforced with a ring beam two years ago.

Point 91 is on the northwest corner of the preheater tower. Approximately 1 1/2 inches of settlement occurred in two years from mid-1982 to mid-1984. The structure was underpinned with caissons and since that time has shown only about 1/2-inch of settlement.

Point 193 represents a paved surface between the finish mill building and the machine shop. This is a drainageway and was previously unpaved. In addition to wetting from surface drainage, a leaky sump and drain lines have also been a problem here. The settlement curve is one of a general wetting that has taken place over a period of time. Total settlement here is about 9 inches in five years. Compare this to the description of the northeast corner of the mill building where settlement of 3 inches occurred in a two-month period of time as a result of a point discharge.

It should also be noted that structures such as the alkali by-pass, blending silos and mobile equipment shop are on spread footings or mats and have not been underpinned and show only minor movement.

Several attempts were made to instrument piles and caissons with only marginal success. Two piles and two caissons have strain gauges that are still providing reasonably reliable data. These data show what might be expected. The loads are increasing at the top of the element and a more gradually increasing load at depth. This is particularly so with the caissons at the preheater unit. The large mat foundation initially took some of the load but gradually became less support and the caissons by now are assuming all of the load.

CONCLUSIONS

The amount of detail collected at this site will provide data for significant analysis for some time. In evaluation of a site in an unproven area, the mode of origin of soils should be considered as well as their relative densities as determined by SPT. Soils that appear to be rapidly deposited and have a high fines matrix should be held in suspect. Positive means of site grading and controlling discharges need to be considered. Where settling soils have occurred or could occur, negative skin friction is a significant factor which can easily be understated. The sleeve method of protecting the upper portion of the piles seems to be very effective. Hand-dug caissons were constructed with ease and provide excellent support for the units so underpinned. It is hoped that a better knowledge of the soils performance and wetting can be passed along to other engineers to prevent problems. It is with this intent that we wish to share this information with the profession.

Proceedings: Second International Conference on Case Histories in Geotechnical Engineering, June 1-5, 1988, St. Louis, Mo., Paper No. 6.58

Performance Evaluation of Pile Foundation Using CPT Data

Keith D. Tucker
Geotechnical Engineer, Southern California Edison Company,
Rosemead, California

SYNOPSIS: The Southern California Edison Company (SCE) has utilized cone penetrometer test (CPT) data for design of concrete drilled shafts and driven piles at various facilities over the plast seven years with substantial cost savings in field exploration and foundation design. This paper incorporates a performance evaluation of drilled shafts and driven piles to predict the uplift load versus deflection curves based on the embedded length to diameter ratio of each foundation. A revised design methodology is presented to correlate the side friction values from CPT data with field uplift load test results in granular and cohesive soils.

INTRODUCTION

The Southern California Edison Company (SCE) has utilized cone penetrometer test (CPT) and exploratory boring results for design of concrete drilled shafts and driven piles along transmission line routes and other facilities within its service territory over the past seven years. Substantial cost savings have been achieved in field exploration and foundation design.

A performance evaluation was made incorporating SCE uplift load tests performed over the past 50 years. Normalized curves are presented which utilize the peak uplift resistance or ultimate uplift capacity at a vertical displacement of one inch (2.5 cm). Thus, the uplift capacity of drilled shafts and driven piles may be predicted with associated deflections based on the shape of the foundation.

A revised design methodology is presented in this paper for use with CPT side friction values. Correlation charts are given for drilled shafts and driven piles to obtain the total side friction resistance of foundations in granular and cohesive soils.

LOCATION OF FIELD LOAD TESTS

A total of 30 uplift load tests were performed at 21 sites within the SCE service territory. The location of three transmission lines, Magunden-Pastoria, Mira Loma-Serrano and Devers-Palo Verde are shown in Fig. 1, along with the Westminster facilities. Also, nine uplift load tests were conducted along the Intermountain Power Project (IPP) transmission line at four sites in Utah, Nevada and California by the Los Angeles Department of Water and Power (LADWP).

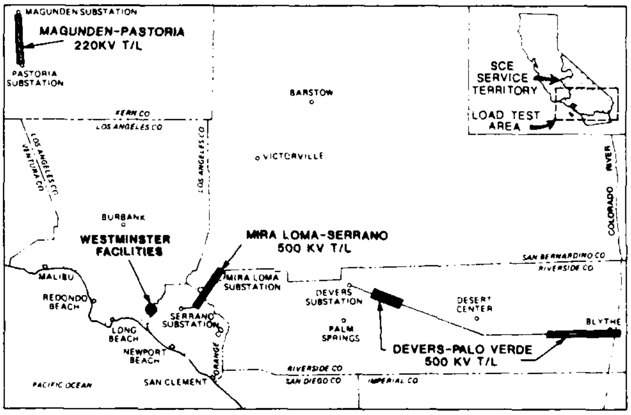
MAGUNDEN SUBSTATION
MAGUNDEN-PASTORIA 220KV T/L
PASTORIA SUBSTATION
BARSTOW
SCE SERVICE TERRITORY
LOAD TEST AREA
KERN CO
LOS ANGELES CO
LOS ANGELES CO
VENTURA CO
LOS ANGELES CO
VICTORVILLE
COLORADO RIVER
BURBANK
WESTMINSTER FACILITIES
MIRA LOMA-SERRANO 500 KV T/L
SAN BERNARDINO CO
RIVERSIDE CO
MALIBU
MIRA LOMA SUBSTATION
REDONDO BEACH
DEVERS SUBSTATION
DESERT CENTER
SERRANO SUBSTATION
LONG BEACH
PALM SPRINGS
BLYTHE
NEWPORT BEACH
ORANGE
DEVERS-PALO VERDE 500 KV T/L
RIVERSIDE CO
SAN DIEGO CO
IMPERIAL CO
PACIFIC OCEAN
SAN CLEMENT

FIGURE 1. LOCATION OF SCE UPLIFT LOAD TESTS

SOIL CONDITIONS

The soil conditions at the four test sites along the Magunden-Pastoria transmission line, southeast of Bakersfield, consisted of loose to medium dense silty sands and silts. Along the Mira Loma-Serrano transmission line, these same conditions were encountered at Sites 4XX and 14AX. Sites 17 and 29X were comprised of surficial silty sands overlying intermixed silty sand and clay layers to a depth of 30 feet (9.1m). Site 27 consisted of medium stiff clay to a depth of 15 feet (4.6m). At site 159, a stiff clay stratum was noted from 3 to 6 feet (0.9 to 1.8m) overlying dense sands with gravel to a depth of 10 feet (3.0m).

During construction of the Devers-Palo Verde transmission line, loose dune sands were encountered at Sites 4018 and 4107, east of Palm Springs. Extreme caving was noted at Site 4018, so a cement slurry was placed in the excavation and the test pier was constructed by drilling through the slurry to the design depth. Between Sites 4722 to 4747, west of Blythe near the Colorado River, the subsurface conditions consisted of loose silty sands overlying intermixed sand and clay strata to depths up to 15 feet (4.6m). Medium dense to dense sands were encountered at depths from 15 to 40 feet (4.6 to 12.2m). Groundwater was located from 10 to 15 feet (3.0 to 4.6m) below the ground surface in this area.

At the Westminster facilities, medium dense silty sands were encountered in the upper five feet (1.2m) overlying intermixed silty sand, silt and clay layers to a depth of 25 feet (7.6m). From 25 to 60 feet (7.6

to 18.3m), dense sand strata were encountered with thin layers of soft clay at various depths. These dense sand layers required predrilled holes so that the precast concrete piles could be driven to the design depths.

Along the Intermountain Power Project transmission line, the Delta and Alamo sites in Utah consisted of stiff to very stiff overconsolidated clay. The Caliente site in Nevada and Baker site in California were characterized by cemented silty sands overlying sands and gravels to a depth of 20 feet (6.1m). Detailed soil conditions for the IPP sites along with pressuremeter data are presented by Briand, et al. (1984).

CONE PENETROMETER TEST RESULTS

The CPT soundings were performed by Earth Technology Corporation and Pioneer Consultants using a standard electric cone pushed at a rate of 0.8 in/sec (2 cm/sec) using a 20 ton (178 kN) reaction truck. Both side friction and point resistance profiles were recorded continuously and used in computing the friction ratios.

UPLIFT LOAD TEST PROCEDURES

Uplift load tests were performed on 30 drilled shafts and driven piles by SCE personnel using a portable steel tripped test frame. This frame is 10 feet (3.0m) high and has three legs spaced 18 feet (5.5m) apart at 120 degree angles from each other. A double acting hollow plunger hydraulic jack with 150 ton (1335 kN) capacity and 8 inch (20.3 cm) stroke was used to apply the tensile loads. The jack has a 3 1/8 inch (7.9 cm) diameter hole through its center and rests on a 1 inch (2.5 cm) thick steel plate at the top of the tripod. A 1 3/8 inch (3.5 cm) diameter, high strength Dywidag bar extends through the jack and was attached to the top of the foundation.

Load tests were conducted by applying a tensile load to the Dywidag bar in increments of approximately 25 percent of the design load. The load was rebounded to zero from 25, 50 and 75 percent of the design load, then the load was re-applied until failure was reached prior to a final rebound, if possible.

Deflections at the top of the test foundations were measured by the use of generally three dial gauges, with an accuracy to 0.0001 inch (0.00025 cm), located at 120 degree spacing around the circumference of the top of the pile. The dial gauges were mounted to a rigid frame which was supported outside the perimeter of the load test frame.

BASIC CONSIDERATIONS

In principle, the uplift capacity of drilled piers in granular soils is shown in Fig. 2a and may be computed from the following vertical equilibrium equation:

$$Q_u = W + Q_s + Q_t \qquad (1)$$

with Q_u = ultimate uplift capacity, W = foundation weight, Q_s = side resistance and Q_t = tip resistance. The side resistance varies depending on the shearing surface and shearing resistance of the granular materials. The tip resistance can be developed from tension and suction stresses at the bottom of the foundation. During drained loading, suction is not present and tip tension is normally very low for cast-in-place concrete drilled shafts as described by Kulhawy (1985). Since the tensile strength of granular soils is usually low, the tip resistance for the drilled shafts and driven piles was assumed to be zero.

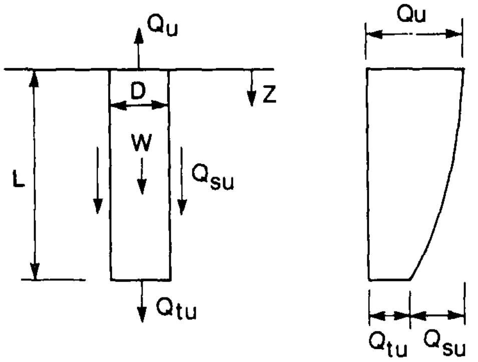

A) FORCE DIAGRAM B) SIDE AND TIP RESISTANCE

FIGURE 2. DRILLED PIER IN UPLIFT

The side resistance, Q_s, is shown in Fig. 2b and may be expressed as:

$$Q_s = Q_u - W - Q_t = \int_0^L (A_s)(f_s)\,dz \qquad (2)$$

where A_s = Surface area of soil-shaft interface, f_s = Average skin friction along soil-shaft interface and L = Embedded length of foundation. The side resistance varies in a parabolic manner along the shaft to a minimum value at the tip of the shaft based on load test results from Reese, et al. (1976), Vesic (1970) and others.

For cast-in-place concrete drilled piers, the soil-shaft interface occurs adjacent to the perimeter of the shaft. Along transmission line routes, belled piers are typically used due to increased uplift resistance as compared to drilled piers of the same length. The generalized failure surfaces for belled piers are shown in Fig. 3a depending upon the embedded length to shaft diameter (L/D) ratio. An equivalent force diagram using a cylindrical shear failure surface is shown in Fig. 3b for belled piers in normally consolidated soils where the uplift "breakout cone" is not likely to develop based on recent studies. The mean diameter for belled piers may be obtained from the following relationship:

$$D_{mean} = D_{shaft} + 1/3\ (D_{bell} - D_{shaft}) \qquad (3)$$

where D_{shaft} = Average shaft diameter and D_{bell} = Diameter at base of pier.

FOUNDATION PERFORMANCE EVALUATION

The performance of drilled shafts and driven piles have been described by many authors in various soil conditions. For this study, field uplift tests by SCE were evaluated based on the foundation geometry (L/D ratios) where the peak capacity was reached. When the peak capacity occurred at larger displacements, the ultimate capacity was selected at a vertical deflection of one inch (2.5cm). This deflection criteria has been used by SCE in design of foundations for transmission line towers and substation steel structures after tower failures occurred in high winds.

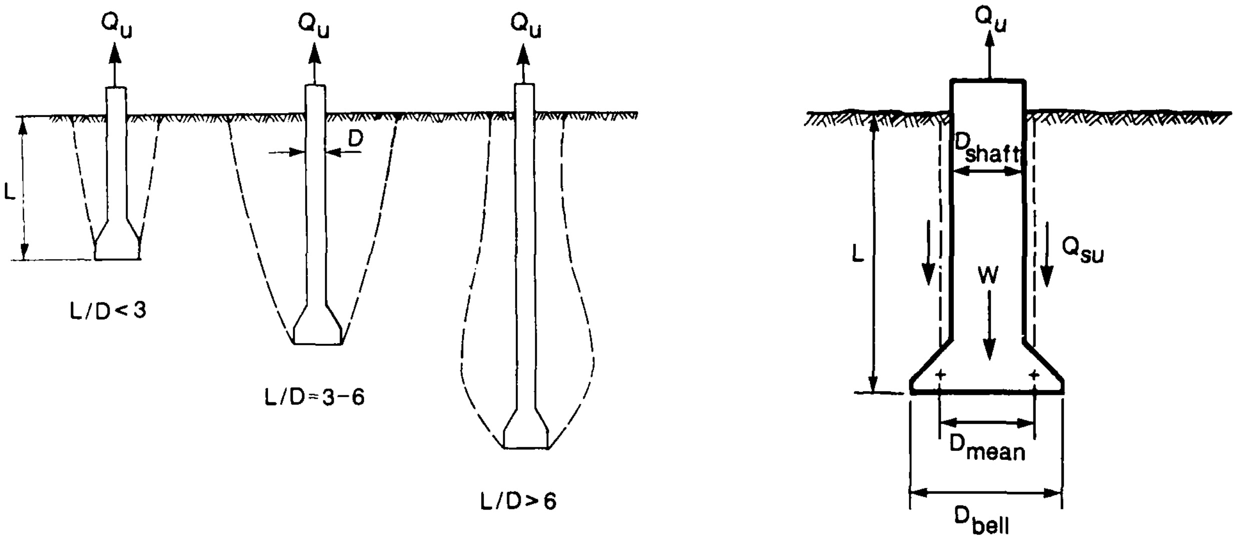

A) GENERAL FAILURE MODES FOR BELLED PIERS

B) EQUIVALENT FORCE DIAGRAM

FIGURE 3. BELLED PIER IN UPLIFT

The load-deflection curves have been normalized based on the peak or ultimate capacity for drilled shafts and driven piles, as shown in Figs. 4 and 5, respectively. A method was developed to estimate the ultimate uplift capacity for test foundations where the peak uplift resistance was not reached during field load tests by using these normalized curves. The measured uplift load at small deflections was compared to the normalized uplift curves based on the type of foundation and embedded length to diameter (L/D) ratio. The ultimate uplift capacity could then be estimated using procedures given by the author (1987) for use in this evaluation.

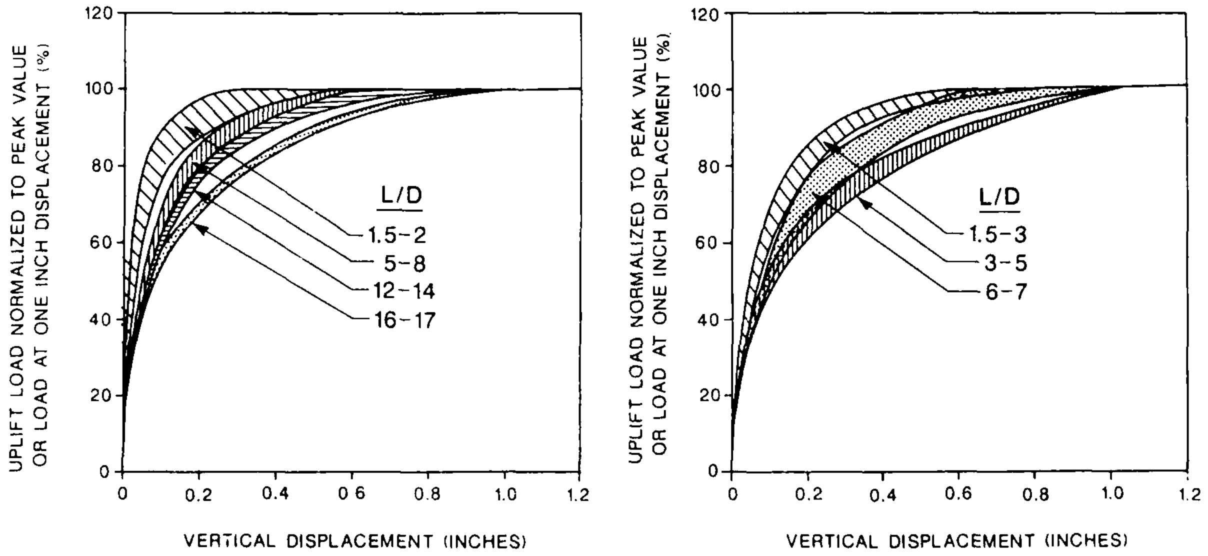

A) DRILLED PIERS

B) BELLED PIERS

FIGURE 4. NORMALIZED UPLIFT LOAD RELATIONSHIP FOR CAST-IN-PLACE CONCRETE DRILLED SHAFTS (1 INCH=2.54 CM)

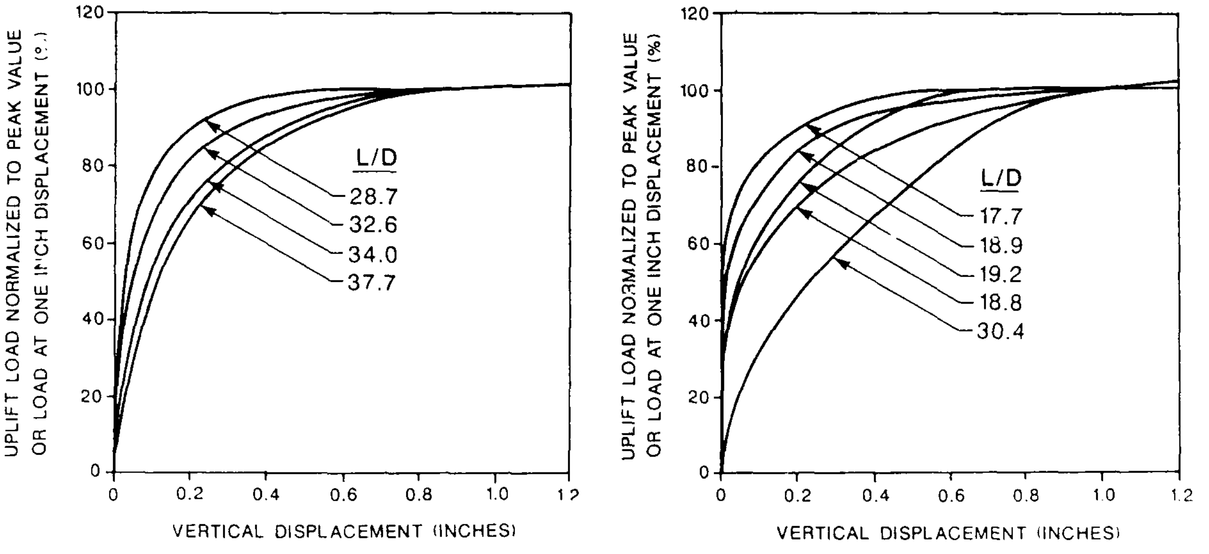

A) CONCRETE SQUARE PILES

B) RAYMOND STEEL STEP-TAPERED PILES

FIGURE 5. NORMALIZED UPLIFT LOAD RELATIONSHIP FOR DRIVEN PILES (1 INCH=2.54 CM)

Belled piers typically require larger displacements to mobilize the ultimate uplift capacity, due to the "breakout cone" failure surface, for piers with L/D ratios less than six. Also, uplift tests on slender steel and concrete driven piles in sand and clay soils indicate that the peak uplift capacity occurred at vertical deflections greater than one inch (2.5 cm). Since most structures are not designed to accommodate these large foundation displacements, the use of a deflection criteria to evaluate the design foundation capacity was incorporated.

FIELD UPLIFT LOAD TEST RESULTS

Field uplift load tests were performed on 16 drilled piers and 13 belled piers using cast-in-place concrete construction, as well as 10 prestressed concrete driven piles. The field load test results are given in Tables 1, 2 and 3 for the drilled piers, belled piers and driven piles in granular soils, respectively. The field load test results on drilled shafts in cohesive soils are listed in Table 4.

TABLE 1. RESULTS OF UPLIFT TESTS ON DRILLED PIERS IN GRANULAR SOILS

Location	Pile Length (Feet)	Pile Dia (Feet)	L/D	Uplift Capacity Total (Kips)	Uplift Capacity Net (Kips)	Vert. Defl (Inch)	TPT Capacity(1) $F_S F_1$ (Kips)	TPT Capacity(1) Actual (Kips)	K(1) $F_S F_1$	K(1) Actual	Ground Water (Feet)	TPT Capacity(2) (Kips)	TPT Capacity(2) Actual (Kips)	K(2) [illegible]	K(2) Actual
SCE Mira Loma-Serrano 500 kV T/L															
Pile [illegible]	35.0*	1.50*	16.7*	162.0	155.4	1.00	95.5	111.8	1.63	1.33	NE	134.7	152.0	1.15	[illegible]
SCE Devers-Palo Verde 500 kV T/L															
Site 4[illegible]A	8.0	4.21	1.9	106.0	89.4	0.56	15.8	40.0	--	--	NE	124.8	272.0	--	--
[illegible]				(110.5)	(93.8)	(1.00)			5.58	2.35				2.72	2.34
Site 4[illegible]	22.8	1.75	13.0	103.0	96.7	0.33	109.9	110.0	0.88	0.88	11	145.7	147.2	[illegible]	[illegible]
				100.0		0.45									
Site 4[illegible]5	34.0	2.85	11.9	124.0	101.0	0.05	306.0	349.3	-	-	10	389.7	439.3	-	-
				(258.3)	(235.3)	(1.00)			0.77	0.67				0.67	0.54
Site 4[illegible]	26.5	2.80	9.5	138.0	119.8	0.10	280.0	362.2	--	--	10	483.9	616.3	-	
				(226.2)	(208.1)	(1.00)			0.74	0.57				0.43	0.34
Site 4[illegible]3A	26.2	1.15	22.8	102.0	99.0	0.97	134.2	162.2	0.74	0.61	10	145.7	173.6	0.68	0.57
Site 4[illegible]3B	22.7	1.70	13.5	120.0	114.0	0.50	144.6	166.7	0.79	0.68	10	177.5	204.4	0.64	0.56
				125.0		5.14									
Site 4[illegible]3C	17.0	2.05	8.3	90.0	73.0	0.53	106.2	128.2	0.69	0.57	10	162.0	194.7	0.45	0.37
				35.0		7.40									
Site 4[illegible]	22.0	1.75	12.6	130.0	123.9	0.65	133.5	138.4	0.93	0.90	15	180.4	187.0	0.69	0.66
				73.0		10.00									
LADWP Intermountain Power Project T/L															
Baker Site															
Pile No. 3	14.0	2.25	6.2	190.0	181.7	0.40	98.1	162.0	--	--	NE	223.1	355.3	--	-
				(200.0)	(191.7)	(1.00)			1.95	1.18				0.86	0.54
Pile No. 4	9.0	2.21	4.1	98.0	92.8	0.58	41.6	72.4	--	--	NE	139.8	224.0	--	--
				(100.0)	(94.8)	(1.00)			2.28	1.31				0.68	0.42

Notes: Numbers in parenthesis are based on estimated ultimate uplift capacity at a vertical deflection of one inch
*Pier dimensions based on design sheets and were not verified in field. NE = Not encountered
1) Values computed using equations 4 and 5, 2) Values computed using equations 6 and 7
(1.0 kip = 4.45 kN, 1 Foot = 30.48 cm, 1 Inch = 2.54 cm)

TABLE 2. RESULTS OF UPLIFT TESTS ON BELLED PIERS IN GRANULAR SOILS

Location	Pile Length (Feet)	Pile Dia (Feet)	Bell Dia (Feet)	L/D	Uplift Capacity Total (Kips)	Uplift Capacity Net (Kips)	Vert. Defl. (Inch)	CPT Capacity¹ $f_{s<f_l}$ (Kips)	CPT Capacity¹ Actual (Kips)	K_{soil}¹ $f_{s<f_l}$	K_{soil}¹ Actual	Ground Water (Feet)	CPT Capacity² $f_{s<f_l}$ (Kips)	CPT Capacity² Actual (Kips)	K_{sand}² $f_{s<f_l}$	K_{sand}² Actual
[illegible]																
[illegible]	[illegible]	[illegible]	3.[illegible]	3.8	65.0	[illegible]	1.00	16.7	[illegible]	3.68	3.59	NE	88.3	[illegible]	0.70	0.67
[illegible]	4[illegible]	[illegible]	3.8	[illegible]	56.0	[illegible]	0.22	51.6	58.5	--	--	NE	149.5	[illegible]	--	--
					(168.0)	([illegible])	(1.00)			3.13	2.76				1.08	0.94
[illegible]	14.[illegible]	[illegible]	3.[illegible]	[illegible]	74.0	67.4	0.13	22.0	22.0	--	--	NE	47.8	47.8	--	--
					(129.8)	(123.2)	(1.00)			5.63	5.63				2.58	2.58
[illegible]	[illegible]	[illegible]	3.[illegible]	[illegible]	74.0	67.4	1.00	44.2	46.0	1.52	1.47	NE	124.7	129.6	0.54	0.52
[illegible]																
[illegible]	[illegible]*	[illegible]*	[illegible]*	[illegible]*	102.0	[illegible]	0.75	40.8	43.8	2.44	[illegible]	NE	94.2	[illegible]	1.06	[illegible]
[illegible]	[illegible]	[illegible]	[illegible]	[illegible]	79.0	76.2	1.00	27.5	28.0	2.77	2.72	NE	73.2	74.8	1.04	[illegible]
[illegible]	[illegible]*	[illegible]*	3.5	3.5*	196.0	188.0	0.22	86.2	125.8	--	--	NE	204.4	306.3	--	--
					(297.0)	(289.0)	(1.00)			3.35	2.30				1.41	0.94
[illegible]	[illegible]	[illegible]	[illegible]*	4.8	206.0	[illegible]	0.14	40.0	70.0	--	-	NE	145.0	325.0	--	--
					([illegible])	([illegible])	(1.00)			9.43	5.39				2.60	[illegible]
[illegible]																
[illegible]	[illegible]	[illegible]	5	2.6	93.6	84.4	0.60	31.4	136.6	2.69	0.62	NE	205.2	[illegible]	0.41	[illegible]
[illegible]	[illegible]	[illegible]	5.[illegible]	[illegible]	124.0	[illegible]	0.56	27.7	112.5	4.23	1.04	NE	176.8	543.0	0.66	[illegible]
[illegible] Power Project [illegible]																
[illegible]	[illegible]	[illegible]	3.0	3.3	145.0	141.0	0.38	27.8	[illegible]	--	--	NE	132.6	[illegible]	1.34	0.35
					(181.3)	(177.3)	(1.00)			6.38	1.69					
[illegible]	[illegible]	[illegible]	[illegible]	4.3	200.0	194.8	0.26	45.4	154.0	--	--	NE	[illegible]	[illegible]	1.68	0.45
					([illegible])	(288.9)	(1.00)			5.36	1.88					

Notes: Numbers in parenthesis are based on estimated ultimate uplift capacity at a vertical deflection of one inch
*These dimensions based on design sheets and were not verified in field. NE = Not Encountered
1) Values computed using equations 4 and 5, 2) Values computed using equations 6 and 7.
(1.0 kip = 4.45 kN, 1 Foot = 30.48 cm, 1 Inch = 2.54 cm)

TABLE 3. RESULTS OF UPLIFT TESTS ON DRIVEN CONCRETE PILES IN GRANULAR SOILS

Location	Pile Length (Feet)	Pile Dia (Feet)	L/D	Uplift Capacity Total (Kips)	Uplift Capacity Net (Kips)	Vert. Defl. (Inch)	CPT Capacity¹ $f_{s<f_l}$ (Kips)	CPT Capacity¹ Actual (Kips)	K_{soil}¹ $f_{s<f_l}$	K_{soil}¹ Actual	Ground Water (Feet)	CPT Capacity² $f_{s<f_l}$ (Kips)	CPT Capacity² Actual (Kips)	K_{sand}² $f_{s<f_l}$	K_{sand}² Actual
GE Metrology Laboratory															
Pile No. 1	28.7	1.00	28.7	70.0	66.4	0.94	88.0	90.6	0.75	0.73	14	114.2	120.4	0.58	0.55
Pile No. 2	34.0	1.00	34.0	101.0	97.0	0.99	132.4	135.6	0.73	0.72	14	158.6	165.4	0.61	0.59
Pile No. 3	37.7	1.00	37.7	138.0	133.7	1.03	148.4	171.5	0.90	0.78	14	174.5	203.2	0.77	0.66
GE Large Apparatus Repair Shop Facility															
Pile No. 2	50.0	1.17	42.9	217.0	210.2	0.65	292.4	344.0		--	10	309.5	363.7	--	--
				(230.9)	(224.0)	(1.00)			0.77	0.65				0.72	0.62
Pile No. 3	49.5	1.17	42.4	215.0	208.1	0.66	272.5	351.4	--	--	10	283.1	362.1	--	--
				(228.7)	(221.8)	(1.00)			0.81	0.63				0.78	0.61
Pile No. 5	58.0	1.17	49.7	212.0	203.8	0.65	356.6	457.3	--	--	10	374.4	476.8	--	--
				(235.5)	(227.3)	(1.00)			0.64	0.50				0.61	0.48
Pile No. 7	57.0	1.17	48.9	210.0	201.7	0.59	371.3	515.7	--	--	10	394.2	541.3	--	--
				(238.6)	(230.3)	(1.00)			0.62	0.45				0.58	0.43
SCE Devers-Palo Verde 500 kV T/L															
Site 4[illegible]A	38.0	1.17	32.6	120.0	113.8	0.80	325.9	380.2	0.35	0.30	15	364.2	431.9	0.31	0.26
Site 4[illegible]B	40.0	1.17	34.3	150.0	143.9	0.10	348.4	406.2	--	--	15	386.7	457.9	--	--
				(254.2)	(248.1)	(1.00)			0.71	0.61				0.64	0.54
Site 4[illegible]35	40.0	1.17	34.3	90.0	84.2	0.10	345.8	417.7	--	--	15	378.8	453.7	--	--
				(152.5)	(146.4)	(1.00)			0.42	0.35				0.39	0.32

Notes: Numbers in parenthesis are based on estimated ultimate uplift capacity at a vertical deflection of one inch
1) Values computed using equations 4 and 5, 2) Values computed using equations 6 and 7
(1.0 kip = 4.45 kN, 1 Foot = 30.48 cm, 1 Inch = 2.54 cm)

The total uplift capacities in these tables represent the peak resistance from the load tests at displacements less than one inch or the estimated ultimate capacity at a vertical deflection of one inch (2.5 cm) based on the normalized curves in Figs. 4 and 5. The net uplift capacity corresponds to the side resistance along the soil-shaft interface.

FRICTIONAL CAPACITY PREDICTION USING CPT DATA

The CPT soundings provide tip resistance and side friction values of subsurface materials with associated friction ratios. An electric cone penetrometer was used at all sites in this study. The computation of shaft friction using CPT data was described by Schmertmann (1978) using the relationship:

$$Q_{sp} = K_{s,c}\left[\sum_{\ell=0}^{8D} (\ell/8D)\,(f_s)(A_s) + \sum_{8D}^{L} (f_s)(A_s)\right] \qquad (4)$$

where Q_{sp} = Predicted side friction resistance using CPT data, $K_{s,c}$ = f_s correlation factors - K_s in sand layers, K_c in clay layers, ℓ = Depth to f_s value considered, D = Shaft diameter, f_s = Unit local

TABLE 4. RESULTS OF UPLIFT TESTS ON DRILLED SHAFTS IN COHESIVE SOILS

Location	Pier Length (Feet)	Pier Dia. (Feet)	Bell Dia. (Feet)	L/D	Uplift Capacity		Vert. Defl. (Inch)	Ground Water (feet)	Ave. Shaft Friction (Ksf)	Ave. Cone Friction (Ksf)	Adherence Coeff.-M [1]
					Total (Kips)	Net (Kips)					
SCE Mira Loma-Serrano 500 kV T/L											
Site 27	9.5	1.5	3.0	6.3	119.0 (126.5)	116.5 (124.0)	0.65 (1.00)	NE	1.95 2.08	2.36	0.83 0.86
LADWP Intermountain Power Project T/L											
Delta Site											
Pile No. 1	9.4	2.17	--	4.3	107.0 (110.0)	101.7 (104.7)	0.50 (1.00)	18	1.59 1.64	4.02	0.39 0.41
Pile No. 2	9.4	2.08	--	4.5	105.0 (108.0)	100.2 (103.2)	0.62 (1.00)	18	1.63 1.68	4.02	0.41 0.42
Pile No. 3	14.4	2.17	--	6.6	160.0 (168.0)	152.0 (160.0)	0.60 (1.00)	18	1.55 1.63	4.30	0.36 0.38
Alamo Site											
Pile No. 4	8.9	2.13	--	4.2	200.0 (213.0)	195.2 (208.2)	0.32 (1.00)	NE	-- 3.50	18.50	-- 0.19
Pile No. 3	13.9	2.13	--	6.5	200.0 (256.4)	192.6 (249.0)	0.16 (1.00)	NE	-- 2.68	23.58	-- 0.11

Notes Numbers in parenthesis are based on estimated ultimate uplift capacity at a vertical deflection of one inch.
NE = not recommended. 1) Values computed using equation 8. (1.0 kip = 4.45 kN, 1 Foot = 30.48 cm, 1 Inch = 2.54 cm)

side friction resistance from CPT data, A_s = Pile-soil contact area per f_s depth interval, and L = Total embedded length of pile.

The K_s and K_c values are shown in Fig. 6 from Schmertmann (1978). K_s represents a correction factor to be utilized with granular soils and is dependent on embedded length, pile diameter and type of material. The correction factor, K_s, for granular materials was derived from load tests on smooth and rough model piles by Nottingham (1975). The rough piles produced much higher K_s values than results from smooth pile tests. The stress history and coefficient of earth pressure at rest, K_0, may be

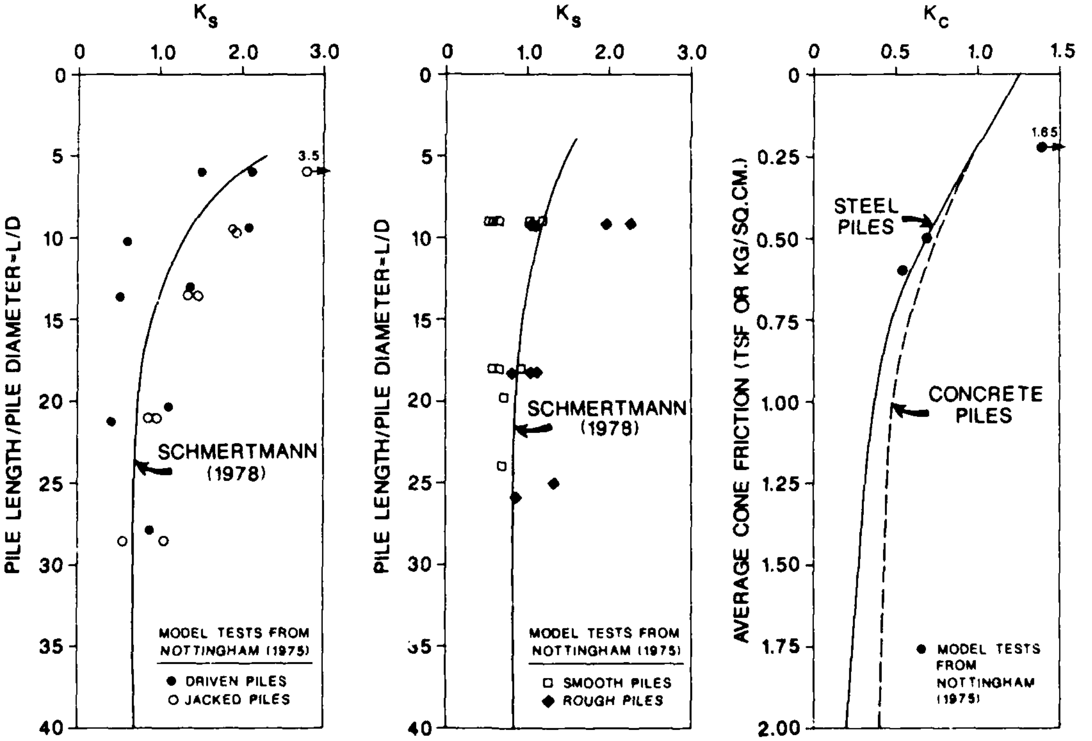

A) STEEL PIPE PILES IN SAND

B) CONCRETE SQUARE PILES IN SAND

C) STEEL AND CONCRETE PILES IN CLAY

FIGURE 6. SIDE FRICTION CORRELATION FACTORS FOR ELECTRICAL PENETROMETER

evaluated using Standard Penetration Test (SPT) blowcounts, CPT results or pressuremeter tests, as described by Kulhawy, et al. (1984).

The K_c value represents a correction factor for cohesive soils which is primarily dependent upon the shear strength of the fine grained soil. Many axial load tests in clay soils have been performed to evaluate the adhesion factors for soft to stiff clays on wood, steel and concrete piles. The correction factor, K_c, for clay soils shown in Fig. 6 was based on test results from Tomlinson (1957) and others where the soil adhesion is compared to the undrained shear strength of the clay soils, as well as limited model tests by Nottingham 1975).

The predicted frictional resistance, Q_{sp}, from CPT data was computed using Eq. 4 with K_c values from Fig. 6 and K_s values set equal to one for each clay and sand layer, respectively. The pile-soil contact area for each interval was calculated using the average diameter for drilled piers and driven piles and mean diameter for belled piers. The side friction values, f_s, were selected for two cases: (1) $f_s \leq f_l$ where f_l = 1.2 tsf (kg/sq.cm.) and (2) f_s = Actual values from CPT data. The limiting side friction value, f_l, was proposed by Schmertmann based on methods used by Dutch engineers.

The peak and estimated ultimate uplift capacities from field load tests were compared to the predicted side resistance capacity from Eq. 4 using the following relationship:

$$K_{soil} = Q_{su} \Big/ \left[\sum_{\ell=0}^{8D} (\ell/8D)\,(f_s)(A_s) + \sum_{8D}^{L} (f_s)(A_s) \right] \qquad (5)$$

where K_{soil} = Correlation factor for granular materials and Q_{su} = Ultimate side friction resistance from uplift load tests. The K_{soil} values are listed in Tables 1, 2 and 3 and are shown graphically in Fig. 7 along with the original design curves from Fig. 6. For the case with $f_s \leq f_l$ = 1.2 tsf, the field uplift test results correlate well with Schmertmann's curve for drilled piers and driven piles with L/D ratios greater than 10. Drilled shafts with L/D ratios less than 10 yield much higher actual capacities than predicted based on model tests by Nottingham (1975). When the actual cone friction values are incorporated into Eq. 4, the field test results are lower than the original design curve for foundations with L/D ratios greater than 10 and somewhat higher for drilled shafts with L/D ratios less than nine. These conclusions from SCE field load tests are consistent with results from Horvitz, et al. (1981) and others.

REVISED DESIGN METHODOLOGY

The predicted side frictional resistance of drilled shafts and driven piles from Eq. 4 incorporates an $\ell/8D$ reduction factor to the side friction values from CPT soundings. Uplift load tests on model piles

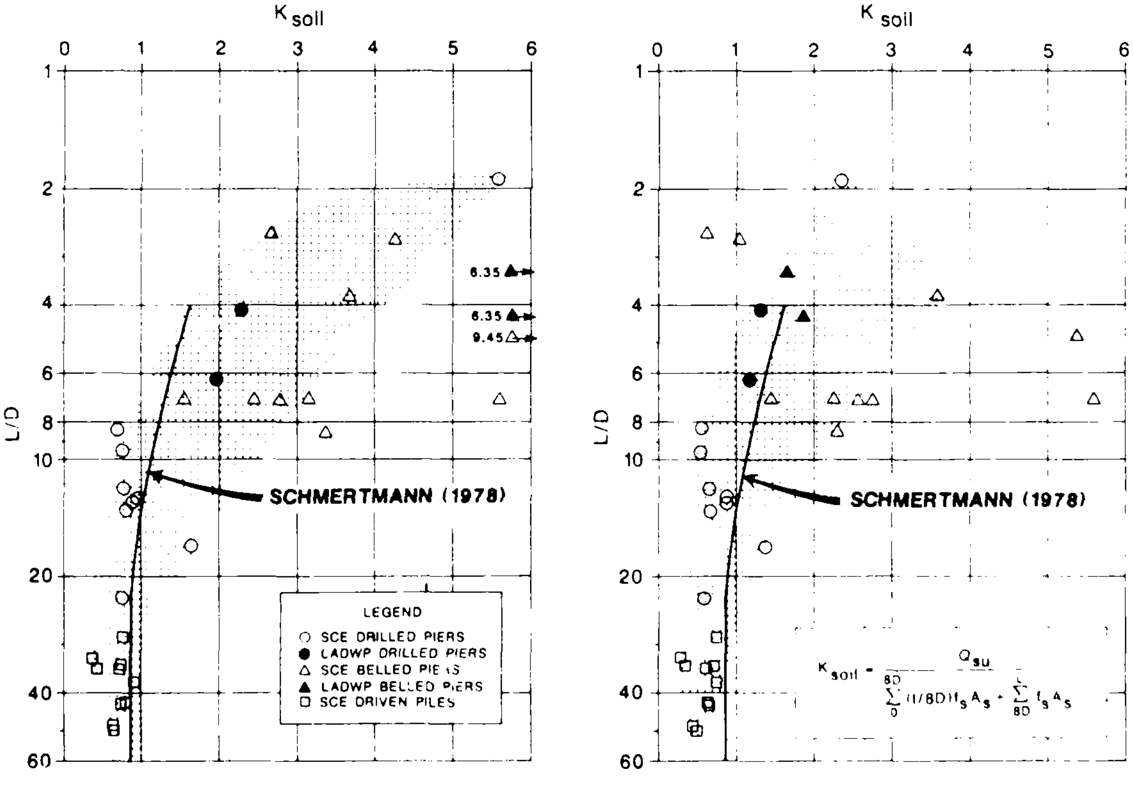

A) WITH $f_s \leq f_l$ = 1.2 TSF OR KG/SQ.CM.

B) WITH f_s = ACTUAL VALUES

FIGURE 7. CPT SIDE FRICTION CORRECTION FACTOR, K_{soil}, FOR SANDS FROM FIELD UPLIFT LOAD TESTS

AD-A213 199 INTERNATIONAL CONFERENCE ON CASE HISTORIES IN 6/8
GEOTECHNICAL ENGINEERING (2.. (U) MISSOURI UNIV-ROLLA
S PRAKASH 30 JUN 89 ARO-25645.2-GS-CF DAAL03-87-G-0129
UNCLASSIFIED F/G 13/2 NL

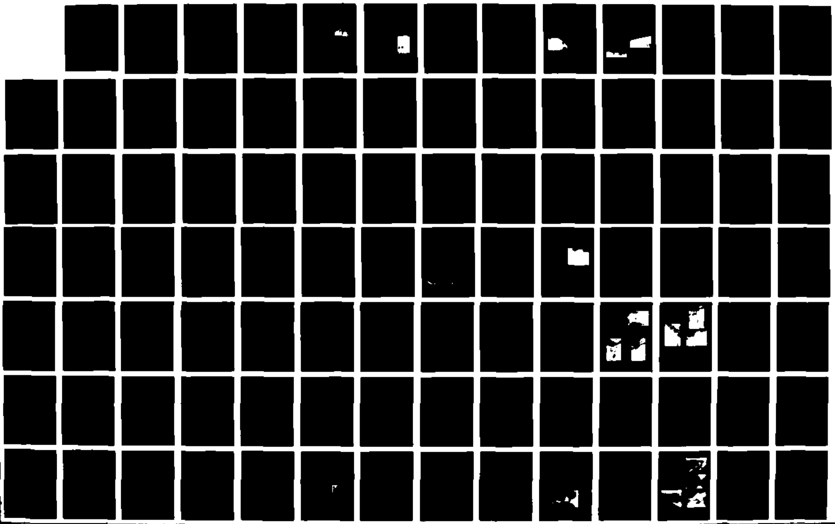

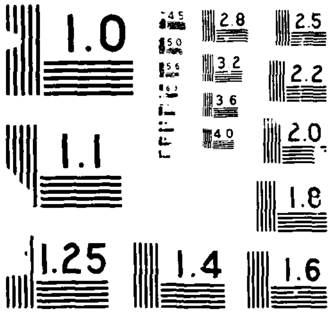
1.0
4.5
5.0
5.6
2.8
2.5
3.2
2.2
3.6
4.0
2.0
1.1
1.8
1.25
1.4
1.6

in granular soils by Das and Seeley (1975), Das and Rozendal (1983), and Meyerhof (1973) indicated that the unit skin friction along the pile increases linearly to a limiting value at a critical depth. This critical depth is dependent upon the soil relative density, shear strength, pile material and roughness along the soil-pile interface. Field axial load tests on circular steel pipe piles conducted by Vesic (1970) and others show that distribution of skin friction along pile shafts is generally parabolic. The limiting skin friction values occurred at embedded length to diameter (L/D) ratios from 6 to 14 in model tests and 2 to 30 in field tests.

Field uplift loads tests performed by SCE over the past 50 years indicate that the average skin friction decreases as the L/D ratio becomes larger in granular soils. These test results were presented by the author (1987) and are shown graphically in Fig. 8. This trend also occurs for drilled shafts in cemented sand and gravels as well as rock materials.

Granular soils - Since field uplift load tests on full scale foundations in granular soils show that a reduction in skin friction for drilled piers with L/D ratios less than 8 is not warranted, the computed side friction resistance in granular soils using CPT data may be obtained from the relationship:

$$Q_{ss} = K_{sand} \sum_{0}^{L} (f_s)(A_s) \qquad (6)$$

where Q_{ss} = Total side friction resistance in sands and K_{sand} = Correlation factor for granular soils. The K_{sand} values from field load tests were computed from the relationship:

$$K_{sand} = Q_{su} / \sum_{0}^{L} (f_s)(A_s) \qquad (7)$$

The Q_{ss} and K_{sand} values from equations 6 and 7, respectively, are given in Tables 1, 2 and 3. Again, two cases were evaluated regarding the CPT side friction values using a limiting condition and actual records as previously discussed. The K_{sand} values are shown graphically versus the L/D ratio of each foundation in Fig. 9. The range of K_{sand} values from Eq. 7 is much less than corresponding K_{soil} values from Eq. 5, indicating that the use of Eq. 6 to predict the side friction resistance with CPT data gives more consistent results as compared to the field uplift test results.

Cohesive Soils - In cohesive soils, field uplift load test results on drilled shafts by SCE and LADWP are tabulated in Table 4. The average skin friction value was computed for each pier from the field load test results using the shaft diameter for drilled piers and the mean diameter for belled piers. The average side friction value from CPT data was calculated at each test site with the adherence coefficient obtained from the relationship:

$$m = f_{ave} / \bar{f}_s \qquad (8)$$

where m = Adherence coefficient in cohesive soils, f_{ave} = Average skin friction along shaft from field load tests, and $\bar{f}_s$ = Average side friction value from CPT data. These values are listed in Table 4 and are

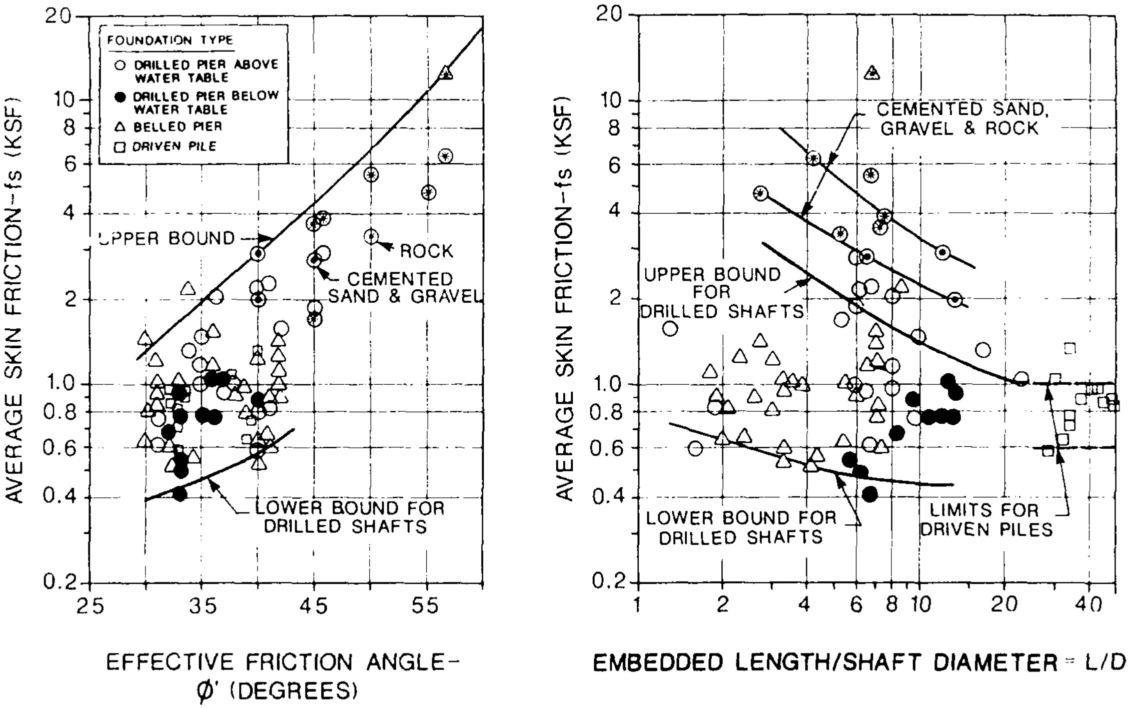

FIGURE 8. VARIATION OF AVERAGE SKIN FRICTION, fs, WITH SHEAR STRENGTH AND FOUNDATION GEOMETRY FROM SCE UPLIFT LOAD TESTS (1 KSF=0.5 KG/SQ.CM.)

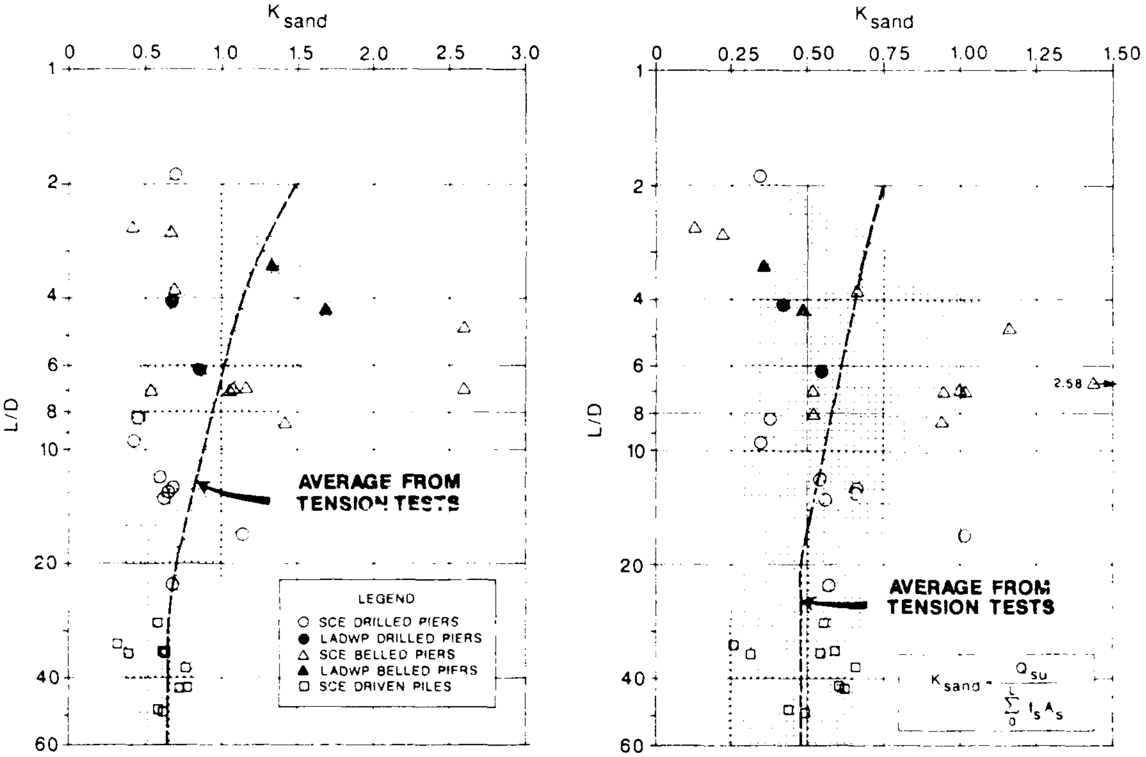

A) WITH $f_s \leq f_l = 1.2$ TSF OR KG/SQ.CM.

B) WITH f_s = ACTUAL VALUES

FIGURE 9. CPT SIDE FRICTION CORRECTION FACTOR, K_{sand}, FOR SANDS FROM FIELD UPLIFT LOAD TESTS

shown graphically in Fig. 10. Field load test results from Tumay, et al., (1983) and O'Neill (1986) in clay soils are also shown in Fig. 10 and compare favorably with the SCE and LADWP test results. Thus, for drilled shafts and driven piles in cohesive soils, the side friction resistance, Q_{sc}, can be computed from the relationship:

$$Q_{sc} = \sum_{0}^{L} (m)(f_s)(A_s) \qquad (9)$$

General Equation - At sites where the soil conditions are predominately sand with some intermixed clay layers, the general equation to obtain the total side friction resistance, Q_{st}, is as follows:

$$Q_{st} = K_{sand} \sum_{0}^{L} (m)(f_s)(A_s) \qquad (10)$$

where: 1) In granular soils, m = 1.0 and K_{sand} is selected from Fig. 9 based on the embedded length to shaft diameter (L/D) ratio, and 2) In cohesive soils, K_{sand} = 1.0 and m is selected from Fig. 10 based on the average side friction value from CPT data for each distinct clay layer.

CONCLUSIONS

A performance evaluation was made based on field uplift load test performed by SCE over the past 50 years. Normalized curves were developed for drilled shafts and driven piles, shown in Figs. 4 and 5, respectively, based on these uplift test results. The ultimate uplift capacity was selected based on an allowable vertical displacement of one inch (2.5 cm) from field load tests where the maximum uplift resistance was obtained. These curves may be used to predict the uplift capacity of drilled shafts and driven piles for various embedded length to diameter (L/D) ratios of the foundation.

Field uplift load tests were performed on 16 drilled piers, 13 belled piers and 10 concrete driven piles by SCE and LADWP at sites with CPT soundings. These test results are given in Tables 1, 2 and 3 for granular soils and Table 4 for cohesive materials. The measured uplift capacity or estimated ultimate uplift capacity from normalized curves were used to obtain the side friction resistance of each test foundation.

A revised design methodology was presented to compute the total side friction resistance of foundations using CPT data. The general relationship is given by Eq. 10 for granular and cohesive soils with associated side friction correlation factors. The correlation factor for granular soils, K_{sand} was obtained from Eq. 7 and is shown in Fig. 9 versus the L/D ratio of test foundations. In cohesive soils, the adherence

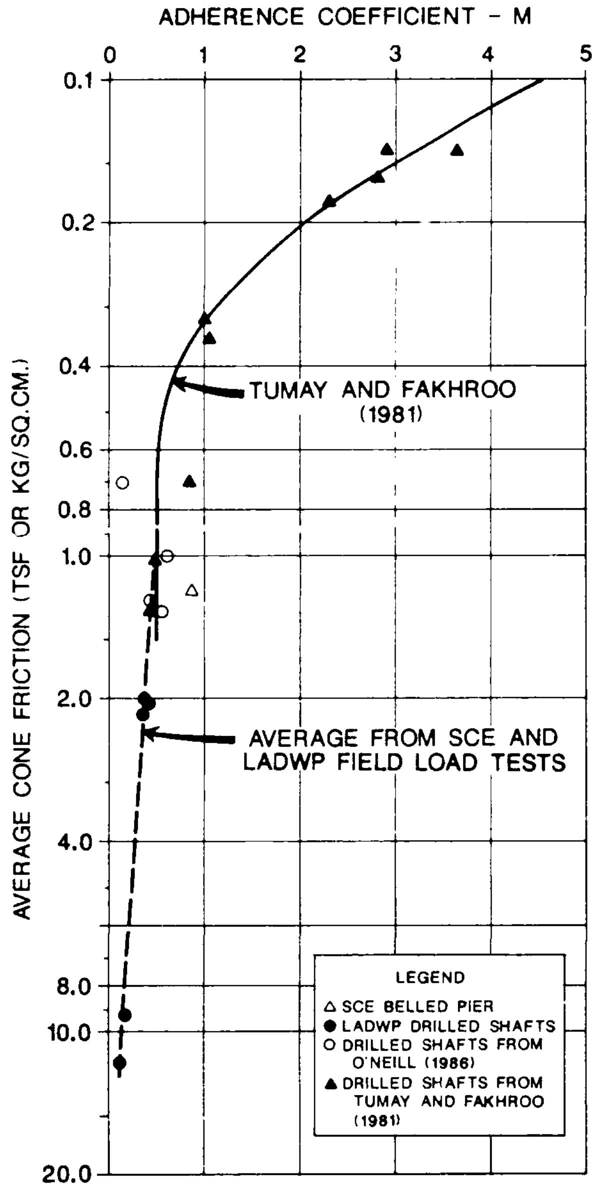

FIGURE 10. CPT SIDE FRICTION CORRECTION FACTOR, M, FOR COHESIVE SOILS

coefficient- m shown in Fig. 10, should be combined with the side friction value from CPT soundings to compute the actual adhesion along the embedded area.

The actual side friction values recorded from electric CPT soundings yield better correlations with the field uplift test results than by using a limiting value of 1.2 tsf (kg./sq.cm.), as recommended by Schmertmann (1978). The K_{sand} values in Fig. 9 range from 0.12 to 1.16 using actual f_s data while a much greater variance, from 0.31 to 2.60, was obtained for K_{sand} values with a limiting value for f_s. Also, no reduction factors should be applied to the computed side friction resistance for drilled shafts with L/D ratios of 8 or less, as shown in Figure 8, based on SCE field load test results.

REFERENCES

Briaud, J. C., Pacal, A. J. and Shively, A. W., "Power Line Foundation Design Using the Pressuremeter," International Conference on Case Histories in Geotechnical Engineering, St. Louis, 1984.

Das, B. M. and Seeley, G. R., "Uplift Capacity of Buried Model Piles in Sand," Journal of the Geotechnical Engineering Division, ASCE, No. GT10, 1975, pp. 1091-1094.

Das, B. M. and Rozendal, D. B., "Ultimate Uplift Capacity of Piles in Sand," Transportation Research Record No. 945, 1983, pp. 40-45.

Horvitz, G. E., Stettler, D. R. and Crowser, J. C., "Comparison of Predicted and Observed Pile Capacity", Cone Penetration Testing and Experience, ASCE STP, October 1981, pp. 413-433.

Kulhawy, F. H. Trautmann, C. H., Beech, J. F., O'Rourke, T. D., McGuide, W., Wood, W. A. and Capono, C., "Transmission Line Structure Foundations for Uplift-Compression Loading," Report EL-2870, Electric Power Research Institute, Palo Alto, CA, November, 1984

Kulhawy, F. H. "Drained Uplift Capacity of Drilled Shafts," Proceedings of the 11th International Conference on Soil Mechanics and Foundation Engineering, San Francisco, California, August, 1985.

Meyerhof, G. G., "The Uplift Capacity of Foundations Under Oblique Loads," Canadian Geotechnical Journal, Vol. 10, No. 1, 1973, pp. 64-70.

Nottingham, L. C., "Use of Quasi-Static Friction Cone Penetrometer Data to Predict Load Capacity of Displacement Piles," Ph.D. Dissertation to the Department of Civil Engineering, University of Florida, 1975.

Reese, L. C. Touma, F. T., and O'Neill, M. W., "Behavior of Drilled Piers Under Axial Loading", Journal of the Geotechnical Engineering Division, ASCE, Vol. 102, No. GT5, May 1976.

Schmertmann, J. H., "Guidelines for Cone Penetration Test, Performance and Design," U.S. Department of Transportation, Federal Administration, Offices of Research and Development, Washington, D.C., Publication No. FHWA-TS-78-209, July 1978.

Tomlinson, M. J., "The Adhesion of Piles Driven in Clay Soils," Proceeding of the 4th International Conference on Soil Mechanics and Foundation Engineering, London, 1957, Vol. 2, p. 66.

Tucker, K. D., "Uplift Capacity of Drilled Shafts and Driven Piles in Granular Materials", Foundation for Transmission Line Towers, ASCE STP, April 1987, pp. 142-159.

Tumay, M. T. and Fakhroo, M., "Pile Capacity in Soft Clays Using Electric QCPT Data,"Cone Penetration Testing and Experience, ASCE STP, October, 1981, pp. 434-455.

Vesic, A. S., "Tests on Instrumented Piles, Ogeechee River Site," Journal of the Soil Mechanics and Foundations Division, ASCE, Vol. 96, No. SM2, Proc. Paper 7170, March, 1970, pp. 561-584.

Proceedings: Second International Conference on Case Histories in Geotechnical Engineering, June 1-5, 1988, St. Louis, Mo., Paper No. 6.59

Foundation Failure of the St. Thomas Church, New Delhi

Devendra Sharma
Scientist Coordinator & Head, Geotechnical Engineering, Central
Building Research Institute, Roorkee, India

SYNOPSIS - The St.Thomos Church was built in 1933 in New Delhi. By oversight it was founded on a graveyard having graves at two levels. The comparatively heavy rains of 1958 and 1964 showed wide spread damage by differential settlement and tilting of tower. During the investigations in 1959 by the Central Building Research Institute, Roorkee, the earlier history of the site and church was examined. It was found that excessive damage had occurred in 1943 also and underpinning of foundations and butressing of walls was done to arrest it. Collapse of graves below the foundations was the reason for damage which reocurred, mainly in the portions which were not underpinned or partially underpinned. Effectiveness and feasibility of remedial measures vis-a-vis the soil investigations are discussed.

THE SITE

Location - The St.Thomos Church is located on Reading Road, now known as Mandir Marg (Fig.1). The area between the Mandir Marg and the Upper Ridge Road is the Eastern slope of the Ridge. The church and the adjacent buildings are situated in a filled up shallow valley near the junction of Panchkuin Road with Mandir Marg. The Ridge is upto 25m higher than the general ground level in the Church compound which is at RL 221.3m.

History of the Site - Delhi is one of the most ancient and historic cities of India. The earliest reference is found in the famous epic Mahabharta, when Delhi was known by the name of 'Indraprastha' and it may be assigned a period of 15th centuary B.C.

There is some evidence that there were stone querry pits around the site of the church. The 'Samadhis' higher up the slopes indicated that the Hindus used to cremate there while the Muslims started using the shallow valley as burial ground.

Delhi was declared the capital of British India in 1911 and New Delhi was laid out. When the construction of the residential quarters in 1915 reached as far as the site of the St. Thomos Church an outcry was raised due to Muslim graves. As a result the graves were covered by clean soil, site was left vacant, and the construction of Clerk's quarters began on the Northern side of the site. This was the site offered to Padre Weller and was accepted. The church was built in 1933 and Walter George was the architect for it. It may be recalled that the period of twenties and thirties was a period of great constructional activity in New Delhi. The famous Viceroy's House, now known as the 'Rashtrapati Bhawan', which is the official residence of the President of India, was designed by Sir Edwin Lutyens and completed in 1929.

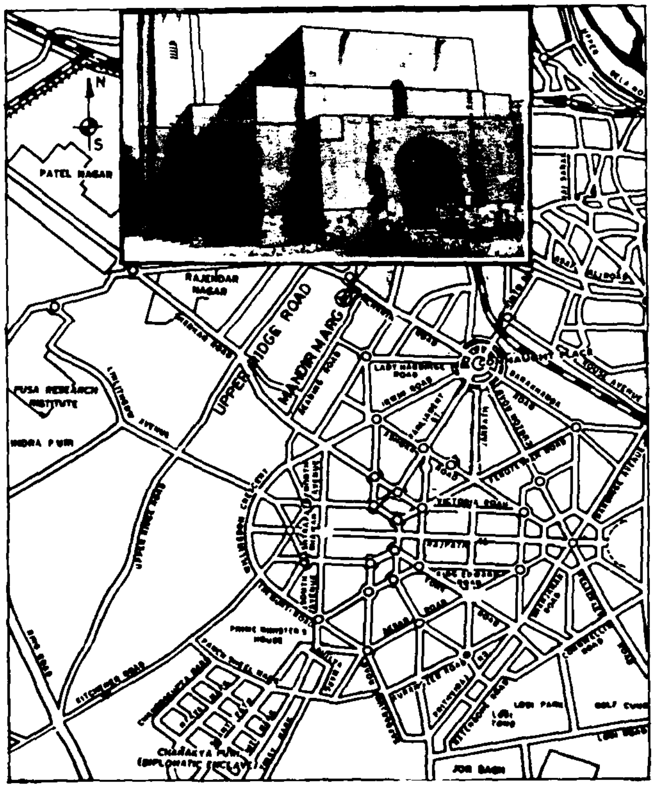

Fig.1 LOCATION OF ST. THOMOS CHURCH, NEW DELHI

THE BUILDING

The church is 103ftx56ft (31.4mx17.1m) in plan (Fig.2). It is a brick structure in lime mortar with a vaulted arch roof. The stone masonry, in local stone, as seen on the outside (Fig.1) is upto 4dt 6in (1.37m) above DPC. The tower was 61ft 10½in (18.86m) high. The butresses (Fig.1) were not an original feature of the building and were added 10 years later in 1943. The tower is accessible through a winding staircase located in the North corner

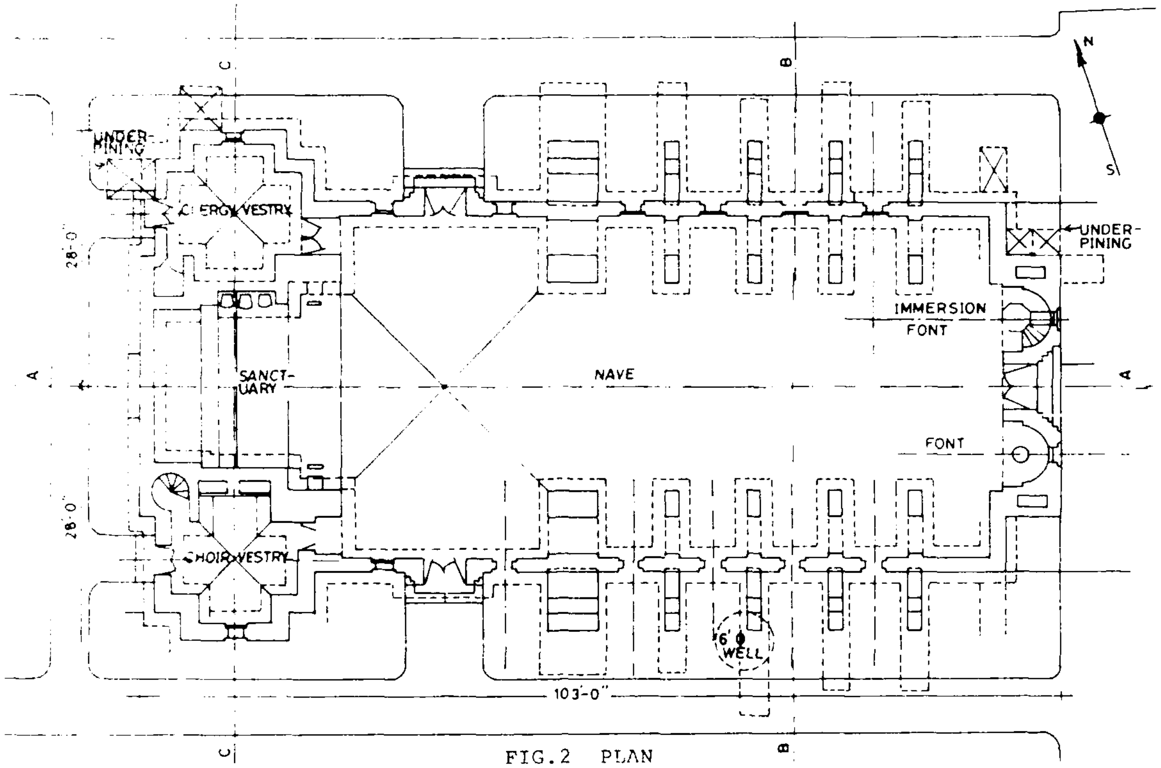

FIG.2 PLAN

of the Choir Vestry. The Nave was provided with 296 seats. The drawings showed that strip footing foundations of 4ft 6in (1.37m) depth below the floor were used originally for the most part of the building. At present the building shows no signs of damage from the outside as it has been repaired from time to time. However, a closer look of the interior will show uneven floors, damage to the railing in the front of the sanctuary, broken door sills and distorted door arches - indicating uneven sinking.

NATURE OF THE PROBLEM

Widespread cracking and sinking occurred after the heavy rains in 1958. The problem aggravated and in early 1959 the Central Building Research Institute was approached for investigations. It was observed that the tower had settled 4in to 6in (10cm to 15cm) showing cracks, wider at top and upto ground, at its junction with longitudinal and transverse walls of the church. The tower tilted away from the building towards the West corner. There was severe cracking of walls of the Clergy Vestry, Fig.3. Floor sills of stone and arches over doors and window also showed cracks. The entire portion comprising of the Choir Vestry, the Sanctuary and the Clergy Vestry separated from the Nave by tilting backward and showing through crack in the roof arch. Majority of cracks were slant along the diagonals. Differential settlements of floors showing sinking along the walls and heaved up centre were conspicuous.

The soil investigations were taken up in March - April, 1959 and findings were reported.

FIG.3 CLERGY VESTRY

The architect of the church provided the details of the problem and remedial measures adopted by him prior to 1958.

The problem of similar damage was again reported in 1964 after the end of rainy season. Cracking reocurred on the locations repaired earlier. As the soil investigations had already been carried out in 1959, only the settlement of the building by taking levels around it was monitored and was discontinued after no change was observed in 1965 and 1966 readings.

THE SOIL STRATA

The Choir Vestry, the Sanctuary and the Clergy Vestry were the most cracked portions. The soil investigations were carried out near these protions. For undisturbed sampling three open pits were dug and five static cone penetration tests were carried out (Fig.4) in March-April 1959. The soil test data are summarised in Fig.5. Undisturbed samples were used for oedometer tests. Additional two pits close to the tower faces were dug for ascertaining the actual depth of the foundations and the examination of the strata. The depth of the foundation below the tower was confirmed at 4ft 6in (1.37m) below ground level. There was a clear evidence of filled up soil. In pit No.4 graves were encountered at 6ft 6in (2m) and 8ft 6in (2.6m) and in pit No.5, these were at 7ft (2.1m) and 8ft 6in (2.6m) depths below ground level.

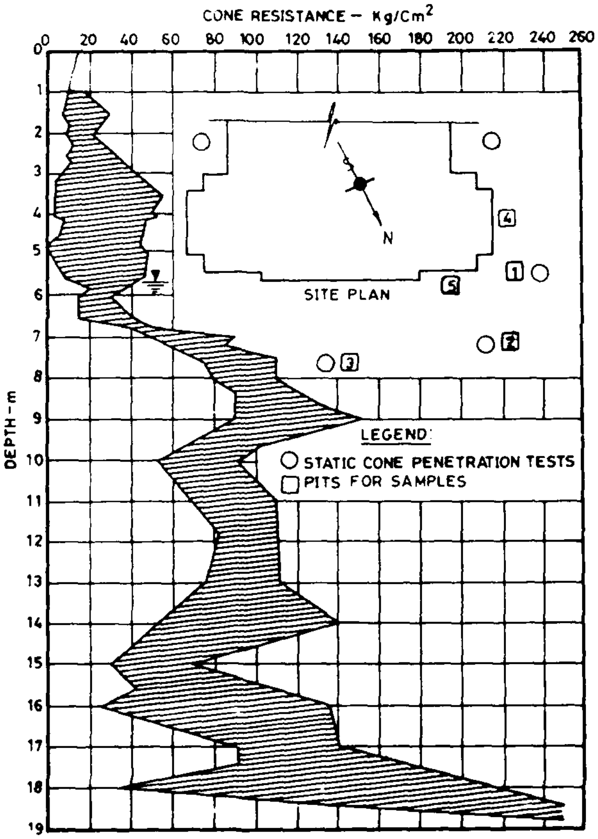

FIG.4 TEST LOCATIONS & STATIC CONE RESISTANCE

THE PROBLEM AND REPAIRS BEFORE 1959

During the course of investigations by the Central Building Research Institute, Roorkee, the architect provided the information about the repairs of the church building since its construction in early thirties. It was reported that severe cracking of the building first occured in 1942. The architect resorted to underpinning of the foundations as shown in some of the sections of the building in Fig. The underpinning was not done below the tower and the Sanctuary. The Clergy Vestry was partially underpinned. The Nave was fully underpinned. The depth of underpinning, depending upon the availability of firm strata, varied from about 11ft (3.35m) to 14ft 6in (4.4m) below the ground level.

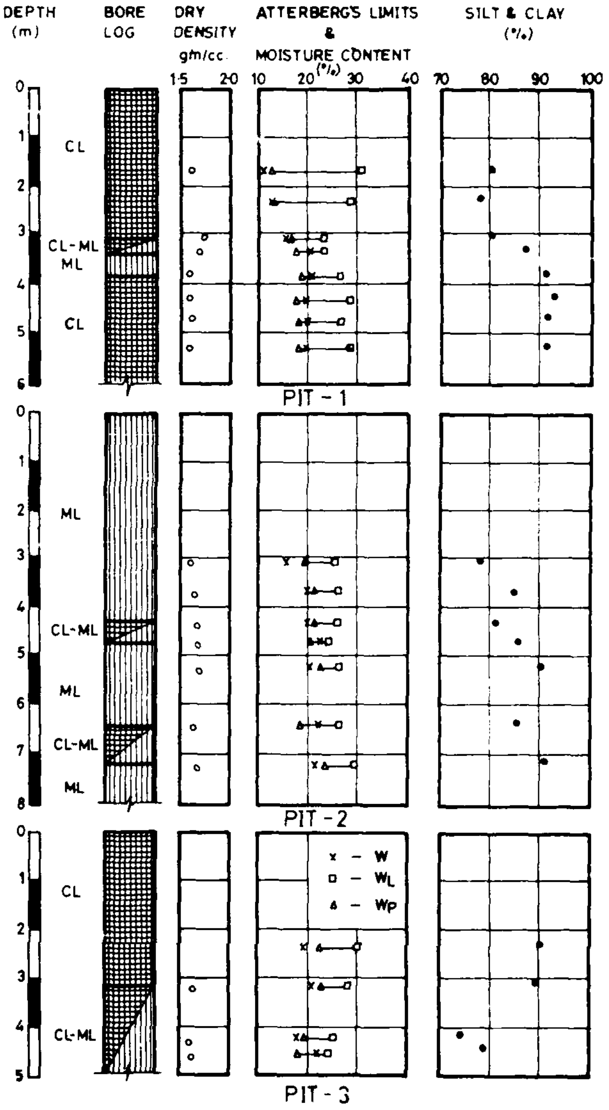

FIG.5 BORELOGS & SOIL TEST DATA

During the course of excavation a number of graves were encountered as indicated in two typical sections (Figs.5 & 6). Barring a few cases, there are two levels of burials at about 2m and 2.6m. It was on record that a pit dug at the Clergy Vestry near the West face revealed a burial at 11ft 3in (3.4m) alongwith a earthen pot containing an egg and two coins of 1835 and 1838, East India Company. The typical orientation, head towards West (direction of the holy 'Kaba') was clearly suggestive of the Muslim burials.

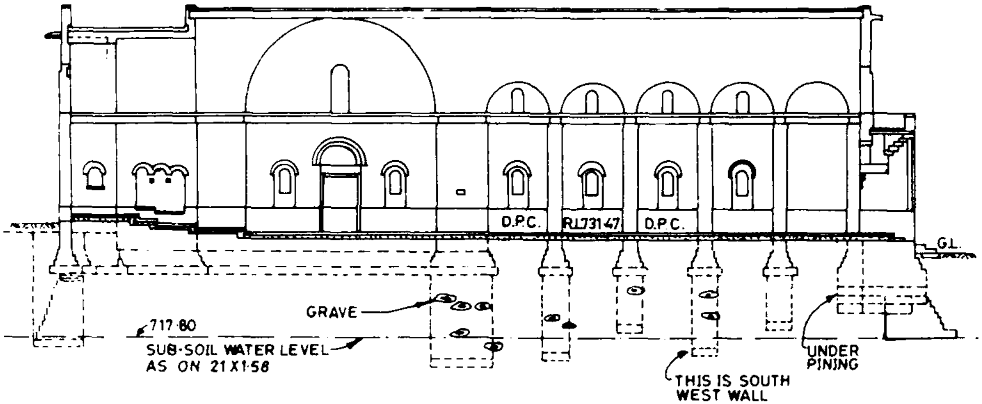

FIG.6 SECTION ON AA

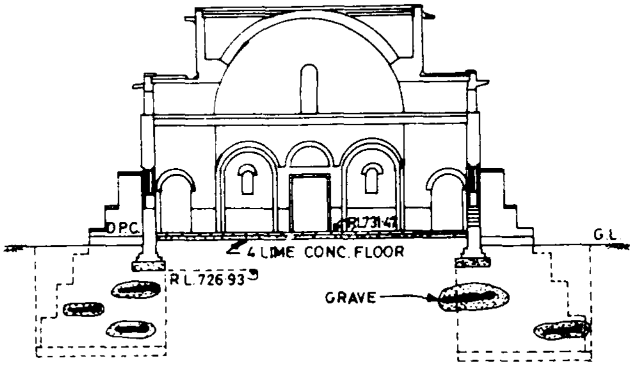

FIG.7 SECTION ON BB

After underpinning operations the butresses (Fig.1) were also provided for additional support for the longitudinal walls. The underpinning of the Clergy Vestry was at the outer accessible corner only.

DISCUSSION ON REASONS FOR DAMAGE

The soil sampling from the open pits showed that it was a filled up ground. However, top yellowish and greyish coloured soils with some 'Kankar' could be easily mistaken to be virgin ground. The architect reported that no soil investigations were carried out as the ground upto about 2m depth showed firm deposit. The site was a couple of feet higher than the surrounding ground at the time of construction, but the architect concluded that there had been a little excavation to get a uniform slope for the road. Thus the site was considered good enough to sustain a pressure of 1.5t/sq.ft (1.5 kg/cm^2) transferred from the footings of the building. Till 1942 when cracking occurred and remedial measures by under pinning were taken up, the existance of graves was not suspected.

The method of burial is such that a hallow space remains at the top of shroud and it gets filled up in due course. The major reason for the collapse of these hollow spaces seems to be the seasonal rise in water table. During the investigations in April 1959 the water table was at a depth of 16ft (5m) and it was reported to be about 6ft (1.8m) during the rains, which is quite close to the footing level. The receding water table caused the collapse of hollows which were indicated by the penetration test showing little or no resistance at certain elevations and confirmed by open excavations. The scatter of curves indicate variability of a filled up ground (Fig.4).

It is worth noting that more damage of sinking and cracking was noticed in 1958-59 in the tower and sanctuary portions which were not on foundations strengthened by underpinning (Fig.8). The Clergy Vestry was partially underpinned at the corner and this resulted in substantial damage. The underpinned corner remained in position while the adjacent portions showed sinking along with the backside wall of the sanctuary.

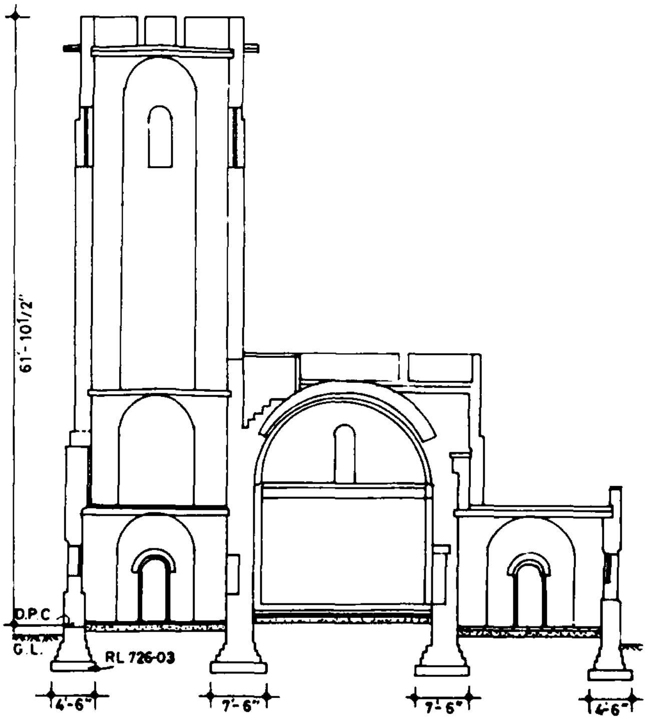

FIG.8 SECTION ON CC

Due to erratic scatter of graves at two levels it is difficult to make a realistic settlement estimates. On 3rd March 1959, the tower had settled by about 5.5in (14cm) at its corner.

The inclination towards South and West were 9.75in (25mm) and 4.5in (11mm) respectively. On 28th September the tilt towards South was 8.35in (21mm) showing a recovery of 4mm.

In June 1964 settlement of the building was monitored at 19 points on the outer walls. The settlements were active upto October 1964 and during a period of three months the Tower, Sanctuary and Clergy Vestry (excluding the underpinned corner) showed settlements of the order of about 8mm while for the longitudinal walls it was less than 2mm. In November 1964 settlements stabilised and there was no further sinking upto 1965 when observation were discontinued. It is worth noting that in both the years 1958 and 1964, the rainfalls were higher than the average.

THE REMEDIAL MEASURES

As stated already the foundations were underpinned in 1943 from the firm ground. But the Tower and sanctuary were left as such. This led uneven support from the bearing strata. Butresses were also provided in 1943, however, they do not seem to fullfil much useful purpose as the problem is more of downward sinking rather than the outward rotation of the walls.

In 1959-60 shoring in Fig.9 was done at the two outer sides of the tower and similarly at the Clergy Vestry walls. The support for shoring at the ground is derived from shallow concrete filled trenches. This shoring has outlived its useful life and as seen in 1986 it is partially rotten and now a relic from the past.

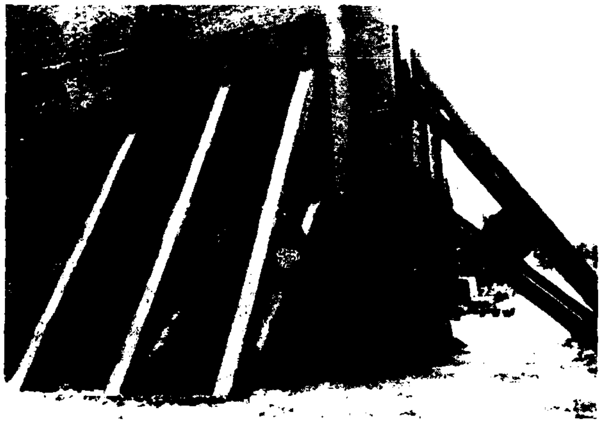

FIG.9 SHORING AT TOWER

Apart from the above measures, there had been a discussion on the feasibility of the other permanent measures as well. Reducing the height of tower for providing a relief in loading on the foundations was a proposal but of marginal help as architectural look was to be preserved. Grouting by cement slurry and underpinning by piles and beams were considered. Grouting was rejected because the strata were predominantly of silt and clay, 80-90 percent, and soil will not accept grout. The pile and beam proposal was not implemented due to specialised handling and the economy considerations. The desirable depth for support from firm strata is around 7m as seen from penetration records (Fig.4) and this means working below water level.

In view of the above no special remedial measures after those of 1943 were taken up. The superstructure and the floors were repaired from time to time. The building is in continuous use.

CONCLUDING REMARKS

The history of the St.Thomos Church once more focusses the attention on the importance of proper soil investigations prior to construction. Also the foundation treatment by remedial measures, by underpinning should be such that it provides uniform support. Otherwise the untreated portions may sink later.

ACKNOWLEDGEMENT

The author is grateful to former Directors, Lt.Gen.Sir Harold Williams and Prof. Dinesh Mohan for their sustained interest in the problem. Thanks are also due to author's former senior colleague Mr.G.S.Jain for his participation in the investigation programme.

The work was carried out as a normal programme of research and the paper is being published with the permission of the Director, Central Building Research Institute, Roorkee, India.

Proceedings: Second International Conference on Case Histories in Geotechnical Engineering, June 1-5, 1988, St. Louis, Mo., Paper No. 6.60

The Case Record of Ba-Yu-Quan Anchor Slab Retaining Wall

Z.S. Zhang
Associate Professor, China Academy of Railway Sciences, Beijing, China

X.X. Zhang
Research Associate, China Academy of Railway Sciences, Beijing, China

D.Z. Luan
Engineer of Shenyang Railway Conservancy, Shenyang, China

SYNOPSIS: Anchor slab retaining wall is a kind of retaining structure, which consists of prefabricated rib-columns, panel slabs, tie-bars and anchor slabs embedded in earth fill. Since the structure was first used and developed in China in 1974, many such structure have been built on railways and other engineering projects. The reviewer of Second International Conference on Case Histories in Geotechnical Engineering gave a comments about this structure as follows: "Chinese method anchor slab the construction should interest the western world".

Ba-Yu-Quan anchor slab retaining wall has been instrumented to measure the load on the tie-bar, the horizontal displacement of the rib-columns, the horizontal earth pressure acting at the panel slabs, and the backfill settlement at different positions. This paper presents project description, construction of the project, data obtained from field observations and the comparison result with analysis and predicted values.

INTRODUCTION

Ba-Yu-Quan anchor slab retaining wall was constructed in the year of 1984-86. It is located in Ba-Yu-Quan harbour, Liaoning province. The wall was constructed for the purpose of retaining the fill at two sections of a railway, each section is a 100 m anchor slab wall, which approaches to an overhead street bridge, as shown in Fig. 1 and Fig. 2, so as to save a great quantity of cropland that is very expensive at the place in question.

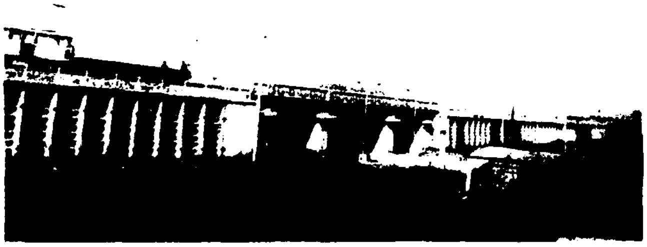

Fig. 1. The Whole Scene of Ba-Yu-Quan Anchor Slab Retaining Wall

The anchor slab retaining wall maintains it-self stabilization through the interaction of face panel, rib-column, tie-bar, anchor slab and backfill, in other words anchor slab structure is an assembled retaining structure.

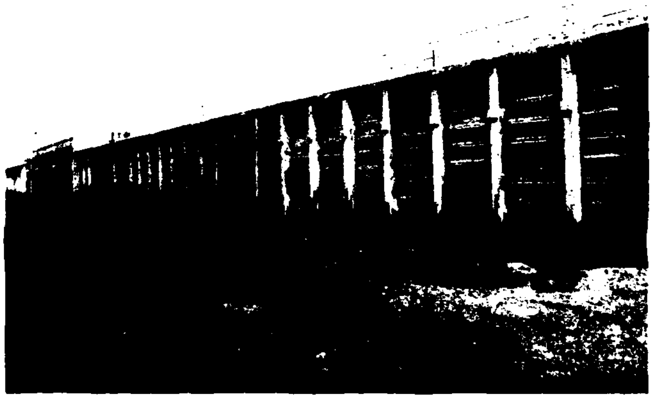

Fig. 2. Photograph of Ba-Yu-Quan Anchor Slab Retaining Wall

As compared with reinforced earth structure, this new type structure is better for protection against corrosion, while it has the advantages of light weight and lower cost. It is suitable to be adopted in regions of low bearing capacity and especially promising in those countries, where reinforcing steel straps is in short supply.

A vibrostand model test has provided information for anchor slab structure that is comparatively flexible and better to against the damage of earthquake than masonry retaining walls.

PROJECT DESCRIPTION

The face panel of Ba-Yu-Quan anchor slab wall consists of reinforcement concrete rib-column and panel slab. The rib-column is 5 m in hight and with 45x25 cm rectangular section. Specing of rib-column is 2 m from center-to-center.

The panel slab is a trough plate 1.96 m in length, 0.5 m in width and 20 cm in thickness.

The foundation of rib-column is a strap concrete footing, 0.8 m in width, 1.25 m in depth, the bottom of foundation is 0.25 m bellow frost depth.

A 55x25 cm top-placed armoured concrete cross beam is placed at the top of rib-column holding it in place.

One rib-column is anchored by two pieces of 1.2 m square anchor slab with 0.25 m in thickness embedded in the earthfill. The rib-column and anchor slab are joined up with *2xΦ28 mm* bar stock. The upper tie-bar is 8 m and the lower one is 7 m in length, the cross section of Ba-Yu-Quan anchor slab wall is shown in Fig. 3.

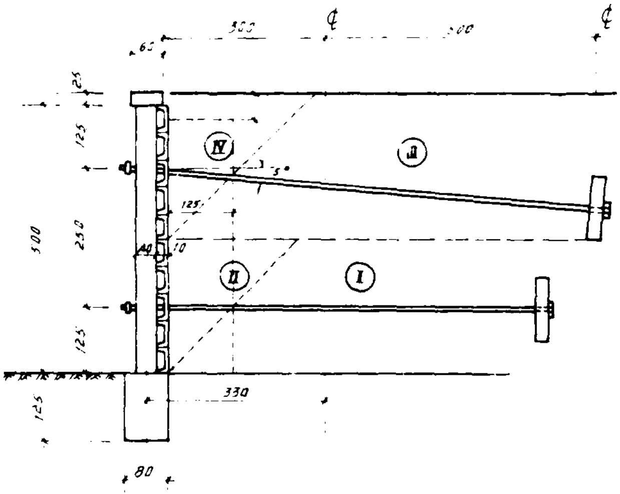

Fig. 3. The Section of Ba-Yu-Quan Anchor Slab Retaining Wall

In design the soil parameters are given as follows,

Unit weight of backfill $\gamma = 1.90$ kN/m^3;

Angle of internal friction $\phi = 30°$;

Angle of wall friction $\delta = 0.5\phi$;

Bearing capacity of subsoil R=120kPa.

Rib-column, panel slab, tie-bar and anchor slab are designed according to lateral pressure acting on panel slab, which consists of Coulomb's active earth pressure and additional lateral pressure caused by external concentrated load. (Casagrande. L., 1973) Both lateral pressure mentioned above were multiplied by a experimental coefficient of 1.2.

The allowable carrying capacity of anchor slab embedded in backfill was chosen as 100-150 kN/m^2 (Lu, Z.J. et.al 1985) at different depth respectively.

The length of tie-bars is designed to extend no less than a distance of 3.5 B beyond the imaginary line of rupture of active earth pressure, in which B denotes the length of one side of the needs of partial and whole stability analysis of anchor slab wall.

CONSTRUCTION

Due to Ba-Yu-Quan anchor slab wall is located in a frigid region, a pervious blanket of 1.25 m in thickness was placed at the back of face panel to protect the wall from frost heave.

The tie-bar were protected against corrosion by coating two layers of rust-resisting paint and winded two layers of spun glass cloth round the bar stock and coated with melted pitch at the same time.

According to the authors' experience, in order to reduce the displacement of an anchor slab wall, the backfill should be compacted and the foundation must not be very soft. The backfill was constructed by a total of 4 stages, which is approximately in order of Ⓘ-Ⓘⓥmarked in Fig. 3. Each layer of earth fill should not be more than 30 cm and compacted to 95% of optimum density.

After the surface of fill reached to the top level of anchor slab, a ditch cut was excavated in backfill to put the tie-bar and anchor slab in place. Plain concrete was concreted in front gap between the anchor slab and ditch wall, then earthfill was placed in the back gap and compacted to the stipulate density.

A temporary wooden support was used to hold the rib-column in right place, after filling the whole backfill, then concreting the cross beam, welding the banisters and stuffing the tie-bar ends with cement morter so as to protect against corrosion.

FIELD INSTRUMENTATION

The instrumented areas were chosen in the rib-columns No. 21-22 and No. 23-24. Both sections between the above columns was sufficiently distant from bridge to make the analyses of data easier.

Totally 30 vibrating wire transducers were installed on above sections, along the rib-column to measure total horizontal earth pressure and its distribution.

On each of the instrumented panel slabs, 3 transducers were mounted between the rib-column and the panel slab, so as to form a state with three sustainers.

16 bar-stock tensiometers were welded on the end of the tie-bar of four rib-columns, located at instrumented area, to measure total tensile force,

To monitor the lateral displacement of the face panel of the wall, on each of rib-columns top and bottom was mounted a mark, in the meantime a reference line for displacement measurement has been established when the rib-column was stood up and the face of backfill reached to the height of half panel slab.

A cup type settlement gauges were also embedded on the anchor slab top to measure its settlement in the backfill.

Field measurement have been made during and after construction and will be measured once or twice each year in the near future.

COMPARISON BETWEEN PREDICTED AND MEASURED VALUES

To examine the predicted value with the field measurement data was the important aim of the field measurement. The tensile force of tie-bar and earth pressure of face panel field measurement data of instrumentation section 1, which is between the rib-column No. 23-24, and its predicted values are shown in Table 1 and Fig. 4.

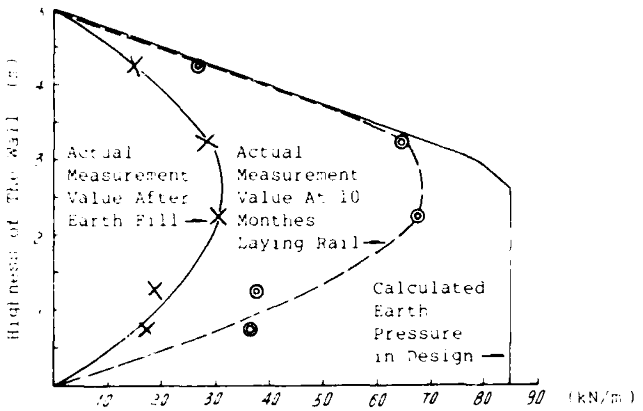

Fig. 4. The Earth Pressure Distribution of Observation Section

TABLE 1. The Predicted and Measured Tie-Bar Force and Observed Earth Pressure

Location	Design Force (kN)			Measurement Tie-Bar Force (kN)		Measurement Earth Pressure (kN)	
	Backfill Weight Only	Include Track Load	Include External Load	After Earth Fill	10 monthes After Laying Rail	After Earth Fill	10 monthes After Laying Rail
The Upper Tie-Bar	56.7	74.0	88.5	48.7	107.6	99.2	212.5
The Lower Tie-Bar	106.5	140.3	202.2	29.0	102.5		
Column Bottom	10.0	12.8	19.1	21.5*	2.4*		
Total	183.2	227.1	309.8	77.7	210.1		

It can be seen from Table 1 that just at the time after backfill was completed, both observation tie-bar tensile force of 77.7 kN and earth pressure of 99.2 kN are about less than a half of the predicted force of 183.2 kN. But 10 monthes after laying rail not only observation tie-bar tensile force of 210.1 kN is about the same, as the earth pressure of 212.5 kN, but als both the above force are the same with design tie-bar force of 227.1 kN, so it can be proved that the earth pressure graph which was shown in Fig. 4 and its quantity adopted in design are conform to the actual situation on the whole.

As compared the actual measurement tie-bar tensile force and earth pressure as mentioned above with total design force, which including the train external load of 309.8 kN, that the former is two-thirds about the latter. It can be borne out that the anchor slab, tie-bar, rib-column and panel slab are all in a state of safety enough.

The authors have measured the tie-bar force at some other anchor slab projects during the train was just parked on the top of earthfill of retaining wall. As a result the tie-bar force had a extreme little increment than the force without the train load. In addition the first author, Z. S. Zhang, had performed finite element analysis on some of the anchor slab structures including the one mentione abcve (Zhang, Z.S. 1985). The results of finite element analysis has shown the same phenomenon mentioned above.

The values with mark * in Table 1. is the calculative values according to the measurement of earth pressure and total tie-bar force, that is to deduct the actual measurement tie-bar force from the actual total measurement earth pressure should be the force supported by the column bottom, there's hardly any difference between the two.

It can be proved that put a column into a shallow nest on foundation, the column bottom could not be formed as a strong support.

The maximum settlement of anchor slab embedded in backfill was [illegible] mm. It is agreed with the result obtained from finite element analysis.

The actual observation data of horizontal displacement of face panel is shown in Fig. 5.

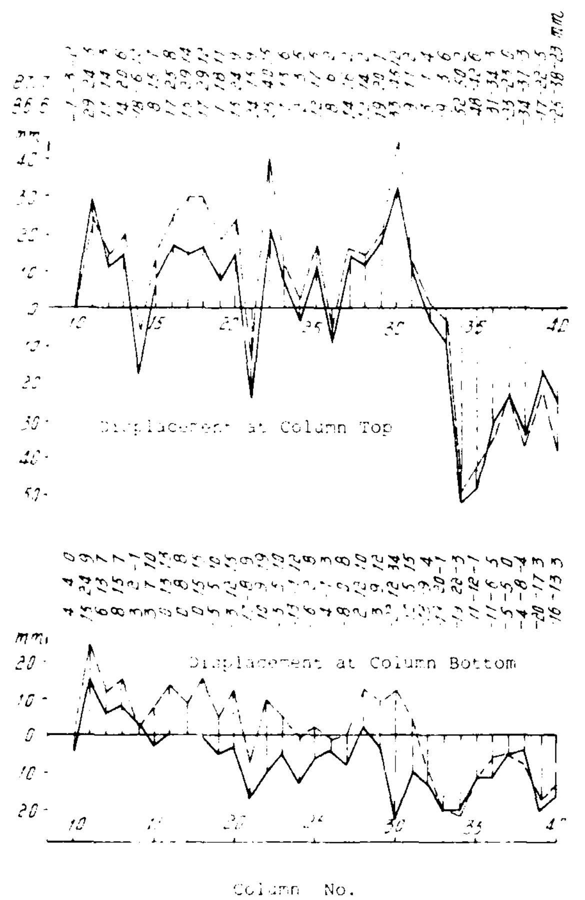

Fig. 5. The Horizontal Displacement Observation Data of Face Panel

When the backfill was just completed, the maximum horizontal displacement of the face panel is 52 mm arised at the top of No. 34 column which is near the end of the wall. It has good reason to say, that this displacement was mainly forming by the hoisting and assembling deviation of the column.

The average horizontal deviation at column top is 18.03 mm and the average horizontal deviation at column bottom is 8.55 mm. Due to the top assembling deviation is only 10 mm greater than that of bottom, therefore the appearance of the face panel of the wall is remain the same smooth.

The last actual displacement observation is 10 monthes after laying rail, which is shown in Fig. 5. The average displacement at top is 6.5 mm and the average displacement at bottom is 8.4 mm. It can be deemed that the column is belong to a small parallel move. This phenomenon and displacement values are quite close to the finite element analysis result.

CONCLUSIONS

The investigations described in this paper have shown:

Anchor slab retaining wall is a kind of assembled retaining structure, it has the advantages of light weight, lower cost and better for protection against corrosion.

In order to reduce the displacement of an anchor slab wall, besides the backfill should be compacted and the foundation must not be very soft, it has to be made the each other gaps between rib-column, panel slab, tie-bar, anchor slab and backfill as close as possible during the wall assembled period.

The dimension of anchor slab must be calculated according to the allowable carrying capacity of anchor slab embedded in backfill, the actual situation of the project makes clear that the value of 100-150 kN/m^2 used in design with ampth factor of safety.

As compared the actual measurement tie-bar force and earth pressure were observed in the project, that can be concluded the column bottom could not be formed as a strong support.

ACKNOWLEDGEMENTS

The authors wish to express their appreciation to the Shenyang Railway Conservancy for permission to publish the results presented in this paper. We would particularly like to acknowledge Mr. C.Z. Zhao, engineer of Shenyang Railway Conservancy, who has taken a part in the design and observation. The authors are gratefully to the engineer in charge of construction, Mr. C.R. Tian, who has provided a powerful backing for the experimental and observational work.

REFERENCES

Casagrande, L. (1973). 'Comments on Coventional Design of Retaining Structure', Journal of the Soil Mechanics and Foundation Division, ASCE, Vol. 99, No. SM2. pp. 181-198.

Lu, Z.J., Wu, X.M. and Zhang, Z.S. (1985). 'Carrying Capacity of anchor slab', Proc. 11th International Conference on Soil Mechanics and Foundation Engineering, Vol. 2, pp. 1135-1138.

Zhang, Z.S. (1985). 'Finite Element Analysis for Retaining Structure', Proc. of the 5th International Conference on Numerical Methods in Geotechnics, Vol. 2, pp. 797-803.

Proceedings: Second International Conference on Case Histories in Geotechnical Engineering, June 1-5, 1988, St. Louis, Mo., Paper No. 6.61

Drilled Pier Load Test, Fort Collins, Colorado

J.B. Hummert, Jr.
USA

T.L. Cooling
USA

SYNOPSIS: A full-scale compressive load test was conducted on a drilled pier in the Pierre Shale Formation near Fort Collins, Colorado, to verify design parameters. The test pier was designed based on presumptive design criteria for both end-bearing and skin friction in the shale. The maximum test load of 6.7 MN (750 tons) resulted in a deflection of approximately 230 mm (9.0 in.). Instrumentation within the pier allowed determination of the actual end-bearing and skin friction values at various applied loads. Based on results of the test, production piers were redesigned for skin friction only and shear rings were added to enhance shaft resistance.

INTRODUCTION

Construction of a new industrial plant approximately 80 km (50 miles) north of Denver, Colorado, USA just east of the City of Fort Collins, Colorado involved installation of approximately 750 drilled piers bearing in the Pierre Shale Formation (Fig. 1). Piers were sized to support column loads ranging from approximately 2.2 to 8.0 MN (250 to 900 tons). Maximum allowable settlement of each pier was approximately 13 mm (1/2 in.). To optimize foundation design rather than rely on presumptive bearing pressures thought to be conservative, the designers recommended that a full-scale instrumented load test be conducted on at least one drilled pier. Considering the large number of piers involved it was anticipated that the load test would result in cost savings.

SUBSURFACE CONDITIONS

The site is underlain by Pleistocene Age glacial, alluvial and aeolian deposits, and the Cretaceous Age Pierre Shale Formation. The profile is relatively consistent across the site. Conditions near the test pier based on test borings B-9 and B-13 are described as follows and shown in Fig. 2.

Aeolian Deposits

The first ±3 m (10 ft) of soils encountered are silty clays with a trace of sand or gravel. The soils are visually classified as medium strength (stiff) and low plastic. They were transported and deposited by wind and can thus be referred to as loess. The upper surface of these materials has been modified and reworked by cultivation.

Alluvial Deposits

The clay is underlain by ±6 m (20 ft) of alluvial sands and gravels. In general these materials are fine to coarse-grained sands with some fine gravel. Layers of silty and/or clayey sands are noted. Blow counts indicate medium dense to dense conditions. Standard Penetration Test (N) values range from 16 to 58 in the two adjacent borings. Groundwater was encountered at the top of this layer in both of the adjacent borings and in the test and reaction piers.

Shale

The sand and gravel is underlain by the Pierre Shale to the depth of exploration, 28 m (90 ft). The upper portion of the shale has weathered to very stiff to hard, olive-tan, highly plastic clay with very fine sand. This weathered zone ranges in thickness from about 1.5 m (5 ft) at the test pier location to about 2.4 m (8 ft) at the nearest adjacent boring. The transition to the unweathered shale is gradual. The unweathered shale is a hard, dark gray, thinly bedded shale with some thin sandstone layers. Blow counts from the Standard Penetration Test range from about 50 blows for 150 mm (6-in.) of penetration to about 50 blows for 64 mm (2.5 in.) of penetration. Pressuremeter and unconfined compression tests in other borings indicates the average undrained shear strength of the unweathered shale is about 1.91 MPa (20 tsf). The water content of the unweathered shale averages 16 percent with a dry density of 2.22 Mg/m^3 (139 pcf). The Pierre Shale is reportedly 2,440 to 3,660 m (8,000 to 12,000 ft) thick and is interbedded with sandstones.

Groundwater

Groundwater was encountered at or near the top of the sand layer (el 1,525 m). The alluvial deposit is an aquifer used by local farmers for irrigation.

LOAD TEST SET UP

Reaction for the load test was provided by two nominally 762 mm (30-in.) diameter drilled piers each located 3.05 m (10 ft) on center from the test pier as shown in Fig. 2. Reaction piers were drilled to depths of 20 m (65 ft) forming rock sockets in the Pierre Shale about 9.2 m (30 ft) long. A 2.1-m (6.5-ft) deep reaction beam centered over the test pier spanned between the reaction piers.

The reference beams consisted of two W8x35 beams, one on each side of the test pier cap oriented normal to the alignment of the test and reaction piers. The reference beams were supported on two 457 mm (18-in.) diameter by 3.05 m (10 ft) deep drilled piers located 3.05 m (10 ft) on center from the test pier.

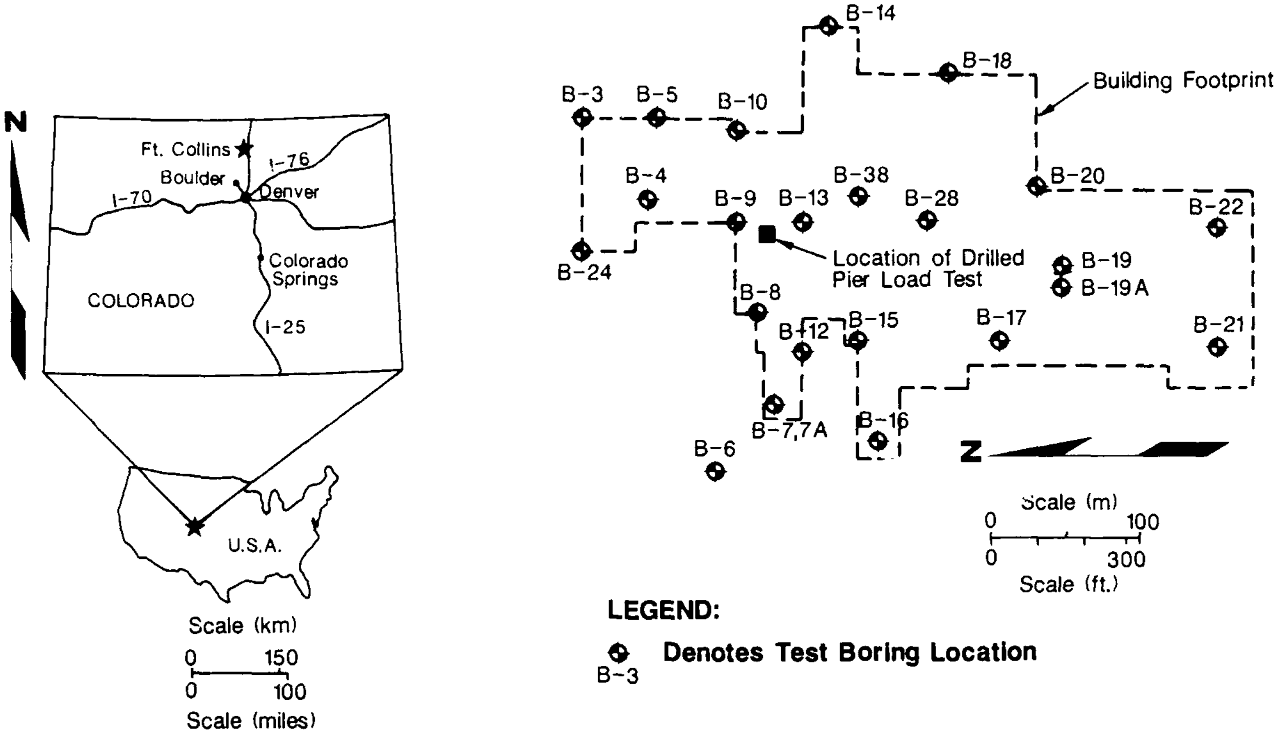
N
Ft. Collins
Boulder
I-76
I-70
Denver
Colorado Springs
COLORADO
I-25
U.S.A.
Scale (km)
0
150
0
100
Scale (miles)
B-14
B-18
Building Footprint
B-3
B-5
B-10
B-4
B-38
B-20
B-9
B-13
B-28
B-22
B-24
Location of Drilled Pier Load Test
B-19
B-19A
B-8
B-12
B-15
B-17
B-21
B-7,7A
B-16
B-6
N
Scale (m)
0
100
0
300
Scale (ft.)
LEGEND:
B-3
Denotes Test Boring Location

VICINITY MAP

SITE PLAN

Fig. 1 Vicinity Map and Site Plan

DRILLED PIER DESIGN

Drilled piers were designed on empirical rules based largely on Standard Penetration Test results. From previous experience with shale in the Denver area, empirical values for the allowable end-bearing and skin friction are calculated as follows (units are in tons per square foot):

$$qa = \text{Allowable end-bearing pressure} = \frac{N}{4} \text{ (tsf)} \quad (1)$$

qa should not exceed 30 tsf (2.9 MPa)

$$fs = \text{Allowable skin friction} = \frac{qa}{10} \text{ (tsf)} \quad (2)$$

Jubenville, et al indicates the same equations, although no limiting values were given.

The Standard Penetration resistance in the unweathered shale was generally in the range of 50 blows for 75 to 100 millimeters of penetration (3 to 4 in.) or an equivalent N-value of 150 to 200. Considering this, design values of qa and fs were 2.9 MPa and 0.29 MPa (30 tsf and 3 tsf), respectively.

LOAD TEST CONSTRUCTION

Construction of the load test consisted of three primary components: 1) construction of the test pier and two reaction piers with pier cap, 2) placement of the reaction beam, and 3) fabrication of the deflection reference system.

Installation of the drilled piers began on October 11 and was completed on October 13, 1983. Piers were installed by personnel and equipment of the Meredith Drilling Company. The contractor used a Williams LDH pier drilling rig to advance the shafts. Conventional flight augers, fitted with 50 mm (2-in.) wide high-strength steel teeth were used to excavate both the soil overburden and the shale bedrock. A 457-mm (18-in.) diameter auger was used to excavate the test pier, and a 813-mm (32-in.) diameter auger was used to drill each of the reaction piers. To provide clearance for the temporary steel casings, a 50 mm (2-in.) wide, angled "side cutter" tooth was inserted on the augers to increase the actual upper excavated shaft diameters to 508 and 864 mm (20 and 34 in.), respectively.

Temporary steel casings were used in each of the three piers. A 9.75 m (32-ft) long by 508 mm (20-in.) (O.D.) by 6.35 mm (0.25-in.) thick steel casing was used for the test pier and a 10.2 m (33.4-ft) by 813 mm (32-in.) (O.D.) by 6.35 mm (0.25-in.) thick steel casing was used for both reaction piers.

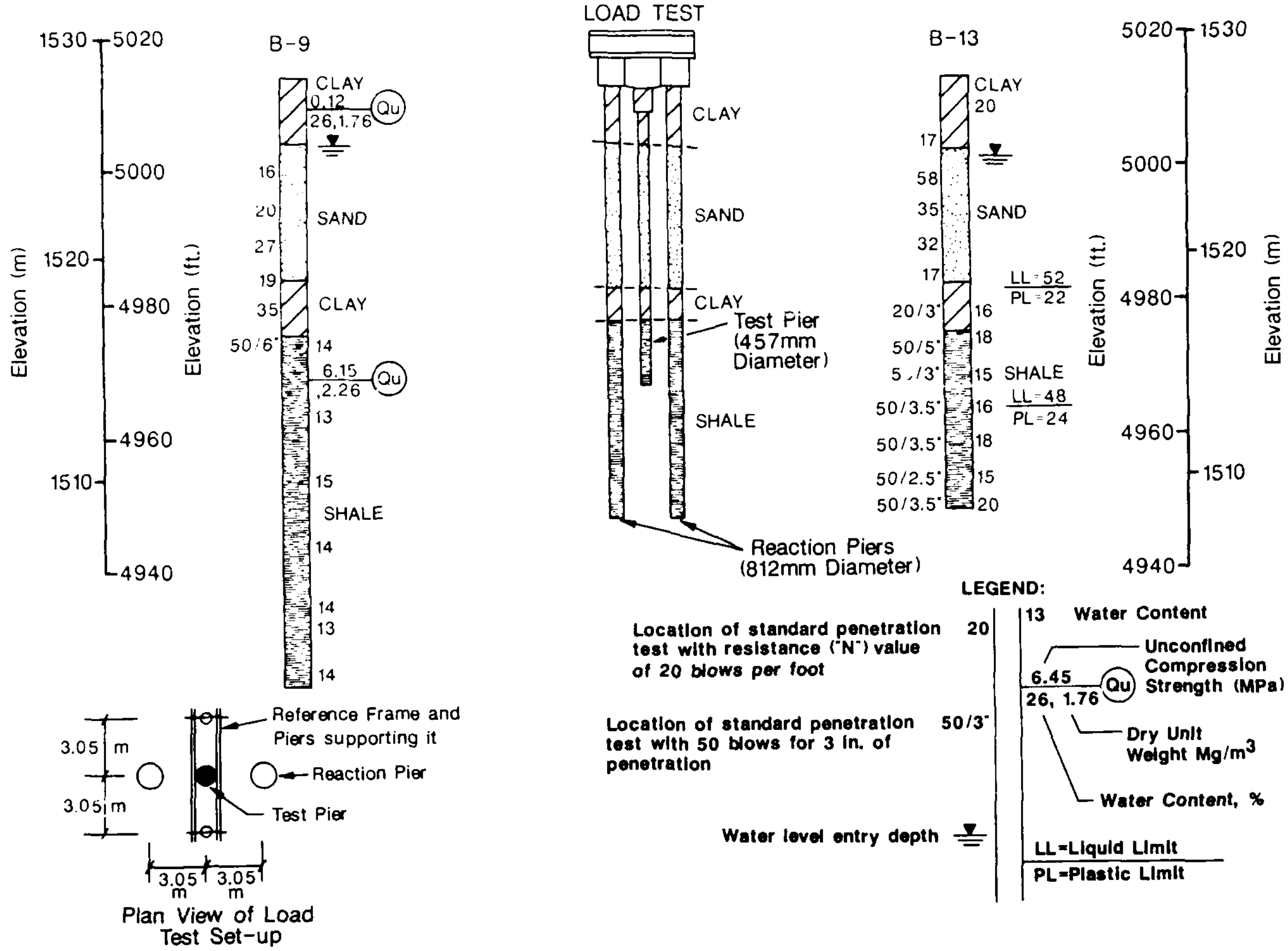

1530
5020
1520
1510
5000
4980
4960
4940
Elevation (m)
Elevation (ft.)
B-9
CLAY
0.12
26,1.76
Qu
16
20
27
19
35
50/6"
SAND
CLAY
14
6.15
2.26
13
15
SHALE
14
14
13
14
LOAD TEST
CLAY
SAND
CLAY
Test Pier (457mm Diameter)
SHALE
Reaction Piers (812mm Diameter)
B-13
CLAY
20
17
58
35
32
17
20/3"
50/5"
50/3"
50/3.5"
50/3.5"
50/2.5"
50/3.5"
SAND
LL=52
PL=22
16
18
15
SHALE
LL=48
PL=24
16
18
15
20
3.05 m
3.05 m
3.05 m
3.05 m
Reference Frame and Piers supporting it
Reaction Pier
Test Pier
Plan View of Load Test Set-up
LEGEND:
Location of standard penetration test with resistance ("N") value of 20 blows per foot
20
Location of standard penetration test with 50 blows for 3 in. of penetration
50/3"
Water level entry depth
13 Water Content
6.45
26, 1.76
Qu
Unconfined Compression Strength (MPa)
Dry Unit Weight Mg/m³
Water Content, %
LL=Liquid Limit
PL=Plastic Limit

Fig. 2 Test Pier Subsurface Profile

Similar drilling procedures were used to construct each of the three piers. The augers were initially advanced through the surficial silty clay layer (3 m thick) to the top of the sand/gravel layer (±6 m thick) where groundwater first entered the shaft. At this depth the contractor added water to the excavation and mixed a drilling slurry. Varying amounts of the surficial clay spoil were added to increase the consistency of the slurry. Drilling continued through the sand/gravel layer and into the weathered shale (±1.5 m thick) by the slurry method. At a penetration of approximately 0.6 to 1 m (2 to 3 ft) into the weathered shale, the temporary steel casing was set and turned an additional 0.3 to 0.6 m (1 to 2 ft) into the weathered shale to form a watertight seal. The contractor then mechanically bailed out the slurry and continued drilling with the auger in the dry hole to the desired bearing elevation. The effectiveness of the casing/shale seal varied. Water flow through the unweathered shale into the excavated shafts was noted in the east reaction pier and in the test pier.

To minimize water softening of the base of the test pier, the drilling contractor halted drilling 0.6 to 1 m (2 to 3 ft) above the desired bearing elevation until the instrumented reinforcing cage was set and concrete arrived on-site. Prior to the final setting of the reinforcing cage, the electrical instrumentation and telltale were attached to the inside of the steel cage. After the instrumentation was attached to the steel reinforcement, the cage was lifted out of the hole, the remaining 0.6 to 1 m (1 to 3 ft) of shale was excavated, and the cage was reinserted into the hole. The delay between final drilling of the pier and placement of concrete was about 30 minutes. Concrete was then placed continuously to the bottom of the pier cap. In an effort to minimize the potential for disturbance of the electrical instrumentation, a full-length, "Elephant Trunk" was used to limit free-fall of the concrete. A log of the test pier is given in Fig. 3.

Concrete Testing

A total of six concrete cylinders were cast from the test and reaction piers. Cylinders were cured in both the field and laboratory and tested for strength and modulus at curing periods of approximately seven to eight days, sixteen to eighteen days, and twenty-two to twenty-four days. The average compressive strength and modulus at the time of the load test were 47.2 MPa and 9,930 MPa (6,840 psi and 1,440,000 psi), respectively.

INSTRUMENTATION

The instrumentation used on the pier load test was divided into three primary categories: 1) pier deformation measurement devices, 2) pier butt displacement measurement devices, and 3) load measurement devices. The two types of pier deformation measurement devices were strain gages and "Carlson Reinforced Concrete Meters." Pier displacement measurements were made using a wire gage, telltale, Brunson automatic level with optical tooling attachment and four optical scales, and three dial gages to measure the vertical displacement of the test pier cap. Load measurements were made using a hydraulic pressure gage and a 8.9 MN (1,000-ton load cell).

Strain Gages Devices

Five strain gages were installed in the test pier: one in the center of the test pier cap, one at the top of the weathered shale, one at the interface between the weathered and unweathered shale, one 1.5 m (5 ft) below the interface, and 2.7 m (9 ft) below the interface (0.3 m above the bottom of the pier). The strain gage device numbers and locations are shown on the Test Pier Log (Fig. 3).

The strain gage located 1.5 m (5 ft) below the interface of the weathered and unweathered shale was found to be defective during the initial loadings and the data are not presented herein.

The purpose of the strain gages was to measure axial deformation of the piers at discrete locations. These measurements were then used to evaluate load transfer with depth. The strain gages ("Micro Measurements" CEA-06-125UT-120) were mounted on 13 mm (0.5-in.) square bars 300-mm (12-in.) long suspended vertically in the center of the reinforcing cage. The linearity and calibration factors for each of the gages were determined in the laboratory using a specially made loading frame. The results of the strain gage device calibration program showed that the devices were linear and within the tolerances published for each of the gages.

Carlson Reinforced Concrete Meters

Three Carlson Reinforced Concrete Meters (Carlson gages) were used to measure axial deformations in the test pier. The first gage was placed near the center of the test pier cap. The second gage was installed at the top of the weathered shale and the third gage was installed at the interface between the weathered and unweathered shale.

The locations of the Carlson gages are shown in the Test Pier Log (Fig. 3). The Carlson gages were installed at the same elevations as strain gages 3A, 3B, and 3C. The purpose of the Carlson gages was to provide alternate measurements of the axial deformations at three locations to verify the measurements of the strain gage devices. A Strain Gage Bridge was used to monitor the output from the Carlson Gages. The Carlson gages were factory calibrated for stress, strain, and temperature. Factory calibrations checked in the laboratory prior to use on the project indicated that the Carlson gages were operating properly.

Telltale

A telltale was installed inside the reinforcing cage of the test pier. The purpose of the telltale was to monitor the displacement of the pier tip.

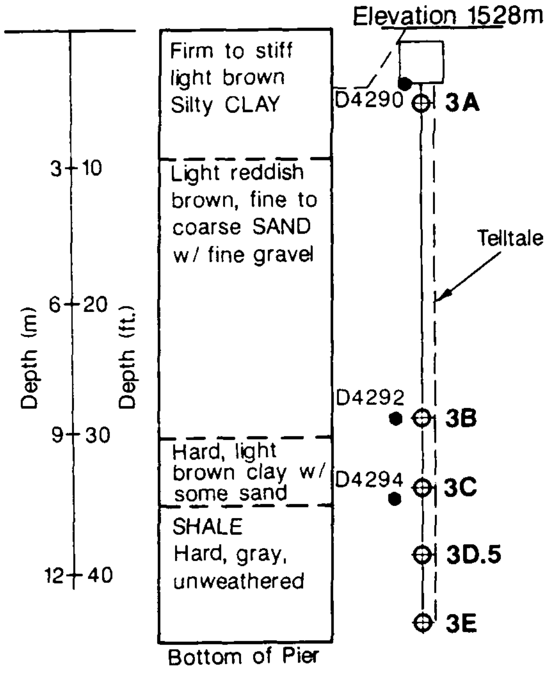
Elevation 1528m
Firm to stiff light brown Silty CLAY
D4290
3A
Light reddish brown, fine to coarse SAND w/ fine gravel
Telltale
3
10
6
20
9
30
12
40
Depth (m)
Depth (ft.)
D4292
3B
Hard, light brown clay w/ some sand
D4294
3C
SHALE Hard, gray, unweathered
3D.5
3E
Bottom of Pier

LEGEND:

- ● **Denotes location of Carlson Gage**
- ⊕ **Denotes location of Strain Gage mounted on 13mm x 13mm Steel Rod**

NOTE:

Pier Diameter 508mm (20-in.) to depth of 6m (20ft.); 457mm (18-in.) diameter below 20 ft. Top of pier of 1.2m (4 ft.) below grade

Fig. 3 Detailed Test Pier Log and Instrumentation

The telltale consisted of a 25 mm (1 in.) I.D. steel pipe which ran the length of the test pier at its center with a 13 mm (0.5-in.) square bar inside. The bar exited the pier horizontally through a pipe tee in the pier cap. Movement of the bar was monitored by a dial gage mounted on the reference frame.

Load Measurement Devices and Jack

Applied load was monitored by a calibrated hydraulic pressure gage on the jack and a 8.9-MN (1,000-ton) capacity electric load cell. Unfortunately the load cell malfunctioned during the test, necessitating use of the pressure gage to monitor load. The test loads were applied by a 10.7-MN (1,200-ton) hydraulic jack. An automatic hydraulic pump was used to increase, decrease, and maintain constant loads throughout the test using nitrogen gas.

To maintain a fairly constant temperature throughout the duration of the test and to provide protection for instrumentation and read-out devices, the test area was enclosed with reinforced polyurethane. A thermostatically controlled propane heater was used as required.

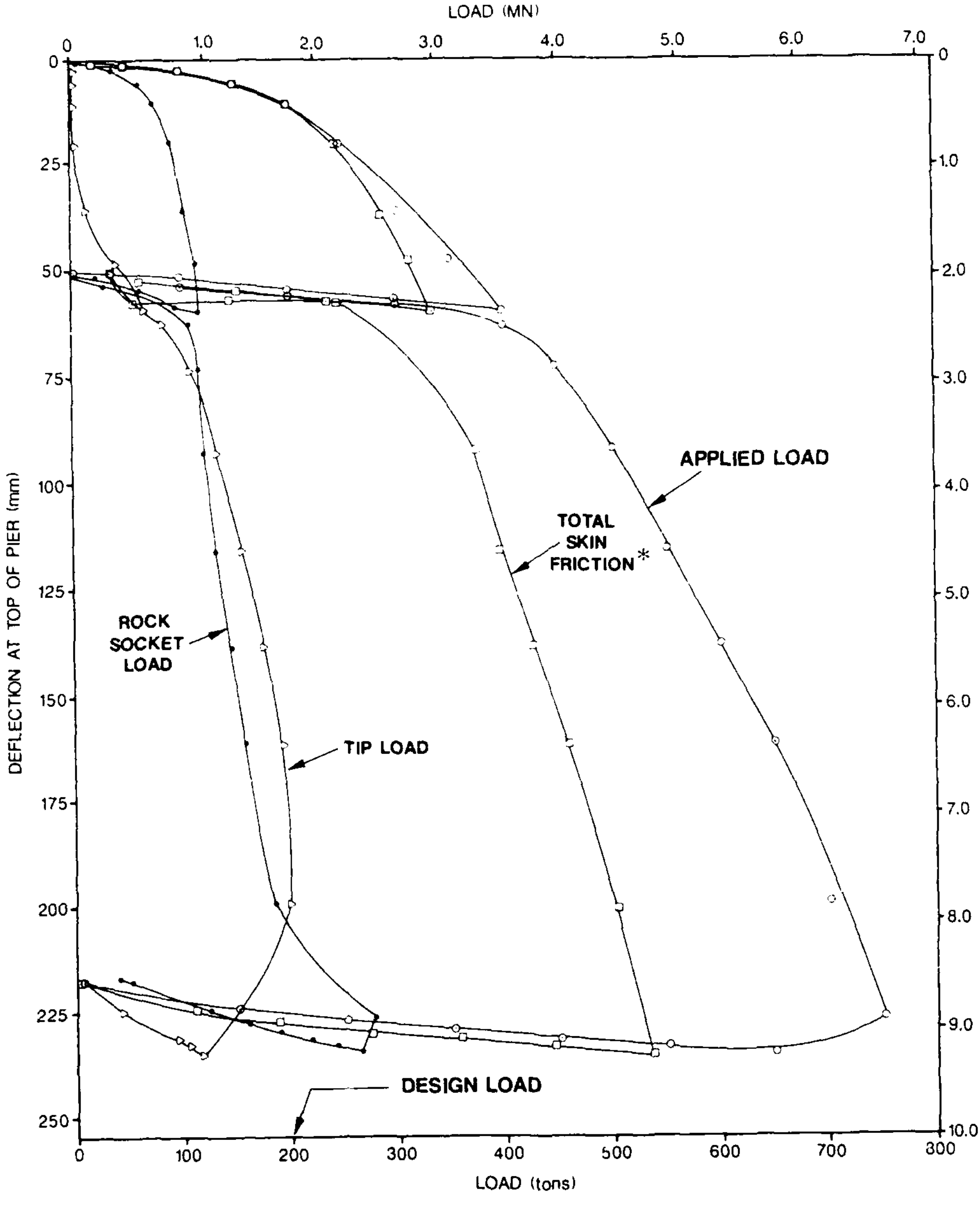

Fig. 4 Load – Deflection Curves

* Total skin friction assumed to be the difference between applied load and tip load.

TEST PROCEDURE

The testing system and loading procedures followed steps outlined by the ASTM standard D1143-81 "Piles Under Static Axial Compressive Load". Loading procedures used during the test were in general agreement with those outlined in Sections 5.1 and 5.3 of the ASTM standard, "Standard Loading Procedures" and "Loading in Excess of Standard Test Load", respectively.

As the test progressed, it was necessary to modify certain ASTM procedures. These modifications regarded the duration of time for maintaining constant load at each increment and the 12-hour holding period at 200 percent of design load. To better define the time-rate of settlement and load-transfer relationships, certain load increments were held in excess of the two hour limit defined in the above standard. The 12-hour holding period for 200 percent of the design load was dropped from the test procedure as a result of the magnitude of settlement already experienced and because the pier was later to be reloaded to failure.

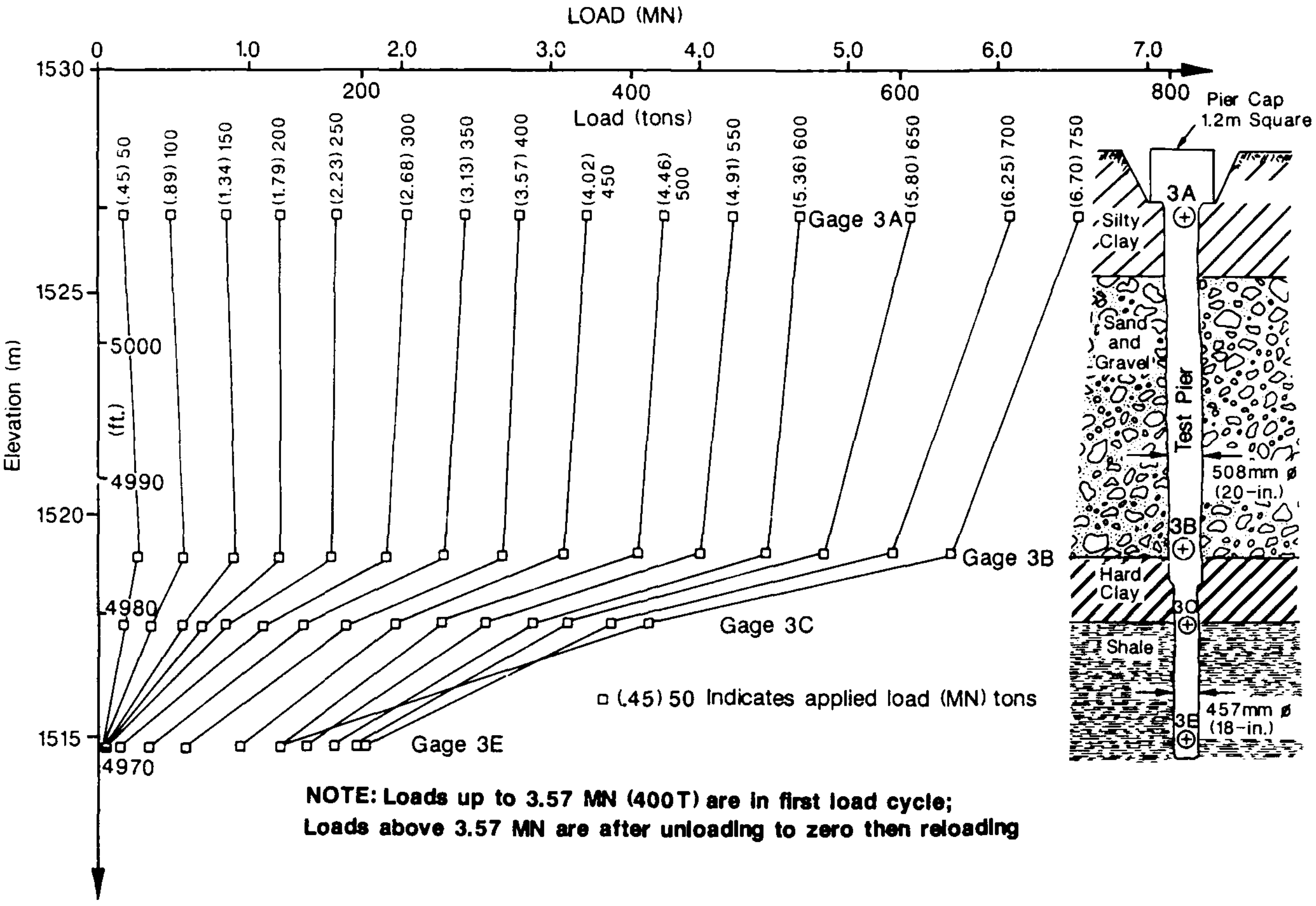

NOTE: Loads up to 3.57 MN (400T) are in first load cycle; Loads above 3.57 MN are after unloading to zero then reloading

Fig. 5 Load Transfer with Depth

Another deviation from the ASTM standard regarded the percentage of design load to be applied in excess of the standard test load. Load increments of 25 percent design load instead of 10 percent were used to define the load-settlement curve for those loads in excess of the standard test load. This was done because of the relatively high maximum test load.

TEST CHRONOLOGY

The load test ran through the weekend of November 4, 5, and 6, 1983. The initial load was applied at 11:13 a.m. on Friday, November 4, and the test was completed 7:30 p.m. Sunday, November 6, 1983. The pier was loaded in 0.45 MN (50-ton) increments to 3.57 MN (400 tons), or 200 percent of the design load. Each load increment was maintained until the rate of axial deflection (herein called axial strain rate) was less than 0.25 mm (0.01 in.) per hour. The load was then removed in 0.89 MN (100-ton) increments to zero load. A minimum period of one hour was used for each of the increments during the unload cycle. The pier was left unloaded for one hour prior to the second load cycle.

During the second load cycle, the pier was loaded in 0.89 MN (100-ton) increments to 3.57 MN (400 tons). Each load increment was maintained until the axial strain rate was less than 1.27 mm (0.05 in.) per hour. From 3.57 MN to 6.7 MN (400 to 750 tons), the loads were added in 0.45 MN (50-ton) increments. The axial strain rate at 6.25 MN (700 tons) held constant at 2.5 mm (0.10 in.) per hour.

The pier experienced rapid and large axial displacement at the maximum load of 6.7 MN (750 tons). The load was maintained until the instrumentation could be read (about 30 minutes). The load was then removed in 0.89 MN (100-ton) increments to 1.34 MN (150 tons) with the last unload increment from 1.34 MN to zero load. The unload increments were maintained until the axial strain rate was less than 0.25 mm (0.01 in.) per hour (typically less than 20 minutes).

LOAD TEST RESULTS

Results of load test are given in Figs. 4 and 5 and information for selected loads are summarized in Table 1. These data are based on loads calculated from the strain gauges and top-of-pier (butt) deflections from dial gauge readings. Strain gauges and Carlson gauges were used to estimate load distribution within the pier. Values between corresponding devices agreed within about ±10 to 20 percent. Only the strain gauge data are shown because the greater number of strain gauges provided more information. Deformation

TABLE 1 Summary of Rock Socket Stress and End-Bearing Stress for Several Loads

Load MN (tons)	Butt Displacement mm (in.)	Rock Socket Bond Stress MPa (tsf)	End-Bearing Stress MPa (tsf)	Remarks
1.79	11.3	0.17	0.11	Design Load
(200)	(0.443)	(1.8)	(1.19)	
3.57	59.4	0.27	3.62	Twice Design Load
(400)	(2.34)	(2.8)	(37.8)	
5.36	138.2	0.34	9.46	Three Times Design Load
(600)	(5.44)	(3.5)	(98.8)	
6.70	226.1	0.62	10.8(2)	Ultimate Load
(750)	(8.90)	(6.5)	(112.4)	

Notes: 1. The data for 1.79 and 3.57 MN are during the first load cycle.
2. Maximum end-bearing stress occurred at a total load of 6.25 MN (700 tons) compared to 6.7 MN (750 tons) for the maximum rock-socket bond stress.

measurements from the dial gages, wire and scale, and Brunson Level were all similar. Movement of the tip determined by the telltale was suspect and the telltale was not functional beyond a movement of 132 mm (5.16 in.).

Data indicate that at the design load of 1.79 MN (200 tons) butt deflection was approximately 11.2 mm (0.44 in.) or about 2.2 percent of the butt diameter of the shaft. Load at that point was carried predominantly by skin friction with negligible contribution from the pier tip. Loading to twice the design load or 3.57 MN (400 tons) increased butt deflections to 59.1 mm (3.3 in.) or 16.5 percent of the butt diameter. At 3.57 MN (400 tons), the load was resisted primarily by skin friction although the end-bearing contribution had begun to increase between approximately 2.2 to 2.7 MN (250 to 300 tons) and by twice design load was 0.60 MN (67 tons). The large deflection (16.5 percent of the butt diameter) necessary to mobilize end-bearing suggests slippage within the rock socket and possible compression of debris- or water-softened shale under the pier tip.

After loading to 3.57 MN (400 tons), the pier was unloaded, then reloaded to failure. Approximately 50 mm (2 in.) of permanent set occurred upon unloading from 3.57 MN (400T). During reload, the load deflection relationship increased at nearly a constant rate with approximately two-thirds of the load resisted in skin friction and about one-third in end-bearing. Between 6.25 and 6.7 MN (700 and 750 tons) strain rate increased indicating failure. Also at that point, the end-bearing contribution decreased and skin friction within the rock socket increased. The maximum end-bearing load of approximately 1.78 MN (199 tons) occurred at a total load of 6.25 MN (700 tons). This corresponds to a maximum end-bearing stress of approximately 10.7 MPa (112 tsf). The maximum skin friction in the rock socket was 2.46 MN (276 tons) which occurred at the maximum applied load, 6.7 MN (750 tons). The maximum bond stress within the rock socket at that load was approximately 0.62 MPa (6.5 tsf). This maximum bond stress corresponds to about 33 percent of the undrained shear strength of the shale.

DISCUSSION

The load-deflection relationship up to the design load of 1.79 MN (200 tons) was within the criteria established by the client. However, above the design load deflections became much greater. These larger deflections are believed to have been caused by slippage of the shaft in the socket. Air and water slaking of the pier shaft during construction may have contributed to shaft slippage.

The test results raised concern that production piers might experience large settlements if constructed with a smooth socket. To limit settlement, it was felt that the shearing resistance between the pier shaft and shale must be increased. A practical means to accomplish this was by use of shear rings which would "key" the pier shaft into the shale. Shear rings would also mobilize a greater percentage of the shear strength of the shale as shown by Horvath, et al. Tests by Horvath, et al (1983) showed that skin friction of 40 to 60 percent of the shear strength of the rock or .76 MPa (8tsf) to 1.15 MPa (12 tsf) in this case was reasonable using roughened sockets. Tests on piers with shear rings by Glos, et al indicated that up to 90 percent of the shear strength of the rock was mobilized. On the other hand, it was felt that there was little that could be done practically to increase end-bearing, especially at small deflections.

Based upon the results of this load test and the references cited, the design parameters were revised for the production piers. It was recommended that production piers be designed for skin friction only, based on an allowable value of the 0.48 MPa (5 tsf) and that shear rings be installed in each pier. It was recommended that shear rings be spaced at approximately 610 mm (24 in.) along the rock socket and that each shear ring be approximately 50 mm (2 in.) deep by 100 mm (4 in.) high. A minimum socket length of 3 m (10 ft) was specified.

In addition, it was recommended that piers be concreted immediately upon excavation of the rock socket to *minimize deterioration of the shale by slaking.*

PRODUCTION DRILLED PIER CONSTRUCTION

Approximately 750 drilled piers varying in diameter from 610 mm (24 in.) to 1.22 m (48 in.) were constructed between February 21 and May 2 of 1985. Typical production using 4 rigs was 18 piers per day with a maximum production rate of 33 piers per day. Piers were installed by similar techniques as the test pier, i.e., slurry drilling and casing through the loessial and granular formations and drilling the rock socket in the dry using earth augers. Shear rings were cut with simple attachments to the drill tools with a minimal increase in time and cost over drilling a smooth rock socket.

The cost of the drilled pier load test including engineering was approximately $100,000. The *modification in the design resulting from the load test,* however, was estimated to have reduced construction cost by about $400,000.

CONCLUSIONS

This study leads to the following conclusions.

> The Pierre Shale is apparently sensitive to air and water slaking which can increase deflections of smooth-socketed drilled piers beyond tolerable values.
>
> Designing based on empirical rules in the Pierre Shale could lead to piers which experience excessive deflections.
>
> Shear rings are recommended on drilled piers in the Pierre Shale to increase bond resistance and *minimize* deflections. The contribution of end-bearing at small deflections is negligible.
>
> A well instrumented load test for a major *project may result in a safer design and* cost savings.

ACKNOWLEDGEMENTS

We wish to thank the many people who contributed to this project and publication of this paper. Particularly, we wish to thank Mr. Howard M. McMaster, for his review and constructive comments. We also wish to thank Mr. Neil Williams and Mr. P. Denny Retter who reduced most of the load test data. Finally, we would like to thank Ms. Tracy Turner and Marian Blumenthal for typing the manuscript and Mr. Kevin D. Williams for preparation of the figures.

REFERENCES

American Society for Testing and Material (1981), ASTM Designation D1143-81, "Standard Method of Testing *Piles Under Static Axial Compressive Load*".

Glos, G.H. III, Briggs O.H., Jr. (1983), "Rock sockets in Soft Rock", Journal of the Geotechnical Engineering Division, ASCE, Vol. 109, No. 4, April.

Horvath, R.G., and Kenney, T.C., (1979), "Shaft Resistance of Rock Socketed Drilled Piers", *Proceedings of a Symposium on Deep Foundations*, Committee on Deep Foundations of the Geotechnical Engineering Division of the American Society of Civil Engineers, Frank M. Fuller, editor.

Horvath, R.G., Kenney, T.C., Kozicki, P., (1983), "Methods of Improving the Performance of Drilled Piers in Weak Rock", Canadian Geotechnical Journal, Vol. 20.

Jubenville, D.M., and Hepworth, R.C. (1981), "Drilled Pier Foundations in Shale, Denver, Colorado Area", Drilled Piers and Caissons, Proceedings of a session sponsored by the Geotechnical Engineering Division at the ASCE National Convention, St. Louis, Missouri October 28, 1981, Michael W. O'Neill, editor.

Proceedings: Second International Conference on Case Histories in Geotechnical Engineering, June 1-5, 1988, St. Louis, Mo., Paper No. 6.62

Caisson Load Test and Instrumentation Program— Sohio Corporate Headquarters

Barry R. Christopher
STS Consultants, Northbrook, Illinois

Clyde N. Baker, Jr.
STS Consultants, Northbrook, Illinois

SYNOPSIS: The Sohio Corporate Headquarters building foundations in Cleveland, Ohio are relatively unique, involving as they do some of the deepest caissons on record, combined with a socket friction design.

This paper reports the performance of a full-scale load test and the results of instrumentation programs performed to evaluate the design and performance of 240-ft (73 m) deep rock socket caissons at the Sohio Corporate Headquarters building project. The load test was carried out to 2.5 times the theoretical design capcacity and the results are reviewed in terms of both total capacity and the individual design parameters, such as socket friction. Details of the instrumentation program used to evaluate concrete strain and corresponding load transference as a function of applied load, caisson depth, and time are also presented. In addition to the load test, the installation details and results of a production caisson instrumentation program to permit long-term monitoring of concrete stress and strain levels are reviewed.

INTRODUCTION

Construction of the Sohio Corporate Headquarters building in Cleveland, Ohio began in early spring of 1983 and was completed in the spring of 1985. Due to the subsurface conditions at the site, caisson (drilled pier) type foundations were required to support the 46-story tower section of the building. Due to the known gas conditions in and over the shale bedrock (the anticipated bearing stratum), it was anticipated that hand clean-up and physical bottom inspection of the caissons would not be practical and that it might be necessary to construct the caissons under water. For this reason, a design based on extending sockets into the shale sufficiently to carry a major portion of the load in socket friction was developed. The loads on the caissons range from 3,000 to 14,000 kips (13 MN to 62.3 MN) including wind loads, resulting in caissons extending to a depth of up to 250 ft (76 m) below street level with shaft diameters of 3.5 to 7 ft (1.1 to 2.1 m) at the socket.

To substantiate the design, a full scale caisson load test with a planned test load at the socket of 2.5 times the design load was performed. To obtain the required loads, the test setup required a reaction load of 1250 tons (11.1 MN). The purpose of the full scale caisson load test was to determine how the load would be carried by the caisson and socket, and to confirm the design capacity, both total capacity and the individual design parameters, such as socket friction. To further evaluate the design, one of the major production caissons was fully instrumented to permit long-term monitoring of stress levels along the full depth of the caisson, both during construction and after completion of the building.

In this paper, a detailed description of the caisson load test is presented, including the physical setup and instrumentation. The results obtained are reviewed and conclusions resulting from the analysis are presented. Also included are details of the instrumentation program for a production caisson and an analysis of measurements taken as of this writing. The results of the load transfer measured in both the load test caisson and the production caisson are then compared.

PROJECT DESCRIPTION

Subsurface Conditions: The subsurface profile at the site is shown in Figure 1. As the figure shows, the subsurface conditions consisted of silty sand to a depth of approximately 30 to 40 ft (9 to 12 m), lacustrine clays and silts to a depth of about 170 ft (52 m), glacial till overlying silty sand, gravel and cobbles to a weathered shale at a depth of 190 ft (58 m), with competent shale at a depth of 220 ft (67 m). The surface water table was located at a depth of approximately 20 ft (6 m) with a deep water table in and over the weathered shale at a depth of approximately 70 to 90 ft (21 to 27 m). To develop sufficient socket friction, the caissons were designed to extend from 1 to 2 diameters into the competent shale layer.

Load Test Setup: The physical load test arrangement is depicted in Figure 2. The plan for the load test consisted of constructing a 3 ft (0.9 m) diameter load test caisson, a non-production caisson, between two production caissons which serve as anchor caissons. The load test caisson was designed to transfer all of the applied load directly to the rock socket by isolating the caisson shaft from the surrounding earth all the way down into the shale socket. This was achieved by placing a 3 ft diameter casing inside the normal top, intermediate and bottom casings required to construct a normal caisson. The 3 ft diameter inner-casing was braced at the top to minimize lateral movement and at the third points to protect against buckling.

FIGURE 1 SUBSURFACE PROFILE AND CAISSON PLAN

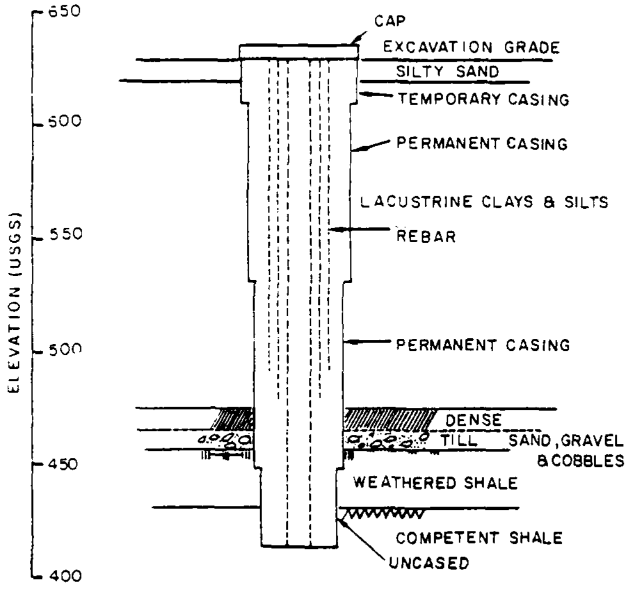
650
600
550
500
450
400
ELEVATION (USGS)
CAP
EXCAVATION GRADE
SILTY SAND
TEMPORARY CASING
PERMANENT CASING
LACUSTRINE CLAYS & SILTS
REBAR
PERMANENT CASING
DENSE
TILL SAND, GRAVEL & COBBLES
WEATHERED SHALE
COMPETENT SHALE
UNCASED

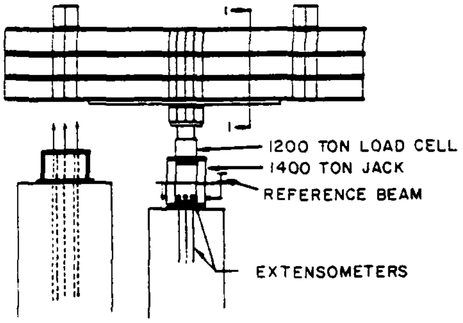
1200 TON LOAD CELL
1400 TON JACK
REFERENCE BEAM
EXTENSOMETERS

FIGURE 2. CAISSON LOAD TEST SET-UP

Several problems occurred during construction that had an influence on interpretation of the test results. A leak developed beneath the top casing which inadvertently resulted in sand and silt in the annular space between the intermediate casing and the inner-casing. Bottom cleaning and sounding, although performed, were hindered by the close steel cage and concern for instrumentation damage. Finally, an overrun in concrete yardage by 6 yards^3 (4.6 m^3) indicated the possibility that a tight seal was not achieved between the inner-casing and the shale socket so that some concrete leakage could have occurred underneath the casing into the annular space outside the inner-casing. It is also possible that the socket drilled in the shale was larger in diameter than assumed because of wobble in the drill auger as the hole is drilled. These possibilities become very important later when analyzing load transfer to the socket.

INSTRUMENTATION SETUP

The instrumentation setup is depicted on Figure 3 and consisted of; two (2) sets of Carlson strain gauges placed at four different levels in the rock socket, wire extensometers, access casing for non-destructive testing, and a seismic pulse transducer (G-Cell). The Carlson gauges are referenced as either D-gauges or A-gauges. The D-gauges are approximately 30 inches (760 mm) in length. As strains are averaged out over the full length of the gauge, they are more representative of average conditions. The A-gauges are 8 inches (200 mm) in length and while more sensitive, can be misleading because they measure strain over a very short distance and may indicate abnormalities rather than average conditions. The gauges were wired to the cage prior to placement

FIGURE 3. INSTRUMENTATION ARRANGEMENT

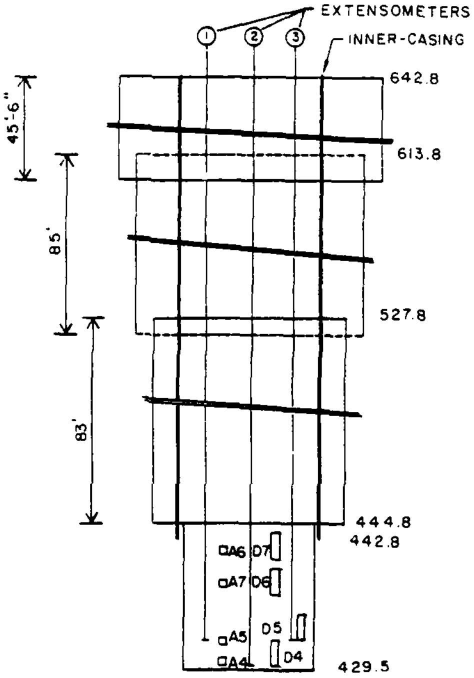
EXTENSOMETERS
①
②
③
INNER-CASING
642.8
613.8
527.8
444.8
442.8
429.5
45'-6"
85'
83'
A6
D7
A7
D6
A5
D5
A4
D4

In order to be able to monitor the tip movement of the caisson during loading, special tell-tales or wire extensometers were installed as shown in Figure 3.

The movement of the caisson bottom was monitored by measuring the movement of the wire cable attached to a plate at the bottom of an outer protective pipe weight pulling on a wire cable.

Unfortunately, in cutting the caisson, the wires to the G cell were destroyed, rendering it inoperable

LOAD TEST RESULTS

The load test procedure consisted of loading the caisson on the first load cycle in increments of 100 tons (890 kN) up to 1,000 tons (8.90 MN) and in increments of 50 tons (450 kN) above 1,000 tons (8.90 MN) to the planned maximum of 1,200 tons (10.7 MN) and then unloading the caisson in three equal increments of 400 tons (3.56 MN). The load vs. deflection was recorded with time using two dial gauges attached to a reference beam with gauges located on opposite sides of the caissons. The dial gauge readings were checked using a wire scale and mirror arrangement with the wire attached to a separate reference from the dial gauges. The load was increased at one (1) hour increments or when the load vs. deflection tended to level off if it occurred in less than one (1) hour.

On unloading from the first load cycle, a small seating load of 70 tons was maintained on the caisson until commencing the second load cycle the next day. On the second load cycle, the first load increment was to 200 tons (1.78 MN) and then each load increment thereafter was 200 tons (1.78 MN) up to 1,200 tons (10.8 MN). With approval of the contractor's engineer, who designed the reaction frame, an additional 50 tons (450 kN) was applied making the maximum load on the second load cycle 1,250 tons (11.1 MN). The unloading sequence was to 800 tons (7.12 MN), 400 tons (3.56 MN) and 0 () MN) tons.

LOAD TEST RESULTS AND ANALYSIS

Load Test: The load test results are summarized on Figure 4 and show the observed deflection of the top of the caisson versus load. Also plotted on the curve are two elastic lines for the concrete. The lower elastic line assumes that all the load is carried from the top of the concrete shaft to the bottom of the concrete with no load dissipation and no deflection at the tip. The upper elastic line assumes full load carried in the concrete shaft to a depth of 20 ft (6.1 m) without dissipation and then gradual linear dissipation of the load to the bottom of the caisson. The modulus of elasticity to develop the elastic lines was obtained by performing laboratory tests on concrete cylinders that were cast at the time of placement of the concrete in the caisson. Allowing for the confinement effect of the steel casing and reinforcement, a modulus of elasticity for the concrete in the caissons of 3.2 million psi (22,000 MPa) was utilized.

It is evident from the load deflection plot that the points plot way above the bottom elastic line. This would indicate that load is being taken out in friction very quickly well above the shale socket where the load was attempted to be transmitted.

In spite of the load apparently carried by friction, at 1,200 tons (10.7 MN) the top deflection falls significantly below the lower elastic line indicating movement of the tip. On unload, a net deflection of 0.8 inches (23 mm) was recorded and the slope of the unload curve is much flatter than the lower elastic line indicating significant locked in friction. This will be discussed further in later sections.

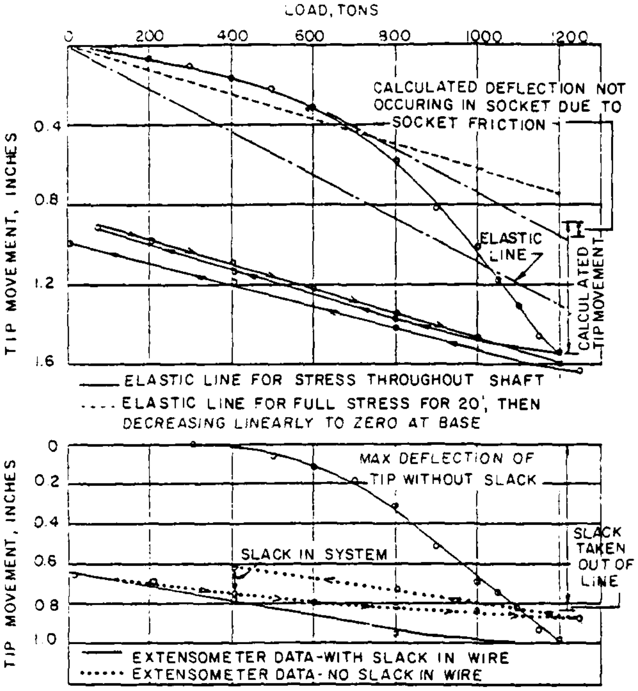

FIGURE 4. CAISSON LOAD TEST RESULTS - LOAD VERSUS SETTLEMENT CURVE

Extensometer Results: The caisson bottom or tip movement as indicated by the tell-tale or extensometer data, is shown on the bottom half of Figure 4. On the initial loading cycle, it appeared that not all of the slack was taken out of the wire lines and that a certain amount of this slack gradually was pulled out as the test progressed. Apparently, kinks in the line that developed during the wire unwinding in installation were not adequately pulled out by the weights that maintained tension in the lines. As this was discovered during the progress of the tests, greater effort was put into pulling the slack out of the line before taking readings for the second load cycle. Thus, the first load cycle is believed to over-indicate the amount of tip movement. Since the measured top movement in the second load cycle went almost to the exact deflection under maximum load as the first load cycle, there could not have been significant increases in the tip deflection of the second load cycle. Thus, the difference in tip deflection measured on the second load cycle using the tell-tales was an indication of slack taken out of the tell-tale system. It is even possible that not all of the slack was yet taken out so that the measured maximum tip deflection of 0.8 inches (20 mm) could still be on the high side. This compares with a calculated tip movement using elastic line analysis and top measured deflection of slightly less than 0.7 inch (18 mm).

Strain Gauge Results: The presumed concrete modulus of 3.2 million psi (22,000 MPa) was also used to calculate the stress level in the concrete at the strain gauge locations. These results are shown in Figure 5.

The stress levels were then multiplied by the transformed area of the caisson shaft at the strain gauge location and the load distribution curves plotted as depicted in Figure 6. The A-strain gauges and the D-strain gauges agree reasonably well for the top 2 strain gauge locations. The second gauges from the bottom appear to not be functioning properly at either

FIGURE 5. STRESS TRANSFER CURVE

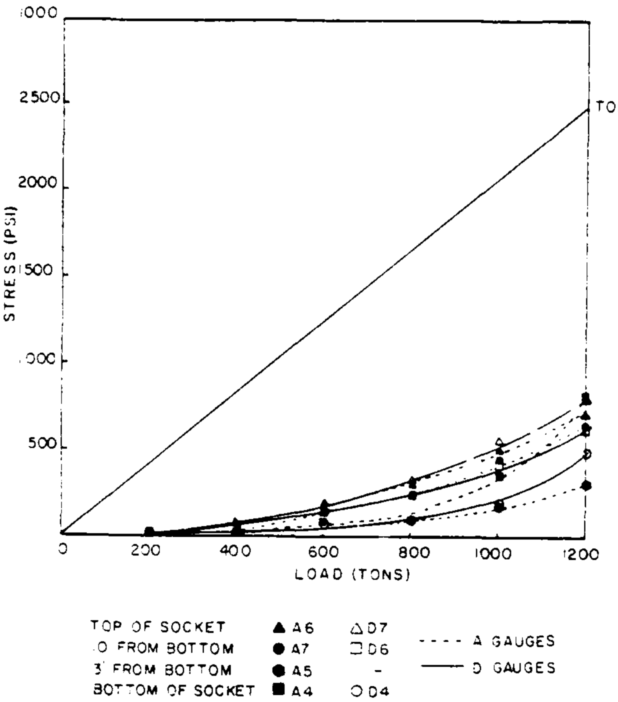

FIGURE 6. LOAD TRANSFER

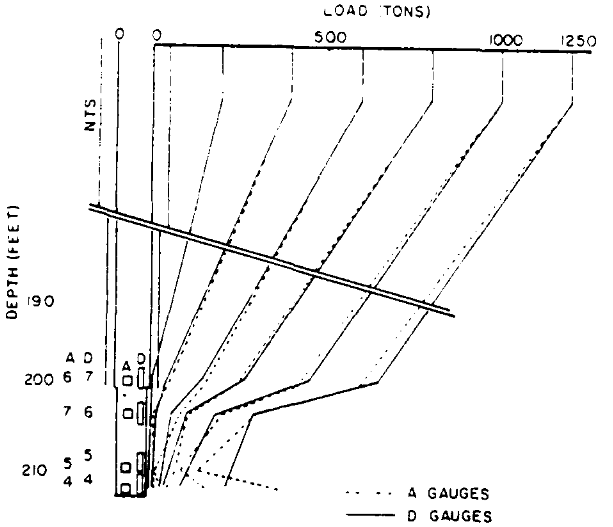

the A or D locations since negligible changes in readings occurred throughout the loading sequence. At the bottom gauge locations, the A-gauge and D-gauge are markedly different with the A-gauge indicating an illogical increase in loading as compared to upper gauges. The D-gauge indicates a reasonable distribution. A possible explanation for the large strain observed in the A-gauge could be contamination of the concrete in the area of the gauge resulting in a much lower modulus than actually used to calculate the stress. Since the D-gauge is larger and averages more concrete, it is believed to be more representative of the conditions and forms the basis of our subsequent analysis on socket friction. Subsequent non-destructive testing with a nuclear gamma logger supported the possibility of bottom contamination.

Measurements during the load test indicated that sand and silt had flowed in all the way up to approximately 20 ft (6.1 m) from the top of the caisson. In order to see if the observed deflections could be theoretically calculated, based on reasonable soil resistance factors, an analysis was performed.

Since the observed deflection was even flatter than the upper elastic line which assumes gradually increasing soil resistance, it is concluded that some load must be taken by the bracing system used between the inner casing and outer casing to avoid lateral deflections and to protect against buckling. By assuming 100 kips (450 kN) load carried in the braces (obtained by straight line extension of the initial points back to 0) and assuming reasonable soil friction parameters of 30 degrees for friction angle and 0.45 for earth pressure at rest, and by further assuming that a maximum friction value is reached at approximately 20 caisson diameters (60 ft (18.3 m) of soil surface or 80 ft (24.4 m) below the top of caisson) (STS Consultants, Ltd., 1983) a reasonable check was made. The calculated deflection is shown by an "X" plotted on the load deflection curve in Figure 4. The calculated deflection almost plots exactly on the curve. This indicates a maximum load being taken in soil friction and bracing friction of 1180 kips (5270 kN) leaving 1220 kips (5410 kN) of load reaching the socket at the point of maximum loading. This agrees reasonably well with the maximum load indicated by the strain gauges of 1190 kips (5310 kN).

Socket Friction Analysis: In order to confirm the design basis for the caissons, a socket friction analysis was made. Calculations indicated that the 1.3 ft (0.40 m) of competent shale above the bottom gauges carries an average friction of 190 psi (1300 KPa) or well above the design assumption of 160 psi (1100 KPa). If this same friction is assumed to continue for the next 1 ft (0.3 m) of competent shale socket, a load of only 162 kips (720 kn) is left remaining for the bottom 1 ft (0.3 m). Theoretically, this should all be carried in the bottom 1 ft (0.3 m) and there should be no tip movement. Since an observed and calculated tip movement on the order of 0.7 inch (18 mm) was believed to have occurred, the data indicates a soft bottom. One possible explanation is that several inches of sand leaked into the bottom underneath the casing prior to concrete placement (as previously indicated). Such a possible sand bottom would be consistent with observed data, particularly with regard to the second load cycle performance and the reaction of the A-gauge at the bottom of the caisson. In the second load cycle, the compressed bottom appears to behave almost elastically and similar to concrete. This is the way confined sand would behave as increasing load were applied. If the A-gauge were partially or entirely embedded in sand, the sand modulus would be much lower than the concrete modulus used to calculate the stress of the gauge. Thus a much lower stress similar to that obtained from the D-gauge would be obtained.

Another interpretation of the data could have a major part of the load on the socket carried at the top of the socket because of the fact that the casing is 3 ft (0.9 m) in diameter and the theoretical socket diameter is 30 inches (760 mm). The gauge reading 3 ft (0.9 m) below the casing appears to confirm a major load transfer occurring in the top 3 ft (0.9 m) of the socket.

CORRELATION OF CAISSON LOAD TEST TO PRODUCTION CAISSONS

Concerning the data and analysis from the load test, the interpretations presented appear to be reasonable on the basis of the observed data. Other assumptions might vary the load distribution calculated, but would not effect the ultimate fact that the caisson was successfully loaded to 2.5 times it theoretical design capacity and that at maximum load, the total system was behaving almost elastically with not even the first signs of approaching capacity limits. Further, whether a disproportionate amount of load is taken out at the top of the socket or whether it is averaged over the thickness of the socket is academic as far as the design of the production caisson is concerned, since the production caissons have the same general geometry with regard to the casing diameter being 6 inches (150 mm) larger than the socket diameter. However, to provide a clearer picture of the actual load transfer mechanism, a production caisson was fully instrumented.

Instrumentation Program: For the instrumentation program, one of the large caissons which was required to carry the largest loads and would involve the most significant change in loading condition under high wind loads was selected. The particular caisson extended to a depth of approximately 245 ft (74.7 m) below street level with a 7 ft (2.1 m) diameter rock socket extending 17 ft (5.2 m) into competent shale.

Figure 7 depicts the instrumentation setup. Strain cells were located at six different levels in the caisson; namely, near the top of the caisson, near the top of the deep dense till layer, at the bottom of the bottom casing, at the top of the socket penetration into the competent shale, at the middle of the socket, and at the bottom of the socket. In addition, a load cell was located near the top of the caisson. For redundancy and checking purposes, three (3) different strain gages were located at each level. The same short and long Carlson gauges (8" long A-gauges and 30" long D-gauges) used in the load test were selected along with Geokon vibrating wire embedment strain gauges. One of each type of gauge was installed at each level. A Geokon vibrating wire total pressure cell was installed at the cold joint, approximately 20 ft below the top of the caisson. This allowed for careful hand placement of the gauge and the embedding it in non-shrinking grout.

Instrumentation Results: Figure 8 and Figure 9 show the results to date (over two years after completion) of the calculated stress levels in the concrete at the strain gauge locations. These results were calculated using a presumed

FIGURE 7 SCHEMATIC OF INSTRUMENTATION FOR PRODUCTION CAISSON

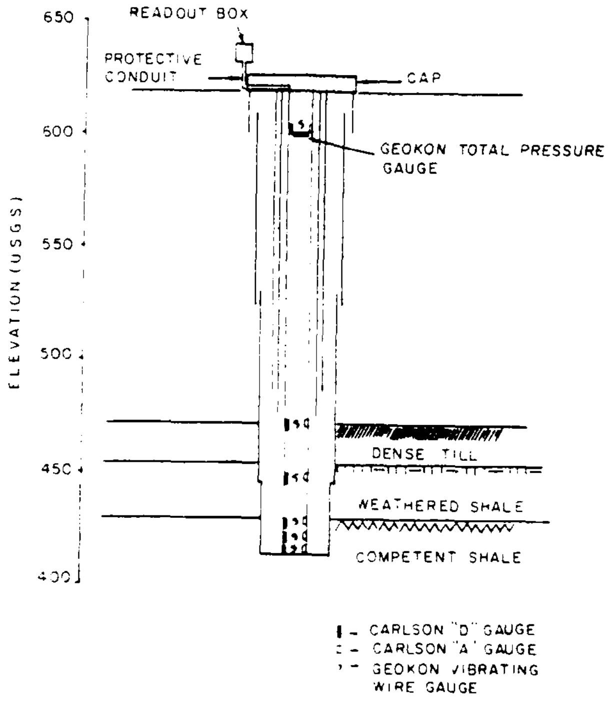

NOT TO SCALE

FIGURE 8. A-GAUGES

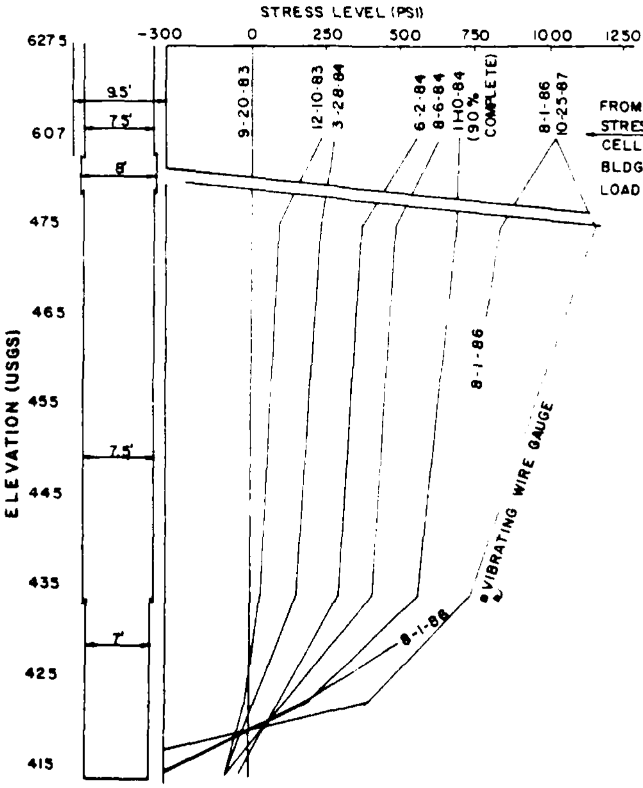

FIGURE 9 D-GAUGES

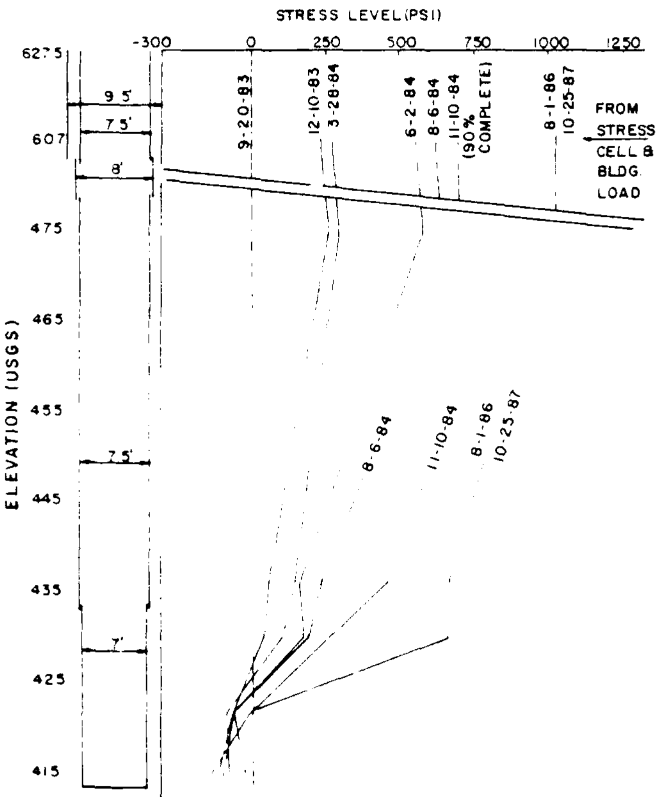

concrete modulus of 3.2 million psi (22,000 MPa). Consideration for creep effects and modulus increase due to age were not included due to evaluation difficulties. Creep under a sustained load would result in an apparent increase in strain while increase in modulus would cause an actual decrease in measured strain. As the influences are somewhat offsetting, the relative trend of stress transfer should not have been highly influenced.

The data shown in the figures indicates comparable stress transfer obtained from both gauges. One obvious anomaly is the negative stress results obtained from the bottom socket gauges. The data shown was calculated from a presumed 0 stress level prior to load application. However, internal stresses can be built into the concrete and gauges during thermal changes in the concrete. If a high residual stress were built into the caisson during thermal expansion, this stress may not be relieved as rapidly as upper level stresses since the socket portion of the caisson is confined by relatively incompressible rock. This stress should be relieved with time and it may be that through relaxation the stress levels are decreasing faster than load is actually being applied. For some as yet unexplained reason, there continues to be an increase in negative values. As it is apparently under no load, the continued increase in negative values at the base may be attributed to minimal concrete shrinkage with age below the level at which load is being carried.

Several gauges are inoperative at this time including most of the vibrating wire strain gauges (apparently damaged during construction), the D-gauge at the top of the till and the D-gauge at the base of the caisson. The A-gauge and the D-gauge at the top of the competent shale rock socket are markedly different with the A-gauge indicating an illogically high stress as compared to the upper gauges and the applied load.

Even with the interpretation problems mentioned above, the data does show certain trends consistent with the previous load test data. It definitely appears that significant load is taken out of the caisson above the socket and that no load is being transferred to the base of the caisson.

CONCLUSIONS

The full scale instrumented test caisson was successfully loaded to 120 tons (11.1 MN) which was 2.5 times the theoretical design capacity, thus confirming the design for the production caissons. However, the actual stress at the base of the caisson was much less than anticipated by design indicating substantial load support through friction in the till and weathered shale layers.

The instrumentation of a production caisson correlates well with the load test results in that negligible load has been recorded at the base of the caisson socket even though the full design building load has been in place for several years. Continued monitoring of the production caisson will certainly reveal more information as to the actual long-term support mechanisms including uplift forces under high wind loading conditions.

The results of this testing may allow for an *even greater increase* in the allowable bearing capacity of caissons in the Cleveland area with confidence that they will provide the necessary load carrying capacity. Hopefully, these results can also be correlated with other tests and design theories on other projects. Only through such hard physical data can theories be verified or modified.

ACKNOWLEDGMENTS

The writers wish to thank the following individuals and organizations for their support in the testing efforts: Brian Smith, STS Field Engineer, and Dennis Wellington, STS Field Technician, who assisted in performance of the field testing; SOHIO Corp. for authorization to present this paper; Urban Investment and Development Co., the Construction Manager; Helmuth, Obata & Kassabaum, Architects for the project; KKBNA, Inc., Structural Engineer; Gilbane Associates, the General Contractor; and Case- Milgard Joint Venture, the caisson contractor for their cooperation and assistance in the performance of the work.

REFERENCES

Bker, C.N. (1983), "Sohio Load Test Report", STS Consultants, Ltd. Report to Urban Investment and Development Co.

Proceedings: Second International Conference on Case Histories in Geotechnical Engineering, June 1-5, 1988, St. Louis, Mo., Paper No. 6.63

Building Design and Construction over Organic Soil

C.N. Baker, Jr.
Vice Chairman, STS Consultants, Ltd., Northbrook, Illinois

S.B. Steinberg
Manager, Market Analysis, STS Consultants, Ltd., Northbrook, Illinois

W. Lam
Principal, KKBNA, USA

SYNOPSIS: A lowrise office building was constructed on a mat foundation over a thick peat deposit that had been preconsolidated beneath surface fill. Environmental restrictions prevented use of deep foundations for fear that penetration through an aquaclude would permit contamination of a deeper water table. This paper describes the laboratory testing and field instrumentation programs, as well as the special geotechnical and structural analysis undertaken for the design and construction of this project. Included in the program were long-term consolidation tests, pressuremeter tests, use of heave markers, inclinometers and pore pressure piezometers. A site history was also developed to define the extent and nature of the surficial fill. To achieve much of the anticipated initial settlement, the basement was temporarily flooded, thus preloading with the full building weight. Water was removed as construction proceeded so that the full building weight was always maintained. Actual settlement was observed to agree fairly well with predicted settlements.

INTRODUCTION

Construction over organic soils has historically been a problem due to the typically low strength and high compressibility that is common to these materials. Designs usually call for supporting the total structure, including floor slabs, on deep foundations extending through the compressible deposits. However, this often leads to difficulties with entering utilities and any attached structures. Alternatively, if the structure is floated over the organic soils in an effort to try to have everything settle together, there is the difficulty of predicting the magnitude and rate of the anticipated settlement.

In the winter of 1984, STS Consultants, Ltd. undertook a project in conjunction with KKBNA, Inc. and Lohan Associates to act as the geotechnical consultant for a proposed office building to be constructed in upstate New York. The building location was to be located over a peat bog buried beneath old surface fill. The design height was to be four stories with a basement, covering approximately 32,500 square feet with column base sizes of 30 feet by 30 feet. The estimated maximum interior column loads ranged from 800 to 1000 kips and the exterior maximum column loads ranged from 550 to 700 kips.

Because of pollutants in the surface fill and the fear of groundwater contamination if deep foundations were used which would puncture the clay aquaclude underlying the organic deposit, only shallow foundation solutions could be considered.

SITE HISTORY

A history of the project area was developed indicating that the site was, at one time, occupied by a chrome tannery plant with operations dating back to the early 1900's. According to early drawings of the site, it appeared that the majority of the area was occupied by hide houses, tannery buildings, small storage sheds and above grade storage tanks. The hide houses were constructed in 1910 and many of the storage buildings were constructed in the 1930's. At the time of the soil boring exploration program for the current structure, no buildings were standing on the site. However, there were remnants of floor slabs and foundation walls throughout. It was discovered from discussions with local people that the buildings were supported on relatively shallow spread footing foundations and that no deep foundation systems had been used on the site. It was also determined that the practice existed at one time of covering the tannery waste in the storage pits with clay fill to minimize odors.

SUBSURFACE CONDITIONS

Analysis of the geologic activity in the region indicated a thick stratum of outwash sand and gravel deposited by glacial stream channels overlying till and bedrock at a depth of about 65 feet. Following deposition of the outwash, it appeared that a channel flowing roughly in a north-south direction was eroded in the outwash by a tributary of a nearby river. This channel appears to have been naturally dammed giving rise to a quiet depositional environment in which clay and silt were laid down. The clay is discontinuous and appears to have been breached by a rejuvenated stream which resulted in deposition of coarse grained alluvial sand and silt. In more recent geologic time, organic soil accumulated in a swampy environment associated with the channel. Aside from this, shallow and deep deposits of fill, associated with the old tannery, were found at various locations.

Fortunately, although organic deposits and peat bogs can vary widely in their physical and chemical properties, depending upon the percent of organic matter and water content, at this site the organic deposit was generally fine grained and contained significant percentages of nonorganic solids. The thickness of the deposit ranged from 0 to 25 feet in the building location and typical water contents were on the order of 100 percent. Due to the age of the tannery plant, it was assumed that the organic deposit had been consolidating under the weight of 10 to 15 feet of fill that had been in place for approximately 80 years. Therefore, the scope of this study was limited to the less compressible end of the organic deposit range and also to a deposit that had been subject to significant preconsolidation. A typical soil profile through the building site is shown on Figure 1 and the range of thickness of peat below the foundation is shown in Figure 2.

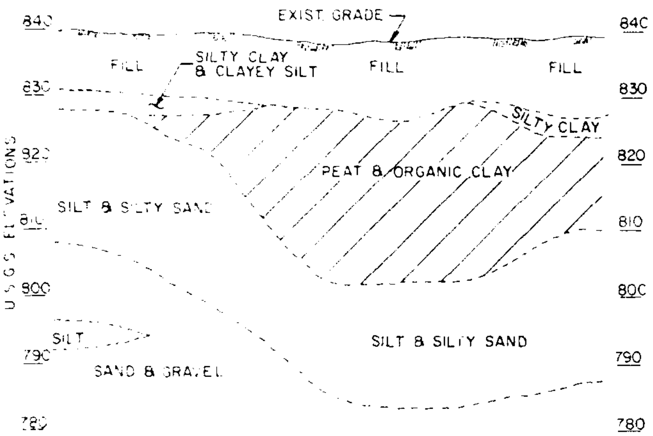

Fig. 1 Typical Soil Profile

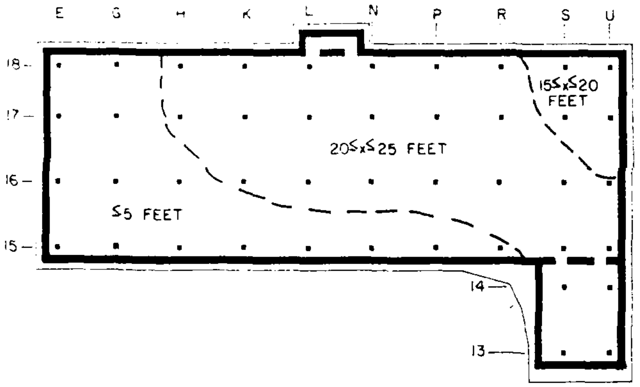

Fig. 2 Peat Thickness Below the Foundation

LABORATORY AND FIELD TESTING PROGRAM

The testing program consisted of performing water content, density, unconfined compressive strength, organic content, Atterberg Limits, consolidation tests and grain size distribution tests on representative soil samples. In addition, in-situ pressuremeter tests were performed to obtain information on the deformation properties of the organic soils in-situ. Average values for the peat are shown on Table 1.

Table 1
Average Values for the Peat

Water Content: 92% (range 64%-146%, 26 samples)
Dry Density: 50 pcf (range 19 pcf-89 pcf, 23 samples)
Unconfined Compressive Strength: 0.54 tsf (range 0.1 tsf-1.0 tsf, 23 samples)
Organic Content: 6.2% (range 2.6%-13.1%, 23 samples)
Atterberg Limits - LL: 73 (range 44-112, 6 samples)
PI: 18 (range 14-24, 5 samples)
Grain Size Distribution
.002mm : 15% passing (range 10%-21%, 5 samples)
.005mm : 23% passing (range 16%-34%, 5 samples)
#200 sieve : 80% passing (range 72%-99%, 5 samples)
#10 sieve : 98% passing (range 94%-100%, 5 samples)
#4 sieve : 100% passing (range 99%-100%, 5 samples)
Consolidation Test Results-Standard Method
P_c : 0.81 tsf (range 0.67 tsf-0.95 tsf, 2 samples)
C_c : 1.8 (range 0.8-3.57, 2 samples)
C_r : 0.15 (range 0.1-0.2, 2 samples)
Pressuremeter Test Results
P_f : 1.5 tsf (range 1.3 tsf-1.7 tsf, 3 tests)
P_1 : 2.8 tsf (range 2.5 tsf-3.0 tsf, 3 tests)
E_d : 25 tsf (range 21 tsf-32 tsf, 3 tests)
E+: 36 tsf (range 31 tsf-45 tsf, 3 tests)

Since anticipated settlement of the organic soils was of primary interest, two types of consolidation tests were performed. The standard consolidation test using a load increment ratio of one and a 24 hour loading sequence was performed, as well as second type of test in which the anticipated design loading condition was placed directly on the sample and left there for the duration of the test.

Initial analysis of the standard consolidation test data did not indicate anything unusual. The deposit appeared to be fully consolidated under the current overburden. The estimated preconsolidation pressure was approximately equal to the calculated overburden pressure. In addition, the time settlement curves showed fairly normal S or C type curves.

In the more unconventional single load long-term test, the results showed signs of A steepening in the slope of the secondary compression curve at about 10,000 minutes. The results of this test are shown in Figure 3.

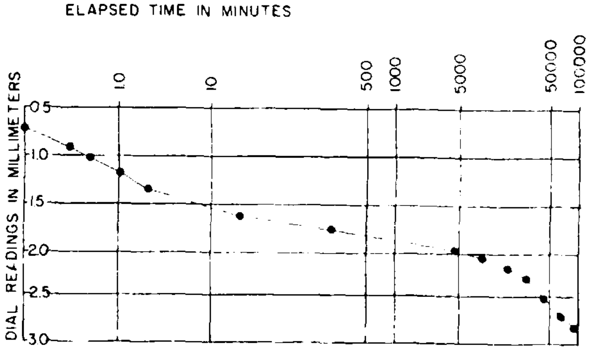

Fig. 3 Single Load Consolidation Test

STRUCTURAL DESIGN CONSIDERATIONS

The project consisted of two L-shaped building facing each other to embrace a well landscaped court, with a bridge link at each end of the building. Because of site limitations, one building (Building A) was located on natural, medium dense granular soils, while the other (Building B) was resting on the deep organic deposit.

Structurally, the floor was concrete fill on composite metal deck supported by composite beams and steel columns. The lateral loads were resisted by the frames. The decision to use this system was based on a cost comparison of many concrete and steel floor framing schemes.

During the foundation analysis, the deep foundation alternative was eliminated to avoid penetration through the underlying aquaclude. In addition, the construction schedule could not allow for removing and replacing over 35, 000 cubic yards of organic material. Therefore, the mat foundation became the apparent solution for Building B and conventional spread footings were used for Building A.

Two major structural problems had to be resolved:

1. How to maintain a stable floor elevation, especially at bridge links between the two buildings, and

2. How to eliminate or minimize the stress induced to the steel moment frames above by the foundation movement (or differential movement).

A mat foundation on top of the organic soil would cause large initial and continual long term (over 50 years) settlements. These large settlements are difficult to predict with the accuracy desired by the architect and structural engineer. To solve these problems, the following steps were undertaken:

A. To maintain a stable building elevation after construction:

A full basement was proposed under Building B, even though the project required only a partial basement for mechanical equipment. The basement was designed to be water tight and was utilized as a floating foundation. It was placed at a calculated depth to balance the weight of the excavated soil and the total weight of the proposed building and its foundation, plus 100% of the superimposed dead loads and 10% of the live loads (the design live load was 80 psf). The anticipated initial settlement due to future transient live load was acceptable.

B. To control the elevation of Building B during construction and to minimize the effects of heave from excavation of the organic deposit and the time required for reconsolidation:

Water was poured into the basement as soon as the basement slab and walls were completed. The amount of water was equal to the weight of the superstructure plus 10% of the live load. It was intended to start the reconsolidation as early as possible so that it could reach a stable condition by the time all floors were installed. Immediately after each floor was completed, the same amount of water by weight was pumped out from the basement to avoid any over consolidation.

Because the organic deposit was not at a uniform depth beneath the building, the reconsolidation was not uniform. In fact, a maximum of 1-3/4" differential settlement was estimated. In order to maintain all floors level, extra long anchor bolts were installed under each steel column with double nuts for adjustments. Adjustments were not made until just before the moment frames were connected together.

C. To avoid or to minimize initial stress in the moment frames caused by the differential settlements:

During the steel erection, all beams to column connections were partially tightened initially. Surveys were made monthly to determine the rate of increase in foundation settlement. Final column height adjustments and tightening of all loose bolts were made after the settlements were considered to be relatively stable.

SETTLEMENT ANALYSIS AND PREDICTION

Since the design concept was based on setting grades such that the weight of the excavated soil was equal to or greater than the total weight of the proposed building including the weight of the planned mat foundation, it was planned that settlements would be limited to reconsolidation of any rebound occurring during excavation for the mat foundation plus continuing long-term secondary compression. Using both the consolidation test data and the pressuremeter test data, calculations were made for the predicted rebound and resettlement under building load. These calculations indicated rebound and resettlement of just over 4 inches.

Based upon past experience of rebound being less than predicted, a heave and resettlement of 3 inches was predicted where the organic deposit was greater than 20 feet, with an additional long-term settlement of 3 inches over the next 50 years as a result of continuing secondary compression. Initially, this 3 inch settlement prediction was based on extrapolation of the straight line portion of the secondary compression line on the long-term load test. However, as the long-term load test results continued to be obtained, a disconcerting trend of ever steepening slope on the secondary compression line was noted. Extension of this slope would result in substantially increased settlement at 50 years. However, if it were assumed that the real current starting point should be the 80 year line so that the true settlement of interest would be the time frame of 80 years to 130 years, the predicted 50 year settlement is only 3 inches. Thus, the 50 year prediction for secondary compression was maintained at a maximum of 3 inches.

CONSTRUCTION INSTRUMENTATION AND PERFORMANCE

In order to monitor building performance, 7 heave markers were installed prior to excavation. These consisted of concrete plugs with slightly protruding steel bars placed in large diameter boreholes to a level just below the planned mat excavation level. The boreholes were backfilled with a bright dye to facilitate finding the heavy markers after excavation. Despite precautions, some of the heave markers were destroyed during excavation.

Inclinometers were also installed just outside the perimeter of the planned excavation to monitor any lateral movements. Unfortunately, the contractor elected to use much steeper excavation slopes than recommended and a classic slope failure occurred destroying the inclinometers, indications of which can be seen in Figure 4 and 5.

After excavation and prior to mat construction, several pore pressure measuring units were installed so that pore pressure build up could be observed and pore dissipation monitored during building construction. Typical results as compared to the vertical movements measured by the heave markers are shown on Figure 6.

Surveys of elevations at the top of all concrete piers were made at the time when the basement was completed; at the time the basement was filled with water, and monthly afterward. The building elevation reached reasonably stable conditions after the third floor steel and metal deck were installed. Column adjustments and final tightening of connections were made at that time.

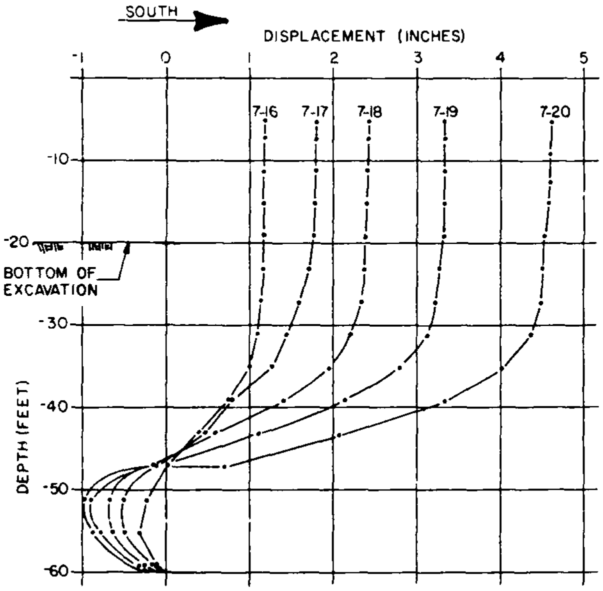

Fig. 4 Inclinometer Movement. North Side

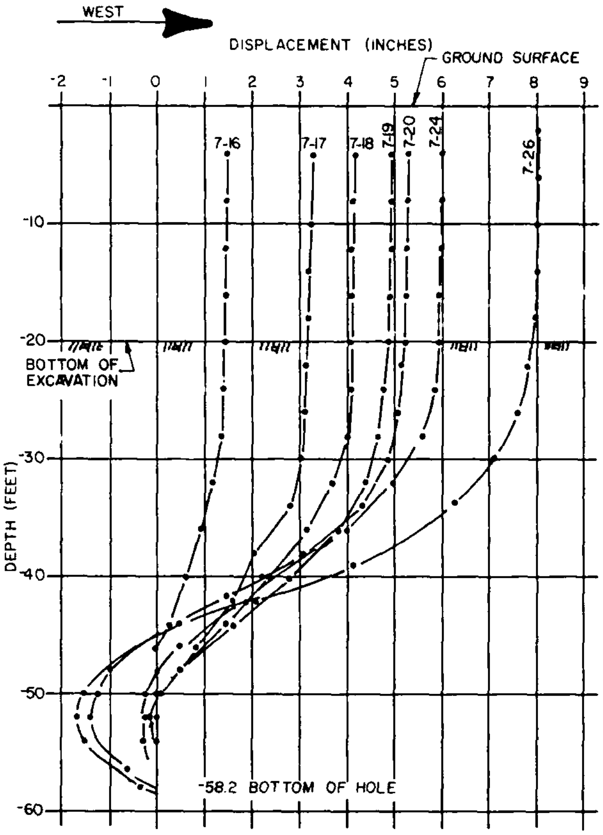

Fig. 5 Inclinometer Movement. East Side

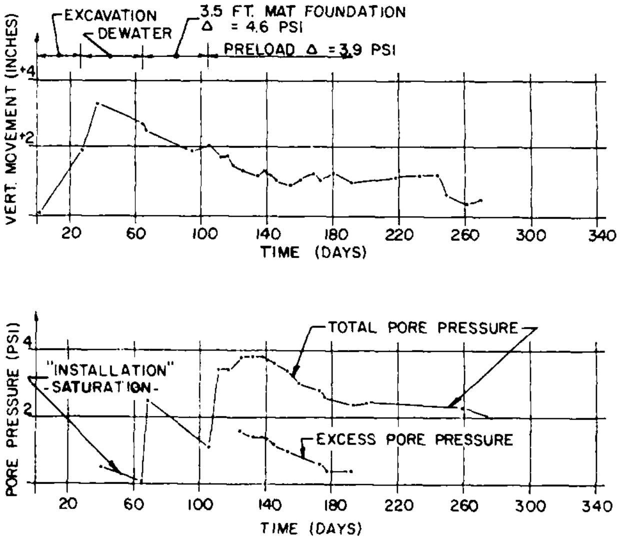

Fig. 6 Typical Heave Marker and Pore Pressure Results

COMPARISON OF PREDICTION AND PERFORMANCE

The comparison of prediction and performance up to 5 months following building completion was remarkably close considering the nature of organic soil. Representative heave markers heaved approximately 3 inches and reconsolidation under a full building load (actual average load of about 1200 pounds per square foot) was also in the 2 to 3 inch range where the organic deposit was thickest.

There were two exceptions to this general performance. The first occurred at the northeast corner of the building where a major slide had taken place during excavation. At this corner there was a sharp increase in settlement during the water loading stage to a point where it appeared that active bearing capacity failure was occurring. In order to decrease the load at that corner, it was necessary to excavate a portion of the backfill placed against the basement walls and replace the heavy backfill with light weight fill. When this operation was completed, the rapid increase in the rate of settlement in the corner decreased to the same rate as the rest of the mat over comparable organic soil thickness. It appeared that the slope failure had so weakened the organic soil as to create the observed rapid settlement phenomenon.

The other anomaly was at the southeast corner of the building where the observed settlement was moderately greater than predicted but where there was not the excess of backfill surcharge. However, a major sump pit and pump had been located at this corner and it is believed that dewatering occurring at this corner may have created additional consolidation effects.

Predicting how long primary consolidation should take was difficult because of significant variations in the laboratory results. The time for 100 percent primary consolidation varied from less than 1 minute to more than 10 minutes. Thus, calculations of 80 percent primary consolidation occurred in time frames ranging from weeks to months. A best guess was made during construction that 80 percent pore pressure dissipation occurred within a two month period. Interpretation of the data was difficult because dewatering was going on during initial mat construction and initial pore pressure observation readings. At first, pumping was going on out of two separate pits. Once the mat and building walls were constructed, pumping on the north side of the building stopped but continued for a while on the south side. Thus, there was a tendency for the water table to build up on the north side of the building and the pore pressure readings rose independent of any building load increase.

During the months following construction, estimates of the actual secondary compression settlement were difficult since 100 percent primary consolidation had not fully occurred and the magnitude of settlement over that time had been within the up and down accuracy of the surveyors. However, it would appear that secondary compression was occurring at a rate no greater than predicted.

CONCLUSIONS

From the data presented herein, it can be concluded that heave and resettlement can reasonably, but conservatively, be predicted in organic soils using consolidation or pressuremeter theory as long as the preconsolidation pressure in the soil is not exceeded. Furthermore, the secondary compression in organic soil does not appear to plot as a consistent straight line on a semi-log plot but rather as an initial straight line followed by a suddenly increasing slope after 2 to 4 weeks followed by a decrease again after an extended period of 6 months to a year on a laboratory 1 inch sample. Finally, the importance of long-term measurements in the laboratory and in the field must be stressed as it is necessary to determine if there are universal relationships that can be applied to the specific organic soils at a given project site.

ACKNOWLEDGMENTS

The authors would like to acknowledge and express appreciation for the assistance of Mr. Richard Caplan of Lohan Associates in Chicago, Illinois in preparation of this paper.

Proceedings: Second International Conference on Case Histories in Geotechnical Engineering, June 1-5, 1988, St. Louis, Mo., Paper No. 6.64

Differential Settlement of Nuclear Power Plant Foundations

M.R. Lewis
Engineering Supervisor, Geotechnical Services, Bechtel Civil, Inc., Gaithersburg, Maryland

C.L. Weaver
Civil Group Supervisor, Bechtel Eastern Power Company, Palm Beach Gardens, Florida

J.R. Davie
Engineering Supervisor, Geotechnical Services, Bechtel Civil, Inc., Gaithersburg, Maryland

SYNPOSIS: A rational approach is presented for evaluating differential settlement of structures at nuclear power plants where settlement monitoring and the associated documentation are important. In nuclear plants, allowable differential settlement is governed by the necessity to prevent architectural and structural damage, equipment malfunction, touching of adjacent buildings during an earthquake, and damage to buried utilities. Measurements of actual settlement of the plant should be taken on a regular basis from start of construction and compared with the allowable values. A description is given of methods for calculating allowable values for differential settlements, and a comprehensive program for obtaining actual settlement data at a nuclear site is outlined. The ratio of measured to allowable differential settlement at which remedial action may be required is discussed.

A case history of differential settlements at a nuclear plant is presented. The settlement patterns exhibited by the major structures can be correlated with foundation conditions at the plant site. Measured differential settlements are small, generally less than 0.25 inch, compared with values of allowable differential settlement which are mainly greater than 0.75 inch.

INTRODUCTION

Predicted settlements for structures are required for a number of reasons. Chiefly, the engineer needs assurance that each structure is stable and can function properly within the predicted settlement range for its design life. Since predicted settlement is a function of the foundation configuration, depth, loading and soils, it generally bears little relationship to the allowable settlement, which is a measure of the settlement the structure can tolerate before damage in one form or another is incurred. For safety-related (Category I) structures, allowable and measured settlement should be compared to ascertain what margin of safety exists, and if remedial action is required. Since settlement monitoring of foundations for safety-related structures at nuclear plants is a requirement, then the main task is to be able to compute allowable differential settlements.

This paper attempts to set forth methods and criteria for determining allowable differential settlements at nuclear plants and describes a program for the regular monitoring of settlement markers to obtain actual differential settlment values. A case history is presented.

ALLOWABLE DIFFERENTIAL SETTLEMENT

In nuclear power plants, allowable differential settlement is governed by the necessity to prevent:

- Architectural or structural damage or equipment malfunction
- Adjacent buildings touching during an earthquake
- Damage to utilities between adjacent buildings and utilities entering buildings from the soil

Architectural or Structural Damage

Three situations resulting from differential settlement are considered under this heading, namely: damage to the base or frame of the structure; damage to the cladding or paneling of the structure; and equipment malfunction. Although these three situations are perhaps the most obvious consequences of differential settlement, they are also the most difficult to define in quantitative terms since each building or piece of equipment will respond in a different manner to differential settlement.

For safety-related structures in nuclear plants, the range of tolerable settlements is in line with industry standards for well-engineered structures, i.e, from 0.0015 to 0.003 radians of slope settlement profile (Navfac DM-7.1, 1982); this range covers structural damage and damage to cladding or paneling.

The most sensitive pieces of equipment in a nuclear plant are the reactor pressure vessel and the turbines. Construction tolerances for the pressure vessel can be less than 0.01 inch level difference over the base of the vessel. Turbines have traditionally presented foundation problems as a result of vibrations caused by out-of-balance forces which can develop during operation. Because of the very conservative standards adopted by equipment manufacturers, both the reactor pressure vessel and the turbines should be able to tolerate more differential settlement under operating conditions than is allowed during construction. However, actual values will depend on the equipment used.

Adjacent Buildings Touching

The situation of adjacent buildings touching during an earthquake arises where individual buildings are separated by only inches, as frequently occurs in the plant powerblock (usually incorporating the reactor, control, turbine and radwaste buildings). During an earthquake, the gap between adjacent buildings will widen and narrow as a function of ground movement. If the buildings have previously settled towards each other resulting in a narrowed gap between the top of the buildings, seismic movement may cause the buildings to make contact. The calculation procedure for allowable differential settlement under these conditions is demonstrated on Figure 1. Settlement values are calculated from the angle of rotation required to close one-half of the remaining gap after deducting the seismic movements of the two buildings from the original gap. For each building, allowable slopes along both axes need to be considered.

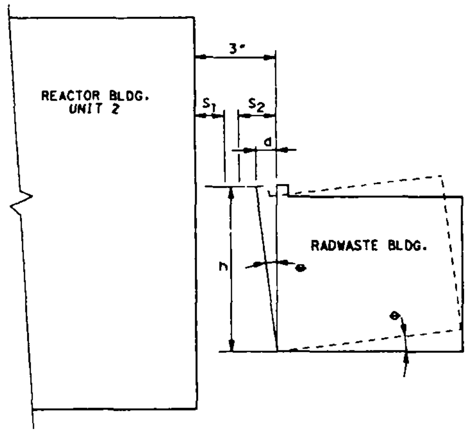

ALLOWABLE SLOPE $\theta = \frac{d}{h}$ (FOR SMALL ANGLES)

AND $d = \frac{3" - (S_1 + S_2)}{2}$

WHERE: θ = ALLOWABLE SLOPE OF THE BUILDING

d = ALLOWABLE HORIZONTAL COMPONENT OF TILT TOWARDS AN ADJACENT BUILDING

h = HEIGHT OF BUILDING

S_1 = SEISMIC DEFLECTION OF BUILDING AT TOP

S_2 = SEISMIC DEFLECTION OF ADJACENT BUILDING AT SAME ELEVATION

Fig. 1 Determination of Allowable Differential Settlement for the Case of Adjacent Buildings

Allowable settlement values calculated by the above method represent the worst case. In order to touch during an earthquake, differential settlement must be such that the buildings represented in Figure 1 lean towards each other, and both must reach or exceed the allowable tilt simultaneously. Thus, the fact that a building has reached the maximum allowable tilt value is only one necessary condition for touching to occur during an earthquake.

Utilities Damage

Buried piping can range from 8 to 15 percent of the total piping within a nuclear plant and can account for as much as 100,000 linear feet in the bigger units. The piping ranges from large-diameter lengths such as cooling water from the intake structure or steam to the turbines, to small diameter service piping. Since the piping system is basically the sole method of transporting vital materials within the plant, it is essential to ensure that overstressing and possible pipe fracturing does not occur under any circumstances. One potential cause of overstressing of the piping as it enters a structure (referred to as a "penetration") is movement of the structure relative to the penetration. This can take the form of differential settlement between structure and soil in cases of isolated structures, or differential settlement between adjacent structures. The amount of differential settlement each penetration can withstand before the pipe becomes overstressed is calculated from the allowable pipe stress criterion (ASME, 1977):

$$\frac{IM_D}{Z} \le 3.0\ S_c$$

where I = Stress intensification factor
Z = Pipe section modulus
M_D = Moment due to building settlement
S_c = Allowable stress in cold condition

In addition to the pipes themselves, pipe anchors and pipe supports must be considered; the moments and stresses due to building settlement must not exceed the anchor and support design moments and stresses. In many cases, the allowable moment in the anchor or pipe support will be the governing factor.

Once the critical moment is established for the penetration, the amount of building settlement which will produce this moment is computed. The authors' experience is that the bending moment and corresponding level of stress produced by actual differential settlement of nuclear plant structures on properly designed foundations is well below the critical overstressing level for most of the penetrations. Only in isolated cases where the penetration design is tailored to satisfy a particular requirement is overstressing liable to occur. The most feasible approach to calculating allowable building settlement, therefore, is to perform for each penetration simple hand computations of structure movement corresponding to the critical bending moment; these computations make simplifying assumptions which produce conservative results, i.e., the computations will indicate critical bending moments that are smaller than they would be in reality. Nevertheless, the settlements calculated by the simplified analysis will in most cases be considerably more than the predicted or measured settlement.

For the few cases where the allowable settlements computed by the simplified manual procedure are close to or less than the predicted or, in some cases, the measured structure settlements, more sophisticated analyses are used. These usually take the form of a computer solution, where factors such as anchor rigidity, assumed complete in the simplified procedure, is relaxed to a realistic level to produce a less conservative result. If this sophisticated analysis produces allowable settlements still less than the measured or predicted settlements, a design to include possible remedial measures is the next step. In most cases, a simple modification to the existing design will increase the allowable settlement to a suitable level. Generally, a change of position or detail change in design of an anchor or support will suffice. It should be noted, however, that any change in the design of one part of a piping system will usually entail re-analysis of the whole system affected by the modified part; this may include reanalyzing the system for seismic effects as well as static loading.

In summary, the steps involved in estimating and dealing with the allowable differential structure settlement with respect to each pipe penetration are:

1. Determine the bending moments in pipe, anchors and supports corresponding to allowable stress.
2. Determine which part of the system is critical.
3. Compute the building settlement required to cause critical bending moment using simplified conservative manual procedures.
4. For penetration where settlement established by 3 is too small, employ more sophisticated analyses using less conservative parameters.
5. For penetrations where settlement established by 4 is too small, consider design of remedial measures.

MEASUREMENT OF DIFFERENTIAL SETTLEMENT

Before the start of construction of a nuclear plant, the location of settlement markers should be carefully planned to optimize the amount of information obtained from the measurement program. Markers should be set at the four corners and at the center of each structure. Additional markers may be required where spacing between markers is much more than 100 feet. This placement program will enable detection of overall tilt or localized sag of the structure; the center marker should also give an indication of the structure rigidity. The markers should be set into the top of the foundation mat as soon as feasible after the mat is poured. Since readings will be taken with conventional surveying equipment, it will be advantageous to make the marker points as accessible as possible. Where the top of the foundation mat becomes difficult to reach after construction of additional floors, e.g., where the foundations are placed in deep excavations, then it may be advisable to transfer the markers to an elevation near ground level. The inaccuracies involved with transfer of the settlement marker, and the differences in settlement measured above the building base compared with at the base, will probably be less than the inaccuracies generated by trying to survey points at inaccessible locations. It is important that any change in marker location or elevation, even if it involves only a slight modification of the marker itself, be fully documented.

Measurement Across Structures

The maximum differential settlement across structures must be measured as a basis of comparison with allowable differential settlement established from structural or architectural damage criteria, equipment malfunction, or adjacent buildings touching during an earthquake. It is important to ascertain the reference dates of the markers, i.e., the date after which differential settlement will affect the performance of the structure or equipment. In other words, the amount of differential movement that has occurred before, say, the turbines are installed, will not affect the turbine operation since the turbines will be leveled during installation. Similarly, any differential movement that occurs before construction of the upper floors of the taller structures will be compensated, since each wall will be plumbed during construction. At the end of construction the gap between the buildings will be as specified, regardless of what movement has already occurred. Thus, differential settlements of the markers will normally be measured with reference to the date of equipment installation or structure completion, not to the date of marker installation.

As discussed previously, a minimum or limiting allowable differential settlement, corresponding to a governing factor such as equipment malfunction, can be calculated for each axis of each building. An additional factor, namely the reference date for measuring this movement must also be considered. For example, the limiting allowable settlement may be 0.5 inch between markers on the north and south ends of the turbine structure, established to prevent the turbine building and adjacent reactor building touching during an earthquake. The differential settlement between north and south ends allowed with respect to satisfactory performance of the turbine is, say, 0.75 inch. However, if the turbines were installed 12 months before completion of the reactor building, then the reference date for turbine operation criterion would be 12 months earlier than for the building touching factor. It must now be established whether more or less than 0.25 inch of north-south differential settlement occurred within these 12 months. If less occurred, the 0.5 inch allowable to prevent the buildings touching still governs; if more occurred, the allowable settlement of the turbines will now be the governing factor.

Measurement of Penetration Settlement

The maximum differential settlement between structures must be measured as a basis of comparison with allowable differential settlements established for penetrations between structures. The penetration locations will not necessarily be close to the settlement markers. It should be sufficient, however, to assume that the movement of the penetrations will be similar to the movement of the nearest marker. Again, it is critical to establish the completion date of the penetration. It is common to install the penetrations during construction of the basement walls prior to backfilling but to wait until nearer plant completion before anchoring the penetrations. Therefore, completion of penetrations can occur over a wide time range.

For movements of penetrations entering buildings from the soil (as opposed to entering from an adjacent building) it is again sufficient to assume that the movement of each penetration is similar to that of the nearest marker. In these cases, only one marker has to be considered instead of two markers for penetrations between buildings. As with other penetrations, it is essential to establish the date on which the penetrations were completed. For all of the penetrations, the structure settlement in question does not have to be differential across the structure since a uniform settlement will produce the same stresses in the pipes and anchors.

In calculating the allowable differential settlement between penetration and soil, it is usual to assume that the soil adjacent to the building is unaffected by the pipe settlement. In fact, some settlement of the soil in the direction of the pipe settlement will occur, especially the soil immediately adjacent to the building. If no soil settlement is assumed, a larger than actual differential settlement between building and soil will be recorded. It may be possible to detect movement of the soil surface adjacent to the building; however, movements will be so small and the soil surface so irregular that measurement may be precluded. In any case, some allowance should be made for soil settlement in order to reduce the amount of conservatism to realistic levels.

REMEDIAL ACTION

During plant design, if predicted differential movements exceed allowable values, then design modifications are made. If, during plant operation, the ratio of measured to allowable differential settlement approaches unity, then some form of remedial action must be considered. Considerable judgment is called for in deciding when and what kind of action is necessary. In this respect, the trend of settlement versus time is most important. This trend will be a function of the foundation type and the foundation soil. For shallow foundations in mainly granular soil, most of the settlement will occur during construction; in clays, consolidation settlement may occur steadily for months or years after construction is completed. Thus, in sands, if the ratio of measured to allowable differential settlement is, say 40 percent after construction, it is very possible that the ratio will never reach much more than 50 percent. On the other hand, if the ratio in clays is 40 percent immediately after construction and reaches 60 percent 3 months after construction, serious consideration should be given to making plans for remedial action in the near future. In any case, under all conditions, if the ratio of measured to allowable differential settlement exceeds about 75%, an engineering investigation should be undertaken. Similarly, if the rate of settlement of a marker begins to consistently increase over a period of several months, the cause should be examined. It is important, therefore, that measured settlement data be plotted on a settlement versus time chart as it is accumulated, and that the chart be reviewed regularly by a geotechnical engineer familiar with the foundation design and subsurface conditions to determine if any action is required.

CASE STUDY

To illustrate an example of differential settlement computation and marker measurement, the differential movement history of the foundations of a nuclear power plant in the southeastern portion of the United States will be described and discussed.

The plant has two units, each having a capacity of approximately 600 MW. The settlement study examined the Unit 2 reactor, turbine, control and radwaste buildings in the powerblock area, and the intake structure, diesel generator building, and main stack outside the powerblock area. For this case study, only the powerblock area will be considered.

The powerblock area is shown in plan view in Figure 2. All of the structures considered were either seismic Category I or related structures. The settlement study entailed computing the minimum or limiting allowable differential settlement of each structure and comparing this with measured values of settlement.

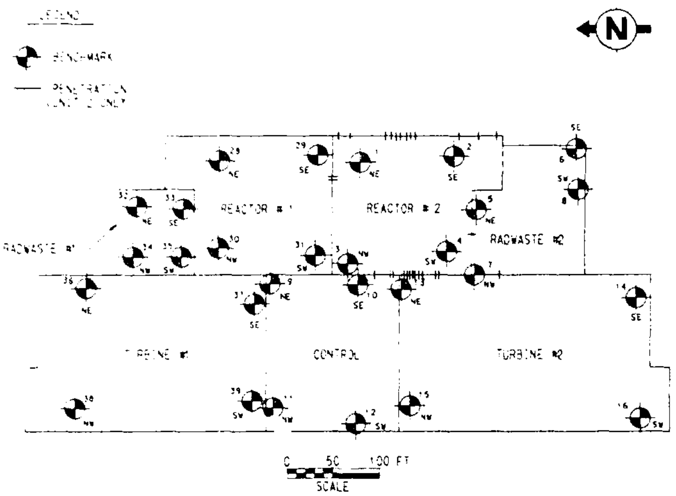
LEGEND
BENCHMARK
PENETRATION (UNIT 2 ONLY)
N
REACTOR # 1
REACTOR # 2
RADWASTE #1
RADWASTE #2
TURBINE #1
CONTROL
TURBINE #2
NE
SE
SW
NW
0 50 100 FT
SCALE

Fig. 2 Plan of Powerblock Area

Foundation Conditions

The site topography prior to construction was gently rolling, with elevations ranging from about 125 to 145 feet MSL with a finished plant grade of 129 feet MSL. The plant site is part of the Atlantic Coastal Plain physiographic province. Relatively unconsolidated materials at the site extend approximately 4,000 feet to a basaltic basement rock of pre-Cretaceous age. No structural features offset the material underlying the site nor do any major or minor fault zones exist near the site.

In the powerblock area, the predominant foundation soils are medium dense to very dense clayey fine sands, extending to about zero elevation; clay layers are found throughout much of the stratum and the sand is partially cemented between about Els. 120 and 75 feet MSL. Hard silty clays exist below the clayey sand. The powerblock structures are built on mat foundations, the deepest being that of the reactor at El. 74 feet MSL. A subsurface profile through a portion of the powerblock structures is shown in Figure 3.

Two distinct water levels exist within the upper formations. The upper (unconfined) level is a "perched" water table which roughly parallels the surface topographhy running 5 to 20 feet below the ground surface. The lower (confined) aquifer exists below about El. 110 feet; the natural potentiometric surface in this aquifer is around El. 70 feet in the powerblock area.

Predicted Settlements

The predicted settlement was computed using an equation based on elastic theory (Bowles, 1968) with an average elastic modulus value. This modulus was estimated from laboratory unconsolidated undrained (UU) and consolidated undrained (CU) triaxial shear tests and also from field standard penetration test N-values. The foundation soils were modeled as one layer with a single modulus value, resting on a rigid base. Total settlements of the reactor buildings for Units 1 and 2 were predicted at about 2.5 inches. Predicted or estimated differential settlements were on the order of 0.75 to 1 inch.

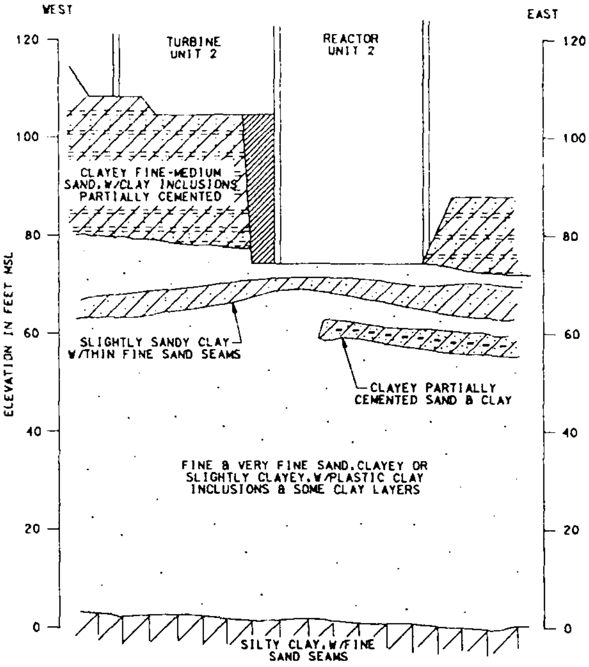
WEST
EAST
TURBINE UNIT 2
REACTOR UNIT 2
120
100
80
60
40
20
0
ELEVATION IN FEET MSL
CLAYEY FINE-MEDIUM SAND, W/CLAY INCLUSIONS PARTIALLY CEMENTED
SLIGHTLY SANDY CLAY W/THIN FINE SAND SEAMS
CLAYEY PARTIALLY CEMENTED SAND & CLAY
FINE & VERY FINE SAND, CLAYEY OR SLIGHTLY CLAYEY, W/PLASTIC CLAY INCLUSIONS & SOME CLAY LAYERS
SILTY CLAY, W/FINE SAND SEAMS

Fig. 3 Typical Subsurface Conditions

Allowable and Measured Differential Settlements

Allowable differential settlements (tilt) across and between structures were computed by the methods explained previously. Table 1 summarizes the differential settlements allowed across each structure in each direction. Prevention of buildings touching during an earthquake governs allowable tilt in the powerblock area. Outside the powerblock area, the allowable tilt is limited by structural and architectural considerations. Computation of the amount of tilt tolerable to installed equipment was beyond the scope of this paper. Table 2 shows the differential settlements allowable for penetrations between Unit 2 reactor and turbine buildings. Similar calculations were made for penetrations between other buildings in the powerblock, and between buildings and the soil. For the majority of the penetrations, the anchor system governs the amount of settlement allowed. A summary of the critical differential settlements between adjacent powerblock buildings and between buildings and soil are shown on Table 3.

The locations of the settlement markers are shown in Figure 2. In some cases, the original markers were preserved. In other instances, the markers had to be transferred to make them accessible as construction proceeded. Sometimes the location of the marker was preserved, but the original bolt had to be replaced, resulting in a small change of levels. The elevations of the markers were normally recorded once a month, but sometimes at longer intervals. Note that settlement markers could not be placed at the center of each structure; thus, no record is available of possible center sag and its relation to structure rigidity.

TABLE I. Summary of Differential Settlements Across Structures

Structure	Reference Date	Direction Of Tilt	Between Benchmark Numbers	Differential Settlement Inches Allowable	Differential Settlement Inches Measured	Ratio Of Measured To Allowable Percent
Reactor	5-76	N-S	1 and 2	0.40	0.01	3
Building		N-S	3 and 4	0.41	0.02	6
Unit No. 2		E-W	1 and 3	1.67	0.12	9
		E-W	2 and 4	1.61	0.11	7
Radwaste	10-75	N-S	5 and 6	1.85	0.30	16
Building		N-S	7 and 8	1.92	0.30	16
Unit No. 2		E-W	5 and 7	1.58	0.02	2
		E-W	6 and 8	0.96	0.02	3
Control	1-75	N-S	9 and 10	1.00	0.07	7
Building		N-S	11 and 12	0.95	0.16	16
		E-W	9 and 11	3.01	0.23	8
		E-W	10 and 12	3.46	0.14	4
Turbine	5-76	N-S	13 and 14	2.69	0.22	8
Building		N-S	15 and 16	2.46	0.34	14
Unit No. 2		E-W	13 and 15	2.96	0.22	7
		E-W	14 and 16	3.37	0.13	3

TABLE II. Summary of Penetration Differential Settlements
Reactor Building Unit 2 and Turbine Building Unit 2

Penetration	Reference Date	Nearest Benchmark Numbers	Differential Settlement - Inches Measured to Date	Differential Settlement - Inches Allowable Pipe	Differential Settlement - Inches Allowable Anchor	Ratio of Measured to Allowable Percent Pipe	Ratio of Measured to Allowable Percent Anchor
10 in. No. 43	5-78	4 and 13	0.08	2.12	1.68	4	5
4 in. No. 44	1-78	4 and 13	0.06	1.30	--	5	--
3 in. No. 57	11-77	4 and 13	0.08	4.17	--	2	--
18 in. No. 57	7-77	4 and 13	0.07	9.55	1.59	1	5
24 in. No. 57 (El. 154.46)	9-76	4 and 13	0.19	25.13	10.59	1	2
24 in. No. 57 (El. 154.55)	9-76	4 and 13	0.19	22.54	9.05	1	2
8 in. No. 84	2-77	4 and 13	0.10	1.13	1.01	8	10
10 in. No. 90	1-78	4 and 13	0.06	2.51	1.77	2	3
3 in. No. 92	12-77	4 and 13	0.04	1.78	1.55	2	2

Figures 4 and 5 show the marker settlement profiles for the Unit 1 and 2 reactor buildings, respectively, from the start of construction to the present. After about June 1977, the general downward settlement trend ceased with no measurable movement taking place. The slight cyclic movements taking place are probably due to the inherent variations associated with optical surveying, including seasonal variation with temperature. A similar pattern was noted for the other buildings.

A comparison of calculated allowable and actual measured differential settlements is also included in Tables 1 through 3. For tilt of the buildings, the ratio of allowable to measured settlement is less than 20 percent in all cases. Since present trends (see Figures 4 and 5) indicate only a small increase, if any, in settlement values, there

TABLE III. Summary of Critical Differential Settlements Between Adjacent Structures and Structures and Soil

Structure to Structure	Reference Date	Nearest Benchmark Numbers	Differential Settlement Inches Allowable	Differential Settlement Inches Measured	Measured to Allowable Percent
Reactor 2 to Turbine 2	2-77	4 and 13	1.01	0.10	10
Reactor 2 to Control	1-78	3 and 10	0.62	0.20	32
Reactor 2 to Radwaste 2	11-77	2 and 5	1.07	0.11	10
	2-77	4 and 5	0.88	0.05	6
Reactor 2 to Reactor 1	1-78	1 and 29	0.53	0.05	9
Reactor 2 to Soil	1-78	1	0.72	0.11	15
	1-78	2	0.56	0.18	32

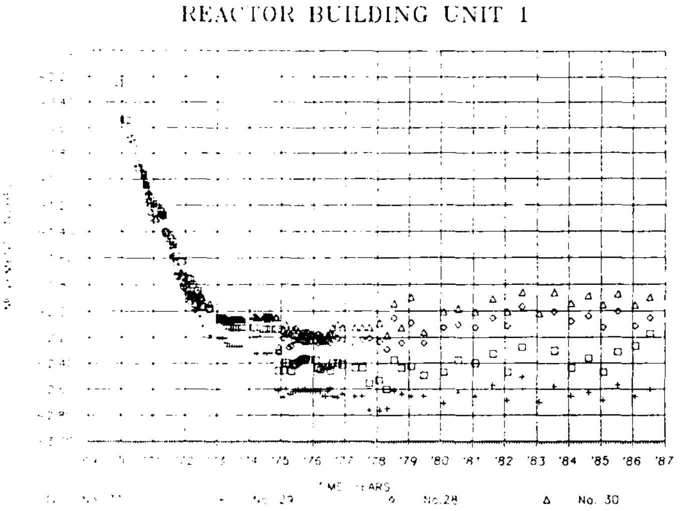

Fig. 4 Reactor Building Settlement - Unit 1

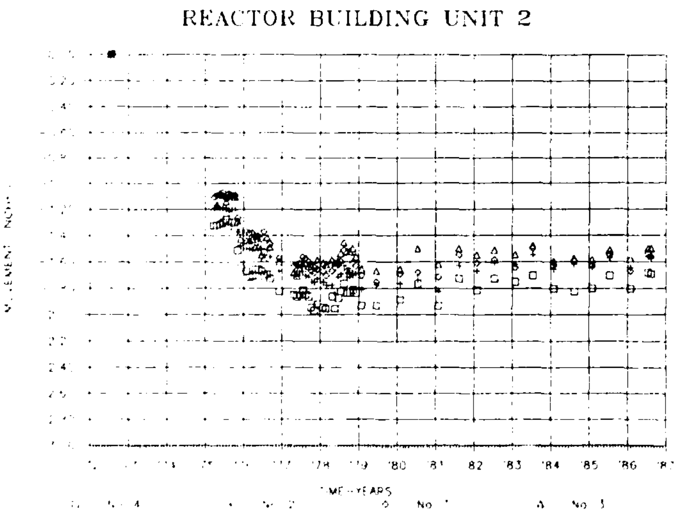

Fig. 5 Reactor Building Settlement - Unit 2

seems to be no cause for concern regarding tilt, either now or in the future. For penetration differential settlements, the ratio of allowable to measured differential settlement in the majority of cases is less than 20 percent.

Discussion

The case studied provides reassuring results concerning the settlement characteristics and trends at a major nuclear plant. The plant rests on mat foundations on dense clayey sands. Due to these foundation conditions, measured differential settlements are much less than the computed allowable settlements in almost all cases. Assuming present settlement trends continue, there appears to be little chance that structures or penetrations will become overstressed due to differential settlement within the lifetime of the plant. However the study revealed a number of points regarding the design of the plant and the existing settlement monitoring program.

First, the differential settlement modes described in this paper were not specifically taken into account in the design of either the structure or the penetrations. Although predicted differential settlement values were provided by the geotechnical consulting engineer during the plant design, allowable differential settlements were not computed.

Second, there was a lack of consistency in the time of placement of the settlement markers in relation to construction. For most of the structures, the markers were placed in the foundation mat; in some cases, however, markers were placed several floors above the foundation. Comparison of settlement of structures was difficult in these cases.

And third, although marker data were recorded and documented monthly, no backup information was provided. A most useful addition for reviewing and analyzing the marker movements would have been a record of the construction phase and activities at the time of measurement. An attempt could then have been made to correlate settlements with events such as start of excavation for adjacent foundations, end of construction dewatering, etc.

CONCLUSIONS AND RECOMMENDATIONS

This paper has described procedures for obtaining values of allowable differential settlement at a nuclear plant and for measuring actual settlements on a regular basis. A case history of differential settlement at an existing nuclear plant has been presented. The following recommendations are made concerning computation and measurement of differential settlement at nuclear power plants:

(1) During plant design, in addition to predicting differential settlements of major structures, computations should be made of the allowable differential settlement governed by architectural and structural considerations, equipment design, touching of buildings during an earthquake, and overstressing of penetrations.

(2) Prior to plant construction, a detailed plan should be developed to place settlement markers in the foundation mats of the major structures. As a minimum requirement, there should be markers at the corners and centers of each structure.

(3) During and after plant construction, the settlement markers should be monitored on a monthly basis. The monthly report should contain all relevant information on construction activities relating to the major structures. The settlement data should be plotted versus time, and then reviewed by a geotechnical engineer who is familiar with the foundation design and subsurface conditions. Whenever differential settlement at a marker consistently accelerates over a period of months, or measured differential settlement reaches 75 percent of the allowable value, an engineering investigation should be performed to find the causes of settlement and if remedial action is necessary.

REFERENCES

ASME Boiler and Pressure Vessel Code (1977), Section 3, Nuclear Power Plant Components, NC-3652.3(b).

Bowles, J.E. (1968) Foundation Analysis and Design, McGraw-Hill, Inc., New York.

NAVFAC DM-7 (1982), Department of the Navy, NAVFAC Facilities Engineering Command.

Proceedings: Second International Conference on Case Histories in Geotechnical Engineering, June 1-5, 1988, St. Louis, Mo., Paper No. 6.67

Reconstruction of the Settlement History of Buildings

G. Hannink
Project-engineer, Delft Geotechnics, Delft, The Netherlands

SYNOPSIS: Although it is a well-known fact that buildings can settle, it is often not known how much settlement has occurred since the construction. Three case studies in the Netherlands are presented which deal with the following questions: has the settlement process stopped or is it continuing and if so, what settlements can still be expected in the future? All three cases show large settlements of up to a maximum of 0.8 m since construction. This paper shows how the magnitude of the settlement since the construction can be reconstructed by analysing settlement data, covering only a relatively short period of time.

INTRODUCTION

The fact that a building is settling is often only recognizable after damage to the walls becomes visible or other harmful effects have been discovered. Questions then arise about the future of the building, and usually only then is a measuring program initiated. The amount of settlement which has occurred since construction is normally not known. Nonetheless the measuring program is required to lead, as soon as possible, to an answer to the question: what is the present rate of settlement? Extrapolation of this measured rate usually makes it possible to predict the settlements to be expected in the future.

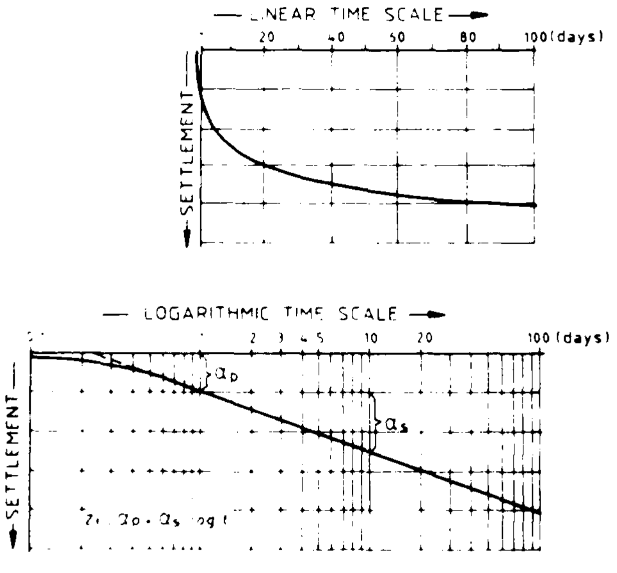

Fig. 1 Settlement according to Keverling Buisman, shown at linear and logarithmic time scales

SETTLEMENT THEORY

The settlement of a building is related to the properties of the subsoil. In 1938 Keverling Buisman presented the following settlement formula which takes into account secular effects, Figure 1; the formula is based on a study of time-settlement diagrams of both structures and laboratory samples.

$$z_t = \sum^{\text{all layers}} d(\alpha_p + \alpha_s \cdot \log t) \cdot \Delta p \qquad (1)$$

where: z_t = total settlement of the soil layers considered, at time t

d = thickness of the particular soil layer

α_p = settlement property of this soil layer, representing the direct effect

α_s = settlement property of this soil layer, representing the secular effect

t = time

Δp = load increment on the particular soil layer (the moment of application of the load is taken as time = 1)

Keverling Buisman states that the settlement process only agrees with this formula, if the excess pore-water pressure in the respective soil layers dissipates in a short period like in a laboratory test. In reality, because of the thickness of the soil layers, this will not be the case, and the increase of the effective stress and therefore the settlement process will be delayed. In practice an increase in load on the subsoil will also take place in a certain period of time. Keverling Buisman therefore introduced the term "equivalent exterior loading time" meaning that (imaginary) point of time when, in the long term, an exterior load, suddenly applied, would lead to a settlement process identical to that which occurs when an exterior load is applied gradually, for example a sand fill.

Keverling Buisman sees the gradual increase of the (internal) effective stress, due to the decrease of the excess pore-water pressures during the hydrodynamic period, as if it were the result of a comparable external increase of the load. An "equivalent internal loading time" can now be introduced as a zero value for the time in the logarithmic settlement process in a similar way as for the external load. The equivalent internal loading time occurs later than the equivalent external loading time. In an analysis of settlement behaviour, it will make little difference if the point of time to be considered is taken with regard to the start of loading or with regard to the equivalent internal loading time, as long as the point of time to be considered occurs a long time after the equivalent internal loading time. The settlement formula proposed by Keverling Buisman was used in the three following case studies.

CASE STUDY I: KAMPEN

Hanze is a post-war extension of the city of Kampen built in the surrounding polder. The site was raised with several metres of sand in 1949 before the construction of houses. The majority of the buildings are two and three storey low-rise blocks of flats founded on continuous footings. Some blocks have raft foundations. Many of the original 30 blocks were built on filled-in ditches in the period 1952-1957. The majority of these blocks show differential settlements and cracks in the brickwork. For this reason one of the blocks was pulled down in 1962. The following soil layers occur:

- the sand fill which was used for raising the site the thickness of which varies between 3 and 6 m;
- compressible layers, consisting of mainly peat and with some clay, the thickness of which varies between 1 and 4 m
- a pleistocene sand layer; the level of the top of this layer varies between 1 and 7 m below New Amsterdam Level.

The ground surface is at present about 3 m above New Amsterdam Level. The sand fill and the sand layer show different pore-water pressures. There have been no major changes in the groundwater regime since the construction of the houses.

Building deformation

Levels of four flat blocks have been taken over a long period; one of these blocks was pulled down in 1962. The measurements of this particular block were started in 1957. In this period 11 sets of measurements were made. Measurements of the other three blocks started in 1961 and, in the period 1961-1983, 19 sets of measurements were made. The measurements show a continuing settlement process. The magnitude of the settlements in the period 1961-1983 varied between 0.05 and 0.14 m. Soil investigations have shown that, by raising the site with the sand fill, the original thickness of the compressible layers was reduced by 30 to 40%. This means, depending on the magnitude of the original thickness of the compressible layers, a settlement of the compressible layers of 0.5 to 3 m. The largest part of this settlement took place before the flats were constructed.

Settlement analysis

The available data indicate that the continuing settlement process, and the related increase in the differential settlements in each block of flats, was mainly caused by the continuing settlement of compressible layers due to raising the level of the site before construction. The settlements of the block which was pulled down and the other three blocks were checked to see if they varied logarithmically with time. It was assumed in this investigation that the hydrodynamic period ended before the measuring period and, therefore, that a secular settlement process took place according to the formula of Keverling Buisman. The following formula was used for the analysis:

$$l(t) = a - b \log t/t_0 \qquad (2)$$

where: $l(t)$ = level of the reference point at time t (m to New Amsterdam Level)
a = constant (m to New Amsterdam Level)
b = constant (m)
t_0 = unit of time (1 year)
t = time of measurement in years after t_1
t_1 = equivalent internal loading time

The equivalent point of time of the application of the external load could be determined rather accurately from the available data, but the equivalent internal time of loading, due to the hydrodynamic period of the compressible layers, occurs some time later and is much more difficult to determine. The relationship between the level of the reference point and the time, that is, the determination of the constants a, b and t_1, was therefore investigated for a number of different points of time t_1. Figure 2 gives the results of the regression analysis for one measuring point. The results of the calculations show a good to very good relationship between the level of the reference point and the logarithm of the time. The equivalent internal loading time has been determined as 1st January 1953 for two blocks of flats and as 1st January 1954 for the other two.

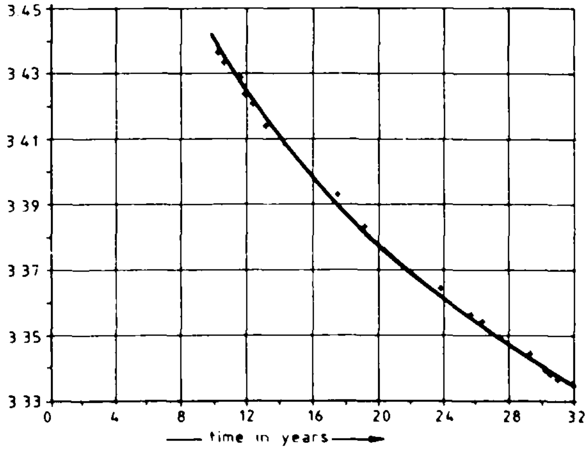

Fig. 2 Time-Settlement behaviour of a measuring point

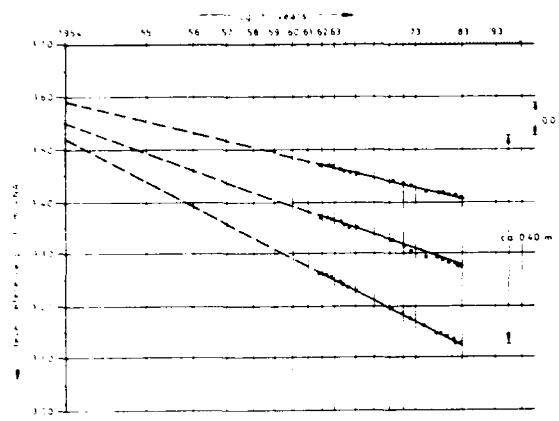

Fig. 3 Determination of the absolute settlement since construction

Because the four blocks were built around 1953/1954, the absolute settlement of each measuring point since construction can be derived directly from the calculated level of the reference points on 1st January 1953 or 1954, Figure 3. The settlement for the three remaining blocks of flats, is about 0.4 m maximum. The constant a in the Keverling Buisman formula which is the calculated level of the reference point in metres relative to New Amsterdam Level on 1st January 1953, should be the same for each block, because the reference points have been placed in the same bed joint. In fact, however, there are differences of up to 70 mm, Figure 3. An accurate prediction of future settlements has been made, based on the reconstruction of the settlement process. Extrapolation of the present logarithmic with time settlement process indicated future settlements which vary between 1 and 3 mm/year. The analysis shows the load on the compressible subsoil as if recorded in a long duration settlement test which satisfies the formula of Keverling Buisman. The measured settlement of the buildings serves as an accurate indication of the settlement process of the subsoil. Such long duration tests are not practicable in the laboratory. It is therefore striking that an empirical formula, introduced about 50 years ago and mainly based on short duration laboratory tests, can describe the settlement process of the houses in Hanze, which has been going on for more than 30 years, so accurately.

CASE STUDY II: VLAARDINGEN

The ROMI factory was originally a sugar refinery which was built on a site outside the dikes of the New Meuse at Vlaardingen. The level of the site was raised shortly before construction. The oldest part of the building dates from 1898. One wing of the building was extended after 1900, the other after 1909; the factory was partially rebuilt in 1937. The building is founded on tapered timber piles about 20 m in length and with a diameter at the top of 280 mm. The brickwork of the building is seriously cracked. The following soil layers occur:

- the sand fill which was used for raising the site the thickness of which varies between 4 and 5 m;
- compressible layers, mainly consisting of clay and peat, with a thickness of about 17 m;
- a pleistocene sand layer in which the piles have been founded; the level of the top of this layer is about 19 m below New Amsterdam Level.

The ground surface is at present about 3 m above New Amsterdam Level. The phreatic groundwater level is about New Amsterdam Level. The piezometric level of the groundwater in the sand layer below the compressible layers is 2 to 3 m below New Amsterdam Level.

Building deformation

Levels of reference points fixed on the outside walls have been taken in the period December 1980 to January 1983. The measured, total, settlements varied between 1 and 11 mm in 25 months, Figure 4. During the rebuilding in 1937 the lower part of the north-west front was replaced, the upper part being maintained. Levels were taken of the top of a decorative "header" course of bricks laid in the brickwork walls constructed in the period 1898-1909. Levels were also taken of a bed joint laid above the part that was renewed in 1937, Figure 5. It is assumed that the bed joint and the header course were horizontal at the time of construction, and that the extensions of 1900 and 1909 were connected, as far as the level of the brickwork is concerned, to the existing building. Measurements will therefore give a clear picture of the differential settlements since the construction: the maximum settlement, up to 1982, was about 575 mm.

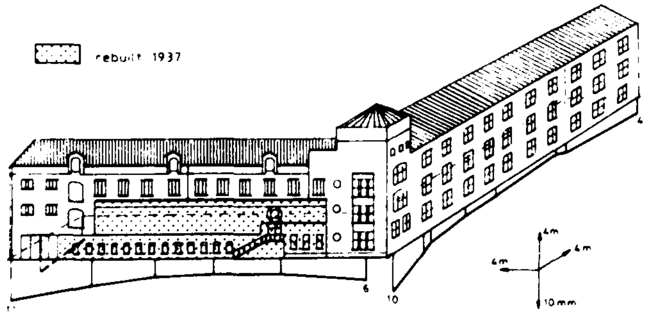

Fig. 4 Settlements in the period December 1980 to January 1983

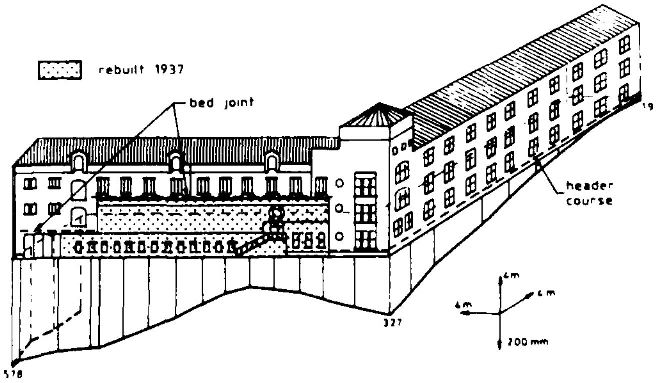

Fig. 5 Differential settlements in the walls constructed in the period 1898-1909

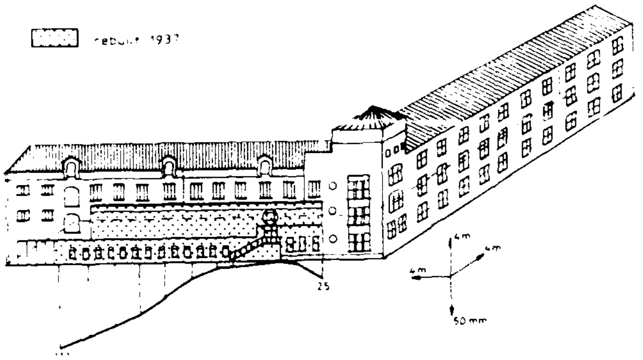

Fig. 6 Differential settlements of the wall rebuilt in 1937

Levels were also taken of the part of the building renewed in 1937, Figure 6. The maximum differential settlement in the period 1937-1982 was about 110 mm.

Settlement analysis

The measured differential settlements of the building are very large for a foundation on piles. The settlement behaviour is, in fact, more like that of a spread foundation. It is sometimes possible to relate the settlement of piles due to negative skin friction to the settlement of the surrounding soil (Hannink and Talsma, 1984). The formula of Keverling Buisman has, therefore, also been used to analyse this case. First the rate of settlement in the period 1980-1983 was determined for each measuring point as accurately as possible. The assumption that settlement is linear with time is reasonable here. The rate of settlement varies between 1 and 5 mm/year. Because only differential settlements were known, it was also necessary to assume here that the lines which represent the settlement process, for each measuring point, according to the formula of Keverling Buisman, intersect each other at the zero of the absolute settlement, Figure 7. The figure shows, for each measuring point, the same ratio between the absolute settlement since the construction and the present rate of settlement Figure 8 shows, for each measuring point on the walls constructed in 1898-1909, the rate of settlement in the period 1980-1983 (x-axis) and the differential settlement since the construction up to 1982 (y-axis). The result is a rectilinear relationship. At x = 0 the y-value can be read from this relationship which should be added to the differential settlement for each measuring point in question to obtain the absolute settlement since the construction up to 1982. The results show that this value amounts to between 24 and 68 mm depending on the number of measuring points accepted, Figure 8. The same approach has been used for the part renewed in 1937. The results show that, depending on whether three or four measuring points are considered, 83 or 98 mm should be added to the differential settlement to get the real settlement in the period 1937-1982, Figure 9.

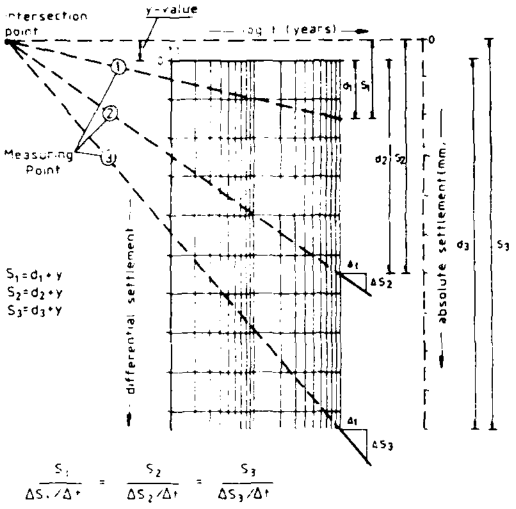

Fig. 7 Assumption for the settlement process

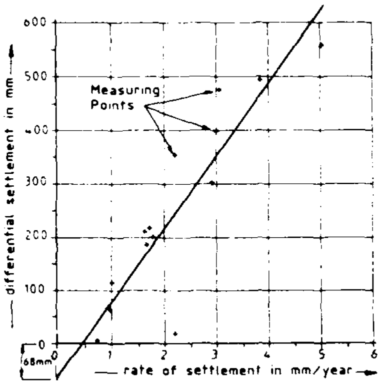

Fig. 8 Relationship between the rate of settlement and the differential settlement in the period 1898-1982

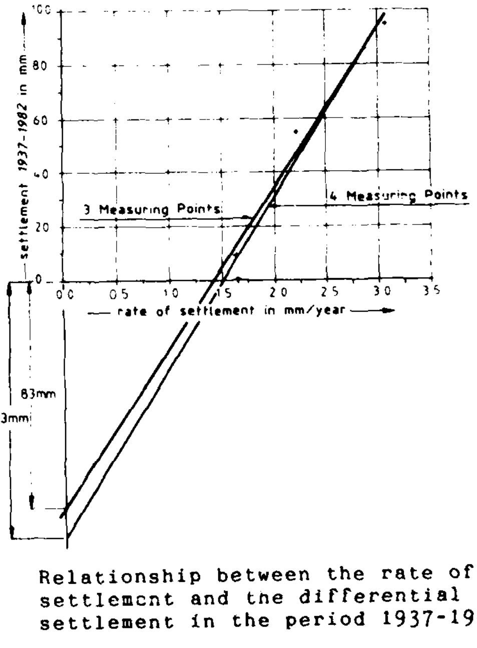

Fig. 9 Relationship between the rate of settlement and the differential settlement in the period 1937-1982

Because of the assumptions which were necessary, the ratio between the absolute settlements since the construction up to 1982, and the settlements in the period 1937-1982 for the part of the building renewed in 1937, was checked for each measuring point to determine whether or not it was the same everywhere, Figure 10. This ratio is indeed everywhere the same and because the line determined by regression analysis should go through the intersection of the axeses, leads even to more accurate results. The minimum settlement of the building, in the period since the construction up to 1982, amounts, according to the calculations, to 68 mm, and the maximum settlement to about 650 mm, Figure 11. In the period 1937-1982 the minimum settlement of the renewed wall was 83 mm, and the maximum settlement about 190 mm. Further analysis showed that the part renewed in 1937 since 1937 has settled almost linear with time and not, according to Keverling Buisman, logarithmically with time. Tracing the cause of this discrepancy was beyond the scope of the investigations. Possible causes are a change of load on the foundation piles in 1937, effects of drainage of the pleistocene sand layer and creep of the timber piles. However, the same ratios presented in Figure 7 also apply when the settlement process is linear with time, and the results of the calculations will therefore not change. A continuation of the settlement process, measured in the period 1980-1983, can, for the larger part of the building, be expected in the near future with a rather large amount of certainty. Settlements which vary between 1 and 5 mm/year must be reckoned with.

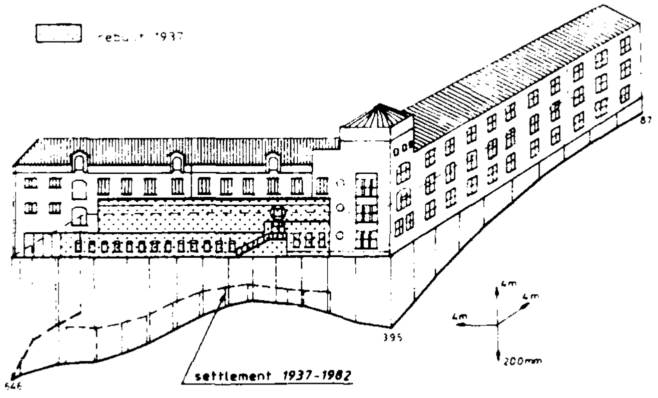

Fig. 11 Calculated absolute settlements up to 1982

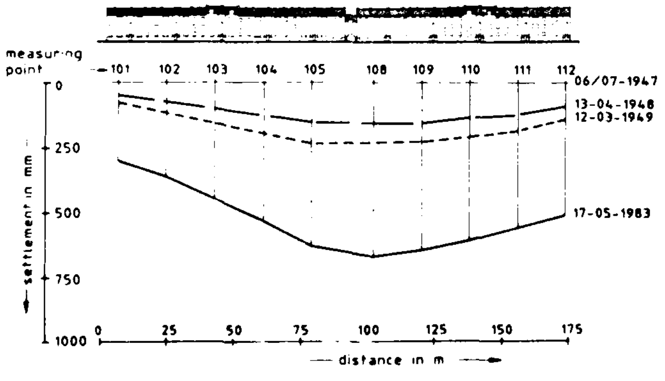

Fig. 12 Settlement of the front side since construction

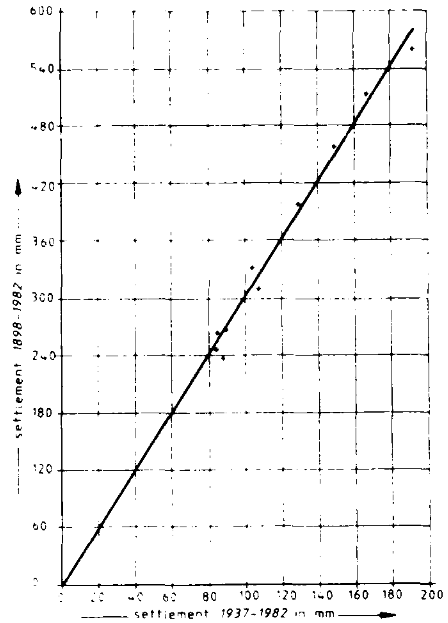

Fig. 10 The absolute settlement in the periods 1898-1982 and 1937-1982 for the part of the building renewed in 1937

CASE STUDY III: DELFT

The flat block in the De Colignystraat was built in 1946/1947 and is founded on raft foundations. The flat block is a three, locally four storey building and contains 58 flats. The flat block is divided into two by a gate, and has a basement floor which is partly below ground level, Figure 12. The basement floor does not continue under the gate. The ground level was raised by 0.7 to 1.0 m of sand at both sides of the building during the construction. The building brickwork is seriously cracked near the gate. The following soil layers occur below the building:

- compressible layers down to about 10 m below New Amsterdam Level, consisting of clay, sandy clay and peat; a sand layer was encountered, however, between about 3 and 6 m below New Amsterdam Level at the southern part of the building;
- sandy clay and clayey sand between 10 and 14 m below New Amsterdam Level;
- compressible layers between 14 and 17 m below New Amsterdam Level;
- a pleistocene sand layer below 17 m below New Amsterdam Level.

The groundlevel at present is about 2 m below New Amsterdam Level.

Building deformation

Since construction, levels of the building have been taken in 1947, 1948, 1949 and 1952. A new measuring program was started in 1982. This case differs from the preceeding cases because the zero-situation is known, and the following absolute settlements of the building were observed for the period 1947-1983, Figure 12:

- south end (front): 300 mm
- middle (front): 650 mm
- middle (back) : 800 mm
- north end (front): 510 mm

The following settlements were measured in the period 1982-1984, Figure 13:

- south end (front): 3 mm
- middle (front): 8 mm
- north end (front): 5 mm

Settlement analysis

The values given above show a clear relationship between the magnitude of the settlement since the construction of the building and the present rate of settlement, similar to that assumed in the analysis of the settlement of the ROMI factory. The continuing settlement process and the related increase in differential settlements are caused by a continuing settlement of the compressible layers. The smaller settlement at the south end of the building is a consequence of the locally better soil conditions. Average rates of settlement, based on different starting-points, are presented in Table I.

TABLE I: Comparison of rates of settlement (in mm/year)

	average from measurements		present rate by extra-polation via Keverling Buisman
	1953-1983	1982-1984	
south end (front)	5	2	2
middle (front)	7	5	3
middle (back)	10	4	4
north end (front)	8	3	3

The results show that the rate of settlement is decreasing as may be expected from the formula of Keverling Buisman. Present rates of settlements, derived from the measurements in the period 1982-1984 and obtained by a logarithmic with time representation of the settlements since the construction, agree rather well, Figure 14. The measurement results seem to indicate that the rate of settlement of the middle part (front) has been increasing over the recent years. In Figure 14 it has been assumed that the point of time t_1 coincides with the point of time of the first measurement. A different time of loading and the presence of a hydrodynamic period has not been taken into account. However, the formula of Keverling Buisman is also very useful in this case for settlement predictions. The expected settlements vary between about 2 and 4 mm/year.

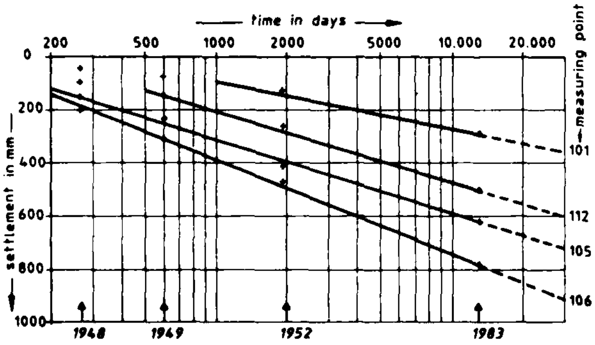

Fig. 14 Time-Settlement diagram

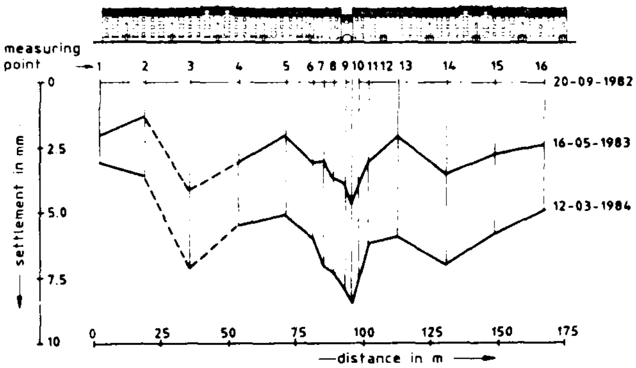

Fig. 13 Settlement of the front side in the period September 1982 up to March 1984

CONCLUSIONS

The settlement of buildings after construction may amount to many decimeters. If this is the case, the building will almost certainly crack, because settlements are never uniform. The causes of settlement may vary. In the present cases the load of sand fill has played the major role in addition to the weight of the building itself. Accurate measurements are essential for the analysis of a settlement process. A period of at least two years is often necessary to establish a rate of settlement with sufficient accuracy. An assumed time-settlement behaviour of a building may deviate from the measured results because of inaccuracies in the measurements, varying groundwater levels and temperature effects during the measurements. A settlement process, once started, continues and *can usually be described correctly* by means of the settlement formula of Keverling Buisman. The three case studies, described here, indicate that, even 30 years or more after construction, the rates of settlement can be 5 mm/year. They also show that the same ratio exists between the settlement since the construction and the instantaneous rate of settlement for the different measuring points. Measuring data, data about structural history, the building itself and the subsoil are indispensable for back-dating the settlement behaviour of a building since its construction. A complete reconstruction of the settlement history of a building, since the construction, is the best base for predicting settlements. Whether there is an acceleration of the settlement process can be discovered in this way, so that measures can be taken in time.

REFERENCES

Hannink, G. and K.W. Talsma (1984), "Geotechnical Consequences to the Environment, by Construction of the Polder Markerwaard", IAHS Publication no. 151, Proc. 3rd International Symposium on Land Subsidence, Venice, 885-897.

Keverling Buisman, A.S. (1936), "Results of Long Duration Settlement Tests", Proc., 1st International Conference on Soil Mechanics, Cambridge (USA), 103-106.

Keverling Buisman, A.S. (1938), "Some Soil Mechanics Concepts, especially related to the Settlement Problem" (in Dutch), de Ingenieur, 12 and 19 August 1938, 133-157.

Proceedings: Second International Conference on Case Histories in Geotechnical Engineering, June 1-5, 1988, St. Louis, Mo., Paper No. 6.68

Large Horizontal Displacements of Houses in Rotterdam

G. Hannink
Project-engineer, Delft Geotechnics, Delft, The Netherlands

A.F. van Tol
Head of Geotechnics Department, Rotterdam Public Works, Rotterdam, The Netherlands

SYNOPSIS: In 1983 it was established that six blocks of terrace houses in Rotterdam had undergone large horizontal displacements. These displacements were caused by insufficient stability of the adjacent quay and as a result one of the blocks had moved as much as 2.5 m since 1958. The foundation piles of the houses were not designed to resist any horizontal loading. As a result of these large horizontal movements the piles had deflected to such an extent that complete failure was feared. This paper describes the remedial measures that were taken to improve the stability of the quay and foundations of the houses. The present displacement behaviour is compared with the horizontal displacement predicted from creep analysis.

INTRODUCTION

In 1983 the Road Management and Surveying Department of Rotterdam Public Works discovered that six blocks of, in total, 41 terrace houses at the north side of a quay, the Zestienhovensekade, had undergone large horizontal displacements, Figure 1. Research by the Department on previous measurements indicated that the horizontal displacements, given in Table I, must have occurred since the houses were constructed. The degree of accuracy of the absolute displacements up to 1975 was estimated at within 0.1 m. The degree of accuracy of the displacements in the periods 1975 - 1983 and 1983 - 1984 was estimated at within 0.02 m. To be more certain about what appears, at first sight, to be incredible figures, the magnitude of the displacements was also established from aerial photos taken for mapping purposes. Based on these measurements, it was concluded, beyond doubt, that large displacements had occurred, and that the maximum rate of displacement was about 0.10 m/year.

TABLE I: Horizontal displacements since construction

Block	House No.	Year of construction	Horizontal displacement (m)		
			up to April 1975	up to Sept. 1983	up to July 1984
0	439	1962	0.8	0.865	0.865
0	447	1962	0.3	0.310	0.310
1	449	1957	0.5	0.525	0.530
1	473	1957	1.3	1.505	1.520
2	475	1958	1.7	2.070	2.150
2	487	1958	1.8	2.440	2.540
3	489	1938	1.2	1.525	1.560
3	499	1938	0.8	1.065	1.100
4	501	1935	0.4	0.460	0.465
4	507	1935	0.1	0.210	0.210
5	509	1938	0.5	0.630	0.630
5	519	1938	1.5	1.730	1.750

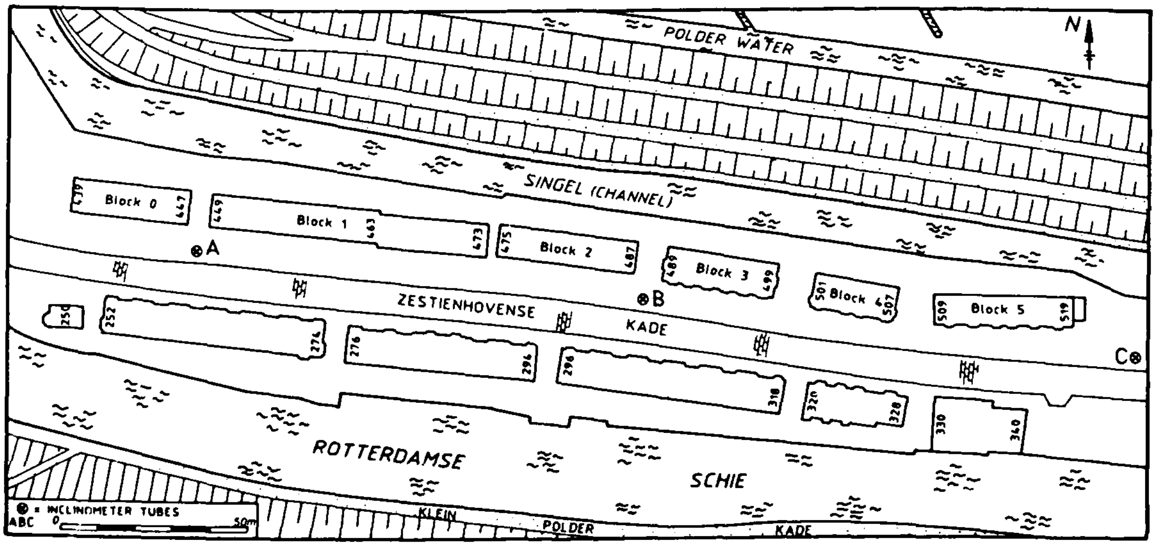

Fig. 1 Situation

Cause of the displacements

The cause of the displacements must be sought in a combination of the following circumstances, Figure 2:

- the level of the ground surface in front of the houses and behind the houses differs by 2.5 m to 3.0 m
- fill with a unit weight of 18 to 20 kN/m³ occurs at the front of the houses down to a level of between 5 m and 6 m below the ground surface and peat with a unit weight of about 10 kN/m³ occurs at the back
- the clay and peat layers under the houses are very soft and have unfavourable friction properties

The effect of displacement on the houses

The first calculations led to the following conclusions for Blocks 1, 2, 3 and 5:

- the foundation piles offer no resistance against the horizontal movements of the quay
- the stresses in the foundation piles have far exceeded the allowable values
- the remaining safety margin of the foundation is difficult to assess. Complete failure in the near future must be feared unless remedial measures are taken.

Remedial measures

Measures which would eliminate the cause of the displacements were given high priority. Two possible solutions were presented:

1. The removal of the inciting load by excavating about 2.5 m of the heavy quay material and replacing it by lightweight material. This solution will be explained below.
2. The absorption of the load by installing an anchored sheet piling along the front side of the blocks. This solution was subsequently not found to be technically feasible and is not discussed further.

An inspection of the condition of the foundations was necessary, which included investigating the top of the foundation piles. It was planned to repair the foundations of the six blocks, if shown to be necessary, after implementing the remedial measures for the quay. The study of the measures was backed by extensive soil investigations and displacement measurements. The soil investigations included field and laboratory work. The field work consisted of cone penetration tests and borings in several cross-sections of the quay as well as the installation of piezometers, and measurements of the pore-water pressure. Cell tests and consolidation tests on undisturbed samples taken in the cross-section with the largest displacements, were carried out in the laboratory. Measurements of the horizontal displacements of the blocks were started on 13th July 1984. Initially these measurements were performed weekly, and then monthly. The vertical displacements of Block 2 were measured from 12th February 1985, and of the other five blocks from 25th March 1985. The frequency of these measurements was almost the same as for the measurements of the horizontal displacements.

IMPROVEMENT OF THE STABILITY OF THE QUAY

Figure 2 shows the composition of the subsoil in a cross-section of the quay. The subsoil consists of soft holocene clay and peat layers to a depth of 16 m below New Amsterdam Level. Below this level fine to rather coarse pleistocene sand is found. The in-situ pore-water pressure was measured in front of Block 2 and an excess pore-water pressure of about 25 kN/m² was found between 10 to 13 m below New Amsterdam Level. The soil investigations confirmed that the holocene layers have very low shear strength. The lowest values occur behind the blocks where the overburden pressure is small. A preliminary stability analysis showed that a slip circle through the soft clay layers around 11 m below New Amsterdam Level, which takes into account the excess pore-water pressure, gives the lowest factor of safety.

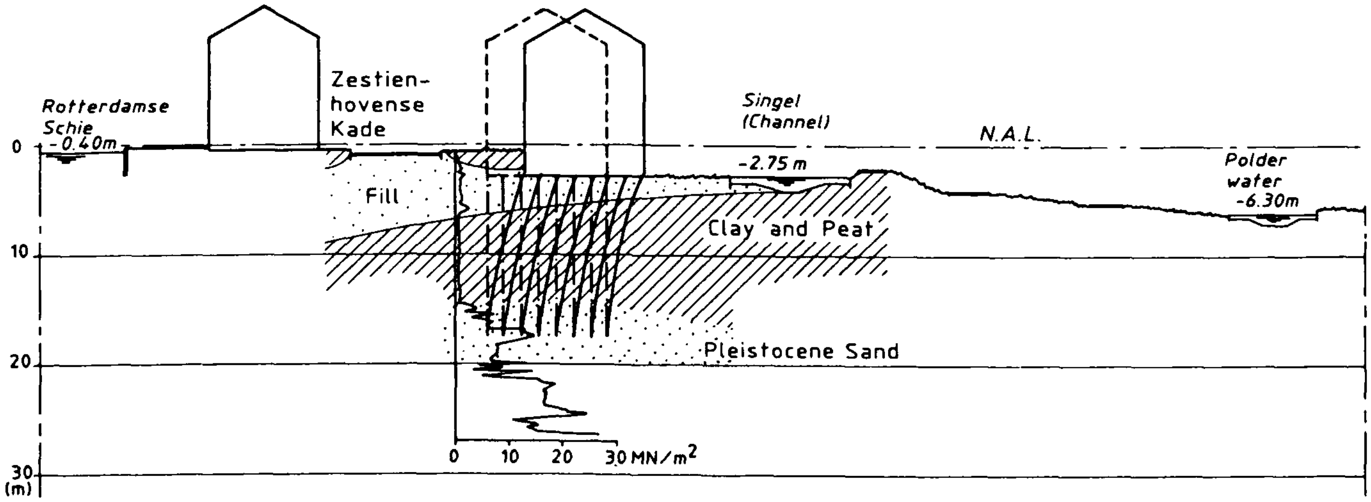

Fig. 2 Cross-section of the quay

Remedial measures

The remedial measures selected, to ensure the stability of the quay, are as follows. Over a total length of 300 m the existing fill was removed and replaced by lightweight material, Figure 3. The original fill had a unit weight of 18 to 20 kN/m³. The backfill consists of light expanded clay aggregate with a unit weight of 6 kN/m³ and polystyrene foam with a unit weight of less than 1 kN/m³. Polystyrene foam and blast furnace slag was placed underneath the road to ensure an adequate foundation. With these measures the surcharge on the subsoil was reduced by 35 kN/m² over a width of at least 12 m. To evaluate the effect of the remedial measures and to find the reasons for the large displacements of the quay, it was necessary to establish the deformation behaviour and the magnitude of the factor of safety in the present and future situation. Two types of analyses were carried out:

- stability calculations according to Bishop's method
- calculations with the Finite Element Method.

Bishop's Method

An analysis of the stability of the situation before remedial measures were taken gave factors of safety which varied from 0.82 to 1.04 depending on the assumed pore-water pressure conditions under and behind the houses. All slip circles go through the deep clay layer. The maximum depth of these slip circles is about 11 m below New Amsterdam Level. The results of stability calculations for the situation after the remedial measures show that, under fully drained conditions, the long term safety factor is about 1.5 to 1.6. If, however, it is assumed that, immediately after the measures are implemented, there is still excess pore-water pressure underneath the houses, the factor of safety falls to between 1.2 and 1.3. The required factor of safety for canal and river dykes in The Netherlands is 1.3. Therefore it can be concluded that the proposed remedial measures will be satisfactory.

Finite Element Method

An analysis with the Finite Element Method was carried out in order to obtain information about:

- the actual and future deformations
- the influence of differences in stiffness
- the factor of safety for non-circular slip surfaces.

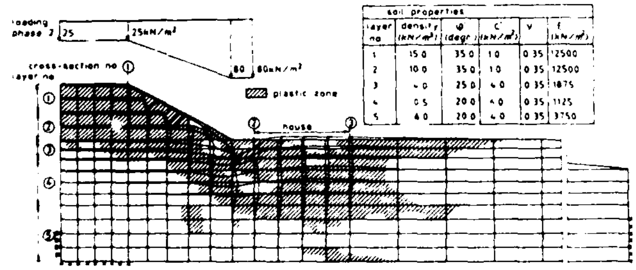

soil properties					
layer no	density (kN/m³)	φ (degr)	c' (kN/m²)	ν	E (kN/m²)
1	15.0	35.0	1.0	0.35	12500
2	10.0	35.0	1.0	0.35	12500
3	4.0	25.0	4.0	0.35	1875
4	0.5	20.0	4.0	0.35	1125
5	4.0	20.0	4.0	0.35	3750

Fig. 4 Phase 2: Displacements and plastic zones after loading

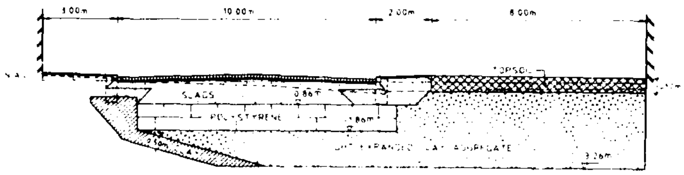

Fig. 3 Design of the improvement of the quay

The analysis was carried out with the help of the DIANA computer program (De Borst, 1984). This program is able to simulate elastoplastic soil behaviour, dilitancy, softening and hardening. In the calculations the Mohr-Coulomb criteria was used for yield; softening and hardening were not taken into account. The element mesh and soil properties are shown in Figure 4. The situation of the quay before the houses were built was simulated in Phase 1. After the construction of the houses, the quay is subsequently filled which is simulated in Phase 2 by introducing a load equal to the fill. Figure 4 also shows the load schedule and the deformations as well as the status (elastic or plastic) of the elements. As can be seen there is a continuous surface of plastic elements (the last iteration step in the Finite Element calculation did not converge).
After Phase 2 the calculated maximum horizontal displacement is 0.73 m. The actual maximum displacement, however, is 2.50 m. This discrepancy may be caused by an incorrect choice of the deformation and yielding parameters, by additional horizontal displacement caused by the dead load on the deflected piles, and by creep. The DIANA program does not take creep into account, and the magnitude of the additional horizontal displacements are unknown. In Phase 3 the load on the quay is reduced by 35 kN/m². Figure 5 shows the deformations and the status of the elements. Table II shows the maximum vertical and horizontal displacements in three cross-sections for the different phases.

TABLE II: Maximum vertical (δ_v) and horizontal (δ_h) displacements (m)

Cross-Section	1		2		3	
Phase	δ_v	δ_h	δ_v	δ_h	δ_v	δ_h
1	0.38↓	0.03→	0.05↓	0.10→	0.04↓	0.05→
2	0.63↓	0.21→	0.31↓	0.73→	0.20↑	0.37→
3	0.54↓	0.19→	0.22↓	0.71→	0.16↑	0.36→

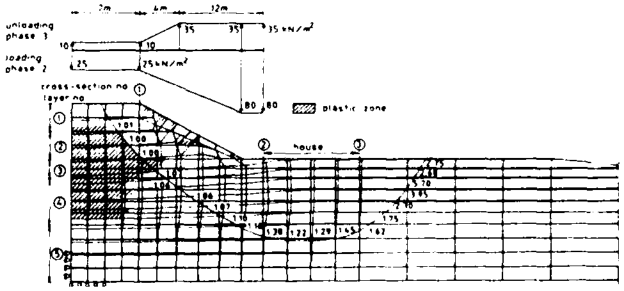

Fig. 5 Phase 3: Displacements and plastic zones after unloading

For the elements which form the imaginary slip surface, the factor of safety is estimated by comparing the mobilized shear strength with the ultimate shear strength. This is expressed by the following equation:

$$\text{factor of safety} = \frac{\sin \Phi'}{\sin \Phi'_{mob}} \qquad (1)$$

where: Φ' = angle of internal friction at failure
Φ'_{mob} = mobilized angle of internal friction

It appears that the elements yielding in Phase 2, which are located underneath the houses, have a factor of safety varying from 1.2 to 1.4 in Phase 3. The calculated displacements in Phase 3 are shown in Table II. Compared with Phase 2 there is only a small decrease in horizontal displacements.

Creep

Singh and Mitchell (1969) presented the following general function for soils that expresses the strain rate, at any time t, after application of sustained deviator stress, Figure 6.

$$\dot{\varepsilon} = A\, e^{\bar{\alpha}\bar{D}} \left(\frac{1}{t}\right)^{m} \qquad (2)$$

where: $\dot{\varepsilon}$ = strain rate
A = projected value of strain rate at zero deviator stress on logarithmic strain rate versus deviator-stress plot for unit time
$\bar{\alpha}$ = dimensionless parameter defined as the value of the slope of the mid-range linear portion of the logarithmic strain rate versus stress level curve, all points corresponding to the same time after load application
$\bar{D}$ = normalized stress level, defined as the ratio of the deviator stress to the deviator stress at failure
t = elapsed time divided by unit time
m = slope of a logarithmic strain rate versus logarithmic time straight line

A general relationship between the creep strain ε and time is obtained by integration of Equation 2.

$$\varepsilon = A e^{\bar{\alpha}\bar{D}} \left(\frac{1}{1-m}\right) t^{1-m} \qquad (m \neq 1) \qquad (3)$$

The effect of unloading on the relationship between strain and time is illustrated in Figure 7. When, at time t_1, a soil sample is unloaded from deviator stress $\bar{D}_1$ to $\bar{D}_2$, it is assumed that the sample will follow the strain rate according to curve $\bar{D}_2$ at time t_2. This is shown by the dotted curve. The principle of the equivalent time concept according to Hanrahan (1973) is used here. The effect of unloading on the strain rate can be calculated as follows. The imaginary point of time t_2 is found by putting the strain at time t_1, according to $\bar{D}_1$, equal to the strain at time t_2, according to $\bar{D}_2$, in Equation 3. It follows that:

$$\frac{t_2}{t_1} = e^{\bar{\alpha}(\bar{D}_1 - \bar{D}_2)/(1-m)} \qquad (4)$$

The ratio between the strain rates follows from Equation 2:

$$\frac{\dot{\varepsilon}(t_1)}{\dot{\varepsilon}(t_2)} = e^{\bar{\alpha}(\bar{D}_1 - \bar{D}_2)} \left(\frac{t_1}{t_2}\right)^{-m} \qquad (5)$$

Combining (4) and (5) leads to:

$$\ln \frac{\dot{\varepsilon}_1}{\dot{\varepsilon}_2} = \bar{\alpha}\, \frac{\bar{D}_1 - \bar{D}_2}{1-m} \qquad (6)$$

The reduction in strain rate can therefore be calculated from Equation 6 if the parameters $\bar{\alpha}$ and m are known, and if the factors $\bar{D}_1$ and $\bar{D}_2$ have been calculated by a stability analysis. Future strains, after time t_2 can be calculated with Equation 3. It follows that:

$$\frac{\varepsilon(t_1)}{\varepsilon(t_2)} = \left(\frac{t_1}{t_2}\right)^{1-m} \qquad (7)$$

The imaginary time t_2 follows from Equation 4. The strain at a selected number of years after t_2 at time t_1 follows from Equation 7 if the strain at time t_2 is known.

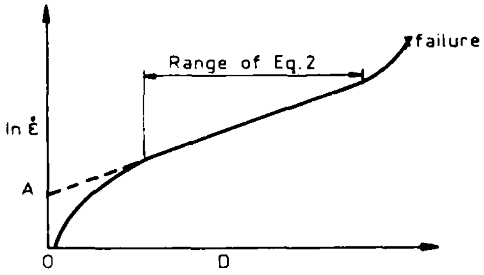

Fig. 6 Relationship between strain rate and deviator stress at given time

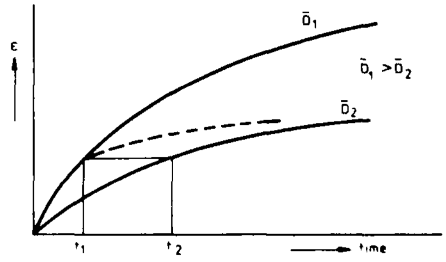

Fig. 7 Effect of unloading on the relationship between strain and time

Prediction of future strain rate and strain

In order to make the predictions extensive laboratory investigations are required to determine the parameters $\bar{\alpha}$ and m. Since only strain rates and strains before and after the remedial measures have to be compared, it was decided that indicative calculations would be sufficient. Therefore values given by Singh and Mitchell (1968, 1969) were used, complemented by data from tests on Oesterdam clay carried out by Delft Geotechnics. These data indicate that the parameter $\bar{\alpha}$ varies between 1.4 and 6.7. It appears that the value of $\bar{\alpha}$ is higher for soft clays than for stiff clays. The parameter m varies between 0.70 for soft soils and 1.30 for stiff. The worst case approach was followed for predicting. Therefore $\bar{\alpha} = 3$ and $m = 0.7$ were taken. The factor $\bar{D}_1 - \bar{D}_2$ is derived from the stability calculations. An increase of the actual safety factor from 1.0 to 1.3 immediately after the remedial measures, indicates $\bar{D}_1 - \bar{D}_2 = 0.23$. If the long term factor of safety is taken as 1.5, it follows that $\bar{D}_1 - \bar{D}_2 = 0.33$. Substituting these values in Equation 6 it appears that the ratio between the strain rates before and just after the remedial measures, is at least 10. This ratio increases to at least 30 in the long term.
To predict the future horizontal displacements of Block 2 the strain was considered for a period of 50 years after the remedial measures. The magnitude of the horizontal displacement was about 2.5 m in the period 1958 - 1984, that is, $t_1 = 26$ years and, from Equation 4, it follows that $t_2 = 260$ years for $\bar{D}_1 - \bar{D}_2 = 0.23$. Taking $t_3 = 310$ years and substituting the values in Equation 7 it appears that the ratio between the strains just after the remedial measures, and 50 years later, is 1.05. The horizontal displacement of Block 2 will therefore increase by 5%, being 0.13 m. Taking $\bar{D}_1 - \bar{D}_2 = 0.33$ leads to a ratio of 1.02 and an expected horizontal displacement of Block 2 of 0.05 m. A horizontal displacement of 0.10 m has been taken into account in the design of the new foundations for the blocks.
The observed strain rate is about 100 mm/year for Block 2. Immediately after the remedial measures the strain rate should reduce to 10 mm/year, and in the long term to 3 mm/year. The analysis of the future strain based on the actual displacement, indicates a strain rate of 2.5 mm/year immediately after the remedial measures and 1 mm/year in the long term. The discrepancy can be explained by the fact that the observed strain rate of 100 mm/year, is not in agreement with Equation 2. This can be explained as follows:

- Equation 2 is only valid for values of $\bar{D}$ between 0.3 and 0.9 and not for the near failure conditions which occur before the remedial measures are applied, Figure 6.
- Additional fills to compensate settlements are not in agreement with the assumption of sustained deviator stress.
- The large horizontal displacements cause a secondary horizontal load on the pile foundations which cannot be neglected and therefore an increase in the strain rate.

Equation 2 is valid for conditions after the improvement of the quay and the foundations, and the prediction of the future strain rate based on the observed horizontal displacement is reliable.

IMPROVEMENT OF THE FOUNDATIONS OF THE HOUSES

Due to the extreme horizontal displacements the stability of at least 4 of the 6 blocks of terrace houses was in danger, the more so since the dead load of the houses on the deflected piles increases the displacements. Data from archives and inspection of some foundation piles showed the following:

- Block 1, consisting of 13 houses, is founded on 55 precast concrete piles, 0.35 m square, and with a length of 19 m. Six pile heads have been inspected. The upper part of these piles have inclinations varying from 6 : 1 till 30 : 1. Several pile heads show serious cracks, Figure 8. Sonic integrity tests on two piles demonstrated that these piles had no cracks on deeper levels.

Fig. 8 A cracked concrete pile

- Block 2, consisting of 7 houses, is founded on tapered timber piles with a precast concrete upper section above water level. Four out of five upper sections inspected were almost vertical; one had an inclination of 6 : 1. The upper part of the timber piles have inclinations of 3 : 1 to 6 : 1.
- Block 3, consisting of 6 houses, is founded on 103 tapered timber piles. The upper part of the piles have inclinations varying from 4 : 1 till 6 : 1.
- Block 5, also consisting of 6 houses, is founded on 93 tapered timber piles. The upper part of the timber piles have inclinations varying from 2 : 1 till 3 : 1.

The following sequence of improvements was chosen as a result of these inspections: Block 2 and then Blocks 5, 3 and 1. Measurements showed that the houses had also undergone vertical displacements. Absolute displacements could not be established, but the differential displacements since construction varied from 0.2 m for Block 3 to 0.7 m for Block 5. It was striking that despite the large horizontal and vertical displacements, the blocks showed so little cracks. This was caused by the relatively stiff cellar floor that was present under all the blocks.

Demands on the foundations

Measures were necessary to guarantee the stability of the terrace houses for the next fifty years. The following aspects had to be taken into account in the design of a new foundation or in the re-use of the existing one:

- there must be an equilibrium of forces and moments without large deformations
- a horizontal displacement of 0.1 m is to be expected in 50 years after the remedial measures for the quay are carried out
- all the parts of the construction must have sufficient strength
- the design must be practicable.

Injection piles

Already in an early stage of the investigation it was decided that if it was impossible to re-use the existing piles injection piles would be installed as replacements. An injection pile is a steel tube pile filled with a hardened grout. During installation the soil is pushed aside, which improves the bearing capacity of the pile. The steel tube is brought to the right depth by hammering, the grout being injected at the same time. The grout is forced down the tube and out of the bottom up the outside. The grout functions as a lubricant during the installation, and in this way, reduces the resistance. After hardening the grout contributes to the strength and the stiffness of the pile, transfers a part of the load to the soil, and protects the steel tube against corrosion. In this project a coupled injection pile was used with an external diameter of the tube of 114.3 mm and a wall thickness of 5.4 mm. The total external diameter of the pile, inclusive the grout will finally amount to about 150 mm.

Possible solutions

Two possible solutions for the design of a new foundation were considered. In the first solution the installation of new raking and vertical piles was studied, Figure 9. In principle an equilibrium of forces is reached if the magnitude of the active earth pressure H_1 and the passive earth pressure H_2 can be determined with sufficient accuracy. However, this solution has the disadvantage that it contains the idea of fixing the position of the house, while some horizontal deformation has to be taken into account.

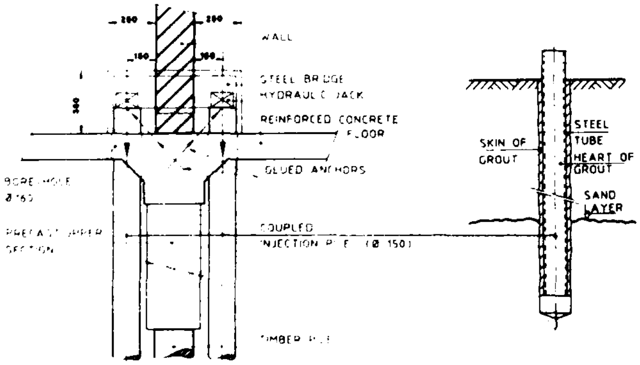

Fig. 11 Design of the foundation improvement and principle of the injection pile (dimensions in mm)

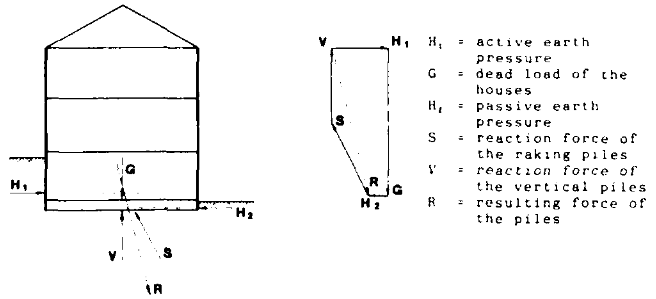

H_1 = active earth pressure
G = dead load of the houses
H_2 = passive earth pressure
S = reaction force of the raking piles
V = reaction force of the vertical piles
R = resulting force of the piles

Fig. 9 Solution with raking and vertical piles

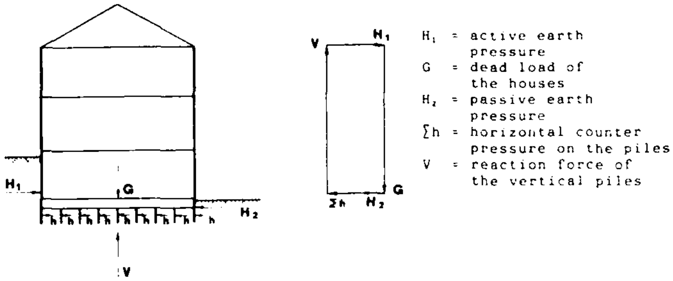

H_1 = active earth pressure
G = dead load of the houses
H_2 = passive earth pressure
Σh = horizontal counter pressure on the piles
V = reaction force of the vertical piles

Fig. 10 Solution with only vertical piles

When deformation of the quay takes place, the soil tends to displace more than the house, and H_1 will increase and H_2 decrease. This solution requires relatively many raking piles and therefore extra piles, and, as a result, is less attractive. However, in the case of a new building this solution, with relatively massive piles, would probably be selected. In the second solution only the installation of vertical piles was studied, Figure 10. An equilibrium of forces is reached if also the soil behind the upper part of the piles delivers some counter pressure. To be able to deliver extra counter pressure, the pile and therefore the house has to be displaced horizontally a little bit more than the soil. The advantage of this solution is that H_1 is smaller than in the first solution, and H_2 is larger. The horizontal loads and the moments and shear forces on the piles will remain small. This solution is practicable because it requires not very many piles and no massive piles. In addition it is a flexible solution. One condition, however, is of great importance; the total horizontal displacement, after the replacement of the foundation piles, must not be excessive. Based on the calculations discussed above this solution was selected for the replacement of the foundation piles.

Design of foundation improvements

The injection piles were installed from the cellar floor at both sides of the bearing walls and then connected to the walls by glued anchors and a steel beam, Figure 11. The designs for the foundation improvements for the various blocks were based on the various requirements discussed above. The result was a complete replacement of the bearing function of the foundation piles under Blocks 2, 3 and 5. The design for Block 1 will probably consist of partial replacement.

Execution of foundation improvements

The injection piles were hammered to a deeper level than the existing piles. However, no serious problems were encountered during the execution of the works. One aspect is interesting. The blocks of terrace houses have not been displaced horizontally the same amount. Block 5, in fact, shows a difference in displacement of about 1 m between the ends. As a result new piles could be hammered accidentally on to the existing piles, Figure 12. Although this was taken into account in the design as much as possible, it did occur a few times, however without consequences. The step-wise transfer of loads from the existing piles to the new piles went as planned.

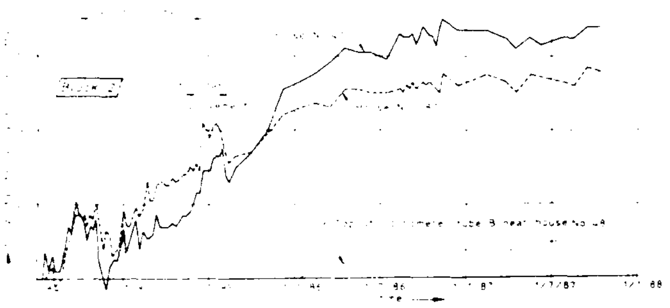

Fig. 13 Horizontal displacements of Block 2

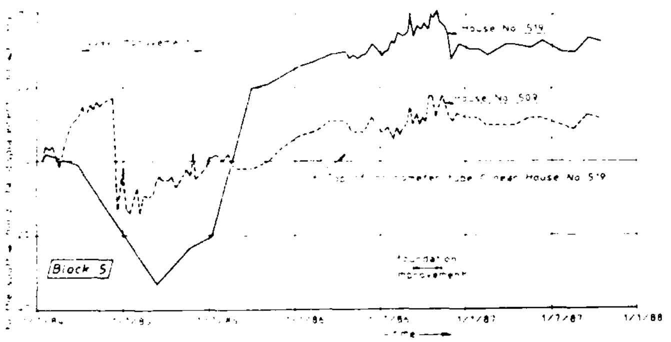

Fig. 15 Horizontal displacements of Block 5

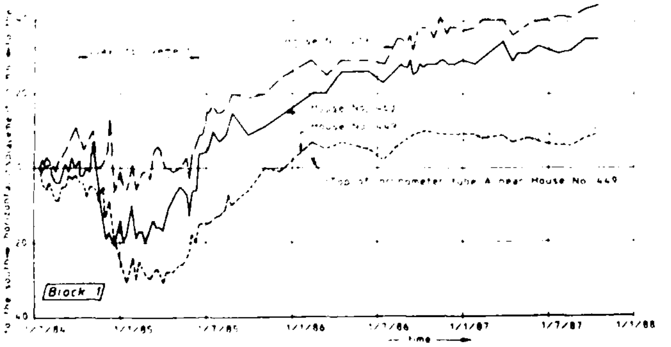

Fig. 16 Horizontal Displacements of Block 1

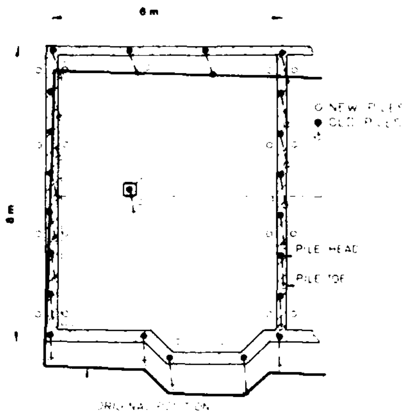

Fig. 12 Location of the new piles relative to old piles

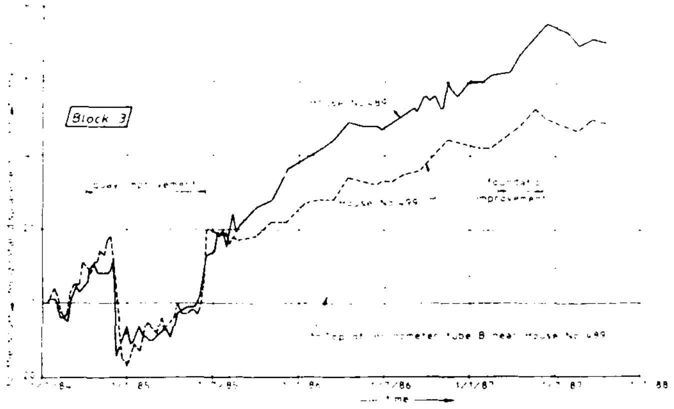

Fig. 14 Horizontal displacements of Block 3

DISPLACEMENT BEHAVIOUR SINCE 1984

Initially the measurements of the horizontal displacements were made relative to a straight line. Both ends of this line were situated outside the area of influence of the soil movements. Since 13th January 1986 another system has been used. The new measuring line is defined as the line between the top of three inclinometer tubes installed with the bottoms in the deep Pleistocene sand layer. The results of the measurements of the horizontal displacements of the blocks of terrace houses are given in the Figures 13 to 16. The horizontal displacements of the top of the inclinometer tubes are given in the same figures. The vertical displacements of Blocks 1, 2, 3 and 5 are given in Figure 17. The following periods are indicated in the figures:

- reconstruction of the quay : 03-10-1984 to 14-06-1985
- new foundation for Block 2 : 14-05-1985 to 05-08-1985
- new foundation for Block 5 : 10-09-1986 to 10-11-1986
- new foundation for Block 3 : 02-03-1987 to 04-06-1987

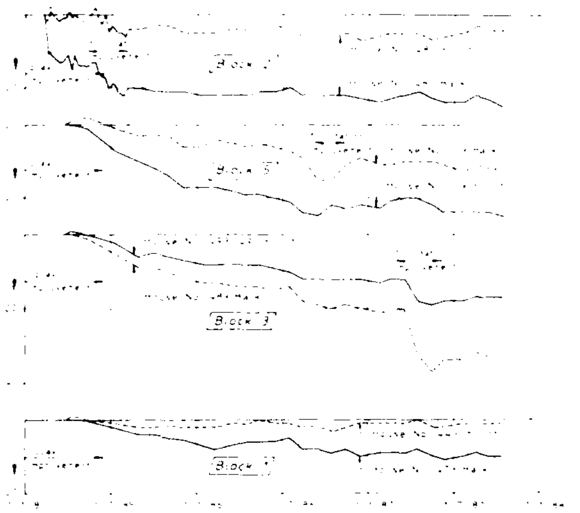

Fig. 17 Vertical displacements of Blocks 2, 5, 3 and 1

Reduction of rate of horizontal displacement

Data given in Table I and those measured since July 1984 indicate the following rates of horizontal displacements, Table III. The data since July 1984 are given in three periods. The division in periods has been made in such a way that temporary influences like foundation improvements occur in only one period.

TABLE III: Rates of horizontal displacement to the north (mm/year)

Block	House No.	date of constr. to 1975	1975 - 1983	9/1983 - 7/1984	13.7.84 - 13.1.86[1]	13.1.86 - 26.1.87	26.1.87 - 14.10.87
0	439	62	8	0	3	12	-1
0	447	23	1	0	-5	7	-3
1	449	28	3	6	2	6	9
1	473	72	24	13	19	11	8
2	475	100	44	101	35[2]	14	1
2	487	106	75	126	31[2]	8	3
3	489	32	38	44	26	21	16[2]
3	499	22	31	44	18	15	10[2]
4	501	10	7	6	2	0	1
4	507	3	13	0	-7	-2	-3
5	509	14	15	0	5	5[2]	0
5	519	41	27	25	17	5[2]	3

[1] = period includes quay improvement
[2] = period includes foundation improvement

The period 1975 - 1983 is taken as the reference period for the horizontal displacements before improvement of the quay for the analysis of the reduction of the rates of horizontal displacement. Table III shows, for Block 2, a reduction of this rate by a factor of 3 to 10, one year after the improvement of the quay and the foundation. One year later the reduction has increased to a factor of 25 to 40, the rate of horizontal displacement amounting to 1 to 3 mm/year. The reduction factor for Block 5 amounts to 3 to 5, one year after the improvement of the quay. One year later, that is also one year after the improvement of the foundation, the reduction has increased to a factor of at least 9, the rate of horizontal displacement amounting to 0 to 3 mm/year.

The reduction factor for Block 3 amounts to about 2, one year and about 3, two years after the improvement of the quay. Improvement of the foundations has only been implemented recently, and future measurements will indicate the effect on the magnitude of the horizontal displacements. House No. 473 of Block 1 shows a reduction factor of about 2 one year and of about 3 two years after the improvement of the quay. Improvement of the foundations is still in the design stage. The inclinometer tubes also show decreasing rates of horizontal displacement. Data before the improvement of the quay are not available. Comparing 1987 with 1986, however, shows a reduction factor of 2 to 3 for the tops of Tubes A and B. Data of 1987 show a rate of horizontal displacement of about 3 mm/year. Tube C shows a variation of measuring results between the two periods, and is therefore not considered here.

CONCLUSIONS

The remedial measures have resulted in a considerable reduction of the rate of the horizontal displacement of the houses. The combined effect of the improvements to the quay and the foundations is a reduction of this rate by a factor of 9 to 40 for Blocks 2 and 5 in a period of two years. The predicted reduction amounted to a factor of at least 10 initially, subsequently increasing to at least 30. Prediction and observation therefore agree rather well. The new foundations were designed on a horizontal displacement of 100 mm to be expected in 50 years, that is an average rate of 2 mm/year. Although the rate immediately after the implementation of the remedial measures turned out to be rather large, this rate has, in the mean time, reduced to 0 to 3 mm/year for Blocks 2 and 5. The present behaviour therefore is satisfactory. After improving the foundations of Blocks 2, 3 and 5 the settlement process, of these blocks, stopped. The inclinometer tubes show some movement of the new quay, but the rate of horizontal displacement is reducing from about 8 mm/year, one year after the improvement of the quay, to about 3 mm/year one year later. The measurements will be continued for the time being.

REFERENCES

Borst, R. de, and P.A. Vermeer, (1984), "Possibilities and Limitations of Finite Elements for Limit Analysis", Geotechnique, vol. 34, 199-210

Hanrahan, E.T., and M. Shahrour, (1973), "Prediction of Strain Rates using Eg. Ek parameters", Proc., 8th International Conference on Soil Mechanics and Foundation Engineering, Moscow, vol.1, 171-175

Singh, A., and J.K. Mitchell, (1968), "General Stress-Strain-Time Function for Soils", Journal of the Soil Mechanics and Foundations Division, Proc. ASCE, vol. 94, no. SM1, 21-46

Singh, A., and J.K. Mitchell, (1969), "Creep Potencial and Creep Rupture of Soils", Proc., 7th International Conference on Soil Mechanics and Foundation Engineering, Mexico, vol. 1, 379-384

Proceedings: Second International Conference on Case Histories in Geotechnical Engineering, June 1-5, 1988, St. Louis, Mo., Paper No. 6.72

Predicting Performance of Large-Diameter Buried Flexible Pipes: Learning from Case Histories

Koon Meng Chua
Assistant Research Engineer, Texas Transportation Institute, Texas A&M University System, USA

Larry J. Petroff
Engineering Supervisor, Spirolite Corporation, Chevron Chemical Company, USA

SYNOPSIS: Analytical approaches to predicting pipe deflections are based on the predetermined pipe properties, the anticipated soil properties and on the assumption that the specified installation configuration can be met. However, in-place pipe deflections do often deviate from the predicted. This paper summarizes the observations made from more than twenty case histories of entrenched large-diameter flexible high density polyethylene pipes and discusses the effects of construction methods and site conditions on pipe performance. Procedures are also presented on how site conditions and construction methods can be accounted for when using the TAMPIPE (Texas A&M PIPE) method and the Spangler's method. Procedures are given for predicting the variability of pipe deflections in the field. The TAMPIPE method is also shown to be accurate in predicting the long-term deflection of the pipe.

INTRODUCTION

Analytical methods of designing large-diameter buried pipes invariably assume that the pipe can be installed according to specifications, without considering the difficulties posed by the actual site condition. For example, providing a vertical trench wall in a loose soil or attempting to achieve specified compaction in a flooded trench are both difficult. This paper attempts to introduce such considerations into the design process in order to bridge the gap between the theoretical and the practical.

THEORETICAL PREDICTIONS

The Spangler's equation (Spangler, 1951) which is a semi-empirical solution, has been the most popular method used in the design of buried flexible pipes for the past several decades. In recent years, the emphasis has been to formulate mechanistic solutions. The TAMPIPE [Texas A&M PIPE] solution (Chua and Lytton, 1987a) which will be considered here is one such method. This is an analytical regression-type solution developed using results obtained from a nonlinear finite element program called CANDE [Culvert ANalysis and DEsign] (Katona et.al., 1976). This procedure will compute the pipe vertical deflection, and the pipe maximum stress and strain for any given time period.

Spangler's Method

The Spangler's equation (also known as the Iowa Formula) is as follows:

$$\Delta D/D = \frac{D_l \; K W}{8E_p I_p/D^3 + 0.061\,E'} \qquad (1)$$

where: $\Delta D/D$ = pipe horizontal deflection (normally assumed to be the same as the vertical),
D_l = time lag factor,
K = bedding constant (0.083 - 0.11),
W = load per unit length of pipe (lb/linear inch)
E_p = the pipe elastic modulus (psi),
I_p = moment of inertia of the pipe wall (in^4),
D = pipe diameter (ins), and
E' = modulus of soil reaction (psi).

TAMPIPE Method

The TAMPIPE procedure considers a pipe buried in a trench of any width, and surrounded by three soil zones - the embedment (or bedding), the backfill and the in situ soils. Figure 1 shows a typical trench condition.

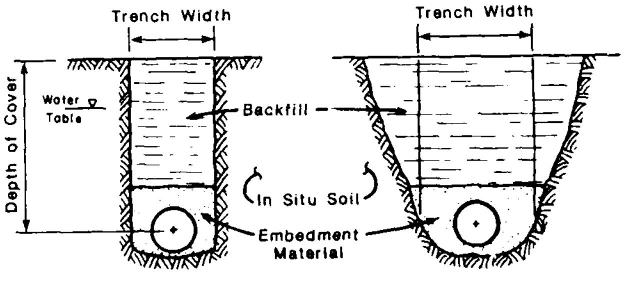

Figure 1. Trench Configurations

The pipe vertical deflection is given by:

$$\Delta D/D = \frac{B_f(1-A_f)\,\gamma z\,(1-W_f)}{8E_p I_p/(1-v_p)D^3 + C_f\,E_1'} \qquad (2)$$

where: B_f = bedding factor (function of Poisson's ratio of soil),
A_f = arching factor ,
γ = unit weight of soil,
v_p = Poisson's ratio of pipe material,
C_f = a coefficient (function of Poisson's ratio of soil),
W_f = a factor to include the effects of a water table. and
E_1' = soil support modulus (psi).

The initial tangent modulus of the soil modeled by TAMPIPE (similar to CANDE) is given by,

$$E_i = K\ P_a\ (\sigma_3\ /P_a)^n \qquad (3)$$

where: K_i = soil modulus number,
n = modulus exponent,
P_a = atmospheric pressure, and
σ_3 = the minor principal stress.

In view of this, the TAMPIPE procedure will require K_e, K_i and K_b which represent the embedment soil, in situ soil and the backfill soil, respectively. The soil support modulus E_1', which is a tangent modulus is calculated for the soil at the springline.

The time-dependent predictions made with TAMPIPE consider pipe material and the three soils to be viscoelastic. For the detailed development of the TAMPIPE procedure, refer to (Chua, 1986; Chua and Lytton, 1987b).

A REVIEW OF CONSTRUCTION PRACTICE

Twenty eight projects were selected from a period of time to form the basis of this study. These projects are representative of the practice with large-diameter high density polyethylene profile wall pipes. The pertinent characteristics of each of the installations are summarized in Table 1 which will be referred to in the following sections. In the case where multiple pipe sizes were used at different depths, only one representative size and depth was chosen and considered in the analysis.

Field Measurements

Pipe deflection ($\Delta D/D$) was determined by measuring the change in vertical diameter ($\Delta D/D$) due to earth and live loading. Typically, two to four measurements were taken per 20 ft pipe length with the total number of data points per project ranging from 50 to several hundreds. Probability plots of diametrical measurements approached a straight line, indicating that the standard deviation assumes a normal distribution. In order to compare projects, the coefficient of variation which is the ratio of the standard deviation to the mean is used. Figure 2 shows the mean pipe vertical deflections as well as the plus one and minus one standard deviation obtained for the various projects.

Installation Configuration

Pipe diameters considered ranges 18" to 72". The pipe stiffness (defined as $8E_pI_p/0.149\ D^3$) considered ranges from 5.4 psi to 49 psi. A trench width to diameter ratio of between 1.25 to 1.5 is usually called for in a design, but as can be seen, over-excavation is not uncommon. Depths of cover (measured from the ground surface to the spring line) considered here range up to 35 ft. Flexible plastic pipes have been installed to depths of over 100 ft in fills.

The vertical and the sloping trench wall configuration is shown in Figure 1. A removable trench box is sometimes used during construction to support the soil in order to keep the trench wall vertical. Column 12 shows whether open, sheeting or braced trench construction was carried out.

Table 1. Project Descriptions

PROJECT	DIAMETER	P.STIFFN.	COVER	(---- TRENCH WIDTH ------>			GROUND	(-- EMBEDMENT -->		IN SITU	CONSTR.	INSPECT.	AVE.DEFL.	STD.DEV.	COEF.VAR.	TIME
NUMBER	(INS)	(PSI)	DEPTH (FT)	NO. DIA.	(---- WALL ----->		WATER	TYPE	COMPACT. METHOD	SOIL	TECHN.	(%TIME)	(%)		(%)	(DAYS)
					TYPE	FIRMNESS										
COL.1	COL.2	COL.3	COL.4	COL.5	COL.6	COL.7	COL.8	COL.9	COL.10	COL.11	COL.12	COL.13	COL.14	COL.15	COL.16	COL.17
1	36	15.2	25	1.6	SLOPE	STIFF	NO	STONE	TAMP	MIXED	OPEN	100	1.6	1.3	81	1460
2	18	49	17	2		MEDIUM	NO	SAND	TAMP	SAND	OPEN	50	2.1	1.9	90	540
3	42	9.7	10	1.4	SLOPE	STIFF	NO	SAND	TAMP	MIXED	OPEN	100	1.7	1.1	65	90
4	42	52	35	1.4	VERT.	STIFF	NO	STONE	TAMP	SAND	OPEN	50	1	0.4	40	14
5	36	15.2	15.5	2		STIFF	YES	STONE	TAMP	SAND	OPEN	100	0.8	0.6	76	3
6	42	9.7	15.5	2	BOX	MEDIUM	NO	STONE	DUMP	CLAY/SILT	OPEN	0	2.5	1.4	59	780
7	36	15.2	15	1.7	SLOPE	V/LOOSE	NO	SAND	TAMP	CLAY/SILT	OPEN	0	0.9	0.9	100	3
8	48	6.5	11	1.8	SLOPE	V/LOOSE	YES	STONE	DUMP	CLAY/SILT	OPEN	FR	1.4	2.3	164	1
9	48	26	20	1.6	BOX	STIFF	DEWATER	STONE	SHOVEL	CLAY/SILT	BRACED	100	2	0.8	40	315
10	36	15.2	11.5	1.7	VERT.	MEDIUM	NO	GRAVEL	TAMP	MIXED	OPEN	50	2.3	1.1	48	730
11	54	18.4	12.5	1.6	BOX	STIFF	YES	CEM-SAND	TAMP	CLAY/SILT	SHEET	50	3.3	0.9	27	450
12	36	8.7	13.5	2.5	SLOPE	MEDIUM	YES	STONE	SHOVEL	CLAY/SILT	OPEN	50	4.1	1.7	41	150
13	54	7.3	20	1.3	SLOPE	STIFF	YES	STONE	DUMP	SAND	OPEN	50	4.2	2	48	300
14	60	5.4	11.5	2	BOX	V/LOOSE	DEWATER	STONE	TAMP	CLAY/SILT	SHEET	100	2.1	1	48	1095
15	24	32.5	13	3	BOX	V/LOOSE	YES	SHELL	TAMP	SAND	BRACED	50	1.5	1.9	127	365
16	18	49	7.5	2			(?)	CLAY(CH)	DUMP	CLAY/SILT	OPEN		5.4	2.8	52	300
17	30	25.9	20	2	BOX	V/LOOSE	DEWATER	MIXED	TAMP	SAND	BRACED	50	1.31	1	79	14
18	48	6.5	12	1.2		MEDIUM	YES	CEM-SAND	DUMP	CLAY/SILT	OPEN	FR	3.3	1.7	52	180
19	48	10.4	8	2	BOX	LOOSE	YES	STONE	DUMP	CLAY/SILT	BRACED	FR	3.5	1	29	1
20	36	8.7	12.5	1.7	BOX	V/LOOSE		STONE	DUMP	MIXED	BRACED	50	2.01	2.4	121	7
21	72	8	26	1.7	SLOPE	STIFF	NO	STONE	TAMP	SAND	OPEN	50	1.5	1	67	90
22	24	21.2	15	2	SLOPE	LOOSE	NO	STONE	TAMP	CLAY/SILT	OPEN	50	2.1	1.3	62	1
23	30	17.1	16	2.4	BOX	V/LOOSE	YES	SAND	TAMP	CLAY/SILT	BRACED	100	1.5	0.8	53	7
24	36	15.2	15	1.3		STIFF	NO	SAND	TAMP	CLAY/SILT	BRACED	50	2.2	2.1	95	1
25	36	24.2	10	1.7	SLOPE	V/LOOSE	YES	SAND	TAMP	CLAY/SILT	OPEN	100	0.31	0.3	97	1
26	24	15.9	17	2	SLOPE	MEDIUM	NO	STONE	TAMP	CLAY/SILT	OPEN	100	2.7	1.1	41	540
27	36	8.7	15	1.7	VERT.	STIFF	YES	STONE	SHOVEL	CLAY/SILT	OPEN	FR	2.49	1.2	48	90
28	24	21.2	6	2				STONE	SHOVEL	CLAY/SILT	OPEN		1.5	0.5	33	30

Footnotes:- V/LOOSE for VERY LOOSE; DEWATER = YES; CEM-SAND =Cement-sand; MIXED implies SAND/CLAY/SILT; FR= Factory Representative

Site Conditions

Column 7 describes the firmness of the site soil. The soil is classified as very loose, loose, and medium to stiff. For instance, a very loose soil indicate a collapsing trench if left open and unsupported. Column 9 shows whether a water table was encountered during construction and whether dewatering was done.

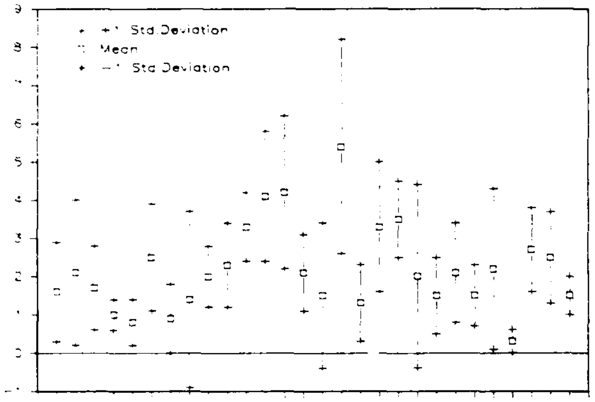

Figure 2. Observed Pipe Deflections and Variability

Embedment Materials

In about 50% of the projects, tamping was carried out to compact the embedment (bedding) materials. Shovel slicing accounts for 25%. However, for the rest of the projects, the embedment materials were simply dumped with no compaction. This practice should be discouraged since the highest deflections observed in this study were dumped embedment materials.

Embedment materials used include sand, crushed stone, pea-gravel, a mixture of sand and stone, and sea-shells. In one case, fat clay from the site itself was dumped around the pipe with no compaction. This resulted in a large pipe vertical deflection (Project 16).

Other Factors

From the measured pipe deflection shown in Table 1, it is evident that where there is good inspection, minimal deflections usually occur. The attitude of the contractor and the efficiency and quality of the construction equipment are important factors and should be considered. The variability of pipe deflection is probably an indicator of how conscientious the contractor is.

CONSTRUCTION CONSIDERATIONS

In developing the construction adjustments which may be required to more accurately predict the mean pipe vertical deflection, the philosophy is to attempt to explain the field data by modifying the design parameters affected rather than the common approach of simply using "add-on" deflections.

Figure 3 shows the pipe vertical deflections predicted using TAMPIPE and the Spangler's equation prior to adjusting for construction factors versus the observed values. The predictions made using Spangler's equation can be seen to be generally lower than the field measurements.

Upon reviewing the factors which may contribute to the difference between the predicted and the observed deflections, the most obvious cause is the condition of the trench. That is, whether it is a loose or wet or both and whether it is sloped (open cut) or braced. In a wet and loose trench, uncleaned wall sloughs and compaction difficulties may lead to increased deflections. These problems may be slightly compounded when a portable shield, or box, is used.

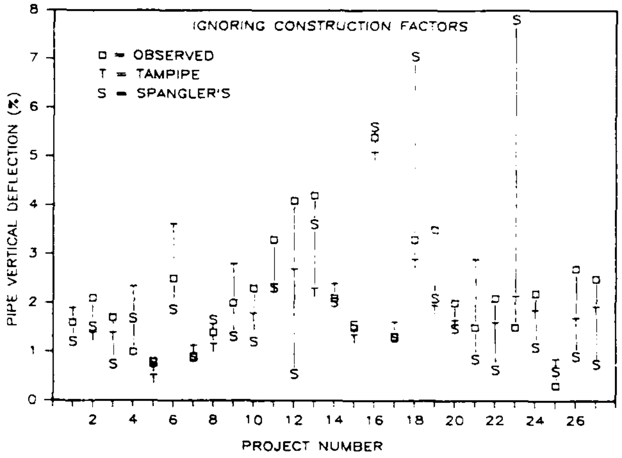

Figure 3. Initial Predictions of Pipe Deflections

Recommendations

TAMPIPE Method

From observations, it appears that the only adjustment required for TAMPIPE is in the modulus number of the embedment material, K_e. By reducing Ke, it was found that the TAMPIPE predictions can be improved to match the wet trench case, and the wet and unstable trench case. For cases in which remedial action such as dewatering of a wet trench, no reduction in K_e was required. Dewatering, when done properly, will allow the installation to be carried out as successfully as a dry one. The Ke-value can be multiplied by the factors shown in Table 2. These factors may be used in CANDE.

Table 2. Recommendations for TAMPIPE

Trench Condition	Reduction Factor
Stable and Wet Trench without dewatering	0.66
Unstable and Wet Trench without dewatering	0.5

Spangler's Method

The coefficients in the Spangler's equation were determined empirically from the field which may explain why the predictions are reasonable in most cases. The soil modulus used in the predictions (Figure 3) are shown in Table 3.

Table 3. USBR Values of the Soil Modulus E'

Soil Type	Compaction, % Proctor			
	Dumped	85	85-95	>90
Fine-Grained, CL, ML, ML-CL				
<25% coarse-grained	50	200	400	1000
>25% coarse-grained	100	400	1000	2000
Coarse-Grained, GW,GC,SM,SC				
>12% fines	100	400	1000	2000
<25% fines	200	1000	2000	3000
Crushed Rock	1000	3000	3000	3000

In order to enhance the accuracy of the predictions, the following recommendations are made.

Table 4. Additional Values of E' Values (psi) for Iowa Formula

Crushed Rock	
Dumped in wet in situ soil	500
Shovel sliced	
only under haunch	1000
in soft clayey in situ soil	500

Results

Figure 4 shows the predictions made using the TAMPIPE and the Spangler's equations after considering construction conditions.

PREDICTING THE VARIABILITY OF PIPE DEFLECTION FOR INDIVIDUAL PROJECT

The coefficient of variation for the each project can be estimated using the decision tree shown in Figure 5.

The standard deviation can be calculated from the coefficient of variation. The pipeline engineer can decide from standard deviation the number of pipe sections which will probably exceed the acceptable deflection. If the risk is unacceptable, the engineer can either (a) ensure that installation specifications are strictly followed, or (b) reduce the mean deflection by using a stiffer pipe or better embedment soil.

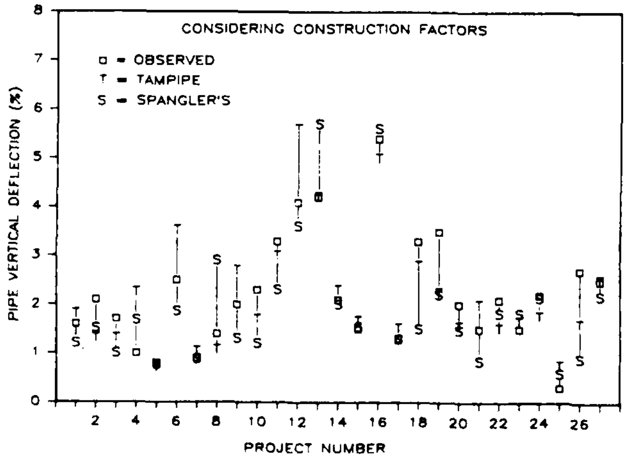

Figure 4. Final Prediction of Pipe Deflections

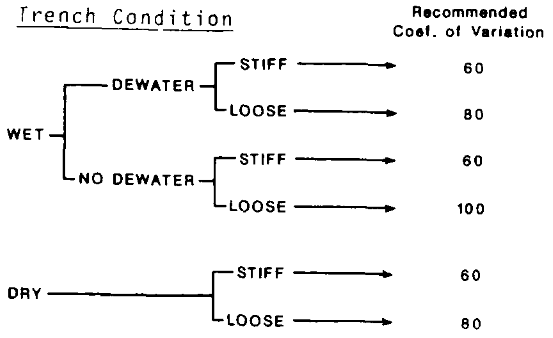

Figure 5. Determining Variability of Pipe Deflections

CONCLUDING REMARKS

Presented herein are case histories of projects involving large-diameter flexible buried pipe in which the mean pipe vertical deflections as well as the variability of the measurements are available. Procedures are presented in which input to the TAMPIPE and the Spangler's equation can be adjusted to reflect the construction methods as well as the site conditions during installation. A method of predicting the variability of the pipe deflections in the field is also presented. Several factors causing in-place pipe deflections to deviate from the predicted were identified. The most critical factor involves the condition of the trench, namely, whether the trench wall is stable and whether a water table is present. It appears that appropriate remedial actions when effectively executed, such as using a trench box or dewatering, can still ensure a proper installation.

This study once again underscores the fact that proper construction procedure is just as important, if not more important, than an accurate design procedure.

REFERENCES

Chua, K.M. (1986). "Time-Dependent Interaction of Soil and Flexible Pipe", A PhD. Dissertation, Texas A&M University, May.

Chua, K.M. and Lytton, R.L. (1987a). " A New Method of Time-Dependent Analysis for Interaction of Soil and Large-Diameter Flexible Pipe", presented at the 66th Annual Meeting, Transportation Research Board, Washington, D.C., January.

Chua, K.M. and Lytton, R.L. (1987b). "Short Communication: A Method of Time-Dependent Analysis Using Elastic Solutions for Nonlinear Materials", Intl.J. for Num. and Analyt.Methods in Geomech., Vol.11 No.4, Jul-Aug.

Katona, M.G.; Smith, J.M.; Odello, R.S.; and Allgood, J.R. (1976). "CANDE - A Modern Approach for the Structural Design and Analysis of Buried Culverts". Report No.FHWA-RD-77-5, Federal Highway Administration, Washington, D.C., October.

Petroff, L.J. (1985). "Stiffness Requirements for HDPE, Profile Wall Pipe", Proc. Advances in Underground Pipeline Engineering, University of Wisconsin, Madison.

Spangler, M.G. (1951). Soil Engineering, Intl. Textbook Co., Scranton, 3rd Ed.

Proceedings: Second International Conference on Case Histories in Geotechnical Engineering, June 1-5, 1988, St. Louis, Mo., Paper No. 6.73

Behavior of Ground Anchors for Taipei Sedimentary Soils

J.C. Li
Director of Planning and Research Department, Taiwan

L.P. Shi
Assistant Engineer of Research Sector, Taiwan

H.L. Yao
Chief of Research Sector, Planning and Research Department, Taiwan

B.I. Shy
Chief of Foundation Construction Office of Taipei Main Station, Taiwan

SYNOPSIS: Seven ground anchors were installed for full scale field tests in Taipei Railway Underground Project. The soil at job site can generally be classified as silty clay or clayey silt. The length of the anchors was about 40 m each, including 23 m bond length. The borehole diameter was 125 mm and the designed borehole inclination was 26 degrees downward. Each of the anchors was expected to share approximately 300 to 400 kN of tie-back force to support the diaphragm wall during excavation. Investigation of the borehole inclination was carried out by using horizontal inclinometer. The distribution of skin friction along the bond anchorage was determined from strain gauges applied on the anchoring strands, and the tensile load was monitored by load cells. It was observed that the average borehole direction deviated with an angle of about 1.5 degrees. It has also been found that most of the design load was carried by the first 10 m of the bond length. For a nearest spacing of about 1.5 m between the anchors, the group effect and the stress interaction among them were negligible.

INTRODUCTION

For designing an anchor in soil, it is generally assumed that a constant skin friction distributes over grout-soil interface along bond anchor length. OSTERMAYER and SCHEELE (1977) have performed the full scale tests on anchors in non-cohesive soils. They have found that the decrease of tendon forces from the front part to the rear part of the bond length corresponds with the load transmission from the tendon into the grouted body. The maximum skin friction shifts from the front part of bond length towards the anchored end when the tensile step loadings were gradually applied. A progressive failure mechanism was used to explain the variation of skin friction with bond length. So far, as the behavior of ground anchors in silty or clayey soil is concerned, the limitations of the application of the various theoretical approaches have been discussed by Ou (1986). In this paper, a field investigation on the behavior of ground anchors in Taipei Sedimentary Soils is reported. The main objectives of this research are:

(i) to observe the borehole inclination after it was driven.
(ii) to understand the stress distribution along fixed anchor length and its variation with respect to time,
(iii) to understand the group effect of anchors and its influence on stress distribution,

FIELD TESTS

Among the many anchors installed in Taipei Railway Underground Project, seven were selected for full scale tests. A schematic arrangement of the test anchors is shown in Fig. 1. According to the requirements on this research, three instrumentation systems, i.e., horizontal inclinometer, strain gauges and load cells, were used in the testing program. The length of the anchors was about 40 m each including about 23 m bond length. The borehole diameter was 125 mm and the designed borehole inclination was 26 degrees. The simplified geotechnical profile of typical Taipei Sedimentary Soils is shown in Table I. A large part of the bond length was situated at a layer of silty clay or clayey silt with undrained shear strength (Su) of about 60 kN/m^2. Some part of the bond length was located in the layers of silty fine sand with effective internal friction angle of 31 to 32 degrees. All test anchors were installed at the elevation lower than the ground water table, which is normally located at 1 to 2 m below the ground surface.

Each of the test anchors was expected to share approximately 300 to 400 kN of tie--back forces to support the diaphragm wall during excavation. Four or five tension strands with diameter 12.7 mm each were used for anchorage. The temperature compensating strain gauges were attached to a steel bar (165 mm in length and 20 mm in diameter). They were protected by several layers of waterproof coatings and an aluminum tube to prevent from stain and damage. This assembly was then connected to one of the tension strands at the pre-selected points. All instruments were calibrated in the laboratory before the field testing. The following are the procedures of installation and measurement in the testing program:

(i) the steel casing was driven down to the design depth,
(ii) the plastic tubes for inclinometer were inserted into the casing and then

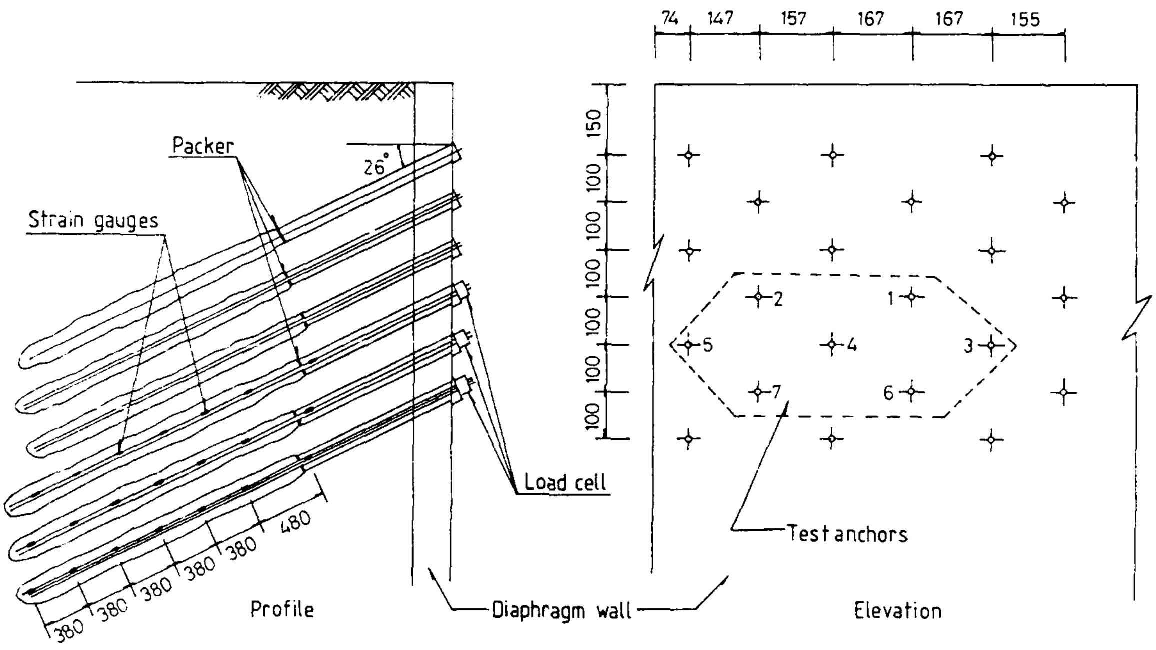

Fig. 1: Test Anchor Arrangement and Instrumentation

Tabale I: Simplified Soil Profile and Parameters

Elevation range, m	Soil Profile Description	N	γ kN/m³	c kN/m²	ϕ deg.	$\bar{c}$ kN/m²	$\bar{\phi}$ deg.	Su kN/m²
Ground Level to -2	Asphalt pavement, balast backfilled soil and silty clayey or clayey silt	5	18.6	20.6	17	0.0	23.0	24.5
-2 to -12	silty fine sand	12	19.0	-	-	-	31.0	-
-12 to -19	silty clay or clayey silt	7	18.6	30.4	15.5	0.0	28.0	58.8
-19 to -28	silty fine sand	12	19.0	-	-	-	32.0	-

Note: N: blow count of standard penetration test,
γ: total unit weight of soil,
c, $\bar{c}$: apparent, effective cohesion intercept,
ϕ, $\bar{\phi}$: apparent, effective internal angle of shearing resistance,
Su: undrained shear strength of soil,
average ground surface at elevation +4.3 m,
permanent ground water at elevation +2.0 m,
temperary ground water at elevation +3.6 m.

the borehole inclination was measured,

(iii) the wire strands with strain gauges were inserted into casing,

(iv) the borehole was grouted from bottom of the casing while retracting the casing simultaneously,

(v) in the free length part, i.e., outside the packer of borehole, the remaining cement paste was flushed out with water,

(vi) the load cell was installed after a waiting period of about 7 days and then the tensile force was applied.

The water/cement ratio of the grout was 0.5 and the grouting pressure was kept at about 0.2 to 0.5 MN/m². The pulling force was applied in steps (LITTLEJOHN, 1981) by a hollow ram jack.

TEST RESULTS

Borehole Inclination

Fig. 2 shows a typical borehole inclination (represented by dashed lines). According to the measurement of inclination (sensor length about 610 mm), the borehole inclination at each advancing length ranges from 23.4 to 27.6 degrees. The average deviation away from the designed inclination was about 1.5 degrees (Fig. 2). On the diaphragm wall, the minimum distance among the anchors was about 1.8 m. While along the bond length of each anchor, the minimum spacing calculated from the measured inclination was about 1.5 m.

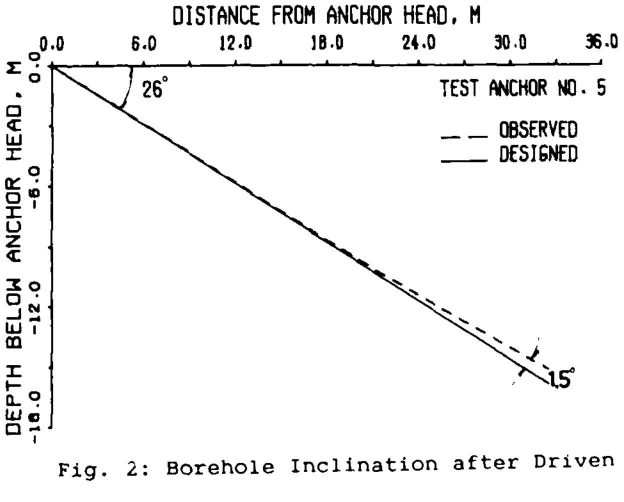

Fig. 2: Borehole Inclination after Driven

Distribution of Tensile Load

A typical distribution of tensile forces in strands and average skin friction along grout-soil interface are represented in Fig. 3. The bond length indicated on the horizontal axis refers to the position of the packer. The skin friction was obtained from the difference of forces at two neighboring points divided by the circumferential area of the grouted body. It is observed that the transmitted forces have decreased from the front to the rear part of bond length (Fig. 3A) and the distributed forces have increased when the load was kept constant for a period of time (about 5 minutes). It is also found that as the load was kept constant at high loading steps, the decrease of skin friction in the front part is accompanied by the increase of skin friction in the rear part of bond length (Fig. 3B). It must be kept in mind that the test anchors have passed through non--homogeneous soils, i.e., the first 6 m of bond length was in the layer of medium dense silty fine sand and the remaining 16 m was in the layer of silty clay or clayey silt. The behavior of test anchors shows a similar phenomenon as that disclosed in the research for non-cohesive soils (OSTERMAYER and SCHEELE, 1977).

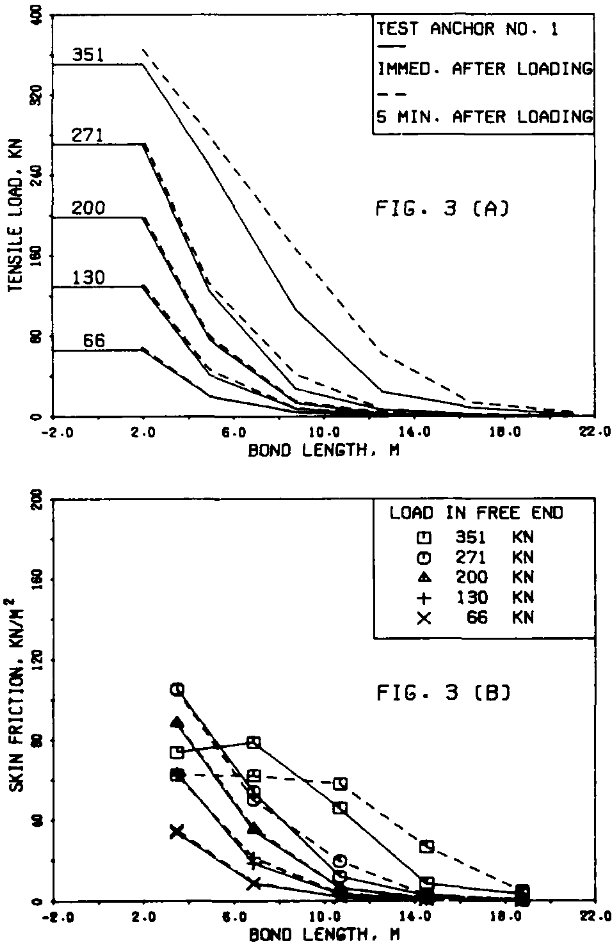

Fig. 3: Tensile Load and Skin Friction Distribution along Bond Length

The progressive failure phenomenon was found when the load applied was approaching 300 kN. It is indicated from Fig. 3 that the first 10 m of the bond length was enough to carry most of the design load. An important issue is to maintain the grout-soil interface well bound.

Continual observations on this field test were performed from February to June, 1987. The excavation work went on until the end of April. The load cell readings with respect to time are shown in Fig. 4. There was a sudden increase of tensile force in the anchor head due to 3 m depth excavation near the test site at the end of March (40 days after February 14). The readings of strain gauges with respect to time are shown in Figs. 5, 6, and 7. It was observed that the influence of excavation can be immediately detected only in the gauges of anchor number 6 (1.8 and 4.5 m away from packer in Fig. 7). The results given by the other strain gauges (over 7 m away from packer) have shown that the tensile force increased gradually at beginning, and then became steady after the end of May (about

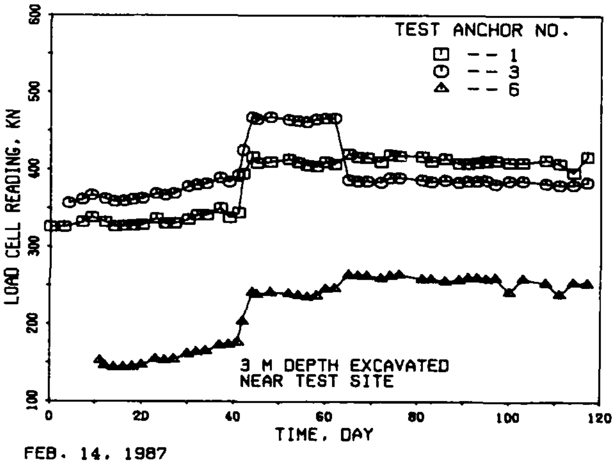

Fig. 4: Load Cell Readings with Respect to Time

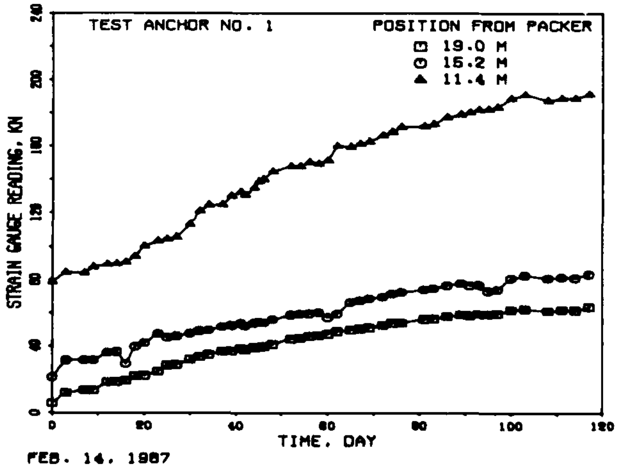

Fig. 5: Strain Gauge Readings with Respect to Time (Test Anchor No. 1)

100 days after February 14). It is noted that the tensile load in anchor number 3 decreased after excavation (Fig. 4). The readings of strain gauges at 7.6 m from packer were also affected by this decrease of tensile load (Fig 6). It has also been found that most of the anchor load was taken by the first 10 m of bond length at long term condition.

Group Effect

In order to know the group effect and stress interaction among these anchors, the stress condition was recorded for all the anchors when one of the anchors was being loaded. It is worth noticing that a particular test sequence was arranged to assure meaningful comparison, i.e., the center one in test group (number 4 in Fig. 1) was loaded until all the others had been installed. Comparing the test results before and after pulling the anchor number 4 (Table II), there was a very small difference between these two test data. The maximum value of the difference was about 22 microstrains (0.5 kN). The same phenomenon was also detected in the other test cases.

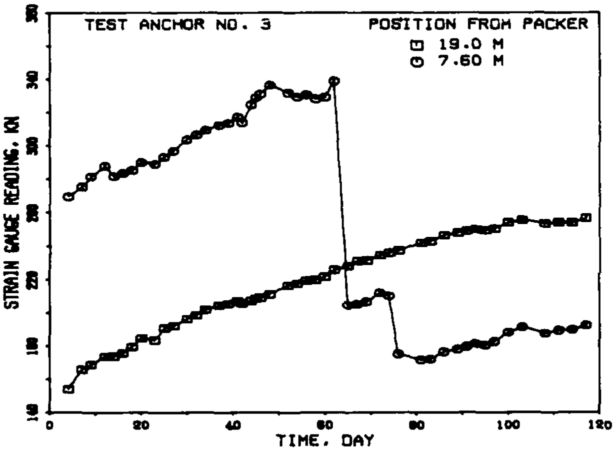

FEB. 14. 1987

Fig. 6: Strain Gauge Readings with Respect to Time (Test Anchor No. 3)

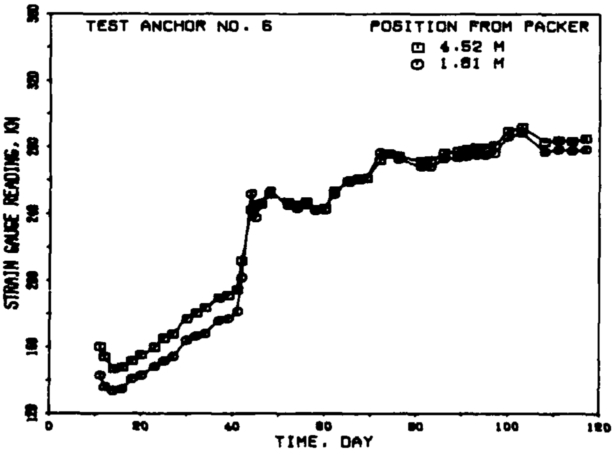

FEB. 14. 1987

Fig. 7: Strain Gauge Readings with Respect to Time (Test Anchor No. 6)

Table II: Strain Gauge Readings (microstrain) Before and After Pulling Test Anchor Number 4

Test Anchor No.	Strain Gauge Position measured from Packer, m				
	3.8	7.6	11.4	15.2	19.0
1	-	938(932)	346(341)	200(205)	-
2	-	593(598)	349(335)	122(139)	347(325)
3	-	2376(2378)	-	-	1581(1583)
5	-	2162(2144)	1688(1676)	-	329(347)
6	-20(-14)	58(58)	-29(-27)	-45(-45)	-107(-104)
7	39(36)	6(5)	19(19)	-19(-17)	-46(-44)

Note: ( ): reading after pulling test anchor 4.

For a nearest spacing of about 1.5 m along bond length, the stress interaction among the test anchors was very small when loading and unloading each one of them. Therefore, the influence of group effect was negligible.

CONCLUSIONS

After investigating the behavior of ground anchors in Taipei Sedimentary Soil, similar phenomenon was observed as that in non-cohesive soil (OSTERMAYER and SCHEELE, 1977). The average deviation away from the designed inclination was about 1.5 degrees. The first 10 m of bond length can carry most of the maximum tensile load if the grout-soil interface was well bound. For a nearest spacing of about 1.5 m along bond length between testing anchors, the stress interaction among them was very small and the influence of group effect was negligible. After five month observation, it is expected that these long term instrumentation results will help in understanding the behavior of ground anchors due to excavation effect. Because of the limited monitoring period, the influence of soil creep to the behavior of ground anchors was not fully understood and a further study is recommended.

ACKNOWLEDGEMENTS

The authors are grateful to Dr. Chin-Der Ou, Shyr Chyang and Gin-Min Wei for their helpful suggestions and contributions.

REFERENCES

LITTLEJOHN, G. S. (1981) "Acceptance Criteria for the Service Behavior of Ground Anchorages", Ground Engineering Vol. 14, No. 3.

OSTERMAYER, H. and SCHEELE, F. (1977) "Researech on Ground Anchors in Non--cohesive Soils", Special Session No. 4, 9th International Conf. on Soil Mechanics and Foundation Engineering., Tokyo.

OU, C. D. (1986) "Design Consideration and Test of Ground Anchor", Sino-Geotechnics, No. 14, April 1986 (in Chinese).

Proceedings: Second International Conference on Case Histories in Geotechnical Engineering, June 1-5, 1988, St. Louis, Mo., Paper No. 6.74

Post-Tensioned Caissons Permit Interstate Construction: A Case History

A. Joseph Nicholson, Jr.
President, National Foundation Company, USA

John R. Wolosick
Chief Engineer, National Foundation Company, USA

SYNOPSIS: Due to severe right of way restrictions associated with the relocation and widening of Interstate 85 in Atlanta Georgia, a special post-tensioned caisson retaining wall was constructed within 12 inches of an adjacent parking garage and office building. National Foundation Company's design for the twenty foot high retaining structure was used in lieu of an L-shaped cantilevered concrete retaining wall that required extensive temporary shoring for construction. The caisson wall was instrumented and monitored during and after construction using slope indicators and optical survey.

PROJECT BACKGROUND

For the past several years, the Georgia Department of Transportation has been involved in a rebuilding program requiring major widening of the existing right-of-way for the Atlanta freeway system. In the first extensive use of Permanently Anchored Retaining Walls by a state highway department, Georgia has implemented cost effective alternatives to more traditional methods of retaining wall construction.

In 1981, the Georgia Department of Transportation let a $63,000,000 contract to rebuild the Brookwood Interchange where Interstates 75 and 85 meet on the north side of Atlanta. Part of the work involved relocating portions of Interstate 85. The old highway was to remain in service parallel to the new Interstate, and would serve as a four-lane feeder road. The width and alignment of old I-85 were changed in some locations, including the area of the subject project. Grade at this

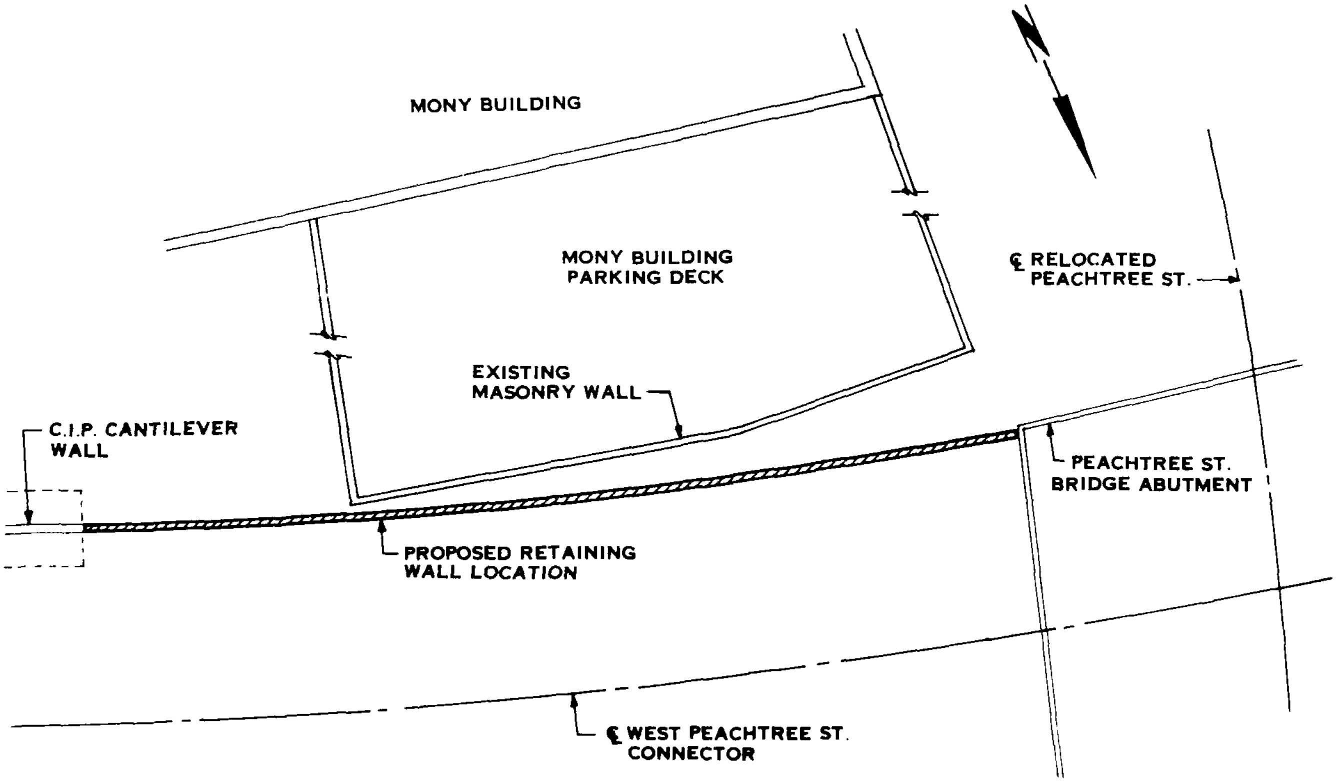
MONY BUILDING
MONY BUILDING PARKING DECK
℄ RELOCATED PEACHTREE ST.
EXISTING MASONRY WALL
C.I.P. CANTILEVER WALL
PEACHTREE ST. BRIDGE ABUTMENT
PROPOSED RETAINING WALL LOCATION
℄ WEST PEACHTREE ST. CONNECTOR

FIGURE 1. PROPOSED RETAINING WALL LOCATION

location was lowered 20 feet but the roadway shoulder was only 5-1/2 feet from an existing masonry wall. Behind this wall was a four story parking deck servicing an attached eleven story office building (see Figure 1.)

The original design drawings issued by the Georgia DOT called for sheet piling to be driven to refusal adjacent to the masonry wall. The contractor was required to design the bracing for the sheet piling to temporarily support the excavation while a concrete cantilever retaining wall was constructed. The cantilever wall was designed as an L-shaped structure due to severe right-of-way limitations which prevented construction of the heel of the footing. To adequately support the wall, the footing was to be founded on bedrock at a depth of approximately 40 feet below grade. Figure 2 illustrates the locations of the proposed temporary and permanent retaining structures. Because the new roadway was only 20 feet below existing grade, 20 feet of additional excavation below design subgrade and then 20 feet of backfill would have been required to construct the L-shaped wall on rock.

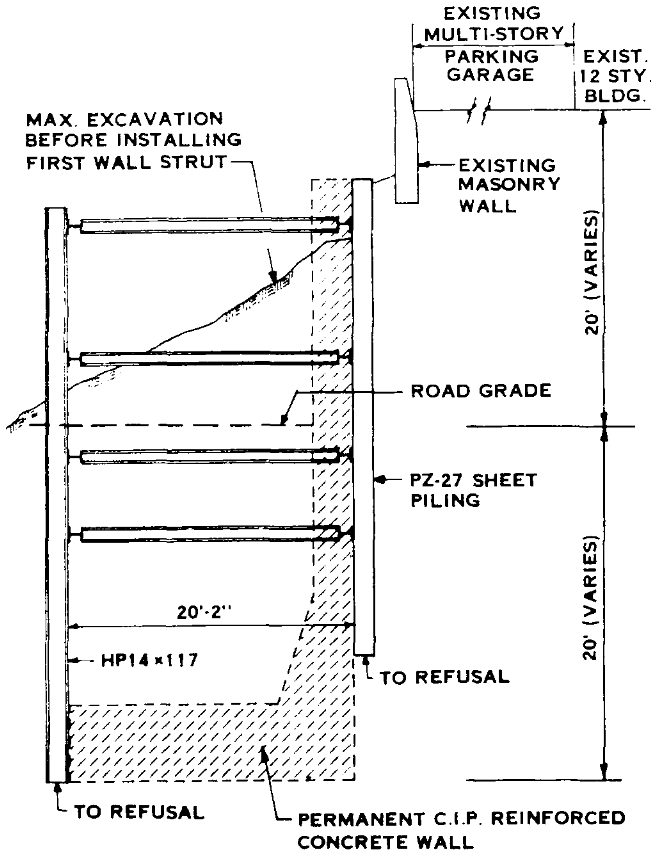

FIGURE 2. ORIGINAL RETAINING WALL SCHEME

The contractor designed a system of struts and reaction piles to support the sheeting during construction of the cantilevered wall. During a review of the shoring design, questions arose concerning the magnitude of possible lateral deflections. The Georgia DOT requested that the contractor investigate the use of temporary tiebacks rather than struts to support the sheeting. It was believed that prestressed tiebacks would greatly reduce lateral movements during excavation. Unfortunately, the owner of the adjacent building would not grant subsurface easements even for temporary tiebacks.

National Foundation Company was originally requested to prepare a cost estimate for installing the temporary tieback wall. When the subsurface easement problem arose, National Foundation proposed an entirely different scheme to limit the anticipated deflections. This scheme was based upon constructing the temporary and permanent walls as one. The proposed design limited the required excavation to 20 feet, or only the amount necessary to reach road grade. This design, which the Georgia DOT eventually accepted, is illustrated on Figure 3 and consisted mainly of the following components:

1. Fifty caissons, 42 inches in diameter, drilled from the ground surface to rock. These reinforced caissons were installed either tangent to each other or spaced 12 to 15 inches apart to form a continuous structural wall.

2. Fifty post-tensioned rock anchor tendons which were installed through a draped conduit cast into the caissons. Below the caissons, the tendons were anchored into the underlying granite gneiss bedrock which was drilled through the conduit from the ground surface. When stressed, the draped tendons imposed an eccentric load on each caisson. This load induced a moment which moved the top of the caisson backward towards the building.

WALL DESIGN

The wall design was performed by Law/Geoconsult International and required extensive coordination between geotechnical and structural personnel due to the complex soil/structure interaction mechanisms involved.

Deflection Calculations

Extensive deflection estimates were calculated to assess the effectiveness of the post-tensioned caisson concept in advance of design. These estimates were based on elastic analyses of caisson deflection using a horizontal modulus of subgrade reaction recommended by Terzaghi (1) and compared with estimates prepared for the sheet pile and strut system. The deflection estimates for the wall were based on theory presented by Kocsis (2).

The designers estimated that the temporary sheet pile and strut system originally designed for the site would deflect about 1.4 inches at the top of the wall. The Georgia DOT felt that this estimate might be optimistic. In any case, they felt that deflections should be less than about 0.75 inches to keep settlement of the adjacent masonry wall within acceptable limits. There was also concern for the adjacent parking garage since visual inspection of the drilled shafts supporting the structure indicated deterioration and cracking.

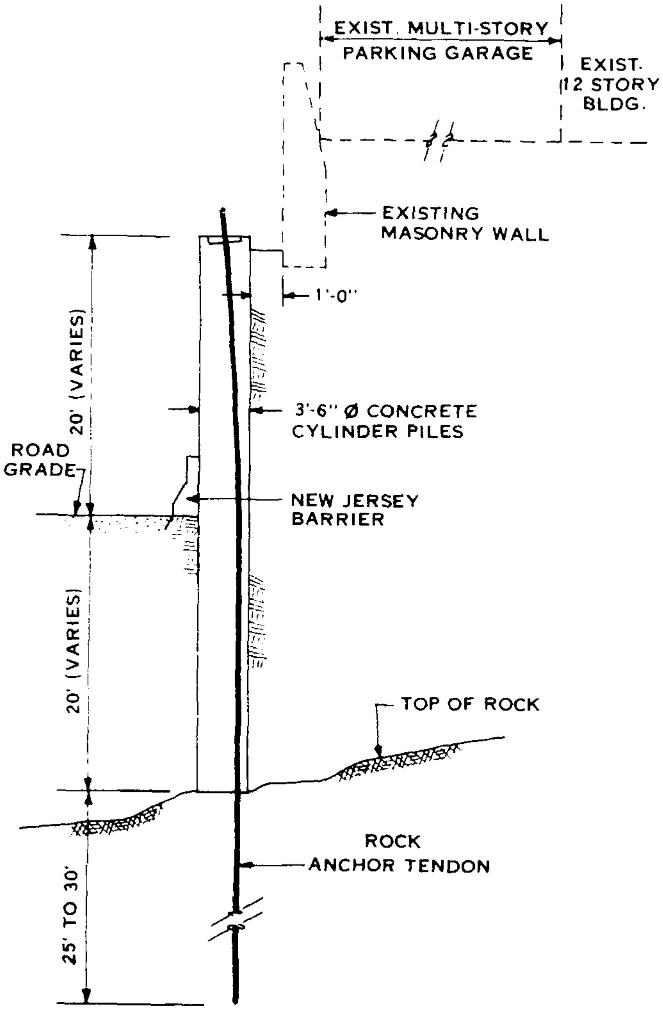

FIGURE 3. POST-TENSIONED CAISSON RETAINING WALL

Deflection calculations for the caisson wall were performed using superposition of elastic theory for the combined effects of surcharge, earth pressure, and post-tensioning. These effects were assumed to generate movements related to cantilevering as well as rotation and deflection expected at the ground line.

Deflection estimates for the caisson wall governed the caisson diameter and spacing with the limited right-of-way as the critical factor. Deflection estimates at the top of the wall were 0.7 inches for the final design caisson diameter of 42 inches.

Earth Pressure Assumptions

Earth pressures were calculated using assumed soil parameters based on standard penetration testing performed in the silty sands and sandy silts located at the site. No shear strength tests were performed on samples from the borings. However, the designers had considerable experience in these soils, so the assumed value for the angle of shearing resistance of 28 degrees had a high degree of confidence associated with it.

The specified at-rest (Ko) earth pressure distribution was added to calculated surcharge loading based on the Boussinesq (3) strip loading solution, doubled to account for stress reflection. Interestingly, the passive resistance against the caissons below grade was estimated based on the elastic horizontal subgrade modulus reactions, with an assumed point of fixity at the bottom of the caissons or at the top of rock. The passive effect was considered a resistance rather than an actual load since the point of fixity was assured by the post-tensioning tendons and/or caisson rock sockets. The resulting passive distribution was triangular shaped with zero points at the excavation line and at the rock line. The designers were comfortable with this conservative assumption since they felt that this distribution better modeled the actual loading conditions. It was felt that the classical triangular distribution which increases from zero to a maximum at the bottom of the structure might overestimate the amount of resistance available.

The groundwater table was located far below final excavation grade near to top of the bedrock, so hydrostatic pressures were not added to the earth pressure diagram. However, positive drainage was provided through the wall to prevent any accumulation of water.

Structural and Geotechnical Design

The structural design relied on theory presented by Kocsis (2) for the determination of shear and moment. The specified at-rest earth pressures and the assumed surcharge loads were used to size the caisson reinforcement and post-tensioning loads. The location of the post-tensioning ducts was governed by the caisson geometry. The ducts were placed as far to the rear of the caissons as possible to maximize the eccentricity and the moment generated by the tendons. However, the ducts were moved toward the center of the caisson near the top of each shaft and reinforcing was added to overcome excessive shear at the back of the caissons. Concrete strengths of 5000 psi were required for the caissons to resist the combined stresses.

The rock anchor tendons consisted of up to 28-0.6 inch diameter steel strands. Maximum working load was about 845 kips. The tendons were up to 88 feet in length with drill holes extending from 25 to 30 feet into sound rock below the bottom of the caissons.

A provision was made for caisson rock sockets when calculations indicated that fixity could not always be achieved with the available soil embedment indicated by the borings. The sockets were designed to be 1 or 2 feet deep, depending on the depth at which sound bedrock was encountered.

Positive drainage was provided along the wall with the use of a prefabricated drainage board placed between the caissons where they were not tangent. At tangent caissons, slotted PVC pipes were covered with filter fabric and placed in drilled holes at the point of tangency at 5 foot vertical intervals and attached to vertical PVC pipes. The drainage board and vertical PVC pipes were connected to weep holes through the New Jersey barrier at the base of the wall.

A cast-in-place, 12 inch thick reinforced concrete facing was designed for the wall. The facing consisted of 19 to 32 foot wide segments. These segments were cast around steel shear studs that were drilled and epoxied into the caissons. The facing was provided with a rusticated finish to architecturally match the adjacent conventional retaining walls.

CONSTRUCTION

Construction began in July of 1984, and took a total of 8 months. Five months were required to construct the caissons and rock anchor tendons. The remaining time was used to excavate in front of the wall and pour the concrete facing. The first phase of work was to drill the caissons, which averaged 42 feet long from the ground surface to the top of rock. Forty-two inch diameter rock sockets in the hard granite gneiss were cored for 25 of the caissons. The sockets were generally 1 or 2 feet in depth, although three of the caissons had sockets of 4, 4.5, and 6 feet in length where seamy rock was encountered. The reinforcing cages were fabricated in advance with the draped metal post-tensioning ducts tied into the proper position. The cages were lowered into the drill holes, and concrete was pumped from the bottom up, maintaining the void space in the post-tensioning ducts. When the caisson concrete had sufficiently cured, a rotary hydraulic drill rig was positioned over the ducts to drill the rock anchor sockets. The drill tools, consisting of a 6 inch diameter down-the-hole hammer and 3 inch diameter drill rods were first lowered through the draped ducts to the bottom of the caissons. The 25 to 30 foot sockets were then drilled into sound bedrock.

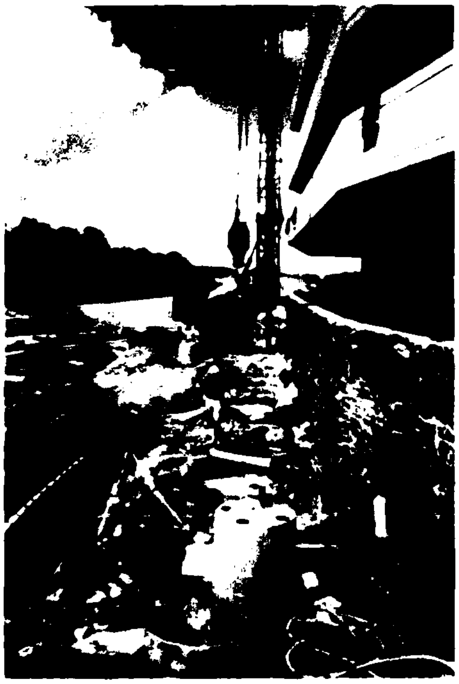

FIGURE 4. CAISSON DRILLING

Water pressure tests were performed in the rock anchor sockets to determine the relative permeability of the bedrock. When these tests all indicated water takes beyond the specified limits, the holes were grouted for water tightness and redrilled.

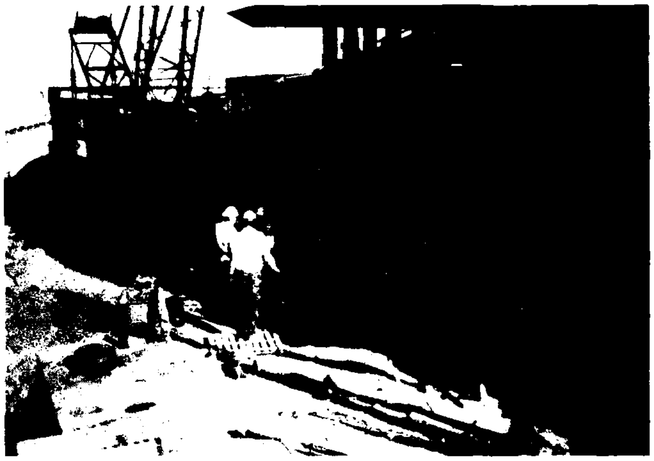

FIGURE 5. ROCK ANCHOR TENDONS

The rock anchor tendons were prefabricated and delivered to the job by truck. The individual strands were "basketed" around centralizers in the bond length to maintain at least 1/2 inch of grout cover over the steel. The tendons were placed with the aid of a crane. Primary grout, consisting of a plain cement-water mix was injected through a plastic tube placed to the bottom of the rock anchor sockets. A predetermined quantity of the mix was injected to fill only the bond length of the anchor. After allowing the primary grout to cure, bearing plates were installed at the top of the

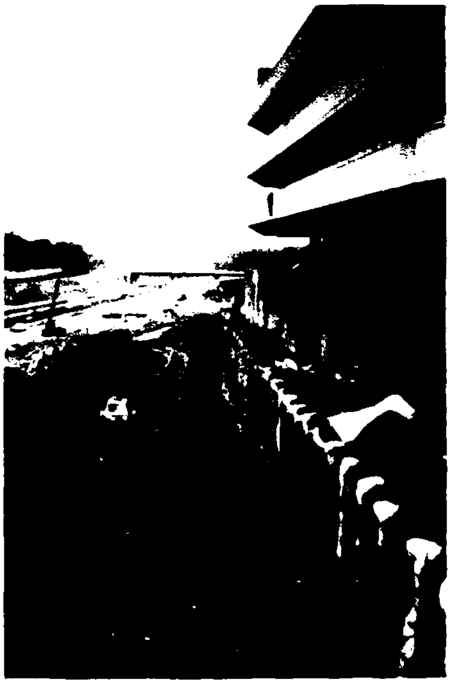

FIGURE 6. EXCAVATION IN FRONT OF WALL

caissons at an angle perpendicular to the drape of the tendons. The rock anchors were tested to 1.5 times the design load (up to 1268 kips) using a large center hole hydraulic jack, which pulled all of the strands simultaneously. Once the anchors were tested and locked off at design load, the strands were cut off and the ducts were filled with secondary grout. The bearing plates and anchor heads were encased in non-shrink grout for corrosion protection.

Excavation was performed in three lifts. As soil was removed from the face of the caissons, two separate operations took place. The drainage board or PVC drainage pipes were placed and the steel shear studs were epoxied into holes drilled into the caissons. When the excavation was complete, the reinforcing steel for the fascia was tied and the facing was cast. The weep holes were cast through a New Jersey barrier which was slip-formed along the base of the wall.

FIGURE 7. CAISSONS AND DRAINAGE BOARD

FIGURE 8. CONSTRUCTION OF CONCRETE FACING

FIGURE 9. COMPLETED RETAINING WALL

INSTRUMENTATION

An instrumentation program was implemented by the Georgia DOT to document the performance of the structure and to provide early warning of unexpected behavior. The instrumentation also provided a means to assess the adequacy of the design including checking design assumptions.

The instrumentation mainly consisted of slope indicator casings placed in four of the caissons. Caisson numbers 16, 28, 37, and 44 had steel pipes tied to the reinforcing steel cages and cast into the shafts. Inclinometer casings were then grouted inside the steel pipes. Also, optical survey measurements were performed at various locations along the wall to check for settlement and tilting.

Several inclinometer measurements were made at each caisson location to establish a baseline for the movements. These measurements were taken several weeks before stressing of the post-tensioning tendons or excavation in front of the wall. Three readings were also made on the day that the instrumented caissons were stressed. These included: 1) before stressing, 2) at 150 percent of design load, and 3) at design load. The instrumentation was read on a weekly basis before, during, and after construction for a total period of 9 months. The instruments were read monthly for a further period of 5 months. The next readings were made at 6 month and 1 year intervals. The instruments were last read in June 1987, more than 2 years after the completion of construction.

The inclinometer data provided the deflected shapes of the instrumented caissons. Plots of the deflected caissons are shown on Figures 10, 11, 12, and 13. The exaggerated horizontal scale of these figures show the evolution of the deflected profile at important milestones throughout construction and up to the most current readings.

The shafts responded to the post-tensioning by bowing backward towards the parking garage at the top and bulging outward at approximately mid-depth. The resulting shape was a smooth curve which looked like an archery bow. When the 20 foot excavation was performed to road grade in front of the wall, the released confinement allowed the tops of the caissons to bow backwards an additional amount towards the parking garage (especially where the caissons were not tangent.) The caissons then deflected and rotated outward in response to earth pressure after excavation. However, the post-tensioning forces were high enough to maintain the caissons in a permanently bowed configuration. Maximum outward deflections of 0.25 to 0.30 inches were measured approximately at roadway grade. The tops of the caissons are currently located either at their original installed positions or slightly more towards the parking garage than when first installed.

Approximately 55 to 65 percent of the outward movement of the caissons occurred within 8 weeks after excavation was complete. In general, these movements occurred uniformly, indicating a gradual application of earth pressure to the wall over an extended period of time.

Caisson 28 experienced a shift in the inclinometer casing at a depth of 37 feet, 12 days after stressing. This caisson contained the deepest rock socket (5 feet) on the project. Very seamy rock was encountered during the drilling of this caisson (a very hard zone was drilled immediately above a soft zone.) The inclinometer casing shift apparently followed the caisson's response to the application of the post-tensioning load in these subsurface conditions.

CONCLUSIONS

1. The design and construction of the wall provided a cost effective alternative to more traditional methods. The scheme used for this wall was advantageous because:
   a. The wall was built from the "top down." No temporary shoring was necessary because the caissons and rock anchor tendons were in place and functioning prior to the start of excavation.

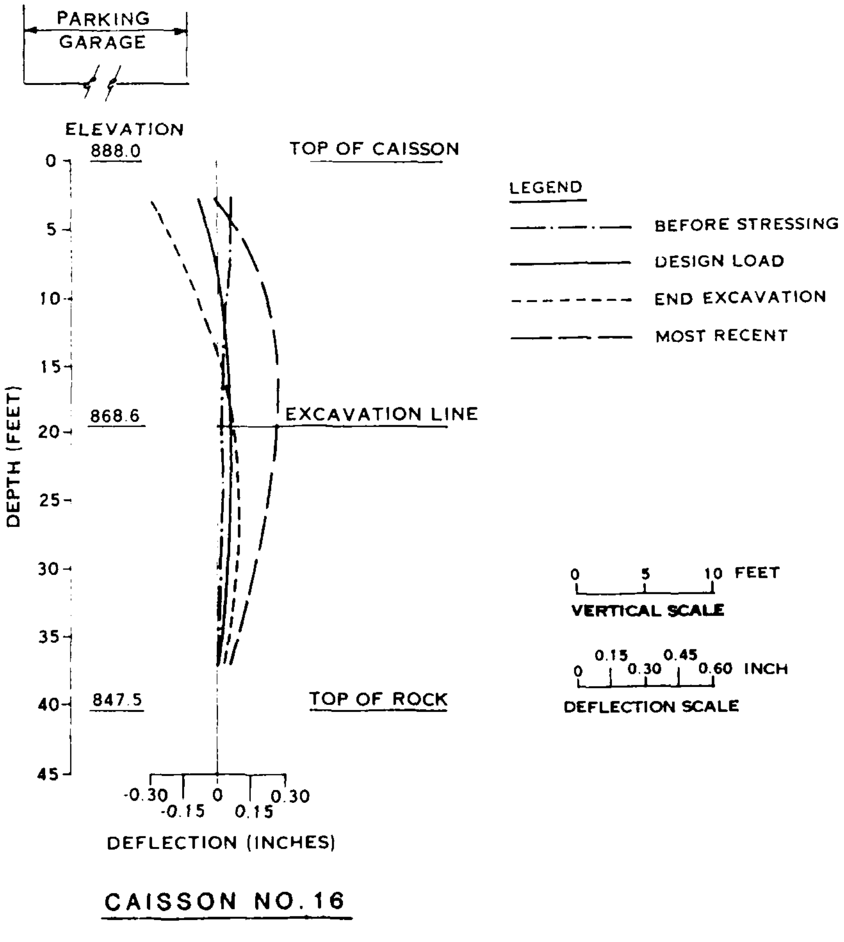

FIGURE 10. SLOPE INDICATOR RESULTS

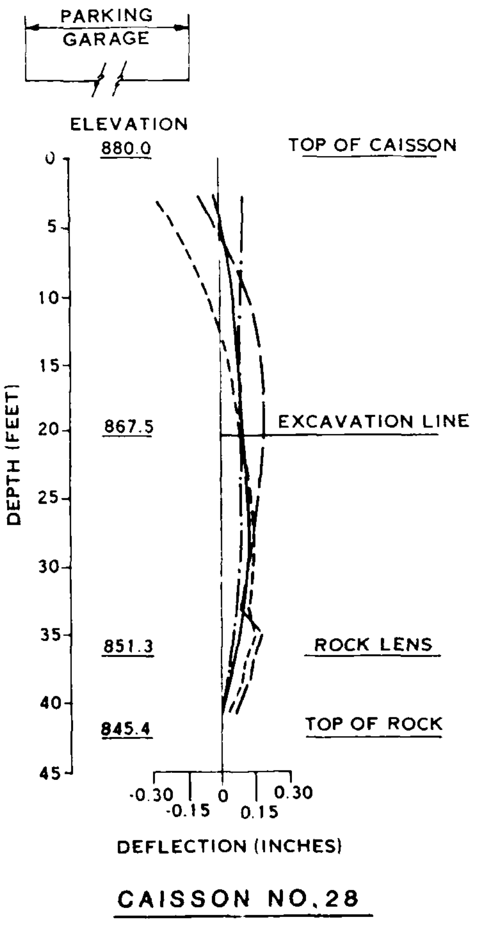

FIGURE 11. SLOPE INDICATOR RESULTS

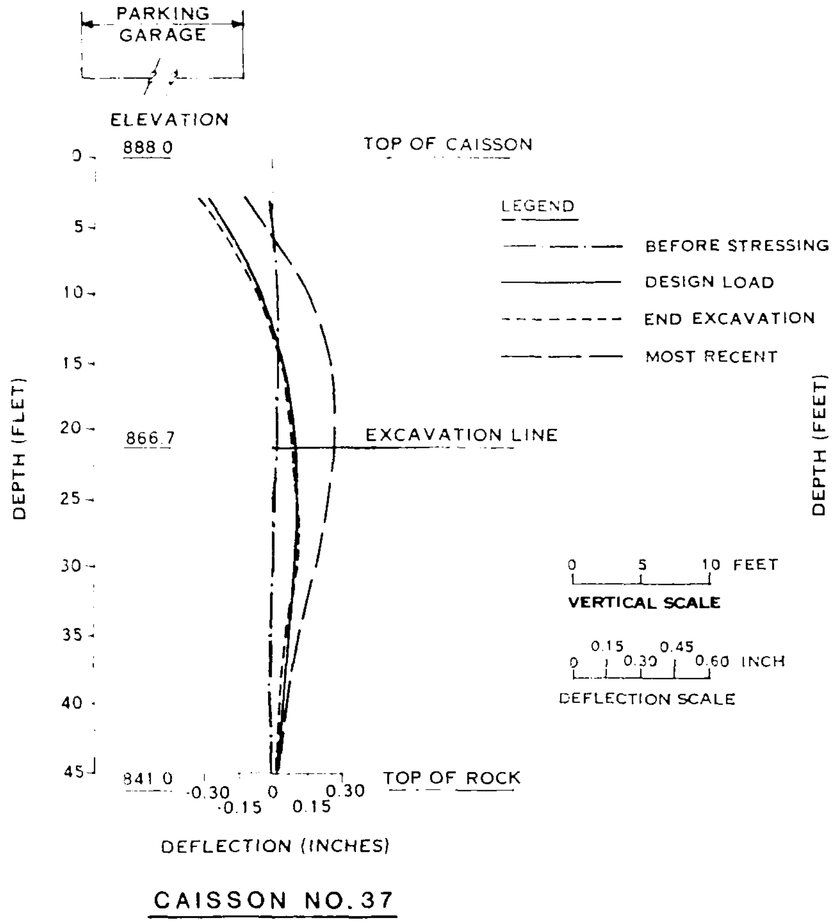

FIGURE 12. SLOPE INDICATOR RESULTS

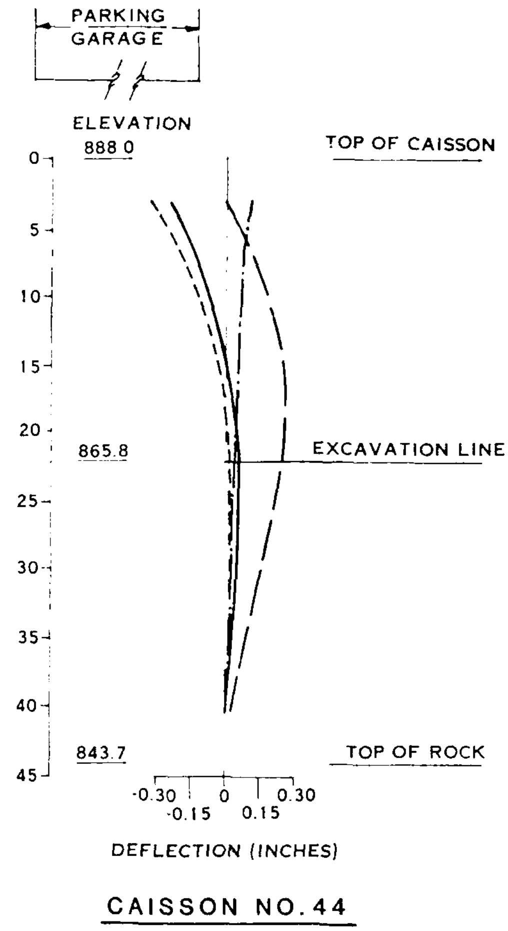

FIGURE 13. SLOPE INDICATOR RESULTS

b. It was not necessary to excavate 20 feet of the 40 foot cut originally planned. This was significant because a sensitive structure was located immediately behind the wall.

c. The rock anchor tendons did not extend behind the rear face of the wall. This feature is noteworthy in urban environments where it is often difficult to obtain easements under adjacent properties.

2. The wall did not deflect outward at the top as much as anticipated, although the pre-excavation response to post-tensioning was predicted accurately during design. The caissons responded to the post-tensioning by deflecting back towards the parking garage at the top; and by bulging outward at approximately mid-depth. The bowed shape became more pronounced after excavation was performed in front of the wall. The post-tensioning force was apparently large enough to retain the bowed shape throughout the project, even after the application of earth pressure. This locked-in shape was responsible for the reduced outward deflections observed at the tops of the caissons.

ACKNOWLEDGMENTS

The writers would like to thank the Georgia Department of Transportation for their foresight in the approval of this project, and for the excellent instrumentation data provided to us. Georgia DOT officials responsible for the project were Mr. Charles Lewis, State Bridge Engineer, and Mr. David Mitchell, Chief of the Geotechnical Branch. Structural design of the retaining wall was performed by Mr. David Shiver for Law/Geoconsult International.

REFERENCES

1. Terzaghi, K., Evaluation of Coefficients of Subgrade Reactions, Geotechnique, Vol. V, December, 1955, No. 4.

2. Kocsis, P., Lateral Loads on Piles, 68 pgs., Chicago, Illinois, 1968.

3. Boussinesq, J., Application des potentials à l'étude de l'equilibre et du mouvement des solides elastiques. Gauthier-Villars, Paris, France, 1885.

Proceedings: Second International Conference on Case Histories in Geotechnical Engineering, June 1-5, 1988, St. Louis, Mo., Paper No. 6.76

Model Test of Reinforced Earth Retaining Wall

A.S. Stipho
Asst. Prof., Civil Engineering Department, King Saud University,
Riyadh, Saudi Arabia

SYNOPSIS: Reinforced Earth techniques are fast growing procedures within geotechnical engineering practice. The ease and flexibility of the techniques make them widely accepted. In the last two decades, considerable advances have been realized in utilization of concepts in retaining structures. The analysis and design procedures for earth reinforced retaining walls had been exercised within Rankin and Mohr Coulomb theory. An earth retaining model wall was designed according to Mohr Coulomb theory with minimum factor of safety. The wall was constructed in the laboratory in much the same way as the large walls in the fields. The wall was then brought to failure by surcharge loading, during which wall behavior was monitored. The maximum surcharge load that induced failure and the mode of failure was observed. Stresses in the reinforcement strips were compared with those predicted by the theory. The efficiency, usefulness and conservativity of the technique was outlined.

INTRODUCTION

In the last five years, thousands of miles of first class highways were constructed in Saudi Arabia. Some were found along the desert flats and others were located in steep mountainous terrain. Due to the rapid construction of this comprehensive development, a great need for flexible, inexpensive convenient-to-build retaining structures arose. Some of these structures were constructed quickly and occasionally on poor foundation conditions.

Reinforced earth retaining walls were considered at various locations. Reinforced earth is a construction material composed of soil fill reinforced with rods bars of the like to strengthen the soil and increase its frictional resistance. Vidal since the early sixties developed the concept of reinforced earth; and demonstrated the beneficial effects of adding small amount of fibrous material to soil.

DESCRIPTION OF THE STRUCTURE

A sketch of the key component of a representative earth reinforced model is shown in Figure 1. The main items of the wall are the backfill materials, face units and the reinforcing elements. The backfill material is characterized by its friction properties and density. Face units need not be of a particular strength so that fabric, metal or precast concrete units are commonly used and generally referred to as the skin (Lee, Adams and Vagneron 1973). The size and type of the face elements is determined by handling convenience, esthetics, cost and technique employed. The reinforcing elements which are normally known as ties are selected by their resistance to corrosion and must be strong enough to prevent failure by breaking in tension. They are sized in such a way as to prevent failure of the structure by preventing extraction of the ties (pull out resistance).

FAILURE MODES OF THE WALL

Failure of reinforced earth retaining wall may take place due to one or more of the modes described below.

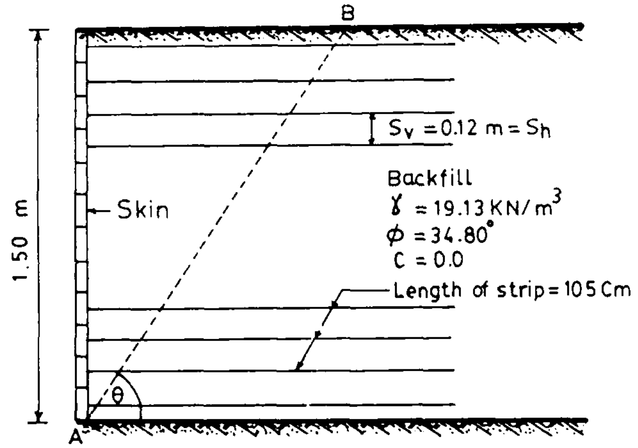

Fig. 1 Design element of the wall

Failure of the wall by slipage along a sliding wedge in the soil mass due to either failure in bond and/or tension of the reinforcing ties. This mode of failure seems to be the most commonly occuring mode of failure observed from model test results (Lee et al 1973, Lee 1976, Banerjee 1975, Al Hussaini and Perry 1978, Ingold 1981, 1982).

Other failure mode of the reinforced earth retaining wall, may be due to failure of its foundation. Such failure may occur when the load intensity on the foundation becomes more than the allowable bearing pressure of the foundation material. Skin units may also fail due to increased lateral earth pressure from possible rise of pore water pressure developed in the backfill material, if drainage by some means becomes blocked.

Once the internal stability requirements of the wall have been satisfied, the external stability of the wall presumed to act as a solid gravity mass against circular slip failure requires investigation as another possible mode of failure.

DESIGN CONCEPT

To solve any problem of soil mechanics, the basic governing equation "constitutive relations" for the soil must be defined. Formulation of such constitutive relations for sophisticated soil behavior including three dimensional anisotropic elasto-plastic constitutive relations were already advanced (Prevost, 1978, Yennis Dafalias 1982, Stipho 1985). Herein, the model wall under study was designed and idealized using a simplified model behavior such as the Mohr Coulomb criteria where,

$$\tau = C' + \sigma_n' \tan \phi' \qquad (1)$$

τ = Shear stress on slip plane

C = apparent cohesion

σ_n = normal stress, and

ϕ = angle of internal friction.

The prime (') indicates that the parameter an effective term.

This model wall was designed to have a minimum factor of safety (F.S. = 1) against snapping of strips. It was assumed that sufficient amount of lateral movement during construction takes place for the mobilization of the skin friction between the strips and the backfill material to develop an active wedge failure.

In this analysis failure of the foundation and the skin was considered not critical because the model wall was built in the laboratory using precast concrete skin units. Within this context the wedge failure occurs along the failure plane AB (Figure 1) passing through the toe and inclined at an angle θ to the horizontal; where,

$$\theta = 45° + \phi/2 \qquad (2)$$

Thus, from consideration of equilibrium, the sum of tensile forces in the reinforcement (ΣT) per metre run of the wall can be found as:

$$\Sigma T = \frac{1}{2} . \gamma . H^2 . \text{Cot } \theta . \tan(\theta - \phi) \qquad (3)$$

or $$\Sigma T = \frac{1}{2} K_a . \gamma . H^2 \qquad (4)$$

where:

ΣT = represents the sum of reinforcement tension per metre run of wall.

H = the wall's height

γ = soil's unit weight

$$K_a = \frac{1 - \text{Sin } \phi}{1 + \text{Sin } \phi}$$

Similarly the tension in each layer of reinforcement varies with depth, and the maximum tension in the mth layer at the bottom per metre run of the wall could be given as (Schlosser and Vidal 1969);

$$T_i = \frac{i}{m+1} . K_a . \gamma . H . S_v \qquad (5)$$

where:

m = number of reinforcing layers

i = variable from 0 to m

S_v = the vertical spacing between each layer of reinforcement.

This T_i should be less than the ultimate tensile strength of the ith layer of reinforcement. Therefore, for a desired factor of safety the reinforcement per metre run can be obtained.

$$T_i = f_s . A . n_{si} \quad (\text{F.S.} = 1) \qquad (6)$$

where

f_s = the maximum tensile strength of the strips.

A = cross section area of the strip.

n_{si} = number of strips per metre run of wall at ith layer.

PULL OUT RESISTANCE

In the design of a reinforced earth retaining wall, the check on the likely bond stress along the strip's effective length that produce adequate pull out resistance is very necessary. The effective strip length (L) is the actual length put to work to resist the pull out. It is mainly the length beyond the proposed failure plane. The pull resistance depends upon the strip size and the angle of friction between the strip and the soil (ψ). The maximum frictional resistance of the strips per metre run at depth (h) can be calculated as:

$$F_h = (2 L . \omega . \gamma . h . \tan \psi) \frac{1}{S_h} \qquad (7)$$

where:

L = effective length of strip

ω = width of the strip

γ = backfill unit weight

h = height above strip's level

ψ = angle of friction between strip and the backfill soil

S_h = the horizontal spacing of strips.

The total horizontal stress at the depth (h) causing the pull out per metre run can be determined as:

$$\sigma_h = K_a . h . \gamma . S_v \qquad (8)$$

MODEL TEST

A reinforced earth retaining wall 1.5 m height, 1.5 m long and 1.5 m wide was constructed at the Civil Engineering Geotechnical Laboratory to examine the behavior of a reinforced earth retaining wall during construction and at failure. The number and size of the strips were calculated from equation (6) and were made from galvanized steel. The strips had a maximum tensile strength ot 120 N/mm^2. The strips were all 7 mm in width and 0.095 mm thick. The length of each strip was taken as 0.7 H or equivalent to 1.05 m. The skin elements were made of units 15 x 15 x 3 cm shaped in such a way as to give an interlocking effect in the four directions as shown in Figure 2.

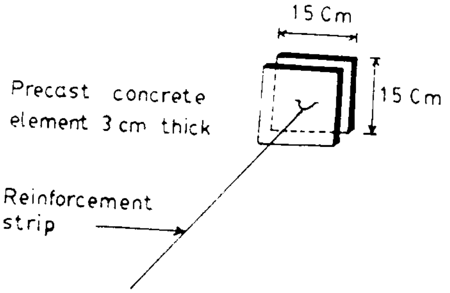

Fig. 2 Details of face units

Each unit has an embedded steel connector to which the strip was tied. The fill material used was clean, well graded coarse sand (G = 2.61) having an angle of internal friction (ϕ) equal to 34.8°, with zero cohesion. The soil's maximum dry unit weight (γ_d) was 19.13 KN/m^3 with an optimum moisture content of 13.2%. To assure maximum sand density during the test, a special concrete roller was designed based on the compaction efforts used during the test. The number of passes for 15 cm lifts were determined according to the size and weight of the roller used. However, field density tests were conducted every 50 cm of the wall height to verify the value of maximum dry density.

The wall was constructed within a steel framed box with three sides made of 18 mm thick clear perspex. The perspex sidings were used to enable monitoring the shape and location of the shear plane. The galvanized steel strips were instrumented with strain gages connected to a read out station. The strain gages were fixed on the strips at points where the expected failure plane cuts at that particular strip level. These were used to measure the tensile strength of the strips at the failure plane during the test. The outward movements of the skin elements were also monitored by a set of mechanical dial gages arranged and fixed on rigid steel tower in front of the wall. After the desired height (1.5 m) was reached, the structure was left for one week protected and undisturbed. A surcharge loading was then presumed by applying linear surcharge load (SL) at D = 50 cm away from the face line, and increased until failure took place.

TEST OBSERVATIONS

The outward deflection of the skin at each reference point of the wall's height at the end of construction was recorded and compared with that value found at the stage surcharge loadings and failure (Figure 3). It can be noticed that very minor movements of the skin took place after construction was complete. An outward movement, particularly at the base, of about 1% of the wall's height was recorded at failure. This movement was sufficient to produce a definite failure surface as indicated by the offsetting of the backfill soil mass. The observed shear plane was compared with that assumed in the theory and shown in Figure 4. A small deviation from the theoretical plane at the bottom part of the wall was noticed. This could well be due to the presence of the ties and disturbance caused by the leads of the strain gages.

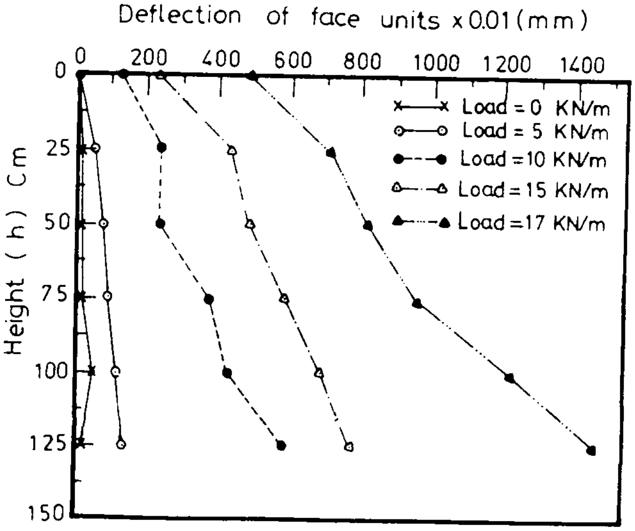

Fig. 3 Stage deflection of the wall

On the other hand to clarify the assumption used in the design of ties, the state of stress acting on the wall at the end of construction and on the ties was recorded. The data observed from the gages, at the theoretical position of the shear surface, was compared with lateral pressure acting on the same section of the wall at that level and presented in Figure 5. The measured pressure seems to follow a pattern reasonably close to the theoretical, dotted line, particularly at the top sections of the wall. At the bottom sections of the wall mixed levels of stresses were observed. This indicates that the maximum tensile stresses in the ties may not necessarily occur at the failure plane as suggested by Lee et al 1973.

The test indicates that model wall supports higher loads than predicted by theory. Using the concept of surcharge loading treated by Schlosser and Long 1974; it could be concluded that this model wall displayed a ratio of actual to theoretical load value to 1.46. This ratio is higher than the ratio, found by Bell

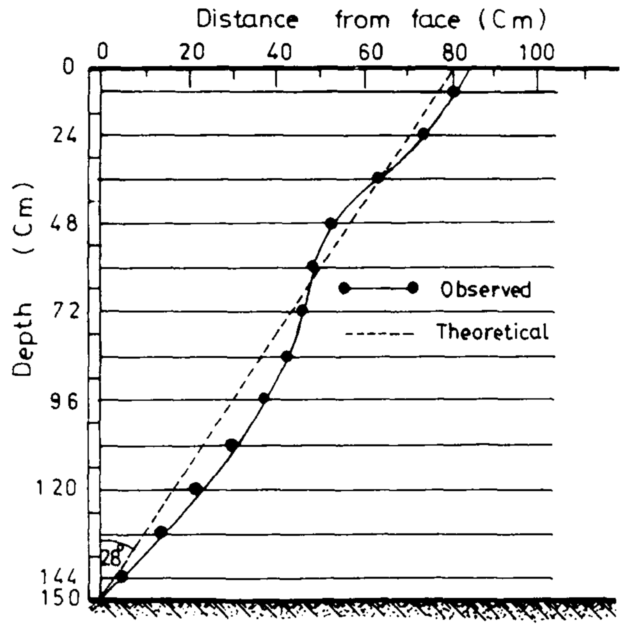

Fig. 4 Comparison between theoretical and observed planes after surcharge loading.

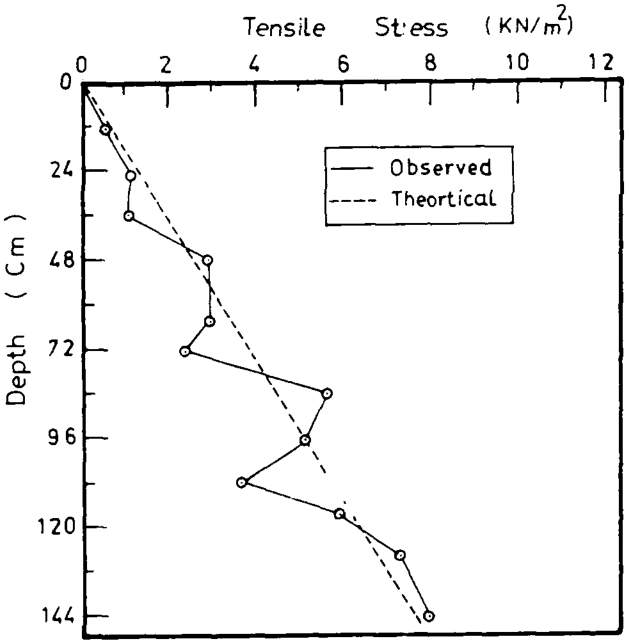

Fig. 5 Comparison between calculated and observed stresses along the failure plan.

et al 1974 testing fabric reinforced earth wall analysed by Rankin theory. However, the model wall demonstrated the feasibility of the design and construction method of such walls. Apart from the serious questions about the boundary effect and the friction constraints at the sides of the model test; it appears that the theory used can produce a conservative earth reinforced walls cheaply.

The author expresses his gratitude to Dr. Al-Dhowalia, Head of Civil Engineering Department for making facilities of the department available for this work, Mr. Waddah Jabr for conducting the test and also Mr. Abdul Sattar who helped all the way during the test and the preparation of the diagrams.

REFERENCES

Al Hussaini M. and Perry, E. (1978), "Field Experiment of Reinforced Earth Wall", J. of Geot. Eng. Div. ASCE, GT3, pp. 307-322.

Banerjee, P.K. (1975), "Principles of Analysis and Design of Reinforced Earth Retaining Walls, J. Int. Higher Engrs. 22, No. 1, pp. 13-18.

Bell, J.R., Stilley, A.N. and B. Vandre (1975), "Fabric Retained Earth Walls", Proc. 13th Ann. Eng. Geological and Soil Eng. Symp. Idaho, pp. 271-287.

Ingold, T.S. (1982), "Reinforced Earth", Pub. Thomas Telford Ltd., London.

Ingold, T.S. (1981), "Reinforced Earth Theory and Design", Proc. Inst. Higher Engrs, 28, No. 7.

Lee, K.L. (1976), "Reinforced Earth - An Old Idea in a New Setting". International Symposium on New Horizons in Construction Materials, held at Bethlehem, Pa. Envo Pub. Co., Vol 1, pp. 655-682.

Lee, K.L. Adams, B.D. and Vagneron, J. (1973), "Reinforced Earth Retaining Walls", J. of Soil Mech. and Found. Eng. ASCE, Vol. 99, No. 10, pp. 7845-764.

Prevost, J.H. (1978), "Anisotropic Undrained Stress-Strain Behavior of Clays", J. of the Geot. Division ASCE, Vol. 104, pp. 1075.

Schlosser, F. and Long, N.T. (1974), "Recent Results in French Research on Reinforced Earth, J. of Const. Div. ASCE, 103, pp. 223-237.

Schlosser, F. and Vidal, H. (1969), "Reinforced Earth" (French) Bulletin de liaison des Laboratories Routiers, Paris, pp. 101-144.

Stipho, A.S. (1985), "Prediction of the Behavior of Natural Clay Deposits", Proc. 5th Int. Conf. on Numerical Methods in Geomechanics, Nagoya, Japan, pp. 309-315.

Vidal, H. (1966), "La terre armee", Arales de Institute Technique du Batiment et des Travaux publics Nos. 223-24, pp. 888-938.

Yennis, F. Dafalias (1982), "An Elastic Plastic Viscoplastic Constitutive Modeling of Cohesive Soils, Int. Symp. of Numerical Models in Geomechancis, Zurich, p. 126.

Proceedings: Second International Conference on Case Histories in Geotechnical Engineering, June 1-5, 1988, St. Louis, Mo., Paper No. 6.77

Repair and Rehabilitation of a Residential Building at Nile River in Cairo

Sayed Abdel-Salam
Assoc. Professor of Structural Engineering, University of Zagazig, Egypt

Mohsen Mashhour
Assoc. Professor of Geotechnical Engineering, University of Zagazig, Egypt

SYNOPSIS: Five floors were added to a six storey building during its construction without carrying out necessary structural calculations. When such calculations were later performed they revealed that both the spread footing foundation and many columns were unsafe. The contact pressure beneath footings exceeded the allowable soil pressure.

The repair method described in this paper depended on disregarding the spread footing foundation and constructing a new deep foundation system for the existing building. This consisted of end bearing bored piles drilled and cast in the voids between the footings using a special low rise rig. The piles were connected to a rigid reinforced concrete raft located above the footings. The raft in turn was connected to the ground floor columns by means of reinforced concrete jackets. Unsafe columns were repaired using reinforced concrete jackets. Settlement observations were carried out for a sufficient period of time after repair with additionally applied test loads which showed satisfactory results.

INTRODUCTION

The problem which is being resolved in this paper has arisen when the owner and contractor of a residential building had decided, during construction, to complete the building to eleven stories. The building was originally designed to consist of six floors only. This was accomplished without carrying out any further structural calculations and soil investigation. The local authorities prohibited the use of the building pending a consultant engineer's report assuring the safety of the building. The structural status of the existing building had to be first carefully determined in order to evaluate its safety. For this end some of the procedures suggested by Bresler (1985) were utilized. The following steps were followed: (1) Soil investigation. (2) Structural survey and (3) Structural calculations for the existing foundations and superstructure.

The above study had shown that the foundations and some other structural elements were unsafe. The contact pressure beneath footings had also exceeded the allowable safe soil pressure. An appropriate method of repair, believed to provide a high degree of safety as well as economy, was designed and constructed.

DESCRIPTION OF THE BUILDING

The building lies at the east bank of the Nile River in Moneib district at Giza zone of the city of Cairo. It is a residential eleven storey building constructed of reinforced concrete skeleton consisting of columns, beams and slabs. Figure 1 shows the ground floor plan. The foundations consisted of isolated and combined reinforced concrete footings, Figures 2 and 3. Foundation level was -2.80 m from ground level. Construction commenced in January 1983 and ended in early 1985.

SOIL INVESTIGATION

The spread footing foundations were designed to support a six storey building. Moreover soil data used in the design were assumed, rather than measured, based on local experience in soil types and formations of this area. It was necessary therefore to carry out a proper soil investigation. Three boreholes were sunk around the building at the locations illustrated in Figure 1. Boring depth was 17.00 m. Figure 4 shows a typical borehole log. The borehole logs unexpectedly revealed that the spread foundations were resting on a layer of fill about 2.00 m thick with relatively low bearing capacity.

STRUCTURAL SURVEY

The building was carefully examined from both outside and inside where no cracks were observed. The strength of concrete composing different structural elements were determined using non destructive testing by means of a rebound hammer device, Clifton (1985). The cross sectional dimensions of columns and beams were measured and compared with those of the original design. The footings were uncovered and their real dimensions were also measured together with the foundation depth. Only slight differences were found between the actual dimensions and those in the original design drawings. However a new set of drawings for the building was prepared based on the real measured dimensions.

STRUCTURAL REDESIGN

The loads acting on different structural elements of the building were calculated for both dead and live load cases. The internal forces and stresses were determined for beams and columns. The normal stress in 10 columns at different floors exceeded the allowable value. The contact pressure beneath each footing was also determined. Its

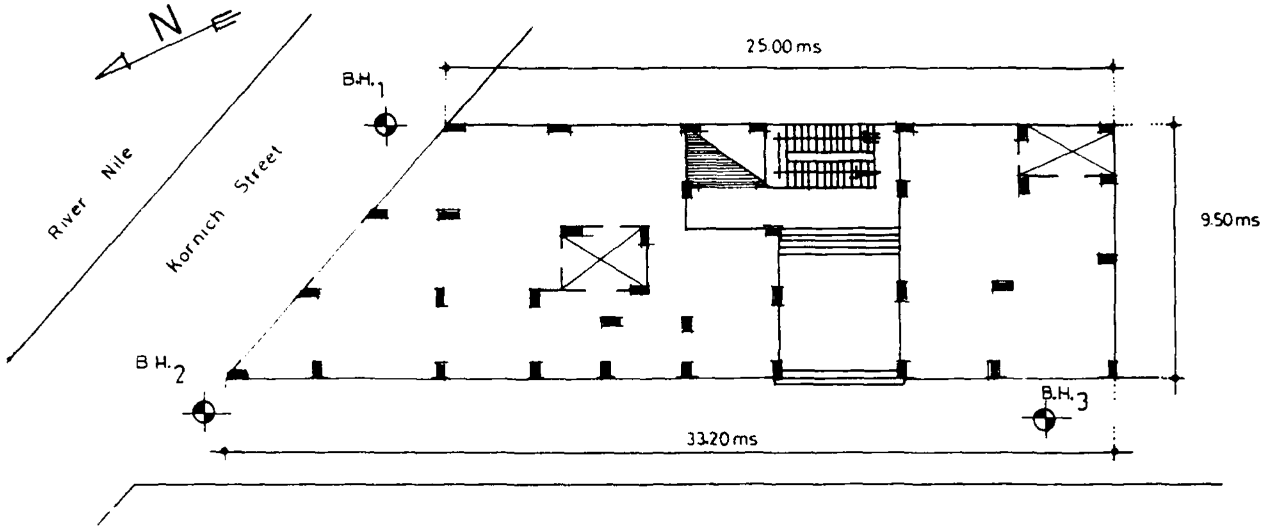
N
River Nile
Kornich Street
B.H.1
B.H.2
B.H.3
25.00 ms
9.50 ms
33.20 ms

Fig. 1 : Plan of the Ground Floor

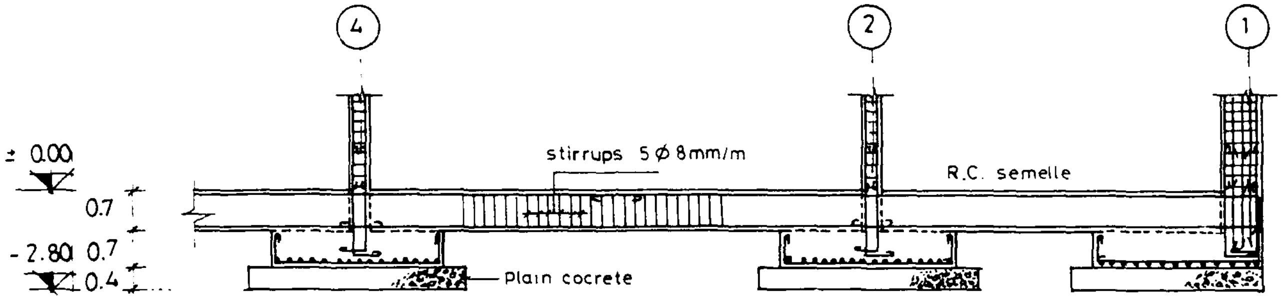
4
2
1
± 0.00
0.7
- 2.80
0.7
0.4
stirrups 5 ϕ 8mm/m
R.C. semelle
Plain cocrete

Fig. 2 : Section A-A in the Old Foundations

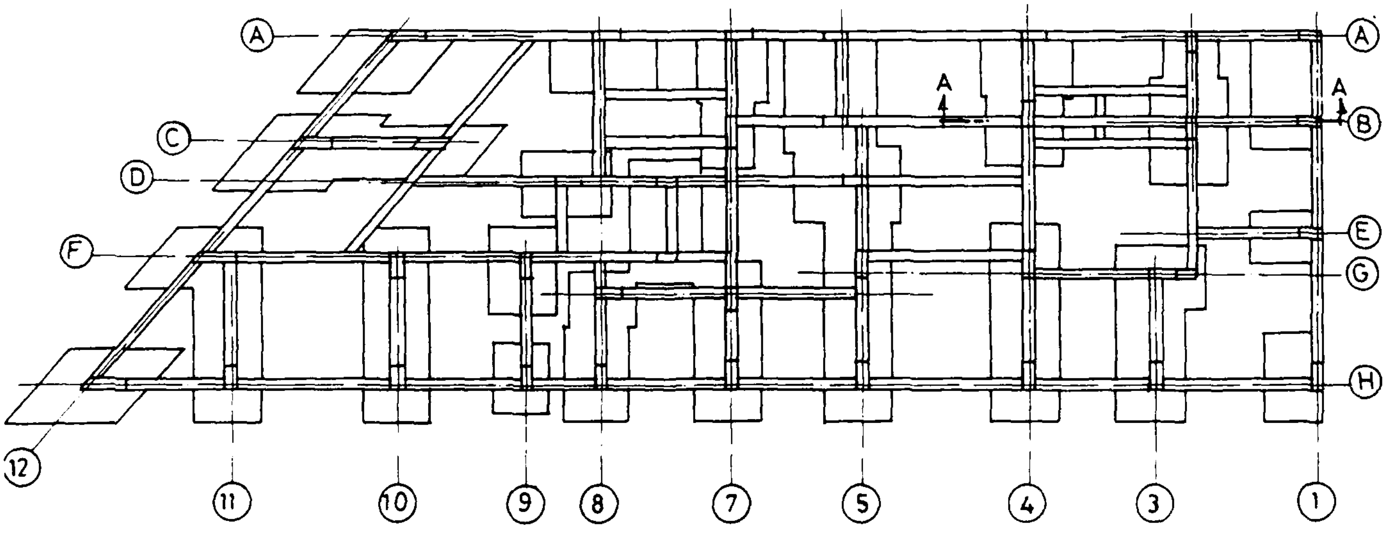
A
C
D
F
B
E
G
H
A
A
12
11
10
9
8
7
5
4
3
1

Fig. 3 : Plan Showing Old Spread Footing Foundation

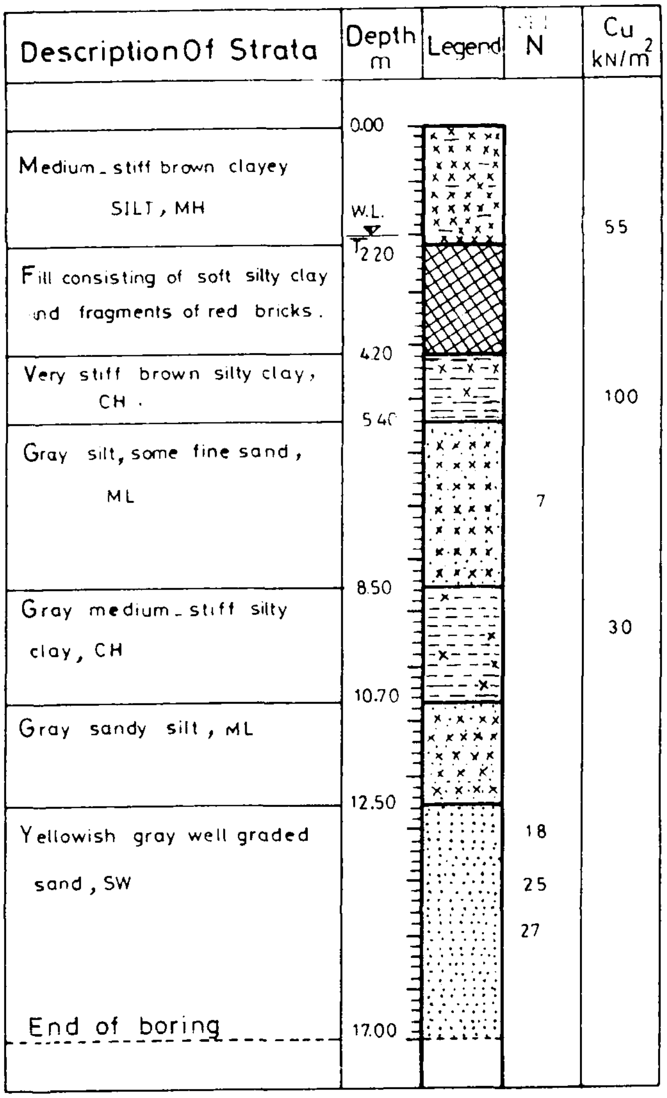
Description Of Strata
Depth m
Legend
N
Cu kN/m^2
0.00
Medium - stiff brown clayey SILT, MH
W.L.
2.20
55
Fill consisting of soft silty clay and fragments of red bricks.
4.20
Very stiff brown silty clay, CH.
100
5.40
Gray silt, some fine sand, ML
7
8.50
Gray medium - stiff silty clay, CH
30
10.70
Gray sandy silt, ML
12.50
Yellowish gray well graded sand, SW
18
25
27
End of boring
17.00

Fig. 4 : Typical borehole Log

value for the case of dead load only ranged betweek 150 and 300 kN/m2 whereas the allowable bearing pressure for the soil below the foundation was 75 kN/m^2.

METHOD OF REPAIR

Common techniques for soil strengthening, such as underpinning, had been considered and ruled out since they would only improve the soil and not the foundation. In the studied case, however it has been proved that the spread footing foundation itself was too weak to support the eleven storey building. The suggested solution depended on disregarding the spread footings, designing and constructing a completely new foundation system for the existing building. This new foundation system consisted of end bearing bored reinforced concreted piles. The piles were bored and cast in the void areas between the footings using a specially manufactured low rise drilling rig. They were 400 mm diameter each and reinforced with five 16 mm diameter rebars and a spiral stirrup 8 mm diameter with 100 mm pitch. Due to the limited head room of the ground floor, reinforcement cage for every pile was divided into three parts each 4.75 m long. The three parts were placed and spliced. The piles rested on the dense sand layer at 14.00 m depth from ground level. Allowable load per pile was 40 t. Figure 5 shows the distribution of piles in plan. Not more than one pile was bored near a footing every day in order to avoid soil deformation beneath the footing due to boring. The piles were connected to a rigid reinforced concrete raft whose bottom was 100 mm above the top of the old foundations. This gap was filled with sand to avoid loading of the old foundations by direct contact.

In order to transfer column loads to the raft, reinforced concrete jackets were used (Abdel - Rahman, 1985). Jackets were also used to repair the overstressed columns. Typical types of the column jackets used are illustrated in Figure 6. The surface of columns to be repaired were first roughened then an adhesive epoxy was applied to the surface. Steel reinforcement was placed in place. Floor slabs above the repaired columns were broken around columns and the slab was supported by timber struts. The resulting gaps were used to cast concrete down into jacket forms. These gaps also allowed the jacket reinforcement to extend to a higher floor level, Figure 7.

Figure 8 shows a cross section in the new foundation system. The distribution of piles was irregular following the location of void areas between the footings. This irregularity was taken into consideration in the design of the raft. The piles, raft and column jackets were designed to carry both dead and live loads including wind forces.

Settlement observations were taken for a sufficient period of time after repair with additionally applied test loads which showed satisfactory results. The building has been safely used since January 1987.

CONCLUSIONS

A residential building subject to failure has been successfully and economically repaired. The susceptibility to failure of the building was attributed to the following three reasons. 1- The spread footing foundation of the building rested on a weak fill layer with contact pressure exceeding the allowable safe soil pressure, 2- reinforced concrete footings were unsafe and 3- the stresses in many columns exceeded the allowable value. The adopted method of repair is thought to be original. It also provides a very high degree of safety to the building since a completely new deep foundation system was designed and constructed. Both the weak fill layer and the old spread footing foundations were disregarded and relieved of loads. Unsafe columns were repaired using reinforced concrete jackets. Since the problem was initially caused by alteration to an existing building, attention is again drawn to the importance of undertaking thorough structural redesign calculations before executing such alterations

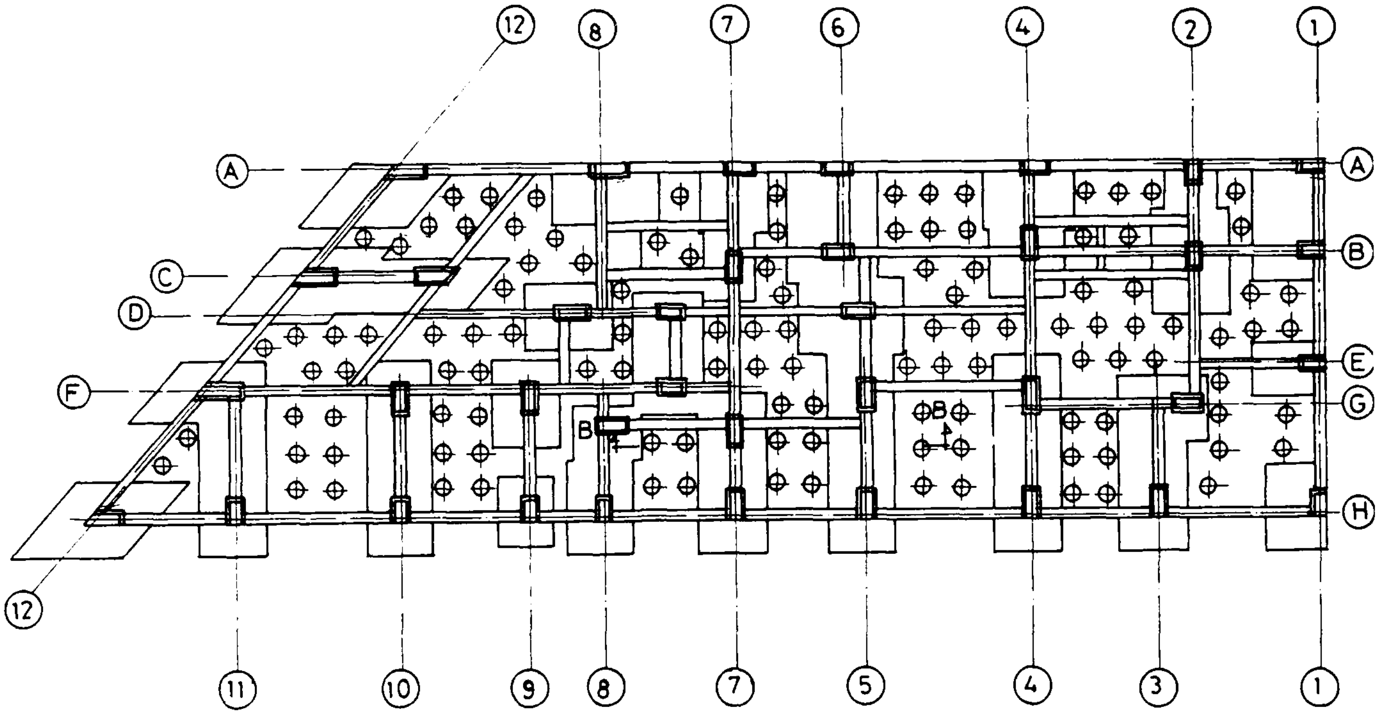
12
8
7
6
4
2
1
A
B
C
D
E
F
G
H
B
B
12
11
10
9
8
7
5
4
3
1

Fig. 5 : Plan of the New Pile Foundation

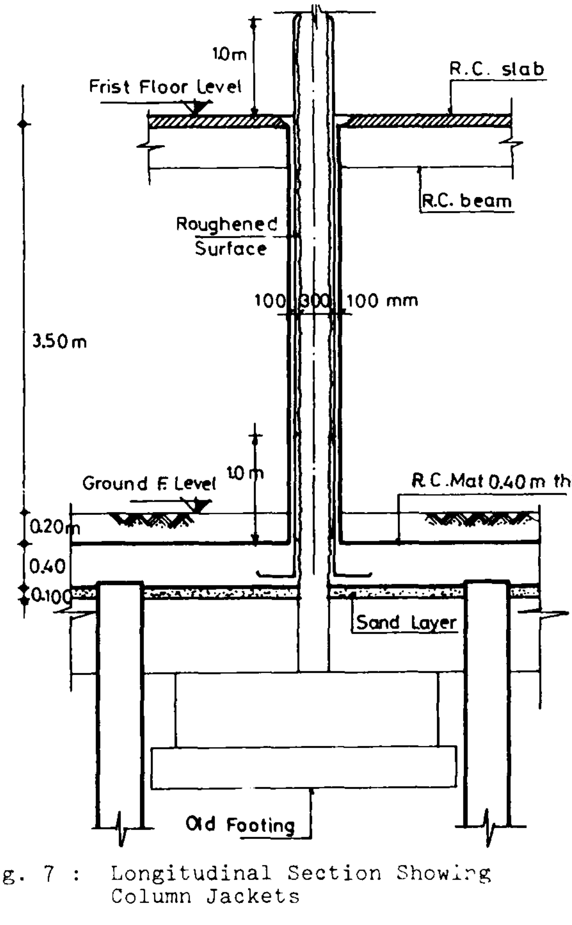
1.0m
Frist Floor Level
R.C. slab
R.C. beam
Roughened Surface
100
300
100 mm
3.50 m
1.0 m
Ground F. Level
R.C.Mat 0.40 m thick
0.20m
0.40
0.10
Sand Layer
Old Footing

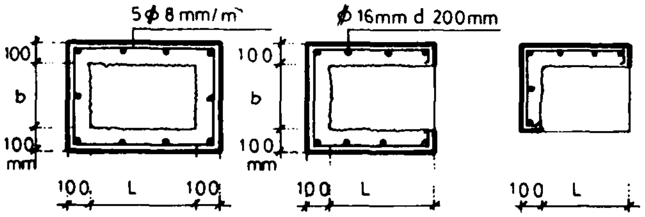
5φ 8 mm/m'
φ 16mm d 200mm
100
b
100 mm
100
b
100 mm
100
L
100
100
L
100
L

Fig. 6 : Typical Sections for the Concrete Jackets Used

Fig. 7 : Longitudinal Section Showing Column Jackets

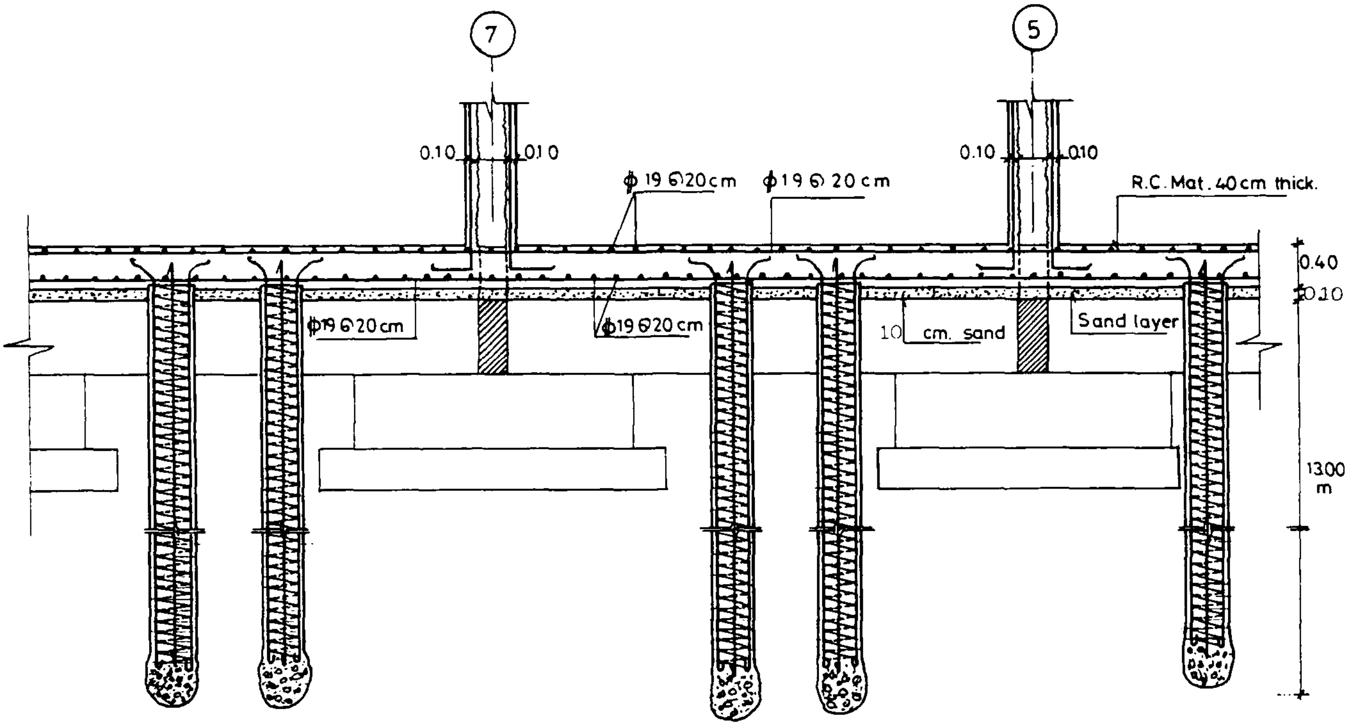
7
5
0.10
0.10
0.10
0.10
ϕ 19 @ 20cm
ϕ 19 @ 20 cm
R.C. Mat. 40cm thick.
ϕ19 @ 20cm
ϕ19 @ 20 cm
10 cm. sand
Sand layer
0.40
0.10
13.00 m

Fig. 8 : Section B-B in the New Pile Foundations

REFERENCES

Abdel-Rahman, A. (1985), "Strengthening of Columns by Concrete Jackets", Proc. I: Arab Structural Engineering Conference, Cairo, 5: 1-17.

Bresler, B. (1985), "Essential Step in Adaptation of Old Buildings", Symposium on Rehabilitation, Renovation and Preservation of Concrete and Masonry Structures, ACI, 1-18.

Clifton, J. (1985), "Nondestructive Evaluation in Rehabilitation and Preservation of Concrete and Masonry Materials", Symposium on Rehabilitation, Renovation and Preservation of Concrete and Masonry Structures, ACI, 19-30.

Proceedings: Second International Conference on Case Histories in Geotechnical Engineering, June 1-5, 1988, St. Louis, Mo., Paper No. 6.79

Behavior of Buried Concrete Box Culvert

Y.S. Kim
Assistant Professor, The Catholic University of America, Washington, District of Columbia

P.Y. Thompson
Chief Scientist, Air Force Engineering and Services Center, Tyndall AFB, Florida

ABSTRACT: The centrifuge model technique is used to evaluate the behavior of a 5-in. X 5-in. concrete box culvert under a 4-in. backfill soil. Two different types of soil installations are studied: embankment and trench. Results of the centrifuge model study for both installations are compared with each other, and with predictions of a finite element code, CANDE (Culvert ANalysis and DEsign). Furthermore, the influence of soil stiffness for backfill is studied. The results of CANDE analyses including a nonlinear constitutive model for characterizing soil and incremental construction with a symmetric mesh are reported.

INTRODUCTION

During the past decade, research on soil-structure interaction of circular culverts under embankments was performed by numerous research groups. Empirical data on soil pressure distributions and structural stresses and deflections has been collected for shallow to moderate depth installations. As a result, the soil- structure interaction problems of circular culverts embedded in embankments are better understood, and new design and analysis procedures are being proposed. However, research on box culverts has been limited, and the behavior of box culverts is not well understood. Due to an increased interest in protective and buried structures, a better understanding of soil-structure interaction and more accurate calculation of soil pressure distributions and concrete section behavior are required.

In recognition of further research needed in these areas, a comprehensive research program has been initiated to study the behavior of box culverts under static and dynamic loadings. This paper presents the results of a series of small scale (1/60) model tests that has been performed with emphasis on: (1) development of an experimental technique using a centrifuge, (2) the influence of installation (embankment and trench) and soil types, and (3) a comparison study between the results of centrifuge and numerical model (finite element method) studies for static structural responses.

CENTRIFUGE MODEL STUDY

Perhaps one of the most ideal approaches for obtaining information on the behavior of prototype structures is full scale model testing. A full scale model with the necessary insrumentation (i.e., soil stress meters, pore water pressure transducers, settlement gages and strain gages, etc.) could give the best results for estimating prototype soil and structural behaviors. Unfortunately, full scale model testing has serious major drawbacks: mainly, cost and time of construction and operation. Because of these reasons, small scale model testing has been a favorite testing method in geotechnical engineering. However, use of small scale model tests in the laboratory is severely limited when the gravity body force of the structure itself is the principal load on the system, such as in dams and embankments. This limitation is due to two major factors. One is that soil characteristics are nonlinear and overburden dependent, and the other involves stress magnitudes. The stresses in a small scale model due to its own weight are much smaller in magnitude than those in the corresponding prototype system. To overcome this limitation, the centrifuge model technique has been introduced and is currently being used as a research tool in geotechnical engineering. The major advantage of using this technique is that the technique provides qualitative information of prototype behavior in a small scale model with a comparatively inexpensive and easy way. It is possible since the state of stress at every point in the centrifuge model under an artificial gravitational field is equal to that at the homologous point in the prototype. Although some difficulties are encountered at present, this technique has been applied to a variety of geotechnical problems (slope stability, reinforced earth, pile foundation, offshore gravity platforms, rockfill dams, tunnels, and buried circular pipes), and the results are reported elsewhere (1,4,7,8,9,10).

The Centrifuge: The geotechnical centrifuge at the University of California, Davis was used for the present model study. The centrifuge (Schaevitz Type B-8-D rotary accelerator) is designed to apply controlled centrifugal accelerations up to 175 g's or 10,000 g-lbs at a nominal radius of 39 inches. It is capable of reaching a maximum speed of 390 rpm.

Model Concrete Box Culvert and Instrumentation: The model box culvert was made of Quikrete, a commercial ready-to-use sand mix, with water-cement ratio of 0.15 (by weight). The model box culvert consisted of a roof, floor, and two side walls. The exterior dimension of the culvert was 9 inches (length) by 5 inches (width) by 5 inches (height). The thickness of these slabs was 0.4 inch.

A commercial strain gage (Gage Type CEA-13-125UW-120) made by Measurements Group, Inc. was used to measure the strains on the surfaces of the culvert. The strain gages were placed at the mid-section of the culvert. Figures 1 and 2 show the dimensions of the model box culvert and location of the strain gages, respectively. A microcomputer based data acquisition system (11) was used to process large quantity of data.

Soil Properties: Monterey No.0 sand was used in this study. The sand is classified as SP in the Unified Soil Classification System. It has a specific gravity of 2.65 and a mean grain diameter of about 0.45 mm (12).

Model Preparation: The following steps were involved in preparing a model:

1. The concrete model box culvert was instrumented, and was then placed in the selected installation type (embankment or trench) (Figures 3 and 4).
2. Monterey No.0 sand was pluviated in the direction normal to the axis of the culvert. In this way, the dry density of 105 lb/ft^3 of soil sample was obtained.
3. The completed model was transferred to the centrifuge and placed in one of the two swing-up buckets.
4. Instrumentation (T.V. monitor and multiplexer) was securely fastened, and both static and dynamic balancing of the rotating arm were performed prior to testing, thus completing preparation of the model system for centrifuge testing.

After a model was placed in the swing-up bucket and all required insrumentation was securely mounted in the centrifuge, the model package was slowly brought up to a rotating speed of 195 rpm, equivalent to 60 gravitational pulls.

NUMERICAL MODEL STUDY (FINITE ELEMENT ANALYSIS)

The computer code, CANDE (Culvert ANalysis and DEsign), used in this study was developed by Katona et al. (5,6). The basic assumptions of the program are: plane strain geometry and loading, small displacement theory, and quasistatic response. The following description summarizes numerical procedures used in the analyses.

Finite Element Mesh and Boundary Conditions: The finite element grid with boundary conditions used in this study is shown in Figure 5: a fixed movement condition in the horizontal direction and free movement condition in the vertical direction. All distances are converted to prototype terms. Since the model and its loading was symmetric, only half of the model was analyzed. The culvert was represented by 20 beam-column elements, and the soil by 110 quadrilateral elements.

Soil-Culvert Interface and Incremental Solution: A fixed condition was used at the soil-culvert interface based on a current study (3). The study (3) demonstrated that the influence of slip conditions for this particular geometrical configuration is insignificant.

The incremental solution procedure for embankment and trench simulated the actual installation process of placing soil layers in a series of lifts. Figure 6 shows the construction increment numbers of element groups entering sequentially into the system. The first construction increment included placing all bedding pad, in situ soil, and the box culvert elements. Subsequent increments, numbers 2 through 10, were gravity loaded elements of fill soil.

Soil Model: The soil model employed in the study is a characterization proposed by **Duncan** et al. (2) which has had a substantial history of development and application over the last decade. Table 1 shows the parameters (2) used for Monterey No.0 sand in the analysis.

RESULTS AND DISCUSSION

The Influence of Installation Type: The bending moments and the thrusts developed in the concrete culvert obtained from the centrifuge model study and finite element analysis are presented. Figure 7 shows the moments for the midspan of the top slab. The moments are initially negligible, and subseqently increase almost linearly with the backfilling process. All the moments are positive throughout the incremental construction due to the vertical soil pressure which induces inward deflection of the top slab. No negative moments are detected during the first six construction increments at which the fill height reaches the same elevation of the top slab of the culvert. This indicates that the box culvert is rigid enough to resist the inward forces on the sides of the culvert under lateral soil pressure. Figure 8 shows the thrusts developed at the midspan of the top slab. The thrusts begin with compressive (positive) forces, but once the depth of fill height exceeds the crown height of the clvert, the thrusts become tensile (negative) forces. Figure 9 shows the compared moments around the culvert under fill height of 20 feet. As expected, the largest moment is developed at the upper corner of the culvert.

No major difference in structural behavior is observed under two different installation types from both centrifuge and numerical model studies except the embankment installation produces slightly greater loading conditions. This result may indicate that the influence of the installation type on overall behavior of the box culvert is minimal although the installation type is one of the important parameters to be considered for circular culverts. In general, the centrifuge model and the numerical model results are in moderately good agreement for shape.

The Influence of Soil Type: Since no major difference in structural behavior was found between embankment and trench soil installations, only embankment condition was considered. Finite elment analysis has been only studied at present time and the predictions are reported here. Two soil types were considered: GW soil type (coarse aggregate) and SM soil type (silty sand). The input parameters for the soil model in CANDE were chosen from standard Duncan's soil parameters (2,6). Table 2 shows the hyperbolic parameters used in the analysis. Figure 10 shows the variation of normal soil pressure at the midspan of the top slab with depth of fill. As shown in the figure, GW soil type (coarse aggregate) exhibits lower values of normal soil pressure until the fill height reaches approximately 7 feet. Beyond this it starts to show high values of soil pressure. At a fill height of 20 feet, the soil pressure of GW soil type (coarse aggregate) is almost twice as large as the soil pressure of SM soil type (silty sand).

Figure 11 shows crown deflection versus the depth of fill. SM soil type (silty sand) shows a rising crown deflection until the fill height reaches the crown level of the culvert, followed by a downward linear deflection due to the vertical soil pressure of backfill. By comparison, GW soil type (coarse aggregate) shows no rising crown deflection. The deflection of GW soil type at 20 feet of fill height is about two times larger than the deflection of SM soil type. With the soil pressure previously observed, this confirms that greater deflection and larger structural stresses (Figure 12) of the culvert would be developed from the higher soil pressure. Figure 13 shows the final shape of deformed culvert under the fill height of 20 feet. Based on the information observed, it is evident that the type of soil is one of major factors governing the behavior of a box culvert, and is an important factor for analysis and design of a box culvert.

SUMMARY AND CONCLUSION

Centrifuge model technique is used to simulate a prototype structural box culvert, and the measured structural responses are compared with predictions of finite element analysis. Based on the results obtained, no major difference in structural behavior is observed between trench and embankment soil installations from both centrifuge and numerical model studies except that embankment soil installation produces slightly higher loadings. However, significantly different shapes of the deformed culverts are observed from the finite element analysis when different soil stiffness is used. This indicates that soil type is one of important parameters to be considered in the analysis and design of box culverts.

Although some differences in magnitude between the results of centrifuge and numerical model studies exist, in general, they agree moderately well in shape. With continuous efforts on the development of accurate small model techniques and larger size of the centrifuge, and the development of sophisticated and more realistic constitutive models for soils in numerical analysis, it is certain that both the centrifuge and numerical model techniques will be useful research tools to check the adequacy of design and verify the theoretical formulation of soil mechanics problems.

ACKNOWLEDGEMENTS

The authors acknowledge the support of the Air Force Office of Scientific Research, Air Force Systems Command, USAF for this research under Grant No. F49620-82-C-0035. Thanks are also due to the geotechnical research group at the University of California, Davis; to Dr. C.K. Shen and Mr. X.S. Li for their help in setting up the data acquisition and recording system; to Drs. J.A. Cheney and B.L. Kutter for their kindness in allowing the use of centrifuge facility.

REFERENCES

1. Coles, C.K., "Centrifuge Models of a Spile-Reinforced Tunnel," M.S. Thesis, University of California, Davis, June, 1982.
2. Duncan, J.M., et al., "Strength, Stress-Strain and Bulk Modulus Parameters for Finite Element Analyses of Stresses and Movements in Soil Masses," Report No. UCB/GT/78-02, National Science Foundation, April, 1978.
3. Gardner, M.P. and Jeyapalan, K., "Preliminary Analysis of the Behavior of Reinforced Concrete Box Culverts," Report No. FHWA/TX-82/50+326-1, September, 1982.
4. James, R.G., and Larsen, H., "Centrifugal Model Tests of Buried Rigid Pipes," Proceedings of the Ninth International Conference on Soil Mechanics and Foundation Engineering, Tokyo, Japan, 1977.
5. Katona, M.G., Smith, J.M., Odello, R.J., and Allgood, J.R., "CANDE - A Modern Approach for the Structural Design and Analysis of Buried Culverts," Report No. FHWA/RD-77/5, Federal Highway Administration, Washington, D.C., October, 1976.
6. Katona, M.G., Vittes, P.D., Lee, C.H., and Ho, H.T., "CANDE-1980: Box Culverts and Soil Models," Report No. FHWA/RD-80/172, Federal Highway Administration, Washington, D.C., May, 1981.
7. Kim, M.M. and Ko, H.Y., "Centrifugal Testing of Soil Slope Models," Transportation Research Record 872, pp. 7-15, 1982.
8. Rowe, P.W. and Craig, W.H., "Application of Models to the Prediction of Offshore Gravity Platform Foundation Performance," International Conference on Offshore Site Investigation, pp. 269-281, Graham and Trotman, London, 1980
9. Scott, R.F., and Morgan, N.R., "Feasibility and Desirability of Constructing a Very Large Centrifuge for Geotechnical Studies," Report 760-170 NSF, California Institute of Technology and JPL, March, 1977.
10. Shen, C.K., Kim, Y.S., Bang, S. and Mitchell, J., "Centrifuge Modeling of a Lateral Earth Support," Proceedings of the ASCE, Journal of the Geotechnical Engineering Division, Vol. 108, No. GT9, pp. 1150-1164, September, 1982.
11. Shen, C.K., Li, X.S. and Kim, Y.S., "Microcomputer Based Data Acquisition Systems for Centrifuge Modeling," Proceedings of the ASTM, Geotechnical Testing Journal, Volume 7, Number 4, pp. 200-204, December, 1984.
12. Yang, F., Personnal communication, Department of Civil Engineering, University of California, Davis, August, 1985.

Table 1. Duncan's Soil Parameters for Monterey No.0 Sand (Reference 2)

Cohesion, c	0.0
Friction Angle, ϕ	35.0°
Modulus Number, K	920.0
Modulus Exponent, n	0.79
Failure Ratio, R_f	0.96

Table 2. Representative Parameter Values of the Modified Duncan Model (References 2 and 6)

	GW Soil	SM Soil
Cohesion, c	0.0	0.0
Friction Angle, ϕ	33.0°	32.0°
Modulus Number, K	200.0	300.0
Modulus Exponent, n	0.4	0.25
Failure Ratio, R_f	0.7	0.7
Bulk Modulus Number, K_b	50.0	250.0
Bulk Modulus Number, m	0.2	0.0

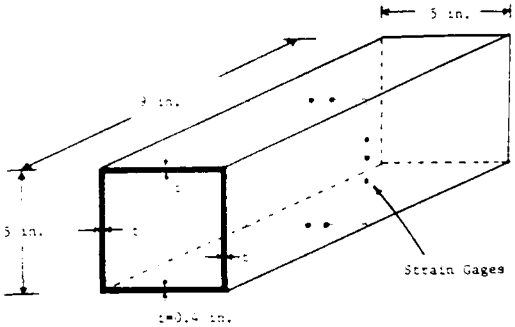
5 in.
9 in.
5 in.
t
t
t
t=0.4 in.
Strain Gages

Figure 1. Dimensions of the Model Box Culvert

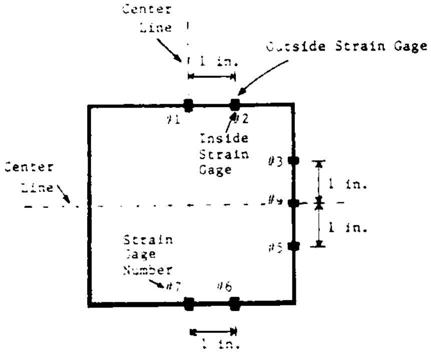
Center Line
1 in.
Outside Strain Gage
#1
#2
Inside Strain Gage
#3
Center Line
#4
1 in.
1 in.
#5
Strain Gage Number
#7
#6
1 in.

Figure 2. Locations of the Strain Gages

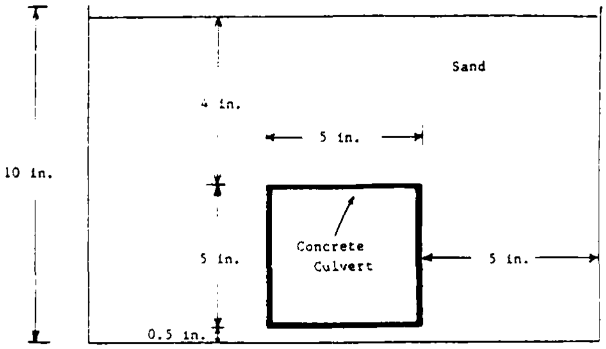
Sand
4 in.
5 in.
10 in.
Concrete Culvert
5 in.
5 in.
0.5 in.

Figure 3. Dimensions of the Model Package (Embankment Condition)

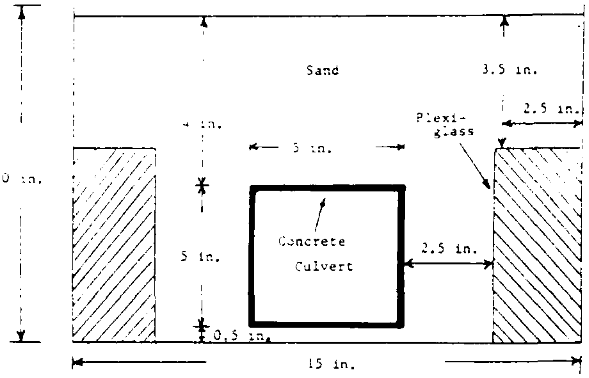
Sand
3.5 in.
2.5 in.
Plexi-glass
4 in.
5 in.
10 in.
Concrete Culvert
5 in.
2.5 in.
0.5 in.
15 in.

Figure 4. Dimensions of the Model Package (Trench Condition)

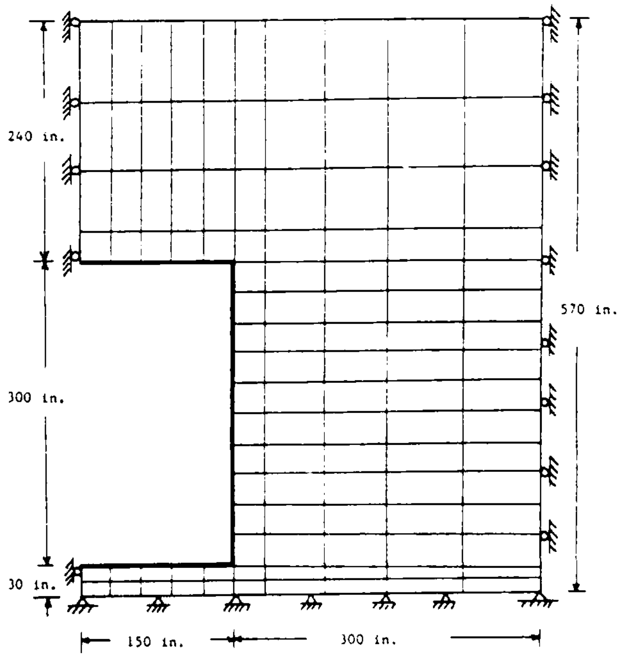
240 in.
570 in.
300 in.
30 in.
150 in.
300 in.

Figure 5. Symmetric Mesh

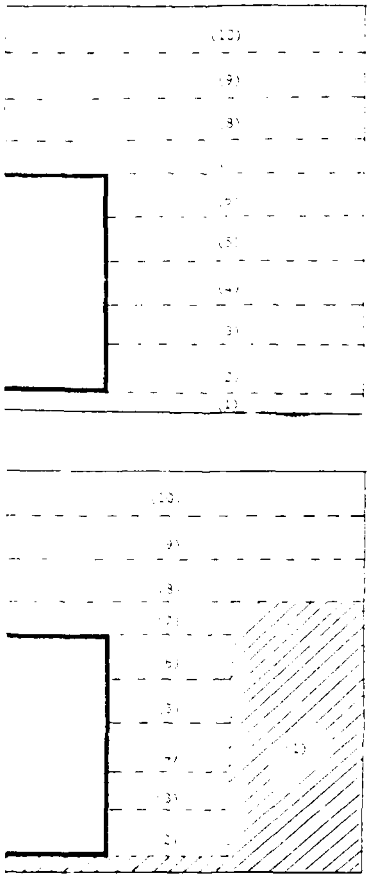

Figure 6. Soil Layers and Construction Increments for Trench Soil Installation

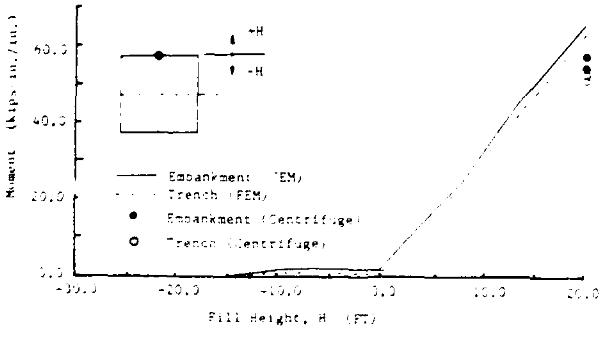

Figure 7. Culvert Bending Moments at Strain Gage #1

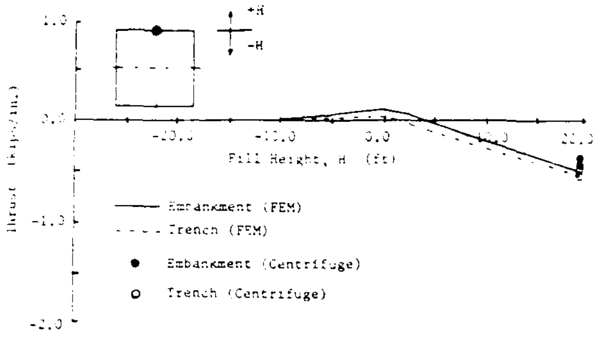

Figure 8. Culvert Thrusts at Strain Gage #1

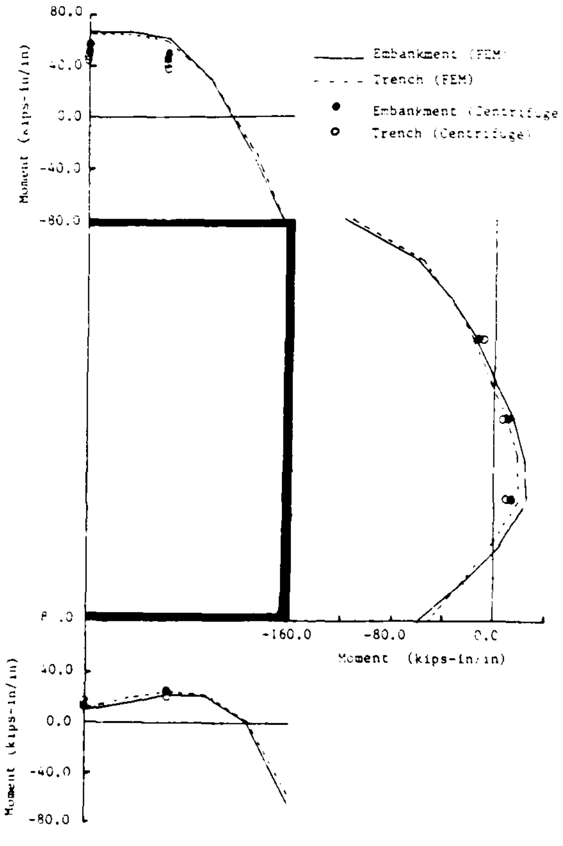

Figure 9. Bending Moments around the Culvert at Fill Height = 20 ft.

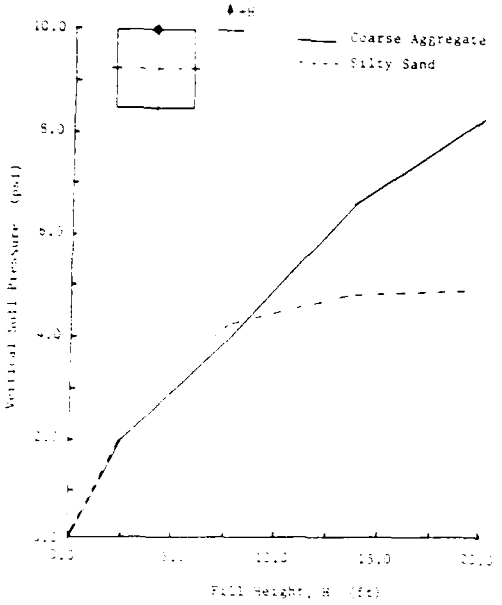

Figure 10. Vertical Soil Pressures at Crown

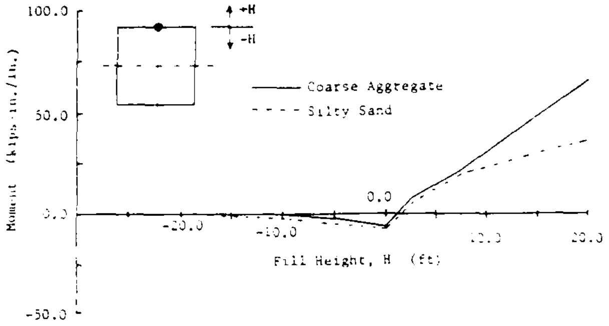

Figure 12. Culvert Bending Moments at Crown

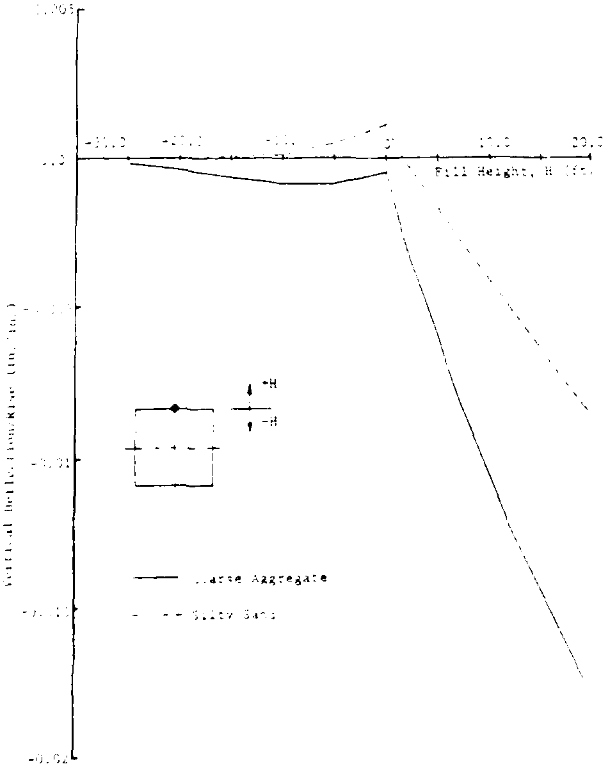

Figure 11. Crown Deflection/Rise vs. Fill Height

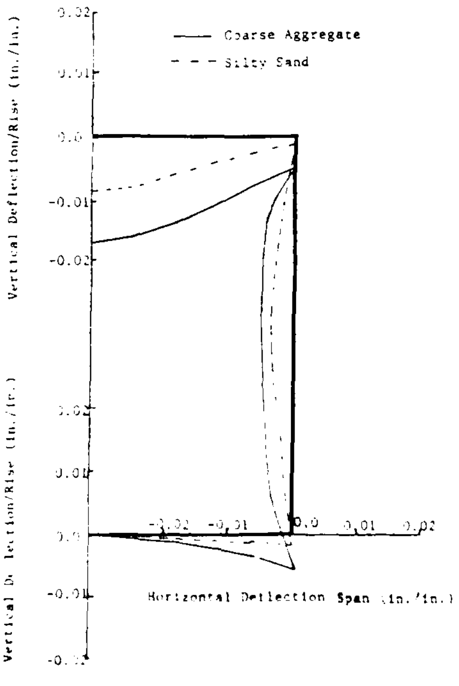

Figure 13. Deformed Box Culvert under
Fill Height = 20 ft.

Proceedings: Second International Conference on Case Histories in Geotechnical Engineering, June 1-5, 1988, St. Louis, Mo., Paper No. 6.83

Settlement Predictions in Residual Soils by Dilatometer, Pressuremeter and One-Dimensional Compression Tests: Comparison with Measured Field Response

Roy H. Borden
Associate Professor of Civil Engineering, North Carolina State University, Raleigh, North Carolina

Weichen Lien
Staff Engineer, Trigon Engineering Consultants, Inc., Greensboro, North Carolina

William J. Sullivan
Senior Engineer, Trigon Engineering Consultants, Inc., Greensboro, North Carolina

SYNOPSIS: A case study investigating settlement predictions based on data from one dimensional compression, pressuremeter (PMT) and dilatometer (DMT) tests is presented. *A relationship is established between PMT and DMT evaluated moduli and the standard penetration N values.* These relationships are utilized in the settlement computations. The predictions obtained by each method are compared to the actual measured settlement. The column location at which settlement observations were made was instrumented with strain gages to measure the actual applied loads. A comparison between actual and design loads is made. Settlement predictions using PMT were performed utilizing two different existing approaches. A distinction is made between the rheological factors, both termed , *used in each of the methods.*

INTRODUCTION

It is generally believed that settlement predictions based on one-dimensional compression test data *often overestimate the observed* settlement of structures constructed on piedmont residual soils. Overestimation of shallow foundation settlements could unnecessarily result in the choice of a more costly deep foundation system. Less traditional in-situ tests such as the pressuremeter and Marchetti dilatometer have been successfully used to more accurately predict settlement. On a recent project by Brookhollow Corporation in Greensboro, North Carolina, for which Trigon Engineering Consultants (TEC) was the geotechnical consultant, TEC performed one dimensional compression tests, pressuremeter tests, and in conjunction with North Carolina State University (NCSU), dilatometer tests. Settlement estimates were then made based on the data from each test. This paper compares these estimates with measured field response.

PROJECT DESCRIPTION

The project consists of a split-level building with four levels in the front and five levels *in the rear of an office building core area.* A single story section wraps around this taller core area. The building was constructed using a steel frame with composite decking and stub girder system. According to Guinnin-Cambell, the structural engineers, the maximum column loads occur at four column locations in the building core area. Total design column loads within this core area range from 180 kips to a maximum of 730 kips. The total design column loads outside the core area, around the single story section, range from 10 to 20 kips.

FIELD INVESTIGATION

Initially, five widely spaced soil borings were performed as part of a preliminary subsurface exploration at the site. Subsequently, an additional eleven soil test borings, five pressuremeter (PMT) tests, and three dilatometer (DMT) profiles were performed. The boring locations and plan view of the building are shown in Figure 1.

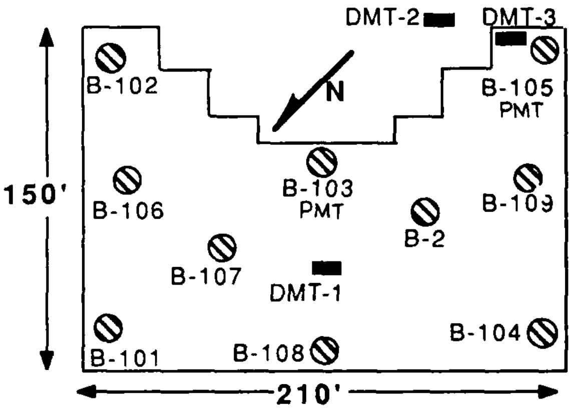

Figure 1. Boring and Test Location Plan

The soil test borings were performed to depths ranging from 15 feet to approximately 75 feet below the ground surface. Standard Penetration Tests (SPT) were performed and Shelby tube samples were recovered from the borings at designated intervals. A generalized soil profile is shown in Figure 2.

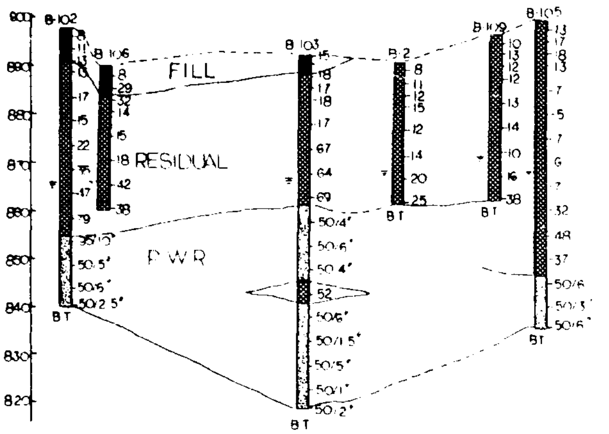

Figure 2. Generalized Subsurface Profile

Based on the SPT profiles, a series of five pressuremeter tests were performed by TEC in borings B-103 and B-105. NCSU and TEC personnel performed a total of three DMT profiles (DMT-1 through DMT-3) adjacent to the previous PMT borings, as shown in Figure 1.

In an attempt to better understand the actual loads transferred to the footings, strain gages were mounted on two columns within the taller building core area. These gages were mounted on the column steel after erection of the first level of steel and placement of the first floor concrete slab.

LABORATORY INVESTIGATION

The supporting laboratory testing program consisted of moisture content determinations, liquid and plastic limit tests, sieve analyses and one-dimensional compression tests. Table 1 shows a summary of the laboratory test results; one dimensional compression curves are shown in Figure 3.

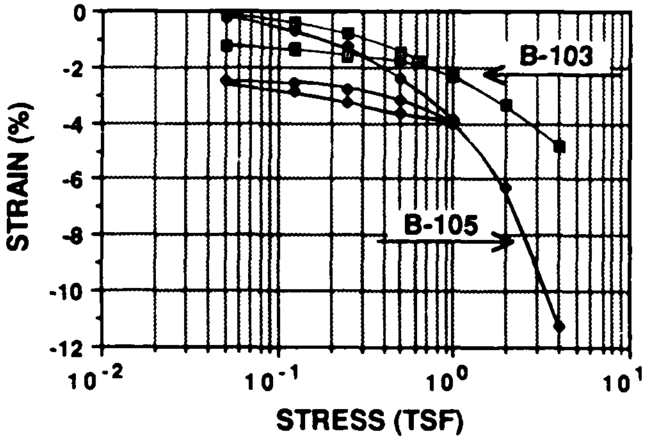

Figure 3. One-Dimensional Compression Tests

Table 1. Summary of Laboratory Test Data

	B-103A	B-105A
Depth	10.0 - 12.0'	18.0 - 20.0'
Natural c	20.9%	59.5%
LL / PL / PI	-----	62 / 45 / 17
Classification	Light gray fine sandy silt	Tan fine sandy clayey silt
Cc	0.09	0.43
wet	104.3 pcf	102.1 pcf
dry	86.7 pcf	64.1 pcf
Saturation	61.5%	99.4%
e_o	0.88	1.51

ANALYSIS OF DATA

The heaviest loaded column is located in the building core area, in the vicinity of B-103. This column was chosen as the focus of this study.

Loads

The loading information noted previously refers to the design loads for the project and those used in determining the footing sizes. For estimating settlement, Guinnin-Campbell initially suggested that these loads be reduced by a factor of 0.64. This resulted in a total column load composed of 87% dead and 13% live load.

Settlement predictions in this study were based on the projected actual dead loads derived from detailed engineering calculations and collaborated by strain gages mounted on the column of interest. The strain gages were monitored during construction as the steel framing and concrete for the second and third floors were completed. The strain gage readings are shown in Table 2. In interpreting the strain measurements, Poissons ratio and Young's Modulus for the 38.8 in^2 column were taken to be 0.27 and 29,000 ksi, respectively.

Teble 2. Measured Column Loads

Date	Reading=2 $_h$	$_v$	(ksi)	P (kips)
09/07/86	0	0	0	0
09/14/86	20x10 E -6	37x10 E -6	1.07	41.6
09/21/86	41x10 E -6	75.9x10 E -6	2.20	85.4
09/28/86	51x10 E -6	One gage loose		
10/05/86	Both gages destroyed			

Because the strain gages were destroyed prior to completion of construction, Guinnin-Campbell was asked to re-evaluate the loading conditions for this study without design live loads or factors of safety. The calculated dead loads for each floor are shown in Table 3.

As noted previously, the strain gages were mounted at the base of the column after the first floor pour. Therefore the readings taken on September 14, 1986, represent the response due to the estimated second floor load of 40.9 kips, as shown in Table 3.

Table 3. Calculated Construction Load for Column C.9-5

ITEM	LOAD (kips)
Load from fourth floor*	40.9
Load from third floor*	40.9
Load from second floor*	40.9
Load from first floor*	18.4

* Due to metal deck, concrete and steel framing

The second reading on September 21 was made after the third floor pour, which brought the estimated load, after gage activation, to 81.8 kips. These values compare quite favorably with the measured values of 41.6 kips and 85.4 kips, respectively. This provided the desired collaboration of the Guinnin-Campbell calculated loads.

Table 4 shows the calculated total column load. The weight of the 5-inch slab-on-grade and soil above the footing was not considered in evaluating settlements since a net stress increase for this load component would be approximately zero. Nor were items 2 and 3, because they were not in place during our settlement readings. For item 5, the difference between the weight of the soil and the weight of concrete was used.

Due to a construction problem, the foundation for column C.9-5 was overexcavated, resulting in a footing area approximately 25% larger than that originally planned. Utilizing this larger footing area with the modified calculated loads shown in Table 4 results in a net bearing pressure of approximately 1.0 ksf. Stress increases in the soil profile were calculated using the Boussinesq theory.

Pressuremeter

A summary of the five PMT tests is shown in Table 5. A ratio of the pressuremeter modulus, E_m, to the "N" value obtained directly below the PMT test elevation was used to interpret pressuremeter moduli at elevations other than the test locations. The highest and lowest E_m/"N" values were excluded, in our calculations and an average of the remaining ratios was calculated to be 9.7 . Table 6 shows the interpretation of the PMT test results. Settlement was calculated using the modulus profile shown in Table 6 and the settlement equation developed by Menard (1975).

The empirical soil factor or rheologic coefficient, α , used in these equations relates the volumetric compression modulus, obtained from the one-dimensional consolidation test, and the shear modulus, obtained from the pressuremeter test. The α coefficient is dependent on the grain size and stress history of the soil. Consistent with the range of E_m/P_l ratios obtained, $\alpha = 2/3$ was used in the analysis.

Table 4. Foundation Dimensions and Calculated Total Loads

ITEM	COLUMN GRIDS C.9-5
1. Total Weight of structural steel, metal deck, concrete and roofing material (kips)	262.3*
2. Weight of elevator equipment (kips)	14+
3. Weight of ceiling, mechanical, shaft walls and fireproofing (kips)	33.4*+
4. Weight of 5" slab-on-grade and soil above footing (kips)	213.7+
5. Weight of footing (kips)	108.6+
6. As built Footing Size: width length depth	11'-6" 22'6" 3'6"
7. Bottom of footing (below top of slab-on-grade)	-8'-6"
8. Load to base of footing (kips)	650+

* Accuracy estimated to be +/- 5%
+ Not used in settlement analysis.

Table 5. Summary of Menard Pressuremeter Tests

Boring	Depth (Ft.)	PMT Modulus, E_m (TSF)	Limit Pressure, P_l (TSF)	$\frac{E_m}{P_l}$	SPT "N"	$\frac{E_m}{\text{"N"}}$
105B	19.0	96.5	6.0	16.0	4*	24.0
105C	8.5	120.9	7.25	16.7	13	9.3
105D	20.75	72.6	6.75	10.8	9	8.1
103C	11.0	257.8	15.25	16.9	22	11.7
103	22.5	291.1	22.5	12.9	60	4.8

* SPT performed from 20' to 21.5'

Table 6. Interpretation of E_m Value by Using PMT Data of B-105

Layer/Depth Below Footing	N (Blows/ft)	N ave (Blows/ft)	E_m=9.7 N ave (TSF)
1R=5.75 ft	13		
2R=11.5 ft	18	15	145.5
3R=17.25 ft	6		
4R=23.0 ft	7		
5R=28.75 ft	6		
6R=34.5 ft.	7	6.5	96.5
7R=40.25 ft	32		
8R=46.0 ft	48	39	260
BELOW 46 ft	>100	>100	300

A second method, introduced and subsequently revised by Martin (1977, 1987), was also used for predicting settlements with the pressuremeter data. In this second method Schmertmann's strain influence factor distribution (1970, 1978) was used with the soil deformation modulus, E_s. Martin uses a rheological factor, which he also calls α, to relate the pressuremeter modulus, E_m to E_s. He suggests that a value equal to 1 be used for piedmont residual soils along with a regional correction factor equal to 0.6. This correction factor is suggested to compensate for the discrepancy between calculated and measured results.

Martin has also developed a relationship between SPT and E_{pm} for piedmont residual soils. This relationship is shown in *Figure* 4. A correlation coefficient equal to 0.788 for line 1, 0.795 for line 2 and 0.790 for line 3 was calculated. The difference resulted from more data points being progressively added for each line. The SPT and E_{pm} values developed for this study were used in conjunction with Figure 4 to develop E_{pm} values at the depths of interest.

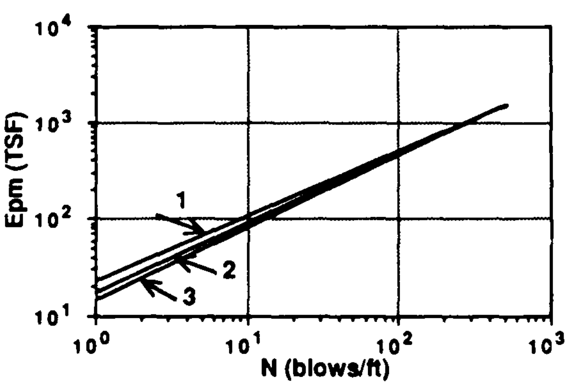

Figure 4. Relationship Between N Values and E_{pm} (After Martin, 1987)

Dilatometer

The computer program "DILLY 4", Schmertmann and Crapps (1986), was used for reduction of the DMT field data. The output of interest includes the dilatometer modulus, E_d, *the material* index, I_d, and a horizontal stress index, K_d. Using this DMT data, a constrained modulus, M, was calculated as suggested by Marchetti (1980) by the equation $M=R_mE_d$, where R_m *is a function of the soil type* (I_d) *and* K_d. This modulus was then used to estimate settlements. The pertinent results of DMT-1 are shown in Figure 5.

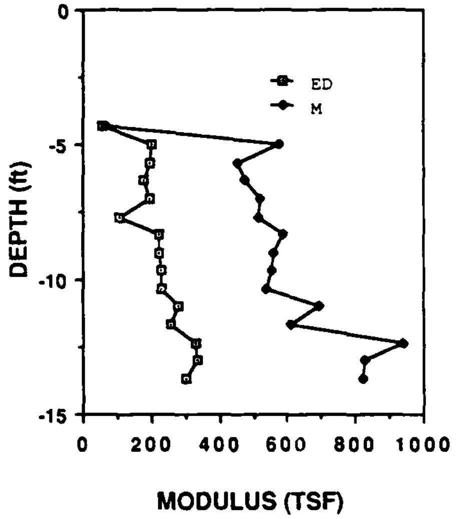

Figure 5. DMT E_d and 1-D Modulus vs Depth

A relationship was established between the DMT M values and SPT N values obtained from adjacent borings, to estimate M values at elevations other than those tested. Figure 6 shows the M/N ratio as a function of depth for locations DMT-1, DMT-2, and DMT-3. It is evident that M/N values are generally in the range of 30-70 for DMT-3 and 45-80 for DMT-1; M/N values for both locations *show* quite comparable results. The M/N ratio between 23 to 33 ft. in Boring DMT-2 is on the order of 10. This layer was identified as a silty clay, and the ratio of 10 indicates that the M/N ratio will be soil type *dependent*. An evaluation of the split spoon samples obtained below Col. C9-5 (Boring 103) shows the profile in this area to be sandy silt to a depth of 19 ft., below which the soil is a silty fine to coarse sand with some fine gravel size quartz (rock) fragments. Based on these observations, it was deemed reasonable to use an M/N ratio of 45 in the subsequent analysis.

Although Marchetti determined the R_m value which relates Ed to M to be a function of soil type and the horizontal stress index, Borden et al (1986), in a study on laboratory compacted and field samples, suggested the use of E_d *as an* upper bound to the anticipated in-situ constrained modulus for piedmont residual soils. This amounts to choosing R_m = 1. Both methods for determining the constrained modulus were used in this study.

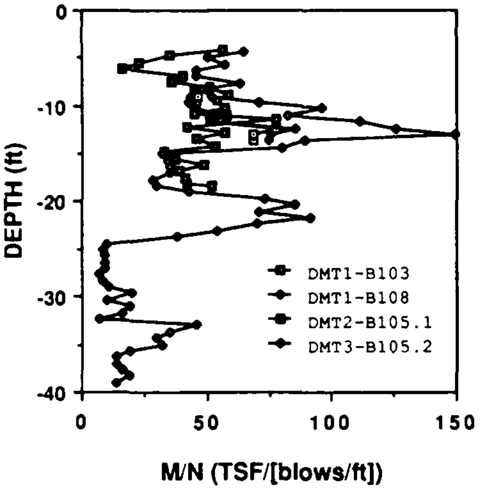

Figure 6. DMT-M/N Ratio Vs. Depth

One-Dimensional Compression

Based on the $\sigma - \varepsilon$ curve from the 1-D compression test of B-103A (Figure 3), the best fit equation for the test data was found to be: $\varepsilon = 0.0114 + 0.006\sigma + 0.000108\sigma^2 - 0.000034\sigma^3$. By differentiating the above equation, the M value is defined by $M = 1/m_v$, where m_v is the coefficient of volume change. The $M - \sigma$ curve is shown in Figure 7. The one-dimensional settlement of each sublayer was then made using the following equation:

settlement = (Δ stress)(thickness)/modulus (M).

The total settlement is obtained by adding the contribution of each sublayer.

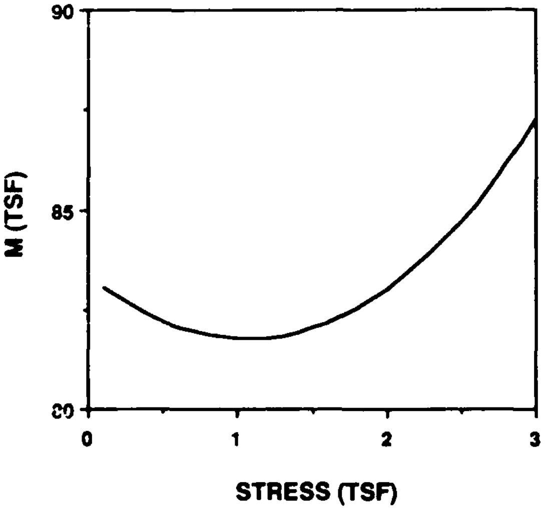

Figure 7. Constrained Modulus vs Vertical Stress

Settlement Comparison

Table 7 shows a summary of the calculated and measured settlements. Figure 8 presents a bar graph comparison of the settlement predicted by the various methods. These results are shown in conjunction with the measured settlement of 0.3 inches.

Table 7. Summary of Calculated and Measured Settlements (inches)

Measured	1-D Compression	DMT		PMT	
		M	$M=E_D$	$\alpha = 2/3$	Martin's $\alpha = 1$ (x0.6)
0.3	0.8	0.11	0.29	0.12	0.22 (0.13)

The predicted PMT settlement using Menard's formula and $\alpha = 2/3$ is 0.12 in. Using Schmertmann's strain influence factor method and Martin's $\alpha = 1$, a settlement of 0.22 in. is predicted. Applying Martin's regional correction factor, results in a settlement of 0.13 in., which further underpredicts the observed settlement.

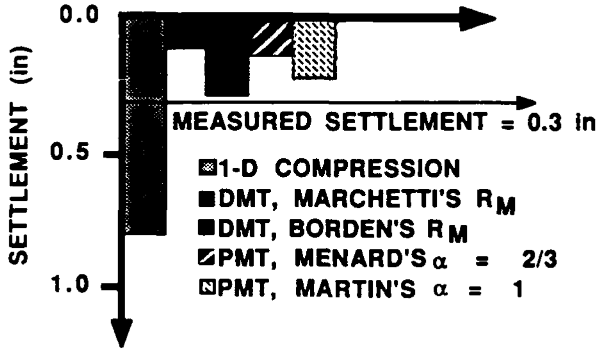

Figure 8. Predicted Vs Measured Settlement

From Figure 8 it can be seen that the predicted DMT settlement using constrained modulus (M) as suggested by Marchetti underpredicts the observed settlement. Utilizing $R_m = 1$, therefore choosing E_d as the upper bound for M, results in a prediction of 0.29 in., which is in good agreement with the 0.3 in. measured.

In contrast to the DMT and PMT prediction methods, using the interpreted M values obtained from the 1-D compression data, resulted in a predicted settlement of 0.8 in. As this overprediction is somewhat typical, it is local practice to multiply this value by 2/3, which would reduce the prediction to 0.53 in., or nearly 1.8 times the measured settlement.

Summary and Conclusions

As a preface to our conclusions, it should be noted that this study is for only one project. The measured settlement was less than one half inch and the accuracy of our measurements is estimated to be ± 0.1 inch. Therefore, additional studies are needed to substantiate the findings. At the time this paper was prepared, additional studies with the same scope of work were being planned. These studies will be reported as they are completed.

The following points can be made concerning the findings in this study:

1. The α factor used in the PMT analyses significantly influences settlement predictions. The α factor used by Martin in conjunction with Schmertmann's strain influence factor method is not the same as that suggested by Menard. The fact that these two factors are both called α could undoubtedly lead to confusion. Further examination of the settlement predictions shows that for Martin's method, applying a regional correction factor of 0.6 is essentially equivalent to using α equal to 2/3 with Menard's formula.

2. The settlement predictions made by using constrained modulus (M) profile obtained from Marchetti's correlation underpredicted the settlement. The prediction made using M equal to Ed shows a much better result. This indicates that Marchetti's M value correlation might overpredict the stiffness of residual soils.

3. Settlement predictions made using the 1-D compression test data overestimated the measured settlement.

4. In evaluating the building loads utilized in the settlement analysis, it was observed that the calculated dead loads were very close to those measured by the strain gages. In contrast, the initial design loads provided for settlement estimates were 165% of the actual loads. The use of the more conservative design loads would have resulted in much more conservative settlement predictions. When using design versus actual loads to predict settlement, one may have the impression that a particular analysis method is conservative or unconservative, when in fact it is not the method which is being evaluated as much as the appropriateness of the assumed loads.

References

Borden, R. H., Saliba, R. E., and Lowder, W. M. (1986), "Compressibility of Compacted Fills Evaluated by the Dilatometer," Transportation Research Record No. 1089, TRB, Washington DC, pp. 1-16.

Marchetti, S., (1980),"In Situ Tests by Flat Dilatometer," Journal of the Geotechnical Engineering Division, ASCE, vol. 106, No. GT3, pp. 299-321.

Martin, R. D. (1977),"Estimating Foundation Settlements in Residual Soils," Journal of the Geotechnical Engineering Division, ASCE, vol. 103, No. GT3, pp. 197-212.

Martin, R. E., (1987),"Settlement of Residual Soils, Foundations and Excavation in Decomposed Rocks of the Piedmont Province," Geotechnical Special Publication No. 9, ASCE, pp. 1-14.

Menard, L. (1975), "The Menard Pressuremeter: Interpretation and Application of Pressuremeter Test Results." Sols-Soils No. 26.

Schmertmann, G., and Crapps, D., (1986), "DILLY 4", Fortran Data Reduction Program User's Manual, GPE INC., Gainesville, Florida.

Schmertmann, J. H., (1970),"Static Cone to Compute Static Settlement Over Sand," Journal of Soil Mechanics and Foundation Division, vol. 96, No. SM3, pp. 1011-1043.

Schmertmann, J. H., Haertman, J. P., and Brown, P. R., (1978),"Improved Strain Influence Factor Diagrams," ASCE, Journal of Geotechnical Engineering Division, vol. 194, No. GT8, pp 1131-1135.

Acknowledgements

The authors wish to express their appreciation for the cooperation of Brookhollow Corporation in allowing the installation of strain gages and subsequent monitoring of settlment during construction, and to Guinnin-Campbell for their interest and effort in supplying building loads. The continued support of Trigon Engineering Consultants, Inc. is greatly appreciated. Thanks are also due to TEC driller Steve Williams. The review and helpful suggestions of Mohammed A. Gabr and Richard C. Wells are appreciated. The effort of Mrs. Kim Tsoumbos in preparing the manuscript is also gratefully acknowledged.

Proceedings: Second International Conference on Case Histories in Geotechnical Engineering, June 1-5, 1988, St. Louis, Mo., Paper No. 6.88

Collapsing Peak Up of a Large Highway Steel Pipe-Arch

Minh Phong Luong
Directeur de Recherche, Ecole Polytechnique, France

SYNOPSIS : This case history reports the collapse of a large highway steel pipe-arch (8.12 m rise - 10.95 m span), occurring just when backfilling reached the top of the arch. No fill was placed on top as backfilling proceeded ; the arch raised, thereby flattening side radius. It shows that stability in a soil-structure interaction system requires not only adequate design of the structure barrel, it also presumes a well engineered backfill. Performance of the flexible steel pipe-arch in retaining its shape and structural integrity depends greatly on placement and compaction of the envelope of earth surrounding the structure and distributing its pressures to the abutting soil masses.

INTRODUCTION

Underpasses or grade separations are an increasingly popular method of eliminating traffic hazards and thereby improving road safety. Soil-steel bridges using corrugated steel pipe are frequently the most economical of the short span bridge alternatives used to achieve grade separations.

Nevertheless installation and contruction procedures are of fundamental importance especially during compaction of the backfill. During the course of examining various buried flexible pipe installation, monitoring their behaviour and, of course, analyzing failure case histories, several observations have been made that are of interest to the pipe designer or constructor.

This paper presents records on the deformation shape of the pipe-arch due to backfill loads causing a collapsing peak up of a large highway steel pipe-arch.

The measurements taken during the construction phase are seen to have been poorly chosen to predict such a problem at an early stage. Nevertheless an experienced engineer should have been able to detect this type of failure by analyzing in details the evolution of appropriate parameters.

PIPE-ARCH LOCATION

The case history describes a vehicular underpass serving as grade separation for automotive traffic promoting the safe movement of vehicles. This local road has been carried under a highway at less cost than by building a bridge.

Figures 1a, b, c show the pipe-arch size, shape and it's alignment, grade with respect to the highway and the diverse characteristics of its installation.

Sectional properties of the arc-and-tangent of corrugation are derived mathematically :

. moment of inertia $I = 33.04\ cm^4/m$
. inertia modulus $I/v = 95.48\ cm^3/m$
. pitch 152.4 mm
. depth 51.5 mm
. thickness 7 mm

Galvanized bolts were used to assemble structural plate sections at the bottom of pitch.

INSTALLATION

The pipe-arch was a large-diameter bolted structure. The bedding fill was constituted with sandy silt of two metre thickness. It has been shaped to the approximated contour of the bottom portion of the structure in order to afford a uniform support for its relatively flat bottom. It was then compacted under the haunches of the structure in the first stages of backfill. The soil adjacent to the corners of pipe-arch was of excellent quality, highly compacted to accommodate the high reaction pressures that can develop at this location.

The backfill material around and near the pipe-arch was well graded gravel of size D less than 80 mm. Excellent control of soil placement and compaction were maintained to fully mobilize soil-structure interaction. The fill was placed alternately to keep it at the same elevation on both sides of the structure at all times. Compaction of the backfill was done with vibrating compactors.

SHAPE CONTROL

The pipe-arch was divided into five sections for which length measurements were taken throughout the backfill procedure. Figure 2 illustrates the sections chosen for controlling the geometry.

The figure 3 shows the length variations for each of the chords during the backfill construction phase. It can be seen that these vary little until just before the onset of failure.

The figure 4 shows that the variation of rise and span measured with respect to a fixed point during the same period gives for an experienced engineer a much earlier indication of the geometrical distortion.

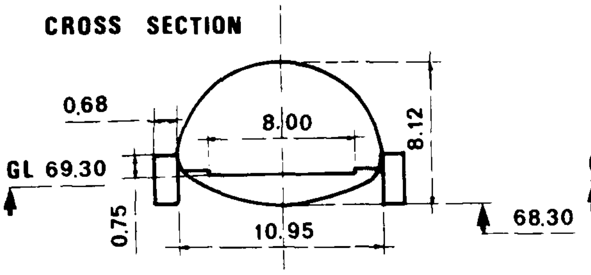
CROSS SECTION
0.68
8.00
8.12
GL 69.30
GL 69.30
0.75
10.95
68.30

Fig. 1a Geometry and Size of the Pipe-Arch

Fig. 1b Sectional Elevation of the Long Span Structure

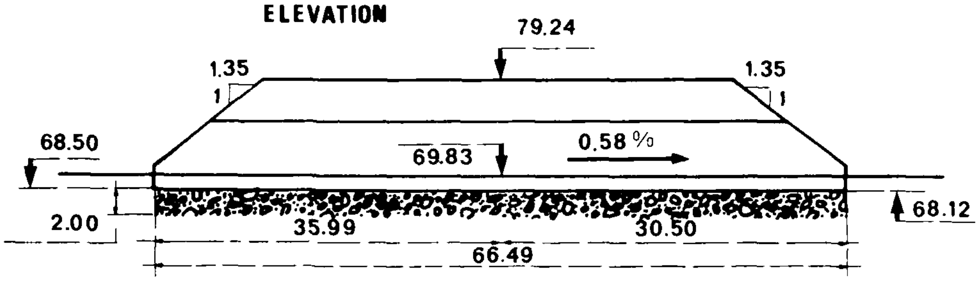
ELEVATION
79.24
1.35
1
1.35
1
68.50
69.83
0.58 %
2.00
35.99
30.50
66.49
68.12

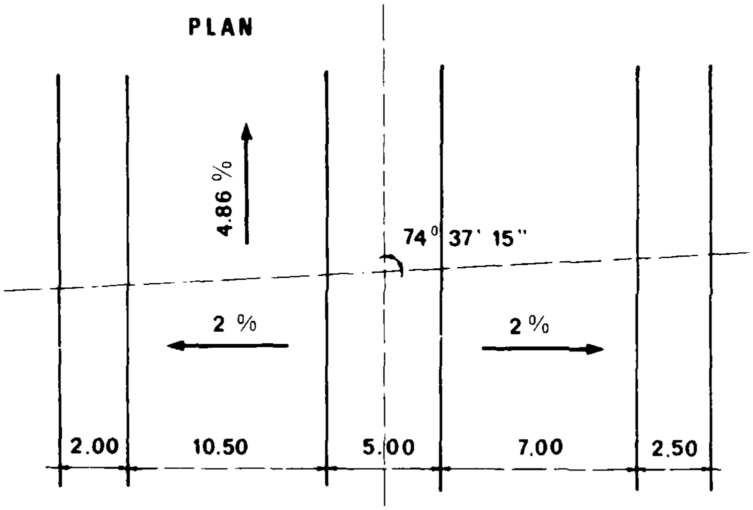
PLAN
4.86 %
74° 37' 15"
2 %
2 %
2.00
10.50
5.00
7.00
2.50

Fig. 1c Pipe-Arch Alignment with respect to the Highway

Fig. 2 Geometry Control from Chord Length Measurements

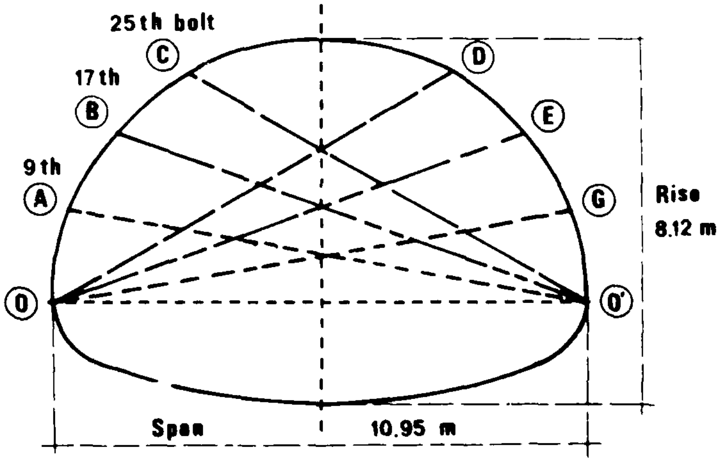
25th bolt
17th
9th
Ⓒ
Ⓑ
Ⓐ
Ⓓ
Ⓔ
Ⓖ
(O)
(O')
Rise
8.12 m
Span
10.95 m

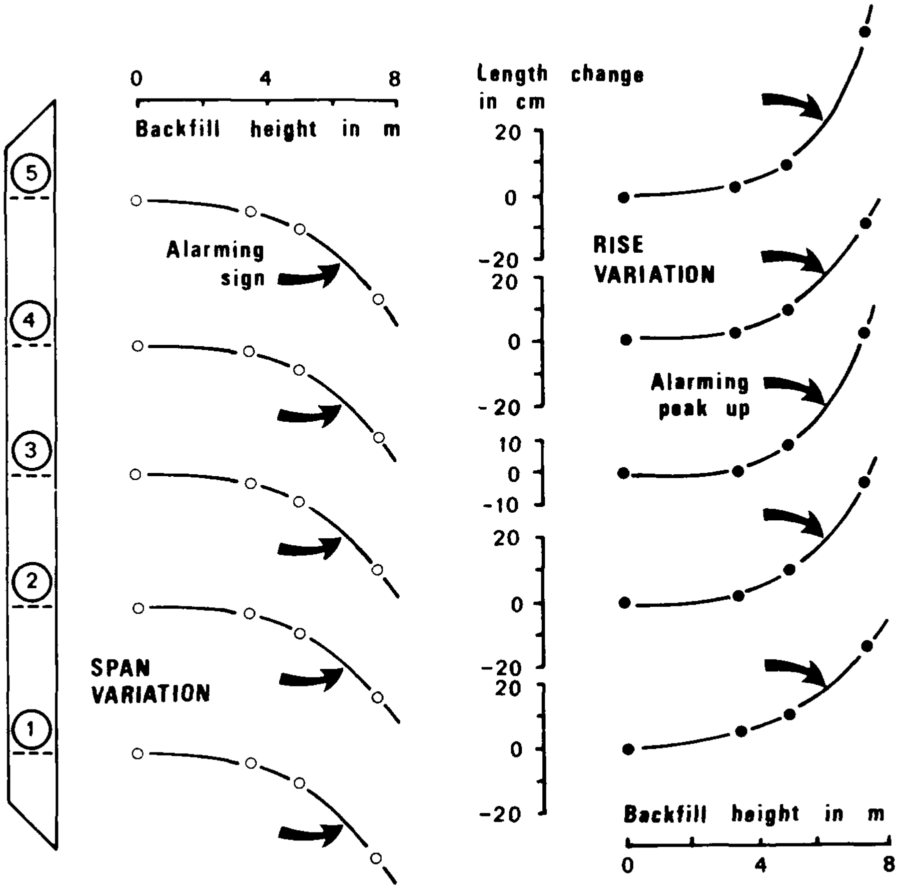

Fig. 4 Span and Rise Variations during Backfilling showing with Evidence a Failure Potential when Backfilling reached Half of its Height

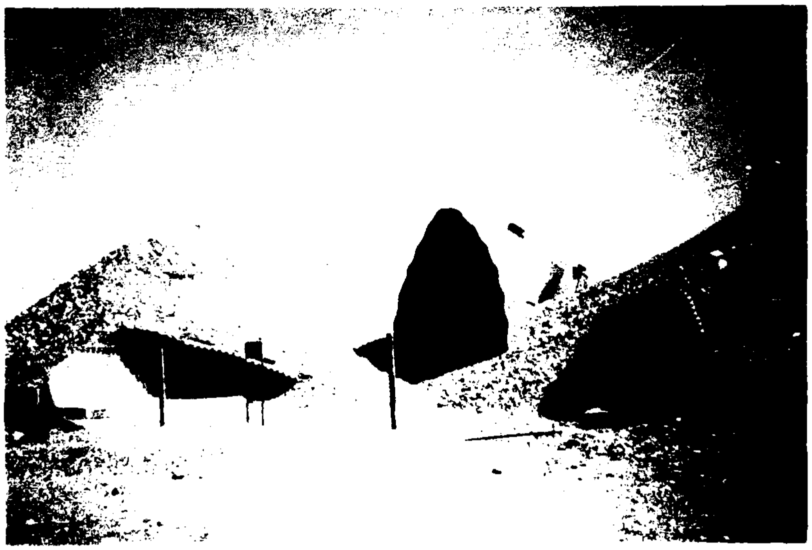

Fig. 5a Cloverleaf Collapse of the Pipe-Arch

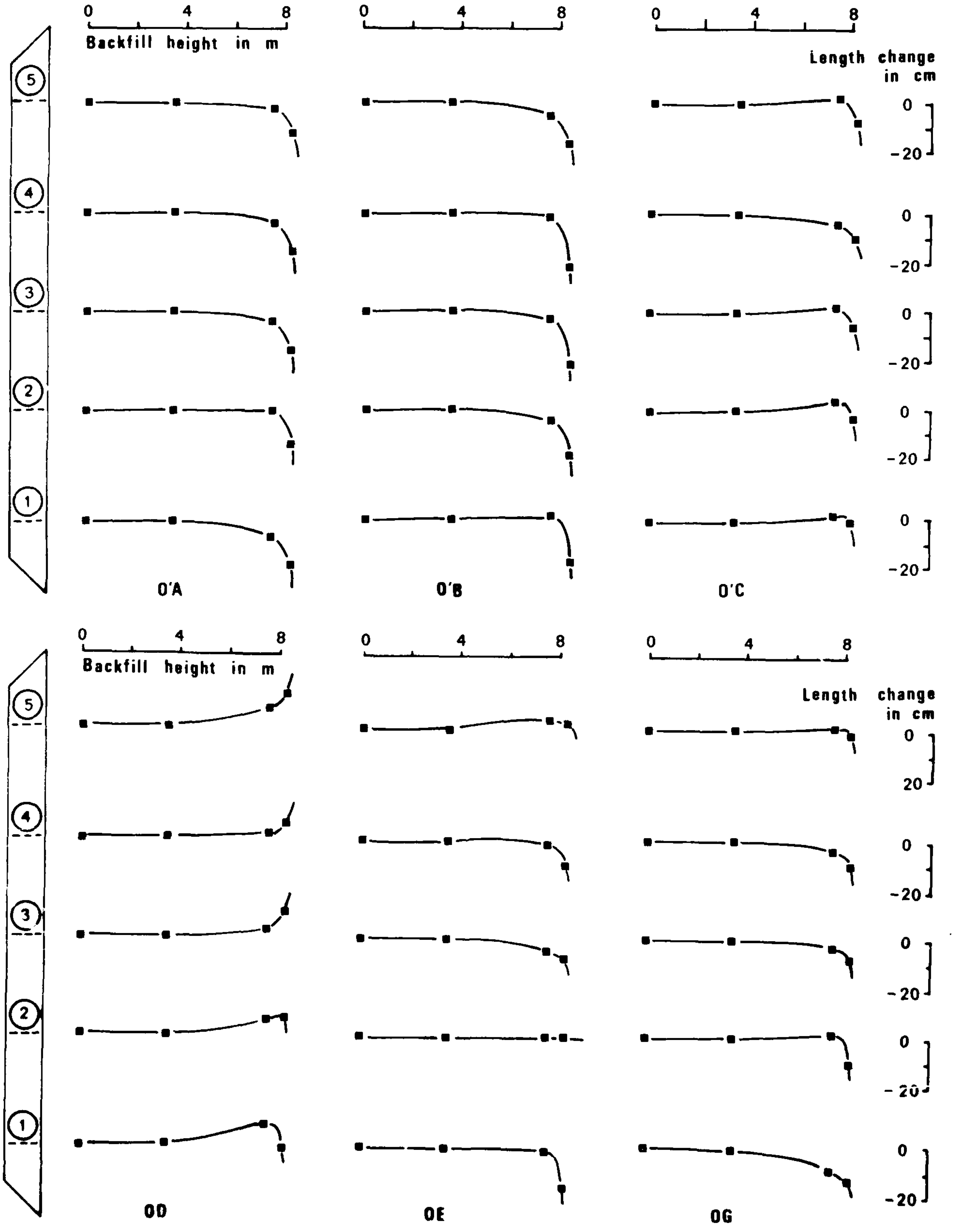

Fig. 3 Length Variations of Symmetrical Chords during Backfilling. No alarming Sign was evident until just before the onset of failure

A REGRETTABLE MISTAKE !

Unhappily, there was a very regrettable mistake. Fill load was not placed on top as backfilling proceeded. The top of the pipe-arch peaked up, thereby flattening progressively the side radius as shown in the figures 3 where the structure shape was checked regularly during backfilling to verify acceptability of the construction. It can be seen that the shape of the pipe-arch was not maintained in admissible condition.

The magnitude of allowable shape changes was specified by the fabricant of the long-span structure. The manufacturer had provided no qualified construction inspector during all structure backfilling to aid the engineer. Nobody advised him on the acceptability of the proper magnitude of the shape.

When the backfill reached the top of the pipe-arch, there was a long pause without having fill load on the arch. Four hours later, the pipe-arch collapsed all along its length as shown in the figures 5.

CONCLUDING REMARKS

This case history illustrates that failures during construction projects can arise simply from inadequate implementation of conventional control procedures (1,2).

REFERENCES

1. Handbook of Steel Drainage & Highway Construction Products, American Iron and Steel Institute, 3rd edition, April 1983.

2. Les Buses Métalliques, Recommendations and rules of the art. SETRA LCPC, Ministry of Transport, September 1981.

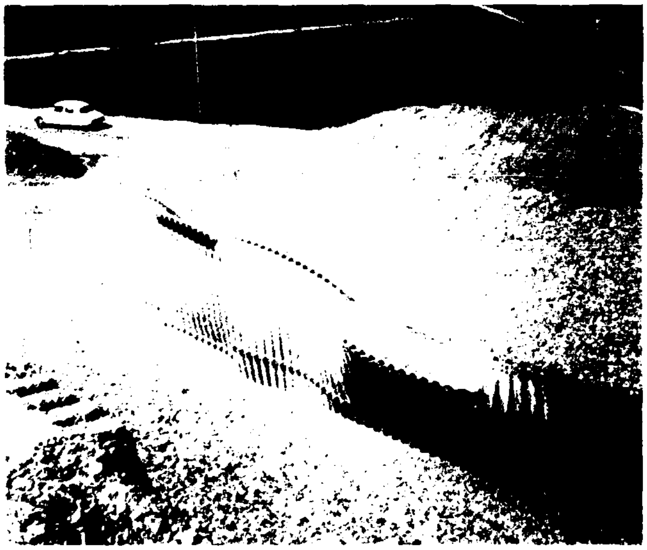

Fig. 5b View evidencing the Peak up of the Pipe-Arch

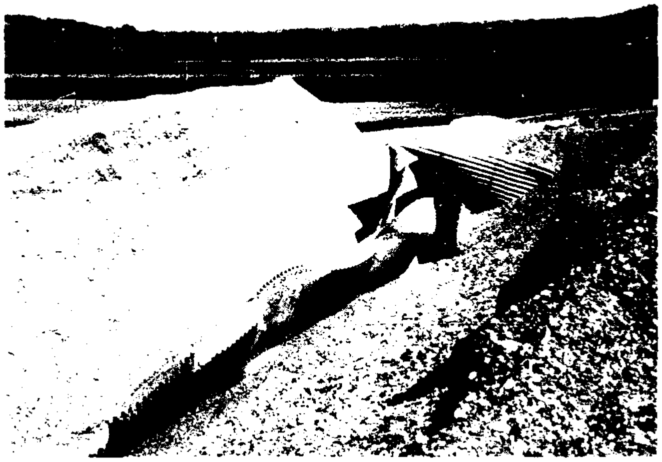

Fig. 5c Final Shape after the Collaspe of the Pipe-Arch

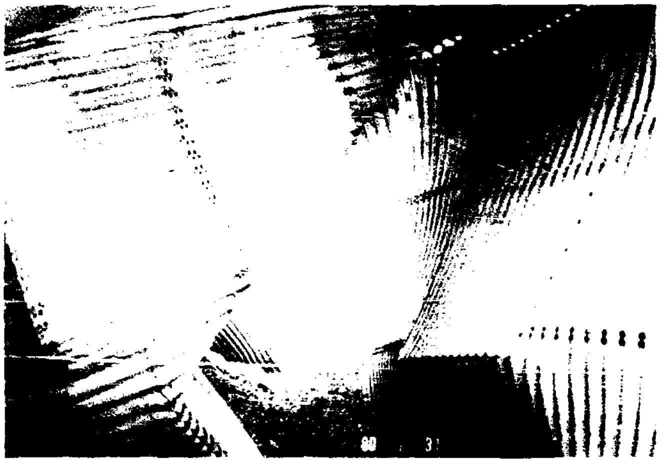

Fig. 5d Detail showing the Flattening of Side Radius

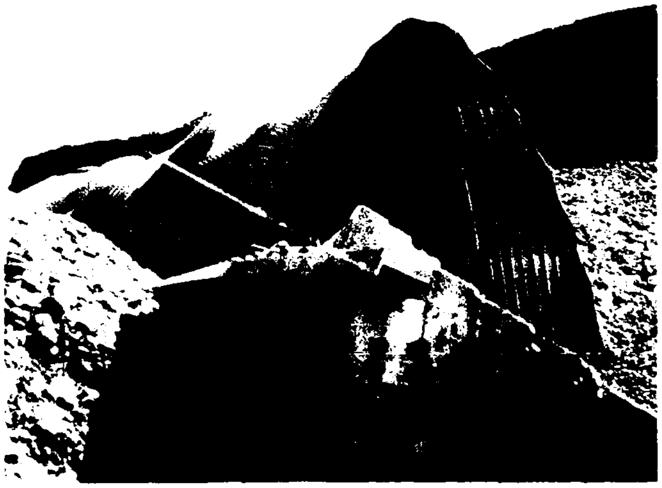

Fig. 5e Distortion of Pipe-Arch End after Collapse

Proceedings: Second International Conference on Case Histories in Geotechnical Engineering, June 1-5, 1988, St. Louis, Mo., Paper No. 6.89

Existing Pile Load Capacity Evaluation

Alan Kropp
Alan Kropp and Associates, Berkeley, California

SYNOPSIS:

An evaluation of the capacity of piles supporting an existing five-story building became necessary when heavy new shear walls were proposed for the structure. Data regarding these piles was obtained from the soil investigation report for the project, from two pile load tests at the site, and from driving records for 229 production piles. Additional information was derived from soil borings and pile load tests for two adjacent buildings. Calculations were made of the anticipated pile capacities of piles at load test locations, and empirical correction factors developed to modify the calculated values to match the load test results. The same calculation methods and empirical correction factors were then used to develop ultimate capacities at each production pile location, and appropriate safety factors applied to estimate allowable pile capacities.

INTRODUCTION

A five-story parking garage was constructed in 1972. In 1982, some cracking in the structure was observed and a detailed evaluation of the original garage design was performed. The evaluation concluded that five shear walls should be added to the facility to provide adequate lateral stability during seismic shaking. A geotechnical evaluation of the existing pile foundation was performed to determine if the piles could carry the additional weight of the new shear walls.

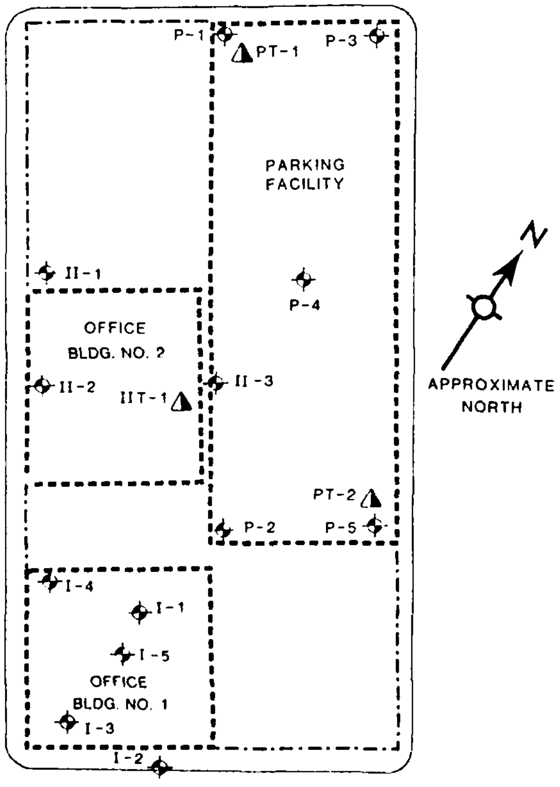
P-1
PT-1
P-3
PARKING FACILITY
II-1
P-4
OFFICE BLDG. NO. 2
II-2
IIT-1
II-3
PT-2
P-2
P-5
I-4
I-1
I-5
OFFICE BLDG. NO. 1
I-3
I-2
N
APPROXIMATE NORTH
LEGEND
Approximate Location of Property Line
Approximate Building Limits
P-1 Approximate Location of Exploratory Boring for Parking Facility
I-1 Approximate Location of Exploratory Boring for Office Building No. 1
II-1 Approximate Location of Exploratory Boring for Office Building No. 2
PT-1 Approximate Location of Test Pile for Parking Facility
IIT-1 Approximate Location of Test Pile for Office Building No. 2
APPROXIMATE SCALE (Feet)
0
100
200

Figure 1. Site Plan

EXISTING DATA

A soil investigation for the parking garage was originally performed in 1970 which provided recommendations for the proposed pile foundations. This study included the drilling of five exploratory borings on the site. Two pile load tests were performed in March 1972, and 229 production piles were driven in March and April of 1972.

Two 13-story office buildings were constructed on piles adjacent to the parking facility. The foundation investigations for these two sites were performed in 1969 and 1972 and included four and three exploratory borings, respectively. One pile load test was performed for the second office building.

The approximate locations of the parking facility, the office buildings, the exploratory borings and the pile load tests are shown on the Site Plan, Figure 1.

SITE CONDITIONS

A. Exploratory Boring Data

The subsurface materials encountered in the borings below the parking facility generally consisted of soft to stiff, silts and clays with sand lenses extending to a depth of about 45 feet. Below this depth, dense sand layers with occasional clay layers were encountered extending to the maximum depth explored of about 95 feet. Gravel layers were encountered in several of the borings, particularly near the bottom of the borings. The borings below the first office building site generally encountered sand layers with silt lenses in the upper 45 feet, and then sand and gravel layers below that depth. At the second office building site, the borings typically encountered clay layers with interbedded sands extending to a depth of about 80 feet, and then sand and gravel layers to the bottom of the borings at a depth of about 100 feet. Thus, the subsurface conditions were somewhat different at each of the three sites.

Although some variability was encountered in the borings, the groundwater was generally present a depth of about 15 to 25 feet at the time of the investigations.

B. Test Pile Data

Two pile load tests on 16-inch square, prestressed concrete piles were performed on the parking garage site. As shown on the Site Plan, one test pile was located adjacent to Boring 1 (in the western corner) and the other was located adjacent to Boring 5 (in the eastern corner). Test Pile 1 (adjacent to Boring 1) was driven to a depth of about 65 feet, while Test Pile 2 (adjacent to Boring 5) was driven to a depth of about 63 feet. Load testing indicated an ultimate capacity of 117 tons for Test Pile 1, and an ultimate capacity of 195 tons for Test Pile 2. Based on this information, the soil engineer said that the proposed heavily loaded production piles (carrying loads of 83 to 97 tons) should be extended to a depth of 77 feet and should have blow counts of at least 30 blows per foot for the last 3 feet.

One pile load test was performed adjacent to Boring 3 on a 12-inch square prestressed concrete pile for the second office building (see the Site Plan). This pile was driven to a depth of about 84 feet (after the upper 40 feet of soil had been predrilled). The pile load test indicated an ultimate capacity of about 325 tons. For the design capacity of 150 tons, the soil engineer recommended all production piles be predrilled to a depth of 40 feet and then driven 10 feet into the dense sand and gravel layer encountered at a depth of about 75 feet.

C. Production Pile Driving

The pile driving records for the parking garage indicated that 229 piles were driven to depths ranging from about 66 to 90 feet (although most tips were at depth between 77 and 80 feet). All piles were 16-inch square, prestressed piles.

EVALUATION AND CONCLUSIONS

A. Soil Layers

On the basis of the pile driving blow counts, and the soil boring logs, rough differentiations were made between types of soil (clay, sand, or gravel) and subdivisions were established between individual soil types (i.e. soft, firm, or stiff clay). These soil categories are presented on Tables 1, 2, and 3. Three types of clay, three types of sand and two types of gravel were identified, and each soil type was given a different letter designation. Differentiation between clay and sand layers was partially based on the blowcount, while distinctions between sand and gravel layers was primarily based on the blowcount.

TABLE 2. CLAY PROPERTIES

Clay Type	Pile Driving Blowcount	Wet Density (pcf)	Undrained Cohesion (psf)	α	Undrained Soil - Pile Adhesion (psf)
A	0 - 2	120	500	0.90	450
B	3 - 6	120	750	0.84	630
C	7 - 10	125	1000	0.71	710

TABLE 2. SAND PROPERTIES

Gravel Type	Pile Driving Blowcount	Wet Density (pcf)	Drained Soil-Pile Friction Angle - ϕ (°)	$K_s \tan \phi'_a$ Vesic (1967)	$K_s \tan \phi'_a$ Corrected Value	f_b/f_s
G	25 - 55	125	38	1.7	0.80	90
H	55 - 100+	130	41	2.4	1.27	120

TABLE 3. GRAVEL PROPERTIES

Sand Type	Pile Driving Blowcount	Wet Density (pcf)	Drained Soil - Pile Friction Angle - ϕ (°)	$K_s \tan \phi'_a$ Vesic (1967)	$K_s \tan \phi'_a$ Corrected Value	f_b/f_s
D	1 - 4	125	30	1.05	0.56	-
E	5 - 14	130	33	1.20	0.64	51
F	15 - 25	130	35	1.36	0.72	65

B. Soil Properties

Very limited soil testing was performed by the soil engineers on samples obtained from the five borings at the parking garage site. Water content and dry density tests were performed on most samples, while five direct shear tests and one consolidation test were performed on other samples. Because of erratic test results, these results were not used to a significant degree in our analyses. Also, very few standard penetration resistance values were recorded, so little information regarding soil properties could be obtained using correlations between blow counts and soil properties.

The soil layers encountered in the borings at the second office building site were somewhat similar to those at the garage site, except the upper sand layers below the parking facility were not encountered in the office building borings. General laboratory tests performed by the soil engineer on samples recovered from the borings included moisture content, dry density, and Atterberg limits tests. In addition, one direct shear test and two consolidation tests were performed. Most samples were obtained with a 3.25-inch diameter sampler driven by a 342-pound weight dropping 18 inches. These values were converted to rough standard penetration resistance (N) values using general correlation factors which considered driving energy and sampler size differences.

The evaluation of the soil property data that existed from previous laboratory testing and rough correlations with standard penetration resistance values indicated that very sparse data on soil properties was available. Therefore, it was concluded that a more reliable procedure to determine load capacity was to estimate soil strength properties based on the pile driving blowcounts, and then modify the strength characteristics of the soil layers using a ratio of the load capacity of the test piles computed using these properties to the actual load capacity determined by the pile load tests.

The initial soil properties selected for the various soil sublayers are presented on Tables 1, 2, and 3. Wet density values were generally obtained by evaluating wet density values recorded on the soil samples tested by the soil engineer at the garage

AD-A213 199 INTERNATIONAL CONFERENCE ON CASE HISTORIES IN GEOTECHNICAL ENGINEERING (2. (U) MISSOURI UNIV-ROLLA S PRAKASH 30 JUN 89 ARO-25645.2-GS-CF DAAL03-87-G-0129 7/8

UNCLASSIFIED F/G 13/2 NL

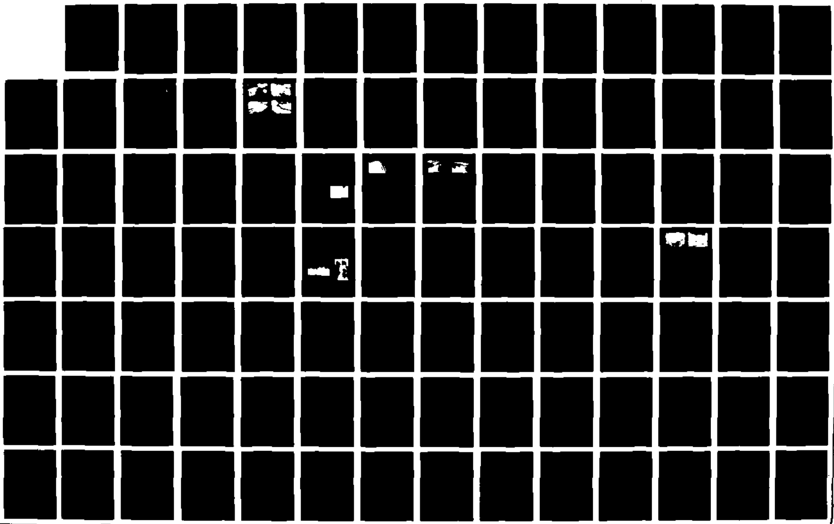

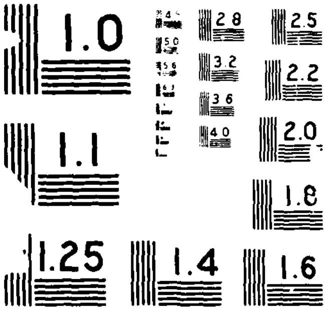
1.0
2.8
2.5
3.2
2.2
3.6
4.0
2.0
1.1
1.8
1.25
1.4
1.6

site. The undrained cohesion values for clay layers, as well as the drained friction angle for sand and gravel layers, were estimated on our experience with similar materials in the area.

C. Shaft Resistance

From Poulos (1980), the following formulas for shaft resistance were obtained:

Clay: $P_{su} = A_s c_a$

Sand and Gravel: $P_{su} = A_s K_s \tan \phi'_a \sigma'_v$

where P_{su} = ultimate shaft resistance

A_s = shaft area

c_a = soil-pile adhesion

K_s = coefficient of lateral pressure

ϕ'_a = drained friction angle between soil and pile

σ'_v = effective stress along shaft

The factors used in our initial capacity calculations for clay layers were determined by interpolation between the factors proposed by Tomlinson (1957) and Kerisel (1965). When sand or gravel layers were present, the relationships between ϕ and K tan ϕ'_a proposed by Vesic (1967) and by Meyerhof (1976) were considered. These two curves are presented on Figure 2. During our initial calculations, the values of Vesic (1967), which had been modified by Poulos (1980), were used. It should be noted that the critical or limiting value of $'_v$ reached along the pile shaft was determined in accordance with Vesic (1967) as a function of the pile diameter and the friction angle of the soil.

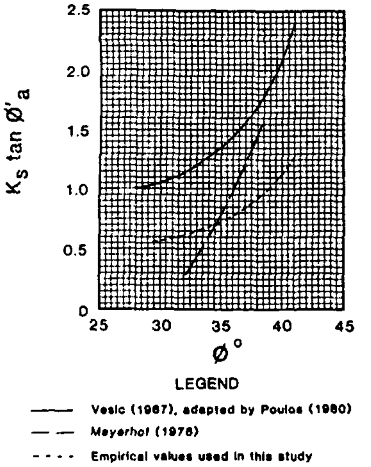

$K_s \tan \phi'_a$ vs. ϕ

Figure 2

D. Tip Resistance

The equations for tip resistance of the pile were also obtained from Poulos (1980). The equations used in this study were:

Clay: $P_{bu} = A_b c_u N_c$

Sand and Gravel: $P_{bu} = A_b f_b/f_s$

where P_{bu} = ultimate base resistance

A_b = base area

N_c = bearing capacity factor

c_u = undrained soil cohesion

f_b/f_s = ratio of base resistance to shaft resistance

In clay layers, the commonly accepted value of $N_c = 9$ proposed by Skempton (1959) was used. Where sand or gravel layers were present, the relationship of ϕ to f_b/f_s proposed by Vesic (1967) was adopted for the study.

E. Correction Factors

Using the equations, soil profiles, and soil properties previously discussed, the ultimate capacity was calculated of the two test piles on the site, as well as the test pile on the second office building site. The calculated capacities were then compared to the values recorded in the pile load tests. The results of these comparisons are presented below.

TP	CUC (Tons)	RUC (Tons)	RC/CC
PT-1	193	117	0.61
PT-2	349	195	0.56
IIT-1	623	320	0.51

TP = Test Pile Designation
CUC = Calculated Ultimate Capacity
RUC = Recorded Ultimate Capacity
RC/CC = Recorded Capacity/Calculated Capacity

This comparison indicates that calculated values were generally about twice the recorded values. It appears that the overestimation of the load capacities resulted primarily from overestimation of the soil properties because of the lack of quality laboratory testing of soils at the site. To a lesser degree, the overestimation might be attributed to the use of the Vesic relationship of ϕ vs $K_s \tan \phi'_a$ rather than the relationship proposed by Meyerhof (see Figure 2). However, the similarity of the ratios between the recorded and calculated values for the three piles is quite good, considering that varying soil profiles were present at the three locations and that PT-1 bears on clay, PT-2 bears on sand, and IIT-1 bears on gravel.

The majority of the calculated pile loads on all of the three test piles were carried by the portions of the pile shaft in sand or gravel layers, while the clay layers contributed relatively minor amounts. Therefore, it was decided to apply an empirical correction factor to the sand and gravel, and not correct the clay values. By applying a correction factor of 0.53 to the $K_s \tan \phi'a$ values originally obtained from Figure 2, the shaft and tip resistance in sand and gravel layers was modified so that the calculated and recorded capacities were nearly the same. The corrected values of $K_s \tan \phi'a$ are presented on Figure 2. The $K_s \tan \phi'_a$ values used are generally between the values proposed by Vesic (1967) and Meyerhof (1976) for sand layers ($\phi = 30° - 35°$), but lower than both values for gravel layers ($\phi = 38° - 41°$). This may mean that the sand properties were accurately estimated originally, but the gravel properties were overestimated.

F. Ultimate Capacity

Using the techniques discussed above, a procedure was developed to estimate the present ultimate load capacity for the existing piles under the five proposed shear walls. The results indicate the piles studied had ultimate capacities which vary from about 160 tons to 384 tons (320 to 768 kips). Soil conditions, pile driving records and load capacity data for the two extreme piers are summarized on Figures 3 and 4.

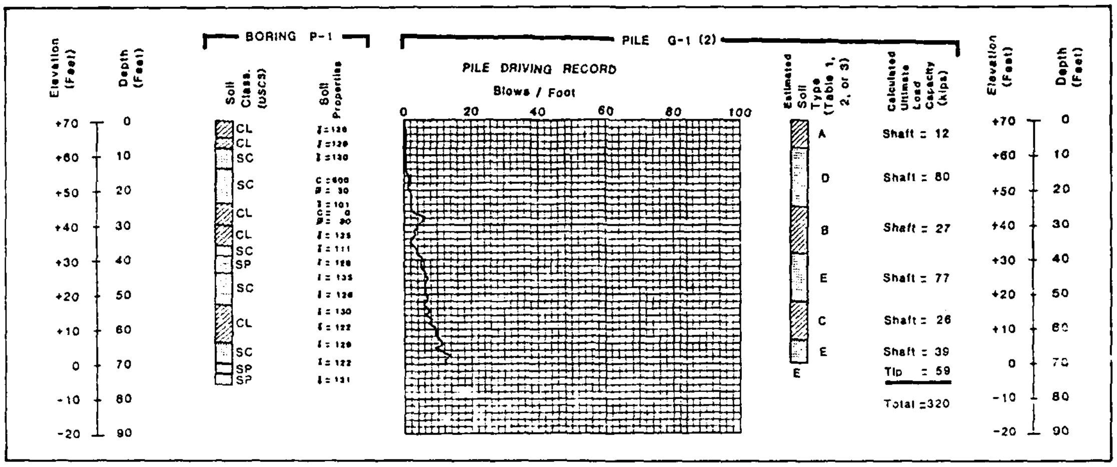

Figure 3. Capacity of Pile G-1 (2)

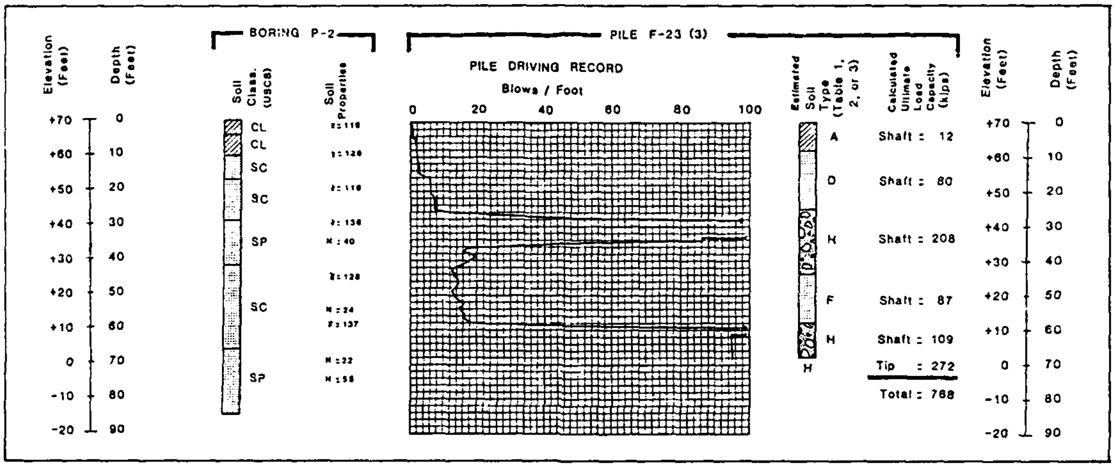

Figure 4. Capacity of Pile F-23 (3)

H. Factors of Safety

Typically, a factor of safety of 2.0 is used to convert ultimate pile capacity to an allowable value for dead plus live loads. However, Terzaghi (1967) indicates that "if the ultimate bearing capacity is determined by means of a load test, the customary factors of safety range between 1.5 and 2." It is our opinion that a factor of safety of 2 is a reasonable value to apply to ultimate capacities determined after soil borings have been drilled and pile load tests performed for a project because large uncertainties still exist about soil profile variations between boring locations. At the garage site, the pile driving records for 229 piles were studied to provide a much more detailed evaluation of soil conditions across the site. Because the level of uncertainty concerning subsurface conditions was substantially reduced for this project, it was recommended that a factor of safety of 1.5 be applied to the ultimate capacities to obtain an allowable capacity for dead plus live loads.

There is little published information about the factor of safety to be applied to ultimate pile capacities to determine the allowable capacity for earthquake loading. Standard practice is often to apply a one-third increase to the allowable capacity determined for dead plus live loads. We recommended that a factor of safety of 1.1 be used to convert ultimate pile capacity to allowable capacity during earthquake loading. We should note that if a one-third increase is used on the allowable dead plus live load capacity obtained using a safety factor of 1.5, then the resulting factor of safety for earthquake loading is about 1.13.

REFERENCES

Kerisel, J., (1965) "Vertical and Horizontal Bearing Capacity of Deep Foundations in Clay," Symposium on Bearing Capacity and Settlement of Foundations, Duke University.

Meyerhof, G.G. (1976) "Bearing Capacity and Settlement of Pile Foundations," ASCE Journal of the Geotechnical Division, Volume 102, No. GT 3.

Poulos, H.G. and Davis E.H., (1980) Pile Foundation Analysis and Design, John Wiley and Sons, New York.

Terzaghi, Karl, and Peck, Ralph B., (1967) Soil Mechanics in Engineering Practice, John Wiley and Sons, New York.

Tomlinson, M.J., (1957) "The Adhesion of Piles Driven in Clay Soils," Proceedings of the 4th International Conference on Soil Mechanics and Foundation Engineering, Volume 2.

Vesic, A.S., (1967), "A Study of Bearing Capacity of Deep Foundations," Final Report, Project B-189, School of Civil Engineering, Georgia Institute of Technology.

Proceedings: Second International Conference on Case Histories in Geotechnical Engineering, June 1-5, 1988, St. Louis, Mo., Paper No. 6.90

Comparisons Between Field and Analytical Behavior of an Experimental Excavation

Roberto Azevedo
Assistant Professor, Universidade Católica do Rio de Janeiro, Rio de Janeiro, Brazil

Nilo Consoli
Auxiliar Professor, Universidade Federal do Rio Grande do Sul, Rio Grande do Sul, Brazil

SYNOPSIS: This paper analyses the behaviour of an experimental unsupported excavation taken to failure in a soft clay deposit near Rio de Janeiro, Brazil. The excavation was originally analyzed by Pontes Filho and Medeiros (1982) assuming undrained conditions. In this paper, the same excavation is analyzed by Biot's coupled theory of consolidation and deformation using linear elastic, non-linear-elastic and elasto-plastic constitutive models and simulating the excavation process in time, without a-priori hypothesis on the drainage conditions. Details of the excavation construction, geotechnical profile and instrumentation are briefly described. Subsequently, the constitutive model calibrations are discussed in view of laboratory tests available. Finally, for each excavation step, comparisons are made between surface settlement profiles, horizontal displacements and pore-pressure measured in the field and analytically calculated.

INTRODUCTION

As part of a research project developed at PUC/RJ, a two-dimensions (2-D) computer program using the finite element method and capable of simulating the construction of excavations as well as embankments, was written. The program uses a coupled deformation-pore pressure dissipation theory (Biot, 1941; Sandhu and Wilson, 1969). It is based on a program developed by Osaimi (1977), the main differences being the implementation of a new version of the hyperbolic stress-strain constitutive model (Duncan, 1980) and the implementation of the Modified Cam-Clay elasto-plastic work-hardening constitutive model (Zienkiewicz and Naylor, 1971).

Parallel to this development, a few years ago (Ribeiro, 1981), an experimental excavation (Sarapui) was executed as part of another research project undertaken simultaneously by the Institute of Highway Research of Rio de Janeiro (IPR) and the Departments of Civil Engineering of PUC/RJ and of the Post-Graduation School of Federal University of Rio de Janeiro (COPPE/UFRJ). Besides the experimental excavation, the research project also included two trial embankments: one taken to failure to investigate strength properties (Ramalho Ortigão et al., 1983) and another one for settlement studies (Figure 1).

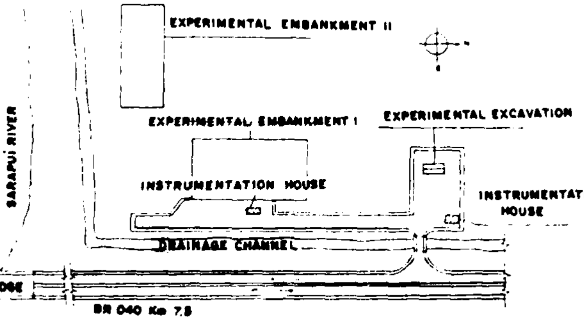

Fig. 1 - Sarapui Experimental Excavation (Pontes Filho and Medeiros, 1982)

The Sarapui experimental was taken to failure in few hours. A first analysis, made with a 2-D uncoupled finite element program with linear-elastic and non-linear-elastic constitutive models, assumed undrained conditions and utilized undrained laboratory tests and soil parameters (Pontes Filho and Medeiros, 1982).

This paper describes the utilization of the coupled finite element program mentioned above in a second analysis of Sarapui experimental excavation. In this second analysis, drained laboratory tests are used to determine soil parameters. The time spent to execute the excavation is taken into consideration, therefore avoiding, a priori, any hypothesis with respect to the drainage conditions of the problem.

Although there are few doubts about these drainage conditions, this second analysis aims, first, to test the coupled model's ability to predict partially drained behaviour and, second, to discuss two different undrained analyses: one made uncoupled with undrained parameters and, another one, made coupled with drained parameters.

Initially, the case history is briefly described. This part was essentially extracted from the work of Pontes Filho and Medeiros (1982) and is included here only to insure completeness. Subsequently, laboratory test results are presented, together with their analytical modeling. Finally, comparisons between field and analytical results are presented.

THE SARAPUI UNSUPPORTED EXPERIMENTAL EXCAVATIONS

The experimental excavation was performed on 4 steps, with failure occuring approximately 5 hours and 45 minutes after the construction beginning (Figure 2).

The instrumentation consisted of 44 surface monuments, 15 piezometers (7 of the Casagrande type and 8 of the hydraulic type), 2 slope indicators and 4 magnetical extensometers (Figure 3).

The soil profile consisted of three layers (Figure 4): a 1 to 1.4 meters thick sandy embankment dumped in the area three years before the excavation, a 3.2 to 3.8 meters thick organic silty clay layer (Sarapui clay) and 10 meters thick stiff sandy clay layer. The sandy embankment consisted of a well-graded sand-gravel mixture excavated from a nearby pit of young gneissic residual soil with average specific unit weight of 2.0 tf/m^3 and moisture content between 9% and 11%. Sarapui soft clay has been investigated by many authors: Costa Filho et al. (1977); Werneck et al. (1977); Ramalho Ortigão and Costa Filho (1982). At excavation site, average liquid limit of 98% and plastic limit of 49% were encountered. Natural moisture content, void ratio, specific unit weight and degree of saturation were equal to 141%, 3.9, 1.33 tf/m^3 and 97%, respectivelly. The organic matter content was about 5% and is responsible for the dark gray color of Sarapui clay (Ramalho Ortigão et al., 1983).

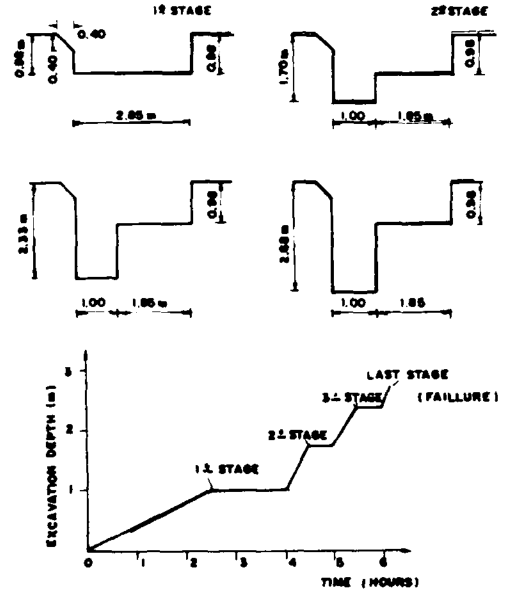
1º STAGE
2º STAGE
0.40
0.98
2.85 m
1.70 m
1.00
1.85 m
2.33 m
2.88 m
1.85
EXCAVATION DEPTH (m)
LAST STAGE
(FAILLURE)
3º STAGE
2º STAGE
1º STAGE
TIME (HOURS)
0
1
2
3
4
5
6

Fig. 2 - Excavation Sequence and Duration (Ribeiro, 1981)

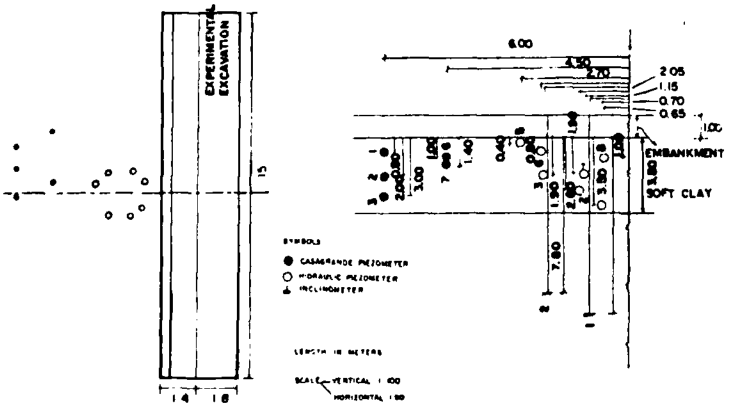
EXPERIMENTAL EXCAVATION
15
1.4
1.8
6.00
4.50
2.70
2.05
1.15
0.70
0.65
1.00
EMBANKMENT
SOFT CLAY
SYMBOLS
CASAGRANDE PIEZOMETER
HYDRAULIC PIEZOMETER
INCLINOMETER
LENGTH IN METERS
SCALE VERTICAL 1:100
HORIZONTAL 1:100

(a) Plan View

(b) Transversal View

Fig. 3 - Excavation Instrumentation

An investigation carried out by Ribeiro (1981) indicated a moderate degree of overconsolidation in the soft clay deposit. However, the sandy embankment constructed three years before the excavation initiated a consolidation process which, based on piezometer readings, was completed before the excavation beginning. Therefore, the deposit to be excavated was normally consolidated (Pontes Filho and Medeiros, 1982).

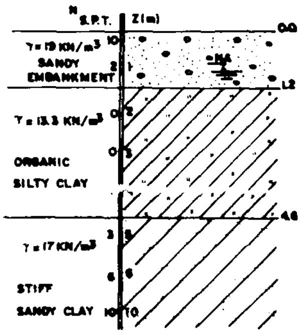
N S.P.T.
Z(m)
0.0
γ = 19 KN/m³
SANDY EMBANKMENT
NA
1.2
γ = 13.3 KN/m³
ORGANIC SILTY CLAY
4.6
γ = 17 KN/m³
STIFF SANDY CLAY

Fig. 4 - Soil Profile and Excavation Site

LABORATORY TESTINGS AND CONSTITUTIVE MODELS

The sandy embankment stress-strain and strength behaviour was investigated by Pontes Filho (1981) who performed two series of drained axisymmetric triaxial tests using a stress-controlled cell (Bishop and Wesley, 1975). The first series consisted of three conventional triaxial compression tests (CTC - increasing axial stress and constant confining pressures of 10, 20 and 30 tf/m^2). The second series consisted of three reduced triaxial compression tests (RTC - constant axial stress of 20, 30 and 40 tf/m^2 and decreasing confining pressure). Only the CTC were used for calibrating the constitutive models.

The Sarapui soft clay stress-strain and strength behaviour was investigated by a series of undrained and drained axisymmetric triaxial tests. The undrained tests were performed by Sayão (1980). A total of 45 tests was executed: 24 rapid tests (UU or CU without pore-pressure measurements) and 21 slow tests (CU with pore-pressure measurements). The drained tests were performed by Bressani (1983). A total of 11 tests was executed, always with volume change measurements: 5 tests were strain-controlled and 6 were stress-controlled.

Only the drained tests were utilized for the hyperbolic calibration of Sarapui soft clay. For the Modified Cam-Clay elasto-plastic model, besides the drained and undrained tests, oedometer tests were also necessary for calibration (Sayão, 1980).

TABLE I

	E (kPa)	ν
SAND	5100.	0.30
CLAY	625.	0.17

TABLE II

	K	n	Rf	c'	φ'	Kb	m
SAND	405.7	0.785	0.71	0	34	–	–
CLAY	9.36	0.36	0.606	0	24	5.53	0.678

TABLE III

	λ	k	M	eo	ν
CLAY	0.73	0.11	1.25	3.90	0.17

COMPARISONS BETWEEN FIELD AND ANALYTICAL PERFORMANCE

Three different finite element analyses were made. In the first one, herein called elastic, both sandy embankment and Sarapui clay were modeled with a linear-elastic model using parameters shown in Table I. In the second analysis, herein called hyperbolic, both sandy embankment and Sarapui clay were modeled with the hyperbolic model using parameters presented in Table II. In the third analysis, herein called Cam-Clay, the sandy embankment was modeled with the hyperbolic model using parameters shown in Table II and the Sarapui clay was modeled with the Modified Cam-Clay elasto-plastic model using parameters presented in Table III.

Figure 5 shows comparisons of surface settlement profiles due to excavation stages: (a) 1, (b) 2 and (c) 3, respectively. The analytical results do not show a good quantitative agreement with the field ones. Results obtained with the hyperbolic and the Cam-Clay analyses are reasonably close and only qualitatively in agreement with the field ones. Field settlement are in general much smaller than the analytical ones. A probable reason for this difference may be found in the analytical simulation of the sand embankment. Due to low stress levels from the beginning of excavation some elements in the embankment fail or become too flexible in the analysis, therefore exaggerating the analytical vertical displacements.

Figure 6 and 7 present comparisons of horizontal displacements due to excavation along vertical lines corresponding to inclinometers I1 and I2, respectively. In this case, results obtained with the hyperbolic and Cam-Clay analyses agree reasonable well with the field ones, except the results from the inclinometer I1, stage 3. The elastic analysis was clearly the worst ones, whereas the Cam-Clay analysis was a little better than the hyperbolic one. It is important to remember that the volumetric response of the sand embankment was estimated, therefore features like dilatancy, that may explain certain observed differences in the horizontal movements, were not either evaluated in the laboratory or modeled.

Figure 8 and 9 present comparisons between pore-pressures analytically calculated and measured in the field by Casagrande and hyperbolic piezometers, respectively. In general, results of the three analyses do not differ much, the largest differences being encountered between the elastic and the other two analyses. The analytical results are in agreement with the field ones specially before failure (time equal to 15:00 hours). After this point some of the piezometer registered an abrupt change in pore water pressure that could not be acounted for in the analysis.

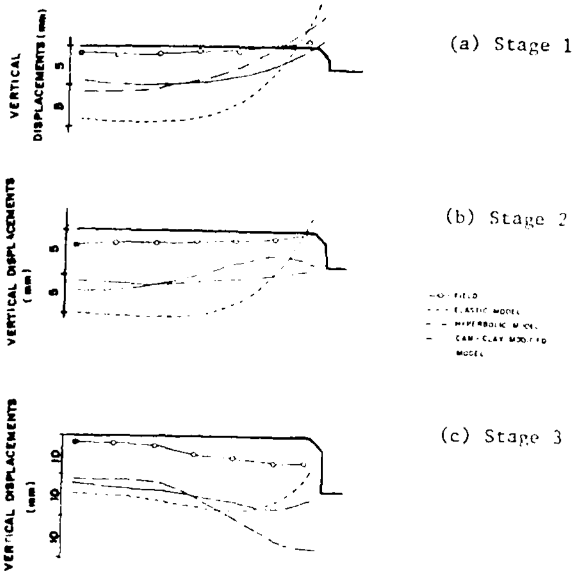

Fig. 5 - Surface Settlement Profile Comparisons

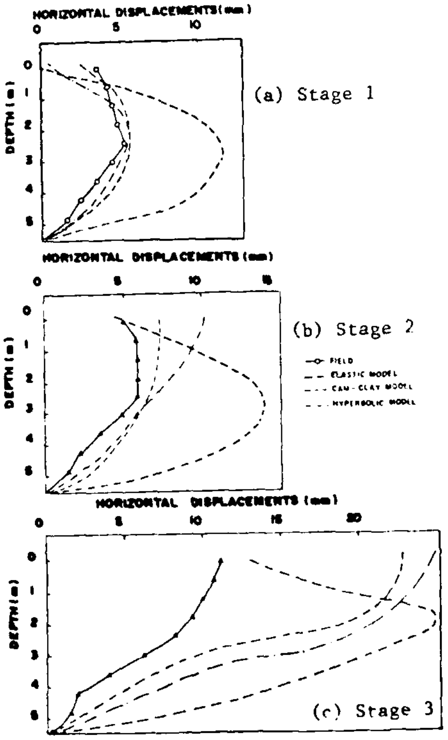

Fig. 6 - Horizontal Comparisons for Inclinometer I1

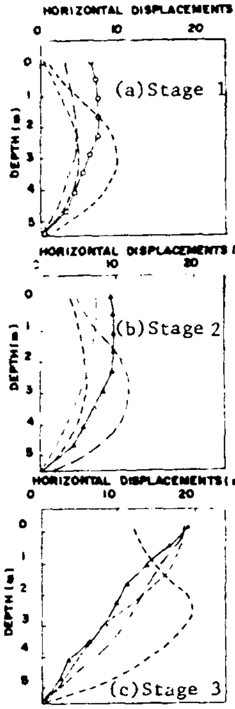

Fig. 7 - Horizontal Displacement Comparisons for Inclinometer I2

CONCLUSIONS

With the exception of the surface settlement profiles, comparisons were, in general, both qualitative and quantitatively good particularly for the hyperbolic and Cam-Clay analyses.

With respect to the pore-pressure comparisons, the three analyses gave rise to close results, therefore not justifying the utilization of more sophisticated models as the hyperbolic and Cam-Clay. However, the displacement comparisons were clearly more favorable for the hyperbolic and Cam-Clay analyses than for the linear elastic one, therefore entirely recommending the utilization of these analyses instead of the linear-elastic one.

The Cam-Clay analysis gave rise to results that were sligthly better than the hyperbolic ones. Nevertheless, the differences were small and, for the case analyzed, there was no major gain in accuracy that justyfied the use of this more sophisticated elasto-plastic model instead of the simpler and widely known hyperbolic model.

Comparisons between results obtained by Pontes and Medeiros (1982) with their uncoupled-undrained analysis with results presented in this paper show small differences justifiable by different values of effective stress in the two analyses. In fact, both analyses induce same total stresses, since they depend on the geometry and equilibrium conditions of the problem. The effective stresses, however, may be different, depending on the pore-pressures. In the analysis made by Pontes and Medeiros (1982) it is assumed, first, that the excavation was executed in undrained conditions and, second, that the pore-pressures generated during the laboratory undrained tests are equal to the field ones while the excavation is being executed. This is only true if the stress-paths in the laboratory tests and in the field are exactly the same which is seldom the case. On the other hand, the pore-pressures generated by the coupled theory are in accordance with the equations governing the behaviour of a two-phase material (Biot, 1941). The main assumptions in this case are, laminar flow and infinitessimal strains during consolidation, and modeling of the effective stress-strain relation observed in drained tests.

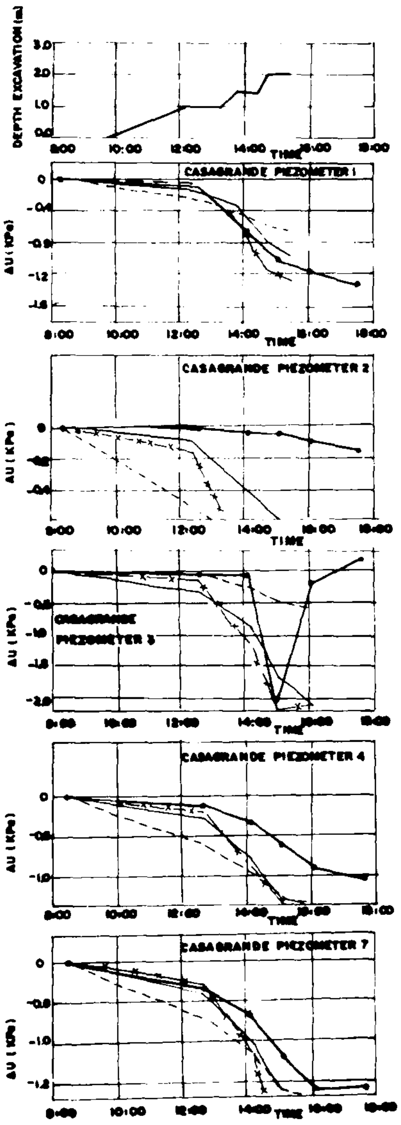

Fig. 8 - Pore-Pressure Comparisons for Casagrande Piezometers

Since results of the two analyses are reasonably close, it is logical to say that they gave rise to values of pore-pressure approximately the same. However, the coupled approach is more attractive because it does not involve an assumption about the drainage conditions in which the excavation is executed which, for pratical rather than experimental excavations, is frequently difficult to determine (Osaimi and Clough, 1979).

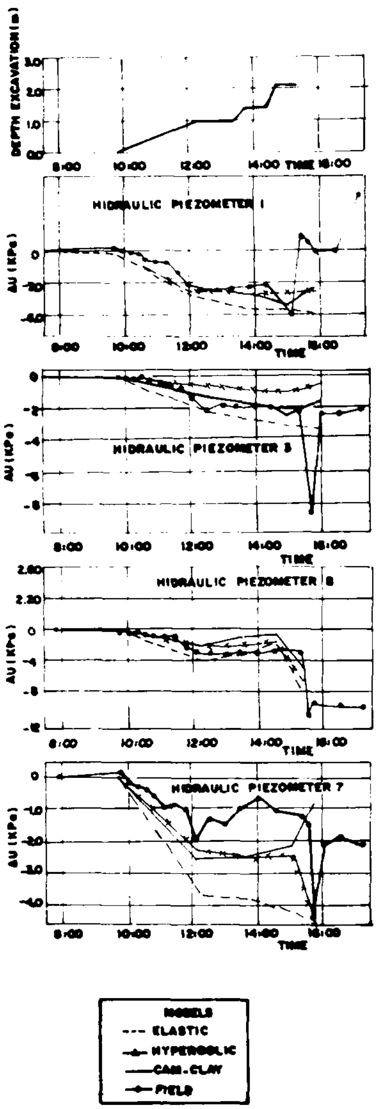

Fig. 9 - Pore-Pressure Comparisons for Hydraulic Piezometers

ACKNOWLEDGMENTS

The subject of this paper is part of the second author M.Sc. thesis who, during his Master program, was awarded with a scholarship provided by CNPq (National Council for Developments and Research, Ministry of Education, Brazil). The writers wish to express their gratitude for this financial support.

REFERENCES

Biot, M.A. (1941), General Theory of Three--Dimensional Consolidation, Journal of Applied Physics, 12, p. 155-164.

Costa Filho, L.M.; Werneck, M.L.G. and Collet, H. B. (1977), The Undrained Strength of a Very Soft Clay, Proceedings, 9th International Conference On Soil Mechanics And Foundation Engineering, Tokyo, 1, p. 69-72.

Duncan, J.M. (1980), Hyperbolic Stress - Strain Relationships, Proceedings, Workshop on Limit Equilibrium, Plasticity and Generalized Stress -Strain in Geotechnical Engineering, Edited by R.K. Yong and H.Y. Ko, McGill University, Canada, p. 443-460.

Osaimi, A.E. (1977), Finite Element Analysis of Time Dependent Deformations and Pore Pressures in Excavations and Embankments, Ph.D. Thesis, Stanford University, California, USA, p. 230 .

Osaimi, A.E. and Clough, G.W. (1979), Pore-Pressure Dissipation During Excavation, Journal of the Geotechnical Division, ASCE, 105, GT.4, p. 481-498.

Pontes Filho, I. (1981), Analysis of Sarapui Experimental Excavation (in Portuguese), M.Sc. Thesis, Pontifícia Universidade Católica do Rio de Janeiro, Rio de Janeiro, Brazil, p. 246.

Pontes Filho, I. and Medeiros, L.V., Finite Element Analysis of an Experimental Excavation, Proceedings, Fourth International Conference on Numerical Methods in Geomechanics, Edmonton, Canada, p. 699-705.

Ramalho Ortigão, J.A. and Costa Filho, L.M. (1982), Discussion of Cam-Clay Predictions of Undrained Strength, by Paul W. Mayne, Journal of the Geotechnical Engineering Division, ASCE, 108, GT. 1, p. 181-183.

Ramalho Ortigão, J.A.; Werneck, M.L.G. and Lacerda, W.A. (1983), Embankment Failure On Clay Near Rio de Janeiro, Journal of the Geotechnical Engineering Division, ASCE, 109, GT. 11, p. 1460-1479.

Ribeiro, J.V. (1981), Planning, Execution, Observation and Preliminar Analysis of an Unretaining Instrumented Excavation (in Portuguese), M.Sc. Thesis, Pontifícia Universidade Católica do Rio de Janeiro, Rio de Janeiro, Brazil, p. 228.

Sandhu, R.S. and Wilson, E.L. (1969), Finite Element Analysis of Flow in Saturated Porous Elastic Media, Journal of Engineering Mechanics, ASCE, 95, p. 641-652.

Sayão, A.S. (1980), Laboratory Testings on the Soft Clay of Sarapui Experimental Excavation (in Portuguese), M.Sc. Thesis, Pontifícia Universidade Católica do Rio de Janeiro, Brazil, p. 201.

Werneck, M.L.G.; Costa Filho, L.M. and França, H. (1977), In Situ Permeability and Hydraulic Tests in Guanabara Bay Clay, Proceedings, Soft Clay Conference, Bangkok, p. 399-418.

Zienkiewicz, O.C. and Naylor, D.J. (1971). The Adaptation of Critical State Soil Mechanics Theory for Use in Finite Elements, Proceedings, Roscoe Memorial Symposium, p. 537-547.

Proceedings: Second International Conference on Case Histories in Geotechnical Engineering, June 1-5, 1988, St. Louis, Mo., Paper No. 6.92

Actual and Predicted Behavior of Large Metal Culverts

David C. Cowherd
President and Chief Geotechnical Engineer, Bowser-Morner Associates, Inc., Dayton, Ohio

Stephen M. Thrasher
Director, Environmental Services, Bowser-Morner Associates, Inc., Dayton, Ohio

Vlad G. Perlea
Senior Engineer, Bowser-Morner Associates, Inc., Dayton, Ohio

John O. Hurd
Hydraulic Research Engineer, Ohio Department of Transportation, Columbus, Ohio

SYNOPSIS The stability of large metal culverts depends on the performance of the backfill around the pipe, which must be considered as a part of the structure when evaluating its safety. A simplified method to evaluate the current stability of such a structure on the basis of the structure's shape is derived. Useful when limited amount of information is available, this method provides an economical procedure for: (1) evaluating the condition of the existing backfill and its capability to provide a safe support for the structure; (2) predicting final movements and determining if additional investigations are necessary to establish the safety of the structure; and (3) determining if measured deflections are in agreement with those predicted and, if not, determining if the safety of the structure is endangered by phenomena other than the expected behavior of surrounding soil (e.g. voids near pipe, soil erosion, non-symmetric loadings).

INTRODUCTION

Several hundred long-span corrugated metal pipes are currently in place across the United States and about one-hundred new pipes are installed each year. Since most of the pipes are installed under highways and the safety of traffic relies on their structural stability, periodic inspection and evaluation is obligatory. Because the stability of these structures depends on the condition of the supporting backfill, and because extensive annual evaluation of the backfill is expensive and impractical in most cases, a simplified method, based on a limited amount of available information, is necessary.

Corrugated metal pipes cannot be rated based on structural capabilities, as can a bridge. These pipes depend on the backfill for their support, and the backfill around the pipe must be considered as a part of the structure. Any evaluation of large corrugated metal pipes must, therefore, take into consideration performance of the backfill. The overall performance of the pipe and backfill can be evaluated by comparing the shape of the pipe with the intended design shape, both at time of installation and periodically thereafter.

The procedure presented describes a relatively simple procedure for evaluating the condition of a long-span pipe based on shape and then, if the shape is approaching a degree of flatness which may be unstable, for utilizing the density of the backfill and the soil type to predict future movement. The method can be used to determine future movements of pipes which are experiencing deflection or to project deflection of a newly installed pipe.

EVALUATION OF PIPE CONDITION BASED ON SHAPE

The important factor to be evaluated in assessing the safety of a corrugated metal structure is the extent to which the pipe wall has lost its curvature and becomes flatter. The extent of flattening can be measured during an annual inspection using the method recommended by Cowherd and Delger (1986). This procedure evaluates the changes in shape to determine whether or not the amount of deflection creates a problem. For this purpose, a computer program entitled "MULTSPAN" was prepared. This program:

- calculates the radii along the structure perimeter based on the chord and mid-ordinate measurements (see Figure 1), determines the average, maximum and minimum values for the chords, mid-ordinates, and radii;
- compares these field values with design values, corresponding to the structure's intended shape;
- where there is no design information available, the program estimates what these dimensions should be using the available field data and calculates estimated mid-ordinates based on the properties of circular areas; and

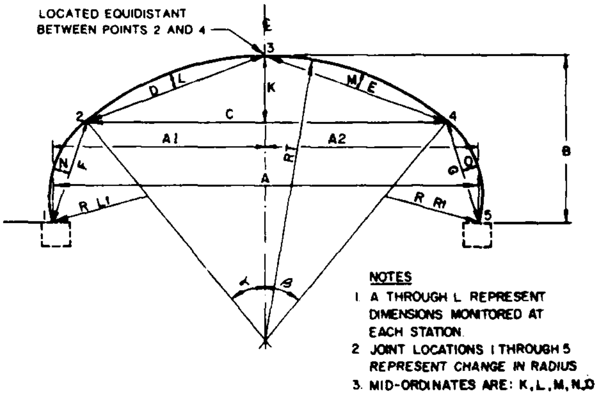
LOCATED EQUIDISTANT BETWEEN POINTS 2 AND 4
℄
1
2
3
4
5
K
D
L
M
E
C
A1
A2
RT
N
F
G
O
A
B
R L1
R R1
α
β
NOTES
1 A THROUGH L REPRESENT DIMENSIONS MONITORED AT EACH STATION.
2 JOINT LOCATIONS 1 THROUGH 5 REPRESENT CHANGE IN RADIUS
3. MID-ORDINATES ARE: K,L,M,N,O

Fig. 1 Measured and Computed Parameters

uses the deflection data and visual observations to assess the degree of flatness and make recommendations of appropriate action.

Details on MULTSPAN can be found in Thrasher and Perlea (1986). The MULTSPAN analysis, along with pipe condition data, can be used to establish a bridge rating. This bridge rating system is compatible with the Bridge Inventory and Inspection Program. The method assesses the deflection (measured in an annual Bridge Inspection Program) to make recommendations relative to remedial action. Table I shows the recommended actions provided by MULTSPAN relative to the various amount of mid-ordinate deflections (Cowherd and Degler, 1986).

TABLE I. Percent Mid-Ordinate Change and Remedial Action

Mid-Ordinate Percent Change	Depth of Cover (ft)	Recommended Action
<15	Any	No action required.
15 - 20	Over 6.0	No action required.
	Under 6.0	Monitor on 6-month interval.
20 - 25	Over 6.0	Reduce legal load to 90% of H-20 and monitor on 6-month intervals.
	Under 6.0	Reduce legal load to 75% of H-20 and monitor on 6-month intervals.
25 - 30	Over 6.0	Reduce legal load to 75% of H-20 and monitor on 6-month intervals.
	3.0 - 6.0	Reduce legal load to 50% of H-2 and monitor on 6-month intervals.
	Under 3.0	Reduce legal load to 50% and do detailed analysis.
>30	Any	Close road until detailed analysis is done.

NOTE: Detailed analysis to include soil borings to determine expected additional movement.

Figure 1 illustrates the measured parameters. The Table I recommendations are based on mid-ordinate deflections and not on total span heights. Such recommendations for corrective action have been based on the extensive experience of the manufacturers and a hand full of practicioners. A more rigorous analysis of these structures can be made, however, based on the assumption that they behave in a manner similar to thin wall tubes subjected to uniform loading.

Defining the factor of safety (F) as the ratio between the critical soil pressure which induces buckling failure and the actual soil pressure, and using relationships between mid-ordinate (m) and other geometrical parameters of the pipe, the following equation may be written (Cowherd et al., 1986):

$$\Delta F/F = (\Delta m/m) \times 3\ (1 - m/r) \qquad (1)$$

Where r is the radius corresponding to the mid-ordinate m.

For standard long-span pipes the factor 3 (1 - m/r) varies generally between 2.3 and 2.8. That means that a pipe having initially a factor of safety of about 5 will have the factor of safety decreased to 2.9-3.3 when the mid-ordinate percent change is 15%, around 2.5 for 20%, around 1.8 for 25%, and close to 1.0 for 30%.

For various types of pipes and other initial factors of safety the results of such an analysis would differ, but not significantly, so that the criteria in Table I appear reasonable.

ESTIMATING STRUCTURE MOVEMENT

If the structure movement is enough to warrant borings to determine the nature of the backfill, the borings are made and appropriate soil data collected. The soil data are then introduced into the computer program to make projections of both magnitude and rate of continued movement. To determine the soil density and soil type, it is necessary to make at least one boring on either side of the pipe in the backfill and preferably at least one boring in the material outside the backfill. The method can use either density measurements directly or standard penetration values which can be correlated to density. The density can be determined with nuclear depth-density gauges throughout the depth of a boring or by taking undisturbed samples. The nuclear density method is by far the most economical.

The accuracy of this method has been evaluated using several different case histories; some of which are presented in this paper. In all cases, good agreement between the predicted and actual movement was observed. The main advantage of the method is that it presents a simple way of assessing the safety of a corrugated metal structure without requiring considerable expensive field and laboratory data and computer time to predict continued movement of a pipe that is experiencing deflection. It can also be used to predict total movement using initial compaction data. As a result, a relatively simple assessment of projected pipe movement can be made. Vertical movement of the structure, when due to the deformation of the pipe and not to a general settlement, is of greatest importance since it is a measure of the degree of flatness of the structures crown.

Except for unusual loading conditions previously noted, the vertical movement of a quasi-circular structure can be related to horizontal or side movement of the structure by a factor of approximately one-half; i.e., the movement of one side of the structure into the backfill is equal to approximately one-half the vertical movement (Spangler, 1951). Actually, the shape factor; i.e., the ratio between the movement of one side of the structure and the corresponding vertical movement, varies for usual shapes between 1.4 and 4.9. The program MULTSPAN makes an evaluation of the shape factor based on the assumption that during small deformations of pipe the mid-ordinates only change, but the chord lengths remain unchanged, which leads to the following relationship (see Fig. 4 for notations):

$$\frac{\Delta R}{\Delta(S/2)} = \frac{1}{2}[(S - S_B)/R_B + S/(R - R_B)] \tag{2}$$

Therefore, determination of the outward horizontal movement will also permit determination of downward movement. The calculation of this horizontal movement may be accomplished by a simplified, three step process:

- Step No. 1 - determine the soil compressibility,
- Step No. 2 - determine the maximum horizontal pressure exerted by the structure on the surrounding fill; and
- Step No. 3 - calculate the horizontal movement using classical theory of consolidation for shallow foundation settlement.

Step No. 1 - Determination of Soil Compressibility

An estimation of the final movement of a structure can be based on the result of a consolidation test with zero lateral movement. This method has been used for many years to evaluate settlement of building foundations. The method can be applied to horizontal (and thus vertical) movement of pipes by considering the side of the pipe as a shallow footing.

This method does not take into account such factors as:

- the variation of the compressibility indexes with the stress level,
- the instantaneous (elastic) compression,
- the secondary compression; and
- the influence of the actual distribution of stresses on the structure.

Experience (with both buildings and long-span corrugated metal pipes) has shown, however, that this method provides an adequate measure of movement for both buildings and pipes. It is the standard method for predicting settlement of shallow foundations. The accuracy of the method is sufficient to provide a basis for making an engineering decision regarding whether or not corrective action is warranted. It is possible to estimate the compressibility of soils without taking undisturbed samples and performing a consolidation test. Empirical correlations which relate the compression index to grain size (soil type) and percent compaction (density) can be made. It is, therefore, possible to determine some characteristics such as grain size and density of the backfill and evaluate the compressibility.

Table II gives a rough estimation of the compression index (C_c) based on the type of soil (seven categories) and relative density or consistency (two limit values and an average one) (Terzaghi and Peck, 1967; Peck et al., 1974; Hough, 1969; Bally and Perlea, 1983; McCarthy, 1977).

For classification in the three density categories, the corresponding void ratio or percent standard Proctor are given in Tables III and IV. An approximate correspondence between void ratio and the results of the standard penetration tests, based also on data in literature, is given in Table V.

TABLE II. Classification of Soil Types and Their Characteristics

Category of Soil	Type of Soil	ASTM D 2487 Class	Average C_c Values For: Loose/Soft Material	Medium Dense	Dense/Stiff Material
I	Gravel	GW GP	0.03	0.01	0.003
II	Silty/Clayey Gravel	GM GC	0.05	0.02	0.008
III	Well Graded Sand	SW	0.06	0.02	0.007
IV	Poorly Graded Sand	SP	0.05	0.03	0.018
V	Silty Sand, Clayey Sand	SM SC	0.33	0.20	0.10
VI	Silty Soils	ML MH	0.40 or based on W_L as below	0.25	0.10
VII	Clayey Soils	CL CH	0.60* or (W_L-10) x 0.012	0.40* or (W_L-10) x 0.008	0.20* or (W_L-10) x 0.006

*Values to be used if liquid limit (W_L) is not known.

TABLE III. State of Density Estimation When (Indirect) Measurements of Void Ratio are Available

Category of Soil	Type of Soil	ASTM D 2487 Class	Void Ratio Corresponding to Loose/Soft Material	Medium	Dense/Stiff Material
I&II	Gravels	GW GP GM GC	0.6	0.5	0.4
III&IV	Sands	SW SP	0.7	0.6	0.4
V	Silty/Clayey Sand	SM SC	0.8	0.7	0.5
VI	Silty Soils	ML MH	0.9	0.75	0.5
VIIa	Clayey Soils ($W_L<50$)	CL CH	1.0 (1.2)*	0.8 (0.9)*	0.6
VIIb	Clayey Soils ($W_L\geq50$)		1.6	1.1	

*Values to be used if liquid limit (W_L) is not known.

TABLE IV. State of Density Estimation Based on Known Degree of Compaction

Category of Soil	Degree of Compaction (Percent Standard Proctor - ASTM D 698-78) Corresponding to: Loose/Soft Material	Medium	Dense/Stiff Material
Any	80	90	100

TABLE V. State of Density Estimation Based on Standard Penetration Results

Category of Soil	Standard Penetration Blow Count, N, Corresponding to: Loose Material	Medium	Dense Material
Cohesionless Soils: I Through V	≤ 10	11-30	≥ 31
	Soft Material	Medium	Stiff Material
Cohesive Soils: VI	≤ 5	6-15	≥ 16
VII	≤ 5	6-10	≥ 11

As an alternate and for research purposes only, the state of density is estimated by the program MULTSPAN using some available correlations for standard penetration test as well as for cone penetration test and accepted relationship between static and standard penetrations (Fardis and Veneziano, 1981, Gibbs and Holtz, 1957, Marcuson and Bieganousky, 1977a and b, Perlea and Perlea, 1983, Schmertmann, 1970, Searle, 1979, Terzaghi and Peck, 1967). A general relationship was considered for estimation of the compressibility index (C_C):

$$C_C = C_{C \cdot av} \times 10^{(A-B)\frac{P-60}{30}} \tag{3}$$

Where:

$A = \log C_{C \cdot av}$

$B = \log C_{C \cdot w}$

$C_{C \cdot av}$ = compressibility index of the soil in average condition, as given by Table II

$C_{C \cdot w}$ = compressibility index of the soil in worst condition of density and moisture content, as given in Table II for loose/soft material.

P = a parameter representing relative density in cohesionless soils and consistency in cohesive soils: $30 \leq P \leq 90$.

Like $C_{C \cdot av}$ and $C_{C \cdot w}$, the parameter P is separately estimated for every type of soil, as shown in Table VI.

TABLE VI. Values of the Parameter "P" Used in the Estimation of Compressibility Index

Soil Category	P: If P > 90, do P = 90 If P < 30, do P = 30
I	$43 \times \log [96.56 \times N \times D_{50}^{-0.284} \times (\sigma'_v)^{-0.56}]$
II	$43 \times \log [72.42 \times N \times D_{50}^{-0.284} \times (\sigma'_v)^{-0.56}]$
III	$11.7 + 0.76 \sqrt{\lvert 222 \times N + 1600 - 0.368\,\sigma'_v - 50\,(C_u)^2 \rvert}$
IV	$21 \sqrt{N/(4.79 \times 10^{-4}\,\sigma'_v + 0.7)}$
V	$43 \times \log [36.21 \times N \times D_{50}^{-0.284} \times (\sigma'_v)^{-0.56}]$
VI	$43 \times \log [24.14 \times N \times D_{50}^{-0.284} \times (\sigma'_v)^{-0.56}]$
VII	$20 \sqrt{N}$

Notations used in Table VI have the following meaning:

N (blows/feet)	- average Standard Penetration Test blow count for the range of depths critical for pipe deformation
D_{50} (mm)	- mean diameter of particles
σ'_v (psf)	- effective overburden pressure at the average depth of SPT measurements taken into account
C_u	- coefficient of uniformity of the soil

Depending on the available information, soil density is estimated by the program MULTSPAN, less or more accurately, by interpolation in Tables III, IV, or V (or relationships in Table VI) and:

- from indirect determination of void ratio by nuclear measurements of soil density and moisture content,
- from design requirements or inspection records, which gives the degree of compaction; and
- from standard penetration tests.

Step No. 2 - Pressure Distribution Around the Structure

A method of estimation of the maximum horizontal pressure, P_h, exerted by the structure on the surrounding fill and the width and the distribution (rectangular, parabolic, or trapezoidal depending on the shape of the structure) of this pressure must be considered (see Figure 2).

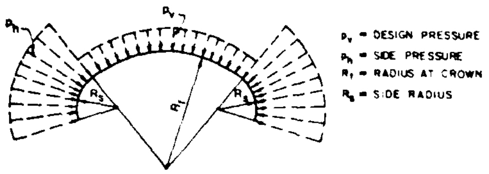
p_v
p_h
R_s
R_t
p_v = DESIGN PRESSURE
p_h = SIDE PRESSURE
R_t = RADIUS AT CROWN
R_s = SIDE RADIUS

Fig. 2 Simplified Hypothesis for Stresses Around the Pipe

An usual approximation for an eliptical shape structure relates p_h to the vertical exerted pressure, p_v, and the ratio of top radius and side radius as follows (Watkins, 1975):

$$p_h = p_v \; R_t / R_s \tag{4}$$

The vertical pressure may be equated with the total overburden acting at the top of the structure.

Step No. 3 - Horizontal Movement Calculation

The classical theory of settlement for a shallow foundation may be used for calculating the horizontal movement. The fill at the side of the structure is considered as a soil column loaded by the pressure generated by the structure onto the fill. Generally, the decreasing of the induced stresses with the distance from the structure must be considered. This may be done using influence charts available for different distributions of the applied stresses (e.g. Fig. 3).

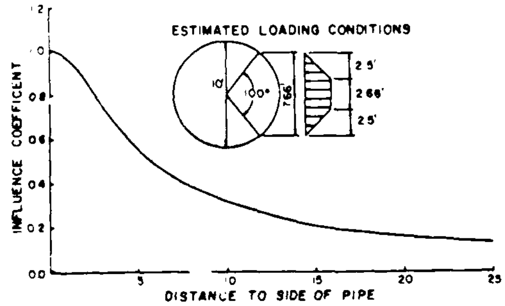

Fig. 3 Stress Distribution in Backfill

If the width of the backfill is small by comparison with the dimensions of the structure (e.g. smaller than the structure span dimension) a uniform distribution of stresses can be conservatively used (Fig. 4). If the width of the backfill is very large, the calculations can be limited to an influence distance of 2.5 rise dimensions.

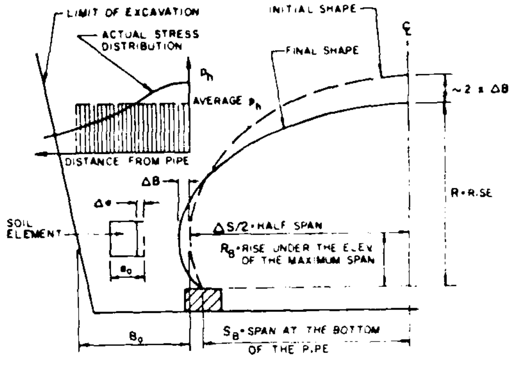
LIMIT OF EXCAVATION
ACTUAL STRESS DISTRIBUTION
INITIAL SHAPE
FINAL SHAPE
℄
p_h
AVERAGE p_h
~2 x ΔB
DISTANCE FROM PIPE
ΔB
Δe
SOIL ELEMENT
B_0
ΔS/2 = HALF SPAN
R_B = RISE UNDER THE ELEV OF THE MAXIMUM SPAN
R = RISE
B_0
S_B = SPAN AT THE BOTTOM OF THE PIPE

Fig. 4 Pipe - Backfill Interaction

The decrease in void ratio at a given distance from the structure may be estimated by the formula:

$$\Delta e = C_c \log \left[(K_0 \, p_v + p_h) / K_0 \, p_v \right] \tag{5}$$

Where:

p_h = the supplementary pressure induced by the structure at a given distance from the structure.

p_v = the effective overburden pressure at the level of calculation (in the middle of the loaded area by the structure; not at the top of the pipe).

K_0 = the coefficient of earth pressure at rest, which largely depends on the method and the intensity of compaction. (0.5 for natural deposits and 0.6 for compacted fills may be used as a rough approximation).

In an incremental layer of initial width B_0, for which the induced stress can be considered constant, the strain ΔB is:

$$\Delta B = B_0 \times \Delta e / (1 + e_0) \tag{6}$$

Where e_0 is the void ratio of the compacted fill not affected by the supplementary pressure induced by the structure; however, if the structure has already begun to deform, the void ratio may be less in the zone of influence of the structure.

Finally, the total horizontal displacement is converted into vertical movement of the pipe crown. For circular or quasi-circular pipes a good approximation is that the vertical movement is equal to the sum of horizontal movements on each side of the pipe. For pipes which significantly differ from the circular shape, a corrective shape factor is applied, as shown in Equation 2.

SOIL EVALUATION - CASE HISTORIES

The previously presented three-step method of calculating structure movement has been applied to many structures including several ODOT structures with predicted results being very close to actual measured deflections. Some case histories demonstrating the use of the soil evaluation analytical program to predict the structure movement are presented in what follows.

Table VII summarizes the results obtained by the use of the proposed method in some cases for which actual measured values were available. Data obtained from borings and nuclear density/moisture content measurements have ben used.

TABLE VII. *Field Measurements of Crown Settlement and Computed Values*

Structure No.	Soil Category in		Measured Vertical Movement (ft)	Computed Movement (ft)
	Backfill	Original Soil		
DEL-37	I	VII	0.91	1.17
BUT-129	IV	VII	0.13[a]	0.57
BRO-62	V	Old Bridge Abutments	0.82	0.82
OKL-25	VII	Rock	0.94	1.00
OKL-78	VII	Rock	1.39	1.22

[a] The measured settlement is suspect since some difficulty was experienced in locating the original bench mark established during erection.

The good agreement between measured and computed movements is partially due to the fact that these case histories were used to evaluate parameters used in the proposed method. More experience is necessary (and probably further adjustment of the parameters) before the method may be used in pipe rating. Until then, only a rough approximation (an order of magnitude) of the deformation of the pipe is expected.

CONCLUSIONS

It can be seen from the above case histories that the simplified method gives very close correlation with actual measured deflections. The example cases have been demonstrated in a research program for the Ohio Department of Transportation. The method offers a simplified procedure for estimating deflection of corrugated metal pipes for a wider range of soil conditions and types. It can be used with initial (during construction) soil compaction data to estimate future deflection or to analyze the additional movement expected in spans already experiencing deflections. The authors have developed a method to rate a structure based on this method. This method uses the same rating system as the Bridge Inventory and Inspection Program.

REFERENCES

Bally, R.J. and V.G. Perlea (1983), Embankment Dams and Levees on Weak Foundation Soils (in Romanian), Ed. Ceres, Bucharest.

Cowherd, D. and G.H. Degler, (1986), Evaluation of Long-Span Corrugated Metal Structures, Prepared by Bowser-Morner Associates, Inc., in cooperation with the Ohio Department of Transportation and the U.S. Department of Federal Highway Administration.

Cowherd, D., S.M. Thrasher, V.G. Perlea, and J.O. Hurd (1986), "An Empirical Approach for Predicting Deflection in Large Metal Culverts", 66th Annual Meting of Transportation Research Board, Washington, D.C. (in print).

Fardis, M.N. and D. Vereziano, (1981) "Estimation of SPT-N and Relative Density", Journal of the Geotechnical Engineering Division, ASCE, Volume 107, No. GT10, pp. 1345-1359.

Gibbs, H.J. and W.G. Holtz, (1957), "Research on Determining the Density of Sands by Spoon Penetration Testing", Proceedings of the Fourth International Conference on Soil Mechanics and Foundation Engineering, London, Volume 1, pp. 435-39.

Hough, B.K. (1969), Basic Soils Engineering, Ronald Press Company, New York.

Marcuson III, W.F. and W.A. Bieganousky, W.A., (1977a), "Laboratory Standard Penetration Tests on Fine Sands", Journal of the Geotechnical Engineering Division, ASCE, Volume 103, No. GT6, pp. 565-588.

Marcuson III, W.F. and W.A. Bieganousky, (1977b), "SPT and Relative Density of Coarse Sands", Journal of the Geotechnical Engineering Division, ASCE, Volume 103, No. GT11, pp. 1295-1310.

McCarthy, D.F. (1977), Essential of Soil Mechanics and Foundations, Reston Publishing Company, Inc.

Peck, R.B., W.E. Hanson, and T.H. Thornburn, (1974), Foundation Engineering, John Wiley and Sons, Inc.

Perlea, V. and M. Perlea (1983), Dynamic Stability of Sandy Soils (in Romanian), Ed. Tehnica, Bucharest.

Schmertmann, J.H. (1970), "Static Cone to Compute Static Settlement Over Sand", Journal of the Soil Mechanics and Foundation Engineering Division, ASCE, Volume 96, No. SM3, pp. 1011-1043.

Searle, I.W. (1979), "Interpretation of Begemann Frition Jacket Cone Results to Give Soil Types and Design Parameters", Proceedings of the Seventh European Conference on Soil Mechanics and Foundation Engineering, Brighton, Volume 2, pp. 265-270.

Spangler, M.G. (1951), Soil Engineering, The Iowa State College, International Textbook Company, Scranton.

Terzaghi, K. and R.B. Peck (1967), Soil Mechanics in Engineering Practice, John Wiley and Sons, Inc., New York.

Thrasher, S.M. and V.G. Perlea, (1986), MULTSPAN - A Computer Program for Evaluation of Large Corrugated Metal Pipes, Bowser-Morner Associates, Inc.

Watkins, R.K. (1975), "Buried Structures", Chapter 23 in Engineering Handbook, Edited by M.F. Winterkorn and H.Y. Fang, Van Nostrand Reinhold Company, New York, pp. 649-672.

Proceedings: Second International Conference on Case Histories in Geotechnical Engineering, June 1-5, 1988, St. Louis, Mo., Paper No. 6.96

Geotechnical Investigation into Causes of Failure of a Gabion Retaining Wall

Edward A. Nowatzki
Associate Professor, Civil Engineering Dept., University of Arizona, Tucson, Arizona

Brian P. Wrench
Principal, Steffen Robertson & Kirsten, Johannesburg, South Africa

SYNOPSIS: This paper describes the post-failure analysis of a 26m long x 4m high gabion retaining wall located in a suburb of Johannesburg, South Africa. The wall had been built just beyond the toe of a natural slope with most of the gabion units resting on the bed of a small river. The river bed soils consisted of approximately 2.5m of soft, dark-grey, silty clay underlain by massive granite bedrock. The water table at the toe of the wall was within 0.1m of the river bed surface. Failure of the wall occurred over the weekend after backfilling to grade behind the wall had been completed.

Stability analyses were conducted using both total (undrained) and effective (drained) shear strength parameters for the clay. The results of the analyses showed that the wall should be stable with FS = 1.2 for effective stress parameters and that the wall should be unstable with FS = 1.0 for undrained strength parameters. The details of the testing program and the selection of strength parameters is described in the paper.

INTRODUCTION

This paper describes the post-failure analysis of a 26m long x 4m high gabion retaining wall located in a suburb of Johannesburg, South Africa. The wall was built as part of the development of an industrial park along the east bank of the *Klein Jukskei River* in Strydom Park.

The original topography of the site sloped steeply downwards to the river. The wall was constructed just beyond the toe of the natural slope with most of the gabion units resting on the river bed, except for a length of approximately 10m near the middle of the wall where the units were founded about 1m below the river bed. Following completion of the wall, an imported fill was placed and compacted between the wall and the natural slope. Final grade was relatively flat with a gentle slope from east to west.

The retaining wall itself consisted of 2m x 1m x 1m gabion cages containing angular rock fill. The front face of the wall was constructed of two rows of gabion units for a length of approximately 26m. The height of the wall along this length was 4m above the river bed. The north and south wing walls of the structure were 9m and 6.5m long, respectively. Figure 1 shows a sketch of the structure prepared by the contractor.

Construction records indicate that backfilling behind the wall was completed on or about 8 July 1983. The wall failed over the weekend of 9-10 July 1983 following a period of heavy rain. The consulting firm of Steffen Robertson and Kirsten (SRK) was retained by the contractor to perform a geotechnical investigation to determine the cause of the failure and to make recommendations for the redesign and/or repair of the wall. A preliminary field investigation revealed that a classic rotational type of failure had occurred along the central portion of the wall. A maximum downward displacement of approximately 1.4m was evident along the intersection of the semi-circular failure surface with the backfill surface. Bulging of the river bed at the toe of the wall was clearly visible. These characteristic features of the failure are shown in Figures 2a and 2b. Reconnaissance of the site revealed the presence of a concrete wall, approximately 3m in height, located just downstream of the retaining structure as shown in Figure 2c. This concrete wall acted as a dam before development in the area took place. Although it was breached at the time of the failure, the wall could back up water under flood conditions. The size of the spans between piers of the bridge located just upstream of the gabion wall, as shown in Figure 2d, suggested that flow in Klein Jukskei River could be substantial. The reconnaissance also revealed the presence of rock outcrops on the opposite river bank and to the north and south of the site. These outcrops formed a natural channel that directed the flow of the river toward the wall. The site conditions described above had a significant impact on the recommendations made by SRK.

METHODS OF INVESTIGATION AND RESULTS

Field Investigation:

Two NX size boreholes were advanced, one (BH-1) on top of the fill 5m behind the retaining wall, the other (BH-2) at the toe of

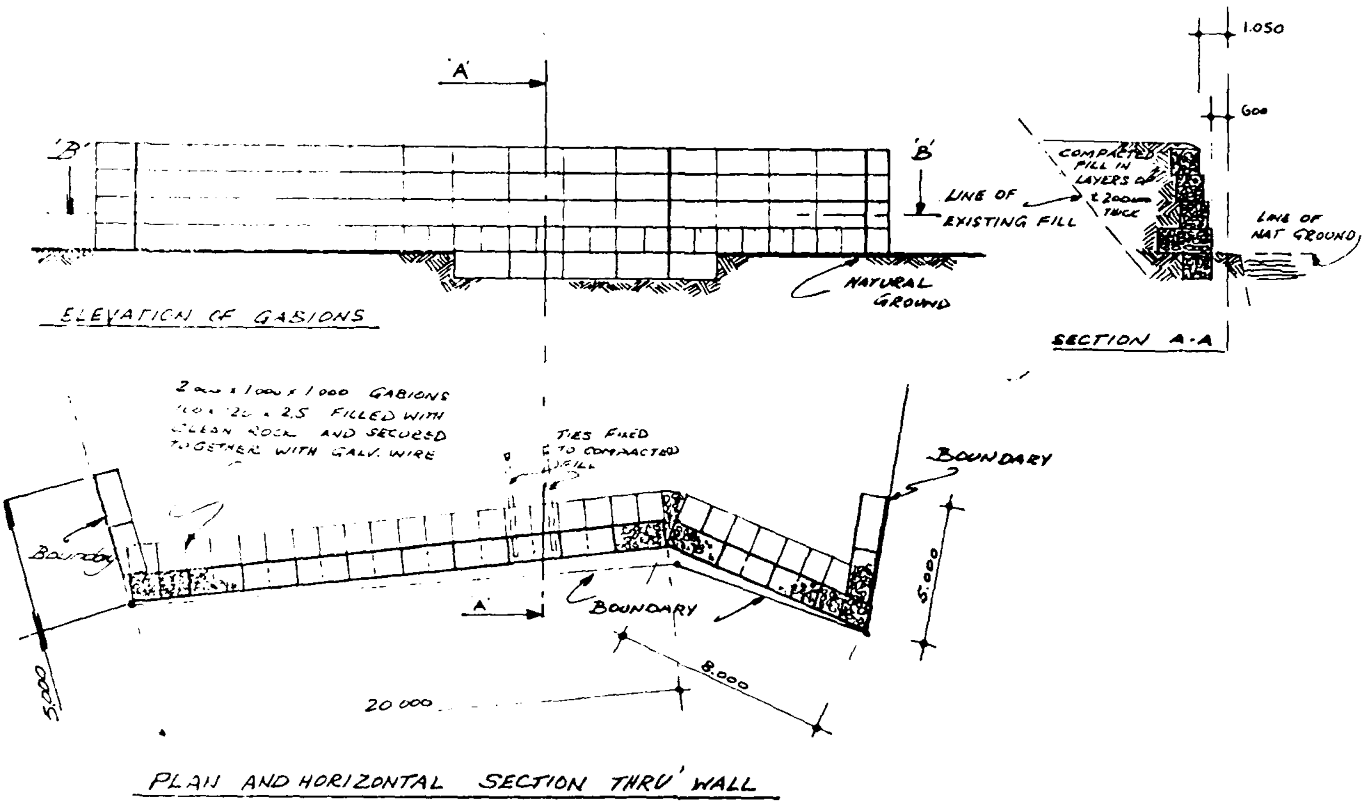
'A'
'B'
'B'
LINE OF EXISTING FILL
NATURAL GROUND
ELEVATION OF GABIONS
1.050
600
COMPACTED FILL IN LAYERS OF ± 200mm THICK
LINE OF NAT GROUND
SECTION A-A
2m x 1000 x 1000 GABIONS 100 x 120 x 2.5 FILLED WITH CLEAN ROCK AND SECURED TOGETHER WITH GALV. WIRE
TIES FIXED TO COMPACTED FILL
BOUNDARY
Boundary
BOUNDARY
'A'
5.000
5.000
8.000
20 000
PLAN AND HORIZONTAL SECTION THRU' WALL

FIG. 1

Sketch of Gabion Wall Showing Configuration and Dimensions

the wall in the river bed. Both boreholes extended through the fill materials and underlying soils and penetrated 2m into the granite bedrock. Standard Penetration Tests (SPT) were carried out to estimate the insitu densities of the fill and subsoils. Disturbed and undisturbed soil samples were recovered from the boreholes for laboratory testing. The results of the field investigation are summarized in Table 1.

TABLE 1
SUMMARY OF RESULTS OF FIELD INVESTIGATION

Borehole	Depth	Average Description	SPT
BH-1	0-4.4 m	Dry to slightly moist medium-dense clayey sand and gravel, fill.	9
	4.4-4.8 m	Moist dark-grey soft clay.	3
	4.8-7.4 m	Unweathered, coarse-grained, widely fractured granite.	-
BH-2	0-2.8 m	Very moist dark-grey clay.	3
	2.8-4.8 m	Unweathered, coarse-grained widely fractured granite.	-

Field vane shear tests to determine the undrained shear strength (s_u) of the clay were also performed. Peak and residual values of s_u were measured.

Laboratory Testing Program:

The following laboratory tests were carried out on selected undisturbed samples retrieved from the site:

1. Saturated unconsolidated-undrained triaxial tests to determine the undrained shear strength (s_u) of the clay.

2. Consolidated-drained shear box tests to determine the drained (effective) cohesion and friction angle ($\bar{c}$ and $\bar{\phi}$) of the clay.

3. Indicator tests (gradation, Atterberg limits) to classify the clay according to the Unified Soil Classification System (USCS).

A summary of the results of the laboratory and field-strength testing program is contained in Table 2.

ANALYSES AND RESULTS

Selection of Shear Strength Parameters:

Two types of stability analyses were performed:

1. Short-term or end-of-construction analysis. This analysis was conducted in

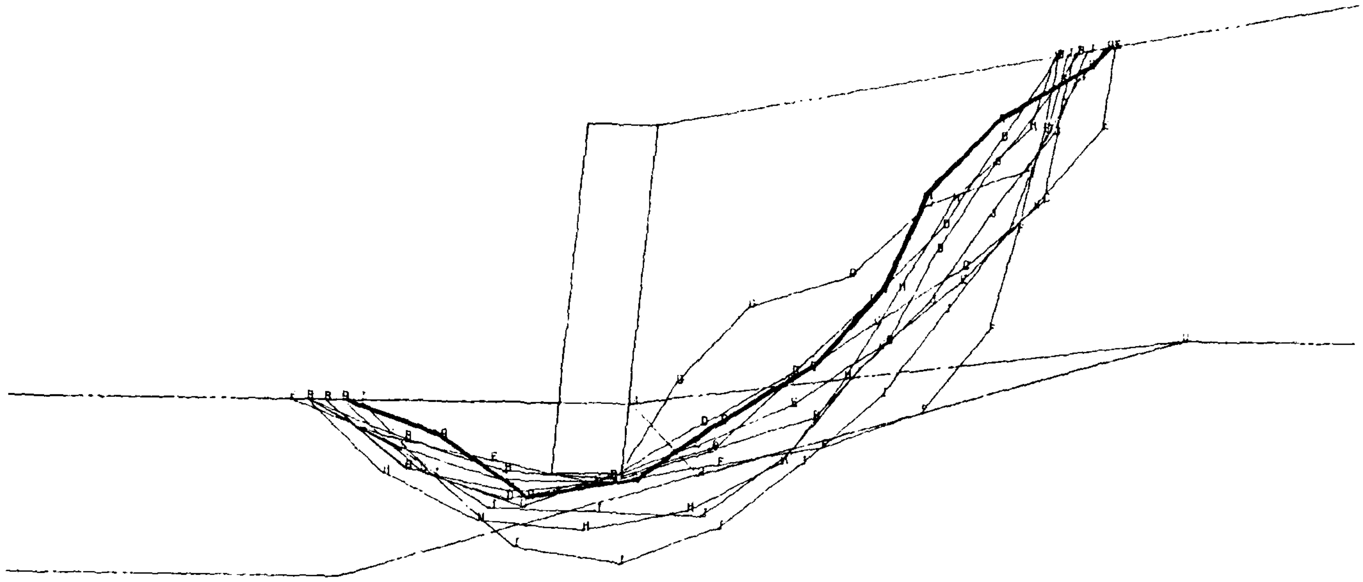

FIG. 3

Failure Surfaces for Short-Term Stability
(s_u = 12 kPa; FS = 1.0)

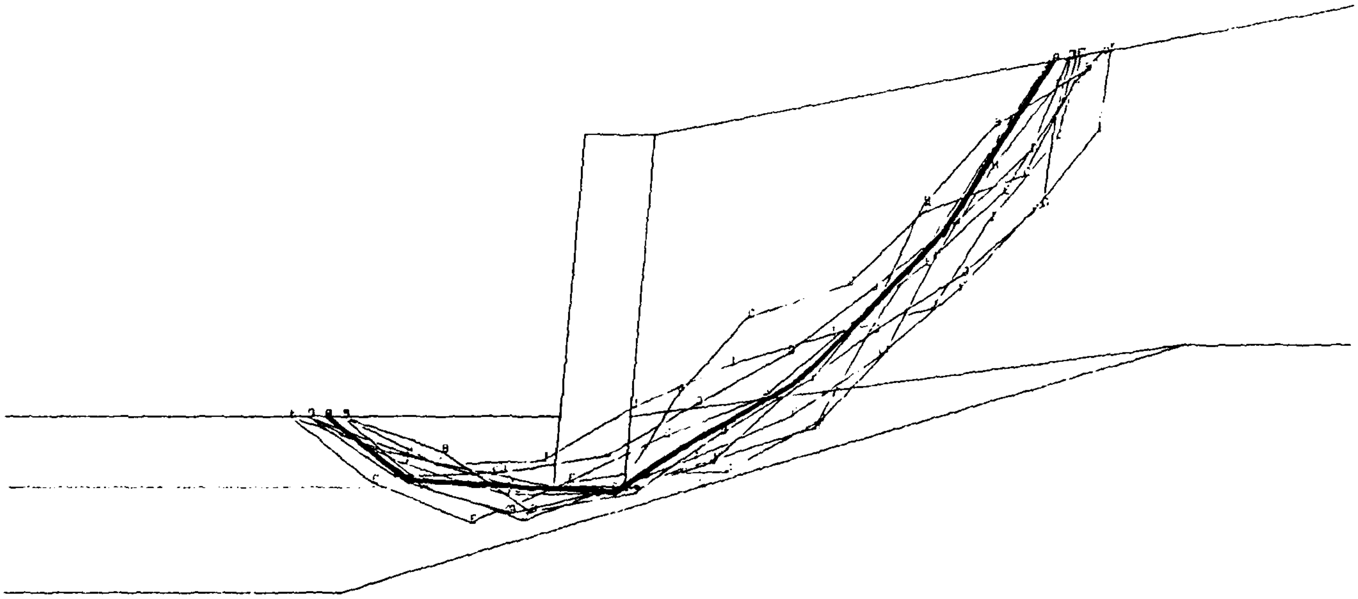

FIG. 4

Failure Surfaces for Long-Term Stability
($\bar{c}$ = 0; $\bar{\phi}$ = 30°; FS=1.2)

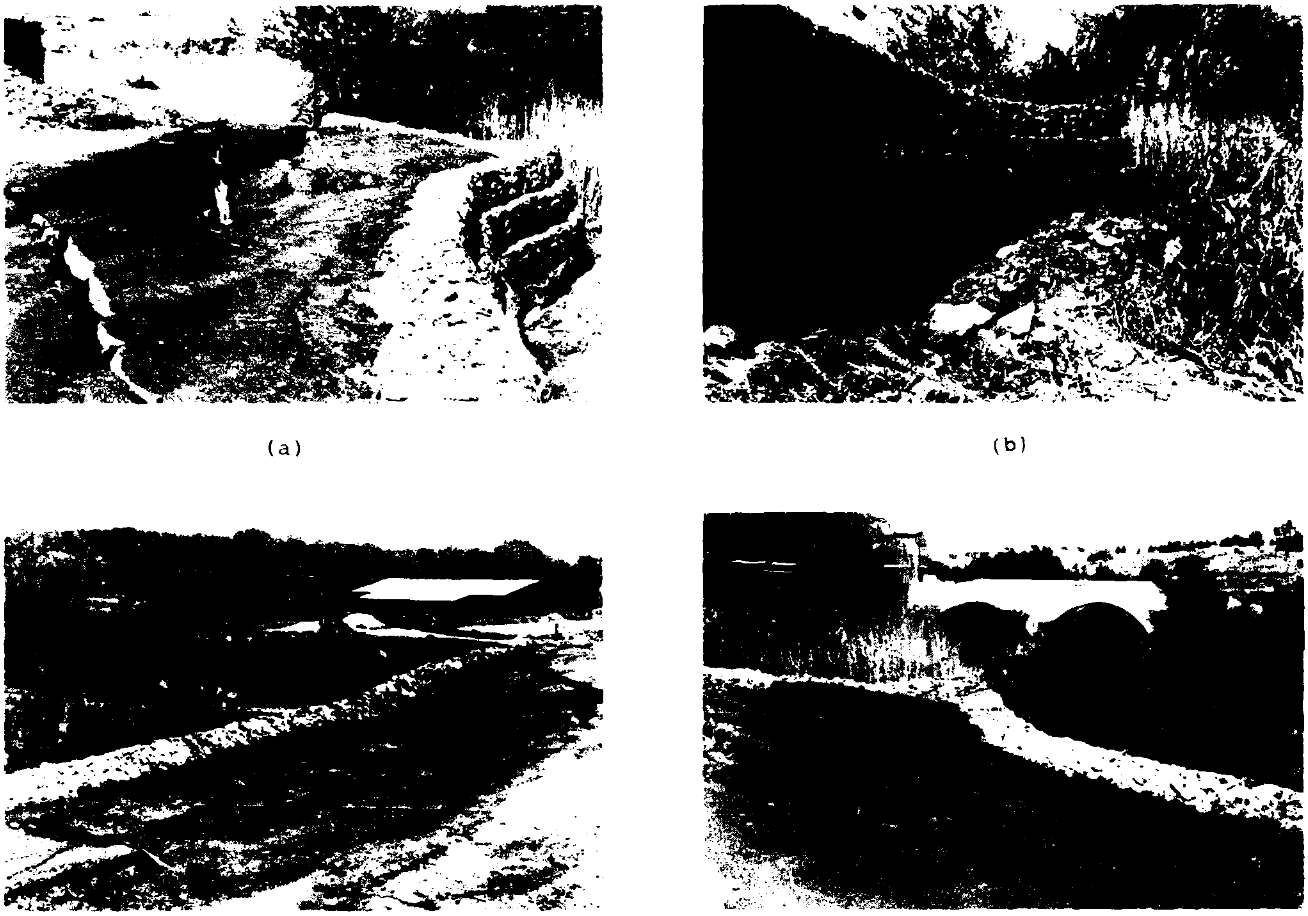

(a)

(b)

(c)

(d)

FIG. 2

Post-Failure Photos of Gabion Wall Showing:

(a) surface displacement of backfill
(b) bulge at toe
(c) view downstream with concrete wall visible
(d) view upstream with bridge span visible

TABLE 2. SUMMARY OF RESULTS OF LABORATORY TESTING PROGRAM

Unit	Test Type	Cohesion (kPa)	Friction Angle (degrees)	Total Unit Weight (kg/m^3)
Fill	SPT	0	35	1880
Clay	Drained Direct Shear	0	30	1550
	Undrained Triaxial	20	0	1550
	Laboratory Vane			
	Peak	6	0	1550
	Residual	3	0	1550
Wall	Assumed[a]	2000	42	2300

(a) Properties of the wall were assumed so as to make the wall rigid relative to the backfill and clay layer in order to model the problem order to determine whether or not the failure could have been predicted had a pre-construction stability analysis been performed. In view of the relatively short construction period and the presence of the near-saturated soft clay as a foundation material, it was clear that the end-of-construction stability of the gabion wall and the backfill should be controlled by the undrained strength of the foundation clay. As indicated in Table 2, the clay exhibited s_u values ranging from 20 kPa, as determined from laboratory UU tests, to 3 kPa (residual), as determined from field vane shear tests. Such discrepancies in measured values of s_u may be attributed to differences in test method (Ladd and Lambe, 1963). Methods that cause greater sample disturbance generally yield lower values of s_u. On the basis of the test results presented in Table 2, it was assumed that the insitu undrained strength along the failure surface would be, on average, between the maximum and minimum values measured. Therefore, a value of s_u = 12 kPa was used for the short-term stability analysis.

2. Long-term analysis. This analysis was conducted in order to evaluate the stability of the gabion wall and the backfill if they had been constructed in stages and if the foundation clay had been given time to consolidate under the intermediate loads. The results of this analysis were of more than academic interest. The recommendations for remedial measures depended heavily on whether or not the gabion wall, even in its failed condition, could ever be expected to become stable enough to allow normal activity to take place behind it. If it could, then only cosmetic measures would be needed to remove evidence of the failure. If it could not, complete removal of the wall and either its reconstruction or replacement with some alternate structure would be indicated. The drained shear strength parameters $\bar{c}$ = 0 kPa and $\bar{\phi}$ = 30° shown in Table 2 were used for the long-term stability analysis.

Analysis Procedure and Results:

All stability analyses were carried out by using the computer program STABL 21 which is based on Janbu's simplified method of slices. One of the features of the program is that it allows irregular failure surfaces to be considered between specified locations on the crest and toe. This feature was particularly useful for the post-failure analyses conducted here since the crest and toe locations of the failure surface were known from measurements made the field. Another feature of the program is that it selects the failure surfaces that result in the ten lowest factors of safety and plots each of them for comparison purposes. The surface having the lowest factor of safety is highlighted.

The results of the short-term stability analysis using s_u = 12 kPa are shown in Figure 3. The highlighted failure surface evident in the figure results in a factor of safety of 1.0. The analysis confirms that failure of the wall occurred because of overstressing of the underlying soft clays. As a matter of interest, analyses were also performed for s_u = 3 kPa and 20 kPa. Factors of safety of 0.7 and 1.2 were obtained, respectively. This suggests that even with the maximum measured value of the undrained strength, the wall and backfill would be only marginally stable.

Analyses were also performed using the effective stress parameters. The results of these analyses are shown in Figure 4. The factor of safety of 1.2 suggests that even if the clay were to drain under the loads existing at the time of failure, the long-term stability of the wall would still be questionable, especially if any of the conditions existing at the time of failure should change. Such changes could occur if, for example, the ground water table should rise, or erosion of the foundation materials should take place, or should additional loads be imposed on the backfill from normal activities of the site user.

CONCLUSIONS AND RECOMMENDATIONS

The stability analyses show that the gabion wall and the backfill failed because the foundation soils were overstressed, and that the wall was only marginally stable in its post-failure condition. In addition, the analyses suggest that further failures could occur if any of the present conditions affecting the stability of the wall should change.

Reconnaissance of the site revealed that the wall was located on the outside sweep of the Klein Jukskei River and effectively served to constrict the channel. Visual assessment of the hydraulic conditions at the site suggested that the gabion wall was in danger of being damaged by erosion of the banks and scour of the foundation materials. Such a danger would be especially acute if the small concrete dam downstream of the wall were to be removed.

On the basis of these two threats to the future stability of the wall, SRK concluded that flood conditions at the site must be established before any remedial measures for the foundation stability of the gabion wall could be evaluated. They recommended that, in the absence of such information, the gabion wall should be removed.

REFERENCES

Ladd, C.C. and T.W. Lambe (1963), "The Strength of 'Undisturbed' Clay Determined from Undrained Tests," ASTM, STP No. 361, pp. 359-371.

Proceedings: Second International Conference on Case Histories in Geotechnical Engineering, June 1-5, 1988, St. Louis, Mo., Paper No. 6.97

Two Case Histories: Performance of Shallow Foundations on Sand

Sreenivasan V. Nathan
Associate, Woodward-Clyde Consultants, Plymouth Meeting,
Pennsylvania

SYNOPSIS: The development of innovative, economical solutions, based on sound principles, as enunciated by Terzaghi some sixty years ago, and on the "design-as-you-go" approach illustrated by Peck in his Rankine lecture, will be the impetus for the Geotechnical Engineer of tomorrow (Nathan, S.V., 1987). Following this theme, two case histories on the performance of shallow foundations on geologically differing sandy subsoils are presented in this paper to illustrate the benefits of economical, unconventional foundation solutions.

QUONSET POINT CASE HISTORY

The first case history involves a mat/continuous footing foundation project for General Dynamics at Quonset Point in Rhode Island. As shown on Figure 1, the site is characterized by 6 to 8 feet of loose sands and silty sands of the recent Coastal Plain deposits mantled by a veneer of fill materials. The loose granular soils were densified in situ by surface applied vibratory compaction, e.g. Ingersoll Rand SP-54/60-DD. The Figure shows a compilation of the Cone Penetration Test (CPT) and Standard Penetration Resistance (SPR) test results both before and after the completion of compaction operations (Nathan, S.V. et al, 1981).

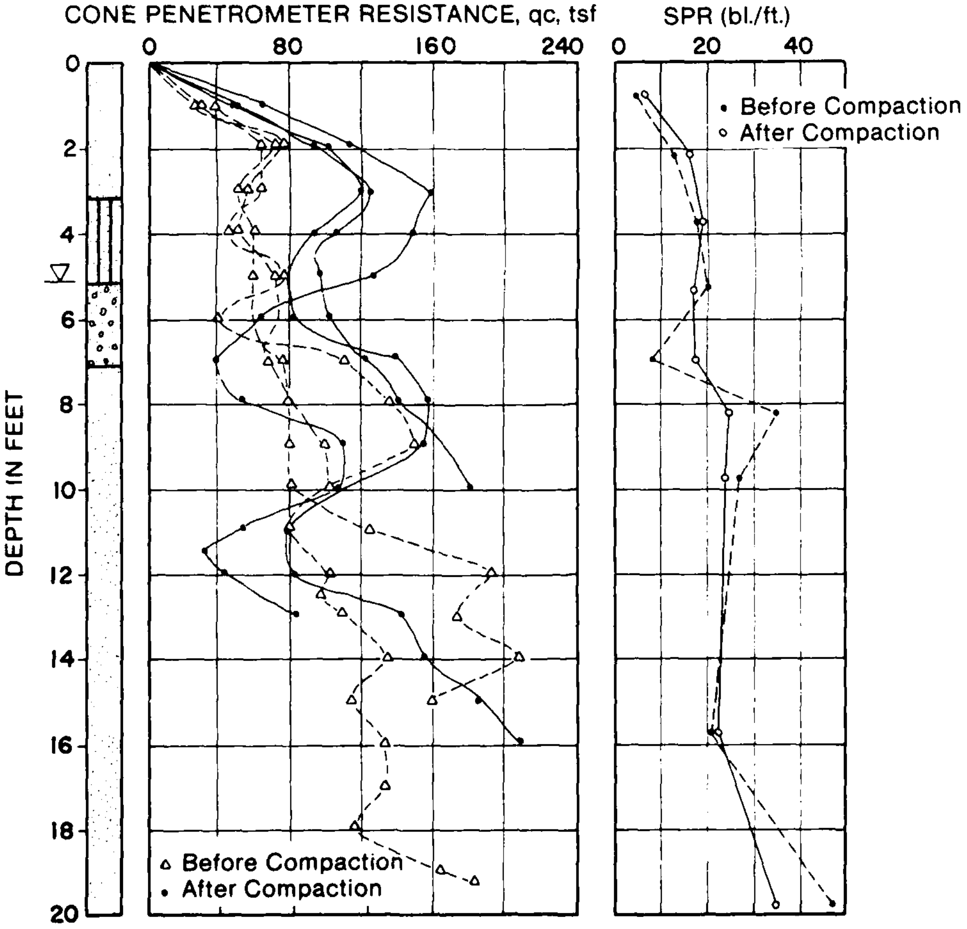

Fig. 1 SCS Records in Coastal Deposits, Quonset Point, Rhode Island (Nathan, S.V.,et al., 1981)

For normally or slightly overconsolidated cohesionless soils, the settlement of a footing, correcting to the one-dimensional compression case, is

$$\delta = \sum_{o}^{H} \Delta h \frac{1.15\,\sigma'_{vo}}{\alpha_2 (1+Dr)^2 q_c} \log \frac{\sigma'_{vo} + \Delta\sigma}{\sigma'_{vo}} \qquad (1)$$

where the correction factor, α_2, in terms of Poisson's ratio, μ is expressed as

$$\alpha_2 = \frac{1-\mu}{(1+\mu)(1-2\mu)} < 0.5 \qquad (2)$$

q_c = CPT value

Dr = Density index (previously known as Relative Density)

Δh = Compressible layer thickness

σ'_{vo} = Existing effective overburden pressure

$\Delta\sigma$ = Applied stress increment

Several case histories have demonstrated that even with the foregoing equations, settlements are significantly overestimated, especially after the densification by vibratory compactors. For example, Schmertmann (1970) concludes that in such cases the settlement, predicted assuming normal consolidation, should be reduced by about one-half. The settlement analysis utilizes the cone to subdivide the profile into discrete layers of thickness Δh. With a thick bearing layer, the subsoils contributing to settlement are assumed to extend below the footing/mat to a depth where the stress increase equals approximately 10 percent of the overburden pressure. Buismann recommends calculating stresses beneath a singular point of a foundation. This point is defined as the point beneath the footing where the stress distribution is essentially independent of the distribution of contact pressure. This approach assumes a rigid footing and enables the use of the average contact pressure to predict an approximate rigid footing stress distribution as per Figure 2.

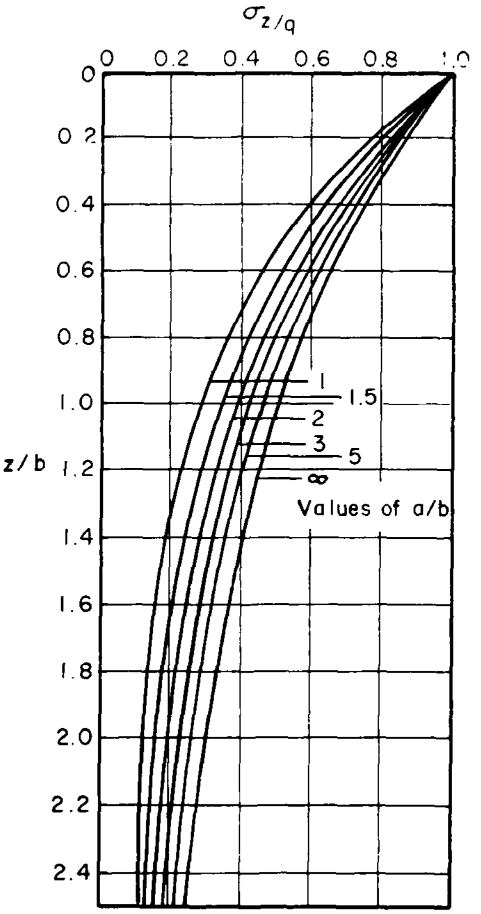

Fig. 2 Mean Vertical Stress Influence Factor for Rigid Rectangular Footings (Buismann, 1954)

Schmertmann (1975) recommends a simplified distribution of vertical strain beneath footings (Figure 3) and uses this strain distribution together with the q_c data to predict settlements from Equation (3)

$$\rho = C_1 C_2 \Delta p \sum_{o}^{2B} \frac{Iz}{\text{[illegible]}} dZ \qquad (3)$$

where $C_1 = 1 - 0.5 \frac{po}{\Delta p}$

$C_2 = 1 - po \log \frac{t}{to}$

Iz = Strain influence factor from the enclosed figure

Izp = peak factor = $0.5 + 0.1 \frac{\Delta p}{\sigma vp}$

Using the above methods for the Quonset Point project, settlements on the order of 3 to 4 inches were predicted for an average contact pressure of 6 ksf before densification of the subsoils. Upon densification, the predicted settlements were on the order of 1 to 1-1/2 inches, which were within acceptable limits for no structural distress or architectural damage was discernible within the completed structure.

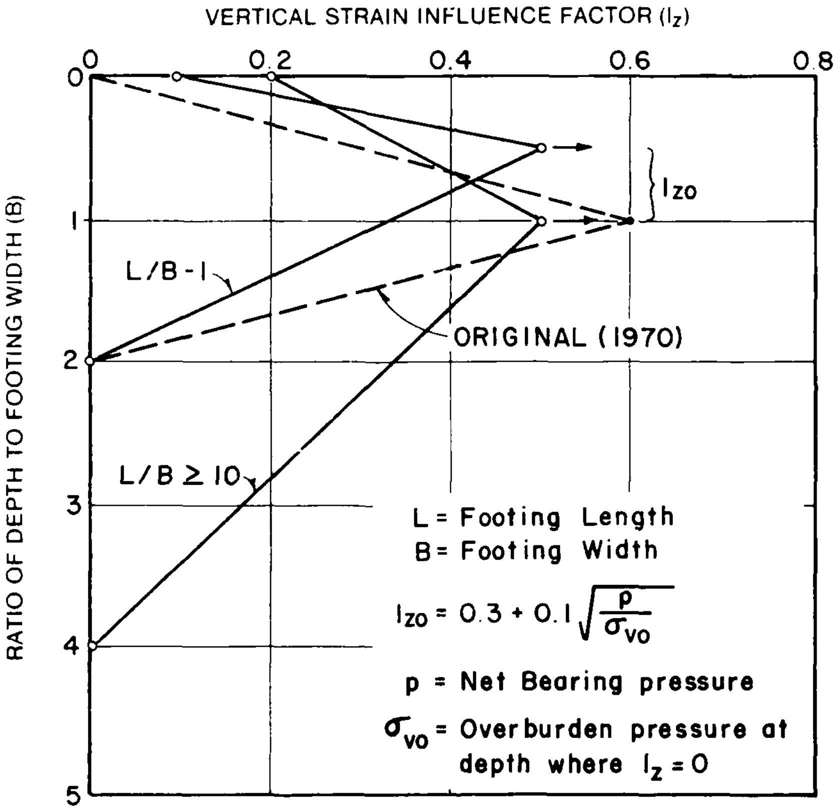

Fig. 3 Modified Strain Influence Factors for Rigid Footings (Schmertmann, J.H.,1975)

It should be noted that in the above predictions, appropriate corrections were applied because of the largeness in size of the mat and footings, in accordance with Figure 4.

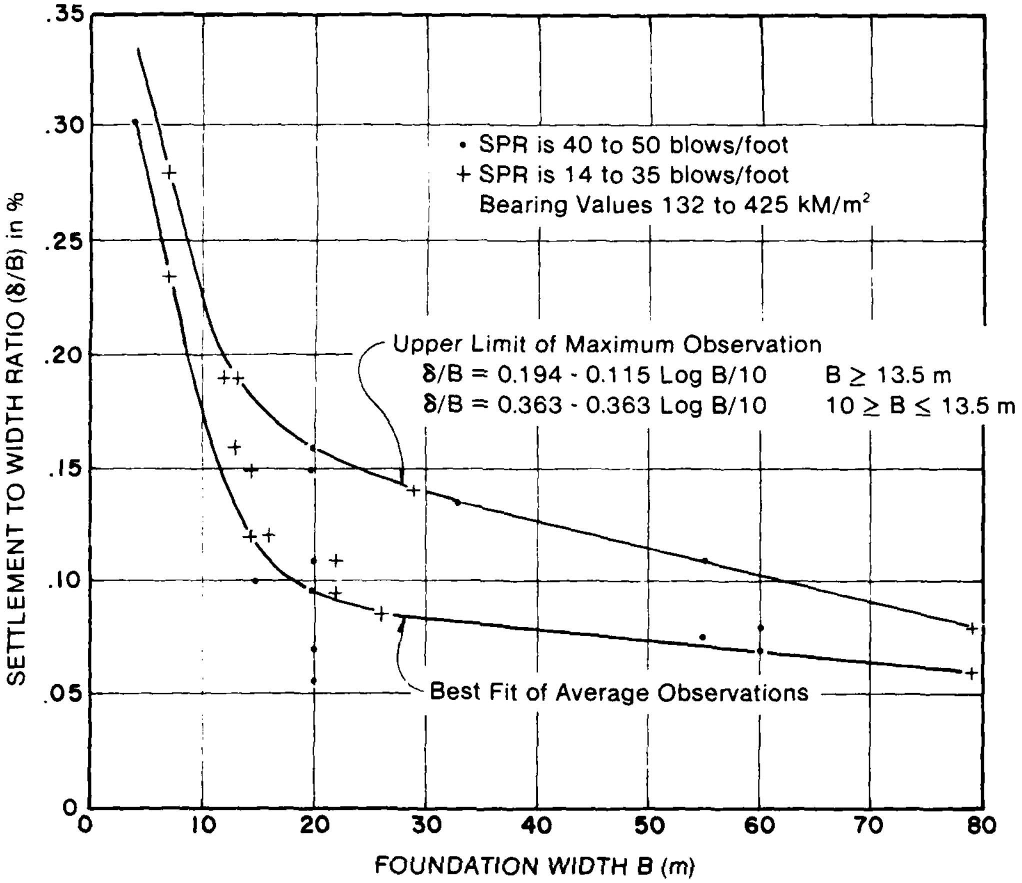

Fig. 4 Settlement of Mats / Large Footings on Sand (Morton, K., 1974)

Field observations suggest that all the previously derived procedures are likely to overestimate the settlements significantly for large footings and mats. This may be attributed to the development of these procedures primarily from the behavior of small footings and test plates and the paucity of similar correlative data from mat-type foundations. It is noted that the average settlement of large, uniformly loaded foundations is primarily a one-dimensional deformation mechanism, unlike that of relatively small footings. Under these conditions, E_s would be expected to increase with stress level consistent with the strain-hardening behavior associated with one-dimensional compression. This behavior is diametrically opposed to that observed during loading of small footings and plates. Here the settlement has a greater shear deformation component and the ratio between the bearing capacity and the bearing value is much less at working loads. In the above Quonset Point Case, observations reported by Morton (1974) and shown on Figure 4 were utilized to apply appropriate corrections.

PHILADELPHIA CASE HISTORY

The second case history concerns the conversion of existing shallow based spread footing foundation system suitable for supporting a 33-story tower imposing additional foundation contact pressures nearly 80% higher than the original design. The project is The Rittenhouse Towers in Center City Philadelphia. As shown on Figure 5, the original structure, with a two-level basement, was abandoned after the foundations and the basements had been constructed. Six years later Woodward-Clyde Consultants (WCC) was approached to explore the feasibility of increasing the original bearing pressure of 6 tsf up to 1 .5 to 11 tsf in order to support 13 additional floors. WCC recommended a "design-as-you-go" approach and an extensive foundation performance monitoring program was initiated. As shown on Figure 5, to date, with more than 95% of the final loads in, the performance of the structure as measured by settlements, is well within established tolerance limits and calculated predictions.

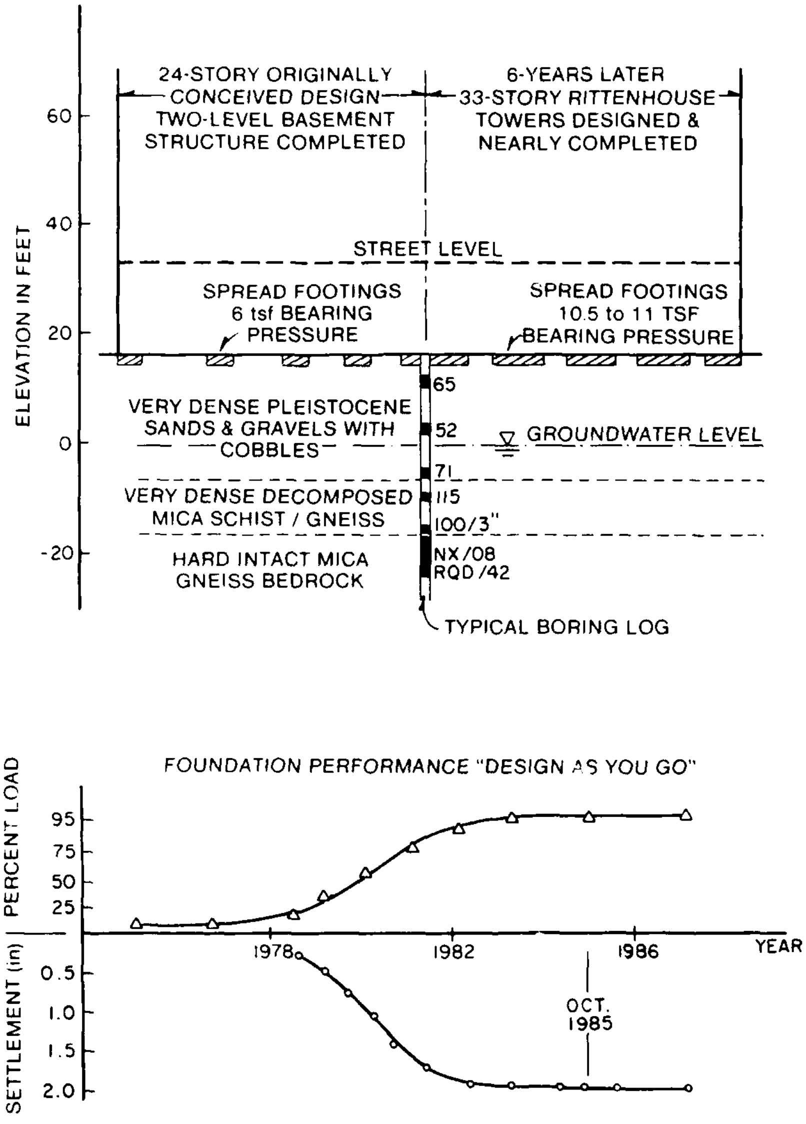
24-STORY ORIGINALLY CONCEIVED DESIGN TWO-LEVEL BASEMENT STRUCTURE COMPLETED
6-YEARS LATER 33-STORY RITTENHOUSE TOWERS DESIGNED & NEARLY COMPLETED
60
40
20
0
-20
ELEVATION IN FEET
STREET LEVEL
SPREAD FOOTINGS 6 tsf BEARING PRESSURE
SPREAD FOOTINGS 10.5 to 11 TSF BEARING PRESSURE
VERY DENSE PLEISTOCENE SANDS & GRAVELS WITH COBBLES
VERY DENSE DECOMPOSED MICA SCHIST / GNEISS
HARD INTACT MICA GNEISS BEDROCK
65
52
GROUNDWATER LEVEL
71
115
100/3"
NX/08
RQD/42
TYPICAL BORING LOG
FOUNDATION PERFORMANCE "DESIGN AS YOU GO"
PERCENT LOAD
95
75
50
25
SETTLEMENT (in)
0.5
1.0
1.5
2.0
1978
1982
1986
YEAR
OCT. 1985

Fig. 5 Rittenhouse Towers, Philadelphia Case History (Nathan, S.V., 1987)

The prediction was mostly based on an in-place load test performed in a nearby site (Mitchell, J.K., et al 1975). The in-place load test was conducted within a 36-inch ID hole drilled to a depth of 18 feet below the existing ground surface at the site of the nearby Holiday Inn site. Subsoil conditions were similar to the Rittenhouse Site and consisted of miscellaneous fill (N=20 blows per foot) to a depth of 12 feet, medium to very dense gravelly silty sand (N=100) to a depth of 20 feet, underlain by very dense sandy gravel and decomposed mica schist. An incremental loading finite element analysis was made using stress increments of 1000 psf and a total final stress of 11 tsf. The results are compared with the measured values in Figure 6. It may be seen that the agreement between prediction and observation is reasonably good. Based on the results of the load test and the methods previously described for the Quonset Point case history, settlement predictions were made for the Rittenhouse project, which to date, have compared favorably with measured performance as discussed before.

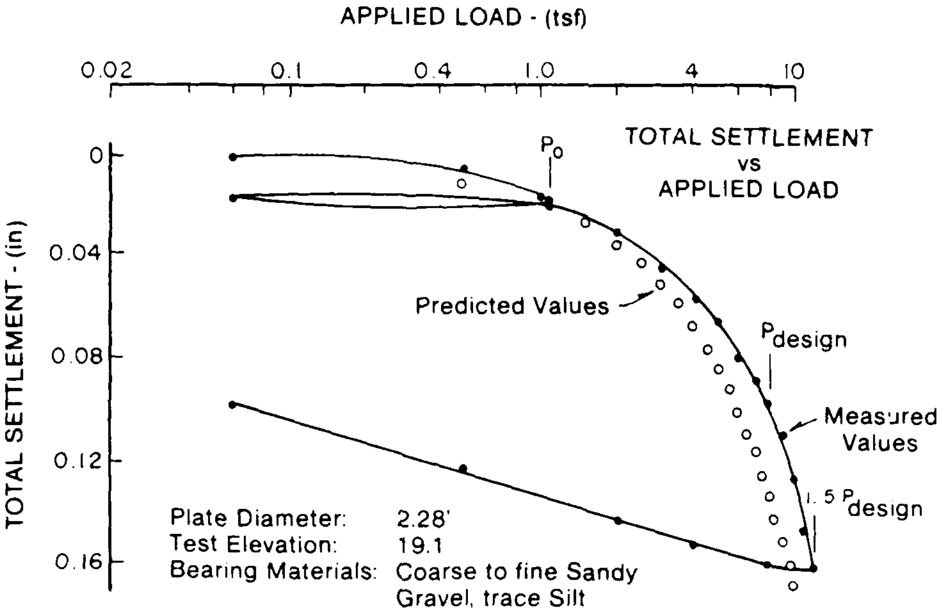

Fig. 6 Holiday Inn Test Results (Mitchell, J.K., et.al.,1971)

ACKNOWLEDGEMENTS

The professional development program of WCC was instrumental in supporting the suitcase cone penetrometer development and the related technical memoranda during 1975-1980. The Author is thankful to Mr. William S. Gardner, Executive Vice President of the firm's professional development practice. Thomas F. Powers did the drafting, and Tina Rissmiller is responsible for the typing.

REFERENCES

Mitchell, J.K. and W.S. Gardner (1971), "Analysis of Load-Bearing Fills over Soft Subsoils," ASCE Journal of the SM and FDF Vol. 97, No. SM11 pages 1549-1572.

Morton, K. (1974), "Discussion, Session I," Proc. of Conf. on Settlement of Structures, British Geotechnical Society, Pentech. press.

Nathan, S.V. (1987), "Innovative Foundation Engineering," Civil Engineering, ASCE, Dec. 1987, Vol. 57 No. 12.

Nathan, S.V. and W.S. Gardner (1981), "The Suitcase Cone System," ASCE Specialty Conference on "Cone Penetration Testing and Experience," October 27, 1981, St. Louis, Mo., 20 pp.

Schmertmann, J.H. (1975), "Measurement of In Situ Shear Strength," ASCE Specialty Conference on In-Situ Measurement of Soil Properties, Proc. Vol. 2, Raleigh, N.C.

Schmertmann, J.H. (1970), "Static Cone to Compute Static Settlement Over Sand," Proc. ASCE, Vol. 96, SM3.

Proceedings: Second International Conference on Case Histories in Geotechnical Engineering, June 1-5, 1988, St. Louis, Mo., Paper No. 6.98

Geotechnical Studies of Foundation of a Tilted Tank at Parikshatgarh, India

G.C. Nayak
India

P.K. Jain
India

B. Singh
India

SYNOPSIS: An overhead tank of 200 KL capacity and 9 m staging was constructed in year 1975 at the ancient historical site at Parikshatgarh, Meerut, India. The depth of foundation is 1.6 m and inner and outer diameters of annular raft is 6.8 m and 10.3 respectively. In year 1978, the overhead tank was observed to be tilted. Detailed geotechnical studies have been conducted in 1987 to find out the causes of tilting of the tank and tilts have been measured every month for last one year. It is interesting to note that inspite of severe tilt of 4.3 cm/meter height the overhead tank has been functioning satisfactorily for last 12 years. A comparison of estimated, permissible and observed total and differential settlements has been made.

INTRODUCTION

Authors visited the tilted tank site alongwith a team of Engineers from U.P. Jal Nigam on 26th May, 1986. Based on the observations and tests it was found that :

a. Concrete of the tank was in very good condition at all levels, the range of cube strength was of the order of 200 to 250 kg/cm^2.

b. Soil investigation report was not available.

c. Maximum tilt was of the order of 4.3 cm meter height at column No.1.

d. There was a leakage of water from the sluice valve chamber which was near the tilted column.

e. The slope of the ground and rain water was also towards tilted columns.

The following recommendations were made for taking the immediate action -

1. The collection of the water in the sluice valve chamber may be eliminated by shifting the chamber to the boundary wall of the water works to prevent the accumulation of water near the overhead tank.
2. Soil test report should be made available or soil investigations should be carried out to find out the causes of tilting and to suggest suitable rehabilitation measures for the safety of the tank.
3. Periodic observations of tilt, both radially and tangentially are to be taken by using plumb bob and theodolite for atleast one year to ascertain stability of the foundation.

A detailed geotechnical investigation programme was planned.

HISTORY OF CONSTRUCTION

The present tank is located at ancient historical site at Parikshatgarh. The small hillock appears to be filled up ground.

The overhead tank of 200 KL capacity at 9 m staging was constructed at this site by U.P. Jal Nigam under Parikshatgarh water supply scheme in the year 1975. It has eight RCC columns of size 35 cm x 35 cm. The depth of foundation is 1.6 m, outer and inner diameters of annular raft are 10.3 m and 6.85 m respectively. Centre to centre spacing between the foundation ring beam is 8.575 m and width of the annular raft is 1.725 m. It was commissioned in 1975. In the year 1978-79, it has come to notice that the overhead tank was started tilting towards one side. A sectional elevation of the tank is shown in Fig. 1.

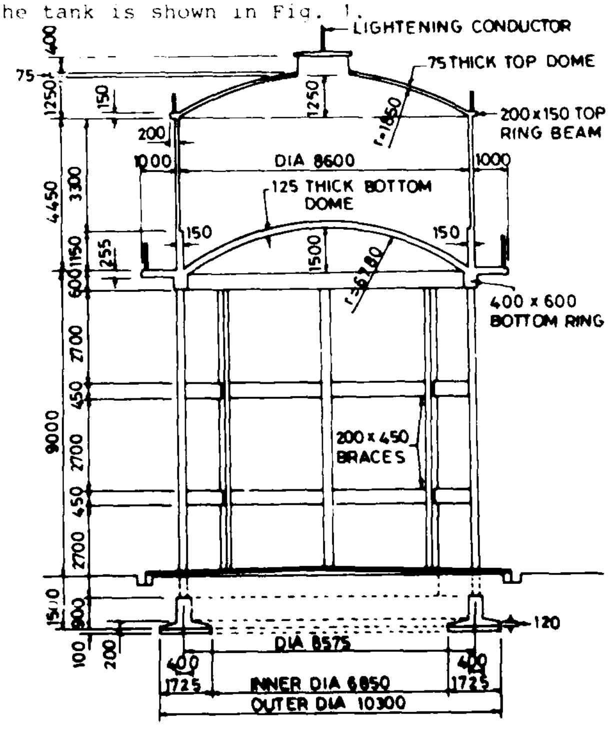

Fig. 1 Sectional Elevation of the Tank

It is important to note that the tank has been serving its function since 1975 inspite of tilting.

PLANNING OF SOIL EXPLORATION PROGRAMME

On the basis of the nature of project, it was decided to carry out soil exploration in order to

(i) obtain soundings of penetration resistance by dynamic penetration test upto 10 m depth or refusal around the tank.

(ii) obtain soundings of penetration resistance by standard penetration test in the bore hole towards tilting and the other sides.

(iii) obtain soil samples, both representative and undisturbed (wherever necessary) for determining soil properties in the laboratory.

(iv) measure tilt every month of all columns.

TESTS PERFORMED AND DATA OBTAINED

The plan of the existing overhead tank is shown in Fig. 2. At this site, the following field tests have been conducted:

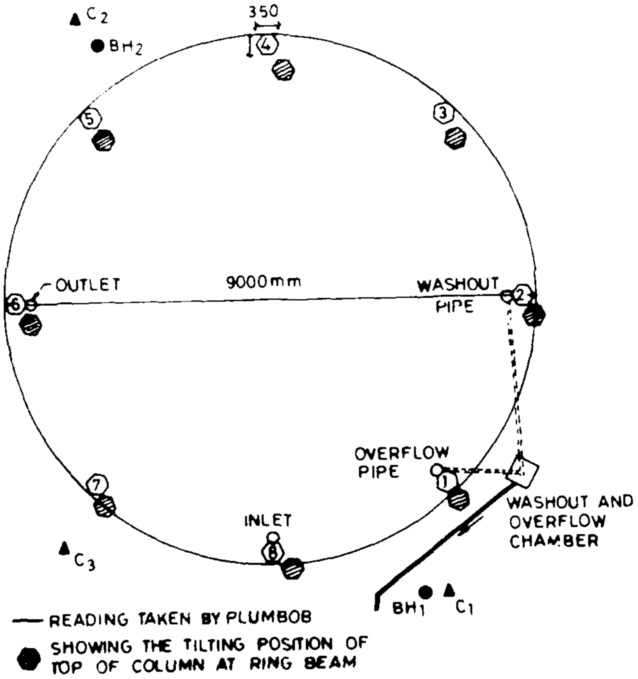

Fig. 2 Plan of the Tank

Two boreholes were made upto the depth of 10 m. One borehole was made towards tilting side of the tank and another borehole was made towards the opposite side of tilting. The location of these boreholes are shown by BH 1 and BH 2 in Fig. 2. The standard penetration tests were conducted at an interval of 1.5 m depth as per Standard Specifications (IS:2131-1981).

Three dynamic cone penetration tests with a 50 mm cone were conducted at locations C1, C2 and C3 as shown in Fig. 2, as per IS:4968 Part I-1976. These tests were performed continuously upto a depth of about 10 m.

Representative samples were collected during the boring from the SPT sampler and the following laboratory tests were conducted.

(i) Sieve analysis, liquid limit and plastic limit tests for classification of soils.

(ii) Water content determination.

Based on the results of laboratory classification tests, the soils were classified as per IS:1498-1970 and the type of soil strata at the site is shown in Figs. 3 and 4. These figures show the values of liquid and plastic limits, natural moisture contents percentage of sand and fines. The soil particles passing from 75 micron sieve are called fines.

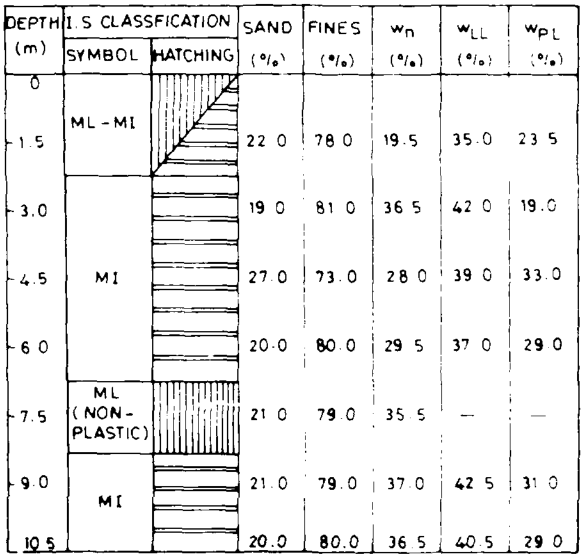

DEPTH (m)	I.S CLASSFICATION SYMBOL	HATCHING	SAND (%)	FINES (%)	w_n (%)	w_{LL} (%)	w_{PL} (%)
0	ML - MI						
1.5			22 0	78 0	19.5	35.0	23 5
3.0	MI		19 0	81 0	36 5	42 0	19.0
4.5			27.0	73.0	28 0	39 0	33.0
6 0			20.0	80.0	29 5	37 0	29 0
7.5	ML (NON-PLASTIC)		21 0	79.0	35 5	—	—
9.0	MI		21.0	79.0	37.0	42 5	31 0
10 5			20.0	80.0	36 5	40.5	29 0

Fig. 3 Bore Log at Location BH 1

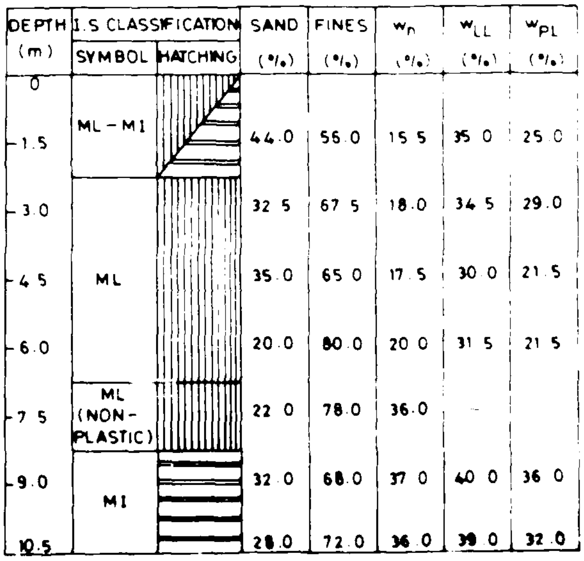

DEPTH (m)	I.S CLASSIFICATION SYMBOL	HATCHING	SAND (%)	FINES (%)	w_n (%)	w_{LL} (%)	w_{PL} (%)
0	ML - MI						
1.5			44.0	56.0	15 5	35 0	25.0
3.0	ML		32 5	67 5	18.0	34 5	29.0
4 5			35.0	65 0	17.5	30.0	21.5
6.0			20.0	80.0	20 0	31 5	21 5
7 5	ML (NON-PLASTIC)		22 0	78.0	36.0	-	
9.0	MI		32.0	68.0	37 0	40 0	36 0
10.5			28.0	72.0	36.0	39 0	32.0

Fig. 4 Bore Log at Location BH 2

Figure 5 shows the standard penetration resistance Ns of locations BH 1 and BH 2. The values observed at the site are shown by the zig-zag curves and average values are shown by vertical straight lines.

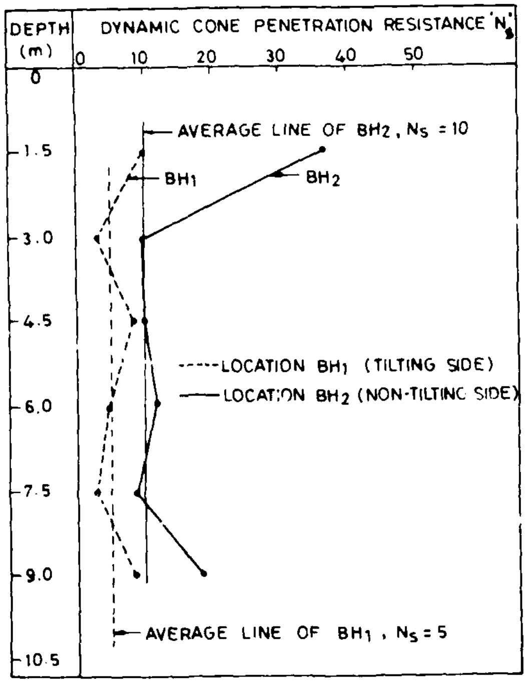

Fig. 5 Standard Penetration Resistance at BH 1 and BH 2

For making a comparison of dynamic cone penetration resistance at tilting and nontilting sides, the values of Nc have also been plotted in Fig. 6.

INTERPRETATION OF RESULTS

Soil Strata

At location BH 1 (tilting side) the soil is sandy silt of low to medium compressibility with brickbats upto about 2.25 m depth. It is followed by sandy silt of medium compressibility upto about 6.75 m depth, further followed by a 1.5 m thick layer of nonplastic sandy silt of black colour, underlain by sandy silt of medium compressibility. The percentage of sand varies from 19 to 27 percent and fines from 81 to 73 percent. The sand is mainly fine and medium. The water content varies from 19.5 to 37.0 percent.

At location BH 2 (nontilting side) the soil is sandy silt of low to medium compressibility with comparatively large percentage of brickbats upto about 2.25 m depth. It is followed by sandy silt of low compressibility upto about 6.75 m depth. It is underlain by a 1.5 m thick nonplastic sandy silt layer of black colour. It is further followed by sandy silt of medium compressibility upto the depth explored. The percentage of sand varies from 20 percent to 44 percent and fines from 80 percent to 56 percent. The water content ranges from 15.5 percent to 37 percent.

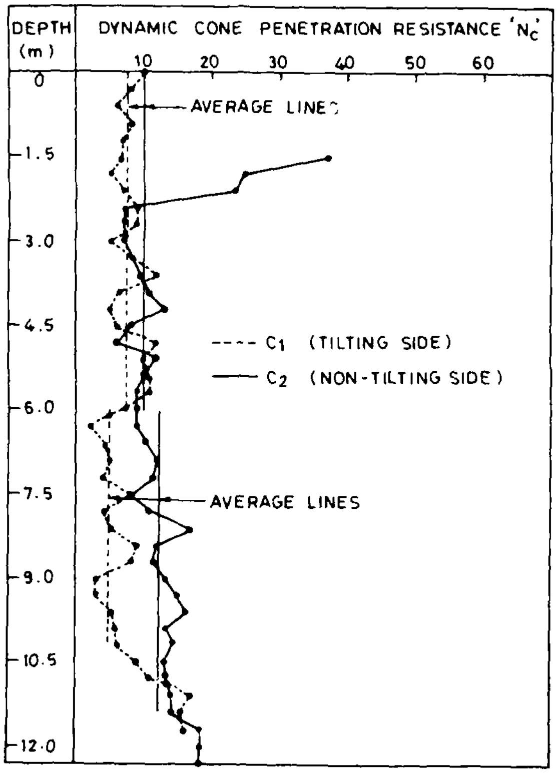

Fig. 6 Dynamic Cone Penetration Resistance at C 1 and C 2

Ground Water Table

The ground water table was not observed upto the 10.5 m depth, in the month of Nov. 1986.

Penetration Test Data

Standard penetration resistance values in general are less towards tilting side (BH 1). However this difference is very large at 1.5 m depth. It is due to large percentage of brickbats present at location BH 2 at 1.5 m depth. The average values of Ns at BH 1 and BH 2 are 5 and 10 respectively.

Dynamic cone penetration resistance is also very poor towards tilting side (BH 1). The average value of Nc is about 7.0 upto about 6.0 m depth and only 5 below 6.0 m depth. Towards opposite of tilting side (BH 2) the average values are 10 and 13. At few depths, the values are as low as 2 and 3 at locations C1 and C3, while the minimum value is 6 at location C2.

Monitoring of Tilt

Regular observations since May 1986 show that tilt has more or less stabilized. There was no significant increase in tilt in last two rainy seasons also. It was further observed that there was elastic rebound of 5 mm when tank was emptied. The tank is still being monitored.

Design Criteria

For satisfactory performance of foundations, the following criteria must be satisfied :

a. The foundation must not fail in shear. A factor of safety of 2.5 - 3.0 is usually applied.

b. The foundation must not settle by more than the permissible settlement.

c. The foundation must not tilt by more than the permissible limit.

IS:1904-1978 specifies the following values of tolerable settlements for rafts of overhead tank.

	Sand and hard clay	Plastic clay
Total settlement	100 mm	125 mm
Differential settlement	0.0025 L	0.0025 L

where L is the length of the deflected part of the raft. The smaller of the bearing pressure obtained according to (a), (b) and (c) above is adopted as the allowable soil bearing pressure.

Computation of Allowable Soil Pressure

The allowable soil pressure is computed using the results of standard penetration test, dynamic cone penetration test and laboratory tests.

The details of the tank (see Fig. 1) are as follows :

Depth of foundation = 1.6 m
Outer dia of the raft = 10.3 m
Inner dia of the raft = 6.85 m
Width of the ring = 1.725 m
Capacity of the tank = 200 KL
Staging = 9.0 m
Numbers of columns = 8
Size of columns = 350 mm x 350 mm

From Fig. 3 the average value of Ns at location BH 1 is only 5.

Shear consideration

From Terzaghi and Peck, (1967) correlations, unconfined compressive strength of the soil corresponding to Ns = 5 is 6.25 t/m^2. Hence from Terzaghi's equation, the net ultimate bearing capacity of soil foundation system is 17.8 t/m^2.

Pressure at the base of the footing is 10.76 t/m^2

Factor of safety = $\frac{17.8}{10.76}$ = 1.65.

This factor of safety is less than the required one.

Settlement calculations

Settlements are calculated from Terzaghi's consolidation theory using Eq. 1.

$$S = \frac{C_c H}{1 + e_o} \log_{10} \left(1 + \frac{\Delta p}{p_o}\right) \qquad (1)$$

where C_c = compression index (0.25)

H = thickness of the soil layer under consideration

e_o = initial void ratio of the soil mass

Δp = increase in pressure at the centre of the layer due to pressures (p) at the base of footing

p_o = effective overburden pressure at the centre of the layer from the ground surface.

$$\frac{C_c H}{1 + e_o} = \frac{0.25 \times 200}{(1 + .9)} = 26.3$$

Settlements are calculated for a pressure intensity of 10.76 t/m^2 in the tabular form as given below :

TABLE 1. Calculation of Settlements

Layer	Thickness (h)	p_o	Δp	$\frac{\Delta p}{p_o}$	$\log_{10}(1 + \frac{\Delta p}{p_o})$	S(cm)
1	200 cm	4	6.81	1.70	0.432	11.35
2	200 cm	7.2	3.92	0.54	0.188	4.96
3	200 cm	10.4	2.75	0.265	0.102	2.69
4	200 cm	13.6	2.127	0.156	0.063	1.66
5	200 cm	16.8	1.73	0.103	0.042	1.12
6	200 cm	20	1.46	0.073	0.030	0.80
7	200 cm	23.2	1.26	0.054	0.023	0.60
8	200 cm	26.4	1.11	0.042	0.018	0.47

Total settlement = 23.65 cm = 236 mm

This settlement does not include immediate subsidence due to soaking of water which is seeping from washout and overflow chamber towards the tilting side (Fig. 2).

Probable differential settlement = 23.65 x $\frac{3}{4}$
= 17.737 cm
(say 177 mm)

Angular distortion = $\frac{177}{10,300} = \frac{1}{58}$

Permissible differential settlement = $\frac{1}{400}$ x 10,300
= 25.75 mm

COMPARISON OF PERMISSIBLE, ESTIMATED AND OBSERVED SETTLEMENTS

The (nearly) estimated, observed and permissible values of differential settlements and angular distortions are listed below :

	Differential settlement	Angular distortion
Permissible	26 mm	1/400
Estimated	177 mm	1/58
Observed	448 mm	1/23

CAUSES OF TILTING

The following may be the possible causes of tilting of this water tank.

Non-uniformity of water content

It was found that the percentage of water content *was higher* upto a depth of 6.0 m towards tilting side than that on the opposite side. Most probably it is due to seepage of water in the ground from washout and overflow chamber and the drain. These sources of seepage were existing towards tilting side.

Non-uniformity and inadequacy of soil resistance

The overall soil resistance was also found very poor towards tilting side of the tank. It is probably due to higher water content at tilting side which in turn is probably due to seepage of water as mentioned above. The strength of plastic and cohesive soils is decreased significantly due to increase in water content. The resistance of the soil, opposite to the tilting side is twice the resistance on tilting side.

The factor of safety of 1.65 against shear failure of soil foundation system is also inadequate at the tilting side.

Suggestions are invited for correcting the tilt and strengthening the foundation if necessary.

CONCLUSIONS

Based on the findings of field and laboratory tests carried out at the site, the following conclusions are made:

1. The soil at the site is sandy silt of low to medium compressibility (ML-MI). There are brickbats also in the soil, the percentage of brickbats are more towards opposite of tilting side and upto a depth of about 2.25 m below the ground level, where as depth of foundation is 1.6.m.
2. The ground water table was not met upto the depth explored i.e. 10.5 m in the month of Nov.1986. Water content was found to be more towards tilting side than the other side. It is perhaps due to seepage of water from washout and overflow chamber and drain in the near past.
3. Penetration resistance, recorded by SPT and DCPT is poor towards tilting side. Average value of standard penetration resistance (Ns) is only 5 at location BH 1 and is 10 at the location BH 2. At few depths towards tilting side the dynamic cone penetration resistance values (Nc) are as low as 2 and 3.
4. The possible causes of tilting of water tank is due to (i) higher water content in the soil mass towards tilting side and (ii) non-uniformity and inadequacy of the soil resistance on tilting side.
5. It is felt that the permissible tilt of 1/400 is too stringent a limit for R.C.C. overhead tanks as it may not create serious eccentricity. The above tank is still functioning inspite of tilt of 1/23 for the last 12 years.

ACKNOWLEDGEMENT

The authors thank Mr. J.A.Joshi, S.E. and Mr. P.K.Jain, E.E., U.P. Jal Nigam for sponsoring the project and taking keen part in discussions. Help rendered by their staff during testing is also acknowledged.

REFERENCES

IS:2131-1981, Method for Standard Penetration Test for Soil, Indian Standard Institution, Manak Bhawan, New Delhi.

IS(4968(Part-I)-1976, Method for Subsurface Sounding for Soils Part I Dynamic Method using 50 mm Cone without Bentonite Slurry, Indian Standard Institution, Manak Bhawan, New Delhi.

IS:1498-1970,Classification and Indentification of Soil for General Engineering Purposes, Indian Standard Institution, Manak Bhawan, New Delhi.

IS:1904-1978, Code of Practice for Structural Safety of Buildings: Shallow Foundations, Indian Standard Institution, Manak Bhawan, New Delhi.

Singh, Bhawani, P.K. Jain and G.C. Nayak (1987), "Report on Geotechnical Investigations for Tilted Water Tank at Parikshatgarh, Meerut", University of Roorkee, Roorkee, India.

Terzaghi, K. and R.B. Peck (1967),"Soil Mechanics in Engineering Practice", John Wiley & Sons, New York.

Proceedings: Second International Conference on Case Histories in Geotechnical Engineering, June 1-5, 1988, St. Louis, Mo., Paper No. 6.99

Lock and Dam No. 26 R, Lock Cofferdam, Construction Sequencing

Robert J. Rapp
Hydraulic Engineer, U.S. Army Engineer District, St. Louis, Missouri

Joseph L. Schwenk
Geotechnical Engineer, U.S. Army Engineer District, St. Louis, Missouri

SYNOPSIS: Construction of a new lock and dam to replace existing Locks and Dam No. 26 required construction to be accomplished in three separate stages. Each portion of the new structure would be constructed inside cellular cofferdams. The construction of each cofferdam would require model tests to determine compatibility with design flow requirements relative to constructabiity of coffercells, scour of riverbed material, and navigation of river vessels.

Compatibility of the lock cofferdam geometry was verified using model studies along with sequence for construction of the cofferdam cells. Construction of the second stage cofferdam was successfully completed in December 1985, followed by dewatering and construction of the 1,200 foot lock structure.

INTRODUCTION

Lock and Dam No. 26, Mississippi River Mile 202.9, Alton, Illinois, is part of the inland waterway system on the Upper Mississippi River, comprised of a series of 28 dams and 34 locks. The Upper Mississippi inland waterway system provides for a channel of 9-foot depth and adequate width between the mouth of the Missouri River and Minneapolis, Minnesota, a distance of about 663 miles. The 28 dams in the system are spaced at irregular intervals varying from 9.6 to 46.3 miles, the average length of pools being 25 miles. The sizes of 34 locks vary in width from 56 to 110 feet and in length from 320 to 1,200 feet, the majority being 110 by 660 feet.

The twin locks at Lock and Dam No. 26, which were opened to traffic in 1938, consists of a 110 by 600-foot main lock and a 110 by 360-foot auxiliary lock located adjacent to the Illinois bank. A gated dam, extending from the locks to the Missouri bank, provides a slack water pool on the Mississippi River to Lock and Dam 25, Mile 241.4, and on the Illinois River to LaGrange Lock and Dam, Mile 80.2.

PROJECT DESCRIPTION

The existing facility was designed and constructed during the transition period when packet-type sternwheelers were being phased out and barge-type tows were just beginning to be used on a large scale. During planning and design of the locks, it was believed that these locks would be capable of meeting the requirements of river transportation until 1988.

Since construction of the project, river traffic has increased beyond expectations due to improvements in the inland waterways system, increase in size and power of barge-tows, and the lower cost of water transportation. These locks pass traffic from and to ports on the Gulf of Mexico, the Great Lakes, the upper Mississippi, the Illinois, the Ohio, the lower Mississippi, and the other tributary systems. River traffic at Locks No. 26 has increased beyond expectation since 1938. Presently, the locks at Alton, Illinois, are considered the "bottleneck" for traffic to and from the Upper Mississippi River and its tributaries.

The practical capacity of the existing locks is limited by many factors such as size of lock chambers, lack of up-to-date operating equipment, poor alinement of the approaches, and severe outdraft. The locks reached their practical capacity of 41,500,000 tons per year in 1968, just 30 years after completion of the project. Subsequently, as the volume of traffic has increased over the practical capacity, tows have experienced progressively longer delay times at the locks. The insufficient capacity of the existing facility has created a significant hindrance to navigation.

Several solutions were investigated to provide adequate facilities for existing and anticipated navigation. Traffic projections of all significant commodity groups were made to determine the required capacity of a 50-year economic life of the improvements. Based on capacity analysis, it was concluded that construction of a 1,200-foot and a 600-foot lock would provide the required facilities. Construction of the new facilities would take place at a site two miles downstream of the existing structure.

GENERAL SITE CONDITIONS

Area Topography

The site of the proposed locks and dam is located approximately five miles upstream from the confluence of the Missouri and Mississippi Rivers, at the northern extension of the alluvial valley known as the American and Columbia Bottoms. The area topography is characterized by the broad alluvial valley of these rivers and the wide, flat plains of the uplands. Maximum local relief approximates 200 feet. The floodplain on the Missouri side is a flat, featureless surface used primarily for agriculture and is some five to six miles wide. The Illinois floodplain, on the east bank of the river, is relatively narrow at the site and upstream, while downstream of the site it becomes wider. Along the river channel, the floodplain ranges in average from Elevation 415 in the vicinity of Alton, Illinois to about Elevation 405 near Dupo, Illinois. Although the floodplain relief is low, frequent changes in the course of the Mississippi River during geologic time have produced a complex variety of landforms and channel deposits. South of the site, crescent-shaped (i.e., oxbow) lakes, curved ridges, and swamps mark the location of former meanders abandoned during the process of the Mississippi River channel migration. Also downstream, alluvial fans, which stand 30 to 50 feet higher than the valley bottom, have been developed below the bluffs where tributary streams have entered the main valley.

Subsurface Materials and Conditions

An extensive investigative program was undertaken by the Corps of Engineers, (St. Louis District) consisting of more than 250 land and overwater borings, geophysical surveys, mineralogical studies, and numerous field and laboratory physical tests, to establish the subsurface materials and conditions at the site of the proposed facility. Other studies, including literature searches of geologic and seismic considerations, were also undertaken to provide general information and aid in establishing the type and properties of the subsurface materials and in predicting the service life conditions at the site.

Cofferdam Development

The selection of the cofferdam plan was based on results from physical model studies of navigation conditions, velocities, and scour patterns; historical hydraulic data: theoretical computations of velocities; the results of foundation exploration program; pumping tests to estimate foundation permeabilities; effects of construction sequence on navigation and project completion; and economic considerations.

CONSTRUCTION SEQUENCE

Project Construction Sequence

A three-stage construction sequencing was planned for the locks and dam. The first stage consisted of construction of six ½ gate bays of the main portion of the dam. The second stage is the construction of the river lock and two-½ gate bays of the main portion of the dam. The third stage will be the construction of the remaining portions of the two gate bays and the auxiliary lock. Each stage incorporates the use of a cofferdam to provide the necessary accessibility and protection during construction.

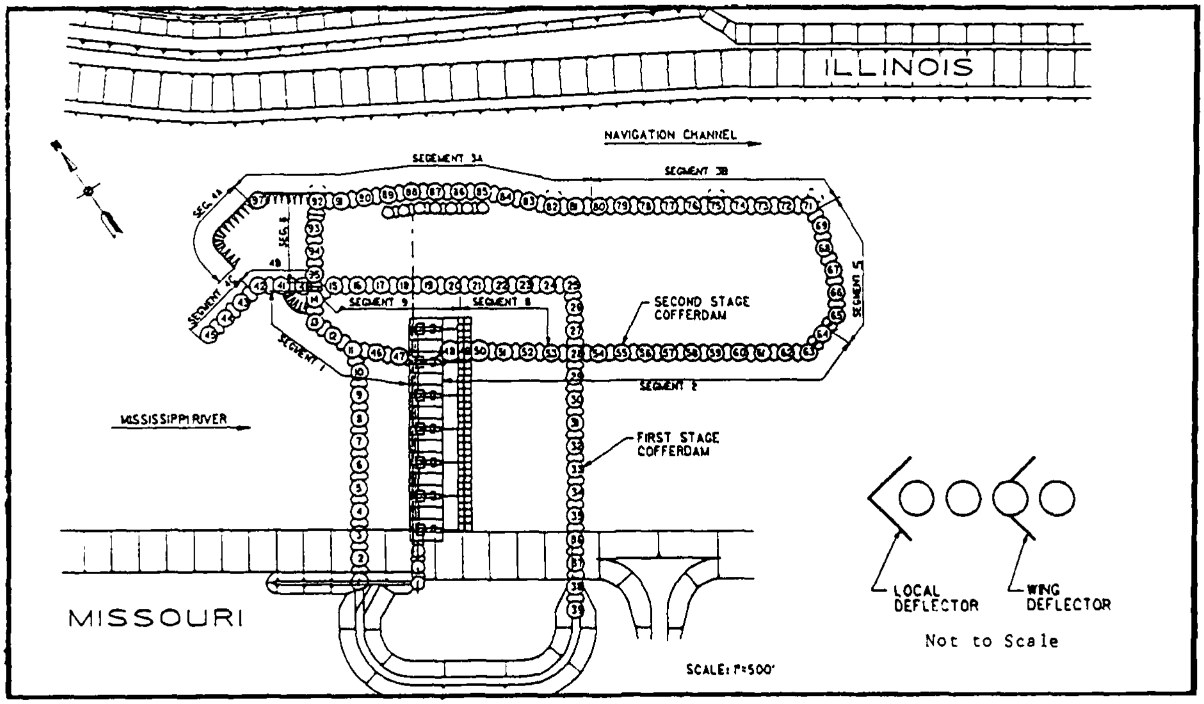

Not to Scale

Fig. 1. Plan for Second Stage Cofferdam

The sequence of construction is considered to be the optimum in order to put the first lock in operation at the earliest date and still permit year-round navigation. The channel width provided during the first stage was 620 feet from the cofferdam to the toe of the Illinois bank. During second stage construction, the channel width is reduced to approximately 330 feet. However, during this stage, five gate bays constructed during the first stage will be available for passage of flow.

During third stage cofferdam construction, the tows will lock through the completed 1,200-foot river lock with the completed portion of the dam operable. Model tests have shown that the proposed cofferdams as sequenced provided optimum combinations of low velocities, minimum scour, and favorable navigation conditions.

The plan for the second stage cofferdam is illustrated in Figure 1. The Missouri leg of the cofferdam was constructed as part of the first stage dam contract. The Illinois leg was located at the center of the two dam gatebays on the Illinois side of the lock. This position provided minimal thorough sufficient work space within the cofferdam while providing the widest possible navigation channel between the cofferdam and the Illinois shore. The upstream and downstream closure walls of the cofferdam are located just beyond the ends of the lock guardwall monoliths.

The cofferdam deflector serves to divert the river currents in the navigation channel away from the Illinois leg of the second stage cofferdam, thus keeping the scoured area away from the upstream Illinois leg of the cofferdam. The deflector also served to provide partial closure of the river channel to aid in construction of the upstream arm of the cofferdam.

ORIGINAL CONSTRUCTION SEQUENCE

The second stage cofferdam has been divided into segments for ease of discussion purposes (see Figure 1). Segment 1 was part of the existing first stage cofferdam. Segment 2 was built under the First Stage Dam Contract. Therefore, the Second Stage Lock Contractor was responsible for construction of segments 3A, 3B, 4A, 5 and 6, and removal of segments 8, 9, 4C and 4B of the first stage cofferdam.

The original concept was that no construction could begin in the river channel until the First Stage Dam Contractor removed cells nos. 1 through 10 and nos. 29 through 39. Removal of these cells would allow passage of flow through the five, 110-foot wide gatebays previously built, thus reducing velocities in the navigation channel.

The construction sequence of the second stage cofferdam was of primary concern. A physical movable bed model located at the Waterways Experiment Station (WES) was used to examine the possibility of beginning any work in the navigation channel before passage of flow through the five gatebays. The model indicated that velocities just downstream of cell No. 25 were low enough to allow cell construction of segment 3B before passage of flow through the recently completed dam. Model velocities in the range of 4 to 6 feet per second were used as a limiting criteria for initiating cell construction activities. Velocities in this range would allow construction of a temporary flow deflector which would provide protection for cell construction. The temporary deflectors will be discussed later.

The next planned activity of the original sequence was the construction of the upstream deflector (segment 4A, cell No. 97, and the portion of the deflector between cells No. 97 and 92). This would begin immediately after flow through the five gatebays was achieved. Under this plan, there was a gap of approximately 2,000 feet between cell No. 92 and segment 3B. When a model tow boat was operated under this condition, regardless of flow conditions, there was a very definite draw into the gap. Figure 2 shows this condition. The draw was caused by flow coming around the upstream deflector and trying to expand back through the gap. This condition was considered a potentially dangerous situation, both to tows and to construction workers. Consequently, a new construction sequence was developed.

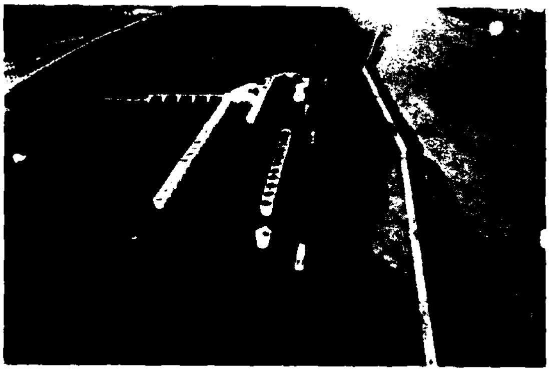

Fig. 2. Navigation Response for Original Construction Sequence

REVISED CONSTRUCTION SEQUENCE

The revised sequence consisted of constructing segments 3A and 3B of the second stage cofferdam prior to construction of the upstream deflector (segment 4A). The model indicated no adverse problems with navigation or scour. Figure 3 shows the model tow headed upstream with segments 3A and 3B complete. Under all flow conditions tested, no problems were identified.

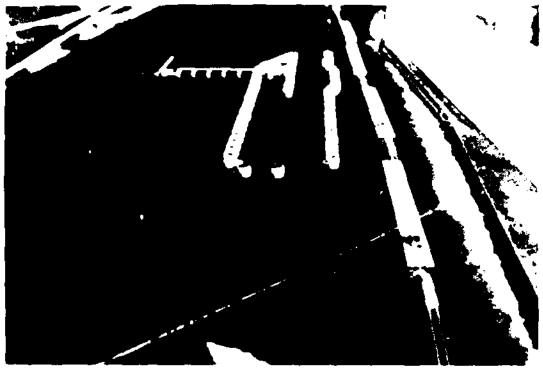

Fig. 3. Navigation Response to Revised Construction Sequence

After the completion of segments 3A and 3B, the remainder of the cofferdam could be completed. The major problem was that a partial river closure would be required in one of three segments. These three segments are segments 5, 6, and 4A (see Figure 1).

Since segments 3A and 3B effectively narrow the navigation channel to approximately 320 feet, segment 5 had to be closed last to provide access to the remaining segments. This would prevent contractor interference with commerical river traffic.

Segment 4A (the upstream deflector) and segment 6 remained as possibilities for partial closure. Originally, the upstream deflector design was to have a continuous flow cutoff to cell No. 42. As Figure 1 depicts, there is a fifty-foot gap between cell No. 42 and the deflector. During model tests to determine the best sequence of construction of the upstream deflector, it was found that velocities would be reduced enough in the area of segment 6 for cell construction if all but fifty feet of the upstream deflector were built. Furthermore, it was determined that the best sequence of constructing segment 6 would be to build cell No. 93, then cell No. 94, followed by cell No. 95 and finally the connecting arcs, starting with the arc between cells Nos. 93 and 92 and continuing on across with the other two arcs. This sequence minimized velocities such that under any flow condition tested, velocities were well within the accepted range for cell construction (4 to 6 feet per second). Therefore, the partial closure was made with segment 6 and the difficulties encountered when trying to close off part of the river were greatly reduced.

MODEL TESTS OF DEFLECTORS

Two other items tested with the model were the local flow deflectors (Figures 1 and 4) and the angle of deflection of the upstream deflector.

Different lengths of the legs of the local flow deflectors were tested to determine their impact on navigation and local scour. The local deflectors have two legs, separated by a 90° angle (see Figure 1). Forty-, sixty-, and eighty-foot legs were tested. The forty-foot legs did not provide sufficient protection to the cell foundation from scour, and the eighty-foot legs produced currents which affected passing navigation. Therefore, a local deflector with sixty-foot legs was decided as best for the given conditions. The sixty-foot legs were long enough to keep the scour away from the cell and thus maintain its stability, and did not affect navigation. The sixty-foot legs provided sufficient protection for three cells immediately downstream. Wing deflectors were then utilized on each side of the third completed cell to provide protection for constructing three more cells. The model revealed that the wing deflectors would be long enough to provide protection similar to the local deflectors (see Figure 1).

Various deflector angles were tested for the upstream deflector. Angles tested ranged from 15° to 60° angled to the direction of the flow. Little differences in results was indicated. The flow separated approximately 500 feet upstream, independent of deflector angles. Therefore, since an angle of 45° to the direction of the flow was used during the first stage without any major problems, it was decided to continue using the same angle.

Prototype Construction

The first local deflector (Fig. 4) was constructed in February of 1985. It was constructed immediately upstream of the location for cell No. 80 (see Figure 2). The construction was accomplished prior to flow through the completed portion of the dam, verifying the model results. Immediately after construction, the river stages began increasing and completely inundated the deflector. In addition, ice began moving down river, subjecting the deflector to ice loads. Normal construction activities did not resume until April 1985, when the template for cell No. 80 was placed. No damage had occurred to the temporary deflector, and the scour patterns which developed correlated well with the model results.

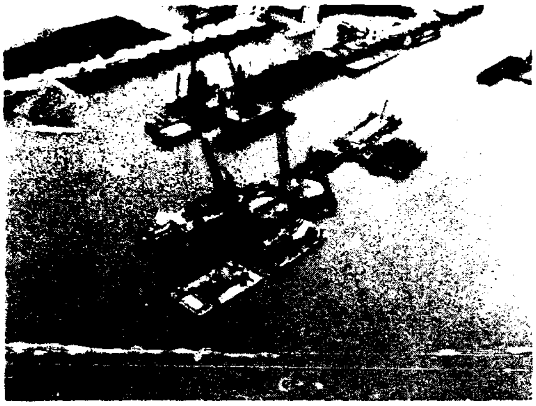

Fig. 4 Local Deflector for Cell Construction

Construction continued throughout the summer of 1985. The sequence of construction followed the specified sequence developed with the aid of the model. By September 1985, the Illinois leg (segments 3A and 3B) and the upsstream deflector (segment 4A) had been completed (see Fig. 5. Visual observations, discussion with towboat pilots, and velocity and flow measurements all indicated very close correlation with the results obtained in the model. The cofferdam was completed in December 1985. During the construction, navigation interference was not a significant factor, and any problems associated with river scour were kept to a minimum. The construction sequence and flow deflectors developed in the model had functioned as designed.

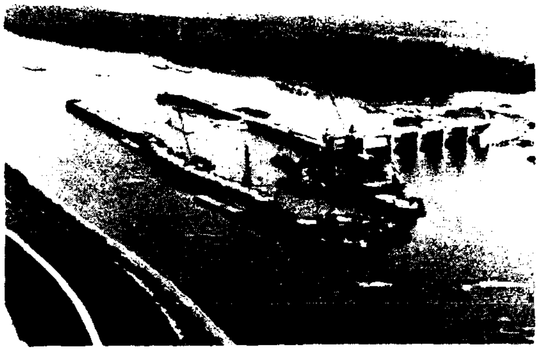

Fig. 5. Illinois Leg and Deflector

CONCLUSIONS

Between April and December of 1985, thirty-one cofferdam cells, the associated arcs between cells, and the upstream flow deflector were constructed in the middle of one of the biggest and busiest rivers in the world. The model tests to develop the construction sequence had lasted well over four years. Much thought and effort went into developing the sequence due to the difficult conditions which would be encountered.

The second stage cofferdam will remain in place until January 1989. Thus far, the cofferdam has functioned as designed. A major flood in October 1986 occurred which required the cofferdam to be completely flooded in anticipation of overtopping. Through all this, actual conditions have reflected those which the model predicted. The model proved to be a very valuable design aid, and has proven its value by the best possible method, prototype performance.

Proceedings: Second International Conference on Case Histories in Geotechnical Engineering, June 1-5, 1988, St. Louis, Mo., Paper No. 6.100

A Study of 15 Cases of Soil-Structure Interaction in China

Xi Hong Zhao
Professor of Geotechnical Engineering, Tongji University, Shanghai, China

Y.A. Yin
Lecturer, Tongji University, Shanghai, China

Y.P. Qian
Lecturer, Tongji University, Shanghai, China

J.G. Dong
Lecturer, Tongji University, Shanghai, China

W.Y. Shen
Lecturer, Tongji University, Shanghai, China

SYNOPSIS: In this paper the first part summarises the results of field experimental studies of deeply embedded box foundations for 10 tall buildings in China, ranging from 10 to 29 storeys. The analyses for deformation characteristic of soil, contact pressure distribution and magnitudes of stresses in foundation reinforcement have been made.

The second part summarises the results of field experimental studies of piled raft and piled box foundation for 4 tall buildings and 1 heavy silo in Shanghai, ranging from 12 to 32 storeys. In this part load-sharing between piles and raft or box and the settlements are analysed, and some suggestions are presented.

INTRODUCTION

With the development of economical construction in China, since 1970's the multi-storey and tall buildings over eight storeys have been gradually increased each year. In recent years the tall buildings around 30 storeys founded on super - long piled raft or piled box foundation have sprung up like mushroom in Shanghai area. The so-called super-long pile means the pile length over 50m which is made of either steel or reinforced concrete.

It is well-known that the field experimental study is significant for monitoring the performance, the design and construction methods, checking the correctness of the existing theory and analyical methods and develping some new ideas in theory and design. For this purpose, in China 10 box foundations and 5 piled raft and piled box foundations were instrumented with settlement measuring systems, including shallow and deep bench markers and heave markers, piezometers, earth pressure cells and bar-stress gauges. Besides, for piled raft and piled box foundations load transducers were installed on the top of piles.

FIELD EXPERIMENTAL STUDIES OF BOX FOUNDATIONS

The summary of box foundations of ten buildings are shown in Table 1.

Settlements of Deeply Embedded Box Foundations

From the typical settlement-time curve for the deep box foundation (see Fig. 1), the loading stages may be simply divided into three main stages for the study of the deformation properties of foundation soil and calculation methods.

(a) Overburden pressure stage (i.e. recompressive deformation stage): The heave and recompressive deformation may be considered as elastic deformation. Recompressive deformation, which is slightly more than the heave, equals 20% - 30% of the total amount of settlement.

(b) Net foundation pressure stage: The foundation soil is still treated as elastic medium although its deformation have entered into the elastoplastic state in some regions. In this stage the rate and increment of settlement increase rapidly. The settlement increment is about 30% - 35% of the total amount of settlement.

(c) Constant foundation pressure stage: The soil deformation varies with time under constant pressure, its characteristics may be expressed by the hyperbola or exponential curve and its magnitude is about 30% - 35% of total amount of settlement.

According to the three main stages, we can carry out the simulation test in the laboratory to obtain the soil parameters, then the total amount of settlement is calculated by the layering summation method as follows:

$$S_{tot} = S_{over} + S_{net} + S_{cons} \qquad (1)$$

The values of allowable settlement for box foundation in China are not restricted to any specific value, and these values depend mainly on the requirements of the building and the effect on the adjacent buildings.

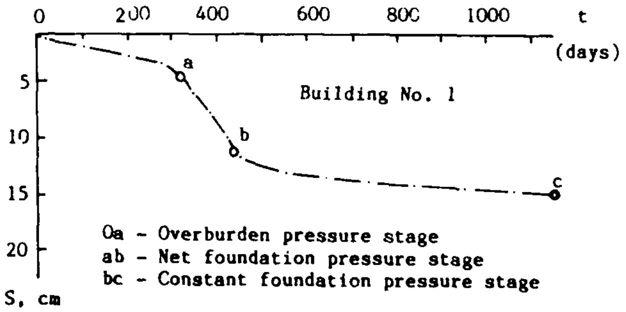

Fig. I Settlement - Time Curve

Table 1 Summary of Box Foundations of Ten Buildings in China

Building No.	Super-structure	Height of Building H, m	Height of box h, m	B/100H	Total pressure p, KN/m²	Allowable pressure, p_a, KN/m²	Average modulous, E_a, KN/m²	Observed settlement S_{ob}, cm	Observed transverse tilt, ‰
	No. of storeys	Dimension of fdn L x B, m	Embedded depth D, m		Net pressure, p_n, KN/m²	Effective pressure p_e, KN/m²		Computed settlement S_{com}, cm	Observed longitudinal deflection, ‰
1	Cross-wall	38.80	5.80	3.6	185.0	300.0	6,100	16.0	2.2
	12	69.6x14.1	5.50		85.0	140.0		21.0	-0.33
2	Cross-wall	35.80	3.68	2.7	188.0	267.0	5,300	12.0	0.5
	12	50.1x9.8	5.20		94.0	146.0		21.0	0.14
3	Frame	37.80	3.65	3.8	156.0	300.0	3,670	24.0	1.7
	12	57.6x14.3	5.65		50.0	110.0		19.2	-0.18
4	Frame	38.98	5.00	4.6	155.0	101.5	2,800	>35.0	2.1
	10	46.0x18.5	5.50		57.0	107.0		35.0	0.10
5	Frame	38.30	5.35	3.4	177.0	200.0	15,730	2.08	0.15
	10	87.4x13.2	5.70		68.7	177.0		7.76	-0.07
6	Cross-wall	30.20	3.30	3.8	150.0	220.0	15,000	1.14	0.30
	12	45.6x11.6	4.41		66.2	150.0		4.41	-0.04
7	Cross-wall	54.70	9.06	2.5	352.0	495.0	7,400	5.39	0.83
	17	36.5x13.8	8.25		222.5	352.0		11.13	0.11
8	Cross-wall	51.80	3.90	3.9	219.0	495.0	15,200	3.14	0.09
	15	62.1x20.3	4.20		102.0	219.0		3.62	0.08
9	Frame cross-w	54.47	5.58	4.7	173.1	207.0	6,500	>30.00	1.58
	16	68.1x25.6	5.58		94.3	157.5		26.42	0.28
10	Tube-frame	104.0	14.50		550.0	$N_{63.5} \cong 60$			
	29		14.50		290.0	550.0			

Table 2 Coefficient of Measured Contact Pressure of Ten Buildings in China

Type	Building No.	Eccentricity due to dead load, cm	0	1	2	3	4	4'	3'	2'	1'	0'
▭ shaped	1	$e \cong 0$		1.146	0.990	0.871	0.911	0.932	0.923	1.080	1.147	
	3	$e_x = 0$, $e_y = 0.3$		1.046	1.028	0.967	0.945	0.957	0.997	1.035	1.025	
	4	$e_x = 0$, $e_y = 16.3$		1.114	1.054	0.985	0.950	0.924	0.908	1.020	1.046	
	5			1.133	0.982	0.945	0.940	0.940	0.945	0.982	1.133	
	6			1.146	0.972	0.946	0.936	0.936	0.946	0.972	1.146	
	7			1.196	0.973	0.921	0.910	0.910	0.921	0.973	1.196	
	8			1.046	0.996	0.981	0.977	0.977	0.981	0.996	1.046	
Cantilever	9		0.810	1.166	1.082	0.977	0.965	0.965	0.977	1.082	1.166	0.810
▭ shaped	2a	$e_x = 0$, $e_y = 23.0$		0.906	0.870	1.015	1.226	1.236	0.977	0.851	0.920	
⌞ shaped	2b					see Table 2a						
Irregular	10					see Reference [2]						

Table 2a

1.015	0.825	0.698	0.603	0.571	0.558	0.558	0.603	0.635
0.444	0.761	0.952	0.952	0.825	0.698	0.666	0.571	0.444
0.635	0.952	1.206	1.396	1.332	1.142	1.015	0.952	0.888
0.952	1.206	1.428						
0.952	1.142	1.301						
1.079	1.079	1.142						
1.206	1.079	1.047						
1.332	1.110	1.047						
1.392	1.142	1.047						
1.459	1.174	1.206						
1.428	1.206	1.904						

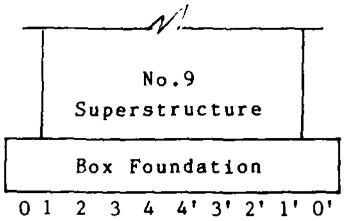

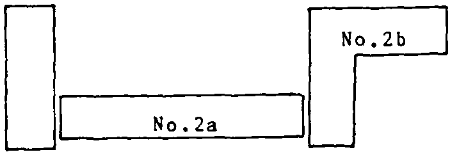

No.2 plan

Longitudinal Deflection and Transverse Tilt of Box Foundations

From the observed data the longitudinal deflection ranges from 0.07‰ - 0.33‰ (see Table 1), and the shape of deflection has been actually completed after the construction of box foundation. During the construction of superstructure (R.C. structure) the deflection basically remains unchanged or changes slightly. This fact shows that rigidity of the box foundation is rather large and the rigidity is even greater when the contribution of superstructure is taken into account. Based on the deflection values, the stress in the box foundation can be calculated using the finite difference method.

From the observed data the tilting value of 0.25% or B/100H may be allowed (see Chinese Code JGJ6-80) in which B and H are the breadth of box foundation and the height of building, respectively.

Table 3 Summary of Piled Raft and Piled Box Foundations of Five Buildings in Shanghai

Building No.	Super-structure	Type of foundation	Dimension of foundation L × B, m	Length of pile, m	No. of piles	Observed settlement S_{ob}, cm	Percentage of load-sharing	
	No. of storeys	Total pressure p, KN/m²	Embedded depth D, m	Dia. or side, m	Spacing m	Computed settlement S_{com}, cm	Raft or box, % *	Piles %
11	Cross-wall	piled box	25.2x12.9	25.5	82	7.1	28	72
	12	228	4.5	45 x 45	1.8-2.1	7.9		
12	Cross-wall	piled box	29.7x16.7	7.5	183	30.0	15	85
	18 - 20	250	2.0	40 x 40	1.2-1.35	30.0		
13	Tube-frame	piled raft	38.7x36.4	53.0	200		30	70
	26	320	7.6	Ø60.9x1.2	1.9-1.95	4.5		
14	Cross-wall	piled box	27.5x24.5	54.0	108		27	73
	32	500	4.5	50 x 50	1.6-2.25	3.0		
15	Heavy silo	piled raft	69.4x35.2	30.7	604	5.8	10 → 0	90 → 100
		288	1.0	45 x 45	1.9	14.5		

Note: * Measured contact pressure included water buoyancy;
Building No.13 and No.14 are under construction.

Contact Pressure Distribution in Longitudinal Direction

The contact pressure distribution is determined by many complex factors, such as the shape and dimension of the foundation and its embedded depth, the stiffness of superstructure and foundation, the properties of soil, construction conditions and the location of the adjacent building etc. The measured results of 10 buildings in some degree may reflect these complex factors.

From the measured results and Table 2 it has been found that there is an evident characteristic, namely, the shape of contact pressure distribution in longitudinal direction has been actually formed under the overburden pressure stage,since then, with the increase of loading, the shape is almost unchanged.

(a) For the individual building with rectangular shape in plan, the shape of contact pressure distribution essentially appears saddle-like.

(b) For the L-shape plan or the building close to the adjacent buildings, the shape is significantly different.

(c) For the cantilever type of box foundation, the shape has another characteristic.

(d) For the irregular plan of box foundation, the shape of contact pressure distribution seems to be parablic (Huang, et al,1986).

These results are helpful to the study of superstructure-box(or raft)-soil interaction. It should be noted that the reasonable layout of building plan is very important.

Stresses in Foundation Reinforcement

The measured results show that the temperature stress in the top slab varies from 20.0MN/m² - 36.5MN/m², in the bottom slab, from 4.0MN/m² - 10.5MN/m²; and the actual stresses including stresses due to overall and local bending are only less than 33.0MN/m². This value is far less than the allowable rebar stress. It is attributable to the superstructure-box-soil interaction. So, the current method to compute the stresses may be conservative.

FIELD EXPERIMENTAL STUDIES OF PILED RAFT AND PILED BOX FOUNDATIONS

Field data on the performance of multi-storey and tall buildings supported on piled raft and piled box foundations is particularly valuable as the amount of reliable data is, as yet,rather limited.

The summary of piled raft and piled box foundations of 5 buildings are shown in Table 3.

Load-sharing between Raft or Box and Piles

It is a complex problem which involves many factors, such as the soil conditions, the dissipation of excess pore pressure (soil consolidation) the number of piles, pile spacing, pile length, pile compressibility, the construction methods and the stiffness of superstructure. However, from the Table 3 and Fig.2 the general conception on load-sharing between raft or box and piles can be obtained as follows:

(a) The proportion of load-sharing between raft or box and piles is different with the increase of construction load, that is, the increment of load carried by piles is greater than that by raft or box. In Shanghai the groundwater level is about 1.0m below the ground surface. So, a common well-point system is usually used during foundation construction. Due to ceasing pumping the water buoyancy has a great effect on the base of raft or box (see Fig.2). The actual soil pressure beneath the base of raft or box, p_s is

$$p_s = p_c - p_w \qquad (2)$$

where p_c = measured value of contact pressure obtained by earth pressure cells;
p_w = water buoyancy.

Actually, the load carried by soil is merely about 10% of the total construction load in conventional spacing of piles.

(b) For the driven precast reinforced concrete piles during piling in soft soils there are often various phenomena happened, such as the heave and horizontal displacement on ground surface, horizontal displacement in soil mass, heave and horizontal displacement of previously driven piles

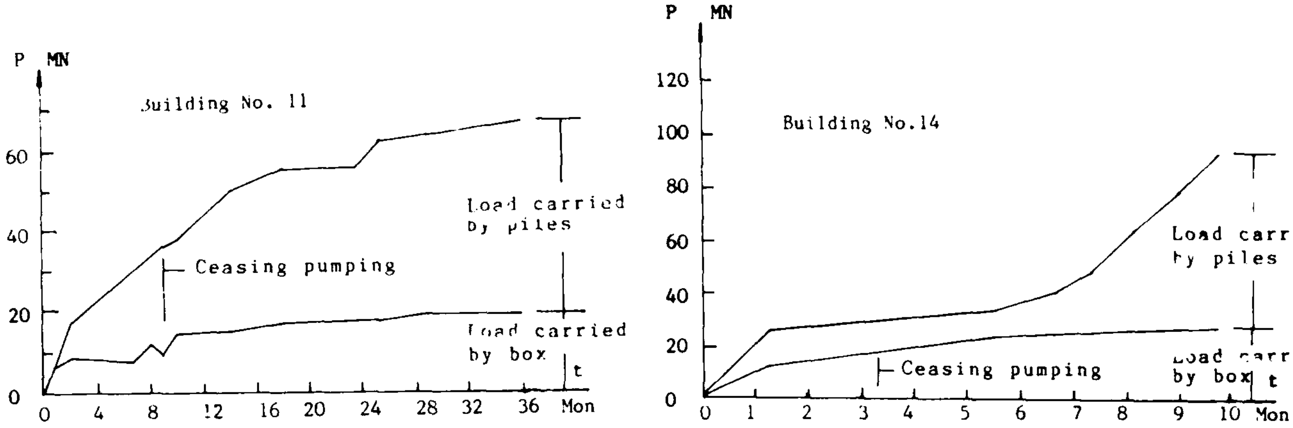

Fig. 2 Load - sharing between Box and Piles

and the high excess pore pressure etc.especially, in large pile groups. For example, in Building No. 15 because of piling speed (604 piles completed in 1.5 months) and large pile groups serious soil deformation both on ground surface and in soil mass were happened, the maximum value of excess pore pressure was 1,4 times the corresponding overburden soil pressure during pile driving into deeply soft clay deposit. With the dissipation of excess pore pressure the base of foundation did not contact with the soil, the contact pressure decreased from $30KN/m^2$ to zero in three years. By excavating the soil below the edge of raft it had found that the gap was 15 cm. It means in this case that the pile and raft interaction seems to be a temporary or transitive characteristic. In Shanghai some case histories in 1930's support this viewpoint.

(c) For the steel pipe pile with open end (see Building No. 13) it has much less disturbance of soil mass than the precast R.C. piles, the height of soil plug in the pipe pile is about 2/3 length of pile, the ratio of maximum value of excess pore pressure to the corresponding soil pressure is 0.69. So, it is hoped that the percentage of load carried by raft will be greater than that used in the precast R.C. piles in same condition.

(d) For the precast R.C. short pile in Building No. 12 the pile tip is located at the sand layer with thickness of 3m, below this layer there is a deeply soft clay. As a result, the settlement is about 30cm. Evidently, the foundation base is in contact with soil and the bearing capacity can be fully mobilized.

Settlements of Piled Raft & Piled Box Foundations

Based on the settlement records of pile-raft and pile-box foundations including the 5 buildings given in this paper, the empirical formulas for predicting the settlement in Shanghai area are as follows:

$S = 0.12\ B_e\%$ for $L = 50m \sim 60m$;

$S = 0.42\ B_e\%$ for $L = 30m \sim 50m$;

$S = 0.35\ B_e\% - 3cm$ for $L = 25m \sim 30m$;

$S = 25cm \sim 30cm$ for $L \cong 8m$.

Where B_e is the equivalent breadth equaling the square root of foundation area and L is the length of pile.

CONCLUSIONS

Analytical results show that Eq.(1) can be used to calculate the settlement of deeply embedded box foundation and analyse the superstructure-box-soil interaction.

In conventional design of pile-raft or pile-box foundations, except short piles in soft soils, the piles and raft or box interaction may be a temporary characteristic in a few years, say 3 years, the piles will eventually carry the total load of building. It should keep in mind that the capacity of piles driven into clay increases with time after driving. So, it has economical significance when piles and raft or box interaction is taken into account, although the settlement is somewhat greater. To mobilize the bearing capacity of soil the pile spacing would be enlarged to 4d - 5d at least.

It is expected that these valuable data presented in this paper will be helpful to geotechnical workers for further study of soil-structure interaction.

ACKNOWLEDGEMENTS

The authers wish to express their hearty thanks to those who provide valuable data, without these data they could not have completed this paper.

REFERENCES

Zhao, X.H. and Y.P. Qian (1983), Some Problems on Foundation Engineering for Multi-storey and Tall Buildings in China, submitted to 4th China Conf. on SMFE, Wuhon (in Chinese)

Huang, X.L. et al (1986), Contact Pressure Characteristic beneath Deep Foundation of Beijing International Hotel, Proc. Inter. Conf. on Deep Foundation, Beijing

Jia, Z.Y. and R.N. Wei (1987), Case History of Soil-Pile Interaction in Soft Soils in Shanghai, submitted to 5th China Conf. on SMFE, Fujian (in Chinese)

Proceedings: Second International Conference on Case Histories in Geotechnical Engineering, June 1-5, 1988, St. Louis, Mo., Paper No. 6.101

Simulation of Drilled Pier Behavior under Three-Dimensional Loading

M.M. Zaman
Assistant Professor, The University of Oklahoma, USA

I. Houssamy
Graduate Research Assistant, The University of Oklahoma, USA

SYNOPSIS: A three-dimensional nonlinear finite element procedure is presented for analysis of drilled (concrete) piers. The procedure allows for tensile cracking and compressive crushing of concrete, nonlinear behavior of soil, and simultaneous application of axial and lateral loads. The procedure is employed to investigate the ultimate capactiy of a 45° underreamed pier. The predicted results are compared with the field test conducted on a similar pier. Also, distribution of displacements and stresses in the soil-pier system and crack pattern in the pier are presented and discussed.

INTRODUCTION

Drilled (concrete) piers are used frequently as foundations for various types of structures such as buildings, bridges, and transmission towers, among others. They may be drilled as straight shafts or shafts with enlarged bottoms, called "underreamed or belled piers," to increase the bearing area of the pier. A schematic of an underreamed pier can be seen in Fig. 1.

Drilled piers are often designed and constructed to provide resistance to axial loads as well as lateral loads and moments from superstructures. An underreamed drilled pier subjected to a general type of loading requires three-dimensional (3-D) analysis. However, due to the complexity involved in the associated soil-structure interaction problems, 3-D analysis has been rarely pursued. Most of the previous studies have been overly idealized in nature (see e.g., Tand and O'Neil, 1977; Farr, 1974; Zaman and Uppal, 1987).

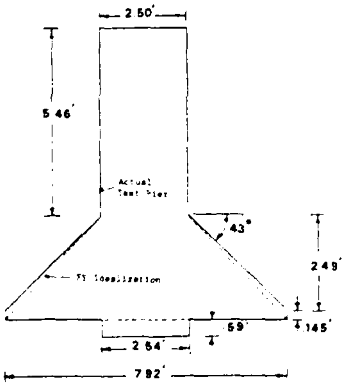

Fig. 1 Schematic of the field test pier

The purpose of this paper is to present a three-dimensional nonlinear finite element analysis of a 45° underreamed drilled pier loaded axially until failure. The generalized plasticity model developed by Desai and Muqtadir (1984) is adopted to describe the nonlinear behavior of soil. Tensile cracking and compressive crushing of concrete are modeled using a linearly elastic fracture model (Chen and Saleeb, 1982). The predicted results for displacements and stresses are compared with the field observations.

3-D FINITE ELEMENT MODELING OF A DRILLED PIER

Nonlinear Finite Element Procedure

A three-dimensional 8-noded hexahedral isoparametric element having twenty four degrees of freedom is used to discretize the required continuum. The soil is assumed to behave as an elasto-plastic material. The concrete is assumed to behave as an isotropic material before cracking and as an anisotropic material after cracking. An incremental iterative scheme is employed for the nonlinear finite element solution. This technique uses the standard Newton-Raphson method in which the system tangential stiffness is updated at the beginning of each iteration. The desired constitutive models are implemented at element integration points rather than having the entire element change properties at one time.

Material Models

The nonlinear behavior of soil is represented by the generalized plasticity model developed by Desai and Faruque (1984). The concrete is assumed to have a perfectly brittle behavior that is modeled by linearly elastic fracture model (Chen and Saleeb, 1982). A brief discussion of this model is presented in this section.

Concrete in Tension

The stress-strain relation matrix for uncracked concrete is described by the generalized Hooke's law.

The tension cutoff failure criterion is used for checking the fracture (cracking) of concrete in tension. A cracking plane is assumed to occur when the tensile stress in a principal direction, at a point in the material, exceeds the tensile strength of concrete, assumed equal to the modulus of rupture of concrete (ASCE, 1981). The cracks are assumed to be smeared rather than discrete and form perpendicular to the principal direction. The normal stiffness of cracked concrete perpendicular to the cracking plane and shear stiffness along the cracking plane are assumed to vanish. It is further assumed that at the instant of cracking, the normal stress perpendicular to the cracking plane and the shear stresses parallel to the cracking plane are released completely and redistributed to the adjacent elements. The incremental stress-strain relation for post-cracking behavior (see Fig. 2) can be expressed as

$$\{\Delta\sigma\} = [T]^T [D]'_{ck} [T] \{\Delta\varepsilon\} - \{\sigma\}_{ck} \qquad (1)$$

where $\{\Delta\sigma\}$ = incremental stress vector, $\{\Delta\varepsilon\}$ = incremental strain vector, $\{\sigma\}'_{ck}$ = released stress vector, $[D]'_{ck}$ = incremental constitutive relation matrix of cracked concrete in the local coordinate system (x'y'z') with x' denoting the offending principal stress direction, and [T] = the desired transformation matrix from local to global coordinate system (xyz).

Once the cracked plane has formed, its direction becomes fixed for subsequent loading. A second cracked plane can form perpendicular to the first cracked plane when the tensile stress in the concrete between the cracks has reached the tensile stress limit. In this case, a new cracking stress-strain relation matrix $[D]'_{ck}$ is formulated to describe the current cracking configuration.

After the cracking of concrete in two directions, the state of stress in the cracked concrete is reduced to uniaxial state. A third cracked plane can form perpendicular to the first and second cracked planes, after which the concrete is assumed to lose its stiffness completely.

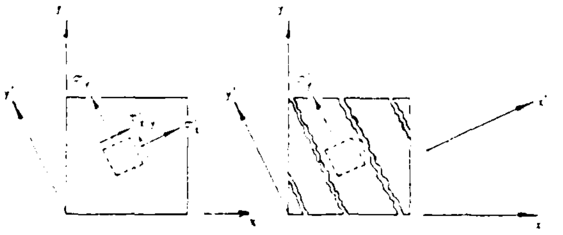

Fig. 2 Cracking of concrete and state of stress after cracking

Concrete in Compression

In this analysis, the concrete is assumed to behave as an elastic material and the Drucker-Prager failure envelope is used to define the elastic limit. The concrete is assumed to crush and lose all its strength once the fracture surface is reached. Also, at the instant of crushing all stresses in concrete are released completely and redistributed to the neighboring elements.

The stress components to be released are converted to nodal forces and applied to the system. The system is reanalyzed and the procedure is repeated until the equilibrium condition is satisfied within some acceptable tolerance. Further details are not presented here because of page limitation but can be found elsewhere (Houssamy, 1987).

NUMERICAL APPLICATION

Finite Element Idealization

The finite element (FE) procedure, described in the preceding section, is used to simulate the field load test of an axially loaded 45° underreamed pier conducted by Sheikh, et al. (1983). Figure 1 shows a schematic of the test pier. Considering the symmetric geometry and loading of the problem, only one half of the pier and surrounding soil block is analyzed in this study. Note that such an idealization is required to analyze a pier under lateral loading although such loading is not specifically considered here. The 3-D (FE) mesh used for the discretization of the pier is shown in Fig. 3. It should be emphasized that for simplicity the finite element idealization adopted herein does not include a reamer seat or toe. The mesh consists of 632 elements connected at 982 nodes. The total number of active degrees of freedom is found to be 2189.

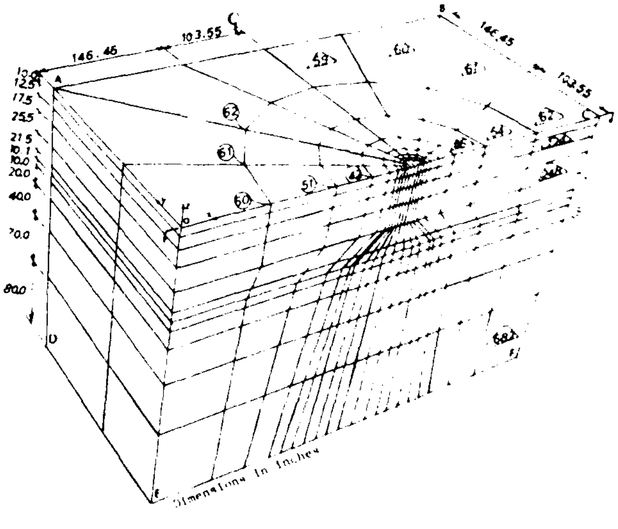

Fig. 3 3-D Finite element mesh

The material properties and constants used for the analysis are summarized below:

Concrete

Compressive strength (f'_c) = 3,250 psi

Modulus of rupture (F_r) = 441 psi

Modulus of elasticity (E_c) = 3×10^6 psi

Poisson's ratio (ν_c) = 0.2

Soil

Modulus of elasticity (E_s) = 4,800 ksi

Poisson's ratio (ν_s) $\approx$ 0.5

The following parameters were assigned for the generalized plasticity model for soil: failure envelope, $\alpha = 0.002$, $\gamma = 0.0008$ ksi, $k = 0.0185$ ksi; hardening parameters, $\beta_a = 0.0001$ and $\eta = 0.01$

The field test failure load (750 kips) was applied in eight increments; the first seven increments were 100 kips each.

DISCUSSION OF RESULTS AND COMPARISON WITH FIELD TEST DATA

Load-Deformation Behavior

The load-settlement curve for the top of the pier is compared in Fig. 4. In the field test, a plunging failure was observed and no evidence of structural failure of the pier shaft or bell could be observed. The failure, defined by a large increase in the rate of settlement of the footing, occurred at a load of 750 kips. The FE model predicted a similar type of failure and the ultimate capacity of the pier was dictated by the failure of soil, however, the FE results underestimated the field observations (see Fig. 4). This can be partly attributed to the fact that an average value of the modulus of elasticity was assumed for the soil medium, although the actual soil was layered.

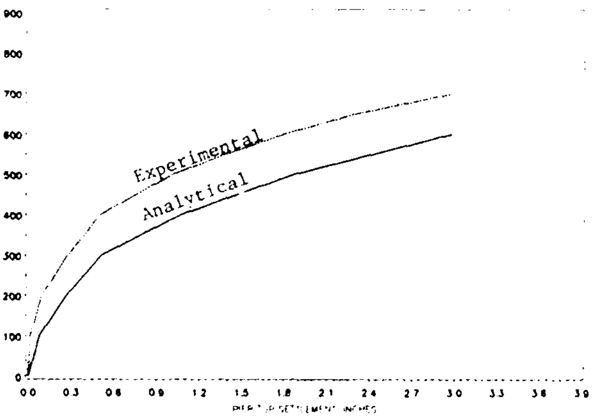

Fig. 4 Load-settlement curve

Typical distribution of displacement field of the pier-soil system at the vertical section I (see Fig. 3) passing through the center of the pier is shown in Fig. 5, for an axial load of 600 kips. It is observed that the pier and surrounding soil experience essentially vertical downward movements. The pier settles down as a rigid body compressing the soil underneath it. A significant settlement of the soil adjacent to the pier is also noticed. This is due to the fact that perfect bond (no slip) is assumed between the pier shaft and soil.

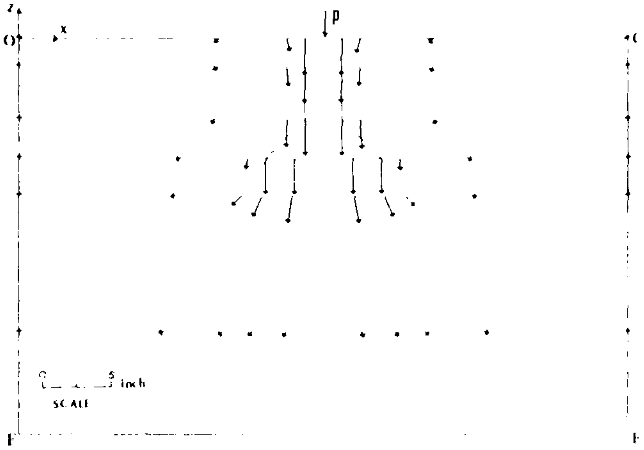

Fig. 5 Displacement field at (P = 600 kips)

Stress Distribution in Soil Mass

The distribution of normal stress component, σ_{zz}, at the integration points of elements surrounding the pier is shown in Fig. 6 at 600 kips load. The normal stresses (σ_{zz}) are symmetrically distributed as expected. The maximum compressive stresses (positive in this analysis) appear to exist beneath the bell with concentration near the edge.

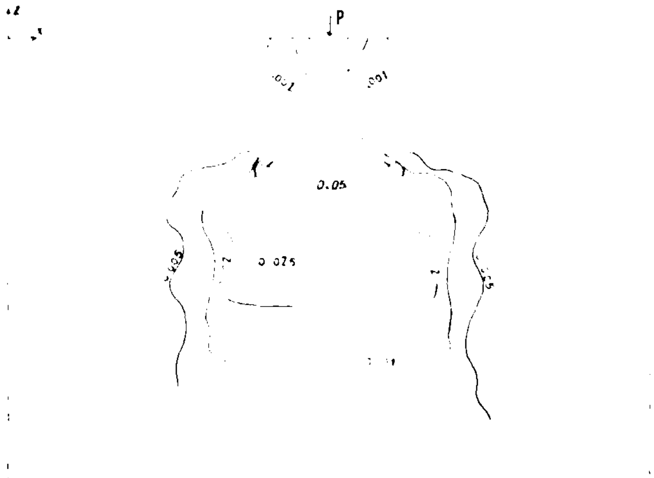

Fig. 6 Distribution of stresses σ_{zz} (ksi) in soil elements at P = 600 kips

Stress Distribution in Pier

The distribution of maximum and minimum principal stresses in the pier are shown in Figs. 7 and 8, respectively, at an axial load of 600 kips. It is observed that the maximum compressive (about 0.8 ksi) stresses in the shaft are not critical and far less than the compressive strength of concrete. From Fig. 8, it is observed that tensile principal stresses of critical magnitudes tend to concentrate at the bottom of underream near the center. This indicates that higher tensile stresses will be induced eventually under increased loads, and cracking is expected to occur in this region. Minor cracking actually occurred, in the present analysis, after the pier was subjected to 700 kips load (considered here as failure load). Fig. 9 shows the crack pattern in the pier.

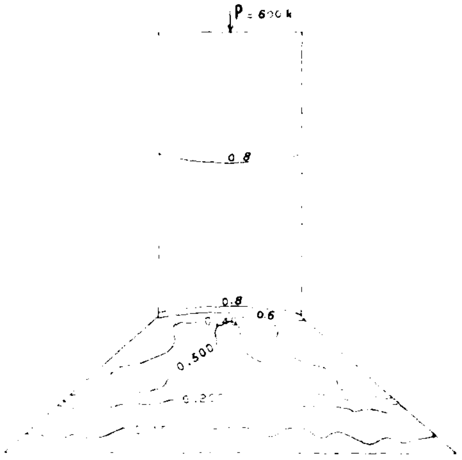

Fig. 7 Distribution of maximum principal stresses (ksi) in the pier

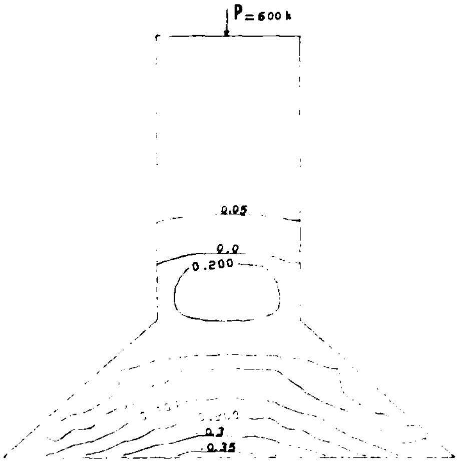

Fig. 8 Distribution of minimum principal stresses (ksi) in the pier

CONCLUDING REMARKS

A nonlinear finite element procedure for three-dimensional analysis of drilled piers is presented. The nonlinear behavior of soil as well as tensile cracking and compressive crushing of concrete are considered. The procedure is used to simulate the field behavior of a 45°-underreamed drilled pier. The predicted results compare favorably with actual observations. The proposed procedure can be used effectively to analyze the deformation response of drilled piers under truly three-dimensional loading.

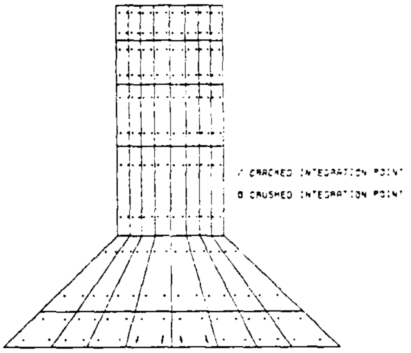

Fig. 9 Crack pattern at P = 700 kips

REFERENCES

ASCE Committee on Concrete and Masonary Structures (1981), "A State-of-the-Art Report on Finite eElement Analysis of Reincorded Concrete Structure," ASCE Special Publication.

Chen, W.F. and Saleeb, A.F. (1982), "Constitutive Equations for Engineering Materials," John Wiley & Sons, Inc., New York.

Desai, C.S. and Faruque, M.O. (1984), "Constitutive Model for Geological Materials," *Journal of Engineering Mechanics Division*, ASCE, Vol. 110, No. 9, pp. 1391-1408.

Farr, J.S. (1974), "Study of the Load Capacity of Plain Concrete Underreams for Drilled Shafts," Master's Thesis, The University of Texas at Austin.

Houssamy, I. (1987), "Three-Dimensional Nonlinear Finite Element Analysis of An Underreamed Drilled Pier," M.S Thesis, University of Oklahoma.

Sheikh, S.A., O'Neil, M.W. and Venkatesan, N. (1983), "Behavior of 45-degree Underreamed Footings," A report to the Association of Drilled Shaft Contractors, University of Houston, Rep. No. 83-18.

Tand, K.E. and O'Neil, M.W. (1977), "Prediction of Load-Settlements Response for Deep Footings," ASCE, Tri-Sectional Meeting, Albuquerque, New Mexico.

Zaman, M.M. and Uppal, A.I. (1987), "A Finite Element Model for Simulation of Field Load Test," Proc. of the Second International Conference on Constitutive Laws for Engineering Materials: Theory and Practice, held at Tuscon, Arizona, Vol. II, pp. 1129-1136.

Zienkiewicz, O.C. (1977), "The Finite Element Method in Engineering Science," 3rd Edition, McGraw-Hill Book Co., New York.

Proceedings: Second International Conference on Case Histories in Geotechnical Engineering, June 1-5, 1988, St. Louis, Mo., Paper No. 6.102

Health of Ammonia Horton Spheres and Foundations—A Case History

Gopal Ranjan
Professor of Civil Engineering, University of Roorkee, Roorkee, India

V.K. Gupta
Reader in Civil Engineering, University of Roorkee, Roorkee, India

S.K. Kaushik
Professor of Civil Engineering, University of Roorkee, Roorkee, India

SYNOPSIS: Liquid Ammonia is stored under pressure in steel Horton spheres (diameter 17 m) under operating pressures of 5-6 kg/cm^2. These spheres are supported on twelve steel columns, concrete pedestals, concrete ring beam and raft or pile foundation depending on the soil conditions. The continuous circular ring beam rests on 72 concrete piles each 45 mm dia and 17 to 20 m long. The second identical Horton sphere is supported on a raft foundation.

The two Horton spheres have been subjected to a hydrostatic loading of 1.7 kg/cm^2 and an additional pressure of 7.3 kg/cm^2 for performance check.

Strains were measured at the crowns, four equatorial points and in six columns. The test results indicate that the spheres and the columns behaved consistent with theoretical values. The concrete in foundations was found to be of good quality corresponding to M20 grade.

The settlements under four columns of the fully loaded actual structure were within anticipated limits i.e. 4-6 mm.

INTRODUCTION

Liquid ammonia required in the production of urea is usually stored under pressure in steel Horton spheres. The operating pressure in these spheres is generally 5 to 6 kg/cm^2 in addition to the liquid head. The safety of these spheres and their foundations is of paramount importance in view of the possible pollution and environmental hazards which may be caused due to the failure of such structures.

The paper reports the actual case record on the performance of the two 17 m diameter spheres and adequacy of foundations when subjected to a loading of 1.7 kg/cm^2 and an additional pressure of 7.3 kg/cm^2. These structures are located in Northern India were commissioned in years 1972 and 1973. These spheres are made of low carbon steel bearing classification No. JIS G 3126 Class 2 SLA 33A and are supported on twelve 570 mm mild steel hollow circular columns, Figure 1. The spheres are reported to have performed satisfactorily so far. However, in view of long time since commissioning and deterioration of shell/concrete due to urea, the assessment of health of sphere was considered essential.

The steel columns are inturn supported by concrete pedestals connected by a ring beam, Figure 2. In one of the spheres, the ring beam was resting on a raft foundation while in the other it rested on 72 concrete piles each 450 mm diameter and 17 to 20 m long.

To assess the health of the Horton spheres strains were measured at the crown, bottom and four equatorial points through suitably pasted electrical resistance gauges. Six of the twelve columns of each sphere were also instrumented for strain measurements. The shell thickness was measured at twelve points to detect the extent of corrosion and also to detect the spread of cracks in welded seams.

The quality of concrete used in the pedestals and ring beam were tested by the ultrasonic pulse technique and Schmidt rebound hammer test. The foundation settlements were also observed at four diametrically opposite columns through suitably mounted dial gauges on independent datums.

FOUNDATIONS

The settlement of the foundations of the Horton spheres was recorded at five equal intervals to achieve a liquid pressure of 1.7 kg/cm^2. The settlements were also recorded when the spheres were pressurised upto 7.3 kg/cm^2 to achieve a total pressure of 9.0 kg/cm^2.

These settlement records are shown in Tables 1 and 2. The settlements were recorded using dial gauges with a least count of 0.01 mm mounted through magnetic bases on independent datums. During the hydro test the load at every stage was maintained constant and the reading recorded when the settlement was complete. The data indicates that the settlements of the four columns were practically equal indicating a uniform settlement of the foundations. The magnitude of settlements was very small and within the permissible limits as specified for water towers and silos (IS:1904-1978). The foundations could thus be considered safe under the stipulated pressure of 9.0 kg/cm^2.

TABLE 1. Settlement Record of Horton Sphere on Piles (Horton Sphere 1)

Sl.No.	Pressure		Col. 1		Col. 4		Col. 7		Col. 10		
			Dial Read	Sett. (mm)	Dial Read	Sett. (mm)	Dial Read	Sett. (mm)	Dial Read	Sett. (mm)	Av. Sett. (mm)
1		0.00	10.24		18.16		17.42		8.73		
2		0.30	14.18*	-	18.29	0.13	17.36	0.06	8.72	0.01	0.07
3	1.5	0.35	14.26	0.08	18.33	0.17	17.35	0.07	8.72	0.01	0.08
4	2.5	0.68	14.33	0.15	18.45	0.29	17.32	0.10	8.75	0.04	0.15
5	3.5	0.85	14.41	0.23	18.47	0.31	17.32	0.10	8.80	0.09	0.18
6	4.5	1.50	14.43	0.25	18.50	0.34	17.21	0.21	8.81	0.10	0.23
7	5.5	1.70	14.45	0.27	18.54	0.38	17.18	0.24	8.85	0.14	0.26
8		2.25	14.47	0.29	18.57	0.41	17.15	0.27	8.87	0.16	0.28
9		4.00	14.50	0.32	18.57	0.41	17.14	0.28	8.87	0.16	0.29
10		6.00	14.53	0.35	18.58	0.42	17.12	0.30	8.87	0.16	0.31
11		7.65	14.53	0.35	18.59	0.43	17.11	0.31	8.87	0.16	0.31
12		9.00	14.60	0.42	18.62	0.46	17.02	0.40	8.87	0.16	0.36

* Dial reset.

TABLE 2. Load/Pressure-Settlement Record of Horton Sphere on Raft (Horton Sphere 2)

Sl.No.	Pressure		Col. 1		Col. 4		Col. 7		Col. 10		Average Sett. (mm)
	Water head (m)	Press. (kg/cm^2)	Dial Read.	Sett. (mm)	Dial Read.	Sett. (mm)	Dial Read.	Sett. (mm)	Dial Read.	Sett. (mm)	
1	0.00		4.25		19.32		9.19		4.47		
2	2.00	0.20	4.03	0.22	19.24	0.08	9.10	0.09	4.29	0.18	0.1425
3	4.00	0.40	3.79	0.46	19.11	0.21	8.98	0.21	4.07	0.40	0.3200
4	4.50	0.45	3.61	0.64	19.00	0.32	8.92	0.27	3.82	0.65	0.4700
5	5.60	0.56	3.14	1.11	18.76	0.56	8.64	0.55	3.25	1.22	0.8600
	5.30	0.53	3.60*	-	18.10*	-	8.80*	-	3.45*	-	
6	5.60	0.56	3.52	1.11**	18.02	0.56**	8.67	0.55**	3.47	1.22**	0.8600
7	6.00	0.60	3.44	1.19	17.89	0.68	8.69	0.57	3.38	1.31	0.9375
8	7.00	0.70	3.24	1.39	17.76	0.81	8.56	0.70	3.20	1.49	1.0975
9	8.80	0.88	3.04	1.59	17.70	0.87	8.20	1.06	3.00	1.69	1.3025
10	9.10	0.91	3.00	1.63	17.65	0.92	8.13	1.13	2.88	1.81	1.3725
11	10.00	1.00	2.68	1.95	17.53	1.04	8.03	1.23	2.40	2.29	1.6275
12	11.00	1.10	2.28	2.35	17.33	1.24	7.95	1.31	1.80	2.89	1.9475
13	13.60	1.36	1.80	2.83	16.52	2.05	7.15	2.11	0.54	4.15	2.7850
14	14.00	1.40	1.70	2.93	16.45	2.12	7.08	2.18	0.42	4.27	2.8750
15	15.00	1.50	1.50	3.13	16.29	2.28	6.95	2.31	0.16	4.53	3.0625
16	16.00	1.60	1.35	3.28	16.20	2.37	6.86	2.40	0.04	4.65	3.1750
17	17.00	1.70	1.30	3.33	16.15	2.42	6.76	2.48	0.02	4.67	3.2250
	17.00	1.70	1.13*	-	16.25*	-	6.98*	-	24.98*	-	
18		2.10	1.15	3.35	15.90	2.77	6.70	2.76	24.83	4.82	3.4250
19		4.00	1.35	3.55	16.00	2.87	6.88	2.78	25.00	4.89	3.5225
20		6.00	1.56	3.76	16.20	3.07	7.00	2.90	25.20	5.09	3.7050
21		7.70	1.72	3.92	16.40	3.27	7.08	2.98	25.30	5.19	3.8400
22		8.80	1.80	4.00	16.45	3.32	7.15	3.05	25.40	5.29	3.9150

* Dial reset
**Readings adopted from earlier loading.

The grade of concrete normally specified for columns and foundations as per IS:456-1978 is M20 and M15 respectively. In the present case M20 grade concrete had been specified for the pedestals as well as ring beams. The quality of concrete in the pedestals and the ring beams, existing for the past 15 yrs, were expected to suffer a strength loss due to urea containmination through air and seepage water. Therefore, non-destructive testing of concrete pedestals and ring beams were carried out. The rebound hammer observations were taken at 2100 points at various positions on the columns and the ring beams of each sphere. The quality of concrete was found to be very good and higher than M20 barring local variations at a few points. The ultrasonic observations were recorded at 50 points and most of the values were found to be more than 3250 m/sec, indicating that the quality of the concrete existing in the foundations was good.

HORTON SPHERES

The Horton spheres are made of low carbon steel as they are required to contain liquid ammonia at a temperature of 3 to 5^{o}C. To obtain this temperature condition the spheres are heavily insulated with an approximately 75 mm thick thermocole layer, aluminium foil and tin sheets. To study the health and behaviour of the spheres during the hydro test, strain gauges were pasted at the crowns and four equatorial points after cutting pockets in the insulation at the desired locations. At each point the meridional and circumferential strains were measured for the two spheres and are given in Tables 3 and 4. A study of these results shows that the strains developed at all stages of hydrostatic loading at all the twelve points were much lower than the yield strain of the material and correspond to a stress of 1125 N/mm^{2}. The strains at the four equatorial points were almost equal indicating symmetrical deformation of the spheres. The theoretical computations of the strains at the twelve locations were found to be in close agreement.

TABLE 3. Measured Strains for Horton Sphere-1 Under Hydrostatic Loading

Sl. No.	Differential Pressure	Pressure at Bottom Crown (Kg/cm^{2})	Temperature (^{o}C)	Date/ Time	Strain in microns											
					Meridional								Circumferential at equator			
					Top		Bottom		Equator							
					EW	NS	EW	NS	N	S	E	W	N	S	E	W
1	0.0	0.0	27	27.5.87 12.30	0	0	0	0	0	0	0	0	0	0	0	0
2	0.4	0.68	25	27.5.87 14.30	138	112	116	116	94	96	89	87	93	105	102	106
3	0.5	0.85	25	27.5.87 17.00	201	203	202	209	107	109	99	108	98	97	102	98
4	0.6	1.087	25	27.5.87 19.00	209	210	295	296	110	113	104	114	107	107	108	107
5	0.8	1.500	25	27.5.87 21.10	229	234	302	303	124	123	117	113	113	124	127	123
6	0.8	1.500	25	27.5.87 23.50	230	235	392	393	165	163	-	153	153	-	-	-
7	1.0	1.700	25	28.5.87 09.30	241	242	405	406	184	187	192	175	176	177	174	178
8	1.0	4.00	25	28.5.87 10.00	302	304	706	707	294	305	307	316	299	296	293	296
9	1.0	6.00	25	28.5.87 10.15	571	572	983	984	402	401	487	401	405	401	400	411
10	1.0	7.65	25	28.5.87 10.30	795	789	1109	1108	517	528	530	538	515	518	517	508
11	1.0	9.00	25	28.5.87 11.00	892	890	1409	1410	609	619	609	619	611	609	607	609
12	1.0	9.00	25	28.5.87 12.00	901	896	1410	1410	608	619	612	620	617	611	615	610

The original thickness of the spherical shells provided ranged from 28 to 32 mm inclusive of a 3 mm corrosion allowance. Since the exterior surfaces of the spheres are epoxy painted no incidence of corrosion is normally expected. Also, as long as the sphere is loaded with ammonia, the oxygen and moisture have no access to the internal surface,minimising the chances of corrosion. Thickness measurements of the spherical shells were taken at twelve locations in May 1987. These thickness values ranged from 32.08 to 33.36 mm indicating the absence of significant corrosion. An inspection of the welded seams of the Horton sphere shells was also undertaken and the spread of cracks in the welds were observed at thirteen locations. Only at one point a prominant crack was observed which was eliminated by grinding the joint by 3.5 mm.

CONCLUSIONS

The future performance of the Horton spheres depends on the extent of corrosion and efficiency of the welded joints. The concrete in the foundations was found to be uneffected by the environmental pollution and to be in accordance with the design specification even after a lapse of 15 years. The design of foundations was found to be adequate and the settlements were found to be small, uniform and within permissible limits.

REFERENCES

Ranjan, G., S.K. Kaushik and V.K. Gupta (1987). "Report on Assessment of Health of Ammonia Horton Sphere - Structure and Foundation", Report No. CE-213/86-87, Department of Civil Engg., University of Roorkee, Roorkee.

Ranjan, G., S.K. Kaushik and V.K. Gupta (1987), "Report on Assessment of health of Ammonia Horton Sphere - Structure and Foundation", Report No. CE-217/86-87, Department of Civil Engg., University of Roorkee, Roorkee.

Neville, A.M. (1975), Properties of Concrete. Pitman Publishing Limited, London.

Whitehurst, E.A. (1951), Soniscope Tests of Concrete Structures. Jour. ACI, Vol.47,

TABLE 4. Measured Strains for Horton Sphere-2 Under Hydrostatic Loading

Sl. No.	Differential Pressure	Pressure at Bottom Crown (kg/cm^2)	Date/ Time	Strain in Microns											
				Meridional								Circumferential at Equator			
				Top		Bottom		Equator							
				EW	NS	EW	NS	N	S	E	W	N	S	E	W
1	0.0	0.00	19.6.87 2030	0	0	0	0	0	0	0	0	0	0	0	0
2	0.2	0.34	2215	75	72	74	78	44	46	47	46	49	55	56	53
3	0.4	0.68	20.6.87 0010	140	113	118	118	96	98	92	93	95	107	103	108
4	0.6	1.087	0325	212	211	290	292	112	115	108	115	110	110	111	109
5	0.88	1.55	1600	235	240	397	395	170	167	162	157	157	153	159	160
6	1.0	1.70	1800	245	246	407	410	189	190	194	179	179	180	177	181
7	1.0	2.00	21.6.87 0200	267	263	498	500	212	210	199	215	197	190	191	199
8	1.0	4.10	0215	305	307	715	717	297	309	312	319	307	303	300	305
9	1.0	6.00	0225	577	579	992	995	407	406	490	450	410	406	406	417
10	1.0	7.70	0235	802	795	1115	1113	520	525	530	540	519	520	522	514
11	1.0	3.80	0315	900	894	1405	1405	608	609	610	612	611	618	620	615

Fig. 1 - HORTON SPHERE

Fig. 2 - CONCRETE COLUMNS AND RING BEAM

pp. 433-44.

IS:1904-1978- Indian Standard-Code of Practice for Structural Safety of Buildings: Shallow Foundations, Bureau of Indian Standards, New Delhi.

IS:456-1978- Code of Practice for Plain and Reinforced Concrete, Bureau of Indian Standards, New Delhi.

State-of-the-Art Papers

Proceedings: Second International Conference on Case Histories in Geotechnical Engineering, June 1-5, 1988, St. Louis, Mo., Invited Paper

Design and Construction of Anchored and Strutted Sheet Pile Walls in Soft Clay

Bengt B. Broms
Professor, Nanyang Technological Institute, Singapore

SYNOPSIS: The design and construction of anchored and strutted sheet pile walls in soft clay are reviewed in the paper based on experience gained mainly in Singapore during the last 10 years where mainly strutted sheet pile walls and contiguous bored piles are used. It is important to consider in the design also the high lateral earth pressures on the sheet piles below the bottom of the excavation when the depth of the excavation is large compared with the shear strength of the clay. The strut loads and the maximum bending moment in the sheet piles can be considerable higher than indicated by a conventional analysis. Different methods to increase the stability have also been investigated. With jet grouting, embankment piles and excavation under water it is possible to reduce significantly the maximum bending moment, the strut loads, the settlements outside the excavated area and the heave within the excavation.

INTRODUCTION

The design of anchored and strutted sheet pile walls in soft clay had to satisfy the following criteria.

- that the sheet pile wall should be stable and the factor of safety be adequate with respect to complete collapse both during and after the construction of the wall (ultimate limit state)
- that the displacements and deformations of the sheet pile wall and of the support system at working loads should be small so that the sheet pile wall will function as intended in the design (serviceability limit state).
- that the settlements or lateral displacements caused by the installation of the sheet piles or of the support system (e.g. the driving of the sheet piles or the installation of the anchors) should be small so that adjacent buildings or other nearby structures are not damaged. The settlements from an unintentional lowering of the ground water level in soft clay due to e.g. pumping can be large.

The main factors affecting the behaviour of anchored or braced excavations in soft clay can be classified as follows :

- Geometry of the excavation
  (depth, width, shape and excavation sequence)
- Soil and ground water conditions
  (strength and deformation properties of the soil and the ground water level)
- Properties of the sheet piles
  (stiffness and depth of sheet piles and the chosen construction method)
- Properties of the support system
  (type, spacing and preloading of ground anchors or of struts)
- Loading conditions
  (surcharge and traffic loads)
- Workmanship

Thus a large number of factors can affect the behaviour of both anchored and strutted sheet pile walls. In this paper experience with strutted and anchored sheet pile walls primarily in Singapore has been reviewed. Limitations of different wall and support systems are analyzed. Methods that can be used to calculate lateral earth pressure and the stability of deep excavations with respect to bottom heave and excessive settlements have been evaluated as well as methods to increase the stability. The following review is mainly based on experience gained in Singapore during the last 10 years where numerous deep excavations in soft clay have been required for high rise building, subway stations and tunnels.

SOILS CONDITIONS IN SINGAPORE

There are extensive deposits of very soft marine clay and organic soil with a thickness of up to 35 m or more along the coast and in the buried river valleys in Singapore. It is mainly these soils that have caused difficulties during the construction of both anchored and braced sheet pile walls, e.g. large lateral displacements and settlements. The organic content of the marine clay is normally 3% to 5%. The water content varies usually between 65% and 100%. The undrained shear strength (c_u) which is usually low close to the ground surface increases approximately linearly with depth. Tan (1983) has reported a c/p - ratio (c_u/σ'_{vo}) of 0.315 based on the results from field vane tests. Tan (1970) and Ahmad and Peaker (1977) have indicated somewhat lower values, 0.27 and 0.25, respectively. The effective friction angle ϕ' as determined by consolidated undrained or drained triaxial tests (CD or CU-tests) has been very consistant, 21 to 22 degrees. Settlement observations and oedometer tests indicate that the clay is slightly overconsolidated. The overconsolidation ratio (OCR) is 1.1 to 1.5. The coefficient of consolidation when the clay is normally consolidated is typically 1 to 2 m^2/year.

WALL SYSTEMS

Different wall systems can be used as illustrated in Fig 1 depending on the soil conditions. In Fig 1a is shown a conventional anchored sheet pile wall. The lateral earth pressure on the wall is transferred to the ground anchors through wale beams, normally U-, H- or I- beams.

Soldier pile and lagging construction is shown in Fig 1b. This support method, also called Berliner wall construction, is commonly used in the United States and in Europe mainly in sand, silt or gravel above the ground water level. The method is not suitable in soft clay. The soldier piles or beams, usually H-piles or channels, are driven or placed in predrilled holes and grouted. The spacing of the piles is normally 1.0 to 2.0 m. Lagging (wooden boards) is placed during the excavation between the flanges of the soldier piles. It is important that the lagging is carefully wedged against the soil behind the boards in order to reduce the settlements around the excavation. Also precast or cast-in-place concrete panels can be used as shown in Fig 1c. The deep excavations required for some of the subway stations in Hong Kong have been stabilized by this method.

In silt or in fine sand there is a risk of erosion of the soil below the ground water level and the resulting settlements can be large. Soldier piles and lagging construction should therefore be avoided in these soils when the ground water level is high. The ground water level can, however, be lowered temporarily with well points or filter wells to prevent erosion and failure of the excavation by bottom heave. In stiff to hard clays it may be advantageous to use pairs of channels as soldier piles instead of steel H-piles (Fig 1c). The wale beams can then be eliminated in order to

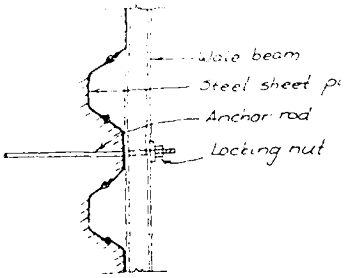
Wale beam
Steel sheet pile
Anchor rod
Locking nut

a Steel sheet piles

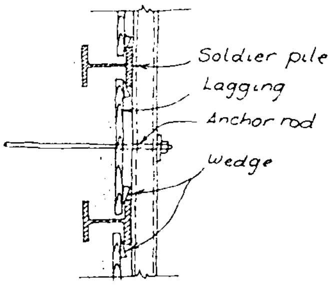
Soldier pile
Lagging
Anchor rod
Wedge

b Soldier piles and lagging

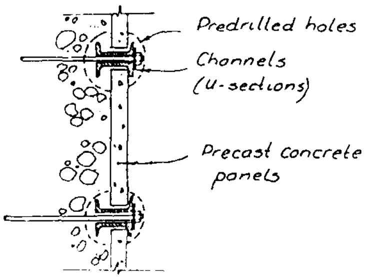
Predrilled holes
Channels
(U-sections)
Precast concrete
panels

c Soldier piles and precast concrete panels

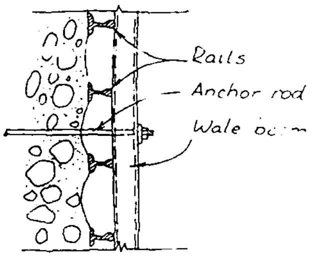
Rails
Anchor rod
Wale be

d. Rails

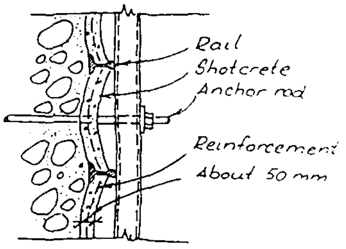
Rail
Shotcrete
Anchor rod
Reinforcement
About 50 mm

e. Rails and shotcrete

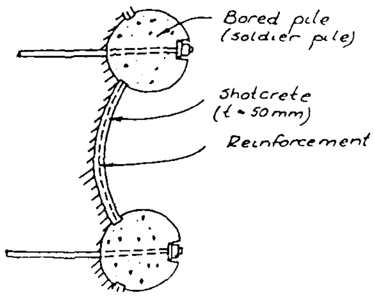
Bored pile
(soldier pile)
Shotcrete
(t ≈ 50 mm)
Reinforcement

f Bored piles and shotcrete

Fig 1a Wall systems

reduce the costs since the anchors can be placed between the two channels.

Rails are used as lateral support in Fig 1d. The spacing is usually 0.2 to 0.3 m. This support method is mainly used in stony or blocky soils above the ground water level. The rails are often placed in predrilled holes when the content of stones or boulders is high since the rails cannot be driven. The rails are often brittle due to the low ductility of the steel (high strength steel). They are difficult to splice by welding. Therefore, bolted joints are often used. In dry sand above the ground water level plywood boards are sometimes placed between the rails to contain the sand. In stiff medium to stiff clays or in silty soils, the soil is normally protected by shotcrete as illustrated in Fig 1e. The reinforced shotcrete arches transfer the lateral pressure from the soil to the rails. The thickness of the shotcrete is normally about 50 mm.

Also bored piles can be used as lateral support in deep excavations as illustrated in Fig 1f. In soft clay the piles should overlap while in medium to stiff clay overlapping is not required. The distance between the piles can be relatively large. The unprotected area between the piles is often covered by shotcrete. Overlapping bored piles, so-called contiguous bored piles, are common in Singapore also in soft clay as foundation for high rise buildings and as lateral support.

ANCHORS AND STRUTS

Different support systems can be used for a deep excavation in soft clay or silt as illustrated in Fig 2 depending on the soil and ground water conditions and on the size (width, length and depth) of the excavation.

The choice of support system depends mainly on the costs, on restrictions at the worksite, on available equipment in the area and on the experience of the consultant or of the contractor. For example, adjacent buildings may be damaged by excessive settlements if a cantilever sheet pile wall is used to support a relatively deep excavation. Also water mains, sewer lines and heating ducts can be damaged by the resulting large settlements and lateral displacements. Excessive settlements can also be caused by the installation of the anchors as well as by the driving of piles inside the excavation. Struts may, therefore, be chosen instead of ground anchors to reduce the risks. The settlements can be reduced further by preloading the struts or the ground anchors. If the anchors are left permanently in the ground they may interfere with future construction such as the driving of sheet piles. However, different anchor systems have been developed during the last few years which can be removed after use and where the settlements caused by the installation of the ground anchors will be small.

The lateral earth pressure behind a cantilever sheet pile wall (Fig 2a) is resisted by the passive earth pressure below the bottom of the excavation while for an anchored or strutted sheet pile wall the lateral earth pressure is resisted by ground anchors or by struts as shown in Fig 2b and 2c, respectively. Ground anchors or struts are normally required in soft clay when the depth of the excavation exceeds 2 to 3 m.

In a large and wide excavation the length of the struts will be large if the struts are horizontal. They had to be braced to prevent buckling as can be seen in Fig 3. The struts will, however, interfere with the work in the excavation and reduce the efficiency. Horizontal bracing is common in Singapore.

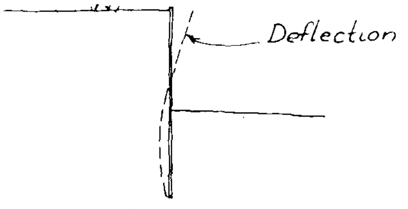

(a) Cantilever sheet pile wall

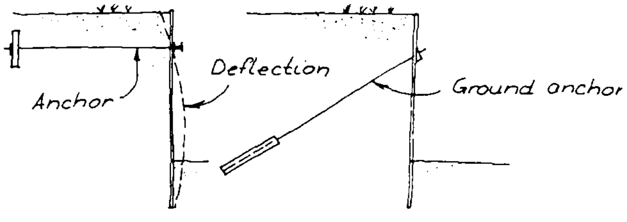

(b) Anchored sheet pile wall

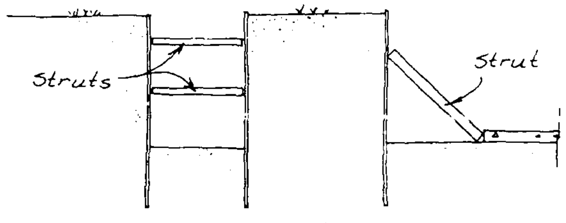

(c) Strutted sheet pile wall.

Fig 2 Support systems

The anchors or the struts can either be horizontal or inclined. In narrow deep cuts horizontal struts are used while in large and wide excavations the struts are often inclined. The inclined struts are generally supported at the bottom of the excavation by a concrete slab or by separate individual concrete footings. It should be observed that the inclined struts or anchors will cause an axial force in the sheet piles which affects the stability of the wall.

A number of different ground anchor systems using bars, wires or strands have been developed during the last 20 years as described by e.g. Hanna (1982). A relatively high pressure is often used in sand or silt for the grouting of the tendons in order to enlarge the hole so that a bulb is formed around the tendons within the grouted section, the fixed anchor length. The tube-à-manchette method can be used especially in sand, gravel and rock to control the grouting. The bore hole can be enlarged mechanically in stiff clay, using a special cutting device in order to increase the tensile resistance of the ground anchors. Also, H-beams have been used as ground anchors in Sweden in very soft clay. The pull-out resistance is high due to the large surface area.

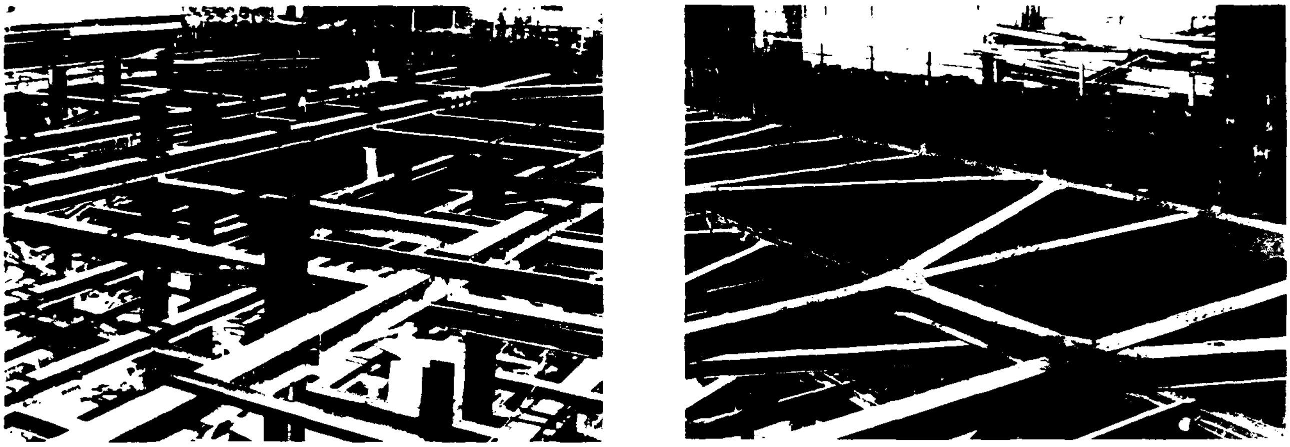

Fig 3 Braced sheet pile wall

Rods (bars) are normally used when the load in the anchors is relatively low, less than about 400 kN, while cables (wires or strands) are utilised as tendons when the load exceeds about 400 kN. The anchor rod or wires are often prestressed in order to reduce the horizontal displacements and the deformations of the wall and thus the settlements during the excavation. Ground anchors are mainly used for temporary structures because of the risk of corrosion of the tendons or of the anchor rods. The corrosion can be reduced for permanent anchors by enclosing the tendons and by introducing a fluid between the covering and the tendons. Also cathodic protection can be used.

A recent development is expander bodies. This new type of anchor consists in principle of a folded thin steel sheet, which can inflated in-situ through the injection of cement grout as shown in Fig 4 (Broms, 1987). The expander bodies can either be driven into the soil or placed in predrilled cased holes depending on the soil conditions. The volume of the grout required for the expansion and the pressure should be measured in order to check the ultimate resistance. The maximum grout pressure in granular soil is 3 to 4 MPa. The main advantage with this new type of ground anchor is that the size and the shape of the anchors are controlled.

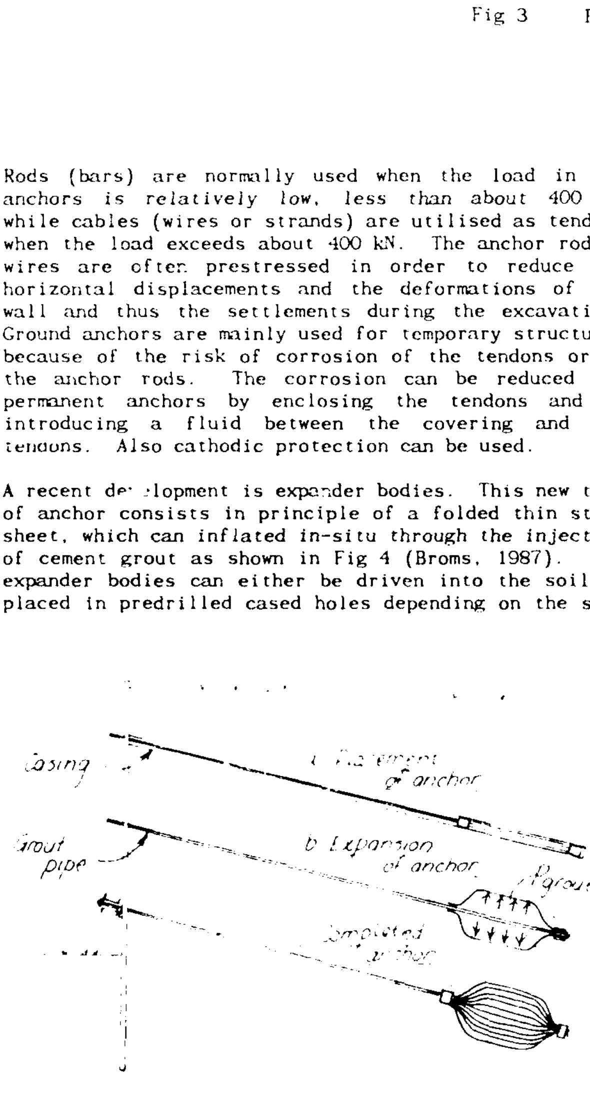

Fig 4 Expander bodies

In Sweden, the Lindö and the JB methods where the casing is provided with a sacrificial drilling bit are used for the drilling of the boreholes. Also different eccentric drilling methods have been developed e.g. Odex, Exier and Alvik to facilitate the installation of the casing and to reduce the costs. An additional method is the In-Situ Anchoring Method where the anchor rods are used as drill rods during the drilling of the boreholes. Casing is not required. However, the allowable load is relatively low for this type of anchor and the method is therefore relatively expensive.

The chosen method of installation of the struts and of the anchors affects both the total lateral earth pressure as well as the earth pressure distribution. When relatively stiff struts are used, the lateral earth pressure can be considerably higher than the active Rankine earth pressure particularly close to the ground surface while at the toe the lateral earth pressure can be lower than the active Rankine earth pressure. The reason for this difference is the relatively small lateral deflection of the sheet pile wall close to the ground surface during the construction since the struts are normally wedged and preloaded.

A certain small lateral deflection is required to mobilize the shear strength of the soil behind the wall and to reduce the lateral earth pressure. In dense sand a lateral displacements of 0.05% of the depth of the excavation is normally sufficient to reduce the lateral earth pressure to the active Rankine earth pressure. When the sand is loose the required lateral deflection is approximately 0.2% of the depth. A much larger deformation is required in soft clay

DESIGN PRINCIPLES

The following four steps are normally followed in the design of a sheet pile wall :

- Evaluation of the magnitude and the distribution of the lateral earth pressure behind the sheet pile wall
- Calculation of the required penetration depth
- Determination of the moment distribution in the sheet piles
- Estimation of the axial force in the ground anchors or in the struts

Extensive investigations are normally required in the field and in the laboratory to determine the depth and the thickness of the different soil strata and of the underlying rock as well as their strength and deformation properties as indicated, for example, in the British Code of Practice (CP2001). Penetration tests are mainly used in cohesionless soils (sand and gravel) in order to estimate the relative density, the angle of internal friction and unit weight. Cone penetration tests (CPT) and weight soundings (WST) are preferred before the standard penetration test (SPT) because of the uncertainties connected with this testing method. However, representative samples are obtained with SPT so that the soil can be classified. The size and the shape of the soil particle are important as well as the gradation since these parameters affect the friction angle of the soil.

The driving of the sheet piles are affected by stones and boulders in the soil. The stone and boulder content of the different strata and the difficulties that may be encountered during the driving of the sheet piles can normally be evalauted from weight (WST) or ram soundings (DP) or from cone penetration tests (CPT). Driving tests with full size sheet piles may be required for large jobs. Stress wave measurements can be helpful to determine the driving resistance and the efficiency of the driving. It is also important to determine the location and possible variations of the ground water level.

For anchored or strutted walls the depth of any soft clay or silt layers below the bottom of the excavation and the variation of the thickness of these layers are particularly important since the stability of the wall depends to a large extent on the passive earth pressure that can develop at the toe of the sheet pile wall. The depth to a firm layer below the bottom of the excavation can usually be determined by penetration tests. Also seismic methods can be used.

Penetration tests especially cone penetration tests (CPT) and weight soundings (WST) are useful in cohesive soils in order to determine the sequence and the thickness of the different layers. The undrained shear strength of the clay is normally evaluated by field vane tests. Undisturbed samples obtained preferably by a thin-walled piston sampler are usually required when the shear strength of the soil is evaluated in the laboratory by, for example, unconfined compression, fall-cone or laboratory vane tests. Undrained triaxial tests are often used to determine the undrained shear strength of stiff fissured clay. The water content, the liquid and plastic limits of the clay should also be measured. Drained triaxial or direct shear tests are required for heavily overconsolidated clays in order to evaluate ϕ_d or ϕ'. The difference between the two angles is usually only a few degrees. An estimate of the long term ground water level and the changes that may occur with time is also necessary. Percussion drilling and coring are normally required in rock. The quality of the rock can often be estimated from the drilling rate. The compressive and tensile strengths can be determined by unconfined compression and or point load tests.

The conditions of the adjacent structures should also be investigated (dilapidation survey). The type of foundation (spread footings, raft or piles) is important since it can affect the choice of support system.

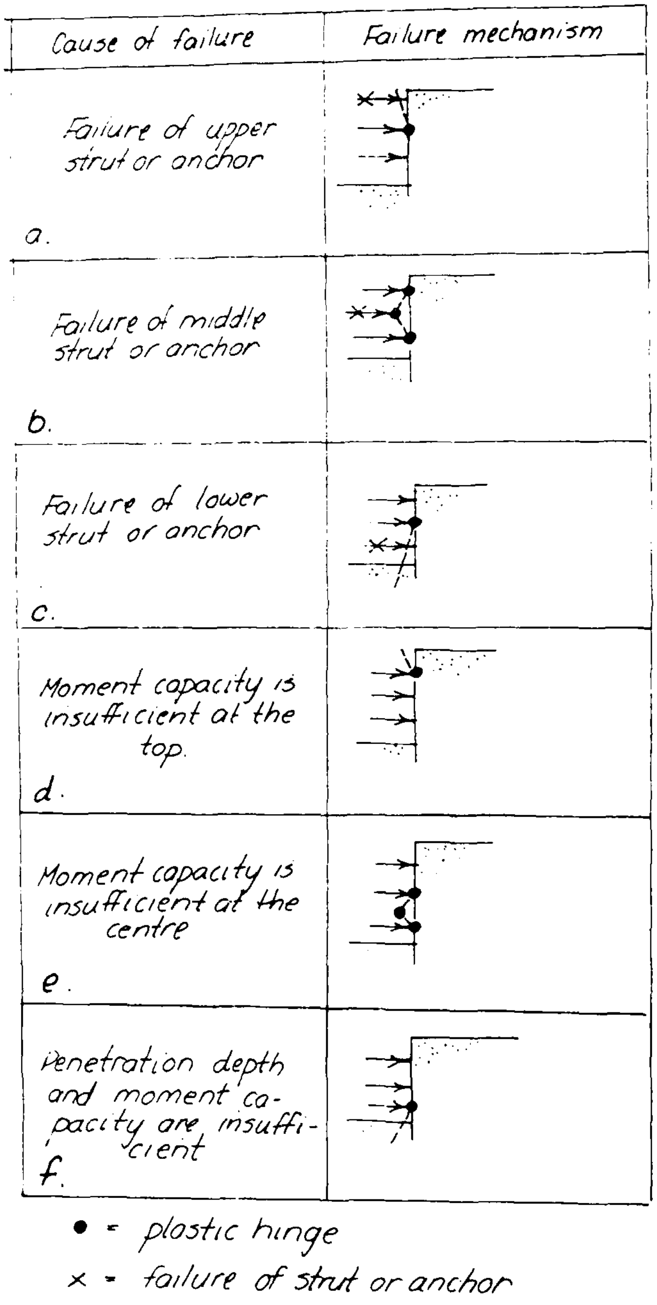
Cause of failure
Failure mechanism
Failure of upper strut or anchor
a.
Failure of middle strut or anchor
b.
Failure of lower strut or anchor
c.
Moment capacity is insufficient at the top.
d.
Moment capacity is insufficient at the centre
e.
Penetration depth and moment capacity are insufficient
f.
● = plastic hinge
× = failure of strut or anchor

Fig 5 Failure mechanisms

In the design of anchored or braced sheet pile walls it is preferable to use characteristic strengths and characteristic loads which takes into account the uncertainties connected with the determination of the shear strength of the soil or of the rock and the loading conditions. A design strength $f_d = f_k/\gamma_m$ is used in the calculation of the lateral earth pressures where f_k is the characteristic strength of the soil or the rock and γ_m is a partial factor of safety larger than 1.0. External loads are treated in a similar way. A design load $F_d = F_k\gamma_f$ where γ_f is a partial coefficient and F_k is the characteristic load, is then used in the calculations of the lateral earth pressures. The probability that the characteristic load will be exceeded in the field should not be greater than 5%. The failure mode or failure mechanism and the deformation required to mobilize the peak resistance of the soil should also be considered when the required partial factor of safety is evaluated as well as cracks and fissures. A statistical analysis of the test results may in some cases be helpful.

A global factor of safety F_s is often used in the design of both anchored and strutted sheet pile walls. A value of 1.5 on F_s is often chosen for clays with respect to the required penetration depth in order to prevent failure by rotation of the sheet pile wall about the anchor level. For cohesionless soils a global factor of safety of 2.0 is normally required.

LATERAL EARTH PRESSURE

Possible failure mechanisms of anchored or strutted sheet pile walls supported at several levels are shown in Fig 5. Failure may occur when the anchors or struts rupture or buckle (Figs 5a, 5b or 5c) or when the moment capacity of the wall has been exceeded (5d, 5e or 5f). The deformations of the sheet piles during the excavation affect both the magnitude and the distribution of the lateral earth pressure behind the wall. The lateral earth pressure can be considerably lower than the active Rankine earth pressure between the support levels due to arching when the lateral deflections of the wall are large. At the strut or anchor levels the lateral earth pressure can be considerably higher that the active Rankine earth pressure as pointed out by e.g. Rowe (1957).

The earth pressure distribution for temporary structures in clay is shown in Fig 6. This distribution is in principle the same as that proposed by Terzaghi and Peck (1967). A trapezoidal earth pressure distribution can be used in the calculation of the force in the anchors and in the struts as well as of the required penetration depth. The lateral earth pressure is assumed to be $[\rho H - 4c_u]$ above the bottom of the excavation when the depth of the excavation exceeds $4c_u/\rho$ and $0.35\rho H$ when the depth is less than $4c_u/\rho$.

Below the bottom of the excavation the net pressure, the difference in the lateral earth pressure on both sides of the wall is $(\rho H - N_{cb}c_u)$ where N_{cb} is the bearing capacity factor of the soil with respect to bottom heave. This factor depends on the dimensions of the excavation (depth, width and length). The net pressure will be negative and contribute to the stability when $\rho H < N_{cb}c_u$ and positive when $\rho H > N_{cb}c_u$.

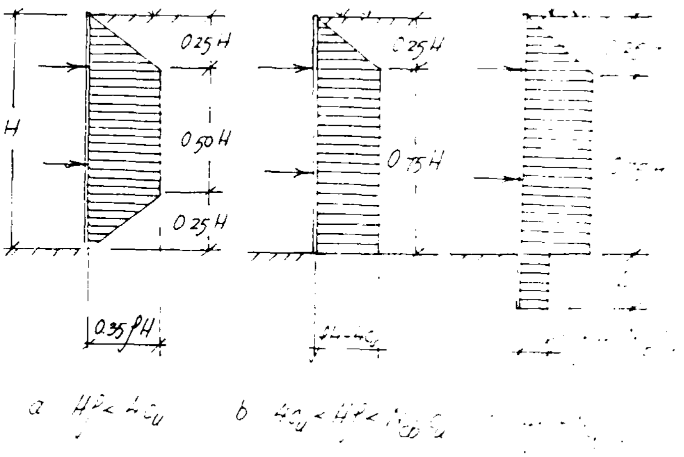

Fig 6 Design of anchored and braced sheet pile walls in soft clay

It is proposed to use the net pressure below the bottom of the excavation at the design instead of the coefficient m as proposed by Terzaghi and Peck (1967) to take into account the increase of the strut or anchor loads when the shear strength of the clay is low below the bottom of the excavation compared with the total overburden pressure. A similar calculation method has been proposed by Aas (1984) and by Karlsrud (1986).

It has been assumed in the calculation of the net earth pressure that the adhesion (c_a) along the sheet piles corresponds to the undrained shear strength of the clay (c_u). The bearing capacity factor N_{cb} will be reduced when $c_a < c_u$. For an infinitely long excavation $N_{cb} = 4c_u$ when $c_a = 0$, a reduction by about 30%.

A relatively large lateral deflection is required to develop the passive lateral earth pressure in front of the wall and thus the net pressure when the shear strength of the clay is low. Adjacent buildings can be damaged by the resulting large settlements. It may therefore be advisable for soft clay to use a lower lateral earth pressure than the net pressure in the calculation of the required penetration depth.

The total lateral earth pressure when the depth of the excavation is less than the critical depth $4c_u/\rho$ corresponds approximately to the lateral earth pressure at rest ($K_0 \approx 0.7$ to 0.8). This earth pressure may be used in the design of permanent structures in soft clay. The preload in the anchors and in the struts should preferably be adjusted periodically especially in soft clay to compensate for creep and consolidation of the soil behind the wall.

In a heavily overconsolidated clay it is important that the lateral earth pressure is sufficiently high close to the ground surface to eliminate any tensile stresses in the soil and to prevent cracking of the clay. Vertical tensile cracks may reduce the shear strength of the clay and increase the lateral pressure when the cracks are filled with water after a heavy rainstorm.

BOTTOM HEAVE

In the design of a strutted or anchored sheet pile walls in soft clay, failure by bottom heave had to be considered as *illustrated in Fig 7*. The *part of the* sheet piles that extends below the bottom of the excavation in Fig 7a must resist a lateral earth pressure that depends on the depth of the excavation and on the undrained shear strength of the clay.

It is proposed to use the net earth pressure as shown in Fig 6 for the part of the sheet pile wall that extends below the lowest strut level. This part of the wall functions as a cantilever which carries the load caused by the lateral earth pressure behind the sheet piles. This load is partly resisted by the passive earth pressure between the two sheet pile walls.

The passive earth pressure is affected by the distance (B) between the two walls. If this distance is less than approximately the penetration depth (D) then the passive earth pressure at the bottom of the sheet piles can be evaluated from the *relationship*

$$\sigma_p = 2\,c_u + D\rho + 2\,c_u D/B \qquad (1)$$

When the distance B between the sheet piles exceeds the penetration depth D (B>D) it is proposed to evaluate the passive earth pressure from the following relationship (Janbu, 1972)

$$\sigma_p = 2c_u\sqrt{1 + \beta} + D\rho \qquad (2)$$

where $\beta = c_a/c_u$. It should be noticed that the passive undrained shear strength as determined from triaxial extension tests should be used in the calculations. This shear strength may be lower than that determined by e.g. field vane tests.

A load factor equal to 1.0 has been used with respect to the unit weight of the soil and the water. In the soft clay below the bottom of the excavation the net lateral pressure is $[\gamma_f q + \rho H_1 - \rho_w H_w - N_{cb} c_u/\gamma_m]$ where N_{cb} is the stability factor with respect to bottom heave (Fig 8). In the intermediate sand layer the net pressure will be positive and contribute to the stability of the wall. The lateral earth pressure will to a large extent depend on the pore water pressure in this layer.

A 2.0 m thick unreinforced concrete slab will be cast below water at the bottom after excavation down to the required depth to prevent heaving when the water level in the excavation is lowered.

If the adhesion (c_a) *along the sheet piles corresponds* to the undrained shear strength (c_u) of the clay, then

$$\sigma_p = 2.83\,c_u + D\rho \qquad (3)$$

When the penetration depth is large compared with the width B, the passive pressure between the two rows will normally be larger than the outside earth pressure and the sheet piles will be supported at least partly by the passive earth pressure between the two walls.

The uplift pressure at the bottom of the sheet pile wall depends on the depth of the excavation H, the penetration depth D, the undrained shear strength of the clay as well as on the shape of the excavation (B/L). The uplift pressure at the bottom of the sheet piles (Fig 7b) can be evaluated from the equation

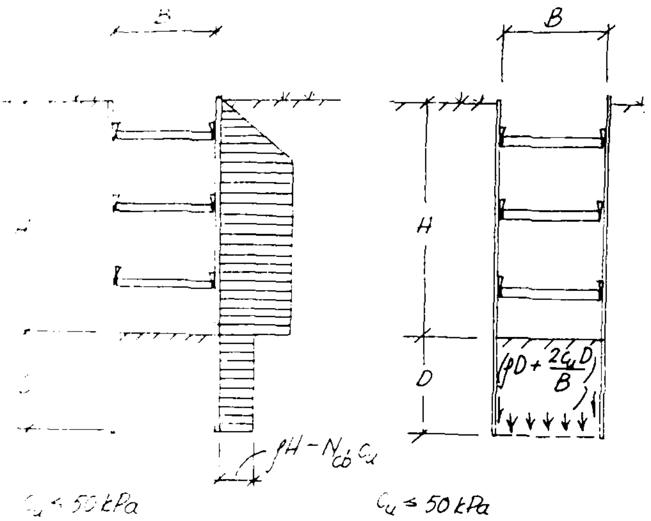

a Earth pressure distribution

b. Bottom heave

Fig 7 Design of braced sheet pile walls in soft clay

$$\sigma_u = (H + D)\,\rho - N_{cb}\,c_u \qquad (4)$$

where N_{cb} is a stability factor (Fig 8) which can be determined from the following relationships (Bjerrum and Eide, 1956).

$$N_{cb} = 5\,(1 + 0.2\,H/B)\,(1 + 0.2\,B/L) \qquad (5)$$

when $H/B \leq 2.5$ and from

$$N_{cb} = 7.5\,(1 + 0.2\,B/L) \qquad (6)$$

when $H/B > 2.5$.

This uplift pressure had to be resisted by the weight of the soil below the bottom of the excavation and by the adhesion c_a of the clay along the sheet piles.

$$\sigma_u = D\rho + 2c_a D/B \qquad (7)$$

In the calculation of the required penetration depth is is advantageous to use load factors (γ_f) and partial safety factors (γ_m) as mentioned previously.

The proposed design method is illustrated in Fig 9a for a braced sheet pile wall. The sheet piles have been driven through soft marine clay (Upper Marine Clay, M) into an underlying intermediate layer with sand (F1). Below this intermediate layer is a second layer with soft marine clay (Lower Marine Clay, M). The shear strength of the clay is low.

It is anticipated that the excavation of the fill and the soft clay will be carried out below water in order to prevent failure of the excavation by bottom heave

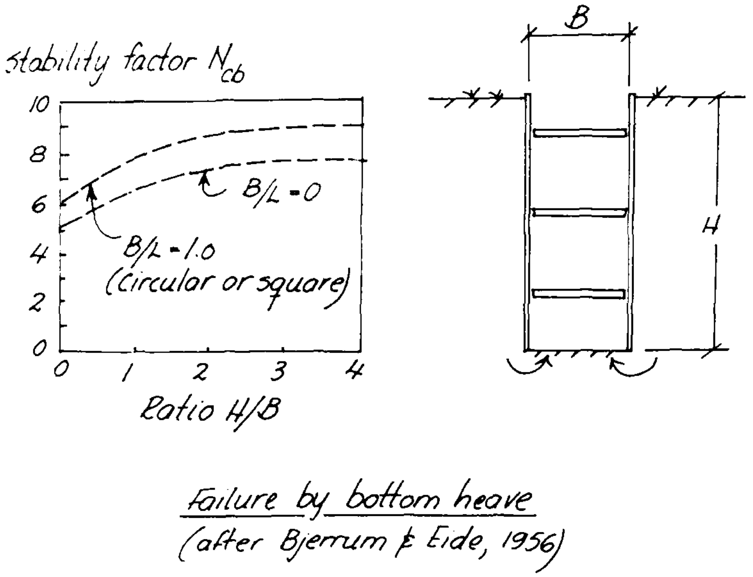

Fig 8 Stability factor N_{cb}

due to the very low shear strength of the clay. The water level in the excavations will be kept at or above the ground level in order to increase the stability of the excavation. Bored piles are used to support the bottom slab. The piles will be installed before the start of the excavation and provided with a permanent casing to prevent necking of the concrete during the casting because of the low shear strength of the clay.

The earth pressure distribution when the excavation has reached the maximum depth is shown in Fig 9a. The lateral earth pressure above the bottom of the excavation corresponds to $[\gamma_f q + \rho H_1 - 4c_u/\gamma_m]$ where γ_f is a load factor and γ_m is a partial factor of safety. The uplift pressure on the concrete slab will vary. A higher uplift pressure (q_1) is expected on the slab next to the two sheet pile walls compared with that (q_3) at the center of the slab as shown in Fig 9b and Fig 9c, respectively.

The uplift pressure q_1 in Fig 9b depends on the total overburden pressure $(\gamma_f q + \rho H_1)$ outside the sheet pile wall at the level of the concrete slab, on the lateral resistance of the sheet piles q_2, on the shear strength

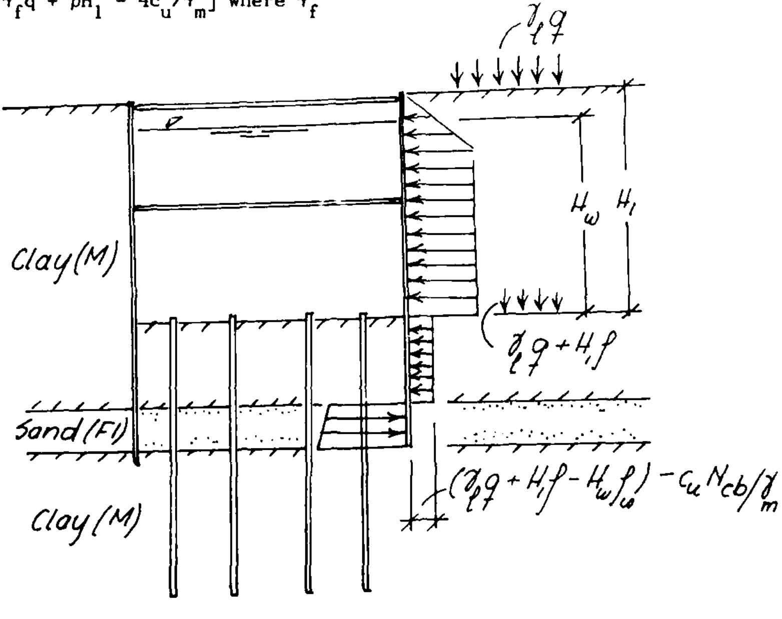

Fig 9a Proposed design method for a strutted sheet pile wall in soft clay

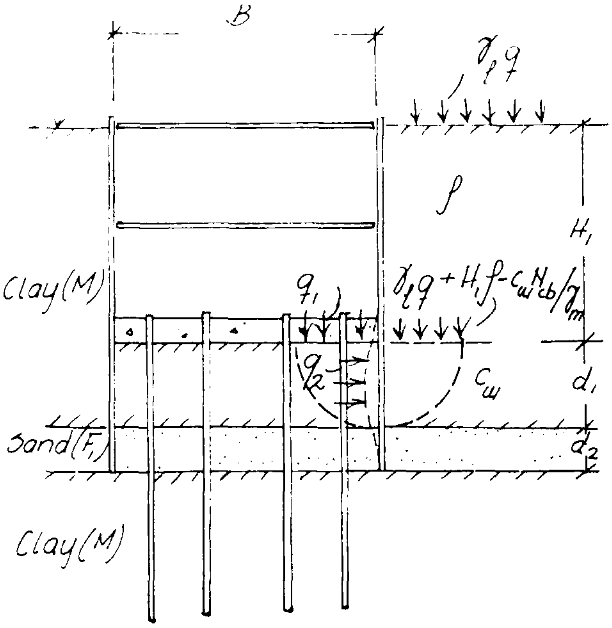

Fig 9b Bottom heave (upper clay layer)

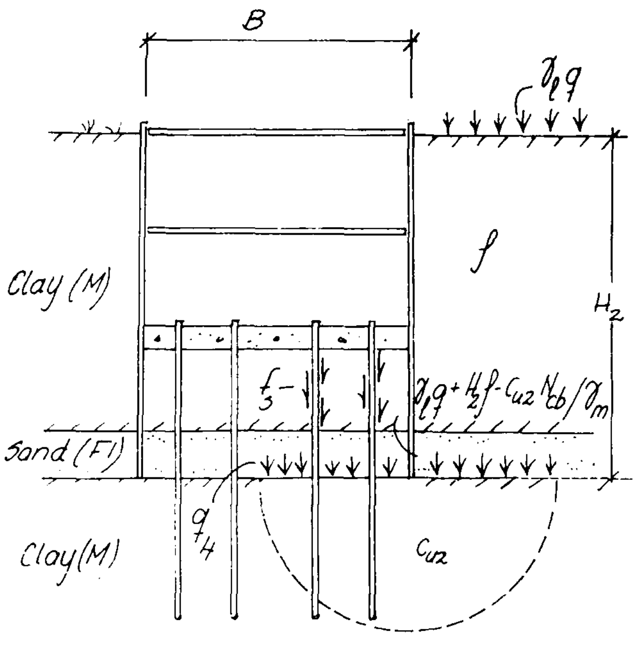

Fig 9c Bottom heave (lower clay layer)

of the clay c_{u1} and on the stability factor N_{cb}. This uplift pressure will act on a strip with a width that corresponds to the depth of the clay layer below the concrete slab.

The stability number for the excavation (D/L = 0.58) is 5.9 when the excavation is long compared with the width (B/L = 0) as can be seen from Fig 7. However, a relatively large deformation will be required to mobilize the average shear strength of the clay. A partial factor of safety of about 1.4 is required to limit the maximum wall movement to 1% of the excavation depth (Mana and Clough, 1981).

The uplift pressure within the center part of the excavation can be estimated as shown in Fig 9c. This uplift pressure q_3 will be lower than that next to the two sheet pile walls (q_1) because of the relatively high shear strength or the lower marine clay (c_{u2}). The overburden pressure at the bottom of the fluvial material F1 depends on the average unit weight of the soil above this layer.

The confining pressure q_4 below the bottom of the intermediate layer (F1) at the centre of the excavation can be estimated from the equation.

$$q_4 = q_3 + d_1\gamma_1 + d_2\gamma_2 + \Sigma Q_s/B \quad (8)$$

where ΣQ_s is the total skin friction resistance per unit length along the sheet piles and the piles in the marine clay and in the F1 material (f_{s1} and f_{s2}, respectively) and B is the total width of the excavation. The adhesion (c_a) along the sheet piles and the piles in the soft clay is estimated to $0.8c_u$, where c_u is the undrained shear strength as determined by e.g. field vane tests. It is suggested that the unit skin friction resistance in the sand (F1) can be taken as 1% of q_c, where q_c is the cone resistance as determined by cone penetration tests (CPT). It has thus been assumed that the total skin friction resistance along the piles and the sheet piles can be distributed uniformly over the total width of the excavation.

SHEET PILE WALLS SUPPORTED BY INCLINED ANCHORS

An anchored sheet pile walls may fail when the vertical bearing capacity of the sheet piles is exceeded as illustrated in Fig 10 in the case the anchors are inclined. The inclined anchors produce a vertical force in the sheet piles which may cause the sheet piles to settle if the embedment depth is not sufficient. A settlement (δ_v) will also cause the wall to move outwards (δ_h) a distance δ_v tan α where α is the inclination of the anchor rods or of the cables at the level of the anchor (Fig 10). The inclination of soil anchors in soil is often 20 degrees while for rock anchors the inclination is normally 45 degrees. The inclination can be increased in order to reduce the length of the anchor rods or of the cables and thus the cost. The vertical component of the anchor force along the sheet piles is, therefore, often higher when the sheet piles have been driven into rock compared with

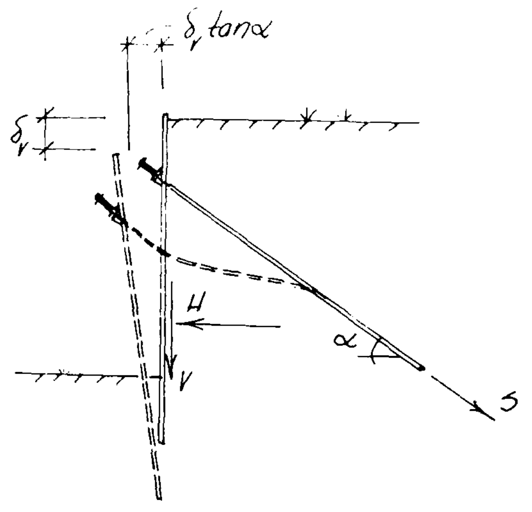

a. Failure mechanism

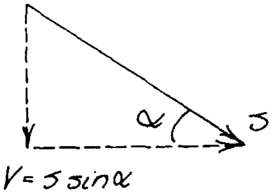

b. Force polygon.

Fig 10 Vertical stability of sheet pile wall with inclined anchors

soil anchors because of the difference in inclination of the tendons. The sheet piles can generally be driven to a higher resistance when competent rock is located close to the bottom of the excavation and rock anchors are used. It is then relatively easy to resist the high vertical force in the sheet piles.

When the depth to rock or to a layer with a high bearing capacity is relatively large and soil anchors had to be used then it is difficult to resist the vertical component of the anchor force by adhesion or by friction along the sheet piles. It may then be more economical to reduce the inclination of the anchors and to increase the length of the anchor rods or of the cables. Then the length of the sheet piles can be reduced because of the reduced axial force.

Figs 11a and 11b illustrate the forces acting on a braced and anchored sheet pile walls in clay, respectively. The normal force N and the shear force T (T is proportional to the active undrained shear strength of the soil c_u) act along the assumed failure plane. The weight (W) of the sliding soil wedge is approximately the same for the two cases. The force (C_a) along the sheet piles depends on the adhesion (c_a) between the sheet piles and the clay below the bottom of the excavation. The inclination and the magnitude of the force (R) in the anchors or in the struts will, however, be different.

It can be seen from the two force diagrams in Fig 11 that both the normal force N on the failure plane and the passive earth pressure force P_p which are required for equilibrium will be larger for an anchored sheet pile wall when the anchors are inclined than for a braced or a strutted wall when the struts are horizontal. Thus a larger penetration depth and a higher passive earth pressure will be required for an anchored wall where the tendons are inclined compared with a braced wall.

The stability of an anchored sheet pile wall can be expressed by the stability factor N_{cb} defined by the

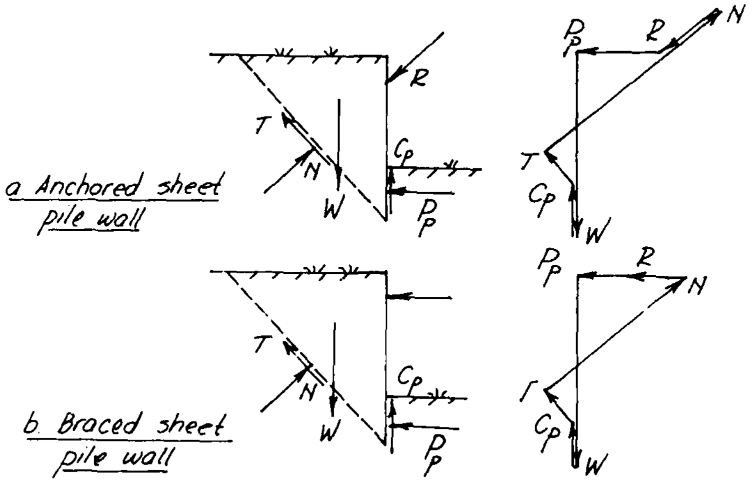

a Anchored sheet pile wall

b Braced sheet pile wall

Fig 11 Stability of anchored and braced sheet pile walls

equation $(\rho H_{cr} + \gamma_f q) = N_{cb}\, c_u/\gamma_m$ where $(\rho H_{cr} + \gamma_f q)$ is the total overburden pressure at the bottom of the excavation H_{cr} is the critical depth and c_u is the undrained characteristic shear strength of the clay. The total overburden pressure depends on the critical depth of the excavation H_{cr} (the maximum depth when the excavation is still stable), the unit weight of the soil ρ and on the surcharge load q.

The stability factor N_{cb} as shown in Fig 12 is a function of the inclination of the anchors (α), the penetration depth (D) of the sheet piles below the bottom of the excavation and the adhesion (c_a) between the sheet piles and the clay. At $\beta_p = 1.0$ the adhesion corresponds to the undrained shear strength of the soil c_u. At $\beta_p = 0$ the adhesion is equal to zero. It can be seen from Fig 12 that the stability factor N_{cb} increases with increasing value on β_p and with increasing force R in the anchors until a critical value has been reached. If this critical value is exceeded then N_{cb} will decrease.

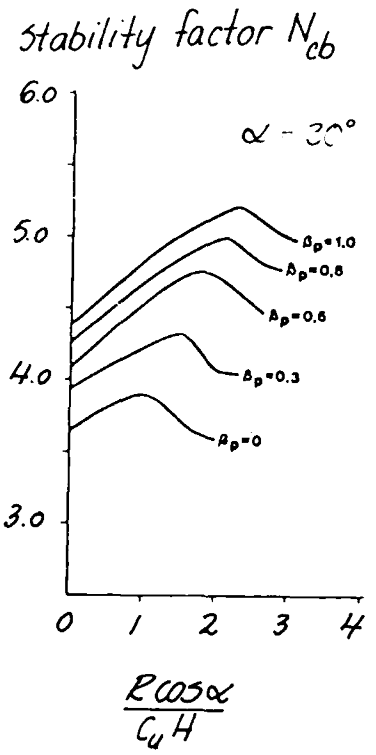

Fig 12 Stability Factor N_{cb}

In order to simplify the calculations Sahlstrom and Stille (1979) have proposed for soft normally consolidated clay that the stability factor N_{cb} should be taken as 5.1 when the sheet piles are driven to a hard stratum so that the end bearing capacity of the sheet piles will be sufficient to resist the axial force caused by the inclined anchors. In the case the sheet piles have not been driven to refusal in a hard layer and the vertical stability of the wall is low then a value on N_{cb} of 4.1 should be used in the calculations.

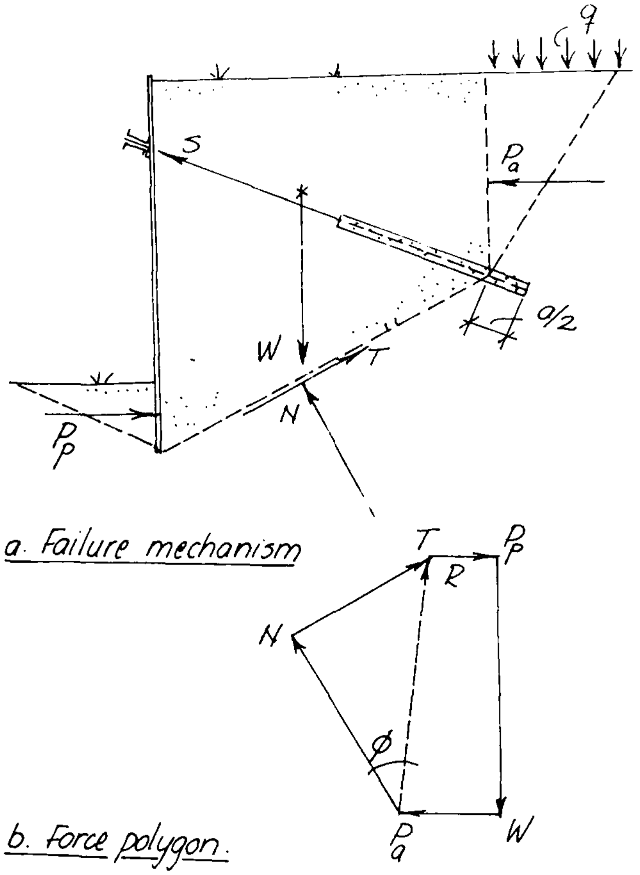

a. Failure mechanism

b. Force polygon.

Fig 13 Total stability of an anchored sheet pile wall

The stability may be reduced especially in silty clays when piles have been driven close to an existing sheet pile wall due to the remoulding of the soil and the resulting increase of the pore water pressures that take place during the driving. In this case a value equal to 3.6 on N_{cb} can be used.

In most cases failure takes place in the undisturbed soil between the flanges ($\beta_p = 1.0$) of the sheet piles since the perimeter area is large. Usually a layer of clay will cling to the surface and come up together with the sheet piles when they are pulled.

The length of the anchors should be sufficient so that the stability of the sheet pile wall will be adequate with respect to a deep-seated failure. In Fig 13 is shown the forces acting on an anchored sheet pile wall in a cohesionless soil and the corresponding force diagram. The rear face of the indicated sliding wedge had to resist the lateral earth pressure P_a. The required passive earth pressure $P_{p'req}$ at equilibrium can be determined as shown in Fig 13 (Broms, 1968) which is a modification of the Kranz method which is widely used in Germany and Austria. It has been assumed in the analysis that the critical failure surface is located (a/2) from the end of the anchors, where a is the spacing of the anchors. It has thus been assumed that the inclination of the failure surface behind the anchors is ($45^{o} + 1/2\ \phi'$). The main advantage with the proposed calculation method is its simplicity.

It is also necesary to check the stability of the wedge located above the fixed anchor length as illustrated in Fig 14. The failure surface has been assumed to extend a distance (a/2) from the end of the anchor block as shown. The passive resistance of the soil in front of the sliding soil wedge should be sufficient to resist the lateral displacement of the wedge. It is proposed to use partial safety factors and load factors in the calculations.

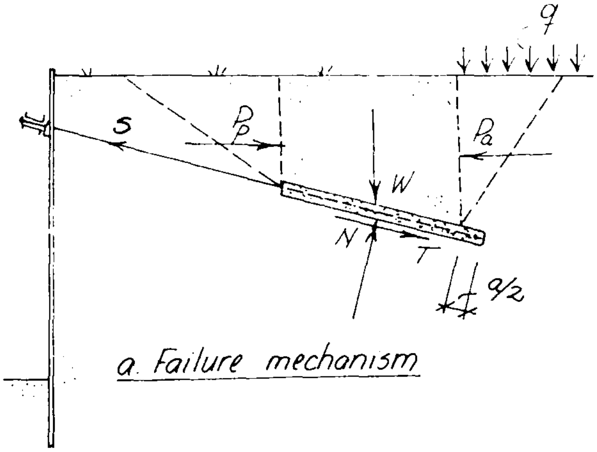

a. Failure mechanism

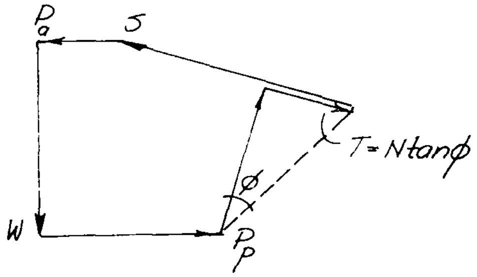

b. Force polygon.

Fig 14 Stability of anchor block

STRENGTH OF ANCHORS

The design of ground anchors has been reviewed by Littlejohn (1970). The method that can be used to calculate the tensile resistance of soil anchors is illustrated in Fig 15. The ultimate tensile resistance Q_{ult} depends on the friction resistance Q_{skin} along the grouted part of the anchor and on the end resistance Q_{end} as expressed by the relationship

$$Q_{ult} = Q_{skin} + Q_{end} \tag{9}$$

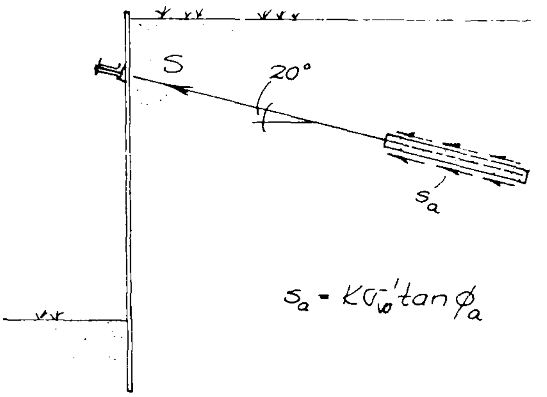

Fig 15 Tensile resistance of ground anchors

The displacement required to develop the maximum skin friction is small, a few mm, compared with the relative large displacement which is required to mobilize the end resistance.

In cohesionless soils (sand and gravel) the pull-out resistance (s_a) depends on the effective overburden pressure σ'_{vo} and on the friction angle ϕ'_a between grouted part of the anchors and the soil as expressed by the equation

$$s_a = K\sigma'_{vo} \tan \phi'_a \tag{10}$$

The friction angle ϕ'_a is normally assumed to correspond to the angle of internal friction of the soil ϕ' or ϕ_d. The coefficient K depends mainly on the relative density of the soil. This coefficient can for dense, coarse and wellgraded sand or gravel be as high as 2 to 3 due to the dilatancy of the soil. In loose fine sand and silt the coefficient K can be as low as 0.5. The assumed value on K should be verified by load tests.

The tensile resistance can also be estimated from the grout pressure used during the installation of the anchors, from the grout pressure required for the expansion of the expander bodies or from the penetration resistance as determined by e.g. cone penetration tests (CPT), standard penetration tests (SPT) or weight soundings (WST).

It is proposed to use the equations suggested by Baquelin et al (1978) for bored piles to estimate the pull-out resistance from the maximum grout pressure (p_{grout}). The tensile resistance of the anchors increases generally with increasing grout pressure especially in hard rock and in dense sand and gravel. The capacity of the anchors will also increase with increasing length of the grouted zone, the fixed anchor length. In sand and gravel there is, however, a maximum effective length. If this effective length is exceeded then there is no further increase of the anchor force. The critical length is about 6 m for sand and gravel. Cyclic loading will, however, reduce this length. The fixed anchor length is usually 3 to 6 m.

According to Baguelin et al (1978) the net base resistance of a bored pile q_{end} can be evaluated from the limit pressure p_ℓ determined from pressuremeter tests

$$q_{end} = k\,(p_\ell - p_o) \qquad (11)$$

where p_o is the initial total horizontal pressure in the ground at the base of the pile and k is a coefficient that depends on the embedment length and on the magnitude of the limit pressure.

It is expected, however, that the limit pressure will correspond to the maximum grout pressure.

$$p_\ell = p_{grout} + z\,\rho_{grout} \qquad (12)$$

where p_{grout} is the grout pressure at the ground surface, ρ_{grout} is the unit weight of the grout and z is the depth.

For the case the tensile resistance corresponds to 70% of the ultimate bearing capacity of a bored pile then the end resistance of the anchors can be calculated from the equation

$$Q_{end} = 0.7\,k\,p_{grout}\,A_{end} \qquad (13)$$

where k is a coefficient that depends on the embedment length and on the magnitude of the limit pressure and A_{end} is the cross-sectional area.

The unit skin friction resistance f_s of a pile in sand or gravel will normally be 0.5% to 2% of the point resistance (Meyerhof, 1956). The skin friction will generally increase with decreasing particle size and increasing cone resistance. It is suggested for sand and gravel that the skin friction resistance should be taken as 1% of the unit end resistance. For silt 2% is proposed.

The total skin friction resistance Q_{skin} of the expander bodies will be 12% of the total end resistance for sand and gravel and 24% for silt. Then for sand and gravel

$$Q_{ult} = 0.78\,k\,p_{grout}\,A_{end} \qquad (14)$$

where k is a bearing capaicty factor which depends on the embedment depth. For silt

$$Q_{ult} = 1.24\,Q_{end} = 0.86\,k\,p_{grout}\,A_{end} \qquad (15)$$

The ultimate pull-out resistance of the expander bodies as determined by Equs (14) and (15) has been plotted in Fig 16 as a function of the maximum grout pressure. It can be seen that the tensile resistance increases rapidly with increasing grout pressure. It should be observed that the depth of the expander bodies should be at least eight times the diameter. Otherwise the resistance will be reduced.

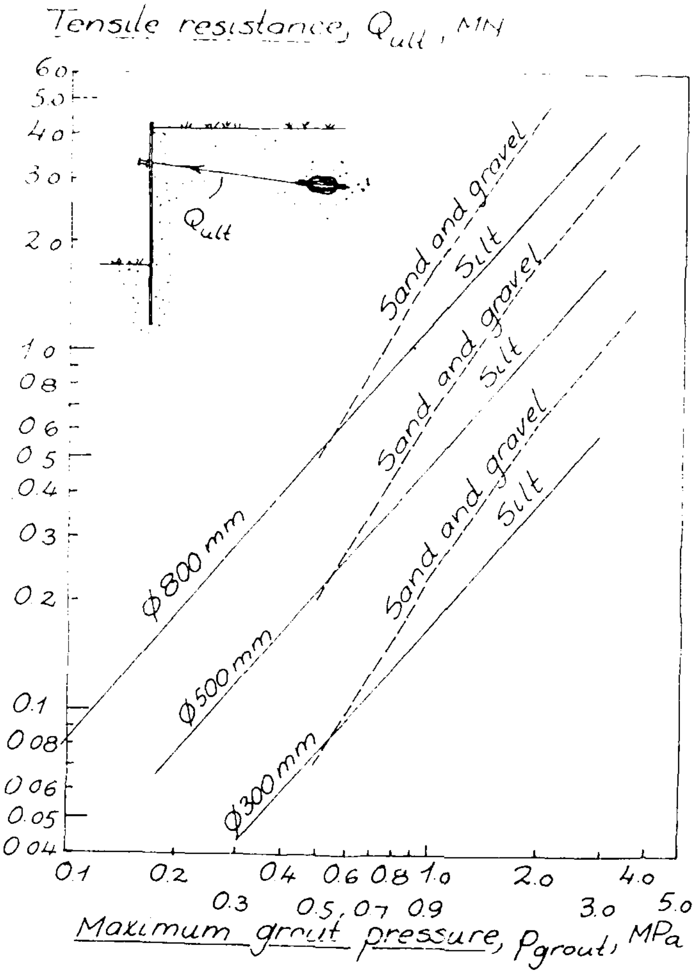

Fig 16 Pull-out resistance of Expander Bodies

The tensile resistance can also be calculated from the penetration resistance of different penetration tests such as cone penetration tests (CPT) standard penetration tests (SPT) and weight soundings (WST). A comparison between the different penetration tests is shown in Table I for cohesionless soils (silt, sand and gravel). For example, a standard penetration resistance (N_{30}) of 30 blows/0.30 m in a medium sand corresponds a cone penetration resistance of about 10 MPa. It should be noted that the results are affected, for example, by the particle size, the depth below the ground surface and the location of the ground water level. For silt, sand and gravel the cone penetration resistance in MPa is approximately 0.2 N_{30}, 0.4 N_{30} and 0.6 N_{30}, respectively.

However, the result from the weight soundings are at large depths (> 10 m) influenced by the friction along the sounding rod since a casing is not used, while at SPT the results are affected by the method used to lift and to release the hammer. The energy delivered by a free falling hammer is considerably higher than that when the rope and pulley method is used.

Load tests indicate that the end bearing capacity corresponds closely to the cone penetration resistance (CPT) within a zone that extends one pile diameter below and 3.75 pile diameters above the pile point (van der Veen and Boersma, 1952). In cohesionless soils the tensile resistance will be lower than the end bearing capacity because of the reduction of the over-burden pressure as mentioned above. It is, therefore,

TABLE I

COMPARISON BETWEEN DIFFERENT PENETRATION TESTS

(after Broms and Bergdahl, 1982)

Relative Density	Cone Penetration Tests (CPT), Point Resistance q_s, MPa	Standard Penetration Tests (SPT), Penetration Resistance N_{20}, blows/30 cm	Weigth Sounding Tests, Penetration Resistance N_w, ht/0.2 m
Very loose	< 2.5	< 4	< 4
Loose	2.5 - 5	4 - 10	10 - 30
Medium	5 - 10	10 - 30	30 - 60
Dense	10 - 20	30 - 50	60 - 100
Very dense	> 20	> 50	> 100

suggested that the tensile resistance of soil anchors should be taken as 70% of the bearing capacity of an equivalent pile.

Test data indicate also that the tensile resistance of the expander bodies will decrease with increasing diameter. It is, therefore, suggested that the unit tensile resistance of 0.5 m and 0.8 m diameter expander bodies should be taken as 80% and 50%, respectively of the resistançe of expander bodies with 0.3 m diameter.

The net end resistance in clay can be estimated from

$$q^*_{end} = 9\ c_u \tag{16}$$

when the anchor is located at least four diameters below the ground surface.

Also the skin resistance (c_a) will depend on the undrained shear strength c_u of the clay

$$s_a = \alpha\ c_u \tag{17}$$

where α is a reduction coefficient which decreases with increasing shear strength. It is suggested that α should be taken as 0.8 for soft clays ($c_u \lesssim 50$ kPa) and as 0.5 for medium to stiff clays when $c_u > 50$ kPa.

It should be noted that the tensile resistance will gradually increase with time after the installation due to the reconsolidation of the clay. Particulary the skin friction resistance is affected. About 1 to 3 months will be required in soft clay to reach the maximum resistance while in medium to stiff clay the calculated tensile resistance usually will be obtained within a few weeks. In weathered rock and residual soils a value 0.45 c_u is commonly used. The tensile resistance can be increased further by enlarging the boreholes by underreaming.

The pull-out resistance of ground anchors in rock has been correlated with the unconfined compressive strength. The allowable shear resistance is often taken as 0.1 q_u where q_u is the unconfined compressive strength of small diameter rock cores. The maximum shear resistance is normally limited to 4 MPa. However, the spacing and the orientation of the joint in the rock can have a large influence on the pull-out resistance. The reduction of the shear resistance has been related to the RQD-value of the rock. Failure of rock anchors located close to the ground surface ($D <$ 1.5 m) often occurs when a cone of rock is pulled out together with the anchor rod or the cable. The tensile resistance will in that case correspond to the weight of the rock cone and thus to the unit weight of the rock mass.

SETTLEMENTS AND LATERAL DISPLACEMENTS

Deep excavations in soft clay can cause settlements around the excavation. As a result surrounding buildings can be damaged. The damage can be related to either the angular distortion, the relative deflection (sagging and hogging) or the lateral deformation of the building. Buildings are in general more affected by large relative deflections or by large lateral deformations than by an angular distortion. Structures are also more sensitive to hogging than to sagging. Buildings located close to an excavation are often loaded in compression while buildings located further away are subjected to lateral tension (elongation) and may therefore crack. The location of the building within the settlement trough around an open excavation is thus important.

The lateral displacement of the soil around deep excavations and its effect on nearby buildings has attracted so far relatively little attention. The resulting lateral movement can damage buildings close to the excavation and other structures. A tensile strain of only 0.1% to 0.2% is often sufficient to cause extensive cracking of masonary structures. E.g. O'Rourke (1981) has observed large lateral strains behind an 18 m deep excavation. The resulting lateral displacements were high enough to cause extensive cracking of masonary structures located up to 9 m behind the excavation.

Some settlements will always occur even when the best available construction technique is been used and the soil conditions are favourable. The installation of the top strut is particularly important. When the costs of different methods to reduce settlements are estimated, it is important to consider also the indirect costs e.g. loss of time and business caused by congestion around the site due to the construction. Grouting and freezing require, for example, space for drilling rigs, mixing and refrigeration units, pipes and pumps as well as for storage of various chemicals and aggregates. For a particular job it is important that the total costs including indirect costs should be as low as possible.

The finite element method (FEM) provides an alternative approach to analyze deep excavations with respect to settlements and lateral displacements. This method can handle complicated soil and boundary conditions. The nonlinear behaviour of the soil and of the support system can be considered as well as the construction sequence. Many case records have been reported in the literature where FEM has been used to analyze the results (D'Appolonia, 1971; Clough and Davison, 1977; Burland et al, 1979; Karlsrud et al, 1980; Mana and Clough, 1981 and O'Rourke, 1981). Both braced and anchored excavations have been investigated (Egger, 1972; Clough and Tsui, 1974; Stroh and Breth, 1976, Clough and Mana, 1977 and Clough and Hansen, 1981). These studies show that the settlements and the lateral displacements of sheet pile or diaphragm walls in soft clay are to a large extent affected by the factor of safety with respect to base heave, by the stiffness of the wall, by the support system (ground anchors and struts), by the geometry of the excavation and by the chosen construction method.

Settlements should be measured frequently during the excavation by level surveying and the results should be plotted and evaluated so that remedial measures, if necessary, can be taken in time. Inclinometers can be e.g. used to determine the lateral displacements of sheet pile or of diaphragm walls. There are inclinometers available with a high resolution (1:10,000) so that lateral displacements as small as 1 to 2 mm can be detected. FEM can be helpful to locate the source of the settlements or of the lateral displacements. Lee et al (1986) have recently described the monitoring of a deep excavation in soft clay in Singapore.

The lateral displacements of braced and anchored sheet pile or of diaphragm walls depend to a large extent on the stiffness of the walls. The displacement is often expressed in terms of a stiffness factor $E_s \ell^4 / E_w I_w$ where ℓ is the vertical spacing of the struts or the anchors, E_s and E_w are the moduli of elasticity of the soil and of the wall material respectively, and I_w is the second area of moment of the sheet piles.

Field observations as well as FEA indicate that it is important to place the struts as soon as possible after the excavation has reached the strut level. Frequently the struts are not installed until the excavation had advanced an additional two to three meters. In that case the settlements and the lateral displacements can easily increase 50% to 100%. It is also important that the wale beams are tightly wedged against the sheet piles in order to reduce the settlements. Gaps should be filled with concrete or be shimmed.

The lateral displacements can be reduced by increasing the stiffness of the wall or by decreasing the vertical spacing of the struts or of the anchors E.g. a diaphragm wall can be used instead of sheet piles. Anchors are very effective since they can be placed close to the bottom of the excavation and be preloaded. Raked struts and temporary berms can then be avoided.

One difficulty with FEM is the choice of parameters since they should reflect both the in-situ behaviour of the soil or of the rock as well as the effect of e.g. workmanship and time. It is important to check the calculations at an early stage with field measurements. The design should be reanalyzed using back soil properties if the discrepancy is large.

INSTALLATION OF SHEET PILES

It is often difficult to drive the sheet piles sufficiently deep into the underlying rock in order to provide sufficient lateral resistance so that the high lateral earth pressure behind the wall can be resisted especially when the depth of the excavation is large. This is frequently the case in Sweden where the soft clay often is underlain by unweathered hard granite with a compressive strength of 150 to 200 MPa or more. Steel dowels are often used which are driven into the rock or placed in predrilled holes and grouted in order to increase the lateral resistance of the sheet piles as illustrated in Fig 17a. The drilling is normally done through steel pipes which have been attached to the sheet piles before the driving. The lateral resistance of the steel dowels depends on the strength of the rock and on the dimensions of the dowels. It is also possible to install additional ground anchors close to the bottom of the excavation as shown in Fig 17b to increase the lateral resistance of the sheet piles in order.

Another common case is illustrated in Fig 18a where it has not been possible to drive the sheet piles sufficiently deep because of stones or boulders in the soil which interfere with the driving. Additional anchors may be required at the toe of the sheet piles in order to increase the lateral resistance. However, an additional row of anchors will increase the vertical force in the sheet pile which has to be considered.

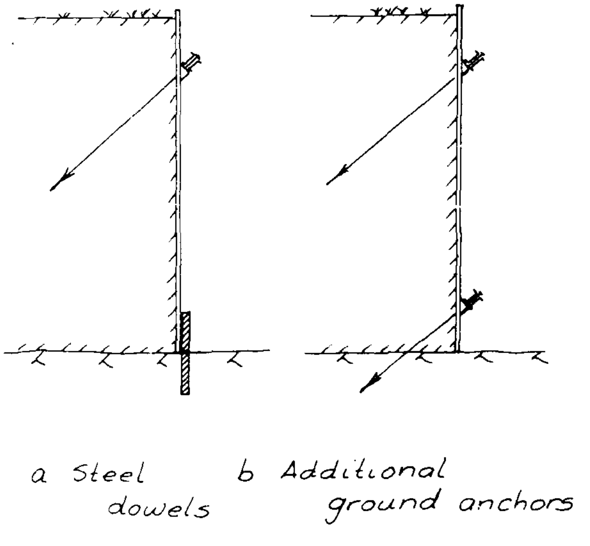
a Steel dowels

b Additional ground anchors

Fig 17 Prevention of toe failure for anchored sheet pile walls

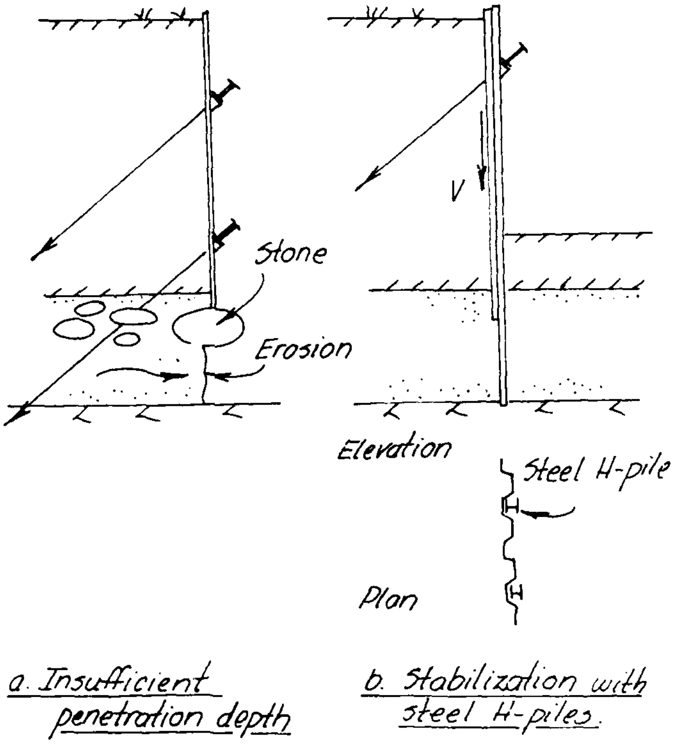

a. Insufficient penetration depth

b. Stabilization with steel H-piles.

Fig 18 Vertical stability of anchored sheet pile walls

Erosion may even occur below the boulders or the stones if the surface of the cut is not protected by, for example, shotcrete. Drain holes will be required to reduce the high water pressure that otherwise may develop behind the shotcrete layer.

Fig 18b illustrates the case when the vertical stability of the sheet pile wall is not sufficient and the vertical force in the sheet piles from the inclined anchors will cause the sheet piles to settle. The vertical stability of the wall can be increased by driving steel H-piles in front of the wall as shown. The H-piles should be welded to the sheet piles so that the vertical force from the anchors can be transferred to the piles. The bearing capacity of the H-piles should be sufficiently high so that they will be able to carry the vertical force.

IMPROVEMENT OF THE STABILITY IN SOFT CLAY

Different methods can be used to increase the stability of braced or anchored sheet pile wall in soft clay as illustrated in Figs 19 through 22. Lime or cement columns have been installed in Fig 19 in front of or between the two rows of sheet piles in order to increase the average shear strenght of the clay and thus the passive resistance of the soil.

The lime or cement columns can also be installed in such a way that they form a series of continuous walls between the two sheet pile walls to keep them apart. The lateral earth pressure acting on the sheet piles below the bottom of the excavation will then be transferred through the walls. In this case, the columns will function as an additional level of struts below the bottom of the excavation. The required spacing of the lime or cement columns depends on the increase of the shear strength that can be obtained with lime (quick lime) or with cement. This can be investigated in the laboratory by mixing the clay with different amounts of lime and cement. The optimum lime content is usually 6% to 10% with respect to the dry unit weight. About 15% to 25% cement is usually required in order to reach the required shear strength of the stabilized soil. Gypsum in combination with quicklime can be beneficial in organic soils.

The columns will increase the average undrained shear strength of the soil. In soft clay the average shear strength can usually be doubled if the 0.5 m diameter lime or cement columns are spaced 1.4 to 1.5 m apart. Lime or cement columns can also be placed behind the sheet piles in order to reduce the lateral earth pressure acting on the wall.

The soil at the ground surface has been excavated in Fig 20 in order to reduce the total overburden pressure at the bottom of the excavation. The reduction of the lateral earth pressure on the wall will be large below the excavation especially when the total overburden pressure at the bottom of the excavation is approximately equal to $N_c c_u$. The excavated soil can be replaced by light weight fill e.g. expanded shale, slag or flyash. In the Scandinavian countries and in Finland sawdust, bark and peat are often used. With slag or flyash, pollution of the ground water might become a problem.

Also jet grouting and quick lime columns can be used to increase the stability as shown in Fig 20 as has been the case in Singapore. At the quicklime column method

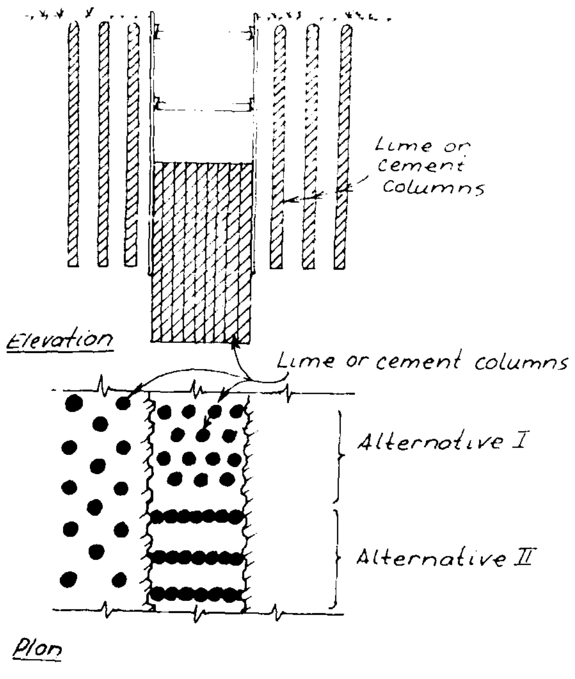

Fig 19 Stabilization with lime or cement columns

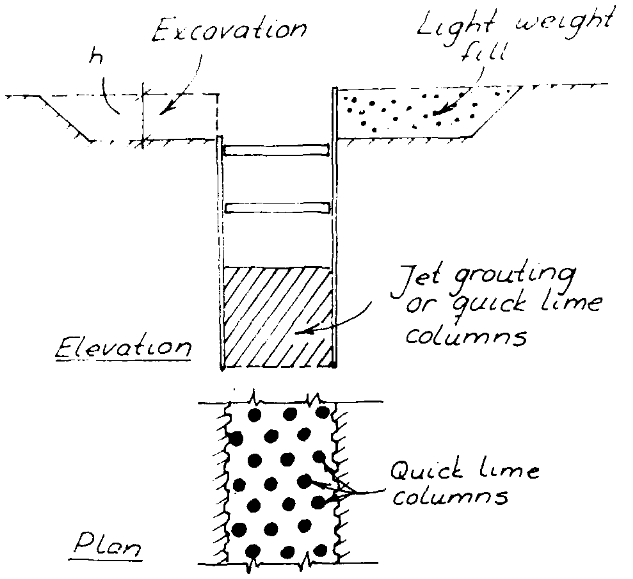

Fig 20 Stabilization with light-weight fill, jet grouting or quicklime columns

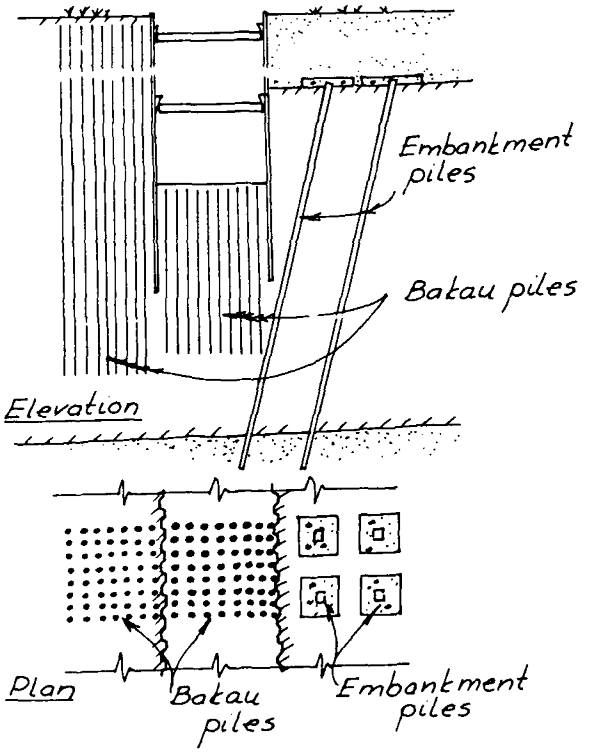

Fig 21 Stabilization with Bakau piles and embankment piles

large diameter holes which are filled with quicklime are used. At this method, the expansion that takes place when the unslaked lime reacts with water is utilized. The method is mainly effective in silty soils with a low plasticity index where a small change of the water content will have a large effect on the shear strength. The effectiveness of the method is, however, reduced when the soil is stratified. Then the expansion of the quicklime columns will occur faster than the consolidation of the soft soil around the columns. As a result, the soil will be displaced and heave rather than consolidate.

Embankment or Bakau piles are used in Fig 21 in order to reduce the lateral earth pressure acting of the sheet pile wall. The piles will carry part of the weight of the clay due to the friction or adhesion along the piles. The efficiency of the embankment piles can be increased if the piles are provided with concrete caps which will transfer the weight of the soil above the caps to the piles. Pile caps are required especially when concrete or steel piles with high bearing capacity are used because of the large length required to transfer the load from the soil to the piles though adhesion or friction along the piles. The transfer length will be large because of the relatively high pile loads which are required in order to make the method economical. Embankment piles are common in Sweden, Finland and Norway particularly in soft clay. Bakau piles are extensively used as embankment piles in Southeast Asia. They have the advantage that the surface area is large, that the transfer length is small and that they are cheap. The diameter is usually 80 to 100 mm. The maximum length is about 6 m. If longer piles are required they had to be spliced.

The stabilizing effect of embankment piles is equivalent to that caused by an increase of the unit weight of the soil below the excavation bottom as illustrated in Fig 22. The equivalent unit weight γ_{eff} of the soil when the embankment piles are used to stabilize an embankment or slope can be estimated from the equation

$$\gamma_{eff} = \gamma + \frac{\pi d c_a}{a^2}$$

where d = diameter of the piles
c_a = adhesion of the clay along the piles
a = spacing of the piles
γ = unit weight of the soil between the piles

An example where an 7.6 m deep excavation in soft marine clay was successfully stabilized with 6 m long Bakau piles has been described by Broms and Wong (1985).

Other methods that have been used to increase the stability with respect to bottom heave are shown in Fig 27. The stability can be improved by driving a few sheet piles to a soil layer with high bearing capacity so that part of the weight of the soil can be carried by the skin friction along the sheet piles. It is also possible to use inclined anchors in order to increase the vertical stability of the sheet pile wall as shown. This method can be economical if there is a concrete slab next to the excavation. The stability can be increased as well by placing the bottom level of struts in trenches below the bottom of the excavation. Thereby the effective length of the sheet piles below the lower strut level will be reduced.

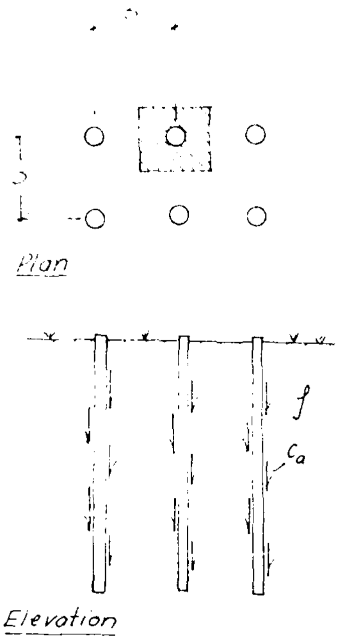

Fig 22 Increase of the equivalent unit weight using embankment piles

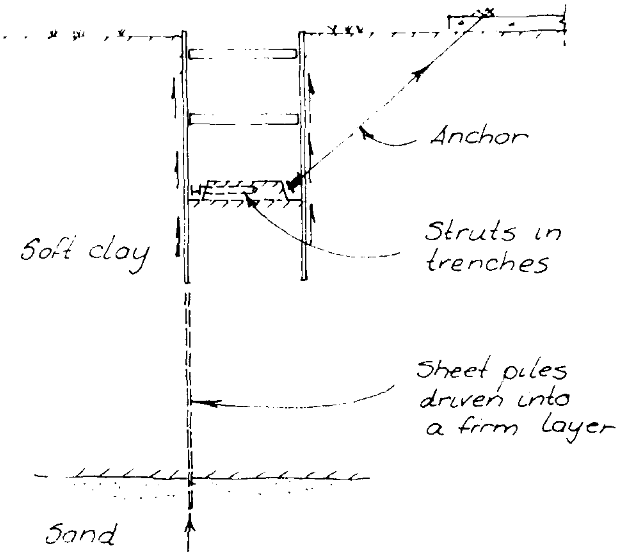

Fig 23 Inclined anchors and lowering of the strut level

FAILURE OF A SINGLE ANCHOR

The redistribution of the load that takes place when one or several of the anchors or struts fail has been investigated by Stille (1976) and by Stille and Broms (1976). In Fig 24 is shown the load redistribution that was observed for an anchored sheet pile wall at Mölntorp, Sweden in a very soft clay with an average shear strength of 18 kPa when one or two of the anchors were unloaded. For this sheet pile wall which was anchored at two levels it was observed that the maximum increase of the load in the adjacent anchors was 9% when one anchor was unloaded and that the load increased by an additional 8% when the load in a second anchor was released. It is interesting to note that the total increase of the load in all anchors was only 36% of the initial load in the unloaded anchor. Thus the total lateral earth pressure on the sheet pile wall decreased by 64% of the initial load in the unloaded anchor. When the second anchor was unloaded then the total increase of the load in the adjacent anchors was only 16% of the initial load in that anchor. Thus the total lateral earth pressure on the wall decreased by 84% with respect to the initial anchor load.

The corresponding load redistribution for a sheet pile wall at Bergshamra, Sweden with three anchor levels is shown in Fig 25. In this case (Panel B1) the maximum increase of load in the adjacent anchors was to 35% of the initial anchor force before the first anchor was unloaded. The total lateral earth pressure on the wall increased by 32% with respect to the initial anchor load. In a second panel (Panel C1) the maximum increase of the anchor force in the adjacent anchors was 14% with respect to the initial load when the load in one of the anchors was released. In this case the total lateral earth pressure on the wall increased by 4% with respect to the load in the unloaded anchor compared with a decrease of 64% at Mölntorp. The behaviour of this sheet pile was thus different. This difference in behaviour can be explained by the difference in mobilized shear strength of the clay behind the wall.

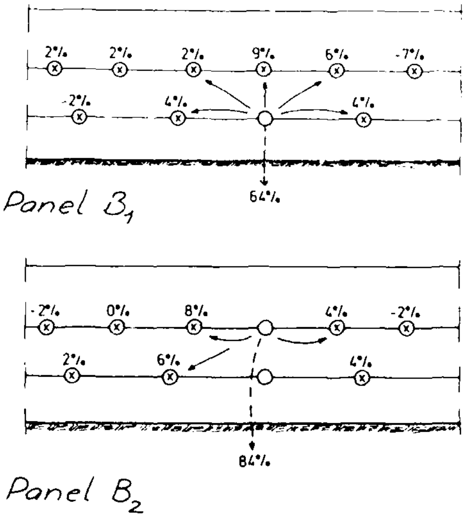

Fig 24 Load redistribution at Mölntorp, Sweden at failure of one or two ground anchors (after Stille, 1976)

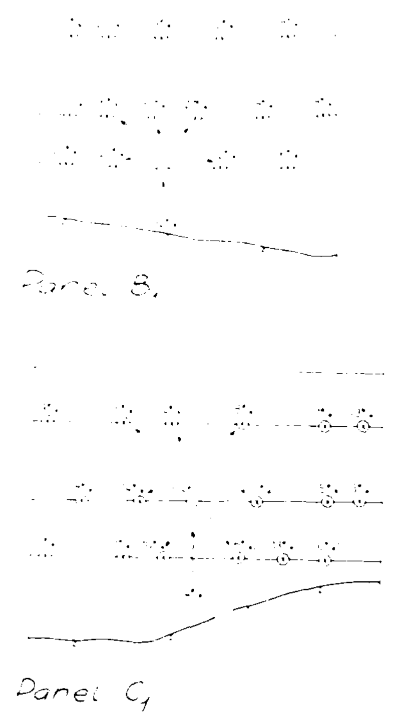

Fig 25 Load redistribution at Bergshamra, Sweden at failure of one or two ground anchors (after Stille, 1976)

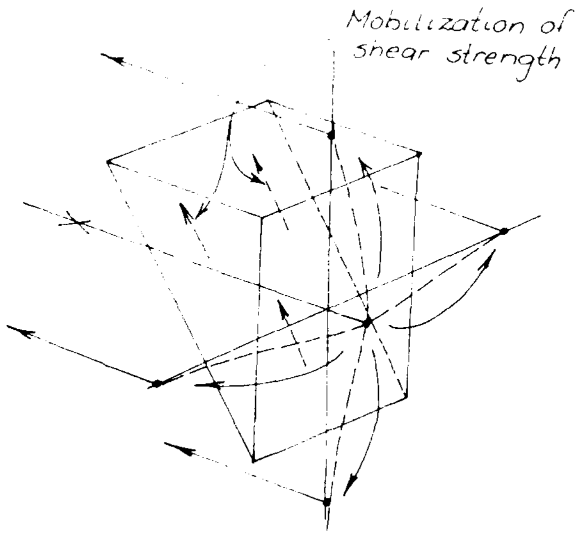

Fig 26 Load redistribution due to mobilization of shear strength

The lateral earth pressure acting on a braced or an anchored sheet pile wall depends on the lateral displacement required to mobilize the shear strength of the soil behind the wall and on the factor of safety used in the design. The wall will deflect laterally when the load in one of the anchors is released or the anchor fails. The increase of the lateral deflection of the wall is generally sufficient to mobilize the shear strength of the clay along a potential failure surfaces behind the wall as illustrated in Fig 26. A relative small deflection is normally required to develop the maximum shear strength of even soft clay compared with the displacement required to develop the ultimate resistance of the anchors or of the struts. In the case the factor of safety initially is relatively high then only a small part of the available shear strength will initially be mobilized. A reduction of the force in one of the anchors will then mainly increase the average shear stress along potential failure surfaces in the clay. In this case, the increase of the load in the adjacent anchors will be small and the total lateral earth pressure on the wall will decrease when one of the anchors is unloaded or fails as was the case at Molntorp.

If on the other hand the factor of safety is low and the shear strength of the clay has been fully mobilized before the release of the force in one of the anchors then the failure of one of the anchor will result in a large increase of the load in the adjacent anchors. The total load on the sheet pile wall may even increase when the peak strength of the clay has been exceeded and the residual shear strength is lower than the peak strength. This was the case at Bergshamra where the total force acting on the sheet pile wall increased when the load in one of the anchors was released.

The consequences when one of the anchors fail will thus depend to a large part on the chosen factor of safety. If a relatively high factor of safety has been used in the design ($\geq$ 1.5) and only part of the shear strength of the soil will be mobilized at working loads then the increase of the load in the adjacent anchors will be small when one of the anchors fails. If on the other hand the factor of safety is close to 1.0 then the failure of one of the anchors will cause a large increase of the load in the adjacent anchors which also may fail. The total lateral earth pressure on the sheet pile wall may even increase and cause a progressive failure of the whole wall (zipper effect).

STABILITY OF THE BASE OF A SHEET PILE WALL

Several failure of anchored walls have been occurred in Sweden in soft clay. In Fig 27 is shown an anchored wall constructed of large diameter bored piles (Broms and Bjerke, 1973). The exposed clay between the piles was shotcreted during the excavation. Clay started to flow into the excavation below the shotcreted part of the wall almost like tooth paste squeezed out of a tube when the depth of the excavation was 5.5 m. Within a few minutes the excavation was filled with soft remoulded clay due to the high sensitivity of the clay. Failure took place when the total overburden pressure at the bottom of the excavation was about 6 c_u where c_u is the undrained shear strength of the clay as determined by field vane tests. The factor 6.0 corresponds to the stability factor N_{cb}. This type of construction using bored piles and shotcrete is therefore not suitable for soft clay when the depth of the excavation is large and the total overburden pressure at the bottom of the excavation exceeds $N_{cb}c_u$

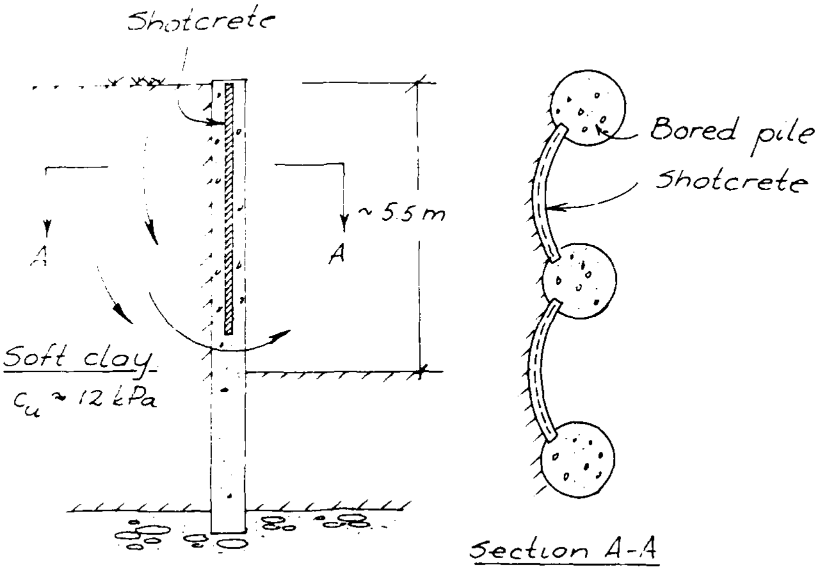

Fig 27 Failure of a vertical cut in soft clay (after Broms & Bjerke, 1973)

(Broms and Bennermark, 1967). Steel sheet piles or contiguous bored piles should have been used instead.

Several failures have also occurred in Sweden when the sheet piles have been driven to rock through a deep layer of soft clay. Because of the high compressive strength of the granite it is not possible to drive the sheet piles into the rock. Soft clay was squeezed into the excavation through the triangular openings which were formed between the bottom of the sheet piles and the rock as shown in Fig 28 since the surface of the rock was inclined. Large settlements were observed outside the wall. The diameter of the depressions corresponded approximately to the depth of the excavation.

STABILITY OF DEEP EXCAVATIONS IN SOFT CLAY IN SINGAPORE

Three deep excavations in soft marine clay in Singapore have been analyzed using a modified version of the computer program EXCAV. In the original program which was developed at the University of California at Berkeley by Chang and Duncan (1977) a non-linear hyperbolic soil model (Duncan et al. 1980) is utilized to describe the soil behaviour. The program can model the excavation layer by layer, the installation and the preloading of the struts and the application of a surcharge load.

The first project involves a braced sheet pile wall, where the sheet piles have been driven into a deep stratum of soft marine clay. In the second project the excessive plastic yielding of a braced sheet pile wall has been investigated. The third project is concerned with the prediction prior to the construction of wall movements for a deep excavation in soft clay.

The short term conditions have been investigated with a total stress analysis using the undrained shear strength of the soft clay. The soft marine clay has been assumed to be saturated and incompressible. A Poisson's ratio of 0.495 has been used in the analysis. The elastic modulus (E_u) that corresponds to undrained conditions has been assumed to 100 c_u to 200 c_u. This equivalent modulus corresponds to the initial tangent modulus, E_i of the soft clay. The tangent modulus, E_t, is a function of E_i and of the stress level.

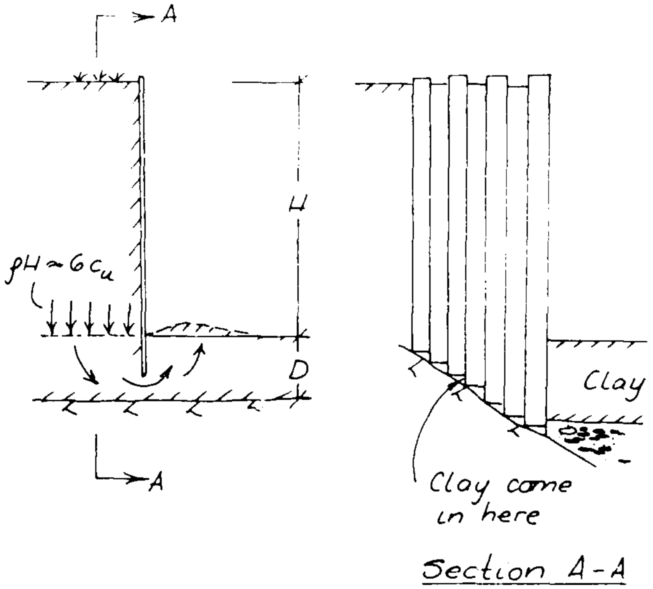

Fig 28 Failure by bottom heave

Project A. This project is located in the Central Business District (CBD) of Singapore (Fig 29). The size of the 11.1 m deep excavation is 42.6 m x 27.0 m. The walls of the excavation were supported by 30 m long sheet piles (FSP IIIA) which were driven 19 m below the bottom of excavation. Six levels of struts supported the wall. The vertical spacing of the strut varied between 1.5 m to 2.5 m. The horizontal spacing was about 6 m.

The excavation proceeded in stages. The struts supporting the sheet piles were installed during each excavation stage 0.5 m above the bottom of the excavation and they were preloaded to 15 percent of the design load. The site was divided into three sections during the excavation. In the present study the behaviour of the sheet pile wall in the middle section of the excavation has been analyzed.

Six slope indicator pipes were installed behind the sheet pile wall as shown in Fig 29. Surface monuments were established to determine the settlements behind the sheet piles. Strain gages were attached to selected struts in order to evaluate the strut loads.

A typical soil profile is shown in Fig 30. A sandy fill about 1 to 2 m thick is located at the ground surface . The fill was followed by a deep layer with soft marine clay which belonged to the Kallang Formation. The clay consists of two distinct members, an upper layer which is approximately 25 m thick and an approximately 7 m thick lower layer. The two layers are separated by a layer of loose to medium dense silty sand. A layer of stiff sandy silt, basically decomposed granite was found below the marine clay.

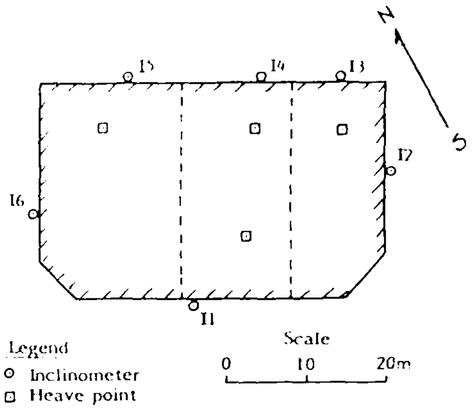

Fig 29 Instrumentation - Project A

The water contents of the upper and lower members of the soft marine clay were 70% and 50%, respectively. The liquid and plastic limits of the upper marine clay varied between 80% and 105% and between 60% and 70%, respectively. The liquid and the plastic limits of the lower marine clay were 70% and 50%, respectively.

Oedometer tests indicated that the marine clay was slightly overconsolidated. The undrained shear strength for the upper and lower members of the marine clay increased almost linearly with depth.

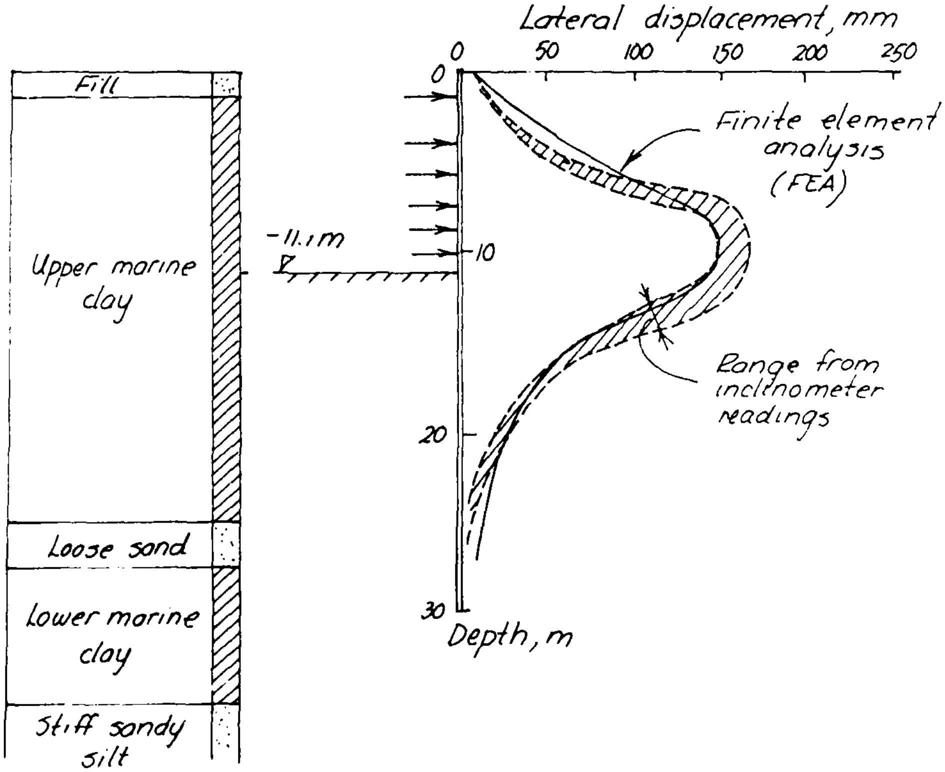

Fig 30 Measured and calculated wall deflections - Project A

Field measurements indicated that the wall gradually moved inwards with increasing depth of the excavation. The maximum deflection of the middle section of the excavation was 150 to 170 mm when the excavation had reached its final depth of 11 m. This is about 1.5% of the excavated depth. A comparison between the measured and the computed deflections is shown in Fig 30.

The observed surface settlements when the depth of excavation was 5.75 m and 11.1 m are shown in Fig 31. The lateral displacements of the wall thus caused large settlements that spread far behind the wall. The maximum settlement was about 1% of the final excavation depth. It occurred at a distance from the excavation equal to about half the excavation depth.

The measured settlements are plotted in Fig 32 as proposed by Peck (1969). It can be seen that the settlements even at a distance of 3.5 times the excavation depth were large. This behaviour can be explained the restraint of the lateral deformations and of the settlements of the sheet pile wall by the sand layer at the toe of the wall as illustrated in Fig 33. This was confirmed by FEM.

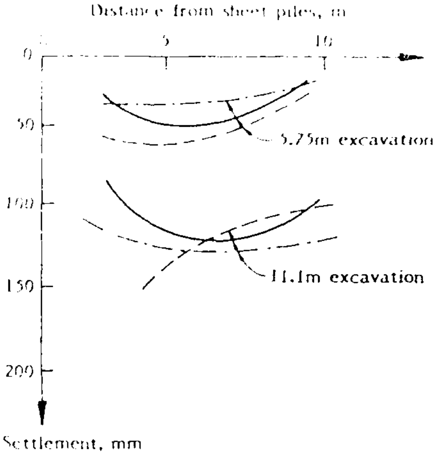

Fig 31 Measured ground settlements - Project A

The maximum bending moment in the wall has been back calculated from the curvature of the sheet piles which was determined from the inclinometer measurements. These measurements indicated that local yielding of the sheet pile occurred during the final stage of the excavation as indicated in Fig 34. The yield moment of FSP IIIA sheet piles is about 380 kN/m/m. The computed maximum bending moment by FEM was 372 kN/m/m. The finite element analysis also indicated that the wall was highly stressed down to about 6 m below the bottom of excavation.

Both field measurements and FEA indicate that the strut load increased rapidly with increasing depth of the excavation. The strut loads reached a maximum just before the installation of the next level of struts. Thereafter, the strut loads decreased slightly with increasing excavation depth.

A comparison between measured and computed strut loads is shown in Fig 35 for the top three levels. The measured strut loads agreed closely with those calculated by FEM. The pressure distribution determined by the tributary area method is shown in Fig 36. It can be seen that the measured and the computed values are in close agreement. It appears that the apparent pressure diagram proposed by Terzaghi and Peck (1967) at m = 0.4 is conservative. A better match is obtained with m = 0.7.

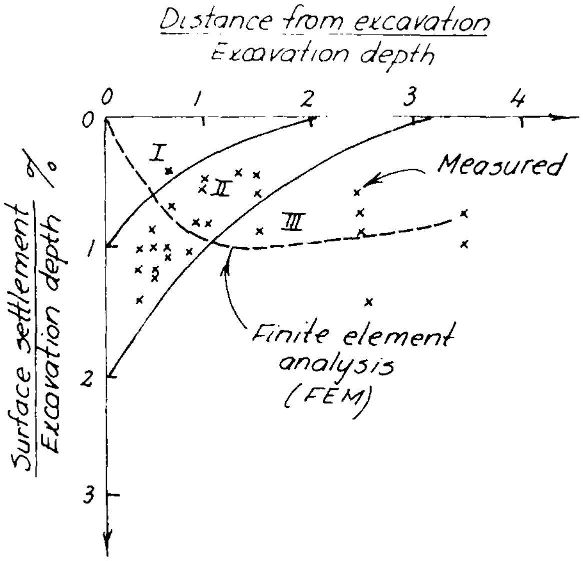

Fig 32 Normalized settlements (Peck, 1969)

The penetration depth of the sheet piles (19 m) below the bottom of the excavation was 1.73 times the depth (11.1 m). An analyses using FEM indicated that the penetration depth could have been reduced by 13.5 m without any significant increase of the strut loads. This conclusion concurs with the observation by Peck (1969) that very little is gained in soft to medium stiff clay by driving the sheet piles far below the bottom of the excavation provided the stability of the excavation with respect to bottom heave is sufficient.

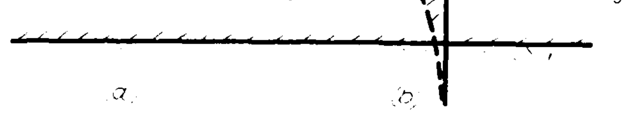

Fig 33 Relationship between settlements and lateral displacements - Project A

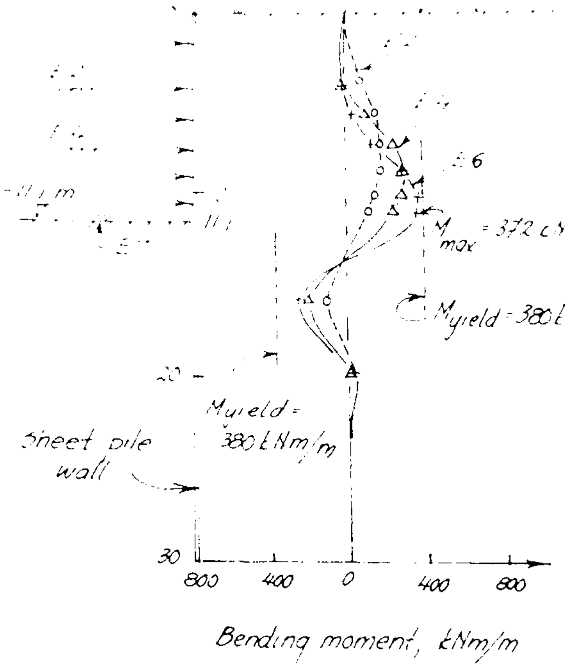

Fig 34 Moment distribution at different stages of construction - Project A

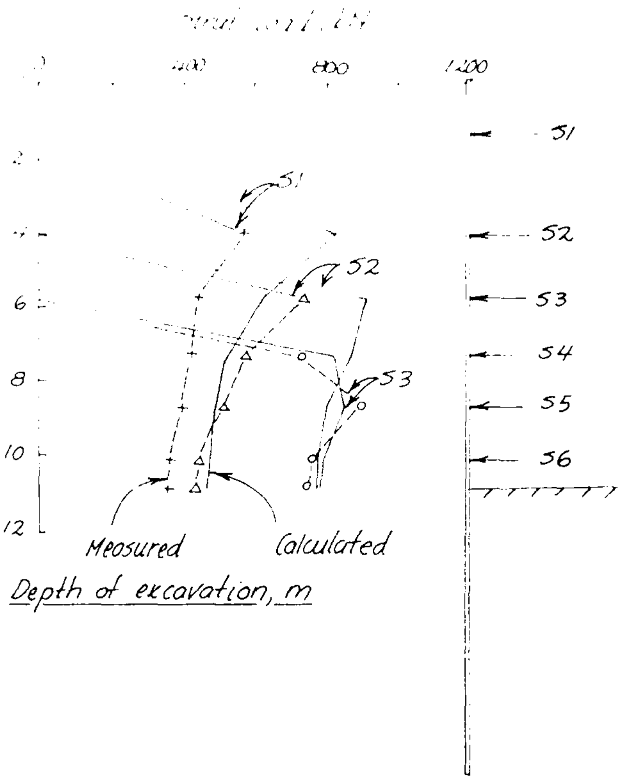

Fig 35 Strut loads - Project A

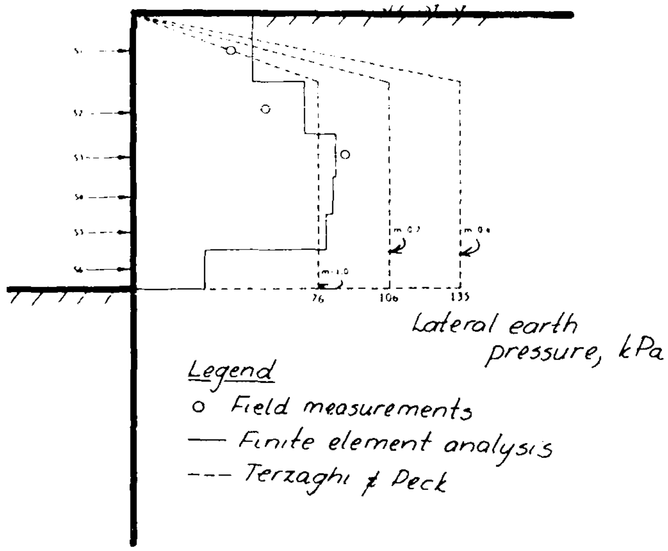

Fig 36 Comparison between measured and calculated strut loads

Project B. This project, which is located just outside the Central Business District in Singapore illustrates the influence of the construction sequence on the performance of braced excavations. The size of the 14.7 m deep excavation was 200 m x 35 m. A cross-section of the excavation is shown in Fig 37. FSP IV sheet piles with a total length of 18.5 m were driven 3.8 m below the bottom of the excavation (D = 0.26H). The sheet piles were supported at six levels. The vertical spacing of the struts varied between 2 m to 2.5 m. The horizontal spacing was about 5.5 m.

The soil condition at this site was highly variable. A soil profile along section A-A is shown in Fig 38. On the west side, the sheet piles were driven into a stiff sandy silt or clay (decomposed granite). On the east side, the soft marine clay extended the full depth of the excavation. The ground water level was located about 1.0 m below the ground surface.

The soil profile on the east side of the excavation is similar to that at Project A. The upper and lower members of the Kallang Formation with soft marine clay are separated by a layer of loose to medium dense sand. Below the marine clay is a deep stratum of decomposed granite, a stiff sandy silt or clay. The upper marine clay is organic (peaty) with an average undrained shear strength of about 10 kPa. The average undrained shear strength of the lower marine clay is 15 kPa. The decomposed granite has an estimated undrained shear strength of about 70 kPa. This material was very difficult to sample and to test.

The soft clay on the east side was adopted in the FEM analysis since it is more critical than the stiff soil on the west side. The excavation was carried out in seven stages. It should be noted that the struts S1 were placed after level E1 had been reached (Fig 37). The excavation proceeded down to level E2 prior to the installation of the struts at this level. This sequence was continued down to level E7. The struts were preloaded to 70% of the design load.

The observed wall movements are shown in Fig 38a. The maximum deflection was 270 mm which is 1.8% of the final excavation depth. This deflection is relatively large since the sheet piles were driven into a stiff soil. The computed maximum deflection was only about 200 mm regardless of the strength and stiffness of the soils when the wall was assumed to be linearly elastic, i.e. non-yielding.

The computed deflections at the different stages of the excavation are shown in Fig 38b for the case when the wall yields. It can be seen that the computed lateral deflections are in good agreement with the measured values.

The maximum settlement, 100 mm, occurred at a distance from the excavation which corresponded to about one-half the excavation depth. The computed settlements fall within Zone I of the normalized settlement chart proposed by Peck (1969).

The measured strut loads were low. A comparison between the measured and computed apparent lateral earth pressures is shown in Fig 40. The measured loads were considerably smaller than those computed by FEM except for the two strut levels at the bottom of the excavation. One possible explanation of this behaviour

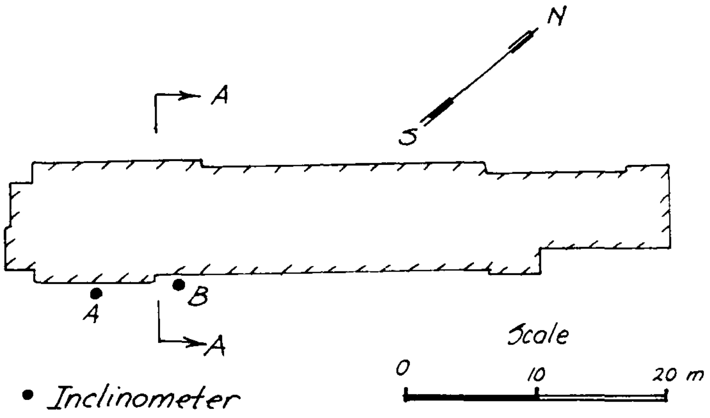
N
S
A
A
B
A
Scale
0
10
20 m
• Inclinometer

Site plan

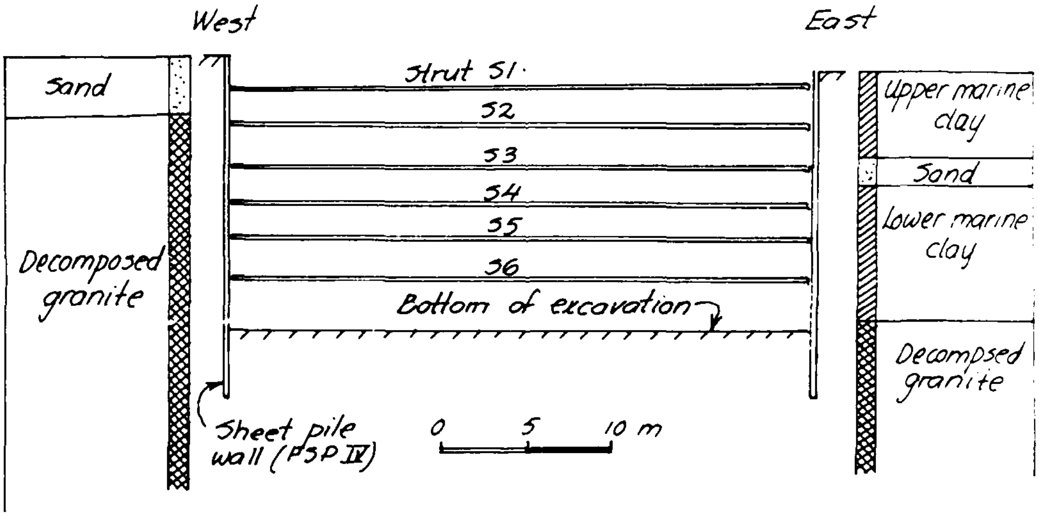
West
East
Sand
Decomposed granite
Strut S1
S2
S3
S4
S5
S6
Bottom of excavation
Upper marine clay
Sand
Lower marine clay
Decompsed granite
Sheet pile wall (FSP IV)
0
5
10 m

Cross-section A-A

Fig 37 Plan and cross-section for Project B

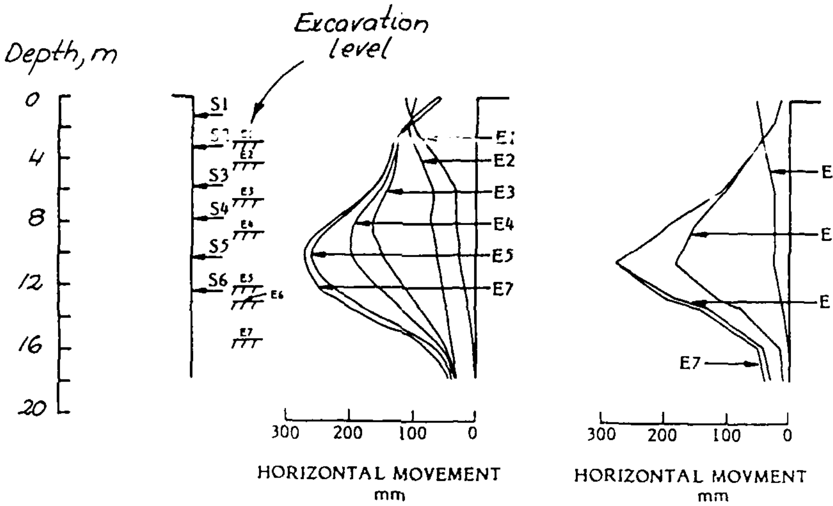

(a) Measured deflection (b) Computed deflection

Fig 38 Measured and computed wall deflections - Project B

is the stiff soil at the west side of excavation. It has been assumed in the analysis that the soft clay extended over the entire excavation.

The measured maximum wall deflection, 275 mm, corresponds to about 1.9% of the depth of the excavation which is rather high for a sheet pile wall driven into stiff soil. This large deflection could have caused by yielding of the sheet piles at an early stage of the excavation.

The analysis indicates that yielding occurred when the excavation reached Level E3, only 7 m below the ground surface due to overexcavation prior to the installation of the struts. Especially the first level of struts is affected.

The installation of the struts lagged behind the excavation of the soft clay by as much as 2.0 m which undoubtly increased the bending moments in the sheet pile wall. It is thus very important to limit the difference between the strut level and the excavation level as much as possible when the struts are installed. This difference should not exceed 0.5 m.

The effect of the construction sequence was also investigated assuming that the depth of the excavation and the strut levels are the same when the struts are installed. In this case, the computed maximum deflection is only 120 mm as shown in Fig 40 which is less than half the measured values. The computed surface settlements and the strut loads were also much smaller. In fact the maximum bending moment in the wall never reached the yield moment of the sheet piles, 590 kN/m/m.

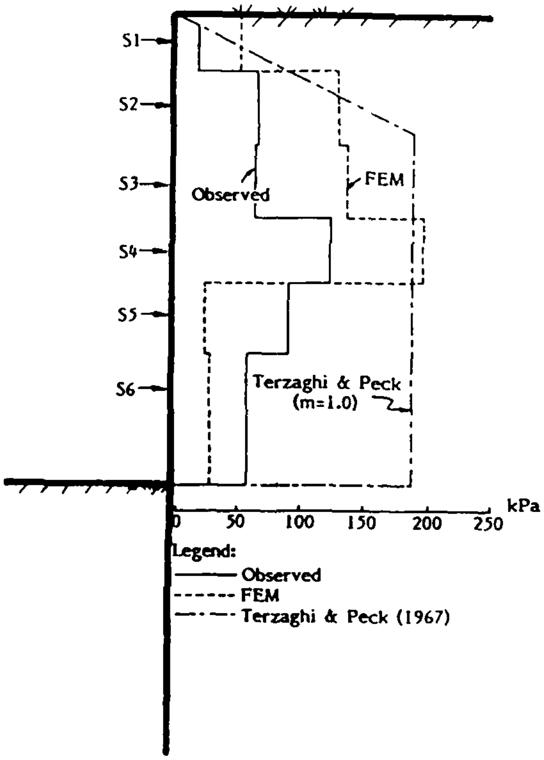

Fig 39 Computed and measured lateral earth pressures - Project B

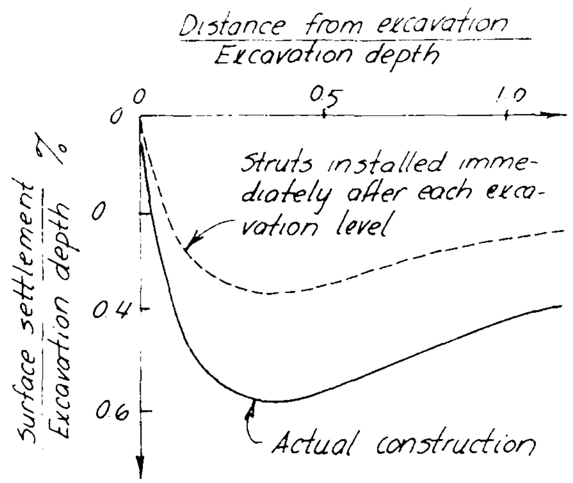

Fig 40 Computed surface settlements - Project B

Project C With the knowledge gained from Projects A and B, an attempt was made to predict the wall movement at Site C prior to construction. This site is located about one kilometer away from Project B. The length of the excavation is about 66 m. The width varies from 6.0 m to about 12.0 m as shown in Fig 42. The total depth is 15.0 m. The field instrumentation included one inclinometer pipe, a number of strain gages attached to selected struts and several survey markers.

Steel sheet piles (FSP VIL) supported at five levels were used as shown in Fig 42. The 26 m long sheet piles were driven 11 m ($D = 0.73\ H$) below the bottom of the excavation. The vertical spacing of the struts varied between 2.0 and 3.5 m. The horizontal spacing was 3.7 m.

Two series of analysis were performed. The first was done prior to construction while the second series was carried out after the excavation had been completed. Soil data from only three boreholes were available prior to excavation. The soil conditions varied considerably between the three holes which were located relatively far from the site (Fig 42). Both the upper and the lower members of the soft marine clay were present in Borehole A whereas only the upper member could be found in Boreholes B and C. The depth to the bottom of the soft clay layer was 16.7 m at Borehole A, 11.5 m at Borehole B and 9.4 m at Borehole C.

The soil conditions at Borehole A was used in the analysis (Case I) since it was the closest of the three boreholes to the investigated section. The average undrained strength of the upper and lower layers of the soft marine clay was 10 and 15 kPa, respectively. This is about the same shear strength as that observed in Project B. Because of the close proximity and the similarity of soil conditions between Projects B and C, the soil parameters in Project B were used in the analysis. An E_u/c_u ratio of 150 was used for the upper layer since the upper marine clay was less peaty than at Project B. A value of 200 was used on the E_u/c_u-ratio for the lower marine clay.

A comparison of the measured and computed wall deflections after the excavation had reached the final depth is shown in Fig 43. The calculated maximum deflection, 75 mm, was only about half of the observed maximum deflection (150 mm).

A parametric study was done prior to the excavation because of the variable soil conditions, in order to assess the effect of the thickness of the soft clay. In one case, the soft marine clay was assumed to extend down to 20 m depth. This assumption was later verified by a cone penetration test (CPT) next to Section A-A. For this case, the computed maximum wall deflection was 142 mm (Fig 44) which agreed closely with the observed maximum deflection of 150 mm. The surface fill as well as the intermediate sand layer were assumed to be absent.

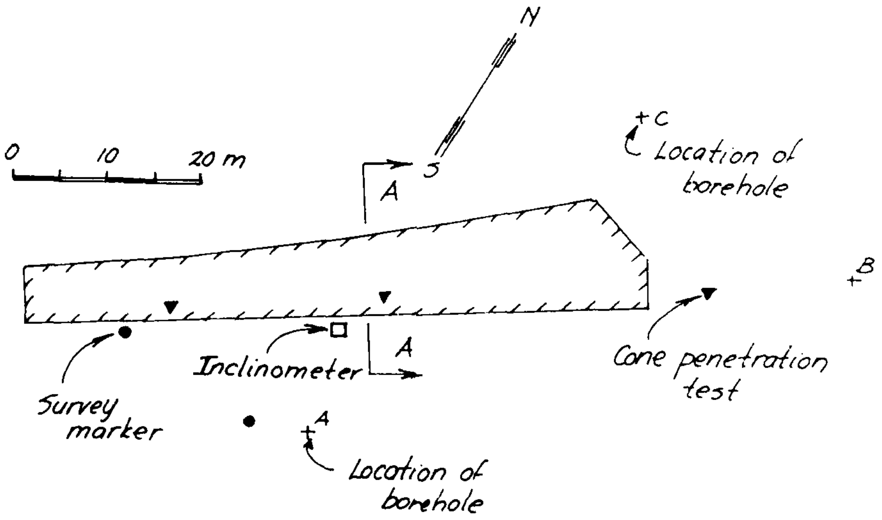

Fig 41 Site plan - Project C

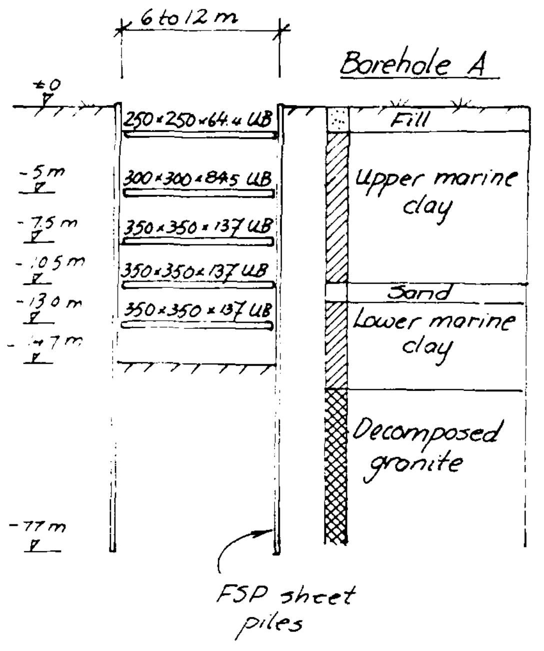

Fig 42 Section A-A - Project C

Shortly after the excavation had been completed, a second series of analyses were carried out using an updated soil profile based on the cone penetration test next to Section A-A. There were no other changes. A comparison between of the computed and measured wall deflections at different stages of the excavation is shown in Fig 45. It can be seen that the computed values were about 20 percent smaller than the measured values. However, the computed shape of the deflected sheet piles compares well with that which was measured.

There are a number of factors that can account for the relatively small computed wall deflections. It has been assumed in the analyses that the excavation depths and the strut levels were the same when the struts were installed. However, the excavation levels during the construction were at least 0.5 m lower than the strut levels. In fact, the first level of struts was not installed until the excavation was 2.0 m to 2.5 m below the ground surface. This accounts for the large lateral deflections observed at the first excavation level as shown in Fig 45. Furthermore, the lowest level of struts (S5) was not installed until the final depth of the excavation had been reached. This accounted for the large observed deflection during the final stage of the excavation. Also the measured ground settlements were much larger than those computed.

The strut loads were not measured at this project. The computed strut loads are shown in Fig 45. The high strut load at level S4 was caused by the intermediate sand layer. A similar phenomenon was observed at Project B.

The analysis indicates that an E_u/c_u-ratio of 100 to 200 gives reasonable results for the soft marine clay in Singapore with respect to settlements, lateral displacements and strut loads and that lateral deflections can be reduced significantly by installing the strut as early as possible and by preloading or prestressing the struts.

For a floating sheet pile wall in a deep stratum of soft clay, the depth of penetration has little effect on the overall behaviour. A penetration depth equal to one-half the excavation depth appears to be adequate provided that the critical depth will not be exceeded.

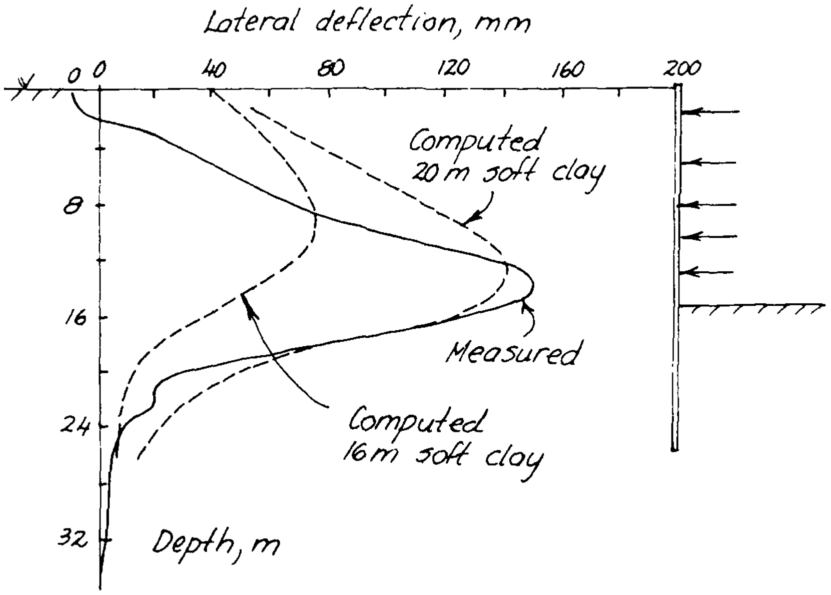

Fig 43 Measured and calculated wall deflections - Project C

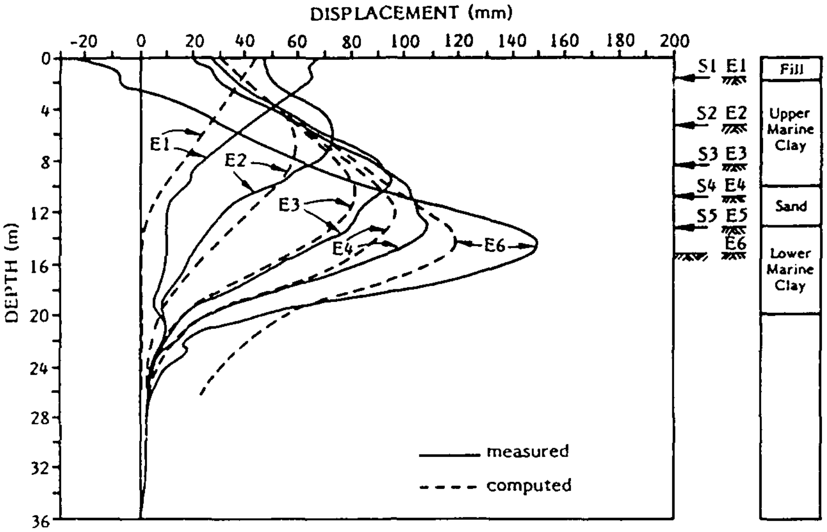

Fig 44 Measured and computed wall deflections - Project C

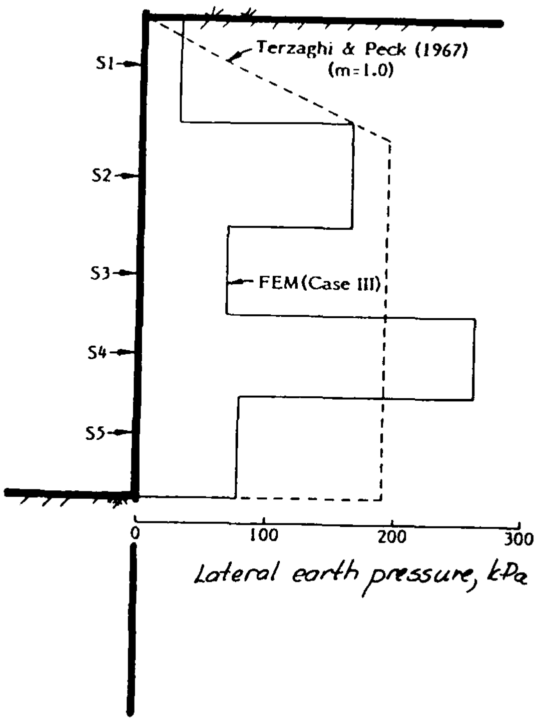

Fig 45 Calculated earth pressures - Project C

STABILIZATION OF DEEP EXCAVATIONS IN SOFT CLAY

Bottom heave is frequently a problem for deep excavations in soft marine clay in Singapore. Failure of bottom heave can occur when the excavation depth exceeds about 5 m to 6 m due to the very low shear strength of the clay. Different methods can be used to increase the stability. The effect of jet grouting, excavation under water and embankment piles (soil nailing) has been investigated for a 11 m deep and 33 m wide excavation in soft clay using a modified version of the computer program EXCAV (Chang and Duncan, 1977). It has been assumed in the analysis that the sides of the excavation are stabilized by 33 m long sheet piles FSP IIIA which have been driven 22 m below the excavation bottom. The sheet piles are supported by struts at four levels. The vertical spacing of the struts is 2.5 m. The top level is located 1 m below the ground surface.

The 50 m deep layer with soft marine clay has been assumed to be slightly overconsolidated down to 11 m depth. Below it is normally consolidated. The undrained shear strength (c_u) is constant, 16 kPa, from the ground surface down to a depth of 11 m. Below, c_u = 16 + 1.25Z kPa where Z is the depth in metres below El. -11 m. The increase of c_u corresponds to a c/p ratio of 0.25 ($c_u/\sigma'_v = 0.25$).

The short term conditions have been evaluated using a total stress analysis. The soft marine clay has been assumed to be saturated and incompressible. A Poisson's ratio of 0.495 has been used in the analysis. The E_u/c_u ratio has been assumed to be 200. A value of 0.9 has been used to estimate the lateral earth pressure at rest (K_o) with respect to the total stress.

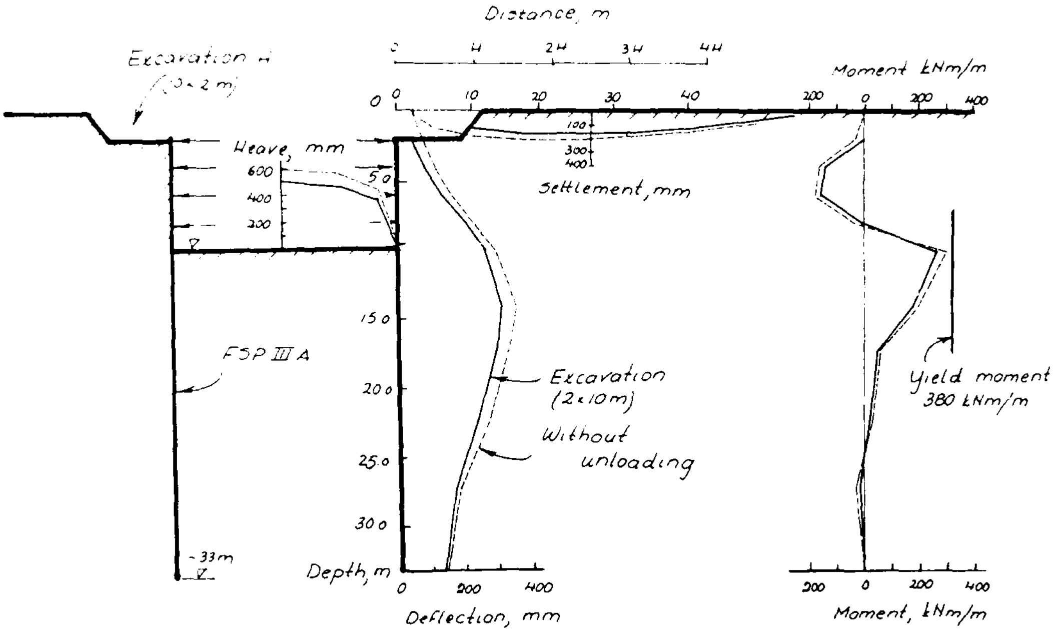

Fig 46 Effect of unloading

These values have been found to be appropriate for deep braced excavations in soft marine clay in Singapore (Broms et al. 1986) and the predicted performance has agreed well with that which has been observed.

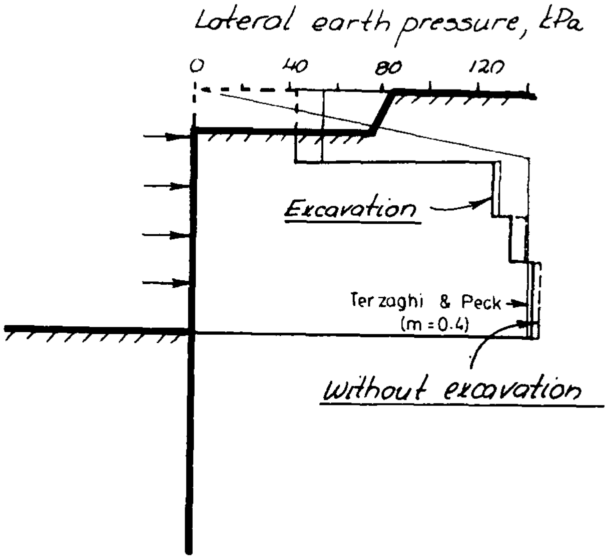

Fig 47 Effect of unloading on strut loads

The lateral deflections of the sheet pile wall are shown in Fig 46 when the depth of the excavation is 11 m. The maximum lateral deflection of the wall is about 400 mm. The ground settlements outside the excavtion and the base heave within the excavation are large as shown in the figure. The calculated maximum settlement and the maximum base heave are about 200 mm and 600 mm respectively. The analysis indicates that the maximum bending moment in the sheet pile wall increases rapidly with increasing depth of the excavation. The maximum bending moment approached the yield strength of the FSP IIIA sheet piles, 80 kNm/m.

The lateral deflection of the sheet piles, the settlements around the excavation and the bottom heave are also shown in Fig 46 when a 10 m wide strip of the soil has been removed along the excavation. It can be seen that the unloading had only a marginal effect on the settlements, the lateral deflections of the sheet pile wall and on the base heave. Also the effect on the strut loads is small as can be seen from Fig 47.

Jet grouting has also been used in Singapore to improve the soft marine clay (Miki, 1985). At this method contiguous or overlapping cylindrical cement columns are formed in-situ in the clay. The diameter of the columns can be up to 2.0 m. The method has, for example, been used to stabilize a 15 m deep excavation for the Newton Circus Station of the Mass Rapid Transit System (MRT) in Singapore and to stabilize tunnels excavated in the soft marine clay and in loose sands.

The construction sequence followed at the jet grouting has been modelled in the FEM-analysis. First the stability of the sheet piles during the installation has been analyzed. Thereafter, the effect of the jet-grouting of a 3 m thick zone of soft clay between the two sheet pile walls below the bottom of the

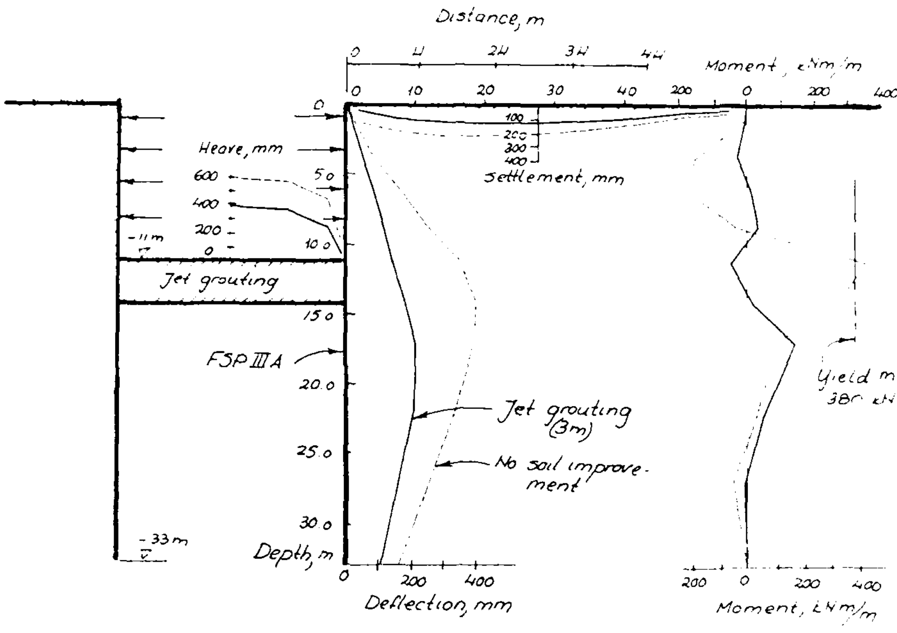

Fig 48 Effect of jet grouting (3 m)

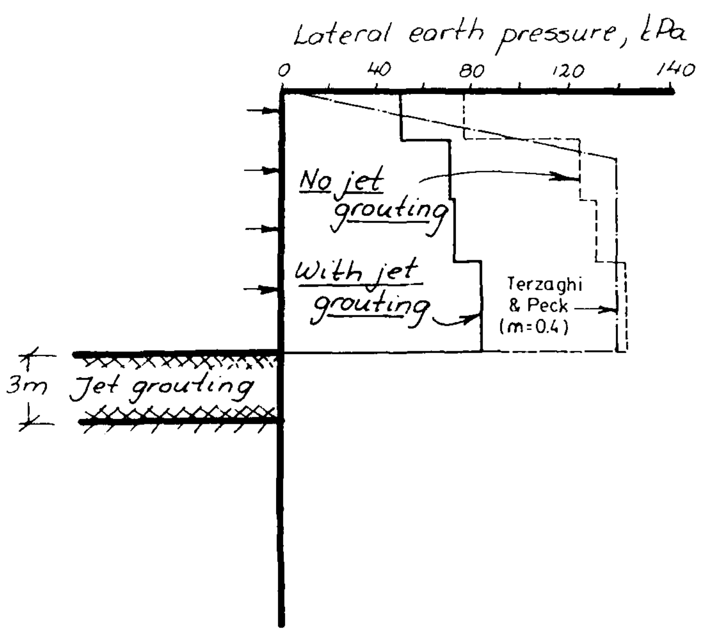

Fig 49 Effect of jet grouting on strut loads

excavation has been investigated. An undrained shear strength of 150 kPa has been assumed for the stabilized 3 m thick layer. Cores of the grouted soil from actual projects indicate that the shear strength of the jet-grouted material can be much higher than 150 kPa

A comparison with the case where no soil improvement has been used shows as indicated in Fig 48 that the performance of the excavation is improved considerably by the jet grouting and that the maximum lateral deflection of the sheet piles is reduced by about 50 percent. Also the settlements and the strut loads are reduced significantly as shown in Fig 49 as well as the maximum bending moment in the sheet piles. Jet grouting has been found to be a very effective method to improve the overall stability of excavations in soft clay.

A further improvement can be obtained by increasing the thickness of the jet grouted zone to 6 m as can be seen in Fig 51. Mainly the deflections of the wall and the bottom heave are reduced. The strut loads are also reduced significantly at all levels (Fig 52). The largest reduction was observed for the bottom level of struts as shown in Table II as could be expected.

FEM has been used to evaluate the stabilizing effect of embankment piles. It was assumed in the analysis that the spacing of the 6 m long Bakau piles with 100 mm diameter is 0.5 m. The piles are driven below the bottom of the excavation using a follower. The tip level is located 17 m below the ground surface. The results of the analysis are presented in Fig 52 and in Table III and compared with the case without soil improvement. The analysis indicate that for a 11 m deep and 33 m wide excavation, four to eight rows of

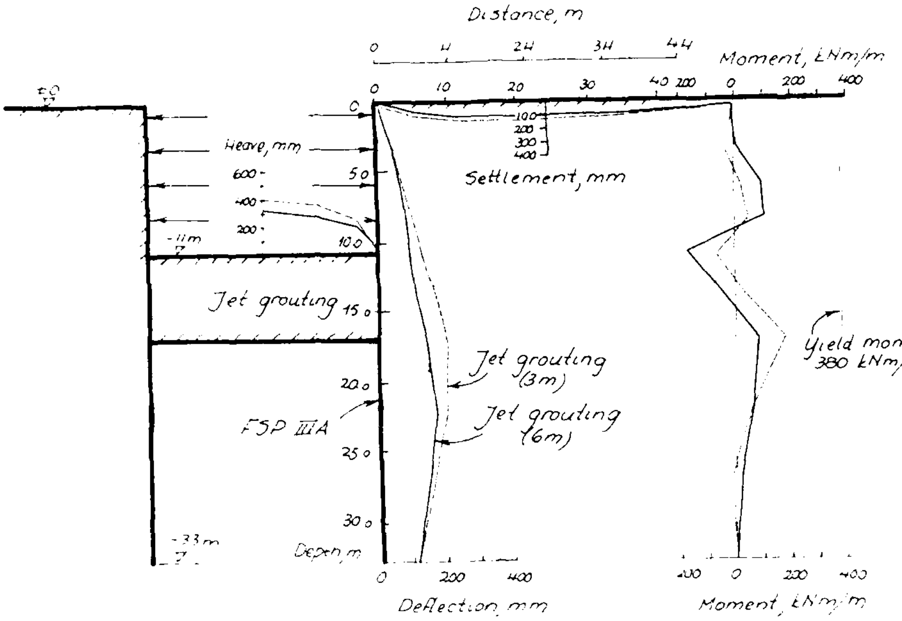

Fig 50 Effect of jet grouting (6 m)

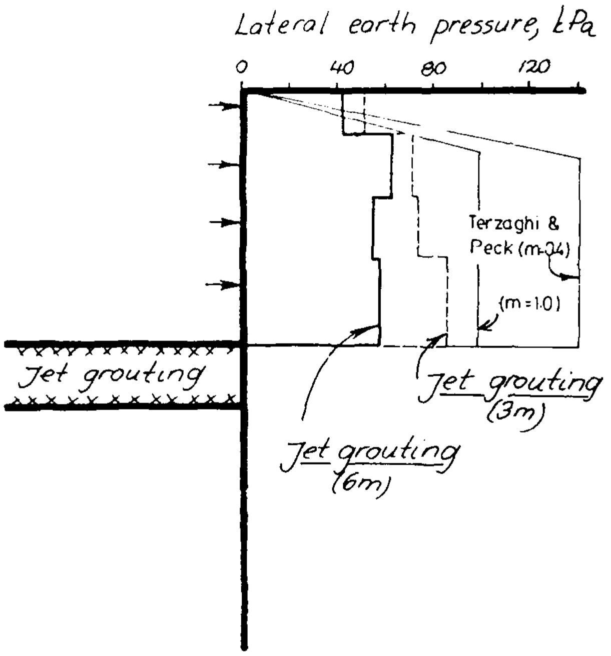
Lateral earth pressure, kPa
0
40
80
120
Terzaghi & Peck (m=0.4)
(m=1.0)
Jet grouting
Jet grouting (3m)
Jet grouting (6m)

Fig 51 Effect of jet grouting (3 m and 6 m) on strut loads

	Without jet grouting	Jet grouting (3m)	Jet grouting 6m
Maximum wall deflection, mm	400mm	208mm	167mm (41%)
Maximum moment, kNm/m	430	180	165 (38%)
Maximum surface settlement, mm	209mm	120mm	100mm (48%)
Maximum base heave, mm	590mm	396mm	320mm (54%)
Maximum strut loads, kN/m			
Level 1	172	126	94 (54%)
Level 2	315	177	153 (48%)
Level 3	329	182	135 (41%)
Level 4	358	209	145 (40%)

Table II Effect of jet grouting on the performance of a 33 m wide and 11 m deep braced excavation

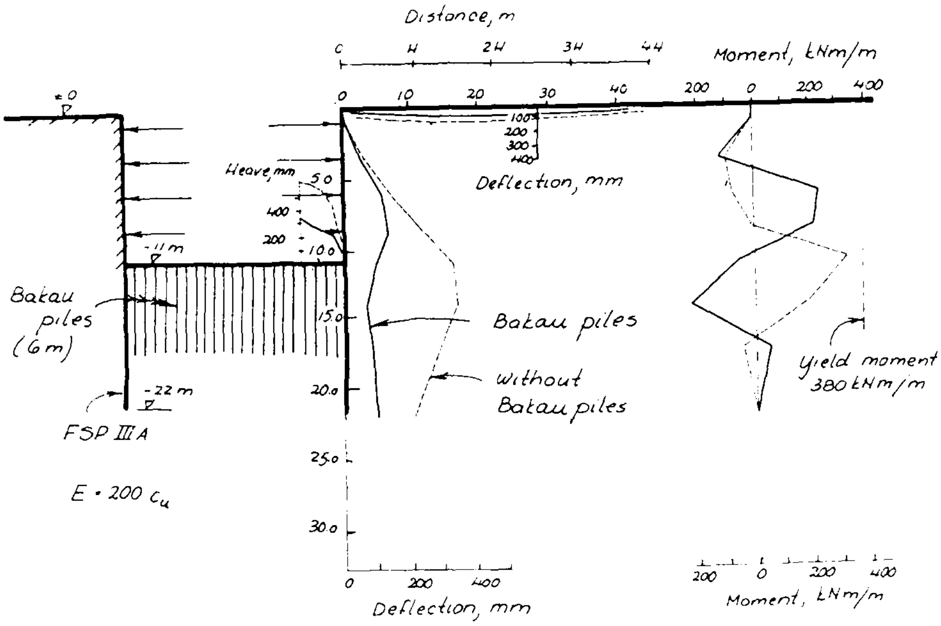

Fig 52 Effect of Bakau piles

Bakau piles in front of each wall could reduce the maximum wall deflection by up to 29% and the maximum bending moment in the sheet piles by 35%. The results also indicate a substantial reduction of the strut loads at the two bottom levels (Fig 53) and an increase of the passive pressure in front of the wall. The effectiveness of the Bakau piles was found to increase with decreasing width of the excavation.

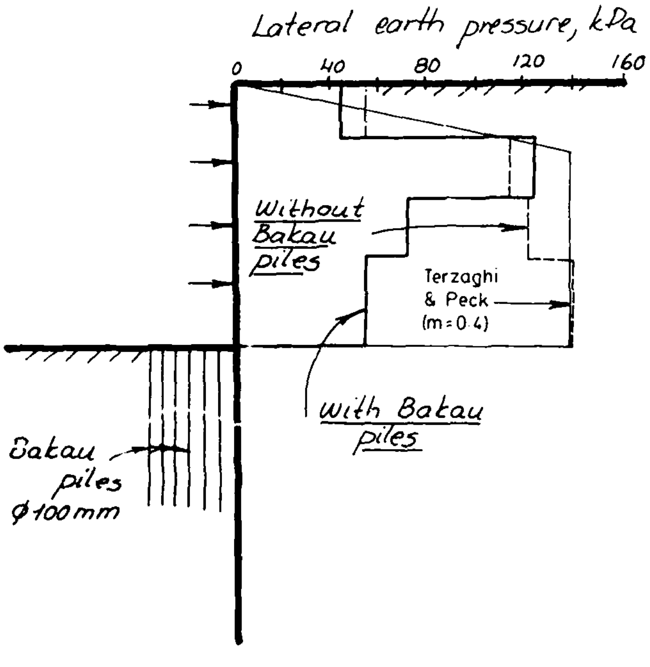

Fig 53 Effect of Bakau piles on strut loads

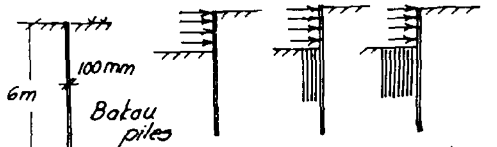

	Without Bakau piles	Bakau piles (4 rows)	Bakau piles (8 rows)
Maximum wall deflection, mm	431 mm	332 mm	306 mm (71%)
Maximum moment, kNm/m	450	306	295 (65%)
Maximum surface settlement, mm	261 mm	220 mm	262 mm
Maximum base heave, mm	594 mm	560 mm	539 mm
Maximum strut loads, kN/m			
Level 1	159	142	128 (80%)
Level 2	324	268	250 (77%)
Level 3	333	264	246 (74%)
Level 4	356	286	272 (76%)

Table III Effect of embankment piles (Bakau piles) on the performance of a 33 m wide and 11 m deep braced excavation

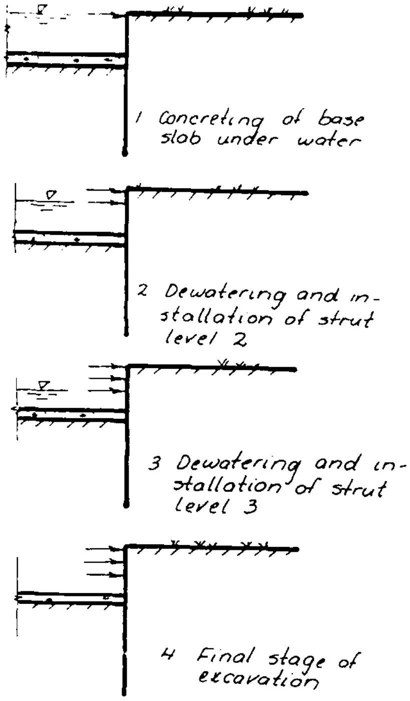
1 Concreting of base slab under water
2 Dewatering and installation of strut level 2
3 Dewatering and installation of strut level 3
4 Final stage of excavation

Fig 54 Construction sequence

The stability of deep excavations in soft clay can also be increased by excavating the soft clay under water. The initial excavation can be done dry until the first one or two rows of struts have been installed. Next, the excavation is flooded so that the soft clay can be excavated down to the final depth. After the base slab has been cast under water the excavation is dewatered and the intermediate struts are installed.

A 15 m deep and 33 m wide excavation has been analyzed using FEM. The sides of the excavation are supported by sheet piles Z-45 with a section modulus (SM) equal to 4500 cm^3/m. Two sets of analysis were conducted. In the first set a conventional excavation method with five levels of struts was investigated. The second set was concerned with the excavation of the soft clay under water. Three levels of struts are used to support the sheet piles. The 2.0 m thick base slab will be cast under water as shown in Fig 54.

The results show a significant improvement of the overall performance (Fig 55). The maximum wall deflection was reduced by 53%. A 44% reduction of the base heave and a 50% reduction of the ground settlement were also obtained. The loads in the second and third level struts are reduced significantly as well (Fig 56 and Table IV). Because the base slab will be installed before the second and third level struts, the axial load in the base slab will be high compared with that in the two levels of struts (Table IV).

The FEM analysis indicates that excavation under water down to 15 m depth is feasible. The calculated maximum wall deflection, 130 mm, and a maximum ground settlement of 150 mm are much less than those observed for actual excavations using conventional methods even when the maximum depth is less than 11 m.

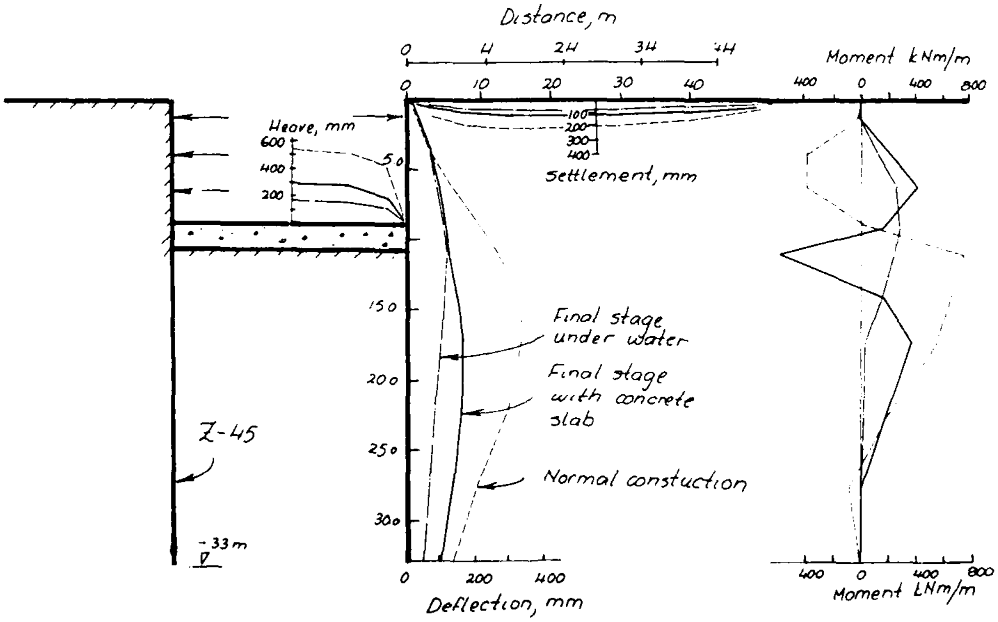

Fig 55 Effect of excavation under water

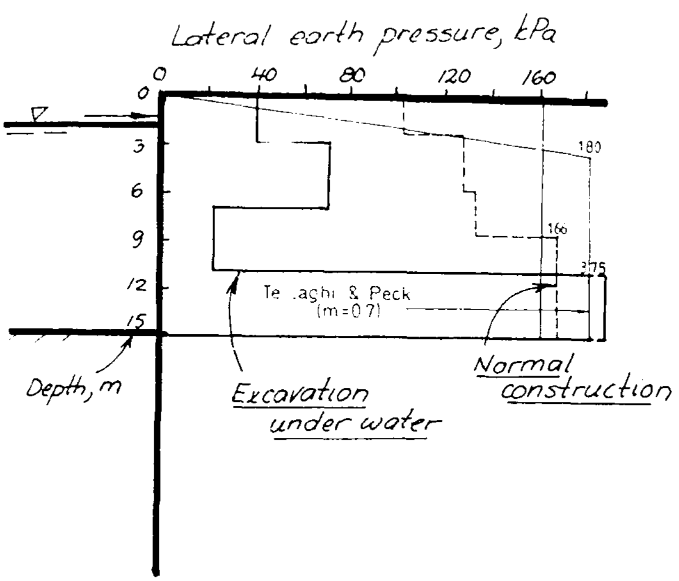

Fig 56 Effect on strut loads of excavation under water

Excavation under water has the main advantage that the stability with respect to base heave is governed by the submerged unit weight of the soft marine clay (about 6 kN/m^3) rather than the total unit weight (about 16 kN/m^3). The wall movements during the dewatering and the installation of the struts after the installation of the base slab under water will mainly occur below the slab. The lateral deflections of the sheet piles above the slab will be small.

	Normal construction	After excavation to 11m, before concreting	Final stage of construction
Maximum wall deflection, mm	347 mm	124 mm	165 mm
Maximum moment, kNm/m	200	80	110
Maximum base heave, mm	540 mm	170 mm	300 mm
Maximum strut loads, kN/m			
Level 1	187	187	158
Level 2	358	–	130
Level 3	363	–	70
Level 4	551	–	953 (slab)

Table IV Effect of excavation under water on the performance of a 33 m wide excavation

SUMMARY

The design and construction of anchored and struted sheet pile walls in soft clay have been reviewed. Most failures have been caused by insufficient penetration depth of the sheet piles when the walls rotate around the level of the anchors or of the struts. Failure can also be caused by rupturing of the anchor rods or by buckling of the struts. The strut or anchor loads can for deep cuts especially at the bottom of the excavation be considerably higher than those calculated by a conventional method. Failure by bottom heave is also a possibility which must be considered in the design.

When inclined anchors are used it is also important to take into account the vertical force caused by the inclined anchors or by the struts. This vertical force can reduce considerably the stability of particularly anchored sheet pile walls. Several failures have occurred which have been caused by insufficient vertical stability of the sheet piles and where the vertical force caused by the inclined anchors was not considered in the design.

Failure of one of the anchors or struts may lead to progressive failure and complete collapse (zipper effect) of the wall. If a sufficient high factor of safety is used in the design then the increase of the load in the adjacent anchors or struts will be small at failure of one of the anchors.

REFERENCES

Aas, G. (1984). "Stability Problem in a Deep Excavation in Clay," Proc. Int. Conf. on Case Histories in Geotechnical Engg., St Louis, Vol. 1, pp 315 - 323.

Ahmad, A. S. and Peaker, K. R. (1977). "Geotechnical Properties of Soft Marine Singapore Clay," Proc. Int. Symposium on soft Clays, Bangkok, Thailand, pp 3-14.

Baguelin, F., Jezequel, J. F. and Shields, D. H. (1978). "The Pressuremeter and Foundation Engineering," Trans. Tech. Publications, Clausthal, Germany, 617 pp.

Bjerrum, L. and Eide, O. (1956). "Stability of Strutted Excavations in Clay," Geotechnique, Vol. 65, No. 1, pp. 32 - 47.

Broms, B. B. (1968). "Swedish Tie-Back System for Sheet Pile Walls," Proc. 3rd Budapest Conf. on Soil Mech. a. Found. Engg., Budapest, pp. 391 - 403.

Broms, B. B. (1984). "Design of Sheet Pile Walls," Proceedings of Seminar on Precautions and Solutions to Environmental Problems Caused by Tunnelling and Excavations organized by ABV-LCM Engineering Pte Ltd, April 1984, Singapore, 27 pp.

Broms, B. B. and Bennermark, H. (1967). "Stability of Clay at Vertical Openings," Journ. Soil Mech. a. Found. Div., ASCE, Vol. 93, No. SM1, pp 71 - 94.

Broms, B. B. and Bergdahl U. (1982). "The Weight Sounding Test (WST)," State-of-the-Art Report, ESOPT II, Amsterdam, 12 pp.

Broms, B. B. and Bjerke, H. (1973). "Extrusion of Soft Clay Through a Retaining Wall," Canadian Geotechnical Journal, Vol. 10, No. 1, pp 103 - 108.

Broms, B. B. and Wong, I. H. (1984). "Foundation of Tall Buildings," Proceedings of Int. Conf. on Tall Buildings, Singapore, pp 547 - 590.

Broms, B. B., Wong, I. H. and Wong, K. S. (1986). "Experience with Finite Element Analysis of Braced Excavations in Singapore," Proc., 2nd Int. Symp. on Numerical Models in Geomechanics, NUMOG II, Ghent, Belgium, pp 309 - 324.

Burland, J. B., Simpson, B. and St. John, H. D. (1979). "Movements Around Excavations in London Clay," Proceedings of Seventh European Conf. on Soil Mechanics and Foundation Engg., Vol. 1, Brighton, pp. 13 - 29.

Chang, C. S. and Duncan (1977). "EXCAV : A Computer Program for Analysis of Stresses and Movements in Excavations," Geotechnical Report No TE 77-4, University of California, Berkeley, 35 pp.

Clough, G. W. and Davidson, R. R. (1977). "Effects of Construction on Geotechnical Performance," Proceedings, Specialty Session III, Ninth Int. Conf. on Soil Mech. a. Found. Engg., Tokyo, 1977, pp. 15 - 53.

Clough, G. W. and Hansen, L. A. (1981). "Clay Anisotropy and Braced Wall Behaviour," Journ. of the Geotechnical Div., ASCE, Vol. 107, No. GT 7, July, pp. 893 - 914.

Clough, G. W. and Mana, a. I. (1977). "Lessons Learnt in Finite Element Analysis of Temporary Excavations in Soft Clay," Proc. 2nd int. Conf. on Numerical Methods in Geomechanics, Blacksburg, Virginia, ASCE, Vol. 7, pp. 496 - 510.

Clough, G. W. and Tsui, Y. (1974). "Performance of Tie Back Walls in Clay," Journ. of the Geotechncial Div., ASCE, Vol. 100, No. GT12, pp. 1259 - 1274.

D'Appolonia, D. J. (1971). "Effects of Foundation Construction on Nearby Structures," Proc. 4th Pan American Conf. on Soil Mech. a. Found. Engg., Puerto Rico, Vol. 1, pp. 189 - 236.

Duncan, J. M., Byrne, P., Wong, K. S. and Mabry, P. (1980). "Strength, Stress-Strain, and Bulk Modulus Parameters for Finite Element Analysis of Stresses and Movements in Soil Mass". Dept of Civil Engg., University of California, Berkeley, 70 pp.

Egger, P. (1972). Influence of Wall Stiffness and Anchor Prestressing on Earth Pressure Distribution," Fifth European Conf. on Soil Mech. a. Found. Engg., Vol. 1, Madrid, pp. 485 - 498.

Hanna, T. H. (1982). "Foundations in Tension - Ground Anchors," Trans Tech Publications, McGraw Hill Book Co., Series on Rock and Soil Mech., Vol. 6, Clausthal, Germany, 573 pp.

Janbu, N. (1972). "Earth Pressure Computations in Theory and Practice," Proc. 5th European Conf. on Soil Mech. a. Found. Engg., Vol. 1, Madrid, Spain, pp. 45 - 54.

Karlsrud, K. (1986). "Performance Monitoring of Deep Supported Excavations in Soft Clay," Proc. 4th Int. Geotechnical Seminar, Field Instrumentation and In-Situ Measurements, Nanyang Technological Institute, Singapore, pp. 187 - 202.

Karlsrud, K., DiBiagio, E., and Aas, G. (1980). "Experience with Slurry Walls in Soft Clay," Proc., Symp. on Slurry Walls for Underground Transportation Facilities, U.S. Dept. of Transportation, Report No. FHWA-TS-80-221, March, pp. 383 - 408.

Lee, S. L., Yong, K. Y., Karunaratne, G. P. and Chua, L. H. (1986). "Field Insturmentation for a Strutted Deep Excavation in Soft Clay," Proc. 4th Int. Geotechn. Seminar, Field Instrumentation and In-Situ Measurements, Nanyang Technological Institute, Singapore, pp. 183 - 186.

Littlejohn, G. S. (1970). "Soil Anchors," Proc. Conf. on Ground Engg. The Institution of Civil Engineers, London, England, pp. 33 - 44.

Mana, A. I. and Clough, G. W. (1981). "Clay Anisotropy and Braced Wall Behavior," Journ. of the Geotechnical Div., ASCE, Vol. 107, No. GT 6, pp. 759 - 778.

Meyerhof, G. G. (1956). "Penetration Tests and Bearing Capacity of Cohesionless Soils," Journ. Soil Mech. a. Found. Div., ASCE, Vol. 82, SM1, pp. 1 - 19.

Miki, G. (1985). "Soil Improvement by Jet Grouting," Proc. 3rd Int. Seminar, Soil Improvement Methods, Singapore, pp. 229 - 236.

O'Rourke, T. D. (1981). "Ground Movements Caused by Braced Excavations," Journ. of the Geotechnical Div., ASCE, Vol. 107, No. GT 9, pp. 1159 - 1178.

Peck, R. B. (1969). "Deep Excavations and Tunnelling in Soft Ground," Proc of Seventh Int. Conf on Soil Mech. a. Found. Engg., State-of-the-Art-Volume, pp. 225 - 290.

Rowe, P. W. (1957) "Sheet Pile Walls in Clay," Proc. of Institution of Civil Enggs., Vol. 7, Jul 1957, pp. 629 - 654, London, England.

Sahlström, P. O. and Stille, H. (1979). "Förankrade Sponter (Anchored Sheet Pile Walls)," Swedish Council for Building Research, Report No T30 : 1979, Stockholm, Sweden, 128 pp.

Stille, H. (1976). "Behaviour of Anchored Sheet Pile Walls," Thesis, Royal Inst. of Tech., Dept. of Soil and Rock Mech., 192 pp.

Stille, H. and Broms, B. B. (1976). "Load Redistribution Caused by Anchor Failures in Sheet Pile Walls," Proc. 6th European Conf. on Soil Mech. a. Found. Engg., Vienna, Austria, Vol. 1.2, pp. 197 - 200.

Stroh, D. and Breth, H. (1976). "Deformation of Deep Excavations," Proc., Conf. on Numerical Methods in Geomechanics, Vol. II, Blacksburg, June, pp. 686 - 700.

Tan, S. B. (1970). "Stability Investigations of the Whampoa Slip," Journ. South East Asia Geotechnical Society, Vol. 1, No. 2, pp. 95 - 101.

Tan, S. L. (1983). "Geotechnical Properties and Laboratory Testing of Soft Soils in Singapore," Int. Seminar on Construction Problems in Soft Soils, Nanyang Technological Institute, Singapore, 1 - 3 December 1983, 47 pp.

Terzaghi, K. and Peck, R. B. (1967). "Soil Mechanics in Engg Practice", 2nd Edition, John Wiley and Sons, New York, 729 pp.

van der Veen, C. and Boersma, L. (1957). "The Bearing Capacity Predetermined by Cone Penetration Test," Proc. 4th Int. Conf. Soil Mech. a. Found. Engg., Vol. 2, pp. 72 - 75.

Proceedings: Second International Conference on Case Histories in Geotechnical Engineering, June 1-5, 1988, St. Louis, Mo., Invited Paper

Case Studies Through Material Modelling and Computation

C.S. Desai
Professor and Head, Department of Civil Engineering and
Engineering Mechanics, University of Arizona, Tucson, Arizona

SYNOPSIS: This paper describes a number of case studies by using numerical procedures conducted by the author and his co-workers over a number of years. The case studies involve a wide range of static and dynamic stress-deformation, seepage and stability, and consolidation problems. The numerical procedures use simple linear and nonlinear elastic models, to advanced but simplified hierarchical plasticity based models for geologic materials and interfaces/joints. The evolution from the use of simple to advanced models is guided by the realization that it is essential to employ models that are capable of handling the complexities in geotechnical systems. In addition to use of the conventional and empirical methods, it is advisable to develop and utilize improved and simplified techniques based on basic principles of mechanics. This approach can allow the geotechnical engineer access to models and procedures towards improved and rational solutions for case studies and for practical applications.

INTRODUCTION

In conventional case studies in geotechnical engineering, the (field) observations are usually examined with the aid of empirical or simplified formulas, or theories to predict the observed behavior and to draw conclusions regarding the performance of the system, the adequacy of design methods used including their limitations, and need for future modifications. As the methods are highly simplified, the analysis performed is usually on a highly idealized system in terms of geometries and material properties that can render itself to simple calculations. Coupled with experience and intuition of the engineer, this approach can provide satisfactory solutions for many problems. However, since it does not allow for factors such as irregular geometries, nonlinear soil properties and complicated loadings, for many other problems, the conventional methods may not be appropriate for realistic solutions.

The notion that the uncertainties in material properties, geometry and loadings in geotechnical problems are high and hence, conventional methods are all that is required, and advanced (computational) methods may not be warranted,and may not be precise! This is because whether one uses a conventional method or an advanced modern method, the uncertainties are essentially the same. While, on the other hand, the modern methods are capable of easy analysis of the effects of uncertainties through parametric studies, and also capable to incorporation in the analysis itself, of newly developing models, e.g. for the material behavior. With this belief, it is considered useful and meaningful from a practical viewpoint of case studies to use modern (computer) methods with improved treatment of material response and other factors.

Scope

The scope of this paper includes:

1. A review of the author's work in case studies involving field measurements using computer (finite element, finite difference) methods for the following problems:

   (a) Static Stress-Deformation

      (i) Axially and Laterally Loaded Piles - 1974, 1980
      (ii) Group Piles - 1974, 1986
      (iii) Tunnels - 1983
      (iv) Retaining Walls - 1983, 1985
      (v) Anchors - 1986

   (b) Seepage and Deformable Flow

      (i) Seepage in River Banks - 1971, 1972, 1983
      (ii) Consolidation of Layered Foundations - 1977
      (iii) Seepage in Dams - 1980, 1983, 1986, 1987
      (iv) Stress and Seepage in Dams - 1983

   (c) Dynamic and Earthquake Analysis

      (i) Model Nuclear Power Plant - 1984

2. Consideration of mechanical behavior of geologic materials and interfaces and joints, starting from simple elastic and nonlinear elastic, to recently proposed new hierarchical and unified plasticity based approach by the author and co-workers. Here, the author has gone through a gradual realization that it is beneficial to think that a nonlinear elastic model, with its simple look, may be appropriate for some problems, only where it is applicable. However, for realistic simulation of the behavior of geologic materials, it is essential to develop improved models from the basic principles of mechanics. The author has found that such models with sound fundamentals need not be complicated if derived through a rational process of simplifications for practical

application. In fact, the hierarchical models [1-4] represent such an approach and involve equal or lesser number of material constants as compared to nonlinear elastic models, and at the same time, are capable of accounting for factors such as volume changes, stress paths, nonassociativeness, softening and anisotropy.

3. With the above viewpoint, in the following, are described a number of case studies, conducted by the author since 1970. Comments are offered on the capability, limitations and improvements in various material models in conjunction with computational methods.

CASE STUDIES

This paper would be too long if all the applications were described in details. Also, case studies involving field problems are related to other studies involving theoretical considerations and laboratory verifications. To overcome this, it is proposed to outline the case studies presented below and the related works in Tables 1, 2, and 3 for Static Stress-Deformation, Seepage and Deformable Flow and Dynamics and Earthquake, respectively. Some related case study topics that are not reviewed herein are also mentioned in these tables. The tables present statements of the problems, constitutive or material model(s) employed and other factors, numerical techniques, and special comments.

In the following, brief descriptions of only selected case studies involving field verifications are given with critical comments on the constitutive models and their gradual progression toward improved characterization and on the numerical techniques and improvements therein. Details of numerical analysis such as meshes are shown only for some problems, whereas for others only typical comparisons of computations and observations are included.

Static Stress-Deformation

Example 1 - Axially Loaded Piles: Figure 1 shows comparisons between predicted* and observed behavior for a typical axially loaded steel pipe pile, outer diameter = 41 cm., length = 16 m, [5] in sand tested in the field at the Arkansas Lock and Dam No. 4 (LD4) site [6]. Here, in the early stage of finite element applications, nonlinear elastic model using hyperbolic simulation [7] was used, which is considered essentially similar to the piecewise representation through data points used before [8] and the spline representation [9] in the sense that they are based on piecewise linear elastic approximation. The constants for these models are found from a set of triaxial test data with cylindrical specimens. The interface element used was a modified version of that with zero thickness as proposed in Ref. 10. A set of design charts (Fig. 11 in Ref. 5) were also prepared for finding bearing capabilities of piles in sands.

The results indicated that for monotonic loading, the finite element scheme with nonlinear elastic models can provide satisfactory predictions of load displacement curves and bearing capacity for piles.

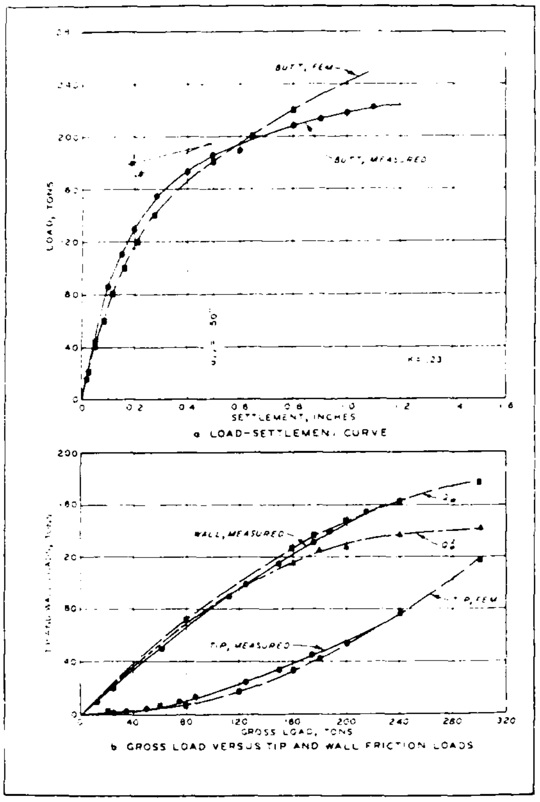

Fig. 1 Comparisons for Pile No. 10, LD4

Although the results allow for nonlinear simulation of a set of the stress-strain curves, the above models can mainly allow for monotonic loading. They are deficient in terms of allowing for factors such as volume change, stress-path, unloading-reloading and nonassociative response. Moreover, these models cannot adequately represent unloading and reloading responses vital in many geotechnical problems. Hence, their use should be tempered with caution.

Example 2 - Pile Supported Lock: Figure 2 shows comparisons between predictions and observations of settlements of different points at various times during sequential construction for the stress-deformation behavior of pile supported Columbia Lock, on the Ouachita River near Columbia, Louisiana, Fig. 3 [11]. Here, the three-dimensional pile foundation system was idealized as structurally equivalent two-dimensional system.

The foundation soils consisted of cohesive backswamp deposits or cohesionless substratum deposits or both, beneath the east wall, and tertiary deposits interfacing with colluvium and substratum deposits beneath the west wall [12]. The stress-strain model used was nonlinear elastic, simulated through hyperbola. The interface model used was the same as in Example 1.

---

*In most cases, predicted imply back predictions of observed response.

TABLE 1. Static Stress Deformation

1 Problem	2 Material Behavior	3 Other Factors	4 Numerical Procedure
1. Axially Loaded Footings	• Nonlinear Elastic - Data Points		2-D Finite Element
2. Axially Loaded Piles	• Nonlinear Elastic - Hyperbolic		2-D Finite Element
3. Laterally Loaded Structures	• Nonlinear Elastic - Ramberg-Osgood	• Construction Sequences	1-D Finite Element
4. Pile Groups	• Nonlinear Elastic - Hyperbolic	• Construction Sequences • Downdrag	2-D Simulation (cf 3-D), Finite Element
5. Pile Groups	• Nonlinear Elastic - Hyperbolic	• New Thin-Layer Interface	3-D Finite Element
6. Tunnels	• Plasticity - Drucker-Prager	• Construction Sequences • Thin-Layer Joint	2-D Finite Element; Displacement, Hybrid Mixed
7. Retaining Walls	• Plasticity - von Mises	• Construction Sequences • Thin-Layer Interface • Flexible Structures	2-D Finite Element, Displacement, Hybrid, Mixed
8. Footings, Walls, Track Mechanics	Options for Non-Linear Elastic and Plasticity - von Mises, Drucker-Prager, Critical State, Cap	• Thin-Layer Interface • Flexible Structures	1-D, 2-D and 3-D Finite Element
9. Anchors	• Hierarchical Associative/ Nonassociative Plasticity	• Thin-Layer Interface • Interaction • Stress Relief	3-D Finite Element

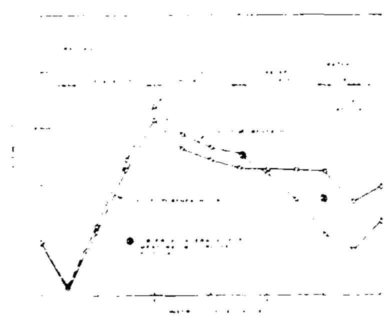

Fig. 2 Settlement Versus Construction Sequences at Typical Nodes, 199 and 483 (1 ft = 0.305 m)

Here the normal stiffnesses during compressive and tensile normal stresses is adopted arbitrarily to very high and very low values, respectively. The shear stiffness is simulated by using the nonlinear elastic, hyperbolic model.

The computer analysis with the nonlinear elastic model provide reasonable to satisfactory predictions of settlements and distribution of loads in the pile groups. They also provided a good prediction for the drag forces on the lock walls which compared well with the observed values [12].

Example 3 - Laterally Loaded Structures: A generalized one-dimensional finite element procedure with idealizations shown in Fig. 4 was used to predict field behavior of a laterally loaded (wooden) pile and a sheet pile retaining wall, Fig. 5, the latter involved (approximate) simulation of construction sequences [13].

The material behavior was simulated by using spring elements to represent translational and rotational components. The nonlinear response was simulated as nonlinear elastic using a Ramberg-Osgood type function, which contains the hyperbola as a special case.

TABLE 2. Seepage and Deformable Flow

1 Problem	2 Material Behavior	3 Other Factors	4 Numerical Procedure
1. Transient Seepage in River Banks	• Darcy's Law	• Steady/Free Surface • Stability	2-D Finite Difference
2. Seepage in Dams	• Darcy's Law	• Steady/Free Surface • Stability	2-D Finite Element 3-D Finite Element - Variable Mesh
3. Seepage in Dams	• Darcy's Law	• Steady/Free Surface • Stability	2-D Finite Element 3-D Finite Element - Residual Flow Procedure - Invariant Mesh
4. Stress Seepage and Stability of Dams	• Darcy's Law • Plasticity: von Mises, Drucker-Prager	• Steady/Free Surface • Construction Sequences	2-D Finite Element - Residual Flow Procedure, - Invariant Mesh
5. Consolidation	• Darcy's Law • Linear Elastic • Plasticity - Critical State	• Construction Sequences • Anisotropy	2-D Finite Element

TABLE 3. Dynamic and Earthquake

1 Problem	2 Material Behavior	3 Other Factors	4 Numerical Procedure
1. Model Nuclear Power Plant Structure in Field	• Plasticity: - Hierarchical and Cap	• Simulated Earthquake • Thin-Layer Interfaces	2-D Finite Element
2. Instrumented Pile Segments	Plasticity - Hierarchical, Anisotropic Hardening	• Thin-Layer Interfaces • Pore Water Pressure	2-D Finite Element

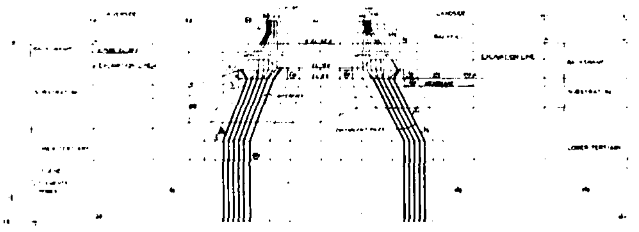

Fig. 3 Finite Element Mesh for Lock and Foundations (1 ft = 0.305 m)

Figure 6 shows comparisons for load-displacement response of the wooden pile tested in the field. Comparisons for the lateral displacements of the sheet pile for one- and two-dimensional predictions and observed response are shown in Fig. 7. This shows that the one-dimensional procedure can provide satisfactory predictions of the field behavior of some laterally loaded structures.

Example 4 - Braced Excavation: Field response of a braced wall for excavation tested in the field in Norway [14] was backpredicted by using displacement, hybrid and mixed finite element procedure [15, 16]. Details of the wall and the finite element mesh are shown in Figs. 8 and 9, respectively.

The construction sequences involving eight stages simulated are given below:

Stage 1: Compute initial stresses, install wall and excavate to el. + 0.2m.
Stage 2: Install first strut A, and excavate to el. -2.0m.
Stage 3: Install struct B, and excavate to el. -3.0m.
Stage 4: Install strut C, and excavate to el. -4.0m.
Stage 5: Excavate to el. -5.0m.
Stage 6: Install struct D, and excavate to el. -6.0m.
Stage 7: Excavate to el. -7.0m.
Stage 8: Install strut R, and excavate to el. -8.0m.

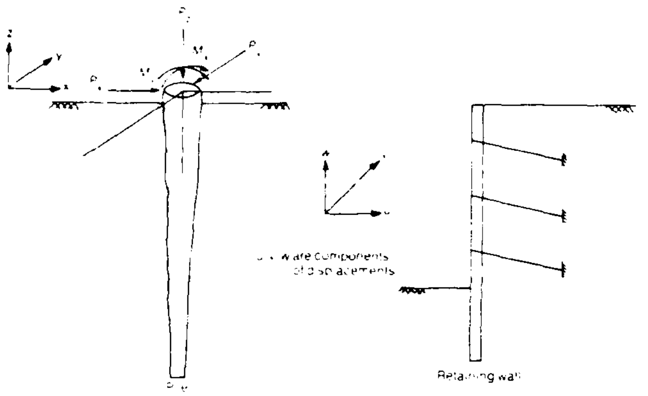
P_z
M_x
M_y
P_x
P_y
z
y
x
u, v, w are components of displacements
Retaining wall
Pile

(a) Piles

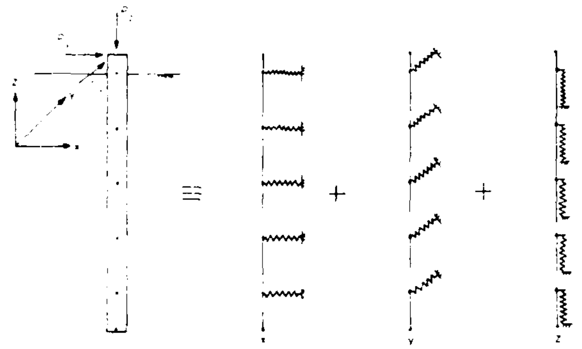

(b) Idealization

Fig. 4 Axially and Laterally Loaded Structures and Idealization

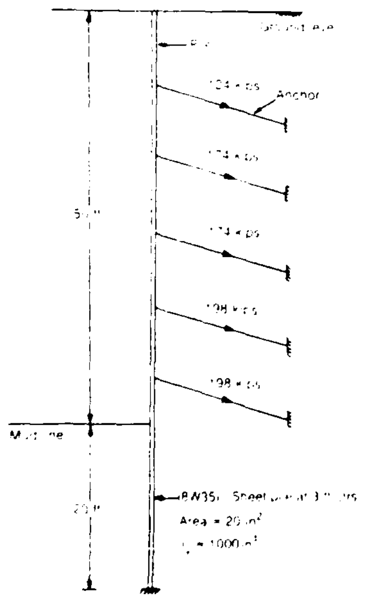
Ground level
P
104 kips
Anchor
174 kips
174 kips
198 kips
198 kips
51 ft
Mud line
20 ft
BW35 Sheet pile at 3 ft ctrs
Area = 20 in²
I = 1000 in⁴

Fig. 5 Sheet Pile Wall

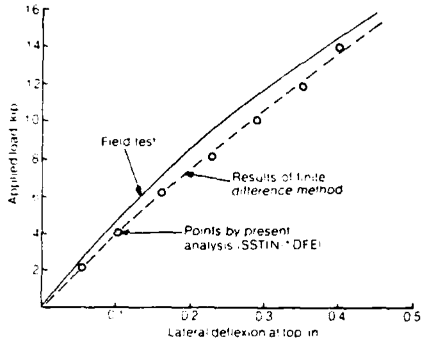

Fig. 6 Comparisons for Wooden Pile; Arkansas River, Lock and Dam No. 4

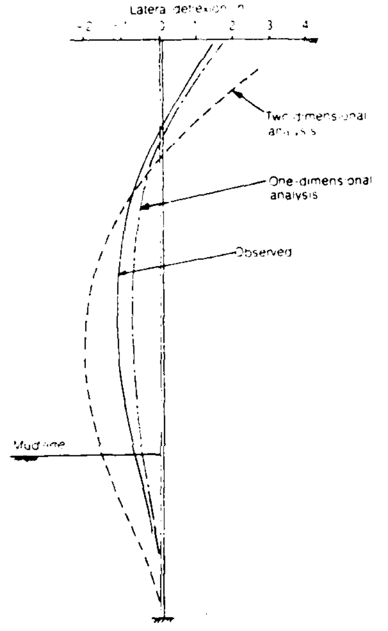

Fig. 7 Comparisons for Lateral Displacements of Sheet Pile Wall

The clayey soils were characterized by using an elastic-plastic model with von Mises yield criterion, while the wall and the struts were assumed to be linear elastic.

The new thin-layer element [17] was used to characterize the behavior of the interfaces.

Figures 10, 11 and 12 show typical comparisons between predictions and observations for wall deflections, heave and wall pressures, respectively.

It can be seen that overall the back predictions are satisfactory. It was found that the zero thickness element [10] adopted for soil-structure problems usually does not provide satisfactory predictions of interface stresses in flexible walls and situations where modes such as debonding other than slippage under compressive

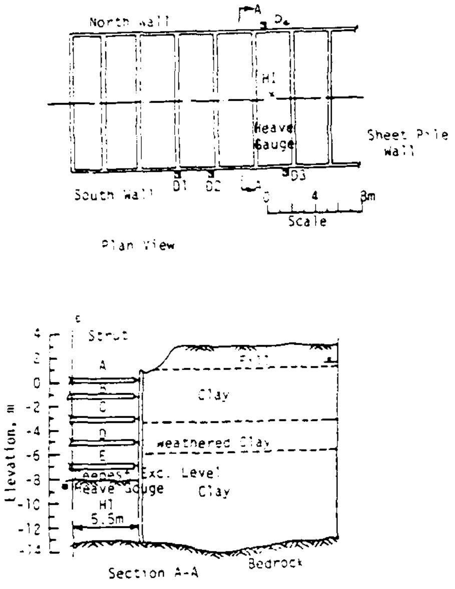
North wall
A
D4
H1
Heave Gauge
Sheet Pile wall
South wall
D1
D2
D3
0
4
8m
Scale
Plan View
Strut
A
B
C
D
E
Fill
Clay
weathered Clay
Exc. Level
Heave Gauge
H1
5.5m
Clay
Elevation, m
4
2
0
-2
-4
-6
-8
-10
-12
-14
Section A-A
Bedrock

Fig. 8 Vaterland 1, Site and Soil Profile (14)

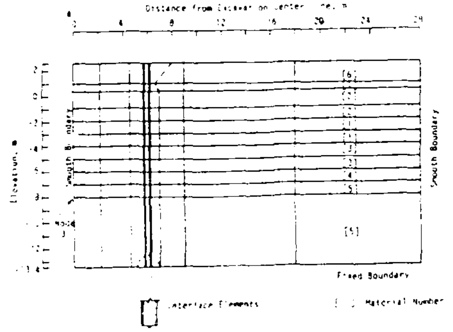
Distance from Excavation Center, m
0
4
8
12
16
20
24
28
Elevation, m
Node 3
South Boundary
Fixed Boundary
Interface Elements
Material Number
[6]
[5]
[4]
[3]

Fig. 9 Finite Element Mesh for Vaterland 1

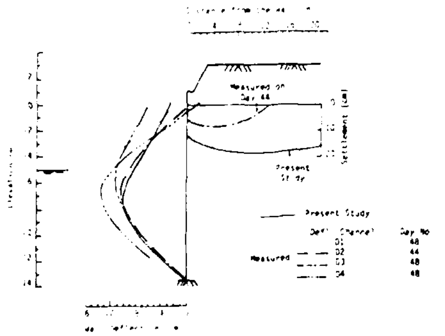

Fig. 10 Wall and Soil Deformations (Stage 5)

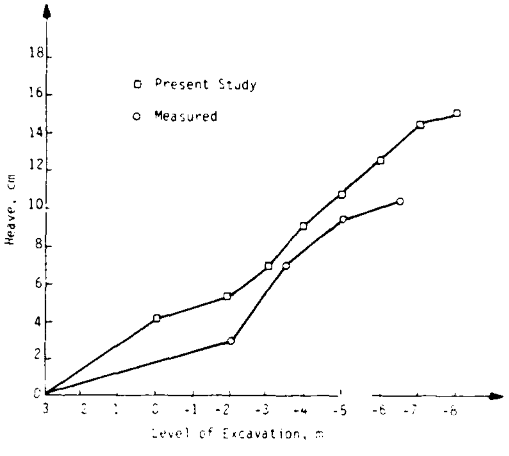

Fig. 11 Comparison of Heave at Node 3 (Figure 9)

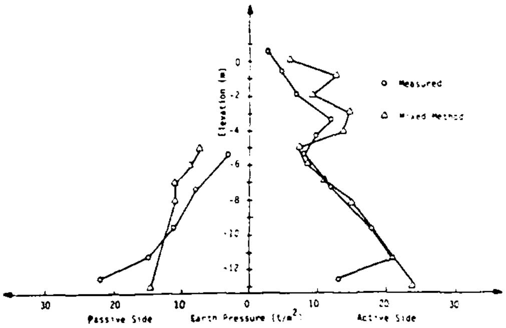

Fig. 12 Earth Pressures (Stage 5)

stresses. On the other hand, the new thin-layer element [17] provides improved predictions for the interface response and wall pressures, and also of various deformation modes. The von Mises plasticity model may be appropriate for essentially undrained response of clays. However, it is not capable of providing satisfactory predictions of volume changes, stress path dependence and dilative response.

Example 5 - Tunnels: The problem of an instrumented section of the tunnel in the Atlanta subway system [18] and the finite element mesh [19] are shown in Figs. 13 and 14, respectively. The construction sequences simulated are discussed in Ref. 19.

The rocks in the system were assumed to be linear elastic with the elastic moduli E and ν found from cylindrical and multiaxial tests [19]. The joints were simulated using the thin-layer element, and its properties were found from laboratory direct shear tests.

Figure 15 shows comparisons for displacements along an instrumented section; this and other comparisons [19] were satisfactory. However, for various reasons such as material modelling

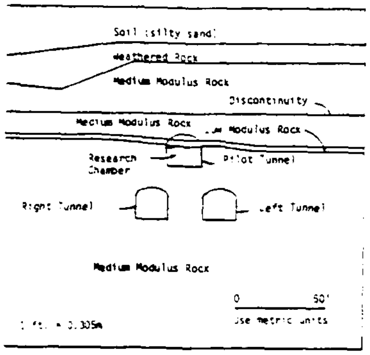
Soil (silty sand)
Weathered Rock
Medium Modulus Rock
Discontinuity
Medium Modulus Rock
Low Modulus Rock
Research Chamber
Pilot Tunnel
Right Tunnel
Left Tunnel
Medium Modulus Rock
0
50'
Use metric units
1 ft. = 0.305m

Fig. 13 Generalized Geologic Section Used for Analysis of Atlanta Subway Tunnels (18)

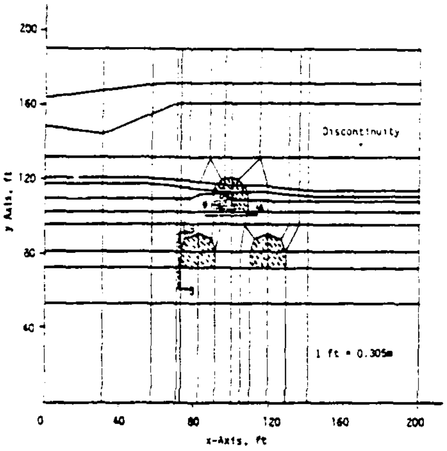
200
160
120
80
40
y-Axis, ft
Discontinuity
1 ft = 0.305m
0
40
80
120
160
200
x-Axis, ft

Fig. 14 Finite Element Mesh

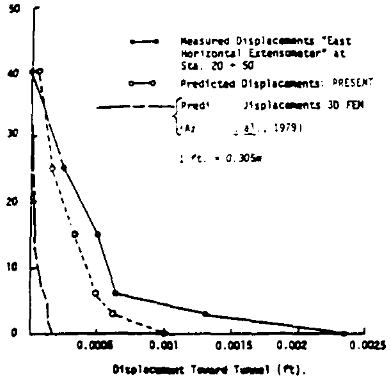

Fig. 15 Comparison Between Calculated and Observed Displacements at EE

and nearby blasting, the extensometer readings at the base of the test cavern were not predicted satisfactorily.

Example 6 - Anchors in Sand: *In the next step* towards improved material characterization, the new general yet simplified hierarchical plasticity based modelling approach [1-4] was used to study three-dimensional field behavior of grouted anchors in sand [20]. The interface response was simulated by using the thin-layer element, Fig. 16.

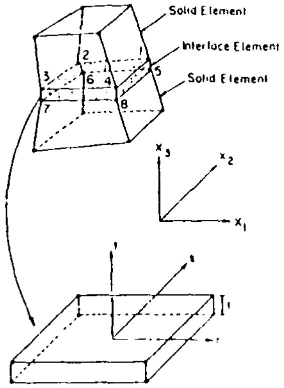
Solid Element
Interface Element
Solid Element
1
2
3
4
5
6
7
8
x_3
x_2
x_1
t
t
t

Fig. 16 Schematic of Solid and Interface Elements

Figure 17 shows details of the anchor-soil system tested in the field [21] and Fig. 18 shows details of the three-dimensional finite element mesh for the anchor-wall system.

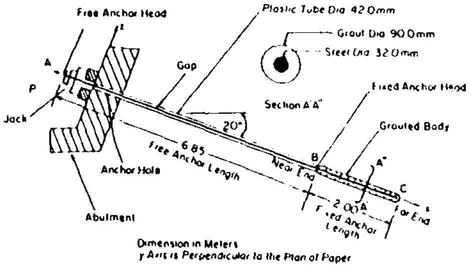
Free Anchor Head
Plastic Tube Dia 42.0mm
Grout Dia 90.0mm
Steel Dia 32.0mm
A
P
Jack
Gap
20°
Section A'A''
Fixed Anchor Head
Grouted Body
6.85
Free Anchor Length
Near End
B
A''
C
2.00
A'
Fixed Anchor Length
Far End
Anchor Hole
Abutment
Dimension in Meters
y Axis is Perpendicular to the Plan of Paper

Fig. 17 Details of Components of Anchor

The loading was simulated incrementally as in the field. Figure 19 shows comparisons between predictions and observations for the load-displacement responses of the fixed anchor head, and Fig. 20 shows load distributions along the fixed (grouted) anchor length. Figure 21 shows distributions of normal and shear stresses in the interfaces between soil and anchor for linear and nonlinear analyses.

It can be seen that the finite element procedure with the hierarchical associative, isotropic hardening model and with the thin-layer element provides very good predictions of load displacement, and stress distribution responses as well

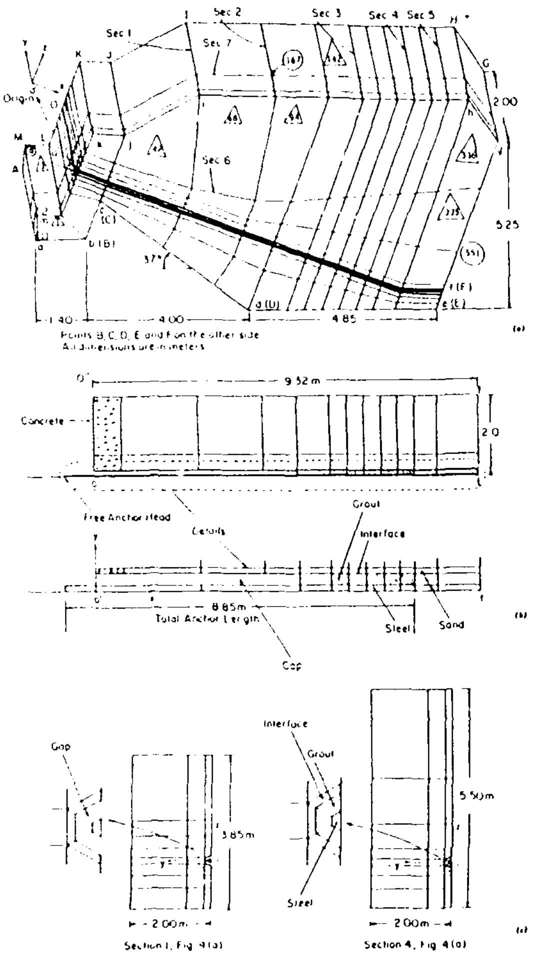
Sec 1
Sec 2
Sec 3
Sec 4
Sec 5
Sec 6
Sec 7
Origin
37°
2.00
5.25
1.40
4.00
4.85
Points B, C, D, E and F on the other side
All dimensions are in meters
(a)
9.32 m
Concrete
2.0
Free Anchor Head
Details
Grout
Interface
8.85m
Total Anchor Length
Steel
Sand
Cap
(b)
Gap
Interface
Grout
Steel
3.85m
5.50m
2.00m
2.00m
Section 1, Fig 4(a)
Section 4, Fig 4(a)
(c)

Fig. 18 Details of Finite Element Mesh: (a) Overall; (b) Along Grouted Anchor; and (c) Across Grouted Anchor

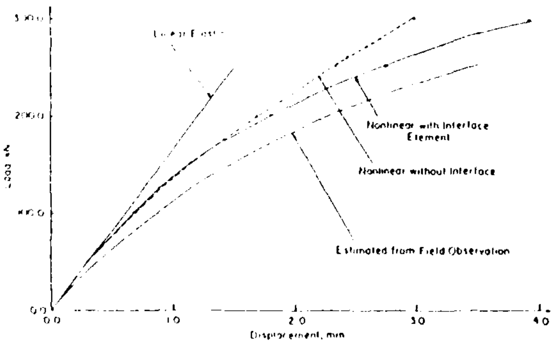

Fig. 19 Load-Displacement Curves at Fixed Anchor Head (Point B in Fig. 17)

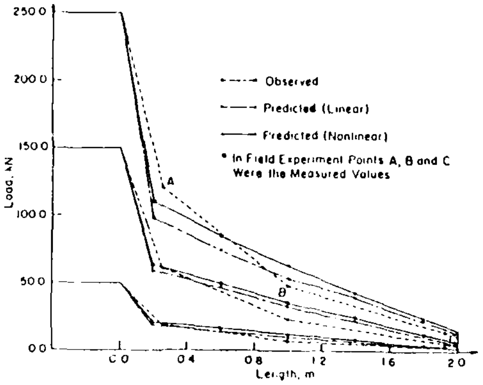

Fig. 20 Axial Load Distribution in Steel Along Fixed Anchor

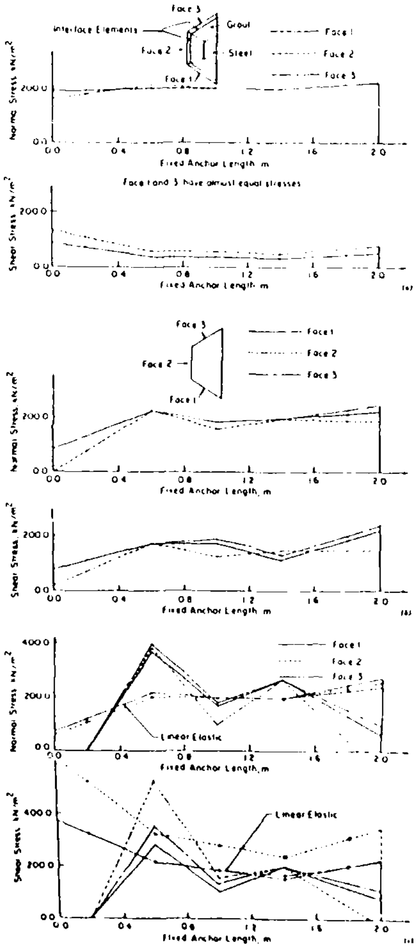

Fig. 21 Normal and Shear Stress Distributions in Interface Elements on Grouted Anchor: (a) At P = 50 kN; (b) At P = 150 kN; and (c) At P = 250 kN

as the phenomenon of stress relief and arching at the ends of the anchor.

FLOW THROUGH (RIGID) MEDIA: SEEPAGE

Steady and transient seepage, confined or unconfined (with free surface) is an important consideration in stable design of slopes, banks and dams. Although nonlinear constitutive laws describing relation between velocity and hydraulic gradient may be required for some problems, the linear Darcy's law is commonly employed in both conventional and computational procedures.

The finite difference and finite element procedures developed by the author and co-workers [22-29] have been applied for predictions of and verifications with respect to a number of analytical, laboratory and field problems. Here typical applications involving field problems and free surface flow are described. The techniques developed involve (a) variable mesh and (b) invariant mesh. The latter is based on a new method, called the Residual Flow Procedure (RFP), proposed by the author [22, 24, 26]. The RFP is mathematically different from methods proposed by other investigators [30] and has been found by Westbrook [31] to be equivalent to the recently proposed variational inequality methods for the flow problem. The RFP involving the invariant mesh is considered to be superior to the variable mesh procedure [23].

Example 7 - River Banks: The variable mesh finite element procedure [23] was used to back-predict transient development of free surfaces due to fluctuations (drawdown) in the Mississippi River Banks; typical instrumented cross section at Walnut Bend 6 with the boring log and fluctuations in the river stages are shown in Fig. 22.

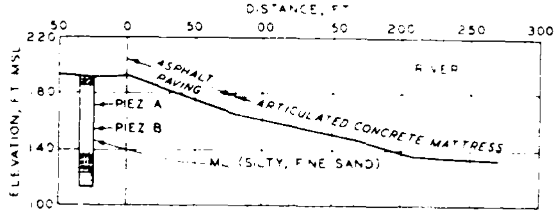

(a) Cross Section

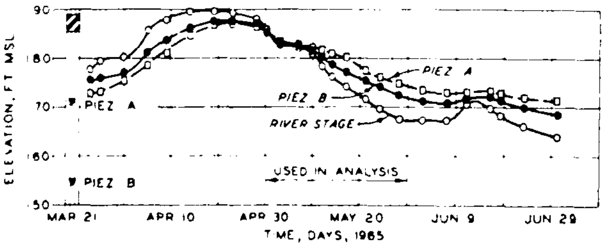

(b) Variation of Head

Fig. 22 Cross Section and Variation of Piezometer and River Heads at Walnut Bend 6

The finite element mesh and typical comparisons between back predictions at two time levels during the drawdown are shown in Fig. 23. The values of permeability k, porosity f and the time step Δt are also shown on Fig. 23. These results indicate that the numerical procedures provide very good predictions of the observed response.

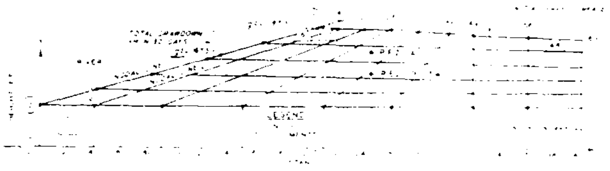

a. Mesh

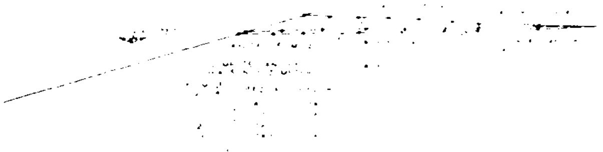

b. AFTER 20 DAYS

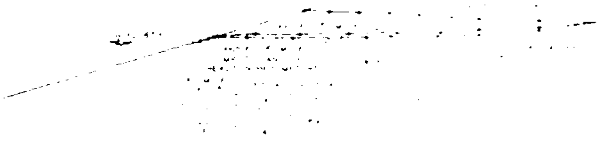

c. AFTER 30 DAYS

Fig. 23 Mesh and Comparisons Between Predictions and Observations

After a comprehensive series of comparisons between predictions and observations in the laboratory (using Hele-Shaw model) and the field behavior, design charts for stability analysis were also prepared [32].

Example 8 - Earth Dam: The field observations and material properties, variation of reservoir head with time and details of the Sherman Dam were provided by the U. S. Bureau of Reclamation [25], Fig. 24. The material in the dam was mostly clay, and the coefficient of permeabilities at various locations, Fig. 24(c), obtained from laboratory permeability and consolidation tests, were used to adopt an average value of k = 0.01 ft/year (0.03 m/yr).

The finite element mesh consisted of 408 nodes and 318 elements, Fig. 25. Comparisons between predictions and observations for computed head for typical piezometer locations are shown in Fig. 26. Despite various approximations such as the adoption of average permeability and assumption of fully saturated condition instead of possible partial saturation, the comparisons show good agreements.

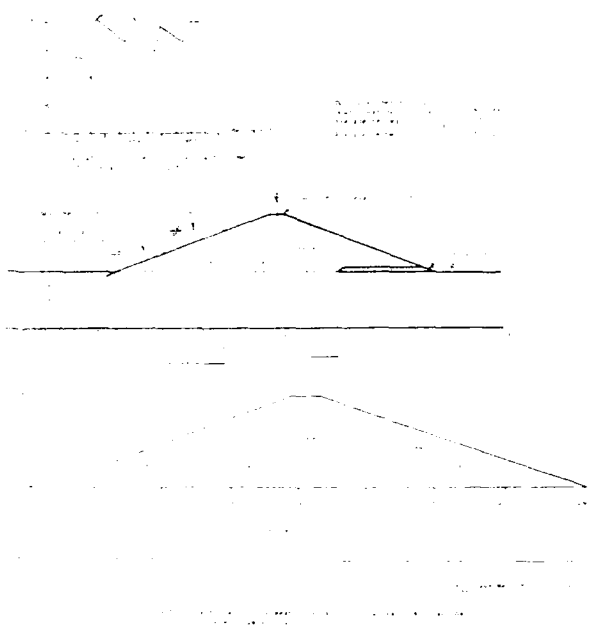

Fig. 24 Details of Sherman Dam

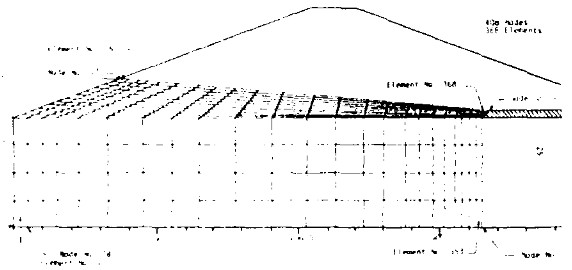

Fig. 25 Finite Element Mesh for the Sherman Dam

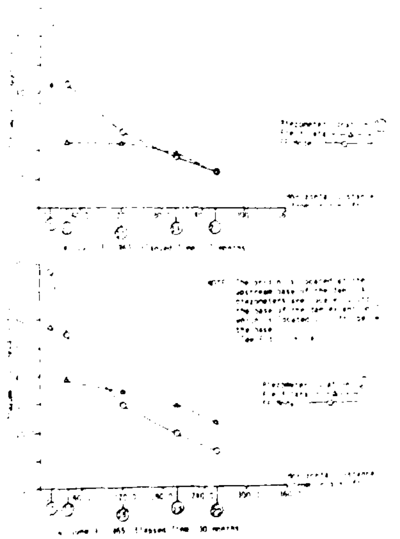

Fig. 26 Comparisons of Computed and Observed Heads

Example 9 - Combined Stress and Seepage in Dams: The assumption of rigid skeleton in conventional seepage may be too restrictive for certain field situations because, in general, soils in dams or slopes experience deformations during seepage. The general way of treating the problem is to use coupled (Biot's) theories for dynamic and static analysis of porous media. For practical analysis, however, it may often be appropriate to use the intermediate uncoupled approach. Here the nonlinear stress analysis is performed by superimposing on it known seepage forces caused by steady or transient seepage.

Applications of the uncoupled approach for back predictions of the field behavior of various dams have been presented in Ref. 27. Here the RFP is coupled with a nonlinear finite element with elastoplastic models for soils. The procedure also allows for sequential construction (embankment) of dams or banks with simultaneous transient change in head, and slope stability analysis.

The procedure possesses a number of advantages: For example, (a) the systematic approach for uncoupled analysis, (b) with RFP the same mesh is used for both stress and seepage analysis, (c) avoids necessity of assuming horizontal (transient) free surfaces in the region between upstream and the core of dam as was done in Ref. 33, and (d) can allow for partial saturation.

Figure 27 shows a cross section of the Oroville Dam [33] and transient locations of free surface due to the hydrograph showing variation of head with time in the reservoir. Figures 28 and 29 show comparisons between computed and observed horizontal movements for two sections, and observed movements of the core section, respectively. The back predictions show good correlation with observations.

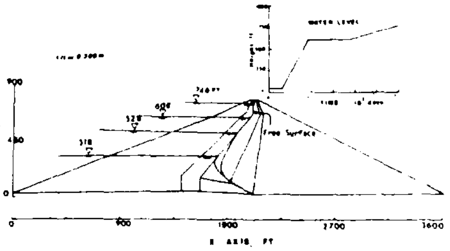

Fig. 27 Section of Oroville Dam, Hydrograph and Computed Locations of Free Surfaces During Reservoir Filling

Example 10 - Consolidation, Seepage in Deformable Soils: In order to allow for full coupling between flow and deformation, Biot's theory of flow through deformable media is often used [34]. Here both the displacements and pore water pressure are assumed to be unknowns in the finite element analysis.

Computations using a two-dimensional finite element procedure based on the Biot's theory were performed for a layered foundation involving clay deposits, Fig. 30 [35], the finite element mesh is shown in Fig. 31.

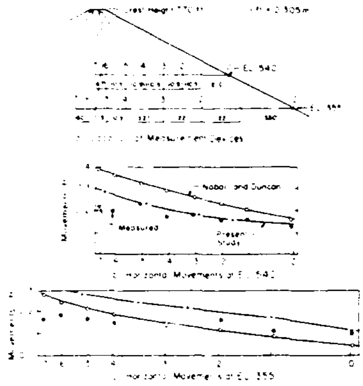

Fig. 28 Comparison of Computed and Observed Horizontal Movements for Two Sections

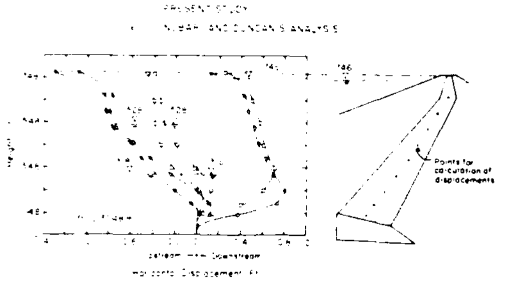

Fig. 29 Comparison of Computed Movements at a Section in Core

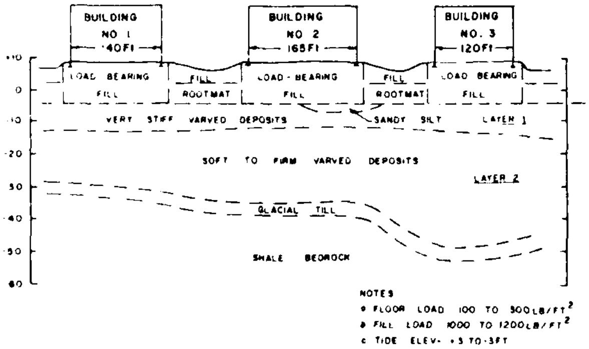
BUILDING NO. 1
140Ft
BUILDING NO. 2
165Ft
BUILDING NO. 3
120Ft
LOAD BEARING FILL
FILL
ROOTMAT
LOAD - BEARING FILL
FILL
ROOTMAT
LOAD BEARING FILL
VERY STIFF VARVED DEPOSITS
SANDY SILT
LAYER 1
SOFT TO FIRM VARVED DEPOSITS
LAYER 2
GLACIAL TILL
SHALE BEDROCK
ELEVATION, FT
+10
0
-10
-20
-30
-40
-50
-60
NOTES
a. FLOOR LOAD 100 TO 300LB/FT²
b. FILL LOAD 1000 TO 1200LB/FT²
c. TIDE ELEV. +5 TO -3FT

Fig. 30 Foundation in Varved Clay (from Reference 35)

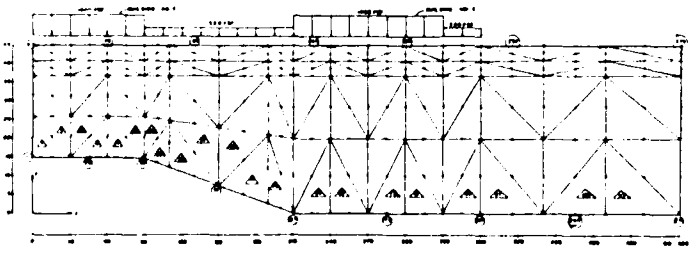

Fig. 31 Finite Element Mesh and Loading

It was found [35] that the settlement computations from the conventional one-dimensional Terzaghi theory were far too smaller than those observed in the field. Among the reasons for the discrepancy are the two-dimensional nature of the system, anisotropic characteristics of the varved clay and the history of loading. The finite element computations included effects of these three factors. In addition, parametric studies were performed in which the ratios of the horizontal to vertical permeabilities of the varved clay were varied. The computed settlements are compared with the observed values at typical locations in Fig. 32. It can be seen that the proposed procedure is capable of predicting the observed response, and that the computations with k_x/k_y = 10 showed the best correlation. This ratio is comparable to that found for many varved clays.

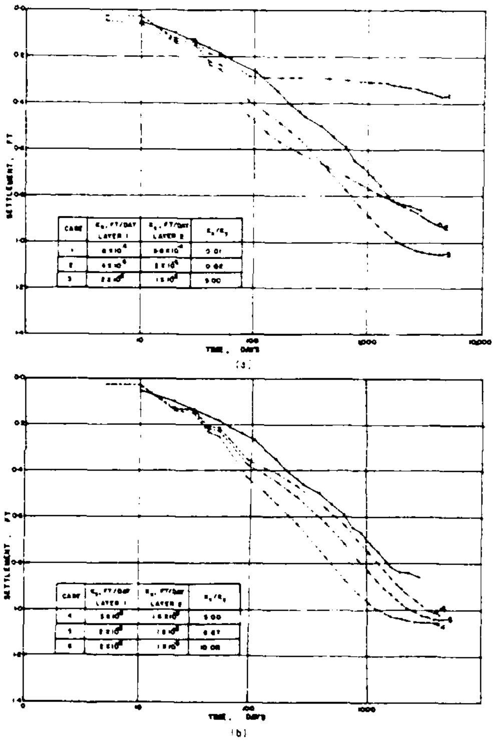

Fig. 32 Numerical Results and Comparison with Field Data for Variations in k_x/k_y

DYNAMIC ANALYSIS (36-42)

For dynamic nonlinear soil-structure interaction problems among other factors, it is necessary to consider the effects of relative motions at interfaces, nonlinear soil response including anisotropic hardening, and appropriate time integration schemes.

The problem of relative motions is handled by using the thin-layer element [17] and laboratory experiments using the cyclic multi-degree-of-freedom (CYMDOF) shear device [36] for determination of nonlinear elastic Ramberg-Osgood type [39] and elastoplastic hierarchical models [41].

The hierarchical model also allows for a general yet simplified model for anisotropic hardening due to cyclic loading [2, 4]. A procedure called Generalized Time Finite Element (GTFEM) is also proposed for improved time integration for nonlinear dynamics problems [42].

The author and co-workers [36-42] have performed comprehensive research on the above factors and applied the finite element procedure for comparisons with analytical solutions, and experimental (laboratory and field) observations.

Example 11 - Model Nuclear Power Plant Structure: A typical application for behavior of a model nuclear power plant structure SIMQUAKE II tested in the field [37, 43] is given below.

Figure 33 shows details of the SIMQUAKE II test structure, involving a 1/8 scale model of a nuclear power plant founded in a cohesionless soil [43]. The structure, interfaces and boundary of the soil island, Fig. 33, were instrumented with displacement, velocity, acceleration and pressure measuring devices. A blast type load was applied in two events at an interval of 1.2 seconds.

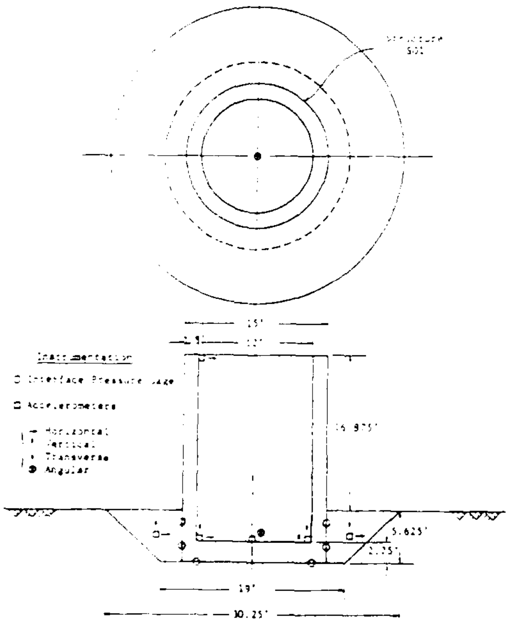

Fig. 33 1/8 Scale Model SIMQUAKE Structure (S01) Including Structural and Near-Field Instrumentation [43]

The interfaces, see mesh in Fig. 34, were characterized by using the Ramberg-Osgood type model and allowed for no slip, slip, debonding and rebonding motions, as well as control of interpenetration. The sand was characterized by using both the cap [43] and the δ_0-version of the hierarchical model [2]. The measured velocities on the boundaries of the soil island were integrated to obtain the displacement vs. time input.

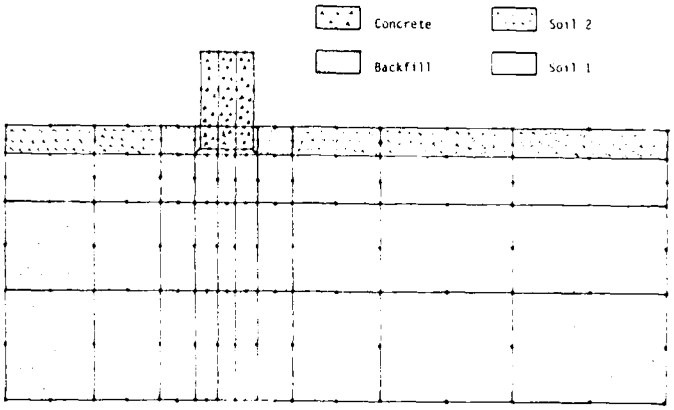

Fig. 34 Mesh Used in Simulation of Soil-Structure Interaction Due to SIMQUAKE II

Figures 35, 36 and 37 show comparisons between predictions and observations for typical horizontal and vertical velocities and contact pressures, respectively. It can be seen that overall the predictions show good comparisons with observations. The interface model assigns arbitrary high or low value for the normal stiffness during bonded and debonded states, respectively. This may be one of the reasons for the discrepancies. It is observed that for realistic simulation of interface response appropriate constitutive models for the normal response should be developed and used [40].

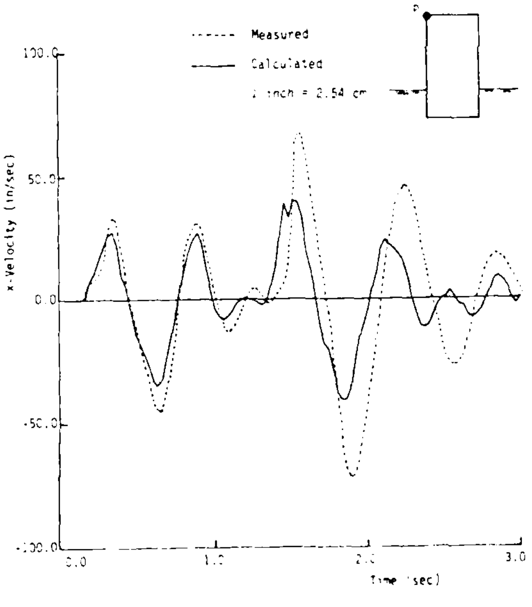

Fig. 35 Comparison of Computed and Measured Horizontal Velocity-Time History at Top of Structure, Point P

AD-A213 199 INTERNATIONAL CONFERENCE ON CASE HISTORIES IN 8/8
GEOTECHNICAL ENGINEERING (2. (U) MISSOURI UNIV-ROLLA
S PRAKASH 30 JUN 89 ARO-25645.2-GS-CF DAAL03-87-G-0129
UNCLASSIFIED F/G 13/2 NL

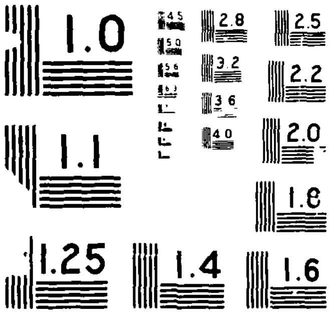
1.0
4.5
5.0
5.6
6.3
2.8
3.2
3.6
4.0
2.5
2.2
2.0
1.1
1.8
1.25
1.4
1.6

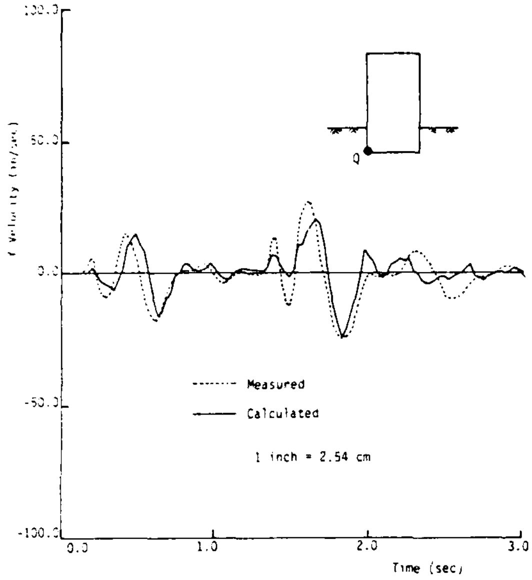

Fig. 36 Comparison of Computed and Measured Vertical Velocity-Time History at Upstream Corner of Structure, Point Q

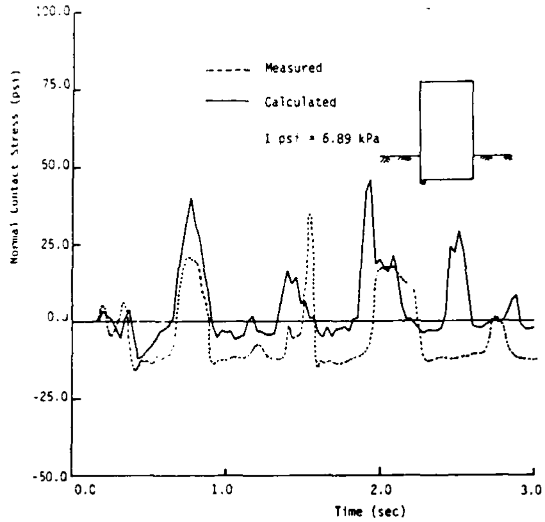

Fig. 37 Comparison of Calculated and Measured Normal Contact Stress-Time Histories Beneath Upstream Corner of Structure

CONCLUSIONS

Use of both conventional and modern solution procedures are important components for development of safe and economical schemes for design, analysis and performance evaluation of field structures. The 'art' of geotechnical engineering toward development of simplified and empirical procedures relies on intuition, experience and scientific thinking. The tradition of using conventional and empirical procedures for case studies is important in our heritage for design of geotechnical systems, and can provide satisfactory solutions for many problems; they need to be used, nurtured, and improved. At the same time, it is essential to continue vigorously to develop innovative and advanced procedures through a process of rational simplification starting with fundamental principles of mechanics and physics so as to reduce or eliminate a number of assumptions inherent in the conventional procedures. This is vital because many complex factors such as nonlinear response, loadings, geometries and environmental effects influence response of geotechnical problems.

This paper presents a summary of the personal experience of the author involving continuous modifications in thinking from use of conventional to advanced computer procedures. One of the main factors in this narrative has been constitutive models for geologic materials and discontinuities. Here the author has gone from use of linear elastic and piecewise linear elastic models about two decades ago to general models that can go beyond the capabilities of the models used in the past. In this growth, the objective of working towards 'simplified' models that can be applied easily in practice, starting from fundamentals, has been followed. The author can conclude that it is possible to develop as or more simplified models than linear and nonlinear elastic that can allow inclusion of many important effects towards more rational case studies of geotechnical problems.

Finally, the author believes that in order to remain competitive and advance into the next century, it is essential to improve our methods through scientific inquiry coupled with intuition and experience, in addition to using and improving on conventional empirical procedures.

ACKNOWLEDGMENTS

The results presented herein represent a part of the author's work over the last two decades. They include participation of a number of his students and colleagues, and support of a number of funding agencies.

REFERENCES

1. Desai, C.S. (1980), "A General Basis for Yield, Failure and Potential Functions in Plasticity," International Journal for Numerical and Analytical Methods in Geomechanics, vol. 4, no. 4.

2. Desai, C.S., S. Somasundaram, and S. Frantziskonis (1986), "A Hierarchical Approach for Modelling of Geologic Materials," International Journal for Numerical and Analytical Methods in Geomechanics, vol. 3, no. 3.

3. Frantziskonis, G., C. S. Desai, and S. Somasundaram (1986), "Constitutive Model for Nonassociative Behavior," Journal of Engineering Mechanics, ASCE, vol. 112, no. 9.

4. Somasundaram, S. and C.S. Desai (to appear) "Modelling and Testing for Anisotropic Behavior of Soils," Journal of Engineering Mechanics, ASCE.

5. Desai, C. S. (1974), "Numerical Design Analysis of Piles in Sands," Journal of Geotechnical Engineering, ASCE, vol. 100, no. 6, 613-635.

6. "Pile Driving and Loading Tests: Lock and Dam No. 4, Arkansas River and Tributaries, Arkansas and Oklahoma," (Sept. 1964) Fruco and Assoc., United States Army Engineer District, CE, Little Rock, Arkansas.

7. Duncan, J. M., and C.Y. Chang (1970), "Nonlinear Analysis of Circular Footings in Layered Soils," Journal of Soil Mechanics and Foundations Division, ASCE, vol. 96, no. SM5, Proc. Paper 7513, 1629-1653.

8. Desai, C.S., and L.C. Reese (1970), "Analysis of Circular Footings in Layered Soils," Journal of Soil Mechanics and Foundations Division, ASCE, vol. 96, no. 4.

9. Desai, C.S. (1971), "Nonlinear Analysis Using Spline Functions," Journal of the Soil Mechanics and Foundations Division, ASCE, vol. 97, no. SM10, Proc. Paper 8462, 1461-1480.

10. Goodman, R.R., R.L. Taylor, and T.L. Brekke (1968), "A Model for the Mechanics of Jointed Rock," Journal of the Soil Mechanics and Foundations Division, ASCE, vol. 94, no. SM3, Proc. Paper 5937, 637-659.

11. Desai, C.S., L.D. Johnson, and C.M. Hargett (1974), "Analysis of Pile-Supported Gravity Lock," Journal of Geotechnical Engineering, ASCE, vol. 110, no. 9, 1009-1029.

12. Montgomery, R.L. and A.L. Sullivan, Jr. (1972), "Interim Analysis of Data from Instrumentation Program, Columbia Lock," Miscellaneous Paper S-72-30, United States Army Engineer Waterways Experiment Station, Vicksburg, Mississippi.

13. Desai, C.S. and T. Kuppusamy (1980), "Application of a Numerical Procedure for Laterally Loaded Structures," Proceedings, International Conference on Numerical Methods in Offshore Piling, Institution of Civil Engineers, London, 93-99.

14. Clausen, C.J.F. (1971), "Finite Element Analysis of Strutted Excavation at Vaterland 1," Report No. 52601-2, Norwegian Geotechnical Institute, Oslo, Norway.

15. Desai, C.S. and S. Sargand (1984), "Hybrid FE Procedure for Soil-Structure Interaction," Journal of Geotechnical Engineering, ASCE, vol. 110, no. 4, 473-687.

16. Desai, C.S. and J. G. Lightner (1985), "Mixed Finite Element Procedure for Soil-Structure Interaction and Construction Sequences," International Journal for Numerical Methods in Engineering, vol. 21, 801-824.

17. Desai, C.S., M.M. Zaman, J.G. Lightner, and H.J. Siriwardane (1984), "Thin-Layer Element for Interfaces and Joints," International Journal for Numerical and Analytical Methods in Geomechanics, vol. 8, no. 1.

18. Rose, D.C. et al. (1979), The Atlanta Research Chamber, Applied Research Monographs, Report No. UMTA-GA-06.007-79-1: U. S. Dept. of Transportation, Urban Mass Transp., Washington, D. C.

19. Desai, C.S., I.M. Eitani and C. Haycocks (1983), "An Application of Finite Element Procedure for Underground Structures with Non-Linear Materials and Joints," Proc. 5th Congress, International Society Rock Mech., Melbourne, Australia.

20. Desai, C.S., A. Muqtadir, and F. Scheele (1986), "Interaction Analysis of Anchor-Soil Systems," Journal of Geotechnical Engineering, ASCE, vol. 112, no. 5, 537-553.

21. Scheele, F. (1981), "Tragfaigkeit von Verpressankern in nichtbinddigem Boden, Neue Erkenntnisse durch Dehnungsmessungen im Verankernungsbereich," Dissertation presented to the Univ. of Munich, W. Germany, in partial fulfillment of the requirements for the degree of Doctor of Philosophy.

22. Desai, C.S. and W.C. Sherman (1971), "Unconfined Transient Seepage in Sloping Banks," Journal of Soil Mechanics and Foundations Division, ASCE, vol. 97, no. 2, 357-373.

23. Desai, C.S. (1972), "Seepage Analysis of Banks Under Drawdown," Journal of Soil Mechanics and Foundations Division, ASCE, vol. 98, no. 11, 1143-1162.

24. Desai, C.S. (1976), "Finite Element Residual Schemes for Unconfined Flow," International Journal for Numerical Methods in Engineering, vol. 10, no. 6, 1415-1418.

25. Desai, C.S. and T. Kuppusamy (1980), Development of Phreatic Surfaces in Earth Embankments, Report to USBR, Virginia Tech, Blacksburg, Virginia.

26. Desai, C.S. and G. L. Li (1983), "A Residual Flow Procedure and Application for Free Surface Flow in Porous Media," Journal for Advances in Water Resources, vol. 6, 27-35.

27. Li, G.C. and C. S. Desai (1983), "Stress and Seepage Analysis of Earth Dams," Journal of Geotechnical Engineering, ASCE, vol. 109, no. 7, 946-960.

28. Desai, C.S. (1984), "Free Surface Flow Through Porous Media Using a Residual Procedure," Chapter 18 in *Finite Elements in Fluids*, Gallagher, R.H. et al. (Eds), John Wiley & Sons Ltd., U.K.

29. Baseghi, B. and C.S. Desai (1987), "Three-Dimensional Seepage Through Porous Media with the Residual Flow Procedure," Report, Dept. of Civil Engg. & Engg. Mech., Univ. of Arizona, Tucson, Arizona.

30. Neuman, S.P. (1973), "Saturated-Unsaturated Seepage by Finite Elements," Journal of Hydraulics Division, ASCE, vol. 99, no. 12, 2233-2250.

31. Westbrook, D.R. (1977), "Analysis of Inequality and Residual Flow Procedures and an Iterative Scheme for Free Surface Seepage," International Journal for Numerical Methods in Engineering, vol. 21, 1791-1802.

32. Desai, C.S. (1977), "Drawdown Analysis of Slopes by Numerical Method," Journal of Geotechnical Engineering, ASCE, vol. 103, no. 7, 667-676.

33. Nobari, F.S. and J.M. Duncan (1972), "Effects of Reservoir Filling on Stresses and Movements in Earth and Rockfill Dams," Report No. S-72-2, U. S. Army Engineer Waterways Experiment Station, Vicksburg, Mississippi.

34. Desai, C.S. and S.K. Saxena (1977), "Consolidation Analysis of Layered Anisotropic Foundations," International Journal for Numerical and Analytical Methods in Geomechanics," vol. 1, 5-23.

35. Baker, G.L. and W. A. Marr (1976), "Consolidation Behavior of Structural Fills on Hackensack Varved Clays," Paper at Annual Meeting of Transp. Res. Board, Washington, D. C.

36. Desai, C.S. (1981), "Behavior of Interfaces Between Structural and Geologic Media," State-of-the-Art Paper, Proceedings, International Conference on Recent Advances in Geotechnical Earthquake Engineering, St. Louis, Missouri.

37. Zaman, M.M., C.S. Desai and E.C. Drumm (1984), "An Interface Model for Dynamic Soil-Structure Interaction," Journal of Geotechnical Engineering, ASCE, vol. 110, 1257-1273.

38. Desai, C.S., E.C. Drumm and M.M. Zaman (1985), "Cyclic Testing and Modelling of Interfaces," Journal of Geotechnical Engineering, ASCE, vol. 111, 793-815.

39. Drumm, E.C. and C.S. Desai (1986), "Determination of Parameters for a Model for the Cyclic Behavior of Interfaces," Journal Earthquake Engineering and Structural Dynamics, vol. 14, 1-18.

40. Desai, C.S. and B.K. Nagaraj (in press), "Modelling for Normal and Shear Behavior of Contacts and Interfaces," Journal of Engineering Mechanics, ASCE.

41. Desai, C.S. and K.L. Fishman (1987), "Constitutive Models for Rocks and Discontinuities (Joints)," Proceedings, 28th U.S. Symposium on Rock Mechanics, Tucson, Arizona.

42. Kujawski, J. and C.S. Desai (1984), "Generalized Time Finite Element Algorithm for Nonlinear Dynamic Problems," International Journal of Engineering Computations, vol. 1, no. 3.

43. Vaughan, D.K. and Isenberg, J. (1982), "Nonlinear Soil-Structure Analysis of SIMQUAKE II," Research Project 810-2, Final Report for Electric Power Research Institute (EPRI).

Proceedings: Second International Conference on Case Histories in Geotechnical Engineering, June 1-5, 1988, St. Louis, Mo., Invited Paper

Movement in the Powerhouse Excavation Saguling Project, Indonesia

George F. Sowers
Senior Vice President, Law Engineering, Atlanta, Georgia
Regents Professor Emeritus, Georgia Institute of Technology,
Atlanta, Georgia

SYNOPSIS: Ground expansion and finally sliding occurred in one corner of the 25 m deep open excavation for the powerhouse. The movement occurred in a slickensided claystone overlain by water bearing sandy gravel. The cause was expansion of the claystone followed by its weakening from water pressure in the open slickensided cracks. The excavation was finally stabilized by drainage plus reinforced sloping walls restrained by cable anchors in the rock below. The paper summarizes the pertinent soil and rock properties and describes the analyses of the movements, the corrective measures and their varied performance, and the professional lessons to be gained.

INTRODUCTION

The Saguling project is the largest hydroelectric plant in the Republic of Indonesia. It is in West Java, about 100 km southeast of the Capital, Jakarta, and about 40 Km west of Bandung, a large industrial and commercial center. The Citurum River rises in a ring of volcanic mountains in West Java. The mountains interrupt the flow of moist air from the Indian Ocean and producing high rainfall within the Citurum watershed. The 98 m high dam creates the reservoir just upstream of the river's fall through a narrow canyon between mountain ridges on its way to the sea. The water is directed around the canyon in twin tunnels 6 km long, down a mountainside in twin penstocks in a cut as deep as 25 m (82 ft), and into the Powerhouse, developing 385 m (1270 ft) of head. The installed generating capacity is 700 megawatts initially with a potential capacity of 1400 megawatts in peaking power. The river profile is shown in Fig. 1.

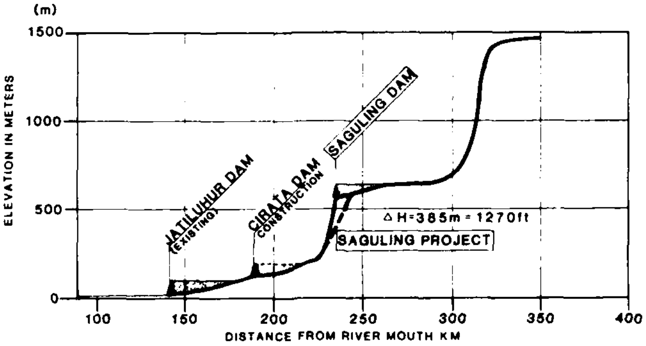

Fig. 1 Profile of the Citurum River

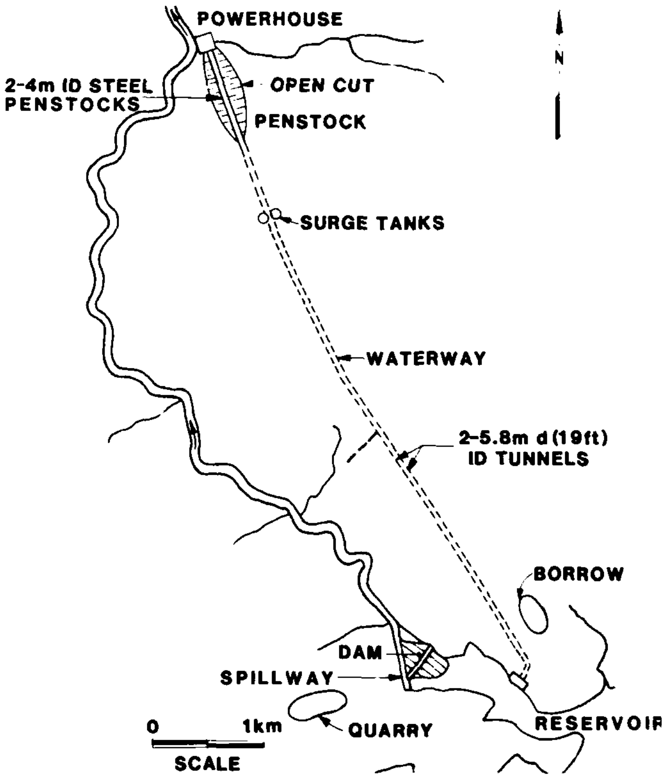

Fig. 2 Layout of Principal Project Components

The major project components are the river diversion tunnels, the rockfill dam with an earth core, waterway tunnels, surge tanks steel penstocks, power house, and switchyard. They extend for about 8 km across low mountains and narrow valleys occupied by rice fields, teak plantations, and occasional jungle, with numerous small villages connected by narrow winding roads. The principal component layout is shown in Fig. 2.

construction required roads for access and housing for personnel, beginning during site exploration and continuing through construction and eventually for project operation.

The design was largely complete in mid 1980 after about 5 years of planning and investigation. Construction commenced in September 1981 and was virtually complete in 1985. The project has been generating power for more than two years, and is a key component of the national electric power company, PLN.

Geotechnical Problems During Construction

Both the site geology and climate present problems for engineering design and construction. Most were anticipated and overcome without incidents. However, landslides were an intermittent hazard to construction works and a cause of construction delay and additional cost.

The site geology is complex. Most of the site formations have a volcanic origin. Many are intrusions and indurated volcanic ash; others are sediments derived from the erosion and redeposition of volcanic/materials in the sea or in a shallow lake basin between the mountains. The formations are comparatively young: the oldest of Tertiary age and the youngest contemporary accumulations of silt from the muddy streams and volcanic ash from still active nearby volcanoes.

There is local limestone of Tertiary Age formed during periods of land subsidence that alternated with violent uplifts of the land. Tectonic forces produced folding and tilting of these young formations, with some of these forces remaining to confound engineers and geologists. Because of recent tectonic movements, many of the more brittle tuffs and similar rocks contain networks of cracks. These are both surfaces of weakness and confined aquifers in which water pressure reduces effective normal stress and shear resistance.

The climate is hostile, particularly to land stability and durability of engineered construction. The average rain of 2320 mm or 91 in. comes largely during the 6 month wet season, beginning in late November and ending in April or May. Rainfall can be extremely intense, including violent thunderstorms. The dry season alternates between periods of no rain of several weeks long periods of predominately dry weather with occasional short wet periods. As a result humidity ranges from moderate to very high, and fluctuates rapidly during the dry season.

The temperature is uniformly high, 30 to 35 C during the day and 18 to 20 C at night. Because of the high rainfall and warm temperature, rock weathering occurs rapidly. The near surface soils and rock either remain saturated or become saturated during the rainy season. Standing water in rice fields and irrigation of all crops during the dry season aggravates the water problems.

The combination of complex formations makes it difficult to accurately characterize the soils and rocks and to analyze stability. Similarly the environmental changes causing weathering and pore pressure increases are difficult to quantify. Therefore, all of the stability problems were not anticipated in project design.

Objective of Paper

Despite the geologic and environmental conditions it has been possible to identify some of the complexities after failure has occurred and to determine how to avoid similar problems in the future. Although instability accompanied excavation at many project locations, this paper is limited to instability in the Powerhouse excavation. The failures have been previously described by Maru and Shaw, 1984. The purpose of this paper is to describe the movements, evaluate the difficulties with their evaluation, and to show what changes are needed in our engineering methods to improve our technology.

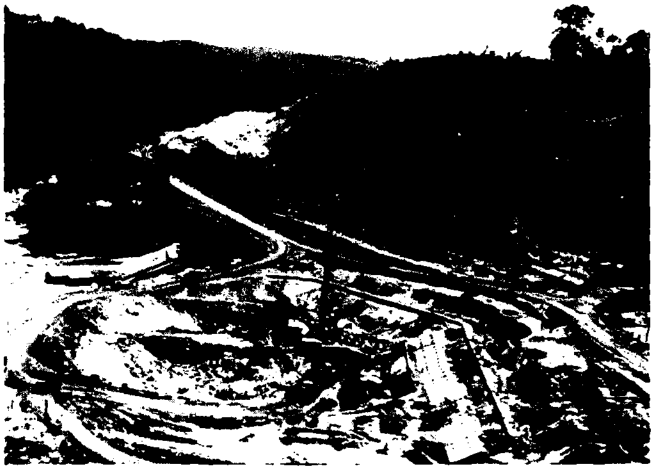

Fig. 3 The Powerhouse Excavation Looking Northwest with the Limestone Ridge in the Background, January 1983, with the Anchored Concrete Restraining System under Construction

THE POWERHOUSE SITE

The Powerhouse is a narrow flood plain and alluvial terrace on the right bank of the river, where the canyon broadens and the slope decreases. The river surface is normally El. 253 m (835 ft), the flood plain, El. 255, and the terrace El. 265, 12 m or 40 ft above the river. Just south of the site a narrow irregular limestone ridge with steep slopes is cut by the river. The ridge crest is about 200 m or 660 ft south of the Powerhouse and it rises to about El. 395, 130 m or 430 ft above the terrace. To the north, the land slopes steeply upward to about El. 700 or 2310 ft. The waterway tunnels exit on this slope and feed twin steel penstock tubes which drop northwestward into the powerhouse. Figure 3 shows the excavation looking north from the lower penstock toward the limestone ridge.

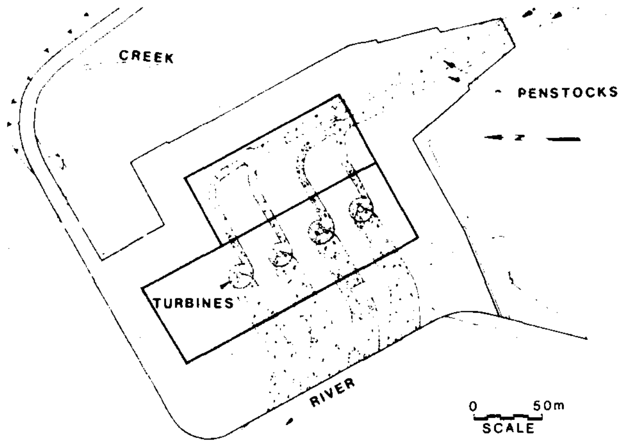

Fig. 4 Powerhouse Plan

The Powerhouse plan is shown in Fig. 4 and a typical cross section through one of the turbine-generator units in Fig. 5. Its long wall is parallel to the river. The penstocks enter the site from the southeast corner, bifurcate and turn toward the river. In order to minimize cavitation the turbine scroll cases are well below river level. This required excavation to EL. 232 m, 33 m or 109 ft below the terrace for the draft tubes and to El. 240, 25 m or about 83 ft below the terrace for the general excavation including the penstocks.

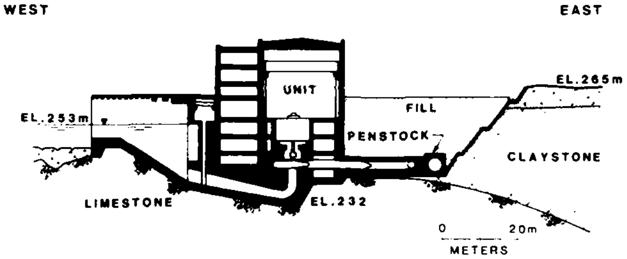

Fig. 5 Powerhouse Cross Section

Soil and Rock Conditions

The soil and rock conditions were explored by seismic refraction profiles, boring with intermittent soil samples and continuous rock coring, and shallow test pits. Laboratory tests for index properties of soil and for the strength of the rock cores were made to define engineering properties for project design. Geologic cross sections were prepared showing the elevations of the strata boundaries for both design and construction planning.

Fig. 6 is a typical excavation cross section, from the contract drawings, depicting three distinct strata. A sandy gravel terrace, about 10 m thick is uppermost. It consists of cobble to fine gravel-size rounded particles of limestone, sandstone, and some volcanics, with a matrix of sand and partially bonded by silt and clay. Below is massive claystone, 15 to 30 m thick. It is well indurated, apparently by consolidation, but without an obvious fissile structure. The clay minerals are dominantly kaolinite and illite. Deeper horizons of the claystone are calcareous, and contain some montmorillonite. The plasticity of the remolded reworked claystone is low, and is classified as CL, even those horizons containing montmorillonite. The stratum is firm to hard with unconfined compressive strengths of 5 to 45 kg/cm^2. The cores show the claystone to be cut by numerous fissures, with random orientations and spacings of between 10 and 100 cm. Many of the fissures are slickensided, as illustrated in Fig. 7.

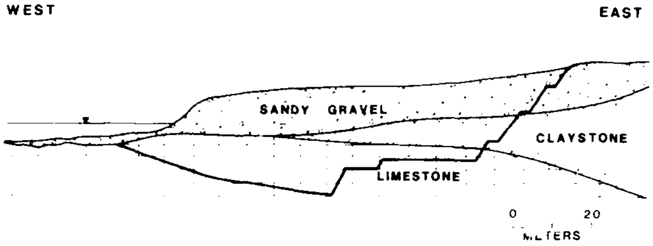

Fig. 6 Contract Design for Excavation Cross Section

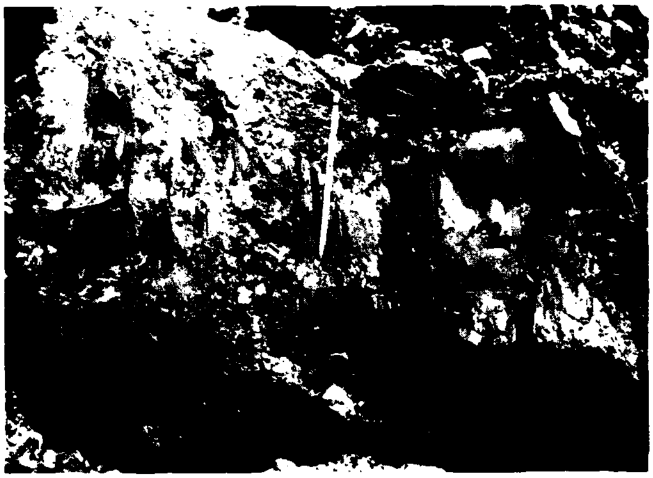

Fig. 7 Slickensided Claystone from Vicinity of the October 1982 Slide

Beneath the claystone is a soft limestone also of Tertiary Age. It has the strength of poor concrete, and is relatively massive with few fissures.

The boundary between the terrace and claystone dips down gently toward the river to the west. The boundary between the claystone and limestone dips down to the east and south, so the claystone rapidly thickens in that direction.

The limestone ridge appears to be supported on the claystone with the boundary between the two materials dipping gently to the southeast. Discrepancies in formational boundaries to the north and east suggest some faulting. However, the fault surface has not been identified. By way of contrast with the deeper limestone, the ridge contains numerous steeply dipping fissures which have been enlarged by solution and are filled with soft red residual silty clay.

Ground Water

The ground water table is typically in the lower sandy gravel about 2 to 4 m above the claystone, and slopes downward toward the river. It is fed by rainfall infiltration and by springs that exit along the base of the limestone ridge at its contact with the claystone below.

Excavation Requirements

The designers adapted the site elevations to the harder lower claystone and the limestone in order to provide a sufficiently rigid foundation for the power house machinery. The optimization of support and excavation dictated the powerhouse orientation. However, with the limestone falling off to the southeast, deep excavation was required in the upper claystone for the penstocks where they entered the powerhouse.

The contract drawings depict the powerhouse excavation to be sloping with intermediate berms as shown in Fig. 6. The cut faces were to be restrained during construction by concrete facings anchored into the claystone and the limestone. After the structures were complete, the excavation was to be backfilled and the anchored facings would have no further function. The basis for the design slopes and the anchoring is not given, but it is presumed that the claystone and limestone strengths included with the contract documents were considered.

Contractors Excavation Plan

The contractor's excavation plan differed somewhat from that of the designer. First, the level of the terrace surface, El. 265 m, was extended to the north 70 m or 230 ft by cutting into the south face of the limestone

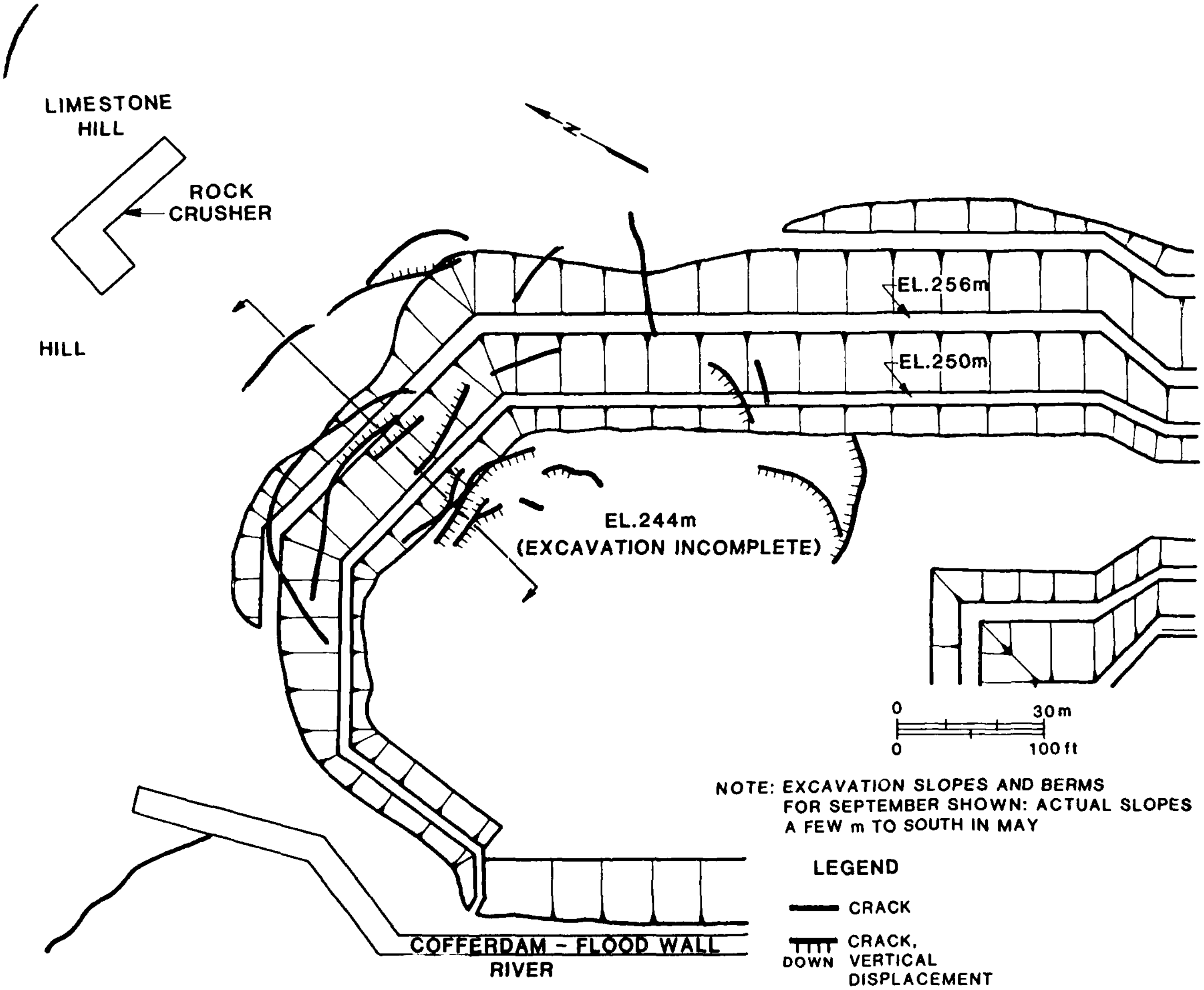
LIMESTONE HILL
ROCK CRUSHER
N
HILL
EL.256m
EL.250m
EL.244m
(EXCAVATION INCOMPLETE)
0
30m
0
100ft
NOTE: EXCAVATION SLOPES AND BERMS FOR SEPTEMBER SHOWN: ACTUAL SLOPES A FEW m TO SOUTH IN MAY
LEGEND
CRACK
CRACK, VERTICAL DISPLACEMENT
DOWN
COFFERDAM - FLOOD WALL
RIVER

Fig. 8 The May 1982 Cracking and Bulging

ridge to provide a space for an aggregate crusher, stockpiles, and the concrete batch plant. This required cutting a near vertical face as deep as 20 m into the limestone. Second, the excavation perimeter was enlarged to provide more gentle slopes in the claystone (2.7 H to 1 V) instead of the 1 to 1 slopes depicted in the contract documents. The objective apparently was to minimize or eliminate the need for the anchored facings. There were no formal drawings nor engineering computations to support these changes, but the high unconfined compressive strengths of the claystone, as given in the contract documents, probably were considered.

MAY 1982 MOVEMENT

Description of Failure

By May 1982 the excavation had reached El. 244 m, a depth of 20.7 m or 68 ft, reaching the upper surface of the limestone over much of the site. As the excavation approached this level, extensive cracking and bulges gradually developed in the slopes of the northeast corner, and in the level work area further to the north and east. These are shown in Fig. 8. Springs developed in the excavated slope at the contact between the gravel terrace and claystone.

The cracks were tensile openings with little or no evidence of vertical displacement. Most were arcuate as well as discontinuous, with their general trend parallel to the excavation faces. The excavation faces bulged upward and outward toward the excavation. However, there was no evidence of overall translation of the cracked materials in a downhill direction.

Cracking to North

A search was made for more widespread cracking. Some additional tension cracks were found in the bench cut for the aggregate and batch plant to the North. Cracks with vertical or shear displacement were found near the top of the limestone ridges nearly 200 m to the North, and directly above the steep face of the limestone cut for the aggregate and batch plant bench. Because there had been no previous search for cracks, it is not known whether these cracks were caused by the bench cutting or by the powerhouse excavation. The evidence of insects nest in the cracks suggests that the cracks occurred before powerhouse excavation. The springs at the toe of the bench excavation continued to seep despite the end of the wet season.

Analysis of Failure

New tests were made of the claystone to define its shear strength in more detail than can be deduced from the unconfined compression tests. The results for saturated samples in consolidated-undrained shear with pore pressure measurements (effective stress) are

ϕ = 23 to 28 deg, c' = 0.14 to 0.31 kg/cm^2 (4 samples)
ϕ = 13 to 15 deg, c' = 0.65 to 1.05 kg/cm^2 (3 samples)

Back analyses were made of the northeast corner slope assuming that it had undergone landsliding with a circular cross section. The circle was presumed to intersect the top of the slope at an observed crack and the toe of the slope, as shown in Fig. 9. The subdivision of the claystone into two units, slickensided and calcareous, is based on new borings made in the cracked zone. Unfortunately there was no evidence of a failure surface in the continuous core samples; the circular failure was assumed for convenience in computation. The ground water levels were deduced from open wells drilled into the slope and from observed seeps in the slope.

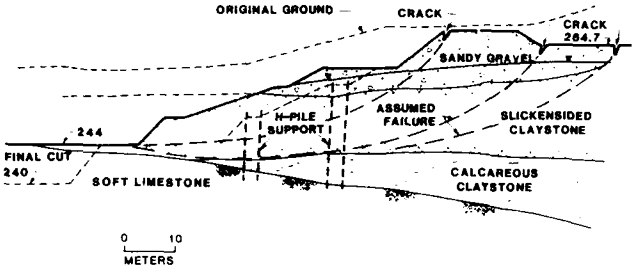

Fig. 9 Cross Section of the May 1982 Movements

The back analysis can be satisfied by various combinations of ϕ' and c' ranging from $\phi'=30$, $c'=0.3\ kg/cm^2$ to $\phi'=15^{\circ}$, $c'=1.0\ kg/cm^2$. The designers arbitrarily selected an intermediate, conservative combination for analysis of corrective measures: $\phi'=22^{\circ}$ and $c'=0.26\ kg/cm^2$.

Counter Measures

Various countermeasures were planned by the designer after discussions with the contractor to increase the "safety factor of 1", presumed in the failure back-analysis, to 1.2. These measures included drains to reduce the ground water level and H-piles to augment the shear resistance of the presumed failure surface. First, the slope was re-excavated to sounder claystone with few cracks, as shown by the dashed line in Fig. 9. Eleven pit wells were excavated through the sandy gravel and about half a meter into the claystone. These were built as concrete box caissons.

Eight 250 mm or 10 in. diameter drilled wells were installed in the northeast corner between the excavation and the concrete plant, spaced 20-40 m apart. These were extended 2 m into the limestone. Each included a 50 mm thick gravel pack throughout the depth to provide for rapid infiltration. The locations of both sets of wells are shown in Fig. 11, the plan of the October sliding.

Horizontal drain holes 10 m long and 50 mm in diameter were planned for the slopes at three different levels to provide additional drainage for the claystone and gravel.

Flattening of the slopes was considered, but space was not available.

The designers analyses based on the arbitrarily selected shear parameters showed that even with drainage, additional shear resistance of 44 tons per meter of slope were required for the desired computed safety factor of 1.2. Four rows of 200 x 200 mm (8 in) H piles were planned. (They were later enlarged to 350 x 350 mm [14 in.].) The piles would penetrate about 2 m into the limestone to fix them against rotation. They were stiff enough to resist bending from the resisting force applied at the level of the assumed circular failure surface. The number of piles was based on adding the shear strength of the steel at its intersection with the failure surface, to the shear resistance of the soil. For conservatism the number of piles required was doubled. No consideration was given to pile claystone shear transfer nor strain compatibility. The locations of the pile rows, two on each of the two intermediate beams, on the re-excavated slope are shown on Fig. 9.

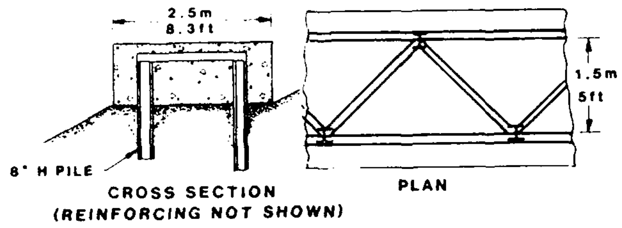

Fig. 10 H-Piles and Capping Beam

The piles on each berm were connected together by steel angles in a simple truss and encased in a reinforced continuous concrete beam, as shown in Fig. 10. The purpose of this beam was to provide some resistance against rotation of the tops of the piles and to transfer loads between areas of greater and less movement.

Critique of Correactive Measures

The analyses upon which the corrective measures were based were flawed. First, the available evidence never showed that a landslide had occurred. The ground bulged upward and outward, without accompanying subsidence and with neither toe bulges nor scarps. No shear surfaces were identified. Instead, the movement appeared to be the result of soil expansion, probably with movement along the existing slickensides, and caused by the stress release from excavation. Later tests showed the claystone to be expansive, with expansive pressures of more than 2.5 kg/cm^2.

The deep wells were too remote from the expansion zone to effectively drain the slickensided cracks in the claystone and the pit wells could only lower the water level in the gravel. The horizontal drains planned were too short and too widely spaced to drain the random claystone cracks. Worse, their installation was halted, when only a few of those first installed produced water. Excavation of the loosened material steepened the slopes and added to the stress release and unbalanced loads in the excavation face.

Finally, the resistance of the H-piles depended on the assumed location of a sliding surface and on adding the shear of the steel to the shear of the soil without regard to load transfer or strain compatibility.

OCTOBER 1982 SLIDING

Failure Description

Slow bulging and cracking continued while the corrective measures were being installed. A failure occurred in the northeast corner with rapid movement on October 18, 1982. By way of contrast with the May cracking, movement developed suddenly, and included both subsidence at the top of the slope and bulging at the toe. It commenced two days after a very intense rain, following two months of very dry weather. Fig. 11 shows the northeast corner of the excavation, with the distortion of the truss connecting the H-piles.

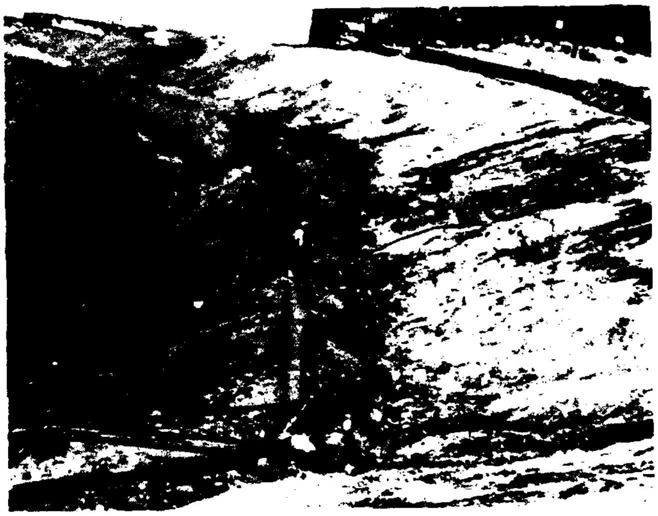

Fig. 11 Buckling of the Truss Connecting the H-Piles by Sliding in the Northeast Corner of the Excavation

Most of the countermeasures planned following the May cracking and bulging had been installed. Installation of horizontal drains had been temporarily stopped because they produced little water. The concrete capping beam for the piles had not been constructed; however, this beam was never considered in the analyses for added stability.

The toe of the slope bulged outward 1 to 2 m; the top of the slope subsided a few cm, opening and extending the previous cracks. The major movements were in the center of the slope where the surface moved more than 1 m horizontally down slope, accompanied by deep cracking and by local subsidence and upheaval, as the claystone mass distorted.

The greatest vertical displacement occurred just downhill of the upper line of H-piles. This displacement was accompanied by a 40 m long arcuate scarp and an open crack 50 to 100 mm wide. Downhill, wedges of claystone moved differentially to form an elongated graben.

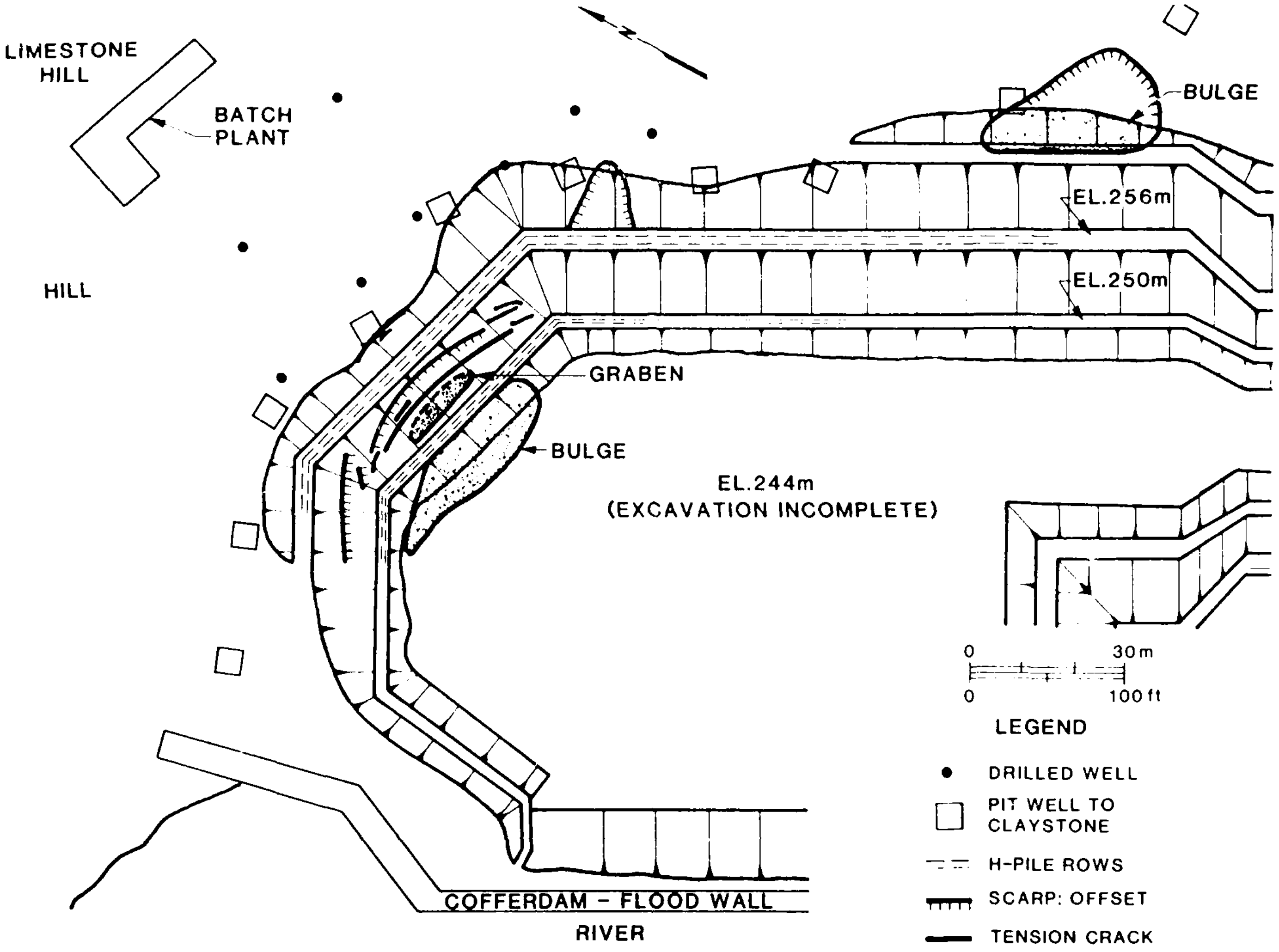

Fig. 12 Plan of the October 1982 Sliding and Earlier Drain System

A plan of the excavation showing the cracking and bulging in the northeast corner as well as two smaller, unrelated slides along the upper west slopes is shown in Fig. 12.

The H-piles were dragged downslope with the movement, but very non-uniformly. The upper rows moved a few cm and tilted downslope only slightly. The truss and the tops of the piles in the lower rows moved downslope up to 1.7 *m* accompanied by partial buckling of the truss from bowing as shown in Fig. 11. Most of the H-piles tilted downhill, one 18 degrees from the vertical, Fig. 13a. The H-piles offered some resistance, but the claystone cracked and tore around them, Fig. 13b.

Excavation into the toe of the slope disclosed a well defined failure surface. It continued to move about 1 cm per hour two weeks after the major movement.

Investigation

The site conditions at the time of the failure were investigated by the designer and by the Author as a consultant to the owner. A number of pertinent facts emerged.

There was no evidence of new cracking or movement at the aggregate-concrete plant nor in the limestone ridge above. The movement was confined to the northeast corner of the excavation. The area involved was smaller than and within the area of the May cracking.

A few of the drain wells were producing water, most were not. The water table rose 1 m following the intense rain in an observation well in the sliding zone, then fell slowly. One of the shaft wells filled with water following the rain and remained full several hours before it could be pumped down. Unfortunately, the caisson walls, excavated into the claystone, had no drain holes to bleed water out of the gravel terrace aquifer. About 1 out of 5 of the horizontal drains produced water (not unusual for horizontal drains).

The H-piles did not penetrate into the limestone as specified. Instead, they stopped abruptly at the top of the calcareous claystone, penetrating into it only 1 to 3 cm. This failure to drive the piles as specified had been overlooked by the designer and was a surprise when it was uncovered.

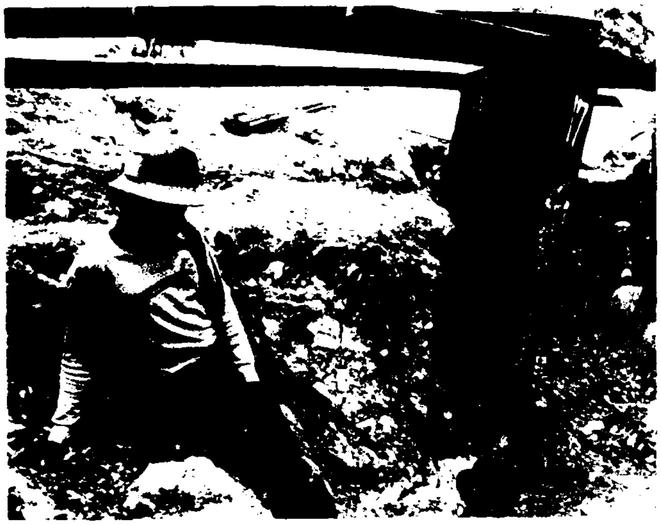

Fig. 13a H-Pile Tilted 18 Deg from Vertical and Heave of Claystone on Slope from the October 1982 Slide

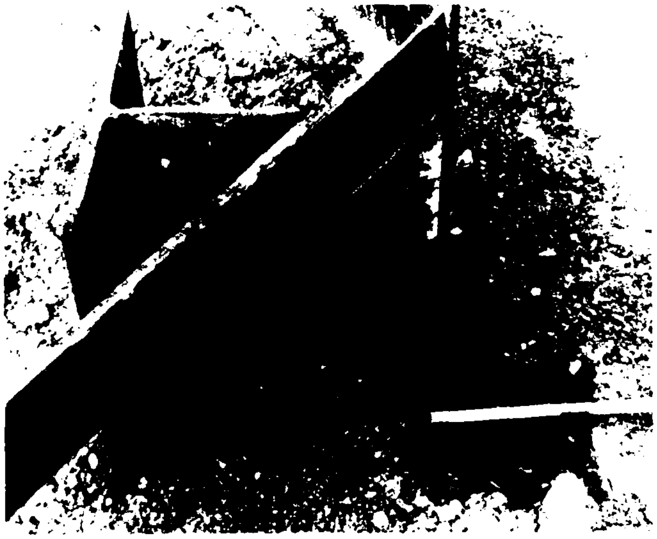

Fig. 13b Claystone Tearing on the Downhill Slide of an H-Pile from Slope Movement in the October 1982 Slide

The tilt of the piles were equivalent to the horizontal movement of their tops. This shows that they had tilted as stiff members, rotating about their tips, driven just into the calcareous claystone.

Added Testing

Additional soil tests were conducted on samples of the slickensided claystone. The earlier tests had all been of intact claystone, between the slickensided cracks. The new tests were of the slickensided cracks. There was a startling contrast with the earlier tests: the effective friction angles were about 12 to 15 deg with little or no cohesion.

Swell tests were conducted of both the slickensided and calcareous claystone: Free swell, 2 to 20%; swell pressure 0.2 to 2.6 kg/cm^2.

The swelling in low plasticity claystone is probably the result of residual stress. It is likely that the slickensides and residual stresses were caused tectonically.

Mechanism of Movements

A cross section of the October slide is shown in Fig. 14. The earlier analyses had presummed a circular cross section of movement, as shown in Fig. 9, and repeated in Fig. 14. However, the pile tilting and ground movement indicate that the motion was nearly linear. A near horizontal surface probably followed the upper limit of the calcareous claystone, connecting with the surface cracks through networks of existing slickensided cracks.

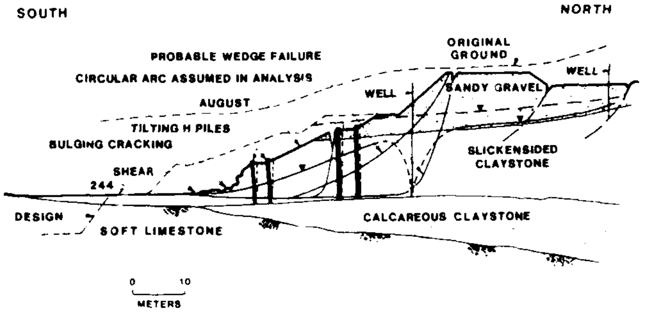

Fig. 14 Cross Section of Sliding in the Northeast Corner of the Excavation

The movement developed in two stages. First, excavation without support allowed the claystone to expand, opening the slickensided cracks within the mass and producing cracks in the ground surface. Second, ground water and surface runoff penetrated the opened cracks, developing pressure. The weakened mass expanded horizontally. Expansion was resisted by the friction on the cracks (reduced by pore pressure) and the resistance of the crack asperities. The H-piles possibly prevented the sliding from becoming catastrophic. However, they tore the slickensided claystone and their lack of embedment caused them to tilt and aggravate the cracking.

Corrective Measures

Further corrective measures were designed considering that no additional space was available for flattening slopes and that the construction of counter measures must be within the capabilities of the powerhouse contractor and Indonesian based contractors because of the time required to mobilize foreign contractors or to import materials. The new data on rock expansion and the continuing movements in the northeast slope indicated that further expansion of the claystone would be likely with further loss of strength.

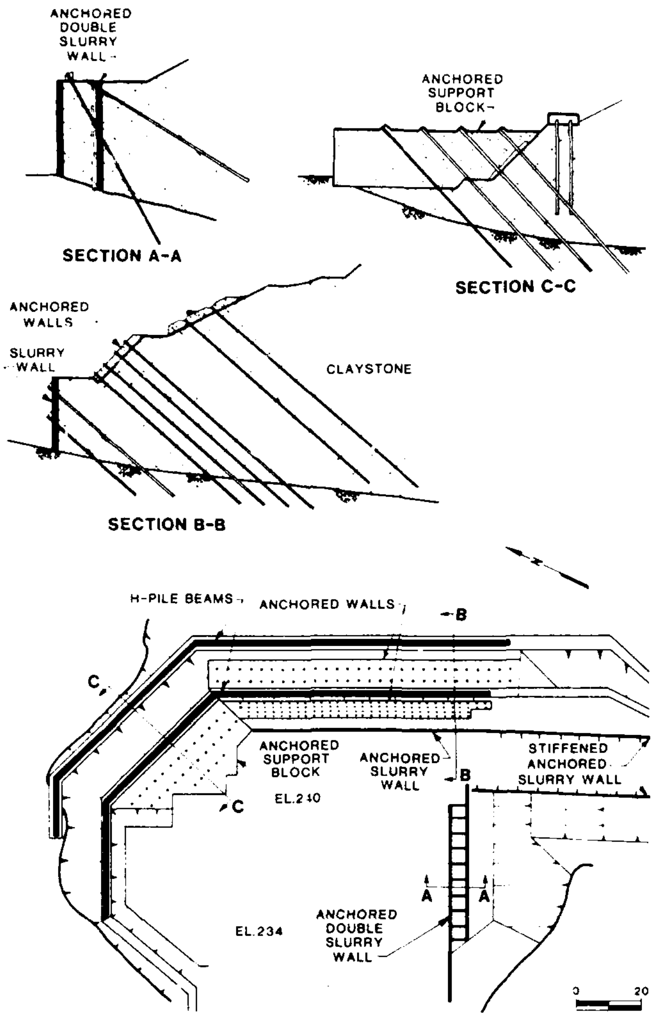

Fig. 15 The Final Excavation Support System

A concrete block, initially restrained by gravity-friction on the limestone was designed to support the northeast corner. Tie back tendon anchors were added when the block moved. Its limited resistance was confirmed when the strength data on the slickensides in the claystone became available. Most of the excavation was supported by sloping concrete walls restrained by tendon anchors into the calcareous claystone and the limestone. At the bottom of the south end of the excavation, vertical tied back walls were added because of limited space. These were installed using slurry supported excavations with the slurry replaced by concrete. These measures are shown on Fig. 15 and Fig. 16.

Small Slides

Two smaller slides occurred in the upper parts of the excavation face shortly after the intense rain of October 13--one at the north end of the east slope and one near the south end of the east slope. Their locations are shown in Fig. 12. Both were confined to the sandy gravel stratum. The cause was excess pore water pressure and weakening of the dried clay bonding in the terrace materials. *Further movement was prevented by horizontal* wood lagging supported by steel H-piles driven as cantilevers into the claystone below.

System Performance

No significant movements occurred in the final support system. The excavations have been backfilled to provide level parking and service areas around the plant. No movements have been noted during 2 years of operation. The cost of the failures and their correction has not been fully identified. Beyond the direct costs are the cost of delay and of acceleration. The estimated total cost probably exceeded $10 million.

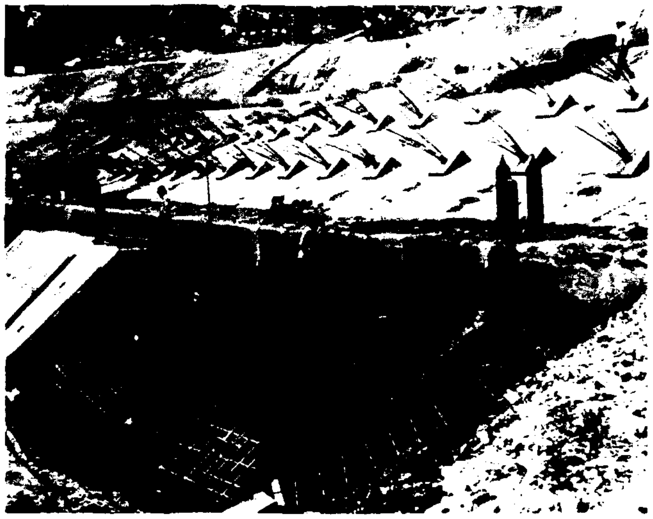

Fig. 16 Constructing the Anchor Concrete Facing Walls to Support the East Excavation Slopes

CONCLUSIONS

Water pressure in the slickensided claystone was the cause of the movements in the powerhouse excavation slopes. Although the slickensides were recognized, their significance was not understood either by those who identified them and those who made analyses and designs. Eventually, the excavation slopes were stabilized, but at considerable additional cost and delay.

These failures and their correction provide a number of valuable lessons for our profession. These include both technical details and broader issues of interdisciplinary action.

Technical Issues

Small fractures that are insignificant geologically can play a key part in soil and rock strength. Testing intact portions of fractured soil or rock is grossly misleading. The strength and rigidity of the mass is largely controlled by the fractures; therefore testing should concentrate on these defects.

Residual stresses play an important part in the design of structures to support the ground. This has been recognized in tunnel support engineering; it is largely ignored in earth pressures on walls and excavation support systems.

The residual stress influences the design three ways. First, if no allowance is made for movement, the lateral pressure can be greater than the vertical stress produced by soil or rock weight. Second, depending on the rigidity of the soil or rock, considerably more movement will be required to reduce the lateral pressure to the active state than is required for materials with gravity stress alone. Such large movements can be intolerable in some situations. Third, the stress release allows existing cracks to open. Those that were initially watertight can accept water, allowing pore pressures to act on the cracked surface. This changes the mass behavior as was demonstrated in the Saguling sliding. Such residual stresses have been largely ignored in geotechnical engineering, because there have been no convenient ways to measure them. With the modern techniques of hydraulic fracturing and the various dilatometers that can be introduced in bore holes, engineers can now measure residual stresses and include them in their analyses.

Back analysis of a failure must be based on accurate information on the kinematics of that failure. If the presumed motion is in error, conclusions based on an analysis of the erroneous motion will also be wrong. If the nature of the movement cannot be determined, then many possibilities must be evaluated--a form of parametric study. The corrective design then is adapted to the range of answers.

Analyses of soil-structure interaction must consider the relative rigidities and strengths of those materials that control their interaction. Assuming that a pile contributes shear resistance to a landslide equivalent to the shear strength of its steel is wrong when it does not consider the possibility that the pile will shear the soil instead.

Drainage design must recognize that real aquifers are highly variable. The failure of some drain holes to find water should not discourage the installation of more drain holes; one hole draining a key aquifer may be sufficient.

Broader Issues

Meaningful interaction between engineers and geologists is essential. The geologists recognized the slickensiding in the mudstone; they did not fully understand their engineering significance. The engineers were informed of the presence of the slickensides, but didn't visualize how they controlled their design. The geologist gave the slickensided soil samples to the laboratory. The laboratory tested the intact material between the slickensides because it was difficult to trim specimens that included the weaknesses. No one informed the laboratory staff of the significance of the slickensides. Thus the importance of the cracks fell through the cracks between the different viewpoints of the geologists, the laboratory engineers, and the design engineers. Instead, geotechnical engineers must have an understanding of geology and engineering geologists must have an understanding of engineering design. Unfortunately, interdisciplinary understanding appears to be declining instead of improving. Jurisdictional jealousy between professions can destroy all, as union labor has demonstrated. The combined knowledge and wisdom of all relevant professions are required to solve the complex problems in geotechnical engineering.

What is economical or practical design in one area at a particular time may not be in another because of local resources of manpower, money, and technology. The H-piles failed to restrain mudstone partially because they could not be installed as the design required. The deficiency was ignored because the contractor had no means to drive them further. The design must fit the resources and capabilities of the moment.

Failure in a civil engineering is more than a problem; it is an opportunity. Failure is the only full scale test of any large engineering system. As a test, it provides valuable lessons to the profession.

As professionals, we should take advantage of the lessons; otherwise, the failure may be repeated. Moreover, we have already paid for the lessons.

The Saguling Project has survived its powerhouse movements and is now generating power as its design anticipated.

ACKNOWLEDGEMENTS

Ir. Husni Sabar was the project manager for PLN during design and construction. He has graciously given his permission to publish this paper. The project designer was the New Japan Engineering Company of Osaka and the contractor, Dumas, of France. The Author was a member of the project's Board of Consultants which included Dr. Leopold Mueller of Austria, Dr. H. Tanaka of Japan and Mr. Ivor L. Pinkerton of Australia. The views expressed in this paper are those of the Author and not necessarily those of others.

REFERENCES

Maru, K. and Shaw, RD: "Ground Instability During Open Excavation of the Saguling Hydroelectric Project, West Java", Proceedings 4th International Symposium on Landslides, Toronto, 1984, vol 2, p. 137-142.

Sowers, G.F., "Report on Powerhouse Excavation Landslide", PLN, November 1982

Proceedings: Second International Conference on Case Histories in Geotechnical Engineering, June 1-5, 1988, St. Louis, Mo., Invited Paper

Lipari Landfill: Leachate Containment System—Geotechnical Considerations

John Ramage
Senior Geotechnical Engineer, CH2M HILL, Inc., Milwaukee, Wisconsin

SYNOPSIS: The Lipari Landfill, located near Pitman, New Jersey, is a 16-acre former sand and gravel and waste disposal site that operated from 1958 through early 1970. This site was ranked the number one site in the U.S. EPA's first National Priority List of uncontrolled hazardous waste disposal sites. Site investigations and analysis of contamination both on- and off-site began in late 1979. Design of the Phase I remediation, consisting of encapsulation utilizing a vertical barrier keyed into a relatively impermeable clay layer and a cover over the entire site, began in late 1982. Construction of the leachate containment system began in the fall of 1983 and was completed in November 1984 at a cost of approximately $2,205,000. U.S. EPA is about to implement the Phase II remedial actions consisting of batch flushing, extraction and treatment of contaminated groundwater and removal and treatment of stream and lake sediments contaminated by leachate migration through surface waters. This Phase II program is expected to cost about $12.3 million and take about 7-1/2 years to complete.

INTRODUCTION

Development and implementation of remedial measures for control and cleanup of the uncontrolled hazardous waste disposal site is unlike anything the geotechnical professional has previously faced. We are dealing with issues that require careful evaluation and understanding in order to implement effective remedial actions. The principal issues that require consideration include:

- o Complex and continually changing regulatory environment at all levels of government--federal, state, and local.
- o Federal legislation dealing with cleanup (CERCLA and SARA) has, as the principal basis for implementing cleanup, the concept of cost recovery from Potentially Responsible Parties (PRP). This means that the ultimate client for technical services in remedial actions implemented under this legislation is the lawyer.
- o The public has greater awareness and interest in the cleanup of hazardous waste sites than any other technical issue facing society today. Citizen groups will monitor and question every step and decision in the remedial action process.
- o The liability issues associated with design and construction of remedial measures are unknown at this point but are potentially monumental. Third party environmental damage suits could be enormous in terms of award and come decades after completion of remedial activities.
- o There are no "standards of practice" for cleanup of hazardous waste sites. While we have standards for various elements of geotechnical practice, such as slurry walls and flexible membrane liner systems, we have not developed standards for the total remedial system. This situation is exacerbated by the public demand for "Complete and Total" cleanup of these sites.

The Lipari Landfill is a 16-acre site used as both a source of sand and gravel and a disposal facility for municipal and industrial wastes located near Pitman, New Jersey. This site, ranked first in U.S. EPA's National Priority List (NPL) in 1982, was the first "Superfund" site where design and initial remedial measures were implemented under the interagency agreement between the U.S. EPA and the U.S. Army Corps of Engineers (USCE). This paper describes the investigative work, feasibility and engineering studies, preparation of contract documents, and construction of the leachate containment system for the Lipari Landfill.

SITE CONDITIONS

History

The Lipari Landfill is located at the southwestern edge of the town of Pitman, New Jersey, approximately 1,500 feet north of U.S. Route 322 and 1-1/2 miles west of Glassboro State College. The eastern limit of the site is about 400 feet west of Chestnut Branch, which flows in a northerly direction toward Alcyon Lake, some 1,000 feet from the site. Chestnut Branch is a tributary of Mantua Creek, eventually discharging to the Delaware River. Features of the area surrounding the Lipari Landfill are shown on Figure 1.

The property was purchased in 1958 by Mr. Nick Lipari who then started a sand and gravel operation on the site. The use of the property for mining and processing of sand and gravel also made the site attractive for use as a landfill. The integration of these two activities began in 1958 with excavation of sand and gravel pits, subsequently filling each pit with waste. Materials from the site were used to cover waste as filling proceeded and for final cover after each pit was filled. These operations were continued until the middle of 1971.

Liquid wastes were dumped from 1958 until approximately December of 1969, and solid wastes were dumped from 1958 through May of 1970, when the landfill was closed (Harrington, 1980). The exact nature and quantities of

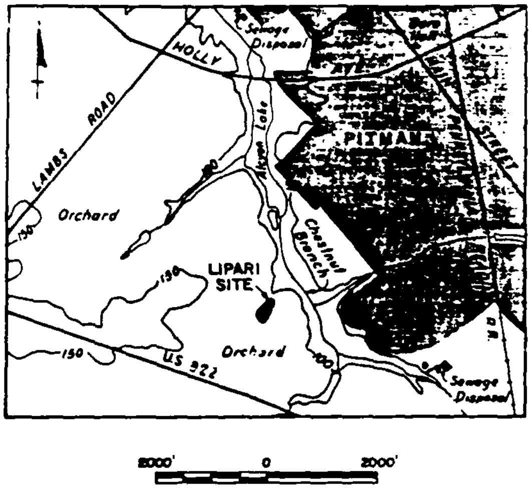

FIGURE 1
Location of the Lipari Landfill (Wright, 1981b)

wastes disposed of at the Lipari Landfill are unknown since detailed records were not kept. Estimates based on records of parties known to have disposed of material at the site suggest that about 12,000 cubic yards of waste are buried on site. Liquid wastes disposed of at the site are estimated at approximately 2.9 million gallons. In most instances, liquid wastes were disposed of uncontained, since drums were emptied and removed from the site for salvage and resale (Harrington, 1980).

Prior to 1971, the operation of the Lipari Landfill was considered to be both legally and environmentally sound by the various regulatory agencies involved. The landfill was inspected on a regular basis by the Department of Health and its successor, the Department of Solid Waste Management beginning in 1963. In 1970, the first signs of problems began to appear, as leachate was observed seeping from walls of the landfill. Official notification for correction was given the operator of the landfill in July, 1971. Attempts to contain and control the seeps had little impact, and the New Jersey Department of Environmental Protection (NJDEP) brought suit against the owners for the facility (Harrington, 1980).

Site Description

The physical characteristics of the landfill are shown on Figure 2. It is estimated that the actual disposal sites covered an area of about six acres, south of the present course of Rabbit Run. The highest point within the disposal area is approximately elevation 134. The disposal site is on a plateau about 30 feet above the Chestnut Branch drainage. The remainder of the plateau area, not disturbed for sand and gravel operations and disposal of wastes, was orchard. Residential areas developed to the east of the site, across the Chestnut Branch Stream channel (Wright, 1980).

Leachate discharges into Rabbit Run were observed along the entire south bank and the stream channel bottom. Leachate was also observed discharging along the eastern wall of the plateau into Chestnut Branch. The leachate discharges occurred in both discrete and nondiscrete flows below elevation 105 (Wright, 1980).

Subsurface Conditions

The Lipari Landfill is underlain by relatively horizontal

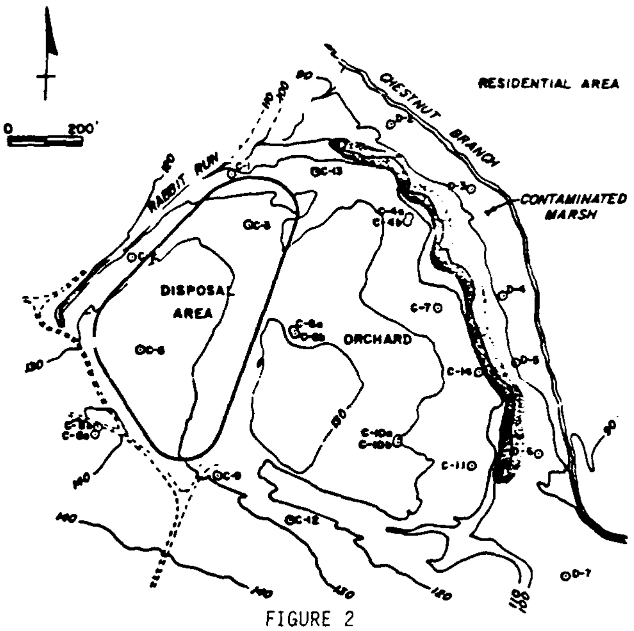

FIGURE 2
Local Setting of the Lipari Landfill
(Wright, 1981b)

geologic units that strike northeast-southwest, and dip slightly to the southeast. The units of concern at the site include (in descending order) Cohansey Sand, Kirkwood Formation, Manasquan Formation, and the Vincentown Formation. Geologic cross-sections of the site are shown on Figure 3.

The landfill site is located in the Cohansey Sand at the northwest boundary of its outcrop. This unit consists of fine to medium silty sand with lenses of clay and gravel. The unit is stratified, with occasional layers of hard iron-cemented sandstone. Based on exploration, sampling and testing done at the site (Wright, 1981a), the Cohansey Sand can be differentiated into upper and lower units.

The upper unit of the Cohansey Sand is exposed in the plateau area of the Lipari Landfill. It generally occurs above elevation 100. This upper unit consists of orange-brown fine to coarse sand and fine to medium gravel, with traces of silt and clay. This unit is the source of sand and gravel mined at the site.

The lower Cohansey Sand outcrops along the eastern bank of the plateau, above the Chestnut Branch marsh. This unit, nearly horizontal, dips slightly to the southeast and is composed of greenish-gray fine to medium sand with some silt. No gravel was encountered in the borings (Wright, 1981a).

The Cohansey Sand is unconfined in the area of the Lipari Landfill, resulting in groundwater recharge through direct infiltration through the outcrop exposure. The water from the Cohansey unit has historically been used in the area for farm and rural domestic water supplies. However, high naturally occurring iron concentrations in the area have made this aquifer unsuitable for domestic use (Wright, 1980).

The Kirkwood Formation underlies the Cohansey Sand, and is approximately 75 feet thick in the area of the Lipari site. The Kirkwood Formation consists of an upper clay unit, ranging in thickness from 8 to 14 feet across the site plateau (Wright, 1981a), underlain by very fine to medium sand unit. The top of the Kirkwood Formation ranges from elevation 92 to about 80 across the plateau.

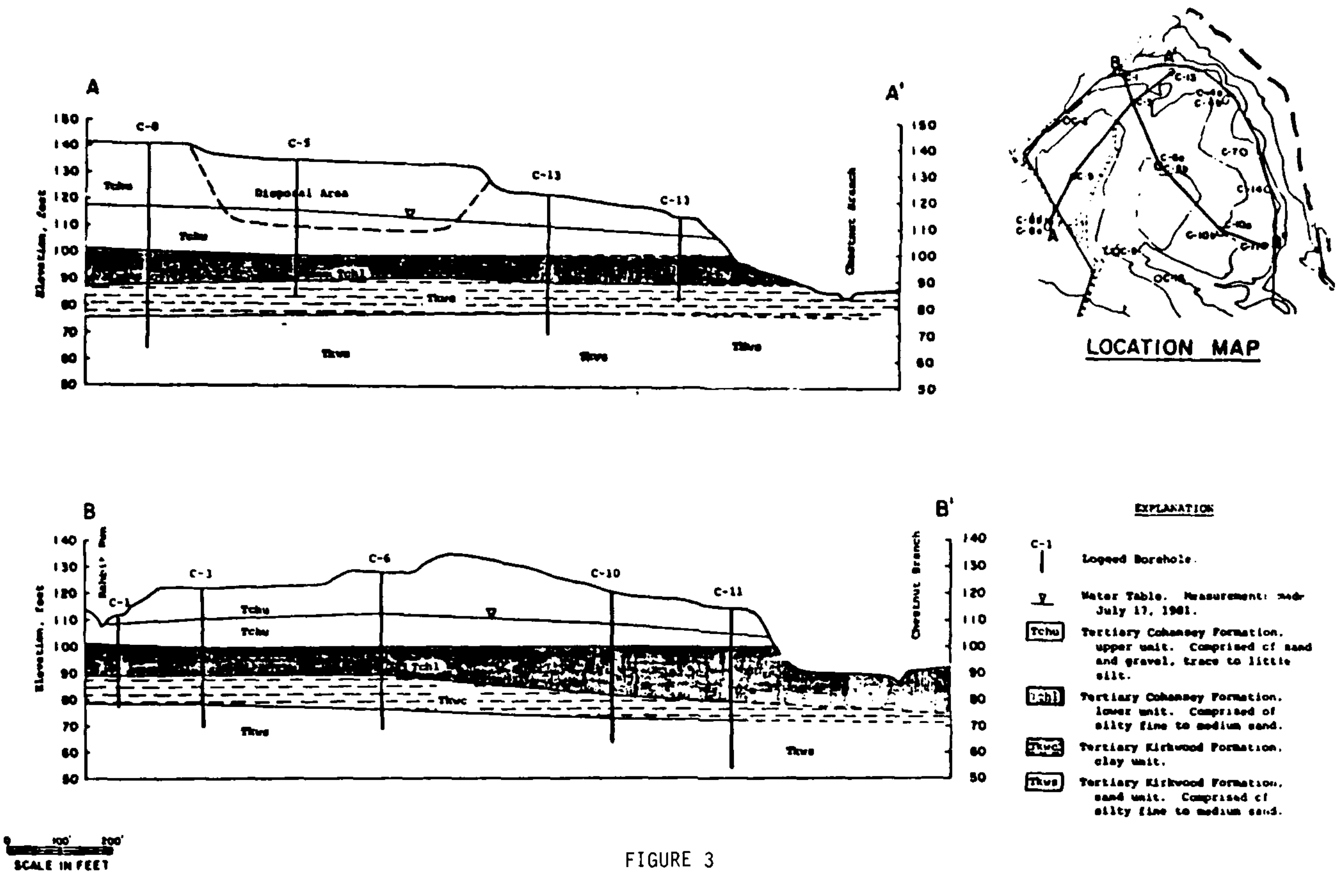
A
A'
C-8
C-5
C-13
C-11
Tchu
Disposal Area
Tchl
Tkwc
Tkws
Chestnut Branch
Elevation, feet
LOCATION MAP
B
B'
C-1
C-3
C-6
C-10
C-11
Elevation, feet
Chestnut Branch
EXPLANATION
C-1
Logged Borehole.
Water Table. Measurement made July 17, 1981.
Tchu Tertiary Cohansey Formation, upper unit. Comprised of sand and gravel, trace to little silt.
Tchl Tertiary Cohansey Formation, lower unit. Comprised of silty fine to medium sand.
Tkwc Tertiary Kirkwood Formation, clay unit.
Tkws Tertiary Kirkwood Formation, sand unit. Comprised of silty fine to medium sand.
0 100' 200'
SCALE IN FEET

FIGURE 3
Geologic Cross-Sections, Lipari Landfill (Wright, 1981b)

The outcrop of the Kirkwood Formation forms a band 2 miles wide, northwest of the site, extending through Alcyon Lake. Groundwater recharge to the Kirkwood Formation occurs through outcrops and by downward seepage from the Cohansey Sand. The Kirkwood is considered a minor aquifer in the area, yielding insignificant flows (Wright, 1980).

The Vincentown Formation underlies the Kirkwood Formation at the site, and is considered the shallowest major aquifer in the area other than the Cohansey Sand (Wright, 1980). The unit is approximately 18 feet thick beneath the site, and consists of fine to coarse sand lithified with clay and small amounts of calcite cement. The unit also contains traces of mica and fossilized shell fragments (Wright, 1981a).

Geologic units occurring beneath the Vincentown Formation are not believed to be threatened by contamination from the Lipari site (Wright, 1981a). Additional investigations are currently being conducted by U.S. EPA as part of the Phase II remedial activities for the site.

Hydrogeology

Contaminated groundwater moved from the disposal area through the Cohansey Sand, discharging as diffuse seepage along the eastern edge of the plateau in Chestnut Branch. This contaminant plume then moved via the surface water regime into Alcoyn Lake. In addition, the downward gradient between the Cohansey Sand and the underlying Kirkwood Formation (sand unit) has introduced contaminants into the lower formation. Groundwater surface in the Cohansey Sand is shown in Figure 4, Piezometric levels in the Kirkwood Formation on Figure 5.

Hydrogeologic parameters used in various alternative analyses and for design of the leachate containment system are as follows (CH2M HILL, 1983):

- All inflow to the encapsulated area results in contaminated leachate.
- Flow through the Cohansey Sand to Chestnut Branch is between 20,000 and 62,000 gallons per day (Wright, 1981a).
- The encapsulation system should reduce flow through the Cohansey Sand by 90 percent.
- The Kirkwood Formation clay layer is approximately 14 feet thick, with a primary permeability of 1.0 x 10-7 cm/sec (Wright, 1981a).
- Upgradient water level elevation of 120.
- Downgradient water level elevation of 100.
- Potentiometric level in the Kirkwood Formation sand unit of elevation 91.

A summary of leachate flows used in the analyses are shown on Table 1, and a summary of significant pollutants found in the Lipari Landfill leachate are listed in Table 2.

INITIAL REMEDIAL MEASURES--BASIS OF DESIGN

Investigations, evaluations, and development of remedial alternatives for the Lipari Landfill began in 1979 and

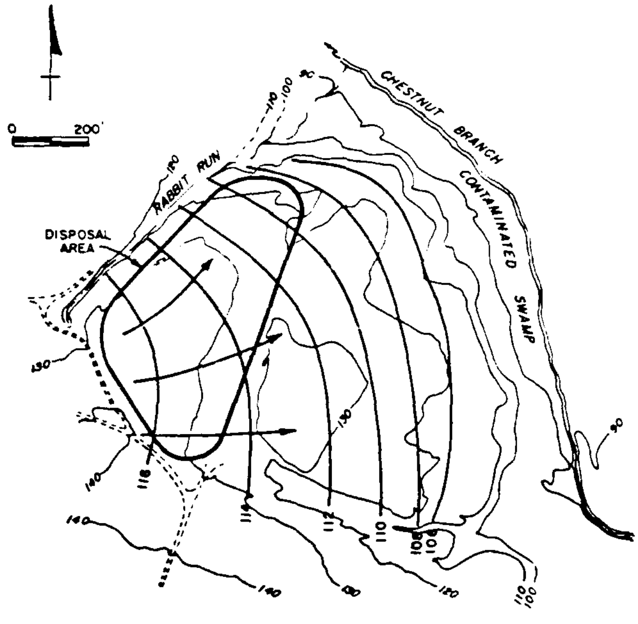

FIGURE 4
Groundwater Surface (Water Table) Contours-
Cohansey Sand, July 17, 1981 (Wright, 1981b)

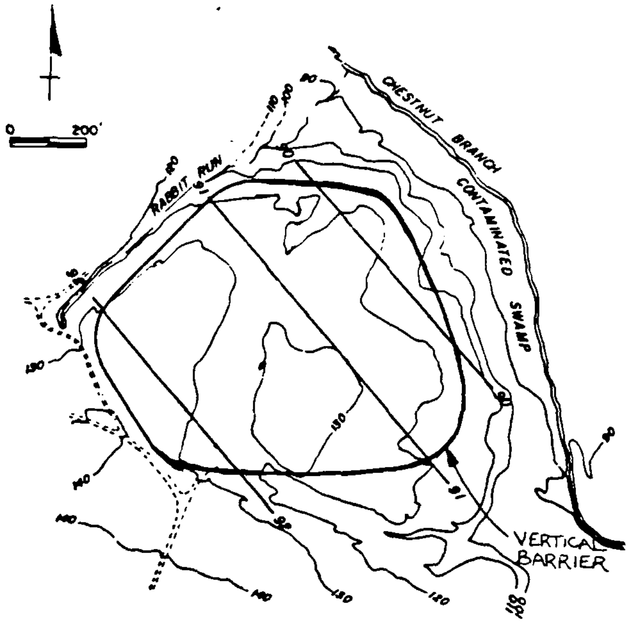

FIGURE 5
Piezometric Head-Kirkwood Formation
(Wright, 1981b)

are ongoing today. Since U.S. EPA began coordinating activities at the site, some 15 different engineering and technical consultants have been engaged in these various investigations, studies, analyses and design.

These activities included site investigations, technical evaluation of abatement alternatives, and development of work scope and specifications for cutoff wall construction by R.E. Wright Associates, Inc. (Wright, 1980, 1981a, 1981b). In addition, Radian Corporation conducted a cost effectiveness assessment of remedial measures and an environmental assessment of the various remedies considered for the Lipari Landfill (Radian, 1982a, 1982b). CH2M HILL conducted detailed engineering analyses and developed plans and specifications for the Lipari Landfill leachate containment system, the Phase I remedial measures program for the site.

The Leachate Containment System for the Lipari Landfill consists of a vertical barrier founded in the Kirkwood Formation clay unit around the entire plateau area (see Figure 5), an impermeable cover system over the area contained by the vertical wall, and a permanent groundwater monitoring system to evaluate the effectiveness of the Phase I remedial program. The following discussion describes the Lipari Landfill Leachate Containment System.

Cover System

Cover systems for the site were evaluated based on the following criteria:

- The native soil at the site is highly permeable; a cover system will provide the only effective barrier to vertical recharge. The cover system shall have an equivalent permeability equal to or less than a 12-inch thick clay layer with a permeability of 1 x 10-7 cm/sec.
- Cover over the barrier shall protect it from vehicular traffic, vegetative root penetration, ultraviolet radiation, ozone degradation, oxidation, microbial attack, and from freeze-thaw and wet-dry cycles.
- The covered area shall have a minimum slope of 2 percent to promote surface runoff.
- All areas within the vertical seepage barrier shall be covered, and the area may be used for construction related activities both before and after cover placement.
- The cover will seal around all openings, such as monitoring wells, and shall seal against the vertical seepage barrier.
- The cover system will not contact contaminated soil or groundwater. Contaminated soil from the vertical seepage barrier construction will be placed within the containment area and covered with noncontaminated soil before construction of the cover system.
- Although a leachate collection and treatment system is not planned as part of the initial remedial measures, the cover system must be designed to accommodate such systems in the future.

Cover systems evaluated included soil-bentonite mixtures, natural clay, synthetic membranes, sprayed-on asphalt emulsion, and rigid systems. Based on detailed analysis and comparison to the design criteria discussed above, flexible synthetic membrane, compacted clay, and soil-bentonite were selected for detailed evaluation (CH2M HILL, 1983). Cost comparisons of these three systems are presented in Table 3.

Both the natural clay and flexible synthetic membrane liner options were designed, with bidders given the option to choose. Details of the cover system designs are shown on Figure 6.

	Rate of Leachate Discharge in gallons per day (gallons per minute)			
Source of Discharge	Groundwater-Flow Method	Area-Discharge Method	Streamflow-Gaging Method	Chemical Mass-Balance Method
Landfill watershed (0.0717 sq. mi.)	87,000 (60)	74,000 (51)	183,000 (127)	62,000 (43)
Landfill (6 acres or 0.0094 sq. mi.)		8,100 (6)		
Landfill, plus polluted area between landfill and Chestnut Branch (16 acres or 0.0250 sq. mi.)		22,000 (16)		
Rabbit Run			43,000 to 108,000 (30 to 75)	
Diffuse leachage seepage	33,000 to 65,000 (23 to 45)	16,000 to 47,000 (11 to 33)	130,000 to 161,000 (90 to 112)	8,640 to 40,000 (6 to 28)
Leachate contribution to Rabbit Run				5,760 to 14,000 (4 to 10)
Vertical leakage through Kirkwood clay unit				
a) Beneath landfill area (6 acres)	550 (0.4)			
b) Beneath affected area (16 acres)	1,460 (1)			

1. Includes discharge to south side of Rabbit Run and to diffuse leachate seepage along Chestnut Branch.

2. Includes groundwater derived from infiltration onto landfill.

TABLE 1
Leachate Flow Analyses (Wright, 1980)

Vertical Barrier

The objectives of a vertical barrier for the Lipari site were to reduce seepage of contaminated groundwater into Rabbit Run and Chestnut Branch, reduce downward migration of contaminants through the Kirkwood Formation, and provide a 50 year design service life. To evaluate cutoff wall alternatives, the following criteria were used:

- The vertical barrier should encircle the contaminated area with a 360-degree enclosure, encapsulating all known burial sites.
- The cutoff wall should enclose as much of the downgradient contamination as possible, essentially maintaining an alignment on the site plateau.

Parameters	Sample 3/ 22 Aug. 79	Sample 3/ 11 Oct. 79	16 April 1980	14 May 1980
pH (units)	-	-	5.2	6.35
Calcium (mg/1)	-	-	27	-
Iron (mg/1)	-	-	100.4	352.6
Potassium (mg/1)	-	-	59.2	-
Sodium (mg/1)	-	-	43	-
Methylene Chloride (mg/1)	0.7	2,890	990	2.8
1, 2-Cichlorolthane (mg/1)	-	1,338	5,800	-
Benzene (mg/1)	1,607	1,190	430	1,200
Toluene (mg/1)	15,500	12,700	3,100	17,500
Ethyl benzene (mg/1)	683.6	583	880	1,600
Bis (2-Chlorethyl) Ether (mg/1)	210,000	23,000	20,000	440
Phenol (mg/1)	4,387	2,400	5,500	1,000

TABLE 2
Chemical Pollutants in Lipari Leachate
(CH2M HILL, 1983)

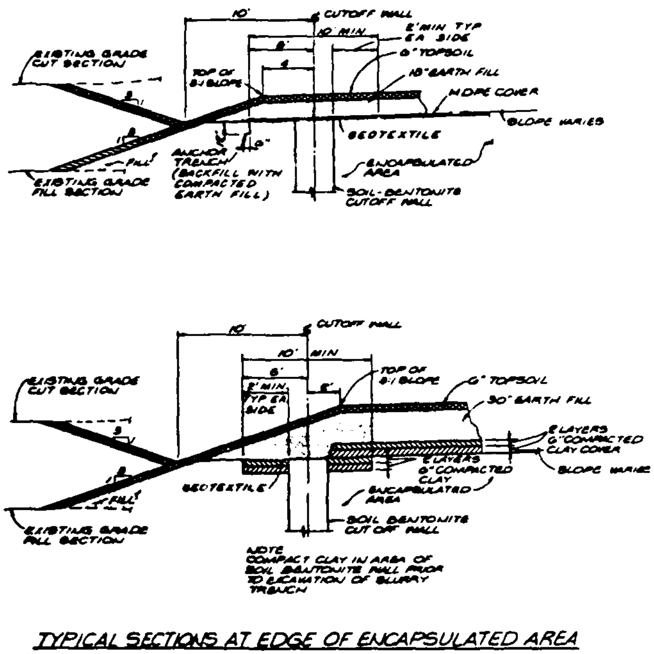
10'
CUTOFF WALL
10' MIN
2' MIN TYP EA SIDE
6" TOPSOIL
18" EARTH FILL
HDPE COVER
EXISTING GRADE CUT SECTION
TOP OF 3:1 SLOPE
SLOPE VARIES
GEOTEXTILE
ANCHOR TRENCH (BACKFILL WITH COMPACTED EARTH FILL)
ENCAPSULATED AREA
FILL
EXISTING GRADE FILL SECTION
SOIL-BENTONITE CUTOFF WALL
10'
CUTOFF WALL
10' MIN
2' MIN. TYP EA SIDE
TOP OF 3:1 SLOPE
6" TOPSOIL
30" EARTH FILL
EXISTING GRADE CUT SECTION
2 LAYERS 6" COMPACTED CLAY COVER
SLOPE VARIES
2 LAYERS 6" COMPACTED CLAY
GEOTEXTILE
ENCAPSULATED AREA
SOIL BENTONITE CUT OFF WALL
FILL
EXISTING GRADE FILL SECTION
NOTE COMPACT CLAY IN AREA OF SOIL BENTONITE WALL PRIOR TO EXCAVATION OF SLURRY TRENCH
TYPICAL SECTIONS AT EDGE OF ENCAPSULATED AREA

b) Synthetic Membrane

FIGURE 6
Cover System Alternates (USCE, 1983)

- The vertical barrier should extend a minimum of 2 feet into the upper clay layer of the Kirkwood Formation, up to 55 feet below ground surface.
- The vertical barrier should have an equivalent permeability equal to or less than a 2-foot thick soil barrier having a permeability of 1 x 10-7 cm/sec.
- Along most of the wall alignment, the groundwater and soil excavated will be contaminated. Spoil excavated from the trench can be disposed of on-site, beneath the cover system.

Two methods of vertical barrier wall construction were evaluated; the slurry trench method and the vibrating beam method.

The primary advantage of the slurry trench method is that the thickness of the wall and trenching method of construction ensure wall integrity and continuity. The keying of the wall into the clay layer can be ascertained by visual inspection of excavated materials. In addition, the techniques are conventional and proven construction technology. However, since the wall is to be constructed in contaminated soil and groundwater, great care would be required to handle and properly dispose of slurry and excavated material. The potential hazard to air quality caused by volatile organics in the excavated materials were of concern. In addition, the impacts of organic contaminants on the permeability of trench backfill materials required evaluation.

The vibrated beam method is a proprietary method of cutoff wall construction developed by Slurry Systems, Inc. In this method, a 2- to 6-inch thick wall is constructed by driving an H-pile to the required cutoff depth and injecting an impermeable slurry mix into the void left as the H-pile is extracted. A wall is completed by overlapping placement of the H-pile.

The vibrated beam cutoff wall has the advantages of rapid construction and no need for handling of contaminated excavation. The method can also be used in steeper terrain than conventional slurry trench construction requiring less site grading along the wall alignment.

The principal disadvantage of the vibrated beam method is that the continuity of the wall between adjacent panels is difficult, if not impossible, to ensure. Installing the H-pile to the best driving tolerances would result in pile plumbness within 1 percent. The installation of a 50-foot deep vibrated beam cutoff to this tolerance would result in a horizontal deviation of 6 inches at the base of the wall. Since the wall is nominally only 4 inches wide, a gap in the cutoff could easily result. Variation in subsurface materials, or natural or manmade obstructions could also cause deviations in vibrated beam panels.

The leachate constituents summarized in Table 2 were used to evaluate the effects of contaminated groundwater on various cutoff wall materials. Materials evaluated included soil-bentonite backfill, asphalt and emulsions, cement-bentonite mixes and concrete (CH2M HILL, 1983). Site-specific laboratory permeability tests for various wall materials were not conducted during the analysis and design phase because of extremely tight implementation schedules. However, information from review of literature (D'Appolonia, 1980 and Anderson, 1981) and of unpublished data collected from other sites was used to develop design recommendations.

Although preliminary engineering analyses and feasibility studies (Wright, 1981b, Radian, 1982a) recommended the vibrated beam method for construction of the vertical

	Soil-Bentonite	**Natural Clay**	**Synthetic Membrane**
Description:	**6" Topsoil** **30" Soil Cover** **4 lb/sf Bentonite**	**6" Topsoil** **30" Soil Cover** **12" Natural Clay**	**6" Topsoil** **18" Soil Cover** **36mil Reinforced Membrane**
Permeability:	10^{-7} **cm/sec**	10^{-7} **cm/sec**	10^{-10} **cm/sec**
Cost :			
Earthwork	**$ 185,000**	**$ 185,000**	**$ 185,000**
Imported Fill	**425,000**	**425,000**	**200,000**
Liner	**370,000**	**540,000**	**470,000**
Grading/Grass	**290,000**	**290,000**	**290,000**
	$1,270,000	**$1,440,000**	**$1,145,000**

TABLE 3
Cost Comparison of Alternative Cover Systems
(CH2M HILL, 1983)

cutoff barrier, the slurry trench method was selected for design. The selected design called for a nominal 30-inch wide slurry supported trench keyed 2 feet into the Kirkwood Formation clay layer and backfilled with a soil-bentonite mixture.

The soil-bentonite mixture was selected because it is conventional, proven technology and provides a plastic, low permeability backfill. The contract specifications required well graded materials with maximum particle size of 3 inches, mixed with a minimum 20 percent by weight of plastic fines. Uncontaminated on site material above the water table was acceptable for the basic backfill material. The plastic fines was imported material passing the No. 200 sieve having a Liquid Limit greater than 20 and a Plasticity Index greater than 4 (USCE, 1983).

INITIAL REMEDIAL MEASURES--CONSTRUCTION

Contract documents for the Lipari Landfill Leachate Containment System were prepared by CH2M HILL for the Kansas City District, U.S. Army Corps of Engineers (USCE) under a U.S. EPA Zone 1 Remedial Response Action Contract. The construction contract was advertised in May of 1983, with bids opened June 30, 1983.

On June 9, 1983, Slurry Systems, Inc., licensee of the vibrated beam method, filed a bid protest with the U.S. Comptroller General, claiming that their technology was unfairly, without authority and with no technical basis excluded from the project. The protest was based on the fact that the U.S. EPA Administrator's decision on containment strategies for the Lipari site incorporated the recommendations from the initial reports (Wright, 1981b) in the Record of Decision. A final decision was rendered by the Comptroller General on December 13, 1983, denying the protest. The denial was based in part on the fact that while various reports were used in evaluation and development of the Record of Decision, it did not state that conclusions of any particular study was adopted (Comptroller General, 1983).

The contract for the leachate containment system was awarded to D'Appolonia Waste Management Services, Inc., with construction beginning in August of 1983. The contractor selected the flexible synthetic membrane cover system. Work was essentially completed in November of 1984 for approximately $2,205,000. One claim concerning leachate overtopping of the vertical wall remains unsettled.

Resident engineering and construction management for the leachate containment system contract were provided by the Philadelphia District USCE, with design interpretations provided by Kansas City District personnel and support as needed from the CH2M HILL design team. In addition, U.S. EPA had oversight responsibilities.

FUTURE REMEDIATION

U.S. EPA has been monitoring performance of the leachate containment system since its completion in late 1984. Detailed analyses of system performance are scheduled for publication in April of 1988. Preliminary indications are that the containment system is behaving as expected.

There are, however, several activities contemplated for the Phase II remedial measures at the Lipari site. These measures include on-site elements and off-site remedial activities. On-site measures are expected to include batch flushing and extraction and treatment of contaminated groundwater within the contained area. Off-site measures include removal and treatment of contaminated sediment in Rabbit Run, Chestnut Branch, and Alcyon Lake. It is also expected that extraction and treatment of contaminated groundwater from the lower Kirkwood Formation sand unit may be required. It is estimated that the Phase II programs will take about 7-1/2 years to complete and cost approximately $12.3 million. The U.S. EPA Administrator's Record of Decision for Phase II remedial measures is expected by April of 1988.

CONCLUSIONS

Approximately 14 years after leachate was first observed seeping from the Lipari Landfill, the construction of a containment system was completed. It is expected that "final" cleanup of this site will not be completed until some 25 years after the initial observation of seepage, at a total cost for remediation for the Lipari Landfill that will approach $15 million.

The technical issues associated with the cleanup of the Lipari Landfill are not overly complex and are, with reasonable expectations, simple to implement. What is difficult for the technologist to fully comprehend and implement in the design and construction process are the public's expectations for hazardous waste site cleanup. We cannot meet these expectations until technology can develop effective means to positively educate the public about the fallacy of "risk-free" solutions and 100 percent removal of contaminants. This situation is compounded by the plethora of public agencies, scores of consultants, and artificial separation of investigation, analysis, design and construction management responsibilities.

The geotechnical profession has made and will continue to make major contributions to cleanup and restoration of uncontrolled hazardous waste disposal sites. Limitations created by institutional constraints have not allowed the implementation of efficient, innovative geotechnical solutions to site remediation. The challenge to our profession is to educate both the regulator and the public as to the benefits of two simple precepts--continuity of thought and the use of the observational method to efficiently and effectively remediate the uncontrolled hazardous waste disposal site.

ACKNOWLEDGEMENTS

This paper expresses the author's opinions and is not intended to represent either U.S. EPA or USCE positions concerning Lipari Landfill. The author wishes to thank Kevin Oates, U.S. EPA, Mat Beatty, USCE and Jim Howey of CH2M HILL for taking time to discuss details of the Lipari Leachate Containment System Project.

REFERENCES

Anderson, D. C., Brown, W. W., and Green, J. (1981), "Organic Leachate Effects on the Permeability of Clay Liners." Proceedings of the National Conference on Management of Uncontrolled Hazardous Waste Sites.

CH2M HILL, (1983), "Predesign Report for Remedial Measures for Lipari Landfill, Gloucester County, New Jersey." Report to U.S. EPA Region II.

Comptroller General, (1983), "Decision in the Matter of Slurry Systems." File B-212033.

D'Appolonia, D. J. (1980), "Soil-Bentonite Slurry Trench Cutoffs," Journal of the Geotechnical Engineering Division of the American Society of Civil Engineers, Vol. 106, No. GT4.

Harrington, W. H. (1980), "Report on Lipari Landfill Investigation and Assessment." Chemical Manufacturers Association.

Radian Corporation, (1982a), "Cost Effectiveness Assessment of Remedial Action Alternatives, Lipari Landfill." Report to U.S. EPA Region II.

Radian Corporation, (1982b), "Draft Environmental Assessment for Remedial Actions at the Lipari Landfill, Pitman, New Jersey." Report to U.S. EPA Region II.

USCE, (1983), "Specifications for Construction of Lipari Landfill: Leachate Containment System." U.S. Army Corps of Engineers, Kansas City District.

R. E. Wright Associates, Inc. (1980), "Abatement Alternatives-Uncontrolled Chemical Leachate Discharge from the Lipari Landfill, Pitman, New Jersey." Report to the Commander, Third Coast Guard District.

R. E. Wright Associates, Inc. (1981a), "Technical Considerations for the Selection of an Abatement System at the Lipari Landfill, Pitman, New Jersey." Report to U.S. EPA Region II.

R. E. Wright Associates, Inc. (1981b), "Work Scope and Specifications, Cutoff-Wall Construction, Lipari Landfill, Pitman, New Jersey." Report to U.S. EPA Region II.

Proceedings: Second International Conference on Case Histories in Geotechnical Engineering, June 1-5, 1988, St. Louis, Mo., Invited Paper

Case Histories in Seismic Response Analysis

W.D. Liam Finn
Professor of Civil Engineering, University of British Columbia,
Vancouver, British Columbia, Canada

SYNOPSIS: The reliability and utility of dynamic response analysis in geotechnical engineering is explored by a series of case histories. A detailed study of the seismic response of Mexico City sites during the 1985 earthquake shows clearly the limitations of present methods for estimating the appropriate input motions for analysis and the necessity of using a suite of representative input motions. Analyses of seismic soil-structure interaction are conducted on centrifuged models subjected to simulated earthquake loading. Finally the seismic response of a tailings dam is investigated using nonlinear dynamic effective stress analysis.

INTRODUCTION

The basic elements in the dynamic analysis of a soil-structure system are input motion, appropriate models of site and structure, constitutive relations for all materials present, and a stable, efficient, accurate, computational procedure. The specification of the input motion and the selection of an appropriate constitutive relation are the most difficult steps in the analysis.

Linear elastic analysis is appropriate for low levels of shaking in relatively firm ground. As the shaking becomes more intense, soil response becomes nonlinear. A great variety of constitutive relations are available for nonlinear response analysis ranging from equivalent linear elastic models to elastic-plastic models with both isotropic and kinematic hardening. An additional complication is the effect of seismically induced porewater pressures. If these become significant, the corresponding reduction in effective stresses will result in significant reductions in moduli and strength which must be taken into account. Therefore, for some problems, the simpler total stress methods of analysis are not adequate; effective stress methods must be used.

The most widely used methods for dynamic analysis are based on the equivalent linear model. Computer programs representative of this approach are SHAKE (Schnabel et al., 1972) for one-dimensional analysis (1-D) and FLUSH (Lysmer et al., 1975) for 2-D analysis. These programs perform total stress analyses only.

In recent years, there has been a distinct shift towards the use of nonlinear total and effective stress methods of analysis. A number of nonlinear 1-D programs are now available which give similar results for a given site (Streeter et al., 1973; Lee and Finn, 1975; Lee and Finn, 1978; Martin et al., 1978; Dikmen and Ghaboussi, 1984). A widely used program of this kind is DESRA-2 (Lee and Finn, 1978) which has been used for site response studies both onshore and offshore.

A number of programs are also available for 2-D nonlinear dynamic effective stress analysis. The simplest kind are based on nonlinear hysteretic models of soil response using hyperbolic skeleton loading curves and unloading-reloading response defined by the Masing criterion (Masing, 1926). A representative program of this type is TARA-3, the third in an evolving series of TARA programs (Finn et al., 1986). This program has been subjected to critical evaluation over the last three years using data from centrifuge model tests sponsored by the U.S. Nuclear Regulatory Commission through the European Office of the U.S. Army Corps of Engineers. Some of these tests have been described previously by Finn (1986). Some results from this study will be presented later.

2-D elastic-plastic models for dynamic effective stress analysis are generally based on Biot's equations (Biot, 1941) for coupled fluid-soil systems. However few of these have been incorporated in commercially available programs. The most widely used program of this type is DYNAFLOW (Prevost, 1981). The elastic-plastic effective stress models offer the most general descriptions of soil response. However, the properties required in some of them are difficult to measure and the programs make heavy demands on computational time. Analyses using these models have been conducted on super computers to cut the turn around time. Recent studies comparing a Japanese program of this type, DIANA-J, with the nonlinear program TARA-3 showed TARA-3 to be a minimum of 50-60 times faster (Yoshida, 1987).

EQUIVALENT LINEAR ANALYSIS OF SITE RESPONSE AT MEXICO CITY SITES

Mexico City is located in the south west corner of the Valley of Mexico on the edge of the former Lake Texcoco. During the 1985 earthquake, ground accelerations were recorded on hard sites in the foothills of the University district (UNAM) and on the soft deposits of the old lake bed. The locations of the accelerograph sites are shown in Fig. 1.

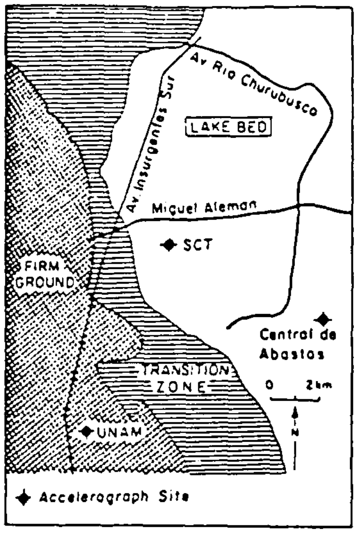

Fig. 1. Soil zones and accelerograph sites in Mexico City (after Mitchell et al., 1986).

Soil conditions in the lake zone are characterized by soft clay deposits overlying dense sands and much stiffer clays with shear wave velocities comparable to those of soft rock. Romo and Seed (1986) characterized the lake zone sites as homogeneous clay layers with the properties shown in Table 1. The CAF and CAO sites are located in Central de Abastos (Fig. 1). The shear wave velocities, V_s, were determined from the natural periods of the sites obtained from the Fourier spectra of the recorded motions (Romo and Seed, 1986). The corresponding shear moduli, G, were obtained from $G = \rho V_s^2$ in which ρ = mass density of the soil. These values compared well with moduli derived from the results of resonant column and cyclic triaxial tests (Romo and Jaime, 1986). The variations of shear modulus and damping ratio of Mexico City clay as a function of shear strain (Leon et al., 1974; Romo and Jaime, 1986) are shown in Fig. 2.

Table 1. Properties of Mexico City Sites for Dynamic Analysis (after Romo and Seed, 1986).

Site	Depth	Shear Wave Velocity	Unit Weight
SCT	35-40m	75-80 m/s	1.2 t/m³
CAO	55m	65-75 m/s	1.2 t/m³
CAF	45m	70 m/s	1.2 t/m³

The response of the lake zone sites will be analyzed in two ways, (1) following the usual procedure of using a scaled acceleration record from another earthquake as a representative input motion and (2) using the rock outcrop motions recorded at UNAM (Finn et al, 1988).

Analysis Using Scaled Motion

Romo and Seed (1986) analysed the three lake bed sites using the program SHAKE (Schnabel et al., 1972). They used the Pasadena record of the 1952 Kern County earthquake (M ≈ 7.6) as a representative input motion after scaling it appropriately for peak acceleration (a_{max} = 0.035 g) and frequency to obtain strong response around a period of two seconds, the period of the SCT site. This scaling resulted in a good match between the computed acceleration response spectrum for the SCT site and the average spectrum of the two horizontal components of acceleration recorded at the site (Fig. 3). This analysis was repeated for the present study with similar results (Fig. 3).

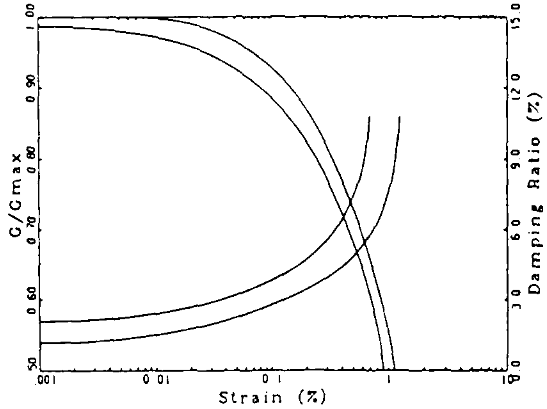

Fig. 2. Range in shear-dependent moduli and damping for Mexico City clay (after Leon et al., 1974 and Romo and Jaime, 1986).

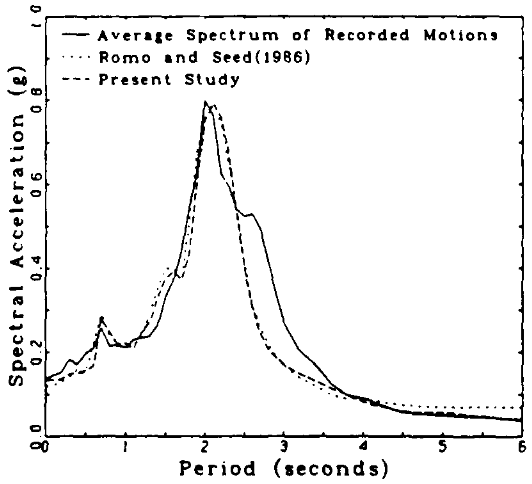

Fig. 3. Response spectra (5% damping) of computed motions and average response spectra of the recorded motions at the SCT site.

The acceleration response spectrum of the scaled Pasadena motions is shown in Fig. 4 together with the spectrum of the motions scaled for peak acceleration only. It is clear that scaling for frequency resulted in a major shift in the period of strong spectral response. Such a major scaling for frequency would probably not have been considered

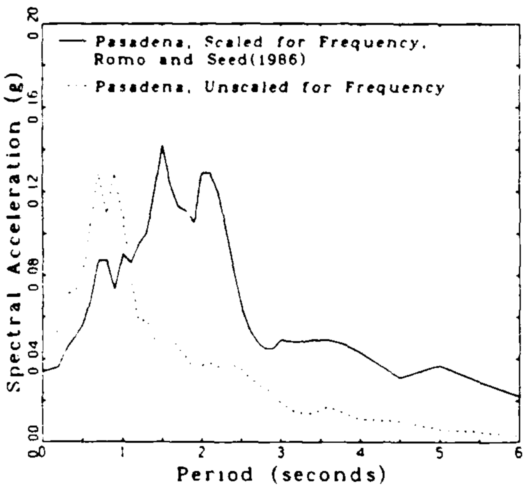

Fig. 4. Response spectra (5% damping) for Pasadena record showing effect of frequency scaling.

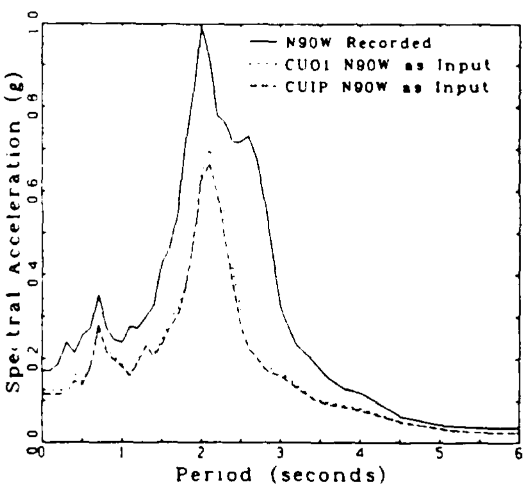

Fig. 5. Response spectra (5% damping) of recorded and computed motions in the N90W direction at the SCT site.

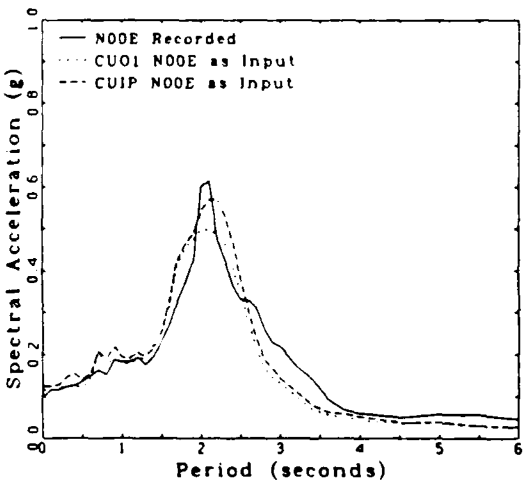

Fig. 6. Response spectra (5% damping) of recorded and computed motions in the N00E direction at the SCT site.

necessary had it not been for the availability of the 1985 ground motion records which showed that the peak response at the SCT site occurred around a period of 2 sec and that the rock motion had relatively high response at the same period. The predominant period of rock input motions would probably have been estimated at around 1.5 sec based on the relationship between predominant period and distance to the causative fault developed by Seed et al. (1969).

Note that uniform scaling of a record for frequency does more than simply shift the period of peak response to the desired frequency. It also enlarges the frequency range in which strong response may be encountered. Therefore input motions with predominant periods greatly different from the required predominant period should not be uniformly scaled unless broad band strong response is desired.

Analysis Using Rock Outcrop Motions

Accelerations were recorded at two hard sites at UNAM. The motions, designated CUO1 and CUIP, were recorded on the first floor of a three storey building and in the free field respectively. The seismic response of the SCT site was analyzed using the N90W and N00E components of these motions as input motions to the SHAKE program. The peak horizontal accelerations of these components are as follows: CUO1-N90W = 0.034 g, CUO1-N00E = 0.028 g, CUIP-N90W = 0.035 g and CUIP-N00E = 0.032 g. Detailed discussions of the characteristics of the recorded ground motions are given by Anderson et al., 1986a, 1986b.

The acceleration response spectra for the computed ground motions are compared with the corresponding spectra of the recorded motions in Figs. 5 and 6. In the N90W direction, both spectra of the computed motions underestimate the spectrum of the recorded motions both in terms of peak spectral acceleration and the range of strong response (Fig. 5). The agreement in the case of the N00E components is much better (Fig. 6). Clearly the motions at the SCT site must have a much greater directional bias than the rock motions recorded at UNAM. This is evident from the acceleration plots in Figs. 7a and 7b, which show the total acceleration paths for the CUIP motions at the UNAM site and the SCT site respectively. Note that the acceleration paths for the SCT site lie in an elongated band inclined significantly more to the N90W direction than to the N00E direction.

A close match between the computed and measured spectra for the N90W direction is obtained if the CUIP input motions are scaled to a peak acceleration of 0.095 g from 0.035 g as shown in Fig. 8. Note that the peak spectral accelerations are approximately equal and the range of peak response is now considerably wider than that obtained using the unscaled motions as input (Fig. 5). Even the shoulder in the recorded response spectrum to

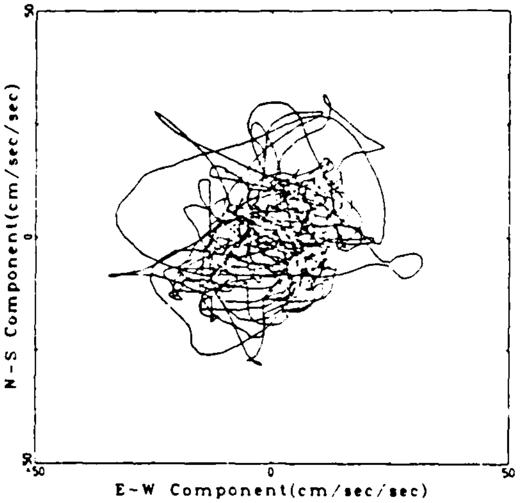

Fig. 7a. Recorded accelerations at the CUIP site.

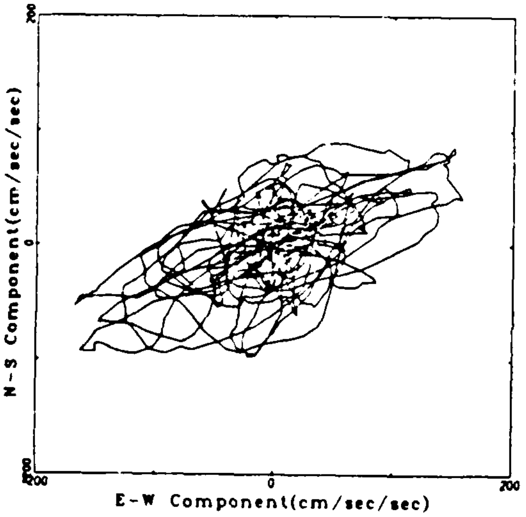

Fig. 7b. Recorded accelerations at the SCT site.

the right of the peak response is now reproduced. When the N90W component of the CU01 motions are scaled also to 0.095 g, the computed response is slightly greater than the recorded response but the correct shape is reproduced. By further refinement in the scaling a closer match could be obtained in the region of peak response. But the lesson is already clear that scaling of the rock outcrop motions by a factor of about 2.5 is necessary to get a good match between recorded and computed spectra in the N90W direction in the region of peak response. Note that the scaling to match peak response has resulted in higher computed responses around a period of 1 sec. It is not possible to get simultaneously a good match in both these regions of the response spectrum. A reasonable match may be obtained in the N00E direction with little or no scaling (Fig. 6).

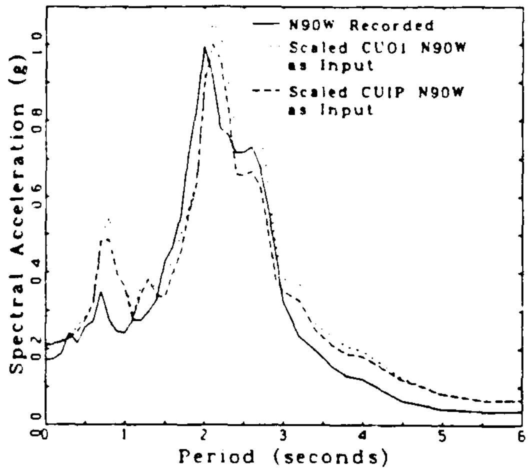

Fig. 8. Response spectra (5% damping) of recorded and computed motions in the N90W direction at the SCT site, scaled outcrop motions as input.

There are a number of possible explanations for the discrepancies between recorded and computed spectra when the rock outcrop motions are used as input. If it is assumed that the shear beam model adequately represents the dynamic response of the sites then it must be assumed that the rock outcrop motions are modified as they pass into the hard sand layer, acquiring a directional bias and a redistribution of peaks. But it seems unlikely that this is the sole explanation. It is probable that surface waves are generated in the stratum above the sand layer with periods dependent on the local thickness and stiffness of the layer. Information on these waves would not be included in the rock outcrop motions, resulting in significant long period differences between computed and recorded responses. An interesting example of this is provided by data from the Oji site in Japan (Ohta et al., 1977).

2-D NONLINEAR DYNAMIC EFFECTIVE STRESS ANALYSIS

2-D dynamic analyses are usually conducted using equivalent linear finite element analyses in the frequency domain. There has been little verification of these methods because of a lack of adequate field data.

There are certain important phenomena in soil-structure interaction outside the scope of conventional frequency domain analysis. Typical examples are uplift during rocking, permanent deformations, the effects of seismically induced porewater pressures, hysteretic behaviour and stick-slip behaviour at interfaces between structure and foundation soils.

The program TARA-3 (Finn et al., 1986) was developed to cope with such problems. The capability of the program will be demonstrated by using it to analyze one of the NRC centrifuge tests which models the response of a heavy two-dimensional structure embedded in a saturated sand foundation to seismic excitation.

ANALYSIS BY TARA-3

In TARA-3, response in shear is assumed to be nonlinear and hysteretic with unloading and reloading stress-strain paths defined by the Masing criterion (Masing, 1926). The response of the soil to uniform all round pressure is assumed to be nonlinearly elastic and dependent on the mean normal effective stress. Porewater pressures during shaking are computed using the Martin-Finn-Seed porewater pressure model (Martin et al., 1975) modified to take into account the effects of initial static shear stress. Moduli and strength are continuously modified during analysis to reflect changes in the effective stress regime. A detailed description of the constitutive relations in TARA-3 is given by Finn (1985).

For analysis involving soil-structure interaction it may be important to model slippage between the structure and soil. Slip may occur during very strong shaking or even under moderate shaking if high porewater pressures are developed under the structure. TARA-3 contains slip elements of the Goodman (Goodman et al., 1968) type to allow for relative movement between soil and structure in both sliding and rocking modes during earthquake excitation.

MODEL STRUCTURE EMBEDDED IN SATURATED SAND

A schematic view of the model structure is shown in Fig. 9. It is made from a solid piece of aluminum alloy and has dimensions 150 mm wide by 108 mm high in the plane of shaking.

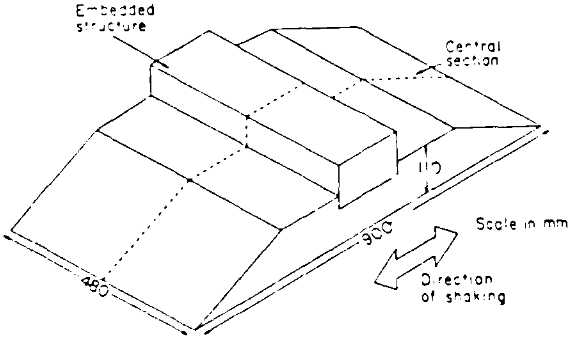

Fig. 9. Centrifugal model of embedded structure.

The length perpendicular to the plane of shaking is 470 mm and spans the width of the model container. The structure is embedded a depth of 25 mm in the sand foundation. Sand was glued to the base of the structure to prevent slip between structure and sand.

The foundation was constructed of Leighton Buzzard Sand passing British Standard Sieve (BSS) No. 52 and retained on BSS No. 100. The mean grain size is therefore 0.225 mm. The sand was placed as uniformly as possible to a nominal relative density $D_r = 52\%$.

During the test the model experienced a nominal centrifugal acceleration of 80 g. The model therefore simulated a structure approximately 8.6 m high by 12 m wide embedded 2 m in the foundation sand.

De-aired silicon oil with a viscosity of 80 centistokes was used as a pore fluid in order to model the drainage conditions in the prototype during the earthquake. If the linear scale factor between model and prototype is N, then excess porewater pressures dissipate approximately N^2 times faster in the model than in the prototype if the same fluid is used in both. The rate of loading by seismic excitation will be only N times faster. Therefore, to model prototype drainage conditions during the earthquake, a pore fluid with a viscosity N times the prototype viscosity must be used. This viscosity was achieved by an appropriate blending of commercial silicon oils. Tests by Eyton (1982) have shown that the stress-strain behaviour of fine sand is not changed when silicon oil is substituted for water as a pore fluid. In the gravitational field of 80 g, the structure underwent consolidation settlement which led to a significant increase in density under the structure compared to that in the free field. This change in density was taken into account in the analysis.

The locations of the accelerometers (ACC) and pressure transducers (PPT) are shown in Fig. 10. Analyses of previous centrifuge tests indicated that TARA-3 was capable of modelling acceleration response satisfactorily. Therefore, in the present test, more instrumentation was devoted to obtaining a good data base for checking the ability of TARA-3 to predict residual porewater pressures.

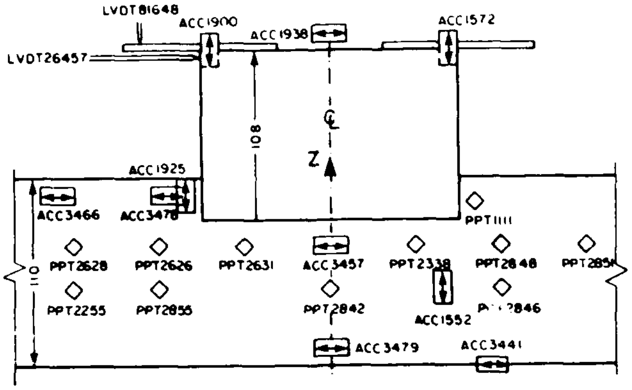

Fig. 10. Instrumentation of centrifuged model.

As may be seen in Fig. 10, the porewater pressure transducers are duplicated at corresponding locations on both sides of the centre line of the model except for PPT 2255 and PPT 1111. The purpose of this duplication was to remove any uncertainty as to whether a difference between computed and measured porewater pressures might be due simply to local inhomogeneity in density.

The porewater pressure data from all transducers are shown in Fig. 11. These records show the sum of the transient and residual porewater pressures. The peak residual pressure may be observed when the excitation has ceased at about 95 milliseconds. The pressures recorded at corresponding points on opposite sides of the centre line such as PPT 2631 and PPT 2338 are generally quite similar although there are obviously minor differences in the levels of both total and residual porewater pressures. Therefore it can be assumed that the sand foundation is remarkably symmetrical in its properties about the centre line of the model. Hence measured and computed porewater pressures are compared only for locations on one side of the centre line of the model only, the right hand side.

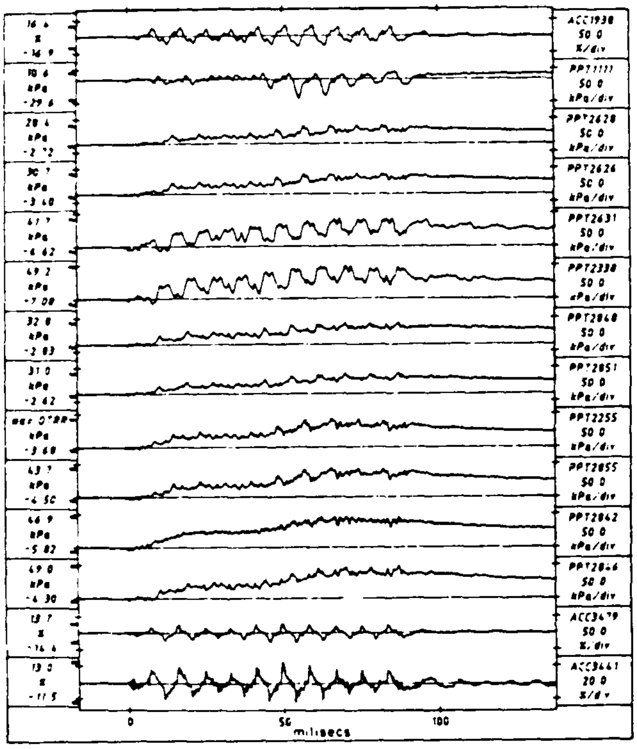

Fig. 11. Complete porewater pressure data from centrifuge test.

COMPUTED AND MEASURED ACCELERATION RESPONSES

The soil-structure interaction model was converted to prototype scale before analysis using TARA-3 and all data are quoted at prototype scale. Soil properties were consistent with relative density.

The computed and measured horizontal accelerations at the top of the structure at the location of ACC 1938 are shown in Fig. 12. They are very similar in frequency content, each corresponding to the frequency of the input motion given by ACC 3441 (Fig. 11). The peak accelerations agree fairly closely.

The vertical accelerations due to rocking as recorded by ACC 1900 and those computed by TARA-3 are shown in Fig. 13. Again, the computed accelerations closely match the recorded accelerations in both peak values and frequency content. Note that the frequency content of the vertical accelerations is much higher than that of either the horizontal acceleration at the same level in the structure or that of the input motion. This occurs because the foundation soils are much stiffer under the normal compressive stresses due to rocking than under the shear stresses induced by the horizontal accelerations.

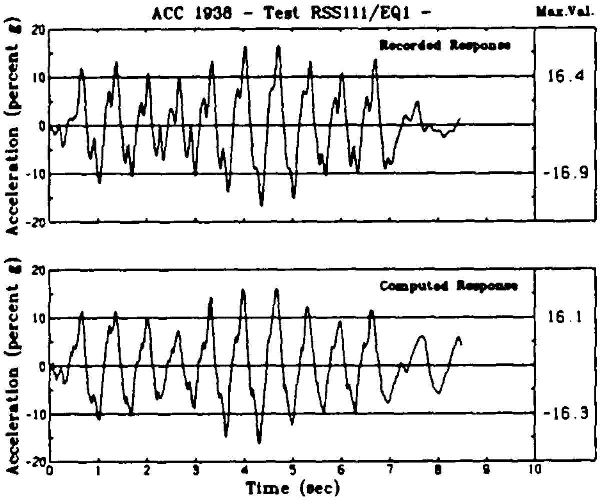

Fig. 12. Recorded and computed horizontal accelerations at ACC 1938.

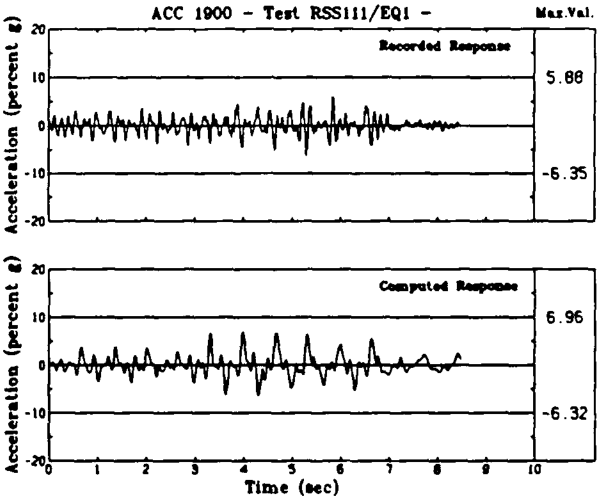

Fig. 13. Recorded and computed vertical accelerations at ACC 1900.

COMPUTED AND MEASURED POREWATER PRESSURES

The porewater pressures in the free field recorded by PPT 2851 are shown in Fig. 14. In this case the changes in the mean normal stresses are not large and the fluctuations of the total porewater pressure about the residual value are relatively small. The peak residual porewater pressure, in the absence of drainage, is given directly by the pressure recorded after the earthquake excitation has ceased. In

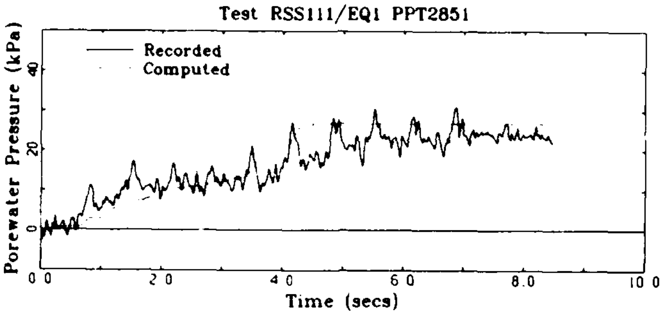

Fig. 14. Recorded and computed porewater pressures at PPT 2851.

the present test, significant shaking ceased after 7 seconds. A fairly reliable estimate of the peak residual pressure is given by the record between 7 and 7.5 seconds. The recorded value is slightly less than the value computed by TARA-3 but the overall agreement between measured and computed pressures is quite good.

As the structure is approached, the recorded porewater pressures show the increasing influence of soil-structure interaction. The pressures recorded by PPT 2846 adjacent to the structure (Fig. 15) show somewhat larger oscillations than those recorded in the free field. This location is close enough to the structure to be affected by the cyclic normal stresses caused by rocking. The recorded peak value of the residual porewater pressure is given by the relatively flat portion of the record between 7 and 7.5 seconds. The computed and recorded values agree very closely.

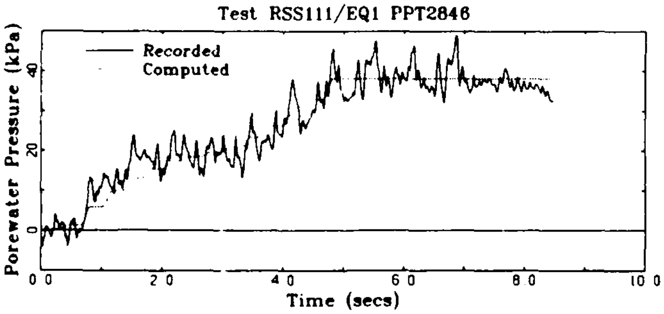

Fig. 15. Recorded and computed porewater pressures at PPT 2846.

Transducer PPT 2338 is located directly under the structure near the edge and was subjected to large cycles of normal stress due to rocking of the structure. These fluctuations in stress resulted in similar fluctuations in mean normal stress and hence in porewater pressure. This is clearly evident in the porewater pressure record shown in Fig. 16. The higher frequency peaks superimposed on the larger oscillations are due to dilations caused by shear strains. The peak residual porewater pressure which controls stability is observed between 7 and 7.5 seconds just after the strong shaking has ceased and before significant drainage has time to occur. The computed and measured residual porewater pressures agree very closely.

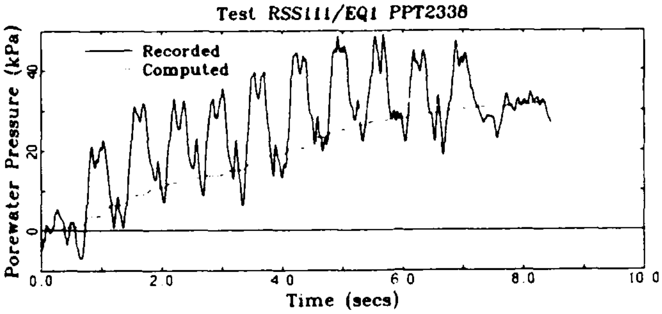

Fig. 16. Recorded and computed porewater pressures at PPT 2338.

Contours of computed porewater pressures are shown in Fig. 17. They indicate very symmetrical distribution of residual porewater pressure. Recorded values are also shown in this figure.

Stress-Strain Response

It is of interest to contrast the stress-strain response of the sand under the structure with that of the sand in the free field. The stress-strain response at the location of porewater pressure transducer PPT 2338 is shown in Fig. 18. Hysteretic behaviour is evident but the response for the most part is not strongly nonlinear. This is not surprising as the initial effective stresses under the structure were high and the porewater pressures reached a level of only about 20% of the initial effective vertical stress.

The response in the free field at the location of PPT 2851 (Fig. 19) is strongly nonlinear with large hysteresis loops indicating considerable softening due to high

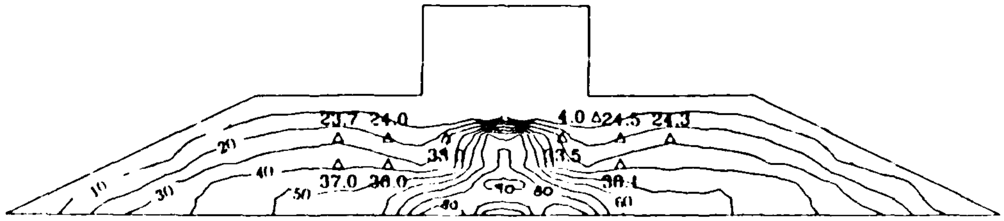

Fig. 17. Contours of computed porewater pressures.

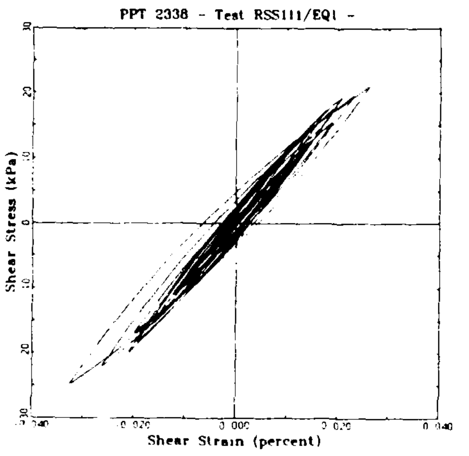

Fig. 18. Stress strain response under the structure.

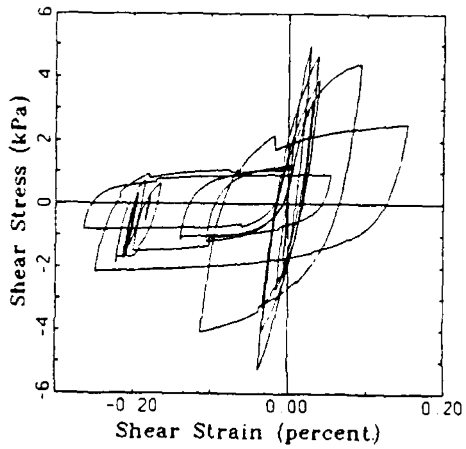

Fig. 19. Stress strain response in the free field.

porewater pressures and shear strain. At this location the porewater pressures reached about 80% of the initial effective vertical pressure.

ANALYSIS OF DAMS

Since the development of TARA-3 in 1986, it has been used to estimate the seismic response of a number of dams. In particular, it has been used to determine the peak dynamic displacements and the post-earthquake permanent deformations. Typical results for the proposed Lukwi tailings dam in Papua New Guinea will be presented to show the kind of data that is provided by a true nonlinear effective stress method of analysis (Finn et al., 1987,1988).

Lukwi Tailings Dam

The finite element representation of the Lukwi tailings dams is shown in Fig. 20. The sloping line in the foundation is a plane between two foundation materials. Upstream to the left is a limestone with shear modulus G = 6.4 x 10^6 kPa and a shear strength defined by c' = 700 kPa and ϕ' = 45°. The material to the right is a siltstone with a low shearing resistance given by c' = 0 and ϕ' = 12°. The shear modulus is approximately G = 2.7 x 10^6 kPa. The difference in strength between the foundation soils is reflected in the dam construction. The upstream slope on the limestone is steep whereas the downstream slope on the weaker foundation is much flatter and has a large berm to ensure stability.

The dam was subjected to strong shaking with a peak acceleration of 0.33 g (Fig. 21). The response of the limestone foundation is almost elastic as shown in Fig. 22 by the shear stress-shear strain response for a typical element.

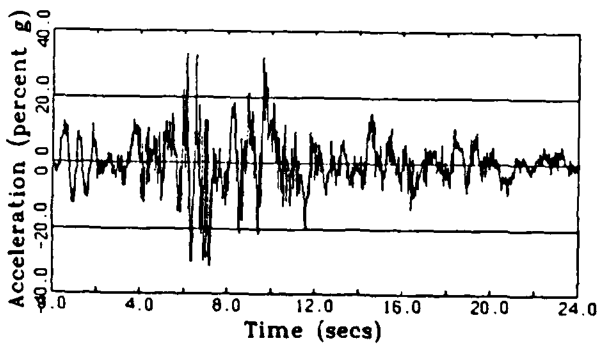

Fig. 21. Input motion of analysis of Lukwi tailings dam.

The response of the siltstone foundation is strongly nonlinear. The deformations increase progressively in the direction of the initial static shear stresses as shown in Fig. 23. Since the analysis starts from the initial

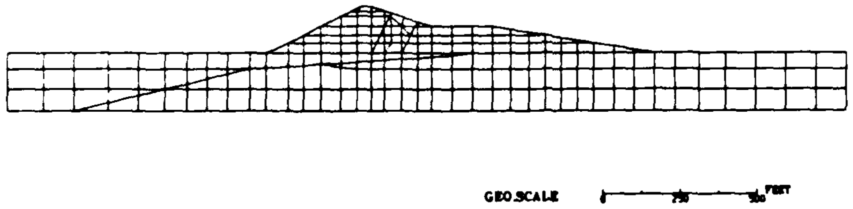

Fig. 20. Finite element idealization of Luwki tailings dam.

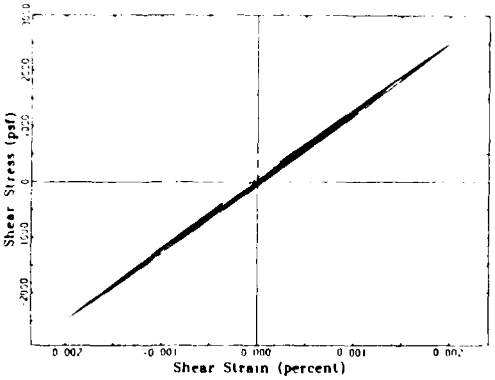

Fig. 22. Shear stress-shear strain response of limestone foundation.

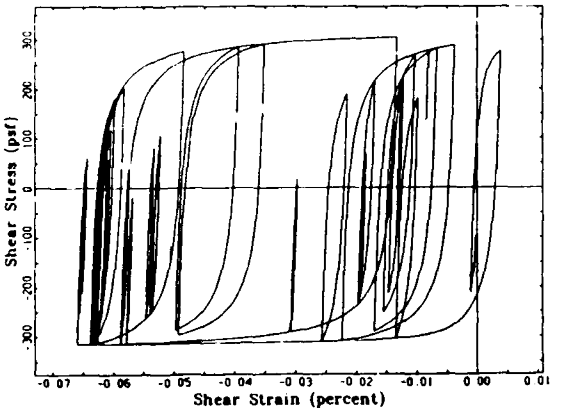

Fig. 23. Shear stress-shear strain response of siltstone foundation.

post-construction stress-strain condition subsequent large dynamic stress impulses move the response close to the highly nonlinear part of the stress-strain curve. It may be noted that the hysteretic stress-strain loops all reach the very flat part of the stress-strain curve, thereby ensuring successively large plastic deformations.

An element in the berm also shows strong nonlinear response with considerable hysteretic damping (Fig. 24).

The acceleration time history of a point near the crest in the steeper upstream slope is shown in Fig. 25. The displacement time history of the point is shown in Fig. 26. Note that the permanent deformation is of the order of 25 cm. Most of this was generated by a large permanent slip which occurred about 8 secs after the start of shaking.

The deformed shape of the central portion of the dam is shown to a larger scale in Fig. 27.

CONCLUSIONS

The selection of representative motions for use as input in seismic response analyses requires considerable skill and a deep understanding of the role of system characteristics

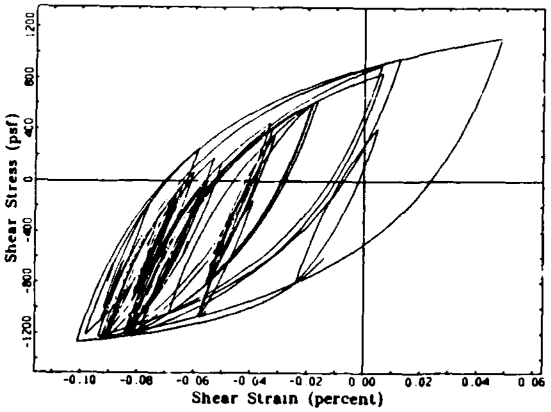

Fig. 24. Shear stress-shear strain response in the berm.

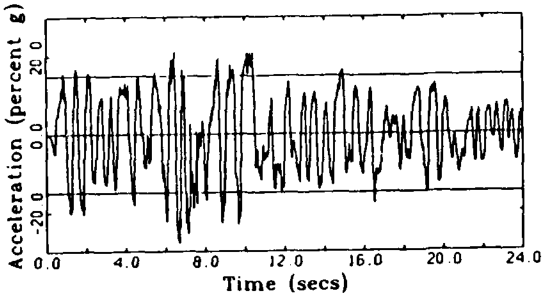

Fig. 25. Computed accelerations of a point near the crest.

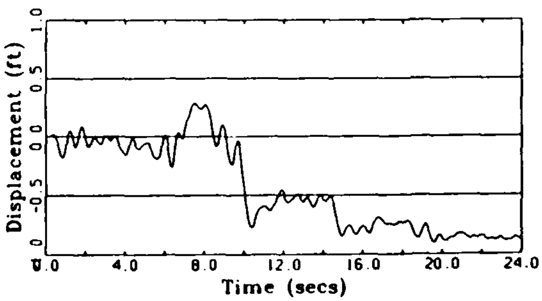

Fig. 26. Displacement history of a point near the crest.

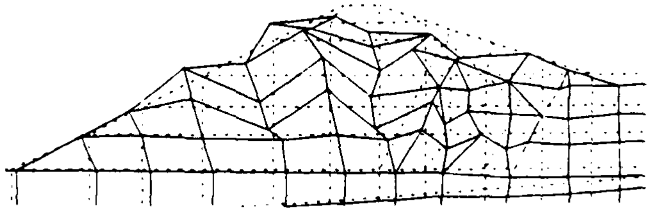

Fig. 27. Deformed shape of the dam after the earthquake to enlarged scale.

in defining seismic response. The practice of selecting just a few candidate motions, which is unfortunately fairly common, may be dangerously unconservative.

The very common practice of modelling the incoming seismic waves as horizontal shear waves propagating vertically is inadequate wherever significant surface waves are present. It may also be inadequate close to the epicentre.

Dynamic analysis provides a constant ordered approach to estimating the characteristics of site specific motions. It allows parametric studies to be conducted which are powerful guides to judgement. Estimating "exact" seismic response parameters is impossible; defining safe but economical design parameters with the help of an adequate supply of representative input motions for dynamic response analysis is feasible and practical.

Phenomenological aspects of soil-structure interaction are clearly demonstrated in centrifuge tests such as high frequency rocking response, the effects of rocking on porewater pressure patterns and the distortion of free-field motions and porewater pressures by the presence of a structure.

The comparison between measured and computed responses for the centrifuge model of a structure embedded in a saturated sand foundation demonstrates the wide ranging capability of TARA-3 for performing complex effective stress soil-structure interaction analysis with acceptable accuracy for engineering purposes. Seismically induced residual porewater pressures are satisfactorily predicted even when there are significant effects of soil-structure interaction. Computed accelerations agree in magnitude, frequency content and distribution of peaks with those recorded. In particular, the program was able to model the high frequency rocking vibrations of the model structures. This is an especially difficult test of the ability of the program to model soil-structure interaction effects.

The program TARA-3 can compute directly the permanent deformations of earth dams under seismic loading. The utility of TARA-3 in practice was demonstrated by the analysis of the Lukwi tailings dam. Computed stress-strain responses show the widely different responses of the different foundation materials to the design earthquake. The computed final deformed shape of the dam itself reflected clearly the influence of dam geometry and the different foundation materials.

The nonlinear effective stress analysis provides a very clear overall picture of the response of the dam to the design earthquake as well as providing the designer with all the details necessary in zones of potential concern.

ACKNOWLEDGEMENTS

The analyses of site response in Mexico City were conducted as part of a study for the Canadian Council on Earthquake Engineering. The development of TARA-3 was supported by the National Science and Engineering Research Council of Canada under Grant No. 1498, and the Exxon Production and Research Company. The centrifuge tests were funded by the U.S. Nuclear Regulatory Commission through the European Office of the U.S. Army Corps of Engineers. The support of these sponsors is gratefully acknowledged. The project was managed by W. Grabau and J.C. Comati of the Europoean Research Office, U.S. Army London; R.H. Ledbetter of USAE Waterways Experiment Station, Vicksburg, Miss.; and L.L. Beratan, Office of Research, U.S. Nuclear Regulatory Commission. The centrifuge tests were conducted by R. Dean, F.H. Lee and R.S. Steedman of Cambridge University, U.K., under a separate contract. The tests were under the general direction of A.N. Schofield, Cambridge University and were monitored by the author on behalf of USAE. Descriptions of the centrifuge model test and related figures are used by permission of Cork Geotechnics Ltd., Ireland. Data from the Lukwi tailings dam analysis are used with permission of Klohn Leonoff Consultants Ltd., Richmond, B.C., Canada. The text was typed by Ms. Kelly Lamb.

REFERENCES

Anderson, J.G., J.N. Brune, J. Prince, E. Mena, P. Bodin, M. Onate, R. Quaas and S.K. Singh. 1986a. Aspects of Strong Motion. The Mexico Earthquakes - 1985, Edited by M.A. Cassaro and E.M. Romero, American Society of Civil Engineers, New York, N.Y., pp. 33-54.

Anderson, J.G., P. Bodin, J. Brune, J. Prince, S. Singh, R. Quaas and M. Onate. 1986. Strong Ground Motion of the Michoacan, Mexico Earthquake. Science, 233, 1043-1049.

Biot, M.A. 1941. General Theory of Three-Dimensional Consolidation. J. Appl. Phys., 12, 155-64.

Dikmen, S.U. and Ghaboussi, J. 1984. Effective Stress Analysis of Seismic Response and Liquefaction: Theory. Journal of the Geotech. Eng. Div., ASCE, Vol. 110, No. 5, Proc. Paper 18790, pp. 628-644.

Eyton, D.G.P. 1982. Triaxial Tests on Sand with Viscous Pore Fluid. Part 2, Project Report, Cambridge University, Engineering Department.

Finn, W.D. Liam. 1985. Dynamic Effective Stress Response of Soil Structures; Theory and Centrifugal Model Studies, Proc. 5th Int. Conf. on Num. Methods in Geomechanics, Nagoya, Japan, Vol. 1, 35-36.

Finn, W.D. Liam. 1986. Verification of Non-linear Dynamic Analysis of Soils Using Centrifuged Models. Proc., International Symposium on Centrifuge Testing, Cambridge University, U.K., 20 pp.

Finn, W.D. Liam and A.M. Nichols. 1988. Seismic Response of Long Period Sites: Lessons from the September 19, 1985 Mexican Earthquake. Canadian Geot. Journal, Vol. 25, No. 1.

Finn, W.D. Liam, R.C. Lo and M. Yogendrakumar. 1987. Dynamic Nonlinear Analysis of Lukwi Tailings Dam. Soil Dynamics Group, Dept. of Civil Engineering, University of British Columbia, Vancouver, B.C., Canada.

Finn, W.D. Liam, M. Yogendrakumar and R.C. Lo. 1988. Direct Computation of Permanent Seismic Deformations. Proceedings 9th World Conference on Earthquake Engineering, Tokyo and Kyoto, Japan, August (to appear).

Finn, W.D. Liam, M. Yogendrakumar, N. Yoshida, and H. Yoshida. 1986. TARA-3: A Program for Nonlinear Static and Dynamic Effective Stress Analysis, Soil Dynamics Group, University of British Columbia, Vancouver, B.C.

Goodman, R.E., R.L. Taylor and T.L. Brekke. 1968. A Model for the Mechanics of Jointed Rock, J. Soil Mech. and Found. Div. ASCE, 94 (SM3), 637-659.

Lee, M.K.W. and Finn, W.D.L. 1975. DESRA-1, Dynamic Effective Stress Response Analysis of Soil Deposits. Department of Civil Engineering, University of British Columbia, Vancouver, B.C.

Lee, M.K.W. and Finn, W.D.L. 1978. DESRA-2, Dynamic Effective Stress Response Analysis of Soil Deposits with Energy Transmitting Boundary Including Assessment of Liquefaction Potential. Soil Mechanics Series No. 38, Department of Civil Engineering, University of B.C., Vancouver, B.C.

Leon, J.L., A. Jaime and A. Tabago. 1974. Dynamic Properties of Soils - Preliminary Studies. Institute of Engineering, UNAM, (in Spanish).

Lysmer, J., Udaka, T., Tsai, C.F. and Seed, H.B. 1975. FLUSH: A Computer Program for Approximate 3-D Analysis of Soil-Structure Interaction Problems. Report No. EERC 75-30, Earthquake Engineering Research Center, University of California, Berkeley, California.

Martin, G.R., W.D. Liam Finn, and H.B. Seed. 1975. Fundamentals of Liquefaction Under Cyclic Loading, Soil Mech. Series Report No. 23, Dept. of Civil Engineering, University of British Columbia, Vancouver; also Proc. Paper 11284, J. Geotech. Eng. Div. ASCE, 101 (GT5): 324-438.

Martin, P.P. and Seed, H.B. 1978. MASH - A Computer Program for the Nonlinear Analysis of Vertically Propagating Shear Waves in Horizontaly Layered Soil Deposits. EERC Report No. UCB/EERC-78/23, University of California, Berkeley, California, October.

Masing, G. 1926. Eigenspannungen und Verfestigung beim Messing, Proc., 2nd Int. Congress of Applied Mechanics, Zurich, Switzerland.

Mitchell, D., J. Adams, R.H. DeVall, R.C. Lo and D. Weichert. 1986. Lessons from the 1985 Mexican Earthquake. Canadian Journal of Civil Engineering, Vol. 13, No. 5, pp. 535-557.

Ohta, T., Niva, M. and Andoh, H. 1977. Seismic Motions in the Deeper Portions of Bedrock and in the Surface and Response of Surface Layers. Proc., 4th Japan Earthquake Engineering Symposium, Tokyo, pp. 129-136 (in Japanese).

Prevost, J.H. 1981. DYNAFLOW: A Nonlinear Transient Finite Element Analysis Program. Princeton University, Department of Civil Engineering, Princeton, N.J.

Romo, M.P. and A. Jaime. 1986. Dynamic Characteristics of Some Clays of the Mexico Valley and Seismic Response of the Ground. Technical Report, DDF, (in Spanish).

Romo, M.P. and Seed, H.B. 1986. Analytical Modelling of Dynamic Soil Response in the Mexico City Earthquake of September 19, 1985. Presented at International Symposium on Mexican Earthquake, Mexico City. To be published in proceeding.

Schnabel, P.B., Lysmer, J. and Seed, H.B. 1972. SHAKE: A Computer Program for Earthquake Response Analysis of Horizontally Layered Sites. Report No. EERC 72-12, Earthquake Engineering Research Center, University of California, Berkeley, California.

Seed, H.B., I.M. Idriss and F.W. Kiefer. 1969. Characteristics of Rock Motions During Earthquakes. Journal of Soil Mechanics and Foundations Division, ASCE, Vol. 95, No. 5, pp. 1199-1218.

Streeter, V.L., Wylie, E.B. and Richart, F.E. 1973. Soil Motion Computations by Characteristics Method. ASCE National Structural Engineering Meetings, San Francisco, California, Preprint 1952.

Yoshida, N. 1987. Presentation at International Symposium on Centrifuge Testing, Cambridge Univerity, U.K.

Proceedings: Second International Conference on Case Histories in Geotechnical Engineering, June 1-5, 1988, St. Louis, Mo., Invited Paper

Cellular Cofferdams—Developments in Design and Analysis

G. Wayne Clough
Professor and Head, Civil Engineering Department, Virginia Polytechnic Institute and State University, USA

James R. Martin, II
Research Assistant, Civil Engineering Department, Virginia Polytechnic Institute and State University, USA

SYNOPSIS: Cellular cofferdams are reviewed from the point of view of recent developments, with a particular focus on movements. It is found that applications for cofferdams are expanding, with uses extended beyond the conventional temporary systems to permanent navigation and retaining structures. Results from instrumented cofferdams show that some conventional analysis procedures for predicting interlock force and internal stability are excessively conservative. Where conditions do not deviate far from the norm, movement patterns for cofferdams can be quantified and predicted. For more exotic cases, finite element procedures are available that yield reasonable predictions of behavior.

INTRODUCTION

Cellular cofferdams are normally temporary, serving to surround an area in a body of water so that it can be dewatered and used for construction. A plan view of this type of system is shown in Figure 1 for the Stage 1 cofferdam used for construction of a portion of the replacement Lock and Dam 26 on the Mississippi River. The cofferdam is formed by means of linked cells, each of which is created by driving interlocking steel sheetpiles. The cell may be circular, diaphragm, or cloverleaf in shape, although circular is the most common. As shown in Figure 1, the circular shape actually only applies to the main cells, with the circular cells connected by smaller arc cells. The wall that the main cell and arc cell share is termed the common wall. Where the common wall joins the converging main and arc cells, a special wye or tee element is used.

For many years, cofferdam technology was relatively static. Design methods remained untested, and in many cases gave conflicting answers. In recent years, this situation has changed. Cofferdams have found use in a wider variety of applications, including retaining structures, waterfront and harbor structures, and floodwalls. This has led to new forms of loading, increased concern about movements, and the use of the cofferdam as a permanent system.

The past 15 years have also seen a number of new investigations of cofferdam behavior. In a few, key cases, cofferdams have been instrumented, leading to data that allows behavior trends to be better understood, particularly as to movements. Also, several groups have adapted the finite element method to cofferdams, leading to insights into the nature of the soil-structure interaction process in these systems, and a linkage of movements in the structure and the soil. Finally, other workers have developed modifications to the conventional design technology. This paper reviews each of these subjects, and assesses the potential for future developments.

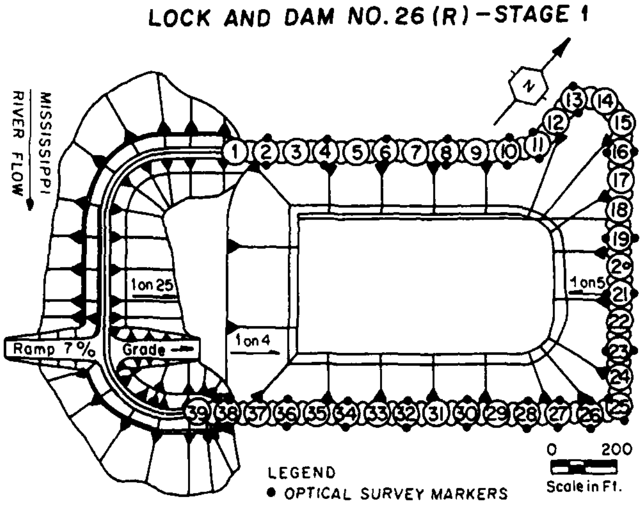

Fig. 1 - Layout and Instrumention of Stage 1 Cofferdam

CONVENTIONAL ANALYSIS AND DESIGN PROCEDURES

Conventional geotechnical design considerations for cofferdams include internal and external stability (Figure 2). Internal stability is concerned with the degree of loading of the sheetpile interlocks and connecting elements, and the possibility of a shear failure developing through the cell fill under the distortions that occur during lateral loading. External stability considers the possibility that the cofferdam behaves as a unit and is subject to bearing failure, sliding on the base, or overturning. Special considerations for cofferdams on rock relate to the possibility of sliding on weak planes in the rock. Broader aspects of cofferdam design involve overtopping, marine impact, ice loading, and construction related problems.

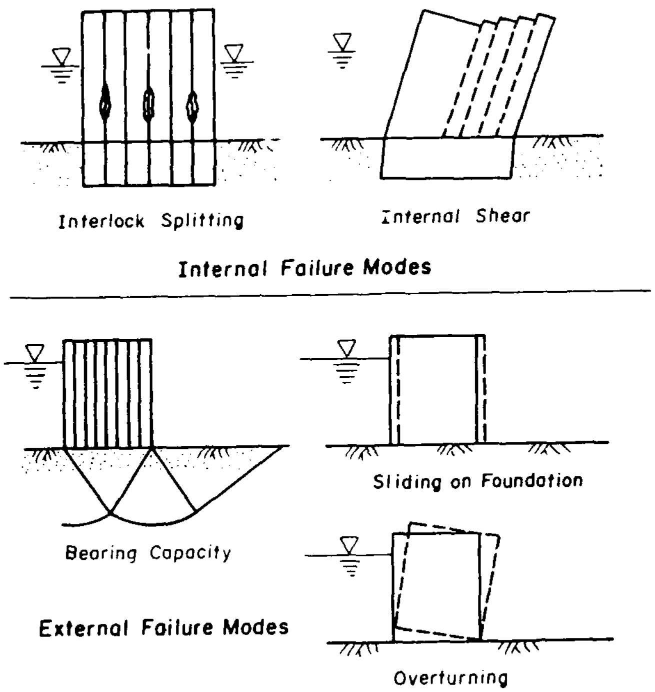
Interlock Splitting
Internal Shear
Internal Failure Modes
Bearing Capacity
Sliding on Foundation
External Failure Modes
Overturning

Fig. 2 - Typical Failure Modes of Cellular Cofferdams

Lacroix, et al. (1970) and Rossow, et al. (1987) have provided thorough reviews of conventional design approaches. These efforts will not be repeated in this section, rather only those areas where some new knowledge has been developed will be discussed. These include methods for calculating interlock loads for main or arc cell elements, interlock loads for the common wall, and internal stability.

There are a number of conventional methods for determining interlock loads. All are based upon the equation:

$$t = p \times r \quad \ldots\ldots\ldots\ldots\ldots \quad (1)$$

in which t = interlock load, p = pressure exerted by the fill, normally as applied to the inboard side of the cell, and r = radius of the cell. Differences in the methods lie in the distribution assumed for the fill pressure, and in the maximum value assigned for the pressure. In Figure 3 four commonly used alternatives are given: Terzaghi (1945), Tennessee Valley Authority (1957), Corps of Engineers, as outlined in NAVDOCKS Design Manual DM7 (1971), and Schroeder and Maitland (1979). For purposes of convenience, these will henceforth be referred to by the symbols TZ, TVA, COE, and S&M. The S&M approach represents the most recent development. As is seen in Figure 3, the TZ and COE methods assume triangular pressure distributions which continuously increase with depth, while the other two increase to a certain depth, and then decrease to zero. It is important to note that the TVA and S&M distributions are not intended to reflect the actual earth pressure distribution. Rather, they are designed to be used to generate the correct distribution of interlock load when using Equation (1). These methods reflect the fact that the interlock load must decrease near the dredge line because of the restraint offered by the embedded portion of the cell. Instrumentation data from cofferdams and finite element analyses support this concept. Further comment on this will be made later in this paper.

The common wall is subjected to a pull from both the main and arc cells. Thus, it is generally accepted that the common wall is subjected to a higher force than either the main or arc cell wall. The calculation of forces in the common wall is usually based on one of two approaches: (1.) The secant formula of the TVA:

$$t_{cw} = p\,L(\sec\theta) \quad \ldots\ldots\ldots\ldots\ldots\ldots \quad (2)$$

in which L = centerline distance between main and are cells; and θ = angle between centerline of main cell and wye connection point; and, (2.) The Swatek (1969) formula:

$$t_{cw} = p\,L \quad \ldots\ldots\ldots\ldots\ldots\ldots\ldots\ldots \quad (3)$$

Of the two, the secant formula gives the larger force prediction, and as will be shown subsequently, field data support the Swatek approach.

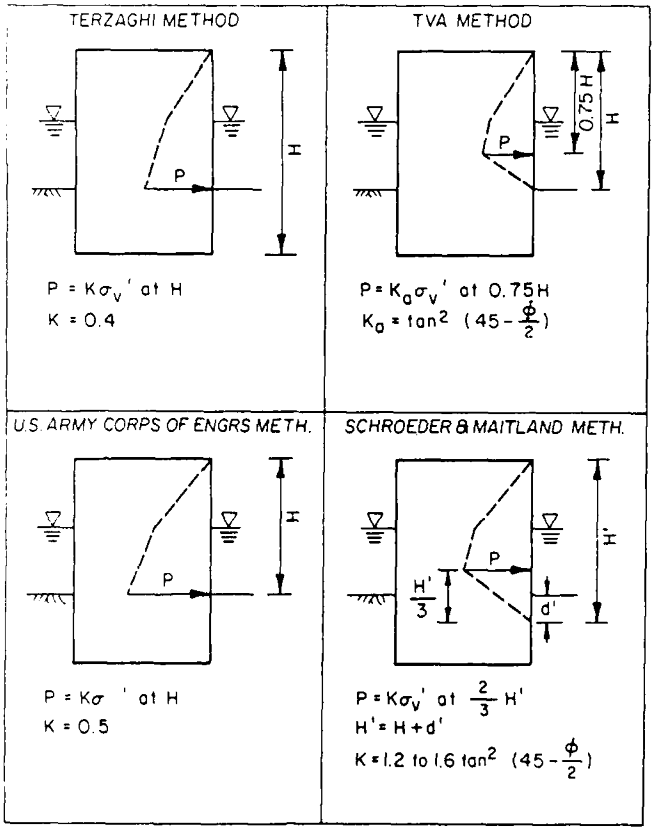
TERZAGHI METHOD
P
H
P = Kσv' at H
K = 0.4
TVA METHOD
P
0.75H
H
P = Kaσv' at 0.75H
Ka = tan2 (45 - φ/2)
U.S. ARMY CORPS OF ENGRS METH.
P
H
P = Kσ ' at H
K = 0.5
SCHROEDER & MAITLAND METH.
P
H'/3
d'
H
P = Kσv' at 2/3 H'
H' = H + d'
K = 1.2 to 1.6 tan2 (45 - φ/2)

Note: σ_v' is vertical effective stress

Fig. 3 - Pressure Distributions for Calculation of Interlock Forces

A number of alternative methods have been proposed for analysis of internal shear failure under the action of lateral loading. Probably the most widely accepted procedure is that postulated by Terzaghi (1945). As shown in Figure 4, he assumes that the soil in the cell undergoes shear along a vertical plane due to the overturning moment generated by the resultant of the lateral loads acting on the cofferdam. The external shear force on the base of the cofferdam fill, Q, is a function of the external or driving moment, M. Q is related to the driving moment as Q = 3M/2b, where b = the diameter of the cell. The force Q is resisted by the internal soil friction on the assumed vertical shear plane, and the friction in the interlocks, and the factor of safety against internal shear failure by this technique is:

$$F = \frac{bH}{3M} K (\tan \; + f)$$

where, f = coefficient of friction on the interlocks, K = the earth pressure coefficient acting on the vertical plane, = unit weight of the soil, and H = the height of the cell. The principal unknown in this approach is the value of the parameter K. Terzaghi assumed it to be 0.5. Schroeder and Maitland (1979) argue that this is too conservative, and that a more reasonable value is 1.0, thus doubling the allowable resultant lateral load. Finite element analyses have tended to support this finding (Singh and Clough, 1988).

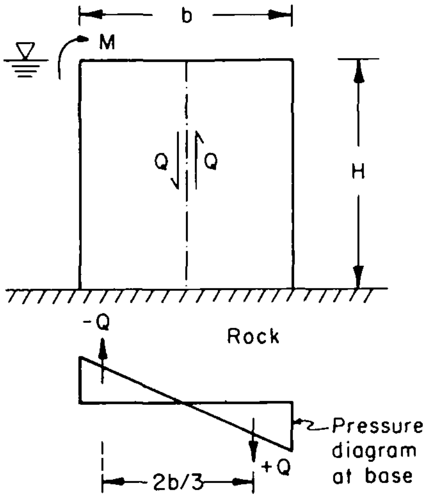

Fig. 4 - Terzaghi's Design Method for Cellular Cofferdams

Alternative methods for internal failure in the fill to that of Terzaghi were proposed by Krynine (1945), Hansen (1953), and Cummings (1957). Reasonable doubt still exists over which of the procedures is correct, and no cofferdam has been documented to have failed in this manner. Model tests by Maitland and Schroeder (1979) support the Terzaghi approach if the earth pressure coefficient used is 1.0, and not 0.5 as suggested by Terzaghi. However, in the model tests, the cofferdam had to be tilted 50 % of the cell height to generate the failure. Thus, it appears that a better approach to design would be to use limiting deformations as the control, since the large movements required to cause internal shear would obviously be unacceptable. In following sections of this paper, methods are suggested to allow calculation of the likely movements of a cellular cofferdam.

FINITE ELEMENT ANALYSIS PROCEDURES

Conventional analysis techniques for cofferdams are largely semi-empirical, and are limited to conditions similar to those for which we have an experience base. The concepts of soil-structure interaction upon which the conventional methods are based are elementary, and do not reflect the true nature of the problem in many instances. Further, they are unable to predict cofferdam movements and deflections. The latter drawback is important in where the cofferdam is deformation sensitive, or in the case deformations are to be monitored and used to judge the performance of the cofferdam.

Early efforts at finite element analyses of cofferdams were conducted without a full appreciation of the complexity of the system, particularly relative to the extra flexibility in the cells provided by the interlocks. Clough and Hansen (1977) first applied the method to a real cofferdam in the analysis of the Willow Island Cofferdam. This effort focused on the effects of lateral loading using a two-dimensional "vertical slice" model. The cell was represented by front and back bending elements connected by a series of flexible springs. The spring stiffnesses were derived on the basis that the cell acted as a perfect pressure vessel. The cell fill model incorporated allowances for nonlinear behavior, and provisions were made for slip between the cell walls and the cell fill. Deformation predictions using this model were reasonable for lateral loading, but were unrealistically small for the filling stage. Stevens (1980) later used the Clough and Hansen model to reanalyze the Willow Island Cofferdam, but he reduced the stiffness of the connecting springs for the front and back walls to allow for more flexibility, and hence to indirectly account for interlock induced deformations in the cell. This approach produced reasonable predictions of movements for both filling and lateral loading, but there was no general method available to determine the degree by which the flexibility should be reduced for interlock influences.

An intensive investigation into finite element analyses of cofferdams was triggered by the construction and instrumentation of the Lock and Dam 26 Replacement (R) cofferdam. Using the results of a series of tests on sheetpile assemblies, the senior author and his coworkers were able to develop three two-dimensional models which incorporated many of the key aspects of cofferdam behavior (Clough and Kuppusamy, 1985; Kuppusamy, et al., 1985). Each of the two-dimensional models addresses a different aspect of the problem. All incorporate allowances for interlock yielding, nonlinear soil behavior, slip between the cell fill and natural soils and the steel sheetpiles, and construction sequence. Further work by Mosher (1988) has extended these concepts to three-dimensional finite element analyses.

Figure 5 shows the results of an axisymmetric analysis of the filling of one of the main cells of Lock and Dam 26 (R). The results are given in terms of radial deflections of the cell, and interlock forces as a function of the degree of flexibility of the cell. The flexibility of the cell is described in terms of the parameter "E-Ratio," which is the ratio of the modulus used for the cell in the horizontal direction to that used for the vertical direction. To allow for interlock stretching, the E-Ratio must be less than one. It can be shown from interlock tests, and by comparison of predicted results to observed that the appropriate E-Ratio for the cell filling stage is in the range of 0.03-0.05. Importantly, with this level of E-Ratio, the cells typically expand enough on filling to cause active conditions within the cell fill, and lead to the lowest possible interlock forces.

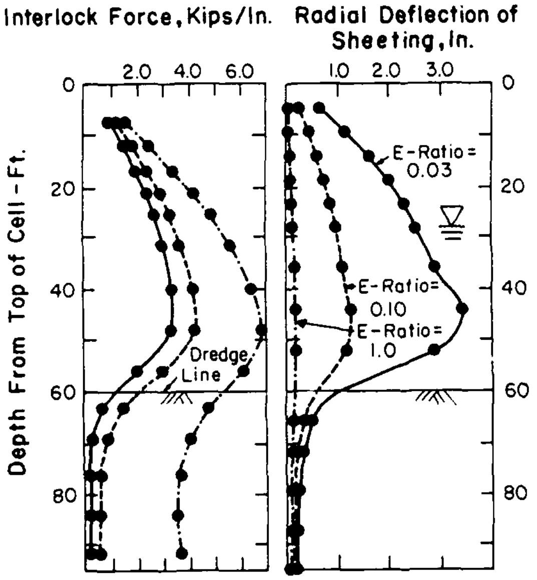

Fig. 5 - Results of Axisymmetric Analysis- End of Cell Filling - Lock & Dam 26 (R)

The contours of lateral stresses predicted for the cell fill for Lock and Dam 26 (R) Stage 1 cofferdam after completion of filling are given in Figure 6. The stress contours reveal a pattern of arching, caused by significant portion of the vertical weight of the fill being picked up by the shear between the cell sheetpiles and the fill. As reported by Clough and Goeke (1986), the arching was reflected in differences in insitu test results performed near the sheetpiles and near the center of the cells for the Lock and Dam 26 (R) Stage 1 cofferdam.

Figures 7 and 8 show comparisons of results predicted by the axisymmetric and three-dimensional finite element models for cell filling, and those obtained in the instrumentation program for Lock and Dam 26 (R) cofferdam. Results from both of the finite element models reasonably match the averages of the observed data for deflection and interlock loads. Movements of the instrumented cells are also closely predicted for differential loading caused by dewatering and flooding, Clough and Kuppusamy (1985). Further analyses of other cofferdams by Singh and Clough (1988) using the finite element tools support the idea that if proper parameters are defined for the models, realistic predictions of cofferdam behavior can be obtained.

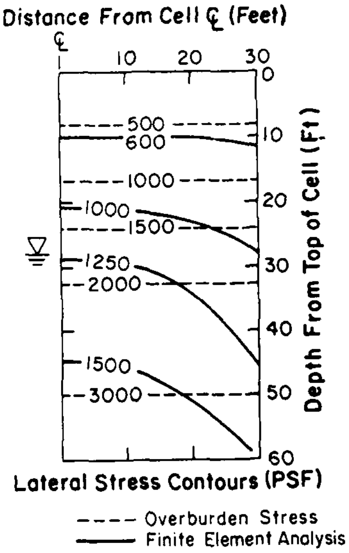

Fig. 6 - Lateral Stress Contours - End of Cell Filling - Lock & Dam 26 (R)

Recent design applications of the finite element models have been made for cofferdams used as floodwalls (Peters, 1987), and waterfront structures. Figure 9 shows predicted deflections for a cell used for a proposed offloading facility in Alaska which is subjected to strong ice loading just at the water line. The ice loading causes the cell to be distorted at the water line, and also to be translated as a unit by the ice loading. Analyses of this type were used to help select cell fill properties and foundation preparation techniques for the offloading facility so as to hold cell deflections within tolerable limits. Instrumentation results will be available in the near future for several projects to check the validity of the finite element predictions. However, the methods have already proven much of their merit in providing information to aid in critical design decisions.

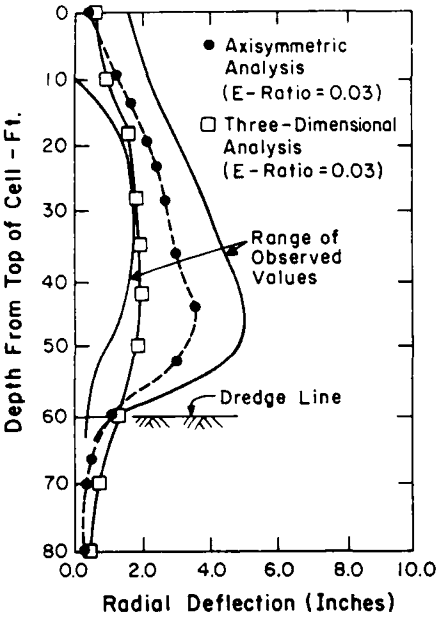

Fig. 7 - Comparison of Radial Deflection from Axisymmetric and Three-Dimensional Analyses - End of Filling

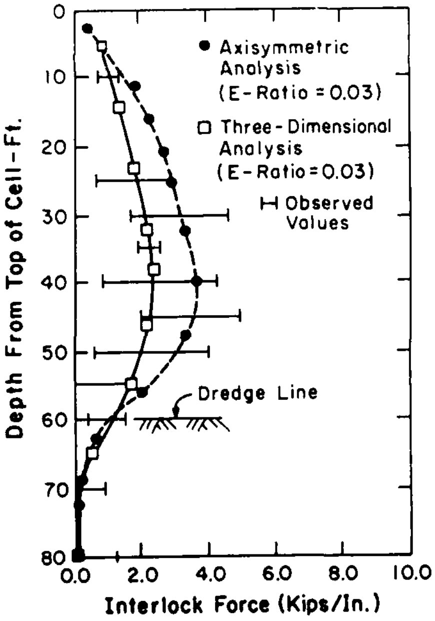

Fig. 8 - Comparison of Predicted Interlock Force from Axisymmetric and Three-Dimensional Analyses - End of Filling

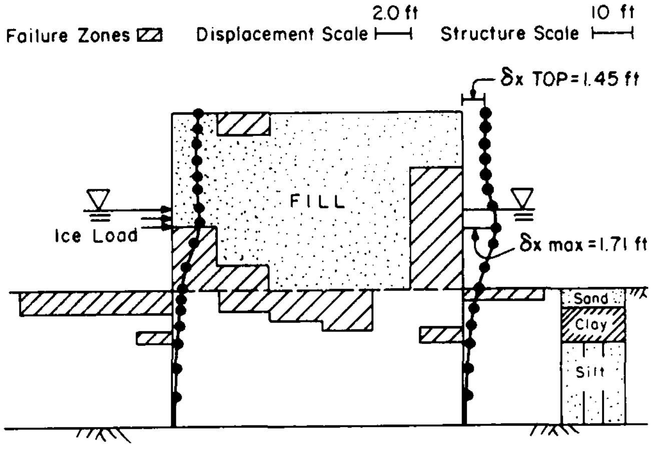

Fig. 9 - Predicted Deflections for Proposed Alaskan Offloading Facility

DESCRIPTION OF COFFERDAMS USED IN CASE HISTORY REVIEW

In Table 1 the key aspects are given for the six cofferdams used in this case history review. The first four are more conventional cases where the cofferdam serves as a temporary system to allow dewatering for construction within a body of water. The latter two are permanent systems, serving as waterfront and soil retaining structures. Instrumentation to monitor the cell filling stage was successfully installed for only two of the cases, the Lock and Dam 26 Stage 1 cofferdam, and the cofferdam for the Trident Drydock.

The diameter of the six cofferdams ranged from 62 to 76 ft, and their height above the dredge line varied from 36 to 80 ft. Sheetpile embedments varied widely, with the smallest at the Willow Island cofferdam where a rock foundation was present, to the largest at the Lock and Dam 26 (R) Stage 1 cofferdam with 35 ft of embedment.

Fill for all of the cofferdams was sand, although in the Seagirt case a 10 ft layer of soft silt soil remained in the cell beneath the fill. In the case of the Trident and Fulton Terminal 6 cofferdams the cell fills were densified using vibratory compaction after they were placed. The Trident case is also unique in that with unwatering of the interior of the cofferdam, the cells themselves were dewatered to increase the weight of the cell fill. In other cases, the cell fill remains partially saturated with water seeping from outboard to inboard side. The Lock and Dam 26 (R) cofferdams used special wellpoints just on the interior of the cofferdam to insure that the seepage water level was kept below dredge line.

Foundations for all of the case histories were generally sound, with the materials composed of dense sands, rock, or hard clays. The poorest foundation was for certain areas of the Seagirt cofferdam, where in some places it was composed of a fissured stiff clay.

TABLE 1. CASE HISTORY INFORMATION

Cofferdam	Cell Ht. (Ft.)	Cell Diam. (Ft.)	Foundation Conditions	Fmc* (K/in.)	Fcw* (K/in.)	Ht. of Fmc (Ft.)	Max. Diff'l Ld.	Max.Defl'n Diff'l Load	Avg.Defl. Max.Diff'l Load	References
Lock & Dam 26 Stage 1	60	63	Sand, med. to dense	4 (1.3 Ka)	5.8	H/4	60 ft. Water	5.7 in. (.8% H)	3.8 in. (.[illegible]% H)	Shannon and Wilson (198[illegible])
Lock & Dam 26 Stage 2	60-80	63	Sand, med. to dense	NA	NA	NA	80 ft. Water	5 in.** (.6% H)	3.5 in.** (.4% H)	Martin and Clough (198[illegible])
Trident Drydock	80	76	Dense Sand & gravel	8 (2.1 Ka)	8	H/8	80 ft. Water	4 in. (.4% H)	3.0 in. (.3% H)	Sorota et al., (1981)
Willow Island	55	65	Rock & Hard Clay	NA	NA	NA	40 ft. Water	1.5 in. (.2% H)	NA	Stevens (1980)
Seagirt Terminal	36	62	Sand & Stiff Clay	NA	NA	NA	55 ft. Slurry	Several Feet	NA	Clough and Duncan (1986)
Fulton Terminal 6	60	66		NA	NA	NA	60 ft. Compacted Backfill	11 in. (1.5% H)	5.7 in. (.8% H)	Schroeder (198[illegible])

*F_{mc}, F_{cw} = Max. Interlock Force after filling: Main Cell, Common Wall, respectively; NA - Not Available

**As of December 1986

Loading was provided by water for most of the cofferdams, except for the Seagirt and Fulton Terminal 6 cases. The Seagirt cofferdam, was designed to support dredged spoil, and the Fulton Terminal 6 cofferdam carried the load of the sand fill used to form the base for a wharf.

REVIEW OF CASE HISTORY DATA FOR CELL FILLING

Relatively few cofferdams have been instrumented and monitored for the cell filling stage. This is attributable to the problems of maintaining workable instrumentation on the sheetpiles as they are driven, and in obtaining reasonable zero readings on them before they are stabilized by filling the cells. Fortunately, as noted earlier, in two instances instrumentation has been successfully implemented during cell filling. In the case of both the Trident drydock (Sorota, et al., 1981) and the Lock and Dam 26 (R) Stage 1 cofferdams (Moore and Kleber, 1985), strain gages were applied to cells to allow determination of interlock forces during filling. Only in the case of Lock and Dam 26 (R) Stage 1 cofferdam were the inclinometers in place to measure cell movements during filling. A section through the Lock and Dam 26 (R) Stage 1 cofferdam is shown in Figure 10. As can be seen from the date in Table 1, the two cofferdams are similar in many characteristics, although the Trident cells had a greater height, less sheetpile embedment, a smaller diameter to height ratio, and was supported by a better foundation material. Notably, after fill placement, the cell fill in the Trident case was densified using a vibratory technique.

Interlock Forces on Filling

In Figure 11 the ranges of the measured main cell interlock forces for the two cases immediately after fill placement are shown. The trend in the data is for the interlock forces to increase with depth to a point slightly above the dredge line, and then to decrease after that. With compaction of the fill for the Trident cofferdam, the interlock stresses showed a clear increase over the placement values. For purposes of comparison with predicted interlock forces the measured values at the completion of cell filling are shown with those determined using the the TVA

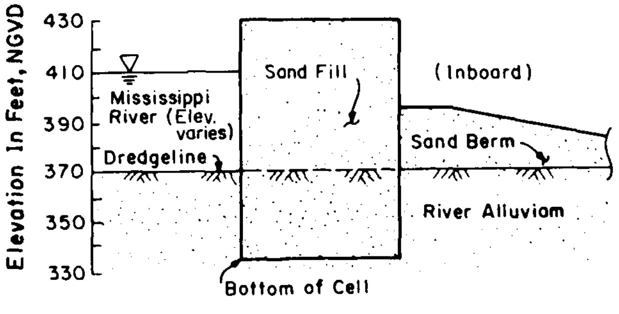

Fig. 10 - Typical Cell Schematic of Lock & Dam 26 (R)

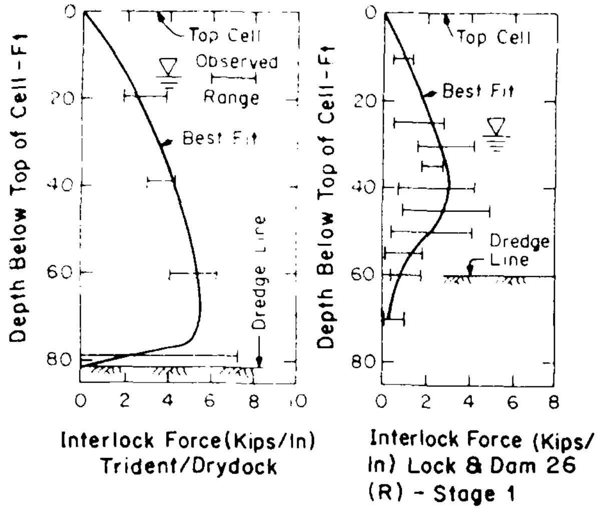

Fig. 11. - Measured Interlock Forces for Trident and Lock and Dam 26 (R) Cofferdams

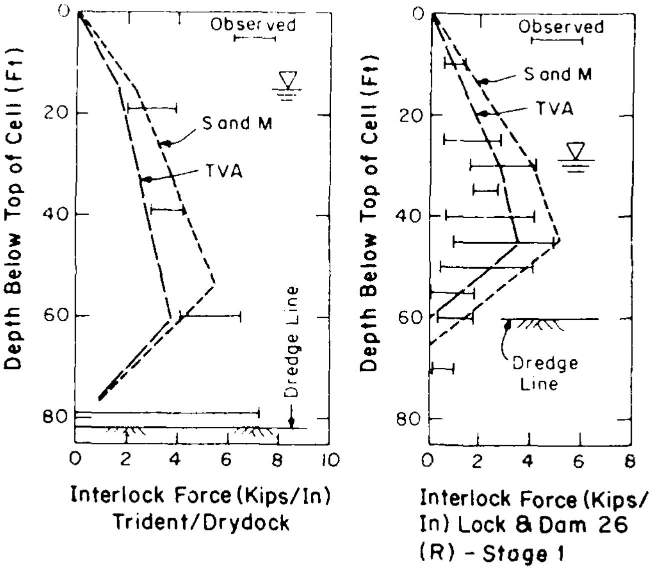

Fig. 12. - Comparison of Predicted TVA and S&M Interlock Forces with Measured Values

and S&M methods in Figure 12. General conclusions that are drawn from the measured interlock forces from the filling stage are:

1.) The observed interlock force distributions follow a similar trend to that defined by the TVA or S&M methods.

2.) The TVA method tends to predict interlock forces for cell placement which fit the average observed values for the Lock and Dam 26 (R) case well, but are on the low side for the Trident case. Conversely, the S&M method is on the high side for Lock and Dam 26 (R), and fits the average well for the Trident case.

3.) The maximum interlock force typically occurs at distances of 0.125H and 0.25H above the dredge line for the Trident and Lock and Dam 26 (R) cofferdams respectively. The higher location for the maximum interlock force is associated with the greater embedment of the Lock and Dam 26 (R) cofferdam versus that of the Trident case.

4.) The earth pressure coefficient for the compacted fill in the Trident cofferdam is higher than could be reasonably predicted by either the TVA or S&M methods. This is likely due to either built-in compaction stresses, or break down of arching effects in the fill as a result of the disturbance in the fill by the compaction.

As would be expected from conventional theory, the measured values of interlock forces in the common walls of the two cofferdams are higher than those in the main cells. However, the measured values are less than would be expected by the TVA secant formula, and more consistent with the predictions of the Swatek approach.

Cell Displacements on Filling

The different measurements of cell displacements generated by filling for Lock and Dam 26 (R) Stage 1 cofferdam inclinometers yielded the same general trends, but there was a rather wide spread in magnitudes (Figure 7). This is likely due to the extreme flexibility of the cofferdam before and during filling. The deflected shape indicates increasing cell bulging down to a point about 0.25H above the dredge line, and decreasing movements after this. The location of the maximum bulge is consistent with the location defined for the measured maximum interlock force, as it should be. This location of maximum bulge is also consistent with that suggested by Lacroix et al. (1970) for other cofferdams with similar conditions.

REVIEW OF CASE HISTORY DATA FOR COFFERDAMS SUBJECTED TO DIFFERENTIAL LOADING BY WATER

The data available for the four temporary cofferdams varies in extent and consistency. In some cases, there was only a survey net to measure movements of the top of the cells (Stage 2 cofferdam of Lock and Dam 26), while in others data were obtained from inclinometers and strain gages as well.

Interlock Forces

In the application of differential loads to the two cofferdams instrumented for interlock force, conditions differed. At Lock and Dam 26 (R) Stage 1, a restraining berm was placed on the interior of the cofferdam before unwatering began. During unwatering, a dewatering system was activated which controlled the underseepage beneath the cofferdam. The Trident cofferdam was unusual in that upon unwatering of the interior, the cell fills themselves were dewatered.

For Lock and Dam 26 (R), the maximum interlock forces showed decreases during berm placement, unwatering, and flooding by percentages of 3, 40, and 27 respectively. These decreases are all counter to conventional theory which would predict no change for berm placement, and an increase on initial unwatering and flooding. Interestingly, the finite element analyses of this cofferdam correctly predicted these trends (Clough and Kuppusamy, 1985). The reason for the lack of agreement between conventional theory and the actual behavior is shown in the finite element analyses to lie in the effects of the stabilizing berm. The initial berm loading works against the pressures exerted by the cell fill, and lowers the net load at a point near the maximum interlock force. Upon unwatering and flooding, the cell walls are pushed against the berm which then mobilizes the strength of the soil in the berm, and generates additional resistance to lower the net loading on the sheetpiles.

In the Trident cofferdam, where no berm was present, unwatering led to an increase of interlock forces on the unwatered or inboard side, and a decrease on the outboard side. This response is consistent with conventional theory, and reflects the fact that there is no element requiring further consideration of soil-structure interaction beyond the simplest concepts. The contrast between the Trident and Lock and Dam 26 (R) Stage 1 cofferdams shows the importance of soil-structure interaction in cofferdam behavior.

Cell Movements

The inclinometer-based movements of the instrumented cells for the Trident and Lock and Dam 26 (R) Stage 1 cofferdams allow the cell wall displacement patterns to be determined. Figures 13 and 14 show the measured profiles for the outboard and inboard sides for two of the typical cells for each cofferdam. The profiles reflect the effects of the unwatering isolated from the previous displacements induced by filling. The Trident cell tended to rotate in a relatively uniform pattern, while the Lock and Dam 26 (R) cell underwent more of a distortion effect with the lower portions of the cells restrained. This difference can be attributed to: (1) The differences in cell embedments, with those for the Trident cell small, and those for the Lock and Dam 26 (R) cell large; (2) The presence of the restraining berm against the inboard sheetpiles for Lock and Dam 26 (R); and, (3) the especially dense condition of the fill at the Trident cofferdam. One notable common trend in the results is that the outboard side moved more than the inboard side, a behavior that is confirmed in other measurements shown subsequently.

The inclinometer measurements are interesting, but they only represent the movement of one cell. Thus, it is also useful to study the survey data for top of cell movement since this is available for many cells, and allows an insight into the scatter of behavior as well as other aspects of response. In Figure 15 the survey data obtained during the unwatering of Lock and Dam 26 (R) Stage 1 cofferdam for

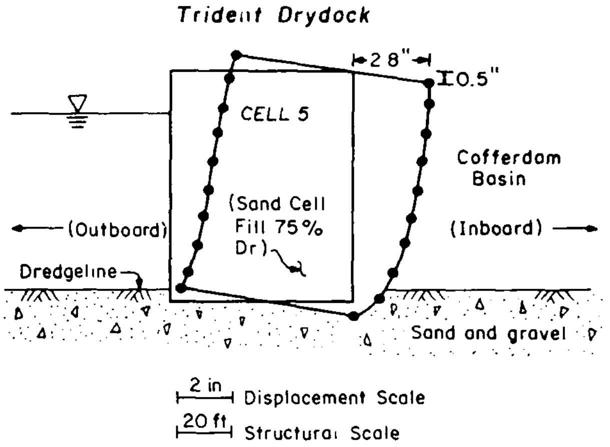

Fig. 13. - Movement of Cell 5 of Trident Drydock Cofferdam during Dewatering

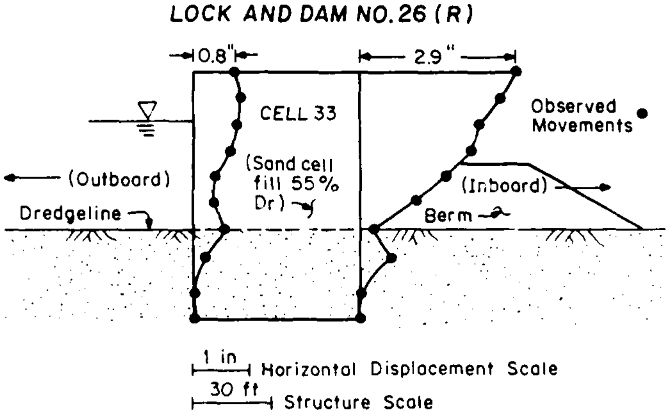

Fig. 14 - Movement of Cell 33 of Lock & Dam 26 (R) during Dewatering

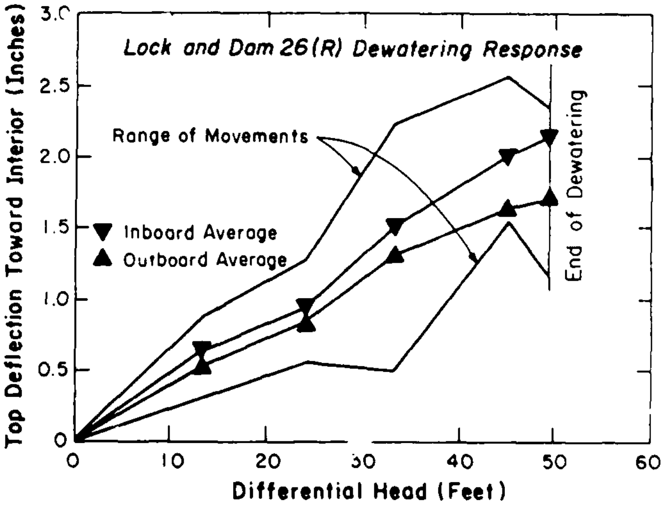

Fig. 15 - Movements of 11 Typical Cells during Dewatering (optical survey)

movements of the tops of 11 typical upstream and downstream cells are plotted versus the differential head between the outboard and inboard side of the cells. The differential head is a simple measure of the loading applied to the cells. The range in cell movements as well as the averages are shown. The following trends stand out:

1.) Although there is scatter in the data, there is a consistent trend for the cell displacements to increase almost linearally with differential head.

2.) The average of the inboard cell movements is uniformly larger than those of the outboard cell movements.

Review of the data from other cofferdams shows the same response as indicated in these conclusions, and a similar response is seen in finite element analyses (Martin and Clough, 1988).

Figure 16 extends the movement data for the 11 typical cells of Lock and Dam 26 (R) Stage 1 cofferdam to include the behavior that was observed as the water levels fluctuated after completion of unwatering. The changes in differential water head first involved a small decrease. This was followed by a flood event in December of 1982. As the head reached essentially 60 ft and threatened to overtop the cells, the Corps of Engineers began voluntary flooding of the interior of the cofferdam using an emergency spillway. This immediately led to a decrease of the differential head acting on the cofferdam. As is seen in Figure 16, the response of the cofferdam to these loadings was not the same as that which developed on initial unwatering. Each event led to cumulative increases in movements. The response to the December high water was particularly sharp with deformations increasing with differential head faster than during unwatering. It is believed that this is caused by the fact that the moment arm of the high water about the cofferdam centerline is greater than that of the normal pool, and that the high water leads to more submergence of the cell fill, thus reducing the effective stresses and stiffness of the fill. It is also notable that the outboard sheetpiles moved more than the inboard sheetpiles during the high water loading, where the opposite was true on unwatering. This reversal is caused by the fact that the high water loading is directly applied to the outboard sheetpiles.

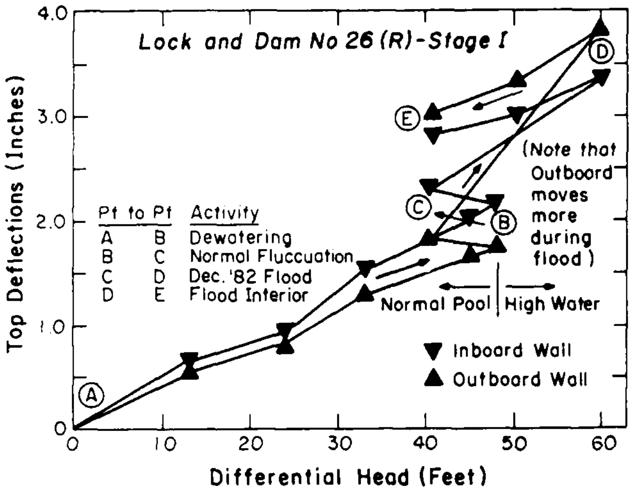

Fig. 16 - Dewatering and Flood Response 11 Typical Cells (optical survey)

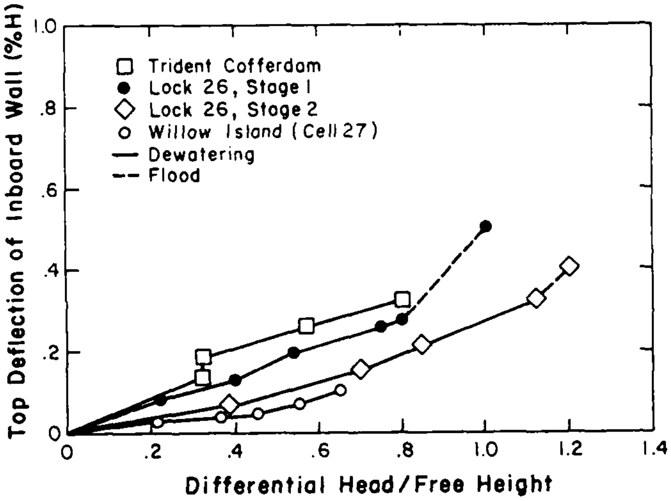

Fig. 17 - Normalized Loads and Movements for Cofferdams under Water Loadings

To compare the four temporary cofferdam movements, the measured displacements of the tops of the cells are normalized by dividing by the free height of the cell, and then plotted against the differential head which is also normalized by the free cell height (Figure 17). The amount of data tabulated for each project varies; only limited inclinometer information was available for Willow Island, but for the others, each point represents the average of many survey measurements. As is seen in the figure, the nondimensionalized movements follow the loading directly, and in an almost linear fashion until the very high levels of loading are reached. In order of increasing nondimensionalized movements, the cofferdams are ranked as Willow Island, Lock and Dam 26 (R) Stages 1 and 2, and Trident. This ranking is consistent with the relative conditions for the cofferdams. Willow Island has the largest diameter to height ratio, the strongest foundation, and a stabilizing berm, and it shows the smallest displacements. The Trident cofferdam has one of the smallest diameter to height ratios, no interior stabilizing berm, and the greatest height, and it shows the largest displacements. The Lock and Dam (R) 26 cofferdams have conditions which fall between the other two, and displacements which do likewise.

The general level of the nondimensionalized movements are of interest since the consistency of the trends shown for the cofferdams suggest that they can be used to help predict the likely level of movement of cofferdams with similar conditions. There are two other reference points of this type worthy of mention. Swatek (1967) reports that in his experience the typical temporary cofferdam moves 1 % of its free height at the top of the cell. This would be high for the average movement data in Figure 17, where none of the values exceeded 0.6 %. However, if the extreme movements were considered at each cofferdam, then the 1 % figure would not be far from the observed value. In finite parametric studies, Singh and Clough (1988) report that the movements should not exceed 0.5 % for a conservatively designed cofferdams, particularly if there is a stabilizing berm present. It would appear from all of the information that for prudent design of a cofferdam on good foundation conditions, a value of 0.5 to 1 % of the free cell height could be used to estimate displacements.

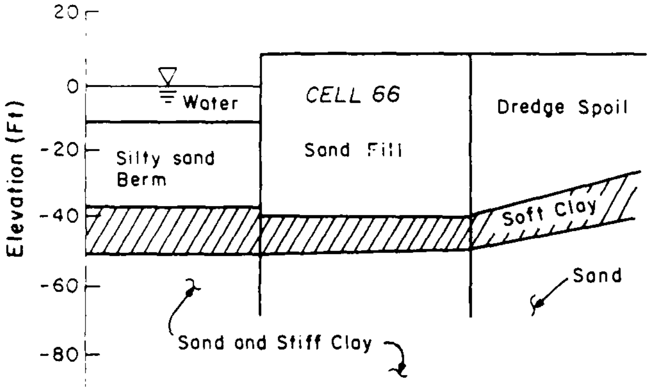

Fig. 18 - Typical Cell Schematic of Seagirt Cofferdam

REVIEW OF CASE HISTORY DATA FOR COFFERDAMS SUBJECTED TO OTHER THAN WATER LOADINGS

The Seagirt and Fulton Terminal 6 case histories represent unique situations in that these cofferdams are subjected to loading other than by water. Figure 18 shows typical section for the Seagirt cofferdam in the area where it was founded on sand. In other areas, this cofferdam was founded on a fissured hard clay. The Seagirt cofferdam was originally intended as a temporary system for the containment of the slurry created by excavation for the I-95 Baltimore Harbor tunnel. Several years subsequent to the construction of the tunnel, it was decided to use the cofferdam and its retained fill as a waterfront terminal. This review focuses on the cofferdam performance before the time changes were instituted to upgrade the system for its permanent use. The upper soils at the site were soft organic clays, and these were underlain by either stiff fissured clays, or dense sands. The cells were driven through the upper soils to a shallow embedment in the underlying stiffer soils. A sand fill was placed into the cells without removing the soft soils that remained inside the cells.

The Fulton Terminal 6 cofferdam case history is described by Schroeder (1987). This structure serves as a container wharf, and is founded on dense sand. Before driving the sheeting, an upper layer of soft silt was dredged. With the sheets in place, fill was dredged into the cells, and in the area behind the cells to create a level working surface. The fills in the cells and behind the cells was vibrated into a dense condition, with an estimated relative density of about 80 %.

Both the Seagirt and Fulton Terminal 6 cofferdams underwent significant deformations as a result of the lateral loads applied to them. In Figure 19, the lateral movements measured at the tops of selected cells for both cofferdams are plotted versus date, with key activities at the sites noted. For the Seagirt case, two sets of data are shown, one for a section of the cofferdam on a clay foundation, and one for a section on the dense sand. The movements for the Seagirt cofferdam do not represent the entire deformation history of this system, since some movement occurred before measurement benchmarks were installed.

Maximum lateral movements for the Seagirt case reached about 5 ft for the cell on founded on clay, and 1 ft for the cell founded on dense sand, values equal to 13 and 3 % respectively of the free cell height. While most of the displacements of the cells occurred during active construction, a significant portion of those for both foundation condition are time-dependent. Because no inclinometers were in place during the construction, the exact sources of the movements cannot be determined. However, it seems reasonable that the large deformations are in part related to the presence of the soft organic silts in the cell and in the soil on either side of the cell. Also, where the hard clay formed the foundation material, it is likely that the sheetpiles in the front of the cells plunged into the clay causing a rotation of the cells forward.

As is seen in Figure 19, lateral displacement due to placement of fill behind the cell was only 1.0 ft, or about 1.5% of the cell height. Inclinometers installed on the cofferdam cells allowed a definition of sources of movements. A significant amount of displacement was observed at the dredge line and below, indicating movements of the embedded portion of the sheetpiles.

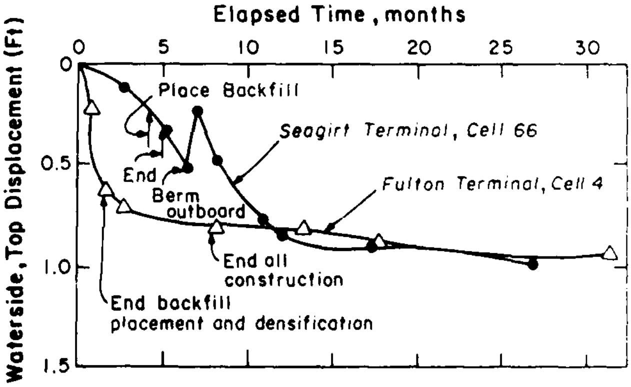

Fig. 19 - Lateral Displacements of Cells Loaded by Soil

The performances of the Seagirt and Fulton Terminal 6 cofferdams lead to the following observations:

1). Despite large deformations of the cofferdams, they continued to perform adequately showing the resilence of these flexible structures.

2.) The lateral movements of the cofferdams loaded by soil were larger than those of the cofferdams loaded by water.

3.) The movements of the Seagirt cofferdam are larger than those for the Terminal 6 cofferdam, presumably due to poorer foundation conditions and the presence of the weak silt in the fill.

SUMMARY AND CONCLUSIONS

Until the early 1970's, the technology for cellular cofferdams was relatively static. Design methods were largely empirical, and the main use for cofferdams was as a temporary structure to allow construction in the dry in a body of water. Since that time, a number of studies of the subject have taken place in the form of model and full-scale instrumentation projects. Also, investigators have developed finite element models with realistic allowances for many of the important aspects of the complex cofferdam problem. Conclusions from the work to date include:

1.) Model studies have led to new methods for calculating interlock forces and internal stability. These generally lead to less conservative answers than are obtained by the early design techniques.

2.) For finite element methods to successfully model the cellular cofferdam, they must account for the nature of the construction process, the nonlinear soil behavior, flexibility added to the system through sheetpile interlock deformations, and slip between the sheetpiles and the soils.

3.) Finite element analyses show that the soil-structure interaction process in the cofferdam is complicated because of the flexibility of the system and the large deformations that occur.

4.) Earth stability berms placed on the interior of the cofferdam have an impact on the behavior both in reducing overall cell deformations, and in limiting the development of interlock forces in the cell by providing a restraint at the location where the interlock forces are usually the largest.

5.) For cells with significant embedment, the maximum interlock force and cell bulge occurs at a distance of about 0.25H above the dredge line.

6.) For cells with small embedments, the maximum interlock force and cell bulge occurs at a distance less than 0.25 H above the dredge line.

7.) The maximum interlock force can be reasonably calculated using either the TVA or S&M methods when a earth berm is not present. If an earth berm is present, then these methods will lead to conservative predictions of interlock forces for conditions after filling.

8.) Average lateral displacements at the top of conservatively designed cofferdams under the action of water loading will be in the range of 0.5 % of the cell height. Repeated loading by high water can lead to cumulative increases of cofferdam movements.

9.) Lateral displacements of cofferdams are controlled by the magnitude of the lateral loading, and follow the loading magnitude almost linearally so long as the factor of safety of the system is well above one.

10.) Densification of the cell fill causes increases in interlock forces and cell displacements over those induced during cell filling.

11.) In the cases considered herein, cofferdams loaded by soil moved more than those loaded by water.

12.) Cellular cofferdams are resilient structures, and are able to sustain large displacements and distortions without failure.

ACKNOWLEDGEMENTS

The authors would like to express their appreciation to many individuals and organizations that have contributed to this effort. Funding for much of the work has come from the U. S. Corps of Engineers, Contract No. DACW 39-86-K-0007. Corps employees who were of special help include Messrs. T. Mudd, R. Mosher, and Brian Kleber. Virginia Tech colleagues who worked with the authors on one phase or the other of the projects mentioned in this paper include T. Kuppusamy, Y.P. Singh, and J. M. Duncan. Thanks are also due to Mr. R. Nelson, Chief Engineer of the Maryland Port Administration for allowing use of the Seagirt Marine Terminal data.

REFERENCES

Clough, G. W. and Duncan, J. M. , "Finite Element Analysis of Cofferdam Movements during Construction of the Seagirt Terminal, Baltimore," STV/Lyon Associates, Baltimore, MD, April, 1986.

Clough, G. W. and Goeke, P. M., "In Situ Testing for Lock and Dam 26 Cellular Cofferdam," Proceedings, Use of In Situ Tests in Geotechnical Engineering, ASCE Speciality Conference, Geotechnical Special Publication No. 6, 1986, pp. 131-145.

Clough, G. W. and Hansen, L. A., "A Finite Element Study of the Behavior of the Willow Island Cofferdam," Technical Report No. CE-218, Department of Civil Engineering, Stanford University, 1977.

Clough, G. W. and Kuppusamy, T., "Finite Element Analyses of Lock and Dam 26 Cofferdam," Journal of the Geotechnical Engineering Division, ASCE, Vol. III, No. 4, April, 1985, p. 521-544.

Cummings, E. M., "Cellular Cofferdams and Docks," Journal of the Waterways and Harbors Division, ASCE, Vol. 83, No. WW3, Paper No. 1366, September, 1957, pp. 13-45.

Department of the Navy, Soil Mechanics, Foundation and Earth Structures, NAVDOCKS Design Manual DM7, Bureau of Yards and Docks, Washington, DC, March, 1971.

Hansen, J. B., "Earth Pressure Calculations," Danish Technical Press, Institution of Danish Civil Engineers, Copenhagen, 1953.

Krynine, D. P., Discussion of "Stability and Stiffness of Cellular Cofferdams," by K. Terzaghi, Transactions, ASCE, Vol. 110, Paper No. 2253, 1945, pp. 1175-1178.

Kuppusamy, T., Clough, G. W. and Finno, R. J., "Analysis of Cellular Cofferdams Including Three Dimensional Cell Interaction," Proceedings, 11th International Conference on Soil Mechanics and Foundation Engineering, Vol. 4, 1985, pp. 1993-1996.

Lacroix, Y., Esrig, M. I. and Luscher, U., "Design, Construction and Performance of Cellular Cofferdams," Proceedings, ASCE Specialty Conference, Lateral Stresses in the Ground and Design of Earth Retain-Structures," June, 1970, pp. 271-328.

Maitland, J. K. and Schroeder, W. L., "Model Study of Circular Sheetpile Cells," Journal of the Geotechnical Engineering Division, ASCE, Vol. 105, No. GT7, July, 1979, pp. 805-822.

Martin, J. R. and Clough, G. W., "A Study of the Effects of Differential Loadings on Cofferdams," Technical Report Prepared for U. S. Corps of Engineers, 1988.

Moore, B. H. and Kleber, B. K., "Multiple Integrated Instrumentation Programs Locks and Dam No. 26, Mississippi River, " Proceedings, Congress on Large Dams, 1985, pp. 621-641.

Mosher, R., "Three Dimensional Finite Element Analysis of Cellular Cofferdams," Thesis to be Submitted in Partial Fulfillment of the Ph.D. Degree, Virginia Polytechnic Institute and State University, 1988.

Peters, J. F., Leavell, D. A., and Holmes, T. L., "Finite Element Analysis of Williamson CBD Sheetpile Cell Floodwall," Prototype Cell Analysis, Task II, Department of the Army, Vicksburg District, Corps of Engineers, February, 1987.

Rossow, M., Edward, D., Mosher, R., "Theoretical Manual for Design of Cellular Sheet Pile Structures (Cofferdam and Retaining Structures)," Department of the Army, Corps of Engineers, Waterways Experiment Station, Vicksburg, Mississippi, May, 1987.

Schroeder, W. L. and Maitland, J. K., "Cellular Bulkheads and Cofferdams, " Journal of the Geotechnical Engineering Division, ASCE, Vol. 105, No. GT7, July, 1979, pp. 823-838.

Schroeder, W. L., "Wharf Bulkhead Behavior at Fulton Terminal 6," Journal of the Geotechnical Engineering Division, ASCE, Vol. 113, No. 6, June, 1987, pp. 600-615.

Shannon and Wilson, Inc., "Summary Report, Instrumentation Data Analyses and Finite Element Studies for First Stage Cofferdam, Lock and Dam 26 (Replacement)," Department of the Army, St. Louis District, Corps of Engineers, November, 1983.

Singh, Y. P. and Clough, G. W., "Finite Element Analyses of Cofferdams, "Technical Report Prepared for U. S. Corps of Engineers, 1988.

Sorota, M. D., Kinner, E. B. and Haley, M. X., "Cellular Cofferdam for Trident Drydock: Performance," Journal of the Geotechnical Engineering Division, ASCE, Vol. 107, No. GT12, December, 1981, pp. 1657-1676.

Stevens, R. F., "Study of the Behavior of a Cellular Cofferdam," Thesis Submitted in Partial Fulfillment of the Ph.D. Degree, Duke University, 1980.

Swatek, E. P., "Cellular Cofferdam Design and Practice," Journal of the Waterways and Harbors Division, ASCE, Vol. 93, No. WW3, Proc. Paper 5398, August, 1967, pp. 109-130.

Tennessee Valley Authority, "Steel Sheet Piling Cellular Cofferdams on Rock," TVA Technical Monograph No. 75, Vol. 1, December, 1957.

Terzaghi, K., "Stability and Stiffness of Cellular Cofferdams," Transactions, ASCE, Vol. 110, Paper No. 2253, 1945, pp. 1083-1202.

Author's Index

Aas, P.M. 1249
Abdel-Salam, S. 1437
Abolhassani, D. 347
Abramson, L.W. 1191
Agarwal, K.B. 645
Ahmad, S.A. 1343
Alberro, J. 467
Al-Yahyai, K.S. 1201
Amano, T. 1099
Amick, D. 811
Amin, D.P. 1165
Anderson, D.G. 443
Angeles, N.P. 1319
Anguelov, K. 299
Antes, D.A. 195
Arcangeli, E. 947
Arya, A.S. 837
Atibu, F.S. 717
Atmatzidas, D.K. 1297, 1303
Atukorala, U. 863
Atwater, J. 55
Aughenbaugh, N.V. 163
Azevedo, R. 689, 1465

Baer, G.R. 355
Bahrami-Samani, F. 347
Bailey, B. 489
Baker Jr., C.N. 1383, 1389
Baliga, B.D. 407
Bandis, S.C. 107
Bandyopadhyay, S. 837
Bapat, A. 825
Barnes, G.E. 1229
Bauer, L.T. 143
Beene, R.R.W. 567
Berggren, B. 1169
Berry, R.M. 885
Betournay, M.C. 291
Bhandari, R.K. 245, 333
Binquet, J. 511
Blendy, M.M. 1233
Blight, G.E. 929
Bloom, E. 489
Borden, R.H. 1449
Borm, G. 953
Boscardin, M.D. 1029
Bosscher, P.J. 63
Bowman Jr., J.C. 795
Brenner, R.P. 347
Broms, B.B. 1515
Bruce, D.A. 1121
Bucher, S.A. 1303
Burgess, A.S. 81
Butler, D.K. 519
Butts, R.L. 201
Byington, M.L. 1087
Byrne, P.M. 863

Cabrera, J.G. 185
Caldwell, J.A. 25
Calle, E.O.F. 533
Cameron, R. 1209
Carr, C.A. 1209
Cazzuffi, D. 1137
Celestino, T.B. 941
Chandrashekhar, K. 253
Chandra, D. 361
Chaney, R.C. 555
Chang, Y.H. 417
Chan, Y.C. 559
Charles, R.D. 1069
Cheng, S.S.M. 1343
Chonggang, S. 729
Chouery-Curtis, V.E. 1063
Chowdhary, G.R. 1133
Christodoulias, J. 457
Christopher, B.R. 1093, 1383
Christos, M. 337
Christoulas, St. 671
Chua, K.M. 1417
Chugh, Y.P. 253
Chukweze, H.O. 935, 1279
Chummar, A.V. 1271
Chung, K.Y.C. 1113
Cincilla, W.A. 495
Ciuffi, F. 877
Clough, G. Wayne 1597
Colleselli, F. 599
Collins, S.A. 977
Consoli, N. 1465
Cooling, T.L. 1375
Coons, L. 25
Corda, I.I. 663
Cordell, D.A. 35
Coulson, A. 683
Courage, L.R. 635
Cowherd, D.C. 683, 1471
Cramer, G.H. 71
Curtis, R.L. 1063

Dailer, D. 1263
Daman, M.M. 1505
Datye, K.R. 1075
Davie, J.R. 1019, 1309, 1395
Deal, C.E. 451
Deaver, C.M. 519
DeFour, S. 1001
Dehner, J.G. 443
Dekker, J. 547
Desai, C.S. 1551
Descour, J.M. 229
Dezfulian, H. 43
Dhowian, A.W. 237, 1117
Dirnberger, M.M. 787
Dominque, L.C. 941
Dong, J.G. 1501
Doria, A.C. 1037
Dovnarovitch, S. 1245
Dube, A.K. 211
Dumas, J.C. 921
Duncan, J.M. 977
de Pee, J. 541

Earley, K.H. 341
East, D.R. 495
Edil, T.B. 63
El-Sohby, M.A. 321
Endicott, L.J. 123
Erol, A.O. 237
Erwin, J.W. 355

Fang-Fu, T. 749
Fan, W. 1047
Farrel, E.R. 1145
Fattohi, Z.R. 159
Fergusson, W.B. 1293
Ferrari, O.A. 941
Findlay, R.C. 401
Finn, W.D.L. 1585
Finno, R.J. 1297
Fowler, J. 977
Fradkin, S.B. 221
Franks, L.W. 977
Fraser, D. 863

Fulan, P. 743

Gado, D.P. 1327
Gallavresi, F. 1121
Gambin, M. 969
Garga, V.K. 1239
Gassios, E. 671
Gates, W.C.B. 1
Gerber, F.A. 411
Ghinelli, A. 1173
Ghosh, D.K. 807
Ghosh, N. 1055
Giannaros, H. 457
Gichaga, F.J. 717
Gilchrist, A.J.T. 627
Gillon, M.D. 841
Glynn, E.F. 1293
Goel, M.C. 423, 433
Goel, R.K. 177
Golder, M.H. 1107
Gonzalez-Valencia, F. 467
Gouda, M.A. 1315
Grainger, G.S. 201
Grice, H. 885
Grosch, J.J. 1201
Gross, D.J. 143
Guatteri, G. 1037
Gupta, M.K. 837
Gupta, V.K. 1509
Gurevich, A.M. 89

Handford, G.T. 829
Hannink, G. 1403, 1409
Hansbo, S. 1337
Hansmire, W.H. 1191
Hardin, D.J. 1087
Harrel, H.C. 997
Harsulescu, A.I. 711
Hartung, S.C. 513
Hasan, B. 271
Hejazi, H. 461
Hempen, G.L. 787
Hepworth, R.C. 1349
Hermosilla, R.P. 677
Houssamy, I. 1505
Hsieh, H.N. 7
Huag, M.D. 55
HuiShan, L. 765
Hummert Jr., J.B. 1375
Hurd, J.O. 1471
Hu, G.A. 137

Ilsley, R.C. 221
Itskowitch, M. 737
Ivanov, Y. 1245
Ivsic, T. 819
Izhar-ul-Haq 705

Jain, J.K. 1289
Jain, P.K. 1489
Jain, S.L. 607
Jethwa, J.L. 147, 177
Jianyun, M. 167
Jiayou, L. 167
Johnson, L.D. 989
Jokhyo, A.M. 279
Jones, C.J.F.P. 1275
Jones, D.L. 1107
Judge, A.S. 1001

Kalteziotis, N. 671
Kapoor, K.K. 285, 657
Karfakis, M.G. 173
Katti, A.R. 527
Katti, D.R. 527
Katti, R.K. 527
Kauschinger, J.L. 1037
Kaushik, S.K. 1509
Keaveny, J.M. 1249
Kelley, G.P. 1327
Keys, R.A. 635
Ke, Z.J. 417
Khare, P.S. 207
Khare, R.K. 1289
Khera, R.P. 985
Kilkenny, W.M. 19
Kim, Y.S. 1443
King, T.B. 443
Kinner, E.B. 503
Kiricenko, A. 819
Kiu, T.K. 1257
Klohn, E.J. 479, 829
Knight, R.B. 55
Knuppel, L. 383
Koga, Y. 721
Kogure, K. 377
Kozicki, P. 55, 1149
Kravits, S.J. 997
Krizek, R.J. 1303
Kropp, A. 1461
Kulkarni, S.G. 207
Kummerle, R.P. 921
Kvasnicka, P. 819
Kwong, J.K.P. 123

Lafleche, P. 1001
Laier, J.E. 993
Laird, G.S. 81, 89
Lakshnaman, N. 855
Lambrechts, J.R. 503
Lam, W. 1389
Lance, D.S. 911
Larson, J.A. 215
Lau, K.C. 291
Lavania, B.V.K. 615, 621
Lengfelder, J. 1349
Leonard, B.D. 593
Leonard, M.S. 81
Lewis, M.R. 1019, 1233, 1309, 1395
Lew, M. 795
Lien, W. 1449
Lifrieri, J.L. 195
Lindquist, R.W. 651
Lippincott, I.W. 1315
Lissey, A. 55
Li, J.C. 1421
Llopis, J.L. 519
Long, P.D. 1169
Lozier, W.B. 89
Lo, R.C. 479, 829
Luan, D.Z. 1371
Lumsden, A.C. 123
Lum, K.K. 479
Luong, M.P. 1455
Lyman, T.J. 911

Macdonald, G.J. 1107
Macedo, G. 467
MacTavish, G.C. 369
Madhav, M.R. 1075
Marsland, A. 695
Martin III, James R. 1597
Mashhour, M. 1437
Mastrantuono, C. 947
Mathur, T. 587
Matsui, T. 1099
Matsuo, K. 377
Matsuo, O. 721
Matthews, W.G. 369
Mattox, R.M. 993
Maurath, G. 811
Mazen, S.O. 321

McElroy, J.J. ... 1327
McGrane, D. ... 13
McLean, F. ... 383
Mehrotra, G.S. ... 245
Meissner, H. ... 953
Miglani, V.D. ... 871
Miller, D.A. ... 1063
Miller, R.J. ... 229
Mills, D.E. ... 35
Mills, S.V. ... 1087
Milne, W.G. ... 829
Mirza, C. ... 291
Missavage, R. ... 253
Mithal, R.S. ... 311
Mitsch, M.P. ... 1257
Mitsuse, C.T. ... 941
Modhwadia, K.E. ... 327
Mokhashi, S.L. ... 207
Montanez, L. ... 467
Moore, B.H. ... 787
Mosley, E.T. ... 885
Mudjihardjo, D. ... 423
Mundell, J.A. ... 489
Murty, A.V.S.R. ... 361
Muthumani, K. ... 855

Nadim, F. ... 1249
Nainwal, H.C. ... 305
Natarajan, T.K. ... 361, 365
Nathan, S.V. ... 1483
Nayak, G.C. ... 1489
Nelson, J.D. ... 699
Nerby, S.M. ... 1297
Neyer, J.C. ... 1025
Nhiem, T.V. ... 889
Nicholson Jr., A.J. ... 1425
Nowatzki, E.A. ... 1477

Ohri, M.L. ... 1133
Olsen, J.M. ... 593
Orr, T.L.L. ... 1145
Otani, Y. ... 1099
Ou, C.Y. ... 1183
O'Donovan, T. ... 1145

Pagotto, A. ... 1137
Pancholi, D.M. ... 327
Pang, P.L.R. ... 559
Patel, N.M. ... 127
Patodiya, S.C. ... 285, 657
Paul, J. ... 1127
Perlea, V.G. ... 683, 1471
Perry, C.W. ... 801
Perry, E.B. ... 1037
Peters, J.F. ... 977
Petroff, L.J. ... 1417
Petschl, R.O. ... 533
Pitts, J. ... 115
Posse, J.A. ... 677
Prabhakar, B. ... 147
Prager, R.D. ... 201
Prasad, C. ... 305
Price, H.R. ... 1025

Qian, Y.P. ... 1501
Qiu, Y. ... 1047

Rager, R.E. ... 25
Raghu, D. ... 7, 51, 195, 1315
Rahim, K.S.A. ... 1117
Ramage, J. ... 1577
Ramamurthy, T. ... 263, 607
Ranjan, G. ... 1509
Ransone, J.W. ... 495
Rao, P.J. ... 365
Rapp, R.J. ... 1495
Ray, M.B. ... 807
Reed, R.F. ... 1159
Richardson, T.L. ... 1011
Richards, D.P. ... 215
Riker, R. ... 1263
Rimoldi, P. ... 1137
Robison, M.J. ... 911
Rodda, K.V. ... 801
Rodriquez-Molina, C. ... 151
Rodriquez-Perez, B. ... 151
Roodsari, A. ... 383
Rosenthal, I. ... 737
Rudenko, D. ... 341
Rupchang, K.V. ... 437

Sahu, B.K. ... 717
Sammy, G.K. ... 651
Santamaria, J.M.M. ... 677
Santos, L.A. ... 689
San, K.C. ... 1099
Sarma, B.S. ... 855
Sarsby, R.V. ... 75
Schaefer, V.R. ... 977
Schneider, J.R. ... 651
Schubert, W. ... 1011
Schwenk, J.L. ... 1495
Scott, M.D. ... 479
Seco e Pinto, P.S. ... 849
Seed, R.B. ... 1183
Shah, D.L. ... 1165
Sharma, D. ... 1365
Sharma, H.D. ... 1149
Sharma, V.M. ... 263
Sheng-sun, X. ... 1285
Shen, W.Y. ... 1501
Shiwei, D. ... 759, 773
Shixuan, Z. ... 575
Shi, L.P. ... 1421
Shi, M. ... 1047
Shorey, E.F. ... 221
Shroff, A.V. ... 1165
Shy, B.I. ... 1421
Simonini, P. ... 599
Singh, A. ... 1133
Singh, B. ... 147, 177, 211, 407, 1489
Singh, V.K. ... 407
Sivapatham, T. ... 581
Smith, R.B. ... 395
Smith, T. ... 451
Solymar, Z.V. ... 369
Song, B. ... 969
Soranzo, M. ... 599
Sowers, G.F. ... 1567
Soydemir, C. ... 1257
Srinivasulu, P. ... 855
Srivastava, L.S. ... 779
Steinberg, S.B. ... 1389
Stipho, A.S. ... 1433
Stoll, U.W. ... 1319
Stroman, W.R. ... 567
Sullivan, W.J. ... 1449
Sundriya, Y.P. ... 305
Suprenant, B.A. ... 173
Surabaya, J.L. ... 433
Swaffar, K.M. ... 1025

Tabba, M.M. ... 1055
Taiping, Q. ... 765, 963
Tepel, R.E. ... 801
Termaat, R.J. ... 533
Testa, S.M. ... 97
Thompson, P.Y. ... 1443
Thornhill, P.D. ... 567
Thrasher, S.M. ... 1471
Tomiolo, A. ... 947
Tsiambaos, G. ... 671

Tsien, S.I. 1219
Tucker, K.D. 1355
Tuttle, D.C. 555

Vaidya, P.H. 327
Van Besien, A.C. 163
Van Order, R.J. 51
Van Quang, N. 1169
Vannucchi, G. 1173
Vaziri, H. 863
Vazquez Castillo, A. 151
Vazquez Castillo, L. 151
Von M. Harmse, H.J. 411
van Herpen, J.A. 541
van Tol, A.F. 1409

Wade, N.H. 635
Wagner, A.B. 1093
Wang, Z.Q. 131
Weaver, C.L. 1395
Weaver, K.D. 143
Weiquen, Z. 963
Wei, L.F. 635
West, T.R. 403
Wietek, B. 905
Willis, R. 587
Wolff, T.F. 787
Wolosick, J.R. 1425
Wrench, B.P. 699, 1477
Wright, P. 1159
Wu, A.H. 1179

Xianjinan, Y. 759
Xikang, W. 755, 759
Yandell, W.O. 395
Yao, H.L. 1421
Yih, C.T. 985
Yiji, W. 1225
Yin, Y.A. 1501
Yong, C.H. 417
Young, L.W. 1019
Yuqing, W. 769, 963

Zainiko, A. 433
Zappi, U. 511
Zhang, R.X. 131
Zhang, X.X. 1371
Zhang, Z.S. 1371
Zhao, X.H. 1501
Zhen-Yu, T. 749